SANDIA REPORT SAND82-0664/1 • Unlimited Release
Printed July 1982

vol. 2

Subseabed Disposal Program Annual Report January to September 1981

Volume II: Appendices (Principal Investigator Progress Reports)

Part 2 of 2

SAND--82-0664 Vol. 2 App-Pt. 2

DE82 020854

Seabed Programs Division

Prepared by
Sandia National Laboratories
Albuquerque, New Mexico 87185 and Livermore, California 94550
for the United States Department of Energy
under Contract DE-AC04-76DP00789



MASTER

DISTRIBUTION OF THIS DOCUMENT IS UNLIMITED

SF 2900-Q(6-82)

DISCLAIMER

This report was prepared as an account of work sponsored by an agency of the United States Government. Neither the United States Government nor any agency thereof, nor any of their employees, makes any warranty, express or implied, or assumes any legal liability or responsibility for the accuracy, completeness, or usefulness of any information, apparatus, product, or process disclosed, or represents that its use would not infringe privately owned rights. Reference herein to any specific commercial product, process, or service by trade name, trademark, manufacturer, or otherwise does not necessarily constitute or imply its endorsement, recommendation, or favoring by the United States Government or any agency thereof. The views and opinions of authors expressed herein do not necessarily state or reflect those of the United States Government or any agency thereof.

DISCLAIMER

Portions of this document may be illegible in electronic image products. Images are produced from the best available original document.

Issued by Sandia National Laboratories, operated for the United States Department of Energy by Sandia Corporation.

NOTICE: This report was prepared as an account of work sponsored by an agency of the United States Government. Neither the United States Government nor any agency thereof, nor any of their employees, nor any of their contractors, subcontractors, or their employees, makes any warranty, express or implied, or assumes any legal liability or responsibility for the accuracy, completeness, or usefulness of any information, apparatus, product, or process disclosed, or represents that its use would not infringe privately owned rights. Reference herein to any specific commercial product, process, or service by trade name, trademark, manufacturer, or otherwise, does not necessarily constitute or imply its endorsement, recommendation, or favoring by the United States Government, any agency thereof or any of their contractors or subcontractors. The views and opinions expressed herein do not necessarily state or reflect those of the United States Government, any agency thereof or any of their contractors or subcontractors.

Printed in the United States of America
Available from
National Technical Information Service
U.S. Department of Commerce
5285 Port Royal Road
Springfield, VA 22161

NTIS price codes
Printed copy: A113
Microfiche copy: A01

SAND82-0664/II
Unlimited Release
Printed July 1982

SUBSEABED DISPOSAL PROGRAM ANNUAL REPORT JANUARY TO SEPTEMBER 1981 VOLUME II APPENDICES (PRINCIPAL INVESTIGATOR PROGRESS REPORTS)

Part 2 of 2

Seabed Programs Division

K. R. Hinga, Editor

Abstract

Volume II of the eighth annual report describing the progress and evaluating the status of the Subseabed Disposal Program contains the appendices referred to in Volume I, Summary and Status. The annual report this year covers the period January to September 1981 because the program is shifting from a calendar year to a fiscal year reporting period. Because of the length of Volume II, it has been split into two parts for publication purposes. Part 1 contains Appendices A-Z; Part 2 contains Appendices AA-TT.

DISTRIBUTION OF THIS DOCUMENT IS UNLIMITED

CONTENTS

Part One
(Under Separate Cover)

Appendix

Systems

A Subseabed Disposal Safety Analysis: C. M. Koplick, T. J. Kabele 9

B A Systems Model for Assessing the Consequences of Release of Radioactive Material into the Ocean: C. M. Koplick 17

C Accident Scenarios and Probabilities for the SDP Transportation System: D. A. Ensminger 61

Waste Package

D Corrosion Studies of Titanium and Iron Base Alloys for Waste Canister Overpack Applications: R. B. Diegle, D. W. Schaefer, J. A. Ruppen, W. L. Larson, T. J. Headley 107

E The Effects of Hydrogen on Mechanical Properties of TiCode 12: S. L. Robinson, N. R. Moody, D. H. Doughty 127

F Effects of Radiation on Corrosion of Titanium: R. S. Glass 131

Site

G Assessment of North Atlantic Seabed Regions for Radioactive Waste Disposal: B. E. Tucholke and R. A. Stephen 139

H Maps of Sediment Thickness and Depth to Basement in the Western North Atlantic Ocean Basin: B. E. Tucholke, R. E. Houtz, W. J. Ludwig 151

I High Resolution Stable Isotope Stratigraphy of the Latest Pleistocene and Holocene of Three Northern Bermuda Rise Cores: L. D. Keigwin, B. H. Corliss 179

J Analysis of Geological and Geophysical Data from Study Locations C_1, B_1, and E_2 in the Northwest PAC 1 Study Region: D. E. Hayes, J. E. Damuth, R. D. Jacobi, R. D. Flood 191

K Site Qualification Activities: E. Laine, J. Fisher, C. Sopher, C. Barton 207

L Paleomagnetic Study of Areas B_1, C_1, and E_2: C. Barton, E. Sopher 235

M Pacific Site Assessment: M. Leinen and T. A. King 335

N Pacific Site Assessment: G. R. Heath, N. G. Pisias, C. Lopez 389

O Ichthyolith Age Correlation of North Pacific Cores: P. Doyle 469

Contents, Part One, Con't.

Appendix

P	In Situ Heat Transfer Experiment: L. O. Olson and T. E. Ewart	483
	Addendum A: ISHTE System Tests at MPG-1, May 1981: J. L. Backes, L. O. Olson, B. M. Bell	507
	Addendum B: Corrosion Test Results for Typical ISHTE Materials: J. G. Harrison	557
	Addendum C: ISHTE Simulation Sensor Calibration and Interpolation Methods: J. Miller	587
Q	Castable Ceramics for Hydrothermal Environments: Materials Evaluation for the In Situ Heat Transfer Experiment: B. C. Bunker	593
R	Heat Transfer and Fluid Mechanics: C. E. Hickox	623
S	Fabrication and Testing of Deep Ocean Piezometer System and Components: R. H. Bennett, J. T. Burns, D. N. Lambert	641
T	URI Geotechnical Program of the In Situ Heat Transfer Experiment: A. J. Silva, S. J. Criscenzo, S. A. Jordan, J. D. Babb, W. P. Levy	647
U	Chemical Experiments on ISHTE: F. L. Sayles	695
V	Experimental and Theoretical Modeling of Hydrothermal Processes in the Near Field Environment: W. E. Seyfried, E. C. Thornton	717
W	Radiolytic Oxidation of Technetium Dioxide: K. L. Nash, S. Fried, A. M. Friedman	807
X	Diffusion of Neptunyl(V) and Pertechnetate Ions in Marine Sediments: F. Schreiner, S. Fried, A. Friedman	815
Y	Far-Field Radionuclide Transport Investigations: K. L. Erickson	825
Z	High Temperature Triaxial Compression Device: N. D. Williams, W. N. Houston, R. Tully, H.-D. Lin, S.-S. Lai, S. L. Green	847

Part Two

AA	Constitutive Properties for Undisturbed Marine Sediments: S. A. Akers	9
BB	Geotechnical Studies for Subseabed Disposal: A. J. Silva, S. A. Jordan, W. P. Levy	99
CC	Physical Simulations Using Centrifuge Techniques: H. J. Sutherland	225
DD	Creep Modeling of Deep Ocean Sediments: P. R. Dawson	235
EE	Preliminary Penetration Studies: S. N. Burchett	289

Contents, Part Two, Con't.

Appendix

FF Hole Closure Calculations Using HONDO II and MARBLE: T. Canfield, S. N. Burchett 301

GG Dynamic Hole Closure Behind a Deep Ocean Sediment Penetrator: P. T. Dzwilewski 335

HH Conceptual Ship Description: M. M. Miller, C. Chryssostomidis, C. Shirley 359

II Environmental Modeling: M. G. Marietta, E. S. Hertel, D. W. Jackson A. R. Robinson, G. L. Weatherly 393

JJ Deep Sea Biophysics: A. A. Yayanos 407

KK Biology of the Central North Pacific: R. R. Hessler, C. L. Ingram 505

LL Deep Sea Scavenging Amphipods: An In Situ Marking Method: C. R. Smith-Zaninovich, T. M. C. Present 511

MM Feeding Activity and Energetics in Orchomene N. Sp.: Project Summary: T. M. C. Present, C. Smith-Zaninovich 535

NN Activity Rates of Abyssal Communities: R. J. Baldwin, K. L. Smith, Jr. 559

Addendum 1: Benthic Boundary Layer in the Central and Eastern North Pacific: I. A Chemical and Biological Characterization: K. L. Smith, Jr., M. L. Laver, N. O. Brown 564

Addendum 2: Benthic Boundary Layer in the Central and Eastern North Pacific: II. Sediment Community Oxygen Consumption and Nutrient Exchange: K. L. Smith, Jr., S. G. Horrigan 610

Addendum 3: Scavenging Deep Sea Amphipods: Effects of Food Odor on O_2 Consumption and a Proposed Metabolic Strategy: K. L. Smith, Jr., R. J. Baldwin 663

Addendum 4: Energetics of the Sablefish Anoplopoma fimbria under Laboratory Conditions: K. M. Sullivan, K. L. Smith, Jr. 703

Addendum 5: A Comparison of Methods of Age Determination of Coryphaenoides acrolepis (Macrouridae) with a Review of Problems: R. R. Wilson, Jr. 732

OO Long Core Facility: Alan H. Driscoll 759

PP Modeling Studies for Long Coring Facility: C. H. Karnes, S. N. Burchett, E. A. Aronson 787

QQ Instrumented Seabed Penetrator Project: L. T. James 797

Contents, Part Two, Con't.

Appendix

Regulatory and Institutional Studies

RR	Sociopolitical Aspects of a Subseabed Disposal Program for High Level Nuclear Waste: J. L. Kildow	803
SS	Public Education and Participation: J. E. Kelly	943
TT	Management System Design Group: L. Susskind	955

APPENDIX AA

CONSTITUTIVE PROPERTIES FOR UNDISTURBED MARINE SEDIMENTS

Stephen A. Akers

US Army Engineer Waterways Experiment Station

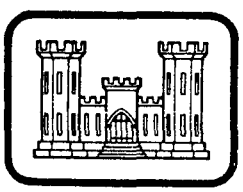
(Contract #74-1174)



CONSTITUTIVE PROPERTIES FOR UNDISTURBED MARINE SEDIMENTS IN SUPPORT OF THE SUBSEABED DISPOSAL PROGRAM

by

Stephen A. Akers



April 1982

Sponsored by Sandia National Laboratories
Albuquerque, New Mexico

Conducted by **U. S. Army Engineer Waterways Experiment Station**
Structures Laboratory
Vicksburg, Mississippi

ABSTRACT

A laboratory material property investigation was conducted on newly acquired undisturbed samples of Pacific illite in order to quantify the effective-stress, stress-strain and strength properties of the material when subjected to high-pressure static and dynamic loading conditions. The laboratory testing program consisted of triaxial shear (TX), hydrostatic compression, and uniaxial strain (UX) tests.

Consolidated-undrained static TX tests with pore pressure measurements resulted in an effective-stress Mohr-Coulomb friction angle and cohesion intercept of 28.6 degrees and 0.004 MPa, respectively. Comparable static and dynamic tests indicated that the undrained shear strength of undisturbed Pacific illite increased nominally 200 percent for an increase in strain rate from 10^{-6}/second to 1/second. In terms of total stresses (up to 35 MPa), Pacific illite was observed to behave as a $\phi = 0$ material in shear.

Constrained modulus values derived from consolidated-undrained test results exhibited an expected dependence on specimen density (and/or effective consolidation stress). UX tests conducted to investigate loading rise time effects, however, produced divergent results. Two dynamic tests (with 36-millisecond rise times) performed on virgin specimens exhibited negligible increases in undrained constrained modulus compared to static test results (with 300-second rise times). In contrast, two multiply-loaded test specimens (with sequential rise times of 300 seconds, 100 milliseconds, and 36 milliseconds) showed a modulus increase of 20 percent by the third load cycle.

Drained UX tests were successfully accomplished to stress levels in excess of 50 MPa and strains in excess of 60 percent.

Representative static and dynamic laboratory test results were selected for future use by constitutive modellers in characterizing the response of undisturbed Pacific illite.

At the request of the sponsoring agency, several drained hydrostatic creep tests were also conducted as part of this investigation.

PREFACE

This report documents the results of a high-pressure, effective-stress laboratory material property investigation conducted for Sandia National Laboratories (SNL) by personnel of the Geomechanics Division (GD), Structures Laboratory (SL), U. S. Army Engineer Waterways Experiment Station (WES), in support of the Subseabed Disposal Program (SDP), Activity D, Emplacement of Wastes in Sediments. The investigation was conducted during the period January 1981 through December 1981 and was funded under SNL Purchase Order No. 74-1174 dated 28 August 1980.

The work was performed and this report prepared by Mr. Stephen A. Akers under the general direction of Dr. J. G. Jackson, Jr., Chief, GD; Mr. J. Q. Ehrgott, Chief, Operations Group, GD; and Dr. Behzad Rohani, principal investigator for the SDP at WES. Dr. J. S. Zelasko provided detached peer review.

The GD technicians and aides and personnel of the Instrumentation Services Division of WES provided invaluable assistance during the course of the testing program and in subsequent data reduction. Special acknowledgement is given to Messrs. L. O. Olson and W. R. Gropper from the Applied Physics Laboratory of the University of Washington for their help during gravity coring operations aboard the USNS De Steiguer. Special thanks are also given to Ms. Kate Moran of the University of Rhode Island and Dr. C. M. Percival of SNL for their assistance during coring operations and core processing.

LTC David C. Girardot, CE, and COL Tilford C. Creel, CE, were the Commanders and Directors of WES during this investigation. Mr. F. R. Brown was the Technical Director. Mr. Bryant Mather was Chief, SL.

CHAPTER 1

INTRODUCTION

1.1 BACKGROUND

Since 1979, personnel of the Geomechanics Division, Structures Laboratory, U. S. Army Engineer Waterways Experiment Station (WES), have been tasked by Sandia National Laboratories (SNL) to conduct research on the static and dynamic high-pressure effective-stress mechanical properties of seabed sediments and to formulate a mathematical constitutive model for such materials using effective-stress concepts, for ultimate application in dynamic waste canister penetration and hole closure simulations for the Subseabed Disposal Program (SDP).

During the period November 1979 to December 1980 a large number of laboratory material property tests were conducted at WES on a variety of undisturbed and remolded samples of Pacific illite. Simultaneously, a three-dimensional effective-stress constitutive model was derived and the numerical algorithm necessary to incorporate it into stress wave propagation codes was developed. Upon completion of the laboratory testing program, this model was fit to selected static effective-stress material property test data. The results of this combined theoretical and experimental work were communicated to SNL in the form of an annual report entitled "Constitutive Properties and Model Development for Marine Sediments in Support of the Subseabed Disposal Program," dated March 1981 (Reference 1).

Reference 1 successfully demonstrated the capabilities of WES (1) to experimentally determine (a) the effective-stress material properties of seabed sediments, and (b) their response to static and dynamic loadings, and (2) to theoretically simulate the observed behavior with an effective-stress constitutive model. The primary deficiency recognized in the work was that an insufficient number of samples were available to generate a consistent set of laboratory test data on undisturbed Pacific illite. Consequently, SNL tasked WES to (1) obtain fresh cores of seabed sediment and (2) conduct the requisite laboratory tests to generate a consistent set of material property data on undisturbed Pacific illite so that the original constitutive model fit of Reference 1 could ultimately be refined.

In May 1981, the author participated in the cruise of the USNS De Steiguer to the North Pacific study site MPG-I (Mid-Plate/Mid-Gyre, Site I) for the purpose of obtaining new cores of seabed sediment. Undisturbed specimens subsampled from two of these cores were subsequently used to generate the laboratory test data requested by SNL.

In order to fit the WES effective-stress constitutive model, the minimum information required consists of (1) the response of the material to hydrostatic loading and unloading for both totally drained and totally undrained conditions, (2) the loading and unloading stress-strain-pore

pressure response from consolidated-undrained triaxial shear tests conducted at several different effective confining pressures, and (3) an effective-stress failure envelope developed from (2) above. If hydrostatic compression data are unobtainable, data from drained and undrained uniaxial strain tests can be used to fit the model.

A laboratory test matrix was planned by WES personnel, in conjunction with SNL, to acquire the above minimum set of material property data during 1981. The completed laboratory test program consisted of 11 consolidated-undrained triaxial shear tests, 1 drained hydrostatic compression test, 14 consolidated-undrained uniaxial strain tests, and 5 drained uniaxial strain tests. The consolidated-undrained tests were performed at three effective confining pressure levels: 0.034, 0.069, and 0.093 MPa. Five of the shear tests and nine of the undrained uniaxial strain tests were loaded dynamically.

In addition to the above test matrix, six drained hydrostatic creep tests were conducted at the specific request of SNL to obtain data on the creep (secondary compression) characteristics of Pacific illite. These tests were performed as auxiliary experiments on six of the above shear test specimens during their consolidation phase.

1.2 PURPOSE AND SCOPE

The purpose of this report is to document the details and results of the 1981 laboratory testing program, and their subsequent analyses.

The report is divided into six chapters and one addendum. Chapter 2 briefly describes the various activities of the author during the De Steiguer cruise and the subsequent core processing. Chapter 3 presents the results of the 11 triaxial shear tests and the 1 hydrostatic compression test. The results of the 19 uniaxial strain tests are presented in Chapter 4. Representative static and dynamic material properties developed from these new experimental data are presented in Chapter 5. Chapter 6 summarizes the work and the findings reported herein. The data obtained from the special hydrostatic creep tests requested by SNL are presented in Addendum A.

CHAPTER 2

CRUISE ACTIVITIES AND CORE PROCESSING

In support of the SDP, the author participated in the May 1981 research cruise of the USNS De Steiguer and was assigned responsibility for coordinating the gravity coring operations aboard ship. The chief scientist was Mr. L. O. Olson of the Applied Physics Laboratory (APL) of the University of Washington. The primary cruise tasks were to launch, test, and recover the APL-designed ISHTE (In Situ Heat Transfer Experiment) hydrostatic corer and to test and evaluate the APL acoustic tracking system. To maximize the use of available ship time, gravity coring activities were planned around ISHTE work periods.

The gravity corer used during the cruise was borrowed from Oregon State University. The weight stand was constructed from a 1.5-meter-long, 10-centimeter-ID metal pipe with a lifting bracket welded at the top. A weighted collar molded around the pipe provided the driving mass, and a threaded coupler at the bottom attached the core barrels to the weight stand. Three-meter lengths of Schedule 40 PVC pipe (10 centimeters ID) were used as core barrels. A metal core cutter with collapsible metal fingers was riveted to each barrel to provide a cutter and catcher for the corer.

Thirteen gravity cores were obtained during the cruise. These cores have been identified by (1) cruise number (DS-1208-81), and (2) gravity core number (GC-01 through GC-13). Table 2.1 lists the latitude and longitude for each of the gravity cores and their ultimate recipients. The first two cores were launched from the starboard side of the ship using a hydrographic winch. During the retrieval of the second core (GC-02), the winch developed mechanical problems and had to be shut down for the remainder of the cruise after the core was recovered. Mr. Olson offered the use of the APL nylon line retrieval system and the assistance of his personnel to conduct the remaining gravity coring operations over the stern of the ship. This system worked well and had a turnaround time of approximately 3.5 hours compared to 3 hours using the winch.

Figure 2.1 is a map of the cruise area upon which the positions of 12 of the 13 cores obtained have been marked. The thirteenth core (GC-04) is located just off the map below GC-03.

After recovery of each gravity core, the core barrel was removed from the weight stand, capped, and stored in a vertical position until it could be processed. Onboard processing involved cutting the barrels and the sediment contained within to lengths appropriate for shipment. Cores sent to the University of Rhode Island (URI) were cut into 1.5-meter lengths and those sent to WES, SNL, and the University of California at Berkeley were cut to 0.75-meter lengths. Each section of core was capped, taped, sealed with wax, and taped again. The sealed sections were stored vertically in the ship's refrigerators for the remainder of the cruise.

Upon the ship's return to Pearl Harbor, the cores were transported to Holmes and Narver, Inc., at Hickam Air Force Base. Here crates were built and the cores were packed and shipped to the appropriate laboratory. At all times special efforts were made to keep the cores in a vertical orientation and refrigerated.

WES received 6 of the 13 gravity cores. Of these, one core (GC-09) has been completely processed and another (GC-08) has been partially processed. A sufficient number of undisturbed test specimens were obtained from these two cores to conduct all of the tests reported herein.

During core processing at WES, water content specimens, vane shear measurements, undisturbed test specimens, and classification specimens were obtained. Figure 2.2 is a plot of water content (corrected for 35 parts per thousand salt content), undrained shear strength determined from vane shear measurements, and wet density for gravity core GC-09. Values of wet density were determined from the undisturbed test specimens. The author believes these data to be typical of illite sediments from MPG-I.

Table 2.1 DS-1208-81 Core Log.

Core Identification	Date (1981)	Local Time*	Location (Latitude, Longitude)	Destination
GC-01	25 May	0250	30°21.22N 157°48.22W	UCB
GC-02	25 May	0740	30°21.24N 157°49.11W	WES
GC-03	25 May	2330	30°17.26N 157°50.55W	WES
GC-04	26 May	0305	30°16.93N 157°50.27W	WES
GC-05**	26 May	1936	30°20.68N 157°50.99W	Sampled on board
GC-06	26 May	2300	30°20.78N 157°52.73W	WES
GC-07	27 May	0148	30°21.24N 157°53.33W	UCB
GC-08	27 May	1350	30°19.90N 157°52.40W	WES
GC-09	27 May	1653	30°20.42N 157°53.87W	WES
GC-10†	27 May	2111	30°20.12N 157°49.95W	URI
GC-11	28 May	1530	30°22.90N 157°50.21W	URI
GC-12††	28 May	1903	30°23.63N 157°51.46W	URI
GC-13††	29 May	1252	30°21.48N 157°51.57W	URI

* Corer at bottom.
** HC-1 (hydrostatic) companion core.
† GPC-3 companion core.
†† Sampled at proposed ISHTE site.

NOTE: UCB is the University of California at Berkeley; WES is the U. S. Army Engineer Waterways Experiment Station; and URI is the University of Rhode Island.

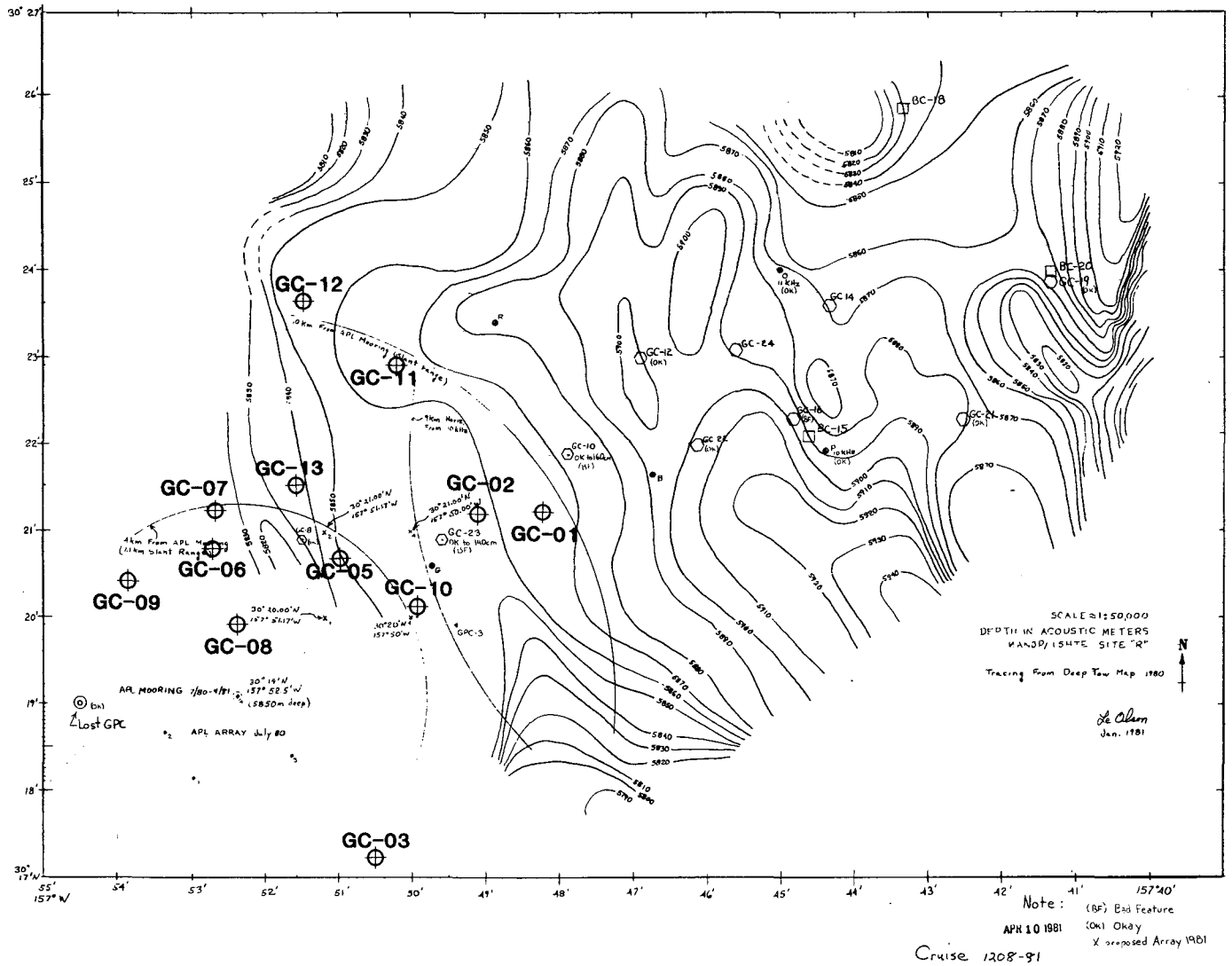


Figure 2.1 Gravity core locations for cruise DS-1208-81.

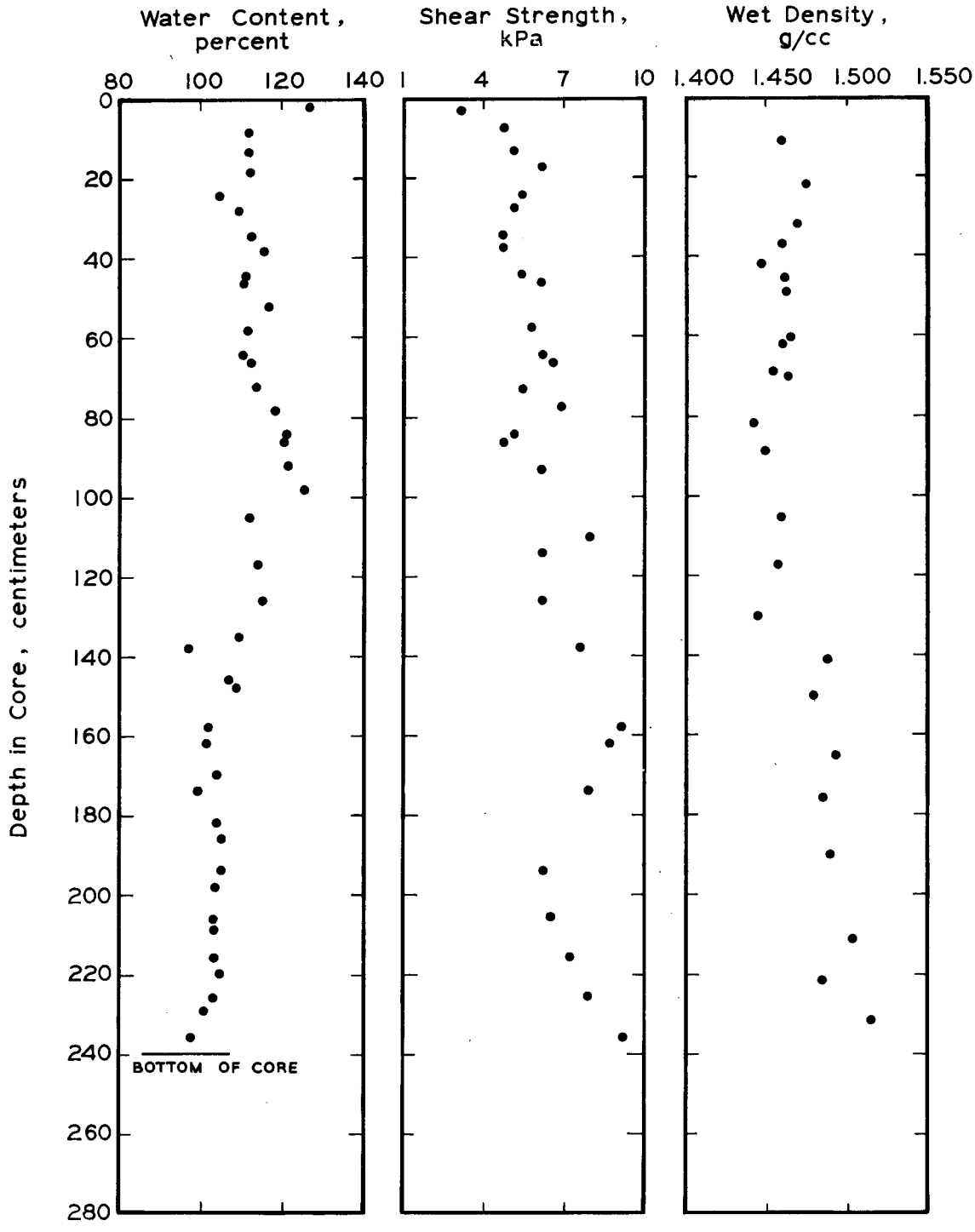


Figure 2.2 Geotechnical properties of gravity core DS-1208-81 GC-09

CHAPTER 3

TRIAXIAL SHEAR TESTS

3.1 GENERAL

A matrix of 11 consolidated-undrained triaxial shear (TX) tests was conducted on the new undisturbed seabed material to determine (1) the static Mohr-Coulomb parameters of effective cohesion, c', and effective internal friction angle, ϕ'; (2) the effects of strain rate on the total-stress shear behavior of the material; (3) the effects of high total pressures on the static shear properties. In addition, one drained low-pressure hydrostatic compression test was conducted to obtain load and unload pressure-volume data. The resulting undrained shear data and consolidation data contributed to the representative mechanical property analysis described in Chapter 5.

The original shear test matrix (as planned) consisted of nine undrained TX tests--three static low-pressure (LPTX) tests with pore pressure measurements, three dynamic LPTX tests, and three static high-pressure (HPTX) tests. However, 11 specimens were ultimately tested to complete the planned matrix because two of the tests were terminated prior to the shear phase due to membrane leaks.

The three specimens of the static LPTX group were consolidated to three different effective stresses (0.034, 0.069, and 0.093 MPa), then statically sheared to establish an effective-stress failure envelope. The three specimens in the dynamic LPTX group and those in the static HPTX group were also consolidated to these same three effective-stress levels. These consolidation stresses insured that the specimens would be normally consolidated prior to shear. The dynamic LPTX tests were conducted to investigate loading rate effects for an increase in strain rate from 10^{-6}/second to 1/second. The static HPTX tests were conducted to determine the effects upon specimen shear behavior of increasing the applied mean normal stress up to 35 MPa.

The single load-unload hydrostatic test was incrementally loaded up to 0.45 MPa and then unloaded to determine the low-pressure drained response of the seabed material. The loading behavior of this specimen can be directly compared with the consolidation behavior of the shear test specimens.

Composition properties calculated for all 12 test specimens using the formulas documented in Reference 1 are listed in Table 3.1. The starred properties have been corrected for a salt content of 35 parts per thousand. A specific gravity of 2.70 was used to calculate volumes of solids. Table 3.1 also lists the type of test conducted on each specimen and its posttest water content.

Pertinent test parameters and results from the 12 tests are presented in Table 3.2. This table identifies the test number, the type of test,

the confining stress (σ_r) and pore water stress (u) at the end of the back-pressure saturation (BPS) consolidation phase, the confining stress σ_r and pore pressure u at the beginning of the undrained shear phase, the principal stress difference at failure $(\sigma_1 - \sigma_3)_f$, the excess pore pressure at failure u_f (when measured), the effective mean normal stress at failure $(J_1'/3)_f$, the pretest water content and wet density, and the posttest water content.

3.2 PROCEDURES

The test equipment and basic procedures used in the 1980 experimental program (see Reference 1) were used again in 1981. The only change made to the equipment was the elimination of the top drainage line in the LPTX equipment. This line was removed to maintain similar drainage conditions in both the LPTX and the HPTX tests.

All 12 test specimens were back-pressure saturated to 0.345 MPa using increments of approximately 0.069 MPa per one-half hour, while an effective stress of 0.007 MPa was maintained. Each test specimen was subsequently consolidated to a desired effective stress level, recording volume change (water expelled) versus time. For 6 of the 12 specimens this consolidation (effective-stress) increment was imposed in one loading. Volume change-time histories are not presented in this report for these six specimens; however, the data are available upon request. For the other six tests (including the drained hydrostatic test, GC-09 185-195 cm) a different procedure was used so that a drained hydrostatic creep (secondary compression) test could be conducted on the specimens. These latter tests are fully described and documented in Addendum A.

Specimen stresses and strains were calculated using the methods documented in Reference 1. No corrections were made for filter strips or membranes.

3.3 STATIC LPTX TESTS

For each of the three successfully completed static consolidated-undrained LPTX tests, individual plots of principal stress difference versus axial strain, pore pressure versus axial strain and A-factor versus axial strain are sequentially presented in Figures 3.1 to 3.9. The total-stress paths and effective-stress paths for these three tests are shown in Figures 3.10 and 3.11, respectively.

Test GC-09 150-160 cm (Figures 3.10 and 3.11, curve 3) did not exhibit the expected stress path responses for this material; i.e., it should follow the pattern set by curves 1 and 2. The principal stress difference values of curve 3 are too low and the pore pressures too high when compared to tests GC-09 173-183 cm and 160-170 cm. Comparing the plots of A-factor (Figures 3.3, 3.6, and 3.9) also shows a correspondingly dramatic difference in response. Curve 3 was therefore eliminated from subsequent analyses. The two remaining tests, GC-09 173-183 cm and 160-170 cm, indicate that the sediment possesses an effective cohesion

intercept c' of 0.004 MPa and an effective friction angle ϕ' of 28.6 degrees. These results agree with values previously reported by URI (Reference 2); specifically three series of static TX tests conducted by URI on undisturbed Pacific illite from MPG-I produced the c' and ϕ' values listed:

URI Test Series	c' MPa	ϕ' deg
MA-02 GC-04 200 cm	0.0	34.8
MA-02 GC-04 100 cm	0.003	33.0
V-32 PC-115 200 cm	0.004	22.9

3.4 DYNAMIC LPTX TESTS

The shear data obtained from the three successful consolidated-undrained dynamic LPTX tests are presented in Figures 3.12 through 3.14 as individual plots of principal stress difference versus axial strain. The total-stress paths for these tests are plotted in Figure 3.15. No dynamic pore pressure measurements were made for these three tests.

The stress-strain curves for the corresponding (equal effective consolidation stress) static and dynamic tests are shown in Figures 3.16 and 3.17. These figures indicate that the ratios of dynamic-to-static shear strength at failure for this material are on the order of 2.40 and 2.03. These ratios show that a significant increase in shear strength occurs for a 6-decade reduction in time to failure. In addition, they are larger than those found previously (0.67 to 1.45, Reference 1) for remolded specimens tested under the same six-decade difference in strain rate.

3.5 STATIC HPTX TESTS

Three static consolidated-undrained HPTX tests were conducted in the 1981 experimental program. A new test chamber was used in the program, but all of the basic measurement features of the previous (1980) system were maintained. The three specimens were back-pressure saturated and consolidated to the same initial effective-stress levels as the LPTX specimens. The back pressure was imposed in one increment due to problems with drift in one of the two pressure regulators. This drift in pressure occurred immediately after resetting the regulator but would stabilize within several minutes. A live confining stress (see Table 3.2) was applied to each specimen before and held constant throughout the shear phase.

Except for volume change burette measurements, all data were recorded with the automatic data acquisition system described in Reference 1. During consolidation and shear, specimen deformations were recorded versus time using vertical and lateral deformeters (Reference 1). Volumetric strains were calculated from these deformeter data as

$\varepsilon_{kk} = \varepsilon_a + 2\varepsilon_r$. Deformeter strains are used in all subsequent data plots.

For the three HPTX tests, plots of principal stress difference versus axial strain, principal stress difference versus principal strain difference, mean normal stress versus volumetric strain, and principal stress difference versus mean normal stress are sequentially presented in Figures 3.18 to 3.29. All stresses in these plots are total stresses and all strains are "total" strains, i.e., strains measured from the start of each test (from the beginning of the back-pressure saturation phase). Pressure transducers with a working range of 34 MPa were used to measure the chamber pressure and pore pressure. During the shear phase, however, these transducers lacked the sensitivity to measure the very small excess pore pressures generated. For this reason no pore pressure or effective-stress results are presented for these tests. The values of principal stress difference at failure for the three HPTX tests are listed in Table 3.2.

Note on the plots of principal stress difference versus principal strain difference (Figures 3.19, 3.23, and 3.27) that at the end of consolidation the principal strain difference is approximately equal to zero (i.e., $\varepsilon_a \simeq \varepsilon_r$) . This observation suggests that the material is essentially isotropic. An anisotropic material would produce noticeable principal strain differences under spherical (isotropic) stress loadings.

At 14 percent total axial strain, test GC-08 70-80 cm (Figure 3.22) exhibits an increase in principal stress difference. This change from decreasing to increasing principal stress difference was caused by the operator who significantly increased the strain rate at that point in an attempt to attain 15 percent axial strain during shear (i.e., 22 percent total strain) in a prealloted time. The principal stress difference at failure for this test was taken as the first peak.

Figures 3.30 and 3.31 each compare an equivalent HPTX and LPTX test (conducted at equal effective-stress levels). Each pair of tests compares very well in spite of differences between the LPTX and HPTX tests due to (1) different methods of calculating deformed specimen cross-sectional areas and hence axial stresses, and (2) differences in initial specimen composition properties. We therefore conclude that over a range of 34 MPa the total-stress failure envelope is unaffected by confining pressure and that Pacific illite behaves as a $\phi = 0$ material. The same conclusion was drawn from the 1980 experimental program conducted on remolded specimens (Reference 1).

3.6 DRAINED HYDROSTATIC TEST

A single low-pressure drained hydrostatic loading test was successfully completed on specimen GC-09 185-195 cm (Figure 3.32), after applying seven loading and four unloading pressure increments. As for the LPTX shear tests, the specimen was initially back-pressured saturated to 0.345 MPa, while maintaining an effective stress of 0.007 MPa; then consolidated. The volumetric strains were calculated from volume-change

burette measurements. Each loading and unloading pressure increment was maintained for approximately 24 hours, except for the 0.093-MPa stress increment which was maintained for several days to determine the amount of secondary compression (see Addendum A).

To demonstrate the scatter (or lack thereof) in the pressure-volume change data obtained from the consolidation phase of the 11 TX tests and the hydrostatic loading test, Figure 3.33 is presented. The asterisks represent the loading and unloading data from the drained hydrostatic test of Figure 3.32, and the "†" symbols represent the volumetric strains for one or more effective-stress loading increments applied in the 11 TX tests. The mean volumetric strain, its standard deviation, and the coefficient of variation at the three effective-stress consolidation levels are as listed:

Effective Consolidation Stress MPa	Volumetric Strain		
	Mean	Standard Deviation	Coefficient of Variation
0.034	10.39	0.68	6.58%
0.069	16.28	0.68	4.20%
0.093	19.77	0.91	4.58%

Note that the coefficient of variation is quite small, indicating a small degree of scatter.

Table 3.1 Summary of Composition Properties for DS-1208-81 GC-08 and GC-09 Triaxial Shear Specimens.

Test Number	Pretest w^* %	γ g/cc	γ_d^* g/cc	V_a^* %	V_s^* %	V_w^* %	Type of Test	Posttest w^* %
DS-1208-81 GC-09 160-170 cm	95.7	1.493	0.763	1.2	28.3	70.5	LPTX/Static Shear	85.5
DS-1208-81 GC-09 173-183 cm	104.4	1.486	0.727	0.0	26.7	73.3	LPTX/Static Shear	74.2
DS-1208-81 GC-09 150-160 cm	110.1	1.479	0.704	0.0	25.1	74.9	LPTX/Static Shear	73.9
DS-1208-81 GC-09 196-206 cm	101.9	1.396	0.691	6.3	25.6	68.1	LPTX/Static Shear**	74.0
DS-1208-81 GC-09 112-122 cm	112.2	1.458	0.687	0.1	25.5	74.4	LPTX/Dynamic Shear	88.6
DS-1208-81 GC-09 136-146 cm	108.6	1.488	0.713	0.0	25.1	74.9	LPTX/Dynamic Shear	75.5
DS-1208-81 GC-09 125-135 cm	110.5	1.446	0.687	1.2	25.4	73.4	LPTX/Dynamic Shear	78.7
DS-1208-81 GC-09 100-110 cm	114.0	1.460	0.682	0.0	24.9	75.1	LPTX/Dynamic Shear**	82.0
DS-1208-81 GC-09 185-195 cm	101.5	1.489	0.739	0.2	27.4	72.4	LPTX/Drained Hydrostat	63.2
DS-1208-81 GC-08 55-65 cm	108.7	1.466	0.702	0.2	26.0	73.8	HPTX/Static Shear	91.0
DS-1208-81 GC-08 70-80 cm	112.0	1.465	0.691	0.0	25.2	74.8	HPTX/Static Shear	77.1
DS-1208-81 GC-08 40-50 cm	108.4	1.462	0.702	0.6	26.0	73.4	HPTX/Static Shear	73.3

* Corrected for 35 ppt salt content. (Specific gravity assumed = 2.70).

** Specimen leaked before shear.

Table 3.2 Summary of Triaxial Shear Test Data for DS-1208-81 GC-08 and GC-09 Specimens.

Test No. DS-1208-81	Type of Test	BPS Consolidation σ_r MPa	BPS Consolidation U MPa	Shear σ_r MPa	Shear U MPa	$(\sigma_1-\sigma_3)_f$ MPa	u_f MPa	$(J_1'/3)_f$ MPa	Pretest w %	Pretest γ g/cc	Posttest w %
GC-09 160-170 cm	LPTX Static Shear	0.379	0.345	0.379	0.345	0.0347	0.0235	0.0225	95.7	1.493	85.5
GC-09 173-183 cm	LPTX Static Shear	0.414	0.345	0.414	0.345	0.0559	0.0464	0.0412	104.4	1.486	74.2
GC-09 150-160 cm	LPTX Static Shear	0.438	0.345	0.438	0.345	0.0431	0.0632	0.0443	110.1	1.479	73.9
GC-09 196-206 cm	LPTX Static Shear*	0.438	0.345	---	---	---	---	---	101.9	1.396	74.0
GC-09 112-122 cm	LPTX Dynamic Shear	0.379	0.345	0.379	0.345	0.0833	NM**	NM	112.2	1.458	88.6
GC-09 136-146 cm	LPTX Dynamic Shear	0.414	0.345	0.414	0.345	0.1133	NM	NM	108.6	1.488	75.5
GC-09 125-135 cm	LPTX Dynamic Shear	0.438	0.345	0.438	0.345	0.1427	NM	NM	110.5	1.446	78.7
GC-09 100-110 cm	LPTX Dynamic Shear*	0.391	0.345	---	---	---	---	---	114.0	1.460	82.0
GC-09 185-195 cm	LPTX Drained Hydrostat	0.352	0.345	NA	NA	NA	NA	NA	101.5	1.489	63.2
GC-08 55-65 cm	HPTX Static Shear	0.400	0.366	34.83	34.80	0.0322	---†	---†	108.7	1.466	91.0
GC-08 70-80 cm	HPTX Static Shear	0.441	0.372	34.08	34.01	0.0535	---†	---†	112.0	1.465	77.1
GC-08 40-50 cm	HPTX Static Shear	0.452	0.359	34.70	34.61	0.0699	---†	---†	108.4	1.462	73.3

* Specimen leaked before shear.

** NM: not measured (see text).

† Lack of sensitivity (see text).

NOTE: NA: not applicable.

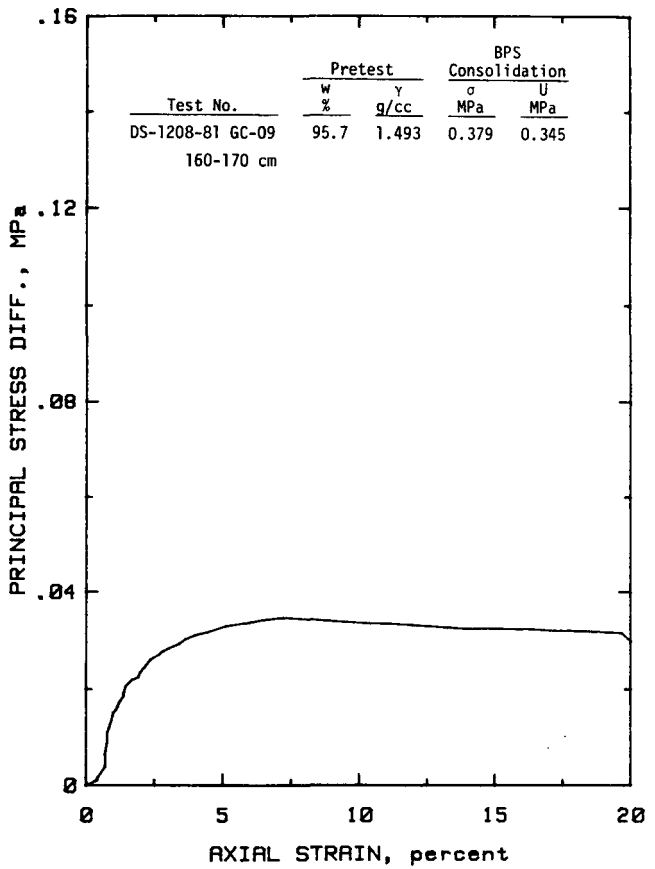


Figure 3.1 BACK PRESSURE SATURATED CONSOLIDATED STATIC UNDRAINED TRIAXIAL SHEAR SPECIMEN DS-1208-81 GC-09 160-170 cm PR. STRESS DIFF. vs AXIAL STRAIN

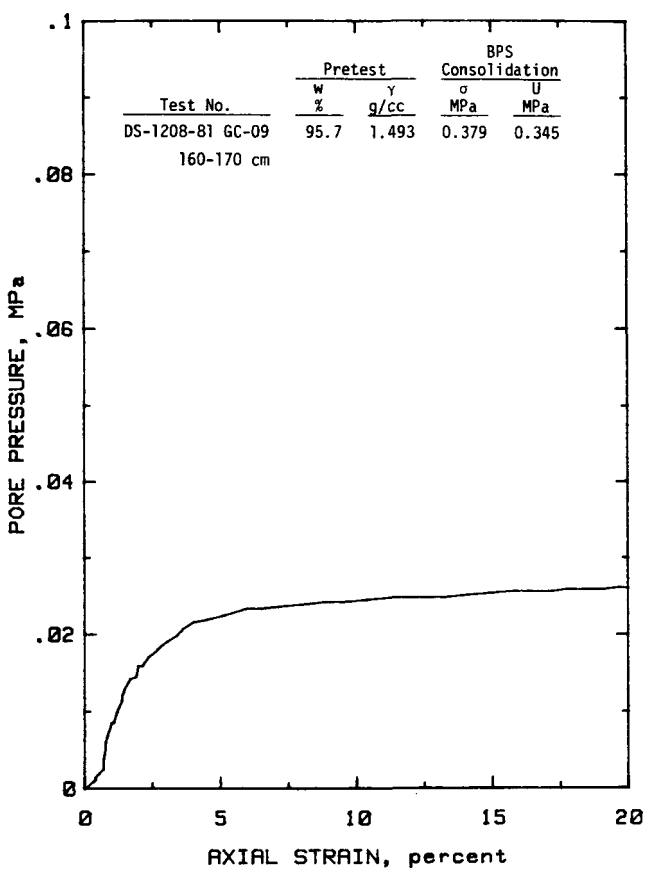


Figure 3.2 BACK PRESSURE SATURATED CONSOLIDATED STATIC UNDRAINED TRIAXIAL SHEAR SPECIMEN DS-1208-81 GC-09 160-170 cm PORE PRESSURE vs AXIAL STRAIN

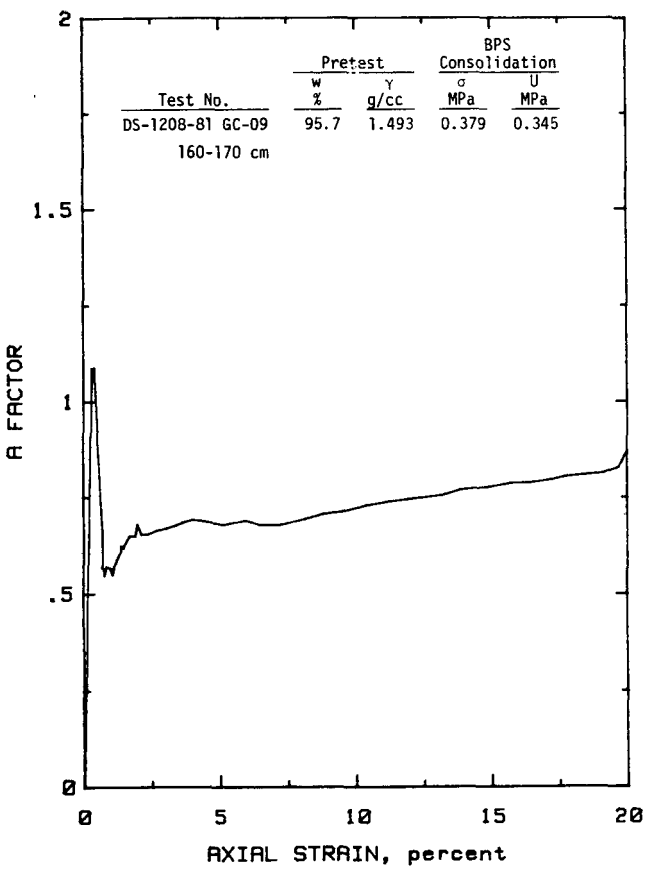


Figure 3.3 BACK PRESSURE SATURATED CONSOLIDATED STATIC UNDRAINED TRIAXIAL SHEAR SPECIMEN DS-1208-81 GC-09 160-170 cm A FACTOR vs AXIAL STRAIN

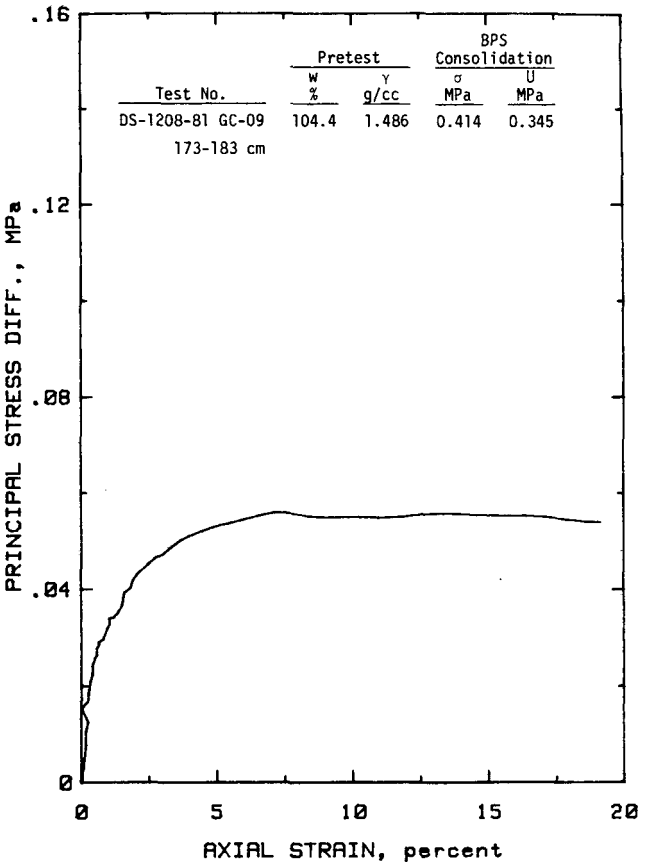


Figure 3.4 BACK PRESSURE SATURATED CONSOLIDATED STATIC UNDRAINED TRIAXIAL SHEAR SPECIMEN DS-1208-81 GC-09 173-183 cm PR. STRESS DIFF. vs AXIAL STRAIN

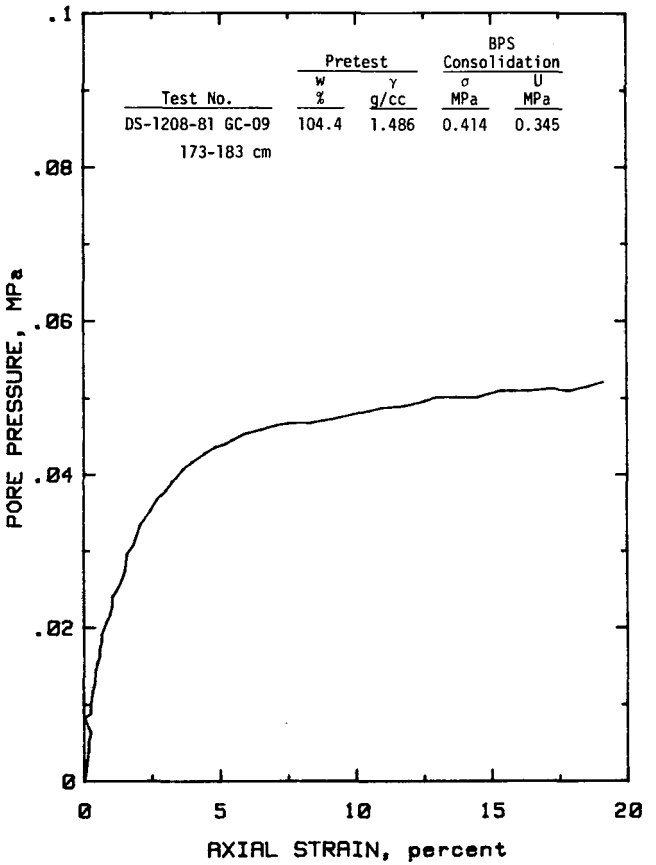


Figure 3.5 BACK PRESSURE SATURATED CONSOLIDATED STATIC UNDRAINED TRIAXIAL SHEAR SPECIMEN DS-1208-81 GC-09 173-183 cm PORE PRESSURE vs AXIAL STRAIN

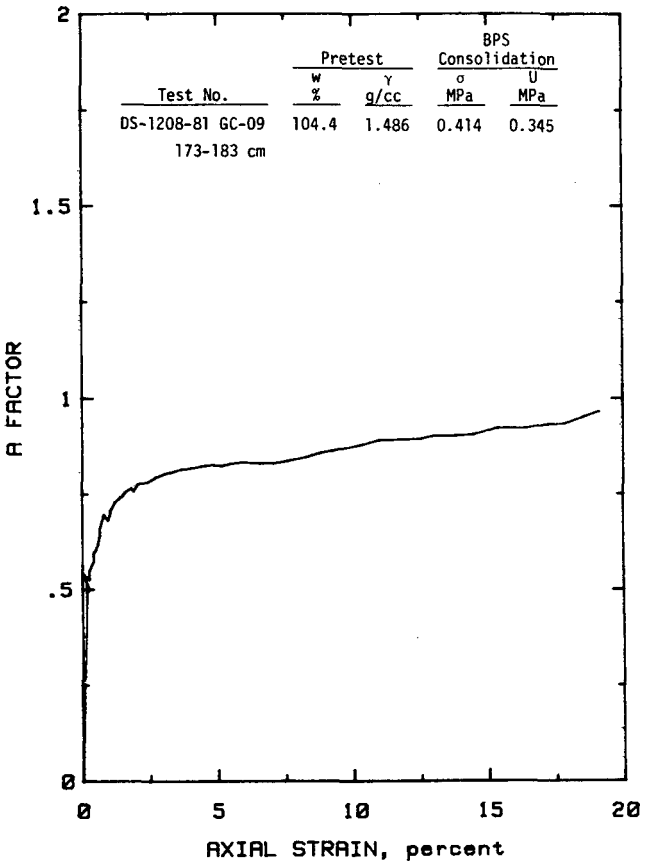


Figure 3.6 BACK PRESSURE SATURATED CONSOLIDATED STATIC UNDRAINED TRIAXIAL SHEAR SPECIMEN DS-1208-81 GC-09 173-183 cm A FACTOR vs AXIAL STRAIN

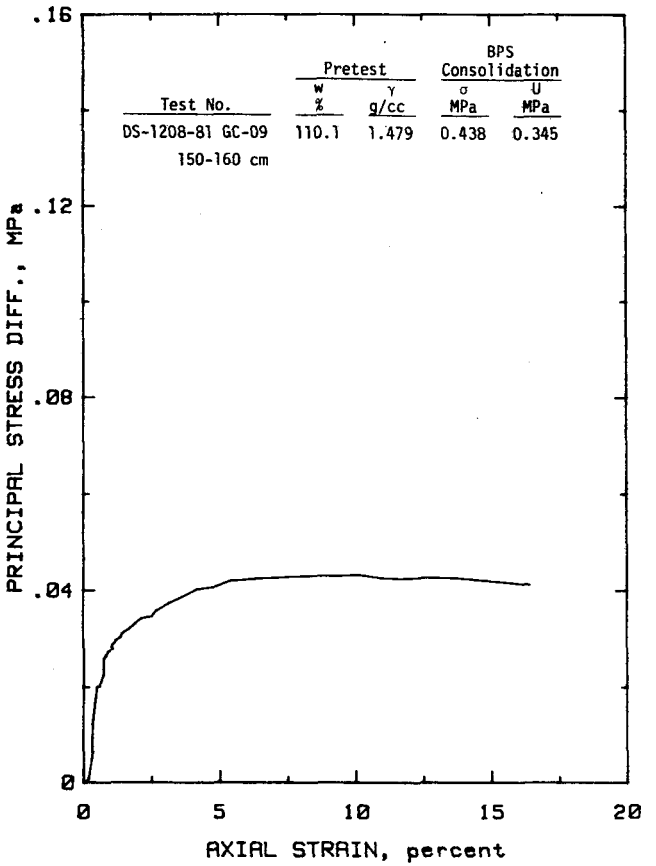


Figure 3.7 BACK PRESSURE SATURATED CONSOLIDATED STATIC UNDRAINED TRIAXIAL SHEAR SPECIMEN DS-1208-81 GC-09 150-160 cm PR. STRESS DIFF. vs AXIAL STRAIN

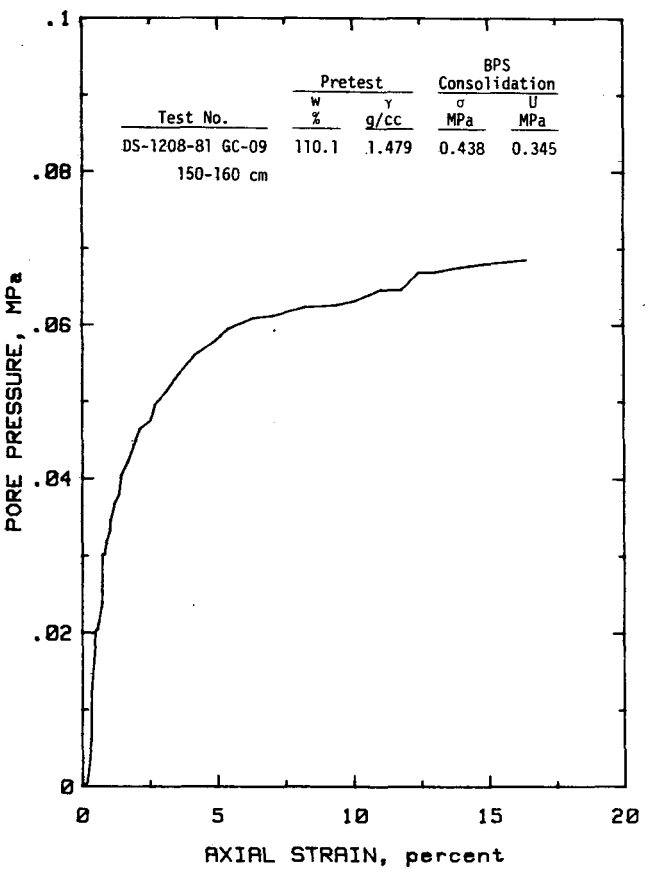


Figure 3.8 BACK PRESSURE SATURATED CONSOLIDATED STATIC UNDRAINED TRIAXIAL SHEAR SPECIMEN DS-1208-81 GC-09 150-160 cm PORE PRESSURE vs AXIAL STRAIN

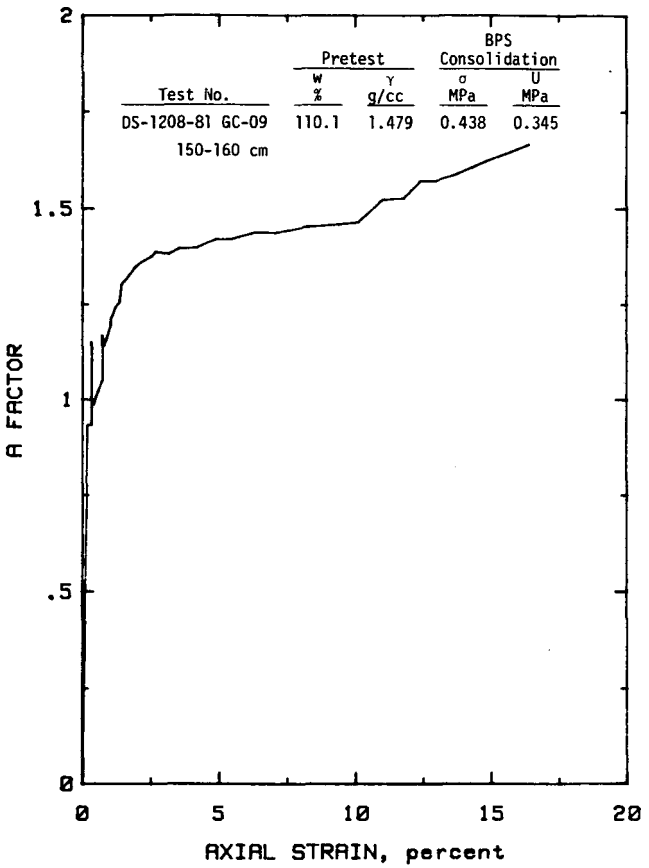


Figure 3.9 BACK PRESSURE SATURATED CONSOLIDATED STATIC UNDRAINED TRIAXIAL SHEAR SPECIMEN DS-1208-81 GC-09 150-160 cm A FACTOR vs AXIAL STRAIN

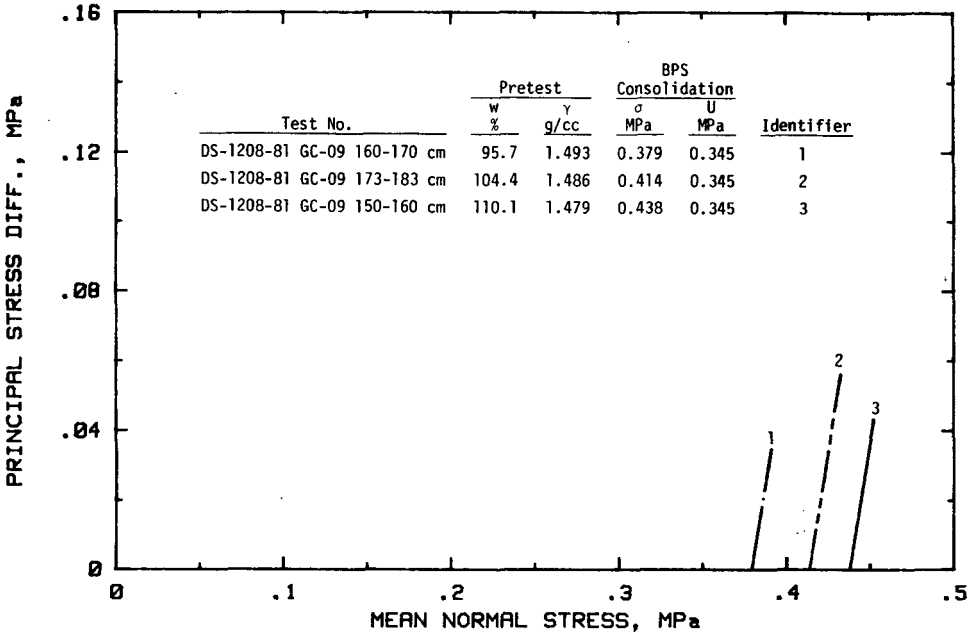


Figure 3.10 BACK PRESSURE SATURATED CONSOLIDATED STATIC UNDRAINED TRIAXIAL SHEAR SPECIMEN DS-1208-81 GC-09 150-183 cm PR. STRESS DIFF. vs MEAN NORMAL STRESS

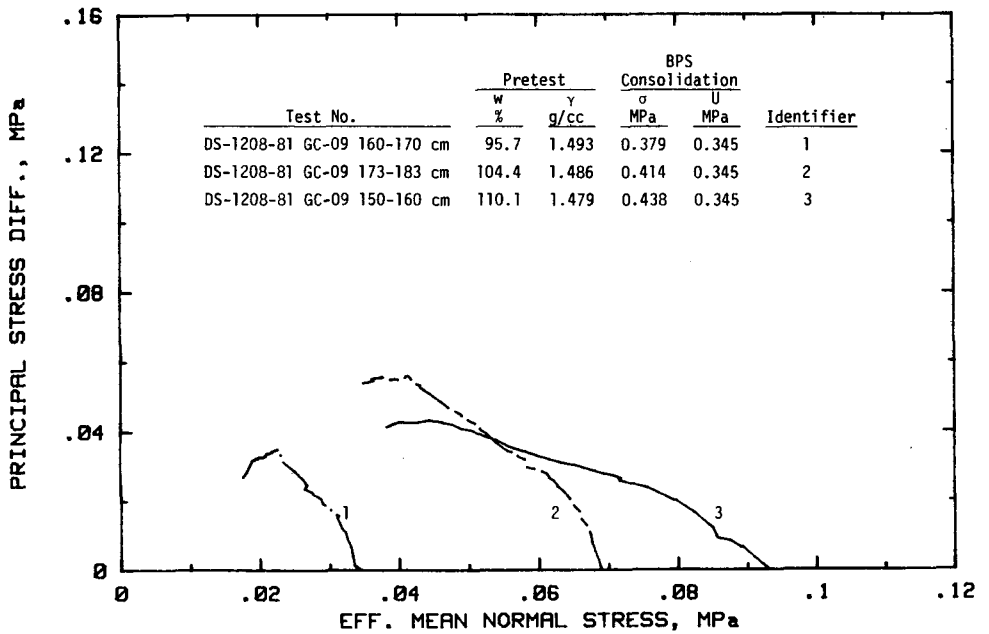


Figure 3.11 BACK PRESSURE SATURATED CONSOLIDATED STATIC UNDRAINED TRIAXIAL SHEAR SPECIMEN DS-1208-81 GC-09 150-183 cm PR. STRESS DIFF. vs EFF. MEAN NORMAL STR.

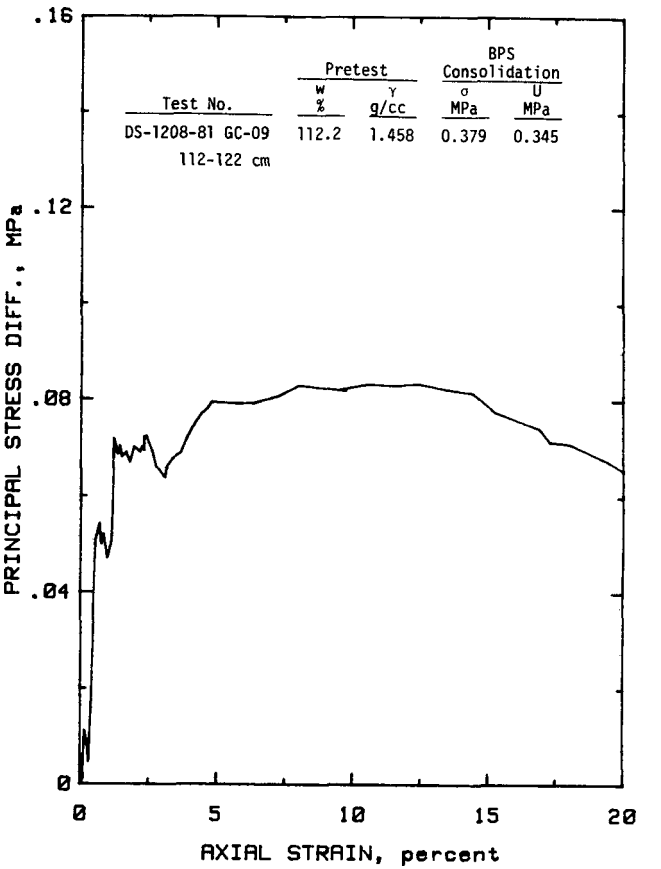


Figure 3.12 BACK PRESSURE SATURATED CONSOLIDATED DYNAMIC UNDRAINED TRIAXIAL SHEAR SPECIMEN DS-1208-81 GC-09 112-122 cm PR. STRESS DIFF. vs AXIAL STRAIN

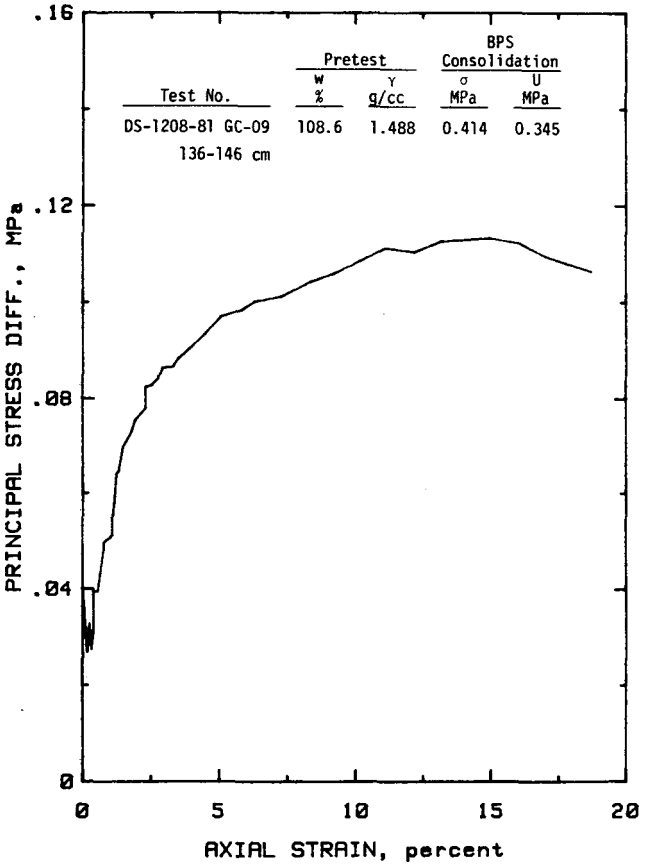


Figure 3.13 BACK PRESSURE SATURATED CONSOLIDATED DYNAMIC UNDRAINED TRIAXIAL SHEAR SPECIMEN DS-1208-81 GC-09 136-146 cm PR. STRESS DIFF. vs AXIAL STRAIN

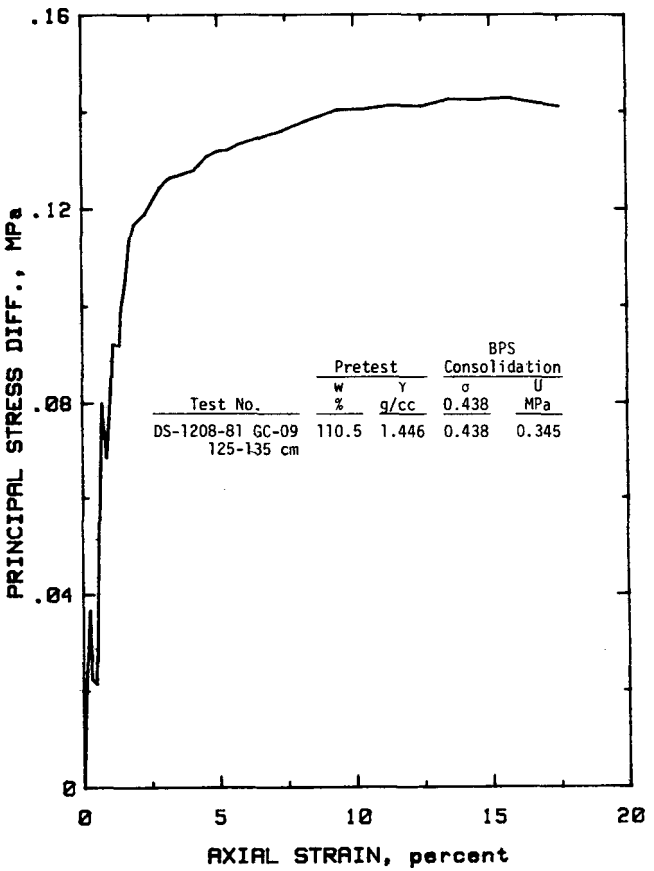


Figure 3.14 BACK PRESSURE SATURATED CONSOLIDATED DYNAMIC UNDRAINED TRIAXIAL SHEAR SPECIMEN DS-1208-81 GC-09 125-135 cm PR. STRESS DIFF. vs AXIAL STRAIN

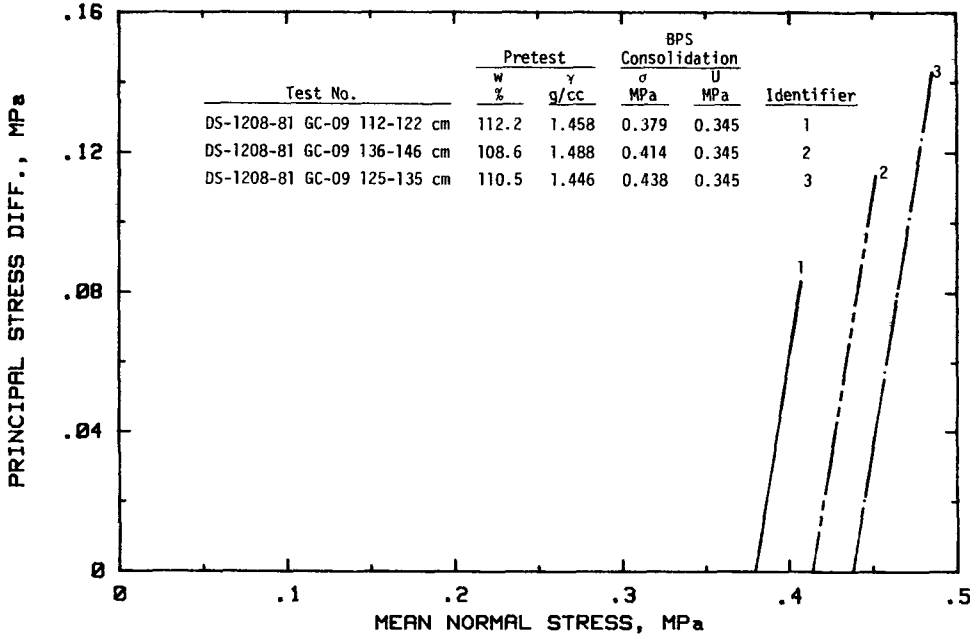


Figure 3.15 BACK PRESSURE SATURATED CONSOLIDATED DYNAMIC UNDRAINED TRIAXIAL SHEAR SPECIMEN DS-1208-81 GC-09 112-146 cm PR. STRESS DIFF. vs MEAN NORMAL STRESS

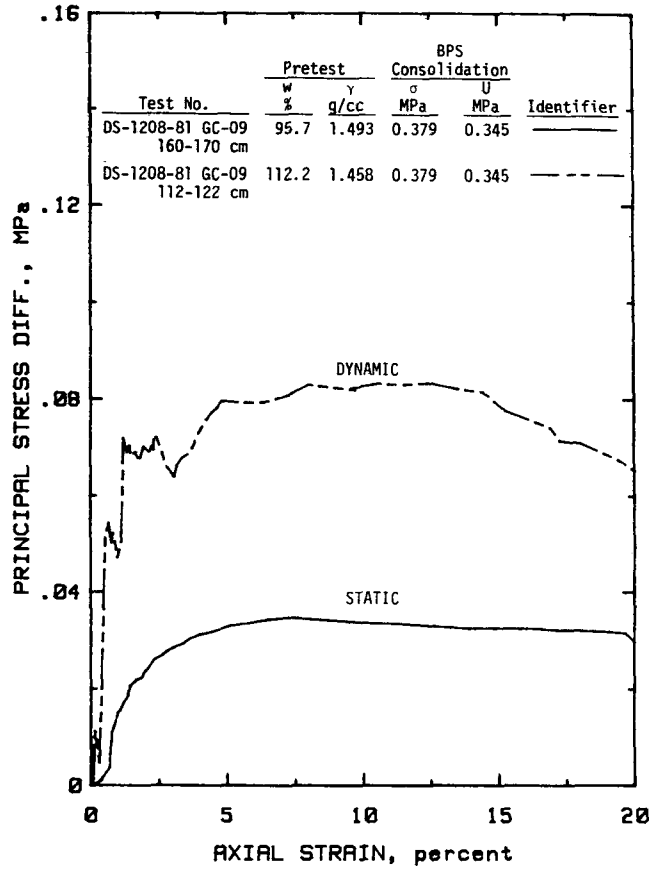


Figure 3.16 BACK PRESSURE SATURATED CONSOLIDATED STAT. & DYN. UNDRAINED TRIAXIAL SHEAR DS-1208-81 GC-09 160-170 & 112-122 cm PR. STRESS DIFF. vs AXIAL STRAIN

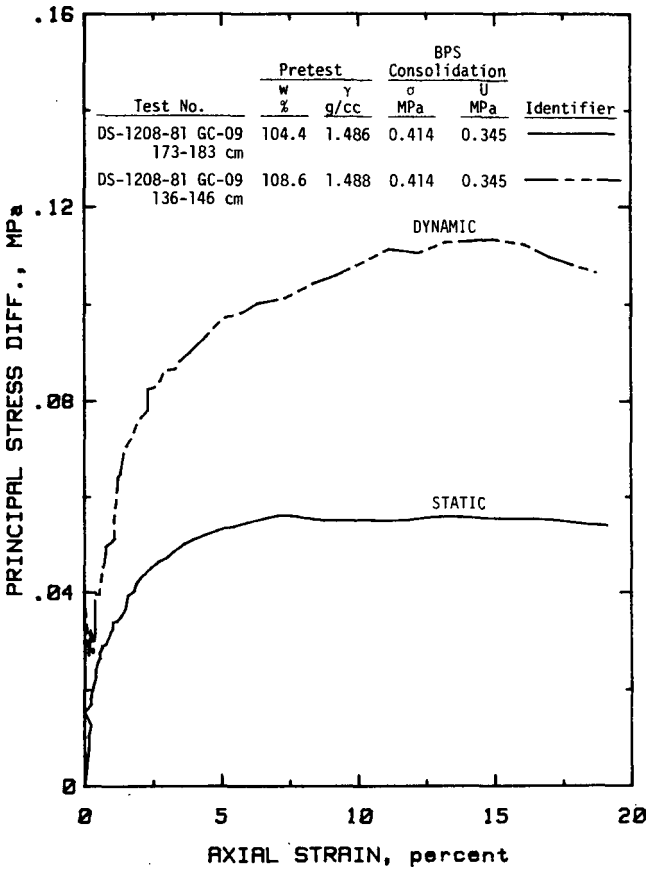


Figure 3.17 BACK PRESSURE SATURATED CONSOLIDATED STAT. & DYN. UNDRAINED TRIAXIAL SHEAR DS-1208-81 GC-09 173-183 & 136-146 cm PR. STRESS DIFF. vs AXIAL STRAIN

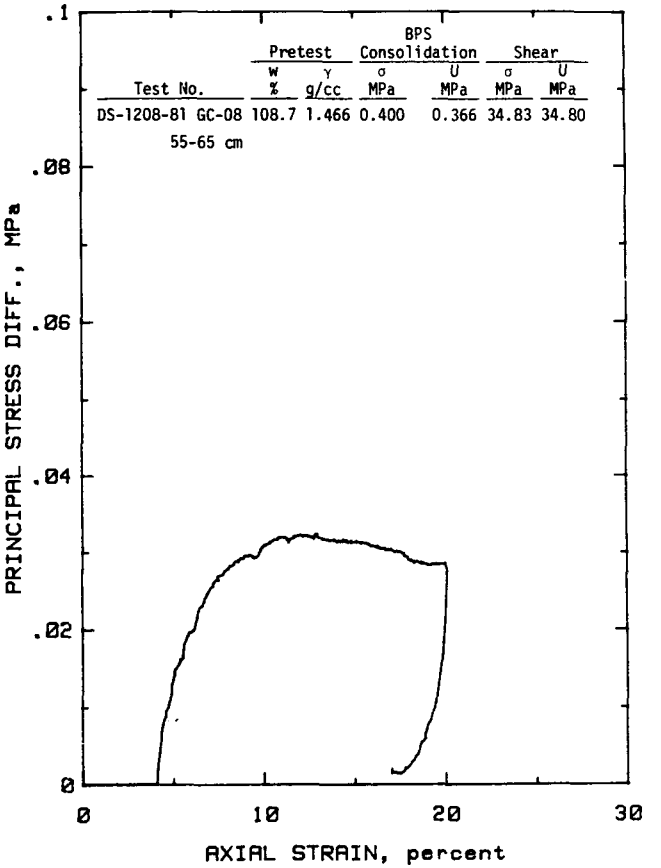


Figure 3.18 BACK PRESSURE SATURATED CONSOLIDATED STATIC UNDRAINED TRIAXIAL SHEAR SPECIMEN DS-1208-81 GC-08 55-65 cm PR. STRESS DIFF. vs AXIAL STRAIN

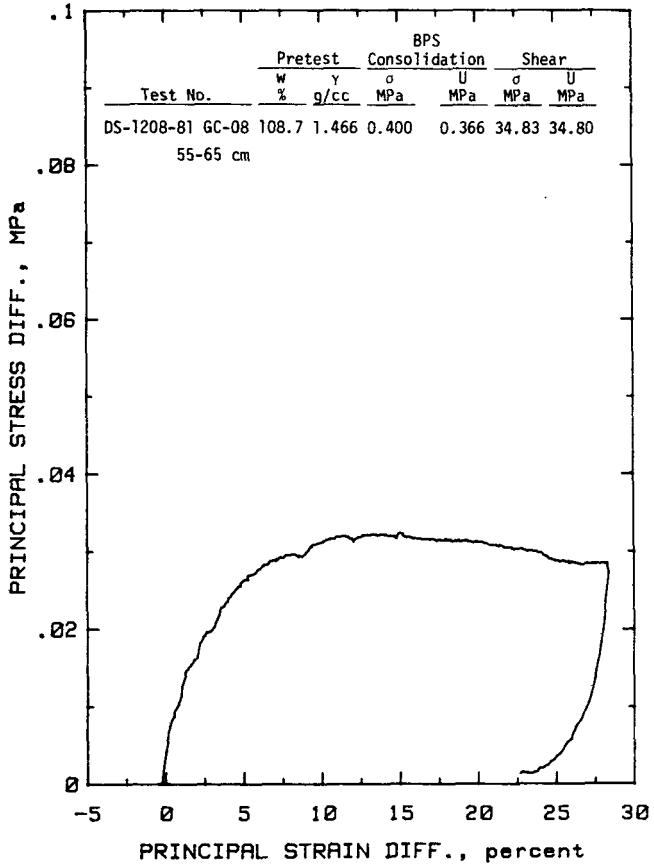


Figure 3.19 BACK PRESSURE SATURATED CONSOLIDATED STATIC UNDRAINED TRIAXIAL SHEAR SPECIMEN DS-1208-81 GC-08 55-65 cm PR. STRESS DIFF. vs PR. STRAIN DIFF.

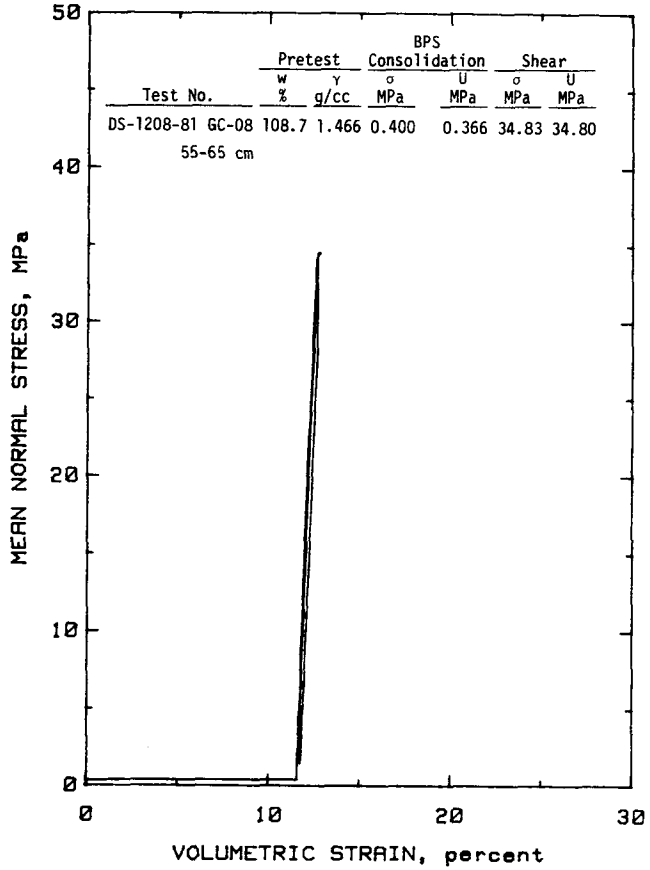


Figure 3.20 BACK PRESSURE SATURATED CONSOLIDATED STATIC UNDRAINED TRIAXIAL SHEAR SPECIMEN DS-1208-81 GC-08 55-65 cm MEAN NORMAL STRESS vs VOLUMETRIC STRAIN

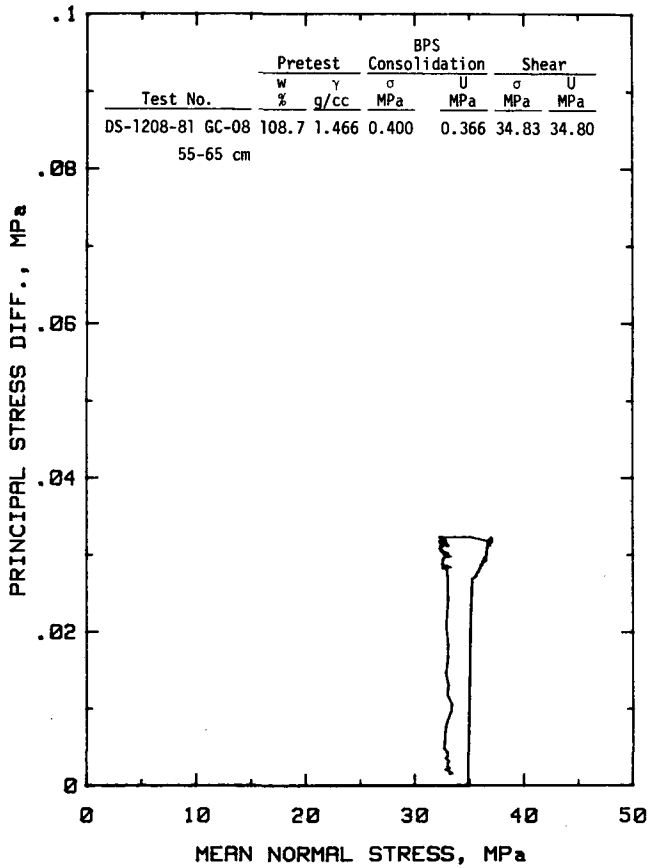


Figure 3.21 BACK PRESSURE SATURATED CONSOLIDATED STATIC UNDRAINED TRIAXIAL SHEAR SPECIMEN DS-1208-81 GC-08 55-65 cm PR. STRESS DIFF. vs MEAN NORMAL STRESS

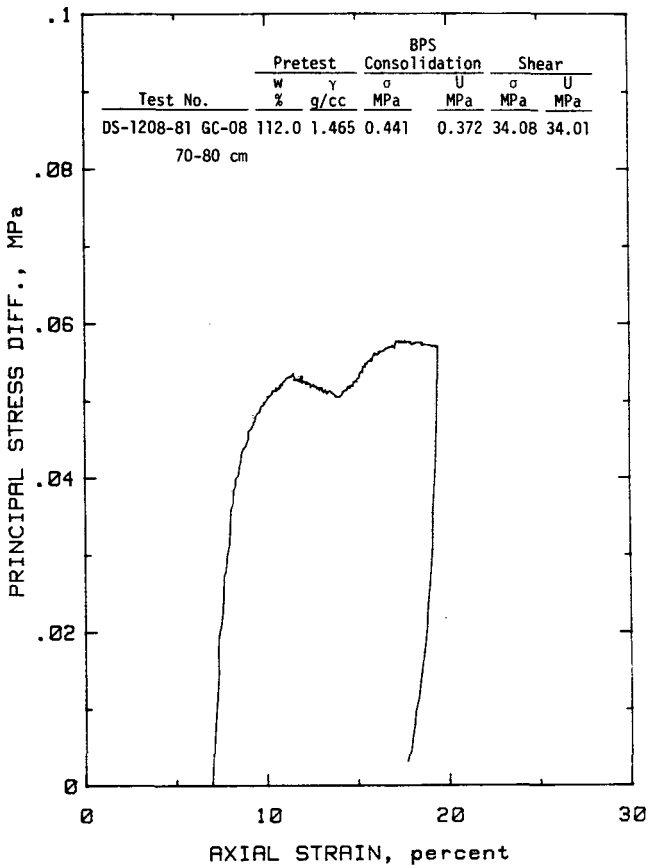


Figure 3.22 BACK PRESSURE SATURATED CONSOLIDATED STATIC UNDRAINED TRIAXIAL SHEAR SPECIMEN DS-1208-81 GC-08 70-80 cm PR. STRESS DIFF. vs AXIAL STRAIN

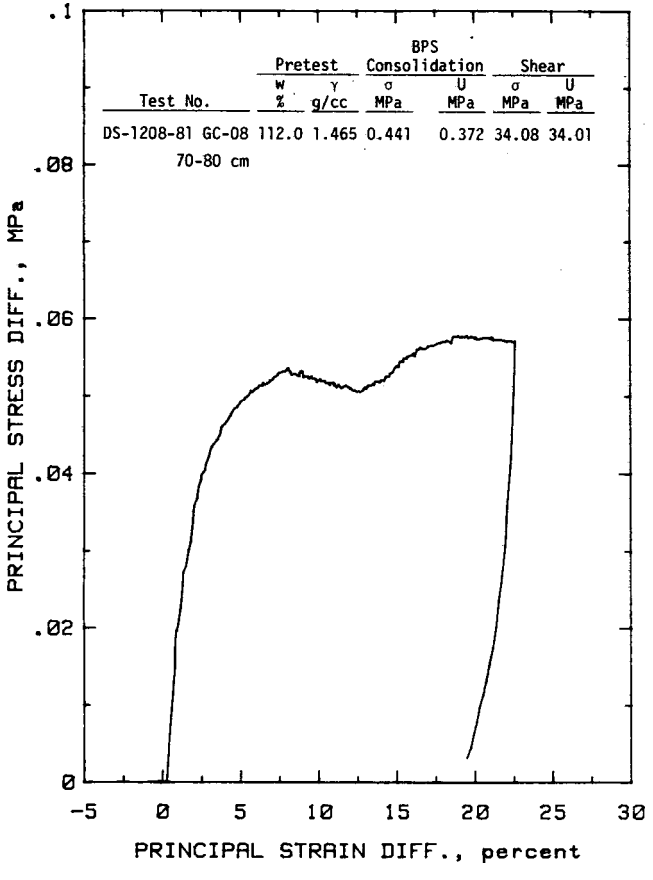


Figure 3.23 BACK PRESSURE SATURATED CONSOLIDATED STATIC UNDRAINED TRIAXIAL SHEAR SPECIMEN DS-1208-81 GC-08 70-80 cm PR. STRESS DIFF. vs PR. STRAIN DIFF.

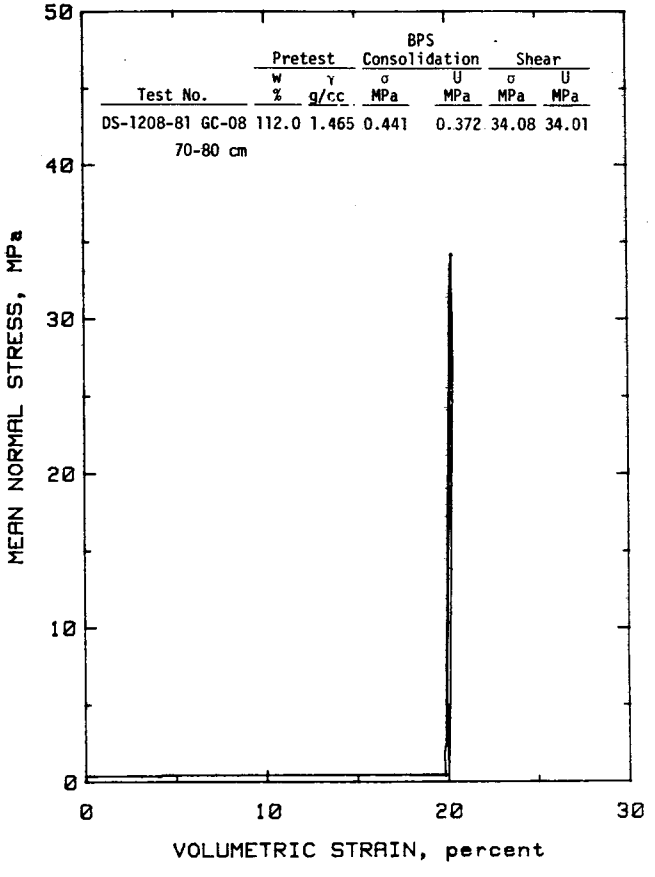


Figure 3.24 BACK PRESSURE SATURATED CONSOLIDATED STATIC UNDRAINED TRIAXIAL SHEAR SPECIMEN DS-1208-81 GC-08 70-80 cm MEAN NORMAL STRESS vs VOLUMETRIC STRAIN

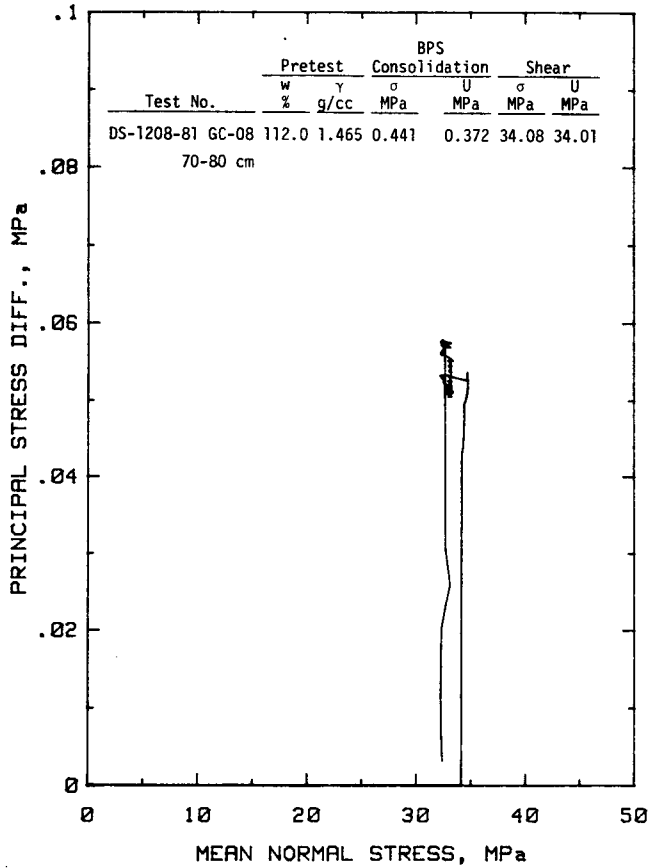


Figure 3.25 BACK PRESSURE SATURATED CONSOLIDATED STATIC UNDRAINED TRIAXIAL SHEAR SPECIMEN DS-1208-81 GC-08 70-80 cm PR. STRESS DIFF. vs MEAN NORMAL STRESS

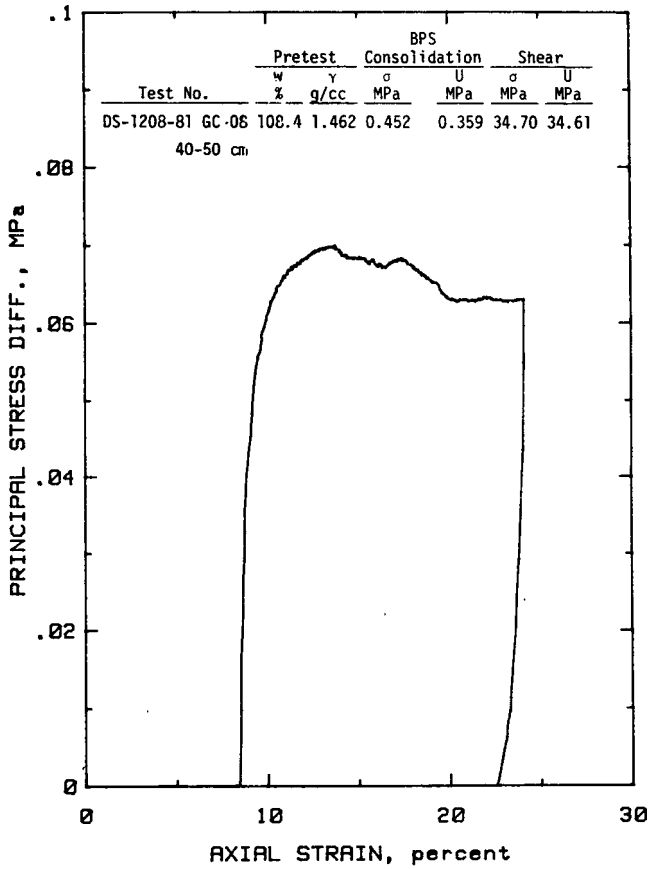


Figure 3.26 BACK PRESSURE SATURATED CONSOLIDATED STATIC UNDRAINED TRIAXIAL SHEAR SPECIMEN DS-1208-81 GC-08 40-50 cm PR. STRESS DIFF. vs AXIAL STRAIN

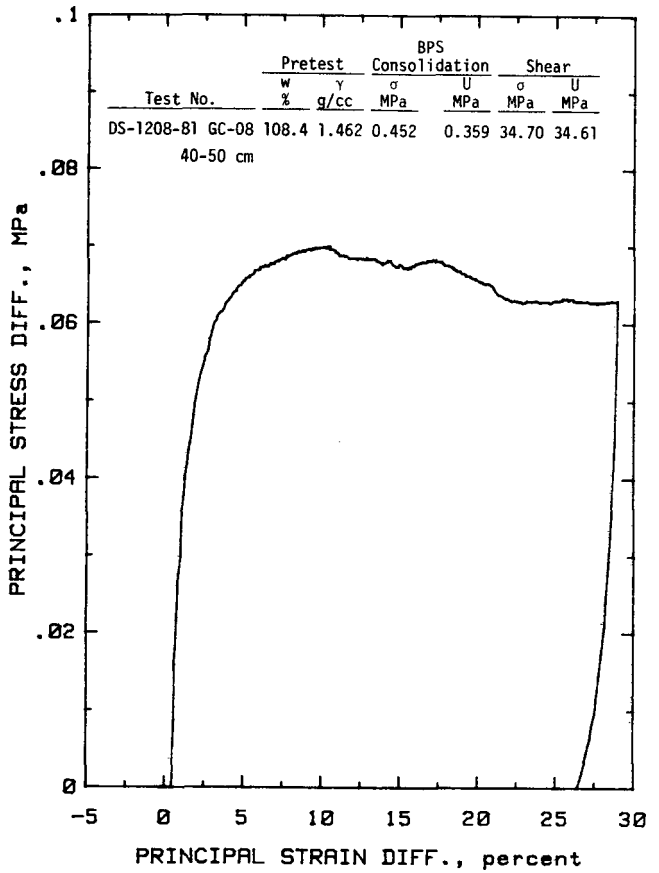


Figure 3.27 BACK PRESSURE SATURATED CONSOLIDATED STATIC UNDRAINED TRIAXIAL SHEAR SPECIMEN DS-1208-81 GC-08 40-50 cm PR. STRESS DIFF. vs PR. STRAIN DIFF.

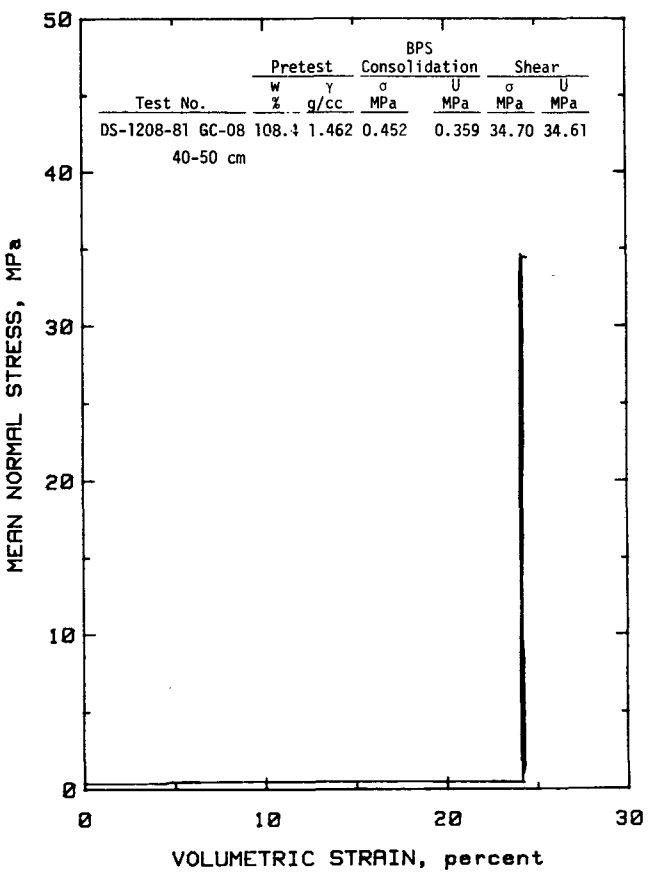


Figure 3.28 BACK PRESSURE SATURATED CONSOLIDATED STATIC UNDRAINED TRIAXIAL SHEAR SPECIMEN DS-1208-81 GC-08 40-50 cm MEAN NORMAL STRESS vs VOLUMETRIC STRAIN

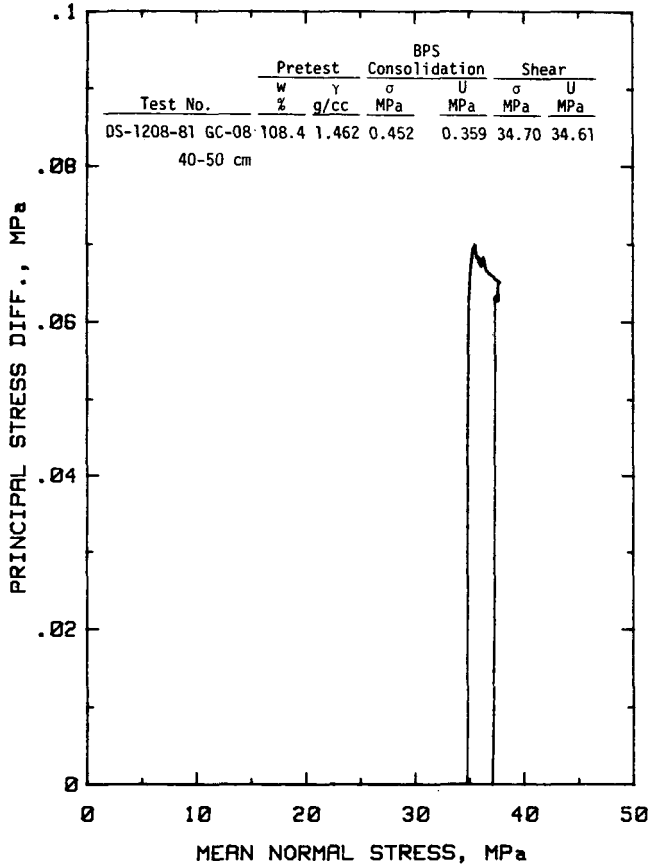


Figure 3.29 BACK PRESSURE SATURATED CONSOLIDATED STATIC UNDRAINED TRIAXIAL SHEAR SPECIMEN DS-1208-81 GC-08 40-50 cm PR. STRESS DIFF. vs MEAN NORMAL STRESS

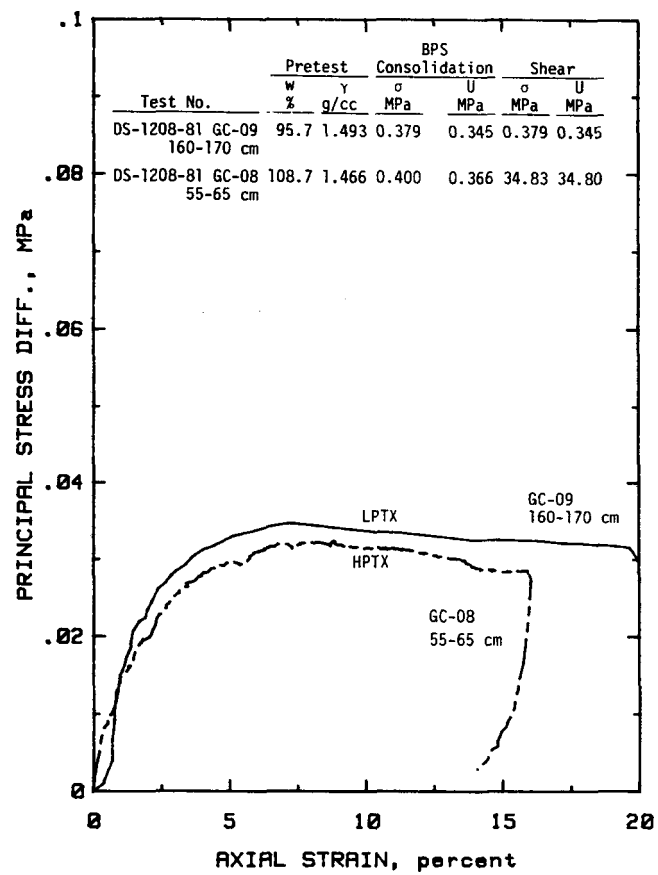


Figure 3.30 BACK PRESSURE SATURATED CONSOLIDATED STATIC UNDRAINED TRIAXIAL SHEAR GC-09 160-170 & GC-08 55-65 cm PR. STRESS DIFF. vs AXIAL STRAIN

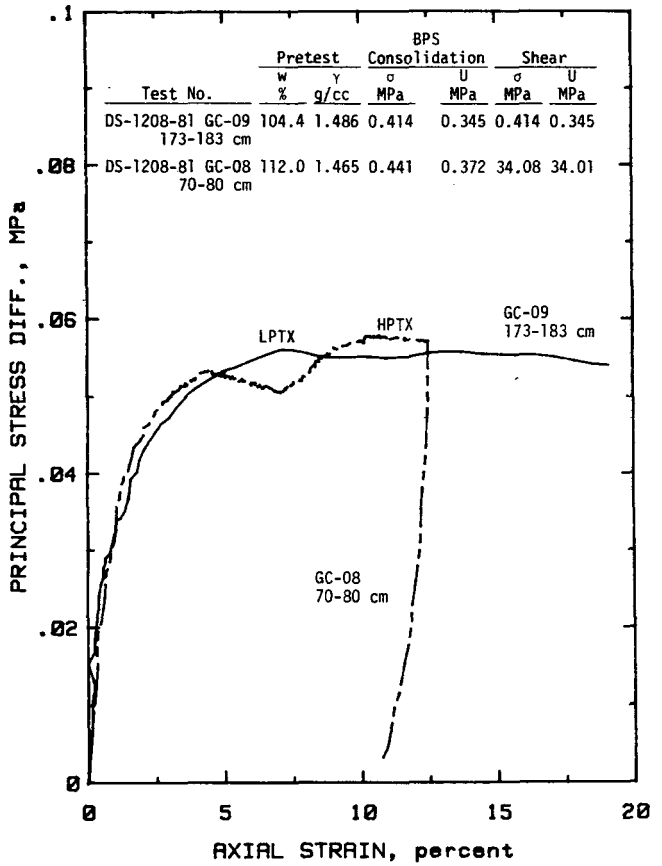


Figure 3.31 BACK PRESSURE SATURATED CONSOLIDATED STATIC UNDRAINED TRIAXIAL SHEAR GC-09 173-183 & GC-08 70-80 cm PR. STRESS DIFF. vs AXIAL STRAIN

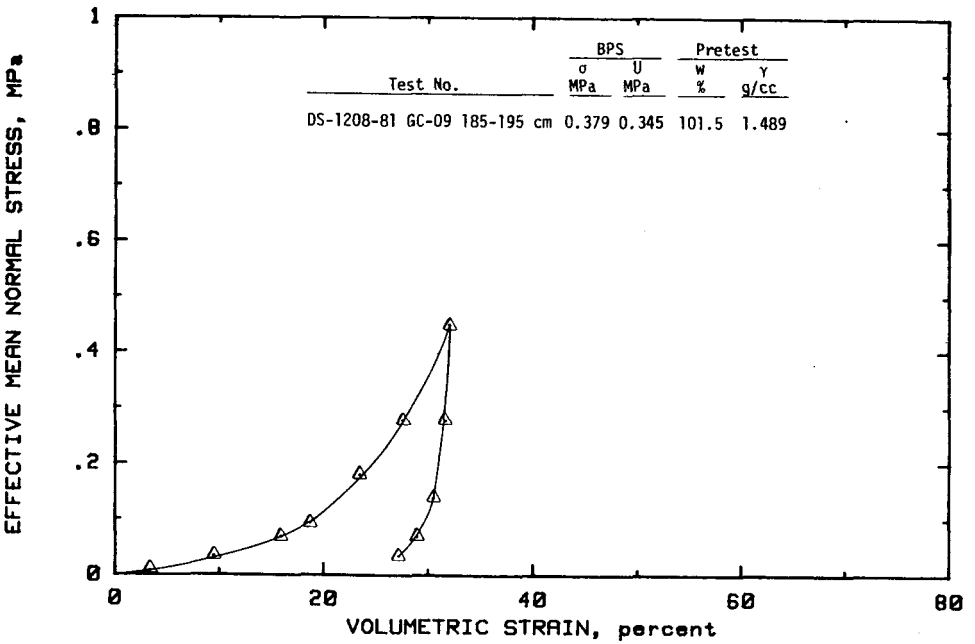


Figure 3.32 BACK PRESSURE SATURATED CONSOLIDATED STATIC DRAINED HYDROSTAT SPECIMEN DS-1208-81 GC-09 185-195 cm EFF. MEAN NORMAL STR. vs VOLUMETRIC STRAIN

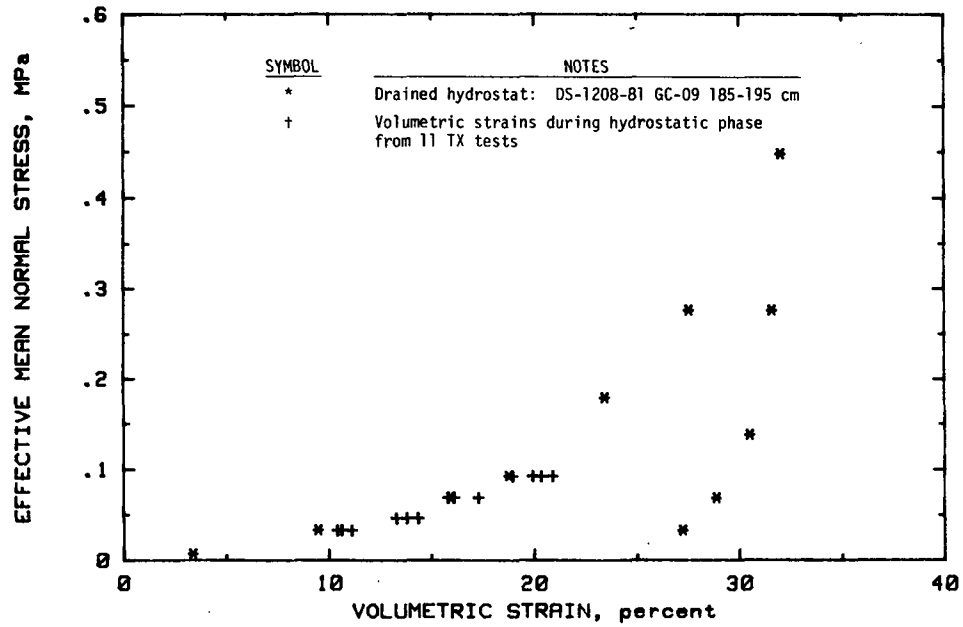


Figure 3.33 BACK PRESSURE SATURATED CONSOLIDATED
STATIC DRAINED HYDROSTATS
DATA FROM TWELVE TX TESTS
EFF. MEAN NORMAL STR. vs VOLUMETRIC STRAIN

CHAPTER 4

PORE PRESSURE UNIAXIAL STRAIN TESTS

4.1 GENERAL

Nineteen pore pressure uniaxial strain (PPUX) tests were conducted on 13 undisturbed Pacific illite specimens obtained from gravity cores DS-1208-81 GC-08 and GC-09. Fourteen tests were conducted on eight specimens to investigate the effects of two test variables (initial effective-stress level and loading rate) on the undrained compressibility of the new material. Two of these specimens were each loaded four times at successively faster rates. Five additional tests were conducted on five specimens to determine the drained compressibility due to incrementally applied static loads.

4.2 COMPOSITION PROPERTIES

Table 4.1 presents the composition properties for the 13 PPUX specimens tested and identifies the type of test conducted on each specimen. Note that two pretest water contents were determined for each specimen. These water content specimens were trimmed from the top and bottom of the actual test specimen during core processing. However, the wet density listed in the table was determined from the specimen itself. Hence, there are two computed values of γ_d , V_a , V_s , and V_w for each test specimen. Each posttest water content was determined directly from the specimen after it had been tested.

4.3 TEST EQUIPMENT

The PPUX test device has been previously described in Reference 1. One modification (an improvement) was made to the test device which enabled us to apply a desired initial effective-stress condition to each specimen before dynamic loading. In last year's program, the initial effective stresses could only be controlled for static PPUX tests. This modification involved drilling a 3/8-inch-diameter hole through the side wall of the top fluid chamber and attaching a permanent control valve to the outside of the chamber. This permitted us to independently apply a static pressure to the chamber fluid when the apparatus was set up under the SECO ram loader (Reference 1).

4.4 UNDRAINED PPUX TESTS

Six of the undrained PPUX tests involved single loadings of individual specimens. Two series of tests were conducted on these six specimens--one static and one dynamic to determine the effects of consolidation stress level on the undrained specimen compressibility. In each series three different effective consolidation stresses were applied (0.034, 0.069, and 0.093 MPa--the same stress levels as in the TX tests of Chapter 3). To isolate the effects of loading rise time, two special multiple-loading tests were conducted on two additional specimens. In

these tests, the specimen was first loaded statically, and then loaded dynamically three times, decreasing the loading rise time for each subsequent load application. It was presumed that each loading would produce only elastic strains and therefore each subsequent loading would be applied to an identical specimen. For all practical purposes this presumption was justified by the experimental results.

All test procedures with the exception of those discussed herein are described in Reference 1. For the two undrained specimens upon which multiple loading tests were conducted, the procedures used were (a) the test device was assembled with the specimen in place and positioned under the WES/SECO 100-kip loader; (b) valves and pressure lines were connected to the device to allow application of fluid pressure from the back-pressure saturation control panel and/or the high-pressure hydraulic pump; (c) the specimen was back-pressure saturated and then consolidated, recording volume changes versus time; (d) the specimen drainage valve was closed; (e) the vertical stress was increased to 62 MPa over a period of about 300 seconds, then decreased over a period of approximately 1 minute (cycle-A); (f) the original effective-stress conditions were reimposed; (g) the SECO loader was set up and fired, applying a nominal 62-MPa vertical stress to the specimen in approximately 100 msec, with a nominal 300-msec decay (cycle-B); (h) steps f and g were repeated with a rise time of approximately 35 msec (cycle-C); and (i) steps f and g were again repeated with a rise time of approximately 6 msec (cycle-D). In each of these two special multiple loading tests, specimen variability was eliminated as a test variable.

Table 4.2 summarizes the undrained PPUX test matrix results, presenting for each test the pretest water content and wet density, posttest water content, stresses imposed during the back-pressure saturation-consolidation phase, vertical strain measured by the LVDT just prior to undrained loading, loading rise time, the undrained constrained modulus, and the 95 percent confidence interval about that modulus.

For each undrained test specimen and for each cycle of the special multiple-loading tests, a plot of vertical stress versus vertical strain and a plot of vertical stress and pore pressure versus time are presented. For the static tests, time is not plotted explicitly on the abscissa; rather, point numbers are plotted for each test. Fifteen hundred digitized points represent one complete static test. In each of the above plots the vertical stresses, pore pressures, and vertical strains are plotted as total stresses and "total" strains, i.e., strains developed from the beginning of the back-pressure saturation phase of the test.

The test results for the single-loaded static tests are presented in Figures 4.1 through 4.6 and the single-loaded dynamic test results are shown in Figures 4.7 through 4.12. Figures 4.13 through 4.28 present the sequential results of the special multiple-loading tests.

In computing the constrained modulus for each undrained test (Table 4.2), a linear least squares line was fit to the loading points of the stress-strain curve. The 95 percent confidence interval for each modulus

was also calculated to determine if any meaningful statistical differences existed among any given tests. Table 4.2 indicates that the constrained modulus values increase as expected with increasing consolidation stress for both static and dynamic loadings. In addition, the special tests show a trend of increasing modulus with decreasing rise time. However, there is a conflict between the dynamic moduli of the single-loaded specimens and the multiple-loaded specimens. Figure 4.29 illustrates this conflict. The single-loaded dynamic moduli (with their 95 percent confidence limits) tend to group with the single-loaded static moduli and the A-cycle moduli of the special tests, which suggests no apparent loading rate effect. On the other hand, the C-cycle moduli from the special tests indicate a definite effect of loading rate (relative to the A-cycle moduli), on the order of 20 percent. The reason for this conflict is not presently understood. More testing is required to better define the effects of loading rate on the undrained constrained modulus of Pacific illite. Feedback from the theoreticians can tell us if this behavior is significant in model calculations.

Theoretically, during undrained loading and unloading, vertical stress and pore pressure should exhibit a one-to-one correspondence. However, there is at least a 1.5-msec time lag between peak vertical stress and peak pore pressure in the PPUX device due to the pore pressure measurement system itself (see Reference 1). We therefore expected close agreement between the vertical stress and pore pressure measurements in tests with rise times of the order 100 msec and greater. Good agreement was exhibited by all of the static PPUX tests, including the A-cycles of the special tests (Figures 4.2, 4.4, 4.6, 4.14, and 4.22). However, the B-cycles of the special tests, with rise times of approximately 100 msec, showed a much poorer correlation than expected (Figures 4.16 and 4.24); in fact, in Figure 4.24, the measured pore pressure is greater than the applied vertical stress during unloading. This indicates some type of heretofore unobserved lag exists in the overall pore pressure measurement system. However, this lag is not consistent in the other dynamic tests. For example, from the D-cycles of the two special tests (the fastest rise times) we observe only a very small difference between the vertical stress and pore pressure measurements (Figures 4.20 and 4.28), suggesting that improved "priming" of the system had occurred by the fourth cycle. Further study and testing are necessary to resolve these dynamic pore pressure measurement difficulties in the PPUX device.

Tests from which questionable pore pressure data were acquired are indicated as such on the corresponding figures. It must be emphasized here, however, that a poor pore pressure response does not affect the stress-strain response.

4.5 DRAINED PPUX TESTS

Five static drained PPUX tests were conducted to determine the drained loading and unloading compressibility response of undisturbed Pacific illite. Of the five tests, two were loaded to a peak effective stress of 54.83 MPa and subsequently unloaded. The other three specimens

developed leaks. Two of the tests which leaked did so during their first loading increment and thus no usable stress-strain data were obtained. Table 4.3 summarizes the data obtained from each of the five drained tests. The table lists the specimen test number, pretest water content and wet density, vertical stress and pore pressure at the end of back-pressure saturation, maximum total vertical stress and pore pressure achieved in the test, maximum strain (calculated by two methods), post-test specimen water content, and final specimen strains calculated by four different methods. The two methods used to calculate volumetric strain during each test are described in Reference 1 but are reviewed below for the sake of convenience.

In one method strains were calculated during the test from vertical deformeter measurements made by an LVDT inside the test device using the formula $\Delta H/H_o$, i.e., change in specimen height divided by original specimen height. In the second method, the volume of water expelled during consolidation was measured in a volume change burette and the volumetric strain was calculated as $\Delta V/V_o$, i.e., change in volume divided by pretest specimen volume. The differences in volumetric strain calculated by these two methods are not significant, as can be observed in Table 4.3 under the column headings "Maximum Strain" and "Final Strain." The observed differences generally developed early in the test during back-pressure saturation and during the first increments of effective-stress loading. These small initial differences then tended to remain constant throughout the remainder of the stress loading history.

In addition to the above two methods, final strains were also calculated (a) from direct physical measurements of the posttest deformed specimen (see column headed "Measured"), and (b) from posttest composition properties. The latter determination, listed under the column headed "Calculated", was computed based on the difference between the posttest and pretest water contents and the volume of solids of the saturated specimen.

Plots of effective vertical stress versus volumetric strain are presented for specimen GC-09 87-90 cm in Figure 4.30, GC-09 220-223 cm in Figure 4.31, and GC-08 35-38 cm in Figures 4.32 and 4.33. In each of these figures, volumetric strains calculated by the two methods are shown. Note that the volumetric strains calculated from the burette measurements are numerically smaller than the LVDT-based strains for all three tests. These smaller strains are attributed to negative volume changes measured by the burette system during back-pressure saturation.

To demonstrate the reproducibility of the drained compressibility tests, several comparison plots are presented in Figures 4.34 through 4.38 for low (0 to 1 MPa) and high (0 to 80 MPa) stress ranges. All of the data shown are for drained PPUX tests except test GC-09 185-195 cm (Figure 4.36) which is the drained hydrostatic test previously presented in Chapter 3. Test MA-12 GC-19 S#8 (Figures 4.37 and 4.38) was conducted on an undisturbed specimen of Pacific illite also taken from a core obtained in MPG-I (Reference 1).

Within the accuracy of the strain measurement systems, it can be stated that all of the curves presented fall on top of one another.

Table 4.1 Summary of Composition Properties for DS-1208-81 GC-08 and GC-09 Pore Pressure Uniaxial Strain Specimens

Test Number	Sample Depth in Core cm**	w* %	γ g/cc	γ_d* g/cc	V_a* %	V_s* %	V_w* %	Type of Test	Posttest w* %
DS-1208-81 GC-09 9-12 cm	8	112.1	1.460	0.688	0.0	25.5	74.5	Static Undrained	92.6
DS-1208-81 GC-09 9-12 cm	13	111.9	1.460	0.689	0.0	25.5	74.5	Static Undrained	92.6
DS-1208-81 GC-09 30-33 cm	28	109.5	1.469	0.701	0.0	25.8	74.2	Static Undrained	87.5
DS-1208-81 GC-09 30-33 cm	34	112.7	1.469	0.691	0.0	24.8	75.2	Static Undrained	87.5
DS-1208-81 GC-09 40-43 cm	38	115.6	1.447	0.671	0.2	24.9	74.9	Static Undrained	81.6
DS-1208-81 GC-09 40-43 cm	44	111.2	1.447	0.685	1.0	25.4	73.6	Static Undrained	81.6
DS-1208-81 GC-09 20-23 cm	17	112.2	1.476	0.695	0.0	24.6	75.4	Dynamic Undrained	92.0
DS-1208-81 GC-09 20-23 cm	24	104.7	1.476	0.721	0.3	26.7	73.0	Dynamic Undrained	92.0
DS-1208-81 GC-09 60-63 cm	58	111.6	1.461	0.690	0.0	25.5	74.5	Dynamic Undrained	90.6
DS-1208-81 GC-09 60-63 cm	64	110.4	1.461	0.694	0.2	25.7	74.1	Dynamic Undrained	90.6
DS-1208-81 GC-09 47-50 cm	46	110.7	1.463	0.694	0.0	25.7	74.3	Dynamic Undrained	80.9
DS-1208-81 GC-09 47-50 cm	52	116.8	1.463	0.675	0.0	23.8	76.2	Dynamic Undrained	80.9
DS-1208-81 GC-09 80-83 cm	78	120.7	1.443	0.654	0.0	23.7	76.3	Static/Dynamic Undrained	103.7
DS-1208-81 GC-09 80-83 cm	84	121.0	1.443	0.653	0.0	23.7	76.3	Static/Dynamic Undrained	103.7
DS-1208-81 GC-09 67-70 cm	66	121.7	1.453	0.655	0.0	22.9	77.1	Static/Dynamic Undrained	83.9
DS-1208-81 GC-09 67-70 cm	72	126.8	1.453	0.641	0.0	21.5	78.5	Static/Dynamic Undrained	83.9
DS-1208-81 GC-09 87-90 cm	86	118.2	1.450	0.665	0.0	24.1	75.9	Static Drained	53.7
DS-1208-81 GC-09 87-90 cm	92	113.8	1.450	0.678	0.3	25.1	74.6	Static Drained	53.7
DS-1208-81 GC-09 230-233 cm	229	100.9	1.514	0.754	0.0	26.5	73.5	Static Drained	---
DS-1208-81 GC-09 230-233 cm	236	97.4	1.514	0.767	0.0	27.8	72.2	Static Drained	---
DS-1208-81 GC-09 220-223 cm	220	104.9	1.484	0.724	0.0	26.6	73.4	Static Drained	29.0
DS-1208-81 GC-09 220-223 cm	226	103.2	1.484	0.730	0.1	27.1	72.8	Static Drained	29.0
DS-1208-81 GC-09 210-213 cm	209	103.3	1.502	0.739	0.0	26.3	73.7	Static Drained	---
DS-1208-81 GC-09 210-213 cm	216	103.5	1.502	0.738	0.0	26.2	73.8	Static Drained	---
DS-1208-81 GC-08 35-38 cm	32	112.1	1.461	0.689	0.0	25.4	74.6	Static Drained	25.2
DS-1208-81 GC-08 35-38 cm	39	112.7	1.461	0.687	0.0	25.2	74.8	Static Drained	25.2

* Corrected for 35 ppt salt content; specific gravity assumed = 2.70.

** Depth of water content specimen.

Table 4.2 Summary of Test Data for DS-1208-81 GC-09 Undrained Pore Pressure Uniaxial Strain Specimens

Test Number	Pretest w* %	Pretest γ g/cc	Posttest w %	BPS Consolidation σ MPa	BPS Consolidation U MPa	BPS Consolidation ϵ_v %	Rise Time sec	Constrained Modulus MPa	95 Percent Confidence Interval MPa
DS-1208-81 GC-09 9-12 cm	112.0	1.460	92.6	0.379	0.345	6.81	300	4252	±147
DS-1208-81 GC-09 30-33 cm	111.1	1.469	87.5	0.414	0.345	11.10	300	4596	±143
DS-1208-81 GC-09 40-43 cm	113.4	1.447	81.6	0.438	0.345	15.06	300	4862	±180
DS-1208-81 GC-09 20-23 cm	108.5	1.476	92.0	0.379	0.345	6.90	0.038	4392	±290
DS-1208-81 GC-09 60-63 cm	111.0	1.461	90.6	0.414	0.345	9.98	0.041	5010	±732
DS-1208-81 GC-09 47-50 cm	113.8	1.463	80.9	0.438	0.345	13.62	0.040	5109	±395
DS-1208-81 GC-09 80-83 cm A	120.9	1.443	103.7	0.379	0.345	5.97	300	4496	±133
DS-1208-81 GC-09 80-83 cm B	120.9	1.443	103.7	0.379	0.345	5.97	0.112	5108	±133
DS-1208-81 GC-09 80-83 cm C	120.9	1.443	103.7	0.379	0.345	5.97	0.037	5328	±233
DS-1208-81 GC-09 80-83 cm D	120.9	1.443	103.7	0.379	0.345	5.97	0.007	4676	±351
DS-1208-81 GC-09 67-70 cm A	124.3	1.453	83.9	0.414	0.345	10.98	300	5005	±229
DS-1208-81 GC-09 67-70 cm B	124.3	1.453	83.9	0.414	0.345	10.98	0.104	5210	±234
DS-1208-81 GC-09 67-70 cm C	124.3	1.453	83.9	0.414	0.345	10.98	0.036	6013	±369
DS-1208-81 GC-09 67-70 cm D	124.3	1.453	83.9	0.414	0.345	10.98	0.006	6286	±781

* Average water content from Table 4.1.

Table 4.3 Summary of Test Data for DS-1208-81 GC-08 and GC-09 Drained Pore Pressure Uniaxial Strain Specimens

Test Number	Pretest		BPS		Maximum Stress		Maximum Strain†		Posttest	Final Strain†			
	w* %	γ g/cc	σ_r MPa	U MPa	σ_r MPa	U MPa	$\Delta H/H_o$ %	$\Delta V/V_o$ %	w %	$\Delta H/H_o$ %	$\Delta V/V_o$ %	Measured %	Calculated %
DS-1208-81 GC-09 87-90 cm	116.0	1.450	0.35	0.34	0.76**	0.34	41.61	41.32	53.7	41.61	41.32	41.84	---
DS-1208-81 GC-09 230-233 cm	99.2	1.514	0.35	0.34	0.38**	0.34	---	---	---	---	---	---	---
DS-1208-81 GC-09 220-223 cm	104.1	1.484	0.35	0.34	55.17	0.34	65.17	63.13	29.0	54.28	48.85	55.78	53.26
DS-1208-81 GC-09 210-213	103.4	1.502	0.35	0.34	0.38**	0.34	---	---	---	---	---	---	---
DS-1208-81 GC-08 35-38 cm	112.4	1.461	0.35	0.34	55.17	0.34	66.94	63.01	25.2	59.82	55.50	61.44	58.32

* Average water content from Table 4.1.
** Specimen leaked at this stress increment.
† See text for explanation.

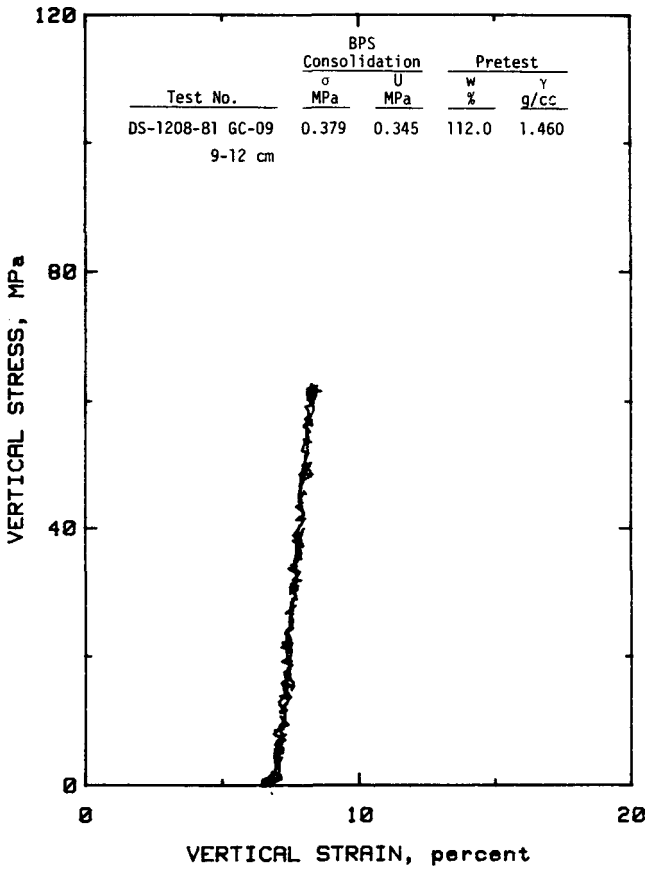


Figure 4.1 BACK PRESSURE SATURATED CONSOLIDATED STATIC UNDRAINED UNIAXIAL STRAIN SPECIMEN DS-1208-81 GC-09 9-12 cm VERTICAL STRESS vs VERTICAL STRAIN

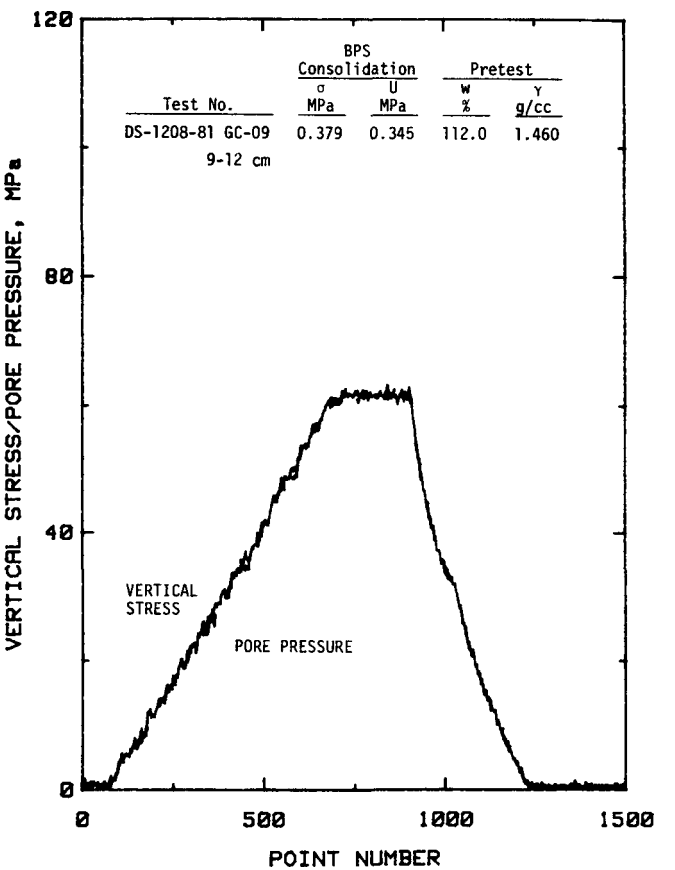


Figure 4.2 BACK PRESSURE SATURATED CONSOLIDATED STATIC UNDRAINED UNIAXIAL STRAIN SPECIMEN DS-1208-81 GC-09 9-12 cm VERTICAL STR./PORE PR. vs POINT NUMBER

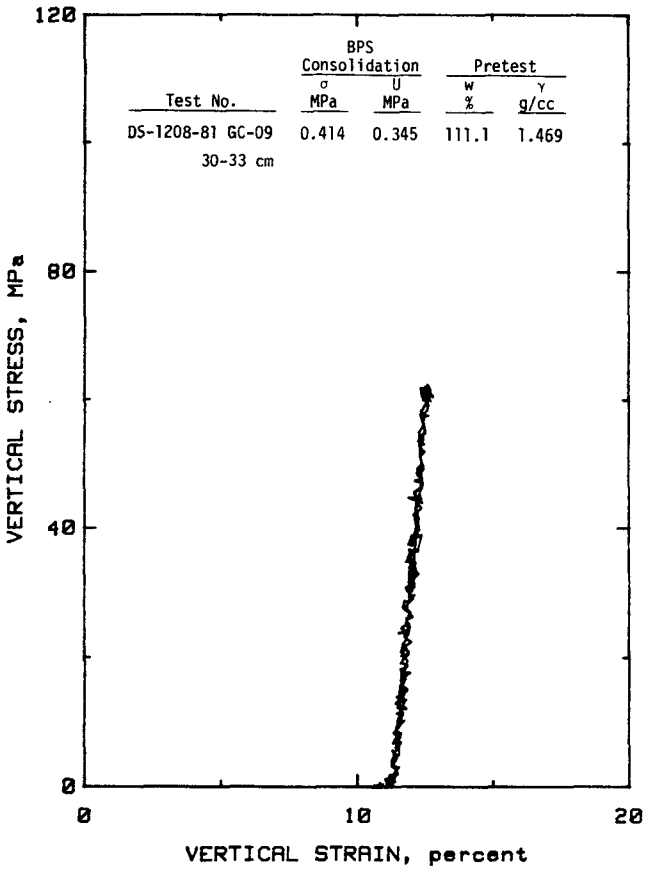


Figure 4.3 BACK PRESSURE SATURATED CONSOLIDATED STATIC UNDRAINED UNIAXIAL STRAIN SPECIMEN DS-1208-81 GC-09 30-33 cm VERTICAL STRESS vs VERTICAL STRAIN

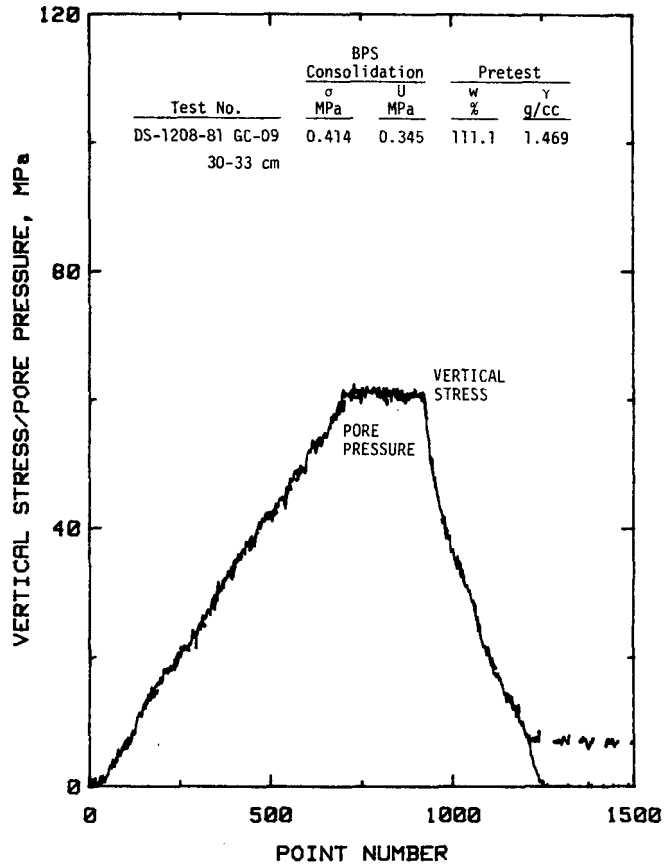


Figure 4.4 BACK PRESSURE SATURATED CONSOLIDATED STATIC UNDRAINED UNIAXIAL STRAIN SPECIMEN DS-1208-81 GC-09 30-33 cm VERTICAL STR./PORE PR. vs POINT NUMBER

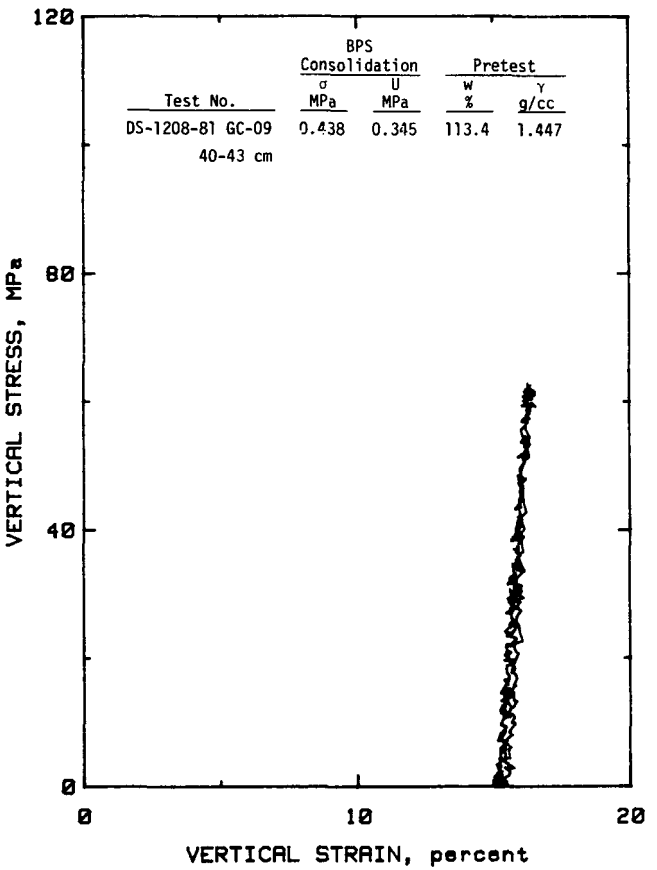


Figure 4.5 BACK PRESSURE SATURATED CONSOLIDATED STATIC UNDRAINED UNIAXIAL STRAIN SPECIMEN DS-1208-81 GC-09 40-43 cm VERTICAL STRESS vs VERTICAL STRAIN

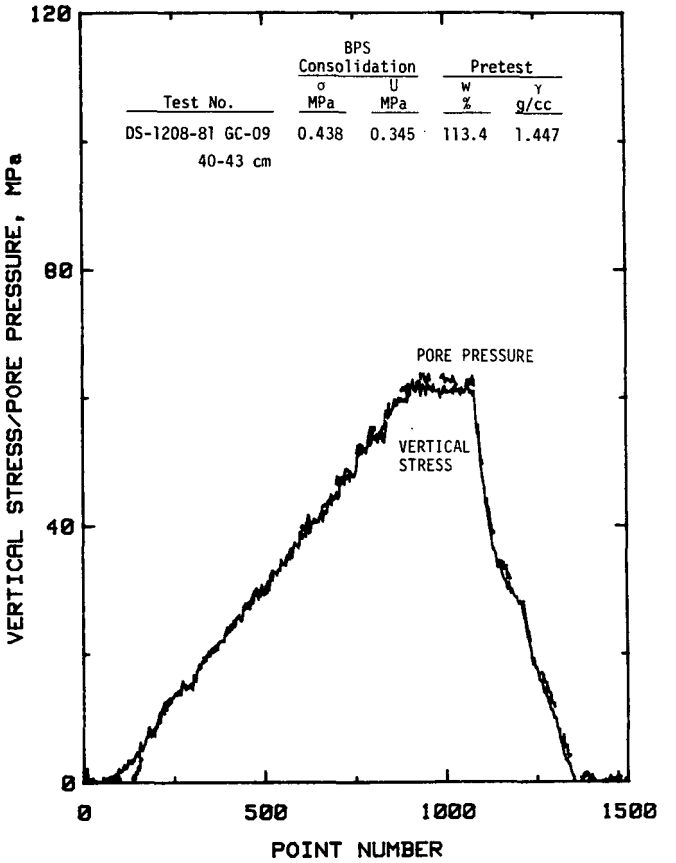


Figure 4.6 BACK PRESSURE SATURATED CONSOLIDATED STATIC UNDRAINED UNIAXIAL STRAIN SPECIMEN DS-1208-81 GC-09 40-43 cm VERTICAL STR./PORE PR. vs POINT NUMBER

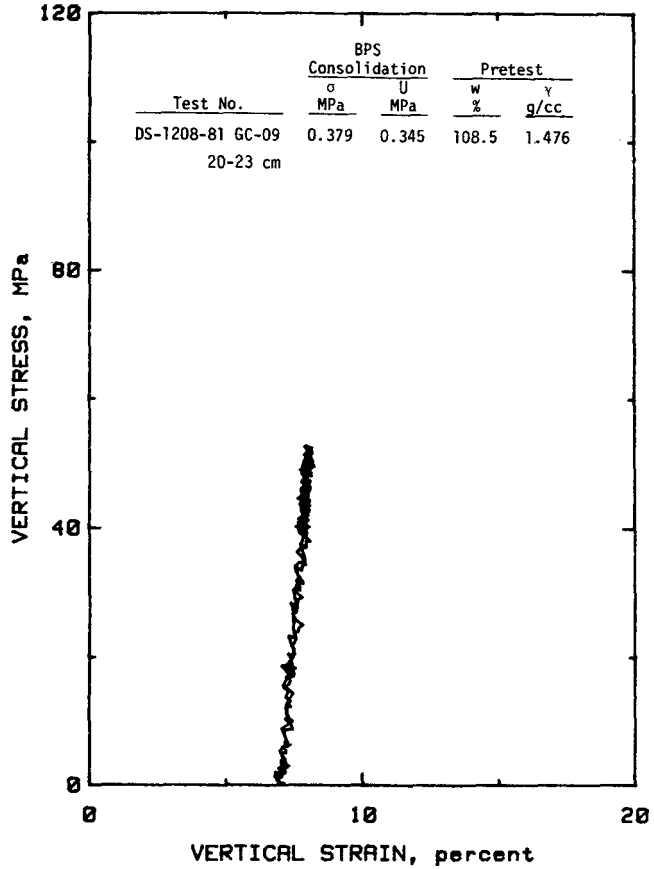


Figure 4.7 BACK PRESSURE SATURATED CONSOLIDATED DYNAMIC UNDRAINED UNIAXIAL STRAIN SPECIMEN DS-1208-81 GC-09 20-23 cm VERTICAL STRESS vs VERTICAL STRAIN

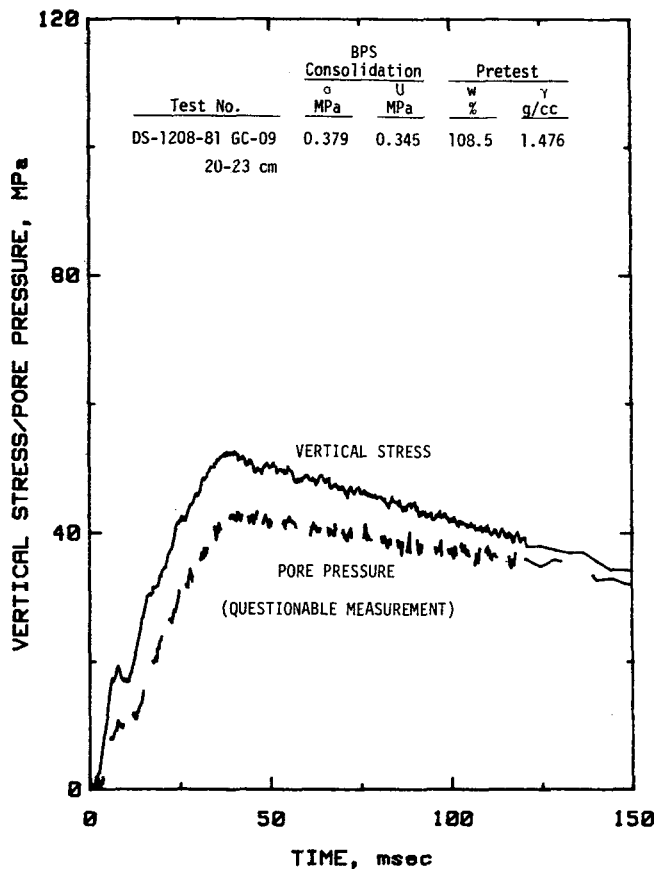


Figure 4.8 BACK PRESSURE SATURATED CONSOLIDATED DYNAMIC UNDRAINED UNIAXIAL STRAIN SPECIMEN DS-1208-81 GC-09 20-23 cm VERTICAL STR./PORE PR. vs TIME

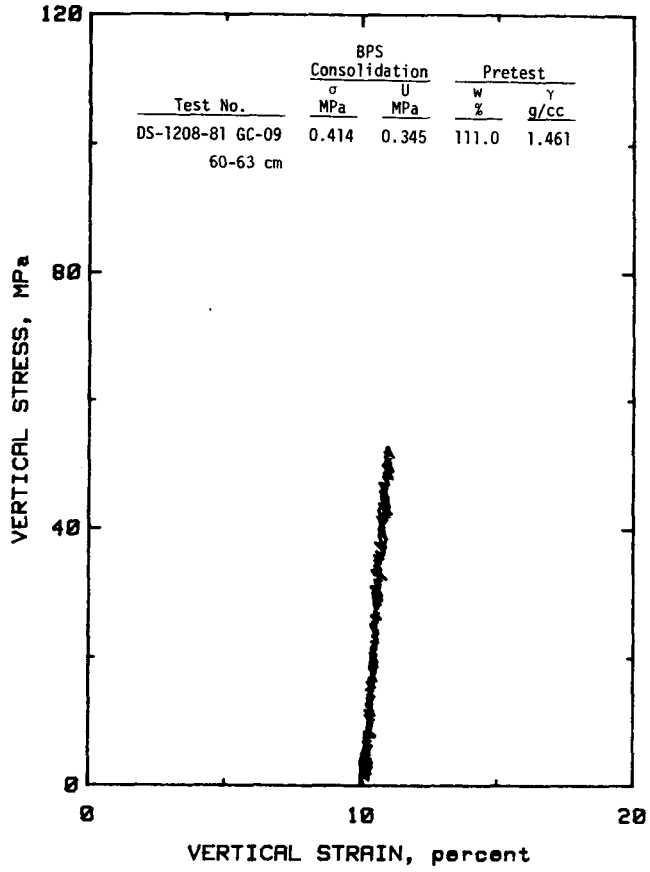


Figure 4.9 BACK PRESSURE SATURATED CONSOLIDATED DYNAMIC UNDRAINED UNIAXIAL STRAIN SPECIMEN DS-1208-81 GC-09 60-63 cm VERTICAL STRESS vs VERTICAL STRAIN

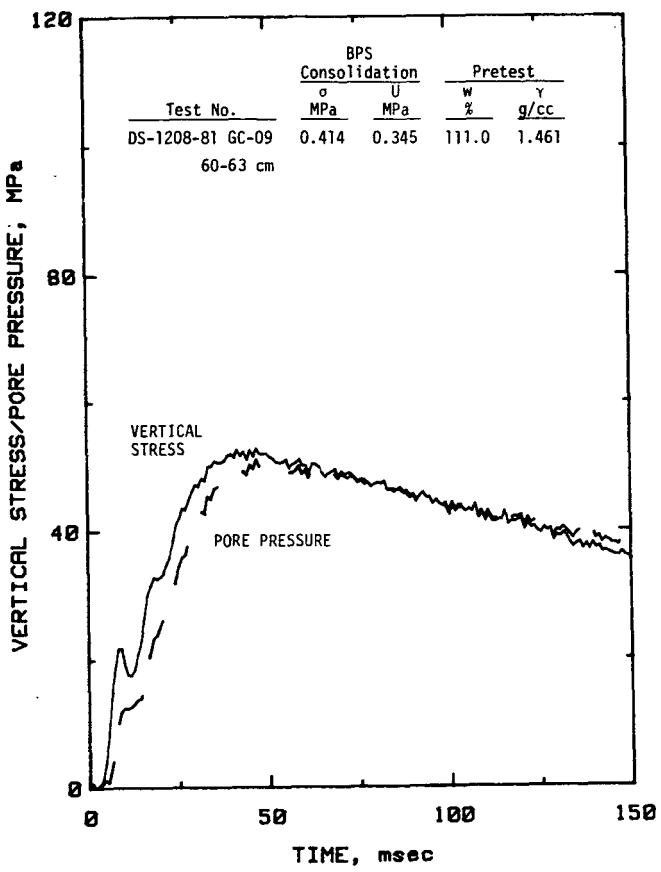


Figure 4.10 BACK PRESSURE SATURATED CONSOLIDATED DYNAMIC UNDRAINED UNIAXIAL STRAIN SPECIMEN DS-1208-81 GC-09 60-63 cm VERTICAL STR./PORE PR. vs TIME

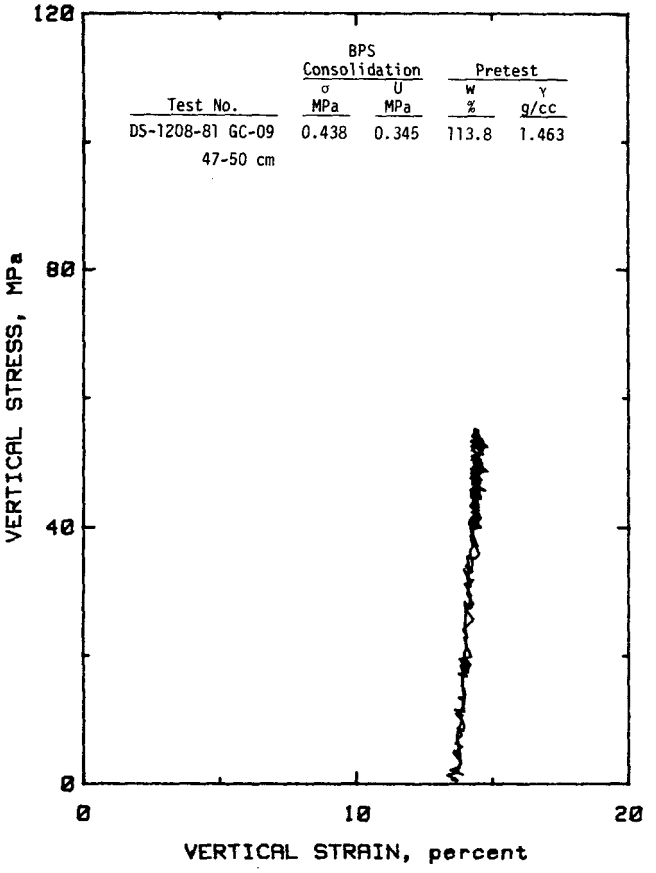


Figure 4.11 BACK PRESSURE SATURATED CONSOLIDATED DYNAMIC UNDRAINED UNIAXIAL STRAIN SPECIMEN DS-1208-81 GC-09 47-50 cm VERTICAL STRESS vs VERTICAL STRAIN

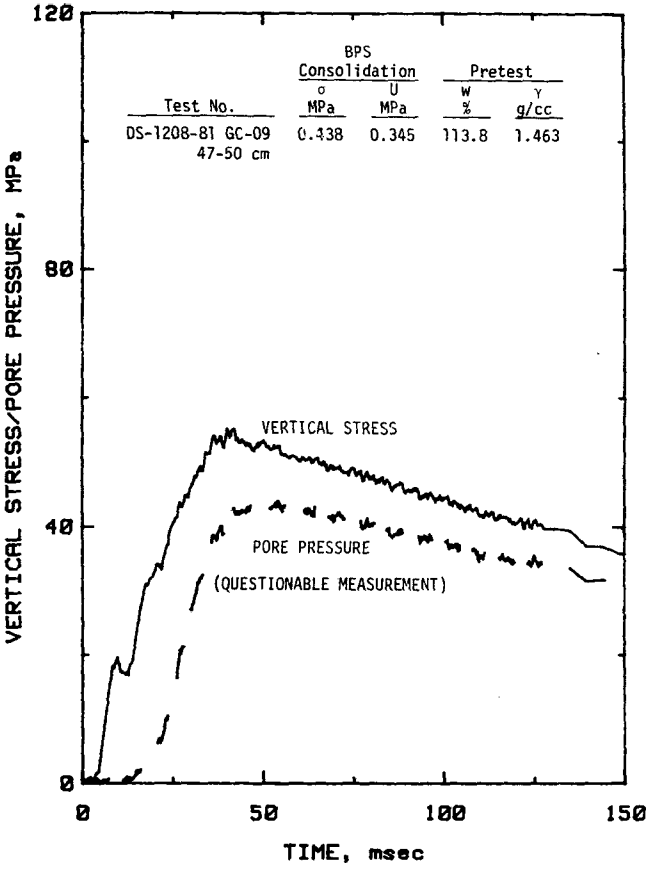


Figure 4.12 BACK PRESSURE SATURATED CONSOLIDATED DYNAMIC UNDRAINED UNIAXIAL STRAIN SPECIMEN DS-1208-81 GC-09 47-50 cm VERTICAL STR./PORE PR. vs TIME

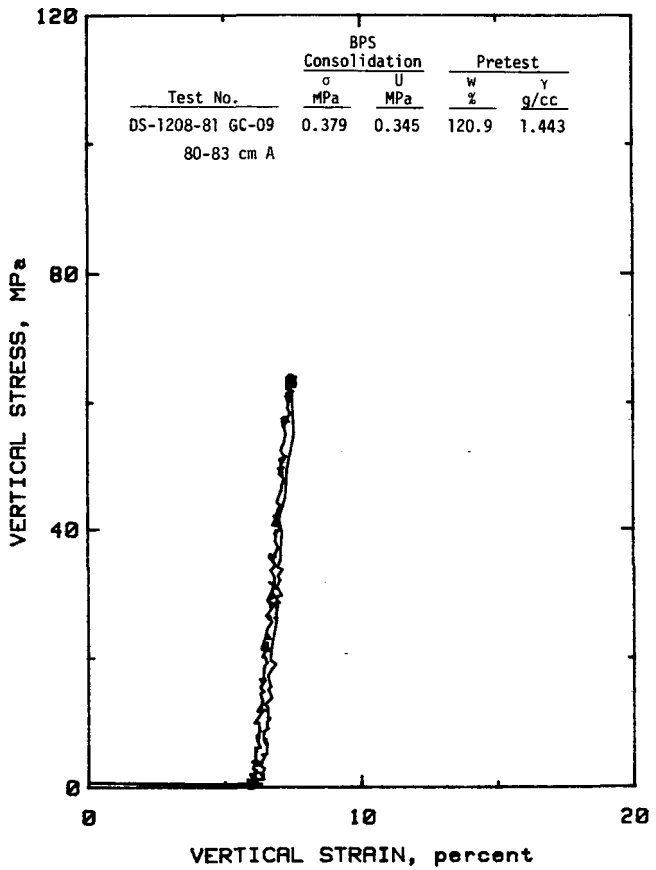


Figure 4.13 BACK PRESSURE SATURATED CONSOLIDATED STATIC UNDRAINED UNIAXIAL STRAIN SPECIMEN DS-1208-81 GC-09 80-83 cm A VERTICAL STRESS vs VERTICAL STRAIN

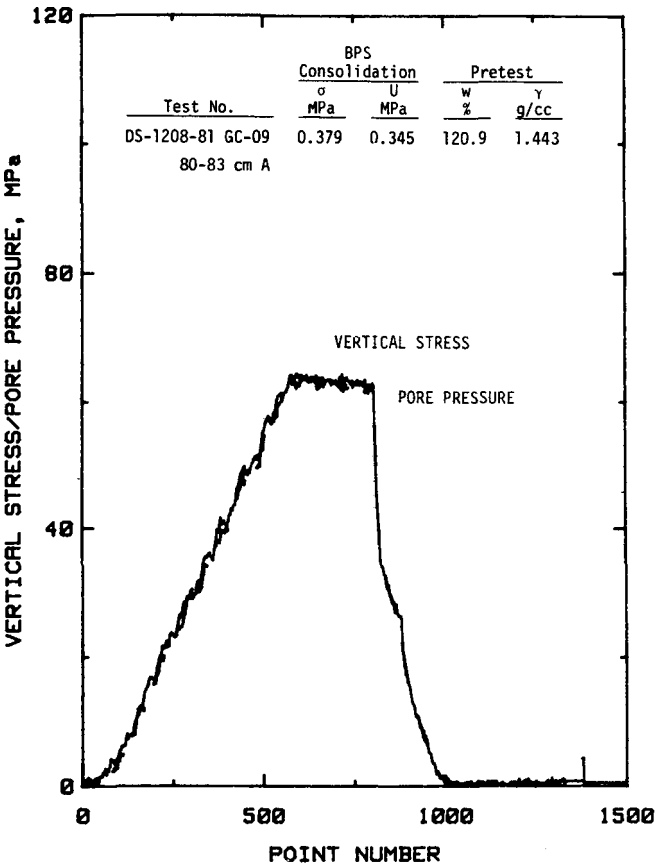


Figure 4.14 BACK PRESSURE SATURATED CONSOLIDATED STATIC UNDRAINED UNIAXIAL STRAIN SPECIMEN DS-1208-81 GC-09 80-83 cm A VERTICAL STR./PORE PR. vs POINT NUMBER

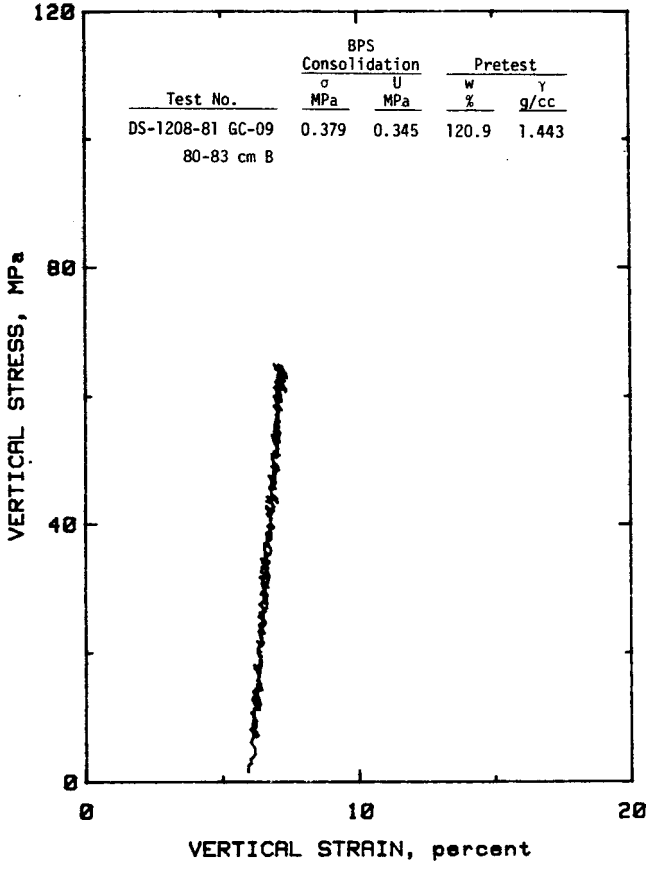


Figure 4.15 BACK PRESSURE SATURATED CONSOLIDATED DYNAMIC UNDRAINED UNIAXIAL STRAIN SPECIMEN DS-1208-81 GC-09 80-83 cm B VERTICAL STRESS vs VERTICAL STRAIN

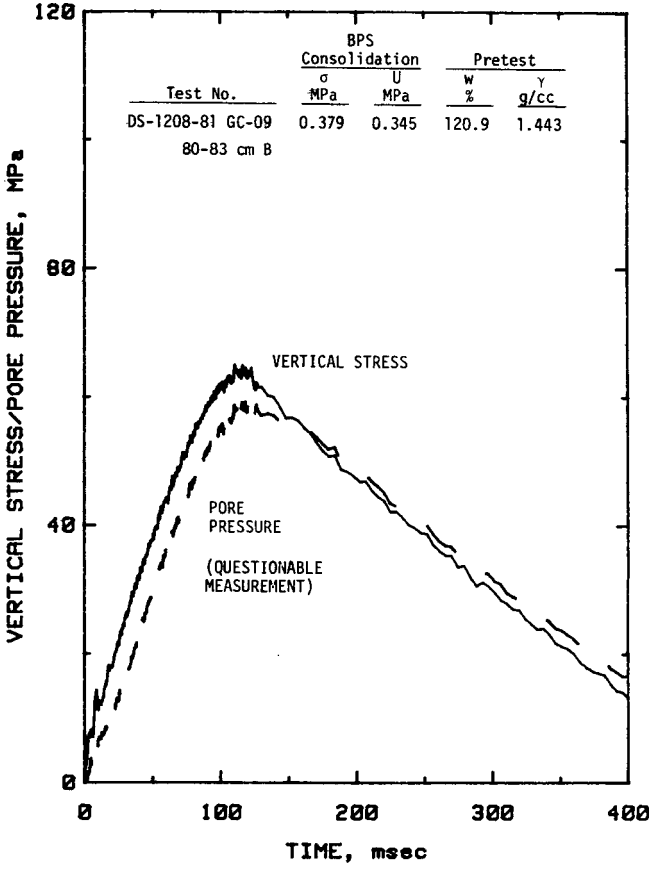


Figure 4.16 BACK PRESSURE SATURATED CONSOLIDATED DYNAMIC UNDRAINED UNIAXIAL STRAIN SPECIMEN DS-1208-81 GC-09 80-83 cm B VERTICAL STR./PORE PR. vs TIME

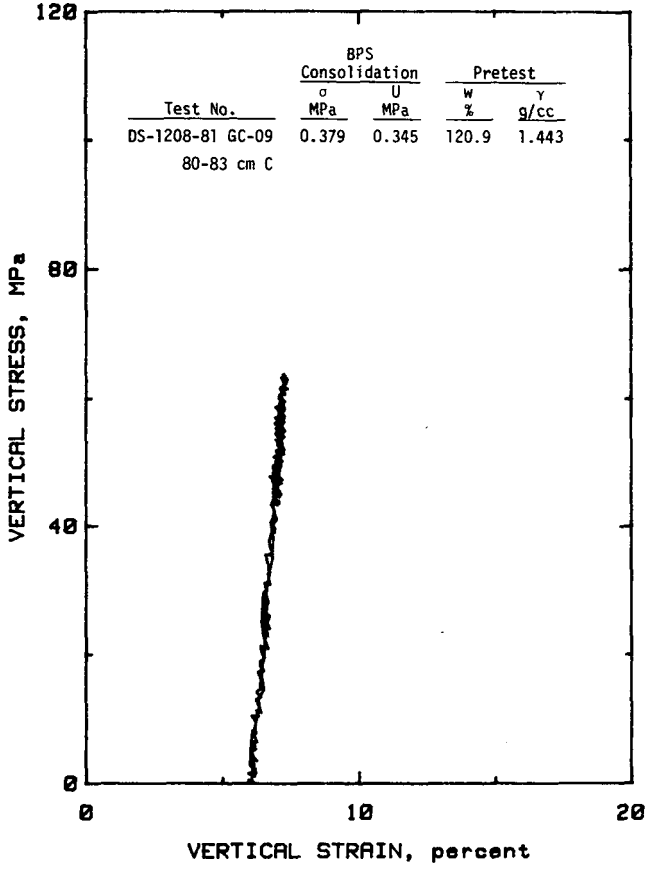


Figure 4.17 BACK PRESSURE SATURATED CONSOLIDATED DYNAMIC UNDRAINED UNIAXIAL STRAIN SPECIMEN DS-1208-81 GC-09 80-83 cm C VERTICAL STRESS vs VERTICAL STRAIN

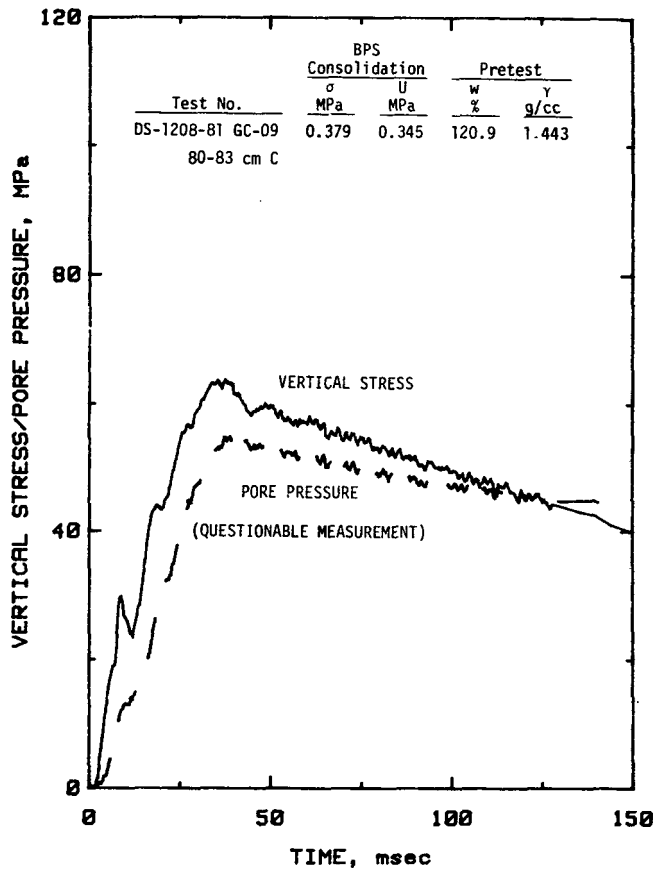


Figure 4.18 BACK PRESSURE SATURATED CONSOLIDATED DYNAMIC UNDRAINED UNIAXIAL STRAIN SPECIMEN DS-1208-81 GC-09 80-83 cm C VERTICAL STR./PORE PR. vs TIME

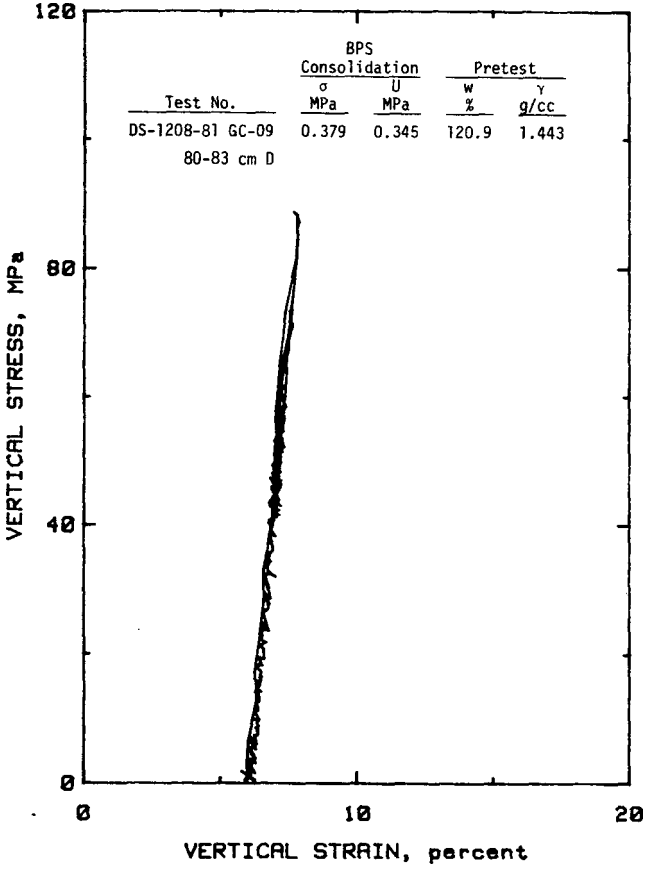


Figure 4.19 BACK PRESSURE SATURATED CONSOLIDATED DYNAMIC UNDRAINED UNIAXIAL STRAIN SPECIMEN DS-1208-81 GC-09 80-83 cm D VERTICAL STRESS vs VERTICAL STRAIN

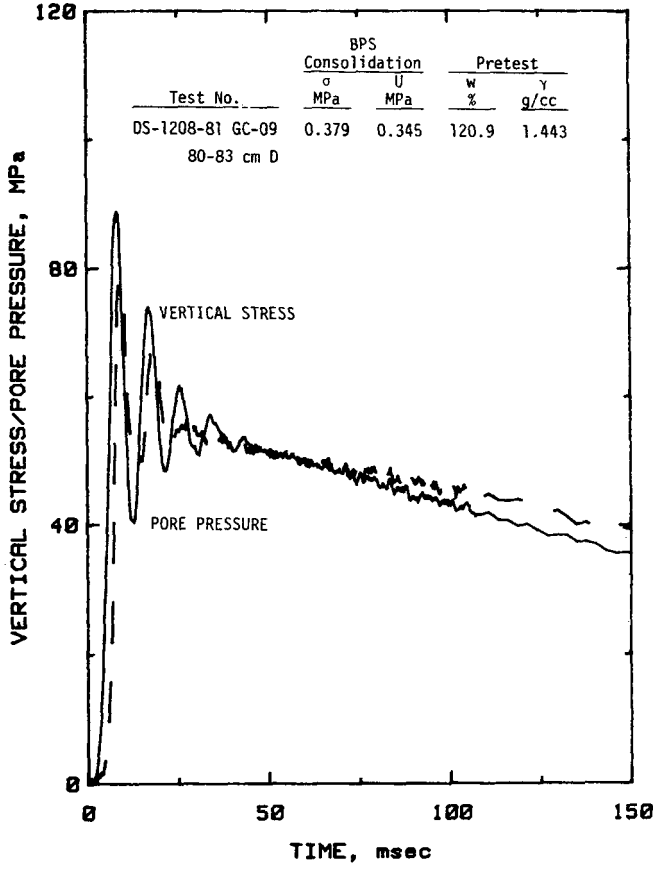


Figure 4.20 BACK PRESSURE SATURATED CONSOLIDATED DYNAMIC UNDRAINED UNIAXIAL STRAIN SPECIMEN DS-1208-81 GC-09 80-83 cm D VERTICAL STR./PORE PR. vs TIME

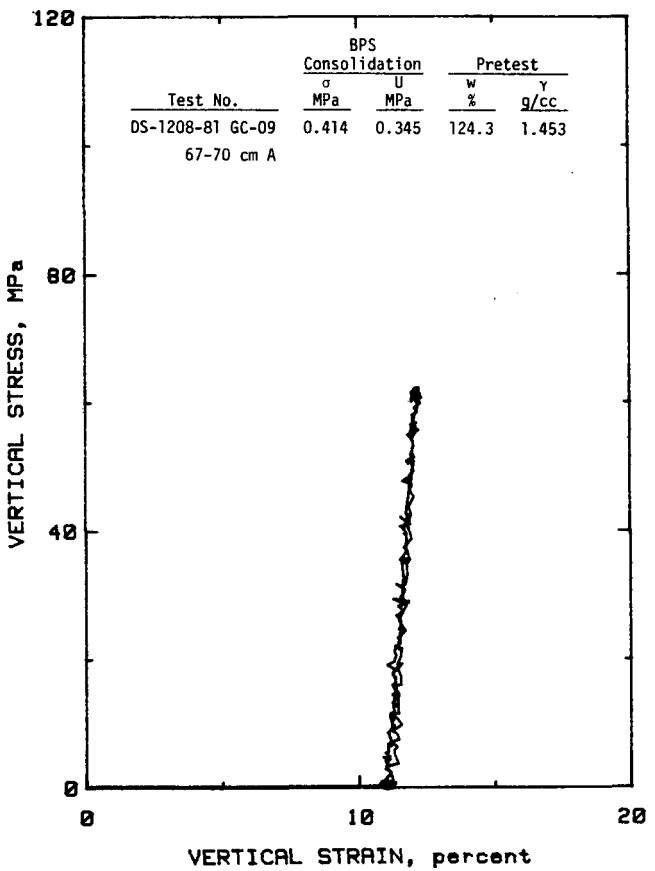


Figure 4.21 BACK PRESSURE SATURATED CONSOLIDATED STATIC UNDRAINED UNIAXIAL STRAIN SPECIMEN DS-1208-81 GC-09 67-70 cm A VERTICAL STRESS vs VERTICAL STRAIN

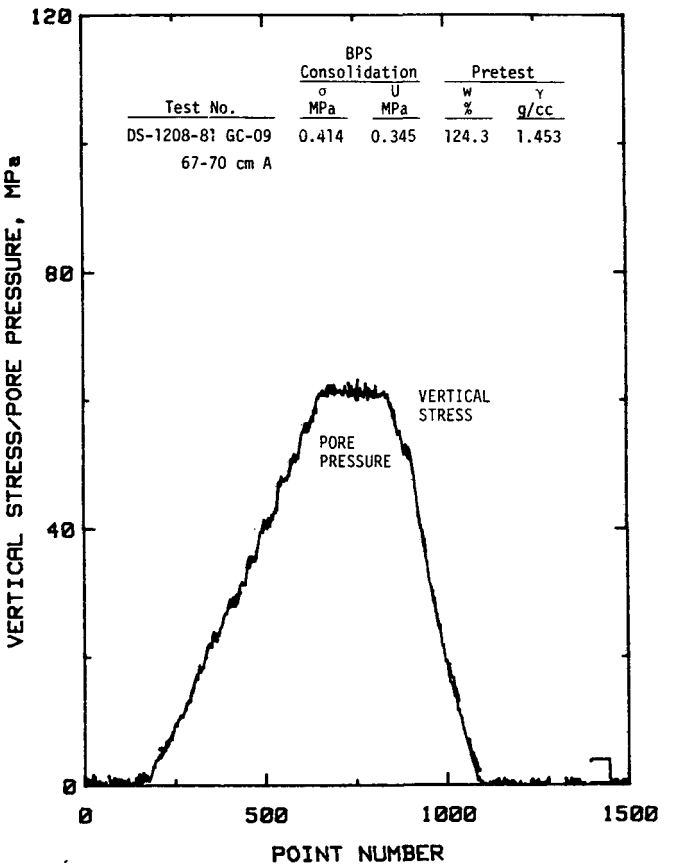


Figure 4.22 BACK PRESSURE SATURATED CONSOLIDATED STATIC UNDRAINED UNIAXIAL STRAIN SPECIMEN DS-1208-81 GC-09 67-70 cm A VERTICAL STR./PORE PR. vs POINT NUMBER

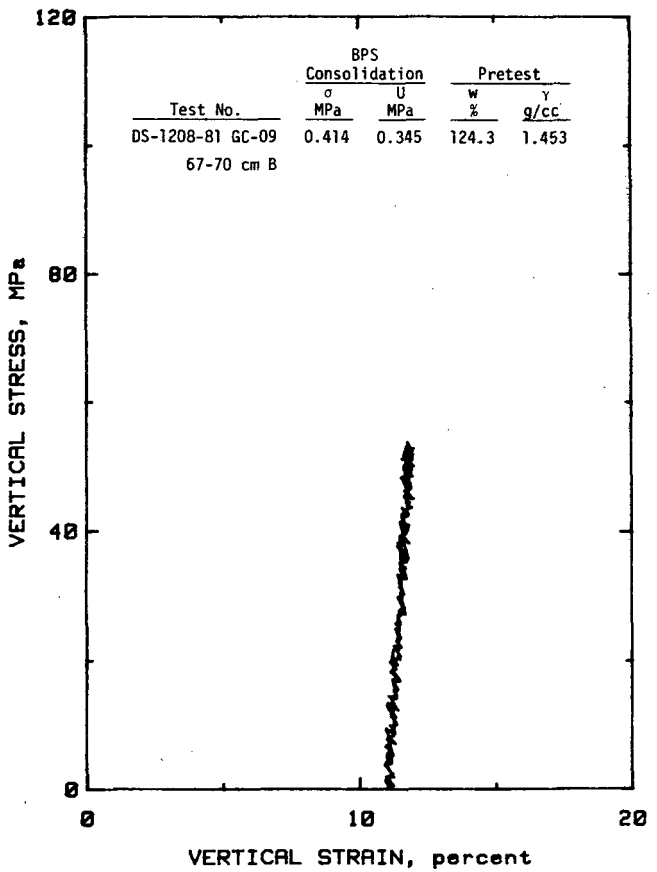


Figure 4.23 BACK PRESSURE SATURATED CONSOLIDATED DYNAMIC UNDRAINED UNIAXIAL STRAIN SPECIMEN DS-1208-81 GC-09 67-70 cm B VERTICAL STRESS vs VERTICAL STRAIN

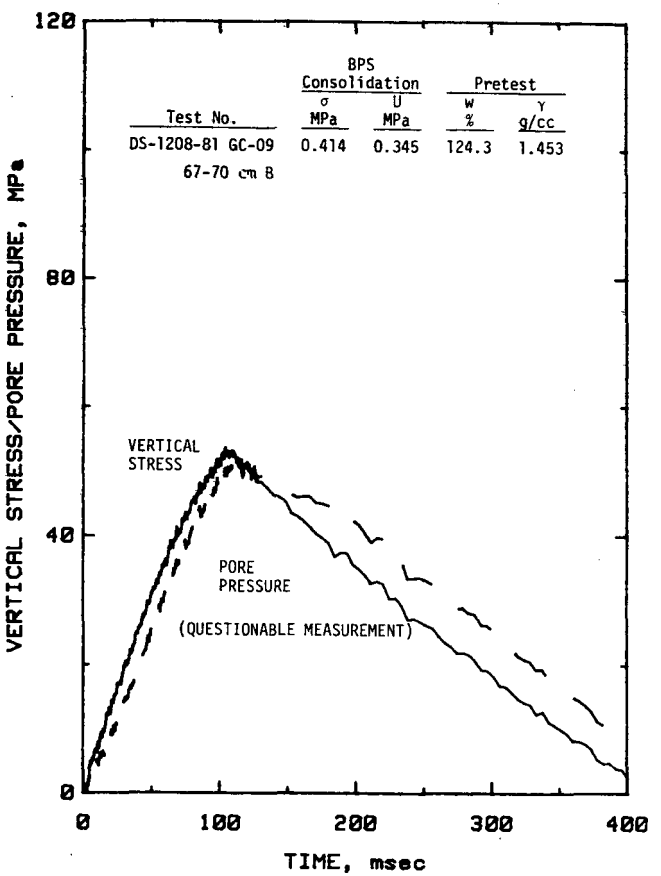


Figure 4.24 BACK PRESSURE SATURATED CONSOLIDATED DYNAMIC UNDRAINED UNIAXIAL STRAIN SPECIMEN DS-1208-81 GC-09 67-70 cm B VERTICAL STR./PORE PR. vs TIME

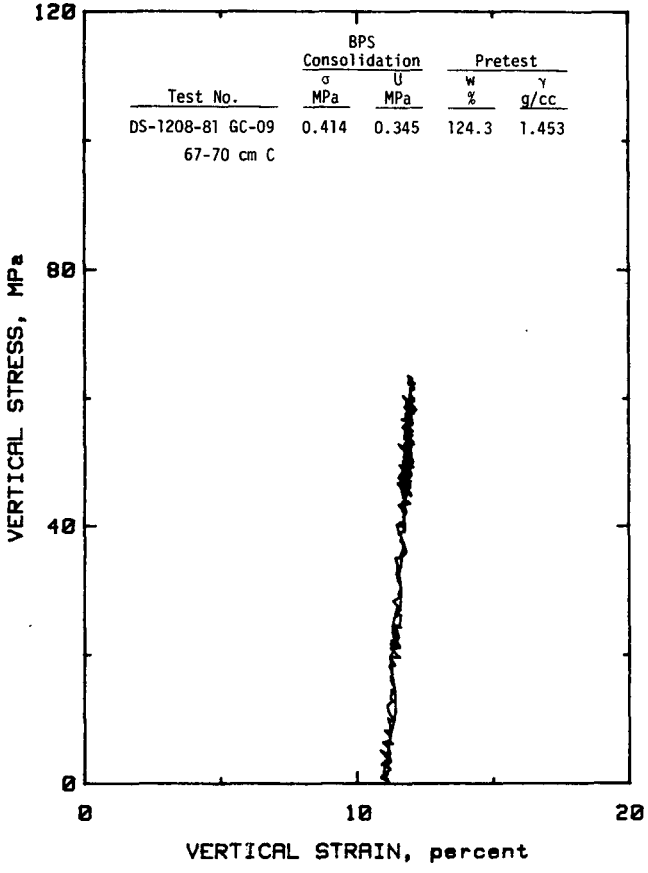


Figure 4.25 BACK PRESSURE SATURATED CONSOLIDATED DYNAMIC UNDRAINED UNIAXIAL STRAIN SPECIMEN DS-1208-81 GC-09 67-70 cm C VERTICAL STRESS vs VERTICAL STRAIN

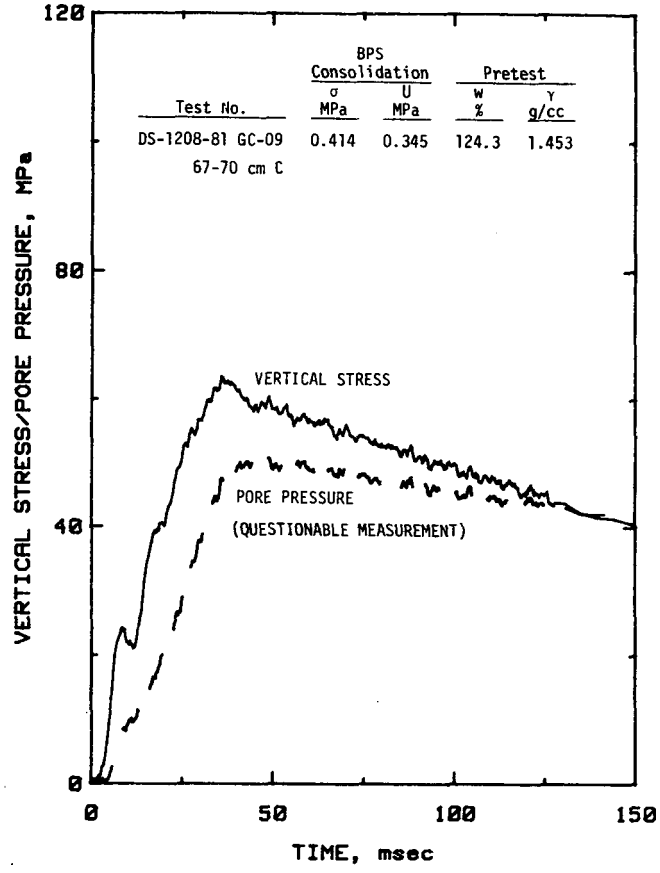


Figure 4.26 BACK PRESSURE SATURATED CONSOLIDATED DYNAMIC UNDRAINED UNIAXIAL STRAIN SPECIMEN DS-1208-81 GC-09 67-70 cm C VERTICAL STR./PORE PR. vs TIME

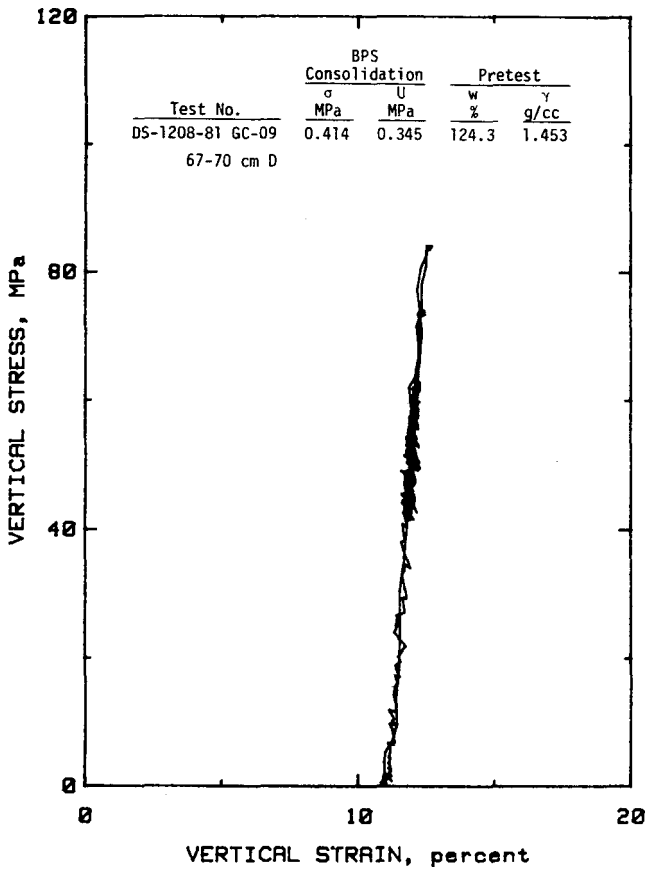


Figure 4.27 BACK PRESSURE SATURATED CONSOLIDATED DYNAMIC UNDRAINED UNIAXIAL STRAIN SPECIMEN DS-1208-81 GC-09 67-70 cm D VERTICAL STRESS vs VERTICAL STRAIN

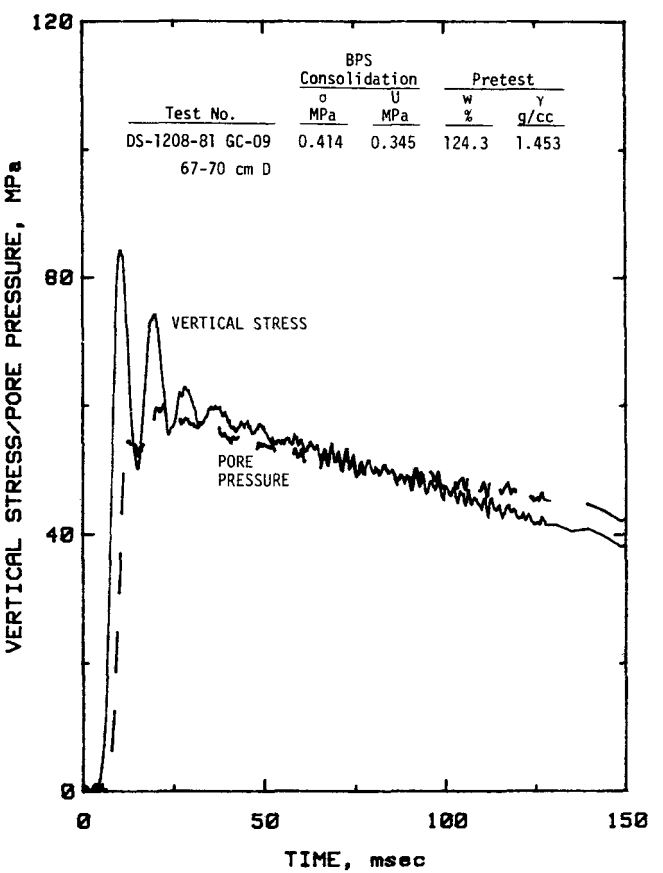


Figure 4.28 BACK PRESSURE SATURATED CONSOLIDATED DYNAMIC UNDRAINED UNIAXIAL STRAIN SPECIMEN DS-1208-81 GC-09 67-70 cm D VERTICAL STR./PORE PR. vs TIME

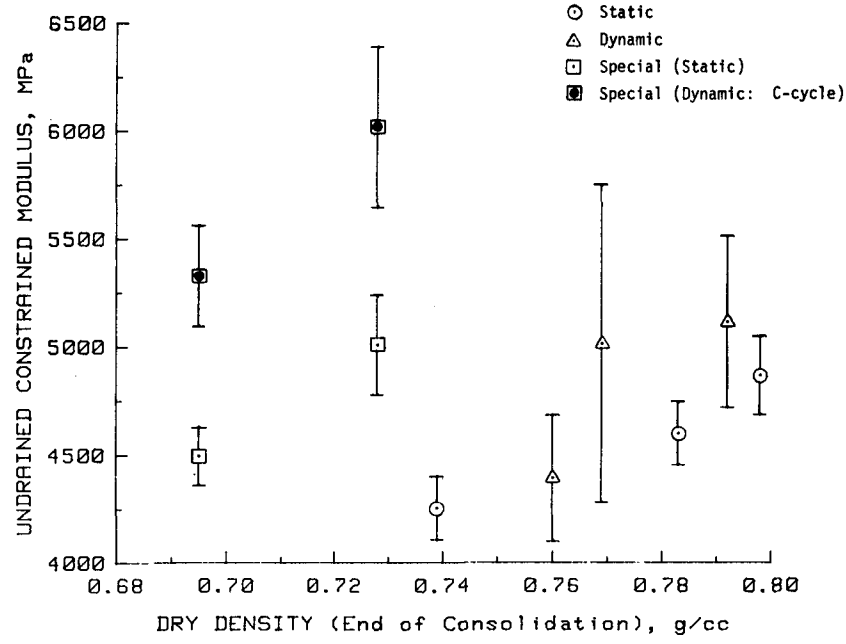


Figure 4.29 Undrained constrained modulus versus dry density relation.

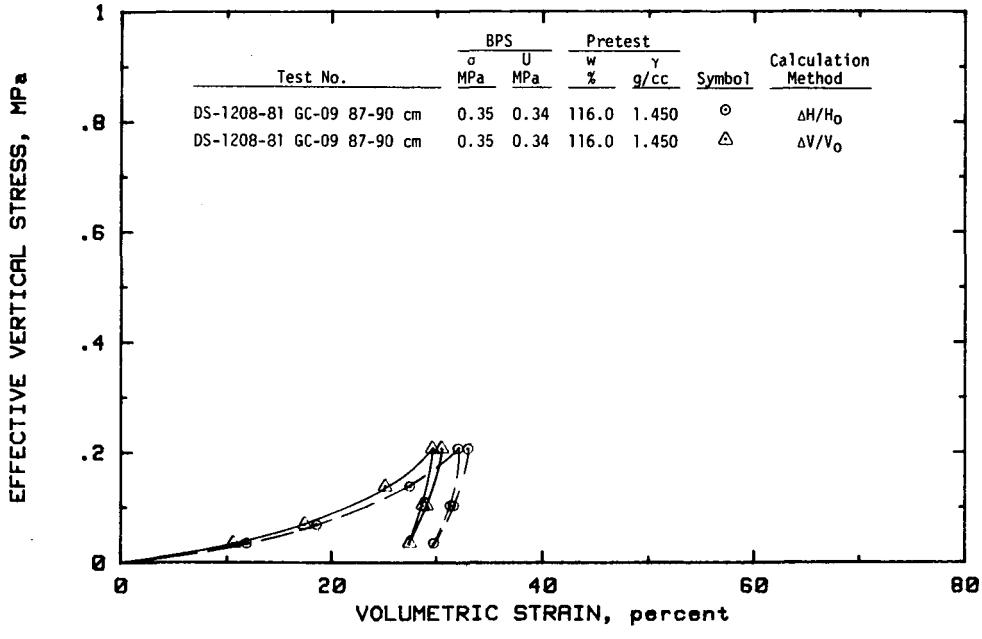


Figure 4.30 BACK PRESSURE SATURATED CONSOLIDATED
STATIC DRAINED UNIAXIAL STRAIN
SPECIMEN DS-1208-81 GC-09 87-90 cm
EFF. VERT. STRESS vs VOLUMETRIC STRAIN

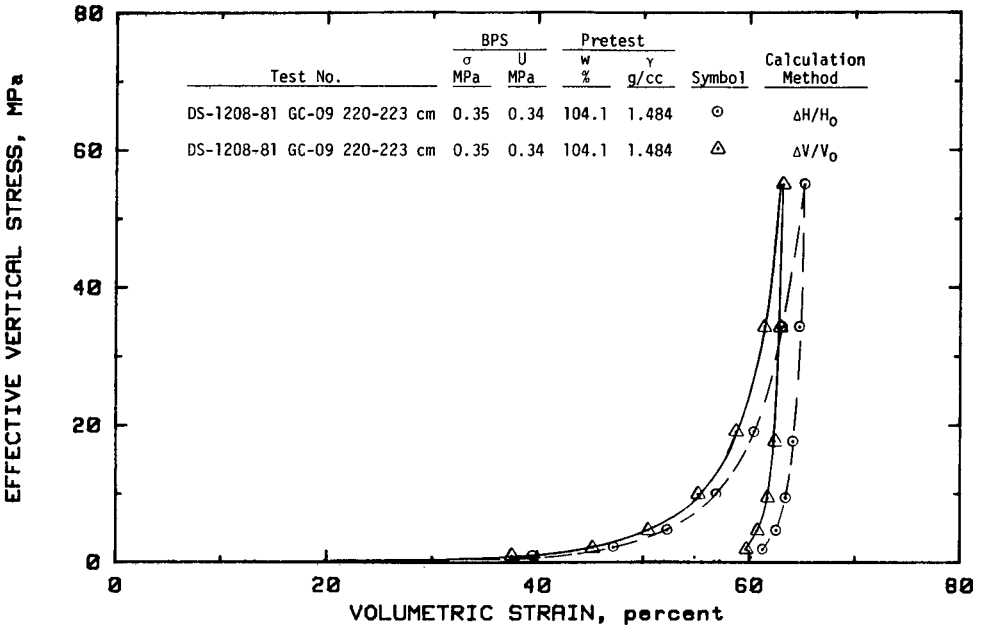


Figure 4.31 BACK PRESSURE SATURATED CONSOLIDATED STATIC DRAINED UNIAXIAL STRAIN SPECIMEN DS-1208-81 GC-09 220-223 cm EFF. VERT. STRESS vs VOLUMETRIC STRAIN

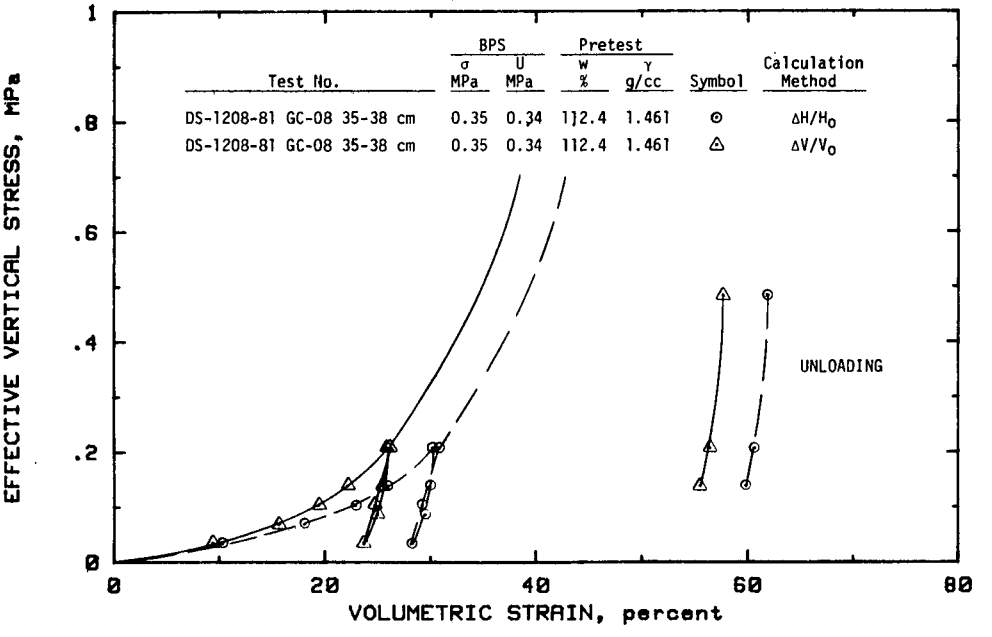


Figure 4.32 BACK PRESSURE SATURATED CONSOLIDATED STATIC DRAINED UNIAXIAL STRAIN SPECIMEN DS-1208-81 GC-08 35-38 cm EFF. VERT. STRESS vs VOLUMETRIC STRAIN

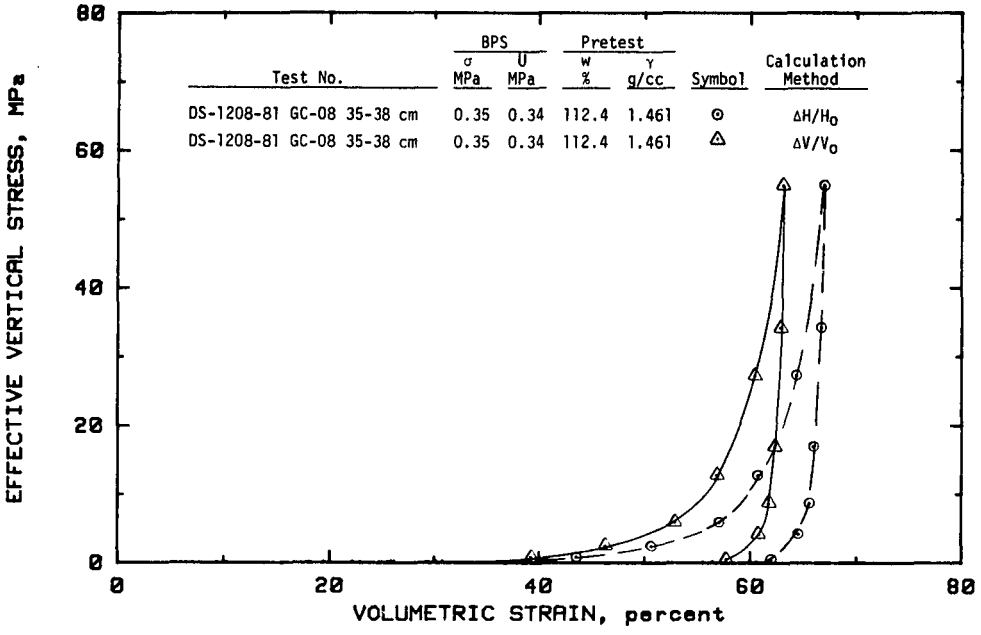


Figure 4.33 BACK PRESSURE SATURATED CONSOLIDATED STATIC DRAINED UNIAXIAL STRAIN SPECIMEN DS-1208-81 GC-08 35-38 cm EFF. VERT. STRESS vs VOLUMETRIC STRAIN

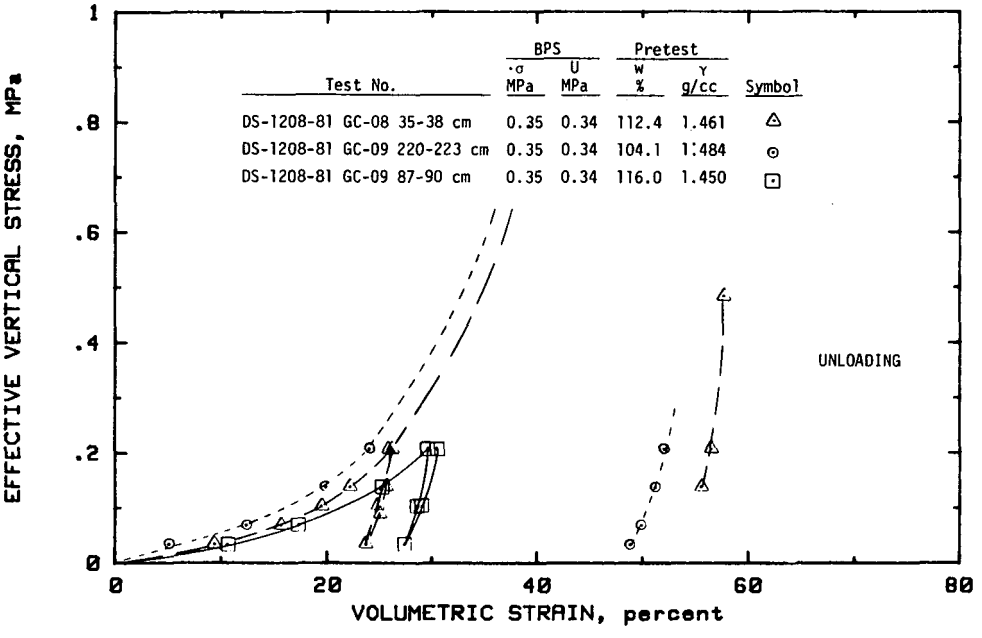


Figure 4.34 BACK PRESSURE SATURATED CONSOLIDATED STATIC DRAINED UNIAXIAL STRAIN SPECIMENS DS-1208-81 GC-08 35-38 cm & GC-09 220-223 cm & GC-09 87-90 cm

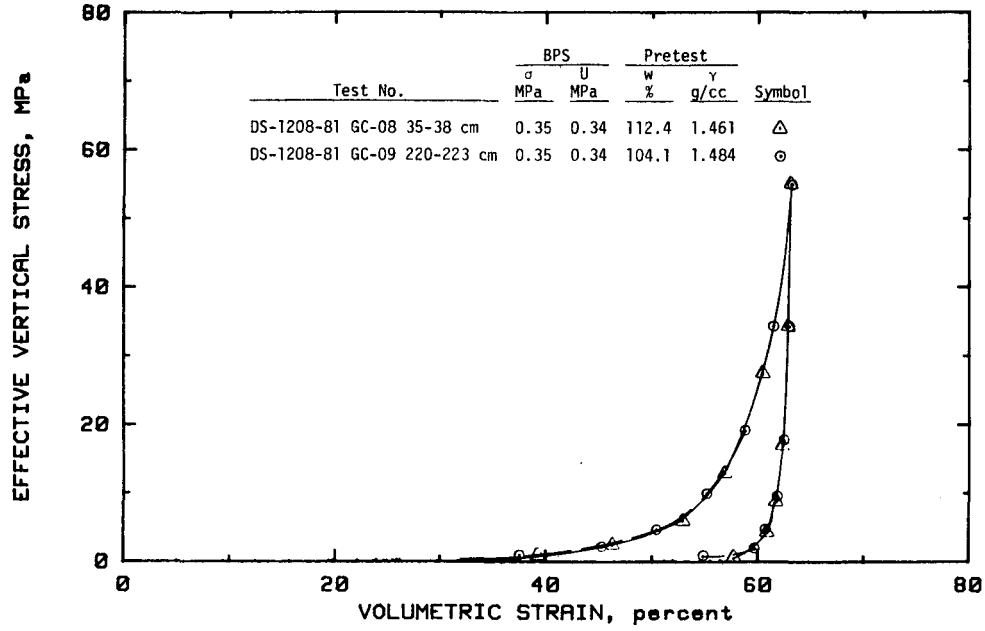


Figure 4.35 BACK PRESSURE SATURATED CONSOLIDATED STATIC DRAINED UNIAXIAL STRAIN SPECIMENS DS-1208-81 GC-08 35-38 cm & GC-09 220-223 cm

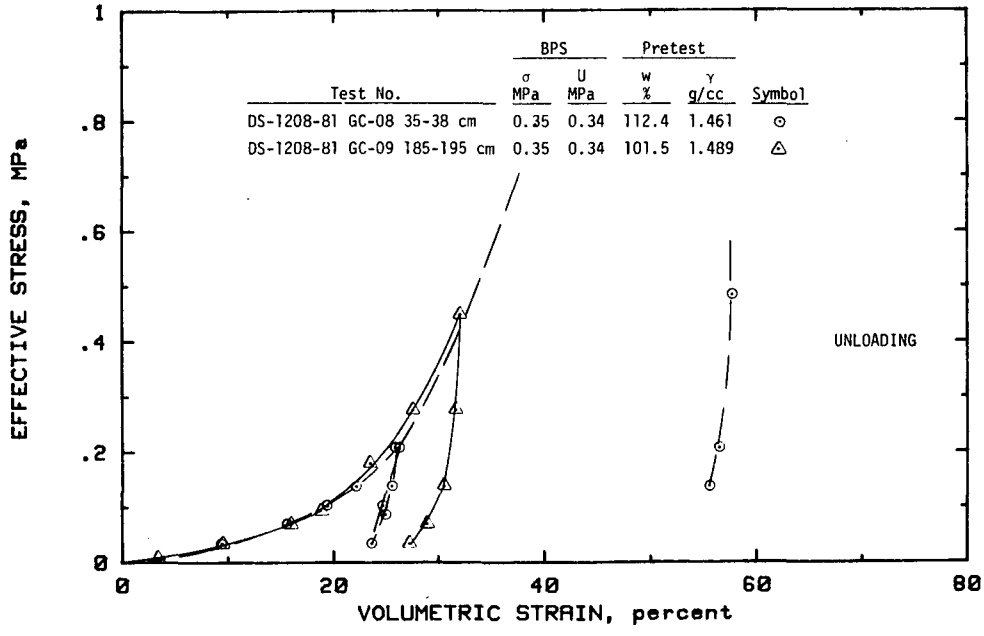


Figure 4.36 BACK PRESSURE SATURATED CONSOLIDATED STATIC DRAINED UNIAX & HYDROSTAT SPECIMENS DS-1208-81 GC-08 35-38 cm & GC-09 185-195 cm

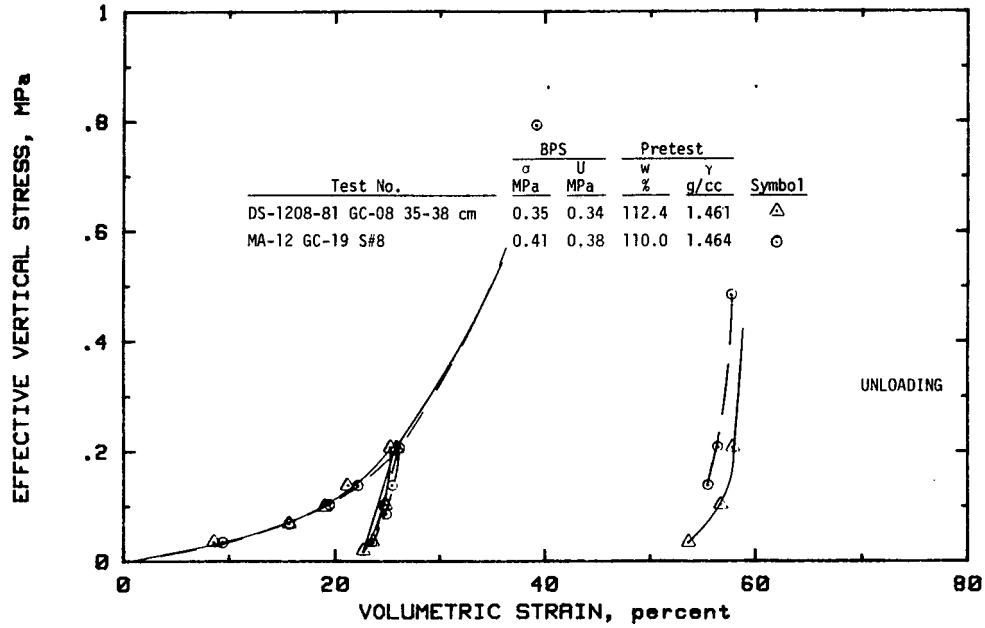


Figure 4.37 BACK PRESSURE SATURATED CONSOLIDATED STATIC DRAINED UNIAXIAL STRAIN SPECIMENS DS-1208-81 GC-08 35-38 cm & MA-12 GC-19 S#8

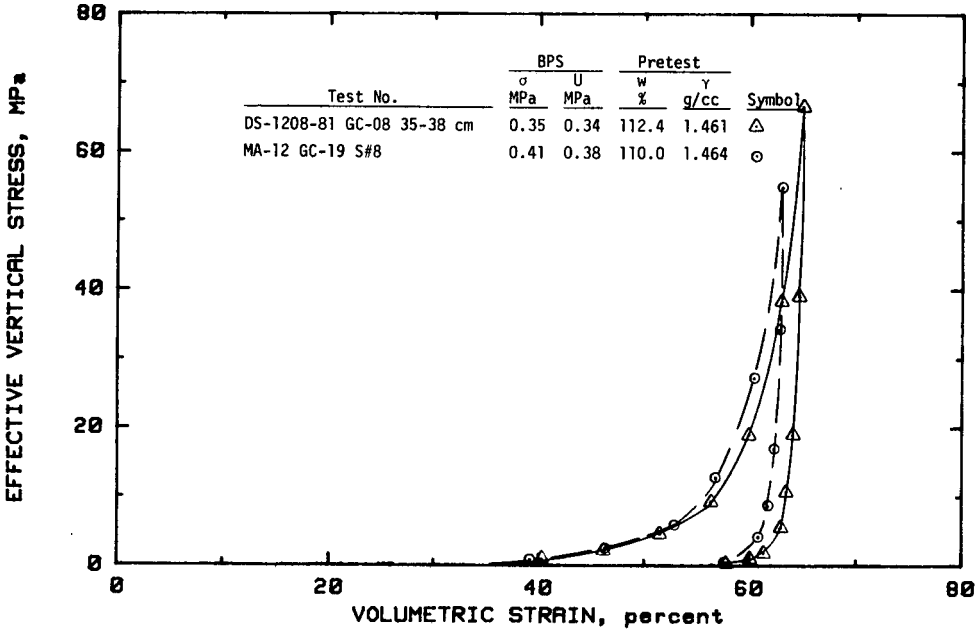


Figure 4.38 BACK PRESSURE SATURATED CONSOLIDATED STATIC DRAINED UNIAXIAL STRAIN SPECIMENS DS-1208-81 GC-08 35-38 cm & MA-12 GC-19 S#8

CHAPTER 5

REPRESENTATIVE MATERIAL PROPERTIES

5.1 REVIEW

The experimental program described in Chapters 3 and 4 resulted in a suite of static and dynamic laboratory material property test data for a consistent set of undisturbed samples of Pacific illite. The ultimate goal of this work was to form a data base from which to select (or develop) representative material properties for use by theoreticians in updating their effective-stress constitutive model (originally fit to remolded Pacific illite data) described in Reference 1.

Recall that in the dynamic laboratory tests conducted for this report, pore pressure measurements were either not attempted (dynamic TX tests, Chapter 3) or were of questionable validity (dynamic UX tests, Chapter 4). Consequently, only the total-stress dynamic behavior of the material was determined in these tests. In contrast, good quality pore pressure data were obtained throughout the static testing program (TX and UX); hence, the total-stress as well as effective-stress behavior of the material was determined from this suite of tests. Comparisons of the total-stress responses of the material under undrained static and dynamic loading conditions (TX and UX) revealed definite quantitative influences of loading rate: (a) the dynamic stress-strain behavior in shear was stiffer and stronger than the static behavior, leading to a nominal factor of two greater undrained strength; and (b) dynamic constrained moduli (from the C-cycles of multiple-loading tests) were stiffer by approximately 20 percent than their static counterparts. Note again that the single-loading dynamic UX tests did not reveal a strong loading rate sensitivity (Chapter 4).

The objective of this chapter is to present the representative static and representative dynamic material properties derived from the new data base.

5.2 COMPOSITION PROPERTIES

Although the actual composition properties of Pacific illite vary somewhat with depth (Chapter 2), an initial set was selected as being "representative" of the range of seabed material tested for this report. These selected properties (which offer a starting point to the modellers) are:

Wet density: 1.460 g/cc

Water content: 111.9%

Dry density: 0.689 g/cc

Specific gravity of solids: 2.70

Volume of air: 0%

Volume of water: 74.5%

Volume of solids: 25.5%

These properties are referenced to a nominal 1-meter depth in MPG-I Pacific illite.

5.3 STATIC DRAINED PROPERTIES

Figures 5.1 and 5.2 present the low-pressure and high-pressure, respectively, drained hydrostatic response of the representative material plotted as effective mean normal stress versus engineering volumetric strain. The low-pressure relation was based primarily on the single hydrostatic compression test discussed in Chapter 3 (Figure 3.32). The high-pressure relation was based on the drained uniaxial strain test results presented in Chapter 4 (Figure 4.35) and the experience gained from conducting the tests reported in Reference 1; viz, high-pressure consolidation data obtained for seabed sediments by means of hydrostatic compression tests or uniaxial strain tests are for all practical purposes indistinguishable from one another.

5.4 STATIC UNDRAINED PROPERTIES

Figure 5.3 depicts the undrained triaxial shear test behavior of the material plotted as principal stress difference versus engineering axial strain for three different effective-stress levels. Figure 5.4 depicts the corresponding plots of pore pressure versus axial strain and Figure 5.5 shows the static effective-stress paths corresponding to Figures 5.3 and 5.4, plotted in terms of principal stress difference versus effective mean normal stress. In all three figures response curves A and B are "smoothed" versions of the actual LPTX test data shown in Figures 3.1 through 3.11. Response curve C was based primarily on the HPTX test data of Figure 3.27, but also on the judgment of the writer in interpreting the LPTX behavior of this material.

The representative static effective-stress failure relation is also shown on Figure 5.5. The static total-stress failure envelopes for specimens consolidated to effective-stress levels of 0.034, 0.069, and 0.093 MPa are shown in Figure 5.6 plotted as principal stress difference versus total mean normal stress.

The representative load-unload, stress-strain relation for consolidated-undrained TX tests is plotted in Figure 5.7 as principal stress difference versus principal strain difference. These curves are both "smoothed" versions of the actual test data and companion curves to those of Figure 5.3.

The recommended UX relationships for static undrained loadings are shown in Figure 5.8. These moduli were developed by first deriving dry density values from Figure 5.1, then fitting an exponential curve to the virgin loaded static test data of Figure 4.29, and finally selecting the representative moduli from the exponential curve at the selected dry densities.

5.5 DYNAMIC UNDRAINED PROPERTIES

Figures 5.9 through 5.11 contain the representative dynamic material properties for undisturbed Pacific illite. Figure 5.9 presents dynamic triaxial shear stress-strain relationships for the material (for a strain rate of 1/sec) plotted as principal stress difference versus axial strain for the three initial effective-stress states. These curves are smoothed versions of the actual undrained test data shown in Figures 3.12 to 3.14.

Figure 5.10 shows the dynamic total-stress failure envelopes for specimens consolidated to effective-stress levels of 0.034, 0.069, and 0.093 MPa. Note that the maximum dynamic stress differences are a factor of two greater than the corresponding maximum static strengths (Figure 5.6).

Figure 5.11 shows the dynamic vertical stress versus vertical strain relationships for undrained UX tests with loading rise times of approximately 36 msec, and consolidated to effective-stress levels of 0.034, 0.069, and 0.093 MPa, respectively. The moduli of these curves were developed by increasing the static moduli of Figure 5.8 by 20 percent. Recall that the undrained constrained modulus increased 20 percent for the A- and C-cycles of the special UX tests.

5.6 COMMENT

We hope that the essentially "massaged" data presented in this chapter will ease the future work of the modellers. However, should they choose to work instead with the individual test results reported in the previous chapters, the information given will assist them in locating the pertinent figures.

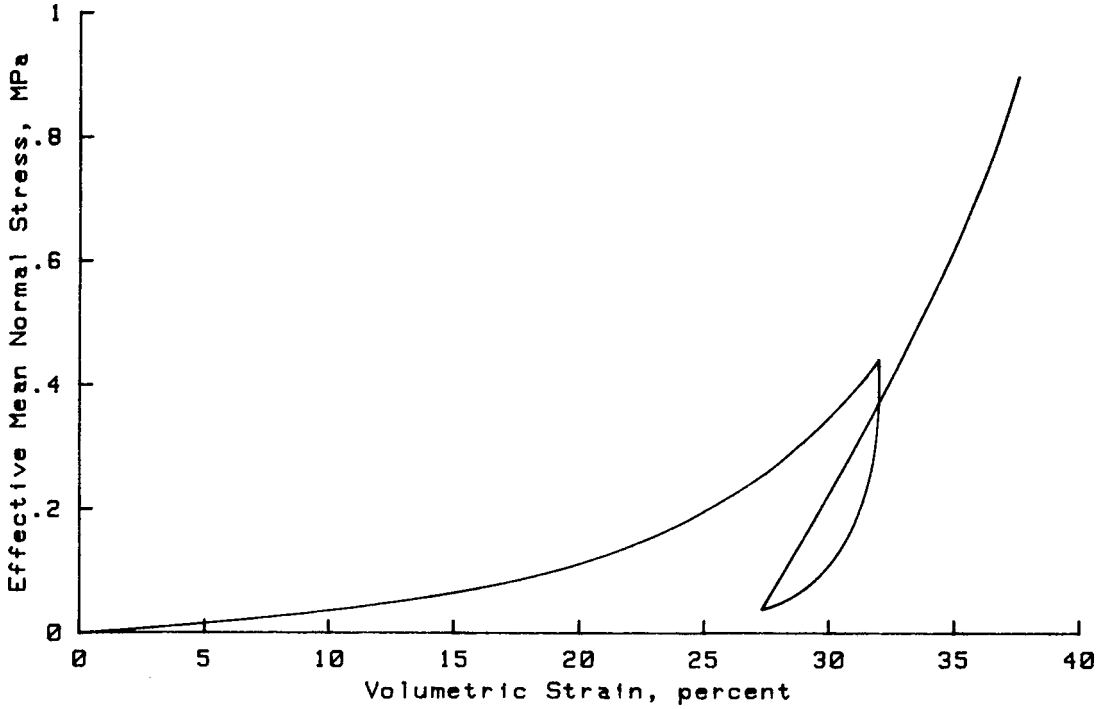


Figure 5.1 Recommended Low-Pressure Hydrostatic Relation for Drained Conditions

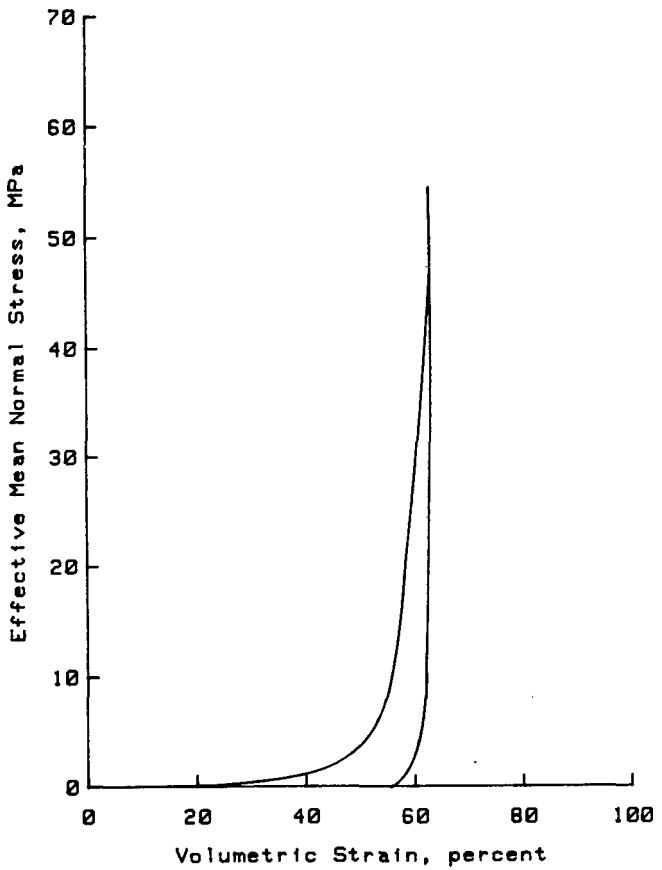


Figure 5.2 Recommended High-Pressure Hydrostatic Relation for Drained Conditions

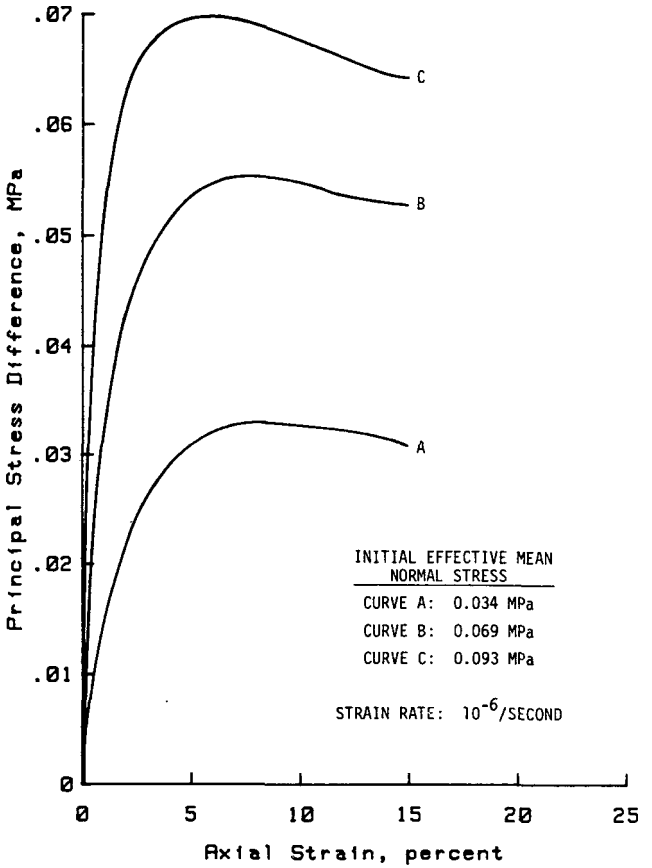


Figure 5.3 Recommended Static Undrained Shear Relationship

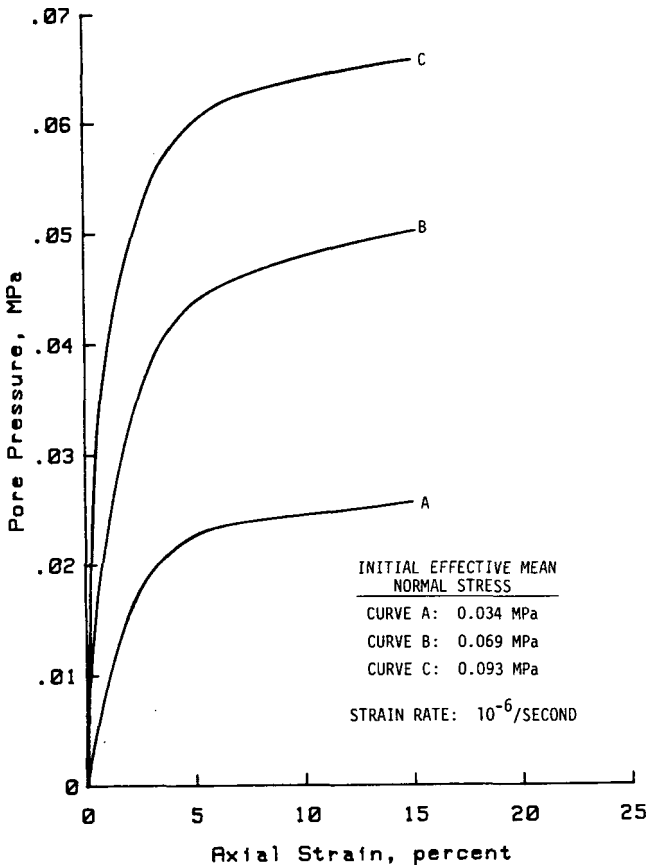


Figure 5.4 Recommended Static Undrained Shear Relationship: Pore Pressure

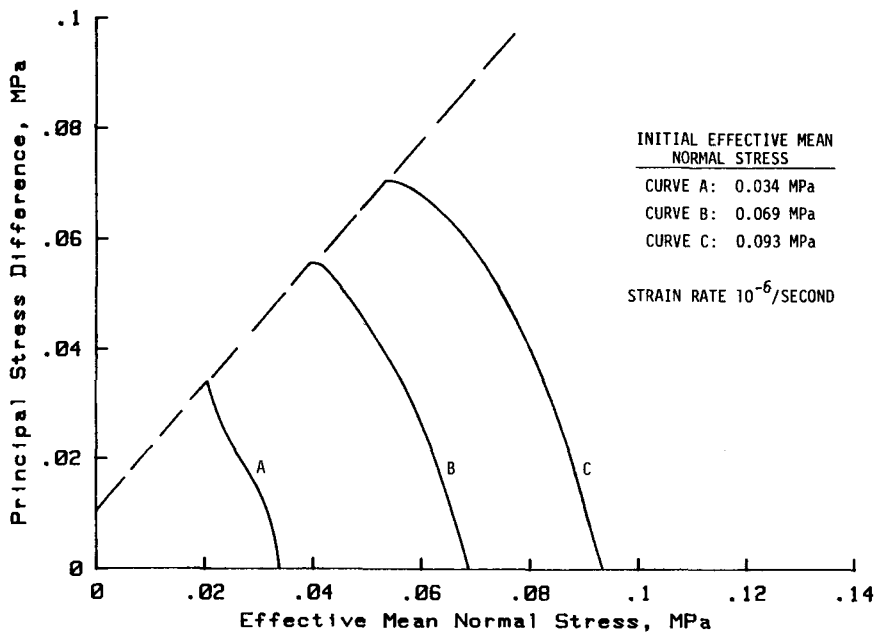


Figure 5.5 Recommended Static Effective Stress Failure Relation and Effective Stress Paths

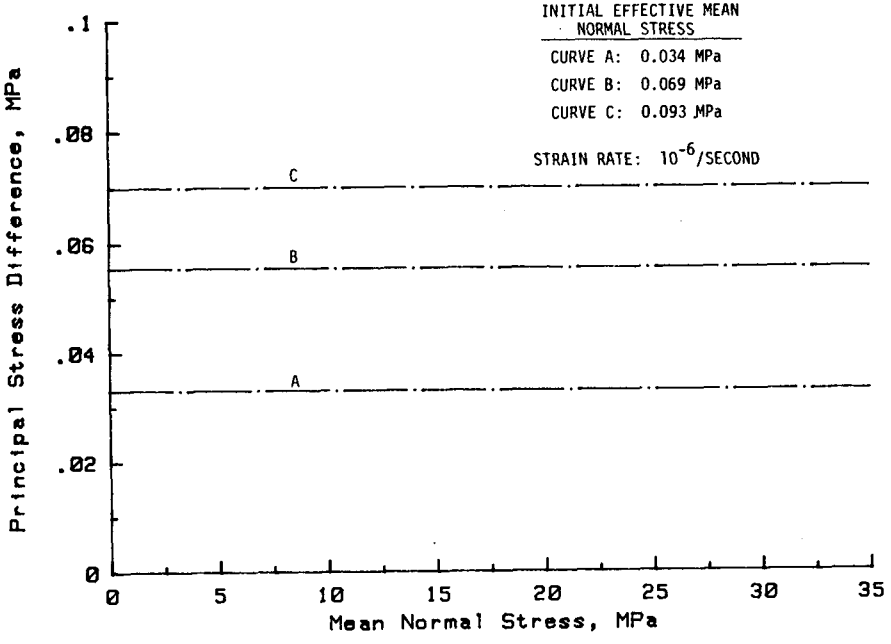


Figure 5.6 Recommended Static Total-Stress Failure Envelope

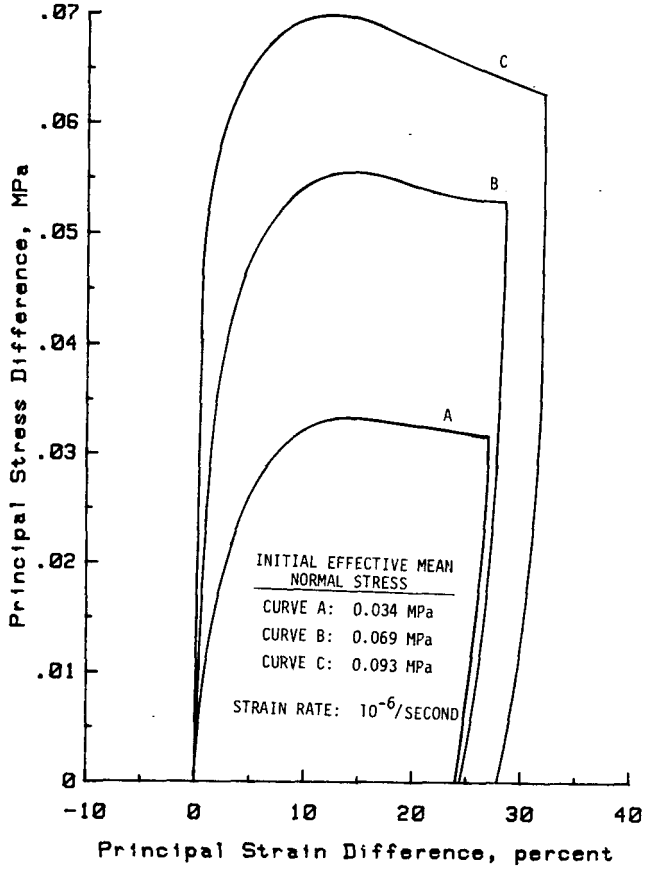


Figure 5.7 Recommended Static Undrained Shear Relation: Stress Diff. vs Strain Diff.

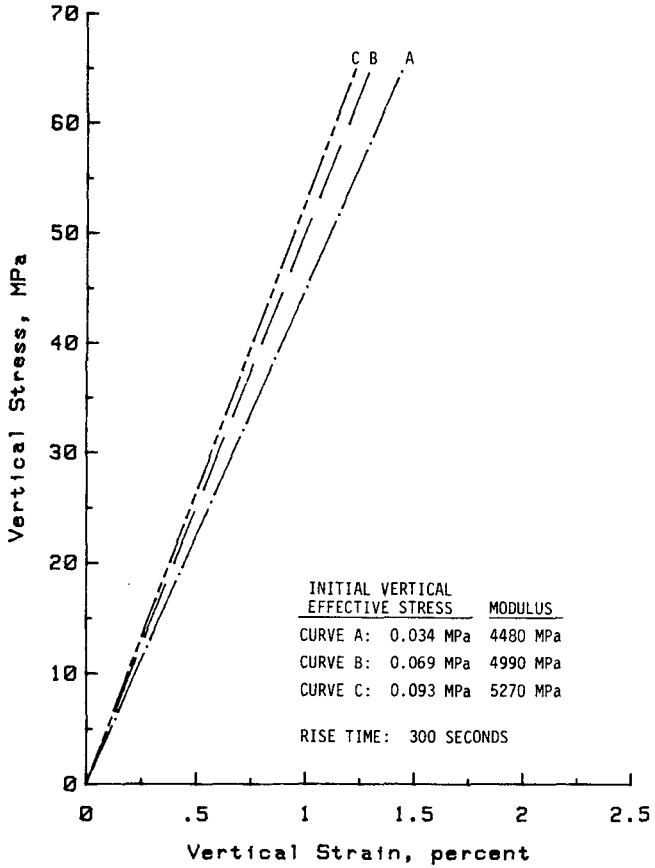


Figure 5.8 Recommended Static Undrained Uniaxial Strain Relation

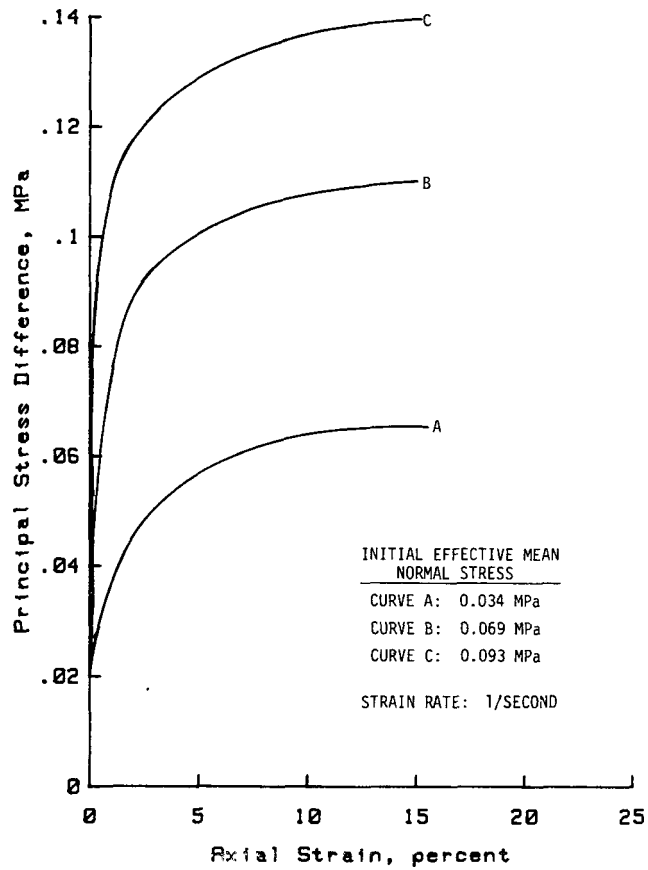


Figure 5.9 Recommended Dynamic Undrained Shear Relationship

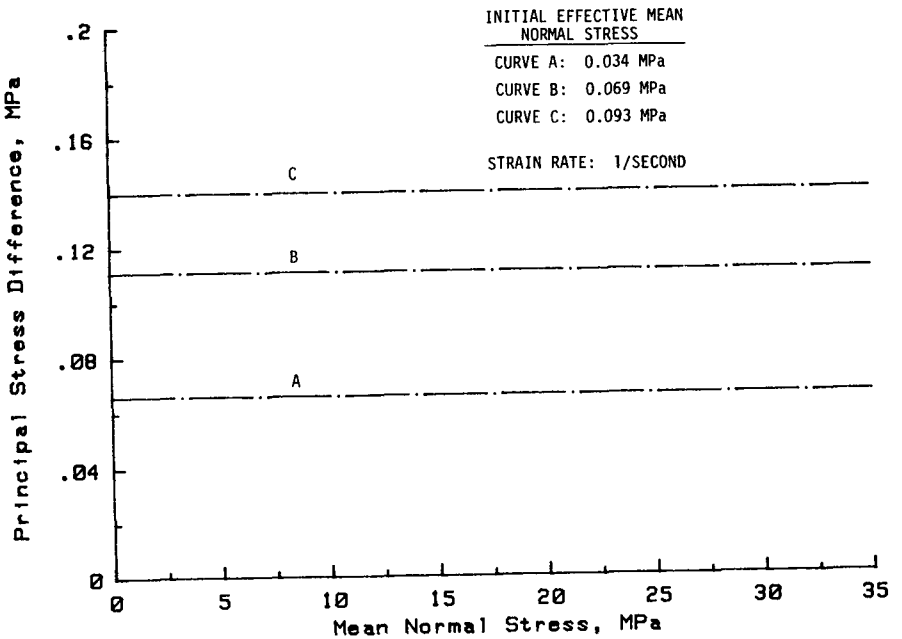


Figure 5.10 Recommended Dynamic Total-Stress Failure Envelope

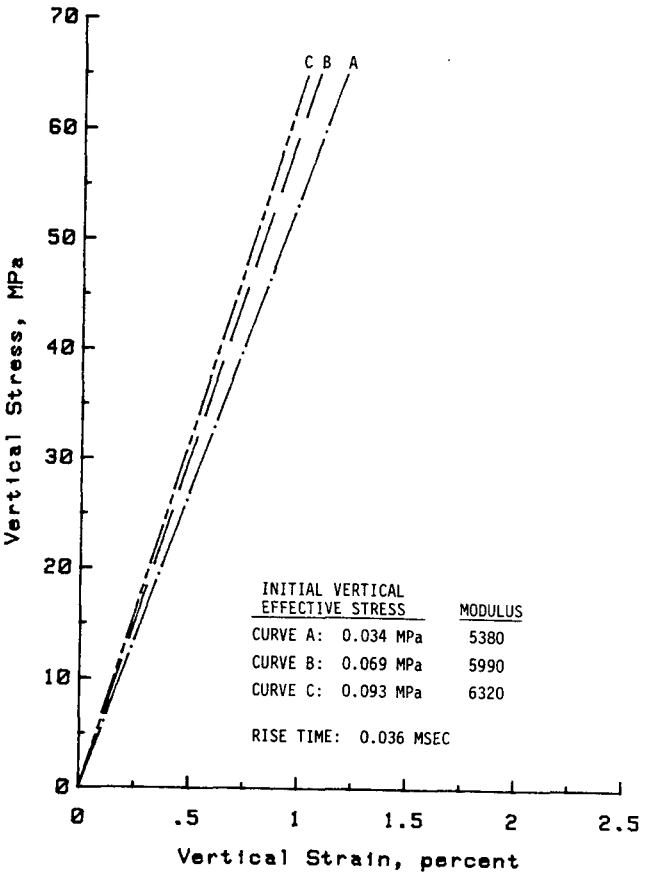


Figure 5.11 Recommended Dynamic Undrained Uniaxial Strain Relation

CHAPTER 6

SUMMARY AND CONCLUSIONS

This report documents the work performed for SNL by WES personnel during 1981. The work consisted of three major activities: (1) the participation by the author in a cruise to MPG-I aboard the USNS De Steiguer to obtain new cores of seabed material, (2) the completion of 38 laboratory material property tests conducted on undisturbed seabed material, and (3) the development of representative static and dynamic laboratory material property data for undisturbed Pacific illite.

During the De Steiguer cruise, 13 undisturbed gravity cores were obtained, 6 of which were shipped to WES. These cores provided sufficient new material to conduct a test program which generated a (heretofore unavailable) consistent set of laboratory test data on undisturbed Pacific illite. The test matrix, using specimens from gravity cores DS-1208-81 GC-08 and GC-09, consisted of 11 consolidated-undrained triaxial shear tests, 1 drained hydrostatic compression test, 19 consolidated-undrained uniaxial strain tests, and 6 hydrostatic creep tests. Representative material properties generated from these undisturbed test data will ultimately be used to revise the current WES effective-stress constitutive model, which was previously fit (in 1980) to laboratory test results primarily obtained from remolded specimens of Pacific illite (Reference 1).

An effective-stress Mohr-Coulomb friction angle and cohesion intercept of 28.6 degrees and 0.004 MPa, respectively, were obtained from two low-pressure static shear tests. These values compare very well with previously published data for undisturbed Pacific illite.

Three high-pressure static shear tests (total stresses up to 35 MPa), conducted at the same effective consolidation stresses as three low-pressure shear tests (total stresses less than 1 MPa), indicated a $\phi = 0$ total-stress failure envelope. This same $\phi = 0$ relationship was obtained in the 1980 experimental program for remolded specimens (Reference 1).

Three low-pressure dynamic shear tests indicated a nominal 200 percent increase in undrained shear strength due to an increase in strain rate from 10^{-6}/second to 1/second. This exceeds previous indications for remolded specimens (67 percent and 145 percent, Reference 1).

Constrained modulus values calculated from undrained virgin loaded static and dynamic uniaxial strain test results showed an expected dependence on effective consolidation stress and no apparent dependence on loading rise time. Dynamic data from multiply-loaded specimens, in contrast, suggested that the undrained constrained modulus increases (nominally 20 percent) with decreasing loading rise time (from 300 seconds to 36 msec). This conflict has not yet been resolved. With respect to hole closure calculations, a 20 percent change in undrained constrained modulus would be insignificant.

Pore pressures measured during undrained uniaxial strain tests (in particular during dynamic tests) were found to be inconsistent with anticipated trends and therefore of questionable validity. We believe the measurements were influenced by the initial specimen/pore-pressure-system setup procedures.

Two uniaxial strain test specimens were successfully consolidated to an effective-stress level of 55 MPa. Both tests exhibited excellent agreement (1) with one another, (2) with lower-pressure test results, and (3) with comparable undisturbed test results obtained in the previous testing program (Reference 1).

The six hydrostatic creep tests conducted were special (add-on) tests requested by SNL for their own use. These tests did not contribute to (or detract from) the main objective of the present WES work. Hence, the creep test results are presented in an addendum.

Based on the new laboratory test data reported herein representative material properties were developed for undisturbed MPG-I Pacific illite. These properties are presented in formats suitable for fitting/revising the WES effective-stress constitutive model described in Reference 1.

REFERENCES

1. Baladi, G. Y. and Akers, S. A.; "Constitutive Properties and Material Model Development for Marine Sediments in Support of the Subseabed Disposal Program"; Annual Progress Report, January to December 1980, to DOE; March 1981; U. S. Army Engineer Waterways Experiment Station, CE, Vicksburg, MS.

2. Akers, S. A. and Silva, A. J.; "Stress-Strain and Strength Properties of Marine Sediments from the North Pacific"; Technical Report, 1980; University of Rhode Island, Kingston, RI.

ADDENDUM A

HYDROSTATIC CREEP TESTS

A.1 GENERAL

As part of the 1981 experimental program, Dr. Joel Lipkin (SNL) asked WES to obtain hydrostatic creep (secondary compression) data from four undisturbed test specimens. Dr. Lipkin's letter is included herein (Plate A.1) to document the work request. In the completed creep test program, six specimens were tested; however, creep data at the designated stress level were only obtained for five of the specimens. One of the specimens leaked after the first effective-stress loading increment. All six specimens were part of the triaxial shear test matrix discussed in Chapter 3; that is, the creep tests were performed at an intermediate stage in the consolidation process of the triaxial shear tests.

A.2 PROCEDURES

All specimens (except the one that leaked) were loaded in one or more increments to an applied effective-stress level of 0.093 MPa (using the procedures outlined in Chapter 3) at which point the creep tests were performed. Upon reaching the 0.093-MPa stress level, volume change measurements were continued for a period of time sufficient to define secondary compression. SNL had requested that two specimens be subjected to identical loading histories so that repeatability could be assessed. In fact, two sets of identical loading histories were applied; i.e., two specimens were consolidated in one increment and two were consolidated in two increments. For intermediate stress increments (those less than 0.093 MPa) the applied effective stress was maintained for a length of time which insured the completion of primary consolidation. All but one of the specimens were obtained from core GC-09.

A.3 TEST RESULTS

The creep test data are presented in tabular form and in figures. Tables A.1 through A.6 document the respective results for each test. For each specimen, the tables list the confining pressure and back pressure for each increment of effective stress, the pretest composition properties, pretest specimen dimensions, posttest water content, volumetric strain during back-pressure saturation, number of stress increments, and the volume-change time histories for each consolidation stress increment up to and including 0.093 MPa. Each time history tabulation includes values of time, incremental volume change, total accumulated volume change, and total volumetric strain.

Table A.7 summarizes the primary consolidation histories of Tables A.1 through A.6 by listing the values of volumetric strain after the completion of each primary consolidation phase. The end of primary consolidation was presumed to occur at t_{100} (the time to 100 percent consolidation as determined from a plot of the volume change versus log of time curve). Figures A.1 through A.12 present plots of volume change

versus log of time and volume change versus square root of time for each stress increment of the six tests.

A.4 COMMENTS

In conducting the creep tests, the idea was to impose and maintain a "constant" effective stress because small changes or fluctuations in this parameter (on the order of 0.7 to 1.4 kPa) can have observable effects on the volumetric strains during secondary compression. Two different techniques were used to control confining pressure and back pressure. Both techniques described herein permit small pressure fluctuations to occur. The better technique involved a 103-kPa differential pressure regulator (used for LPTX tests GC-09 100-110 cm, 125-135 cm, 150-160 cm, and 196-206 cm), which is capable of controlling differential pressures to within an estimated ±0.3 kPa. This differential regulator was not used for HPTX test GC-08 40-50 cm and the drained hydrostat GC-09 185-195 cm. Instead, two independent regulators, each with an estimated accuracy of ±1.7 kPa were used to control the back pressure and confining pressure. Greater confidence should therefore be placed in the creep test results obtained with the differential regulator.

In Table A.7, volumetric strains at the end of primary consolidation exhibit a relatively small amount of scatter for the various initial water contents and wet densities encountered. The mean total volumetric strains at 0.093 MPa, its standard deviation, and the coefficient of variation are 19.98, 1.19, and 5.96 percent, respectively. The 5.96 percent coefficient of variation is considered small. Specimen repeatability is therefore considered very good. Analysis of the secondary compression data is to be performed by SNL individuals who requested the tests.

Sandia National Laboratories
Albuquerque, New Mexico 87185

July 1, 1981

Mr. Stephen A. Akers
Geomechanics Division
Structures Laboratory
US Army Engineer
Waterways Experiment Station
Vicksburg, MS 39180

Dear Steve:

In reference to our telecon of June 29, 1981, I would like to request that your upcoming test series on undisturbed illite be modified somewhat to provide Paul Dawson and myself with additional hydrostatic creep data (i.e. consolidation characteristics). As we discussed, four tests of four different triaxial samples should be adequate for our purposes. In each test the consolidation stress should be applied in increments up to a final value of 93 kPa (13.5 psi). After each load increment is applied, volume change (water expelled) data should be taken over a period of two to three days to insure that the secondary compression region is identified. I will leave the actual choice of increments up to you, but I would request that two of the samples have identical histories so that reproducibility can be investigated. Prior to testing, an accurate water content measurement representative of the specimen material should be made. If possible the data should be reported as volumetric strain (natural measure) vs. time in seconds. However, if this is not convenient we can handle any other measures in our own data reduction scheme.

If you have any questions, please contact me.

Best regards,

Joe

J. Lipkin
Seabed Programs Division 4536

JL:4536:saf

Copy to:
B. Rohani, WES
J. Q. Ehrgott, WES
P. R. Dawson, Cornell
4536 D. R. Anderson
4536 D. M. Talbert
5511 J. W. Nunziato
5531 S. L. Passman
4536 J. Lipkin

PLATE A.1

Table A.1 Secondary Compression DS-1208-81 GC-08 40-50 cm

Confining Pressure = 0.452 MPa Back-Pressure = 0.359 MPa

Specimen Composition Properties:

w, %:	108.4	V_a, %:	0.6
γ, g/cc:	1.462	V_s, %:	26.0
γ_d, g/cc:	0.702	V_w, %:	73.4

Pretest Specimen Dimensions:

Height, cm: 9.65 Diameter, cm: 4.95 Volume, cc: 185.97

Posttest Water Content: w, %: 73.3

Volumetric Strain During Back-Pressure Saturation: 3.86%

Total Number of Stress Increments: 1

Effective Mean Normal Stress: 0.093 MPa

Time min	ΔVolume cm^3	ΔVolume Total cm^3	$\Delta V/V_o$ %
0.0	0.0	7.17	3.86
0.25	0.57	7.74	4.16
0.50	0.94	8.11	4.36
1.0	1.60	8.77	4.72
2.0	2.17	9.34	5.02
3.0	2.64	9.81	5.28
4.0	3.11	10.28	5.53
6.5	3.96	11.13	5.98
9.0	5.20	12.37	6.65
16.0	7.07	14.24	7.66
25.0	8.77	15.94	8.57
36.0	10.47	17.64	9.49
54.0	12.82	19.99	10.75
83.0	15.65	22.82	12.27
117	18.90	26.07	14.02
167	20.37	27.54	14.81
704	26.50	33.67	18.11
913	28.54	35.71	19.20
1195	31.68	38.85	20.89
2708	33.47	40.64	21.85
4195	33.76	40.93	22.01
5376	33.94	41.11	22.11
6468	33.94	41.11	22.11
7200	34.04	41.21	22.16
7948	33.94	41.11	22.11

Table A.2 Secondary Compression DS-1208-81 GC-09 196-206 cm

Confining Pressure = 0.438 MPa Back-Pressure = 0.345 MPa

Specimen Composition Properties:

w, %:	101.9	V_a, %:	6.3
γ, g/cc:	1.396	V_s, %:	25.6
γ_d, g/cc:	0.691	V_w, %:	68.1

Pretest Specimen Dimensions:

Height, cm: 9.65 Diameter, cm: 4.95 Volume, cc: 185.97

Posttest Water Content: w, %: 74.0

Volumetric Strain During Back-Pressure Saturation: 3.24%

Total Number of Stress Increments: 1

Effective Mean Normal Stress: 0.093 MPa

Time min	ΔVolume cm^3	ΔVolume Total cm^3	$\Delta V/V_o$ %
0.0	0.0	6.03	3.24
0.25	0.74	6.77	3.64
0.50	1.07	7.10	3.82
1.0	1.49	7.52	4.04
2.0	2.17	8.20	4.41
3.0	2.71	8.74	4.70
4.0	3.14	9.17	4.93
6.5	4.18	10.21	5.49
9.0	4.95	10.98	5.91
16.0	6.72	12.75	6.86
30.0	9.59	15.62	8.40
48.0	12.10	18.13	9.75
76.0	15.17	21.20	11.40
156	21.32	27.35	14.71
195	23.12	29.15	15.68
274	25.75	31.78	17.09
462	28.74	34.77	18.70
557	29.82	35.85	19.28
1140	31.60	37.63	20.24
1418	31.78	37.81	20.33
1645	31.89	37.92	20.39
2615	32.07	38.10	20.49
3020	32.21	38.24	20.56
4432	32.35	38.38	20.64
6692	32.35	38.38	20.64
7200	32.43	38.46	20.68
9786	32.51	38.54	20.72

Table A.3 Secondary Compression DS-1208-81 GC-09 100-110 cm

Confining Pressure = 0.391 MPa Back-Pressure = 0.345 MPa

Specimen Composition Properties:

w, %: 114.0 V_a, %: 0.0

γ, g/cc: 1.460 V_s, %: 24.9

γ_d, g/cc: 0.682 V_w, %: 75.1

Pretest Specimen Dimensions:

Height, cm: 9.65 Diameter, cm: 4.95 Volume, cc: 185.97

Posttest Water Content: w, %: 82.0

Volumetric Strain During Back-Pressure Saturation: 2.49%

Total Number of Stress Increments: 1

Effective Mean Normal Stress: 0.047 MPa

Time min	ΔVolume cm^3	ΔVolume Total cm^3	$\Delta V/V_o$ %
0.0	0.0	4.63	2.49
0.25	0.57	5.20	2.79
0.50	0.73	5.36	2.88
1.0	1.06	5.69	3.06
2.0	1.51	6.14	3.30
3.0	1.88	6.51	3.50
4.0	2.23	6.86	3.69
6.5	2.94	7.57	4.07
9.0	3.61	8.24	4.43
16.0	5.07	9.70	5.21
27.0	6.81	11.44	6.15
39.0	8.39	13.02	7.00
50.0	9.53	14.16	7.61
81.0	11.94	16.57	8.91
100	13.14	17.77	9.55
130	14.72	19.35	10.41
180	16.51	21.14	11.37
325	18.99	23.62	12.70
1235	21.49	26.12	14.04
1875	22.03	26.66	14.34
2553	22.35	26.98	14.51
3185	22.68	27.31	14.69

Table A.4 Secondary Compression DS-1208-81 GC-09 125-135 cm

Confining Pressure = 0.391 MPa; 0.438 MPa Back-Pressure = 0.345 MPa

Specimen Composition Properties:

w, %:	110.5	V_a, %:	1.2
γ, g/cc:	1.446	V_s, %:	25.4
γ_d, g/cc:	0.687	V_w, %:	73.4

Pretest Specimen Dimensions:

Height, cm: 9.65 Diameter, cm: 4.95 Volume, cc: 185.97

Posttest Water Content: w, %: 78.7

Volumetric Strain During Back-Pressure Saturation: 3.11%

Total Number of Stress Increments: 2

Effective Mean Normal Stress: 0.047 MPa

Time min	ΔVolume cm^3	ΔVolume Total cm^3	$\Delta V/V_o$ %
0.0	0.0	5.78	3.11
0.25	0.43	6.21	3.34
0.50	0.59	6.37	3.43
1.0	0.84	6.62	3.56
2.0	1.25	7.03	3.78
3.0	1.60	7.38	3.97
4.0	1.89	7.68	4.13
6.5	2.55	8.33	4.48
9.0	3.03	8.81	4.74
16.0	4.22	10.00	5.38
25.0	5.43	11.21	6.03
39.0	6.89	12.67	6.81
51.0	7.85	13.63	7.33
87.0	10.18	15.96	8.58
110	11.29	17.07	9.18
240	15.60	21.38	11.50
465	18.09	23.87	12.83
1184	18.92	24.70	13.28

Effective Mean Normal Stress: 0.093 MPa

Time min	ΔVolume cm^3	ΔVolume Total cm^3	$\Delta V/V_o$ %
0.0	0.0	24.70	13.28
0.25	0.12	24.82	13.35
0.50	0.21	24.91	13.39
1.0	0.30	25.00	13.44
2.0	0.49	25.19	13.55
3.0	0.62	25.32	13.61
4.0	0.74	25.44	13.68
6.5	0.98	25.68	13.81
9.0	1.18	25.88	13.92
16.0	1.74	26.44	14.22
27.0	2.32	27.02	14.53
38.0	2.83	27.53	14.80
54.0	3.44	28.14	15.13
82.0	4.34	29.04	15.61
107	4.97	29.67	15.95
170	6.20	30.90	16.62
384	8.54	33.24	17.88
677	9.84	34.54	18.57
1170	10.54	35.24	18.95
1465	10.81	35.51	19.09
2021	10.96	35.66	19.18
2627	11.00	35.70	19.20
4054	11.03	35.73	19.21
5565	11.07	35.77	19.23

Table A.5 Secondary Compression DS-1208-81 GC-09 150-160 cm

Confining Pressure = 0.391 MPa; 0.438 MPa Back-Pressure = 0.345 MPa

Specimen Composition Properties:

w, %:	110.1	V_a, %:	0
γ, g/cc:	1.479	V_s, %:	25.1
γ_d, g/cc:	0.704	V_w, %:	74.9

Pretest Specimen Dimensions:

Height, cm: 9.65 Diameter, cm: 4.95 Volume, cc: 185.97

Posttest Water Content: w, %: 73.9

Volumetric Strain During Back-Pressure Saturation: 3.62%

Total Number of Stress Increments: 2

Effective Mean Normal Stress: 0.047 MPa

Time min	ΔVolume cm^3	ΔVolume Total cm^3	$\Delta V/V_o$ %
0.0	0.0	6.73	3.62
0.25	0.33	7.06	3.80
0.50	0.45	7.18	3.86
1.0	0.66	7.39	3.97
2.0	0.98	7.71	4.15
3.0	1.24	7.97	4.28
4.0	1.53	8.26	4.44
6.5	1.93	8.66	4.66
9.0	2.34	9.07	4.88
16.0	3.24	9.97	5.36
31.0	4.76	11.49	6.18
56.0	6.48	13.21	7.10
92.0	8.31	15.04	8.09
120	9.41	16.14	8.68
205	11.81	18.54	9.97
271	13.04	19.77	10.63
371	14.34	21.07	11.33
708	17.42	24.15	12.99
1472	18.92	25.65	13.79
1908	19.34	26.07	14.02
2897	19.75	26.48	14.24

Effective Mean Normal Stress: 0.093 MPa

Time min	ΔVolume cm^3	ΔVolume Total cm^3	$\Delta V/V_o$ %
0.0	0.0	26.48	14.24
0.25	0.15	26.63	14.32
0.50	0.23	26.71	14.36
1.0	0.30	26.78	14.40
2.0	0.48	26.96	14.49
3.0	0.59	27.07	14.56
4.0	0.68	27.16	14.60
6.5	0.90	27.38	14.72
11.0	1.25	27.73	14.91
17.0	1.57	28.05	15.09
28.0	2.12	28.60	15.38
60.0	3.26	29.74	15.99
84.0	3.90	30.38	16.34
126	4.85	31.33	16.85
276	7.07	33.55	18.04
443	8.46	34.94	18.79
720	9.59	36.07	19.39
1386	10.56	37.04	19.92
1920	10.97	37.45	20.14
2804	11.16	37.64	20.24
3595	11.32	37.80	20.33
4886	11.38	37.86	20.36
7140	11.32	37.80	20.33

Table A.6 Secondary Compression DS-1208-81 GC-09 185-195 cm

Confining Pressure = 0.379 MPa; 0.414 MPa Back-Pressure = 0.345 MPa

Specimen Composition Properties:

w, %:	101.5	V_a, %:	0.2
γ, g/cc:	1.489	V_s, %:	27.4
γ_d, g/cc:	0.739	V_w, %:	72.4

Pretest Specimen Dimensions:

Height, cm: 9.65 Diameter, cm: 4.95 Volume, cc: 185.97

Posttest Water Content: w, %: 63.2

Volumetric Strain During Back-Pressure Saturation: 3.36%

Total Number of Stress Increments: 3

Effective Mean Normal Stress: 0.034 MPa

Time min	ΔVolume cm^3	ΔVolume Total cm^3	$\Delta V/V_o$ %
0.0	0.0	6.26	3.36
0.25	0.16	6.42	3.45
0.50	0.25	6.51	3.50
1.0	0.37	6.63	3.56
2.0	0.62	6.87	3.70
3.0	0.78	7.04	3.78
4.0	0.86	7.12	3.83
9.0	1.38	7.63	4.11
16.0	1.97	8.22	4.42
25.0	2.54	8.80	4.73
36.0	3.14	9.42	5.06
49.0	3.73	9.99	5.37
69.0	4.47	10.73	5.77
141	6.23	12.49	6.72
215	7.36	13.62	7.33
360	8.98	15.24	8.19
840	10.95	17.21	9.25
1404	11.33	17.59	9.46

Effective Mean Normal Stress: 0.069 MPa

Time min	ΔVolume cm^3	ΔVolume Total cm^3	$\Delta V/V_o$ %
0.0	0.0	17.59	9.46
0.25	0.11	17.70	9.52
0.50	0.17	17.76	9.55
1.0	0.25	17.84	9.59
2.0	0.38	17.97	9.66
3.0	0.49	18.08	9.72
4.0	0.58	18.17	9.77
6.5	0.79	18.38	9.88
9.0	0.99	18.58	9.99
18.0	1.51	19.10	10.27
25.0	1.85	19.44	10.46
43.0	2.55	20.14	10.83
78.0	3.58	21.17	11.38
126	4.64	22.23	11.95
268	6.73	24.32	13.08
376	8.35	25.94	13.95
685	9.59	27.18	14.61
2063	11.26	28.85	15.51
3426	11.89	29.48	15.85
4275	12.00	29.59	15.91

(Continued)

Table A.6 (Concluded)

Confining Pressure = 0.438 MPa Back-Pressure = 0.345 MPa

Specimen Composition Properties:

w, %: 101.5 V_a, %: 0.2

γ, g/cc: 1.489 V_s, %: 27.4

γ_d, g/cc: 0.739 V_w, %: 72.4

Pretest Specimen Dimensions:

Height, cm: 9.65 Diameter, cm: 4.95 Volume, cc: 185.97

Posttest Water Content: w, %: 63.2

Volumetric Strain During Back Pressure Saturation: 3.62%

Total Number of Stress Increments: 3

Effective Mean Normal Stress: 0.093 MPa

Time min	ΔVolume cm^3	ΔVolume Total cm^3	$\Delta V/V_o$ %
0.0	0.0	29.59	15.91
0.25	0.06	29.65	15.94
0.50	0.07	29.66	15.95
1.0	0.08	29.67	15.96
2.0	0.14	29.73	15.99
3.0	0.18	29.77	16.01
4.0	0.22	29.81	16.03
6.5	0.30	29.89	16.07
9.0	0.39	29.98	16.12
16.0	0.48	30.07	16.17
24.0	0.62	30.21	16.25
48.0	0.91	30.50	16.40
75.0	1.21	30.80	16.56
109	1.49	31.08	16.71
160	1.86	31.45	16.91
310	2.62	32.21	17.32
570	3.44	33.03	17.76
763	3.80	33.39	17.96
1476	4.49	34.08	18.32
1966	4.94	34.53	18.57
2833	5.07	34.66	18.64
3592	5.38	34.97	18.80
5770	5.67	35.26	18.96
6248	5.52	35.11	18.88
7218	5.35	34.94	18.79
8980	5.41	35.00	18.82
10080	5.31	34.90	18.76

Table A.7 Volumetric Strain (ε_{kk}, Percent) After Completion of Primary Consolidation for Several Stress Increments

Effective Mean Normal Stress MPa	Test Number					
	GC-08 40-50 cm	GC-09 196-206 cm	GC-09 100-110 cm	GC-09 125-135 cm	GC-09 150-160 cm	GC-09 185-195 cm
0.007	3.86	3.24	2.49	3.11	3.62	3.36
0.034	---	---	---	---	---	9.25
0.047	---	---	14.04	13.28	13.79	---
0.069	---	---	---	---	---	15.85
0.093	21.85	20.24	---	18.95	19.92	18.96
Pretest Composition Properties						
w, %	108.4	101.9	114.0	110.5	110.1	101.5
γ, g/cc	1.462	1.396	1.460	1.446	1.479	1.489

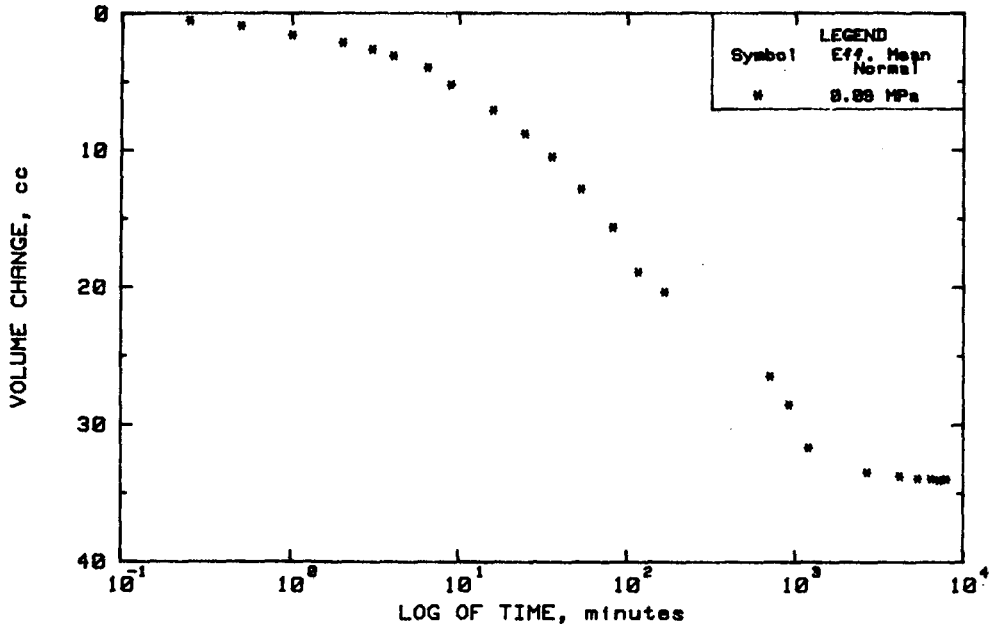


Figure A.1 BACK PRESSURE SATURATED CONSOLIDATED
STATIC DRAINED HYDROSTAT
SPECIMEN DS-1208-81 GC-08 40-50 cm
VOLUME CHANGE vs LOG OF TIME

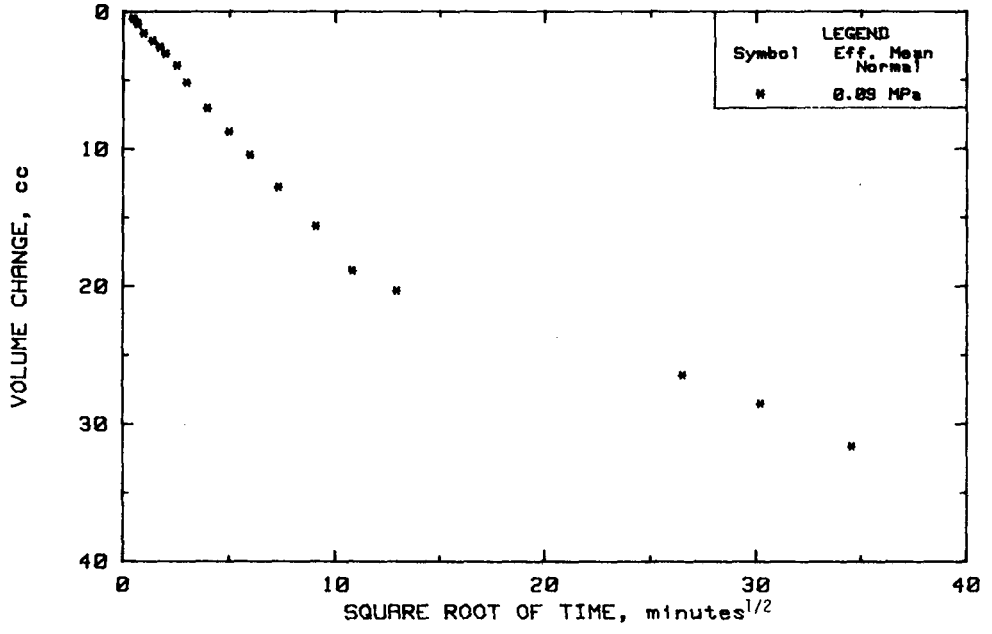


Figure A.2 BACK PRESSURE SATURATED CONSOLIDATED
STATIC DRAINED HYDROSTAT
SPECIMEN DS-1208-81 GC-08 40-50 cm
VOLUME CHANGE vs SQUARE ROOT OF TIME

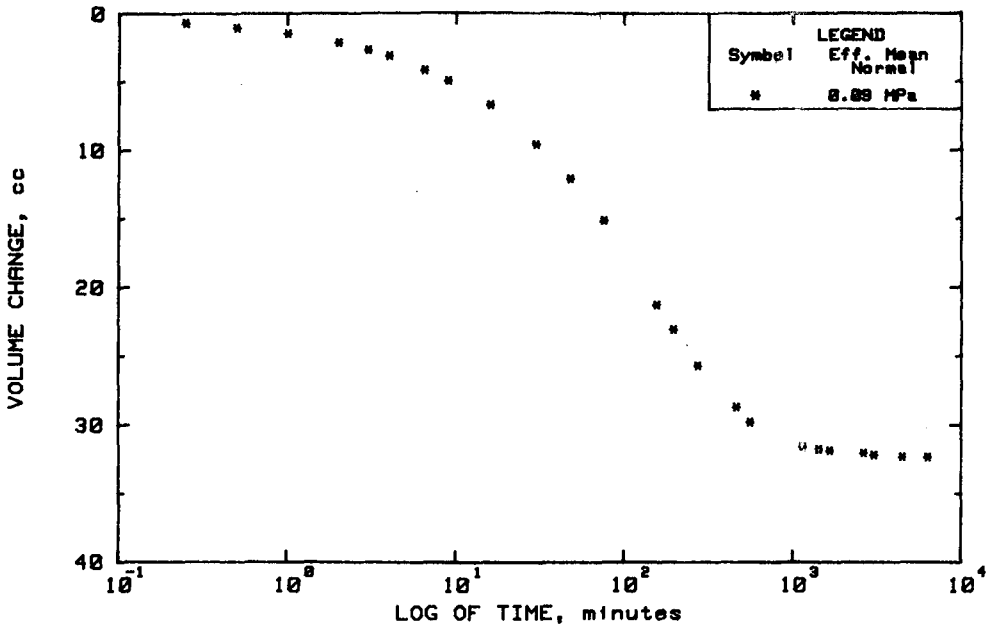


Figure A.3 BACK PRESSURE SATURATED CONSOLIDATED
STATIC DRAINED HYDROSTAT
SPECIMEN DS-1208-81 GC-09 196-206 cm
VOLUME CHANGE vs LOG OF TIME

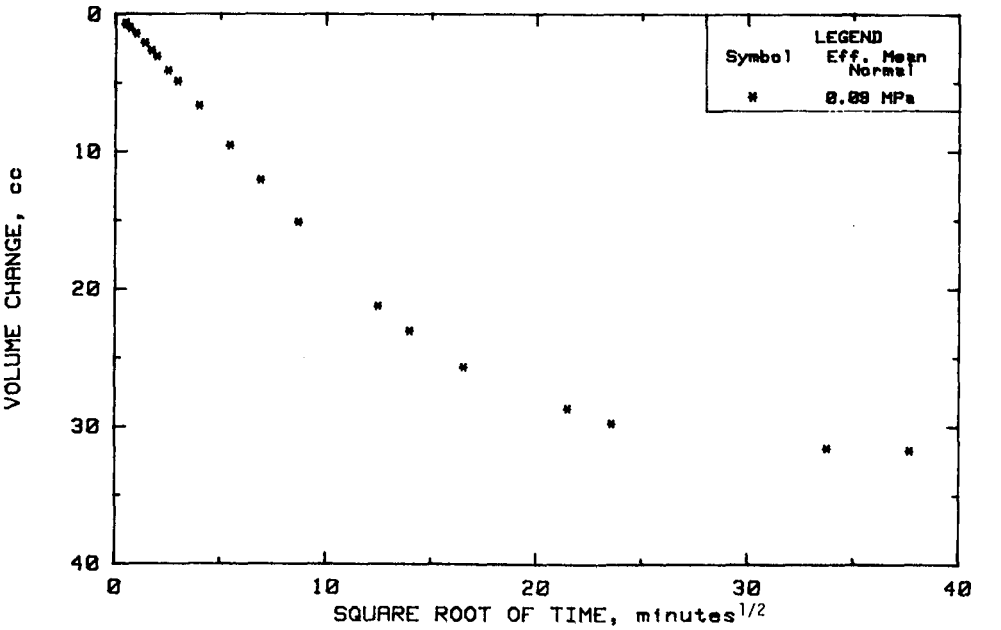


Figure A.4 BACK PRESSURE SATURATED CONSOLIDATED
STATIC DRAINED HYDROSTAT
SPECIMEN DS-1208-81 GC-09 196-206 cm
VOLUME CHANGE vs SQUARE ROOT OF TIME

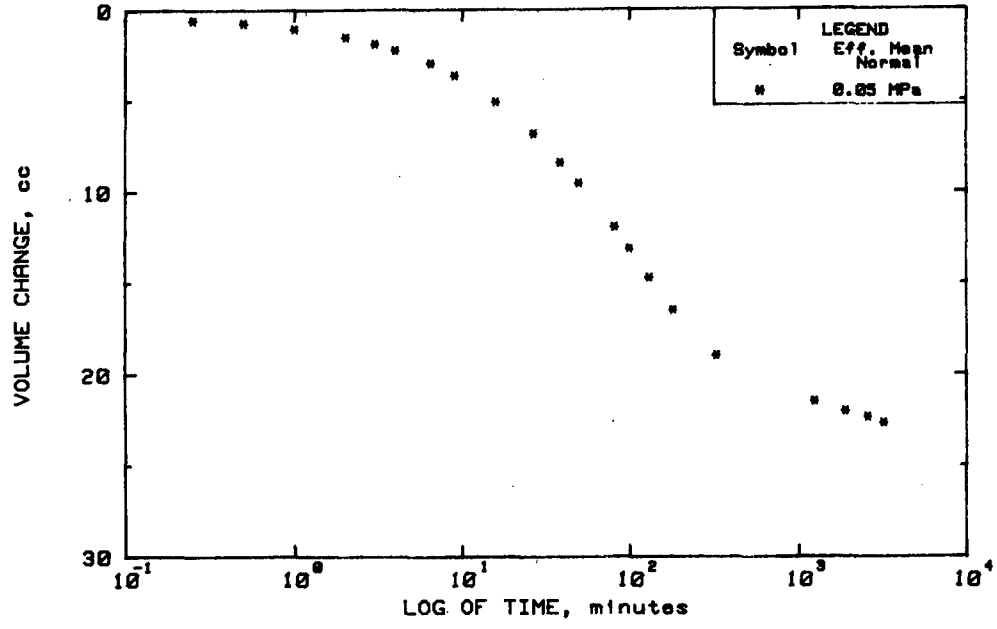


Figure A.5 BACK PRESSURE SATURATED CONSOLIDATED
STATIC DRAINED HYDROSTAT
SPECIMEN DS-1200-81 GC-09 100-110 cm
VOLUME CHANGE vs LOG OF TIME

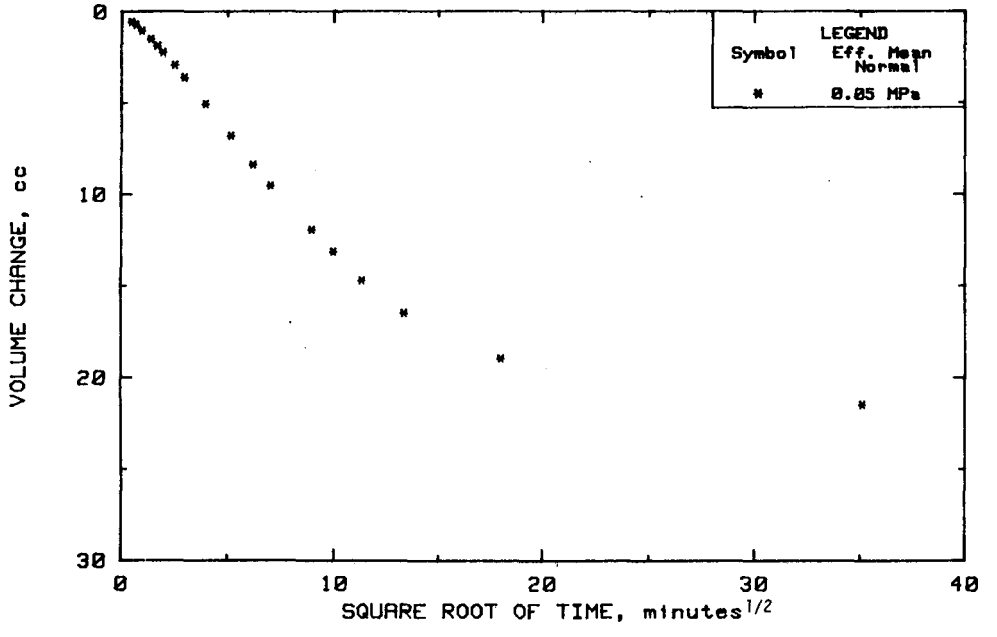


Figure A.6 BACK PRESSURE SATURATED CONSOLIDATED
STATIC DRAINED HYDROSTAT
SPECIMEN DS-1200-81 GC-09 100-110 cm
VOLUME CHANGE vs SQUARE ROOT OF TIME

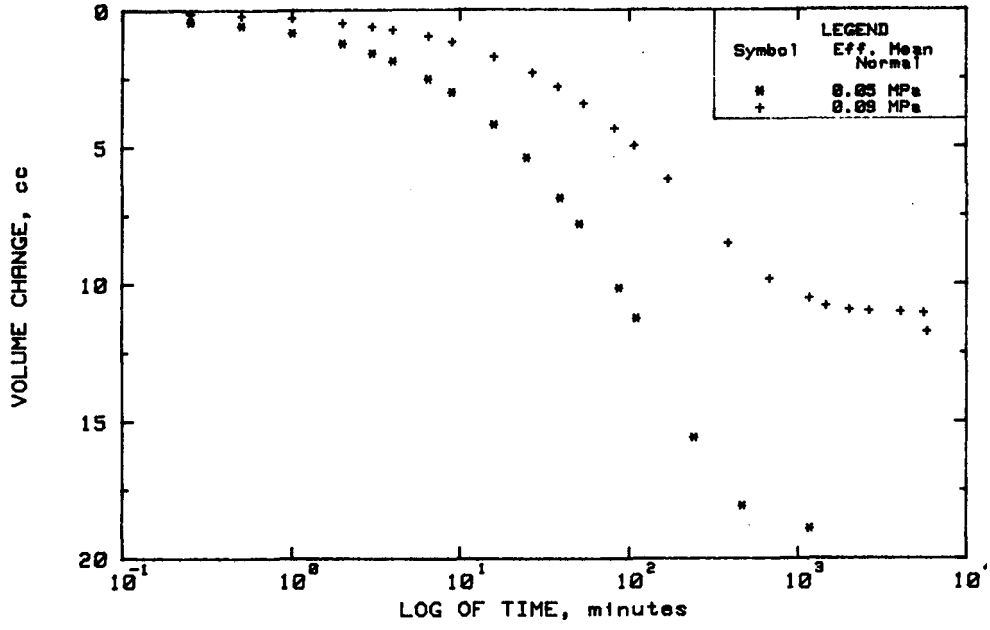


Figure A.7 BACK PRESSURE SATURATED CONSOLIDATED
STATIC DRAINED HYDROSTAT
SPECIMEN DS-1208-81 GC-09 125-135 cm
VOLUME CHANGE vs LOG OF TIME

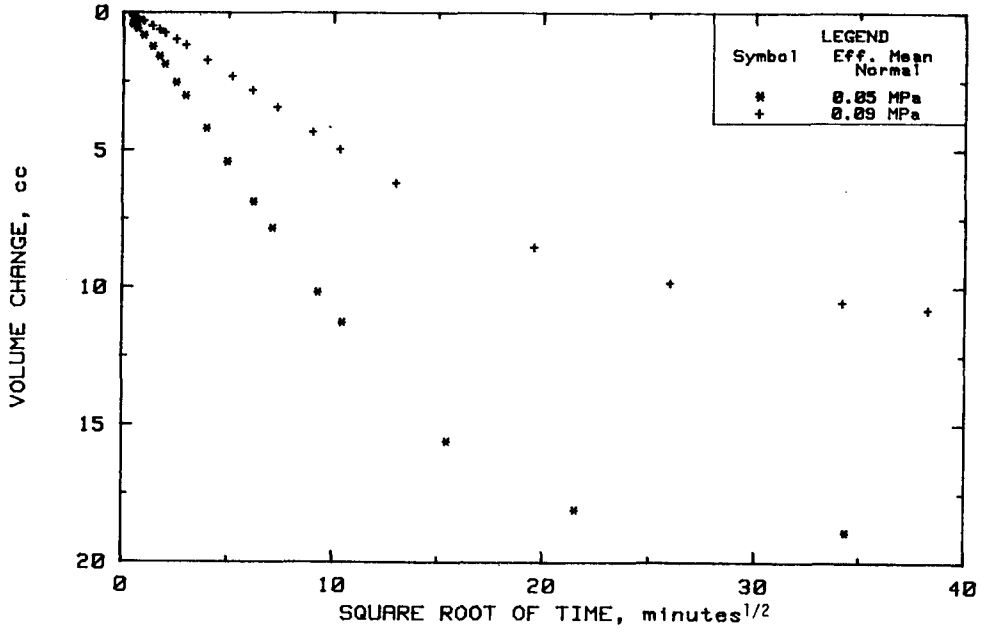


Figure A.8 BACK PRESSURE SATURATED CONSOLIDATED
STATIC DRAINED HYDROSTAT
SPECIMEN DS-1208-81 GC-09 125-135 cm
VOLUME CHANGE vs SQUARE ROOT OF TIME

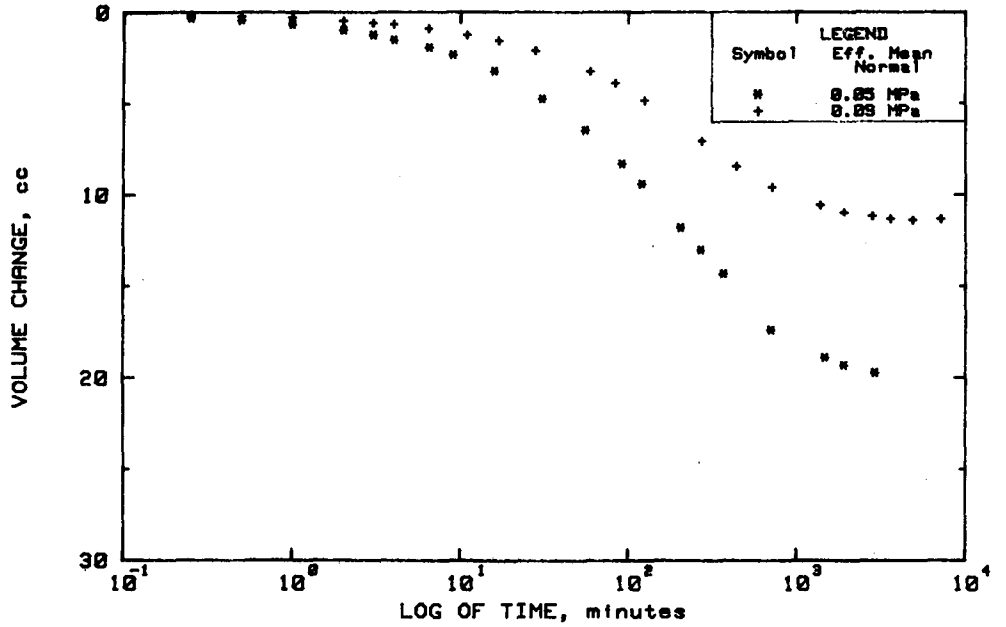


Figure A.9 BACK PRESSURE SATURATED CONSOLIDATED
STATIC DRAINED HYDROSTAT
SPECIMEN DS-1208-81 GC-09 150-160 cm
VOLUME CHANGE vs LOG OF TIME

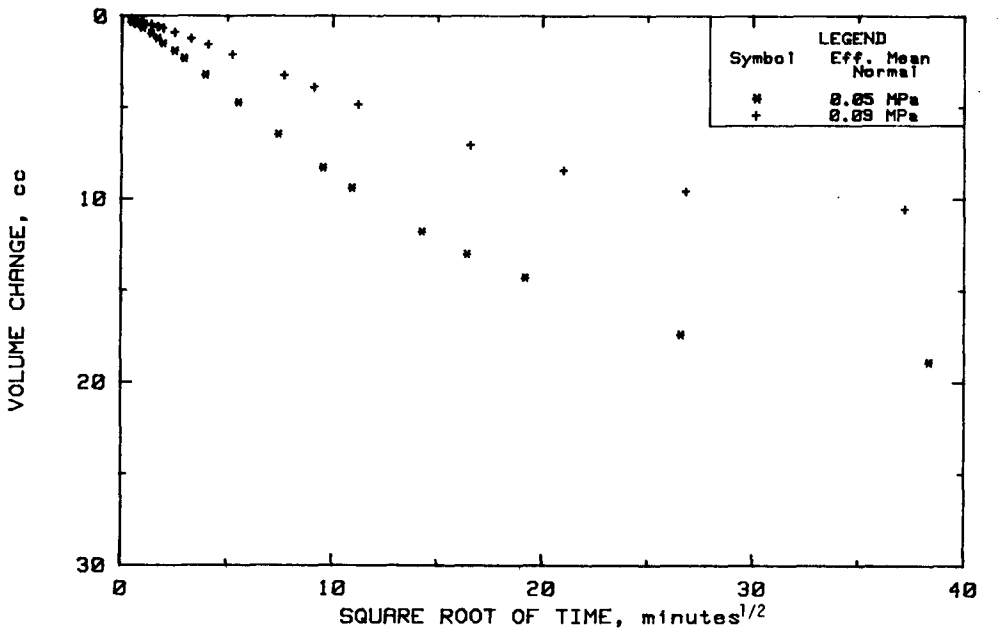


Figure A.10 BACK PRESSURE SATURATED CONSOLIDATED
STATIC DRAINED HYDROSTAT
SPECIMEN DS-1208-81 GC-09 150-160 cm
VOLUME CHANGE vs SQUARE ROOT OF TIME

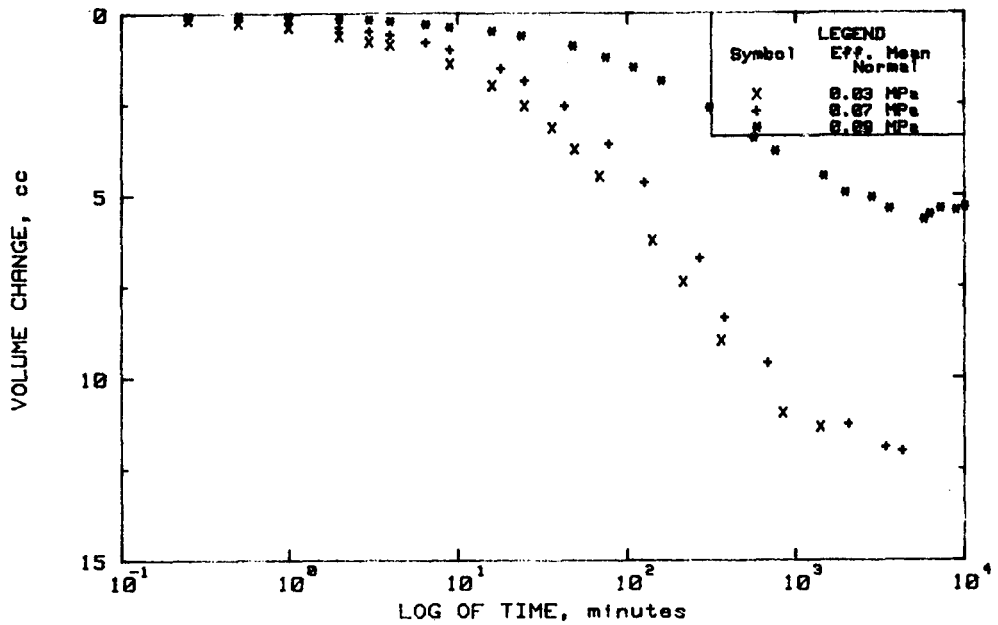


Figure A.11 BACK PRESSURE SATURATED CONSOLIDATED
STATIC DRAINED UNIAXIAL STRAIN
SPECIMEN DS-1208-81 GC-09 185-195 cm
VOLUME CHANGE vs LOG OF TIME

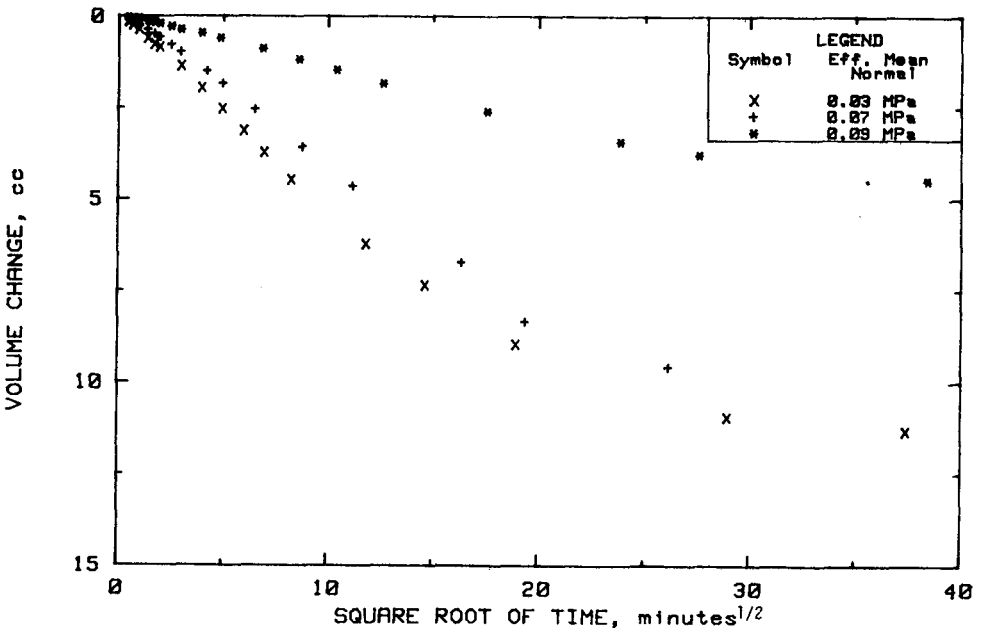


Figure A.12 BACK PRESSURE SATURATED CONSOLIDATED
STATIC DRAINED HYDROSTAT
SPECIMEN DS-1208-81 GC-09 185-195 cm
VOLUME CHANGE vs SQUARE ROOT OF TIME

APPENDIX BB

GEOTECHNICAL STUDIES FOR SUBSEABED DISPOSAL

Armand J. Silva, Stephen A. Jordan, and William P. Levy

University of Rhode Island

(Contract #74-1098)

Progress Report

GEOTECHNICAL STUDIES FOR SUBSEABED DISPOSAL HIGH LEVEL RADIOACTIVE WASTES

for period

January 1, 1981 through September 30, 1981

by

Armand J. Silva

Stephen A. Jordan

William P. Levy

DEPARTMENTS OF OCEAN AND CIVIL ENGINEERING

University of Rhode Island

DOE/SLA Contract No. 74-1098

for

Department of Energy

in cooperation with

Sandia National Laboratories

Albuquerque, New Mexico

December, 1981

ABSTRACT

This is the eighth annual progress report, for calendar year 1981, of the University of Rhode Island geotechnical program which is part of the Subseabed Disposal Program concerned with disposal of high level radioactive wastes. Detailed data and results are presented for several activities.

Sediment characterization results (used for site evaluation) are presented for three areas; MPG-I, MPG-IIIN, and MPG-IV. New results in the N. Central Pacific MPG-I area agree well with previous data which show that this site is feasible, from a geotechnical point of view, for waste disposal. However, the W. Atlantic MPG-IIIN area showed appreciable concentrations of sand size material below 10 meters which may have an adverse affect on dynamic penetration and fluid migration. The W. Pacific MPG-IV results completed on sites B_1, C_1 and E_2 indicate favorable conditions for waste disposal with E_2 as the most desirable.

The triaxial program centered on assessing radiation, high pressure and overconsolidation effects on stress-strain properties and behavior. Results showed that the radiation history on remolded smectite had no significant effect on the properties nor the behavior. High consolidation pressures of 270 and 689 kPa on remolded illite generated a brittle failure when sheared with a slickensided failure surface occurring at 689 kPa. Overconsolidating samples of remolded illite did not produce the classical strain softening behavior after failure and, at an OCR value of 8, the material became dilatant.

A creep program is continuing to study the long term stress-strain-time properties and behavior under both triaxial (at various temperatures) and uniaxial conditions. Variable temperature tests (up to 200°C) have shown the occurrence of instabilities at intermittent times and a change in the creep behavior. At the end of FY 81, a planned one-year creep test at room temperature was still in progress. Results show instabilities at intermittent times with the magnitude of strain rate decreasing after each instability. Results from the uniaxial creep test show behavior similar to that observed under triaxial conditions, however, as compared to standard consolidation results, it appears the effect of long term straining reduces the preconsolidation stress.

Compressibility tests are continuing in the three study areas; MPG-I, MPG-IIIN and MPG-IV. Apparent overconsolidation was recognized (as in previous reports) in the surficial material (upper 3 meters) in all areas. There was also significant overconsolidation in some of the deeper samples in MPG-IV. Some underconsolidation was indicated below 1000 cm in MPG-IIIN. There is need for additional study of stress history and implications to SDP.

Permeability measurements in the MPG-I area agree well with those reported previously. Results from the MPG-IIIN permeability tests show values similar to MPG-I. However, MPG-IV tests reveal permeabilities consistently higher than in MPG-I. High temperatures (up to 220°C) and/or high pressures (up to 60 MPa) do not seem to have any discernible effects on permeability except for predicted effects on physical properties of the constituents.

Simple shear equipment has been assembled and calibrated and preliminary testing is underway.

1.0 INTRODUCTION AND PROGRAM DESCRIPTION (A. Silva)

1.1 Introduction

This is a progress report of the geotechnical program at the University of Rhode Island, Marine Geomechanics Laboratory (URI/MGL) covering the period from January 1, 1981 to September 30, 1981. The work is part of the Subseabed Disposal Program (SDP) sponsored by the Department of Energy (DOE) through Sandia National Laboratories (SNL). The research is a continuing effort since 1974 and therefore this report supplements and extends what was reported previously in SDP annual reports on file at SNL, Albuquerque, N. M. (Dr. D. R. Anderson).

The basic concept of the SDP is that waste canisters will be buried in soft, fine-grained sediments of certain deep sea regimes. It is therefore necessary to know and understand the properties and behavior of the sediments under a variety of conditions. The geotechnical aspects include a) stress-strain-time behavior for short duration (penetration) events, quasi-static behavior and long-term behavior associated with canister-sediment interactions, b) compressibility characteristics associated with the natural sediment column and perturbations to the sediment, c) permeability characteristics and associated water flow due to both natural conditions and the presence of the waste canister, d) changes in all the physical properties and behavior as a result of heat and radiation and e) the use of geotechnical properties as part of site characterization studies and selection of potential disposal locations. The geotechnical information is also part of the modeling work aimed at prediction of sediment response in the context of the SDP.

1.2 Outline of Activities

The primary focus of the program during 1981 continues to be on experimental studies of geotechnical properties and behavior of deep sea sediments in relation to the Subseabed Disposal Program. Following is a brief description of each task along with some comments on how the studies relate to various aspects of the overall program.

Sediment Characterization: This task consists primarily of general geotechnical analyses which are useful to characterize sediments and determine vertical and areal variability of study sites. The results provide sediment data which together with other information, can be used in preliminary evaluations of sites as potential SDP study areas.

Triaxial Compression Studies: (Quasi-static stress-strain behavior): Previous studies have been augmented and some new work initiated. A test series was completed to determine the effects of radiation history on stress-strain behavior and a program is underway to study the effect of high consolidation stresses and stress history on basic parameters.

All these studies are important in overall evaluation of the sediments as an effective barrier.

Creep Studies (long-term stress-strain behavior): Because of the nature of the waste disposal problem it is essential to consider the long-term behavior under a variety of environmental and physical conditions. The URI/MGL role includes a study of stress-strain-time behavior at "room" and variable temperatures with varying stress conditions.

Compressibility Studies: Experimental studies are continuing to determine consolidation characteristics of core samples from the various SDP study sites to help characterize the sediment, determine the stress history of the sediment, determine the stress history of the sediment column, and provide compressibility parameters. The results are used to help evaluate the sites as potential containment media and for geotechnical analyses related to bottom supported structures.

Permeability Studies: Experimental programs are continuing to determine the permeability characteristics of deep sea sediments from SDP study sites. Permeability is a crucial property since the rate of water movement, and hence the effectiveness of the sediment as a barrier, is a direct function of this parameter.

High Pressure, High Temperature Permeability and Conductivity Studies: Since the temperatures in the vicinity of a canister would be quite high and the hydrostatic pressure in the pore fluid is also great, it is important to understand the relationships between permeability as well as thermal conductivity and these two variables. Special laboratory equipment is being used in this program.

Simple Shear Experiments: As part of the program to understand the full range of stress-strain behavior sediments, a special simple shear device has been purchased for use during FY'82. The results will be directly applicable in penetration and hole closure studies.

1.3 Personnel

The following URI/MGL personnel actively participated in the Seabed Disposal Program during FY'81 and contributed to the writing of this report. Graduate Research Assistants (GRA) devote half-time to research and half-time to studies during the academic year and full-time on research during most of the summer months. Research Assistants devote most of their time to research and are generally finishing up their theses. Included are telephone extensions of each individual (401-792-X)

Armand J. Silva, Principal Investigator, 6191, 6194, 2684
Stephen A. Jordan, Research Program Manager, 6200, 6194
William P. Levy, Geotechnical Research Specialist, 6200, 6194
David I. Calnan, Research Associate III (part-time), 2684

Bradford Howe, Research Technician, 6196
Kathryn Dady, GRA (from 9/81), 6148
Kathryn M. Moran, RA, Geotech. Properties (to 6/81)
John Moriarity GRA (from 9/81), 2684
Roger Morin, GRA, 6148
Sasson Salehipour, GRA (from 9/81), 6196
Pamela Sargent, GRA, (to 7/81)

Supporting staff includes Dolores Provost, Prin. Clerk Steno. (part-time), Cynthia M. Thomas, Chief Clerk (part-time) an Cynthia D. Read, Clerk Typist (part-time). Part-time undergraduate technicians also participate on a need basis and URI staff technicians helped in many aspects.

1.4 Publications, Reports and Presentations

Publications

Baldwin, K. C., Celikkol, B. and Silva, A. J., "Marine Sediment Acoustic Measurement System," Ocean Engineering Journal, M. E. McMormick, R. Bhattacharyya, Vol. 8, No. 5, pp. 481-488, 1981.

Silva, A. J., J. R. Hetherman and D. I. Calnan, "Low-Gradient Permeability Testing of Fine-Grained Marine Sediments," Permeability and Groundwater Contaminant Transport ASTM STP 746, T. F. Zimmie and C. O. Riggs, Eds., Am. Soc. of Testing and Materials, pp. 121-136, 1981.

Morin, R. and Silva, A., "The Effects of High Pressure and High Temperature on Some Physical Properties of Ocean Sediments" abstract for AGU Fall meeting, 1981.

Reports, Theses

Moran, K., "Drained Creep of Deep Sea Sediments", M. S. Thesis University of Rhode Island, 1981.

Schwartz, S., "Undrained Stress-Strain Behavior of Anisotropically Consolidated Deep Sea Surficial Sediments", M. S. Thesis University of Rhode Island, 1980.

Walker, G. R., "Geotechnical Properties of Deep Sea Sediments in the Northwestern Pacific Ocean", M. S. Thesis University of Rhode Island, 1981.

Wildman, J. C., "Effect of Temperature on Creep Behavior of Deep Sea Sediments", M. S. Thesis University of Rhode Island, 1981.

Presentation:

Bedford Institute of Oceanography, Dartmouth Nova Scotia; June 1981: Presentation to approximately thirty staff members and area engineers on geotechnical aspects of high level radioactive waste disposal.

2.0 SEDIMENT CHARACTERIZATION (S. Jordan, K. Dadey)

2.1 Introduction

Sediment characterization properties (such as natural water content, Atterberg limits, undrained shear strength, specific gravity and grain size) are primarily used for classifing a type of material. However, these properties can often be qualitatively correlated to other properties and used as indicators of the type of behavior that can be expected under a variety of conditions (such as compression and stress-strain behavior).

Results from tests on sediments within the MPG-1, North Central Pacific (MARA-02, MARA-12 and RAMA-01 cruises), MPG-III- N, Atlantic Abyssal Plain (HUDSON-80016 cruise) and MPG-IV, Northwestern Pacific (VEMA-36 cruise) are reported here. In addition, some data from previous annual reports are repeated for purposes of obtaining averages and identifying trends. All data from the RAMA and HUDSON cruises are being reported for the first time. A table (Table 2.1-1) is included which lists all cruises, cores and core locations from which samples were taken and tested.

2.2 Test Methods

Laboratory classification tests are conducted according to ASTM specifications. Atterberg limits were determined by approved standard procedures for liquid (ASTM D 423-66) and plastic (ASTM D 424-59) limits. Specific gravity measurements were performed by standard procedure ASTM D 854-58. Grain size was determined using the pipette procedure for fine grained soils (ASTM D 422-63). All water contents were salt corrected for 35 ppt salt content.

2.3 Results

2.3.1 MPG-I

Table 2.3-1 is a listing of grain size (percent sand, silt and clay) and Atterberg limit (liquid and plastic) results for the MARA-02 cruise. Grain size determinations clearly show that the sediment is fine-grained with an averaged percent clay (<.002mm) at 68.4 percent. Sand sized particles (<.062mm) show insignificant percentages.

The liquid limit (ω_L) which is the bound between plastic state and viscous flow show values ranging between 74 and 190 percent with most falling below 100. These values generally vary directly with clay percentages, however, the type of clay mineral also has a significant affect. The sample with a liquid limit of 190 percent (MARA-02, GC-08, 206-218 cm) probably has appreciable concentrations of smectite

mineral. The lower bound of plastic state or plastic limit (ω_p) show values ranging between 32 and 71 percent with most around 40. These values show variability in the same way as the liquid limit. Values of plasticity index (I_p) and activity (A) listed in this table will be discussed in section 2.4.

Specific gravity (G_s) and buoyant unit weight (γ_b) determinations for MARA-02 are presented in Table 2.3-2. Specific gravity results show some variability (2.49-3.02) with the higher values (>3.00) accountable by concentrations of heavy metals; such as Mn, Fe and Ni (Leinen and Heath, 1980). Ship-board and laboratory natural water content results are used with specific gravity to find buoyant unit weight. The range of γ_b (403-507 kg/m^3) is relatively small which indicates an overall consistency within MPG-I; this being a reflection of homogeneity previously recognized and discussed in prece ding annual reports.

Tables 2.3-3 and 2.3-4 show results of Atterberg limits and specific gravity, respectively, for the MARA-12 cruise samples. The range of values (79-109 % for ω_L, 28-46 % for ω_p and 2.61-2.99 for G_s) is somewhat less than the MARA-02 results, however, the number of tests is also less. It should be noted that the trends previously discussed for MARA-02 hold true for MARA-12 sediments.

Tables 2.3-5 and 2.3-6 contain Atterberg limit and specific gravity results of RAMA-01 cruise sediment. The greatest significance of these determinations is that many surficial samples (especially above 50 cm) were tested. The ranges of liquid limit (71-102%) and plastic limit (24-48 %), Table 2.3-5, are not significantly different than those reported for MARA-02 and 12, however, the water contents of superficial sediments tend to be significantly higher. Derived properties utilizing this data are discussed in section 2.4. Specific gravity results in combination with natural water content (Table 4.3-6 -RAMA-01) show a range of 379 to 477 kg/m^3 and an average of 432 kg/m^3 for buoyant unit weight which is much less than that of MARA-02 and 12; (average values of γ_b are 456 kg/m^3 for MARA-02 and 450 kg/m^3 for MARA-12). This is directly reflected by a significant increase in natural water content of the extreme surficial sediment with a relatively unchanged specific gravity.

2.3.2 MPG-III N

Grain size and Atterberg limit determinations on sediment sampled from cores retrieved during the HUDSON-80016 cruise (1980) are listed in Table 2.3-7. Grain size results show high percentages and sand size (<.064 mm) at depths below 1000 cm and of silt size (.002 mm $<\phi<$ .064 mm) at various depths. This data confirms the many layer changes that were visually observed during extrusion and on the important fluctuations in water content and undrained shear strength reported by Silva, Jordan and Levy (1981); sharp reductions in water content occurred at depths of increasing sand and decreasing clay quantities. Liquid and plastic limits have lower values and narrower ranges

(34-86 % ω_L and 18-38% ω_p) than for MPG-I. In some cases, the sand content was too nigh to obtain limits indicating the material is essentially non-plastic.

Table 2.3-7 also contains a summary of specific gravity and buoyant unit weight results for HUDSON cruise sediments. Specific gravities range between 2.71 and 2.84 which is much narrower than reported for MPG-I. This may be an indication of a more consistent type of clay mineral. The low water contents (due to lower percentages of clay content) result in nigher buoyant unit weights with depth and a higher overall average (633 kg/m^3) than reported for MPG-I.

2.3.3 MPG-IV

Reported in tns section are the results of tests conducted during 1981 on sediment from the Nortnwestern Pacific (MPG-IV) area. The majority of data and additional details are contained in the Master of Science Thesis of G. Walker (1981).

Of the three locations investigated, the greatest recovery of good cores was obtained in E_2. The exact positions of the cores which were utilized for sediment characterization are indicated in Table 2.1-1. Sediment loss was suspected for most cores in all locations. Two different schemes were employed to estimate this loss. Results are shown in Table 2.3-8 and Figure 2.3-1. One core from each location was assumed to have lost no sediment, and all others in that location were referenced to it. The more conservative method (Method I) matches peak water contents from different cores, and the other (Method II) utilizes a constant average sedimentation rate based on paleomagnetic reversal data. The latter is actually two variations of one method, one which uses the sedimentation rate for the period between the Brunnes/Matuyama and Upper Yaramillo boundaries (Method II-A in Table 2.3-8) and the other employing the rate from the Brunnes/Matuyama to the lower Yaramillo boundary (Method II-B).

Sediment loss may be due, in part, to overpenetration, intermittent coring due to cable oscillations and actual core shortening due to compression. Although there is good correlation between the two methods for several cores in Location E_2, relatively large differences in calculated sediment loss for the cores in Location B_1 imply that the assumption of no loss in PC 38 was incorrect. Two cores from location E_2 (PC-49 and PC-51) were analyzed in detail (Table 2.3-9).

Atterberg limits were in good agreement for these two cores of with averages of 120 % or liquid limit and 47 % and 46 % for plastic limit, indicating a predominantly illitic clay (Mitchell, 1976). Both liquid and plastic limits tend to increase with depth.

Specific gravity results ranged from 2.45 to 2.95, the mean being 2.73, (Table 2.3-9). In general, PC 49 exhibited lower values than did PC 51. Grain size determinations indicate a decreasing clay content

with depth, and a corresponding increase in sand and silt, denoting a silty clay, underlain by clayey silt and silt.

In addition to the red clay of which Location E_2 is composed, a siliceous green/gray clay was found in PC 43 of Location B_1, thought to be the result of high biological productivity. The results of classification tests of two cores (PC 43 and PC 45) are shown in Table 2.3-10. The differences between Atterberg limits for the two probably signify different sediment types. In addition, large increases in limits with depth in PC 43 suggest the presence of smectite below approximately eleven meters, while values above that depth and throughout PC 45 indicate a predominantly illitic clay (Mitchell, 1976).

One core from location C_1 was examined consisting primarily of red clay with some evidence of the green/gray material similar to location B_1 (see Table 2.3-11). A silty layer is present below 2.5 meters, as reflected by a much lower liquid limit (53) as opposed to an average of 90 for the overlying sediment. From grain size analysis, the sediment is seen to be predominately silty, with sand size generally decreasing with depth and clay increasing, except for the deepest sample (below 2.5 meters) which exhibits a large increase in silt and sand-sized particles.

2.4 Analysis, Conclusions and Comparisons

2.4.1 MPG-I

Averaged values of liquid and plastic limits for the MARA and RAMA cruises are shown in Tables 2.3-2, 4, and 6. Mitchell (1976) indicates a range of 60-120% for liquid limit and 35-60% for plastic limit for clays with illite as the dominate mineral. The above averages fall within this range. The plasticity index (I_p) shown in these tables provide a range of water content over which the sediment is plastic and is calculated by taking the difference between the liquid and plastic limits. Averaged values of 51 (MARA-02), 52 (MARA-12) and 51 (RAMA-01) are high and point out the extent over which plastic behavior can be expected during strength-deformation testing. Figure 2.4-1 is a plasticity chart (ω_L vs. ω_p) from Terzaghi and Peck (1948) which classifies sediment in respect to plasticity, compressibility and organic content. MPG-I sediments fall between inorganic clays and silts of high compressibility and high plasticity.

The activity (A) which is the ratio of plasticity index to clay fraction (<.002 mm) is shown in Table 2.3-2. Mitchell (1976) shows illites typically possessing values between .5 and 1. All activity values fall within this range except two (1.1 and 1.6). These higher activities is an indication of increasing smectite mineral. Generally, activities between .75 and 1.25 (which most values fall in) are classified as "normal" indicating a common clay-water electrolyte system. Activity can be correlated with percent clay fraction to assess the swelling potential of the sediment. Figure 2.4-2 (Seed,

Woodward and Lundgren, 1962) shows the MPG-I sediment to possess a very high swelling potential.

Liquidity index (I_L) which is the ratio of the difference between natural water content and plastic limit to the plasticity index is listed in Tables 2.3-4 and 6 for MARA-12 and RAMA-01, respectively. The liquidity index scales the natural water content such that a brittle, plastic or viscous behavior can be expected; $I_L < 0$-brittle, $0 \leq I_L \leq 1$-plastic, $1 \leq I_L \leq 2$-viscoplastic, $I_L > 2$-viscous. Most of the liquidity indexes listed in both tables fall between 1 and 2 indicating a viscoplastic material, however, the near-surface sediments shown in the RAMA-01 data suggest a material that may behave as a viscous fluid when sheared. Liquidity index correlates well with sensitivity. Values between 1 and 2 (within which most of MPG-I results fall) generally imply a material that is slightly to very sensitive which coincides with previous reported data attained through a miniature vane apparatus.

Calculations to determine the in situ stress (needed to examine stress history) requires knowledge of the buoyant unit weight. Averaged values were found for each cruise and are listed in the appropriate table, however, Figure 2.4-3 shows plots of buoyant unit weight vs. depth for each cruise. Here, each data point represents the norm of all data above the depth of that particular point (Tables 2.3-3, 4 and 6). A least-squares fit to the data is shown including intercept (b), slope (m) and correlation (r). The in situ effective stress can be obtained by simply multiplying the value of buoyant unit weight (read off the linear regression line) by its appropriate depth. A general plot which involved 90 data points of the entire MPG-I area is included in the figure.

2.4.2 MPG-III N

Table 2.3-7 shows mean values for liquid limit (57 %), plastic limit (28 %), and plasticity index (31 %) for HUDSON cruise sediments. These averages are much less than those reported for MPG-I material and is a direct results of lower clay and higher silt and sand contents in MPG-III N (HUDSON) sediments. A point on the plasticity chart (Figure 2.4-1) illustrates that for the average, these sediments are inorganic clays of lesser plasticity and compressibility (than MPG-I).

Activity values shown in Table 2.3-7 basically lie within a range expected for an illitic clay (.5-1). In addition, all activities are less than .75 which imply a material that is relatively inactive. Figure 2.4-2 is a classification chart for swelling potential (A vs. % $< 2\,\mu$) where HUDSON sediments display a medium to high swelling potential.

Figure 2.4-4 includes a buoyant unit weight vs. depth plot and least-squares fit for the HUDSON cruise sediments. The significant scatter is a clear representation of the different types of sediments retrieved in the Atlantic/Abyssal Plain. One should be cautious in

using this fit to find in situ effective stress because of poor correlation, however, a quick reasonable estimation can be made. It would be more accurate to use averages within the individual core of interest.

The new results and analysis previously presented pose some important disadvantages to disposal of nuclear waste in the Atlantic/Abyssal Plain (HUDSON cruise). The friction resistance to dynamic penetration will be high due to significant amounts of silt and sand content. Also, fluid migration may be more probable in this sediment due to the presence of sandy and silty layers. Also, the data used for hole closure analysis conducted for MPG-I will not apply to MPG-III N since these sediments will probably show different strength, deformation and creep properties and benavior.

2.4.3 MPG-IV

A summary of sediment characterization results for the N.W. Pacific MPG-IV are presented in Table 2.4-1. Although plastic limit averages were similar for all three sites, the mean liquid limit for E_2 was much greater than that for C_1, with the B_1 value nearer to that of E_2. The average of specific gravity is greatest for Location E_2 and least for B_1. The much wider range of values for Location E_2 as compared to the other locations may be attributed, in part, to the greater number of measurements taken, but the low values probably correspond to ash-rich layers. Grain size analysis reveals that more clay is present in Location E_2 cores, while the percentages of sand and silt tend to be higher in Locations B_1 and C_1.

Figure 2.4-5 is a plasticity chart with data from the three locations plotted for classification purposes. Nearly all the points fall close to the line dividing clays of high plasticity and clays of high compressibility (A-line). Examination reveals that values for cores from Location E_2 are on the upper side of the A-line, and the majority of other points fall to the high compressibility side.

In general, average values of Atterberg limits determined for cores in the N.W. Pacific MPG-IV area were greater than those obtained in both MPG-I and MPG-III. In addition, MPG-IV grain size analyses reveal a higher silt content and lower percentage of clay than in MPG-I or MPG-III. This apparent contradiction may be explained by a difference in the variations of type of clay mineral comprising the total clay content. It may be further hypothesized that a greater percentage of smectite in the N.W. Pacific produced higher values in liquid limit and it should be noted that only a small quantity of the smectite mineral is necessary to change index properties significantly.

2.5 Future Work

A final report on sediment characterization properties will be completed during FY'82. Some additional testing is required to "fill the gaps". Characterization testing will continue in the MPG-III and MPG-IV study areas to supplement existing data in an overall effort to assess these sites for disposal of nuclear waste.

Table 2.1-1

Core Locations
MPG-I, MPG-III N
and MPG-IV

CRUISE	CORE	LATITUDE	LONGITUDE
MARA-02	GC-04	30° 6.3'N	157° 51.7'W
	GC-07	30° 30.9'N	158° 0.7'W
	GC-08	31° 3.0'N	157° 49.4'W
	GC-09	31° 2.5'N	157° 48.6'N
MARA-12	GC-22	31° 4.8'N	159° 3.5'W
	GC-23	30° 40.6'N	159° 0.4'W
	GC-24	30° 20.1'N	158° 59.8'W
RAMA-01	BC-15	30° 22.1'N	157° 44.6'W
	BC-18	30° 25.9'N	157° 43.3'W
	BC-20	30° 24.0'N	157° 41.4'W
	GC-08	30° 20.9'N	157° 51.5'W
	GC-10	30° 21.9'N	157° 47.9'W
	GC-12	30° 23.0'N	157° 46.9'W
	GC-14	30° 23.6'N	157° 44.3'W
	GC-16	30° 22.3'N	157° 44.8'W
	GC-19	30° 23.9'N	157° 41.3'W
	GC-21	30° 22.3'N	157° 42.5'W
	GC-22	30° 22.0'N	157° 46.1'W
	GC-23	30° 20.9'N	157° 49.6'W
	GC-24	30° 23.1'N	157° 45.6'W
HUDSON-80016	BC-02	32° 30.8'N	55° 57.0'W
	PC-01	32° 30.8'N	56° 0.7'W
	PC-02	32° 31.1'N	55° 57.9'W
	PC-03	32° 30.0'N	55° 56.3'W
	BC-03	32° 32.1'N	55° 57.0'W
VEMA 36-12	GC-39	30° 27.10'N	151° 49.90'E
	PC-43	33° 44.84'N	151° 45.91'E
	PC-45	33° 5.63'N	152° 16.38'E
	PC-49	34° 24.00'N	164° 16.00'E
	PC-51	32° 38.00'N	164° 46.00'E

TABLE 2.3-1

MARA-02 - MPG-I

Grain Size and Atterberg Limits

Core	Depth (cm)	Sand %	Silt %	Clay %	ω_L %	ω_P %	I_P %	A
GC-04	76-84	trace	33.6	66.4	94	38	56	0.8
	86-94	trace	34.8	65.2	83	36	47	0.7
	95-105	trace	30.3	69.7	86	44	42	0.6
	105-115	0.9	26.1	73.0	88	37	51	0.7
	115-121	0.1	31.4	68.5	90	36	54	0.8
	160-165	--	--	--	81	33	48	--
	180-185*	0.1	35.5	64.4	88	44	44	0.7
	203-214	trace	30.3	69.7	90	40	50	0.7
	215-225	trace	29.9	70.1	99	48	51	0.7
	226-236	trace	29.7	70.3	87	46	41	0.6
	237-247	trace	30.0	70.0	100	51	49	0.7
	247-254	0.1	34.3	65.6	83	38	45	0.7
GC-07	60-65*	trace	32.2	67.8	85	32	53	0.8
	80-94	trace	30.3	69.7	99	44	55	0.8
	94-105	--	--	--	81	39	42	--
	123-127	0.1	31.3	68.6	93	43	50	0.7
	145-150*	--	--	--	82	42	40	--
	210-215*	0.1	33.3	66.6	--	--	--	--
GC-08	15-20	0.1	33.5	66.4	85	40	45	0.7
	20-25	trace	32.7	67.3	82	35	47	0.7
	66-73	--	--	--	86	40	46	--
	76-84	0.1	33.5	66.4	74	39	35	0.5
	87-98	0.0	35.0	65.0	--	--	--	--
	100-109	0.1	34.0	65.9	83	37	46	0.7
	140-150*	--	--	--	89	33	56	--
	162-166	0.1	31.0	68.9	98	48	50	0.7
	169-180	0.1	31.0	68.9	101	41	60	0.9
	188-197*	0.1	27.7	72.2	130	54	76	1.1
	206-218	0.9	26.0	73.1	190	71	119	1.6
GC-09	13-20	0.1	32.7	67.2	82	35	47	0.7
	35-40*	--	--	--	89	39	50	--
	77-87	trace	33.0	67.0	87	37	50	0.7
	80-90	trace	30.2	69.8	92	48	44	0.6
	104-110	0.5	32.1	67.4	81	37	44	0.6
	125-135*	--	--	--	93	40	53	--
	152-162	1.2	31.6	67.2	85	39	46	0.7
	170-180	--	--	--	85	39	46	--
	180-190*	0.1	27.0	72.9	88	44	44	0.6
	190-200	0.1	32.4	67.5	86	34	52	0.8
	215-223*	--	--	--	94	41	53	--
AVG. MARA-02		0.2	31.4	68.4	92	41	51	0.7

* NEW DATA

TABLE 2.3-2

SPECIFIC GRAVITY AND UNIT WEIGHTS, MPG-I

MARA-02

CORE	DEPTH (cm)	WATER CONTENT ** %	SPECIFIC GRAVITY G_s	BUOYANT UNIT WEIGHT γ_b kg/m^3
GC-04	76-84	120	2.72	415
	86-94	124	2.71	403
	95-105	118	2.97	449
	105-115	113	2.73	434
	180-185*	105	2.80	471
	203-214	104	2.86	480
	215-225	105	3.00	493
	226-236	105	3.00	495
	237-247	106	3.02	493
	247-254	102	2.75	471
	247-252	102	2.73	468
GC-07	10-20	115	2.83	442
	12-16	115	2.72	428
	35-40*	111	2.89	463
	60-65*	112	2.80	448
	80-94	111	2.87	457
	94-105	117	2.88	441
	107-120	115	2.77	435
	123-127	113	2.65	425
	145-150*	106	2.86	475
	210-215*	101	2.75	479
GC-08*	15-20	108	2.73	451
	20-25	108	2.73	451
	45-50	114	2.83	440
	76-85	104	2.70	460
	100-109	100	2.76	482
	140-150	98	2.88	507
	102-166	103	2.76	472
	189-180	102	2.77	477
	188-197	132	2.91	408
GC-09*	35-40	110	2.75	448
	125-135	100	2.49	440
	180-190	99	2.68	474

MARA-02 AVG..456

*New Data

**All water content data has been previously reported.

TABLE 2.3-3
MARA-12 - MPG-I

Atterberg Limits

CORE	DEPTH (cm)	ω_c %	ω_L %	ω_P %	I_P %	I_L
GC-22	0-3	118	109	29	80	1.1
	15-25 #	110	79	36	43	1.7
	110-120	113	96	35	61	1.3
	160-170#	102	90	42	48	1.3
	184-194	106	80	28	52	1.5
	265-275	103	82	39	43	1.5
GC-23	60-70	115	96	37	59	1.3
	102-112	116	89	37	52	1.5
	114-124	115	89	32	57	1.5
	125-135#	117	87	46	41	1.7
	142-152	116	80	40	40	1.9
	184-194	110	81	38	43	1.7
GC-26	78-85	117	95	39	56	1.4
	90-105#	114	94	41	53	1.4
AVG. MARA-12		112	89	37	52	1.5

Previously reported

TABLE 2.3-4

SPECIFIC GRAVITY AND UNIT WEIGHTS, MPG-1

MARA-12

CORE	DEPTH (cm)	WATER CONTENT** %	SPECIFIC GRAVITY G_s	BUOYANT UNIT WEIGHT γ_b kg/m^3
GC-22	0-3	118	2.75	423
	15-25#	110	2.77	448
	48-52	113	2.76	440
	110-120	119	2.63	407
	148-158#	110	2.73	443
	160-170#	102	2.78	476
	184-194	106	2.82	470
	194-204	107	2.65	441
	265-275	103	2.67	459
GC-23	60-70			
	102-112	116	2.74	429
	114-124	115	2.99	462
	125-135	118	2.77	427
	142-152	116	2.71	425
	184-194	110	2.62	430
GC-24	15-20	111	2.66	433
	139-149#	109	2.62	431
	151-161#	109	2.62	431
	162-172#	100	2.68	468
	173-183	103	2.61	447
	255-260#	100	2.67	470

MARA-12 AVG...450

(averged with GC-28, previously reported by Silva, Jordan and Levy, 1981)

#Previously reported

TABLE 2.3-5
RAMA-01 MPG-I

Atterberg Limits

CORE	DEPTH (cm)	$\omega_{\%C}$	$\omega_{\%L}$	$\omega_{\%P}$	I_{P} %	I_{L} %
BC-15	0-2	165	86	39	47	2.7
	13-16	120	94	30	64	1.4
	22-25	123	91	30	61	1.5
BC-18	14-18	122	102	29	73	1.3
BC-20	0-2	130	80	37	43	2.2
	23-27	131	90	33	57	1.7
	40-44	105	86	32	54	1.4
GC-08	10-15	122	83	34	49	1.2
	53-58	104	82	33	49	1.5
	113-118	105	78	31	47	1.6
	197-203	116	83	33	50	1.7
	260-266	104	84	32	52	1.4
GC-10	0-9	121	78	40	38	2.1
	6-12	121	79	34	45	1.9
	28-34	107	76	32	44	1.7
	84-91	110	93	33	60	1.3
	129-136	115	76	38	38	2.0
	173-178	115	93	29	64	1.3
	279-285	104	71	37	34	2.0
GC-12	64-70	113	86	41	45	1.6
	168-173	104	82	29	53	1.4
	204-216	104	83	32	51	1.4
GC-14	2-7	125	82	44	38	2.1
	70-75	117	81	40	41	1.9
	240-243	104	84	32	52	1.4
GC-16	0-7	121	81	32	49	1.8
	60-66	103	79	38	41	1.6
	117-125	110	81	29	52	1.6
	170-176	106	83	44	39	1.6
	227-233	107	82	35	47	1.5
	266-272	107	82	35	47	1.5
GC-19	19-23	102	90	35	55	1.2
GC-22	0-5	118	83	38	45	1.8
	130-137	116	93	40	53	1.4
	188-192	124	94	36	58	1.5
	255-260	103	94	36	58	1.2
	282-286	103	88	24	64	1.2
GC-23	4-12	123	81	32	49	1.9
	62-68	113	88	32	56	1.4
	127-133	124	92	48	44	1.7
	279-283	103	99	30	69	1.1
GC-24	82-88	121	90	29	61	1.5
	122-129	122	85	27	58	1.6
	177-183	117	88	31	57	1.5
AVG. RAMA-01		115	85	34	51	1.6

TABLE 2.3-6

SPECIFIC GRAVITY AND UNIT WEIGHTS, MPG-I

RAMA-01

CORE	DEPTH (cm)	WATER CONTENT %	SPECIFIC GRAVITY G_s	BUOYANT UNIT WEIGHT γ_b kg/m^3
BC-20	3-8	125	2.71	401
	10-14	125	2.84	417
GC-08	3-8	122	2.66	403
	10-15	122	2.58	392
	53-58	104	2.68	451
	197-203	116	2.62	413
	260-266	104	2.66	454
GC-10	0-9	121	2.79	421
	6-12	121	2.65	404
	28-34	107	2.77	460
	84-91	110	2.70	441
	129-136	115	2.77	436
	173-178	115	2.73	430
	225-230	102	2.71	468
	279-285	104	2.64	451
	300-310	100	2.72	476
GC-12	64-70	113	2.66	427
	120-126	113	2.73	436
	168-173	104	2.69	458
	204-210	104	2.65	451
	240-243	125	2.71	401
GC-14	2-7	125	2.71	401
	14-19	117	2.72	424
	70-75	117	2.66	416
	79-84	110	2.75	448
	110-115	119	2.86	435
	162-168	121	2.83	426
	240-243	104	2.61	446
GC-19	19-23	102	2.77	477
	38-43	107	2.74	456
	50-55	107	2.60	436
	110-115	118	2.83	434
	195-200	111	2.79	450
GC-21	0-5	130	2.62	379
	69-74	110	2.67	437
GC-24	82-88	121	2.63	401
	122-129	122	2.68	405
	177-183	117	2.76	429
	250-256	106	2.68	451

RAMA-01 AVG.432

TABLE 2.3-7

HUDSON-80016 - MPG-III N

Grain Size, Atterberg Limits, Specific Gravity and Unit Weights

Core	Depth (cm)	ω (%)	Sand %	Silt %	Clay %	ω_L %	ω_P %	I_P %	A	G_s	γ_b kg/m^3
BC-2	31-35	75	--	--	--	34	29	5	--	--	--
	35-40	100	0.6	29.0	70.4	67	33	34	.5	2.82	491
PC-01	290-300	87	0.1	56.6	43.3	53	25	28	.7	2.75	531
	610-620	69	0.3	65.7	34.0	--	--	--	--	2.80	632
	890-900	52	trace	38.3	61.7	37	23	14	.2	2.82	760
	1048-1052	84	3.6	31.4	65.0	58	28	30	.5	2.76	546
	1057-1061	72	--	--	--	--	--	--	--	2.82	619
	1062-1069	49	28.0	31.7	40.3	37	18	19	.5	2.82	787
	1160-1170	49	64.5	26.1	9.4	sandy	N.P.	--	--	2.75	768
PC-02	290-300	85	0.5	27.3	72.2	74	31	43	.6	2.74	538
	400-410	50	trace	39.8	60.2	54	28	26	.4	2.78	767
	600-610	79	--	--	--	60	26	34	--	2.78	574
	860-870	64	1.3	38.8	59.9	60	25	35	.6	2.81	666
	1060-1070	24	54.0	35.4	10.6	sandy	N.P.	--	--	2.75	1090
PC-03	280-290	81	--	--	--	74	38	36	--	2.77	502
	610-620	87	trace	50.6	49.4	53	22	31	.6	2.76	533
	930-940	58	0.2	25.8	74.0	65	26	39	.5	2.76	697
	1060-1070	78	--	--	--	62	26	36	--	2.84	589
GC-03	120-130	98	0.2	25.3	74.5	86	36	50	.7	2.71	482
	130-140	99	--	--	--	--	--	--	--	2.71	478
AVG. HUDSON		72	10.9	37.3	51.8	57	28	31	.5	2.78	633

Table 2.3-8

Sediment Loss and Recalculated Sedimentation Rates[1]
Using Three Methods

CORE	METHOD I[2] SED. RATE mm/ky	METHOD I[2] SED. LOSS cm	METHOD II A[3] SED. RATE mm/ky	METHOD II A[3] SED. LOSS cm	METHOD II B[4] SED. RATE mm/ky	METHOD II B[4] SED. LOSS cm
PC 35	5.5	80	7.9	253	8.6	303
PC 45	10.6	70	14.9	379	15.3	406
PC 46	10.3	150	8.1	- 9	9.5	88
PC 47	9.4	165	9.9	198	10.7	257
PC 48	9.9	195	9.9	195	9.9	195
PC 49	7.3	110	9.6	275	10.2	318
PC 51	8.8	250	9.2	278	10.5	372

[1] Rate since B/M boundary to present.

[2] From water content profile matching.

[3] Using sedimentation rate for period between B/M and U/J boundaries.

[4] Using sedimentation rate for period between B/M and L/J boundaries.

Table 2.3-9

Sediment Characteristics
MPG-IV Location E_2

CORE	AVERAGE DEPTH m	W_L %	W_P %	SAND %	SILT %	CLAY %	SPECIFIC GRAVITY G_s
PC 49	0.65	103	43	1.9	45	53	--
	1.75	--	57	2.3	43	54	--
	1.90	119	54	--	--	--	2.66
	2.00	--	--	--	--	--	2.62
	3.15	95	36	Trace	45	55	2.63
	3.72	117	46	1.0	49	50	2.68
	4.40	113	39	--	--	--	--
	5.10	--	--	Trace	49	51	2.78
	5.62	111	45	--	--	--	--
	6.20	--	--	1.8	51	47	2.72
	6.85	126	52	--	--	--	--
	7.35	--	44	2.3	60	37	--
	8.05	140	54	1.7	52	47	2.74
	8.95	133	43	Trace	55	44	2.66
	9.75	--	32	11.0	70	20	2.49
	10.60	--	42	Trace	48	51	--
	11.25	135	51	2.1	59	39	2.45
	11.70	121	54	4.0	63	33	2.76
	11.85	--	--	--	--	--	--
Average	TOTAL	120	47	2.0	52	46	2.66
	<6m	110	46	1.3	46	52	2.68
	>6m	131	47	3.0	58	39	2.64
PC 51	0.14	--	37	3.0	35	62	2.84
	0.42	95	--	--	--	--	2.69
	0.82	95	36	Trace	37	63	2.92
	1.30	92	40	3.1	37	60	2.85
	1.75	108	45	2.8	38	60	2.85
	2.66	130	39	Trace	40	60	2.69
	3.64	--	--	Trace	38	61	2.78
	4.20	131	44	Trace	53	46	2.70
	4.60	127	44	--	--	--	2.72
	4.70	123	43	2.3	42	55	2.80
	5.00	--	--	--	--	--	2.76
	5.65	135	45	Trace	49	51	--
	7.35	128	44	Trace	33	67	2.72
	9.05	133	51	8.2	60	32	--
	10.10	--	44	2.7	53	45	2.76
	10.42	143	45	1.6	44	55	--
	10.78	95	53	Trace	46	53	2.86
	11.77	119	37	Trace	37	63	2.95
	12.00	134	54	1.7	62	36	2.71
	12.24	152	51	1.1	45	54	2.83
	12.38	127	47	3.5	59	37	--
Average	TOTAL	120	46	3.0	45	52	2.79
	<2m	97	41	3.0	37	61	2.81
	>2m	127	47	1.8	47	51	2.77

Table 2.3-10

Sediment Characteristics

MPG-IV Location B_1

CORE	AVERAGE DEPTH (m)	ω_L %	ω_P %	SAND %	SILT %	CLAY %	SPECIFIC GRAVITY G_s
PC 43	1.22	95	41	--	--	--	--
	4.60	120	54	Trace	58	41	2.73
	4.70	94	54	1.2	51	48	2.66
	8.36	125	44	2.7	58	39	2.67
	8.48	117	45	1.9	61	37	2.63
	11.18	132	54	2.2	52	46	2.68
	11.28	150	52	7.5	52	40	--
	11.80	150	55	8.5	57	35	2.69
	11.90	155	54	11.1	64	25	2.67
Average	TOTAL	126	50	4.0	57	39	2.68
	<11m	110	48	1.6	57	41	2.67
	>11m	148	54	7.3	56	37	2.68
PC 45	4.28	83	40	10.8	55	34	2.64
	4.40	100	43	8.8	56	35	2.62
	8.94	95	47	12.6	47	41	2.67
	9.04	89	39	9.2	52	39	--
	12.34	98	36	16.1	54	30	2.77
	12.44	91	31	5.3	66	29	2.68
Average	TOTAL	94	39	11.0	54	35	2.68

Table 2.3-11

Sediment Characteristics
MPG-IV Location C_1

CORE	AVERAGE DEPTH (m)	ω_L %	ω_P %	SAND %	SILT %	CLAY %	SPECIFIC GRAVITY G_s
GC 39	0.19	86	45	12.2	60	28	2.75
	0.52	94	41	9.3	47	44	2.64
	0.90	89	49	8.2	51	41	2.79
	1.26	92	45	0.9	55	44	2.70
	1.62	89	41	2.8	49	48	2.75
	2.10	91	41	0.9	51	48	2.66
	2.57	53	47	14.8	61	25	2.69
Average	TOTAL	85	44	7.0	53	40	2.71

Table 2.4-1

SEDIMENT CHARACTERIZATION SUMMARY - MPG-IV

AREA	CORE	DEPTH	AVERAGE SAND %	SILT %	CLAY %	ω_L %	ω_p %	G_s
E_2	All Cores	TOTAL	2	49	49	120	46	2.73
	PC-49	TOTAL	2	52	46	120	47	2.66
		<6 m	1.3	46	52	110	46	2.68
		>6 m	3.0	58	39	131	47	2.64
	PC-51	TOTAL	3	45	52	120	46	2.79
		<2 m	3.0	37	61	97	41	2.81
		>2 m	1.8	47	51	127	47	2.71
B_1	All Cores	TOTAL	7	56	37	110	45	2.68
	PC-43	TOTAL	4	57	39	126	50	2.68
		<11 m	1.6	57	41	110	48	2.67
		>11 m	7.3	56	37	148	54	2.68
	PC-45	TOTAL	11	54	35	94	39	2.68
C_1	All Cores	TOTAL	7	53	40	85	44	2.71

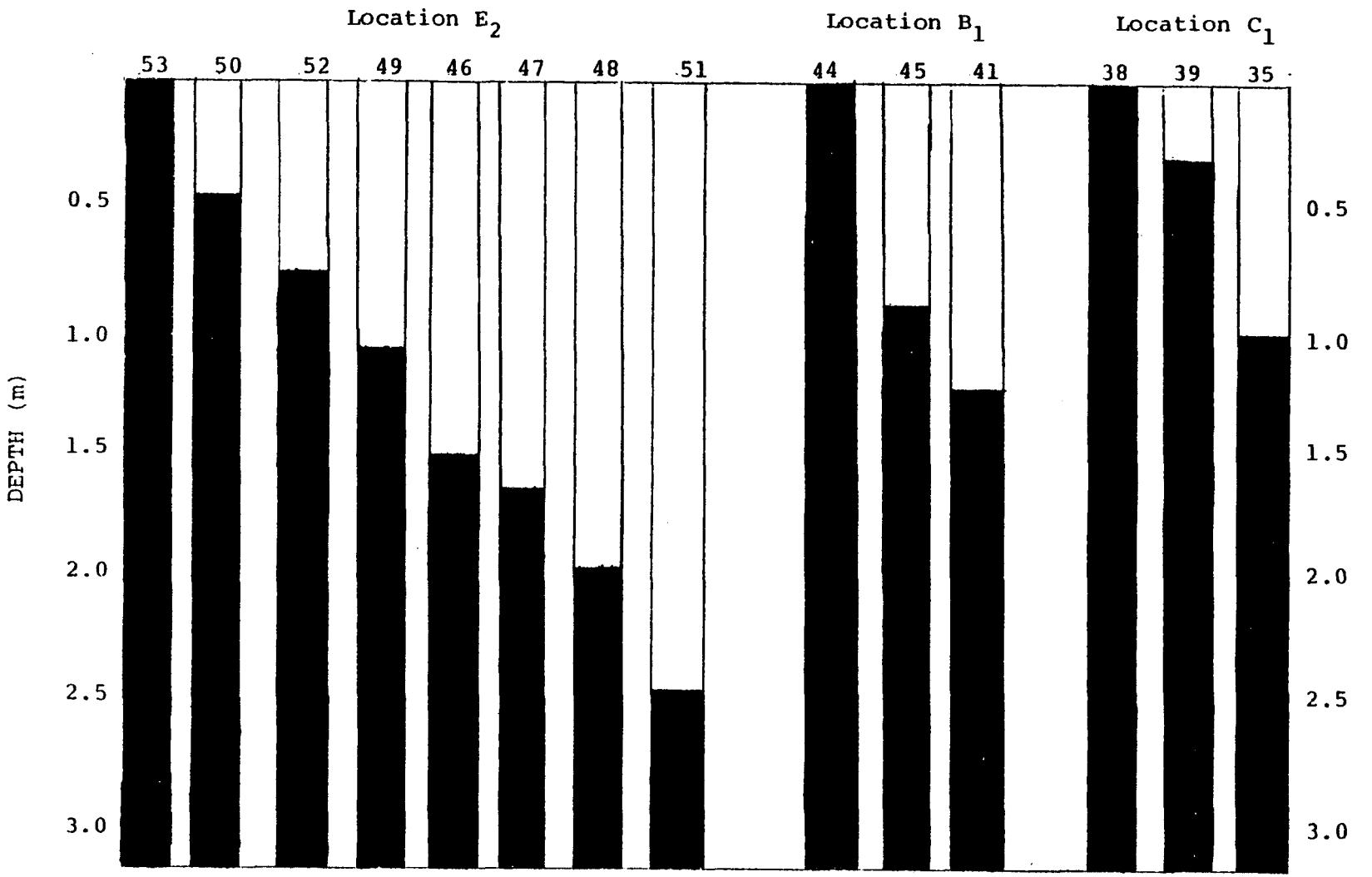
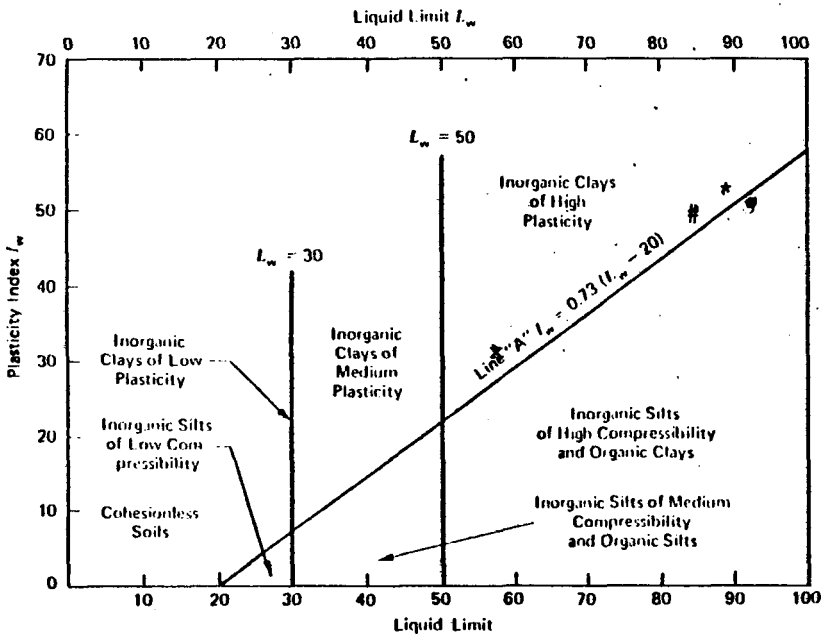


Figure 2.3-1 Corrected depths from water content profile matching.



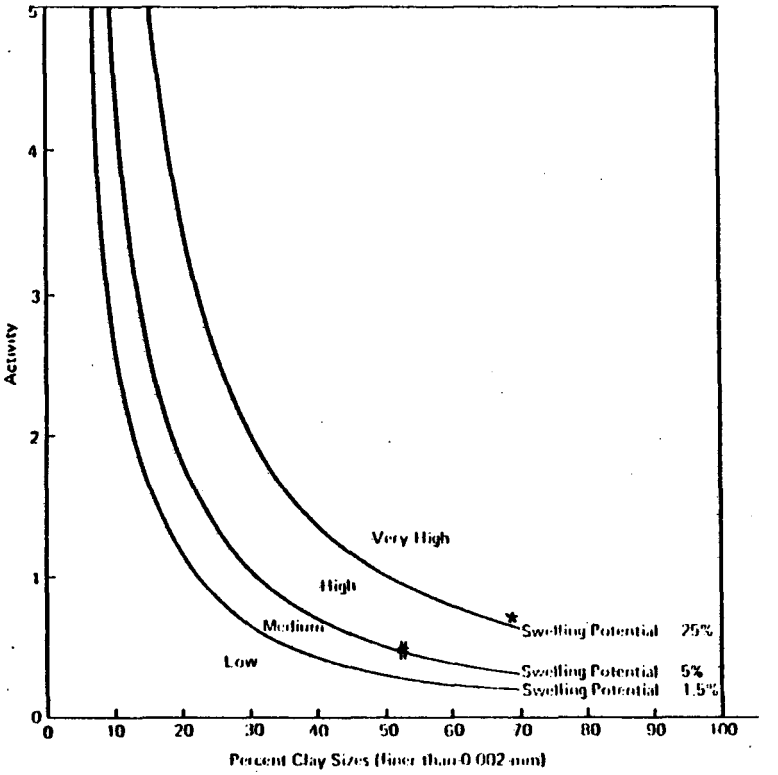
● MARA-02

* MARA-12

\# RAMA-01

x HUDSON

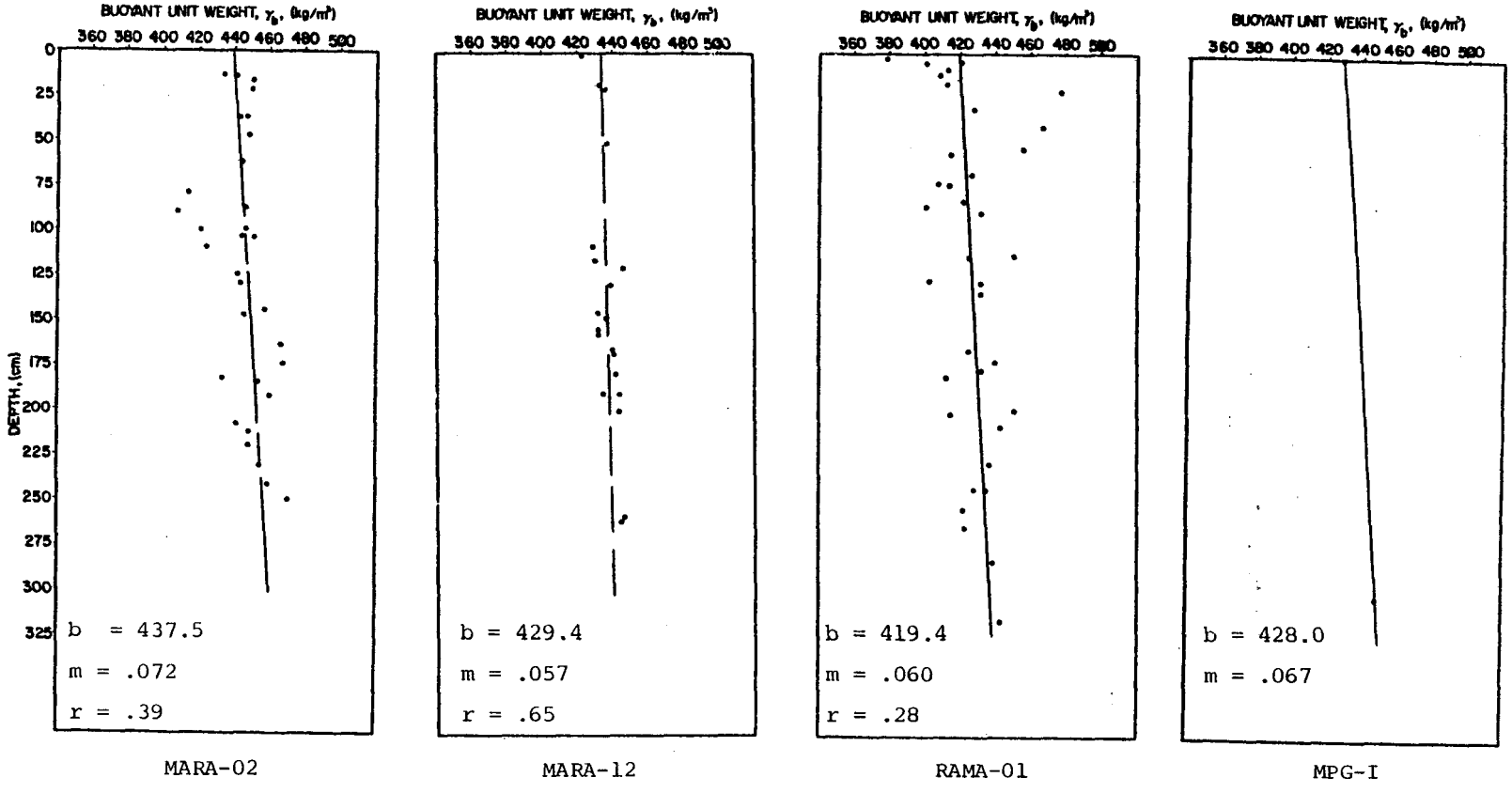
Figure 2.4-1 Plasticity Chart



* MPG-I (MARA and RAMA cruises)

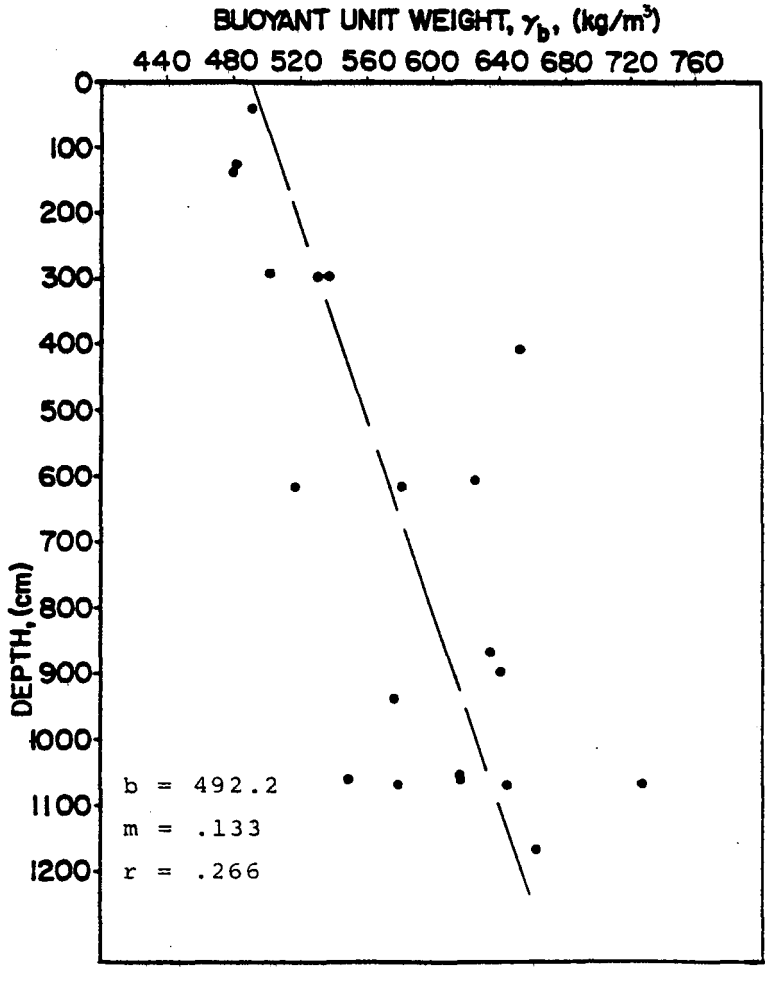
\# MPG-III N (HUDSON cruise)

Figure 2.4-2 Classification Chart for Swelling Potential



b = intercept m = slope r = correlation

Figure 2.4-3 Buoyant Unit Weight vs. Depth - MPG-I sediments



b = intercept m = slope r = correlation

Figure 2.4-4 Buoyant Unit Weight vs. Depth MPG-III N, HUDSON sediment

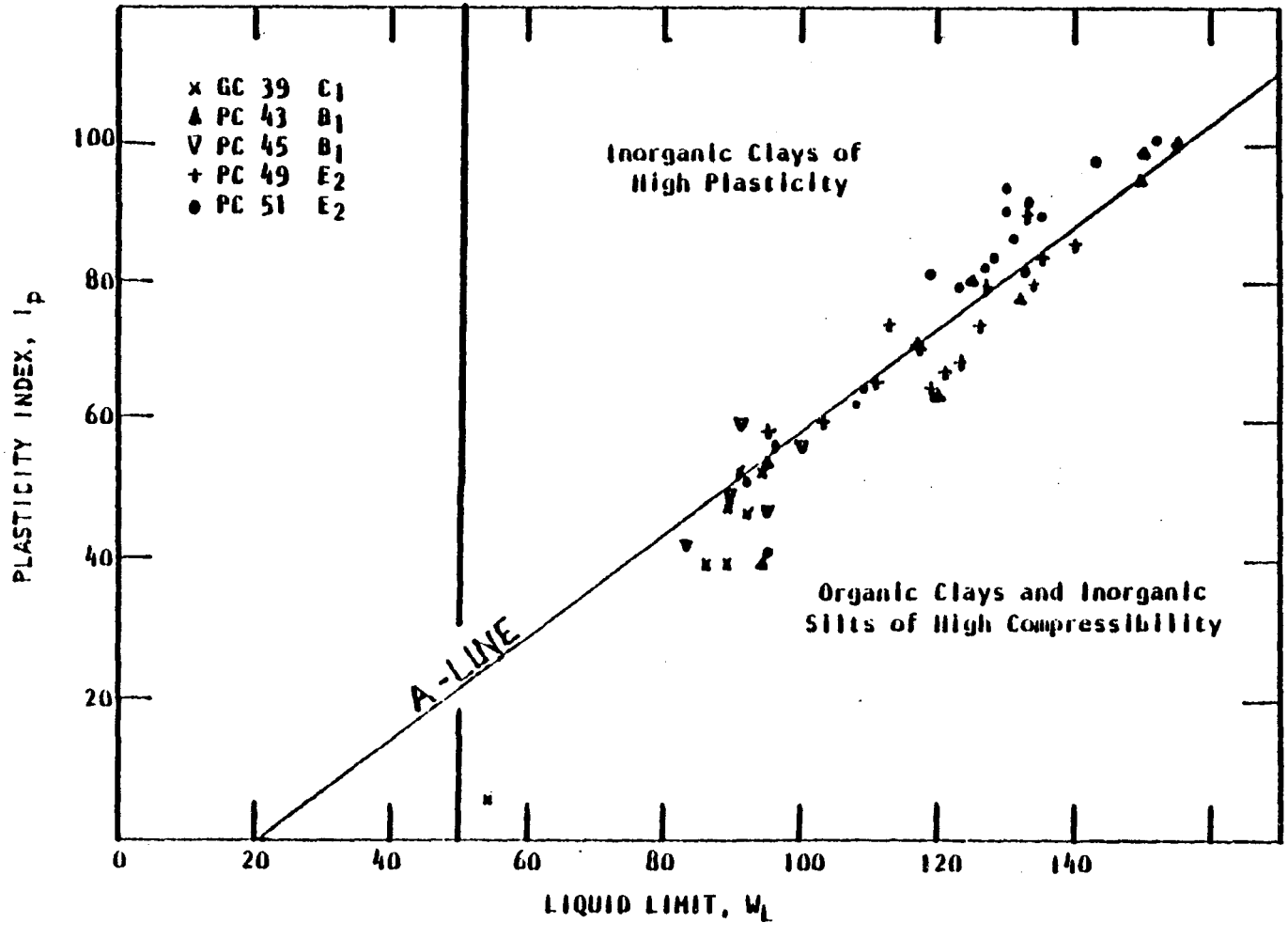


Figure 2.4-5 **Plasticity Chart-All Areas**

3.0 TRIAXIAL COMPRESSION (W. Levy, D. Calnan)

3.1 Effects of Radiation History on Stress-Strain Properties.

3.1.1 Introduction

The effects of possible changes in sediment stress-strain behavior due to high level radiation exposure is of considerable interest to the Subseabed Disposal Program. However, no work of this nature has been previously reported in the literature and therefore a program is underway to determine what changes in properties may occur in the near field around the canister. The materials used were from the MPG-I site.

3.1.2 Materials and Methods

Five triaxial subsamples of reconstituted-reconsolidated Pacific smectite were exposed to a Cobalt-60 radioactive source for various lengths of time at SNL. This source was chosen because it gives off a steady dose rate of 1 Mrad/hr with an insignificant amount of decay over time. The samples used were hole-closure tank subsamples, reconsolidated to a simulated 9 meter depth or 41.2 kPa (Bamford, 1979). One sample was exposed to 8 hrs. of radiation, two to 100 hrs. and two to 1000 hrs. The samples were stored and transported at approximately 4°C, but due to the proximity to the radioactive source they were subjected to a thermal cycle where some drying took place because it was necessary to provide a vent hole in the sample cap. Temperature at the exposure site steadied at 43°C after 8 hrs. and remained at that temperature until removal and re-refrigeration.

One of the 1000 hr. specimens was too dried out to test. Isotropically consolidated undrained triaxial compression tests (CIU) were performed on the four remaining samples and a control group of non-irradiated specimens had been previously tested on similar material (Akers and Silva, 1980). Consolidation stresses were chosen so as to allow direct comparison with the control group. Three samples were consolidated to approximately 134 kPa and one of the 100 hr. exposure samples was tested at 77 kPa to allow a two-point determination of the effective cohesion ($\bar{c}$) and effective internal angle of friction ($\bar{\phi}$). All samples were effectively saturated under back pressure to B values greater than 98%. The shear phase of the tests were strain-controlled at a loading rate of 0.03 mm/min. Corrections for membrane and filter strips have been applied to all data in this study.

3.1.3 Results

Due to the thermal cycle and duration of exposures some of the samples were returned for testing at URI/MGL in less than optimum condition. Some differential drying out of the specimens was noted in the initial water content measurements with as much as 12 % difference between top and bottom. Some horizontal cracking was also noted in the 100 and 1000 hr. specimens. In spite of this, satisfactory saturation

was acnieved (B >99 %) and post-test water content profiles were much more uniform (4 % maximum differential).

Figure 3.1-1 shows the results from the series. The differences in stress-strain behavior (a), pore pressure response (b), and the stress paths (c), among the three tests at a consolidation stress of 134 kPa are minor and may be an artifact of the poor initial sample condition. Normalized parameters reflect this similarity even more clearly. Skempton's A_f varies from .73 - .74 for the three tests, S_u/p varies from .42 to .45 and σ_1/σ_{3f} varies from 3.2 to 3.8.

A summary of the test results is presented in Table 3.1-1 along with results from the control series. A crude two point determination of $\bar{c}$ and $\bar{\phi}$ for the irradiated series yielded a $\bar{\phi}$ of 31.4° and $\bar{c}$ of 6 kPa. This compared relatively well with the two point and four point determinations from the control series as indicated on Table 3.1-1. It should be noted that the control samples were taken from a tank to a simulated 18 meter depth (82.4 kPa).

3.1.4 Discussion

Based on these results it appears that radiation history has no significant effect on the stress-strain properties of the material. Similarly, the actual radiation dosage also appears to have no significant effect on the stress-strain properties.

Future studies should address the problem of examining stress-strain behavior during actual radiation exposure to better simulate the Seabed Disposal conditions.

3.2 Effects of High Consolidation Stress.

3.2.1 Introduction

The Subseabed Disposal Program is concerned with the effect of high consolidation stresses on the stress-strain properties of deep sea sediments. URI/MGL is tasked to perform isotropically consolidated undrained triaxial tests (CIU) on remolded deep sea illite to consolidation stresses of 2640 kPa. This will overlap with similar tests to even higher pressures being run at Waterways Experiment Station.

3.2.2 Materials and Methods

Reconstituted-reconsolidated tank subsamples of deep sea illite consolidated to a simulated 5 meter depth (22.1 kPa) were used for the high pressure tests (PI5-8). Wykeham-Farrance triaxial cells were fitted with special aluminum chambers for the high pressure tests. A preliminary series of consolidation stresses ranging from 270 to 1240 kPa were performed to give a general idea of the stress-strain behavior to be expected. Consolidation stresses were applied in steps and

volume change measured until the desired test pressure was reached. Shearing was strain controlled at a rate of 0.03 mm/min. A fourth test at 1777 kPa was performed but the pore pressure measurements were questionable. However, hydrostatic response and total stress data for this test is still useable in establishing trends though the results do not appear on figures and tables.

The low pressure data reported was done on similar material with the tanks being consolidated to simulate 2 meter (PI-2) and 18 meter (PI-18) depths (Akers and Silva, 1980). Only CIU tests where the samples were reconsolidated well into the normally consolidated range are reported.

3.2.3 Results

The results of these preliminary tests show some interesting effects. Figure 3.2-1 shows there is a pronounced change in stress-strain behavior with increasing consolidation stress. Figure 3.2-2 shows undrained shear strength (q or S_u) plotted against effective consolidation stress ($\bar{\sigma}_c$) for normally consolidated conditions. The closeness of the linear least squares fit to this data (R_f = 0.993) appears to allow future use of the Normalized Soil Parameter-concept for predicting soil strength with depth or increasing $\bar{\sigma}_c$. The best fit $S_{u/p}$ ratio for this sediment is 0.31.

Table 3.2-1 summarizes most of the results of the testing to date. For those samples showing distinct failure planes (689 and 1240 kPa) the axial strain at failure becomes constant at about 5 percent.

3.2.4 Discussion

Figure 3.2-3 shows the Mohr-Coulomb failure circles and the failure envelope derived from them. As can be observed, some slight curvature occurs with the $\bar{\phi}$ angle decreasing with increasing stress. This can be better defined upon further testing. Curvature of this type for clays is not uncommon.

This initial series indicates a definite change in the mode of failure from plastic or "barrel-shaped" at 270 kPa and below to brittle with well-developed shear planes between 270 and 689 kPa and above. At consolidation stresses of 689 kPa and above, actual "slickensided" surfaces are observed on the shear plane at failure.

Hydrostatic behavior during this initial series is as expected. A transition in volume change behavior occurs at a critical consolidation stress for clays (Mitchell, 1976). Once the consolidation pressure reaches this critical point (between 270 and 689 kPa) the amount of additional water that can be squeezed out of the specimen is negligible.

Further testing will take the reconsolidated-reconstituted illite samples towards an upper limit of approximately 2640 kPa consolidation pressure. Additional tests will also attempt to better define the

transition in mode of failure between 270 and 689 kPa. The next test series will use undisturbed samples from the 1981 DeSteiger cruise.

3.3 Effects of Overconsolidation on Stress-Strain Behavior

3.3.1 Introduction

In a previous study, a series of consolidated anisotropically undrained (CIU) triaxial tests were conducted on undisturbed illite and remolded smectite (Silva and Schwartz, 1981). Stress-strain results from these tests showed a significant "strain-softening" effect (stress decrease after failure) which cannot be easily incorporated into the strain-hardening material model currently formulated through SNL for the SDP. In an effort to gain a better understanding of this softening behavior, a series of triaxial tests were conducted on overconsolidated material.

3.3.2 Methods and Materials

Equipment and procedures used to perform the tests are described in detail by Akers and Silva (1980) (CIU tests series) with the following exceptions. The equipment cells used in these tests involved two types of triaxial cells; a specially designed, frictionless bushing cell and a high-pressure solid bushing cell. The test procedure differed in that the specimen was consolidated to an effective stress ($\bar{\sigma}_o$) that was higher than the consolidation stress ($\bar{\sigma}_c$) during shear. A ratio OCR (where OCR = $\bar{\sigma}_o/\bar{\sigma}_c$) was used to identify the stress conditions of each specimen.

Four tests were conducted on reconstituted/reconsolidated (remolded) illite-rich clay sampled from the sediment structure interaction testing (SSIT) tank PI-5-8. Specimens (designated as PI-5-8)_ were tested at overconsolidation ratios of 1, 2, 4 and 8 where $\bar{\sigma}_c$ = 28.25, kPa was used as the consolidation stress that all tests were unloaded to.

3.3.3 Results

The results of this series are shown on Figures 2.2-1, 3.3-2 and 3.3-3. As expected, the material strength increases with increasing degree of overconsolidation. From an OCR of 1 to an OCR of 2 the strength almost doubles. This doubling occurs again between OCR's 2 and 4 (Figure 3.3-1). The tests at OCR's of 1 and 2 both behave normally consolidated in shear as can be seen on the p-q plot (Figure 3.3-3). Pore pressure developed during shear decreases with increasing OCR (Figure 3.3-2). The test at OCR of 8 (which terminated prematurely due to equipment malfunction) is the only test where a definite shear plane developed during failure (after 10% ε_a). These results are summarized in Table 3.3-1.

3.3.4 Discussion

A preliminary analysis has been completed and is discussed below. Skempton's A factor at failure decreases as expected with increasing OCR and at OCR of 8 is approaching zero (Table 3.3-1). Of interest is the transition between OCR of 4 and 8 in pore pressure response where the speciment exhibits a dilative tendency. The test at OCR of 8 shows a peaking of excess pore pressure at 0.6% axial strain followed by a rapid falling off till at 6% strain where the pore pressure actually goes negative (thus dilatancy). This type of behavior is indicative of a dense particle packing arrangement and expansion on shear planes during yielding.

When the normalized shear strength (S_u/ρ) is plotted against OCR on a log scale it appears as an almost linear function. This is to be expected in such relatively homogeneous material.

No significant strain softening was observed in this series as was seen in previous CAU tests (Schwartz, 1981) and similarly, during CAU tests no dilatent behavior was observed in the pore pressure response. Thus, these two sets of tests data appear quite different and assessing a relationship between the two types of sediment mechanical behavior will require additional analysis. However, this data could be useful as is in the modelling the sediment mechanical response to the stress history effects.

TABLE 3.1-1

EFFECTS OF RADIATION HISTORY
ON STRESS - STRAIN PROPERTIES

EXPOSURE TIME(HRS)	ω_I (%)	ω_F (%)	$\bar{\sigma}_c$ (KPA)	ϵ_{AF} (KPA)	$(\bar{\sigma}_1 - \bar{\sigma}_3)_F$ (KPA)	$\bar{\sigma}_1 / \bar{\sigma}_3{}_F$	A_F		
			RECONSTITUTED - RECONSOLIDATED SMECTITE: PS-9						
8	174	119	136	11	113	3.8	.86		
100	180	128	77	14.8	73	4.1	.73	}	$\bar{\phi} = 31.4^0$
100	160	115	137	13.2	124	3.7	.74	}	$\bar{c} = 6$ KPA
1000	130	118	131	9.4	112	3.2	.73		
			RECONSTITUTED-RECONSOLIDATED SMECTITE: PS-18 (AKERS AND SILVA, 1980)						
0	128	112	9.5	10.2	26	3.8	.01		
0	134	131	28	10.4	42	4.1	.32		$\bar{\phi} = 33.5^0$
*0	126	123	78	9.8	66	3.4	.73	$\bar{\phi} = 30.6^0$	$\bar{c} = 1$ KPA
*0	133	117	134	16.0	123	3.6	.68	$\bar{c} = 0$	

* DIRECTLY COMPARABLE WITH IRRADIATED SERIES

TABLE 3.2-1

EFFECTS OF HIGH CONSOLIDATION STRESS

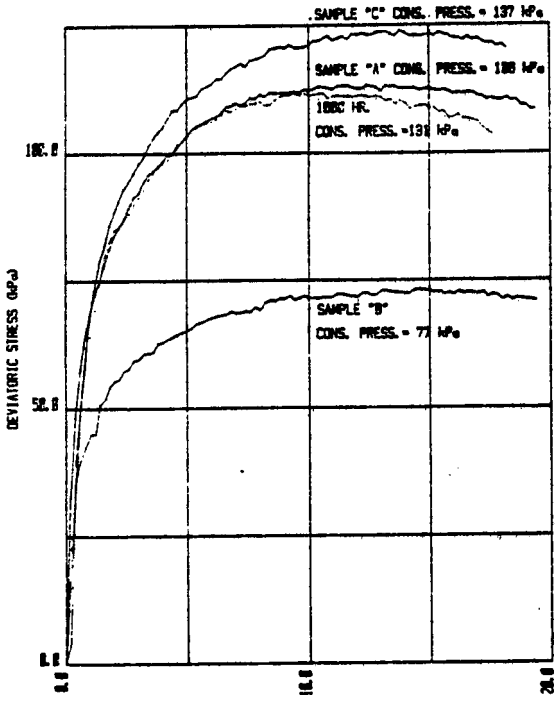
SAMPLE NAME	σ'_c (KPA)	ε_{a_f} (%)	Q (KPA)	P (KPA)	$\bar{A}_f$	ω_i (%)	ω_f (%)
* PI-2	29	1.8	9.7	22.7	.81	91.9	74.4
* PI-2	55	1.4	16.7	39.4	.97	87.3	68.9
* PI-18	99	6.8	49.6	83.4	.66	67.3	66.9
* PI-18	155	8.6	74.1	132.2	.66	70.4	60.1
PI-5-8	270	14.6	105.7	193.8	.86	87.5	56.7
PI-5-8	689	5.0	257.6	586.7	.77	93.9	51.6
PI-5-8	1240	5.6	383.6	1007.9	.80	86.8	48.1

* AKERS AND SILVA, 1980

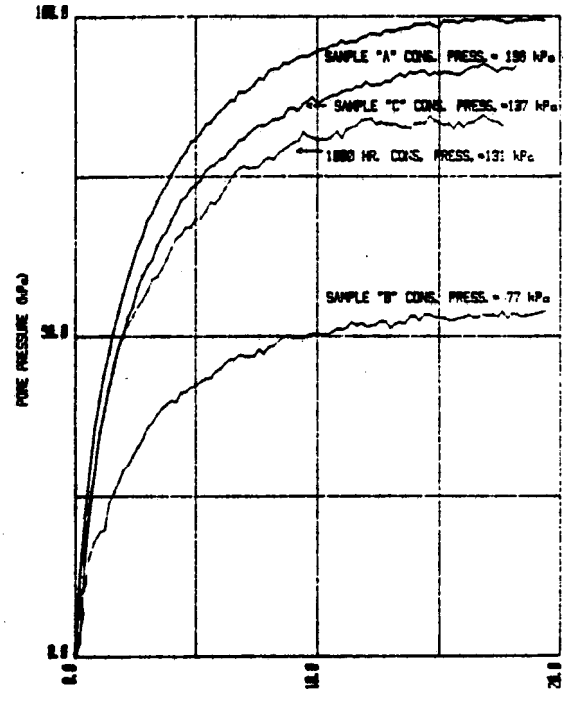
TABLE 3.3-1

OCR SERIES - CIU TRIAXIAL TESTS

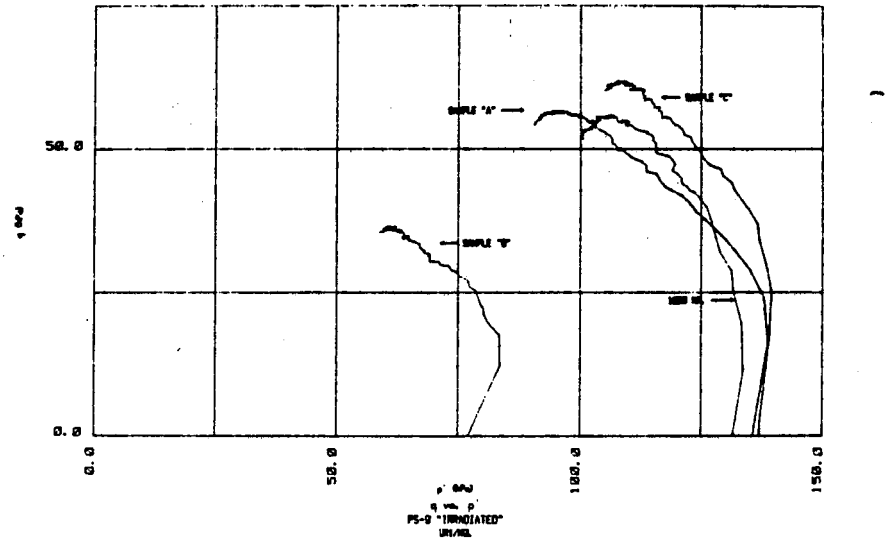
OCR	$\bar{\sigma}_c$ (kPa)	A_f (%)	q_f (kPa)	p_f (kPa)	$\bar{\sigma}_1/\bar{\sigma}_3)_f$	S_u/p	$\bar{A}_f$	ω_i (%)	ω_f (%)
1	28.3	2.6	12.1	22.5	3.3	0.43	0.74	90.5	79.4
2	28.3	15.8	23.6	35.0	5.2	0.83	0.33	81.7	73.9
4	28.3	7.2	38.6	53.4	6.2	1.36	0.17	89.4	69.5
8	28.3	13.0	51.5	78.4	4.8	1.82	0.01	83.7	62.2



(a)

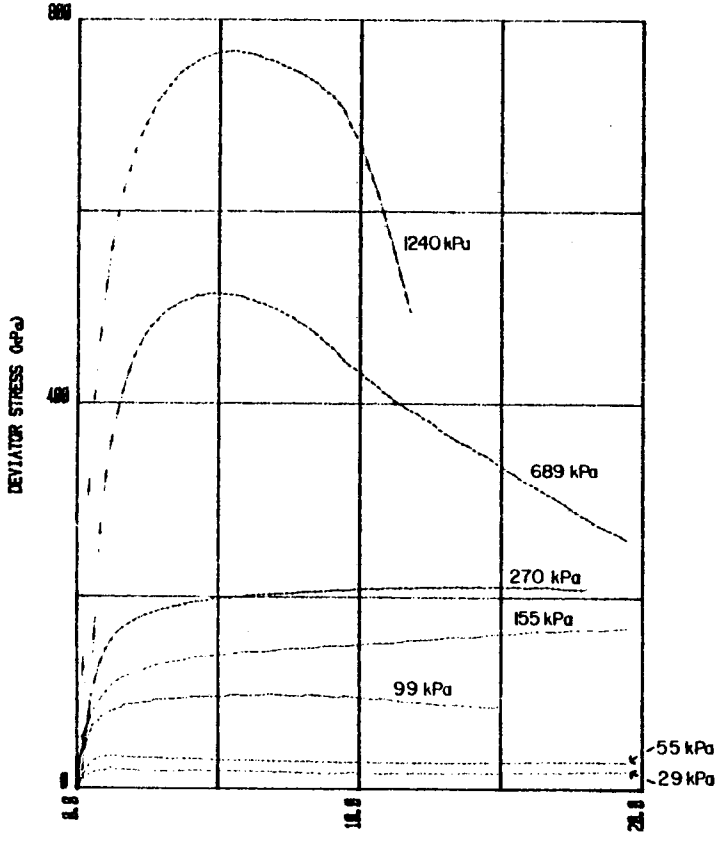


(b)



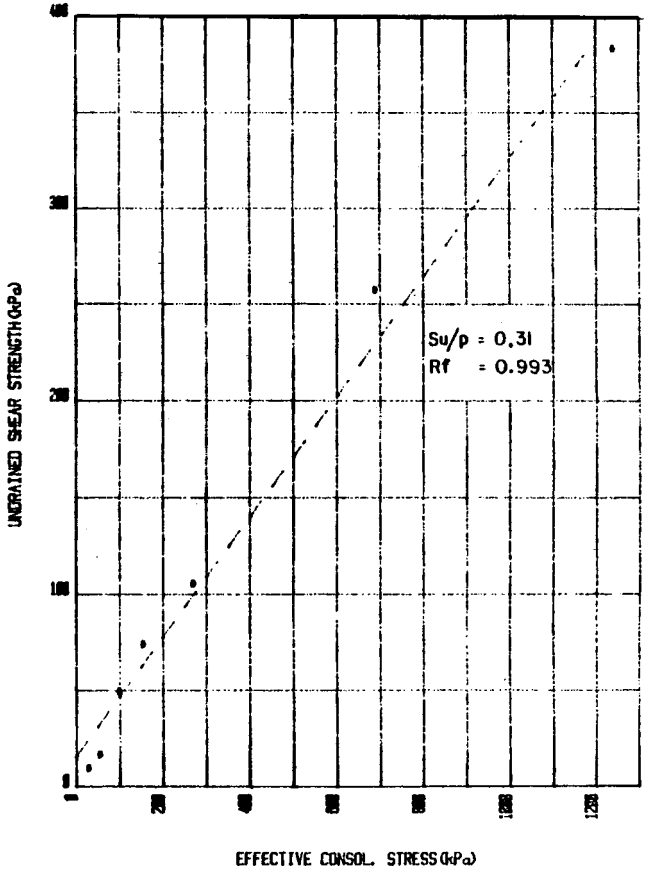
(c)

Figure 3.1-1



DEVIATOR STRESS vs. AXIAL STRAIN
HIGH PRESSURE TRIAXIAL PGM: REMOLDED ILLITE
URI/MGL

Figure 3.2-1



HIGH PRESSURE TRIAXIAL PGM: REMOLDED ILLITE

Figure 3.2-2

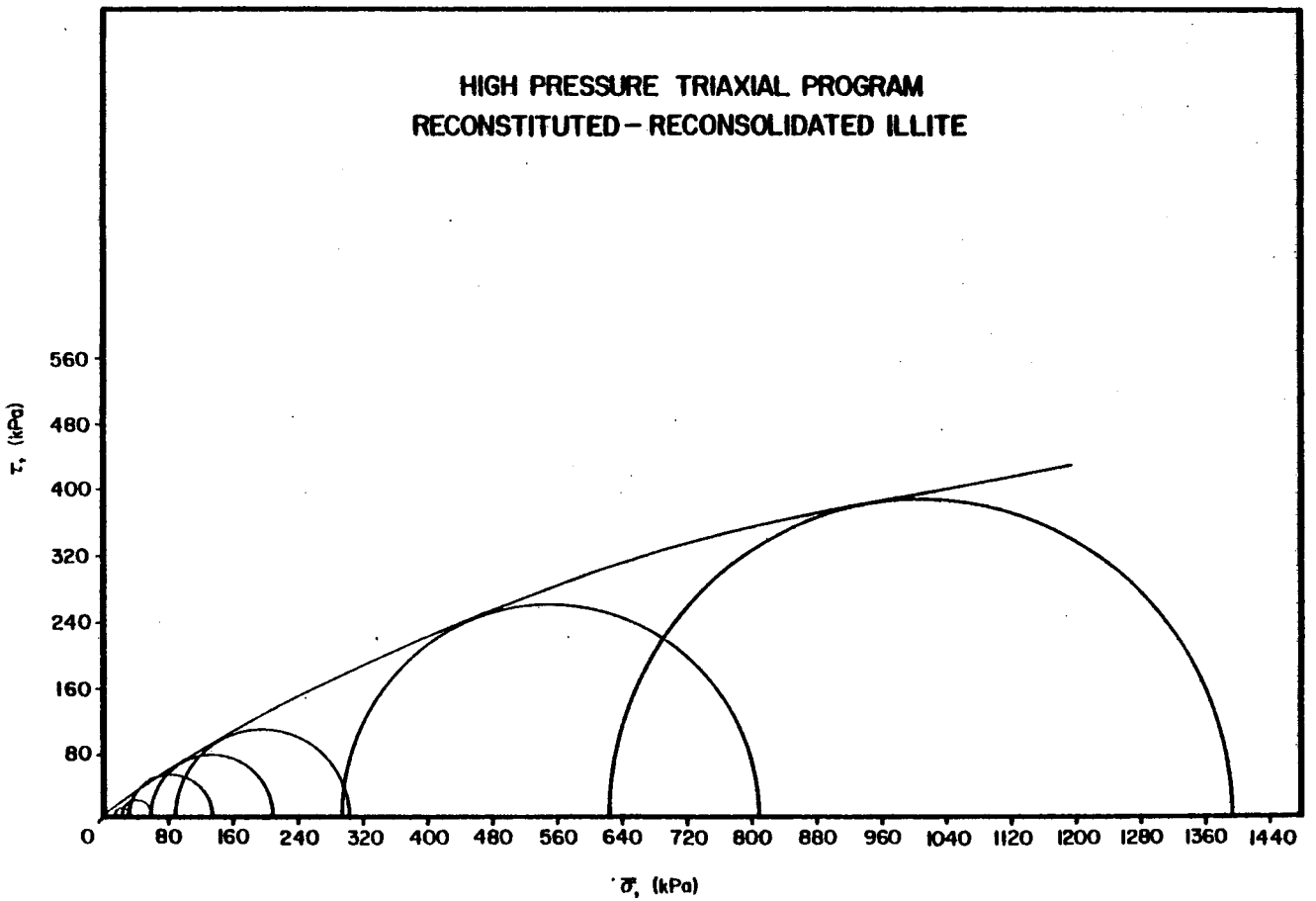
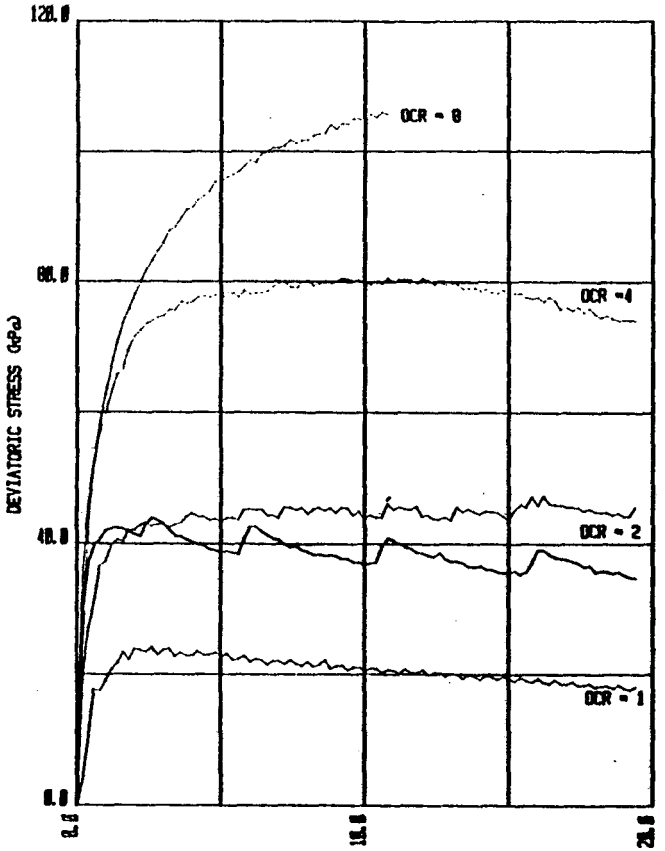


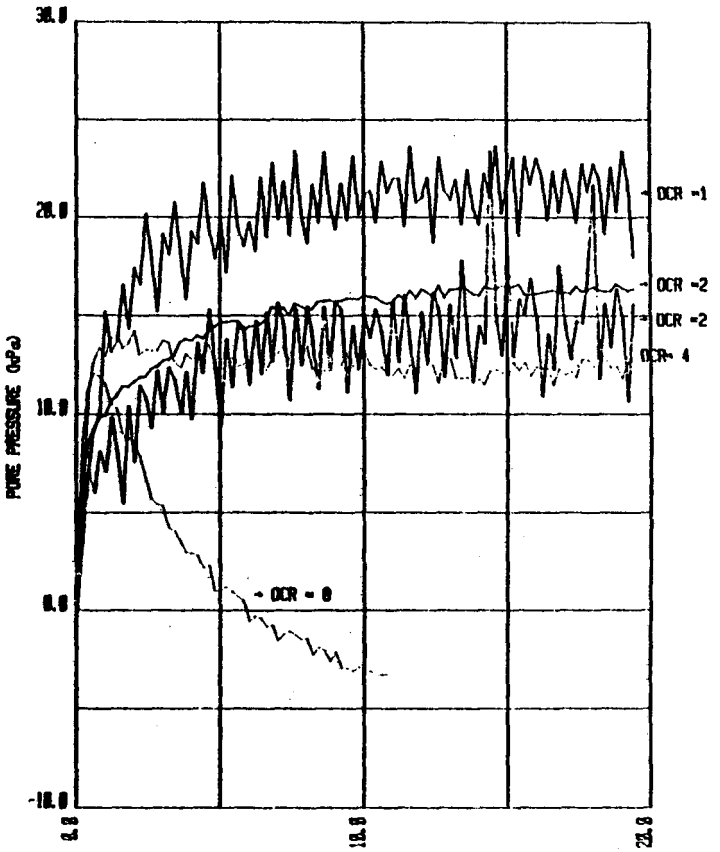
Figure 3.2-3

Mohr-Coulomb Plot



DEVIATORIC STRESS vs. STRAIN
PI-5-8, OCR SERIES
URI/MGL

Figure 3.3-1



PORE PRESSURE vs. STRAIN
PI 5-8, OCR SERIES
URI/MGL

Figure 3.3-2

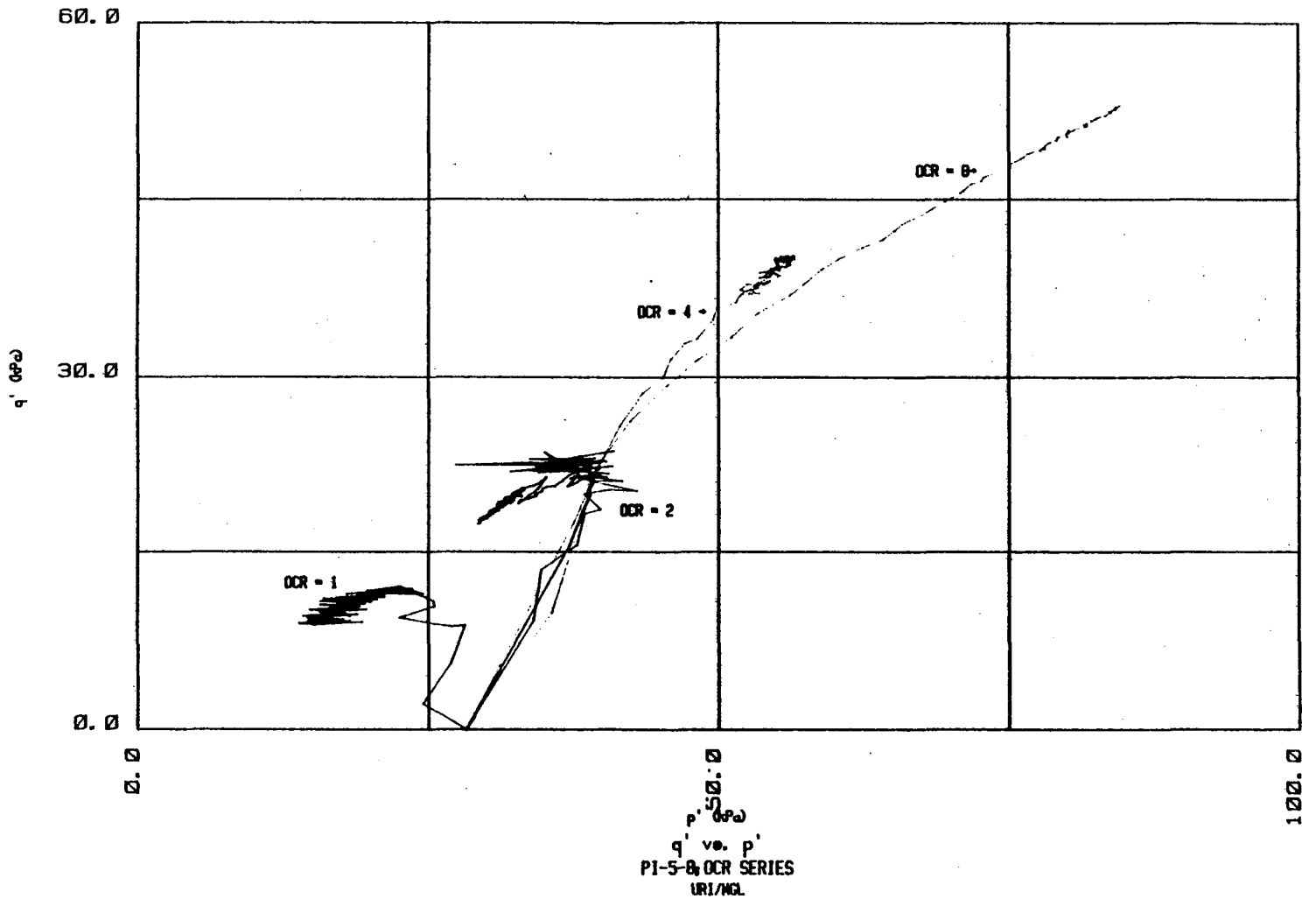

60.0
30.0
0.0
q' (kPa)
OCR = 8
OCR = 4
OCR = 2
OCR = 1
0.0
50.0
100.0
p' (kPa)
q' ve. p'
PI-5-8, OCR SERIES
URI/MGL

Figure 3.3-3

4.0 CREEP STUDIES (W. Levy, S. Jordan)

4.1 Variable Temperature Creep Program

4.1.1 Introduction

The study of effects of temperature on creep behavior is vital to the subseabed program due to the strong temperature dependence of the creep models and the wide range of temperatures expected in the canister vicinity. This report summarizes work to date. Details can be found in the M.S. thesis by Wildman (Wildman, 1981).

4.1.2 Materials and Methods

The equipment for a variable temperature creep test consisted of a main test cell, two constant pressure cells, a volume change burette system, a temperature control system and transducers. Different main cells and temperature control systems were used for the lower temperature (4°, 23°C) and higher temperaure (75°, 150°C) tests. The lower temperature tests used the equipment from the room temperature creep program (Moran, 1981). For both tests (4° and 23°) the apparatus was placed in a temperature controlled room. The higher temperature tests used specially fabricated Hastalloy main cells which are described by Silva and Calnan (1980). The temperature of the main cell was controlled by a heating jacket and thermocouple system. The equipment has since been modified so that pressure is supplied to the system by an air compressor since it was found that the constant pressure cells were inadequate for high temperature work. Back up air and emergency power have also been added to the system.

The samples used were undisturbed Pacific illite from the gravity cores taken in MPG-1 during MARA-12 as indicated below:

Samples	Core	Deptn (cm)	Core Location
triax samples (3)	GC-28	104-150 152-162 164-174	30°20.1'N 159°59.7'W
4	GC-22	194-204	31°04.8'N 159°03.5'W
23	GC-23	102-112	31°00.5'N 159°25.2'W
75	GC-23	142-152	31°0-0.5'N 159°24.2'W

100	GC-27	158-168	31°00.5'N 159°59.7'W
150	GC-23	184-194	31°00.5'N 159°24.2'W

Since it was not possible to use only samples from one core and depth, it can be expected that variations in properties exist between test samples.

The procedure differed between the lower and higher temperature tests. The lower temperature tests were first brought to the proper temperature, then consolidated, backpressured and loaded. The higher temperature tests were backpressured, then the temperature was increased and finally the sample was consolidated and loaded. A consolidation stress of 93 kPa was applied in all tests. All tests were step loaded in the sequence 10, 20, 40, 50 and 70% of drained strength based on room temperature CIU triaxial results. All tests were conducted under triaxial, constant stress, drained conditions.

4.1.3 Results

a) 4°C Test: The 4°C sample was subjected to three loadings until it failed in creep rupture after a duration of 37 days, with an ultimate axial strain of 12.9%. As can be seen by Figure 4.1-1, the first loading seems to contain some irregular strain increase during days 2 and 3. The 20% loading is very smooth and contains no irregularities. The strain increase was slight (0.5%). The 40% loading is very linear in the preliminary stages and then shows considerable increase in strains resulting in sample failure.

Volumetric strain versus time follows the axial trends during strain jumps within the 10% loading. The 20% loading surprisingly does not show the increase in volume change usually associated with addition of load as is seen upon addition of the 40% load. Some leakage is believed to occur later during the secondary creep portion of the 40% load.

The log of strain rate versus time shows steady decreases during the 10 and 20% loads but irregular behavior under the 40% where it eventually failed.

b) 20°C Test: This test had a total duration of 98.2 days. The sample was subjected to five stress levels: 10, 20, 40, 50 and 70% with the 70% stress causing failure (Figure 4.1-2). The 10 and 20% loadings each showed an initial increase during primary loading, then secondary creep. For the 40% stress level it seems as though two loadings occurred on both axial and volumetric plots. The 50% load was again very regular though during this time a leak in one of the lines developed. Application of the 70% load resulted in the almost immediate failure of the sample.

The strain rate with time for each load show distinct decreasing trends in the strain rate after applications of each load. The intermediate strain increase during the 40% loading shows signs of the above mentioned strain increase though not as large as for an actual loading.

c) 75°C Test: This test lasted only 13 days during which the sample eventually failed under the 10% loading. In this test unusual jumps in both axial and volumetric strain are seen which are difficult to explain (Figure 4.1-3). There were no obvious problems with the equipment which would explain the irregularities. The strain rate versus time plot again points to unstable behavior, not exhibiting the steady decreasing trends observed in the 4 and 20° test.

d) 100°C Test: At the time of this writing (Dec., 1981) a 100°C test is in progress using the same test procedures as in the 75°C and 150°C tests. It has been loaded to 70% stress level with no appreciable change in axial strain beyond what was attained upon the 10% loading (Figure 4.1-4). This test indicated that the 75°C test may not be representative of creep behavior in this temperature range.

e) 150°C Test: Axial strain data similar to the 100° test was encountered during the 150° test. After an initial large strain the addition of the 20 and 40% load had no significant effect on either axial or volumetric strain (Figure 4.1-5). The sample was then loaded to failure in 20% stress level increments. Brittle failure occurred at 210% of drained strength. After the usual decrease after initial loading is observed in the early stages of this test, the strain rate data fluctuations are due mostly to noise in the DCDT used to measure axial deformation.

4.1.4 Discussion

Several factors prevent our making any final conclusions about the relationship between creep behavior and temperature. Some of the more significant factors are:

- Stress levels are based on room temperature drained strengths. It would be more logical to use CIU test data at identical temperatures.
- In comparing these undisturbed samples, it should be noted that pretest sample differences may have existed.
- Since this was the first time that the equipment was used, there is a distinct possibility of mechanical problems affecting the results. Problems associated with leakage are very difficult in long term testing. Temperature control during the 4°, 23°, and 150° tests was not perfect. Piston handup could be a problem at high temperature.

Some tentative conclusions that can be made are:

- Instabilities due to structural rearrangement were present in

most tests. This is similar to observations made in previous tests at room temperature (Moran, 1981).
- A possible change in creep behavior is occurring at elevated temperature.
- Step loading is a good technique in creep testing. Also, measurements of volume change versus temperature increase show the increased and predicted volume changes to coincide for each high temperature test. Thus, after temperature increases, it is possible to assume that these samples were at approximately the measured initial volume, since all volume change measured was due strictly to the expansion of water under temperature.

Further testing is recommended with these changes:

- Use remolded deep sea samples to minimize differences in initial conditions.
- Temperature should be applied after backpressuring and consolidation.
- Tighter temperature and measurement control should be effected. Each step load should be shorter in duration.

4.2 Long Term Drained Uniaxial Test

4.2.1 Introduction

A long term drained uniaxial test was initiated on an MPG-I sediment sample in an effort to examine the secondary compression (creep) behavior for various water contents and applied effective stresses. The results can be used to compare with existing triaxial (2-D) creep data currently entered into creep models developed by others for the SDP. In addition, the results will aid in the analysis of secondary compression (settlement) of the ISHTE platform (see ISHTE annual report).

4.2.2 Methods and Materials

A long-term test was set-up and conducted according to ASTM procedure D 2435-70 (one-dimensional consolidation) with the following exception. The sample was incrementally loaded (as in a typical consolidation test) to a stress approximately equal to the in situ effective overburden stress ($\approx$ 2.2 kPa). At that stress and all subsequent applied stresses the specimen is allowed to experience secondary compression for a minimum of 50,000 min (35 days) before the next load is applied. Axial strain vs. time readings are recorded at appropriate intervals to properly define the strain rate function.

The sample selected for this test is an undisturbed illite from the MARA-12 cruise, Core GC-22 at a depth of 48-52 cm. Classification data for this sample are:

ω	= 117%	ω_p	= 35%	A	= 0.6
ω_L	= 96%	G_s	= 2.77	I_L	= 1.28

Atterberg limit data incorporated onto a plasticity chart (Figure 2.4-1) show the specimen to be of very high plasticity and compressibility.

4.2.3 Results

Figure 4.2-1 is a composite plot of axial strain (ε) vs. time (t) at four incrementally applied effective stresses ($\bar{\sigma}$). A small zone of primary creep (decreasing $\dot{\varepsilon}$) can be seen during the initial application of load; generally, less than 1000 min. This should not be interpreted as primary consolidation. According to Terzaghi and Peck (1948), primary consolidation occurs very quickly at low applied stresses, especially below the preconsolidation stress (which for this material is approximately 10.5 kPa). This behavior has been confirmed in many consolidation tests at URI/MGL on deep sea sediments.

Two zones of secondary creep (constant $\dot{\varepsilon}$) can be identified on each curve of constant applied effective stress. The latter being of lesser magnitude in each curve. It is suspected that a microstructural instability may have occurred between these two areas of secondary creep since this manner of behavior is precisely the same as that observed in the room temperature triaxial series (Moran, 1981).

The curve representing secondary compression under a constant effective stress of $\bar{\sigma}$ = 8.34 kPa shows a sudden jump in axial strain after approximately 17,300 min (12 days). This behavior could be attributed to the destruction of some cementation and/or interparticle bonds at the platelet contacts since this sample does lie within the surficial range of "apparently" overconsolidated sediments as discussed in section 5.0. Also, it is noted that this stress (8.34 kPa) is approaching the preconsolidation stress (approximately 10.5 kPa).

4.2.4 Analysis

Table 4.2-1 lists the applied effective stresses ($\bar{\sigma}$) initial water contents (ω_i) (end of primary consolidation but, before secondary compression) and both stages of secondary creep ($\dot{\varepsilon}_i$ and $\dot{\varepsilon}_f$) as well as some pertinent classification data. It appears that the magnitude of strain rate in the first region of secondary creep is relatively unaffected by the applied effective stress. However, except for the higher stress condition, the second region shows an increase in strain rate with $\bar{\sigma}$. The sudden jump in axial strain for $\bar{\sigma}$ = 8.34 kPa seems to have had a significant effect on strain rate. Possibly, the effect of long term straining on cementation and/or interparticle bonding may have reduced the preconsolidation stress below 10.5 kPa and therefore the strain rates shown at the higher stress may be for a normally consolidated rather than "apparently" overconsolidated material. Continued testing on this specimen will provide data at higher stresses to further explain these preliminary results.

4.3 Long Term Drained Triaxial Creep Test

4.3.1 Introduction

Drained creep tests have been successfully completed and analysed at URI/MGL (Moran, 1981) for the SDP. These tests have provided parameters necessary for incorporation into creep models (developed through SNL for SDP) used to predict the long term behavior of the canister-sediment system. In an effort to experimentally examine long term creep properties and behavior, a drained triaxial test is underway with the intention of maintaining a constant stress for several months.

4.3.2 Methods and Materials

Equipment used in long term creep tests is the same as room temperature tests (Moran, 1981) except for some re-routing of drainage lines and an extra sample membrane (3 total).

The test procedure involved back-pressuring the sample first, then consolidating to an effective stress of 93.1 kPa (13.5 psi). Deviatoric loading was then applied at a selected stress level and maintained during the duration of the test. For this test, a stress level of 25% (63.4 kPa) of drained failure strength was attained in one increment. The automatic data acquisition records cell pressure, back-pressure and axial displacement hourly. Volume change is entered by hand daily and values of axial, lateral, and volumetric strain are computed daily in order to make appropriate load adjustments for maintaining a constant stress condition.

The sample selected for this test (designated as UI-8) is an undisturbed illite from the MARA-02 Cruise, Core GC-08 at a depth of 66-73 cm. Classification data for this sample are:

ω	= 111%	G_S	= 2.73
ω_L	= 86%	A	= .6
ω_P	= 40%	I_L	= 1.54

A point on the plasticity chart (Figure 2.4-1) shows this specimen as being of high plasticity and compressibility.

4.3.3 Results and Analysis

Figure 4.3-1 is a plot of axial strain ($\dot{\varepsilon}$) vs. time (t) for the long term creep test UI-8 up to 118,000 min. (82 days). A zone of primary creep (decreasing $\dot{\varepsilon}$) is seen to occur in a relatively short period of time (< 10,000 min.) Three zones of secondary creep (constant $\dot{\varepsilon}$) can be identified with minor jumps (instabilities) in axial strain occurring between them. These jumps are viewed as microstructural instabilities due to a breakdown of the material structure to a lower energy state resulting in a more stable material. The times at which the instabilities occurred coincide with sudden changes in volumetric strain shown in Figure 4.3-2. It appears a

fourth zone of secondary creep is occurring at approximately 115,000 min. (80 days), however, sufficient time has not passed to be sure.

Preliminary strain rates ($\dot{\varepsilon}$) are determined at the zones of secondary creep. It is clear that the strain rate decreases after each instability which suggests that the microstructure did move into a more stable state.

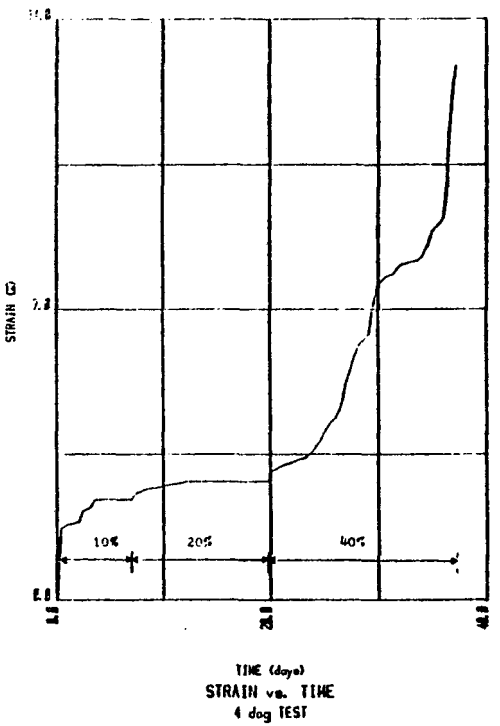
TABLE 4.2-1

Long-Term Uniaxial Creep Test

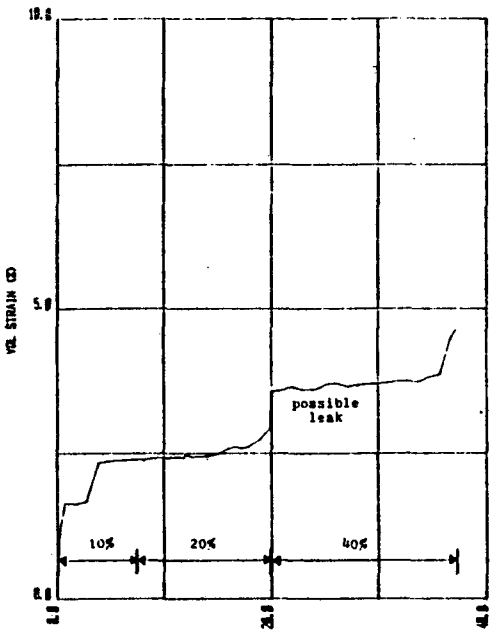
MARA-12 GC-22 48-52 cm

Stress $\bar{\sigma}$ (kPa)	Initial Water Content ω_i (%)	Initial Stage Secondary Creep $\dot{\varepsilon}_i$ (x 10^{-5}%/min)	Final Stage Secondary Creep $\dot{\varepsilon}_f$ (x 10^{-6}%/min)
2.45	116	1.40	4.02
3.92	115	1.82	5.96
5.40	114	1.57	7.80
8.34	112	1.73	3.50

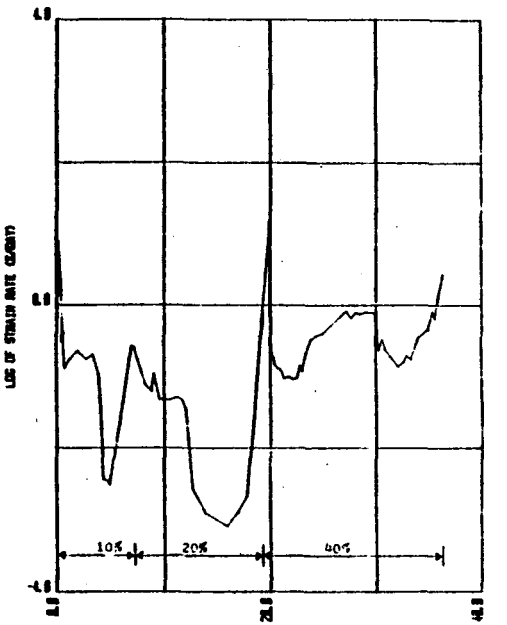
Note: $e_o = 3.23$; $G_s = 2.76$; $\omega_{i_s} = 117$ %; A = .6



STRAIN vs. TIME
4 deg TEST



VOL STRAIN vs. TIME
4 deg TEST



LOG OF STRAIN RATE vs. TIME
4 deg TEST

Figure 4.1-1

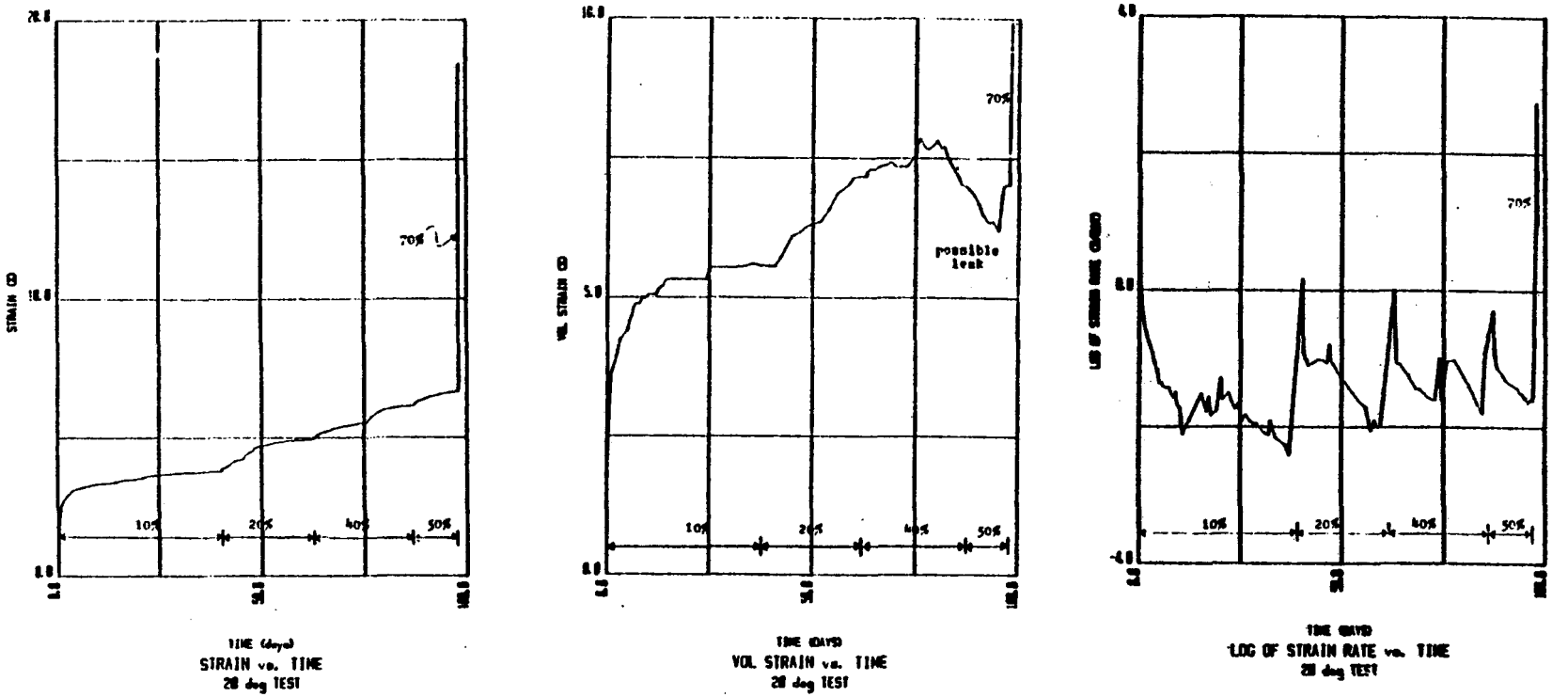
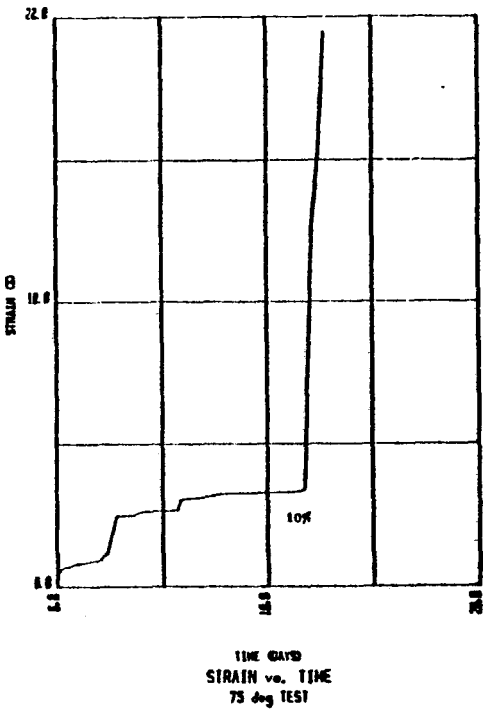
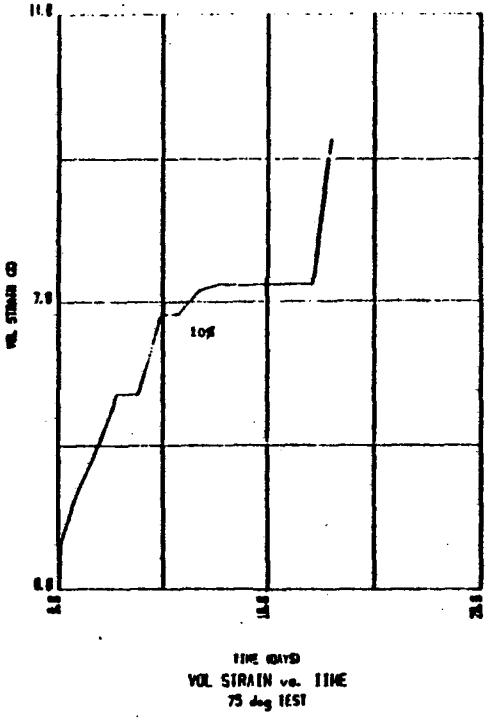

70%
10%
20%
40%
50%
STRAIN vs. TIME
28 deg TEST
70%
possible leak
10%
20%
40%
50%
VOL STRAIN vs. TIME
28 deg TEST
70%
10%
20%
40%
50%
LOG OF STRAIN RATE vs. TIME
28 deg TEST

Figure 4.1-2


22.0
10.0
0.0
10%
0.0
10.0
20.0
TIME (DAYS)
STRAIN vs. TIME
75 deg TEST


11.0
7.0
0.0
10%
0.0
10.0
20.0
TIME (DAYS)
VOL STRAIN vs. TIME
75 deg TEST

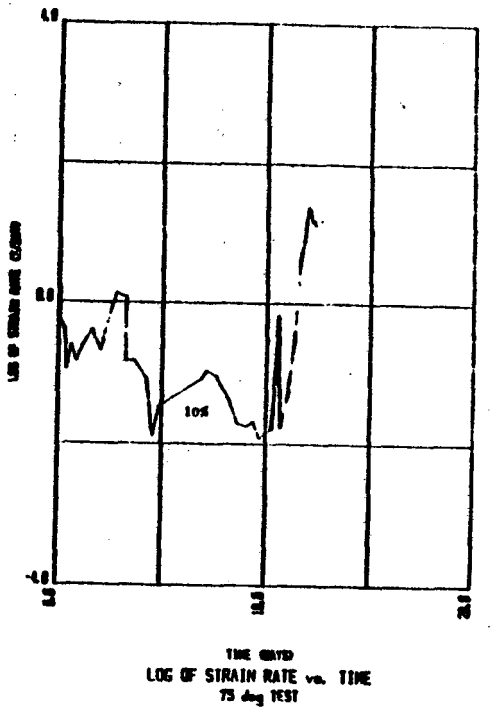
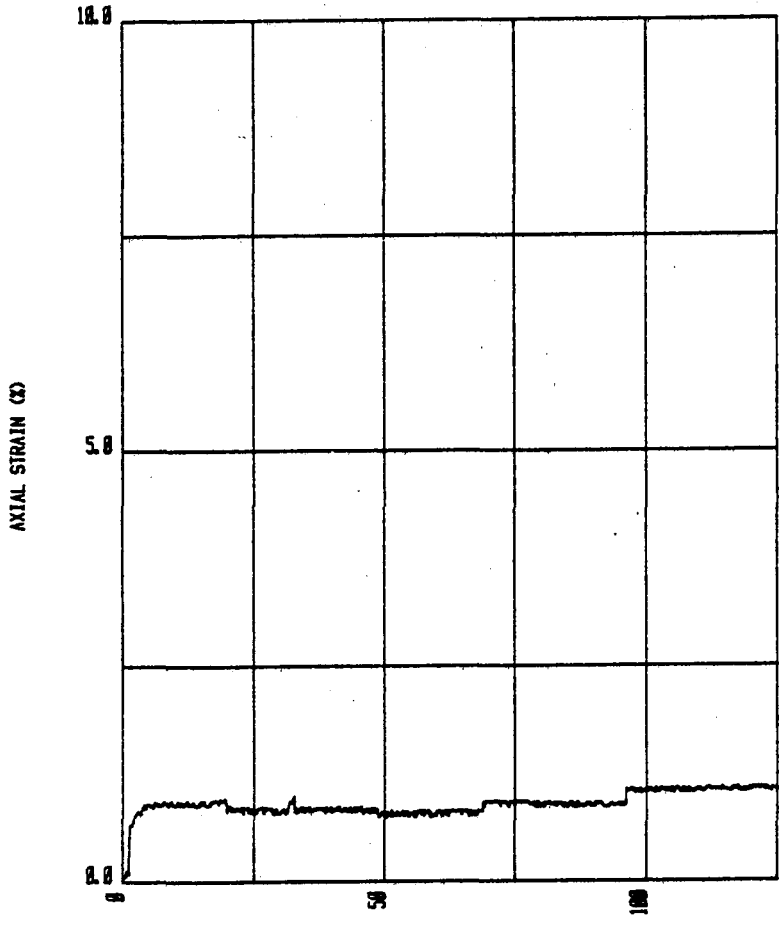

4.0
0.0
-4.0
10%
0.0
10.0
20.0
TIME (DAYS)
LOG OF STRAIN RATE vs. TIME
75 deg TEST

Figure 4.1-3



AXIAL STRAIN vs. TIME
VARIABLE TEMP. CREEP
URI/MGL

Figure 4.1-4

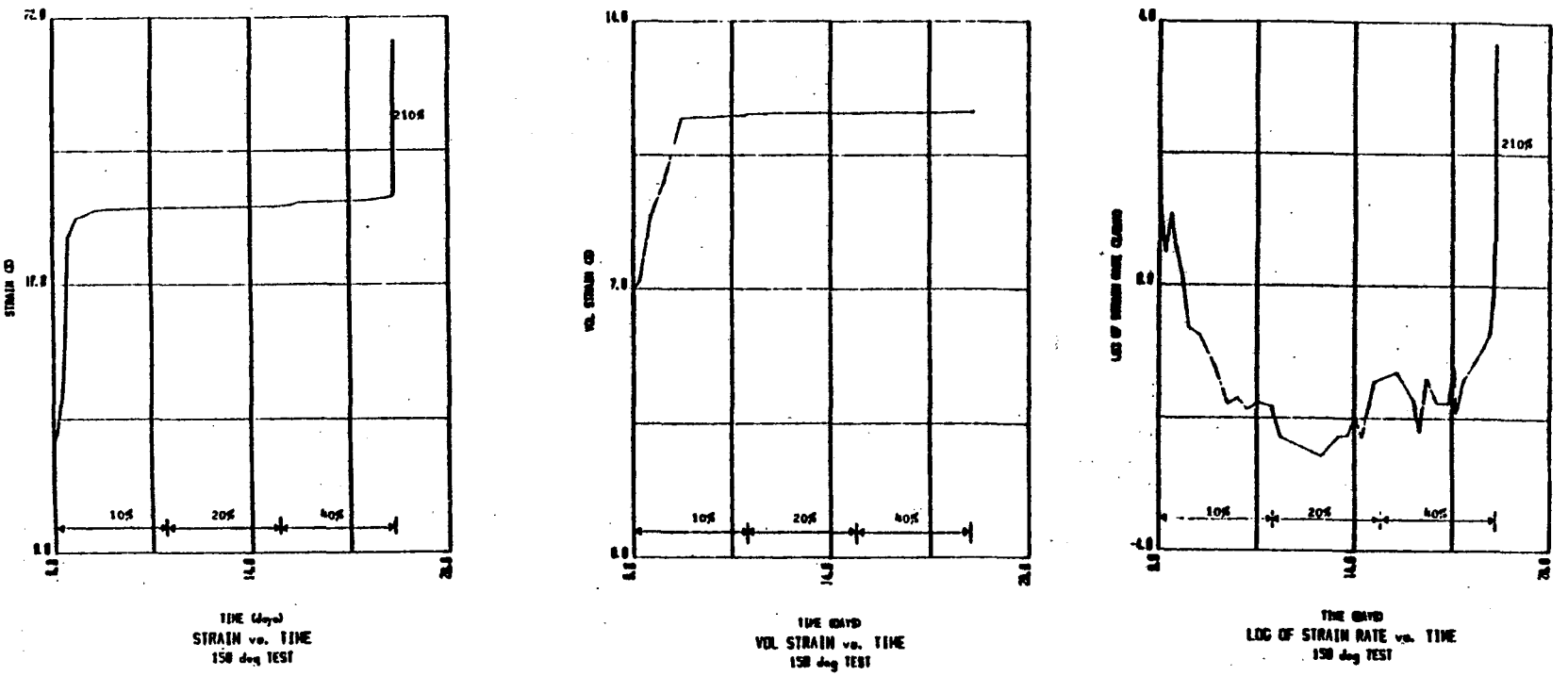
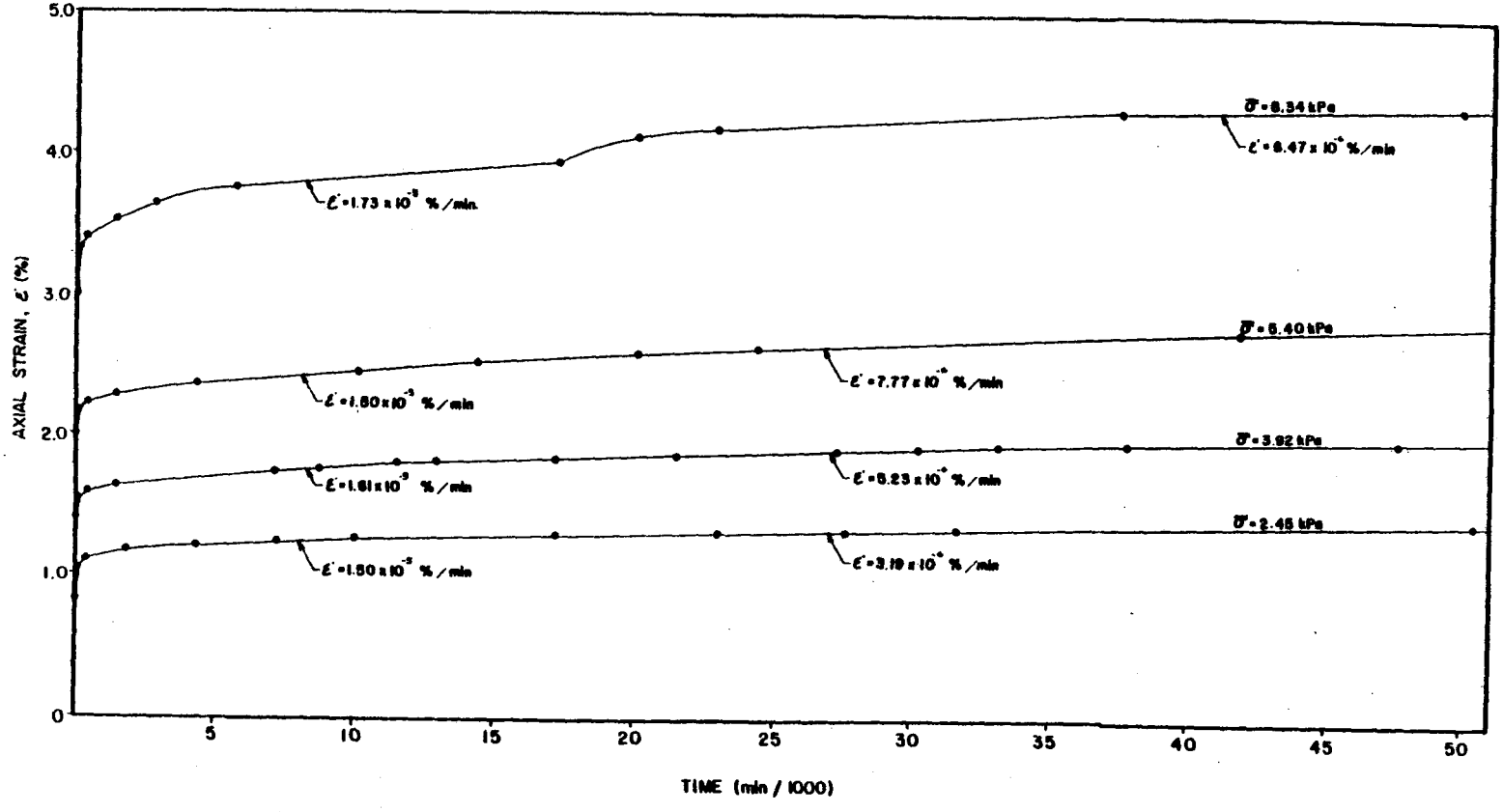

210%
10%
20%
40%
STRAIN vs. TIME
150 deg TEST
VOL STRAIN vs. TIME
150 deg TEST
LOG OF STRAIN RATE vs. TIME
150 deg TEST

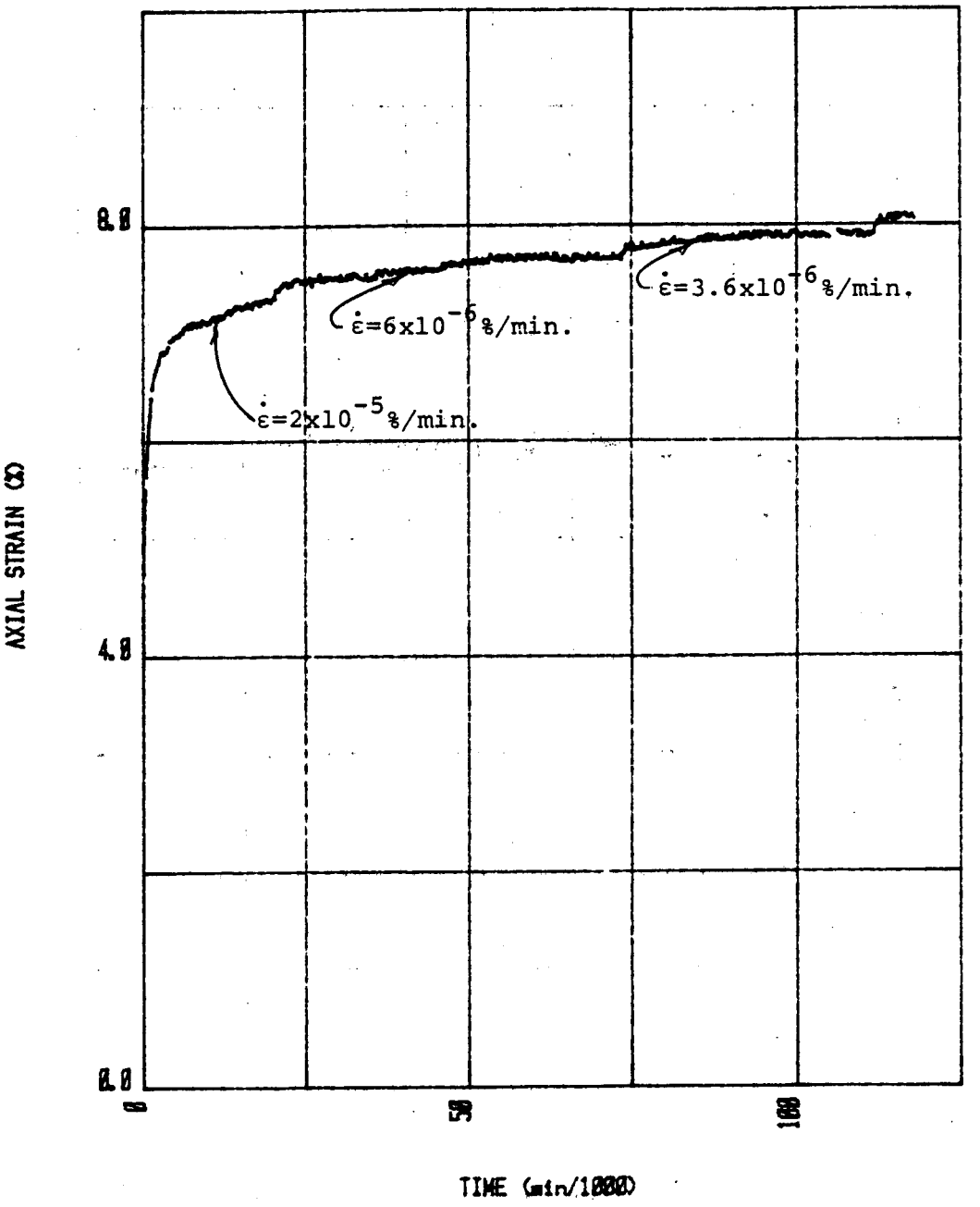
Figure 4.1-5



LONG-TERM UNIAXIAL CREEP

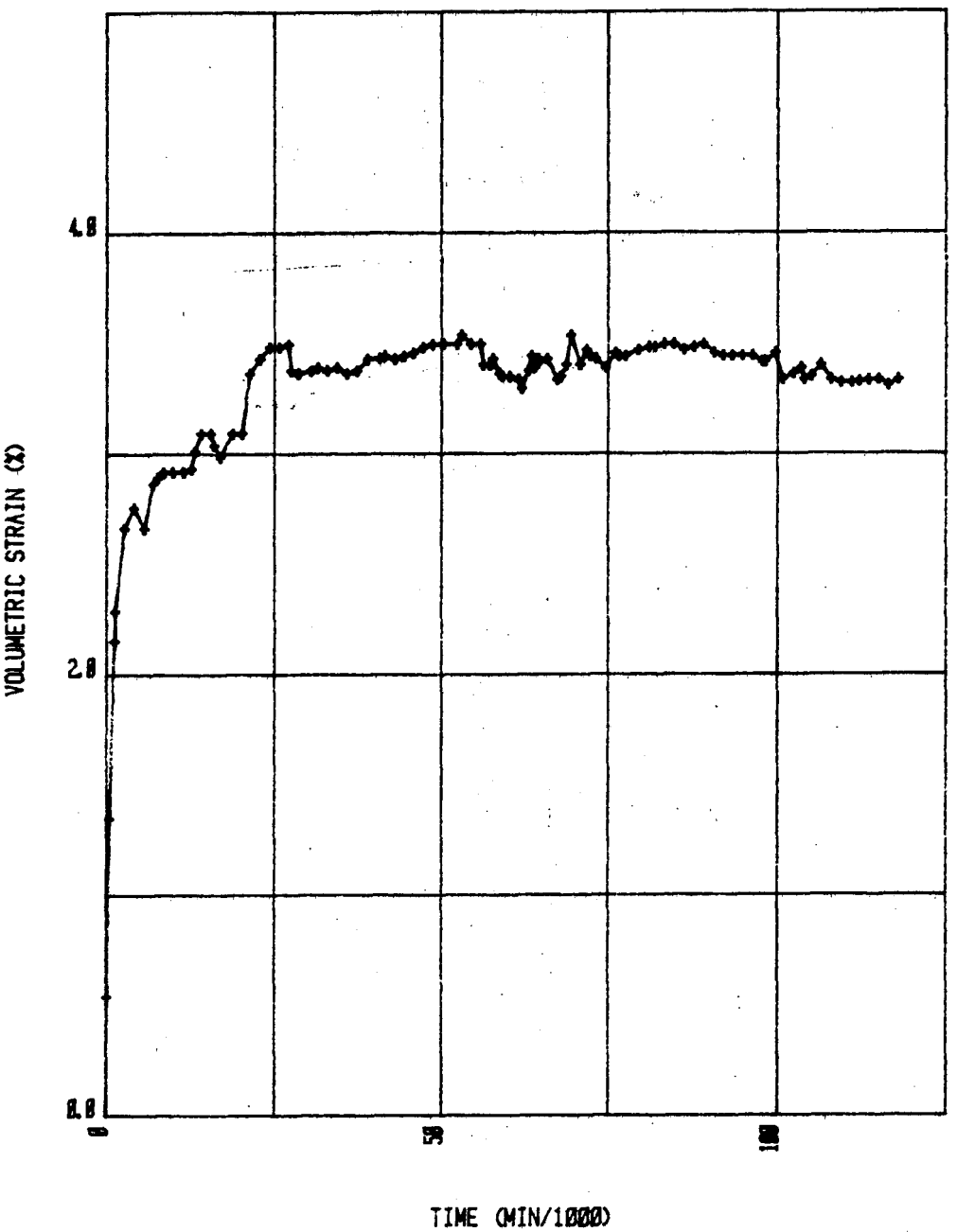
MARA 12 GC-22 48-52 cm

Figure 4.2-1



AXIAL STRAIN vs. TIME
LONG TERM, UI-8
URI/MGL
MARA-02 GC-08 66-73 CM

FIGURE 4.3-1



VOLUMETRIC STRAIN vs. TIME
UI-8, LONG TERM CREEP
URI/MGL
MARA-02 GC-08 66-73 cm

FIGURE 4.3-2

5.0 COMPRESSIBILITY STUDIES (S. Jordan, K. Dadey)

5.1 Introduction

Investigation of material compressibility is necessary to assess the stress history of the sediment column and to provide parameters used in settlement analysis related to bottom supported structures. Research for FY 81 concentrated on sediments from MPG-I North Central Pacific (MARA-02 and RAMA-01 cruises); MPG-III N, Atlantic/Abyssal Plain (Endeavor-023 and HUDSON-80016 cruises); and MPG-IV, Northwestern Pacific (VEMA-36 cruise). Tests conducted on RAMA-01 samples are of special interest in that the derived consolidation parameters are used to predict the total settlement expected during deployment of the ISHTE platform (see ISHTE annual report for details). Geographic locations of the cores from which samples were taken and tested are shown Table 2.1-1.

5.2 Test Methods

Both standard and back-pressured, one-dimensional consolidometers were used to conduct consolidation tests. Standard consolidation tests follow ASTM procedure D 2435-70 with some minor modifications. Back-pressured units provide direct pemeability measurements as well as consolidation data and are described in detail by Silva, Heatherman and Calnan (1981).

5.3 Results

5.3.1 MPG-I

Figures 5.3-1 through 5 show void ratio (e) vs. log applied stress $\bar{\sigma}_v$ plots for five tests on samples from MARA-02 and RAMA-01 cruises. Some figures contain dashed lines (due to slight testing errors such as loading plate friction) indicating the most probable path of consolidation.

Figure 5.3-1 is an e vs. log $\bar{\sigma}_v$ curve for near-surface sample (3-8 cms deep) from box core BC-20 retrieved during the RAMA-01 cruise. Box cores typically provide high quality, undisturbed samples which here is reflected by the sharp parabolic shape during initial compression and a nearly perfect straight line representing the virgin compression curve. This sample shows a very high overconsolidation ratio (OCR >>1) which will be further discussed in section 5.4.

Figure 5.3-2 is another box core specimen from the RAMA-01 cruise at a depth taken between 15 and 19 cm. Again, this curve illustrates a curve indicating an undisturbed sample. The sample also shows overconsolidation but of a lesser degree than the one at 3-8 cms.

Figures 5.3-3 and 4 are consolidation curves of large-diameter gravity core samples from the MARA-02 cruise; one being near the surface (15-20 cm) and the other also surficial but relatively deeper (162-166 cm). Both curves are of good quality. The two anomolous points near the dashed portion of Figure 5.3-3 are either due to load-plate or dial guage "hang-up". These surficial samples also show varying amounts of overconsolidation. Several cycles of decompression and recompression were applied to these samples in an attempt to examine the swelling behavior of MPG-I sediments under various initial conditions of load and void ratio. This data indicates that C_s increases with increasing $\bar{\sigma}_v$ and decreasing e.

Figure 5.3-5 is a consolidation curve of a reconstituted/reconsolidated (remolded) sediment sampled from the sediment-structure interaction testing (SSIT) tank, PI-5-8 at a depth of 30-35 cm. The overconsolidation ratio ($OCR = \bar{\sigma}_{c\ max}/\bar{\sigma}_v$) equals 1 which shows that the tank was completely consolidated. This was expected because the effective "in situ" stress ($\bar{\sigma}_v$) should equal the maximum past consolidation pressure ($\bar{\sigma}_{c\ max}$) in the SSIT tanks. In fact, OCR equaling 1 for this sample is an indication of the reliability in the use of Casagrande graphical procedure to determine $\bar{\sigma}_{c\ max}$.

5.3.2 MPG-III N

Figures 5.3-6 through 5.3-9 show e vs. log $\bar{\sigma}_v$ curves for four tests on specimens from the Endeavor-023 and Hudson-80016 cruises. Consolidation tests on HUDSON samples are being reported for the first time.

Figure 5.3-6 is a consolidation plot of an Endeavor-023 sample taken from gravity core LGC-06 at a depth of 338-343 cm. Little disturbance can be intuitively seen in this sample depicted by the clean parabolic shape during initial compression which results in a small range for determining precompression. This sample is concluded as normally consolidated which does agree with data previously reported on the same material at comparable depths (Silva, Jordan and Levy, 1981 and Silva and Calnan, 1980).

Figures 5.3-7, 8 and 9 represent three e vs. log $\bar{\sigma}_v$ curves of HUDSON cruise sediment sampled from a box core (BC-03, 31-35 cm) and standard piston core (PC-01; 1048-1052 cm and 1057-1061 cm), respectively. The box core sample (Figure 5.3-6) is of good quality with some disturbance and shows significant "apparent" overconsolidation. The other two curves (piston core) show a considerable amount of disturbance, especially the shallower one (1048-1052 cm). Therefore, the range of precompression is quite high. The arrow on these plots points to an estimated single value of preconsolidation from which OCR can be determined. The OCR values are surprisingly low indicating a condition of underconsolication occurring at these depths. Even using the upper limit of range in preconsolidation to find OCR, the implication of underconsolidation is clear. This phenomenon will be furtner discussed in sections 5.4.

5.3.3 MPG-IV

Presented in this sub section is a summary of work completed on N.W. Pacific (MPG-IV) samples during FY 81. More detail may be found in the Master of Science thesis by G. Walker (1981). Contained within the text of this report are representative examples of consolidation plots for the three locations; the remainder of graphs are located in the addenda.

Twelve samples from location E_2 were tested. The plot for PC 51, 1211-1215 cm (Figure 5.3-10) shows a sample of good quality and significant overconsolidation. Another sample at nearly the same depth (PC 48, 1247-1251 cm, Figure 5.3-11) is seen to be disturbed and indicates a normally consolidated sediment.

Six tests were performed on samples from two cores in location B_1. One from PC 45, 893-877 cm (Figure 5.3-12) displays a curve parabolic shape during initial compression, suggesting a sample of high quality and little disturbance. This sample shows significant underconsolidation with an OCR of 0.6. Graphs of the other two, both from PC 43, at 117-121 cm (Figure 5.3-13) and 468-472 cm (Figure 5.3-14) are of a lower quality, probably due to disturbance of the samples. The shallower sample shows significant apparent overconsolidation (OCR=5.2) while the deeper one is normally consolidated.

Of the six samples from location C_1, five were above 5 meters. Two, taken from gravity cores show fairly good plots; indicative of relatively undisturbed samples (Figures 5.3-15 and 16). Both show apparent overconsolidation; the surficial one, GC 39, 17-21 cm having an OCR of 18 and the deeper one, GC 36, 133-137 cm an OCR of 9.7.

5.4 Analysis, Conclusion and Comparisons

5.4.1 MPG-I

Table 5.4-1 is a summary of compressibility results obtained during FY'81. The type of consolidometer used for a particular test is indicated by an S (standard) or B-P (back-pressured) under the abbreviated heading for apparatus. The table shows compression index (C_c) values to be considerably less for the RAMA-01 box cores compared to the gravity cores of MARA-02. However, normalized C_c (with respect to void ratio) reveal little difference in the compressibility of the surficial sediments. This is an indication of the homogeneity in MPG-I. Figure 5.4-1 is a plot of compression index vs. depth for all compresibility testing (to date) on MPG-I sediments with the new data indicated by a special symbol. The new box core data fits in well but does extend the variability somewhat. The remaining C_c results agree quite well with previous data. It should be noted that the significant increase in C_c with depth is a direct result of the increasingly higher concentrations of smectite mineral with depth (Silva and Calnan, 1980) which is known to result in higher compressibilities.

The remolded sample shown in Table 5.4-1 possesses a compression index approximately the same as the undisturbed material (Figure 5.4-1). Generally, an undisturbed material that is disturbed by remolding and subsequently tested would show a compression index significantly lower. It is hypothesized that the method of reconstituting-reconsolidating and thixotropic behavior prior to testing resulted in a material similar to the undisturbed case.

The magnitude of swelling index (C_S) listed in the Table 5.4-1 is not significantly different between samples, however, averaged values were determined for the MARA-02 specimens because decompression/recompression occurred several times. As discussed in the previous section (5.3), these samples were used to assess the one dimensional swelling behavior of MPG-I sediments. Referring to Figures 5.3-3 and 4 the following points are suggested. Schmertmann (1955) states that there exists a unique void ratio (.42 e_0) in clay materials of the same mineral type regardless of the initial conditions; such as initial void ratio and consolidation state. A unique void ratio does occur for these two tests at approximately $\bar{\sigma}_V$ = 1000kPa ($e \simeq 1.3$). Also, clay specimens of the same mineral type should show increasing swell indexes (C_S) with increasing effective consolidation stress and decreasing void ratio. Here, the swelling index not only increases with decreasing void ratio for both samples but a combination of the two curves (providing eight different initial conditions before swell) follow the same trend. In terms of stress-strain behavior, these results point out that the unloading modulus is not a constant. These observations further support the conclusion that MPG-I sediments are essentially homogeneous.

Table 5.4-1 summarizes the overconsolidation ratios for the various tests. Previous annual reports have indicated "apparent" overconsolidation primarily in the surficial sediments (upper 3 meters). The new results support this conclusion. The "apparent" overconsolidation is a result of cementation and/or high interparticle bonding at the points of platelet contact which restricts consolidation due to overburden. Figure 5 4-2 is an illustration of OCR vs. depth of all compressibility tests completed to date. Here, the indication of "apparent" overconsolidation is quite clear to a point where the curve becomes asymptotic to the seafloor.

5.4.2 MPG-III N

Table 5.4-2 lists all the compressibility results obtained during for FY'81 on Atlantic/Abyssal Plain (MPG-III N) sediments. As in the previous table for MPG-I sediments, the appropriate consolidometer used is noted. Compression index (C_C) results show a high value (1.2) for the Endeavor sample. This was not unexpected because results previously reported (Silva and Calnan, 1980) for EN-023 core LGC-06 showed higher plasticity and compressibility than HUDSON samples. Compression index values for the HUDSON sediment show some variability. However, normalized results indicate that the material is similar.

The overconsolidation ratios (OCR) shown in the table present some interesting findings. The normal (OCR=1.0) consolidation for the EN sample is in agreement with previous testing on similar material. The HUDSON box core sample implies "apparent" overconsolidation in the surficial material which is in agreement with previous results and is attributed to cementation and/or high interparticle bonding. However, as discussed in the results section, underconsolidated material was found in the HUDSON piston core PC-01 at depths averaging 1050 and 1059 cm. Several contributing factors to this phenomonem are suggested below.

A combination of factors such as upward gradients, "apparent" overconsolidation of the upper few meters, high sedimentation rates, and low permeabilities can induce under-consolidation of the sediment column. The phenomenon of hydraulic gradients due to thermal gradients can cause an upward fluid flow which would restrict full consolidation and contribute to some portion of the underconsolidation indicated by our data. Cementation and high electrical interparticle bonding is most likely the cause of the pseudo-overconsolidation in the surfical sediments of MPG-III N. It has been hypotnesized (Silva et al., 1976) that the existence of a zone of "apparent" (pseudo) overconsolidation could contribute to a reduction of the consolidation process in the deeper due to the longer drainage path imposed on the system. Additional compressibility tests are scheduled at intermediate depths during FY'82 to help assess this possibility. High sedimentation rates in combination with low permeability would certainly tend to generate underconsolidation in the deeper sediments. High sedimentation rates (≈ 22cm/1000 yrs.) have been recognized in this area (Vilks, personal communication) nowever, analyses in similar depositional areas displaying underconsolidation reveal that even greater sedimentation rates are required (than acknowledged here) to bring about OCR values of these low magnitudes.

With the available data it is impossible to determine the exact magnitude and cause of underconsolidation in this area. However we feel that there are definite indications of significant consolidation which must be properly considered in the context of the SDP. We feel that additional experimentation is warranted and the system should be modeled to determine the effects on water migration.

5.4.3 - MPG-IV

Based on our analyses, (section 2.3) nearly all cores in the N.W. Pacific (MPG-IV) area had sediment loss. Consequently, values calculated for existing overburden pressure ($\bar{\sigma}_o$) and overconsolidation ratio tend to be greater than they truly are. Corrected values are reported on all consolidation plots and in Tables 5.4-3 through 5.4-5. The method of water content profile matching (Method I, Table 2.3-9) was utilized to determine correct depths. Dashed lines indicate cores for which corrected depths and OCR's are not available. Because of the many uncertainties associated with coring results and possible sample disturbance, it is difficult to draw any definitive assessment concerning the stress history of these areas. However, some observations and tentative conclusions are offered.

In location E_2, it appears that all but one sample exhibit overconsolidation (see Table 5.4-3). Based on the high overconsolidation ratios for the deeper samples (except in PC 48) it seems that the sediment column is overconsolidated. Although cementation is a possible explanation, we do not feel this is probable. Compression indices (C_c), averaging over 2.3, fall into the range predicted for Pacific smectites (Silva and Calnan, 1979). However, the Atterberg limits for these cores are lower (see section 2.3-3), and more similar to those of illite (Mitchell, 1976). Further, there is no consistent relationship between C_c and depth, this variance suggesting a changing mineralogy.

The higher C_c values in PC-43 of Location B_1 (see Table 5.4-4) indicate a different mineralogy than for PC-45. The relatively constant values within each core however, imply that each core is fairly homogeneous. In general, these compression indices resemble those of Pacific illites (Silva and Calnan, 1979). The low C_c value at the shallowest depth, 117-121 cm, in PC-43 may to be caused by a different mineral type. On the other hand, greater than normal overconsolidation ratios at depths of approximately twelve meters imply erosion as a cause, although other evidence of this is present. Another anomaly, the underconsolidated sample at 893-897 cm in PC-45 is also unexplainable by other properties.

All samples from Location C_1 exhibited overconsolidation, including the single deep sample (PC 34, 1125-1129 cm). In fact, the OCR'S are abnormally high, even as compared with hose from Locations E_2 and B_1, suggesting the occurence of erosion or mass wasting.

All three of the locations show some extent of overconsolidation at depth. Possible explanations include underestimation of sediment loss, incorrect determination of preconsolidation stress ($\bar{\sigma}_c$), the existence of abnormally strong bonds or cementation which would inhibit consolidation or actual removal of overburden.

The major difference between compressibility of the MPG-IV and MPG-I areas is that the N.W. Pacific cores exhibit overconsolidation as deep as 13 meters, while those from MPG-I are normally consolidated below 5 meters. The small number of tests performed on MPG-III N samples make a real comparison impossible.

5.4 Future Work

As part of our FY'82 tasks, URI/MGL will provide a compressibility report involving all testing on MPG-I sediments. Limited additional testing on selected samples may be required to supplement existing data. In addition, several selected specimens will be tested from HUDSON cruise cored sediments discussed in an effort to assess the underconsolidation phenomenon in Sections 5.2 and 5.3. Limited testing will be performed on samples from the VEMA cruise to further characterize the three areas.

TABLE 5.4-1

SUMMARY OF CONSOLIDATION TESTS RESULTS, MPG-I

CRUISE	CORE NO.	DEPTH (cm)	TYPE OF APPAR.	INIT. VOID RATIO e_o	COMPRESS. INDEX C_c	NORMALIZED COMP. INDEX $C_c / 1 + e_o$	SWELL INDEX C_s	MAX. EFFECT PRECONSOL. $\bar{\sigma}_{c\ max}$ (kPa)	OVERCONSOL RATIO OCR
RAMA-01	BC-20	3-8	S	2.76	.53	.14	.05	6.5	30.1
		15-19	B-P	2.56	.46	.13	-	7.2	10.4
MARA-02	GC-08	15-20	S	3.02	.86	.17	.06	12.8	17.5
		162-166	S	2.96	.71	.17	.08	8.6	1.1
REMOLDED	PI-5-8	30-35	S	3.01	.85	.21	.07	24.9	1.0

TABLE 5.4-2

SUMMARY OF CONSOLIDATION TESTS RESULTS, MPG-III N

CRUISE	CORE NO.	DEPTH (cm)	TYPE OF APPAR.	INIT. VOID RATIO e_o	COMPRESS. INDEX C_c	NORMALIZED COMP. INDEX $C_c/1+e_o$	SWELL INDEX C_s	MAX. EFFECT PRECONSOL. $\sigma_{c_{max}}$ (kPa)	OVERCONSOL. RATIO OCR
EN-23	LGC-06	338-343	S	2.91	1.2	.31	.15	14.2	1.0
HUDSON	BC-02	31-35	S	2.54	.75	.21	.04	14.9	9.1
	PC-01	1048-1052	B-P	3.02	.87	.22	.18	13.2	.21
		1057-1061	S	2.31	.67	.20	.26	21.5	.36

TABLE 5.4-3

CONSOLIDATION RESULTS

VEMA 36-12

LOCATION E_2

CORE	DEPTH (cm)	$\frac{\Delta P}{P}$	C_c	C_s	$\bar{\sigma}_{c_{max}}$ kPa	$\bar{\sigma}_v$ kPa	OCR	DEPTH (cm)	$\bar{\sigma}_v$ kPa	OCR
PC 46	902-906	0.5	2.19	0.11	79	36	2.2	1052-1056	41.4	1.9
PC 47	885-889	0.5	2.30	0.08	97	35	2.8	1050-1054	41.0	2.4
PC 48	570-574	0.5	1.77	0.10	68	21	3.2	765-769	28.0	2.4
	1247-1251	0.5	2.83	0.19	65	60	1.1	1442-1446	67.0	1.0
PC 49	186-190	0.5	3.70	0.22	14	4.8	2.9	296-300	8.2	1.7
	368-372	0.5	1.37	0.16	22.5	10.7	2.1	498-502	14.1	1.6
	1176-1180	0.5	1.61	0.10	51	35	1.5	1286-1290	38.4	1.3
PC 51	115-119	0.5	2.17	0.11	20	3.5	5.7	365-369	12.5	1.6
	446-470	0.5	2.22	0.11	41	14.4	2.8	716-720	23.4	1.7
	1050-1054	0.5	2.60	0.23	91	31.7	2.9	1300-1304	40.7	2.2
	1211-1215	0.5	3.09	0.15	98	36.4	2.7	1461-1465	45.4	2.2
	1224-1228	0.5	3.31	0.18	88	37	2.4	1474-1478	46.0	1.9
GC 53	9-13	1.25†	2.40	0.07	18.6	0.4	49	29-33	1.1	17
	160-164	1.25†	1.91	0.10	17.5	5.8	3.0	180-184	6.5	2.7
	172-176	0.5	1.64	0.06	25.0	6.2	4.0	192-196	6.9	3.6

* Depths corrected from water content profile comparisons.

† Rate applied before $\bar{\sigma}_c$. Rate was 0.5 after $\bar{\sigma}_c$.

TABLE 5.4-4

CONSOLIDATION RESULTS

VEMA 36-12

LOCATION B_1

CORE	DEPTH (cm)	$\frac{\Delta p}{P}$	C_c	C_s	$\bar{\sigma}_{c_{max}}$ (kPa)	$\bar{\sigma}_v$ (kPa)	OCR	DEPTH (cm)	$\bar{\sigma}_v$ (kPa)	OCR
PC 43	117-121	0.5	1.24	0.06	21	4	5.2	--	-	-
	468-472	0.5	1.93	0.08	15	14.5	1.0	-	-	-
	845-849	0.5	1.80	0.09	60	26.5	2.3	--	-	-
	1188-1192	0.5	1.82	0.10	82	35	2.3	--	-	-
PC 45	429-433	1.0	1.10	0.09	25	16	1.6	499-503	18.6	1.3
	893-897	1.0	1.14	0.08	20	33.5	0.6	963-967	36.1	0.6
	1242-1246	1.0	1.17	0.07	90	45.5	2.0	1312-1316	48.1	1.9

* Depths corrected from water content profile comparisons.

TABLE 5.4-5

CONSOLIDATION RESULTS

VEMA 36-12

LOCATION C_1

CORE	DEPTH (cm)	$\frac{\Delta p}{p}$	C_c	C_s	$\bar{\sigma}_{c_{max}}$ (kPa)	$\bar{\sigma}_v$ (kPa)	OCR	DEPTH (cm)	$\bar{\sigma}_v$ (kPa)	OCR
PC 34	1125-1129	0.5	1.74	0.12	100	37.6	2.7	-	-	-
PC 35	408-412	1.0	2.90	0.12	100	14.6	6.8	498-502	17.5	5.7
GC 36	133-137	0.5	1.61	0.09	50	5.2	9.7	-	-	-
	251-255	0.5	1.78	0.12	18.5	9.3	2.0	-	-	-
GC 39	17-21	0.5	1.36	0.06	22	0.6	36	37-41	1.2	18.0
	255-259	0.5	0.92	0.06	17	9.5	1.8	275-279	10.2	1.7

* Depths corrected from water content profile comparisons.

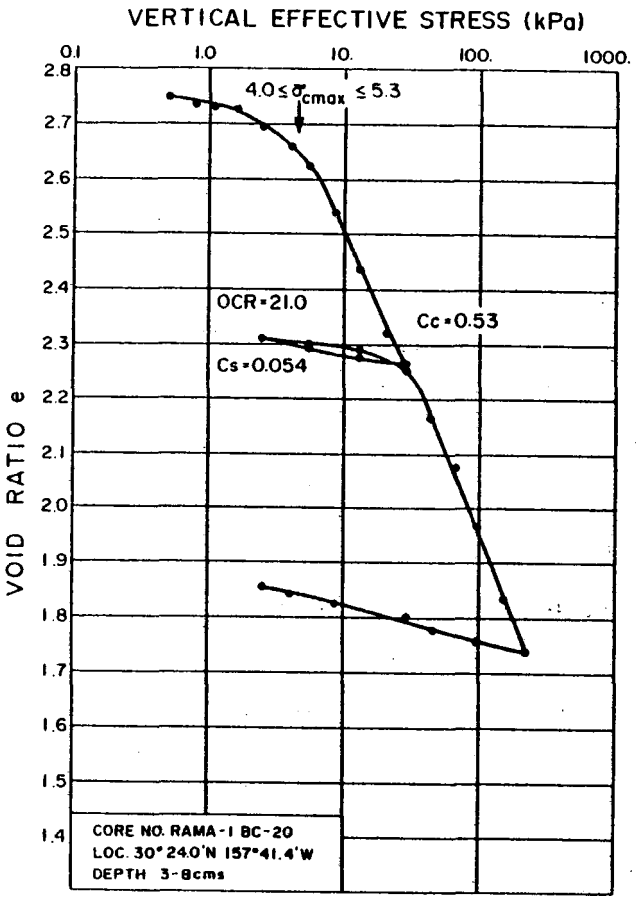


Figure 5.3-1

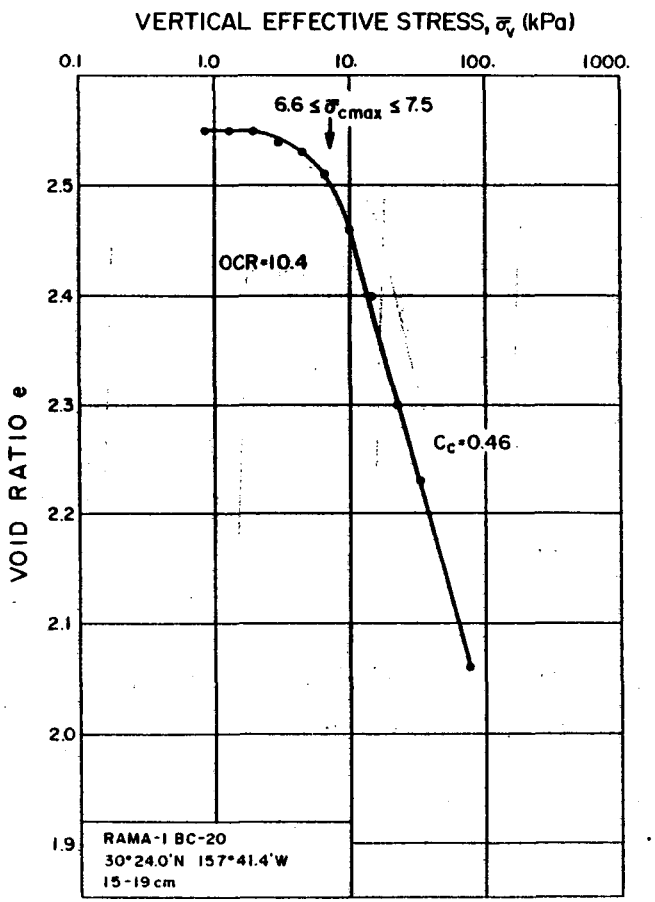


Figure 5.3-2

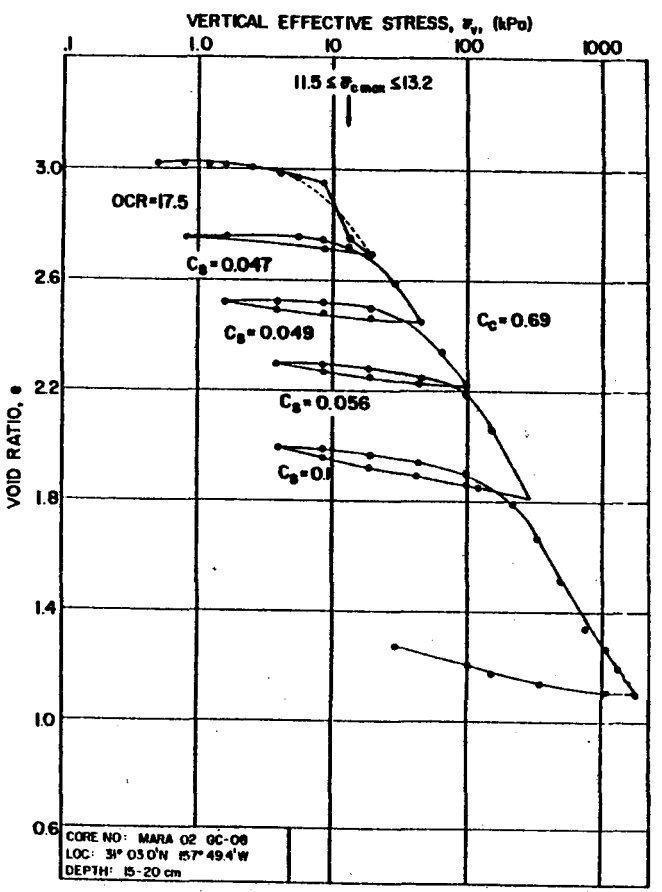


Figure 5.3-3

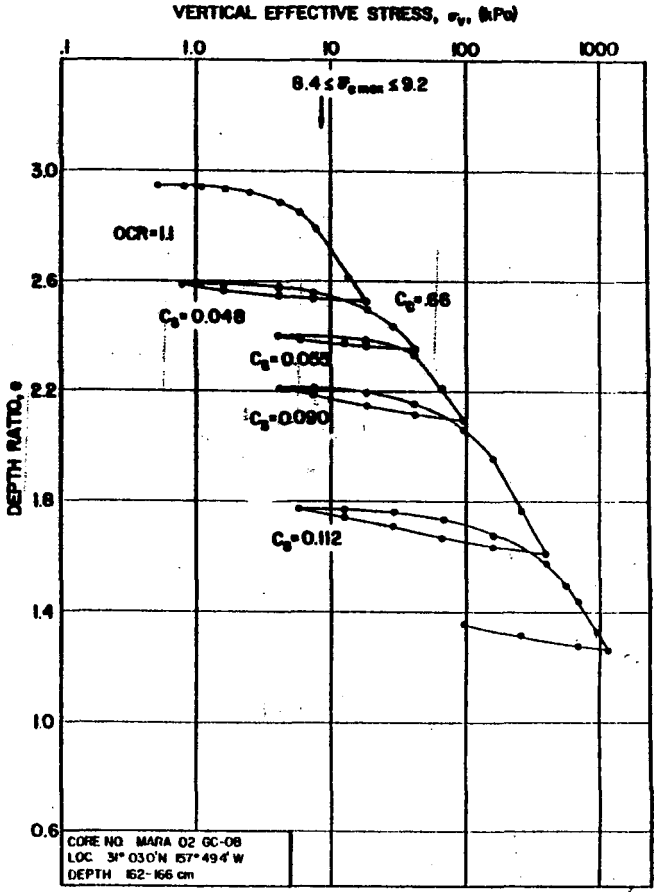


Figure 5.3-4

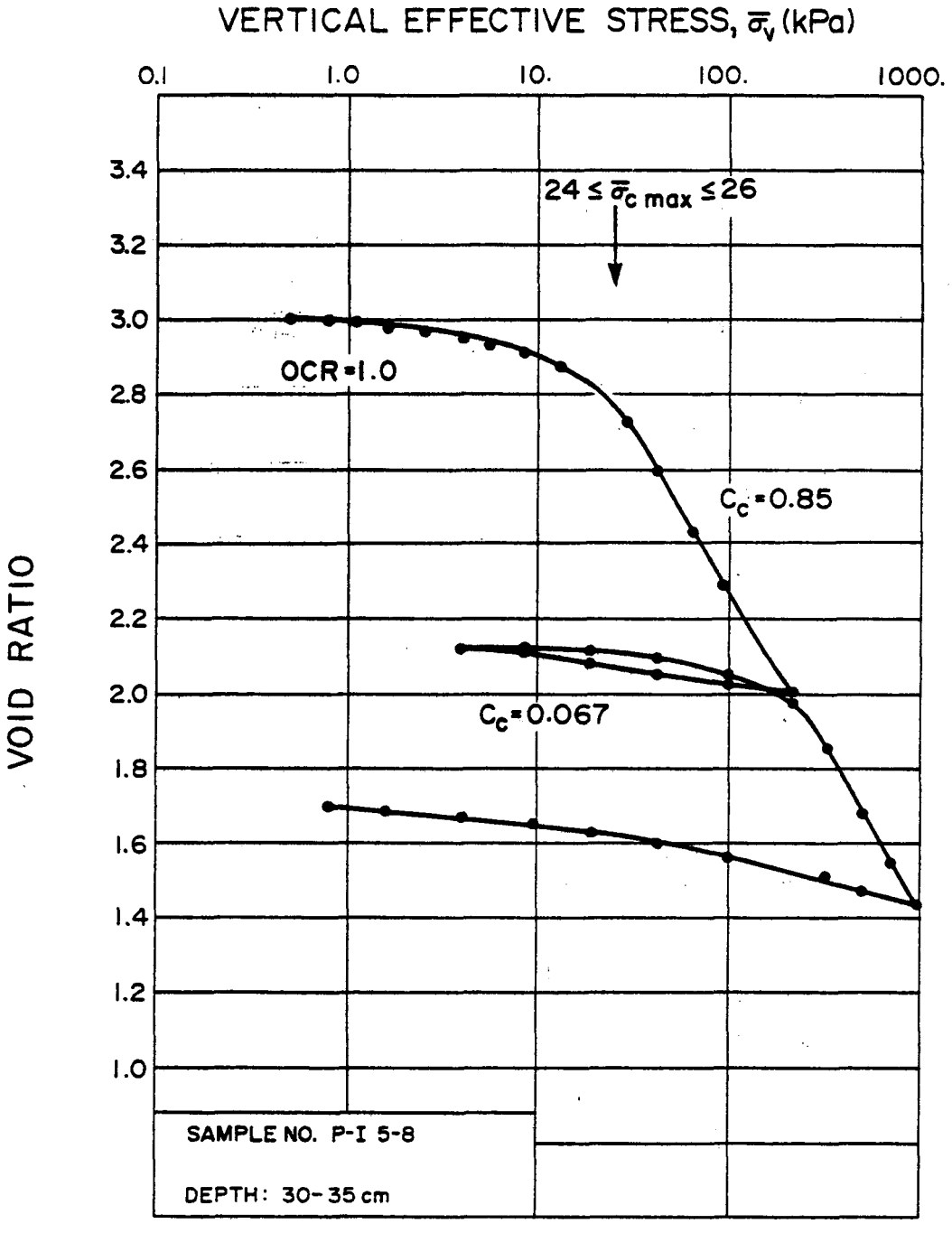

VERTICAL EFFECTIVE STRESS, $\bar{\sigma}_v$ (kPa)
0.1
1.0
10.
100.
1000.
VOID RATIO
3.4
3.2
3.0
2.8
2.6
2.4
2.2
2.0
1.8
1.6
1.4
1.2
1.0
$24 \leq \bar{\sigma}_{c\ max} \leq 26$
OCR=1.0
C_c=0.85
C_c=0.067
SAMPLE NO. P-I 5-8
DEPTH: 30-35 cm

Figure 5.3-5

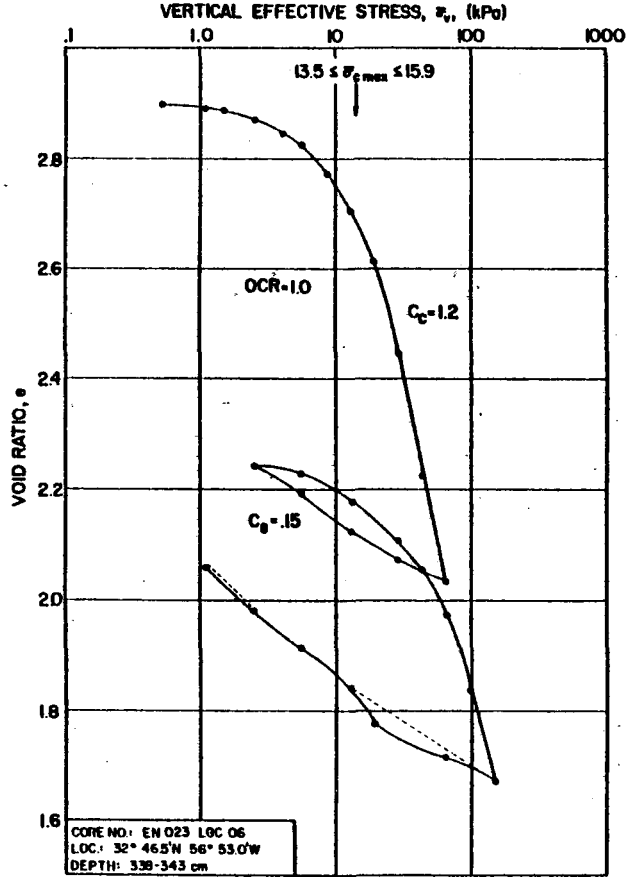


Figure 5.3-6

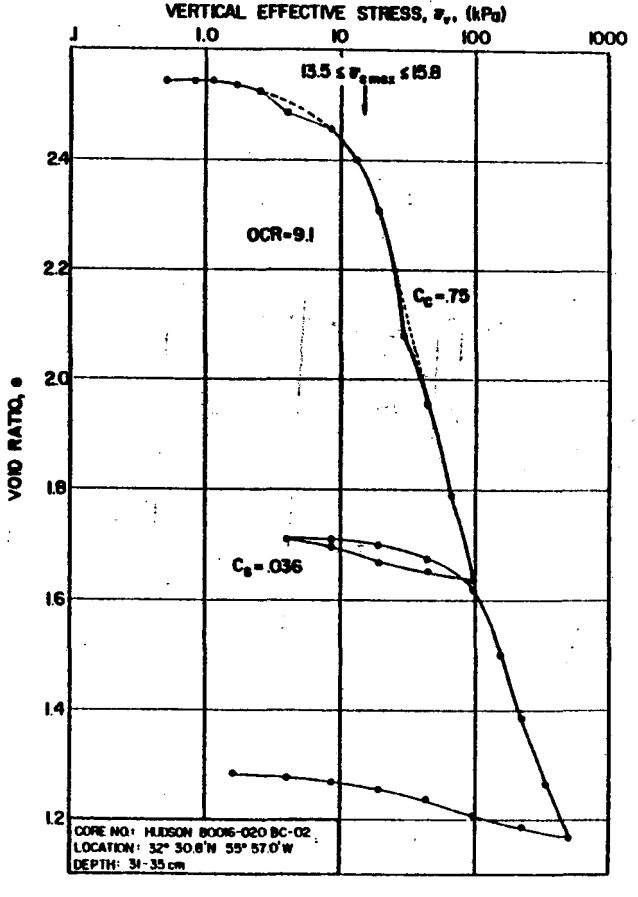


Figure 5.3-7

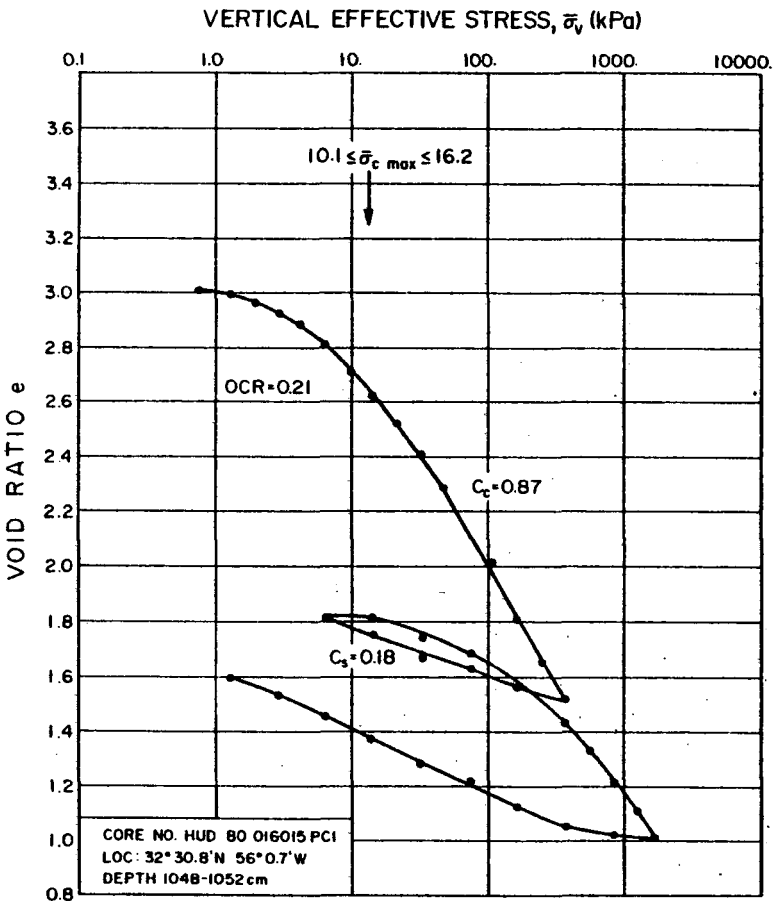


Figure 5.3-8

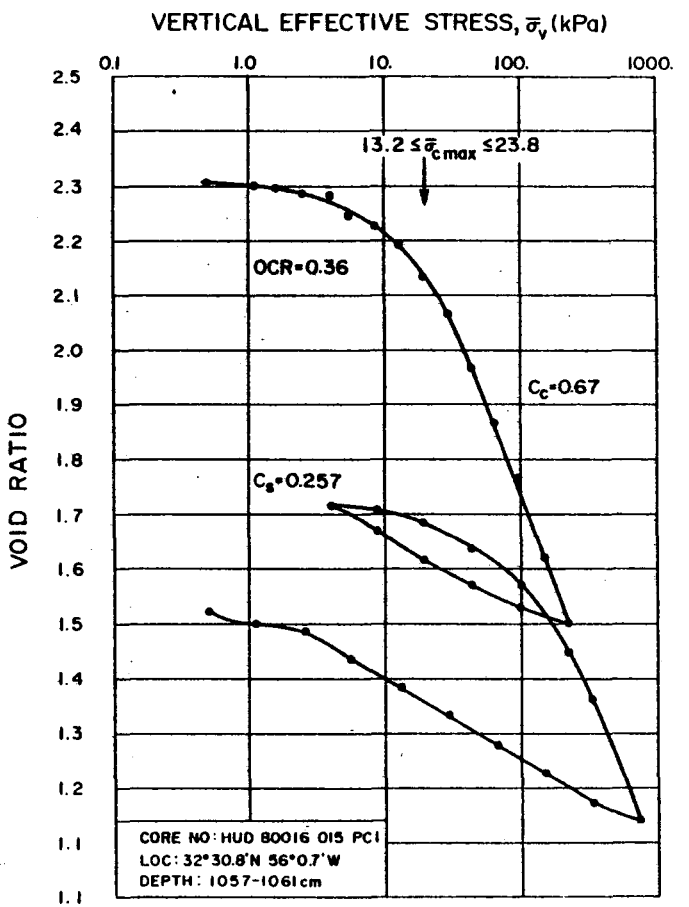
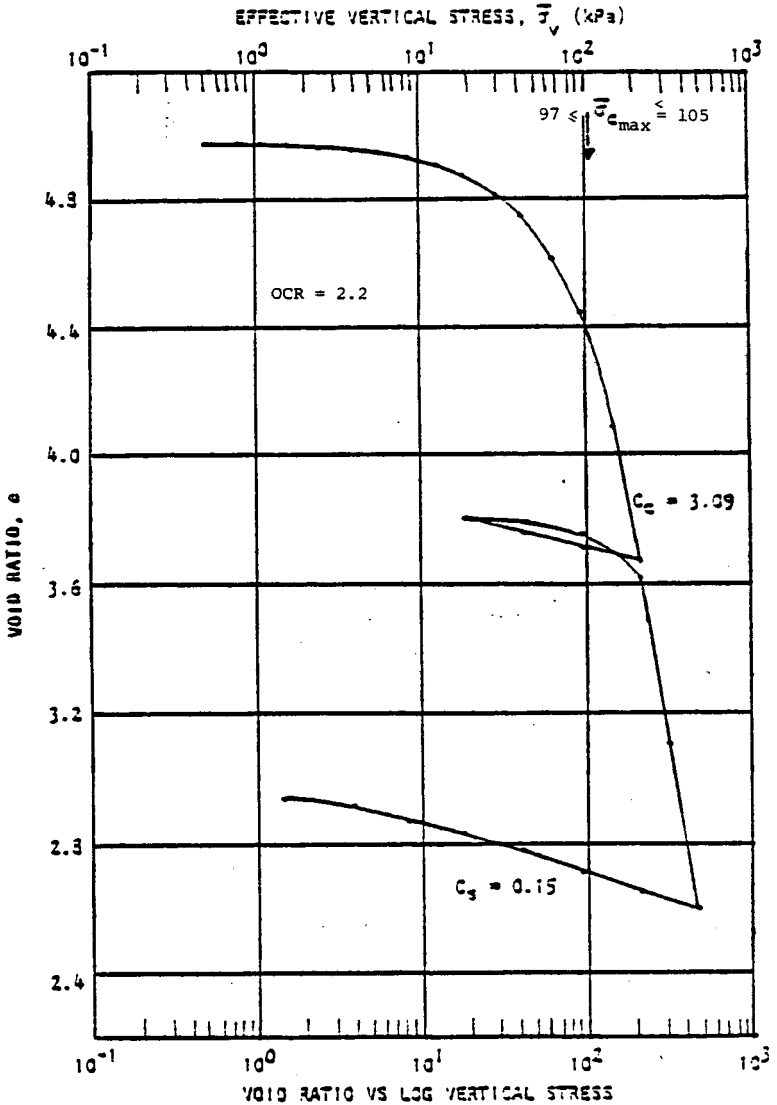
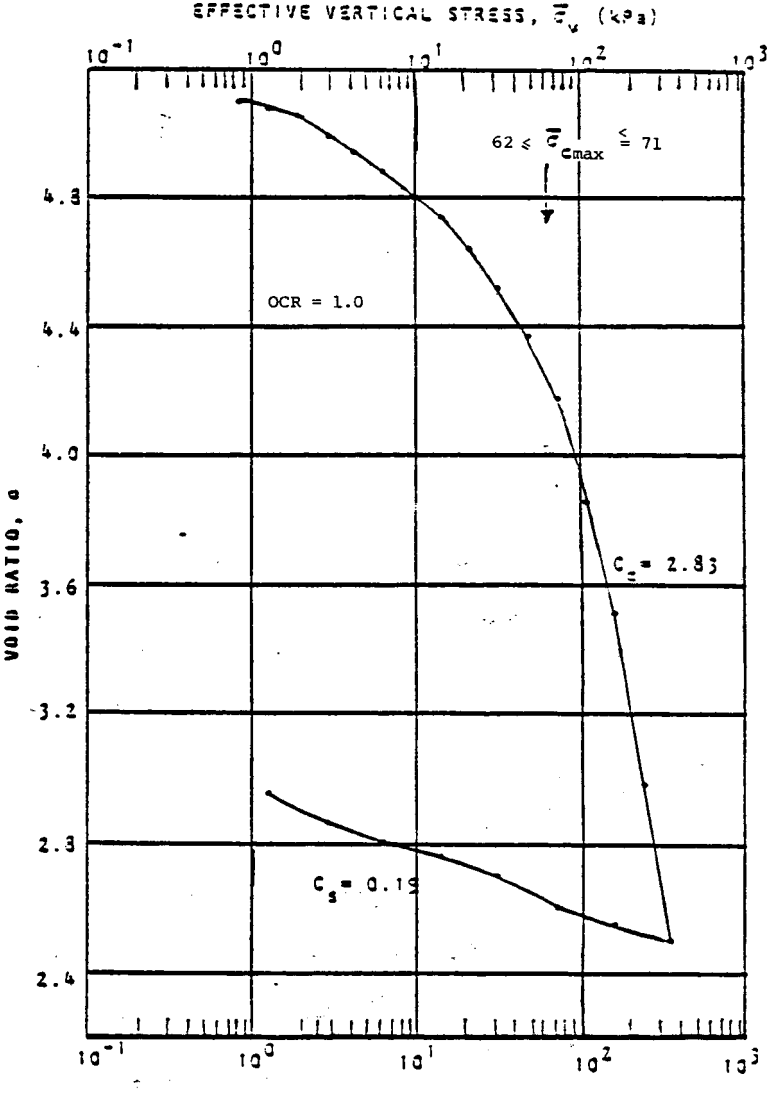


Figure 5.3-9



VOID RATIO VS LOG VERTICAL STRESS
VEMA 36-12
PC 51 1211-1215 cm.
Location E_2

Figure 5.3 - 10



VOID RATIO VS LOG VERTICAL STRESS
VEMA 36-12
PC 48 1247-1251 cm.
Location E_2

Figure 5.3-11

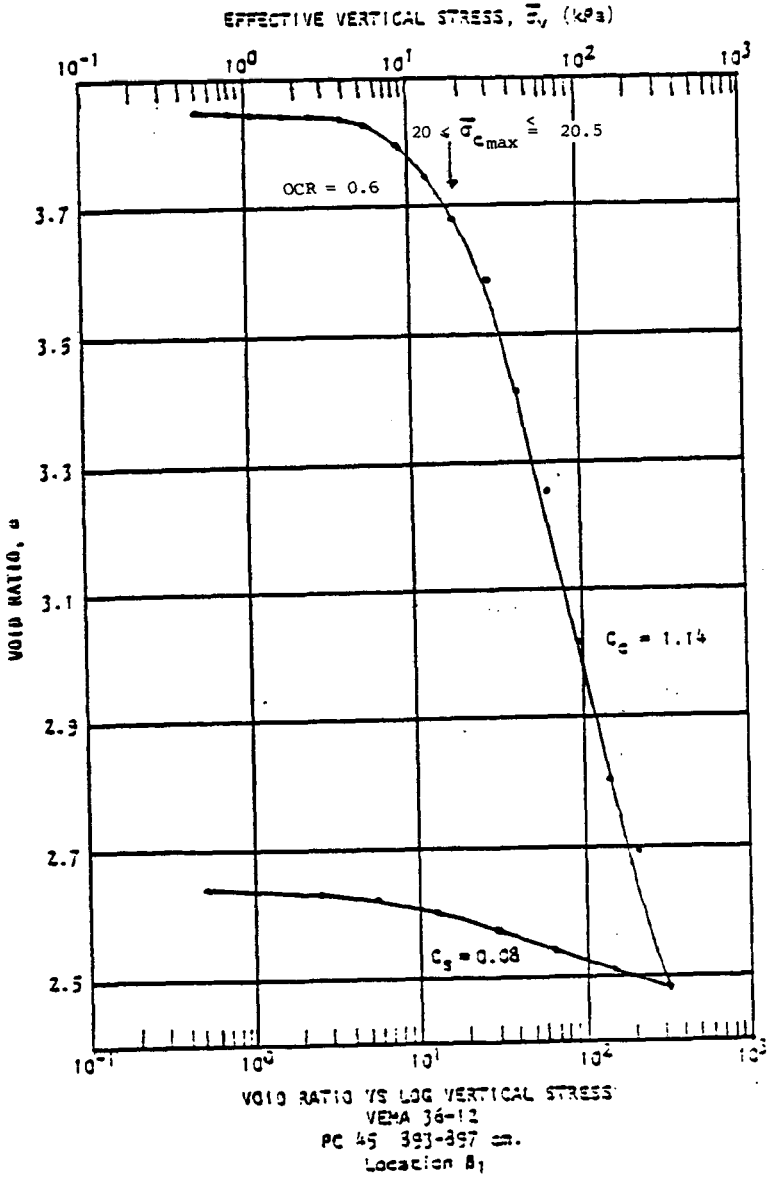


Figure 5.3-12

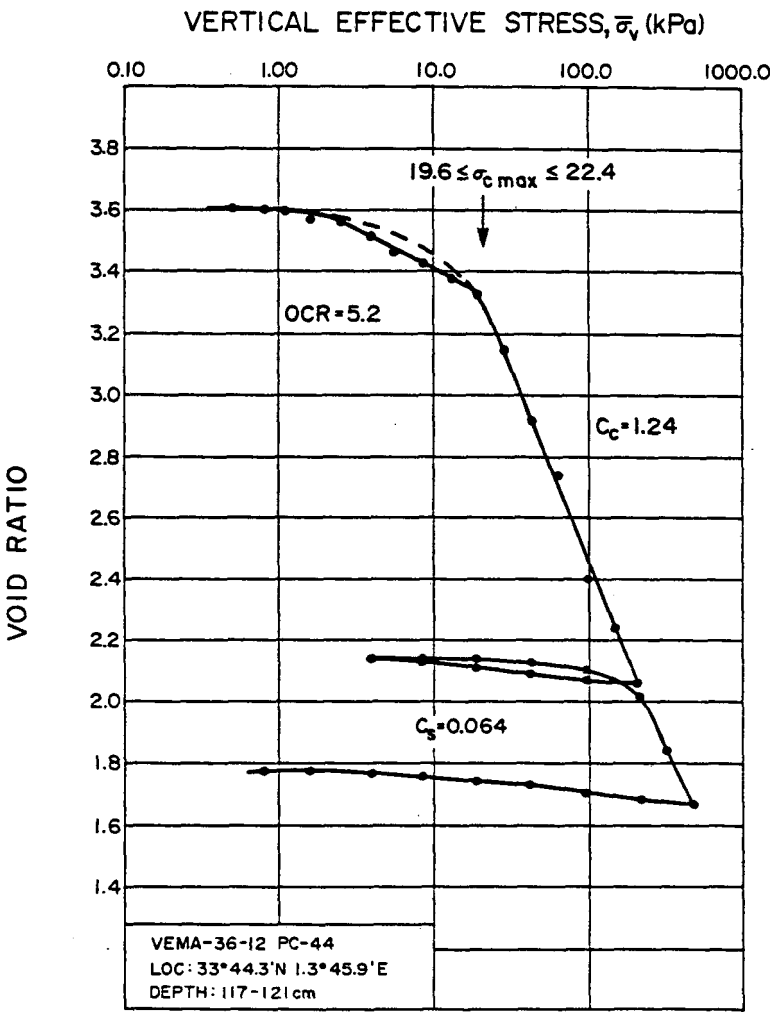
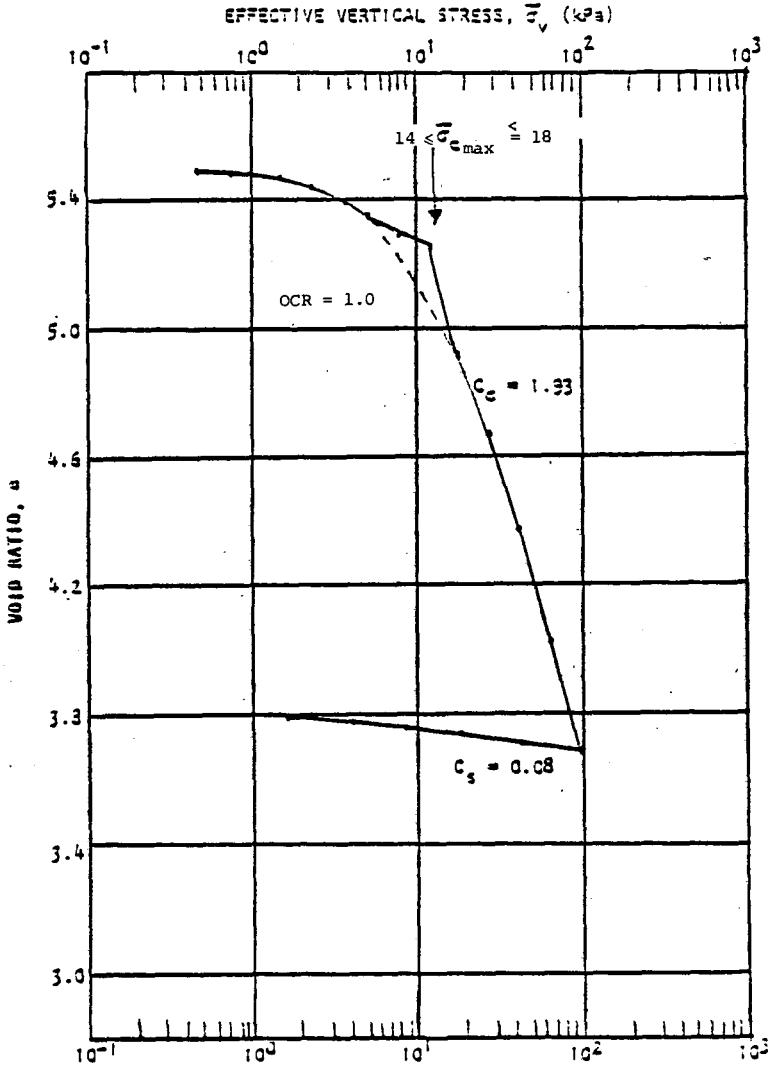
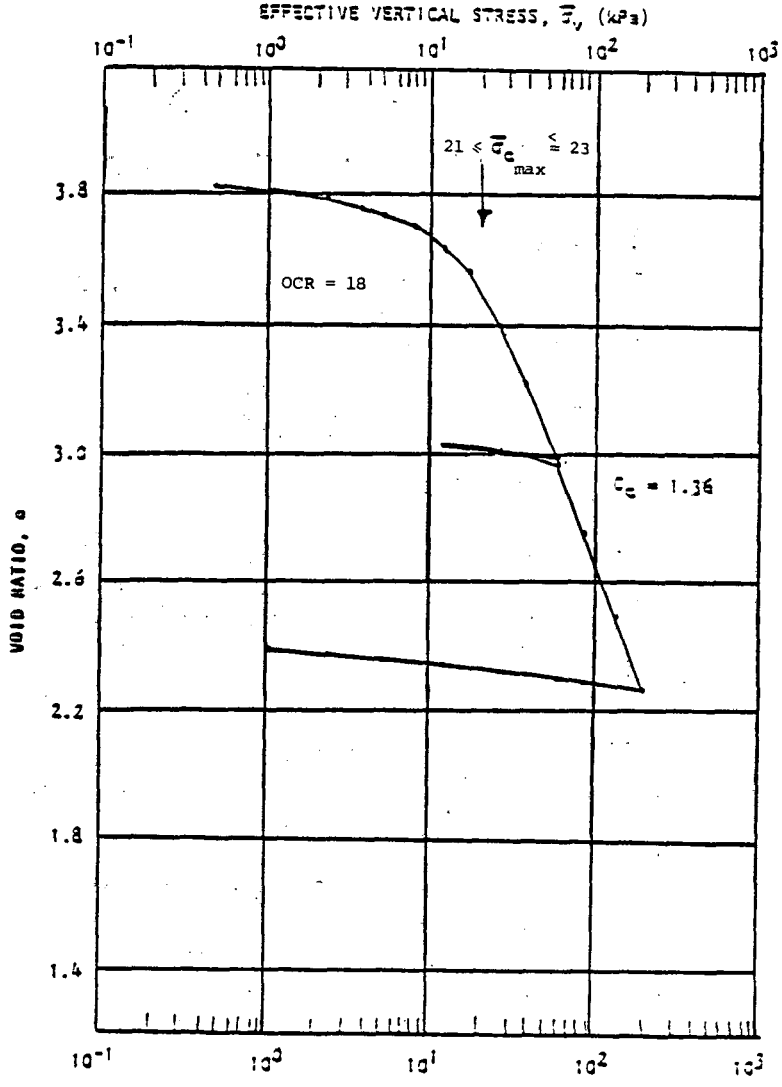


Figure 5.3-13



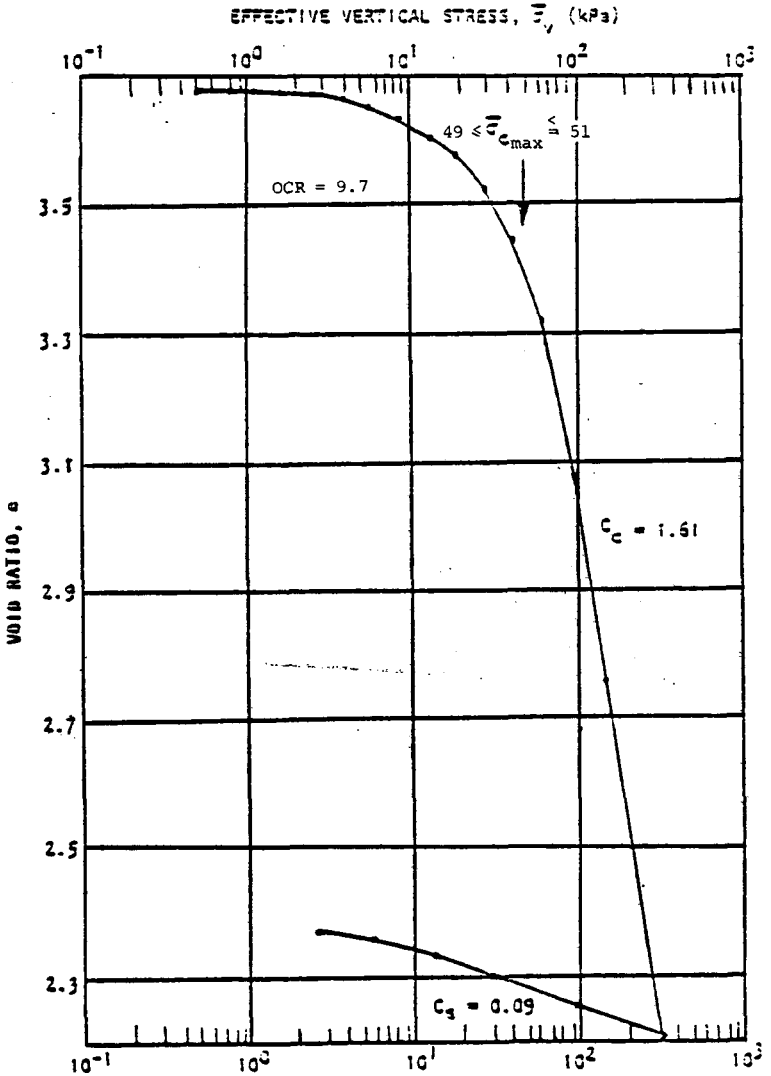
VOID RATIO VS LOG VERTICAL STRESS
VEMA 36-12
PC 43 468-472 cm.
Location B_1

Figure 5.3-14



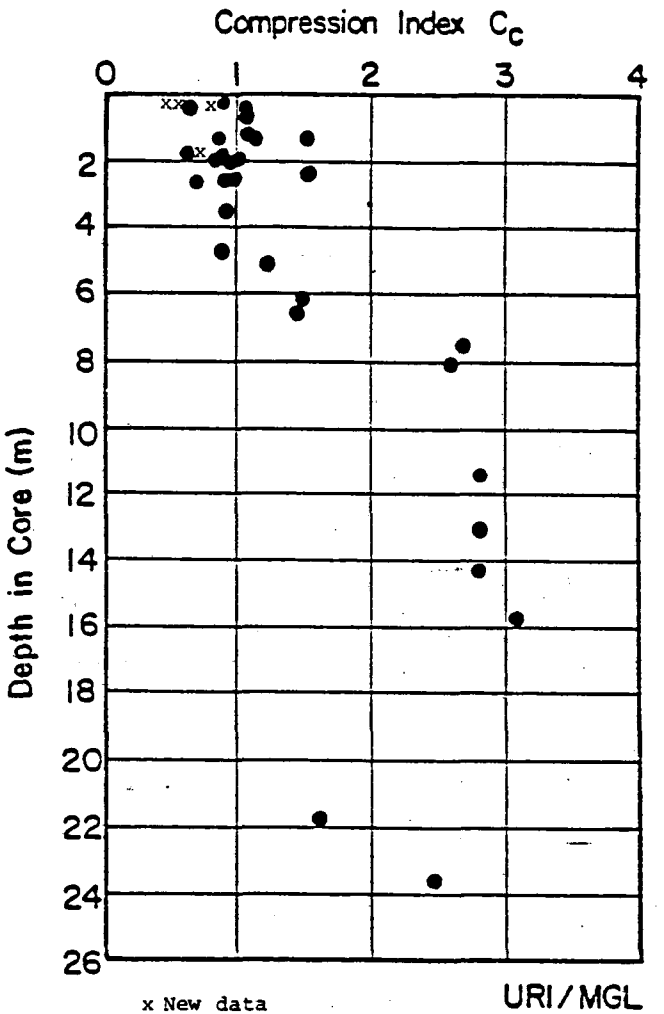
VOID RATIO VS LOG VERTICAL STRESS
VEMA 36-12
GC 39 17-21 cm.
Location C_1

Figure 5.3-15



VOID RATIO VS LOG VERTICAL STRESS
VEMA 36-12
GC 36 133-137 cm.
Location C_1

Figure 5.3-16



Compression Index, C_c, vs. Depth - MPG-I

Figure 5.4-1

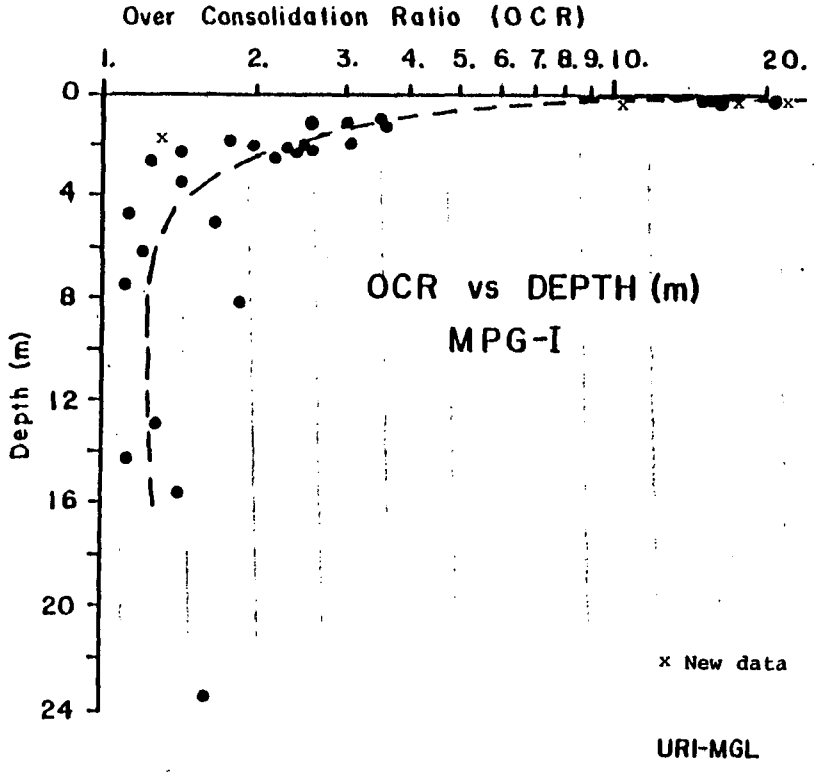

Over Consolidation Ratio (OCR)
1.
2.
3.
4.
5.
6.
7.
8.
9.
10.
20.
0
4
8
12
16
20
24
Depth (m)
OCR vs DEPTH (m)
MPG-I
× New data
URI-MGL

Figure 5.4-2

6.0 PERMEABILITY STUDIES: ROOM TEMPERATURE
(K. Dadey, S. Salehipour, S. Jordan)

6.1 Introduction

Data is presented from three locations in the Northwest Pacific MPG-IV area, as well as additional permeability results from the MPG-I and MPG-III N areas. The reader is referred to previous URI/MGL technical reports and student theses for additional details (Walker, 1981; Silva, et al., 1981, Silva and Calnan, 1980).

6.2 Methods and Materials

6.2.1 Methods

Two methods were used to determine permeability, one by direct measurement at low hydraulic gradients using a modified permeability/consolidation, (Silva et al. 1981) and the other is calculated from one dimensional consolidation theory using both the square root of time and logarithm of time data.

Determination of permeability at in situ conditions was estimated by extrapolating from an extended linear least square fit (L.L.S.F.) of void ration versus the logarithm of permeability back to the in situ void ration.

6.2.2. Materials

MPG-I: The sediments used in the permeability tests are illite rich clays with specific gravities between 2.70 and 2.76. Specimens were taken from either a large diameter gravity or box core (50 cm x 50 cm) at depths from 3 to 166 cm (see Table 6.3-1 for details). The locations of the cores are shown in Table 2.1.1.

MPG-IIIN: The samples for this work were obtained from the Abyssal Plain area east of Bermuda on the HUDSON and ENDEAVOR cruises. The HUDSON samples were from 50 cm x 50 cm box cores whereas the ENDEAVOR samples were from large-diameter gravity cores (see Table 6.3-2 for details). The dominate mineral is illite with a specific gravity of solids of approximately 2.6. The core location is shown in Tables 2.1-1 and 6.3-2.

MPG-IV: Gravity core and piston core samples were taken from three locations (E_2, B_1, C_1) in the Northwestern Pacific. Specific gravities of the sediment range from 2.5 to 2.9, with illite being the main constituent. Specific locations of the cores used for permeability studies may be found in Table 6.2-1.

6.3 Results, Analysis and Comparisons

6.3.1 MPG-I

Figures 6.3-1 through 4 show void ratio (e) vs. log of permeability (k) plots on undisturbed samples from the MARA-02 and RAMA-01 cruises. Figure 6.3-5 is an e vs. log k plot for a reconstituted/reconsolidated (remolded) sample from the Sediment Structure Interaction Testing (SSIT) tank, PI 5-8 at a depth of 30-35 cm. All permeability determinations were calculated using the square root of time method. All of these plots indicate a linear relationship between log k and e; therefore a linear least squares fit was made to the data and is shown in the figures.

Tables 6.3-1 is a summary of all permeability results obtained during FY 81. Values listed for coefficient of permeability are determined from the linear least squares fit shown in the respective figure at the in situ void ration (determined using water content and specific gravity samples trimmed from the undisturbed samples during the sample setup process). The magnitude of k is relatively high for the RAMA-01, BC-20, 3-8 cm and MARA-02 GC-08, 162-166 cm samples. However, similar values have been previously reported in the surfical sediments (Silva, Jordan, and Levy, 1981). A plot of log k vs. depth for all permeability data to date in MPG-I is shown in Figure 6.3-6.

Figure 6.3-6 shows a broad range of permeability of 1.6×10^{-5} cm/sec to 2×10^{-7} cm/sec in the surficial sediments (< 2m) with an average near 3×10^{-6} cm/sec. Below 2 m the range is significantly less (1×10^{-6} cm/sec to 1.5×10^{-7} cm/sec.). The value of permeability of the remolded sample falls within these ranges which supports the belief that reconstituting and reconsolidating this material seems to have little effect on permeability.

6.3.1 MPG-III N

Figures 6.3 7 through 10 show void ratio vs. log of permeability measurements on undisturbed samples from the Endeavor-023 and Hudson-80016 cruises. Direct measurements of permeability as well as determinations using the square root of time and log time methods are indicated. Generally, values determined through the square root of time method are higher than those using the log time method which agrees with previously reported results. The least squares fit line is indicated for purposes of obtaining permeabilities at in situ void ratios.

Table 6.3-2 lists the in situ permeabilities obtained during FY 81 in this area. It appears the variability of permeability is significantly less than in the MPG-I study site but this may be a function of the fewer samples tested. These values as well as all previous results in MPG-III N are plotted in Figure 6.3-11 with respect to sample depth. Overall, the trend of permeability with depth does not differ significantly from MPG-I, although the dramatic increase in permeability is not seen in the surficial material. However,

additional testing in the surfical zone is required to expand the data base in order to make a more positive assessment. Also, additional tests at intermediate depths will be conducted.

6.3.3 MPG-IV

A comprehensive analysis of all geotechnical data from MPG-IV is contained in the recent M.S. thesis by G. Walker (1981). The following is only a brief summary of permeability results.

The results of permeability studies for locations E_2, B_1, and C_1 are summarized in Table 6.3-3. In addition to the direct measurements, values of coefficient of permeability (κ) were calculated from consolidation tests results.

a) Location E_2: Six cores were examined from location E_2 and the results for in situ void ratio conditions are summarized in Figure 6.3-12 (a). Althouogh there is some scatter at various depths, values of coefficient of permeability are fairly constant from two meters through eleven meters, with an average k of 2.66×10^{-6} cm/sec. Futhermore, direct measurements correlate well with values calculated by the square root of time method although there is no consistent relationsnip between calculated and measure values.

b) Location B_1: The coefficient of permeability was calculated by square root of time and logarithm of time methods for PC-45; only the former was employed to compute k for PC-43. The results are plotted versus depth in Figure 6.3-12 (b). The coefficient of permeability is relatively constant, ranging from 1.6×10^{-6} to 6.0×10^{-6} cm/sec. Of the two procedures utilized to calculate the permeability coefficient for PC-45, the logarithm of yields slightly higher values.

c) Location C_1: Six samples of four cores from this location were examined. Of these, the coefficient of permeability was calculated by both analytical methods (square root of time and logarithm of time) and obtained directly for one sample. These results are plotted in Figure 6.3-12 (c). Values for the remaining samples were computed by square root of time. As indicated in Figure 6.3-12 (c), the coefficient of permeability is fairly constant for this location, although there seems to be a trend of slightly decreasing permeability from approximately 4×10^{-6} near the surface to 10^{-6} cm/sec at 11 meters depth. However, because of the limited number of samples involved, this conclusion is difficult to substantiate.

d) Comparisons: Table 6.3.3-1 shows the average permeabilities for locations C_1 and E_2 to be almost identical (2.8 and 2.6×10^{-6} cm/sec) and for location B_1, only slightly higher with an average value of 3.6×10^{-6} cm/sec. The coefficient of permeability does show variability in location E_2, but this may be due to the greater number of values obtained. Initial void ratios observed in location E_2 tend to be greater than those in locations B_1 and C_1 (also see section 2). However, no real correlation was discovered

between the coefficient of permeability and initial void ratio for any of the three locations. Furthermore, the plot of initial void ratio versus coefficient of permeability for all three locations (Figure 6.3-13) does not reveal any consistent relationship between the two parameters for any of the three locations or the area as a whole.

In relation to permeability results of the MPG-I area (Table 6.3-6), the k values for MPG-IV are consistently higher. Initial void ratios from the latter area tend to exhibit less scatter than those from the former.

Table 6.2-1

Core Locations

MPG-I

LOCATION	CORE	LATTITUDE	LONGITUDE
E_2	PC-46	33° 41.12 N	163° 31.70 E
	PC-47	32° 5.8 N	164° 31.0 E
	PC-48	32° 9.0 N	163° 29.0 E
	PC-51	32° 38.0 N	164° 46.0 E
	GC-53	32° 24.57 N	164° 8.9 E
B_1	PC-43	33° 44.84 N	151° 45.91 E
	PC-45	33° 5.63 N	152° 16.38 E
C_1	PC-34	30° 45.59 N	152° 16.24 E
	PC-35	30° 30.13 N	151° 48.74 E
	GC-36	30° 29.57 N	151° 46.21 E
	GC-39	30° 27.1 N	151° 49.9 E

TABLE 6.3-1

SUMMARY OF PERMEABILITY RESULTS, MPG-I

CRUISE	CORE*	DEPTH (cm)	IN SITU VOID RATIO	Coefficient of Permeability (cm/Sec) at in situ void ratio: SQUARE ROOT OF TIME METHOD
RAMA-01	BC-20	3-8	2.76	1.25×10^{-5}
RAMA-01	BC-20	10-14	3.07	1.10×10^{-6}
MARA-02	GC-08	15-20	3.02	6.00×10^{-6}
MARA-02	GC-08	162-166	2.96	1.55×10^{-5}
(PI 5-8)**	-	30-35	3.01	1.00×10^{-6}

* See table 2.1-1 for coordinates

** Reconstituted-reconsolidated sample from laboratory tank consolidated to 25 kPa.

TABLE 6.3-2

SUMMARY OF PERMEABILITY RESULTS, MPG-III

CRUISE	CORE*	DEPTH	VOID RATIO	Coefficient of permeability (cm/sec) at in situ void ratio		
				SQUARE ROOT OF TIME	LOGARITHM OF TIME	DIRECT
EN-23	LGC-06	338-343	2.91	6.5×10^{-7}	2.2×10^{-7}	-
HUDSON	BC-2	31-35	2.54	2.0×10^{-6}	6.2×10^{-7}	-
HUDSON	PC-1	1048-1052	3.02	-	-	3.1×10^{-7}
HUDSON	PC-1	1057-1061	2.31	2.3×10^{-7}	-	-

* See table 2.1-1 for coordinates.

TABLE 6.3-3
PERMEABILITY RESULTS

VEMA 36-12

Location E_2

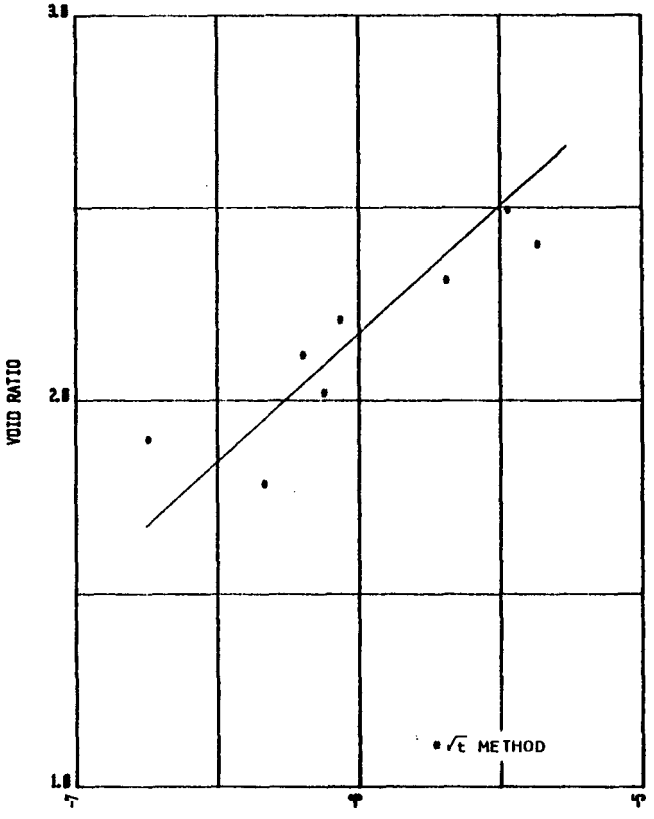
CORE	DEPTH (cm)	IN SITU VOID RATIO e_o	COEFFICIENT OF PERMEABILITY AT e_o (cm/sec) SQUARE ROOT TIME	DIRECT MEASUREMENT
PC 46	902-906	3.70	4.8×10^{-7}	--
PC 47	885-889	4.41	1.1×10^{-6}	--
PC 48	570-574	4.39	1.8×10^{-6}	--
	1247-1251	5.00	3.4×10^{-6}	5.9×10^{-7}
PC 49	186-190	6.25	2.7×10^{-6}	--
	368-372	4.22	--	3.5×10^{-6}
	1176-1180	5.1	9.7×10^{-7}	--
PC 51	115-119	4.65	1.0×10^{-6}	--
	466-470	4.50	1.8×10^{-6}	--
	1050-1054	5.0	2.3×10^{-6}	1.4×10^{-6}
	1211-1215	5.14	2.5×10^{-6}	--
	1224-1228	5.15	5.32×10^{-6}	1.7×10^{-6}
GC 53	9-13	4.22	5.0×10^{-6}	--
	160-164	4.57	1.1×10^{-5}	--
	172-176	4.08	1.8×10^{-6}	2.2×10^{-6}
AVERAGE		4.69	2.7×10^{-6}	

Location B_1

			COEFFICIENT OF PERMEABILITY AT e_o (cm/sec.) SQUARE ROOT TIME	LOGARITHIM TIME
PC 43	468-472	5.55	2.5×10^{-6}	--
	845-849	3.86	6.0×10^{-6}	--
	1188-1192	4.17	3.1×10^{-6}	--
PC 45	429-433	3.43	3.7×10^{-6}	5.9×10^{-6}
	893-897	3.88	2.3×10^{-6}	--
	1242-1246	2.81	1.6×10^{-6}	3.9×10^{-6}
AVERAGE		3.95	3.6×10^{-6}	

Location C_1

			COEFFICIENT OF PERMEABILITY AT e_o (cm/sec.) SQUARE ROOT TIME	LOGARITHM TIME	DIRECT MEASUREMENT
PC 34	1125-1129	3.80	1.0×10^{-6}	--	--
PC 35	408-412	4.17	1.8×10^{-6}	1.4×10^{-6}	2.3×10^{-6}
GC 36	133-137	3.81	2.7×10^{-6}	--	--
	251-255	4.25	3.6×10^{-6}	--	--
GC 39	17-21	3.84	5.4×10^{-6}	--	--
	255-259	3.10	4.0×10^{-6}	--	--
AVERAGE		3.83	2.8×10^{-6}		



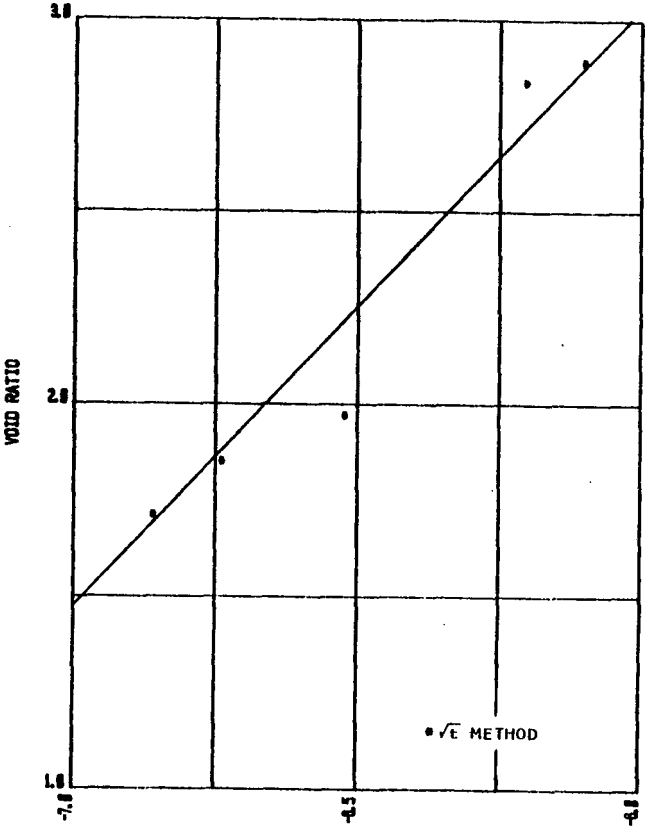
LOG. OF PERMEABILITY (cm/sec)

VOID RATIO vs. LOG. OF PERMEABILITY

RAMA-1 BC-20 3-8cm

URI/MGL

Figure 6.3-1



LOG. OF PERMEABILITY (cm/sec)

VOID RATIO vs. LOG. OF PERMEABILITY

RAMA-1 BC-20 10-14cm

URI/MGL

Figure 6.3-2

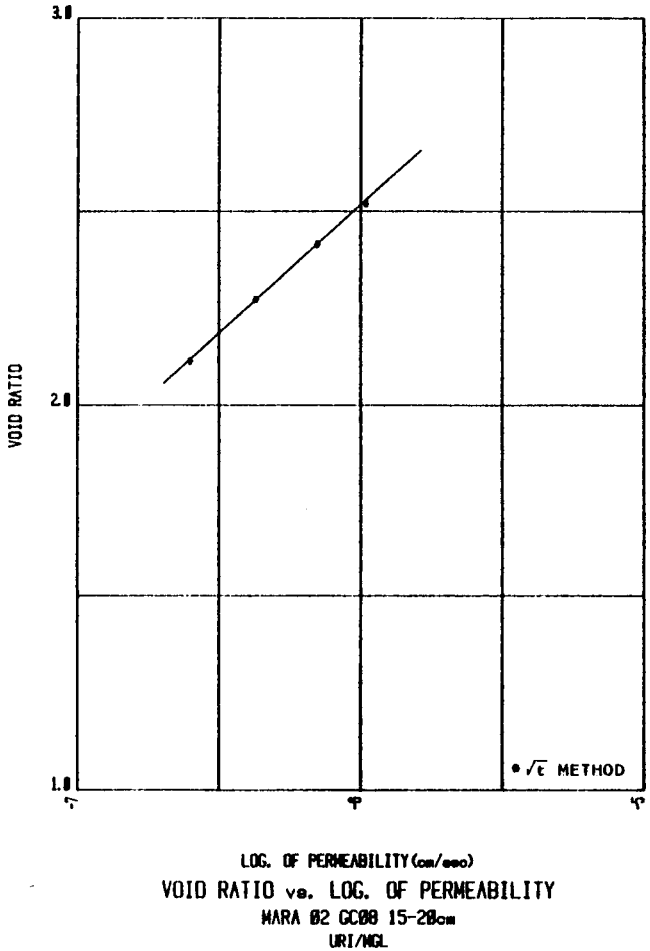


Figure 6.3-3

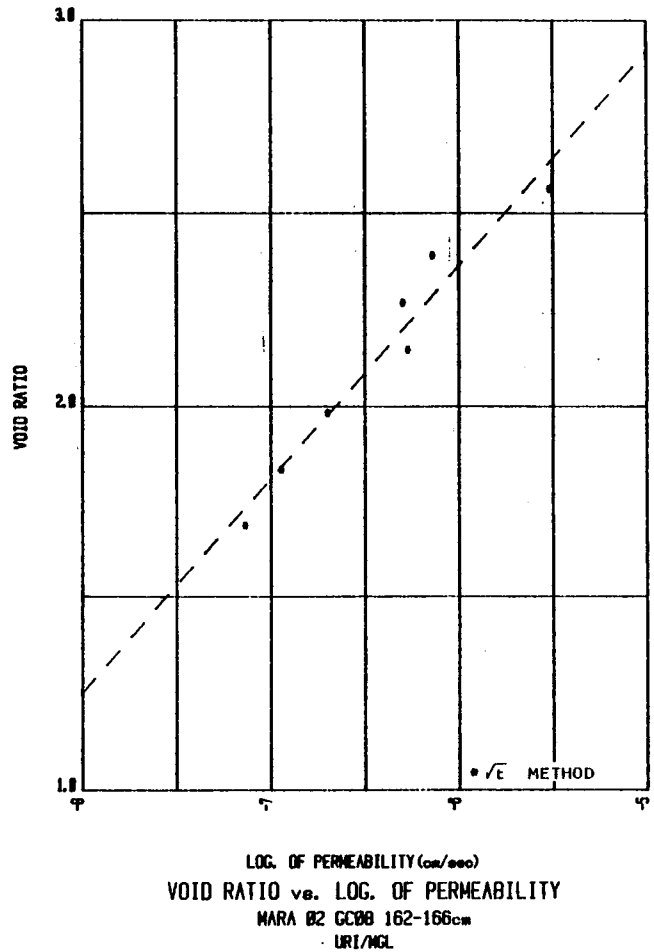
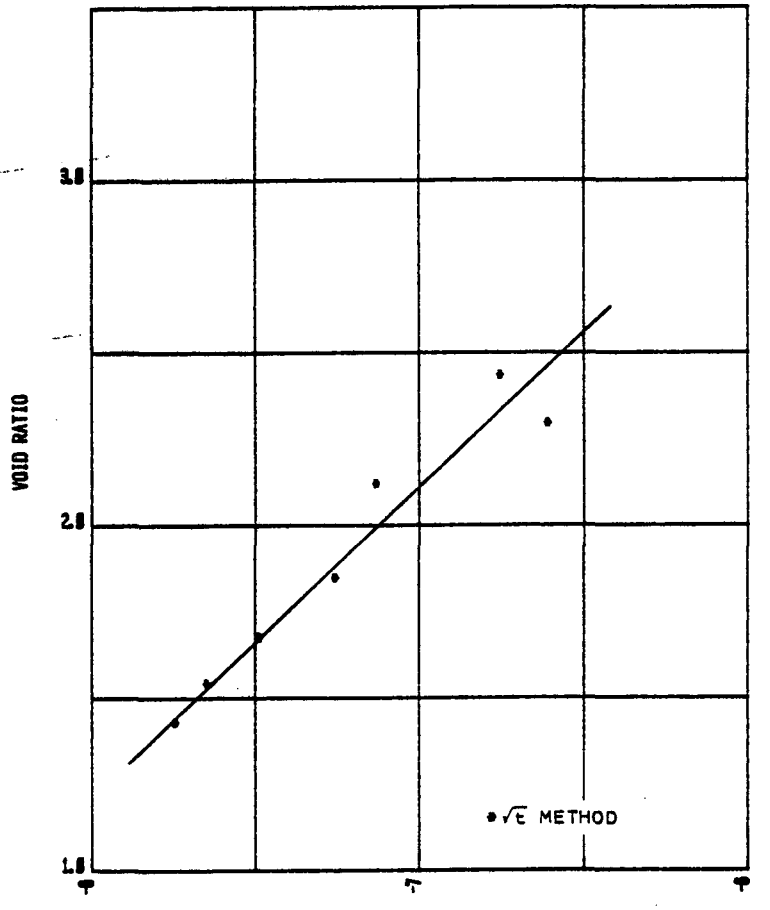


Figure 6.3-4



VOID RATIO vs. LOG. OF PERMEABILITY
PI-5-8, #68, 30-35cm
URI/MGL

Figure 6.3-5

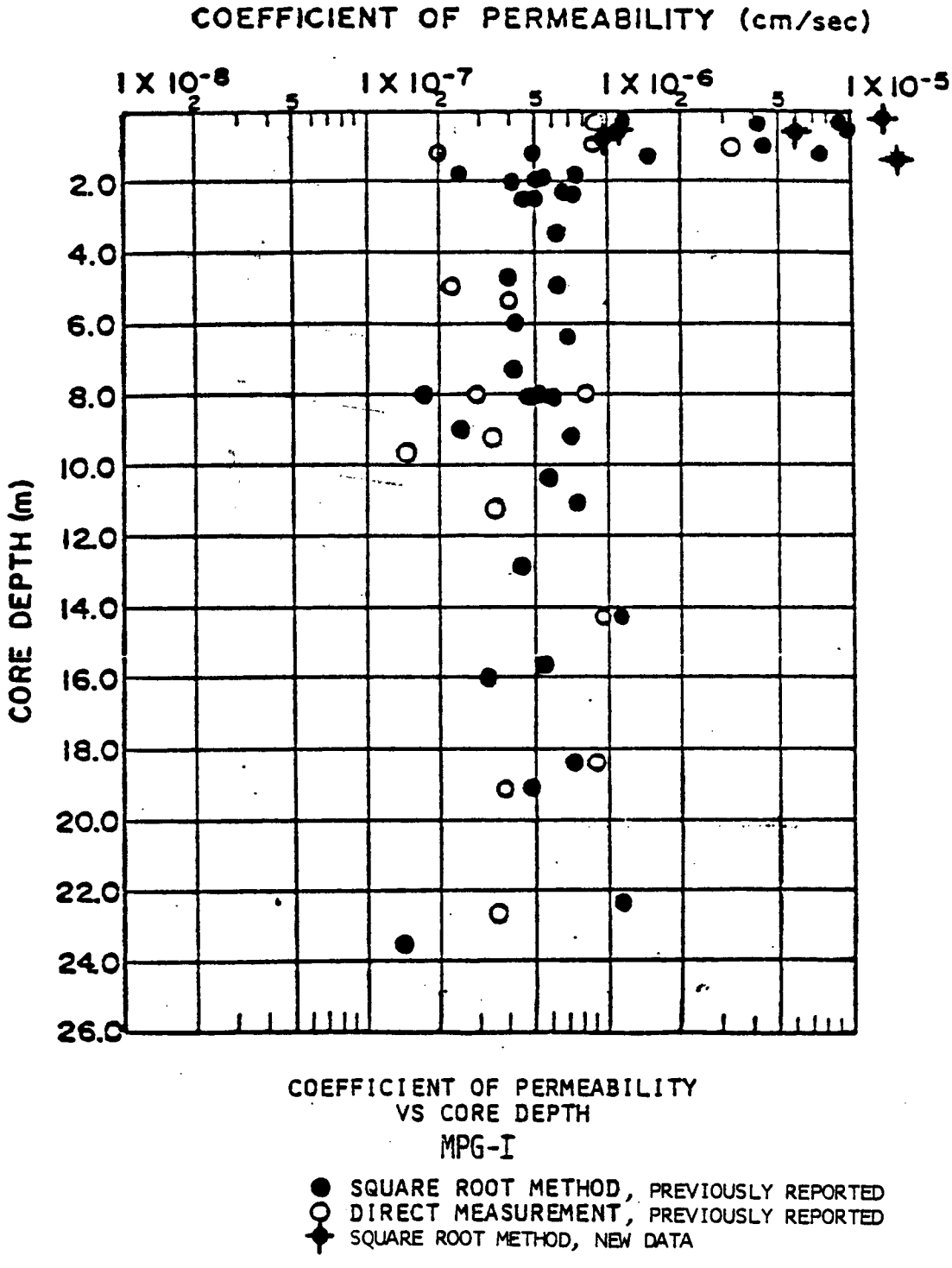
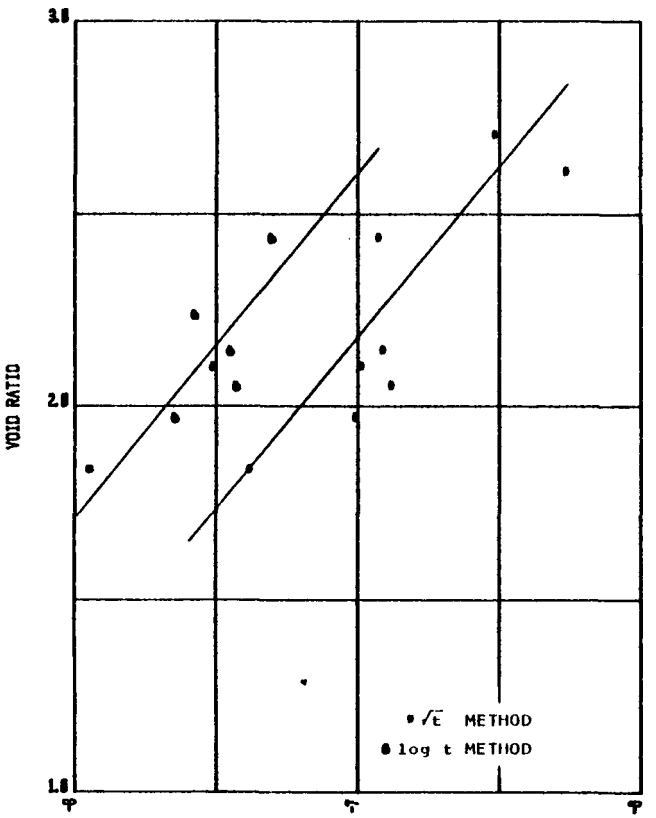
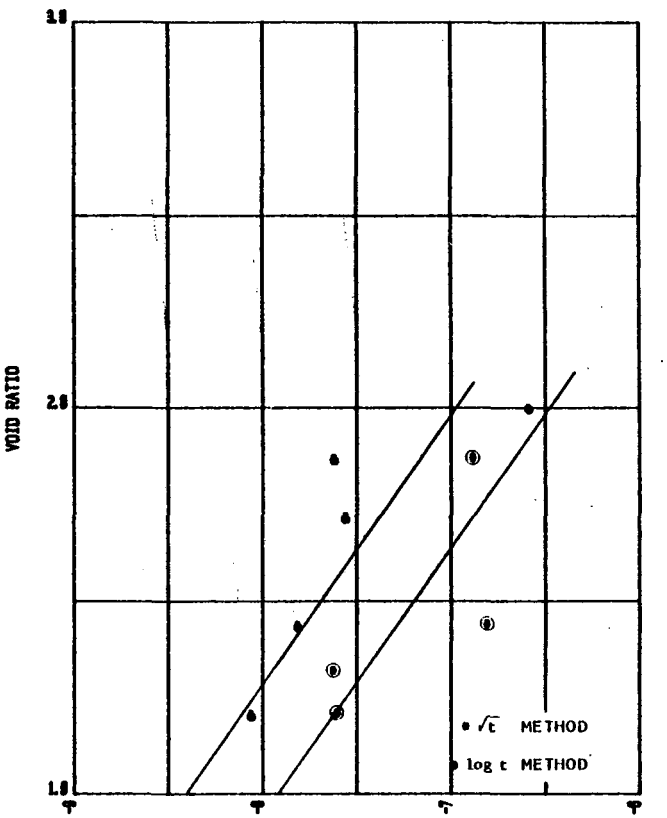

COEFFICIENT OF PERMEABILITY (cm/sec)
1 X 10-8
1 X 10-7
1 X 10-6
1 X 10-5
2
5
2.0
4.0
6.0
8.0
10.0
12.0
14.0
16.0
18.0
20.0
22.0
24.0
26.0
CORE DEPTH (m)
COEFFICIENT OF PERMEABILITY
VS CORE DEPTH
MPG-I
SQUARE ROOT METHOD, PREVIOUSLY REPORTED
DIRECT MEASUREMENT, PREVIOUSLY REPORTED
SQUARE ROOT METHOD, NEW DATA

Figure 6.3-6



VOID RATIO vs. LOG. OF PERMEABILITY
EN023 LGC06 330-343cm
URI/MGL

Figure 6.3-7



VOID RATIO vs. LOG. OF PERMEABILITY
HUD BC-2 31-35cm
URI/MGL

Figure 6.3-8

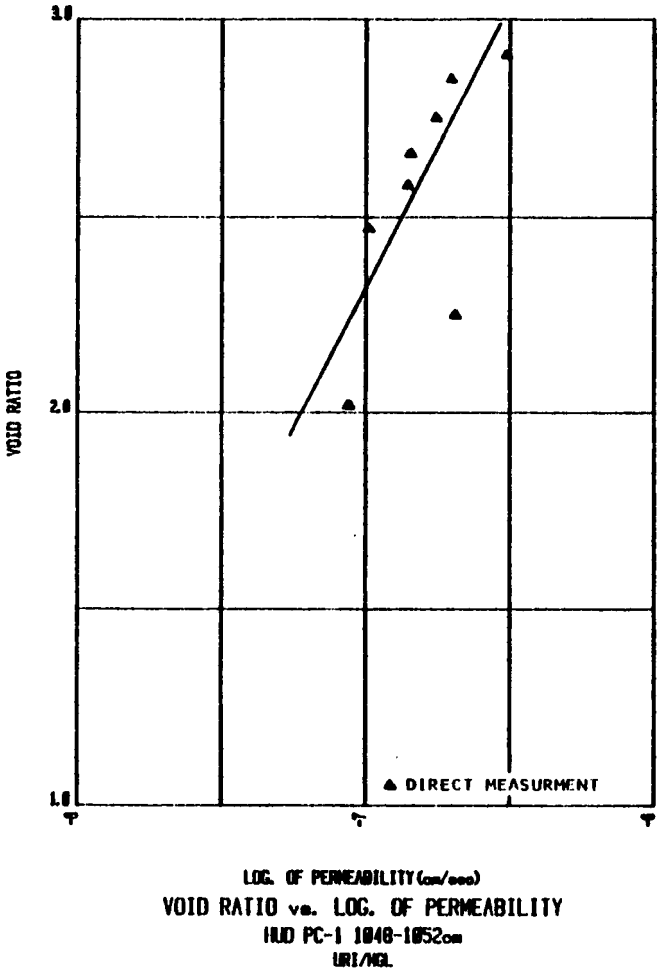


Figure 6.3-9

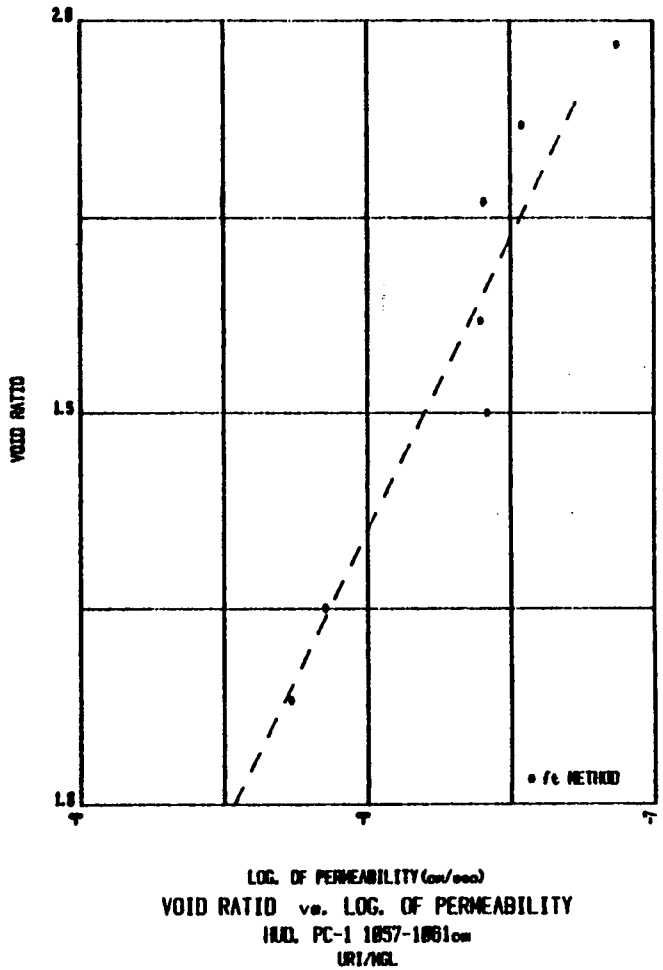
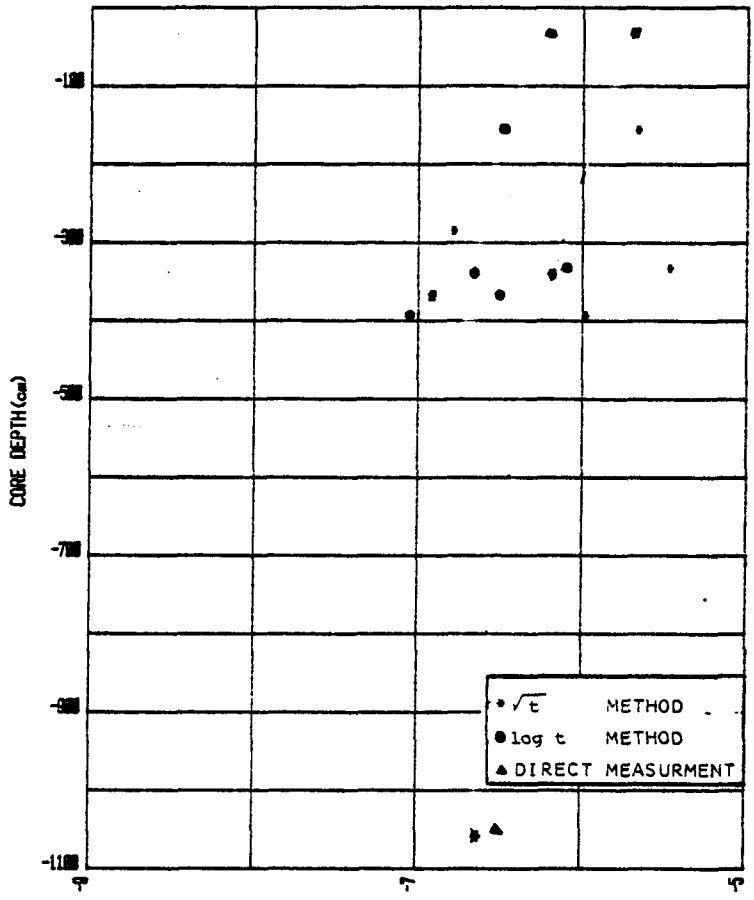


Figure 6.3-10



LOG. OF PERMEABILITY(cm/sec)

CORE DEPTH vs. LOG. OF PERMEABILITY

PERM. RESULTS MPG-3

URI/NGL

Figure 6.3-11

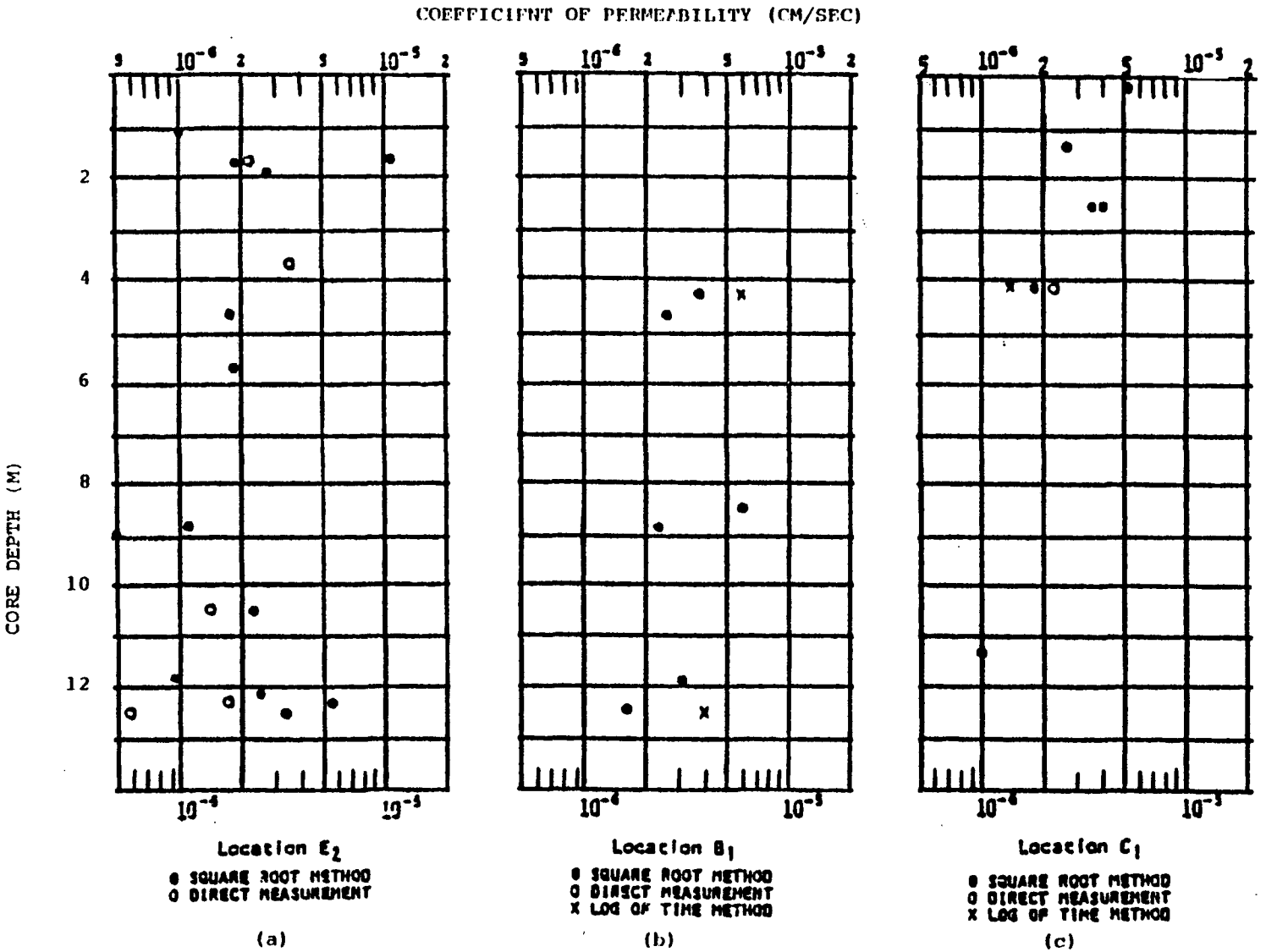

COEFFICIENT OF PERMEABILITY (CM/SEC)
CORE DEPTH (M)
2
4
6
8
10
12
Location E_2
● SQUARE ROOT METHOD
○ DIRECT MEASUREMENT
(a)
Location B_1
● SQUARE ROOT METHOD
○ DIRECT MEASUREMENT
X LOG OF TIME METHOD
(b)
Location C_1
● SQUARE ROOT METHOD
○ DIRECT MEASUREMENT
X LOG OF TIME METHOD
(c)

Figure 6.3-12

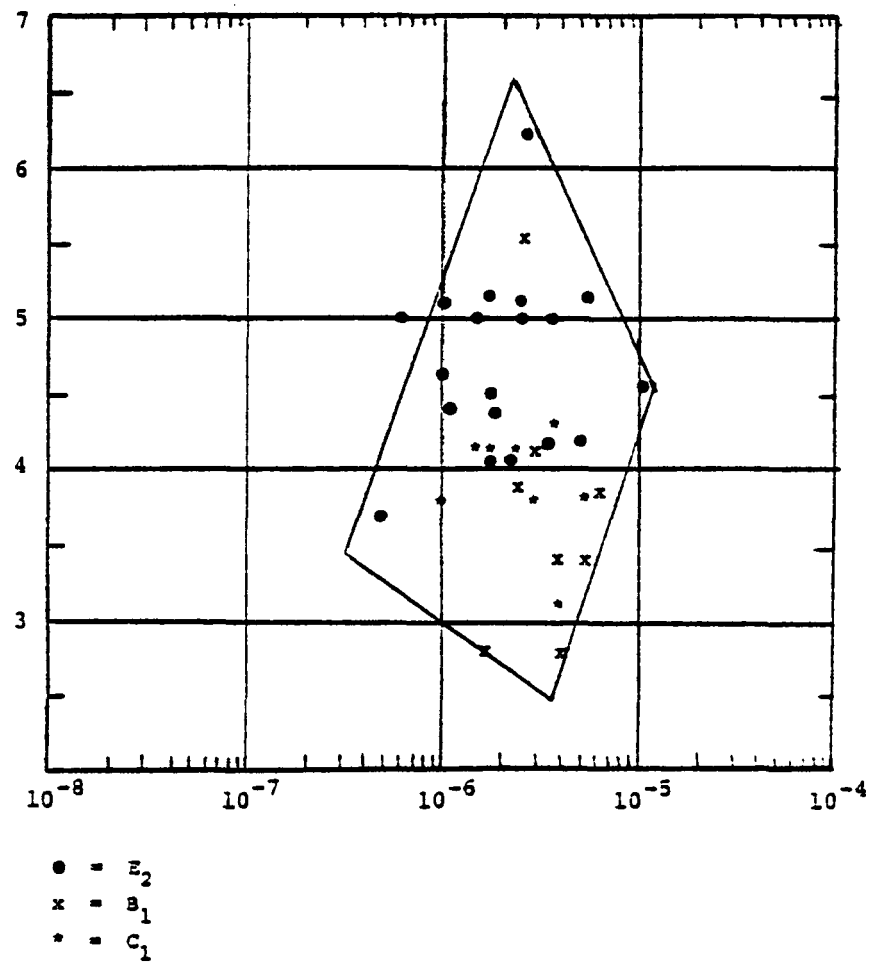

7
6
5
4
3
10^{-8}
10^{-7}
10^{-6}
10^{-5}
10^{-4}
● = E_2
x = B_1
* = C_1
COEFFICIENT OF PERMEABILITY
cm/sec.
VEMA 36-12
COMBINED AREAS

Figure 6.3-13

7.0 HIGH PRESSURE/HIGH TEMPERATURE THERMOPHYSICAL PROPERTIES (R. Morin)

7.1 Introduction

In order to properly analyze the coupled flow of heat and pore fluid in the vicinity of a heat source buried in the seabed, the response of sediments to significant thermal fluxes at large hydrostatic pressure must be determined. This rationale prompted the initiation of a thermophysical properties program at URI/MGL in 1979. The purpose of the laboratory program is to measure the permeability and the thermal conductivity of a few sediment types at their in situ conditions of large hydrostatic pressure and high temperature, and to determine the effects of these environmental parameters upon the sediment physical properties.

Laboratory studies have shown that tests designed to measure sediment permeability directly should be performed under hydrostatic pressures large enough to assure complete pore fluid saturation (Nickerson, 1978; Crowe and Silva, 1981). This back-pressure, usually .5 to 1.0 MPa, is necessary to dissolve gas bubbles which tend to impede water flow through voids. There has been speculation that much larger hydrostatic pressures (beyond 30 MPa) might affect sediment permeability by producing physico-chemical changes in the sediment skeleton.

Studies to determine the effect of temperature on thermal conductivity of sediments have only been performed for a narrow range of temperatures. Ratcliffe (1960), and MacDonald and Simmons (1972) found approximately a 6 % increase in this property from $4^{o}C$ to 25^{o} C. Preliminary work designed to determine the dependence of permeability on temperature has also been performed over a relatively narrow range. Silva et al (1981) found the increase in permeability of an illitic clay at $80^{o}C$ to be due entirely to a decrease in the viscosity of the permeating medium, the change in permeability could be accounted for by applying a viscosity correction within this temperature range. The variation in permeability and thermal conductivity of sediments at much higher temperatures has not been determined.

One possible effect of temperature is the actual thermal alteration of the sediment samples. Muler (1967) has attempted to correlate the chemical-mineralogical changes of various sediment types with depth and duration of burial, pressure, and temperature. He finds that, for the two sediment types analyzed in this study, the one more susceptible to diagenesis is smectite. Weaver (1979) provides a similar assessment. He concludes that smectites are the most likely to be affected by heat because of their high water contents and relatively rapid reaction rates at low temperatures.

This diagenesis, however, may only occur provided there is a sufficient source of potassium in the sediment. Illite is produced when potassium becomes lodged between the contracting layers of smectite. Khitarov and Pugin (1966) confirmed this condition by subjecting a number of montmorillonite samples to elevated temperatures. For samples containing only

trace amounts of potassium, no detectable amount of illite was formed. For samples moistened beforehand with a 10% solution of potassium cloride, however, a smectite to illite transformation was easily initiated. It is not likely that the deep-sea smectite samples tested in this study contained only significant amount of potassium and, consequently, no thermal alteration is expected.

Muller (1967) notes that the transitional zone between diagenesis and metamorphism, where significant mineralogical changes begin to occur in biogenic oozes and illitic clays, is not reached until a critical transition temperature of 300°C is acheived. Testing at this temperature is beyond the scope of this study and, therefore, metamorphic changes are not considered. It is not anticipated that thermal alteration became a factor in influencing the final results. Pre-test and post-test mineralogy analyses of both sediment types will be performed in order to confirm this condition.

7.2 Methods and Materials

The laboratory equipment which was fabricated for this investigation is specially designed to measure sediment permeability and thermal conductivity at hydrostatic pressures ranging from atmospheric to 62 MPa and at temperatures from 22°C to 220°C. Permeability is measured directly by producing a differential pressure across a specimen and measuring the corresponding volume of fluid which permeates through the sample (see Figure 7.2-1). This differential pressure can be controlled to within $\pm$ 3.5 KPa at absolute pressures to 62 MPa.

A stainless steel hypodermic needle, .15 cm in diameter, is mounted vertically through the base of the pressure cell and the sediment sample is pushed down axially over it. The needle contains a thermistor and a nickel-chromium resistor wire, and is filled with a high temperature epoxy resin which allows tests to be performed at temperatures up to 220°C. Thermal conductivity is measured by the needle probe technique (Jaeger, 1958; Von Herxen and Maxwell, 1959). In this method, the temperature response of the thermistor to a specified heat input form the resistance wire is monitored as a function of time and directly related to the sediment thermal conductivity.

A detailed description of the laboratory equipment has been presented in past reports and a photograph of the completed apparatus is included as Figure 7.2-2.

A systematic series of experiments was conducted with each of two clay types, illite and smectite. The undisturbed illite samples were obtained form a gravity core retrieved from MPG-I (MARA-12 cruise). A

series of four cylindrical samples, 5 cm. in diameter by 10 cm. long, was obtained along the length of the core; the specimens were taken in close proximity to one another in order to minimize any mineralogical variations among them. The smectite samples, also 5 cm. by 10 cm., were reconstituted and reconsolidated (remolded) and had originally been obtained from MPG-I as well (LL-44 cruise). Both clays are identified in Table 7.1-1 below.

Table 7.1-1

SAMPLE IDENTIFICATION

SAMPLE	LOCATION	WATER DEPTH (m)	GRAIN SIZE ANALYSIS SAND (%)	SILT (%)	CLAY (%)	MEDIAN (m)	MEAN (m)	SPECIFIC GRAVITY
ILLITE	31°04'N, 159°03'W	5900	0.6	34.6	64.8	0.9	0.8	2.78
SMECTITE	30°24'N, 157°50'W	5900	0.9	27.1	72.0	0.8	0.7	2.74

Each series of samples from the two sediment types was tested at 22°, 80°, 150°, and 220°C. The initial experiment, which was performed at room temperature, also included the variable pressure work. In this study, permeability and thermal conductivity were measured at a constant void ratio as the sediment sample was exposed to hydrostatic pressures ranging from 2 to 60 MPa. The tests conducted at the higher temperatures were performed at constant pressure; the in situ hydrostatic pressure of the clay sample. In these latter tests, the specimens were also consolidated through a series of void ratios to determine the effect of water content upon the physical properties.

7.3 Results

The first series of laboratory tests was designed to address the possible phenomenon of a pressure-induced breakdown of the double layer, along with its effect on permeability. The results are shown in Figure 7.3-1, with experimental accuracy being ± 10%. These data show negligible pressure effects upon the permeabilities of the clays. Permeability is affected by the viscosity of the permeating medium which, in this case, is sea water. Horne (1965) shows approximately a 1% decrease in the relative viscosity of an aqueous, .5N NaCl solution at 60 MPa and 25°C. This viscosity correction for pressure was not applied, since it is well within the accuracy of the test. It is interesting to note that the viscosity of water at room temperature, unlike that of any other liquid, decreases with increasing pressure, again implying an effective breakdown in its structure.

Bridgman (1949) has found that the thermal conductivity of water is primarily a function of density. As its density increases with increasing pressure, so does its thermal conductivity. The results of the thermal conductivity versus pressure tests for both sediment types are depicted in Figure 7.3-2, with the data closely paralleling the behavior of water alone as a function of pressure (Lawson et al, 1959). The effect of pressure on the thermal conductivity of solids is much less than and that of liquids. This was confirmed by Bridgman's work with both metals on non-metals. Since these sediments are primarily water, with porosities ranging from .70 to .88, and since the effect of pressure upon the thermal conductivity of the solid matrix is minimal, the results are expected to reflect the pressure effects upon the liquid phase alone.

Temperature Effects

The results of the permeability tests as a function of temperature are displayed in Figures 7.3-3 through 7.3-6. The values are corrected for pore fluid viscosity effects (Keenan et al, 1978), and graphs of absolute permeability are presented for each sediment type in Figures 7.3-4 and 7.3-6. The absolute permeability incorporates a temperature correction for the viscosity of sea water and carries the units of length squared .

$$K_{abs} = K \frac{\upsilon}{g}$$

K_{abs} = absolute sediment permeability

K = sediment permeability

υ = kinematic viscosity of pore fluid

g = gravitational constant

Although a reduction of the clay double layer has been indicated from the literature, the results show no obvious dependence of absolute permeability upon temperature for these sediments.

Information relating the effect of temperature upon the thermal properties of rocks has been presented by Birch and Clark (1940). Their results show that the thermal conductivity of all the rocks tested decreases gradually with increasing temperature up to 350°C. Keenan et al (1978), on the other hand, predict that the thermal conductivity of water increases with temperature until it reaches a maximum at about 150° and then begins to decline with increasing temperature. Some of these latter data on water are included in Figure 7.3-7. The temperature at which the thermal conductivity is a maximum shifts slightly as the hydrostatic pressure changes. As in the case with the variable pressure analysis, the effect of temperature upon the thermal conductivity of the sediments is dominated by the behavior of the liquid constituent alone.

Consolidation Effects

After initial pressurization and heat-up, each test specimen was consolidated through a series of decreasing porosities in order to simulate compaction through the sediment column. At each prescribed stage, its permeability and thermal conductivity were measured. The permeability data plotted in Figures 7.3-3 through 7.3-6 closely approximate the results of prior studies performed on consolidated marine sediments (Bryant, et al., 1975, Silva et al., 1981).

The results of the thermal conductivity versus void ratio experiments for the two sediment types are presented in Figures 7.3-8 and 7.3-9. The expected trend of increasing conductivity with decreasing water content is consistent with previous work (Ratcliffe, 1960). The graphs illustrate how the solid phase constituents, with their higher thermal conductivities, begin to influence the two-phase conductivities of the sediments to a greater degree as porosity decreases. Various mixture theories have been proposed to predict the thermal conductivity of saturated porous media in terms of the constituent properties and the porosity. Both parallel and series conduction models, along with various combinations of the two, have been developed and are examined by Bear (1972). Although Horai (1971) has measured the thermal properties of a large number of rock-forming minerals, determining the conductivity of the actual solid matrix has continued to be a problem for investigators. Hadley et al. (1981) have presented a best fit curve relating thermal conductivity to porosity for a wide variety of geologic materials, ranging from crustal rocks to soft sediments. This information indicates that the relationship between the two is best approximated by some combination of the parallel and series models. Within the narrow range of high porosities relevant to this study, however, both models tend to coincide and are reasonably accurate.

7.4 Analysis and Conclusions

The results of both the permeability and thermal conductivity tests as a function of void ratio are consistent with previous laboratory studies performed by other investigators on similar sediments. This agreement is important, since it lends confidence to our experimental technique and apparatus. No inconsistencies due to inherent differences in laboratory equipment design were discovered.

Previous studies seem to strongly indicate that, in the case of clays, the diffuse double layer is directly affected by large variations in pressure and temperature. The existence of this phenomenon was not verified in this study and there appears to be no discernible influence upon sediment permeability. This conclusion shows that more conventional laboratory permeability procedures at much lower hydrostatic pressures are valid and the results can be used for higher pressure conditions.

Because of the high porosities encountered in these tests, pressure and temperature effects upon sediment thermal conductivities where found to be dominated by the behavior of the liquid phase. If values of permeability and thermal conductivity are known at room temperature and at few MPa hydrostatic pressure, additional values at more severe environmental conditions can be predicted by simply correcting for the variation in the water properties. Temperature induced diagenesis, however, is still poorly understood and long-term physical properties experiments at relatively high temperature would improve our knowledge of the process.

Further test results obtained within a much lower range of sediment porosities would be helpful in analyzing the role of the solid matrix in dictating sediment conductivity responses to large pressures and high temperatures. This information would facilitate the development of proper thermal conduction models and would extend our predictive capabilities to greater depths within the sediment column.

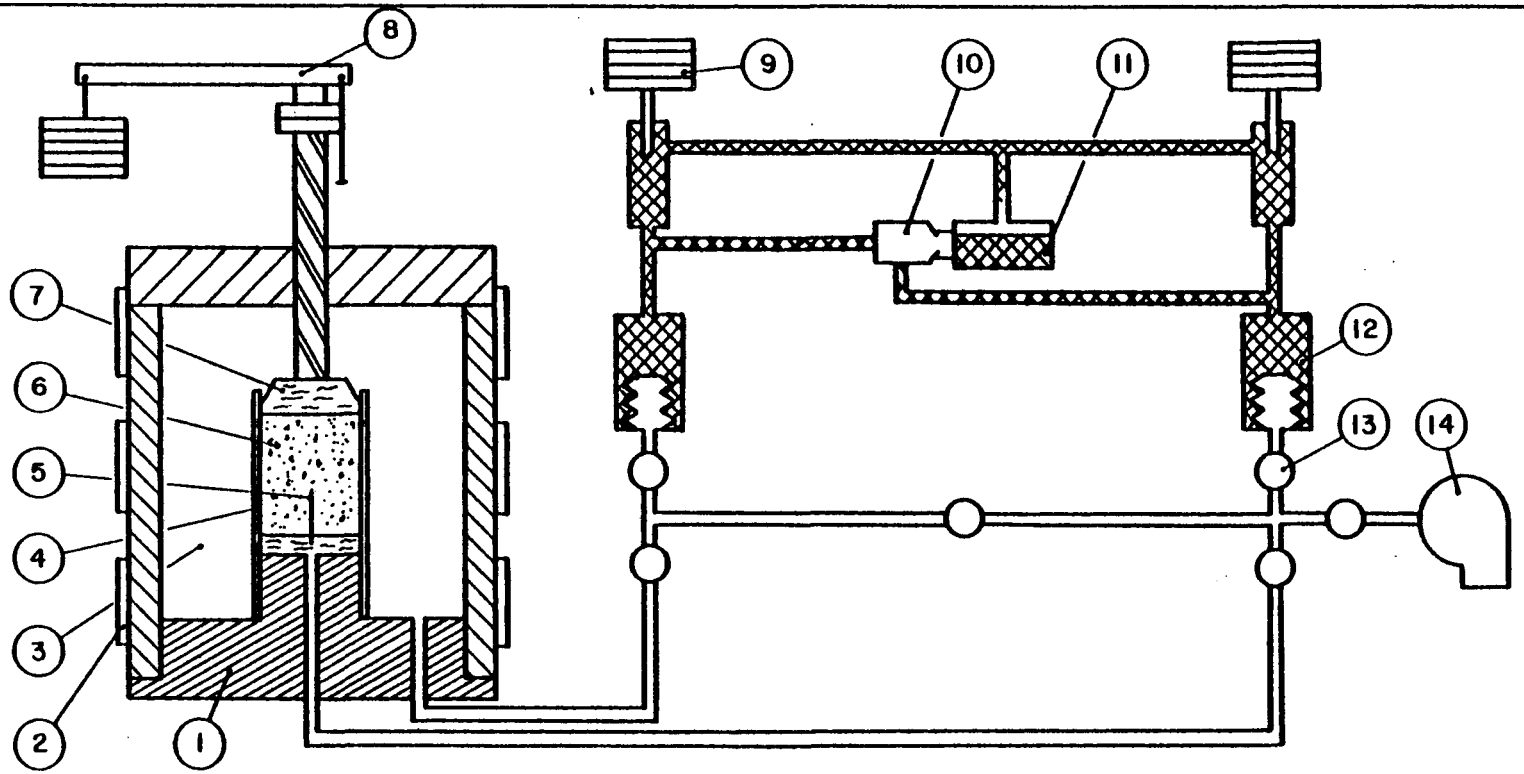
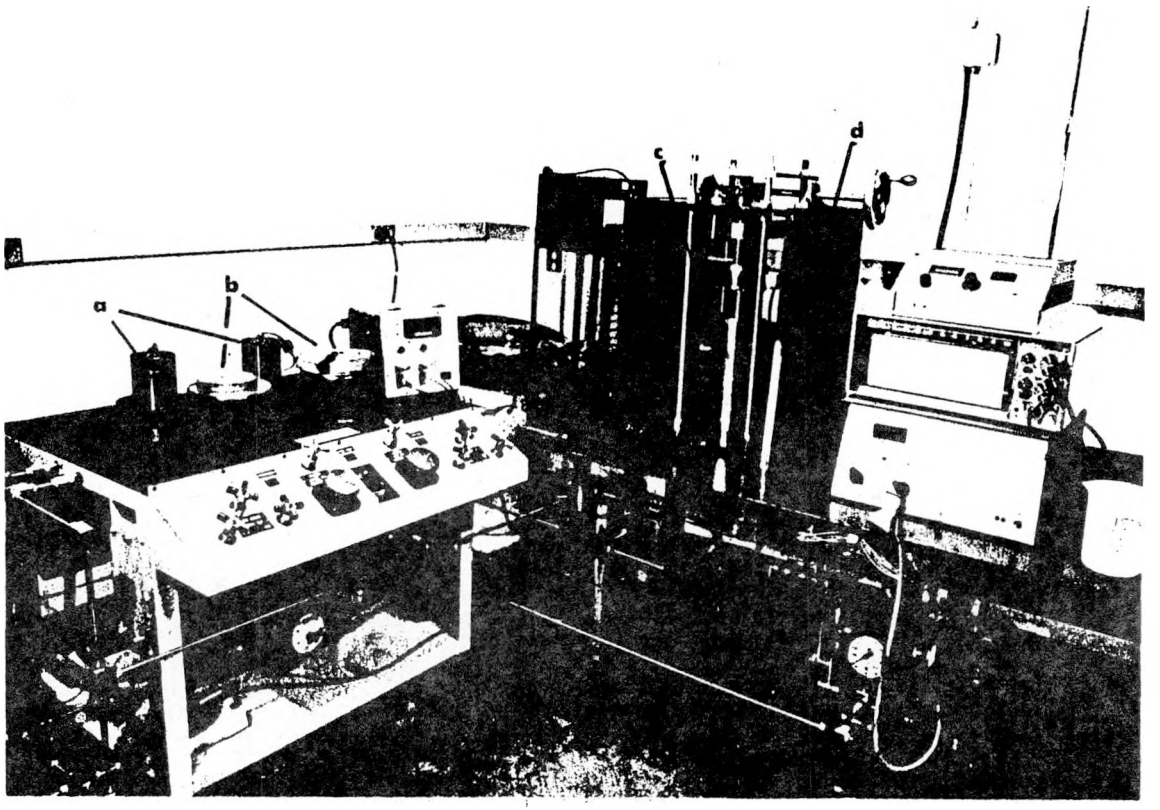


DIAGRAM OF APPARATUS

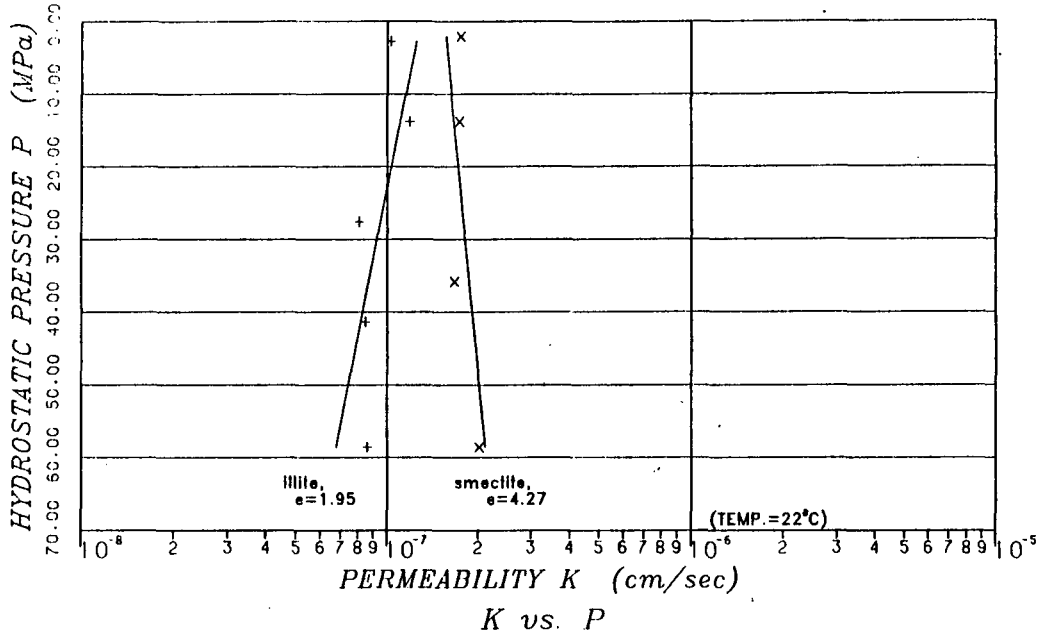
1. High Pressure Triaxial Cell
2. Heating Band
3. Sea Water
4. Cinfining Ring
5. Thermal Conductivity Probe
6. Sediment Sample
7. Porous Filter
8. Loading Frame with Weights
9. Dead Weight Tester
10. Recirculating Hydraulic Pump
11. Oil Reservoir
12. Volume Change Device with Bellows
13. High Pressure Valve
14. High Pressure Roughing Pump

Figure 7.2-1



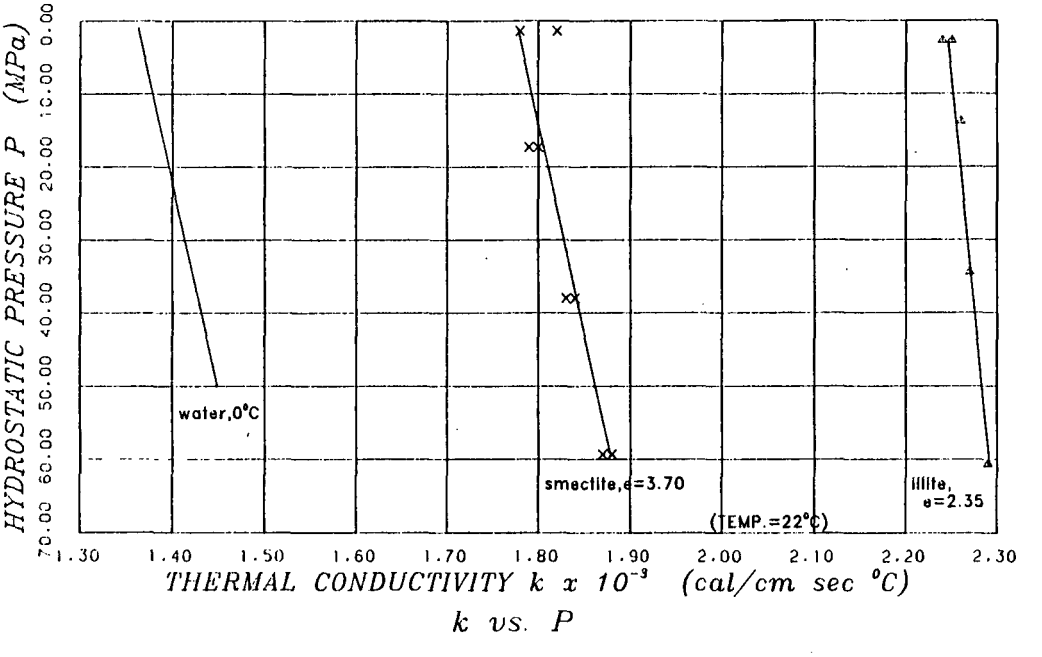
Unit at left contains two volume change devices (a) behind the two dead-weight testers (b), a 5 HP motor and a hydraulic pump. Pressure cell (c) is shown inside loading frame (d) and electronic instrumentation controls are at right.

Figure 7.2-2



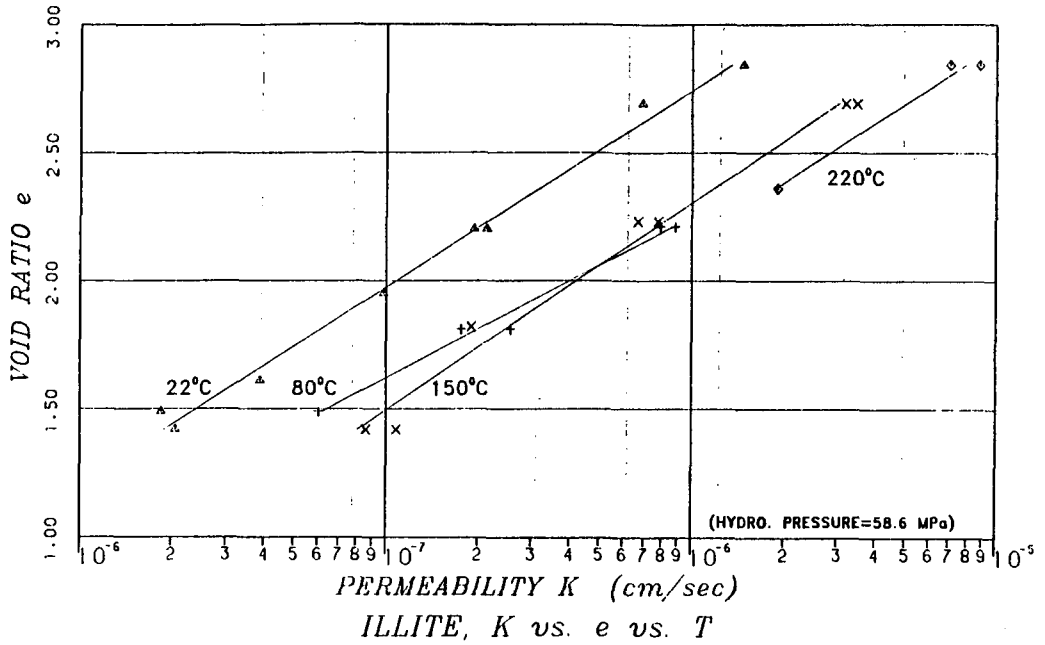
K vs. P

Figure 7.3-1



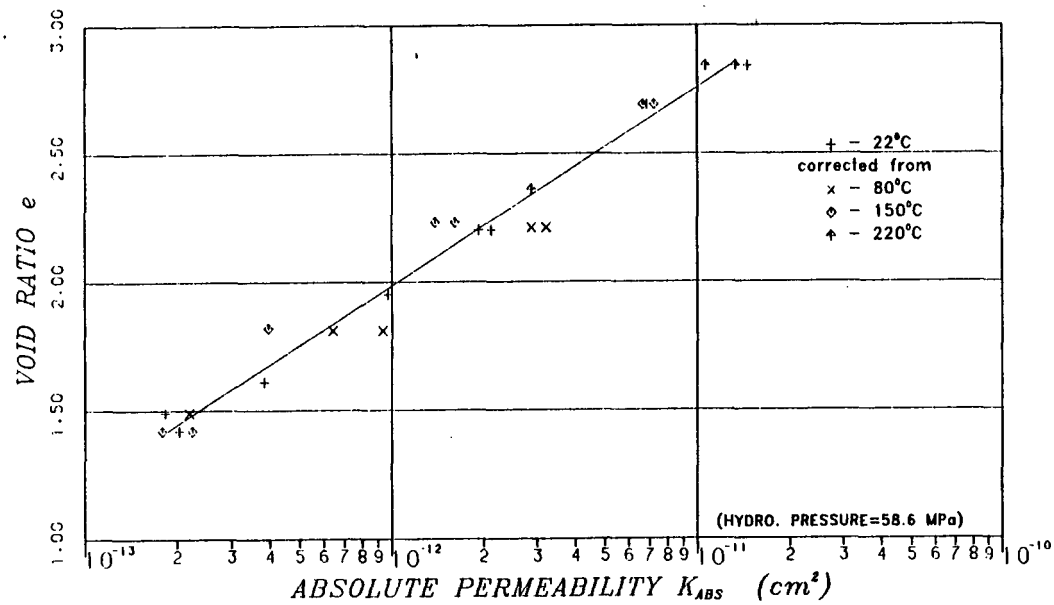
k vs. P

Figure 7.3-2



ILLITE, K vs. e vs. T

Figure 7.3-3



ILLITE, K_{ABS} vs. e

Figure 7.3-4

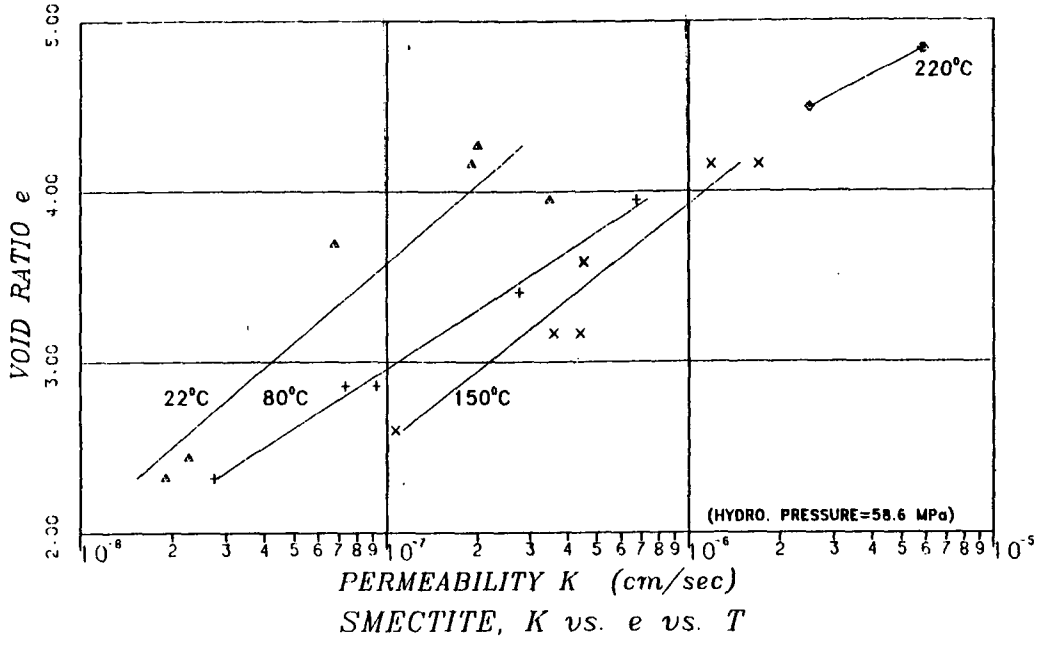


Figure 7.3-5

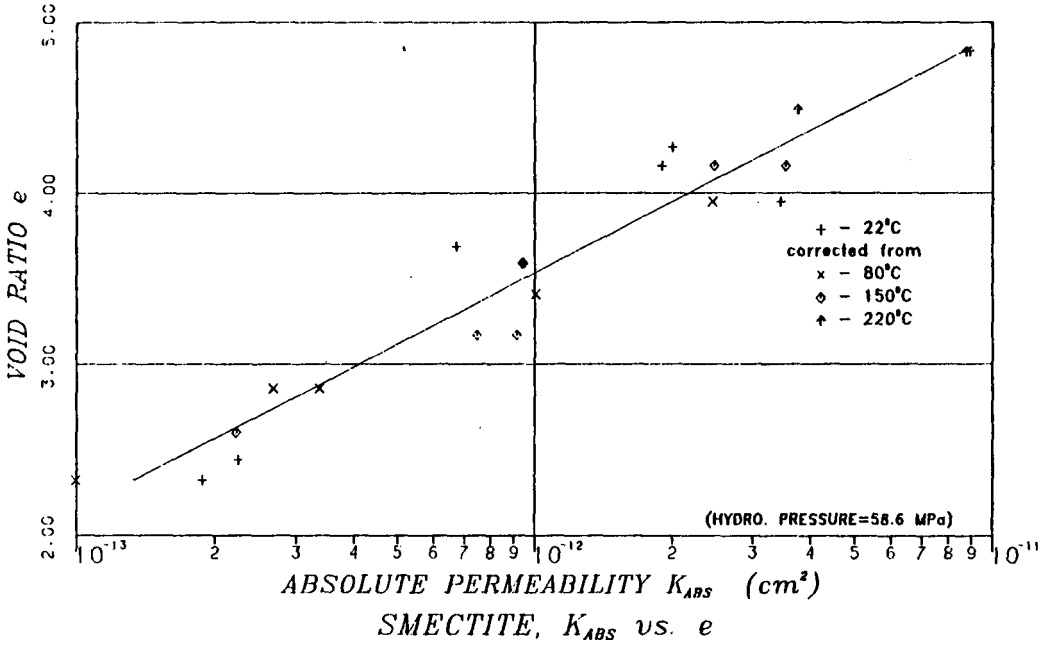


Figure 7.3-6

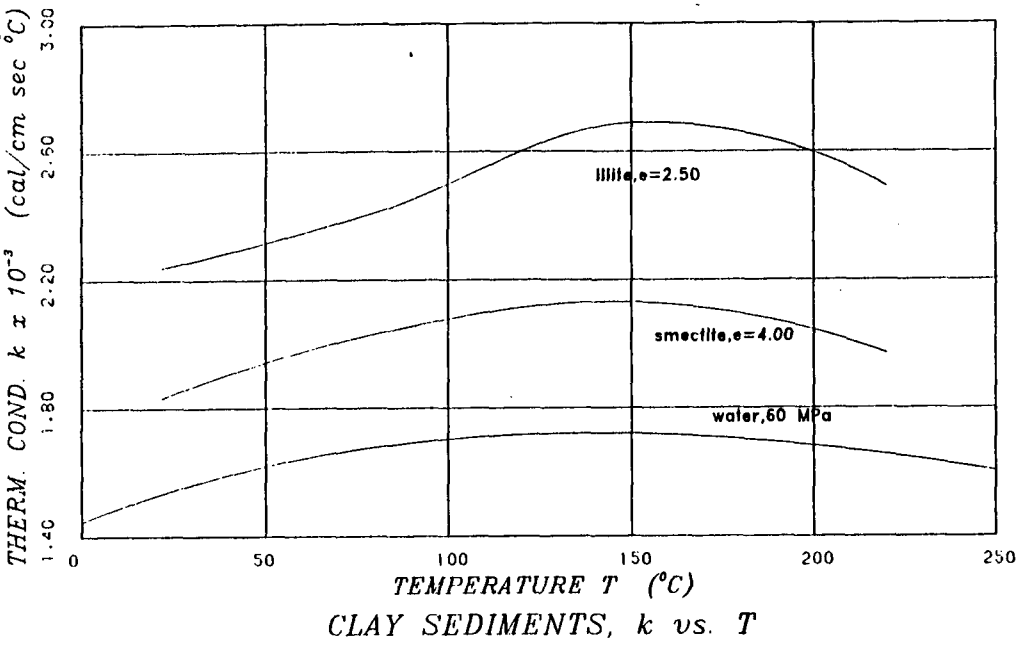


Figure 7.3-7

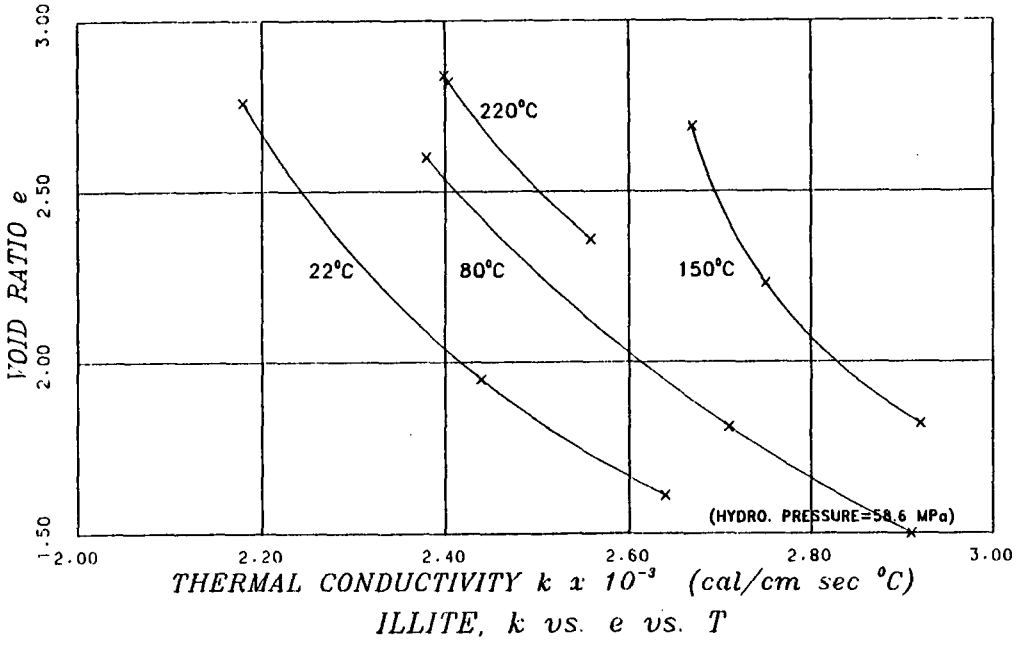


Figure 7.3-8

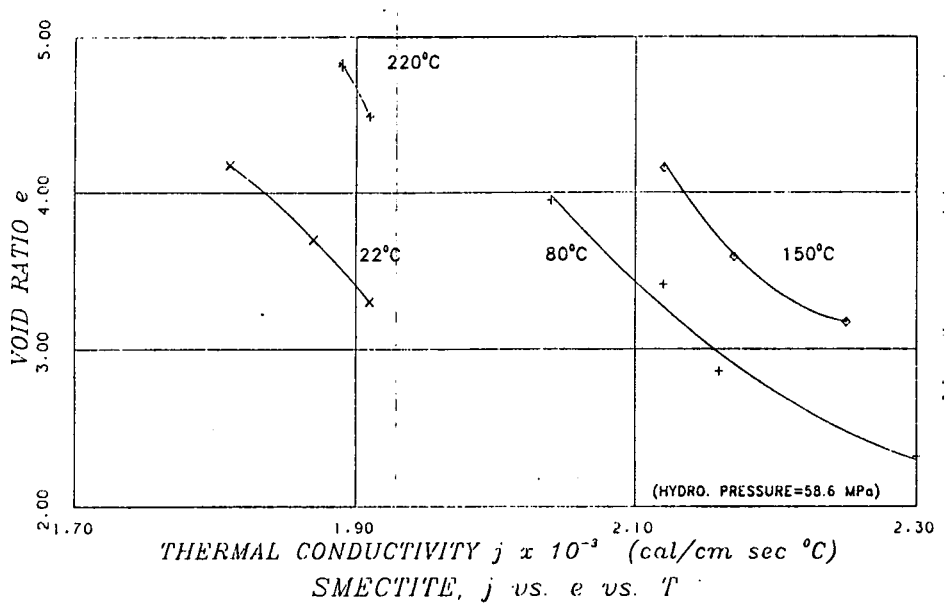

220°C
22°C
80°C
150°C
(HYDRO. PRESSURE=58.6 MPa)
VOID RATIO e
5.00
4.00
3.00
2.00
1.70
1.90
2.10
2.30
THERMAL CONDUCTIVITY j x 10⁻³ (cal/cm sec °C)
SMECTITE, j vs. e vs. T

Figure 7.3-9

8.0 SIMPLE SHEAR STUDIES (B. Levy, S. Salehipour)

8.1 Introduction

Under simple shear conditions the stresses acting upon the specimen are in totally different orientations than previously examined in soil testing as part of the SDP. For this reason simple shear behavior is of interest to modelling efforts aimed at characterizing soil behavior under all types of boundary conditions that may occur during canister emplacment.

The objective of this initial program is to run a series of tests on undisturbed and remolded Pacific illite samples, analyze the results and then develop a more extensive program examining simple shear behavior using the De Steiger cruise samples.

8.2 Equipment Description

The equipment used for this testing was specially designed for URI/MGL by Geotechnical Equipment, Inc. (Figure 8.1-1). The unit has a pressure chamber similar to a triaxial cell. This is an important improvement on the older NGI equipment that has been more commonly in use, as this allows independent control of the horizontal and vertical stresses as well as the ability to back-pressure saturate, consolidate and shear with pore pressure measurements. The flexibility of the system allows stress path testing to be done. K_o consolidation (no lateral straining) can be easily performed prior to shear either by restraining the specimen in wire-reinforced membranes or within articulated Teflon-coated rings. Plain triaxial membranes are available so any anisotropic combination of horizontal and vertical stresses can be applied as well.

Loading can be done statically or dynamically. Static loads in the horizontal direction can be stress or strain controlled. Dynamic loads can be applied in either the horizontal or vertical direction or both. The cyclic loaders are pneumatically actuated Bellofram sealed pistons. Amplitude, frequency, and shape of waveform (triangular, square or sinusoidal) are accurately controlled by a function generator.

Special allowances for accurate measurement have been built right into the system. Both the vertical and horizontal load cells are pressure compensated and set inside the cell so that friction effects of the piston are bypassed. Special hermetically sealed DCDT's pass completely through the cell to directly contact the top and bottom platens. Besides allowing for very accurate sample deformation measurements this also takes any equipment compliance into account by measuring the relative deformation between the two platens.

8.3 Program Status and Test Schedule

The simple shear apparatus has now been totally assembled and calibrated. A preliminary set of remolded specimens were used to check out the system in both static and cyclic modes. Based on these tests further minor modifications to the system were needed and are underway.

A preliminary set of remolded Pacific illite (PI 5-8) will be tested under K_o conditions at various consolidation pressures in strain controlled static shear. These results will then be compared with triaxial compression data. Several of these samples will be tested in bidirectional low frequency cyclic shear as well. A similar test program using undisturbed illite from the MPG-I area will then follow. Finally, remolded smectite and DeSteiger cruise subsamples will be examined towards the latter part of FY'82.

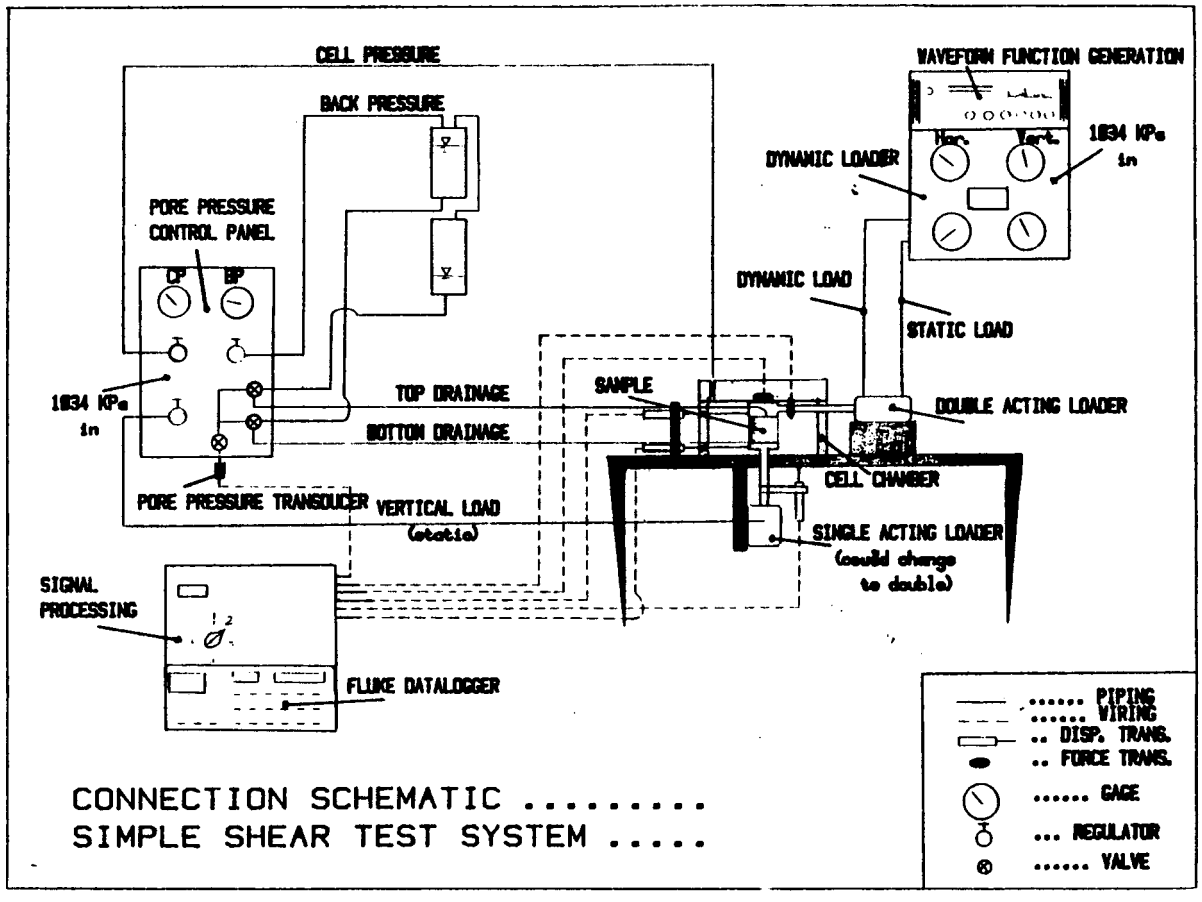


Figure 8.1-1

REFERENCES

Akers, S.A. and Silva, A.J., Stress-Strain and Strength Properties of Marine Sediments from the North Pacific, URI Tech. Report., June 1980.

Banford, S.R. and Silva, A.J., Hole Closure Behavior of Marine Sediments Following Projectile Penetration, URI Tech. Report, June 1980.

Bear, J., Dynamics of Fluids in Porous Media, Am. Elsevier, Inc., 1972.

Birch, F. and H. Clark, The Thermal Conductivity of Rocks and its Dependence upon Temperature and Composition, Am. J. of Science, 238, 529-558, 1940.

Bridgman, P.W., The Physics of High Pressure, G. Bell and Sons, Ltd., 1949.

Bryant, W.R., W. Hottman and P. Trabant, Permeability of Unconsolidated and Consolidated Marine Sediments, Gulf of Mexico, Marine Geotech., 1, 1-13, 1975.

Crowe, J. and A.J. Silva, Permeability Measurements of Equatorial Pacific Carbonate Oozes Using a Direct Measurement Back-Pressured Technique, in press in J. Geophys. Res., 1981.

Duncan, J.M. and Seed, H.E., Errors in Strength Tests and Recommended Corrections, Report No. TE-65-4, Dept. of Civil Eng., Univ. of California, Berkeley, 1965.

Hadley, G.R., D.F. McVey and R. Morin, Thermophysical Properties of Deep Ocean Sediments, in press in Marine Geotech., 1982.

Horai, K., Thermal Conductivity of Rock-Forming Minerals, J. Geophys. Res., 76, 1278-1308, 1971.

Horne, R.A., The Physical Chemistry and Structure of Sea Water, Water Resources Res., 2, 263-276, 1965.

Jaeger, J.C., The Measurement of Thermal Conductivity and Diffusivity with Cylindrical Probes, Trans., Am. Geophys. Union, 13, 708-710, 1958.

Keenan, J.H., F.G. Keyes, P.G. Hill and J. G. Moore, Steam Tables: Thermodynamic Properties of Water including Vapor, Liquid, and Solid Phases, John Wiley and Sons, 1978.

Khitarov, N.I. and V.A. Pugin, Behavior of Montmorillonite Under Elevated Temperatures and Pressures, Geochem. International, 3, 62-626, 1966.

Lawson, A.W., R. Lowell and A.L. Jain, Thermal Conductivity of Water at High Pressures, 3. of Chem. Phys., 30, 643-647, 1959.

Lambe, T.W., and Whitman, R.V., "Soil Mechanics," John Wiley & Sons, Inc., New York, 1969.

Leinen, Margaret and Heath, G. Ross, "Paleochemical Signatures in Cenozoic Sediments from the Central North Pacific," Geochemica et Cosmochimica Acta, 1980.

Mac Donald, K. and G. Simmons, Temperature Coefficient of the Thermal Conductivities of Ocean Sediments, Deep-Sea Res., 19, 669-671, 1972.

Mitchell, J.K., "Fundamentals of Soil Behavior," John Wiley and Sons, Inc., 1976.

Moran, K., Atlantic/Abyssal Plain-HUDSON Cruise, URI Geotechnical Report, 1980.

Moran, K., Drained Creep of Deep Sea Sediments, M.S. Thesis, URI, 1981.

Muller, G., Diagenesis in Argillaceous Sediments, Chapt. 4 in Developments in Sedimentology 8, Diagenesis in Sediments, G. Larsen and G.V. Chilingar (eds.), Elsevier Publishing Co., 1967.

Nickerson, C.R., Consolidation and Permeability Characteristics of Deep-Sea Sediments: North Central Pacific Ocean, M.S. Thesis, Worcester Polytechn. Inst., 1978.

Ratcliffe, E.H., The Thermal Conductivities of Ocean Sediments, J. Geophys. Res., 65, 1535-1541, 1960.

Seed, H.B., Woodward, R.J., and Lundgren, R. "Prediction of Swelling Potential for Compacted Clays," J. of Soil Mech. and Found. Div., ASCE, Vol. 90, No. SM4, 1962.

Schmartmann, J.H., "The Undisturbed Consolidation Behavior of Clay," Trans. ASCE 120.

Schwartz, S., Undrained Stress-Strain Behavior of Anisotropically Consolidated Deep-Sea Clays, M.S. Thesis, URI, 1980.

Schwartz, S. and Silva, A.J., Undrained Stress-Strain Behavior of Anisotropically Consolidated Deep Sea Clays, URI Tech. Report, 1981.

Silva, A.J. and Calnan, D.I., "Geotechnical Aspects of Subsurface Seabed Disposal of High Level Radioactive Wastes," Annual Progress Report No. 4, DOE/SLA Contract No. 05-7899, May 1978.

Silva, A.J. and Calnan, D.I., "Geotechnical Aspects of Subsurface Seabed Disposal of High level Radioactive Wastes," Annual Progress Report No. 5, Contr. No. 05-7899 and 13-2561, 1979.

Silva, A.J. and Calnan, D.I., "Geotechnical Aspects of Sub-seabed Disposal of High Level Radioactive Wastes," Annual Progress Report No. 6, DOE/SLA Contr. No. 13-2561 and 13-9927, May, 1980.

Silva, A.J., J.R. Hetherman and D.I. Calnan, Low-Gradient Permeability Testing of Fine-Grained Marine Sediments, Permeability and Groundwater Contaminant Transport ASTM STP 756, T.F. Zimmie and C.O. Riggs, Eds., Am. Soc. of Testing and Materials, P. 121-136, 1981.

Silva, A.J., Jordan, S.A., Levy, W.P., "Geotechnical Aspects of Subseabed Disposal of High Level Radioactive Wastes," DOE/SLA Contracts Nos. 13-9927 and 74-1098, March 1981.

Terzaghi, K., "Theoretical Soil Mechanics," J. Wiley & Sons, New York, 1943.

Terzaghi, K. and Peck, R.B., "Soil Mechanics in Engineering Practice," New York (J. Wiley), Second edition, 1967.

Von Herzen, R.P. and A.E. Maxwell, The Measurement of Thermal Conductivity of Deep Sea Sediments by a Needle-Probe Method, J. Geophys. Res., 64, 1557-1563, 1959.

Walker, G.R., "Geotechnical Properties of Deep Sea Sediments in the Northwestern Pacific Ocean," M.S. Thesis, URI, 1981.

Weaver, C.E., Geothermal Alteration of Clay Minerals and Shales: Diagenesis, Tech. Rept. ONWI-21, Office of Nuclear Waste Isolation, Battelle, 1979.

Winterkorn, H.F. and Fang, H.Y., "Foundation Engineering Handbook," Van Nostrand Reinhold Co., New York, 1975.

ADDENDA

Remaining compressibility results
for VEMA-36 cruise, MPG-IV, See Chapter 5.0.

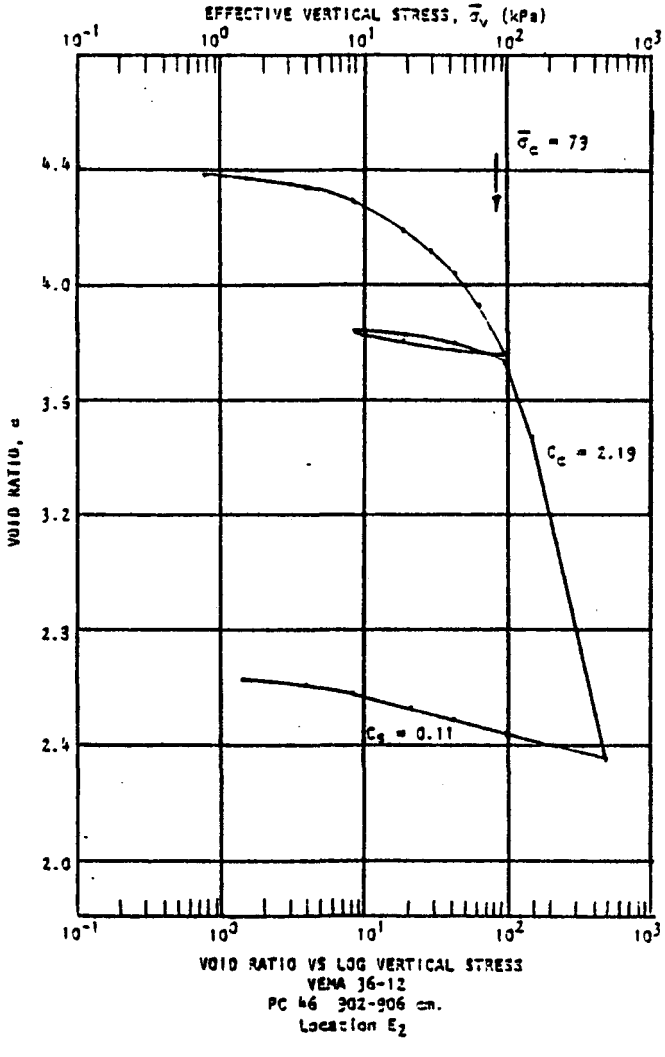


Figure A-1

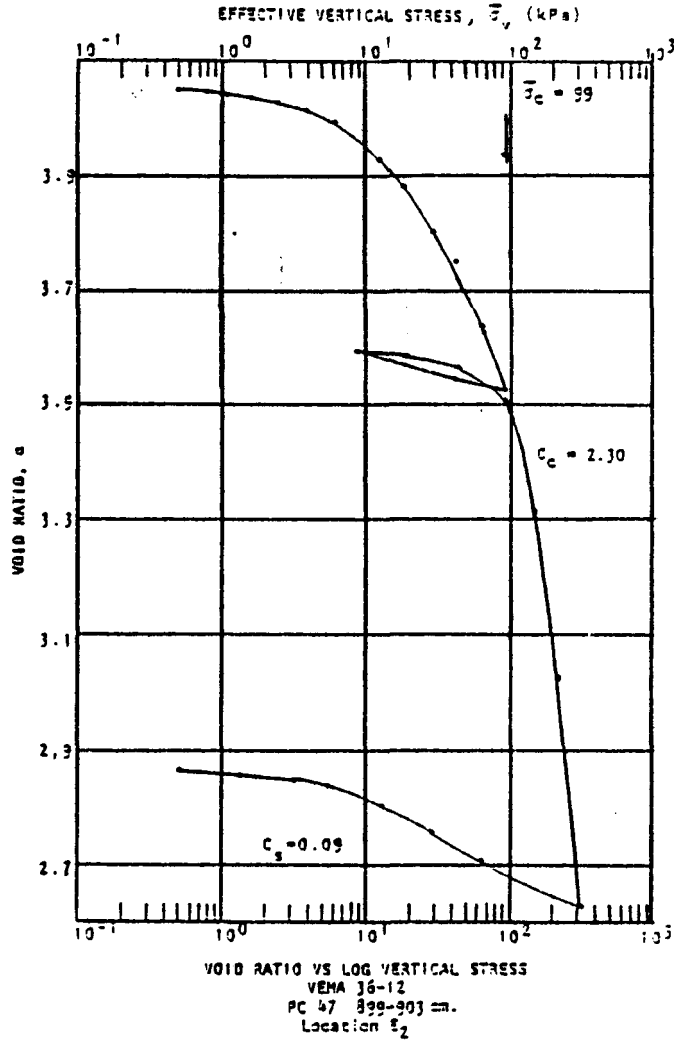


Figure A-2

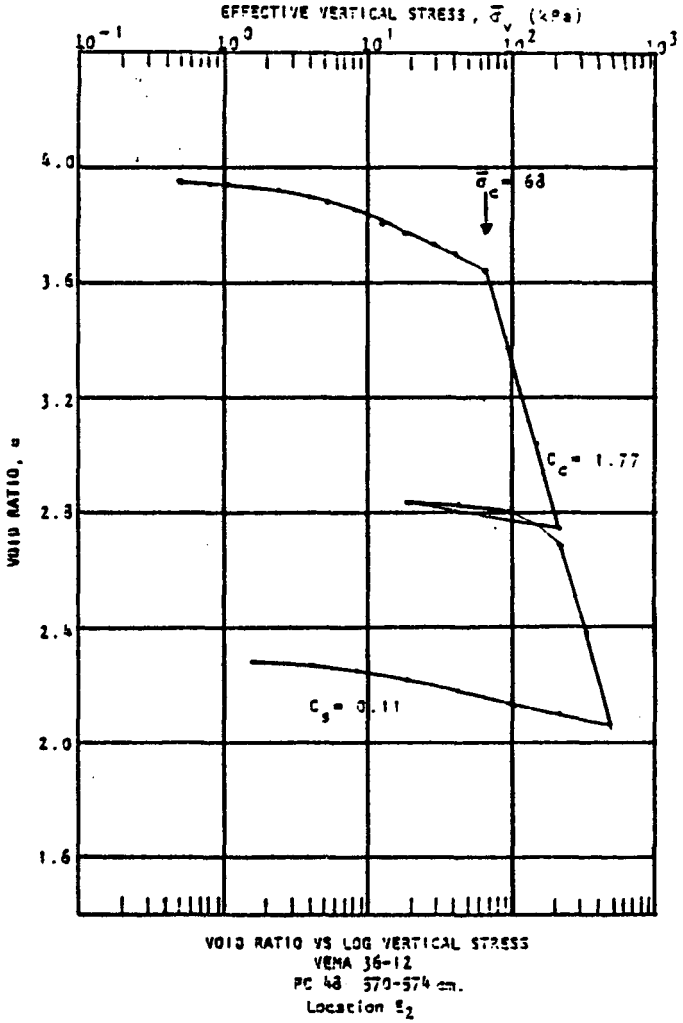


Figure A-3

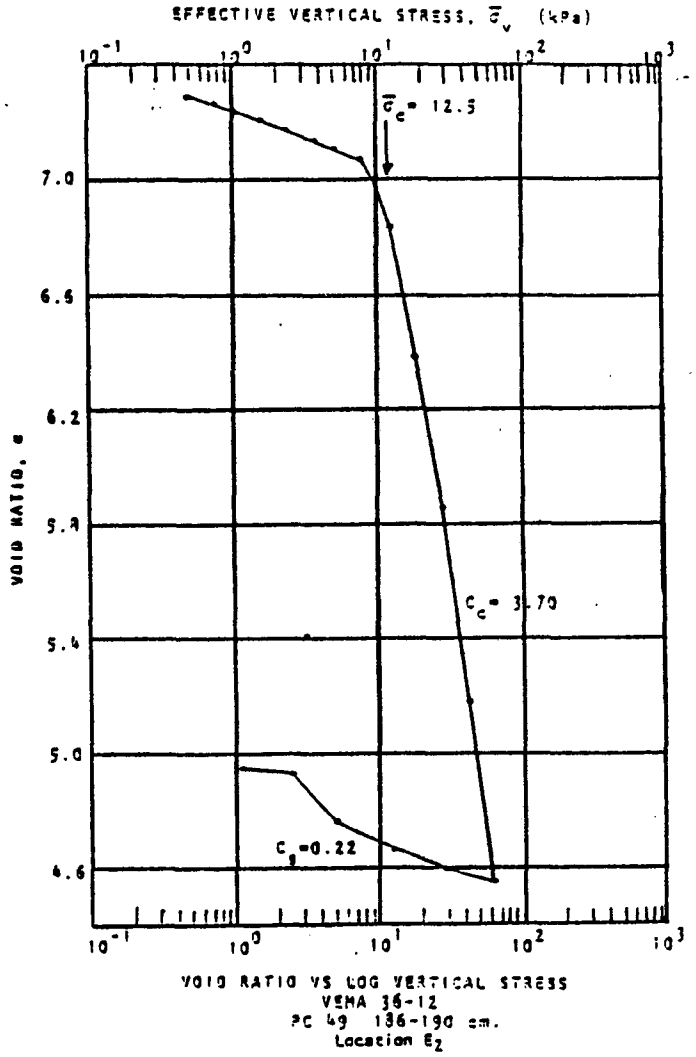
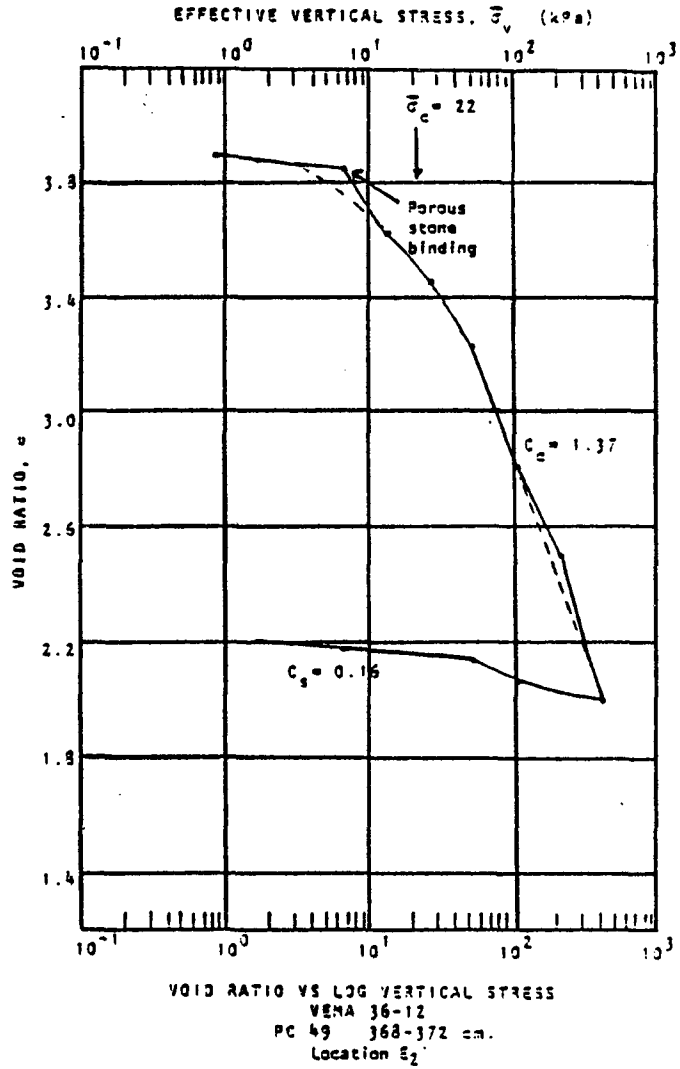
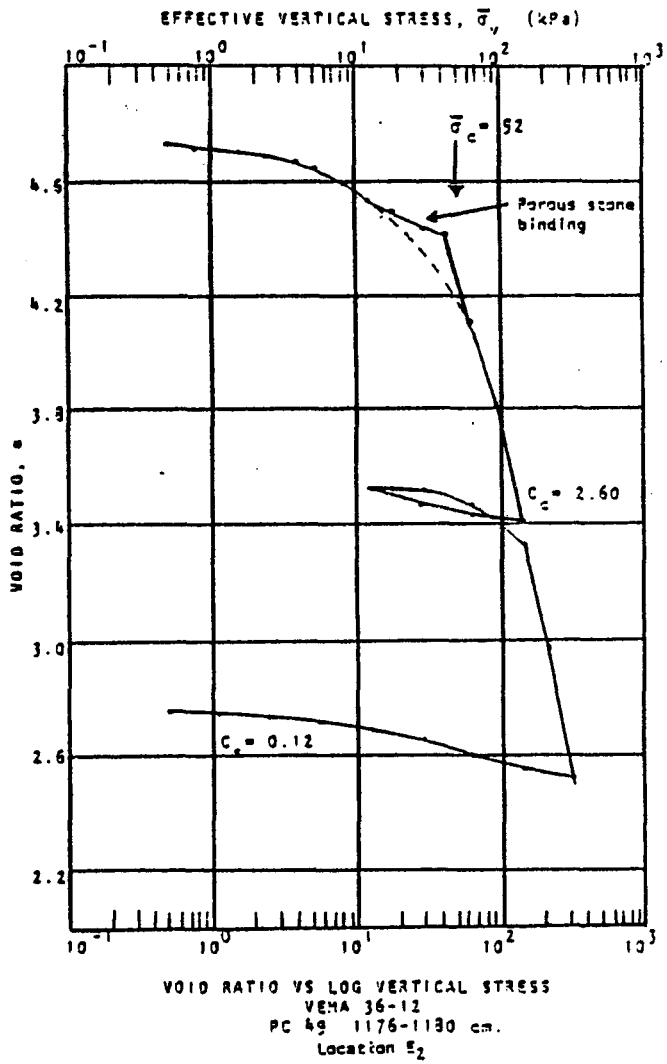


Figure A-4



VOID RATIO VS LOG VERTICAL STRESS
VENA 36-12
PC 49 368-372 cm.
Location E_2

Figure A-5



VOID RATIO VS LOG VERTICAL STRESS
VENA 36-12
PC 49 1176-1180 cm.
Location E_2

Figure A-6

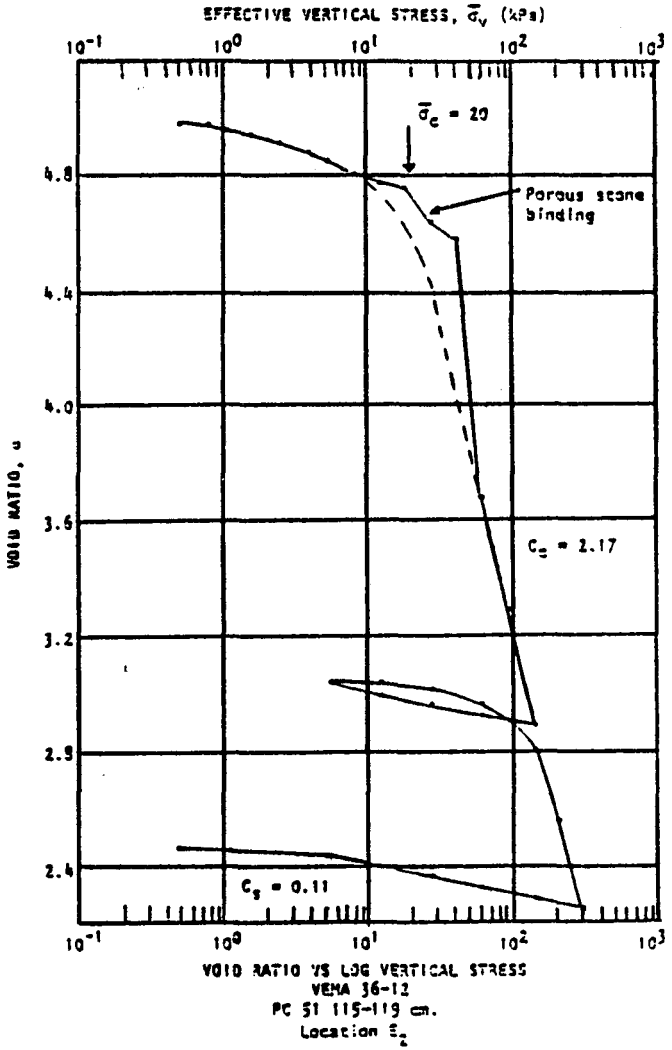


Figure A-7

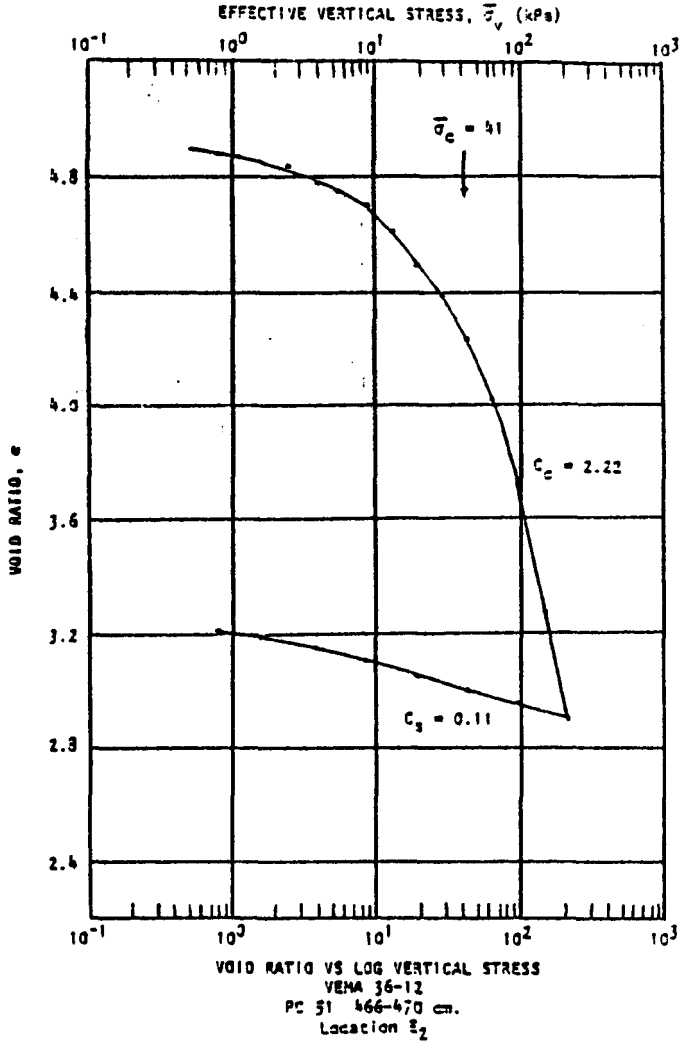


Figure A-8

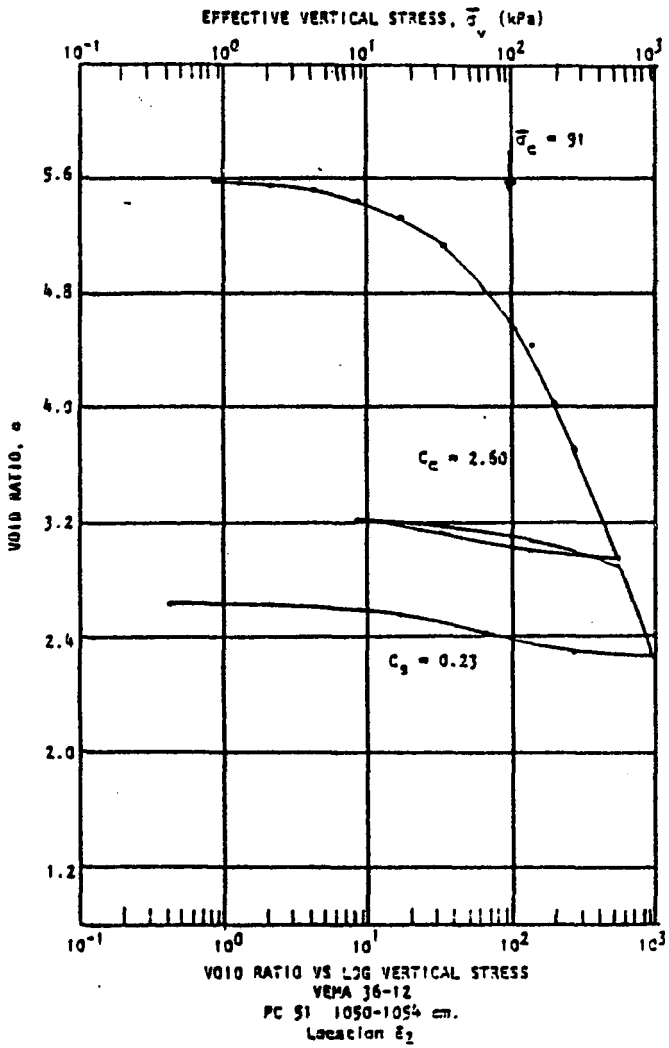


Figure A-9

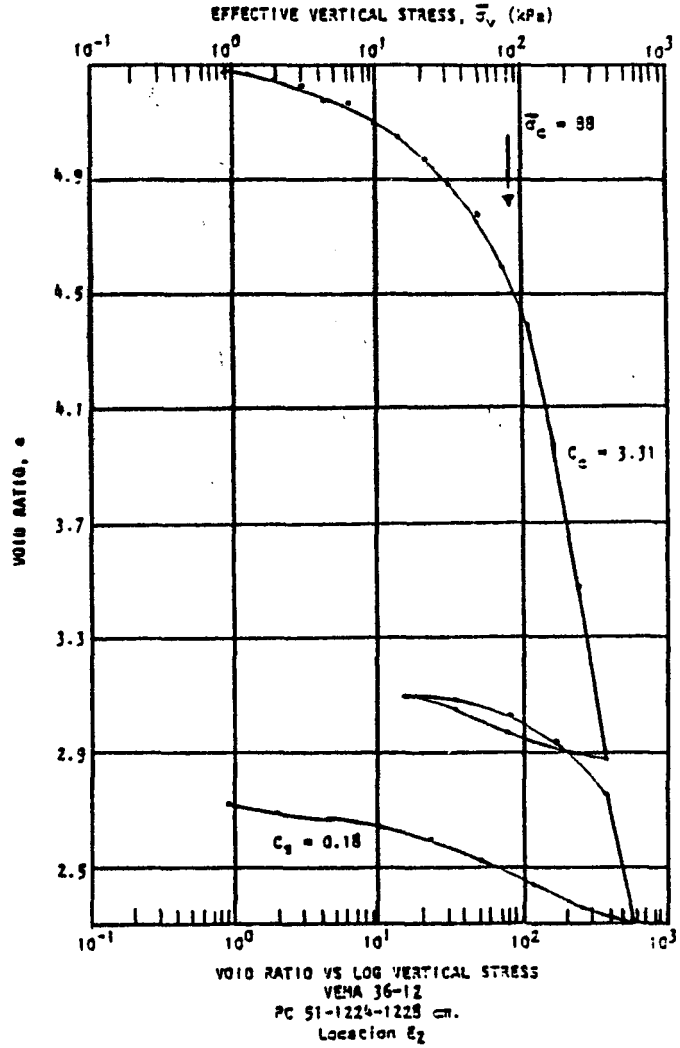


Figure A-10

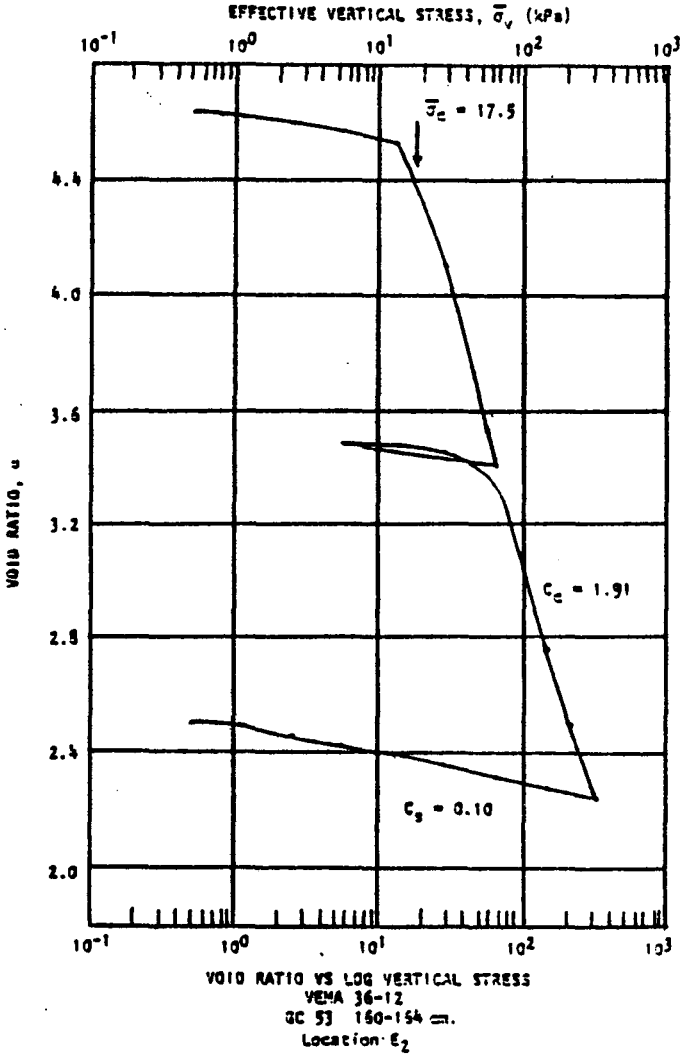


Figure A-11

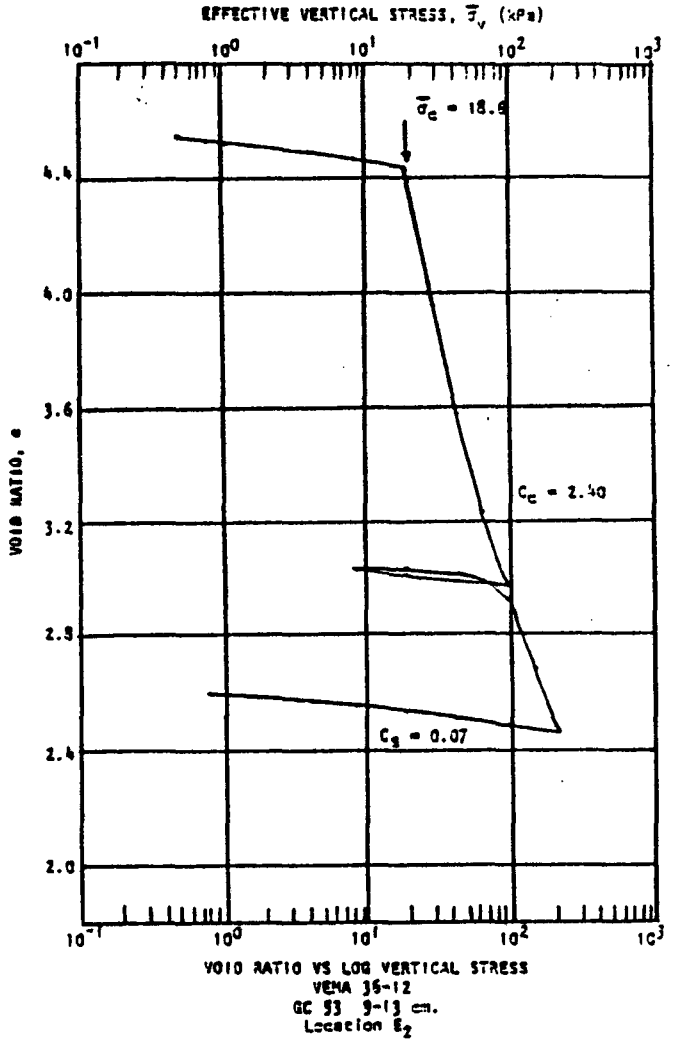


Figure A-12

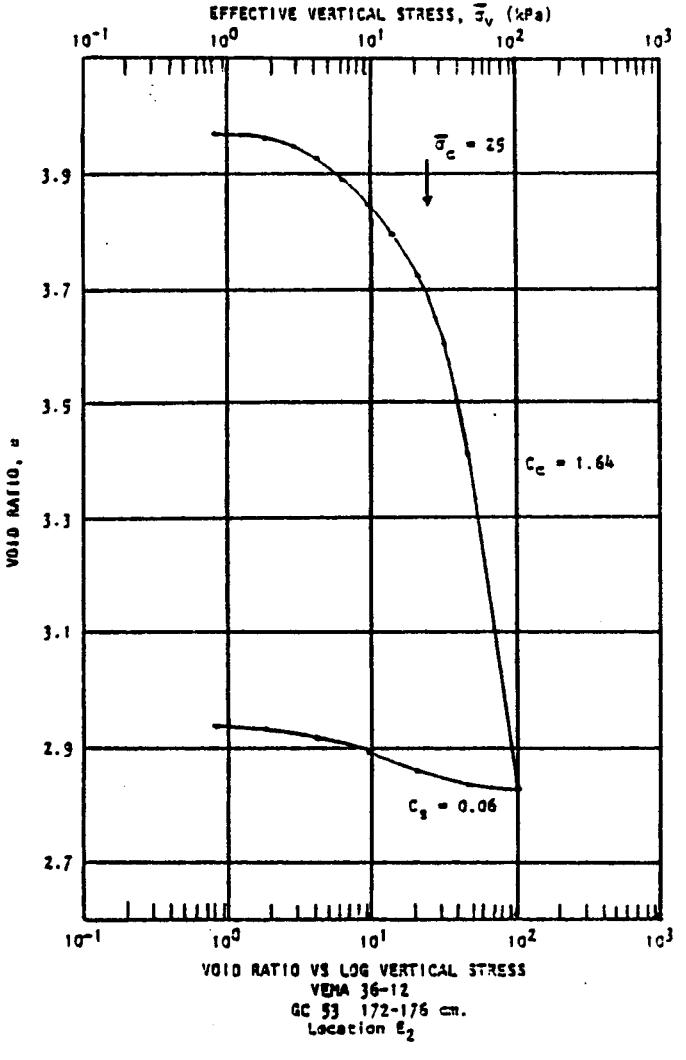


Figure A-13

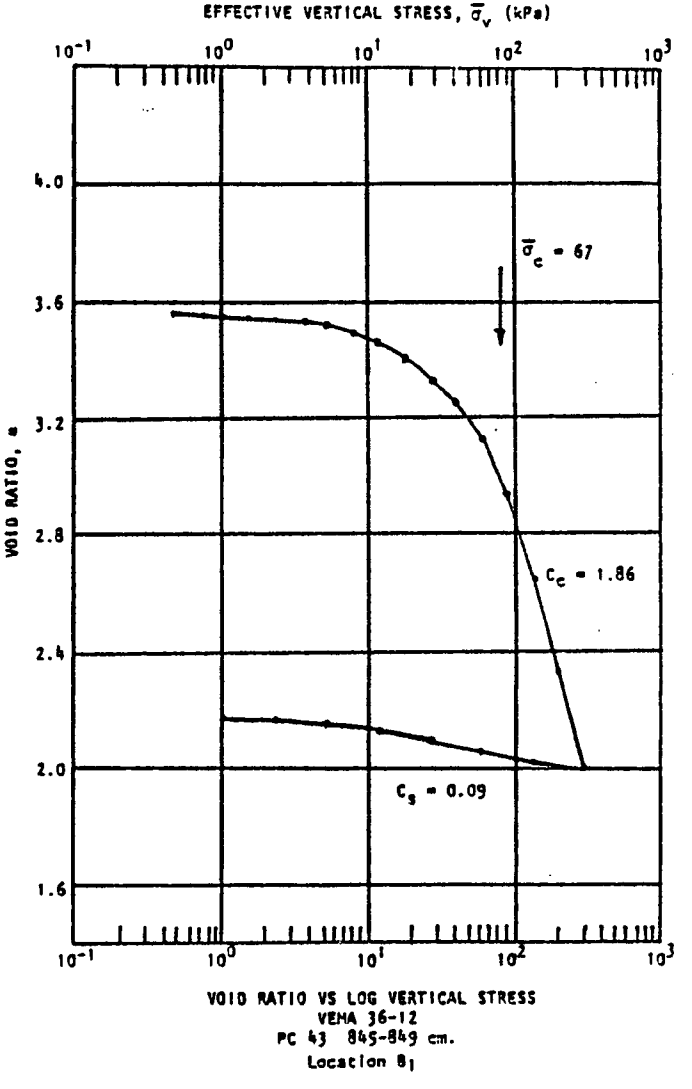


Figure A-14

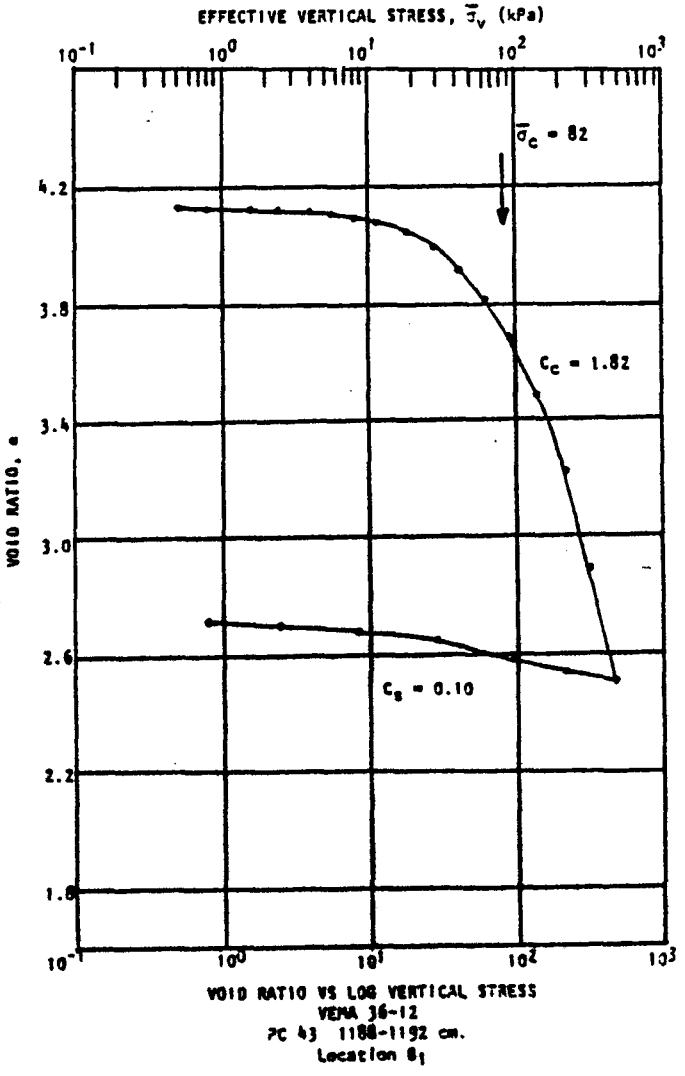


Figure A-15

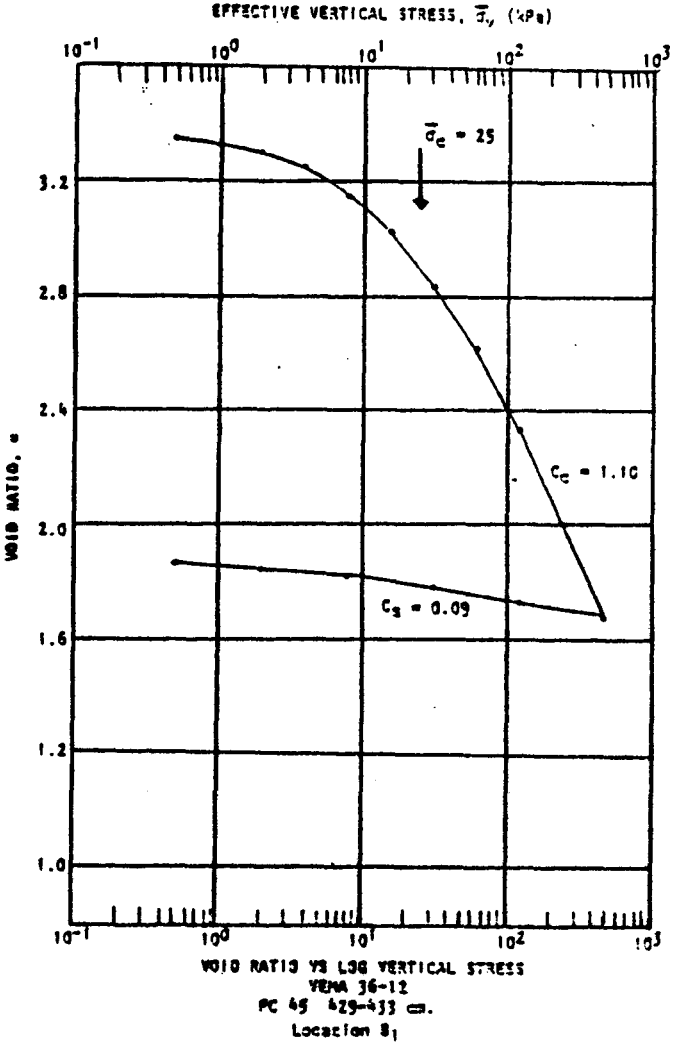


Figure A-16

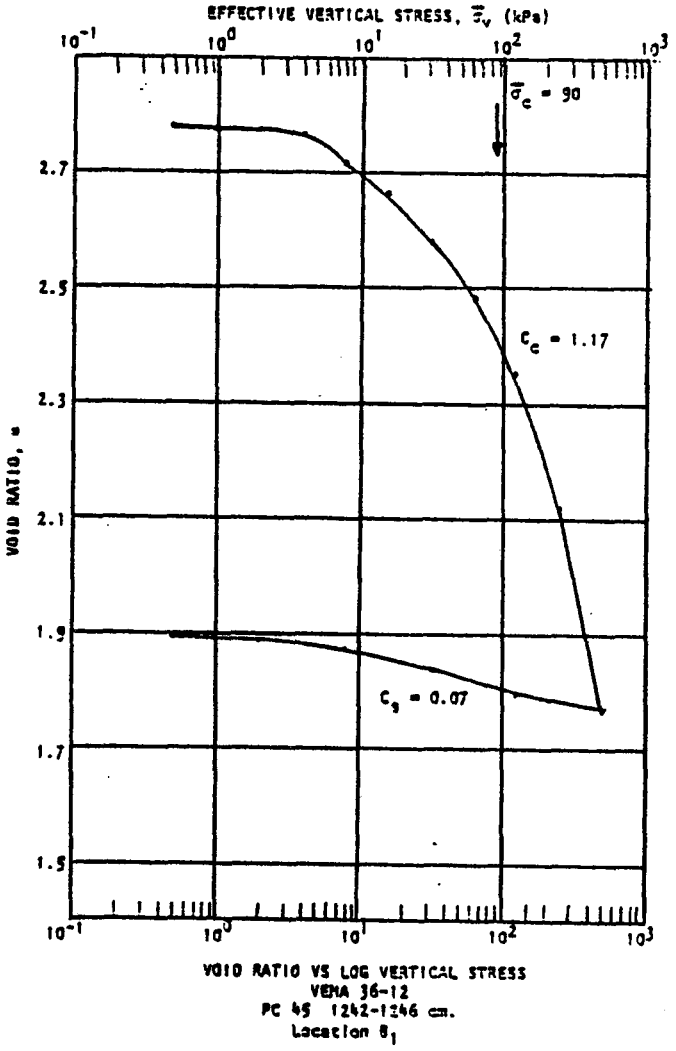


Figure A-17

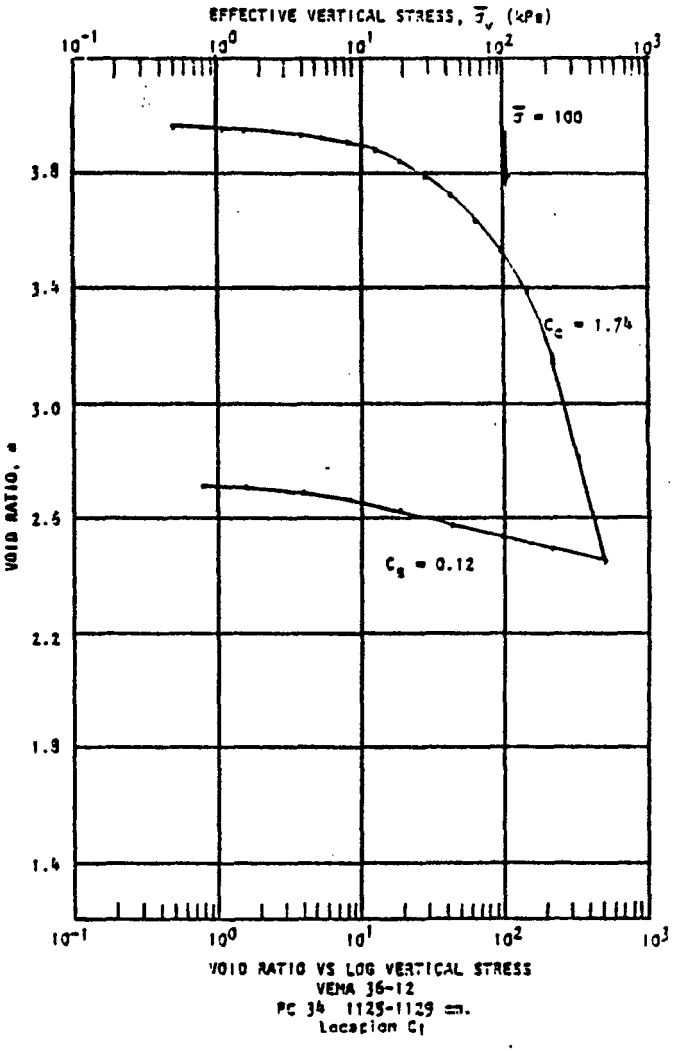


Figure A-18

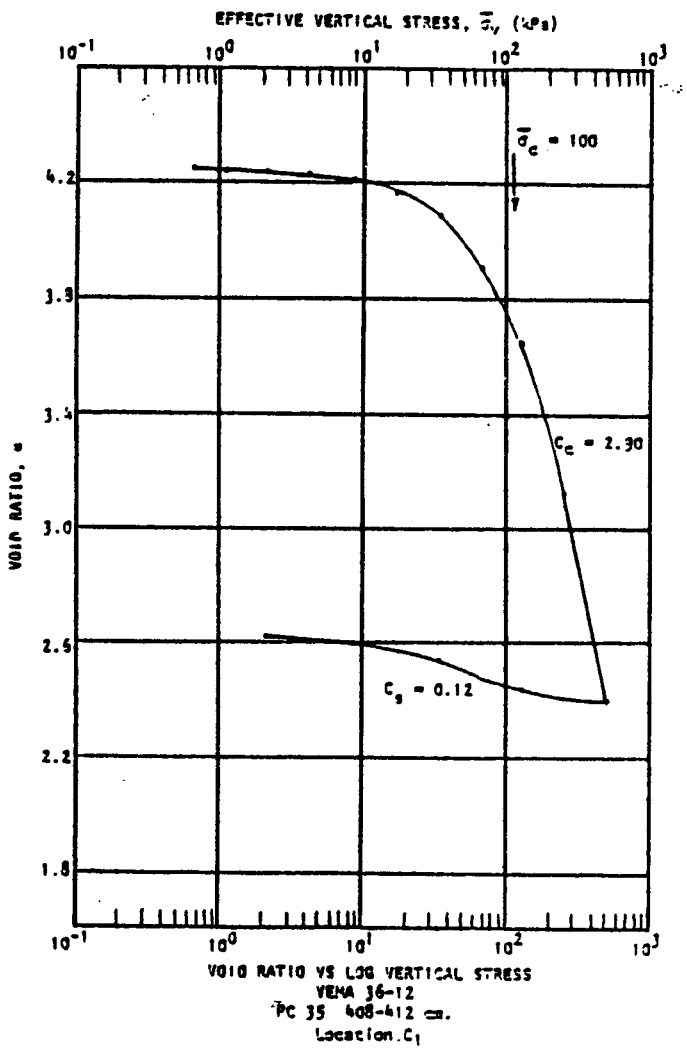


Figure A-19

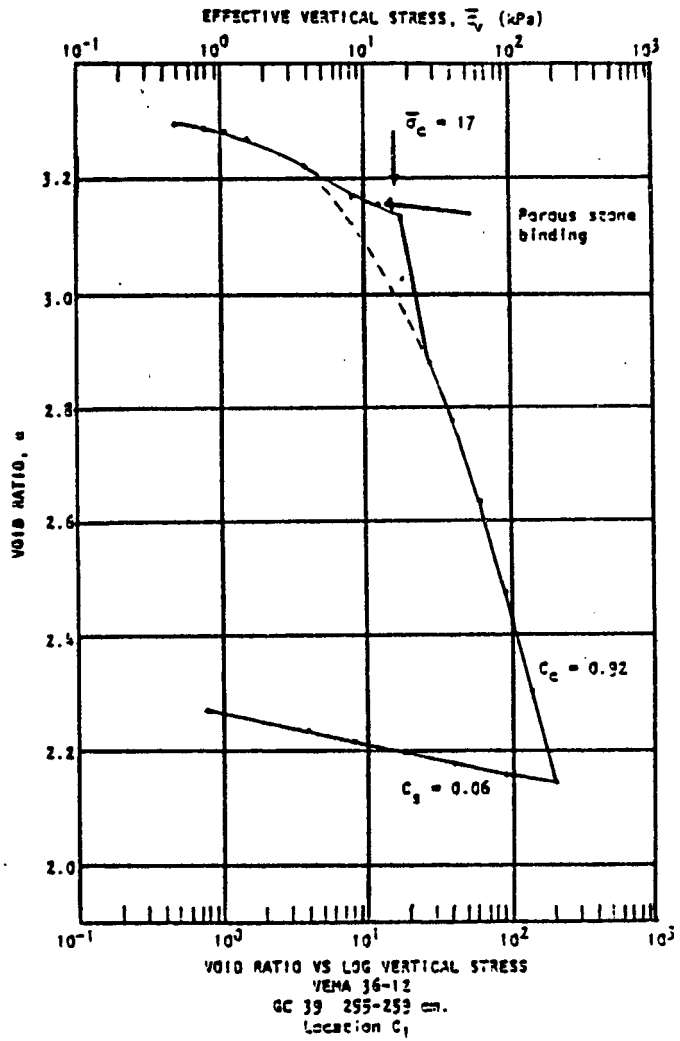


Figure A-20

APPENDIX CC

PHYSICAL SIMULATIONS USING CENTRIFUGE TECHNIQUES

Herbert J. Sutherland

Sandia National Laboratories

PHYSICAL SIMULATIONS USING CENTRIFUGE TECHNIQUES

by

Herbert J. Sutherland

The long-term mechanical response of deep ocean sediments to the emplacement of waste canisters and to the temperature gradients generated by them involve phenomena that are driven primarily by the force of gravity. This driving mechanism involves body forces interacting with the geometry of canister emplacement and temperature gradients to create an overburden stress distribution which, in turn, interacts with structural configurations, material properties, and tectonic activity (which defines boundary conditions) to produce horizontal stress states. This complicated stress state may be duplicated in a reduced-scale model if the body force (apparent force of gravity) acting on the model is increased in the same proportion that the scale is decreased.[1] A centrifuge can be used to increase the body force in the model. And, if sediments from the field site are used to construct the centrifuge-loaded scale model, then regardless of the complexity of the materials' stress-strain behavior, the displacement and strain field will be reproduced in the model as well.

A relatively simple example (slope stability) of this physical scaling is given in Figure 1. For this case, the nondimensional stress N can be written in terms of the specific gravity γ, the height H, and the cohesion C. The design safety factor F can then be posed in terms of N, the shear angle ϕ, and the geometry of the slope. In this simulation, all linear dimensions are reduced by the scaling factor n (n = 100 in Figure 1) and the body force is increased by the same factor. As seen in this figure, this technique keeps the stress distributions in the model equal to that in the prototype, and by using materials from the site, all material constants remain the same. Thus, all parameters in the model duplicate those in the prototype, and the design of the structure may be verified.

The scaling factor n carries over to the other parameters.[2] Some of these scaling relations are shown in the table. Of prime importance are the relations for time. These relations vary depending on the physical processes involved. As an example, diffusion processes scale as n^2, i.e., one hour on the centrifuge at n = 150 is equivalent to approximately 2.6 years for the prototype structure. Thus, time scaling may provide a technique for "accelerated-life-testing" of full-size prototype structures.

Table: Scaling Constants

Parameter	Symbol	Scaling
Length	L	n
Area	A	n^2
Volume	V	n^3
Stress	σ	1
Modulus	E	1
Time	t	1, n, n^2
Force	F	n^2
Moment of Inertia	I	n^4
Weight of Explosive Charge	C_e	n^3
Period of Oscillation	T	n

As summarized in Figure 2, centrifuge simulations provide the experimenter/designer with a method for predicting large-scale field events. And, when this technique is combined with computer simulations, the field event can be predicted by two independent methods. Moreover, the centrifuge simulations with their closely controlled models and boundary conditions can be used to refine and/or verify computer models, and the computer models with their versatility can be used to identify all important features of the prototype which must be modeled in the physical simulations. Thus, more confidence in the predictions of both models is obtained.

To accurately simulate the mechanical response of the canister/sediment system requires (1) a large centrifuge with the necessary fixtures for testing geotechnical structures, (2) an understanding of the laws that govern the scaling of all phenomena pertinent to the problem, and (3) an understanding of how to build and instrument small scale physical models. The first two topics have been addressed in previous annual reports and the third was started this past year.

PREVIOUS RESULTS

Centrifuge Simulations

Sandia's 25 ft-radius centrifuge was modified to accept two different specimen boxes. Both boxes were designed to test two-dimensional (slab geometry) models to 150 g scaling. The medium-scale box will accept specimens 20.5 in. x 13.5 in. x 3 in. and the large-scale box will accept specimens 48 in. x 36 in. x 8 in. The test radius at the base of the model is approximately 27 ft for the medium-scale box and 29 ft for the large-scale box. The medium-scale box attaches to a fixed strong back and the large-scale box attaches to a swing platform. This swing platform was designed to keep the total acceleration vector acting on the model perpendicular to the base of the model at all times.

The medium-scale specimen box has been used in the hole closure experiments (discussed later).

Scaling Relations

The interpretation of the results from a centrifuge simulation of the canister/sediment problem is not straightforward because the stress and strain states produced in the sediment are functions of time. In particular, these states change with pore pressure buildup and dissipation, thermal gradients, and flow of the sediment, to name a few. Thus, to relate the time of a particular measurement on the model to a homologous (equivalent) time in the prototype requires an understanding of the time scaling laws for all of the phenomena involved in the problem. Moreover, if the scaling laws are not the same for all the phenomena, then a homologous time for the prototype may not exist.

The scaling relations that are pertinent to the canister/sediment problem may be developed along experimental and/or theoretical lines. Previous work has centered on theoretical developments that are based on one of two techniques. The first technique (see Ref. 2 and the 1979 Annual Report) develops the scaling relations directly from the solution of the differential equation(s) that describe the particular

process(es) of interest. The second technique for developing scaling relations (see Ref. 3 and the 1980 Annual Report) is a dimensional analysis technique that is based on the Buckingham Pi Theorem.

The results of these two analyses have shown that the model time t_m scales to a homologous prototype time t_p by the scaling factor n (g load) squared; namely,

$$t_p = n^2 t_m. \tag{1}$$

This relation has been shown to hold for such pertinent phenomena as Darcy flow through porous media, the development of a temperature field near a heat source (sink), and the cross terms between Darcy flow and temperature fields. These results imply that this centrifuge modeling technique may be used to do "accelerated-life-testing" of proposed configurations; i.e., long-term studies may be done in relatively short times.

HOLE-CLOSURE EXPERIMENTS

Before the thermal/mechanical interactions of the canister and the sediment can be investigated using centrifuge simulation techniques, the scaling relations for all pertinent phenomena must be understood. This understanding may be achieved from theoretical considerations (discussed earlier) or from a series of centrifuge experiments. In the latter case, a single prototype is modeled at several scaling factors. The results are then cross-correlated to obtain the scaling relations.

To begin the experimental investigation of scaling relations for the canister/sediment system, a hole-closure experiment is being conducted. This experiment, which was designed to investigate the mechanical scaling relations for the sediment, is shown schematically in Figure 3. Using the medium-scale specimen box, a sample of sediment is first packed against the weir assembly. Then at g, a pin is pulled allowing the moveable weir to fall, thus creating a hole in the sediment. The movement of the sediment into this cavity is observed using a video camera, high-speed motion picture cameras, and pore-pressure and total-pressure measurements at selected sites. The thickness of the wier (dimension a in Figure 3) will be 0.5 in., 0.375 in. and 0.25 in. for loadings of 75 g, 112 g, and 150 g, respectively.

During the past year, two simulation experiments were conducted. The first experiment was used to investigate the operation of the wier and the second was used to set up and calibrate instrumentation. In both tests, the 0.5 in. wier was used at 150 g scaling and the ocean sediment was simulated with kaolinite.

Experiment SB-1

The kaolinite was consolidated into the test fixture using a kaolinite/water slurry (above the liquid limit). First, the fixture was filled with the slurry and then centrifuged at 150 g for 30 min. More slurry was then added to the clear water above the thickened slurry and then centrifuged for 15 min. This addition/centrifuge process was repeated until the consolidated kaolinite had built up to the top of the wier. The mix was then centrifuged for an hour.

The plexiglass cover plate was then removed and the wier mechanism was cleaned without disturbing the consolidated keolinite. After replacing the cover, the fixture was returned to 150 g's for 30 min. and the test was run. The mechanism did not operate correctly on first try, but after several adjustments the problem was corrected and the mechanism operated correctly.

High-speed motion pictures of this experiment were used to monitor the movement of the wier. This analysis showed that the wier built to a velocity of 11.4 in/s in the first inch of travel and continued at this velocity for 0.2 s. At that time, the wier encountered a kaolinite slurry in its travel cavity (kaolinite had leaked into the water-filled cavity during the adjustments in the wier mechanism) and was slowed to a velocity of 8.6 in/s for the remainder of its travel.

An observation made during the course of this experiment was that although the kaolinite slurry had been packed for over 8 hours, (20.6 homologous yr) on the bottom and at least 4 hours (10.3 homologous yr) on the top, the consolidated material would flow readily under the influence of a single gravity. This observation implies that the slurry needed additional consolidation.

Another observation was that the kaolinite beside the fixed plate (see Figure 3) did not move when the wier was released. Thus, this section in the bottom of the fixture could be replaced with a solid and thereby greatly reduce the time required to consolidate the kaolinite in the fixture.

Experiment SB-2

Based on Experiment SB-1, two changes were made in the kaolinite consolidation procedure. First, a plexiglass plate (6 in. x 20 in. x 2.75 in.) was fixed into the bottom of the fixture, and second, a layer of felt was placed in the fixture between the cover plate and the slurry. The plexiglass plate reduced the height of the consolidated kaolinite layer from approximately 12 in. to 6 in. The felt reduced the maximum path length for water migration to 3 in. Then by using the consolidation/build up technique described for experiment SB-1, the consolidated keolinite layer was built to within 1 in. of the top of the fixture in only 3.5 hours. The felt was then removed and the kaolinite was packed for 45 min. At this time, the consolidated kaolinite would hold a vertical slope overnight in one gravity.

After consolidation, the cover plate was removed and the wier mechanism was cleaned. The cover was replaced and the fixture was taken to 150 g for one hour. Again wier problems were encountered, but were quickly rectified. The fixture was returned to 150 g for 0.6 hr and the test was run.

The instrumentation package for this test included high-speed motion pictures, video, marker pins, and total and pore pressure measurements. The location of the markers and the pressure transducers are shown in Figure 4. The video showed that the wier moved down with an approximately constant velocity of 5.4 in/s. The movements of the marker pins are

shown in Figure 4. These measurements illustrate that the radius of influence for movement is approximately 10 in. (20 wier thicknesses) and that the movement of the consolidated kaolinite is nearly horizontal. The pressure gauges recorded a 2 psi pressure change that coincided with the movement of the wier. The rise time was of the order of 4s and was recorded on both the pore pressure and total pressure gauges.

An examination of the pressure histories recorded by the transducers revealed two problems. First, the signal-to-noise ratio was low (approximately 2) for the 2 psi pressure change. The electronics have been analyzed and the noise reduced by a factor of 2. Also, the transducers can now be properly sized to maximize their output (a 2.5 increase in output). The second problem concerned the positioning of the pressure gauges. In particular, as all the transducers were located in the consolidated kaolinite, the total pressure head acting above the kaolinite was not measured. Thus, the 2 psi pressure change may be the result of two different processes: a change in pore pressure associated with the closure of the hole created by the wier, and a change in the total pressure head associated with the pumping of water by the movement of the wier. To rectify this situation, the holding tank used to pressurize the fixture will be modified to insure a constant water head and an additional pressure gauge will be added (see below).

As a result of this experiment, three additions have been made to the instrumentation package. First, an automated, large-format, framing camera will be added to provide high resolution photos of the experiment in flight. Second, the gauging will be expanded to include a displacement transducer to measure the displacement history of the kaolinite/water interface. And third, a pressure gauge will be added to measure the total water head acting in the fixture (above the kaolinite).

CONCLUDING REMARKS

Centrifuge techniques offer a method for doing physical simulations of the long-term mechanical response of deep ocean sediment to the emplacement of waste canisters and to the temperature gradients generated by them. Theoretical investigations of the scaling laws for pertinent phenomena indicate that the time scaling will be consistent among them and equal to the scaling factor squared. This result implies that this technique will permit "accelerated-life-testing" of proposed configurations; i.e., long-term studies may be done in relatively short times.

During the past year, the techniques for conducting and monitoring centrifuge simulations of hole closure in ocean sediment have been devised and tested. In the coming year, these techniques will be used to investigate the mechanical scaling relations for flow of the sediment.

REFERENCES

1. P. B. Bucky, "Use of Models for the Study of Mining Problems," Am. Inst. of Mining & Metallurgical Engineers, Tech. Pub. No. 425, (1931), 3-28.

2. G. I. Pokrovsky and I. S. Fyokonov, Centrifuge Model Testing in the Construction Industry, 2 vols, draft translation, Building Research Establishment Library, England (1975).

3. W. E. Baker, P. S. Westine, and F. T. Dodge, Similarity Methods in Engineering Dynamics, Spartan Books, 1973.

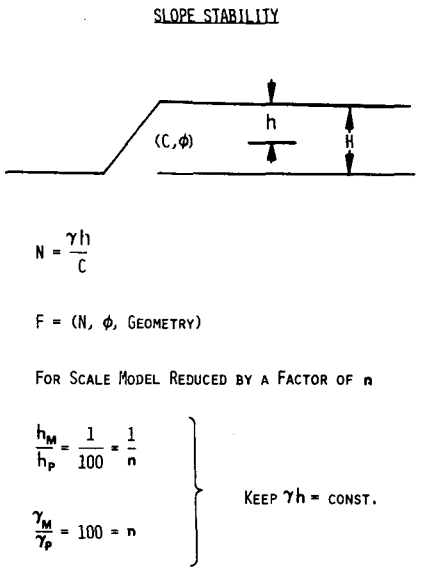


Figure 1. Slope Stability Analysis

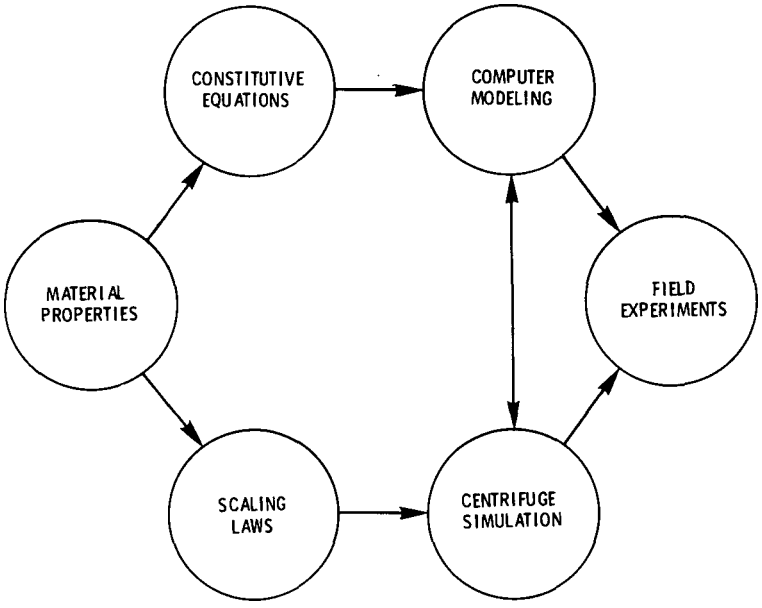


Figure 2. Numerical and Centrifuge Simulation Techniques

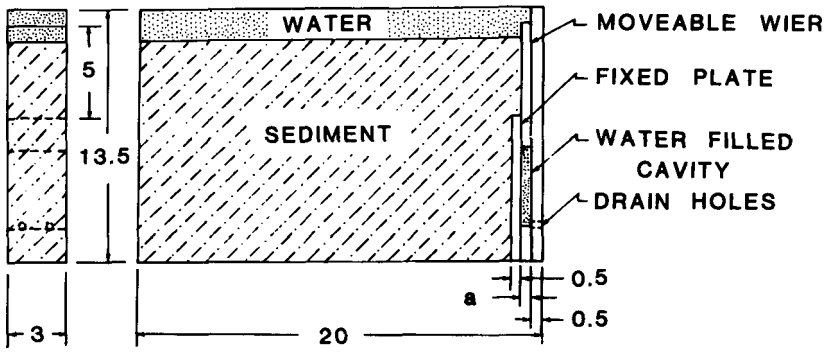


Figure 3. Schematic Diagram of the Hole-Closure Experiment

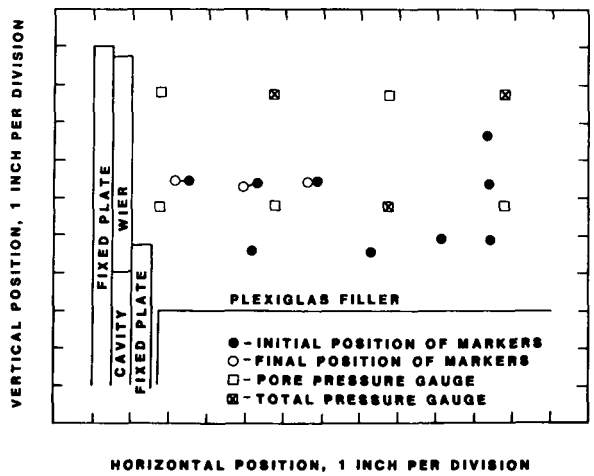


Figure 4. Instrumentation for Experiment SB-2

APPENDIX DD

CREEP MODELING OF DEEP OCEAN SEDIMENTS

Paul R. Dawson

Cornell University

(Contract #74-1077)

Creep Modeling of Deep-Ocean Sediments

Paul R. Dawson
Consultant
Sibley School of Mechanical and Aerospace Engineering
Cornell University

Abstract

Deep-ocean sediments creep when subjected to stress for long periods of time. The purpose of the modeling work reported here is to (1) develop numerical methods capable of analyzing creep of fluid-saturated sediments, (2) develop constitutive models that describe the sediment creep, and (3) apply the methods and models to Subseabed Disposal problems. During the past year progress on all three of these activities has been made.

TABLE OF CONTENTS

Abstract
Table of Contents
List of Figures

Introduction

I. NEPTUNE Development and Documentation

II. Constitutive Models for Sediment Creep Behavior

    A. General Discussion
    B. Empirical Evaluation of the Creep Model Parameters from the Laboratory Data
    C. Triaxial Consolidation Simulation

III. Application of NEPTUNE to Subseabed Applications

Summary

Meetings and Reports

Figures

LIST OF FIGURES

Figure Number	Title
2.1	Typical Static and Creep Behavior of Sediments
2.2	Specimen Volume During Consolidation Test #72
2.3	Specimen Volume Change Rate During Consolidation Test #72
2.4	First Invariant of Strain During Consolidation Test #72
2.5	First Invariant of Strain-Rate During Consolidation Test #72
2.6	Specimen Porosity During Consolidation Test #72
2.7	URI Creep Test UI-2C Axial Strain Data
2.8	URI Creep Test UI-2C Lateral Strain Data
2.9	URI Creep Test UI-2C First Invariant of Strain
2.10	URI Creep Test UI-2C Second Invariant of Deviatoric Strain
2.11	URI Creep Test UI-2C First Invariant of Strain-Rate
2.12	URI Creep Test UI-2C Second Invariant of Deviatoric Strain-Rate
2.13	Stress Dependency in Hydrostatic Compression Consolidation Behavior
2.14	Empirical Fit of Strain-Rate History of Consolidation Test #59
2.15	Empirical Fit of Strain-Rate History of Consolidation Test #72
2.16	Empirical Fit of Strain-Rate History of Consolidation Test #55B
2.17	Empirical Fit of Strain-Rate History of Consolidation Test #55C
2.18	Empirical Fit of Strain-Rate History of Consolidation Test #55D
2.19	Empirical Fit of Strain-Rate History of Consolidation Test #40B
2.20	Parameter K_0 For Varying m^+ (n^+=7) from Consolidation Test #72
2.21	Parameter A_3 For Varying m^+ (n^+=7) from Consolidation Test #72
2.22	Parameter B_3 For Varying m^+ (n^+=7) from Consolidation Test #72
2.23	Parameter β_0 For Varying m^+ (n^+=7) from Consolidation Test #72
2.24	Parameter K_0 For Varying n^+ (m^+=-4) from Consolidation Test #72
2.25	Parameter A_3 For Varying n^+ (m^+=-4) from Consolidation Test #72
2.26	Parameter B_3 For Varying n^+ (m^+=-4) from Consolidation Test #72

LIST OF FIGURES (Cont.)

Figure Number	Title
2.27	Parameter β_0 For Varying n^+ (m^+=-4) from Consolidation Test #72
2.28	Internal Variable β History for Consolidation Test #72
3.1	Canister Centerline Temperature
3.2	Sediment Temperature 0.6 m from Canister Centerline
3.3	Sediment Temperature 1.2 m from Canister Centerline
3.4	Sediment Temperature 4.3 m from Canister Centerline
3.5	Canister Velocity History for Case A
3.6	Canister Velocity History for Case B
3.7	Canister Velocity History for Case C
3.8	Canister Velocity History for Case E
3.9	Sediment Velocity in Case A at 0.6 m from Canister Centerline
3.10	Sediment Velocity in Case A at 4.3 m from Canister Centerline
3.11	Pore Fluid Relative Velocity in Case A at 0.6 m from Canister Centerline
3.12	Pore Fluid Relative Velocity in Case A at 4.3 m from Canister Centerline
3.13	Sediment Velocity in Case B at 0.6 m from Canister Centerline
3.14	Sediment Velocity in Case B at 4.3 m from Canister Centerline
3.15	Pore Fluid Relative Velocity in Case B at 0.6 m from Canister Centerline
3.16	Pore Fluid Relative Velocity in Case B at 4.3 m from Canister Centerline
3.17	Sediment Velocity in Case C at 0.6 m from Canister Centerline
3.18	Sediment Velocity in Case C at 4.3 m from Canister Centerline
3.19	Pore Fluid Relative Velocity in Case C at 0.6 m from Canister Centerline
3.20	Pore Fluid Relative Velocity in Case C at 4.3 m from Canister Centerline
3.21	Sediment Velocity in Case E at 0.6 m from Canister Centerline
3.22	Sediment Velocity in Case E at 4.3 m from Canister Centerline
3.23	Pore Fluid Relative Velocity in Case E at 0.6 m from Canister Centerline
3.24	Pore Fluid Relative Velocity in Case E at 4.3 m from Canister Centerline

INTRODUCTION

The creep of sediments around an emplaced canister is an important aspect of any Subseabed Disposal concept for several reasons. First, it is crucial that the sediment form a continuous barrier around a canister. Although it is felt that the emplacement method should guarantee this, it would be a significant advantage if the sediment around a canister deformed naturally to complete the barrier if any opening or water pocket were to remain following emplacement. Further, the overall magnitude of the motion induced by the heating of sediments (and subsequent natural convection) must be assessed to ensure that this motion is small relative to the dimensions of the sediment barrier. Another important aspect is the effect that sediment deformations near a canister (due to an increased consolidation rate as the sediments heat, for instance) could have on the porosity, permeability and sediment platelet bonding. Sediment motion of this type could have significant consequences on any pore water or ion migration away from the isolated wastes.

Over the past several years the Subseabed Disposal Program has sponsored the development of numerical capabilities for analyzing the creep deformations of the sediments. This development is coordinated with laboratory testing of deep ocean sediments to identify the manner in which sediments deform and to quantify this behavior in the form of constitutive equations. This report deals with several aspects of the total creep modeling effort. The computer code NEPTUNE has been written to analyze the creeping motion of saturated porous materials. During this past year numerous improvements were made in NEPTUNE and the code's capabilities were documented. Further, the creep behavior of the sediments has been studied in the context of models that will be incorporated into NEPTUNE. Interpretation of the laboratory observations through fitting of the model parameters to consolidation behavior of triaxial specimens was initiated and produced several important findings. Finally, the application of modeling techniques to subseabed applications continued. Thermally induced buoyancy and hole closure computations were performed. Each of these activities is summarized in the following sections.

I. NEPTUNE DEVELOPMENT AND DOCUMENTATION

NEPTUNE is a finite element computer code for analyzing the creeping motion of saturated sediments of either planar or axisymmetric geometries. It has been formulated on the premise that effective stresses drive the motion of the sediment skeleton and that pore fluid pressure gradients induce flow of the pore fluid through the skeleton. Large motions of both the skeleton and the pore fluid are permissible. Because the Subseabed Disposal Program is directed principally at the isolation of high level wastes, NEPTUNE is formulated to evaluate the thermal response of the saturated system in conjunction with its motion.

The thermomechanical response of the sediments and pore water system is described by conservation of mass, momentum, and energy and constitutive equations for each material. Conservation of mass and momentum are used

to evaluate the motion of the saturated sediment while conservation of energy is used to determine its thermal response. The deformations and temperatures are closely coupled, however, through convection, dissipative heating, temperature-dependent buoyancy forces, and temperature-dependent material properties.

During the past year the governing equations in NEPTUNE have been closely compared to the mixture theory models being developed by J. W. Nunziato and S. L. Passman (SNL). The mechanical response of the sediments and pore fluid are determined by

System Conservation of Mass:
$$d_{ii} + \frac{\partial}{\partial x_i}(\alpha w_i) = 0 \tag{1.1}$$

System Conservation of Momentum:
$$\frac{\partial}{\partial x_j}((1-\alpha)\,\bar{\sigma}_{ji}) - \frac{\partial p}{\partial x_i} + F_i^s + F_i^f = 0 \tag{1.2}$$

Pore Fluid Conservation of Momentum:
$$\alpha \frac{\partial p}{\partial x_i} + b w_i - F_i^f = 0 \tag{1.3}$$

Kinematics:
$$d_{ij} = \frac{1}{2}\left(\frac{\partial u_i}{\partial x_j} + \frac{\partial u_j}{\partial x_i}\right) \tag{1.4}$$

and

Constitutive Model:
$$\bar{\sigma}_{ij} = 2\mu d_{ij} + \kappa d_{kk}\delta_{ij} \tag{1.5}$$

Here d_{ij} is the deformation rate; u_i is the sediment velocity; w_i is the fluid velocity relative to the sediment; α is the porosity; $\bar{\sigma}_{ij}$ is the effective stress; p is the pore fluid pressure; F_i^s and F_i^f are the volume fraction weighted body forces on the skeleton and pore fluid, respectively; δ_{ij} is the Kronecker Delta; and b, μ, and κ are constitutive model parameters that may be functions of the sediment state. Boundary conditions are specified for the surface tractions or material motion to complete the system of equations.

The sediment thermal response is modeled using a form of the energy equation that describes conductive-convective heat transfer of a two phase system:

$$\frac{\partial}{\partial x_i}\left(k_e \frac{\partial \theta}{\partial x_i}\right) - \frac{\partial \theta}{\partial x_i}\left(\alpha \rho_f Cp_f v_i + (1-\alpha)\rho_s Cp_s u_i\right) + \dot{Q}_e = (\rho Cp)_e \frac{\partial \theta}{\partial \tau} \tag{1.6}$$

where

$$k_e = \alpha k_f + (1-\alpha)k_s \tag{1.7}$$

$$(\rho Cp)_e = \alpha \rho_f Cp_f + (1-\alpha)\rho_s Cp_s \tag{1.8}$$

and

$$\dot{Q}_e = \alpha \dot{Q}_f + (1-\alpha)\dot{Q}_s. \tag{1.9}$$

Here, θ is the temperature; v_i is the pore fluid velocity; τ is time; $\dot{Q}_e$, $\dot{Q}_s$, and $\dot{Q}_f$ are the effective, sediment, and pore fluid heat rates, respectively; k_e, k_s, and k_f are the effective, sediment, and fluid conductivities; ρ_s and ρ_f are the sediment and fluid densities; and Cp_s and Cp_f are the sediment and pore fluid specific heats (other variables are as defined previously). Known heat fluxes or temperatures are imposed at the boundaries to complete the equations. Temperatures of the sediment and pore fluid are assumed to be equal at coincident points and the effects of chemical reactions are neglected.

The equations solved by NEPTUNE are a special subset of the more general mixture theory equations for a saturated porous system. In particular, the mixture theory equations reduce to the equations in NEPTUNE when the system inertia is small and the sediment minerals and pore fluid are incompressible. (Note that this does not imply that the skeleton is incompressible). Volume fraction gradient terms that arise in the mixture theory have been embodied in the constitutive models that describe the motion of the skeleton in the NEPTUNE formulation.

Details of the development of the governing equations for NEPTUNE are given in the documentation manual which is in its final stages of preparation [1]. The assumptions associated with the governing equations are discussed and the finite element formulation is presented. The mathematical development required to obtain the matrix equation for skeleton and pore fluid velocities, and the matrix equation for the system temperatures from the variational statements is presented in its entirety. Specific numerical algorithms for solving the matrix equation are also discussed.

The constitutive models used to approximate the sediment and pore fluid behavior can be simple or complicated, depending on precision to which the real behavior must be reproduced. A variety of models are now available in NEPTUNE that provide for different levels of complexity of the constitutive equations. The parameters b, μ, and κ presented in Equations (1.3) and (1.5) may be designated as constants (that give linear fluid type response of the pore fluid and skeleton) or they may be nonlinear functions of the motion, temperature, and sediment structure. Power law models involving the strain, porosity or internal variables for describing the sediment's dependence on the history of its motion have been implemented in NEPTUNE. Details of these models are presented in the second section of this report. The internal variable model requires a special integration of the differential equation governing the internal variable's behavior. An integration technique using sub-stepping of the time domain has been applied for this purpose.

Volumetric deformation response of the sediment to the application of shear stresses (shear-induced dilation) has been addressed this year. To model this behavior, an additional term is incorporated in the flow law (Equation (1.5)) so that the equation becomes

$$\bar{\sigma}_{ij} = 2\mu d_{ij} + (\kappa d_{kk} + \Omega d'_{II})\delta_{ij} \qquad (1.10)$$

Ω is a material parameter and d'_{II} is the second invariant of the deviatoric deformation rate. This additional term produces a normal stress in the presence of shearing motions.

Volumetric response caused by the relative motion of pore fluid through a matrix having porosity gradients appears in the mixture theory description of saturated porous media developed by Nunziato and Passman (SNL). This response has been implemented in NEPTUNE by incorporating this term in the constitutive model for the skeleton. Equation (1.5), when written to include both the shear-induced dilatancy and the porosity gradient term becomes

$$\bar{\sigma}_{ij} = 2\mu d_{ij} + (\kappa d_{kk} + \Omega d'_{II} + \phi w_k \frac{\partial \alpha}{\partial x_k})\delta_{ij} \qquad (1.11)$$

where ϕ is a material parameter. The contribution of these terms to the response of the system can be included with any of the material models available in NEPTUNE by specifying that the material parameters Ω and ϕ are nonzero.

The incorporation of nonlinear constitutive models in NEPTUNE necessitated the implementation of methods for solving nonlinear matrix equations. Nonlinearities that arise as a result of the skeleton viscosity (μ or κ) being a function of the motion can be solved using either a modified Newton-Raphson technique or a variable stiffness method. The user can specify his preference when solving nonlinear problems of this type. Nonlinearities associated with the shear-induced dilation or porosity gradient effects are treated with a corrective force, iterative method.

The pore fluid pressure is determined explicitly in NEPTUNE as the Lagrange multiplier associated with the conservation of mass constraint. The selection of the approximating function for the pressure affects the manner in which conservation of mass is enforced. A constant pressure within an element gives an averaged mass balance over an element, while a pressure approximation that is linear within an element, but is not continuous from one element to another, satisfies conservation of mass at all points in an element. Another possibility is to use a linear pressure distribution, but require that it be continuous between elements. For systems having only a single constituent (for example, incompressible viscous fluid flow) this choice often gives particularly accurate (and smooth) results (for linear material models). Based on this experience it was decided that a continuous pressure option would be added to NEPTUNE to complement the discontinuous linear approximation already available. To accomplish this, the mesh generator and pre-frontal preparation programs were modified to generate elements with the correct positioning of pressure points and to arrange them in the solution process in a proper order. New approximating functions were defined in the finite element formulation and the matrix assembly procedure was modified so as to allow for the continuous or discontinuous pressure option.

A number of modifications were implemented to improve the efficiency of NEPTUNE as well as make it easier for others to use. For example the use of LCM storage on the CDC 7600 version of NEPTUNE was made more flexible by allowing the size of data transfers to be variable, based on the problem size. The input data was also reorganized and streamlined. Input files now contain information for

1. Mesh Generation
2. Frontal Solution Preparation
3. Thermomechanical Simulation
    a. Material Property Specification
    b. Initial Condition Specification
    c. Boundary Condition Specification
    d. Program Option Specification
    e. Simulation Limit Definition
4. Vector and Scalar Field Plotting
5. Variable History or Profile Plotting

In each of these groups the required information was reduced and formatted to allow easier execution.

A user's manual has been written during the past year. It currently is being revised to incorporate the comments provided by J. Nunziato and D. McTigue (SNL) and to incorporate better sample problems. As written it contains a description of the theoretical background of the equations solved by NEPTUNE and of the finite element formulation utilized in reaching the matrix equation ultimately solved to obtain the sediment and pore fluid velocity field, the pore fluid pressure distribution, and the skeleton temperature field. The constitutive equations that can be selected to model the sediment are also discussed and the parameters necessary to use them are defined. Instructions for applying the program are given in terms of a card-by-card explanation of the input files and the system control language necessary to execute the program on the CDC computing system at Sandia National Laboratories (Albuquerque). Several appendices provide thorough documentation of the finite element and matrix solution details.

Several one-dimensional problems with known analytical solutions were studied in more detail this year. NEPTUNE provided accurate solutions to both uniaxial strain and radial (axisymmetric) compression examples. In these cases both the skeleton velocity and pore fluid velocity throughout the body were accurately predicted. A steady-state temperature field that included convection of heat by motion of the fluid and the skeleton was also simulated accurately by NEPTUNE. These three examples are presented in reference [2].

II. CONSTITUTIVE MODELS FOR SEDIMENT CREEP BEHAVIOR

A. General Discussion

Under constant stress, deep-ocean sediments typical of those found in the Subseabed Disposal Program study areas demonstrate strains that increase

with time. Such deformations can be a result of creep and as such would not be recovered if the stress were removed from the sediment body. However, it might also be possible that the strains would be recovered fully after removal of the load. This fundamental difference in behavior has serious implications for the constitutive model development. First, tests that can characterize the basic nature of the material deformation (be it elastic or inelastic, rate-dependent or rate-independent, etc.) must be conducted, and, second, the mathematical description of the behavior (i.e. the constitutive equation) must provide a relationship between the appropriate variables so that this basic behavior is implicit in the model itself. The model must distinguish between elastic and inelastic components of the deformation, as well as faithfully reproduce the laboratory observations of a particular type of test. Frequently it is possible to fit a given test result using models that are not appropriate for that material by introducing variable moduli (model parameters). However, since an inappropriate model would not properly characterize the material it would fail to perform well on other types of tests (where the stress and strain histories could be quite different), or even be able to predict the response of the specimen to removing the load in the test used to evaluate the material moduli. Thus, the choice of the form of the equations cannot be based on the material behavior from only a single type of test.

The deep-ocean sediments examined as part of the Subseabed Disposal Program exhibit relatively large strains during creep testing (5 to 25%). The test specimens do not recover any appreciable amount of this strain after removal of the load. Further, the rate of creep observed in the secondary compression is proportional to the stress. Principally for these reasons, models are being evaluated in this portion of the Subseabed Program that mathematically relate the applied stress to the rate of deformation, the internal structure of the material, and to the temperature. Equations of this type represent the inelastic component associated with creep of the skeleton. An elastic component of strain occurs in addition to this. The elastic component may be neglected without significant error in situations in which the inelastic component dominates. A creeping viscous flow assumption of this nature has been made in development of the NEPTUNE computer code. The applicability of this assumption can be specified in terms of the material's elastic and viscous moduli and the rate of change of the applied stress.

Assume that the deformation rates are additive:

$$d = d^e + d^v. \tag{2.1}$$

If we define effective elastic (G) and viscous (creep) moduli (μ) each component of the total deformation rate can be written as

$$d^e = \frac{\sigma}{2G}, \tag{2.2}$$

and

$$d^v = \frac{\sigma}{2\mu}. \tag{2.3}$$

The viscous behavior will dominate given that

$$d^v >> d^e \tag{2.4}$$

or

$$\frac{\sigma}{2\mu} >> \frac{\dot{\sigma}}{2G} \tag{2.5}$$

which implies that

$$\left|\frac{\dot{\sigma}}{\sigma}\right| << \frac{\mu}{G} \quad . \tag{2.6}$$

Thus, the relative change in stress must be appreciably less than the relaxation time (defined by the ratio of the effective moduli, μ/G) for the creeping viscous flow assumption to be valid.

Not all laboratory tests satisfy this condition. For instance, a relaxation test is characterized by $|d^e| = |d^v|$. However, a well-executed creep test maintains a constant stress and thus is an ideal application of a viscous approximation. The crucial question is whether field applications associated with the Subseabed Disposal Program can be modeled accurately using a viscous approximation. Preliminary analyses indicate that, except perhaps at time immediately following emplacement, the stress field changes very slowly, supporting the validity of the creeping flow approximation.

For the remaining portion of this section only the creep component of the total deformation will be addressed. This discussion in itself does not require any creeping flow type of assumption be made.

The creep models being studied consist of two basic parts. First is a set of equations involving invariants of the stress and the deformation rate (as well as structure and temperature) that characterize the nonlinear behavior of the sediment. The second part is another set of equations that relate specific components of the skeleton effective stress to the skeleton motion. The latter equations take the form

$$\bar{\sigma}_{ij} = 2\mu d_{ij} + (\kappa d_I + \Omega d'_{II} + \phi w_k \frac{\partial \alpha}{\partial x_k})\delta_{ij} \tag{2.7}$$

where μ, κ, Ω, and ϕ are material parameters that can be written as functions of the motion, temperature and structure of the sediment. These functions are used to describe nonlinear rate dependence, strain hardening and/or softening behavior, thermal history or thermal activation effects, and the effects of deformation histories. (Here the deformation rate d represents the creep component of the total motion.) It is important to note that although the pore water and clay platelets are each considered incompressible, the sediment as a porous structure is, of course, compressible. Changes in the volume may be induced by the mean stress, the shear stresses, or by pore fluid motion in the presence of porosity gradients.

The first part of the creep model provides the function for the material parameters μ, κ, Ω and ϕ. The laboratory data are empirically fit to one equation that gives the mean effective stress (first invariant) and one that gives the second invariant of the effective deviatoric stress tensor. Namely,

$$\bar{\sigma}_I = f(d_I, d'_{II}, w_k \frac{\partial \phi}{\partial x_k}, \beta, \alpha, \theta) \tag{2.8}$$

and

$$\bar{\sigma}'_{II} = g(d_I, d'_{II}, w_k \frac{\partial \theta}{\partial x_k}, \beta, \alpha, \theta). \tag{2.9}$$

The above equations are in general nonlinear, as will be discussed later. The material parameters, μ, κ, Ω, and ϕ are determined by noting that the flow law presented in Equation (2.7) is equivalent to

$$\bar{\sigma}_I = 3Kd_I + 3\Omega d'_{II} + 3\phi w_k \frac{\partial \phi}{\partial x_k} \tag{2.10}$$

and

$$\bar{\sigma}'_{II} = 3\mu d'_{II} \tag{2.11}$$

where

$$K = \frac{2\mu+3\kappa}{3} . \tag{2.12}$$

Comparison of Equation (2.8) to (2.10) and Equation (2.9) to (2.11) allows one to infer the functional form of the material parameters μ, κ, Ω and ϕ once the functions f and g have been explicitly stated.

To date the specific forms of Equations (2.8) and (2.9) that have been examined are

(a) Models involving the porosity

$$\bar{\sigma}_I = A_1 e^{Q_1/R\theta} (1-\alpha)^{m_1} d_I^{n_1} \tag{2.13}$$

$$\bar{\sigma}'_{II} = A_2 e^{Q_2/R} f(\varepsilon) d'^{n_2}_{II} \tag{2.14}$$

(b) Models involving an internal variable

$$\bar{\sigma}_I = A_1 e^{Q_1/R\theta} \beta^{m_1} d_I^{n_1} \tag{2.15}$$

$$\bar{\sigma}'_{II} = A_2 e^{Q_2/R\theta} \beta^{m_2} d'^{n_2}_{II} \tag{2.16}$$

$$\dot{\beta} + A_3 = B_3(1-\alpha) . \tag{2.17}$$

where β is the internal variable. In each of the above models the power law dependence on the deformation rate can be replaced with a logarithmic form that would provide an exponential increase in deformation rate as a function of stress. The effects of shear-induced dilation and porosity gradients have been neglected. These forms apply to the sediment structure provided that the sediment is achieving greater resistance to flow with increased deformation. This implies that the sediment continues to strain-harden. However, in many undrained constant strain rate tests and in a few drained constant stress tests, it has been observed that after several percent strain there is an abrupt change in the behavior. Typically the sediment then loses its capacity to carry higher loads and deformations occur more readily. Such behavior typically is accompanied by qualitatively different behavior of the volumetric component of the motion. For example, a sediment that is compacting may suddenly dilate. The models shown in Equations (2.8) and (2.9) do not address this behavior. However, it may be possible to append limits to these equations in which the magnitude of the motion prior to the change in behavior can be physically represented by an internal structure variable. When this internal variable reaches a specified limit, the sediment begins to soften. This is manifested as a transition to tertiary creep under drained constant stress conditions, and as strain softening following constant rate undrained loading. For example, published literature frequently shows constant strain-rate curves of the form shown in Figure 2.1. The peak strength usually increases modestly with strain rate but occurs at a lower strain magnitude. Similarly, creep data for fine-grained clays often show strain-rate versus strain behavior that diminshes at constant stress to some minimum before increasing as the material enters tertiary creep. These suggest the possible use of an internal structure variable that characterizes sediment conditions in a manner that is appropriate to determine whether or not additional stress can be carried by the sediment. Once that point of transition of behavior can be evaluated it is possible to introduce a different functional form that can properly describe the lesser capacity of the sediment to carry additional load. This aspect of the modeling will be examined in more detail later.

B. Empirical Evaluation of the Creep Model Parameters from the Laboratory Data

The Subseabed Disposal Program currently has several active groups engaged in the testing of fine-grained clay sediments that are principally from Pacific study sites. Most of this testing uses illitic material that has been remolded, but in some instances undisturbed illite and smectite (either in a remolded or undisturbed conditions) are used.

A variety of standard laboratory tests are being performed on these materials. These include

(1) Triaxial undrained, constant strain-rate tests (quasi-static strength tests)

(2) Triaxial drained and undrained constant stress tests (creep)

(3) Triaxial undrained relaxation tests (relaxation)

(4) Undrained constant stress shear tests

In tests that utilize remolded material, the water content is reduced from the freshly remolded state by a stress equivalent to the overburden load that is to be approximated. Such a process may be done isotropically with equal stresses in each direction, or it may be done anisotropically so that their motion of one or more directions is constrained. An often used example is anisotropic consolidation characterized by uniaxial strain that is done to simulate compacting conditions in a sediment column. The consolidation process can yield very important data for evaluation of the first invariant (bulk) behavior.

The above tests provide specific information relative to equations of the model.

Tests	Variables
Consolidation Phase of Testing	First invariant of stress and deformation rate only
Quasi-static Strength	Second invariant of deformation rate only, first and second invariants of effective stress
Creep Tests	
Drained	First and second invariants of both the stress and deformation rate
Undrained	Second invariant of the deformation rate, first and second invariant of the effective stress
Relaxation Test	Second invariant of the deformation rate, first and second invariant of the effective stress
Shear Test	Second invariant of deformation rate, first and second invariants of stress

As is evident from the above table, most tests involve more than just the first invariants of the effective stress and deformation rate or just the second invariants of the effective stress and deformation rate. It is thus difficult to separate effects of the second invariant of the effective stress on the deformation rates from those of the first invariant of the effective stress. The isotropic hydrostatic consolidation phase of the various tests, however, involves only the first invariants

of the stress and motion. From it, the parameters of Equation (2.13) can be evaluated. The first invariant portion of the model is then applied in the data reduction to separate the first and second invariant effects of tests having both contributions active.

Thus, the strategy for evaluating material parameters of the constitutive models adopted can be summarized as

1. Fit the hydrostatic compression data

    a. Convert the time-volume data to plots of deformation rate and porosity.

    b. Fit the first invariant expressions of Equation (2.13) or (2.15) by a least square technique to determine the material parameters for individual phases of the consolidation process.

    c. Determine the optimal set of parameters for all tests.

2. Fit the drained creep behavior

    a. Convert data to plots of invariants of deformation rate and strain.

    b. Fit the first invariant behavior.

        i) Use hydrostatic compression results to separate shear and mean stress effects

        ii) Determine fits for shear induced dilatency.

    c. Fit the second invariant behavior using Equation (2.14) or (2.16).

The procedure for fitting the models to the data was first implemented for the drained creep tests performed by the University of Rhode Island. Steve Akers (WES) provided the consolidation histories for several tests performed on Pacific illite. According to the identification system for his tests, the tests examined were

	Depth of column where sample taken
PI 5-8#40	28 - 38 cm
PI 5-8#55	28 - 38 cm
PI 5-8#59	28 - 38 cm
PI 5-8#72	40 - 50 cm

Tests #55 and #72 had initial water contents of approximately 85% while #40 and #59 were approximately 100%.

Initially, an equation having an exponential dependence of the porosity was fit to the four stages of #55. This is of the form:

$$d_I = Ke^{m\alpha}$$

where K is a constant for constant stress and temperature. Data points for times earlier than 500 seconds were not used in the least squares procedure since this period was characterized by large changes in the pore pressure. (In more recent efforts this time was increased to approximately 2000 seconds.) Although the effective stress was increasing during a particular test (and thus the parameter K would not truly be constant over a test), the trends observed were judged to be valid. These were:

(1) The empirical factor appearing with the porosity in the exponential term was large (averaging approximately 132).

(2) The variation in the factor from one stage of test #55 to another was also large (ranging from 55 to 200).

This made it impossible to fit one stage of the test with parameters determined from another, or from average values of the parameters from all tests. The exponential curve also did not appear to give a particularly accurate reproduction of the data. This may be in part due to the inclusion of data at times when the pore pressure was still high. Even though adjusting the time of the first data considered to 2000 seconds might improve the form of the fit, it would serve to increase the parameters' magnitude, and thus compound the basic flaw of their form.

A second function involving the porosity was also evaluated. In this case a power law of the form

$$d_I = K\alpha^m$$

was fit to the consolidation data for test #55. Again, the coefficients determined by the fit were not satisfactory. First, the exponent of the porosity was large (averaging 103) as was the range of this parameter (from 33 to 111). It is evident that with such large coefficients in the model, small errors in evaluating the initial porosity could lead to enormous errors in the predicted deformation rate. The test-to-test data did not support a conclusion that such great differences in the initial deformation rates would occur as a result of small differences in the initial porosity. However, it is evident from the data that large changes in deformation rate can result from small changes in the porosity of a particular specimen as it deforms.

The tedious chore of performing least squares fits of the various models to the data can best be accomplished by a digital computer. To this end, the tabulated volume/time data for the consolidation tests were entered into files. A detailed outline for data reduction

was prepared that provided instructions for

(a) computing specimen volume as a function of time
(b) computing the strain
(c) computing the strain rate (deformation rate) as a function of time
(d) computing the specimen average porosity as a function of time
(e) performing a least squares fit for an equation of the form

$$d_I = A_o f(\bar{\sigma}_I) g(\alpha).$$

In a similar fashion, test records from the URI drained triaxial creep tests were obtained. For this data, the reduction procedure consisted of

(a) converting engineering strain measures to natural strain measures
(b) modifying the sign convention to have a consistent convention for all components of the strain
(c) computing the first invariant of the strain
(d) computing the deviatoric strain
(e) computing the second invariant of the deviatoric strain
(f) computing the rates of change of the first and second strain invariants
(g) plotting:
    strain versus time
    strain rate versus time
    strain rate versus strain
(h) performing a least squares fit to evaluate the coefficients of the creep models
(i) simulating the creep test using the model and parameters to verify that the model faithfully reproduces the observed response.

Hank Lauson (SNLA) assisted in accomplishing the data reduction. As of the end of the reporting period, the hydrostatic consolidation data had been analyzed and the creep data was ready for performing least squares fitting. However, since the results of the hydrostatic consolidation modeling are necessary to interpret the creep data, the fitting procedure for the creep data has been postponed until a satisfactory model is available for this aspect. The programs prepared for the data reduction process by Hank Lauson are available for further analysis of data.

Typical results from the reduction of both the consolidation data and creep data are presented in Figures 2.2 to 2.12. Figures 2.2 to 2.6 show the specimen volume, time rate change of volume, strain, time rate change of strain, and porosity from Test #72. Figures 2.8 to 2.12 show the behavior observed during the URI creep test UI-2C on undisturbed illite. Similar plots are available from the other consolidation and creep tests.

Based on the experience gained in prior attempts to fit a model to the consolidation phase of triaxial tests, the model was modified to incorporate the volume fraction of the clay platelets rather than the pore water. In this form the model becomes

$$d_I = A_o e^{Q/R\theta}\, \bar{\sigma}_I^{-n}(1-\alpha)^m.$$

The least squares fit to data points after 2000 seconds provides a rather consistent set of parameters as indicated in the Table below.

Test	m-n	B_2
59	-100.5	-109.2
72	-99.98	-115.5
55B	-98.40	-106.0
55C	-103.2	-98.6
55D	-92.5	-106.1
40B	-88.99	-93.44

$$B_2 = \ln[A_o e^{Q/R\theta}\, \bar{\sigma}_I^{-n}]$$

However, the exponent of the $(1-\alpha)$ form is quite large, leading to the same difficulties as encountered with prior models. Further, when the parameter B_2 was plotted as a function of $\ln \bar{\sigma}_I$ to determine the exponent n (Figure 2.13) the resulting value of n was approximately 17 (using an odd integer). This value also seemed high relative to the known behavior of other geological materials even though there is no justification from the present data to discount it. Specific fits of these curves are provided for completeness in Figures 2.14 to 2.19. These show the data points and corresponding fits for the tests enumerated in the preceding table.

The apparent shortcomings of the previous work motivated a search for alternative formulations for describing the observed consolidation behavior. Based on some concepts from creep of crystalline materials, a model that incorporates internal variables (such as a back stress or equilibrium structure) were considered. By considering the general behavior of various types of models to the idealized conditions of a creep test and a quasi-static strength test several forms were eliminated. In addition, by considering what the implications of reducing the stress to a lower value during a test could have on the remaining models several more were eliminated from further consideration.

The internal variable model that was selected for study can be written as shown in Equations (2.15) to (2.17). In this model the internal variable β is used to describe the internal state of the sediment. In it are embodied the effects of prior consolidation history. As shown, it includes only the mechanical effects, but thermal effects could also be included.

Initial attempts to fit such a model to the consolidation phase of the tests indicated that the general nature of the porosity-time behavior could be simulated. Further, the magnitude of coefficients in the fit were much more reasonable than the models discussed previously. To

perform the fits, Equations (2.15) and (2.17) were reduced to a single second order differential equation in the variable α_s ($\alpha_s = 1 - \alpha$) by noting that the stress can be written as a constant divided by α_s for isotropic consolidation. Rewriting the equations gives

$$d_I = \kappa_o \beta^{m^*} / \alpha_s^{n^*}$$

and

$$\dot{\beta} + A_s \beta = B_3 \alpha_s$$

where κ_o, A_s, B_3, m* and n* are material parameters. Conservation of mass requires that

$$d_I = - \dot{\alpha}_s / \alpha_s .$$

Combining these equations in a manner that eliminates β gives

$$\ddot{\alpha}_s = - \left\{ \frac{(n^*-1)\dot{\alpha}_s^2}{\alpha_s} + \frac{m^* B_3 K_o}{\alpha_s^{n-2}} \left(- \frac{\dot{\alpha}_s}{K_o} \alpha_s^{n-1} \right)^{(1 - \frac{1}{m^*})} + m A_3 \dot{\alpha}_s \right\} .$$

Defining K_1^* and K_2^* to be

$$K_1^* = - m^* A_3$$

$$K_2^* = \frac{m^* K_o B_3}{|K_o|^{(1 - \frac{1}{m^*})}}$$

gives

$$\ddot{\alpha}_s = \dot{\alpha}_s \left\{ \frac{(1-n^*)}{\alpha_s} + K_2^* \frac{\alpha_s^{(1 - \frac{n^*}{m^*} + \frac{1}{m^*})}}{\dot{\alpha}_s^{(\frac{1}{m^*} + 1)}} + K_1^* \dot{\alpha}_s^{-1} \right\} .$$

There are five parameters for this model (K_1^*, K_2^*, K_3^*, m* and n*) that are evaluated by selecting the combination of values that give the best fit to the data. Hank Lauson used several fitting techniques to evaluate these parameters. First, using the data to define initial conditions for $\dot{\alpha}_s$ and α_s, he performed a least squares fit to obtain their values. Second, he allowed the initial values of $\dot{\alpha}_s$ and α_s to be determined by the fitting process while imposing values for m* and n*. Numerous combinations of m* and n* were evaluated, with n* ranging from 1 to 7 and m* ranging from -2.25 to -4.0. The third approach used by Hank Lauson was to perform simultaneous solutions of two first order differential equations. These again come directly from the constitutive equations

(Equations (2.15) and (2.17)) and conservation of mass. They become, after correcting for the change in stress with porosity,

$$-\frac{\dot{\alpha}_s}{\alpha_s} = K_o^+ \beta^{m^+} \alpha_s^{-n^+}$$

and

$$\dot{\beta} + A_3\beta = B_3\alpha_s.$$

(Conservation of mass has been used to relate d_I to α_s and $\dot{\alpha}_s$.) Here K_o, m^+ and n^+ are determined directly from Equation (2.15) by algebraic manipulations (and imposing isothermal conditions). The initial conditions for α_s and α were evaluated as part of the fitting procedure while n^+ and m^+ were fixed. The values of n^+ used ranged from 1 to 7 while m^+ ranged from -2.0 to -5.0. It was observed that the system of two first order equations (in α_s and β) were more stable and converged more quickly than the single second order equation (in α_s). In cases where the selection of fixed parameters (m^+ and n^+) coincide, the two approaches yield the same values for the other parameters being evaluated.

Some of the results from fitting the two first order equations to Text #72 are shown in Figures 2.20 to 2.28. In this case n^+ was varied from 1 to 7 while m^+ was held constant at -4.0. Then m^+ was varied between -2.0 to -5.0 while holding n^+ constant at 7. The values of the parameters K_o, A_3, B_3 and the initial value of β determined from the fitting procedure have been plotted in Figures 2.20 to 2.27 for $n^+ = 7$ with m^+ varying and for $m^+ = -4$ with n^+ varying. These plots indicate that variations in β_o, A_3 and B_3 diminish as $|m^+|$ increases, but $|m|$ has little effect on the variations in K_o. The variations in β_o, A_3 and B_3 are nearly constant with respect to n^+, but K_o depends on n^+ nonlinearly. The implications that these trends have on the selection of parameters is still being studied. The internal variable β is plotted as a function of time in Figure 2.28 for Test #72. It is evident that β is monotonically increasing, but at an ever diminishing rate. Over the 25 ks time frame of Text #72, β increases from a value of approximately 1.25 to more than 2.50. The predicted sediment volume fraction, α_s, also matches the data quite closely. However, the number of data points is not adequate to give a high degree of confidence in the model parameters. More recent experiments will provide data for tests of longer duration. The increased number of points for each consolidation history, as well as the longer time spans, will help greatly in increasing the confidence of the model parameters.

C. Triaxial Consolidation Simulation

An underlying assumption of the data reduction process has been that the stress and deformation states are uniform throughout the sample. This actually cannot be the case since pressure gradients must

exist in order to expel pore fluid from the sample. Spatial variations in the effective stress probably exist that tend to produce non-uniform deformations in the specimen. Since this is a difficult problem to address analytically, the computer code NEPTUNE is being used to simulate the triaxial experiments. With this code it is possible to model directly the spatial variations in stress and deformation since the skeleton motion and pore fluid motion are coupled. During this year the triaxial simulation was defined and the input files for NEPTUNE were created. These files contain the description of the specimen geometry constitutive model parameters, test boundary conditions (for loads and drainage), and simulation controls necessary in NEPTUNE. As discussed in the first section of this addendum, the internal variable model was implemented in NEPTUNE. The computations have been initiated, but are awaiting completion of the NEPTUNE modifications for further efforts.

The results of fitting the internal variable model to the consolidation behavior of Test #72 are being used initially in the NEPTUNE simulation. The coefficients that appear in Equations (2.15) and (2.17) are (using the $m^+ = -4.0$ and $n^+ = 5$ results):

$$A_1 = 3.457 \times 10^{6} \qquad A_3 = 5.743 \times 10^{-5}$$

$$Q_1 = 0.0 \text{ (isothermal)} \qquad B_3 = 4.667 \times 10^{-4}$$

$$n_1 = 0.2$$

$$m_1 = 0.8$$

with initial values of α_s and β of

$$\alpha_{s_o} = 0.651$$

$$\beta_o = 1.027.$$

The results of these computations will help assess the validity of using uniform stress and deformation assumptions for evaluating the constitutive model parameters.

III. APPLICATION OF NEPTUNE TO SUBSEABED APPLICATIONS

NEPTUNE has been constructed for analyzing the creeping motion of saturated marine sediments. As discussed earlier, this limits the application of NEPTUNE to slower, longer-term motions that have slowly-changing stress fields and negligible inertia. Two examples have been studied that fall into this category. These problems have received some attention in past years as well. The first is the response of the sediment to a heat-producing canister. In this application the heat produced by high level radioactive wastes in a canister would elevate the temperature of sediment in the vicinity of the canister as well as heating the

canister itself. Raising the sediment temperature would tend to accelerate the consolidation process in the heated area. Further, the reduction in density associated with thermal expansion lessens the gravitational forces acting on the sediment relative to unheated sediment. The differential body forces between heated and unheated sediments drive convective flow of water through the skeleton as well as causing the skeleton itself to flow. This motion occurs concurrently with the sinking of the canister (and waste form) relative to the sediment because of the canister's greater density. The second application addresses the rate of closure expected in a residual cavity left open by the emplacement process. In this case the hole is expected to close following the emplacement by the nature of the design of the penetration vehicle. However, knowledge of whether or not a hole closes by a creeping mechanism even after the penetration event has concluded would provide additional confidence in understanding the overall system.

A heat producing sphere emplaced in a sediment column was modeled with NEPTUNE. The purpose of the effort was to gain a more thorough understanding of the capability of NEPTUNE to simulate complex two-dimensional problems important to the Subseabed Disposal Program. The porosity, permeability, heat load, and sediment constitutive law parameters were varied to test the behavior of NEPTUNE. An idealized geometry in which the canister is a sphere having a 0.5 m radius was chosen so that the isothermal velocities could be compared to existing analytical solutions. A temperature-dependent shear viscosity and a constant bulk viscosity have been assumed. These simplifications limit the applicability of the results relative to expected behavior of an actual emplaced canister, but they are a necessary step in making the numerical simulation transition from one-dimensional verification examples to two-dimensional design applications in which the material nonlinearities are modeled fully.

The sediment in the simulation extends radially 10 m from the canister (there are 20 canister radii to the outside radius of the region). The canister is positioned at the midheight of a 10 m deep sediment column. (This depth will be increased when modeling actual Subseabed Disposal applications.) The top and outside radius of the region are held at a constant 277 K, while an adiabatic condition is imposed at the bottom surface. The bottom and outside radius surfaces have zero normal velocities imposed on both the skeleton and pore fluid. (The tangential shears are also zero.) The traction vectors on the top surface are zero. Initially, the sediment, pore water, and canister are 277 K and the sediment porosity throughout the region is 0.80. The canister produces heat at an initial 0.5 kW rate. However, this rate decays according to a thirty year half-life.

The mesh used is relatively coarse. 128 elements discretize the sediments with an additional 16 elements for the canister. The material properties for the sediment and canister are summarized in Table 3.1. The viscosity, μ, is based on data reported by Bishop and Lovenbury while the viscosities, λ, were chosen to give a reasonable consolidation rate

of an undisturbed sediment column.

Initially NEPTUNE was used to predict the instantaneous velocities of the sediment and pore fluid immediately after emplacement (assuming emplacement left no effects). The porosity and viscosity (κ) were varied over wide ranges (α: 0 to 0.8 and λ: 0 to 10^{22}). With $\alpha = 0$ and $\kappa = 0$, the equations simplify to those for a single incompressible constituent. In this case the predicted velocity compared closely to a Stokes sphere solution for the same problem. Increasing α (κ constant) caused higher downward velocities of the canister because of the larger density differences between the saturated sediment and the canister. Increasing κ (α constant) produced smaller downward velocities of the canister since the skeleton exhibits a greater resistance to flow.

Several cases have been simulated with NEPTUNE for longer periods of time. A number of these simulations are presented in Table 3.2. In these cases the canister density, the skeleton viscosity (κ) and the drag coefficient (b) have been varied. In all of the simulations, the thermal response was dominated by conduction, rather than by convection of the pore fluid or the skeleton. The temperature response of several points located at the midheight (but at different distances from the centerline) are shown for Case A for a sixteen year period. Figures 3.1, 3.2, 3.3 and 3.4 correspond to radial positions of approximately 0.0, 0.60, 1.2 and 4.3 m, respectively. It is evident that the temperatures are higher closer to the canister and that the peak temperature at each position occurs later at larger radius values. Because the problems are conduction dominated, the thermal responses of the other cases are essentially the same, so they are not shown.

The velocity of the canister has been plotted for Cases A, B, C and E (Figures 3.5 to 3.8). As noted before, increasing the viscosity κ tends to diminish the canister velocity since the sediment is stiffer. (Compare Cases A and C or E and F in Table 3.3.) Changing the canister density changes the relative buoyancy of the sediment and canister. Canisters with greater density exhibit higher velocities. (Compare Cases A and B or C and E.) The drag coefficient showed relatively little influence on the rates of motion, since pore pressure gradients were quite small.

The sediment skeleton and pore fluid velocities show the combined effects of thermal softening and buoyancy changes. For Cases A, B, C and E the skeleton and pore fluid velocities at two radial positions have been plotted (Figures 3.9 to 3.24). The downward pull by the canister is offset by the upward lift from buoyancy. As the material softens from the heating, the motion often tends to accelerate.

The emplacement cavity closure analysis was initiated, but to date the results are not satisfactory. A much larger region was discretized than used earlier. The size of the region presented difficulties in obtaining adequate resolution close to the cavity while keeping the problem size manageable. NEPTUNE provided acceptable results for plane

strain models (i.e. a trench) but the velocity fields were qualitatively poor for axisymmetric models (a hole). The difficulties could be traced to the inability of the approximating functions to model the gradients of pore pressure at small radii. Better resolution and constraints on the pore fluid pressure (i.e. continuous pressures) are being implemented to counter this difficulty.

SUMMARY

A variety of activities over the past year have contributed to the increased ability to model the long-term motion of saturated marine sediments. The finite element code NEPTUNE was expanded and improved. Documentation of the program's capabilities was prepared and instructions for using it were written. Several forms of constitutive equations for the creep behavior of sediments were investigated. An internal variable model has shown promise for characterizing the strain-dependence of creep. The application of NEPTUNE to long-term canister motion analyses has demonstrated the ability of NEPTUNE to incorporate the effects sediment shear and volumetric deformation, pore water motion, and heating in problems that have complicated two-dimensional geometries.

MEETINGS AND PUBLICATIONS

1. Subseabed Disposal Program Creep Modeling Workshops

   a. January 1981 — Sandia National Laboratories, Albuquerque
   b. May 1981 — University of Rhode Island, Kingston, RI

2. Reports and Publications

   (1) Dawson, P. R. and P. F. Chavez, "NEPTUNE - A Finite Element Code for Creeping Flow of Saturated Cohesive Porous Media," Sandia Report in preparation.

   (2) Dawson, P. R. and P. F. Chavez, "Thermomechanically Coupled Creeping Flow of Saturated Cohesive Porous Media," Finite Elements in Fluids, Ed. R. H. Gallagher, in press.

Table 3.1. Material Properties

	Skeleton	Pore Fluid	Canister	
Density:	2800.	1000.	4000.	(kg/m^3)
Heat Capacity:	880.	4500.	864.	(Watt/kg K)
Conductivity:	1.92	0.625	1.25	(W/m^2K)
Expensivity:	5.0×10^{-4}	*	0.0	(1/K)

Porosity = 0.8

Drag Coefficient, $b = 1 \times 10^{12}$ and 1×10^{13} ($Pa \cdot s/m^2$)

Skeleton Viscosities: $\mu = 0.17 \times 10^{-7} e^{14700/\theta}$ ($Pa \cdot s$)

$\kappa = 10^{20}$ and 10^{21} ($Pa \cdot s$)

$*\alpha_{exp} = 2.5 \times 10^{-4} + 4.4 \times 10^{-6} (\theta - 273)$

Table 3.2. Heating Sphere Simulations

Case	Canister Density (kg/m^3)	Viscosity (κ) ($Pa \cdot s$)	Drag Coefficient (b) ($Pa \cdot s/m^2$)
A	2280	10^{20}	10^{13}
B	4000	10^{20}	10^{13}
C	2280	10^{21}	10^{12}
D	2280	10^{20}	10^{12}
E	4000	10^{21}	10^{12}
F	4000	10^{20}	10^{12}

Table 3.3. Peak Canister Velocity

Case	Peak Canister Velocity (pm/s)
A	-5.8
B	-27.5
C	-1.59
D	-5.8
E	-9.5
F	-27.3

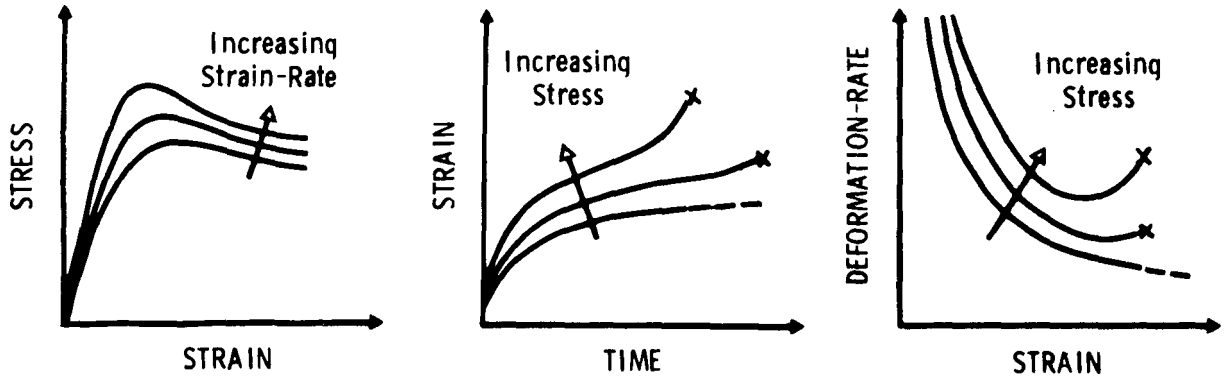


Figure 2.1 Typical Static and Creep Behavior of Sediment

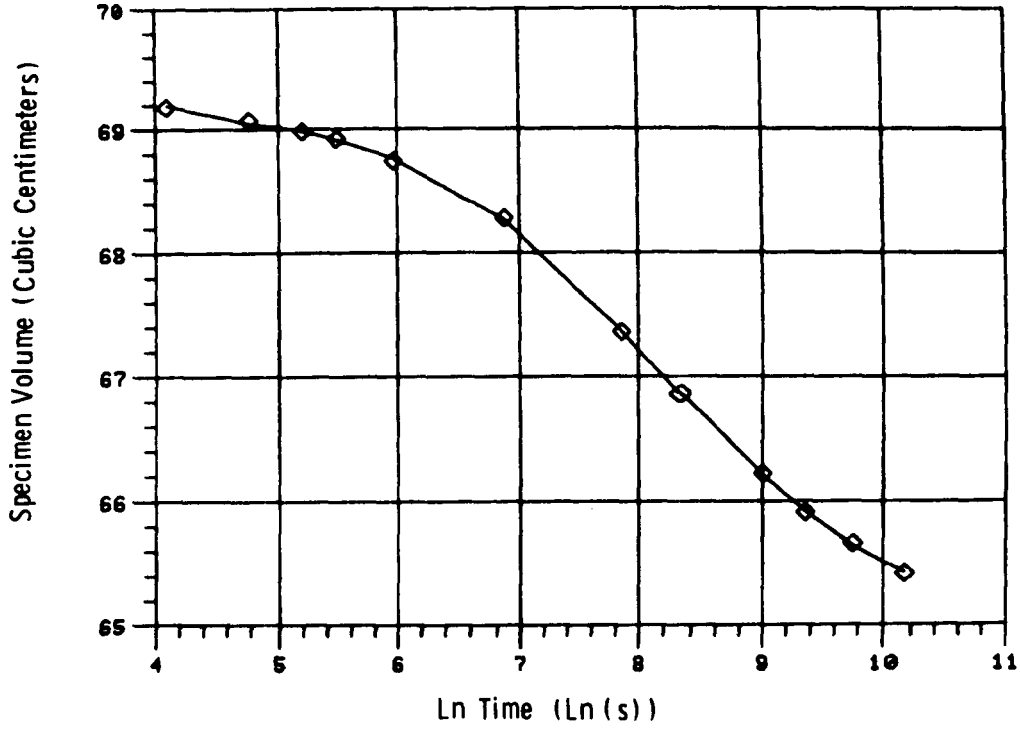


Figure 2.2 Specimen Volume During Consolidation Test #72

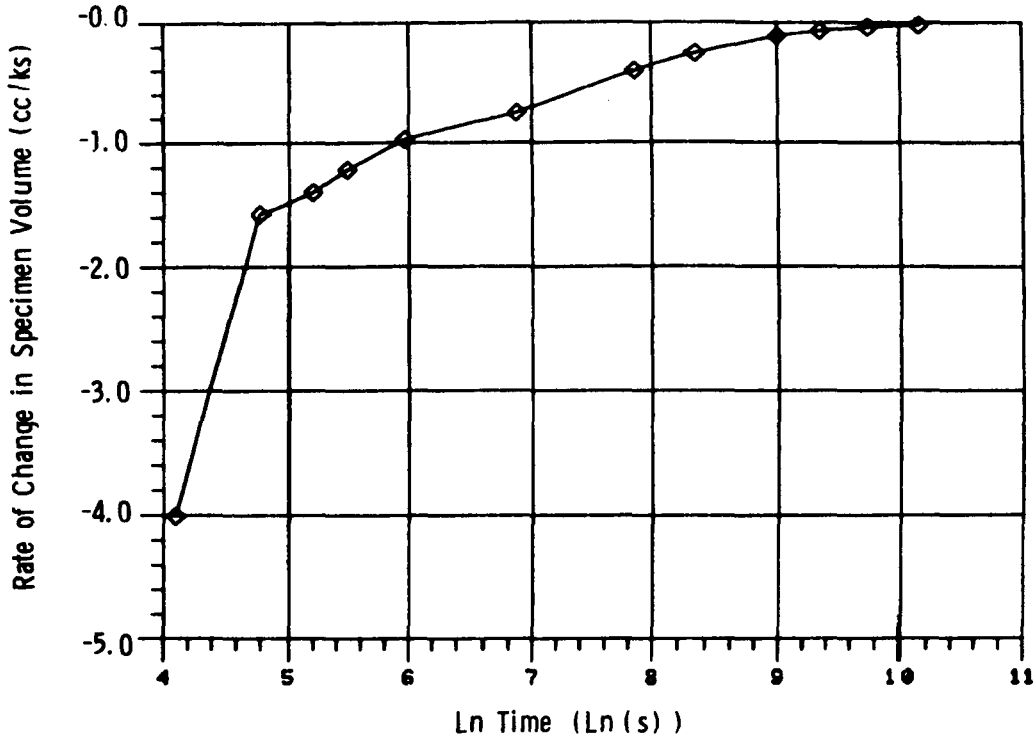


Figure 2.3 Specimen Volume Change Rate During Consolidation Test #72

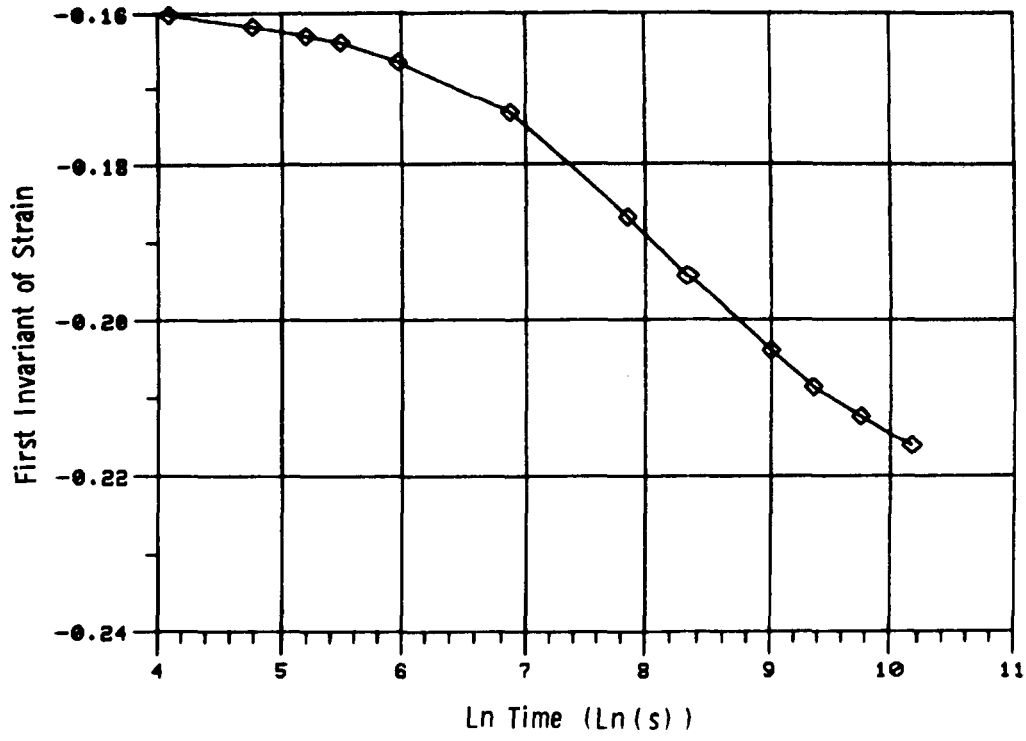


Figure 2.4 First Invariant of Strain During Consolidation Test #72

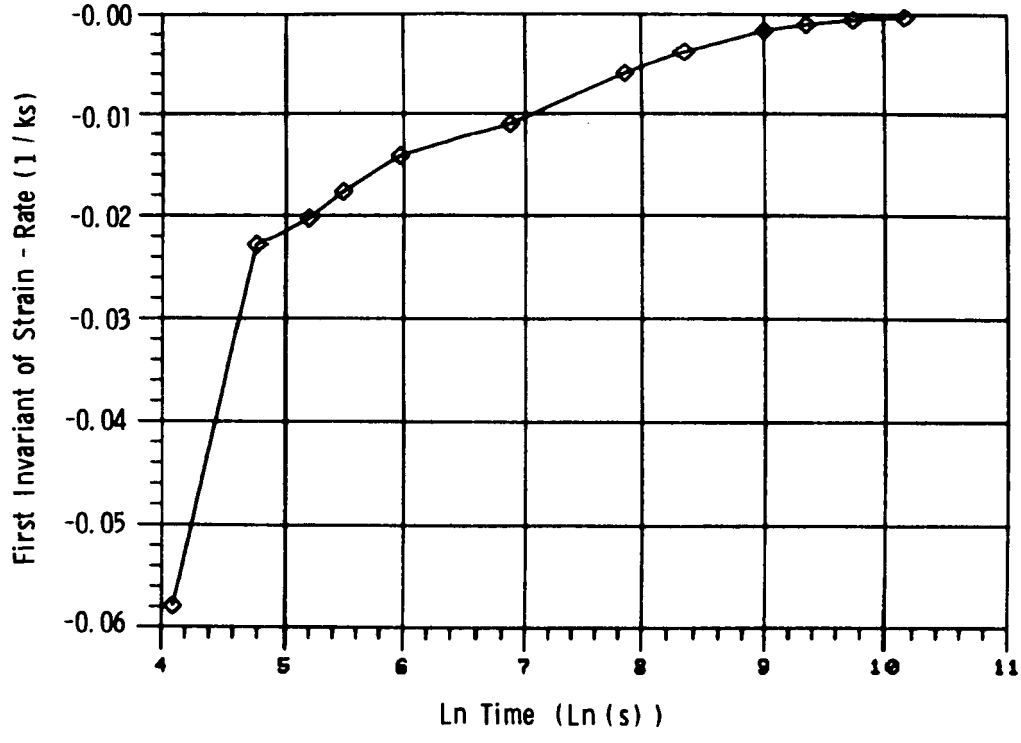


Figure 2.5 First Invariant of Strain - Rate During Consolidation Test # 72

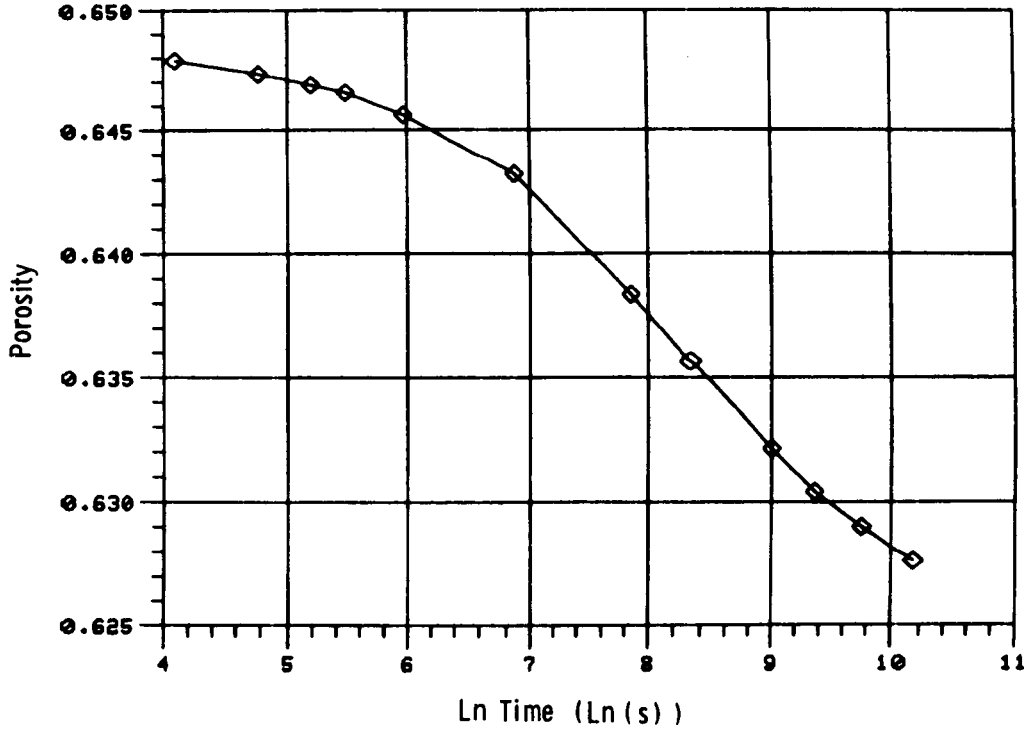


Figure 2.6 Specimen Porosity During Consolidation Test # 72

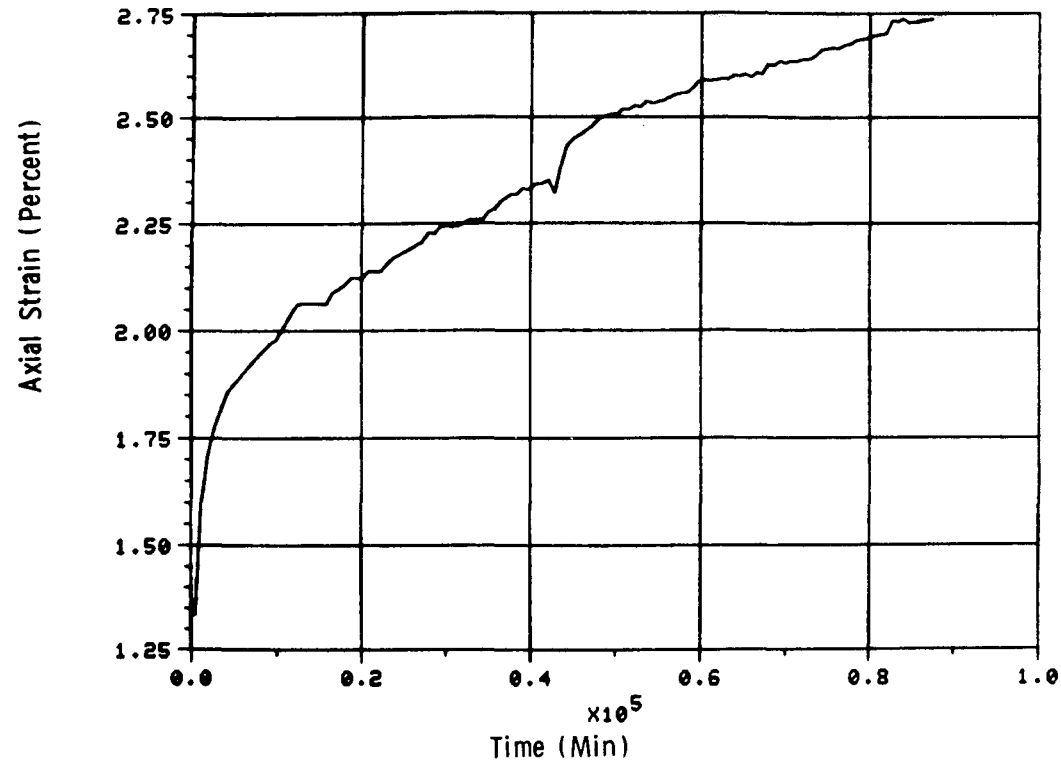


Figure 2.7 URI Creep Test UI-2C Axial Strain Data

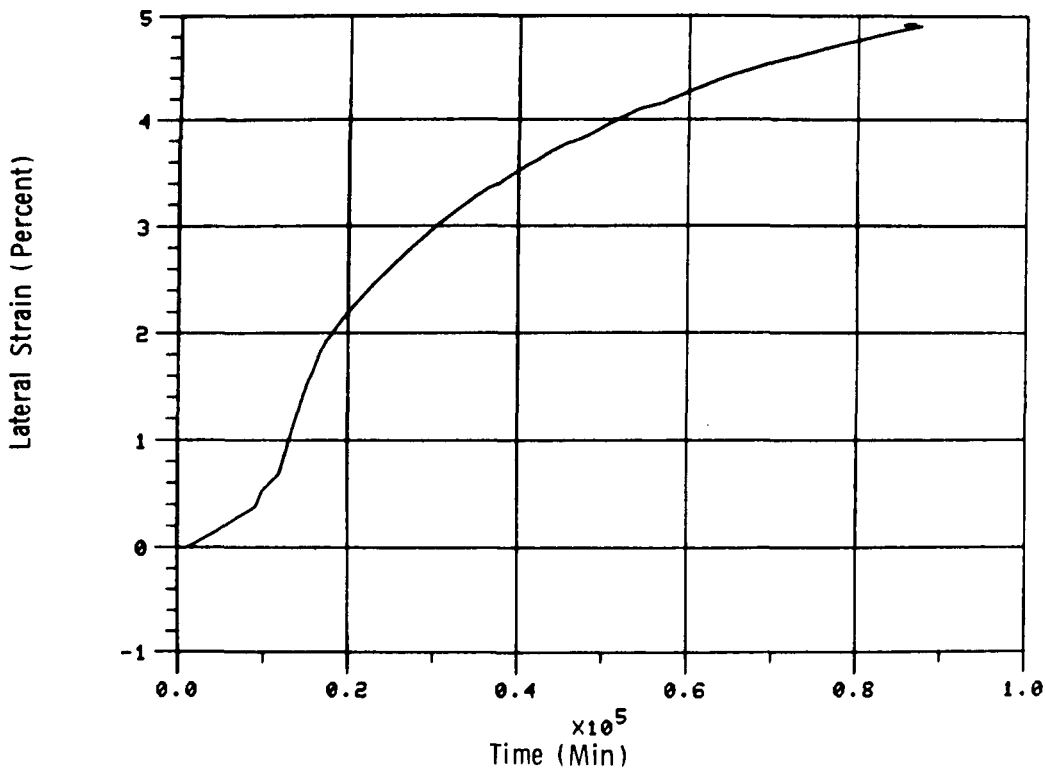


Figure 2.8 URI Creep Test UI-2C Lateral Strain Data

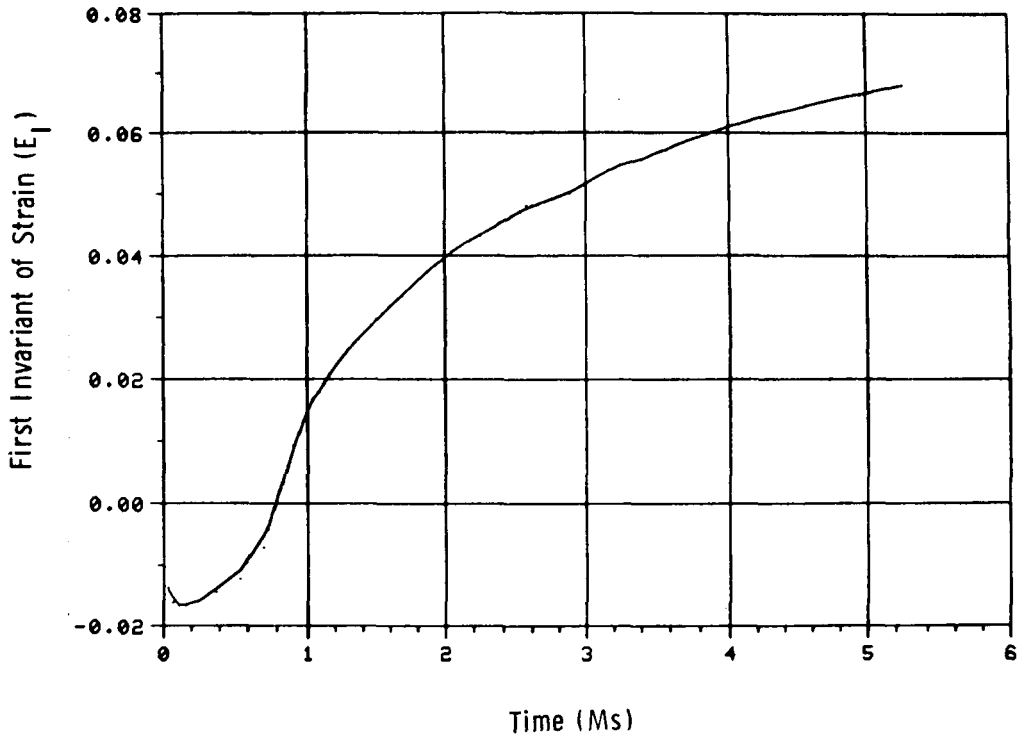


Figure 2.9 URI Creep Test UI-2C First Invariant of Strain

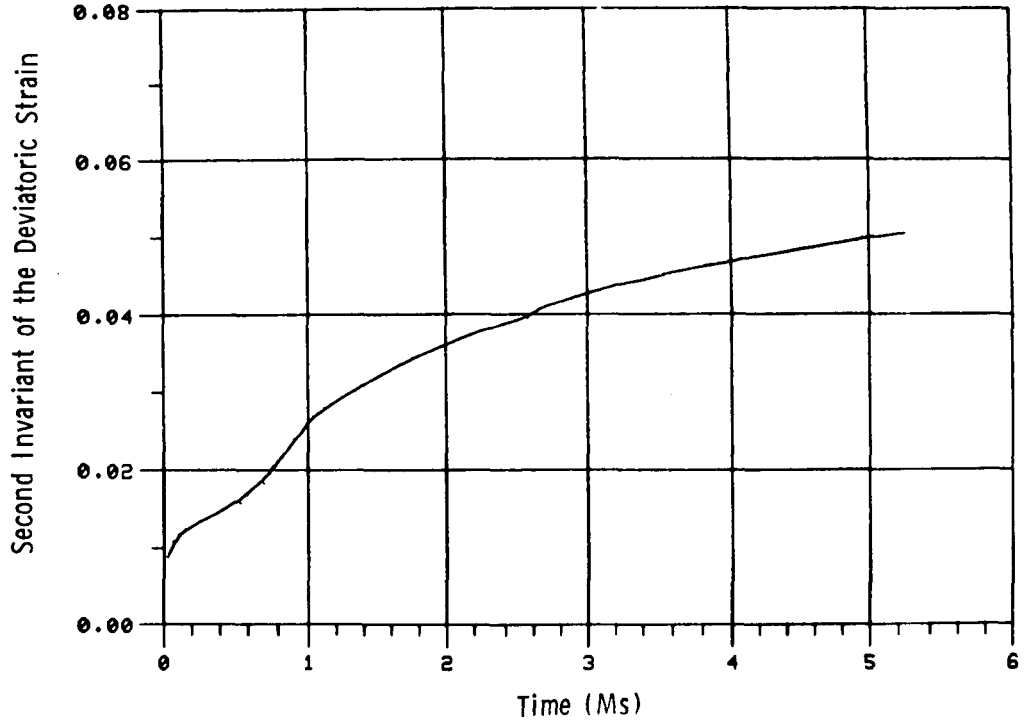


Figure 2.10 URI Creep Test UI-2C Second Invariant of Deviatoric Strain

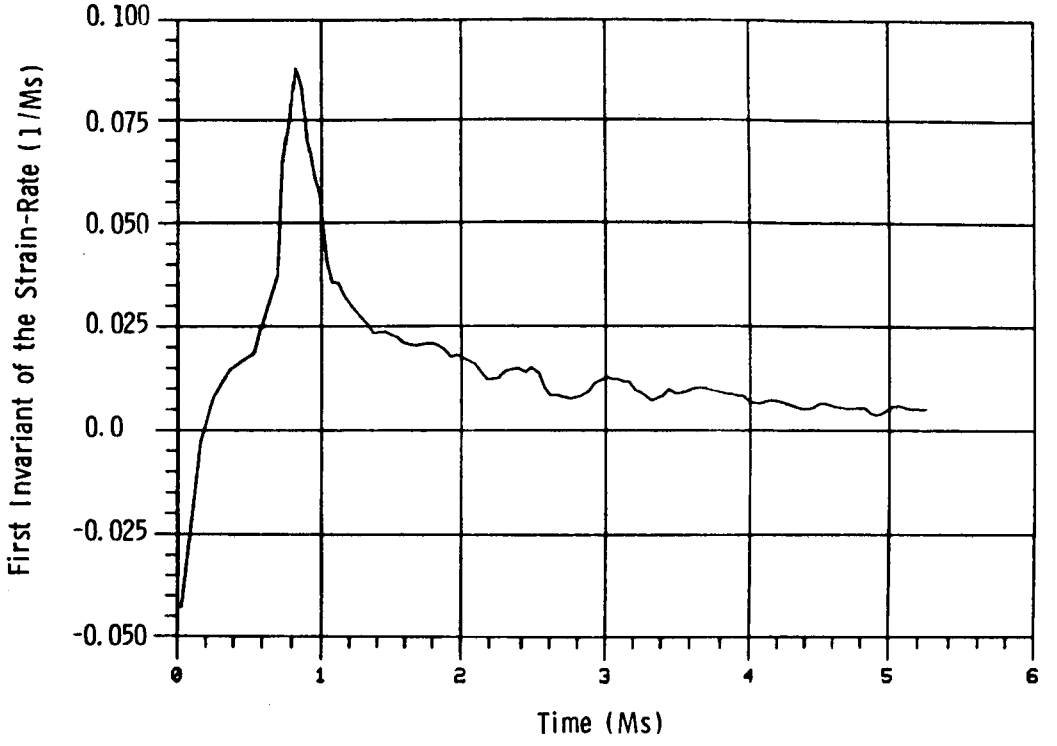


Figure 2.11 URI Creep Test UI-2C First Invariant of Strain-Rate

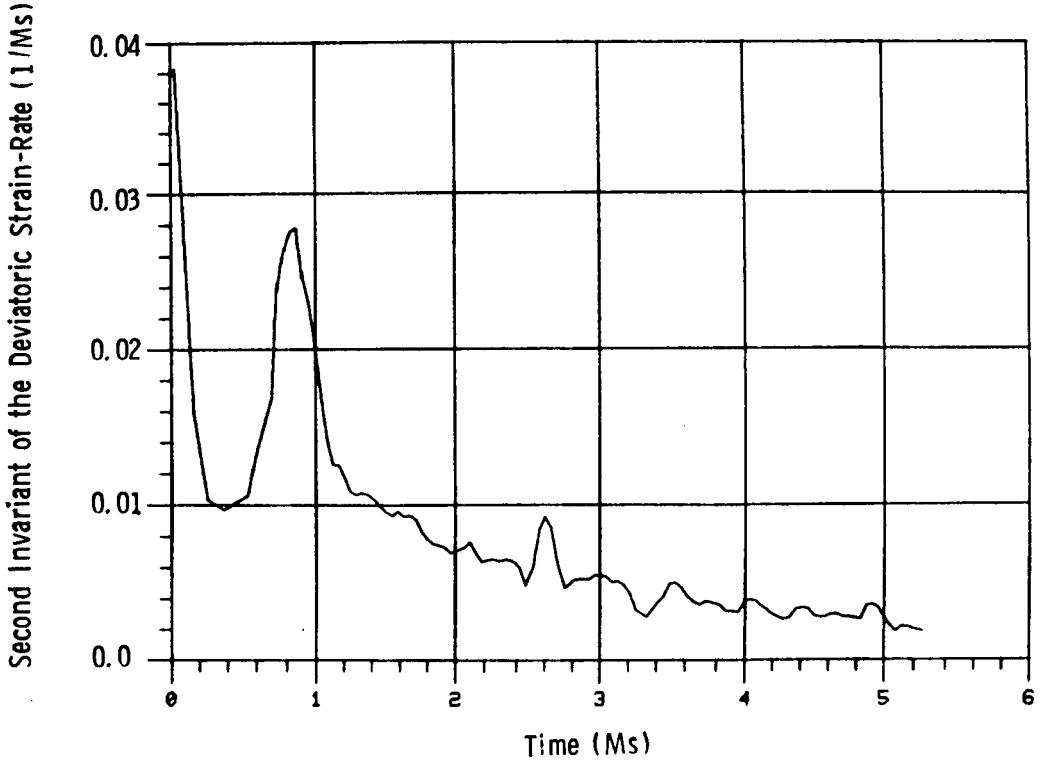


Figure 2.12 URI Creep Test UI-2C Second Invariant of Deviatoric Strain-Rate

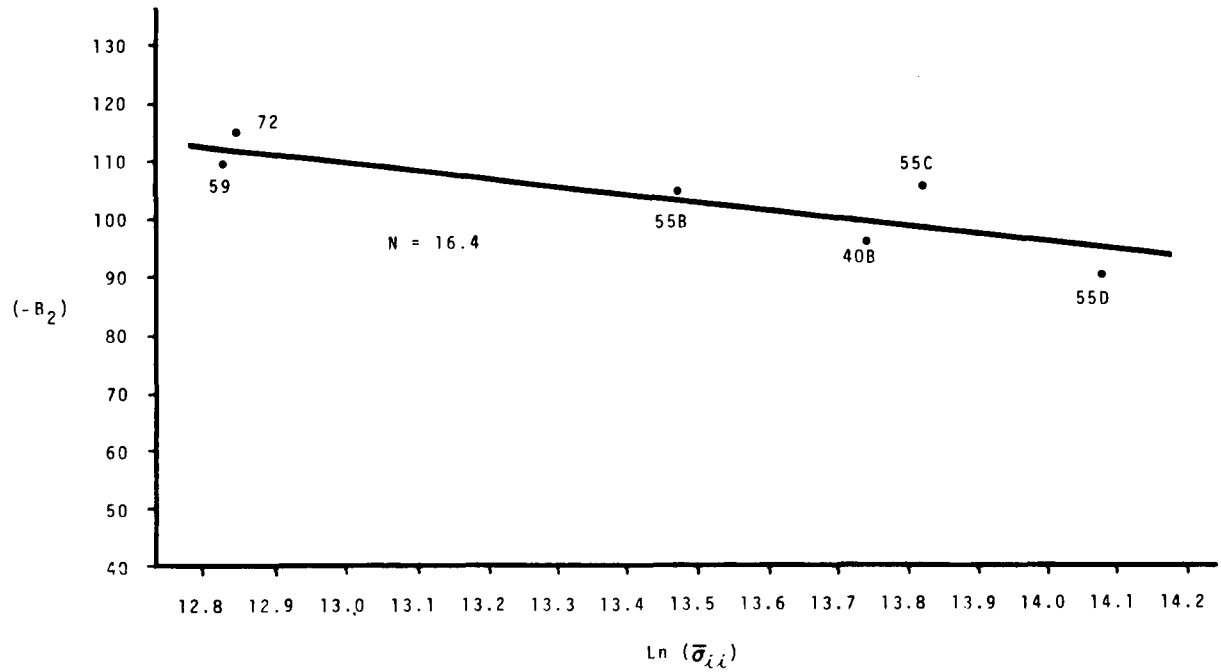


Figure 2.13 Stress Dependency in Hydro Static Compression Consolidation Behavior

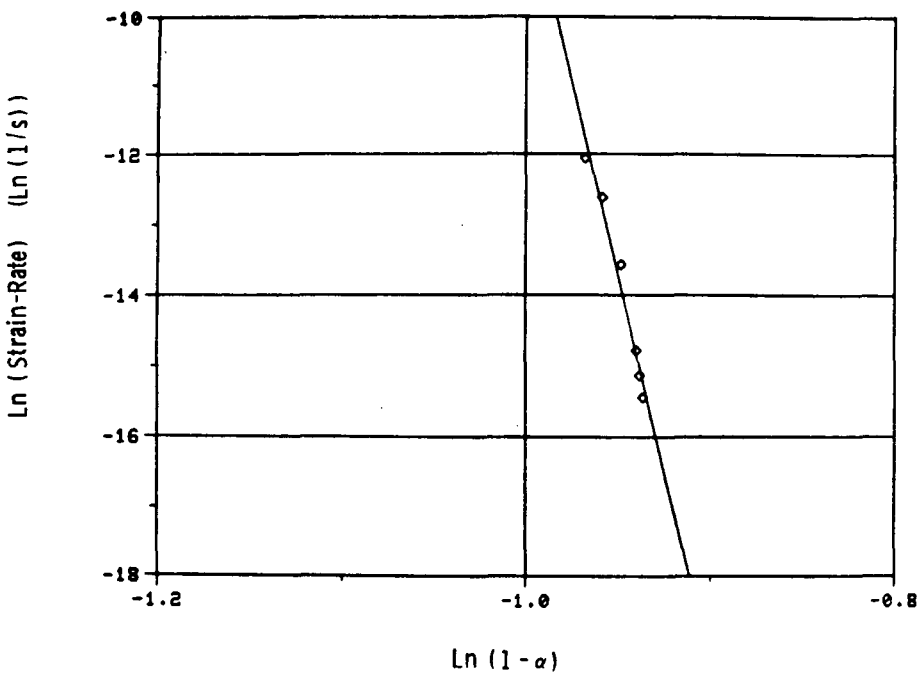


Figure 2.14 Empirical Fit of Strain-Rate History of Consolidation Test #59

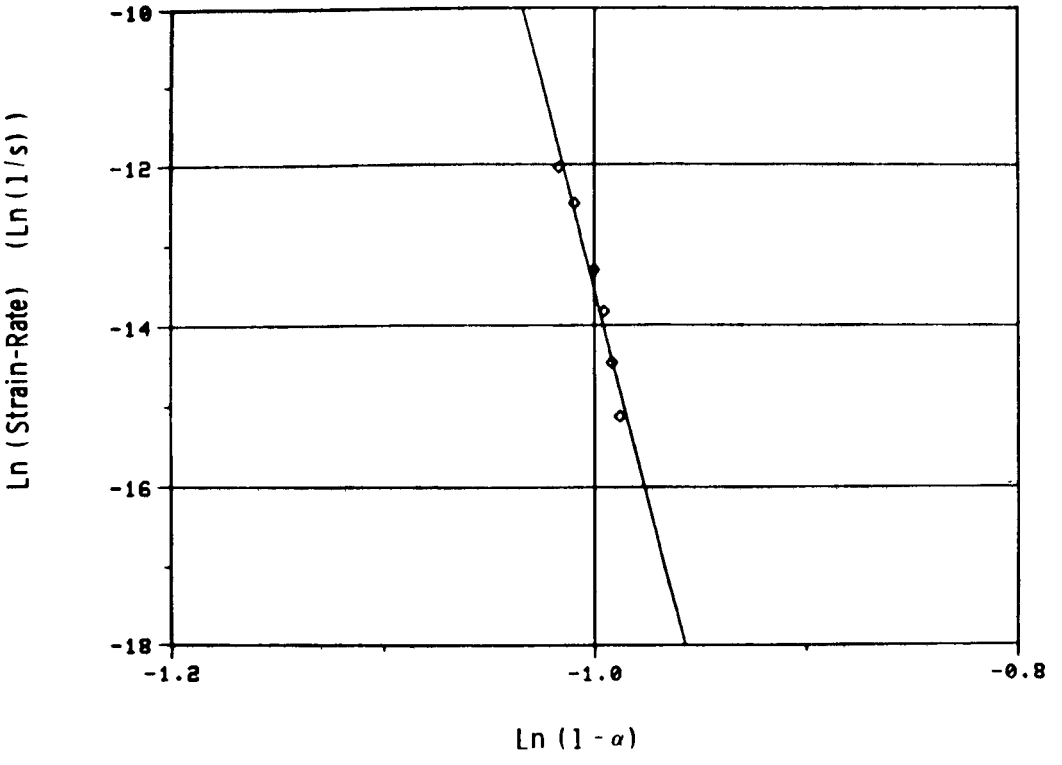


Figure 2.15 Empirical Fit of Strain-Rate History of Consolidation Test #72

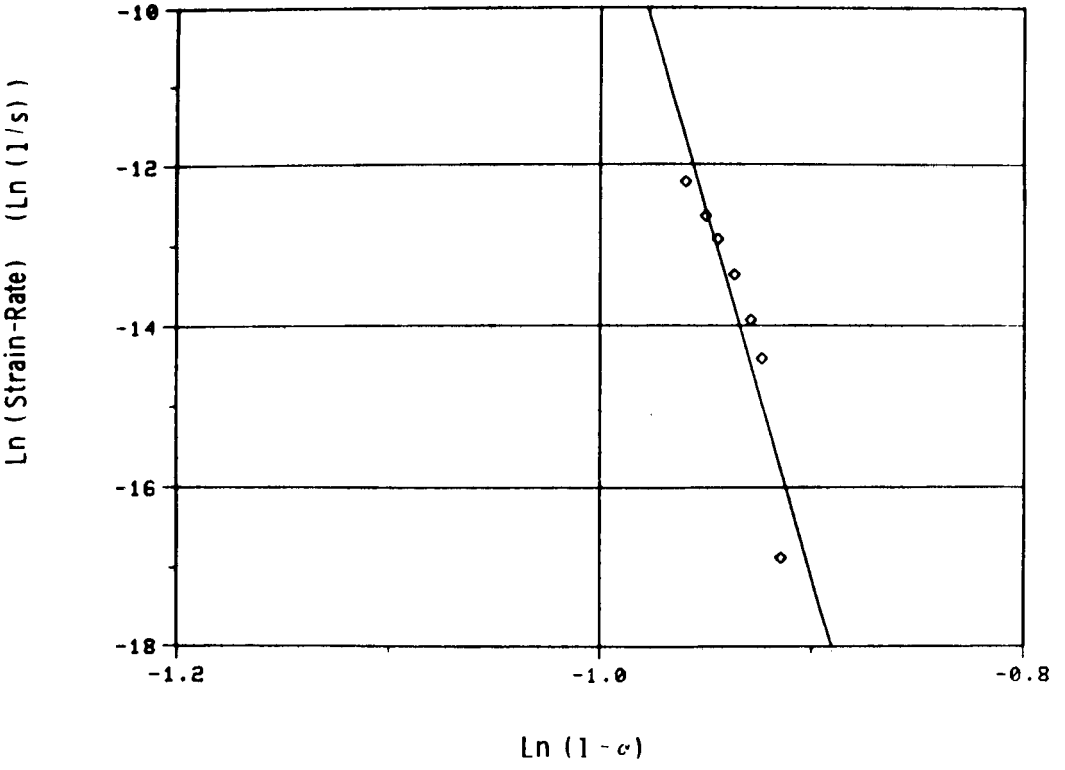


Figure 2.16 Empirical Fit of Strain-Rate History of Consolidation Test #55B

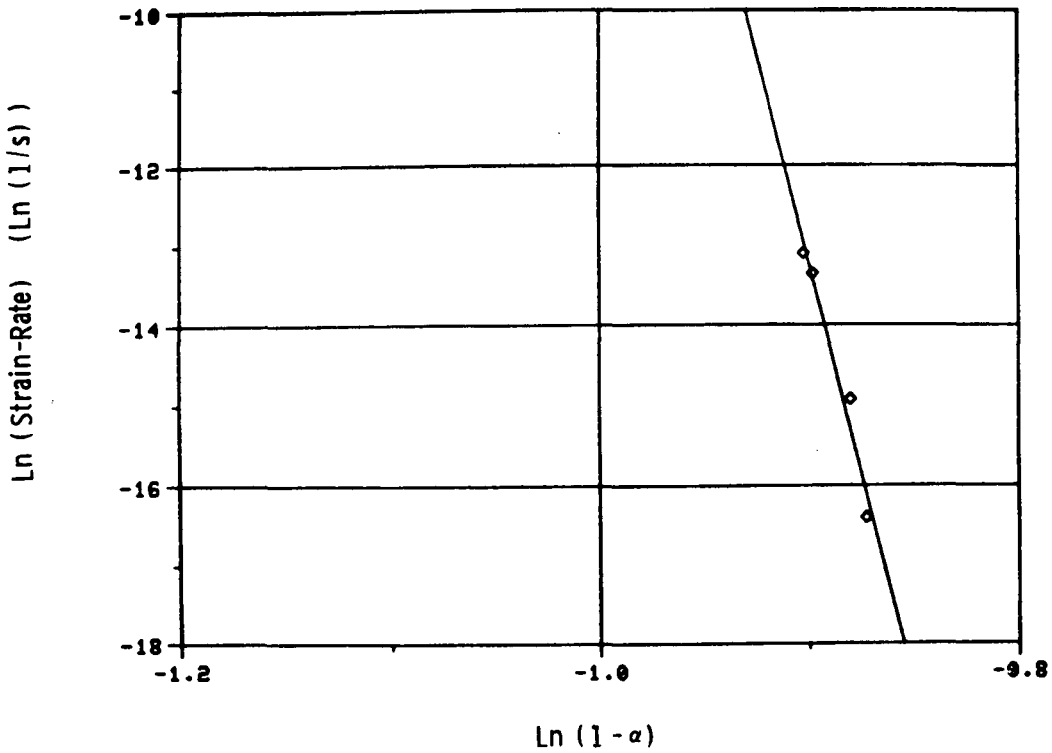


Figure 2.17 Empirical Fit of Strain-Rate History of Consolidation Test #55C

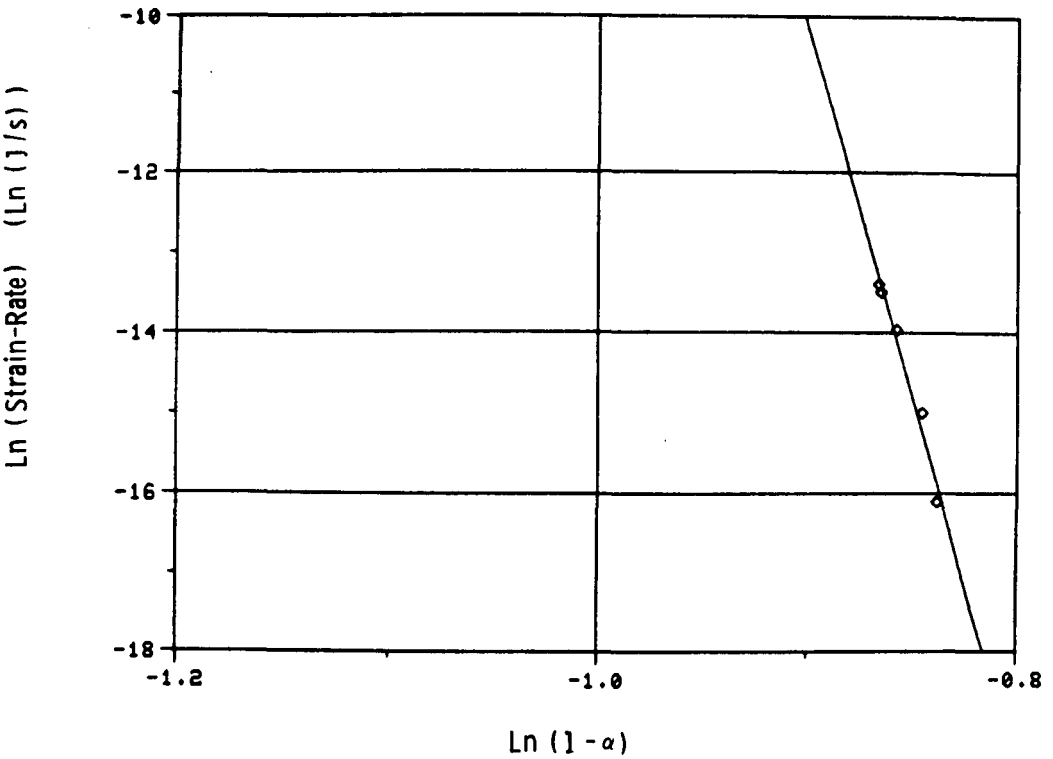


Figure 2.18 Empirical Fit of Strain-Rate History of Consolidation Test #55D

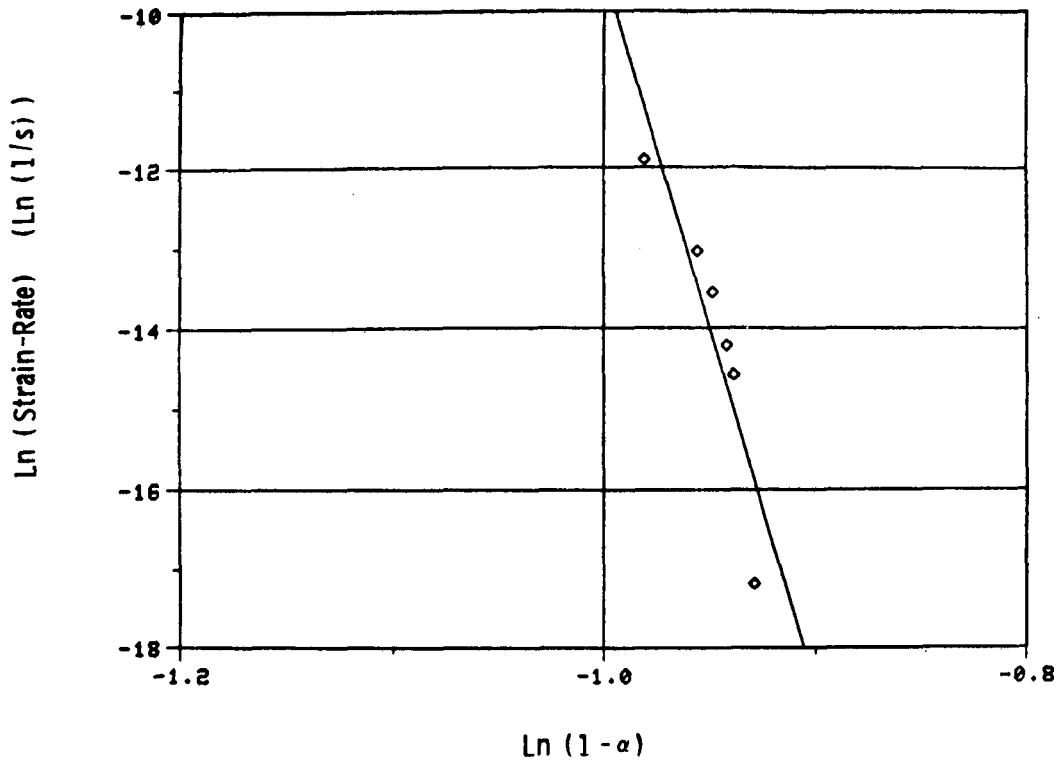


Figure 2.19 Empirical Fit of Strain-Rate History of Consolidation Test #40B

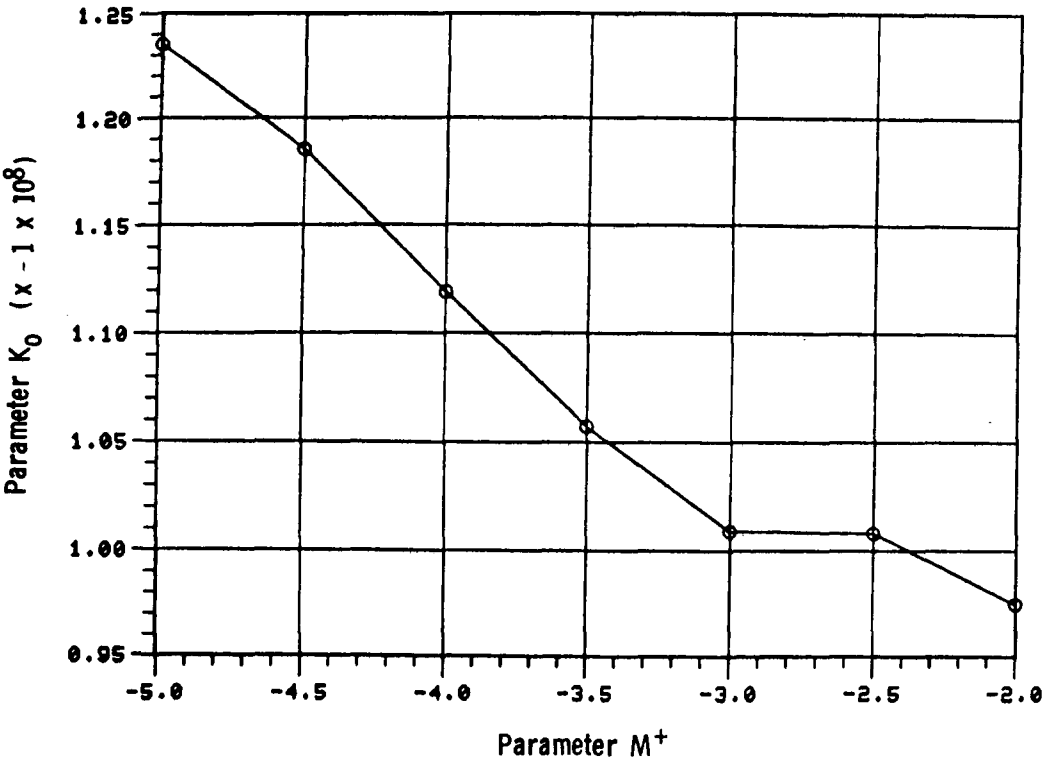


Figure 2.20 Parameter K_0 For Varying M^+ (N^+ = 7) From Consolidation Test #72

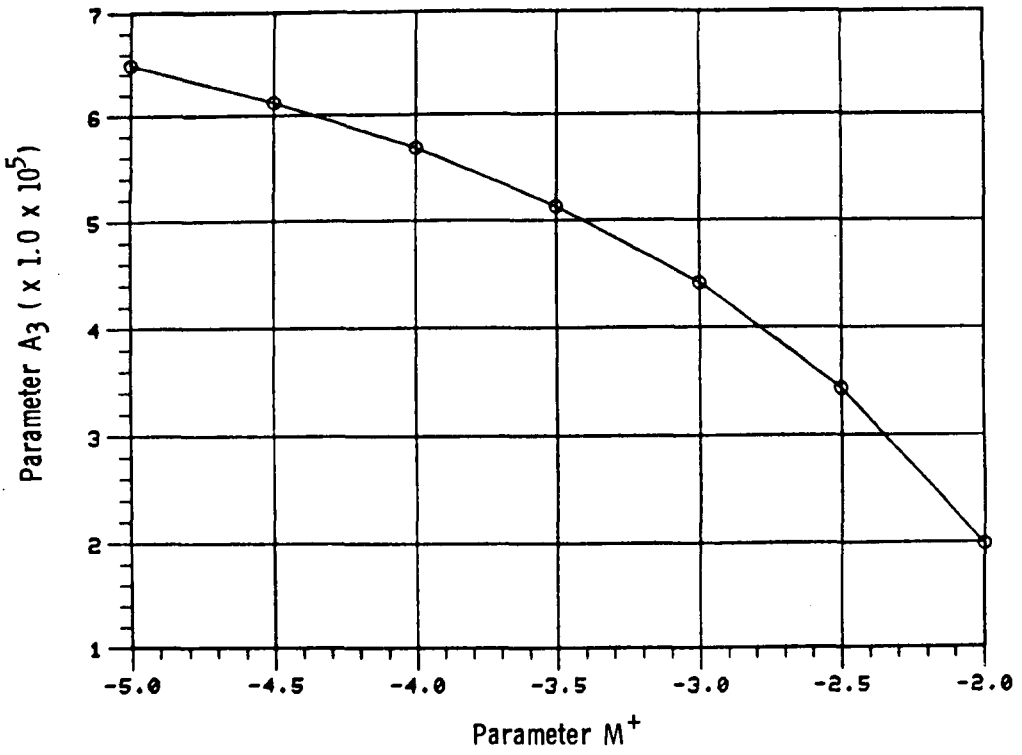


Figure 2.21 Parameter A_3 For Varying M^+ (N^+ = 7) From Consolidation Test #72

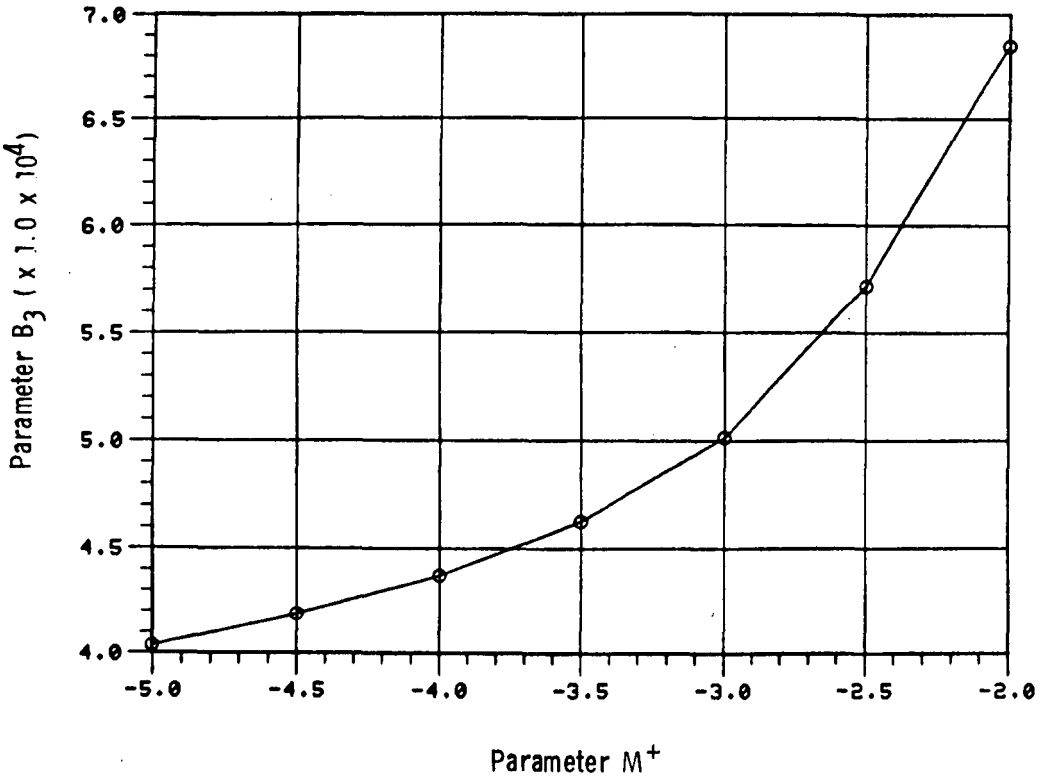


Figure 2.22 Parameter B_3 For Varying M^+ (N^+ = 7) From Consolidation Test #72

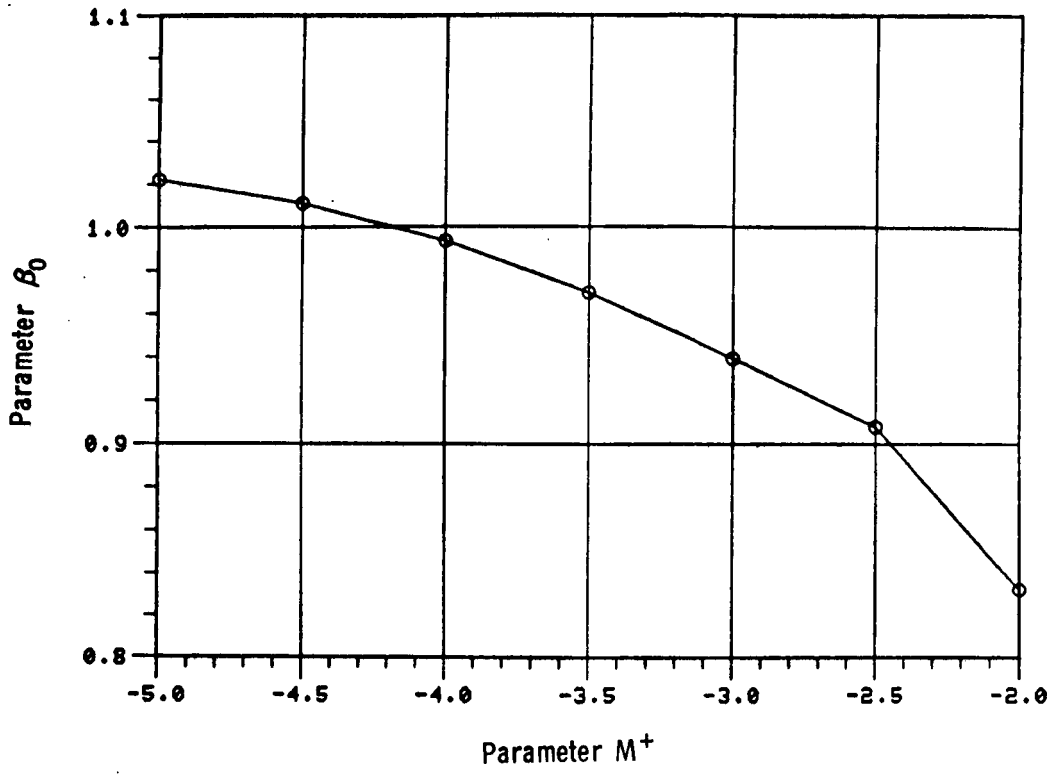


Figure 2.23 Parameter β_0 For Varying M^+ (N^+ = 7) From Consolidation Test #72

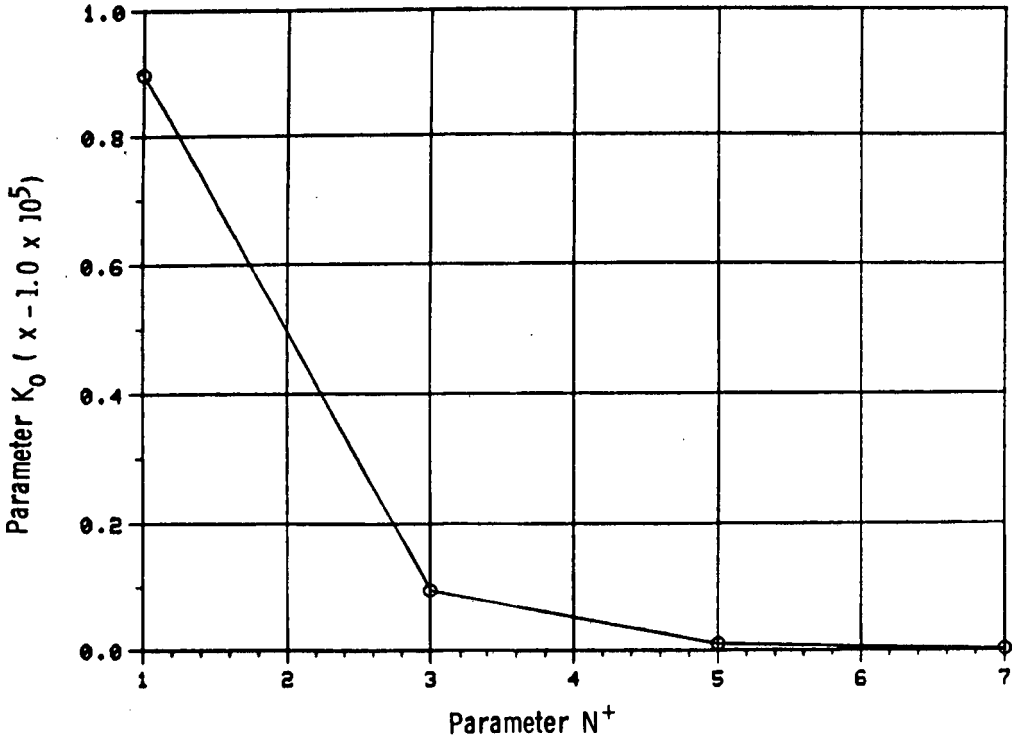


Figure 2.24 Parameter K_0 For Varying N^+ (M^+ = -4) From Consolidation Test #72

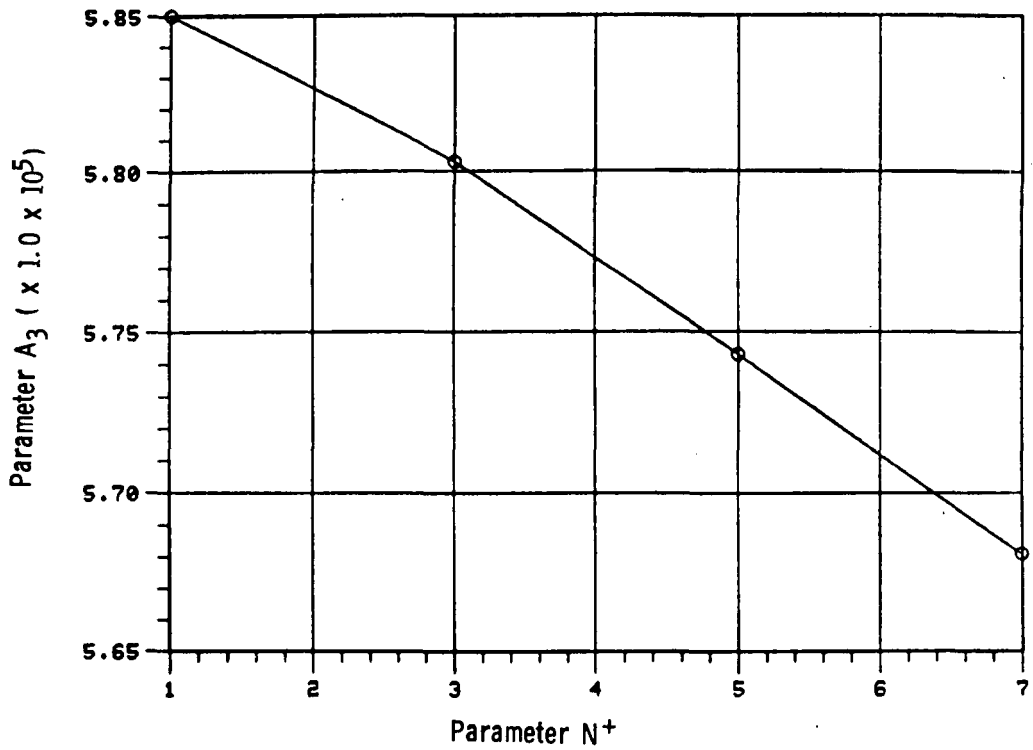


Figure 2.25 Parameter A_3 For Varying N^+ (M^+ = $^-4$) From Consolidation Test #72

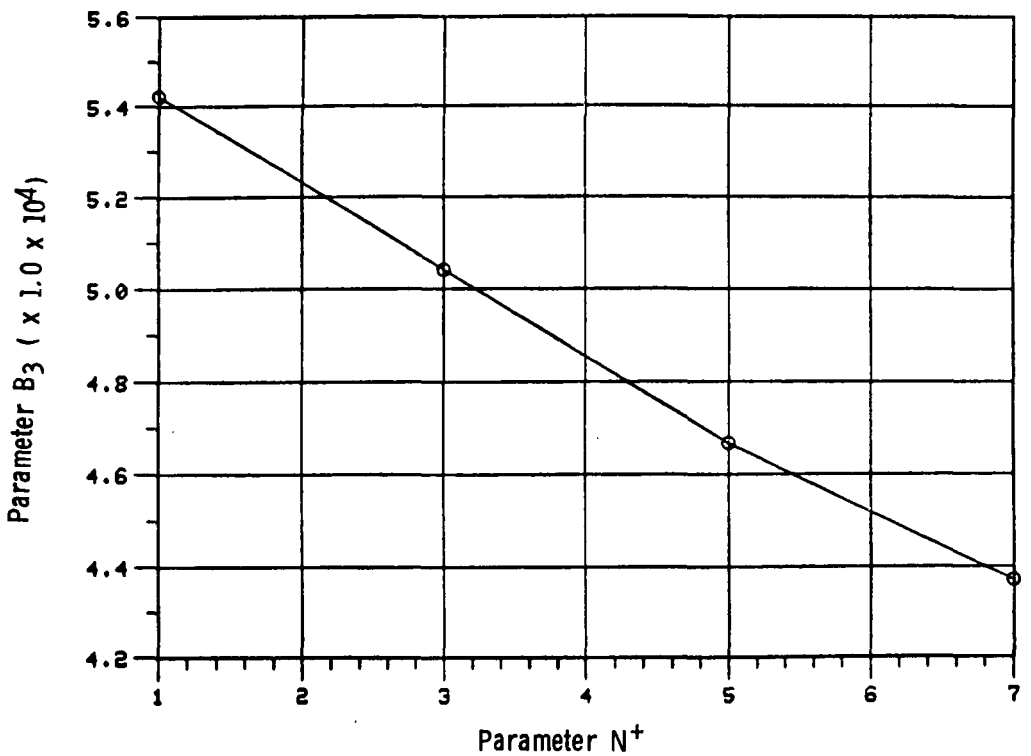


Figure 2.26 Parameter B_3 For Varying N^+ (M^+ = $^-4$) From Consolidation Test #72

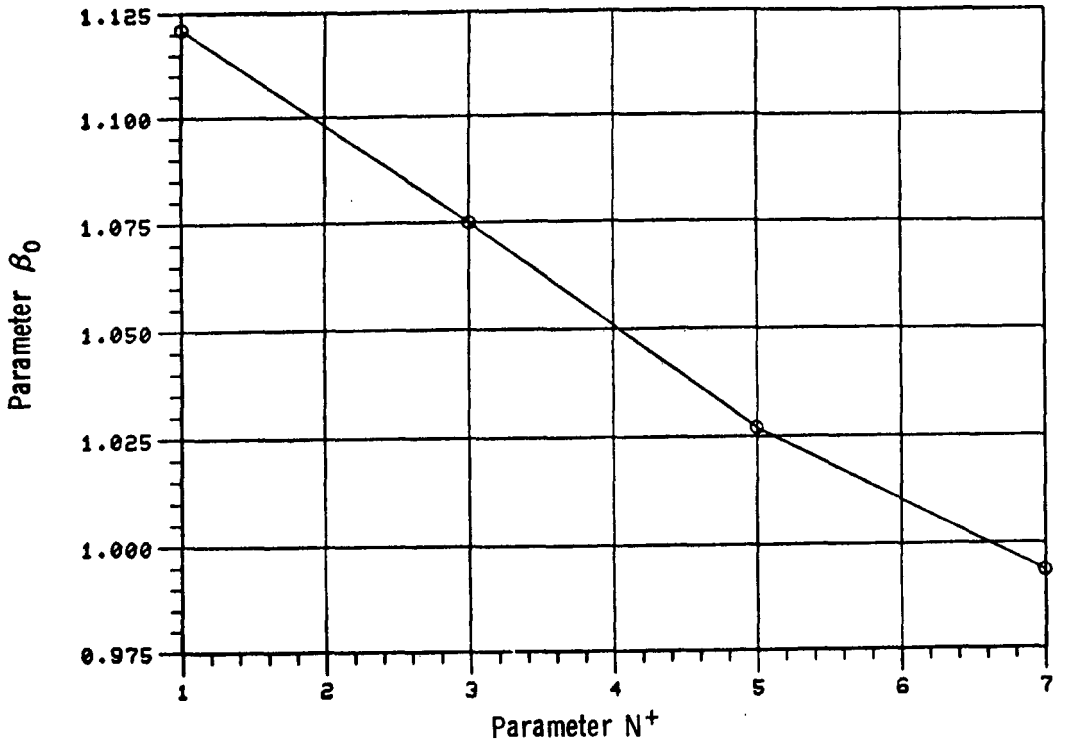


Figure 2.27 Parameter β_0 For Varying N^+ ($M^+ = -4$) From Consolidation Test #72

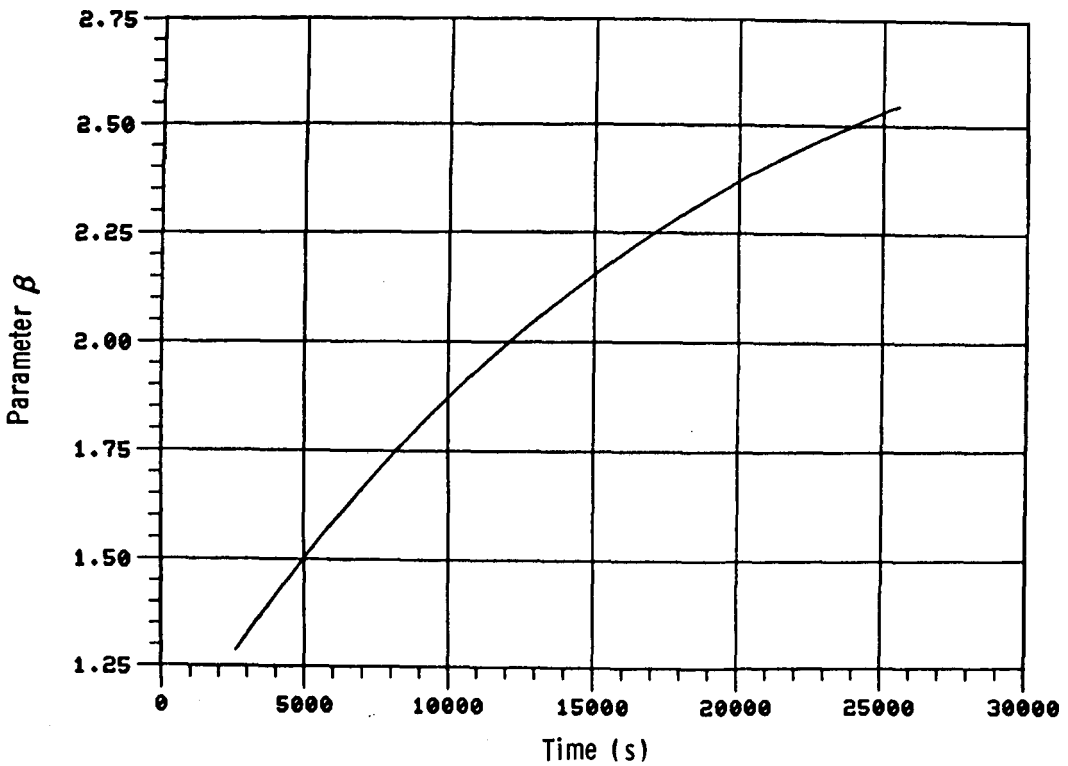


Figure 2.28 Internal Variable β History For Consolidation Test #72

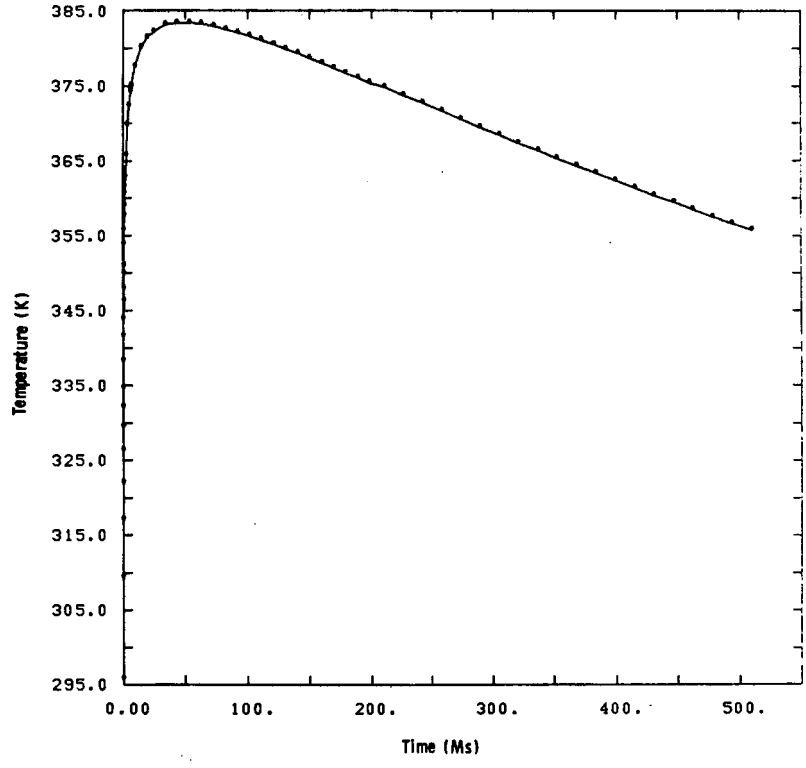


Figure 3.1 Canister Centerline Temperature

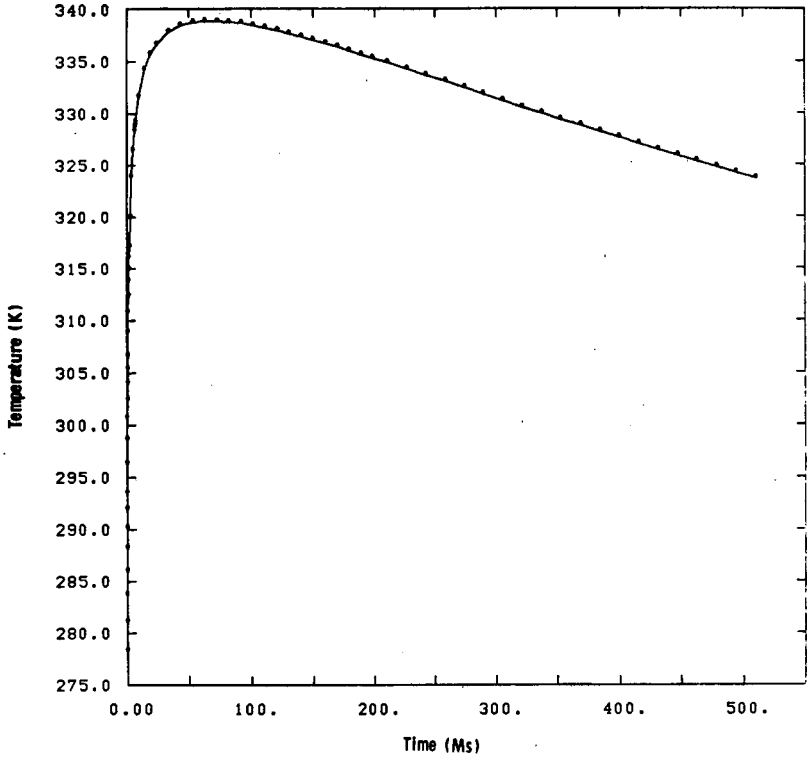


Figure 3.2 Sediment Temperature 0.60 m From The Canister Centerline

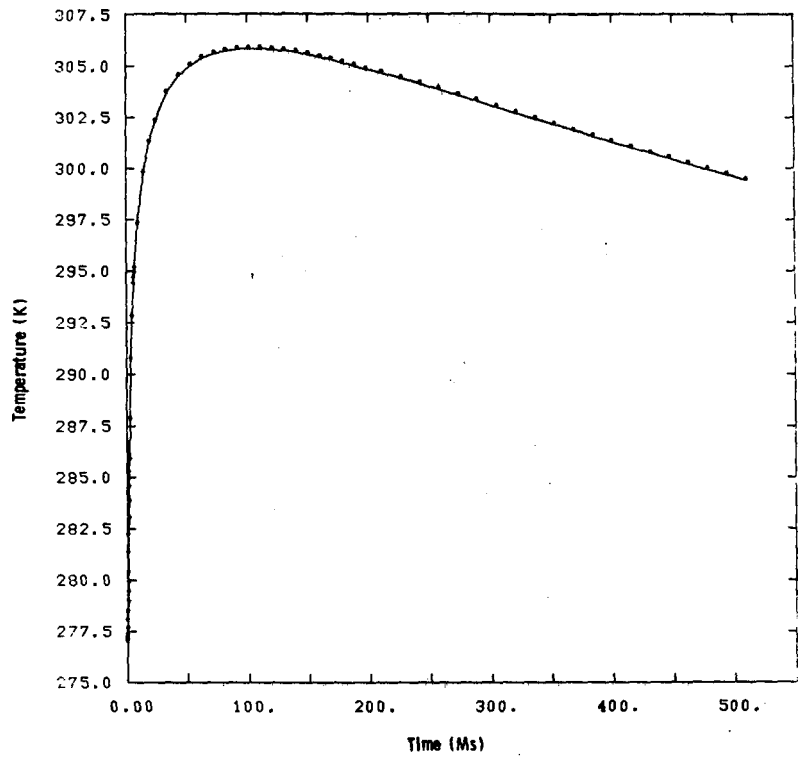


Figure 3.3 Sediment Temperature 1.2m From The Canister Centerline

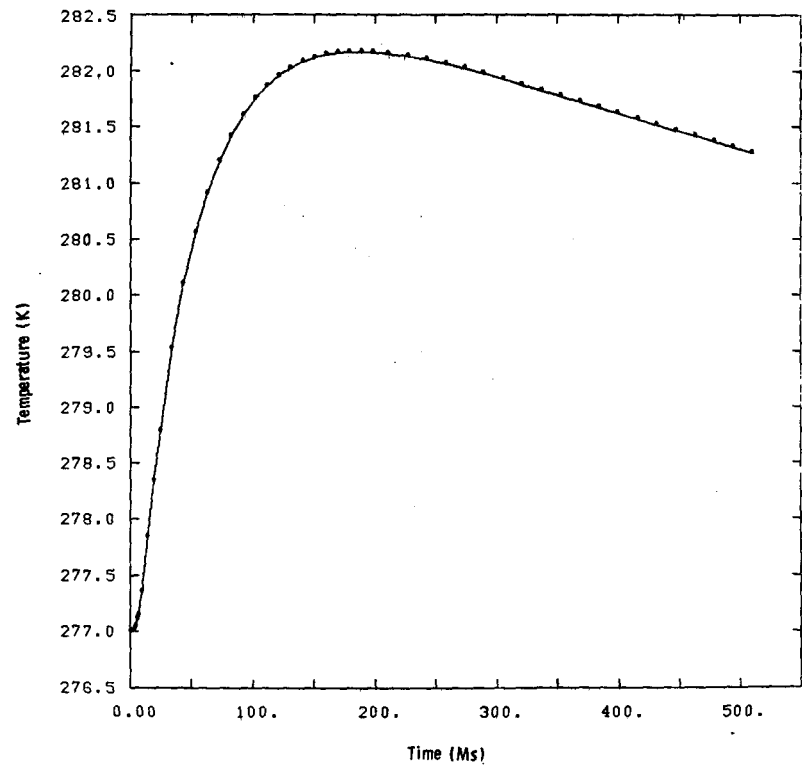


Figure 3.4 Sediment Temperature 4.3m From The Canister Centerline

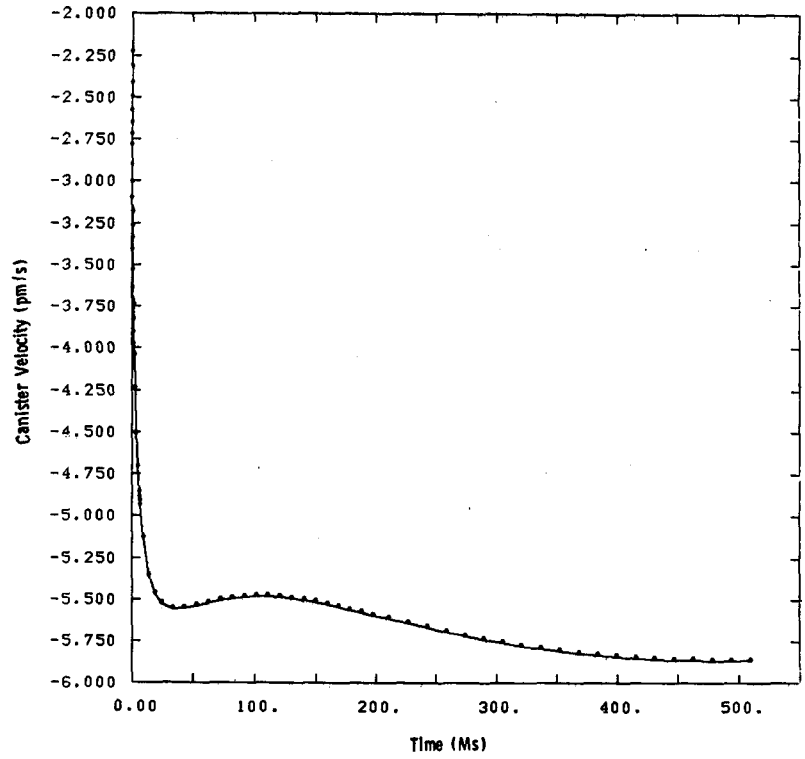


Figure 3.5 Canister Velocity History For Case A

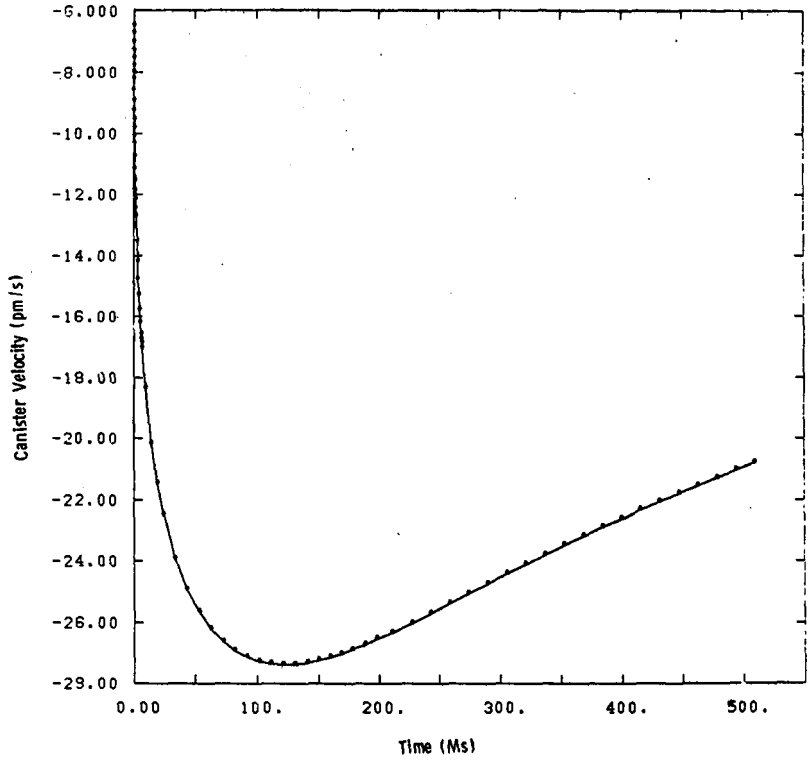


Figure 3.6 Canister Velocity History For Case B

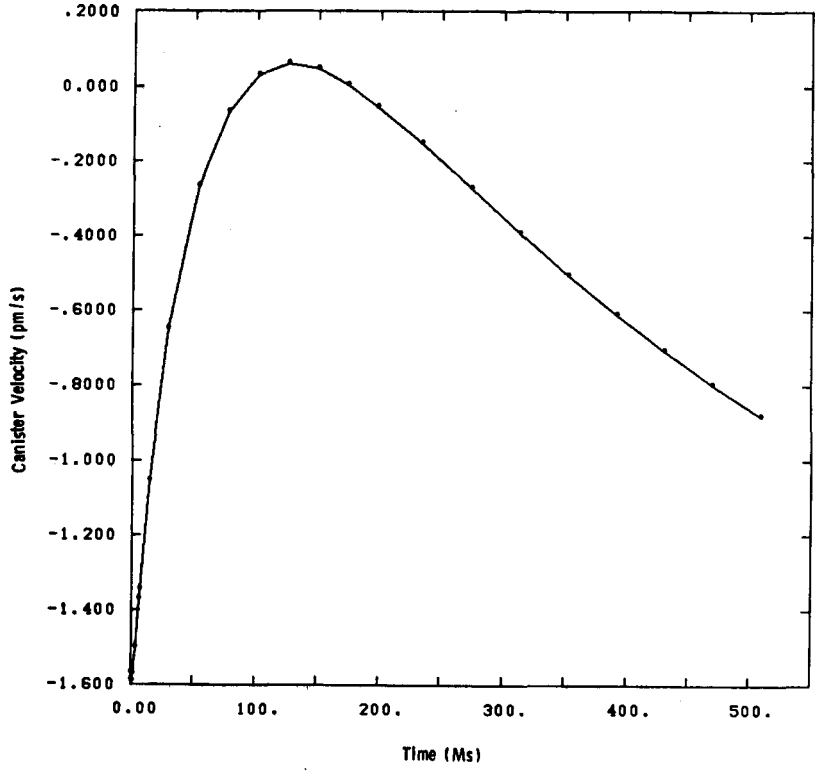


Figure 3.7 Canister Velocity History For Case C

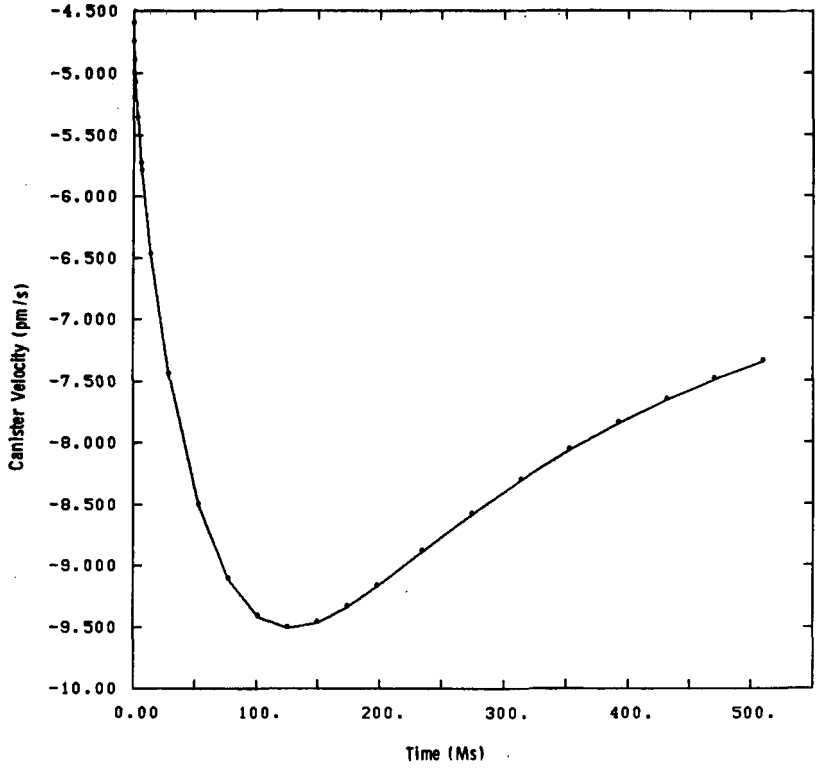


Figure 3.8 Canister Velocity History For Case D

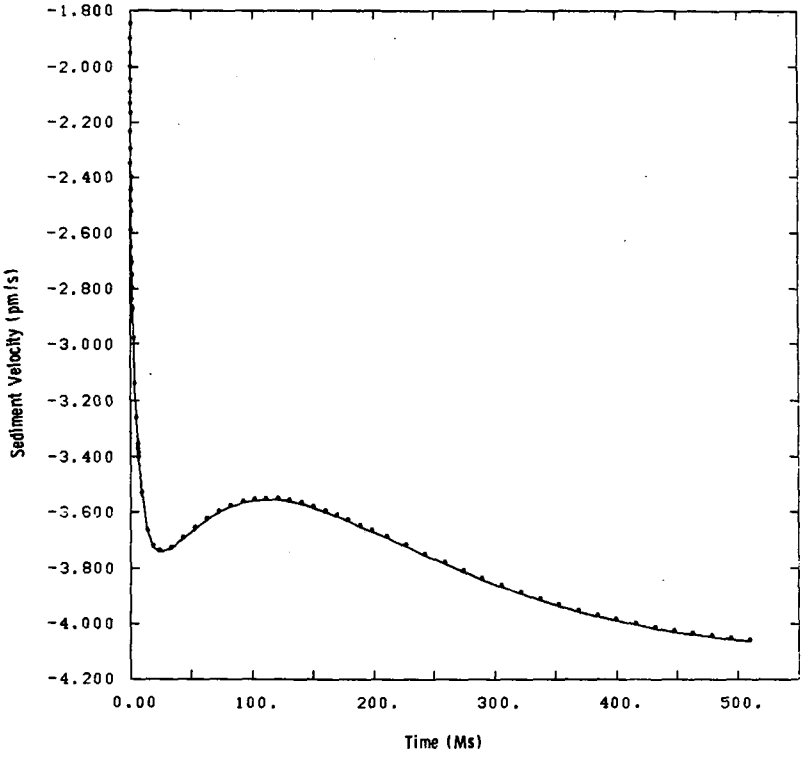


Figure 3.9 Sediment Velocity In Case A At 0.6m From Canister Centerline

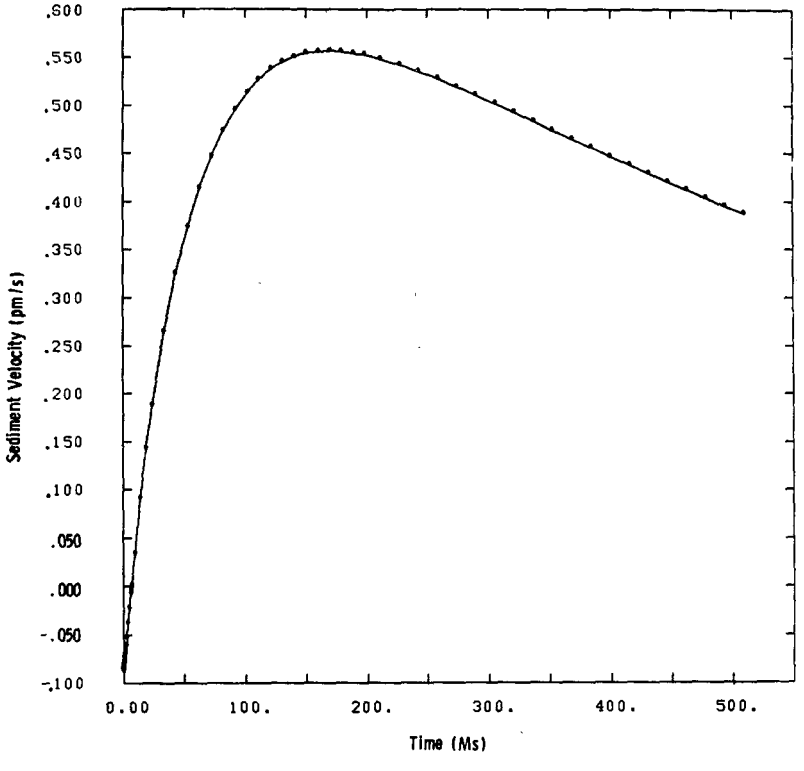


Figure 3.10 Sediment Velocity in Case A at 4.3m From Canister Centerline

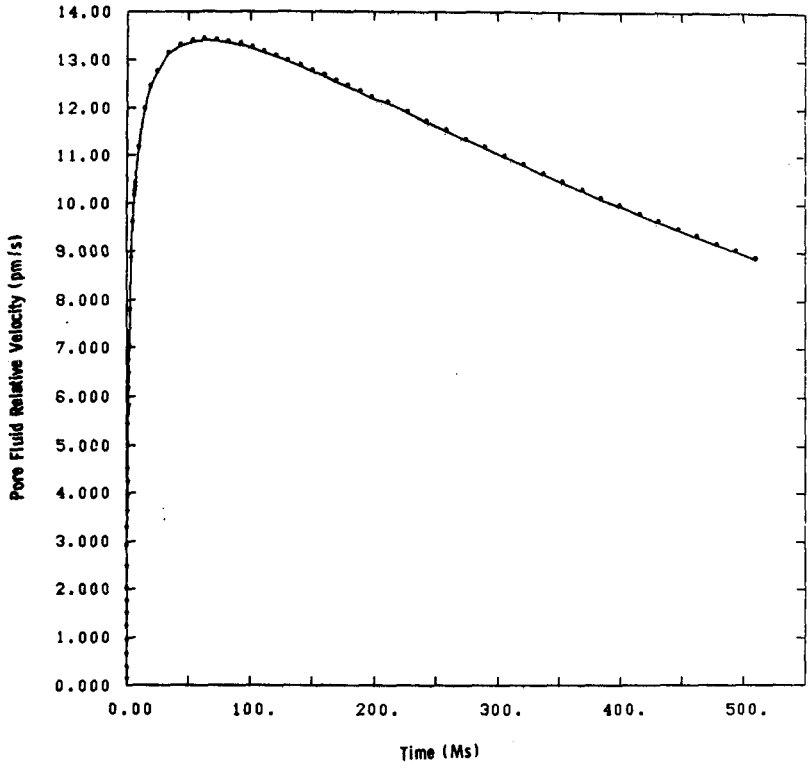


Figure 3.11 Pore Fluid Relative Velocity in Case A at 0.6 m From Canister Centerline

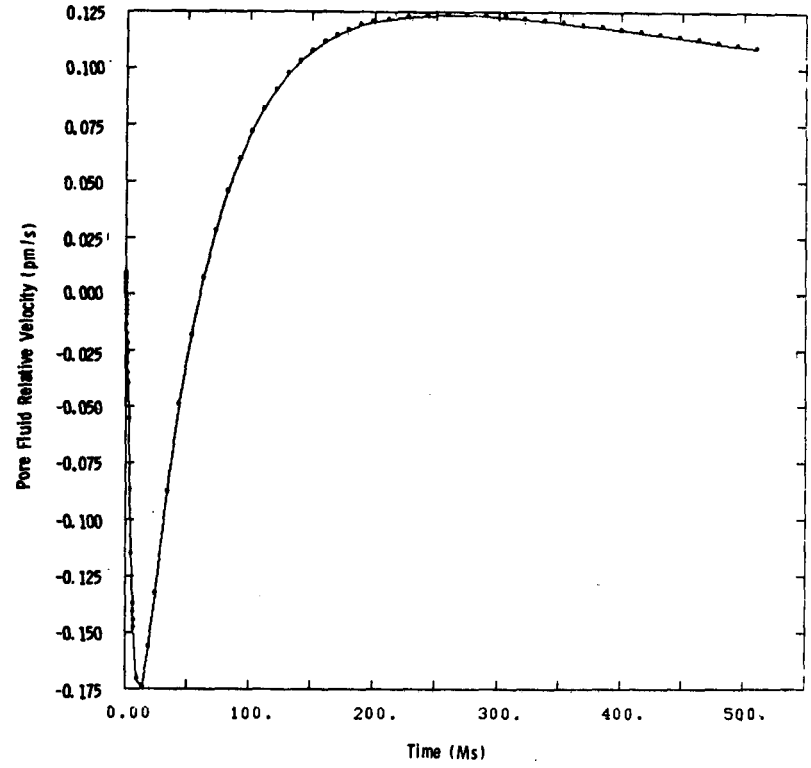


Figure 3.12 Pore Fluid Relative Velocity in Case A at 4.3 m From Canister Centerline

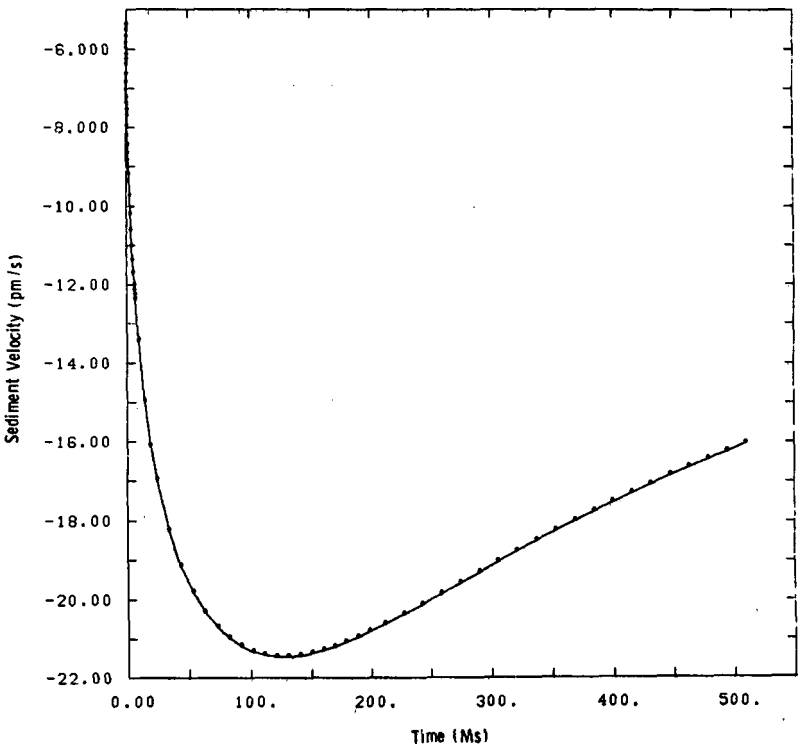


Figure 3.13 Sediment Velocity in Case B at 0.6 m From Canister Centerline

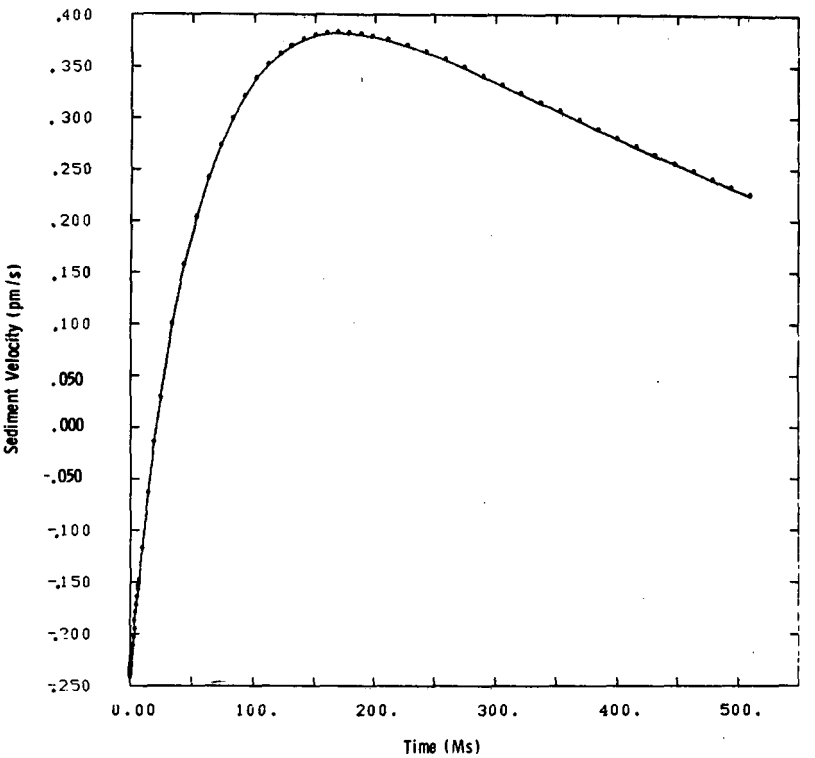


Figure 3.14 Sediment Velocity in Case B at 4.3 m From Canister Centerline

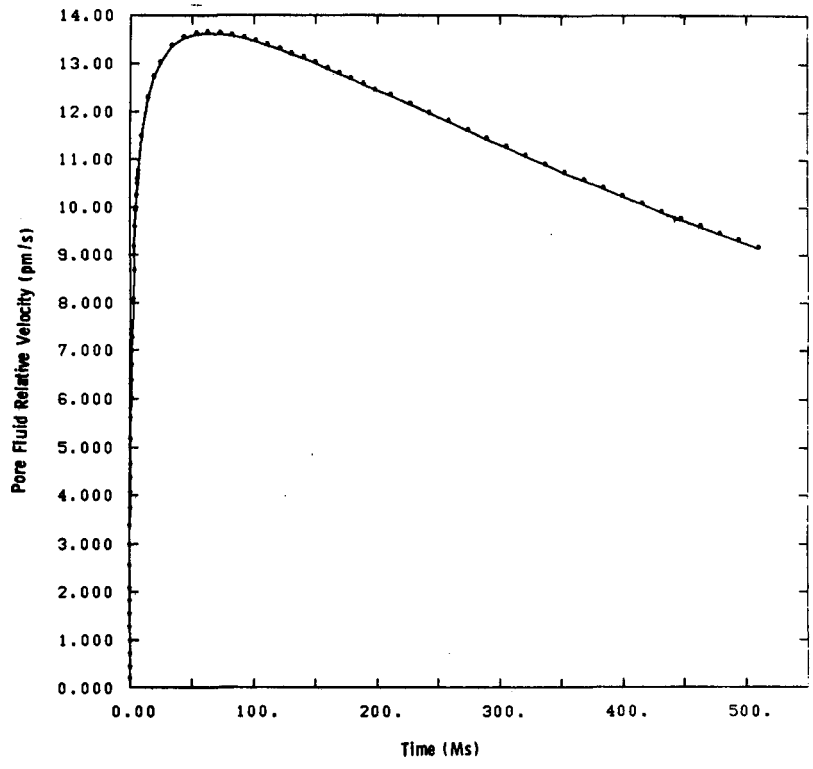


Figure 3.15 Pore Fluid Relative Velocity in Case B at 0.6m From Canister Centerline

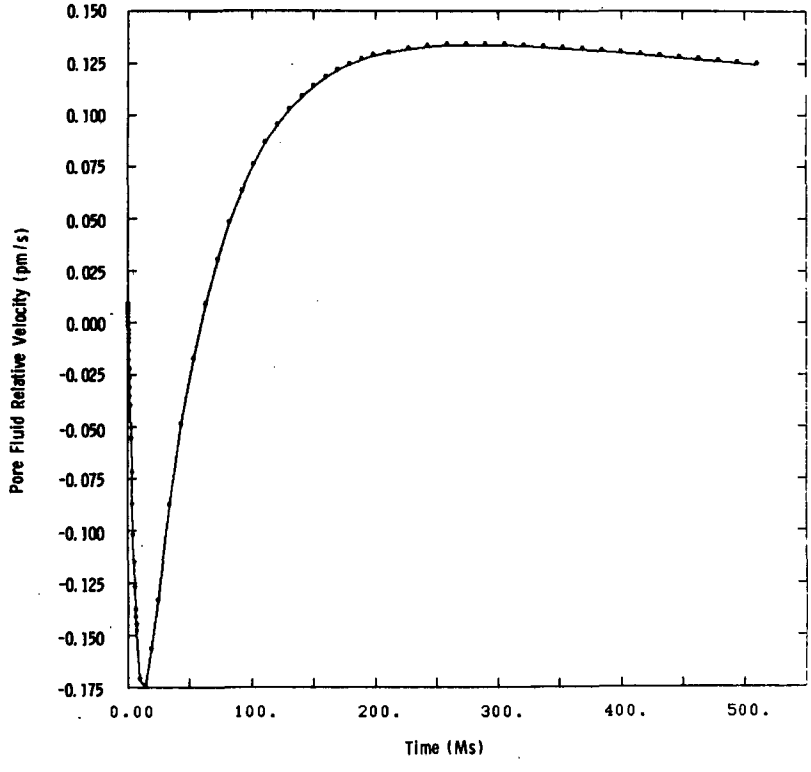


Figure 3.16 Pore Fluid Relative Velocity in Case B at 4.3m From Canister Centerline

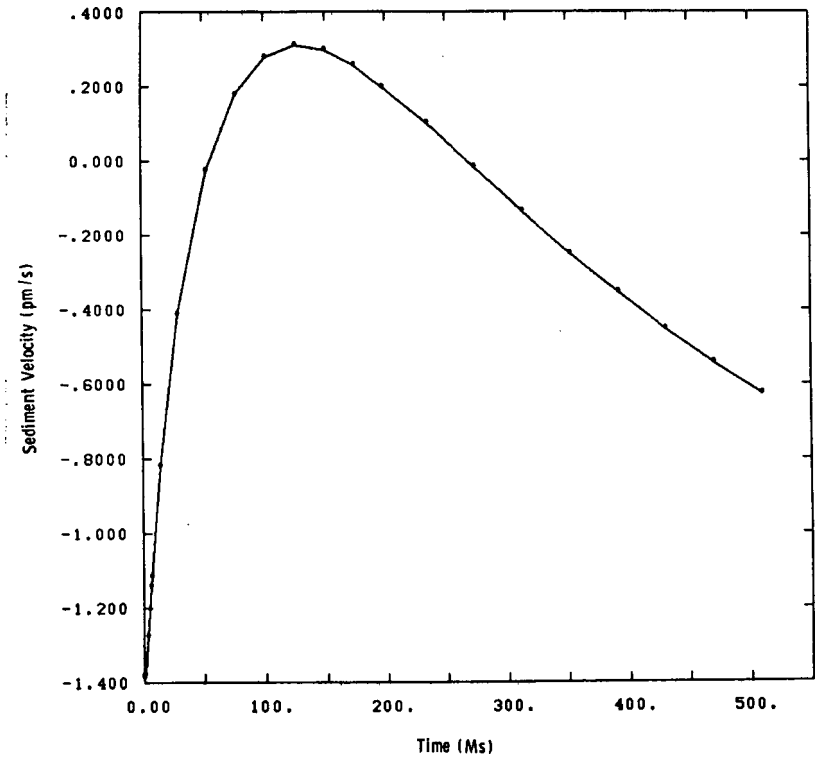


Figure 3.17 Sediment Velocity In Case C at 0.6 m From Canister Centerline

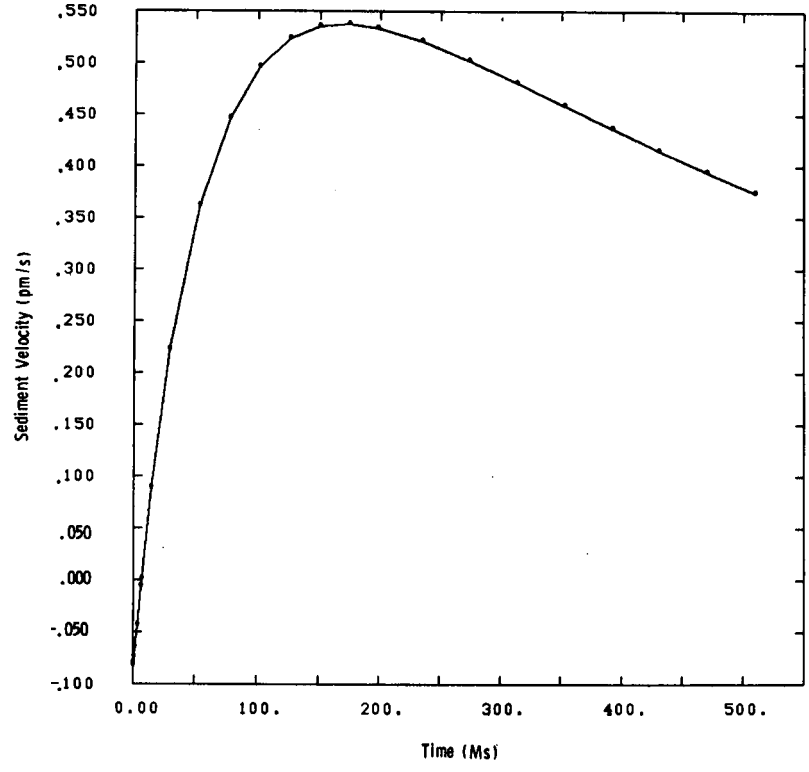


Figure 3.18 Sediment Velocity In Case C at 4.3 m From Canister Centerline

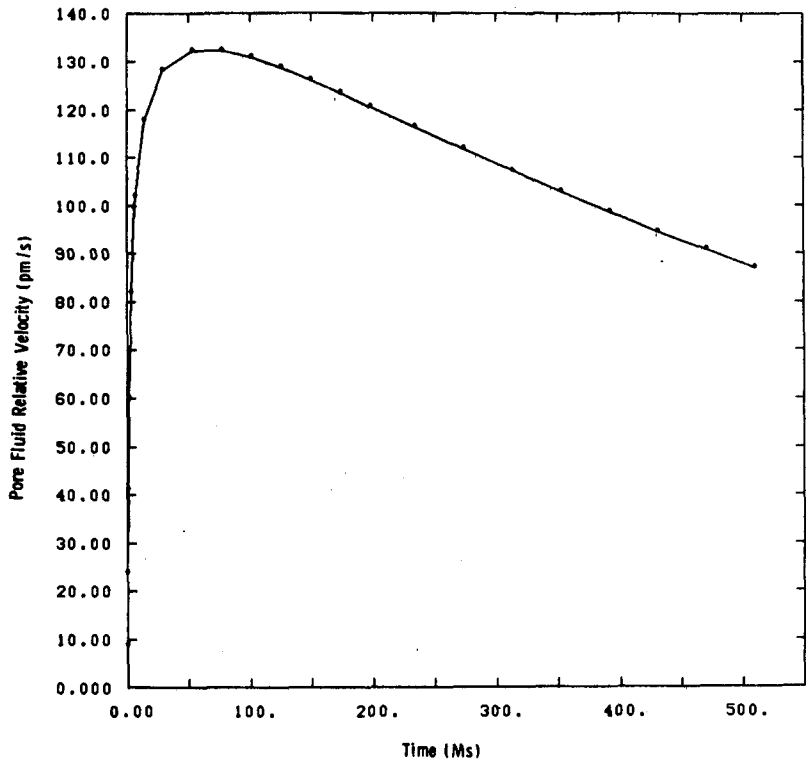


Figure 3.19 Pore Fluid Relative Velocity in Case C at 0.6 m From Canister Centerline

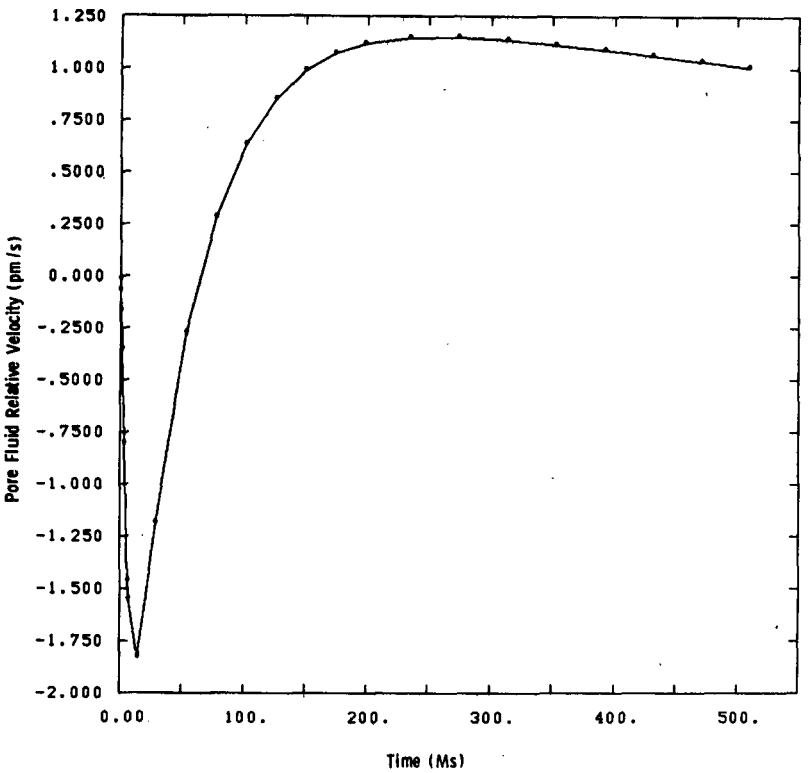


Figure 3.20 Pore Fluid Relative Velocity in Case C at 4.3 m From Canister Centerline

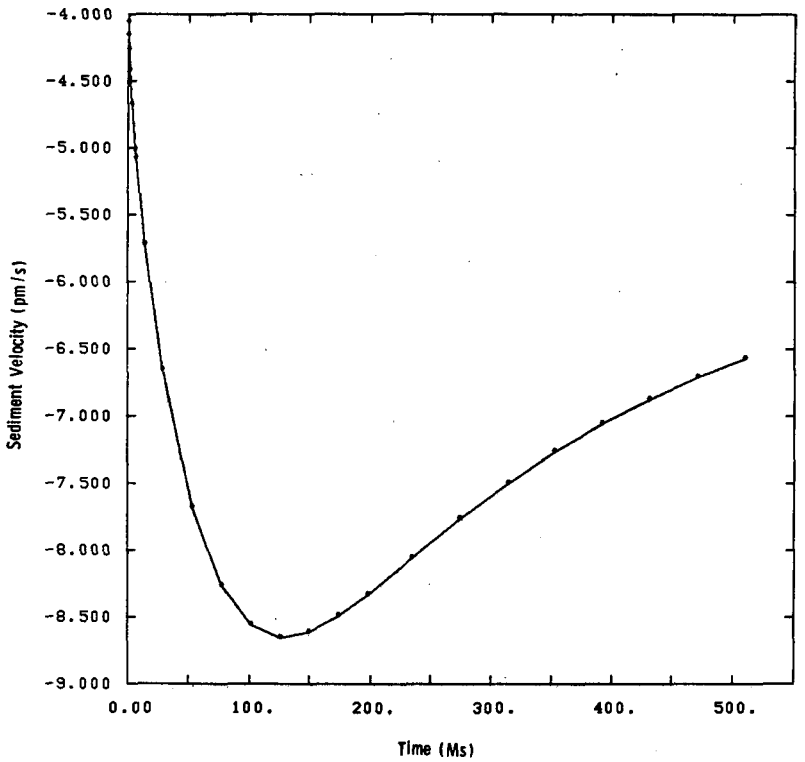


Figure 3.21 Sediment Velocity in Case E at 0.6m From Canister Centerline

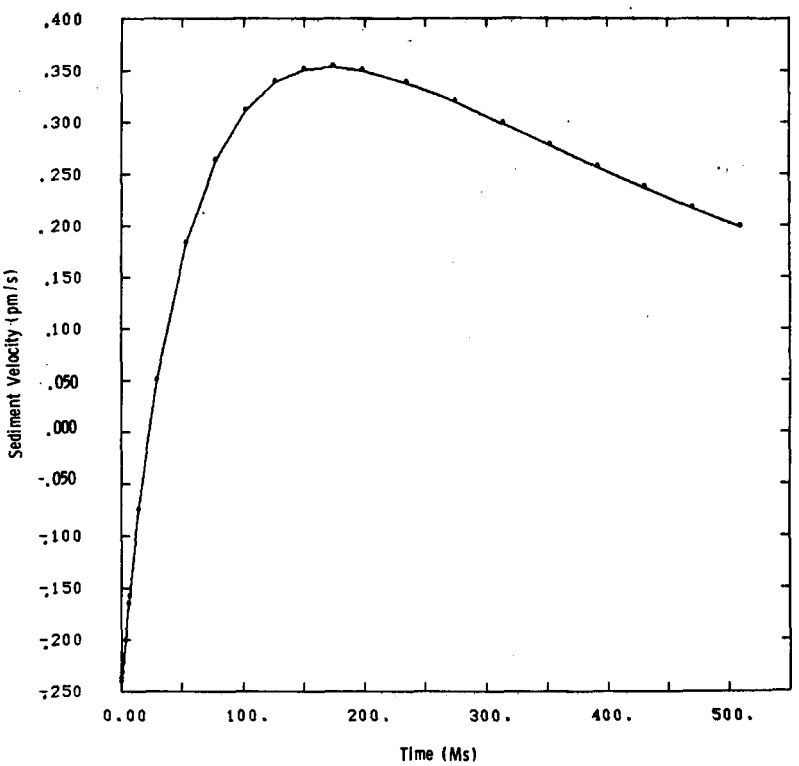


Figure 3.22 Sediment Velocity in Case E at 4.3m From Canister Centerline

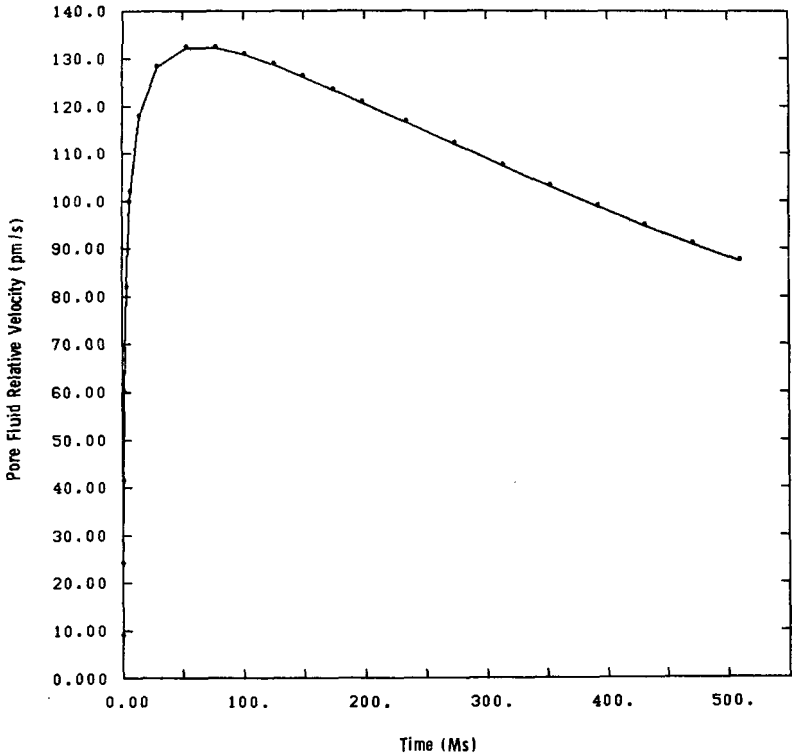


Figure 3.23 Pore Fluid Relative Velocity in Case E at 0.6 m From Canister Centerline

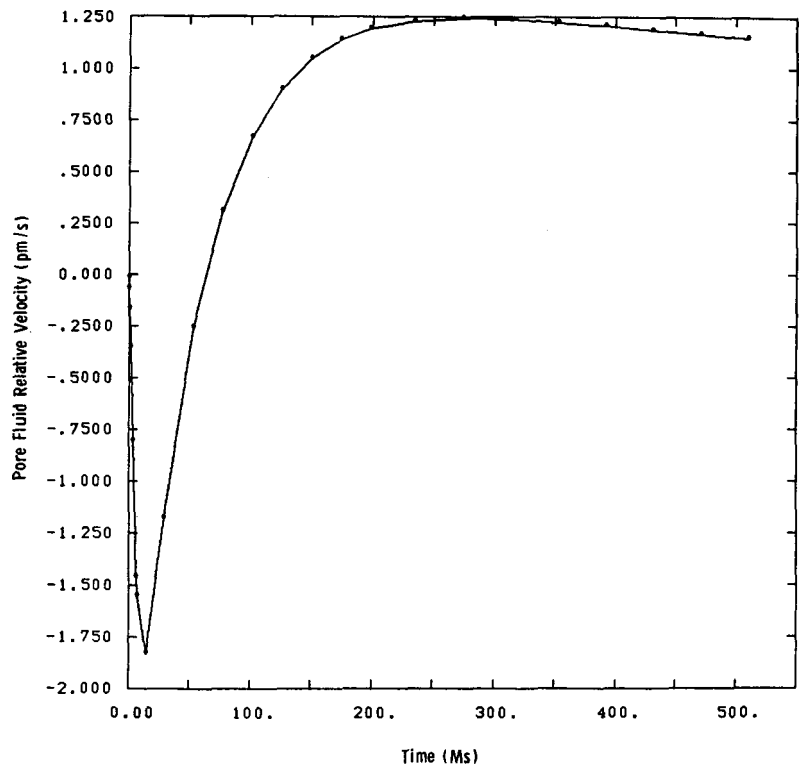


Figure 3.24 Pore Fluid Relative Velocity in Case E at 4.3 m From Canister Centerline

APPENDIX EE

PRELIMINARY PENETRATION STUDIES

Steven N. Burchett

Sandia National Laboratories

PRELIMINARY PENETRATION STUDIES

Steven N. Burchett
Sandia National Laboratories
Albuquerque, New Mexico 87185

Abstract

One of the methods proposed to emplace nuclear waste canisters into subseabed sediment is the use of penetrator technology. For this method to be viable, however, it must be shown that the canisters can be emplaced to the required depth. During this past year, two preliminary penetrations studies were completed. First, a parameter study to determine the ball park performance of a general emplacement vehicle was done. Secondly, a study to estimate the effect of sand layers on penetration was done. The results show that reasonable emplacement depths can be obtained with reasonable vehicle geometries for both free fall and boosted systems and that sand layers have significant effect on depth of penetration and must be evaluated further.

Introduction:

One of the methods proposed to emplace nuclear waste canisters into subseabed sediment is the use of penetrator technology. For this method to be viable, however, it must be shown that the canisters can be emplaced to the required depth. During this past year, two preliminary penetration studies were completed. First a parameter study to determine the depth of penetration as a function of emplacement vehicle geometry and impact velocity. The mass of the emplacement vehicle was also a function of the vehicle geometry. Secondly, a study to estimate the effects of sand layers on depth of penetration study was done. This brief report summarizes these studies.

Penetration Parameter Study:

The assumed geometry of the emplacement vehicle is shown in Figure 1. The steel (ρ = 7800 kg/m^3) vehicle/canister was assumed to be cylindrical in shape with a hemispherical nose. The waste package was assumed to be cylindrical and have a density of 2500 kg/m^3. Five sets of calculations, corresponding to D_o = 0.3 m to D_o = 0.7 m, were done. It was assumed that the diameter of the waste package, D_{op}, was 0.05 m less than the vehicle diameter, (vehicle wall thickness = t_w = 0.025 m = 1.0"). The total vehicle length, ZLT, was defined by specifying the length to diameter ratio (ZLT/D_o).

The waste package length was assumed to be 80 of the total vehicle length (ZLP = 0.8 * ZLT).

The forces tending to stop the emplacement vehicle are the end bearing load at the nose of the penetrator, the wall shearing force and the hydrodynamic drag. The forces are defined in Figure 2.

The sediment properties used in this study were from MPG-1 as obtained from LL44-GPC3. The density is ρ_s = 1400 kg/m^3 and the cohesion is

$$C = 19540 \ln (1 + 0.1189z) \text{ Pascals}$$

where Z = depth below water/sediment interface, m.

The results of this study are shown in Figures 3-5. In Figure 3, the calculated emplacement depth is plotted as a function of impact velocity for a vehicle with an outer diameter of D_o = 0.4 m for a variety of vehicle lengths. The calculated terminal velocities for each of the vehicles are also indicated. This plot shows, for a given emplacement vehicle, the impact velocity required to emplace to a certain depth and if boosting is required. The results for an emplacement vehicle with outer diameters of D_o = 0.3 m, 0.5 m, 0.6 m, and 0.7 m are shown in Figures 4a, 4b, 5a, and 5 b respectively.

The results of this study are preliminary ball park estimates. In general, the results indicate that to obtain reasonable emplacement depths with reasonable emplacement vehicle geometries either free fall or boosted systems could be used. Greater flexibility of possible geometry parameters could be obtained, however, by use of a boosted system.

Effect of Sand Layers:

It has been postulated that preliminary suitable sites in the Atlantic may have sand layers through which the emplacement vehicle must pass. Field evidence has suggested that sand layers or clay/sand layers are difficult to penetrate. This study presents a preliminary evaluation of the effect of sand layers on the penetration capability of an emplacement vehicle.

The forces tending to stop an emplacement vehicle are the end bearing load at the nose of the vehicle, the wall shearing force, and the hydrodynamic drag. In this study, it was assumed that the end bearing load and the wall shearing force was equal to the so-called point resistance and shaft resistance used in deep foundation pile capacity equations. The total capacity of a pile in sand and in clay are given in Figure 6. Using these equations with typical values and

neglecting hydrodynamic drag, the resisting forces on a specific emplacement vehicle can be plotted as a function of penetration depth (Figure 7). The area under these curves is the energy required to penetrate to a certain depth. The effect of sand layers can be estimated by combining the curves and evaluating the energy loss due to sand layer as was done in Figures 8a and 8b.

The penetration capability of an emplacement vehicle obviously depends upon site specific stratigraphy and material properties. This study indicates that sand layers have a significant effect and must be evaluated further.

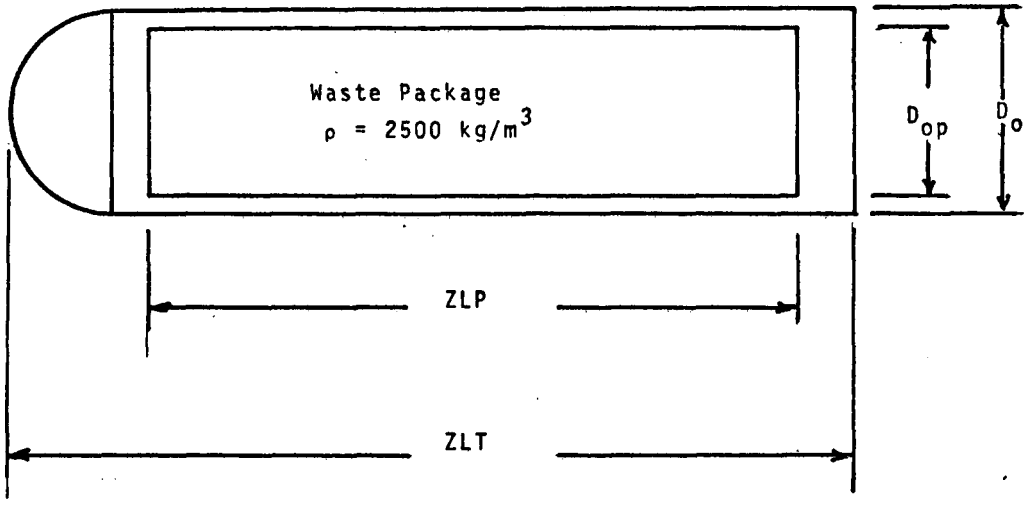


Figure 1: Assumed Geometry of Emplacement Vehicle

END BEARING FORCE:

$$F_{END} = (N_C C + N_Q \sigma')A$$

WHERE C = COHESION OF SEDIMENT

σ' = EFFECTIVE STRESS

N_C, N_Q = BEARING CAPACITY FACTORS, $N_C = 9$, $N_Q = 1$

AND A = FRONTAL AREA.

WALL SHEARING:

$$F_S = \pi D_O \int_{z_1}^{z_2} \alpha C \, dz$$

WHERE D_O = OUTSIDE DIAMETER OF PENETRATOR

C = COHESION OF SEDIMENT

α = EMPERICALLY DETERMINED FACTOR = 0.26

HYDRODYNAMIC DRAG:

$$F_D = 1/2 \, \rho_{SW} \, C_D \, AV^2$$

WHERE ρ_{SW} = DENSITY OF SEAWATER = 1030 KG/M^3

C_D = DRAG COEFFICIENT = $C_{BP} + C_{SF}$

C_{BP} = BASE PRESSURE DRAG COEFFICIENT

C_{SF} = SKIN FRICTION DRAG COEFFICIENT

A = FRONTAL AREA

AND V = VELOCITY

Figure 2: Force Assumptions - Penetration Calculations

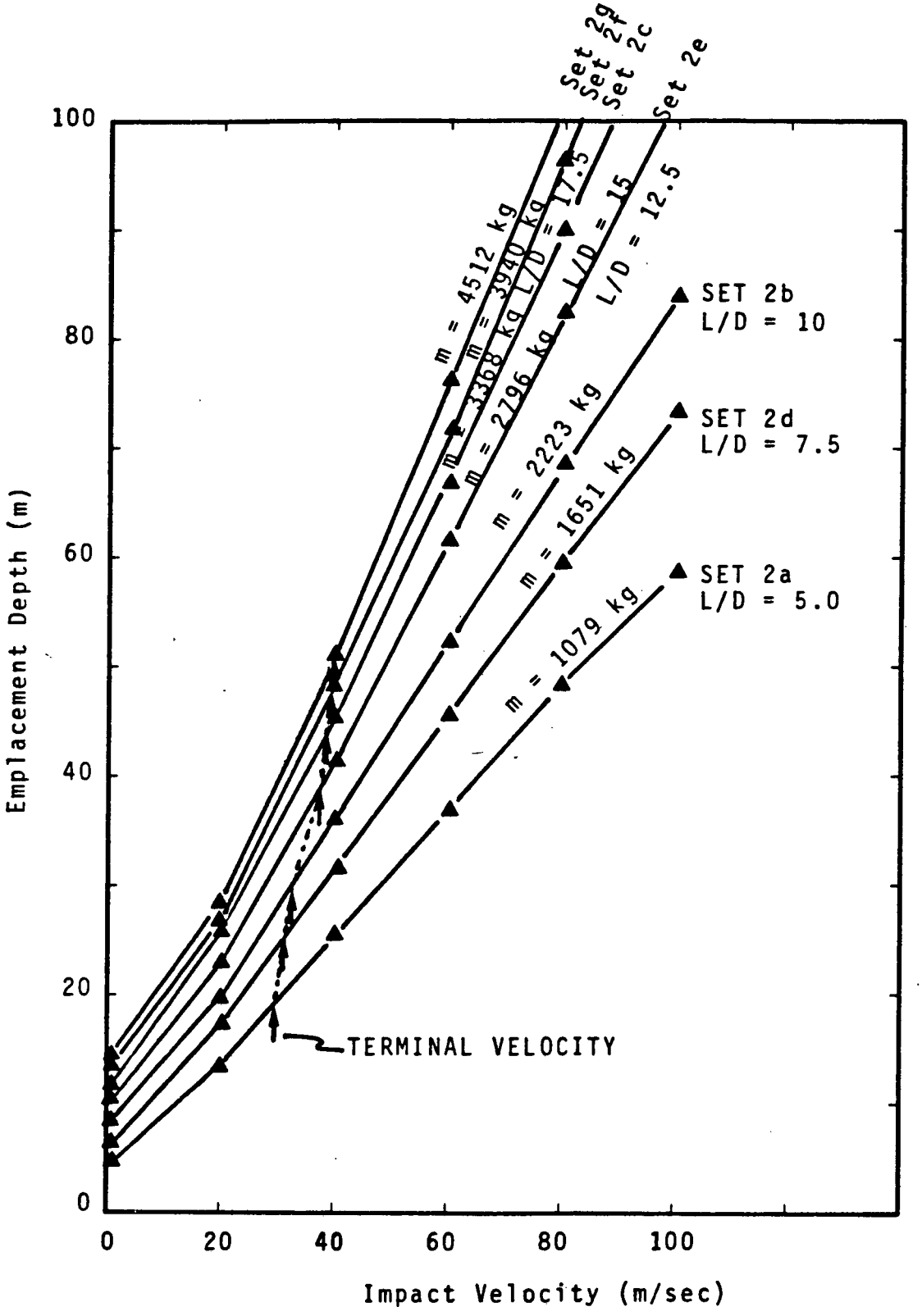


Figure 3: Results - Emplacement Depth vs Impact Velocity D_o = 0.4 m

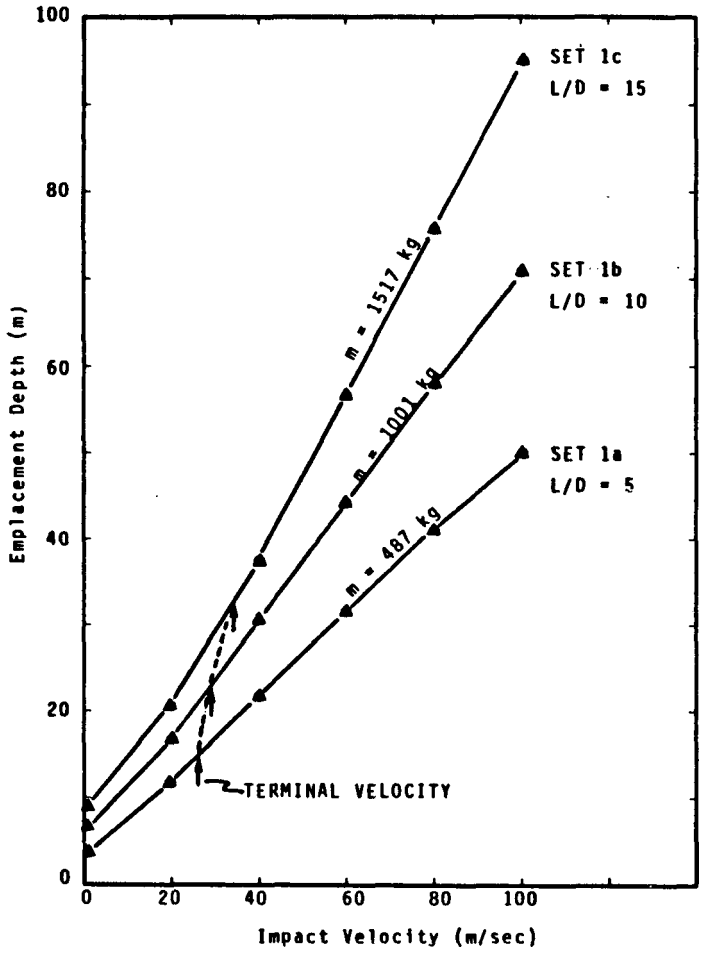


Figure 4a: Results - Emplacement Depth vs Impact Velocity D_o = 0.3 m

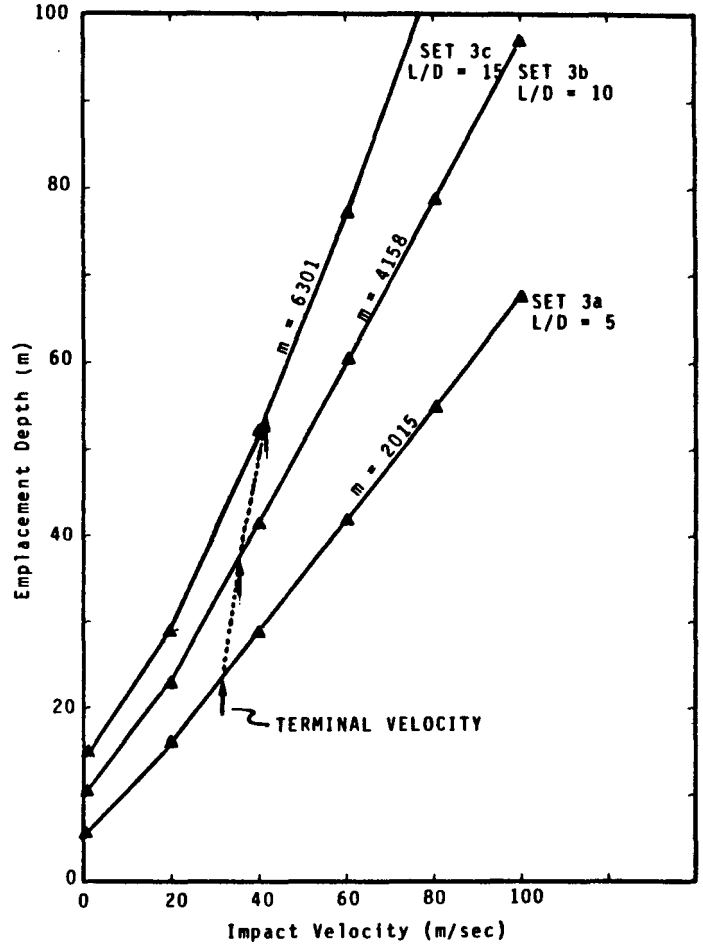


Figure 4b: Results - Emplacement Depth vs Impact Velocity D_o = 0.5

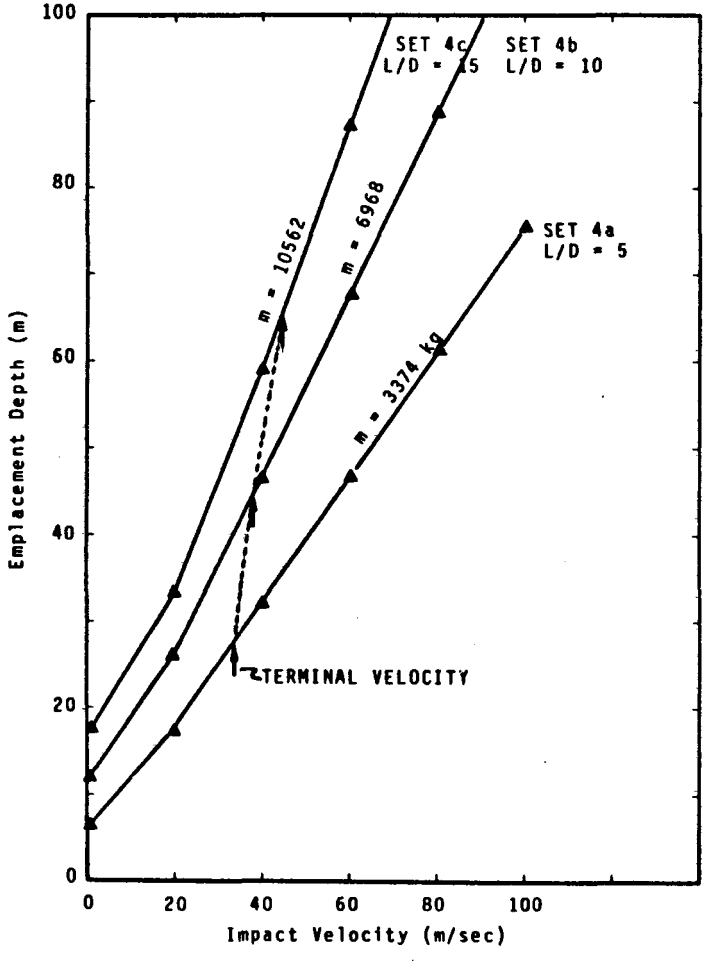


Figure 5a Results - Emplacement Depth vs Impact Velocity D_o = 0.6

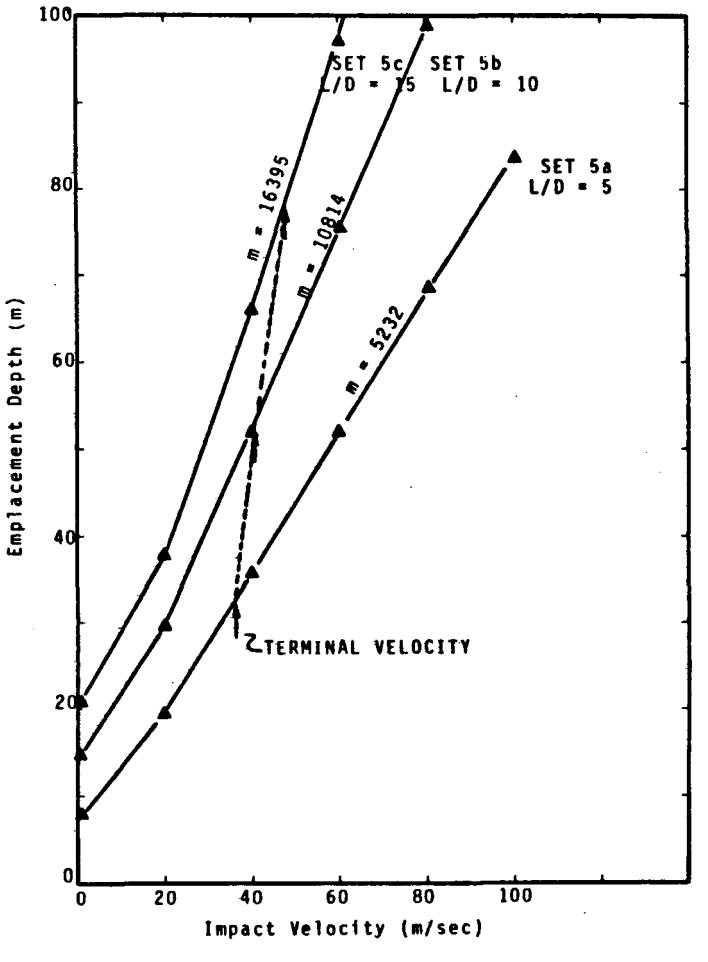


Figure 5b Results - Emplacement Depth vs Impact Velocity D_o = 0.7 m

SAND:

$$Q = A_P(\rho_S-\rho_{SW})GZ\ N_Q + \sum(\Delta LA_S)\ K\ (\rho_S-\rho_{SW})GZ\ \text{TAN}\ \phi_\mu$$

N_Q = BEARING CAPACITY FACTOR = $F(\phi)$ = 15→400

ϕ = FRICTION ANGLE AT ULTIMATE STRENGTH = 25°→35°

K = DENSIFICATION FACTOR 1→3

ϕ_μ = PARTICLE TO PARTICLE FRICTION ANGLE 20°→30°

CLAY:

$$Q = A_P[CN_C + (\rho_S-\rho_{SW})GZ] + \sum\Delta LA_S\ \mu C$$

N_C = BEARING CAPACITY FACTOR = 9.0

C = COHESION = 19540 ℓN (1.0+0.1189Z) PASCALS

μ = EMPERICALLY DETERMINED FACTOR = 0.26

ASSUMPTIONS:

$\rho_{SAND} = \rho_{CLAY} = 1400 KG/M^3$

$\rho_{SW} = 1020\ KG/M^3$

$D_O = 0.4$ M

L = 3.35 M

Figure 6: Force Assumptions - Sand Layer Study

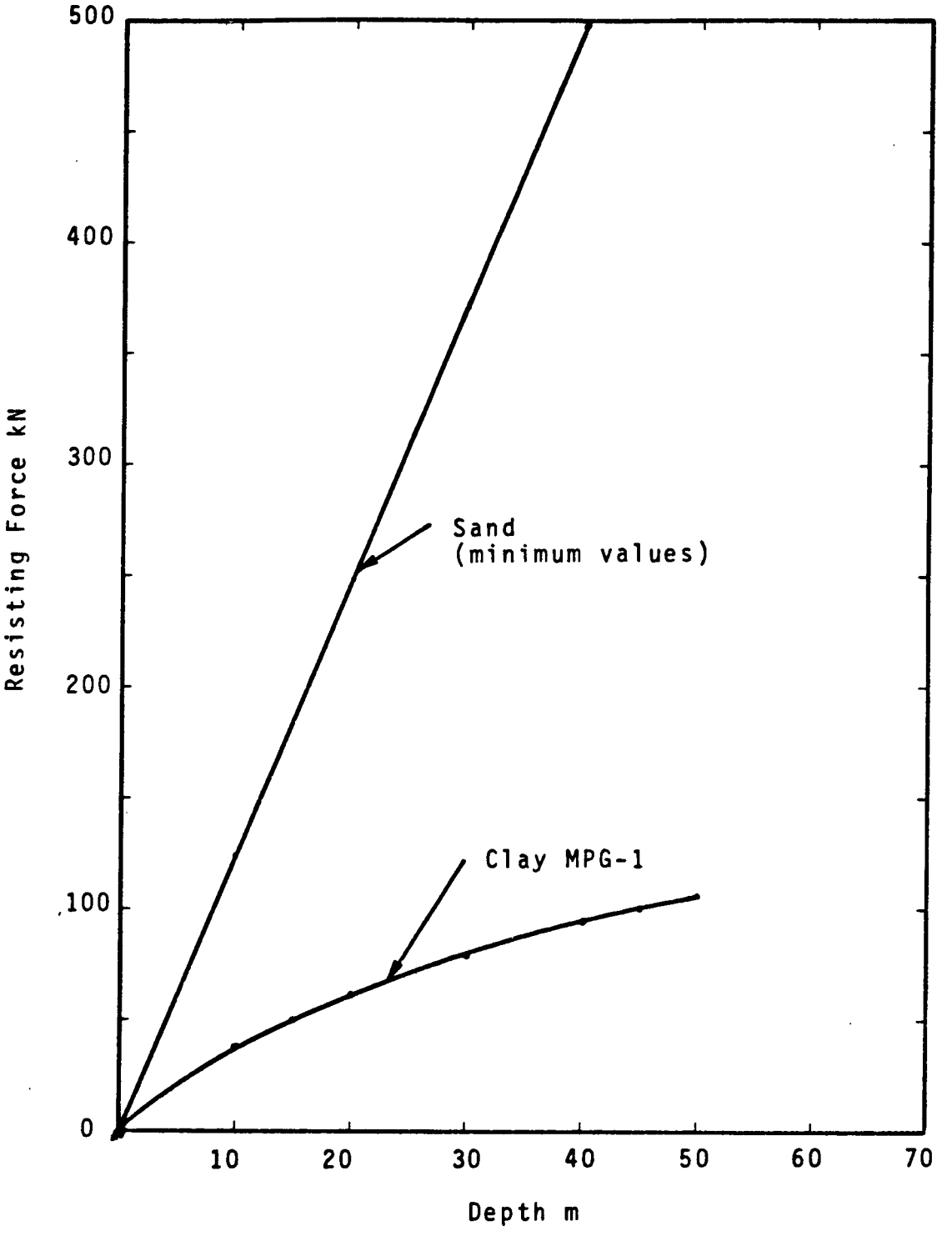


Figure 7 : Comparison of Resisting Forces

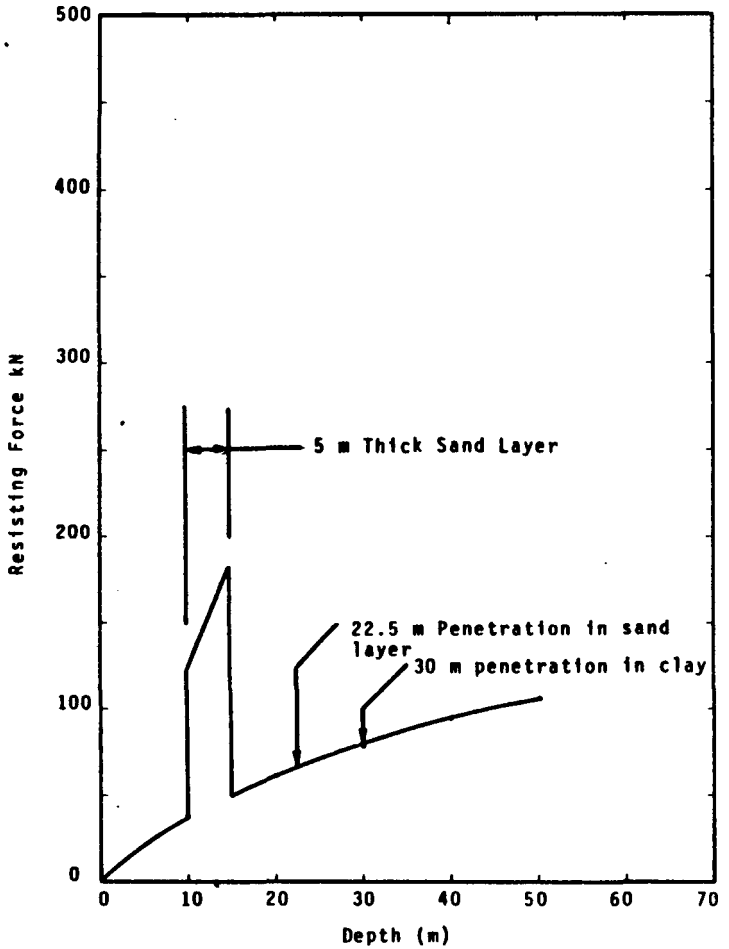


Figure 8a: Resisting Forces in Idealized Stratigraphy
5 m Thick Sand Layer in Clay

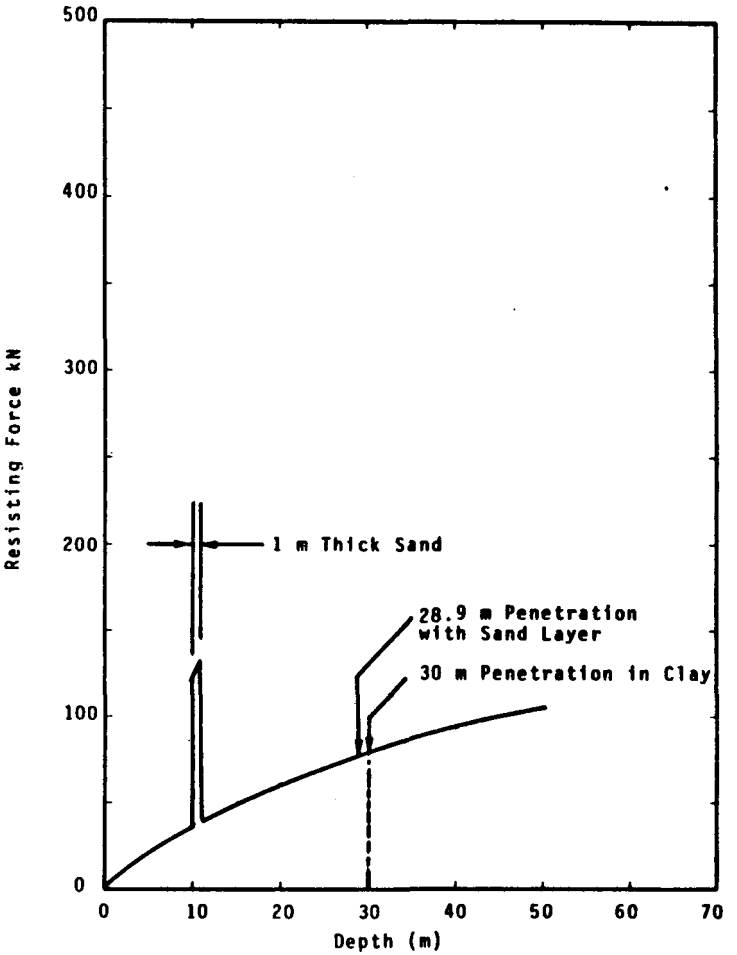


Figure 8b: Resisting Forces in Idealized Stratigraphy
1 m Thick Sand Layer in Clay

APPENDIX FF

HOLE CLOSURE CALCULATIONS USING HONDO II AND MARBLE

Thomas Canfield and Steven N. Burchett

Sandia National Laboratories

HOLE CLOSURE CALCULATIONS USING HONDO II AND MARBLE

Thomas Canfield
Steven N. Burchett

Sandia National Laboratories
Albuquerque, New Mexico 87185

Abstract

One of the methods proposed to emplace nuclear waste canisters into subseabed sediment is the use of penetrator technology. For this method to be viable, however, it must be shown that the canisters can be emplaced to the required depth and that the hole created by the emplacement vehicle closes. This report summarizes the numerical studies done during the past year utilizing the finite element computer program HONDO II and MARBLE to evaluate the hole closure problem. The results to date show that the hole closes, however, additional calculations are needed to couple penetration and hole closure and to determine the sensitivity of material parameters.

INTRODUCTION

Several potential methods have been proposed to emplace nuclear waste canisters into subseabed sediments. Of these, the penetrometer (either free fall or boosted) is the simplest concept. For this method to be viable, however, it must be shown that waste can be emplaced to the required depth and that the hole created by the emplacement vehicle closes (heals itself) without mechanical aids. Numerical calculations are being done to determine the response of the sediment to the passage of an emplacement vehicle. Currently, three numerical techniques are being used. First, one- and two-dimensional calculations using the STEALTH (Ref. 1) finite difference computer code have been done by Peter D. Dzwilewski. In these calculations, the constitutive model assumed was elastic-perfectly plastic using a Mises yield criteria. Secondly, one- and two-dimensional calculations using this HONDO II (Ref. 2) finite element computer code have been done. In the HONDO II calculations, the constitutive model assumed was either elastic-perfectly plastic or an effective stress constitutive model for marine sediments developed by the U.S. Army Engineer Waterway Experiment Station (WES) (Ref. 3). Finally, one- and two-dimensional calculations using the arbitrary Lagrangian-Eulerian (ALE), finite element computer

code MARBLE have been done. In the MARBLE calculations, the WES effective stress constitutive model was used.

The following sections will present a summary of the results obtained from HONDO II and MARBLE during the past year. This will be followed by a summary section.

HONDO II HOLE CLOSURE CALCULATIONS

Introduction:

This report is a review of the status of the hole closure calculations done as part of the Subseabed Disposal Program emplacement task using the finite element computer program HONDO II. The tasks to be done during this reporting period were as follows:

1) Complete the implementation of WES marine sediment constitutive model into HONDO II.

2) Verify that HONDO II with the WES marine sediment constitutive model is correctly implemented by comparing HONDO II calculations to sediment material test results.

3) Perform a series of axially symmetric one-dimensional calculations to investigate the factors influencing hole-closure.

4) Investigate the feasibility of performing axially symmetric two-dimensional hole closure calculations.

Implementation of WES Marine Sediment Constitutive Model:

The marine sediment, effective stress, constitutive model developed by Dr. George Baladi at the U. S. Army Engineer Waterways Experiment Station (Ref. 3) was initially implemented into HONDO II by Ray Krieg (SNL) in April of 1980. During this past year modifications, recommended by WES, have been made to the model. The material constants, recommended by WES to fit the constitutive model to representative material properties obtained from tests of Pacific Illite were incorporated.

Constitutive Model Verification

To verify that constitutive model is correctly implemented into HONDO II, the results obtained from HONDO II were compared to the fit of the model to representative material properties from 1) an isotropic consolidation test, 2) an undrained

isotropic compression test, and 3) a consolidated-undrained triaxial test. The results of these calculations indicate that the WES effective stress sediment constitutive model is properly implemented into HONDO II.

Hole Closure Study - Model Response:

The finite element computer program HONDO II was used to investigate the response of the sediment due to the passage of an emplacement vehicle. First, a study to investigate various geometric models was done. The first model chosen, shown in Figure 1a, is a thin axisymmetric disc subjected to plane strain conditions. At r = 0, displacement boundary conditions are applied to open a cavity. The displacement boundary conditions simulate an ogive of order 3 followed by a short cylindrical section. At t = 0.030 sec, the displacement boundary conditions was removed and a pressure boundary conditions was simultaneously applied. The magnitude of the pressure was equal to the head loss due to water flowing at a constant velocity in a smooth pipe plus the difference in overburden between water and sediment, $P_2 = (\rho_{sw} - \rho_{sed})gy - 1/2\ \rho_{sw}V^2 + P_o$ (P_o = in-situ overburden pressure). The pressure in the water column in therefore a function of both depth in the sediment and the velocity of the water flowing in the column. The minimum value of V is equal to the velocity of vehicle. This pressure tends to close the cavity created by the vehicle.

The second model investigated is shown in Figure 1b. This model is identical to Model 1 with the exception that an absorbing or quiet boundary was implemented at r = 10 m.

The third model investigated is shown in Figure 1c. In this one-dimensional model, it was assumed that the hole created by the emplacement vehicle was already open. The effect of hole opening on the stress state in the sediment was neglected. An absorbing boundary at r = 20 m was also employed. At t = o, the pressure boundary condition, P_2, was applied to the inner surface of the model.

The fourth and final model investigated is shown in Figure 2d. This model is two-dimensional and assumes that the hole created by the emplacement vehicle was again, initially open. A pressure was applied as a function of time to the inner surface of the model to simulate passage of the emplacement vehicle. Absorbing boundaries were also used in this model.

In this series of calculations, the hole closure at a depth of y = 3.0 m below the sediment/water interface was investigated. It was assumed that the emplacement vehicle was traveling at a constant velocity of 30 m/sec. The constitutive model assumed for the sediment was elastic/perfectly plastic

using a Mises yield criteria with the yield strength corresponding to the shear strength obtained by shear vane measurements of LL44-GPC3 sediment. The results of these calculations are shown in Figures 2-5, and are compared in Figure 6. In Figure 2, the calculated response obtained using Model 1 is plotted. In Figure 2a, the calculated radial stress in element 1 (the center element) and element 40 (r = 10 m) are plotted as a function of time. In Figure 2b, and 2c, the calculated velocity and displacement of the center node are respectively plotted as a function of time. The results (Figure 2c) show that the hole closes in approximately 28 msec after passage of the emplacement vehicle.

Calculated radial stress, velocity, and displacement response obtained using Model 2 are plotted in Figure 3a, 3b, and 3c, respectively. The radial stress response of the center element obtained from Model 1 (Figure 2a) and the radial stress response obtained from Model 2 (Figure 3a) are essentially identical, indicating the effectiveness of the absorbing boundary. Using Model 2, the results show that the hole closes in approximately 28 msec after passage of the emplacement vehicle.

Calculated radial stress, velocity, and displacement response obtained from Model 3 are plotted in Figure 4a, 4b, and 4c, respectively. In this model, the hole was assumed to initially open and the material in an "undisturbed" condition when the pressure reduction corresponding to the passage of the emplacement vehicle was applied. The calculated response shows that the hole closes in approximately 28 msec.

In Figure 5, the calculated radial displacement response at various locations on the inside surface of the two-dimensional model (Model 4) are plotted as a function of time. In this model, it was again assumed that the hole was initially open and the sediment was undisturbed. The results of the two-dimensional calculation show that the hole closes in approximately 17 msec after passage of the emplacement vehicle.

The results of the model variation study are compared in Figure 6. In this figure, the radius of the hole is plotted as a function of time (t = 0.0 = passage of emplacement vehicle) for all four models. The results show: 1) the hole created by the emplacement vehicle closes, 2) for the assumed conditions, the hole closure times for the three 1-D models are essentially identical (t = 28 msec) indicating that the absorbing boundary is effective and that initial precondition (opening the hole) is not critically important, and 3) the hole closes faster when a two-dimensional geometry is used.

Hole Closure Study-Baseline Vehicle:

For a given emplacement vehicle, penetrating into a known sediment, a certain impact velocity (energy) is required to penetrate to a specified depth. For the waste package emplacement vehicle, defined in Figure 7, penetrating into seabed sediment, defined by a logrithmetic shear strength distribution with depth as follows:

$$\tau = 19540 \ln (1.0+0.119z) \text{ pa}$$

where z = depth (m),

simple penetration calculations indicate an impact velocity of 37 m/sec is required to emplace to a depth of 30 m. The calculated motion paramters of the vehicle for these assumptions are shown in Figure 8. At a depth of 3 m into the sediment, the calculated velocity is V = 36.9 m/sec. One- and two-dimensional hole closure calculations were done for this baseline vehicle at a depth of 3 m into the sediment. The model used for the one-dimensional calculations corresponded to model 2 of the previous section. The results of the one-dimensional calculations are plotted in Figure 9. Two calculations, one assuming an elastic/perfectly plastic constitutive model, YS = 0.01032 MPa, and one assuming an effective stress sediment constitutive model, WES3, were done for the baseline sediment. These calculations show that the hole closes in 20.5 - 21 msec. Two additional calculations, utilizying an elastic/perfectly plastic constitutive model, were done in which the yield strength was arbitrarily increased 5x and 10x the baseline yield strength. The calculations show that the hole still closes and that hole closure is not critically dependent on the magnitude of yield strength.

The model used for the two-dimensional calculations corresponded to Model 4 of the previous section. The results of the two-dimensional calculations are plotted in Figure 10. The calculated results for the baseline sediment for both the elastic/perfectly plastic constitutive model and the WES effective stress constitutive model are identical and show that the hole closes in approximately 11 msec. Arbitrarily increasing the yield strength of the sediment by 5x and 10x increases the hole closure time to 15 msec and 26 msec, respectively. The yield strength variation has a much more significant effect on hole closure times for two-dimensional response.

Summary, Conclusions, and Recommendations:

Several conclusions can be drawn from the HONDO II hole closure calculations done to date. First, and most important, the results of these calculations show that the hole created by

an emplacement vehicle into deep ocean seabed sediment closes (heals itself). Although not discussed in this report, the dominant factor causing the hole to close is the dynamic pressure reduction due to water flowing into the cylindrical cavity created by the vehicle. The elastic/perfectly plastic constitutive model and the WES effective stress constitutive model predict essentially identical results.

A two-dimensional model enhances hole closure compared to a one-dimensional model. The reason for this is that a 1-D model is dominated by bulk response while a 2-D model is dominated by deviatoric response. Since the sediment has an extremely low yield strength, failure and flow occur more readily in a 2-D model.

The calculations suggest that hole closure is not significantly dependent upon yield strength variations, however, additional systematic studies to investigate material parameter variations need to be done, expecially for a 2-D model.

In these calculations, penetration and hole closure response has been decoupled. To accurately predict the depth of penetration of an emplacement vehicle, decoupling is not valid. To numerically determine the entire emplacement event (or a substantial portion of the event) will be difficult. The prospects are enhanced however by the incorporation of an absorbing boundary capability into HONDO II.

MARBLE HOLE CLOSURE CALCULATIONS

Introduction:

MARBLE (Mixed ARBitrary Lagrangian-Eulerian is a finite element computer program specifically derived to treat dynamic penetration and hole closure problems for the Subseabed Disposal Program. It employs an ALE formulation to describe fluid regimes and a large deformation Lagrangian formulation for solid regimes making it capable of treating a complete problem including sediment, seawater and emplacement vehicle. The program is built upon the framework of the fluid-structural interaction program EURDYN-II (Ref. 5) with substantial additions and improvements. Among them are the addition of quadralateral solids, extension to a large deformation formulation, addition of an ALE slide line, improvement in the velocity smoothing algorithm for the ALE mesh, addition of Lysmer (Ref. 4) absorbing boundary conditions, improved pressure and shear traction histories and the addition of velocity histories for fluid nodes.

In the past year a number of subtasks have been completed with MARBLE for the Subseabed Disposal Program:

1) Implement the WES constitutive model of marine sediments into an ALE code (MARBLE).

2) Verify the proper implementation of the model by comparison with experimental test data and model curve fits provided by WES.

3) Perform one-dimensional axisymmetric hole closure calculations to check performance of the Lagrangian solid formulation of MARBLE with that of HONDO-II.

4) Begin two-dimensional axisymmetric penetration and hole closure calculations which includes both sediment and seawater.

Implementation of the WES Cap Model

The WES model of marine sediment was incorporated into the EURDYN-II code in December of 1980 but it soon became apparent that large strain capability was necessary to carry out these types of calculations. Large strain capability was developed for triangular elements and completed by April of 1981. At this time the material constants for Pacific Illite were available from WES and were employed in testing and verification.

Verification of the WES Cap Model

Proper implementation of the constitutive model in the ALE code was checked by running simulations of drained and undrained

isotropic consolidation tests followed with unloading. A simple axisymmetric model consisting of two triangular Lagrangian solid elements was employed in these calculations. The results were compared with model curve fits of experimental data produced by the WES driver program (SANDR). Excellent agreement was obtained between the finite element calculations and the driver curves. The constitutive model had been successfully installed in the ALE code.

One-Dimensional Axisymmetric Calculations

One-dimensional axisymmetric modeling was achieved by allowing a thin disk of finite elements to displace only in the radial direction in much the same way indicated for the HONDO-II calculations. The disk was 0.1 m thick centered at a depth of 3 m below the ocean floor 6000 m below the surface. Passage of the emplacement vehicle was simulated by application of a displacement boundary condition to open up the hole which was then replaced with a dynamic pressure to simulate the effect of water flowing into the hole after passage. An expression for this pressure is presented in the section on model response for HONDO-II calculations.

The first calculations employed 120 triangular elements in 60 rectangular regions with geometric growth factor of 1.08 in the radial direction. The disk in these calculations extended out to 125 m where fixed boundary conditions were applied. This distance was sufficiently removed from the center of the disk so that stress waves would not be reflected during the computation. Transit time was on the order of 80 msec. The emplacement vehicle was approximated by a second order ogive 0.2 m in diameter without a cylindrical body. It completed its passage in 11 msec. Hole closure occurred quickly after application of the dynamic pressure and was finished in 41 msec. When the dynamic pressure term, $-\frac{1}{2}\rho_{sw}V^2$, was ignored, the hole continued to expand with no indication of reversal.

Time to hole closure after vehicle passage was longer in these calculations than computed with HONDO-II. Several factors are responsible for the difference. Most important was geometry. The second order ogive was nearly half the length of the third order ogive used in HONDO-II calculations. Following release with no cylindrical body the hole continued to expand and did not reverse for 8 msec. Closure had to occur from a larger diameter. Finally, triangular elements are inherently more stiff than quadralaterals representing the same geometry. Displacements of top and bottom nodes initially located at the same radius differed because of element arrangement.

Stress distributions predicted with triangular elements tended to have large oscillations that were not present in

similar calculations with HONDO-II quadralateral solids. This coupled with uncertainties of accuracy resulted in the adaptation of a large deformation quadralateral for the MARBLE code. New calculations were done with 60 quadralateral elements and an emplacement vehicle similar to the one employed in HONDO-II calculations. Nearly identical results were obtained with both codes.

The number of elements required to solve a two-dimensional axisymetric hole closure calculation, without allowing reflections, could number in the tens of thousand for necessary accuracy. The cost and time would be unrealistic for the current program. By incorporation of an incremental form of the Lysmer (ref. 4) absorbing boundary condition an infinite region could be modelled with a much smaller region. An algorithm was incorporated into MARBLE and tested in hole closure calculations using 34 elements in a 15 m radius disk and 21 elements in a 5 m radius disk. The results were encouraging as were HONDO-II calculations with quiet boundaries. It was discovered that more internal reflections were produced by the geometric refinement than with Lysmer boundaries. Calculations are shown for a disk 5 m in radius. Forty Quadralateral elements are employed with no geometric refinement. Lysmer boundaries are applied at the outer radius.

Figure 11 shows the MARBLE calculations of displacement and velocity histories when the disk was penetrated with a vehicle having a third order ogival nose and cylindrical body. Node numbers increase with increasing radius. The vehicle passed in 50 msec traveling at 40 m/sec. Reflection of the stress wave is only slightly perceptable as a kink in the velocity profile of nodal point 1, 8 msec after penetration. Hole closure occurs quickly after passage of the vehicle and is completed in 22 msec.

The corresponding bulk pressures and true volumetric strain histories for elements 1, 5, 10, 15, and 20 are shown in figure 12. Element numbers increase with increasing radius. Element 1 is nearest the hole. Bulk pressures vary with decreasing magnitude for elements initially at larger radii. Only element 1 undergoes substantial volumetric change. This results from the incremental nature of the WES model. When bulk pressures are plotted as a function of incremental volume, $\Sigma d\varepsilon_{kk}$, there is an almost linear relationship with no hysteresis, figure 13.

Finally, figure 14 shows the effective pressure and pore pressure histories that combine to yield the bulk pressure in figure 12. Of significance is that effective pressures are substantially lower than the pore pressures, less than three orders of magnitude. It was also observed that principle stress differences and $\sqrt{J_2}$, both measures of shearing stress, are of the same order of magnitude as effective pressure

indicating the skeleton is not highly stressed and the response is nearly hydrodynamic.

Two-Dimensional Axisymmetric Calculations

Motivation to proceed with two-dimensional calculation is manyfold. Primarily one wishes to employ a model which gives a realistic representation that does not neglect some subtlety which could unfold into an important phenomenon. Inclusion of a region of water above the sediment insures proper impedance at this interface, incorrectly modelled with a pressure boundary condition. Pressure tractions ignore inertial effects. A better representation of the fluid dynamics behind the emplacement vehicle is achieved by drawing fluid column behind and into the hole. There are also shearing effects that result from the geometry of the emplacement vehicle not included in one-dimensional calculations. Finally, effects such as overburden and entrance length are present without need for specific modelling.

Along with advantages there are difficulties in two-dimensional analysis that must be surmounted. Size has been mentioned above. Lysmer boundaries and the geometric adaptivity of the finite elements has been employed to model a smaller spherical region about the point of penetration. Also, some geometric refinement has been employed to minimize the number of elements employed. This geometry is shown in figure 15. It employs 818 finite elements to model a spherical region 5 m in radius. A uniform cylindrical grid covering the same region with no geometric refinement would require 3200 elements not including the emplacement vehicle and water column.

Proper treatment of the water column posed a couple of problems. The first was proper coupling of the fluid dynamics between the large region of seawater above the sediment and the column. Water had to flow across an interface whose geometry changed as the column expanded. This was accomplished by the development of an ALE slide-line. ALE formulations allow the mesh to move independent of the fluid. Proper control of the mesh in the column required refinement of a velocity smoothing algorithm as an alternative to manual control.

Preliminary results are shown in figures 15 through 20 for times 0 through 50 msec at 10 msec intervals. The geometry is 5 m in radius with the lower hemisphere composed material modelled by the WES cap model with the constants determined for Pacific Illite. The upper portion is seawater modelled with an equation of state for water modified to have the proper initial density. The emplacement vehicle is modelled as a rigid body moving downward with constant velocity of 40 m/sec. The water column is attached to the vehicle with ALE sliding node pairs as is the sea water-sediment interface. An ALE

slide line is employed for interaction of the vehicle and water column with the larger regions of seawater and sediment. Finally, this simulation was executed at 60 m depth rather than the 6000 m required in final simulations.

Two satisfying features should be noted. The water column is unfolding properly behind the vehicle and the sediment is being penetrated without violent ejection of sediment into the fluid regime. The unfolding indicates success of the velocity smoothing algorithm on the ALE mesh and the ALE slide line. The second observation is physical and is predicted in part by the low effective pressures of the one-dimensional calculations and the propagation of pressure waves into the fluid regime.

The calculation terminated after 58 msec of penetration. A small jet of sediment had been ejected into the fluid regime. No doubt complete penetration could have been achieved with a modest amount of rezoning or extension of the ALE formulation into the sediment regime. Still 2.32 m of penetration had been achieved. This particular calculation took 41 hrs of CPU time on our VAX 11/780 which is roughly equivalent to 2 hrs of CPU time on the CYBER76.

Summary and Conclusions

The WES marine sediment constitutive model has been successfully implemented and tested in the ALE code MARBLE. It has been employed successfully in one- and two-dimensional axisymmetric penetration and hole closure calculations. Results of one-dimensional axisymmetric hole closure calculations indicate that hole closure should occur rapidly when dynamic pressure losses are included. Two-dimensional calculations are underway but have not been completed. Feasibility of performing these two-dimensional calculations which include sediment seawater and penetrator has been demonstrated.

Ref. 1. Ronald Hofman, "STEALTH, A Lagrange Explicit Finite-Difference Code for Solids, Structural, and Thermohydraulic Analysis," EPRI NP-260, Vols. 1, 2, and 3, Electric Power Research Institute, Palo Alto, California, August 1976. Prepared by Science Applications, Inc., San Leandro, California.

Ref. 2. Samuel W. Key, Zelma E. Beisinger, Raymond D. Krieg, "HONDO II, A Finite Element Computer Program for the Large Deformation Dynamic Response of Axisymmetric Solids," Sandia National Labroatories, SAND78-0422, October 1978.

Ref. 3. George Y. Baladi and Stephen A. Akers, "Constitutive Properties and Material Model Development for Marine Sediments in Support of the Subseabed Disposal Program," U. S. Army Engineer Waterways Experiment Station, Vicksburg, Mississippi, March 1981.

Ref. 4. John Lysmer and Roger L. Kuhlemyer, "Finite Dynamic Model for Infinite Media," J. Eng. Mech. Div., Proc. ASCE. Vol. 5, No. EM4, 859-877, 1969.

Ref. 5. J. Donea, P. Fasoli-Stella, S. Giuliani, J. P. Halleux, and A. V. Jones, "The computer code EURDYN-1M for transient dynamic fluid-structure interaction," EUR6751EN. Commission of the European Communities Joint Research Center Ispra Establishement, Italy 1980.

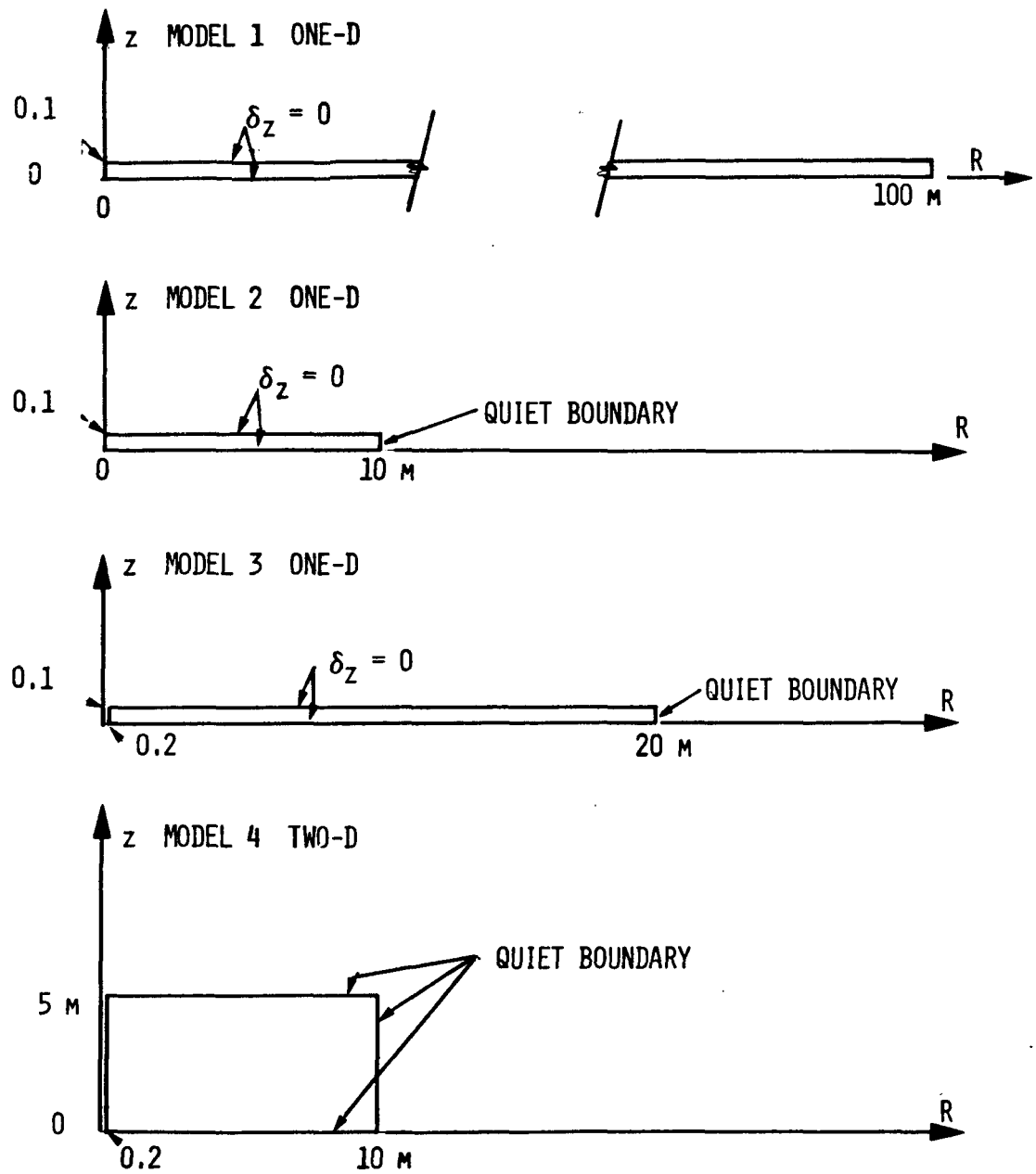


Figure 1: Assumed Models - Model Study

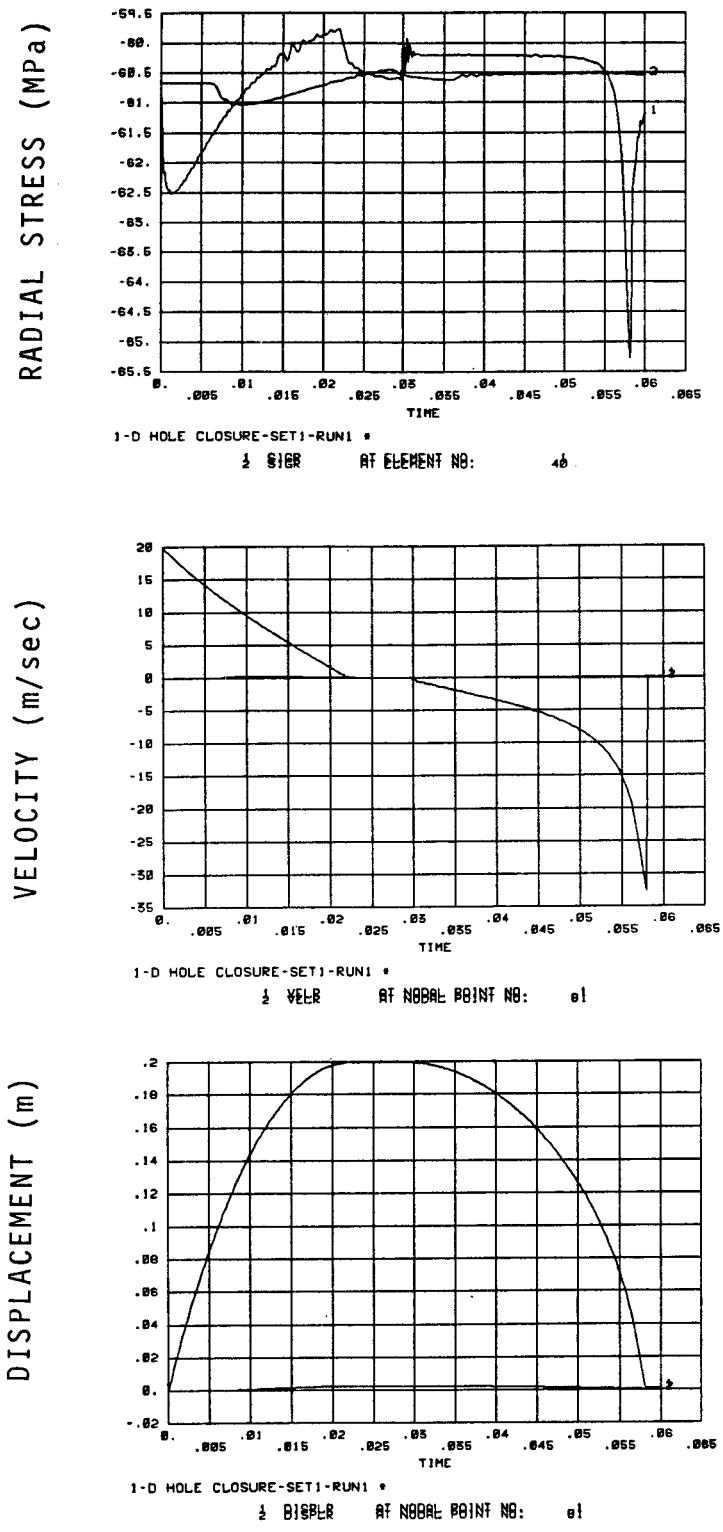


Figure 2: Results - Model 1

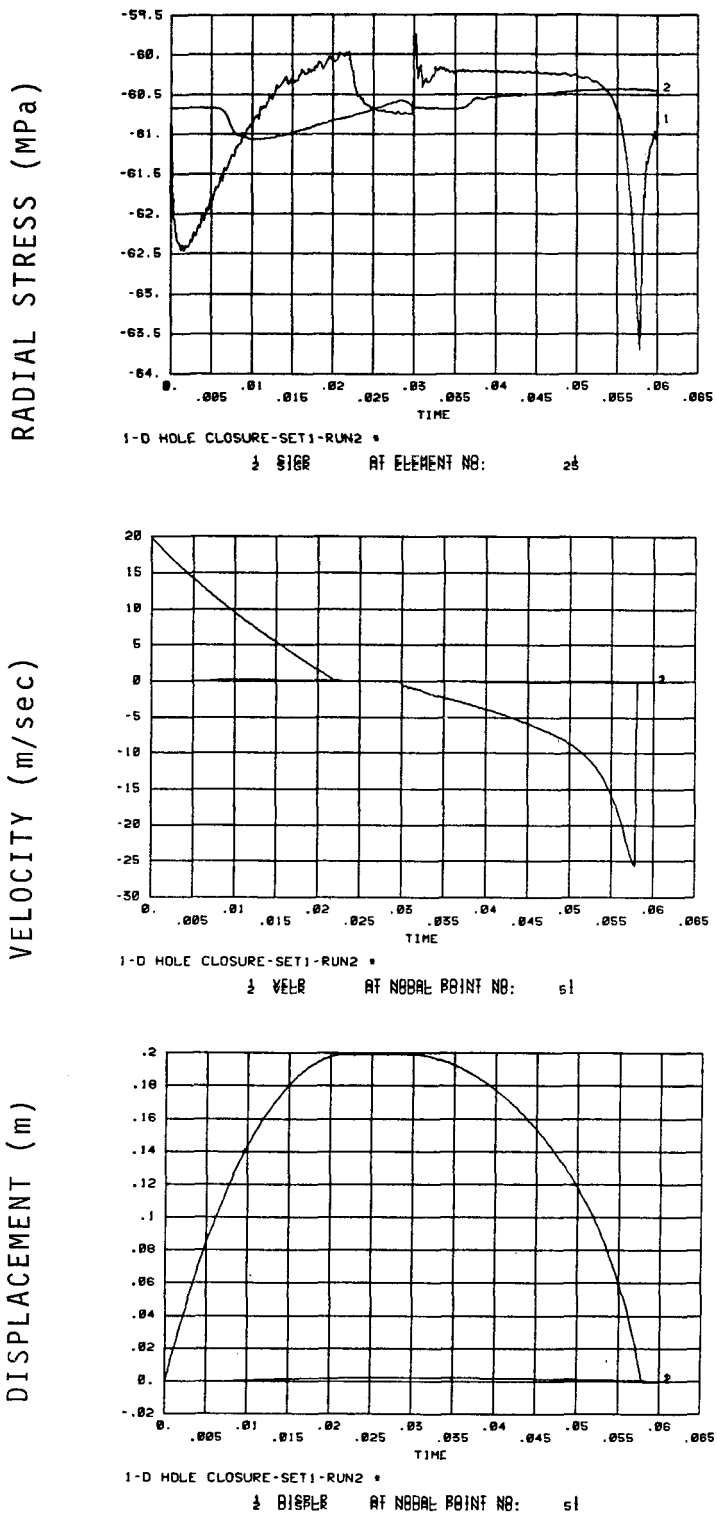


Figure 3: Results - Model 2

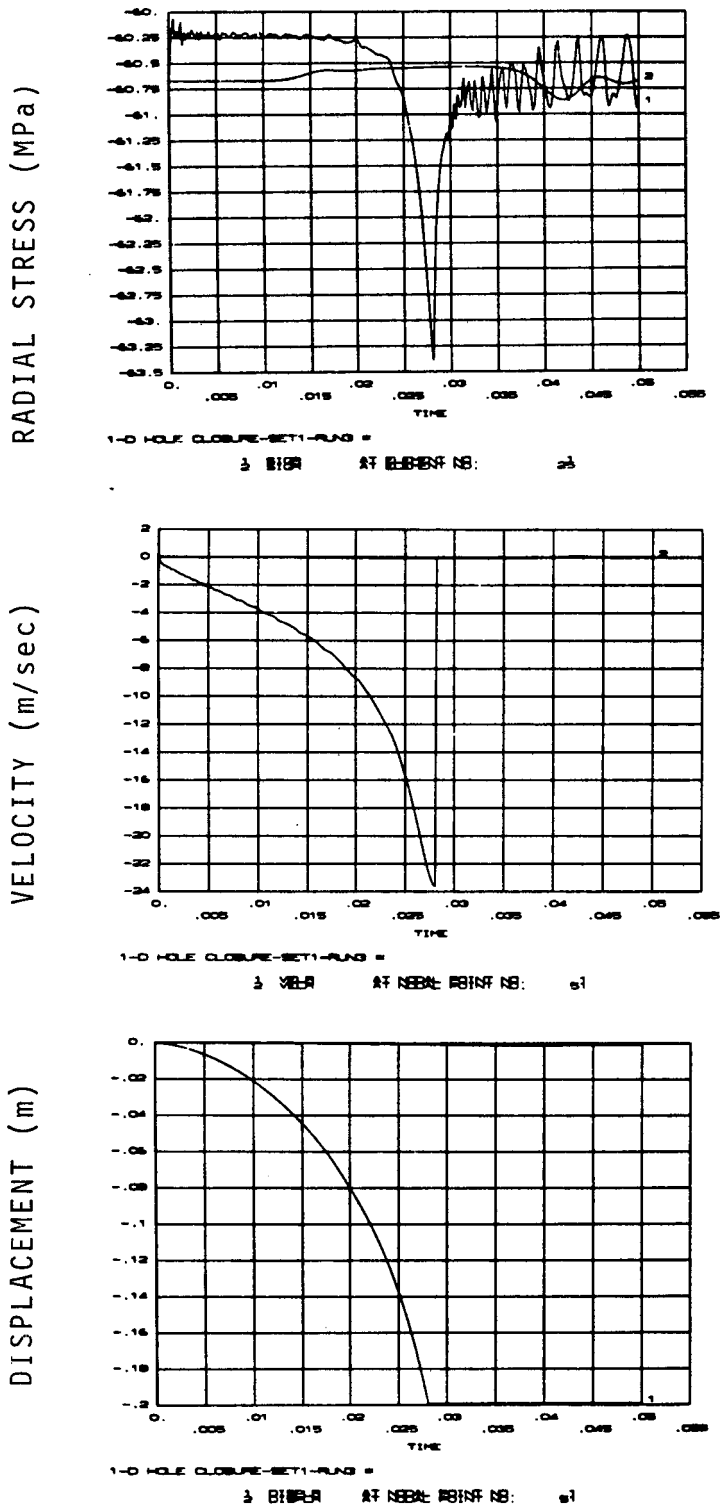


Figure 4: Results - Model 3

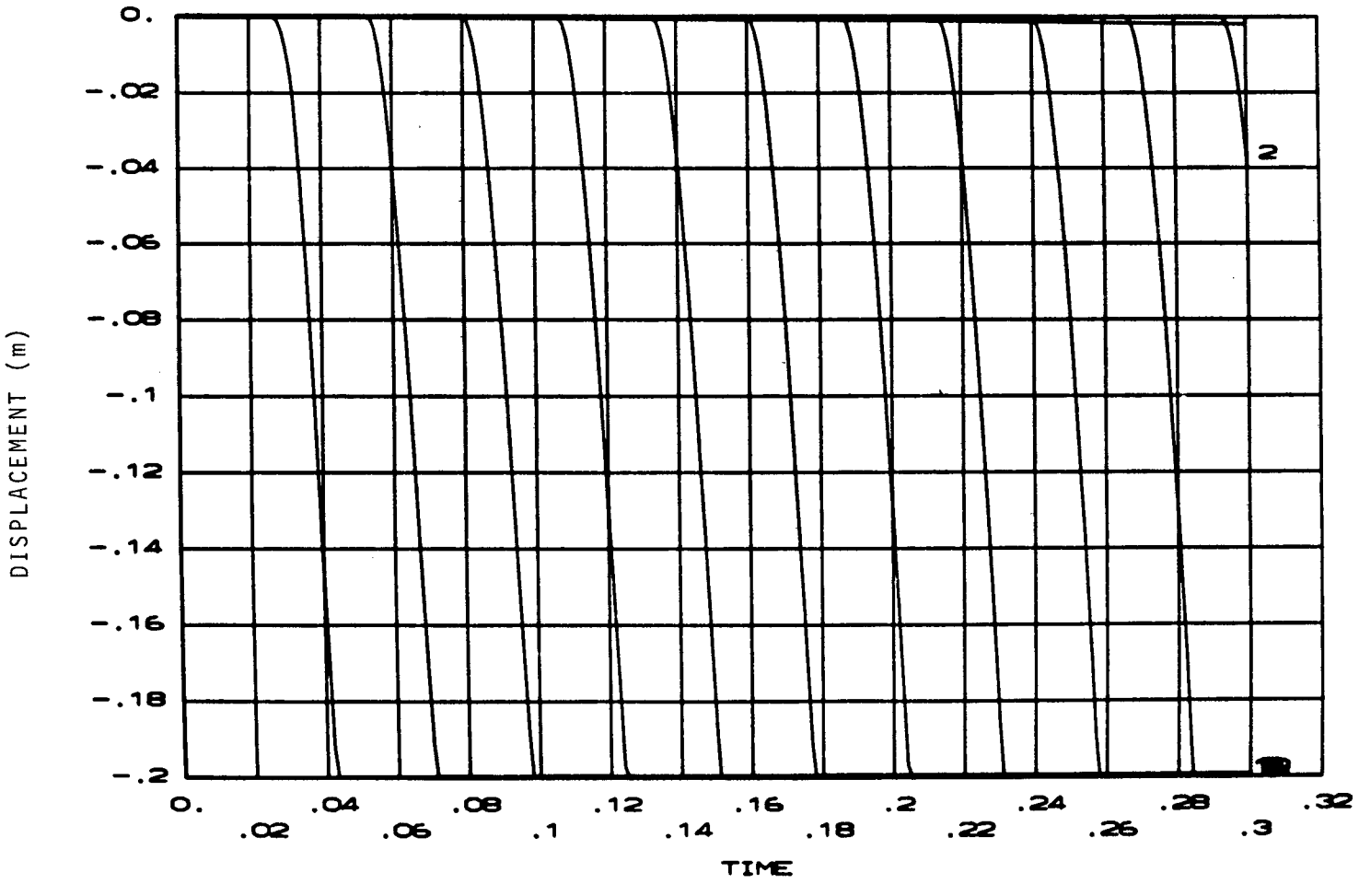


Figure 5: Results - Model 5

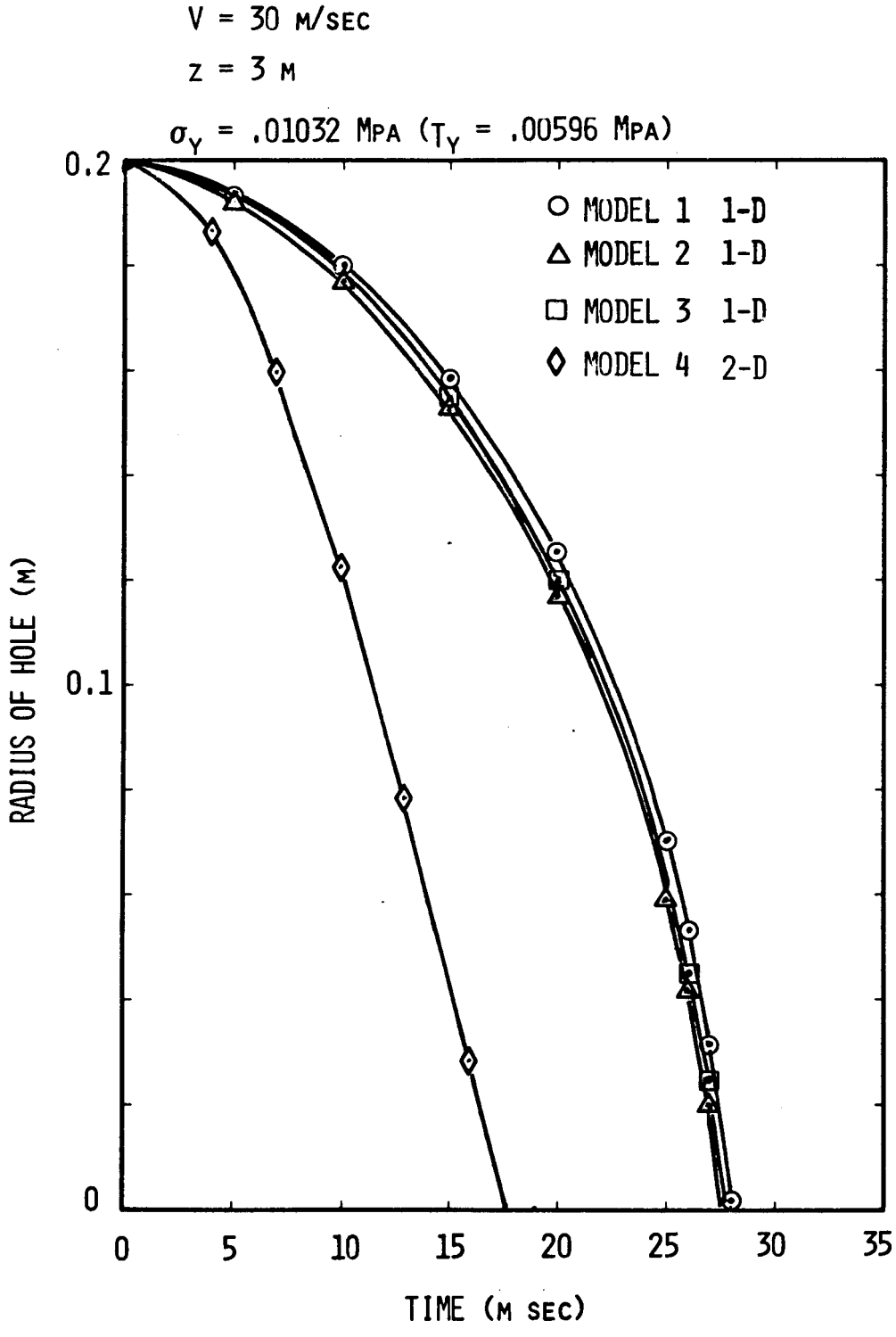
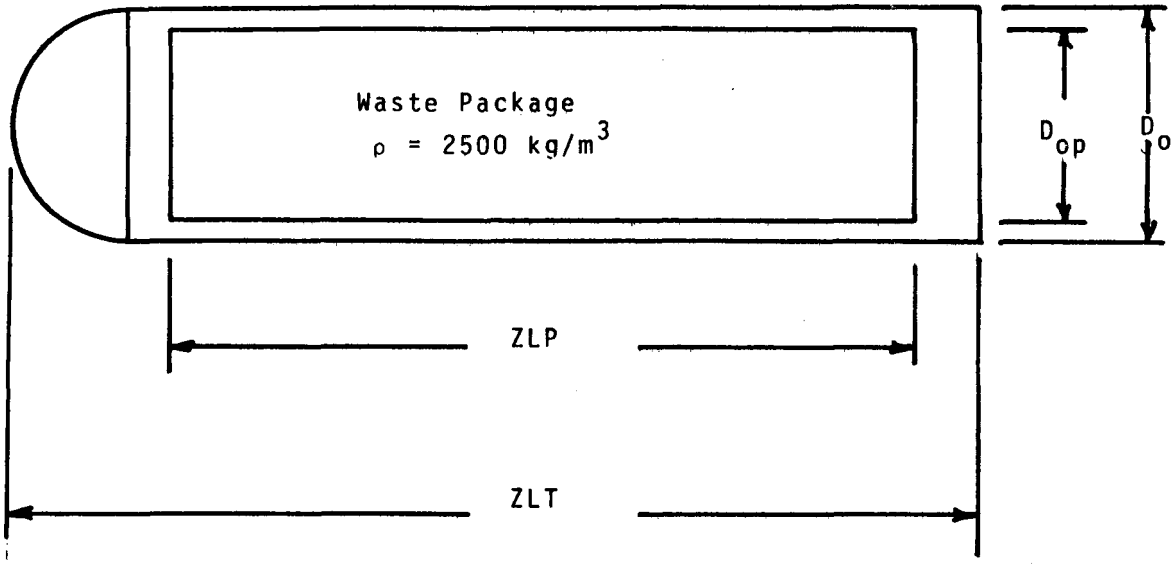


Figure 6: Comparison of Results Geometry Model Study



CORER MASS	=	1800.671
OUTSIDE DIAMETER	=	0.400
FRONTAL AREA	=	0.126
VEHICLE LENGTH	=	3.350
VEHICLE VOLUME	=	0.413
DRAG COEFFICIENT	=	0.212
VEHICLE BOUYANCY	=	0.764
VEHICLE WEIGHT	=	13495.589
TERMINAL VELOCITY	=	31.361
PACKAGE MASS	=	668.668
PACKAGE DIAMETER	=	0.350
PACKAGE LENGTH	=	2.780
PACKAGE VOLUME	=	0.267
VOL P / VOL T	=	0.648

Figure 7: Assumed Geometry of Emplacement Vehicle

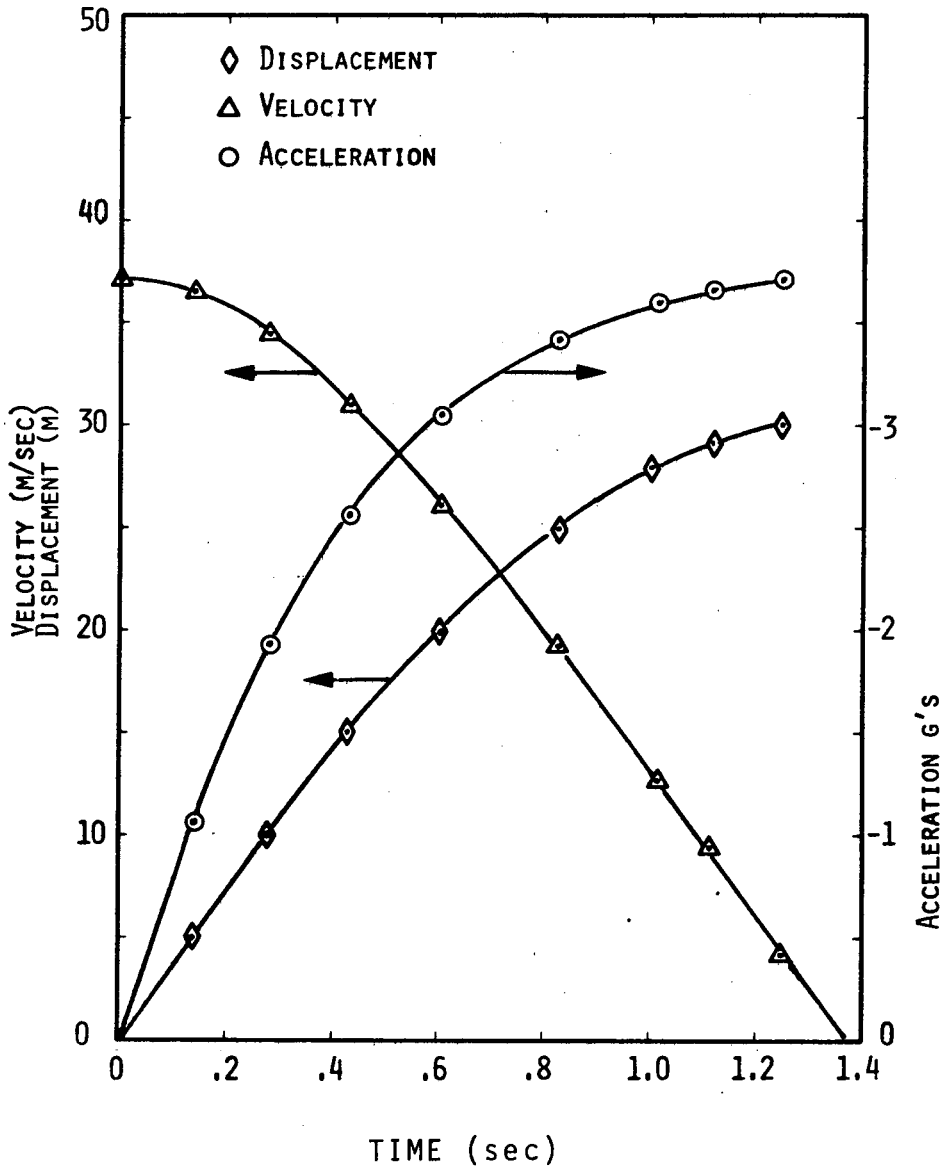


Figure 8: Penetration Response for Baseline Emplacement Vehicle

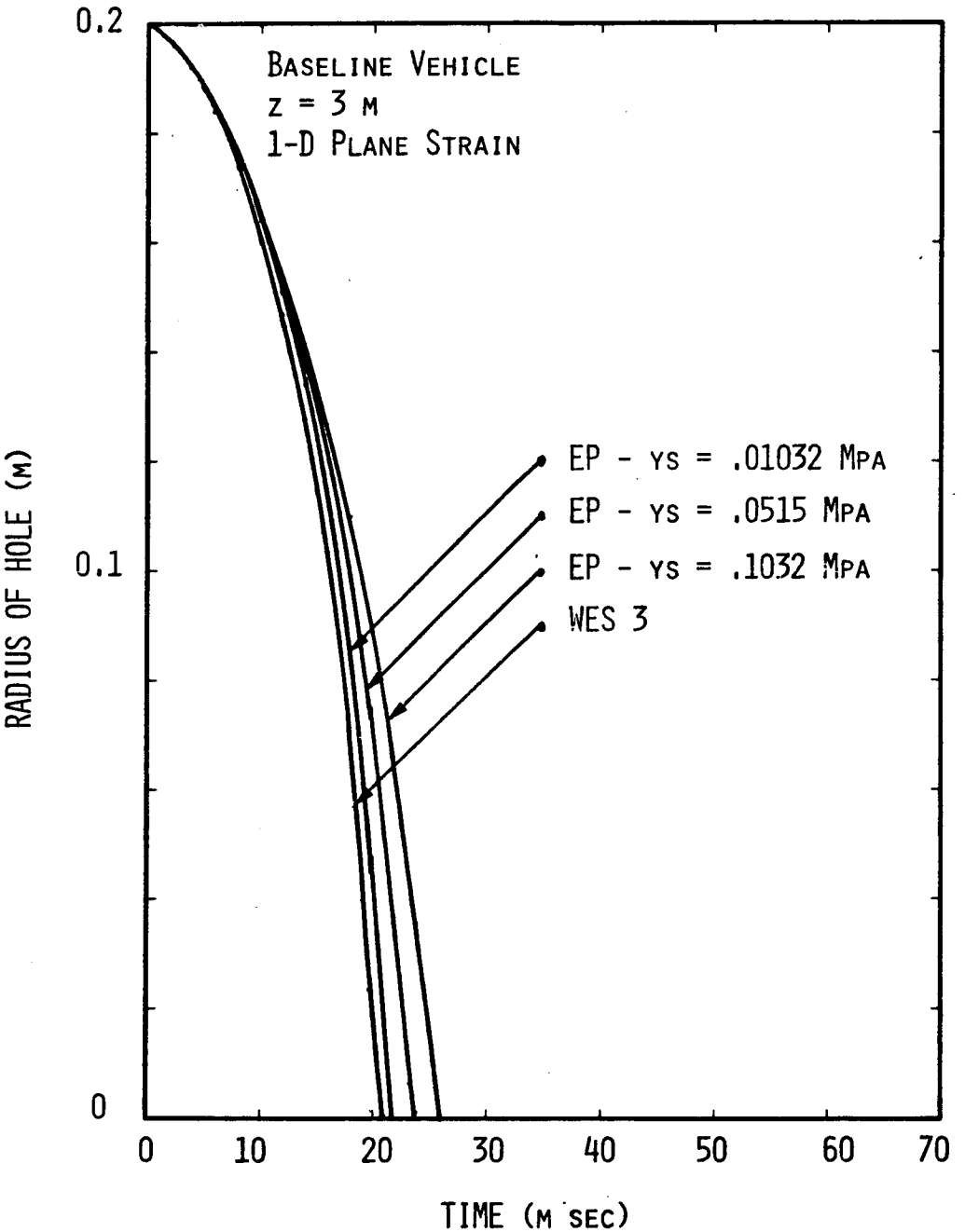


Figure 9: Summary - One-Dimensional Hole Closure Calculations - Baseline Vehicle

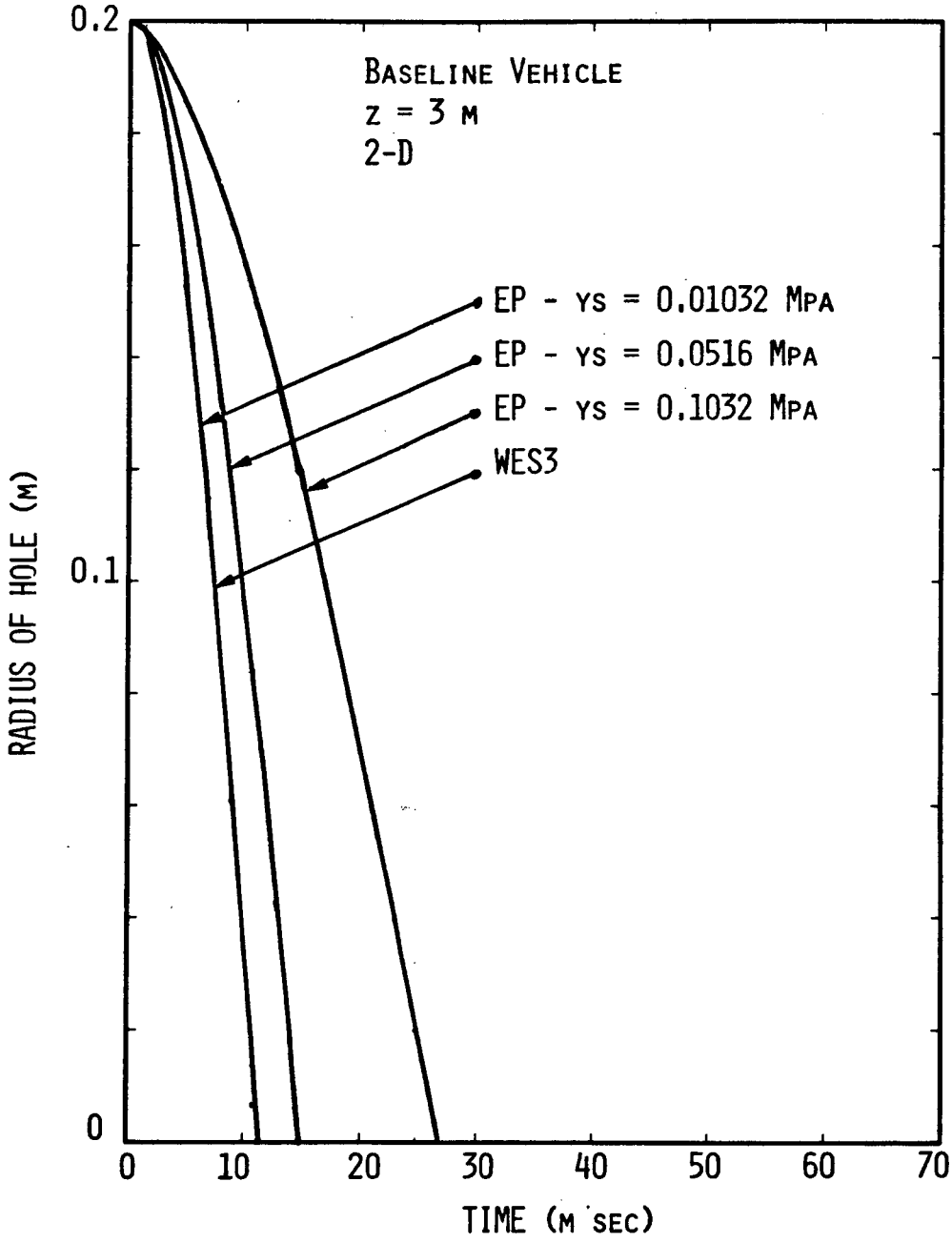
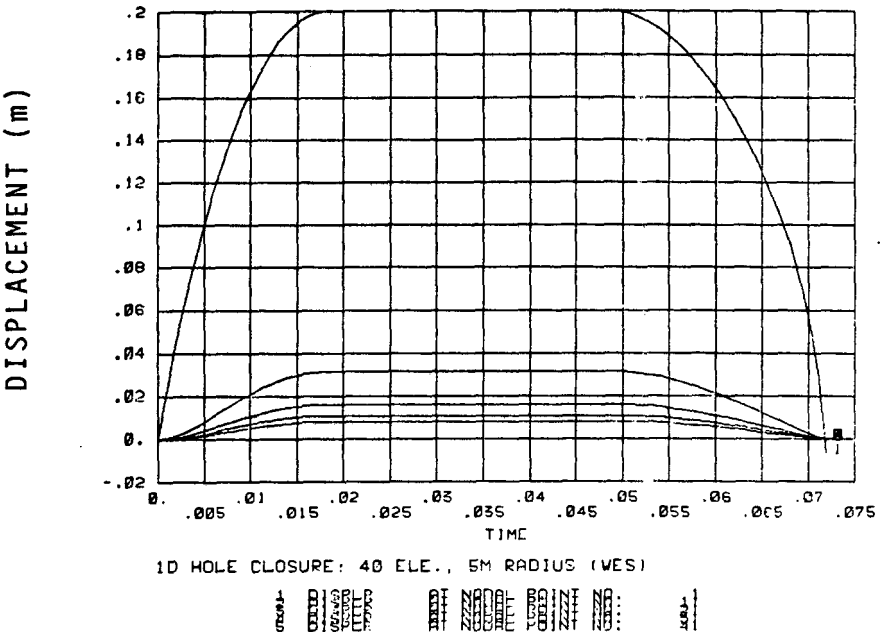


Figure 10: Summary - Two-Dimensional Hole Closure Calculations - Baseline Vehicle



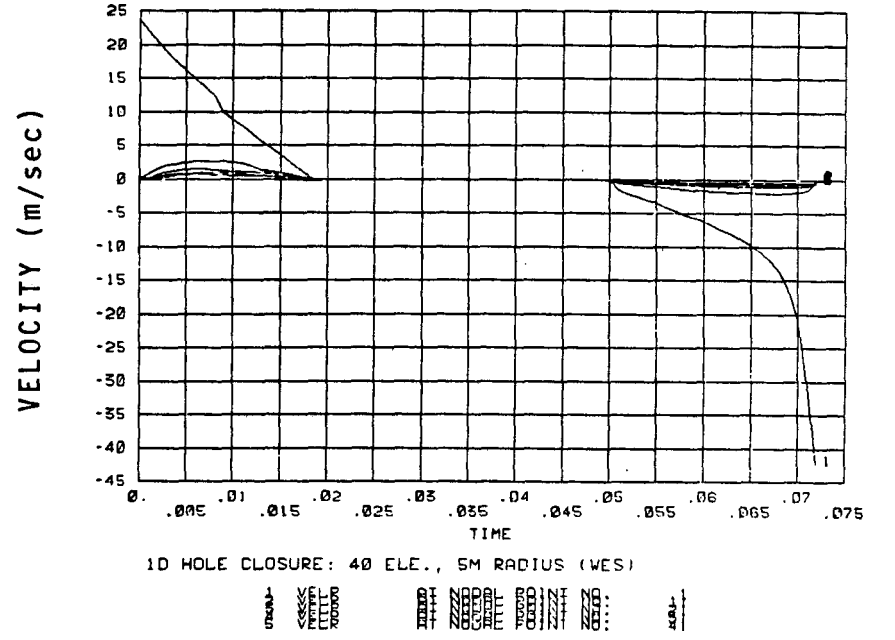


Figure 11: MARBLE Calculations

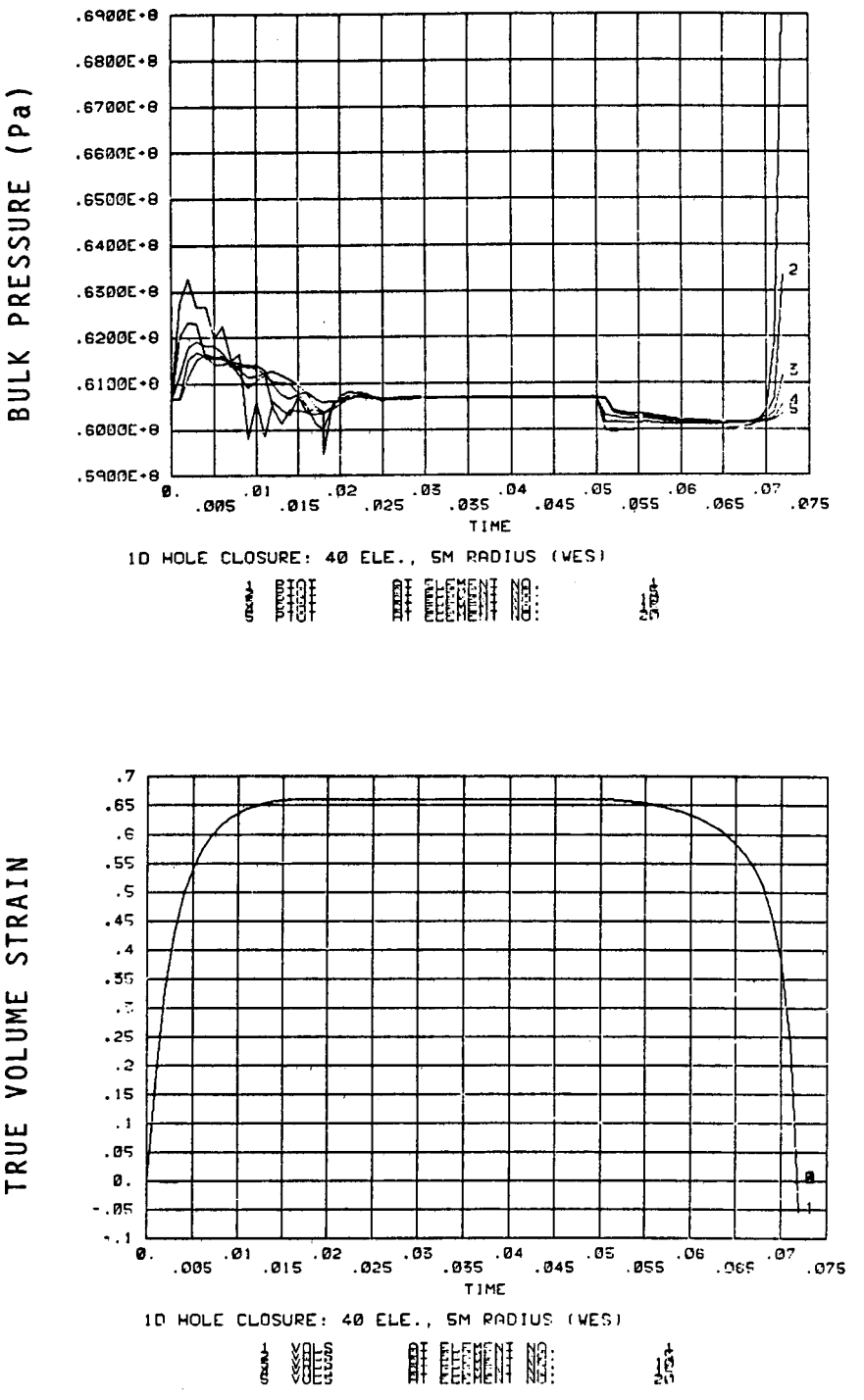


Figure 12: MARBLE Calculations

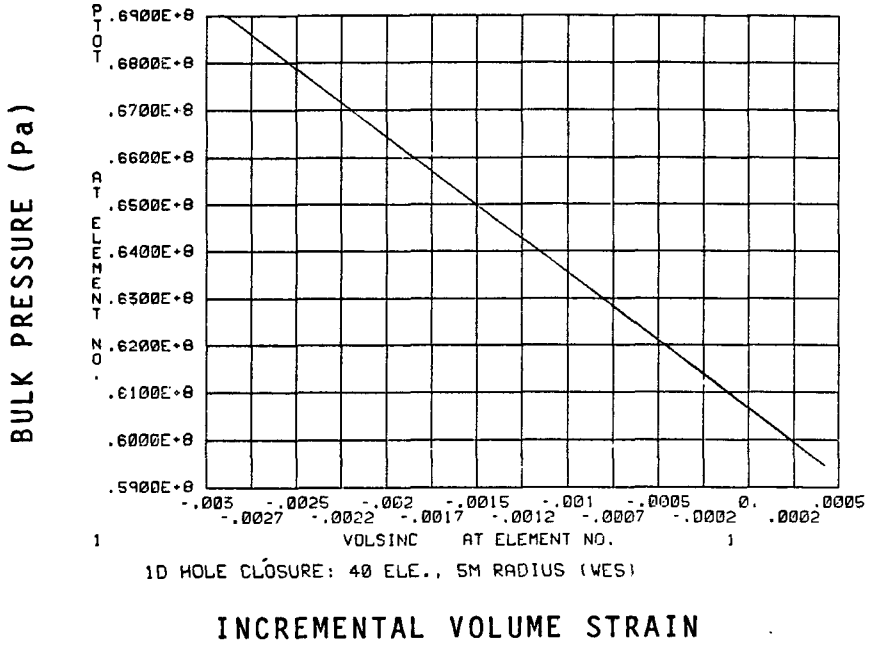
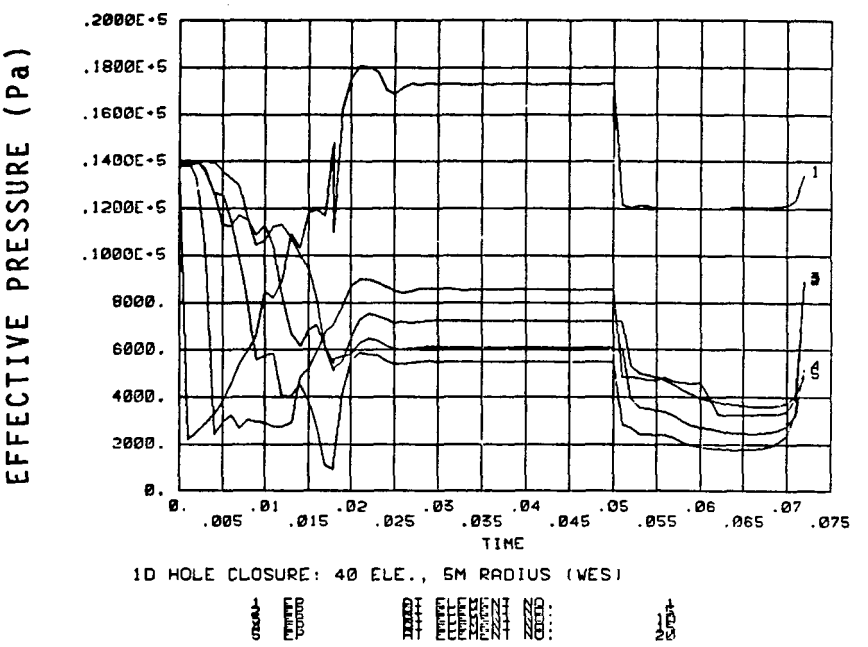


Figure 13: MARBLE Calculations



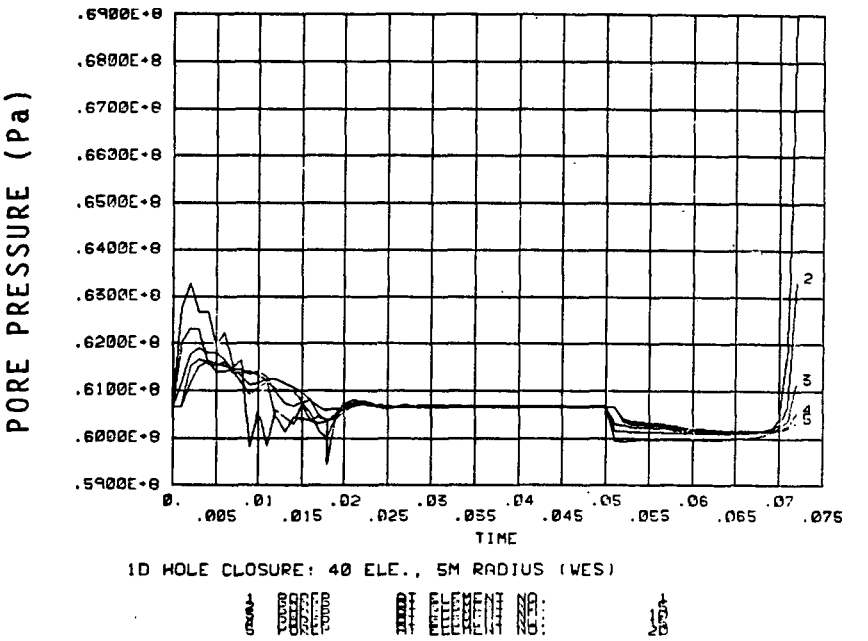
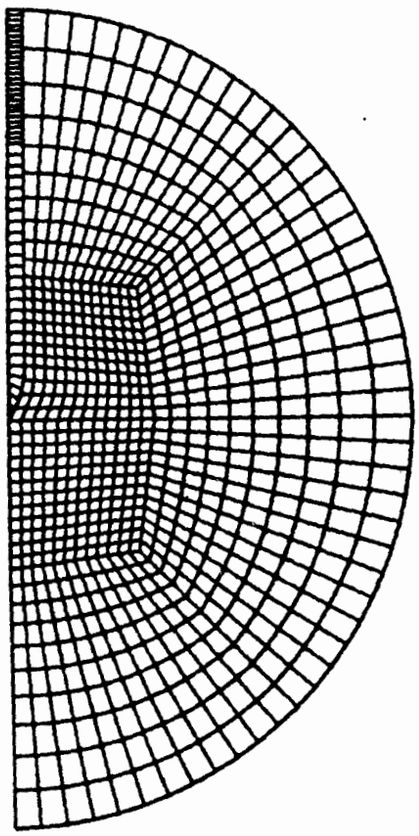


Figure 14: MARBLE Calculations



t = 0

Figure 15a:

2-D axisymmetric penetration calculation, 5 m spherical model.

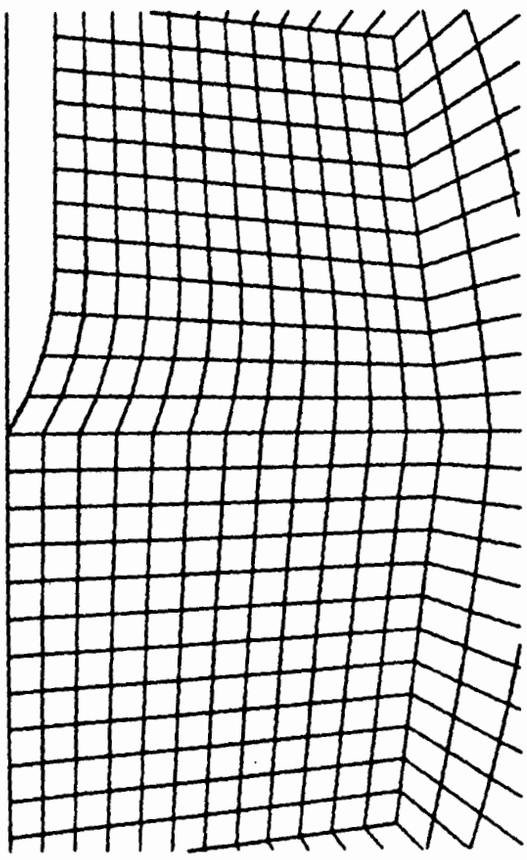


Figure 15b: 3x magnification

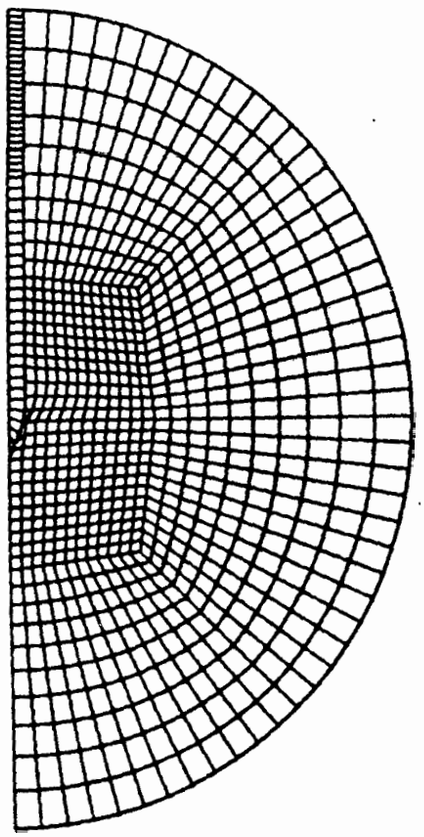


Figure 16a:

2-D axisymmetric penetration calculation, 5 m spherical model.

t = 10 msec

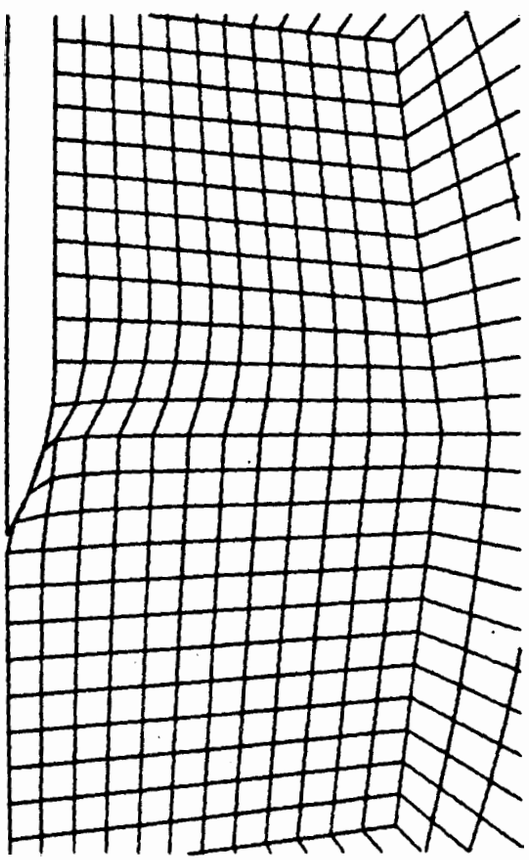
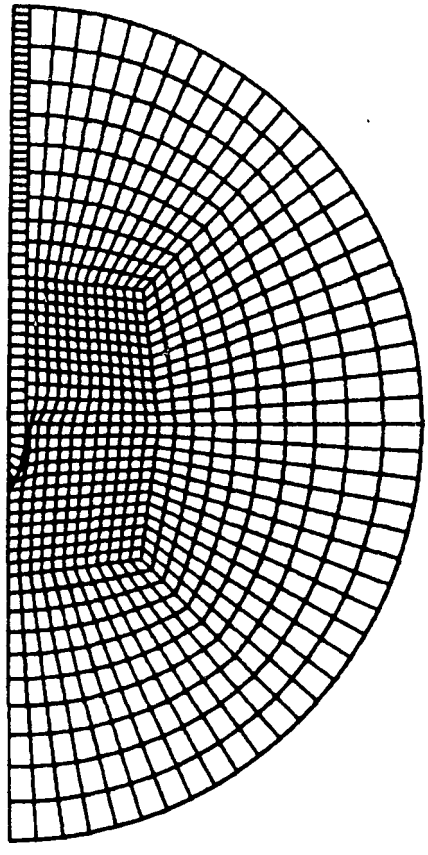


Figure 16b: 3x magnification



t = 20 msec

Figure 17a:

2-D axisymmetric
penetration calculation,
5 m spherical model.

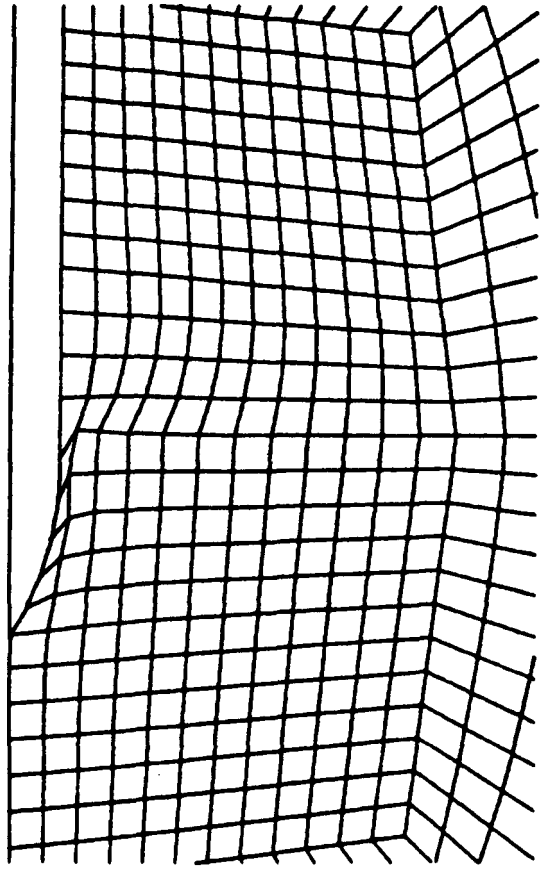
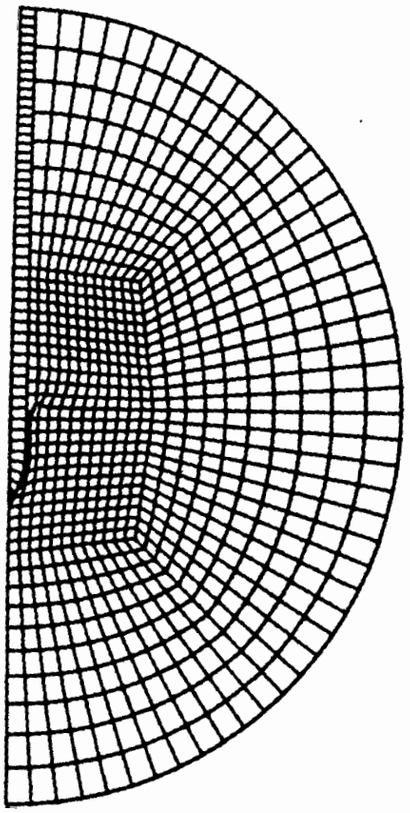


Figure 17b: 3x magnification



t = 30 msec

Figure 18a:

2-D axisymmetric penetration calculation, 5 m spherical model.

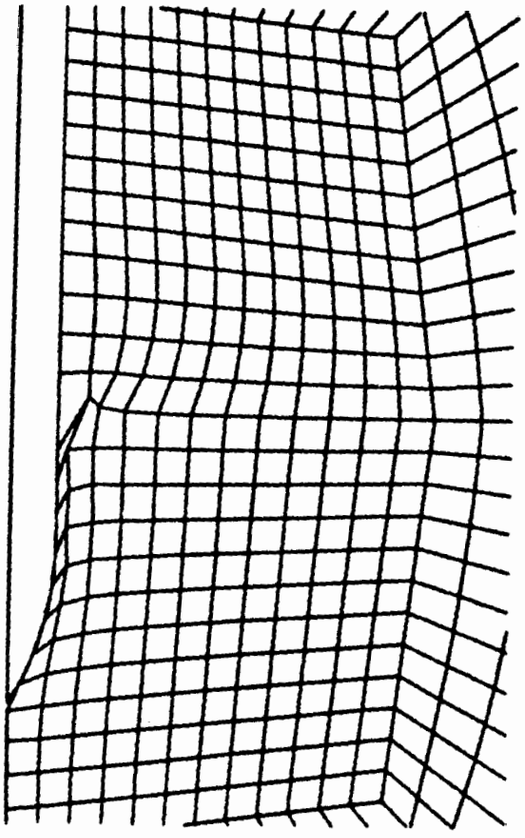
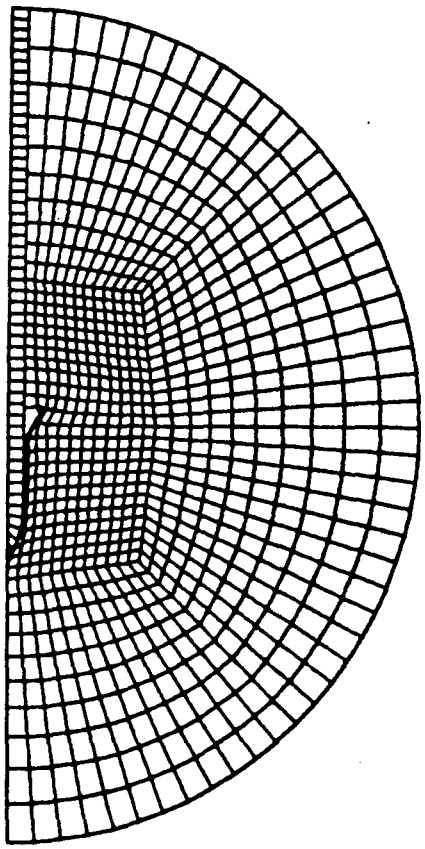


Figure 18b: 3x magnification



t = 40 msec

Figure 19a:

2-D axisymmetric penetration calculation, 5 m spherical model.

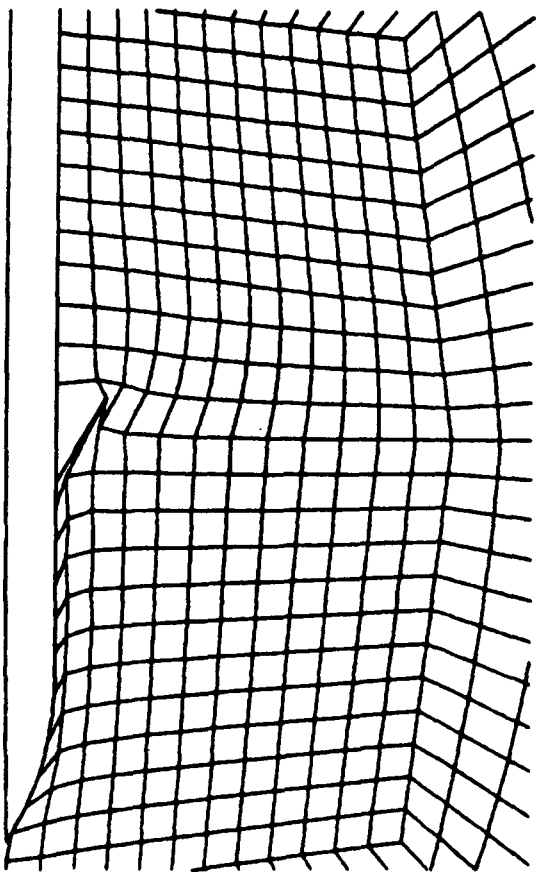
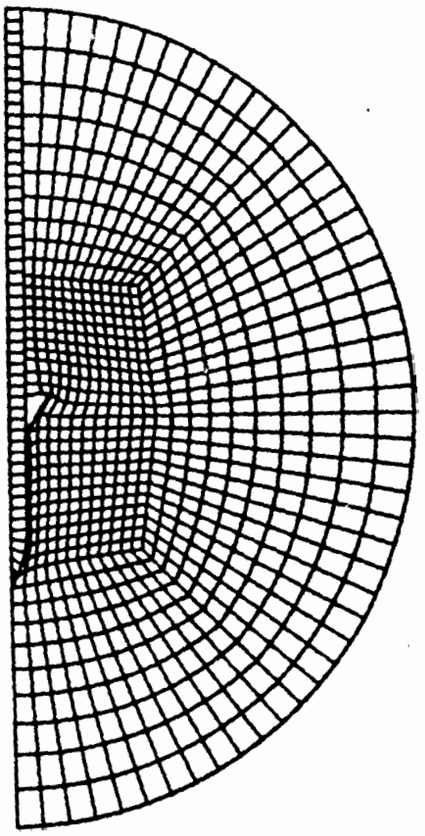


Figure 19b: 3x magnification



t = 50 msec

Figure 20a:

2-D axisymmetric penetration calculation, 5 m spherical model.

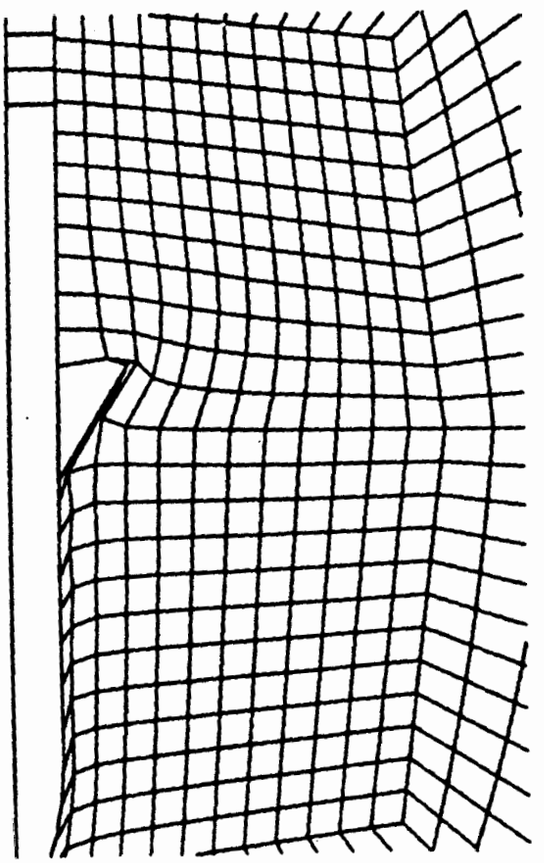


Figure 20b: 3x magnification

APPENDIX GG

DYNAMIC HOLE CLOSURE BEHIND A DEEP OCEAN SEDIMENT PENETRATOR

Peter T. Dzwilewski

Applied Research Associates, Inc.

(Contract #73-7851)

Charles H. Karnes

Sandia National Laboratories

DYNAMIC HOLE CLOSURE BEHIND A DEEP OCEAN SEDIMENT PENETRATOR

Peter T. Dzwilewski
Applied Research Associates, Inc.
Albuquerque, New Mexico 87110
Contract 73-7851

Charles H. Karnes
Sandia National Laboratories
Albuquerque, New Mexico 87185

ABSTRACT

A freefall or boosted penetrator is one concept being considered to dispose of nuclear waste in the deep ocean seabed. For this technique to be acceptable, the sediment must be an effective barrier to the migration of radioactive nuclides, which means that the hole behind the advancing penetrator must close. One mechanism which can cause the hole to close immediately behind the penetrator is the reduction in water pressure in the wake as water tries to follow the penetrator into the sediment. An approximate solution to this complex problem is presented which analyzes the deformation of the sediment with a nonlinear, large displacement and strain, Lagrangian finite-difference computer code (STEALTH). The water was treated by Bernoulli's Principle for flow in a pipe resulting in a pressure boundary condition applied to the sediment surface along the path after passage of the penetrator.

Two one-dimensional and eight two-dimensional calculations were performed with various penetrator velocities (15, 30, and 60 m/s) and sediment shear strengths. In two of the calculations, the dynamic pressure reduction was neglected to see if geostatic stresses alone would close the hole. The results of this study showed that geostatic stresses alone would not close the hole but the dynamic pressure reduction would. The largest uncertainty in the analysis was the pressure conditions in the water behind the penetrator in which frictionless, steady-state flow, in a uniform diameter pipe was assumed. A more sophisticated and realistic pressure condition has been formulated and will be implemented in the computer code in the near future.

INTRODUCTION

For many decades, the ocean sediments have been penetrated by various objects such as anchors, coring devices, seismic instrumentation packages, pilings, and drill strings. Some of these objects have been buried completely, and coring devices and instrumentation packages have been recovered. However, there has been little, if any, interest in these situations as to whether the sediment filled in around the penetration path and effectively closed the hole or that the path was mostly filled with water.

The Subseabed Disposal Program[1] is investigating the technical and environmental feasibility of disposing of nuclear waste materials in deep ocean clay sediments. Various emplacement methods[1] are possible, the simplest being with a canister encased in a hydrodynamically shaped penetrator which enters the sediment with a sufficient velocity to penetrate the sediment to the required depth of a few tens of meters. Because the clay sediments are considered the primary barrier to migration of radionuclides from the canister to the biosphere, the penetration path in the sediment must be shown not to be a breach of the sediment barrier which could allow radioactive ions to migrate rapidly to the water column and possibly back to humankind.

If the hole is assumed to remain open containing a column of seawater after penetration has ceased, then it might close in time by a combination of sediment slumping, caving in, and creep. These mechanisms may, however, be considered too unreliable to create conditions in the path which would represent an adequate ion migration barrier. This would necessitate an engineered closure such as backfilling or tamping by a maneuverable deep water vehicle.

It has been proposed[2] that for a penetrator entering the sediment with sufficient velocity to penetrate to an adequate depth, the sediment will be sucked into the path by the reduced pressure in the wake of the penetrator. If it is assumed that the hole remains open behind the penetrator during penetration, then seawater must flow down the hole with a flow rate sufficient to keep up with the penetrator because the ambient pressure in deep water will prevent the water from cavitating. The required high water flow rate will produce a reduced pressure in the water behind the penetrator due to a combination of Bernoulli's Principle and frictional drag. The resulting difference between the sediment farfield and wake pressures should be sufficient to force the sediment inward thereby pinching off the water flow and closing the hole.

Computing the behavior of the water and sediment in this problem is difficult because of the extreme range of deformation states involved: the water must be treated as a flowing liquid while the sediment experiences deformations ranging from very large inelastic deformations verging on flow to purely elastic deformations. The computational techniques required to consider this range of

deformation states include both an Eulerian formulation to accomodate the flow of the water and part of the sediment and a Lagrangian formulation for the deformation of the remainder of the sediment. These capabilities must exist in either the same or in two, coupled computer codes. An existing computer code is being modified to accomplish this analysis but it is incomplete[3].

The purpose of this paper is to obtain an approximate solution to this problem, treating the problem as one of flow of water in a non-uniform diameter pipe, the pressure in which is coupled to the sediment deformation as a boundary condition in an existing large deformation two-dimensional finite-difference computer code[4]. It is further intended to determine if the dynamic pressure in the wake of the penetrator is sufficient to close the hole in the sediment and to determine the sensitivity of the hole closure phenomena to changes in boundary conditions, penetrator velocity, and sediment descriptive parameters.

GENERAL ASSUMPTIONS

A schematic diagram of the problem is shown in Figure 1. The rear of the penetrator has reached a depth, h, and is moving downward with a velocity, v_p. If the seawater pressure at the surface is P_o, then from Bernoulli's Principle[5], the pressure at a depth, z, within the wake where the water is moving with a velocity, v_w, is:

$$P = P_o + \rho_w \; g \; z - \frac{1}{2} \rho_w \; v_w^2 \qquad (1)$$

where ρ_w is the water density and g is the gravitational acceleration. The local water velocity, v_w, is a function of depth, z; and the pressure, P, is employed as a boundary condition for the lateral surface of the hole above the penetrator. In order to be conservative (and to simplify the analysis), all frictional effects and entry pressure losses have been neglected since both would cause a further reduction in the pressure, P. Neglecting the entry losses results in an assumption of an ideally rounded inlet[5] through which the water flows from above the sediment surface into the hole.

It is apparent that the pressure at a point in the sediment at a depth, z, removed from any influence of the wake is:

$$P_z = P_o + \rho_s \; g \; z \qquad (2)$$

where ρ_s is the density of the sediment. The pressure difference which forces the hole to close becomes:

$$P_z - P = \frac{1}{2} \rho_w v_w^2 + g \; z \; (\rho_s - \rho_w) \qquad (3)$$

If the hole remained open and the same diameter as the penetrator, then the flow rate of the water which must fill the hole is:

$$q_w = A_w v_w = A_p v_p \tag{4}$$

where A_w equals A_p and are the cross-sectional areas of the water and penetrator, respectively. If the sediment is moving in and closing the hole slowly, the water velocity computed from Equation 4 would be an adequate approximation from which to calculate the required boundary pressure from Equation 1. However, for more rapid sediment motion, the fact that sediment is filling the volume swept out by the penetrator must be considered. The rate at which the sediment is filling the hole is given by:

$$q_s = 2\pi \int_0^h R(z)\, v_s(z)\, dz \tag{5}$$

where $R(z)$ is the local radius of the hole, and $v_s(z)$ is the local radial velocity of the sediment evaluated at the hole radius. The flow rate of the sediment must be compatible with that of the water and the volume being swept out by the pentrator:

$$q_w + q_s = A_p v_p \tag{6}$$

where q_w is the total flow rate of the water (assumed incompressible) so that

$$q_w = A_w v_w \tag{7}$$

Equations 5, 6, and 7 are then used to determine the local water velocity from which the required boundary pressure is calculated from Equation 1.

As a first step in the computer analysis of the hole closure problem, it was assumed that the water velocity was equal to the penetrator velocity which implies that the flow of sediment is negligible relative to the flow of water. This is a good assumption right after the penetration passes a given point but becomes progressively worse as the hole proceeds to close. As far as the hole closure process is concerned, the effect of this assumption is not clear. While the water flow, q_w, will be in too high, the assumed cross section area, $A_w = A_p$, will also be too high. The water velocity v_w is proportional to q_w and inversely proportional to A_w. Therefore, the errors will tend to cancel each other. The more realistic analysis which uses Equations 5 - 7 is more complicated and is currently under development.

The penetrator that was used for this analysis is a cylinder 3 m in length and 0.4 m in diameter that had a one caliber ogive nose. The velocity of the penetrator was assumed to be constant with depth and was varied in different computer runs to study the effects. Values of 15, 30, and 60 m/s were used. The 15 and 30 m/s velocities

can be attained by freefall while the 60 m/s velocity must be boosted. The constant velocity assumption is good as can be seen from the velocity versus depth plot in Figure 2 of a similar but slightly smaller penetrator than was used in this study. The two-dimensional computer calculations were run to a penetration depth of approximately 6 m. For the penetrator in Figure 2, the velocity would have dropped from 28.7 to 28 m/s. The penetrator was not specifically modeled; actually the grid boundary was moved radially to match the sediment displacement due to the penetration process. A rigid body penetrator could have been modeled in the code but the point of this study was to determine the response of the sediment. Therefore, this unnecessary complication was not included.

STEALTH[4], which is a nonlinear, large displacement and strain, Lagrangian finite-difference computer code, was used for the calculations because it had many of the necessary features for the calculations and it is modular which made modifications relatively easy. Some of the standard features of the code that were used were the one- and two-dimensional modes, automatic rezoning (continuous and row dropping), restart capability, elastic-plastic material models, and velocity and pressure boundary conditions. Some of the modifications that were implemented were a depth dependent shear strength for the sediment, the logic to switch from velocity to pressure boundaries to model the penetration, inclusion of geostatic stresses, and nonreflecting boundaries to reduce the size of the grid and hence computer costs. Many of these features will be discussed later.

The sediment which is a saturated clay, was modeled as an elastic-plastic material. The density was 1400 kg/m^3; the bulk modulus was 3.2×10^9 Pa; the shear modulus was 2.0×10^8 Pa and Poisson's ratio was 0.48. The baseline shear strength[6] varied with depth according to:

$$Y = 19{,}540 \ln (1 + 0.1189 z), \text{ Pa} \quad (8)$$

where z is depth in meters. The shear strength which is the most important material property as far as hole closure is concerned was varied. The above relationship (Eq. 8) was multiplied by 5 and 20 in some of the calculations. Because Equation 8 is based on the undrained shear strength from a core taken with a piston coring device, the near surface shear strength may be low. Therefore, in one of the calculations the shear strength at 5 m of depth (from Eq. 8) was used for the 0 - 5 m depth to represent an upper bound of the near surface shear strength.

ONE-DIMENSIONAL CALCULATIONS

In order to scope out the hole closure problem, two one-dimensional calculations in cylindrical coordinates were performed. The advantage of this approach was that the special

features needed for the calculations could be developed easier and quicker in one-dimension than in two. The one-dimensional calculations simulated the response of the sediment to a passage of a penetrator traveling at a velocity of 30 m/s at a depth of 10 m. The two calculations differed in that the first included the dynamic pressure ($1/2\ \rho_w\ v_w^2$ in Eqs. 1 or 3) while the second one did not. The purpose of the second calculation was to see if the hole would close just due to geostatic stresses.

The initial zone size was 0.1 m growing geometrically by 8 percent. There were a total of 30 zones out to a radial distance of 11.3 m at which point a nonreflecting boundary of the Lysmer type was used[7]. No rezoning was employed in these calculations although it could have shortened the computer run time by enlarging the zone size near the penetrator and hence, increasing the allowable time step.

The radial velocity boundary condition for the axis that simulated the penetrator nose was:

$$v(t) = \frac{\sqrt{3}\ v_p\ r_p - v_p^2\ t}{\left(r_p^2 + 2\sqrt{3}\ v_p\ r_p t + v_p^2\ t^2\right)^{1/2}} \qquad 0 \le t \le \frac{\sqrt{3}\ r_p}{v_p} \qquad (9)$$

where, v_p is penetrator velocity, and r_p is the penetrator radius. For v_p = 30 m/s and r_p = 0.2 m, Equation 9 becomes:

$$v(t) = \frac{(10.4 - 900t)}{\left(0.04 + 20.8t - 900t^2\right)^{1/2}} \qquad 0 \le t \le 0.0115\ \text{s} \qquad (10)$$

When Equation 10 was used in the one-dimensional calculations, the artificial viscosity term in the force equation, which is used to smear pressure discontinuities over several meshes[8] dominated the sediment response. The reason for this is that at time equal zero the radial velocity is equal to 52 m/s. This jump in velocity from rest conditions induced a large volumetric strain rate and, hence, a large artificial viscosity term. To reduce this effect the velocity was made to be continuous by using the following equation:

$$v(t) = 4.14 \times 10^7\ t^2 \qquad 0 \le t \le 0.001\ \text{s} \qquad (11)$$

Summarizing, Equation 11 was used from time zero to 0.001 s and Equation 10 from 0.001 s to 0.0115 s. However, the velocity from Equation 10 had to be increased by approximately 20 percent to account for the reduction of displacement because of the use of Equation 11 and thereby attain the 0.2 m outward displacement of the penetration radius. After a time equal to $\sqrt{3}\ r_p/v_p$ (0.0115 s) the radial velocity was set equal to zero until a time of $L_p/v_p + \sqrt{3}\ r_p/v_p$ (0.1115 s), where L_p is the penetrator side length. This accounts for the sides of the penetrator and implies that cavitation

is not possible under the 60 MPa ambient pressure. After the penetrator has passed a given point, the pressure boundary is imposed.

The boundary pressure from Equation 3 for Calculation 1 (including dynamic pressure) is:

$$P_z - P = \frac{1}{2} \rho_w v_w^2 + gz (\rho_s - \rho_w) = 502 \text{ kPa} \quad (12)$$

The pressure boundary for Calculation 2 (geostatic pressure only)

$$P_z - P = gz (\rho_s - \rho_w) = 36 \text{ kPa} \quad (13)$$

The results for Calculation 1 are shown in Figure 3 and 4. The radial velocity of the point next to the penetrator is in Figure 3. The velocity is zero at time equal to zero and increases to approximately 41 m/s outward velocity and decreases to zero as the ogive nose passes the point of interest at 0.0115 s. Then the velocity is zero (penetrator side) until 0.1115 s when the pressure boundary is applied. The velocity becomes negative (inward) increasing to approximately 12 m/s. The hole closes and the velocity becomes zero at approximately 0.143 s. The radial position plot (Fig. 4) shows the same phenomena; the hole is opened, remains open until the pressure boundary condition is imposed and then closes in approximately 0.031 s after passage of the rear of the penetrator.

Calculation 2 (geostatic stresses only) results are shown in plots of the radial velocity and displacement, Figures 5 and 6, respectively, and show that the hole remains open. This is a significant finding because it demonstrates that the overburden (at least to a depth of 10 m) is not sufficient to cause hole closure in the short term and that the dynamic pressure is important in the hole closure process. Also, it demonstrates the importance of modeling the dynamic pressure properly (Eqs. 3 and 5 - 7).

For completeness the following statistics are provided on the required computer time. As previously mentioned rezoning would help reduce computer time as would an activation check but to a lesser extent.

	Calculation 1	Calculation 2
Simulation Time, s	0.160	0.2
Cycles	13,199	19,334
Computer Time (CDC 7600) s	193	267
Cost, $	26	35

TWO-DIMENSIONAL CALCULATIONS

Having accomplished the one-dimensional calculations, the development of the two-dimensional axisymmetric calculational scheme was begun. The development paralleled the one-dimensional effort except that some of the coding needed to be generalized for two-dimensions. Much of the one-dimensional coding was directly applicable to the two-dimensional version of STEALTH because both are structured the same. Eight calculations were performed to cover a range of sediment strengths and entry velocities as shown in the following matrix:

Shear Strength	Penetrator Velocity, m/s			
	15	30 Baseline	30 Without Dynamic Pressure	60
Baseline, Eq. 8	X	X	X	X
5X Eq. 8		X		
20X Eq. 8	X	X		
at 5 m depth		X		

Five calculations were done with a penetrator velocity of 30 m/s with four different sediment shear strengths. This velocity is approximately the maximum freefall velocity of these penetrators. One of the calculations at 30 m/s and with the baseline shear strength was performed without dynamic pressure to see if the hole would close under geostatic stresses alone. The hole did not close in one-dimension but it was felt that it may in two-dimensions because there may be more shearing and hence plastic flow. Two calculations were done with a 15 m/s penetrator velocity to see the effects of reducing the dynamic pressure ($1/2\ \rho_w\ v_w^2$) by a factor of four from the baseline penetrator velocity (30 m/s). One calculation was performed for a boosted penetrator (60 m/s) as it is a possible alternative to the freefall deployment method.

All eight calculations were set up the same except for the sediment shear strength and the radial boundary condition (velocity and pressure). The initial zone size was 0.2 m both horizontally and vertically growing geometrically by 10 percent. The grid was 10.2 m square (19 x 19 zones) with nonreflecting boundaries imposed on both the bottom and side. An automatic continuous rezoner was used which attempts to keep the grid points equally spaced. Ten percent of the rezone block is rezoned each cycle which means that each point is rezoned once every ten cycles. The rezone block extended from the second column ($i = 2$) to the fifteenth column ($i = 15$) horizontally and the second row ($j = 2$) to the fifteenth row ($j = 15$) vertically.

The boundaries are not rezoned and the rest of the grid not specified as in the rezone block is Lagrangian.

The boundary conditions to simulate the penetrator are essentially the same as earlier reported in the one-dimensional calculation section (Eqs. 9 and 11) except the time parameter, t, that is used is given by:

$$t = t_c - \frac{z}{v_p} \qquad t_c \geq \frac{z}{v_p} \tag{14}$$

where t_c is the time in the computer simulation, z is the depth, and v_p is the penetrator velocity. Equation 14 takes into account the time required for the penetrator to arrive at a given point. For t_c less than z/v_p, the radial (or horizontal) velocity is set to zero although the vertical velocity can be nonzero as the stress wave propagates down from the penetrator. Because Equation 11, which is used for the first millisecond, was utilized for all the two-dimensional calculations, the velocity from Eq. 10 had to be increased by 9 percent, 20 percent and 49 percent for the 15, 30, and 60 m/s calculations, respectively. After the penetrator passes a given point, the pressure boundary condition is applied (Eq. 1).

The geostatic stresses were loaded into the stress tensor prior to the calculation by assuming the sediment was normally consolidated and hence the vertical stresses were equal to:

$$\sigma_{zz}(z) = \rho_s \, g \, z \tag{15}$$

The horizontal stresses (σ_{xx} and σ_{yy}) were related to the vertical stress by:

$$\sigma_{xx} = \sigma_{yy} = \frac{\nu}{1 - \nu} \sigma_{zz} \tag{16}$$

where ν is Poisson's ratio (0.48 for these calculations). With this high Poisson's ratio the geostatic stresses are nearly hydrostatic. To be compatible with the initial compressive strains, the volumetric strain was calculated from the pressure [1/3 (σ_{xx} + σ_{yy} + σ_{zz})] and the bulk modulus, K.

The calculations for the baseline sediment shear strength (Eq. 8) and penetrator velocity (30 m/s) with and without dynamic pressure, Calculations 3 and 4, respectively, will be presented in some detail while the other six calculations will only be discussed briefly. The grid and velocity vector plot at 0.014 s of Calculation 3, which includes the dynamic pressure term is shown in Figure 7. The penetrator can be seen in the bottom left of the grid heading upward (gravity is also upward). The grid is inverted because it was easier to load the geostatic stresses that way in the code. The effect of rezoning is evident in the bottom left part of the grid, since the columns are moving outward to the right, and the rows are moving

upward in an effort to maintain equal spacing in the zones that are being deformed near the penetrator nose.

At a later time (0.092 s), the grid for the first ten rows and columns are shown in Figure 8. The penetrator is at a depth of about 2.8 m. Notice the zones at the point of entry at the very bottom left of the grid. The jetting of this zone, which was caused by the high pressure induced by the penetration process, has resulted in severe distortion and collapse of the zone immediately to the right. This collapse has reduced the time step from 1×10^{-4} to 6.6×10^{-7} s. This reduction in time step effectively stopped the computer run in that it would have taken over 100,000 additional cycles to complete the problem to a simulation time of 0.200 s. To overcome this problem, the grid line defined by $i = 2$ was removed using a standard feature of STEALTH. An exploded view of the grid with the grid line removed is shown in Figure 9. The zones are much better proportioned which allowed the time step to grow by at least a factor of fifty. With the larger time step the calculation was continued.

Figure 10 shows the grid at a time of 0.122 s, a short time after the pressure boundary was applied. The hole does begin to close. Later in time at 0.173 s, the penetrator tip is at a depth of 5.2 m and the hole is closed for the top 1.3 m (Fig. 11). This calculation was run to a time of 0.200 s at which time the penetrator tip was at a depth of 6 m and the hole was closed for the top 2+ m. The time step from the time of the i-line removal at 0.092 s remained approximately constant to the end of the problem (0.200 s). The hole closure process actually helped maintain the large time step in that the zones that were badly deformed by the penetrator nose were pulled back to tne axis which reduced their distortion.

Calculation 4 was the same as Calculation 3, which was just presented except that the dynamic pressure was not included in the boundary pressure after the penetration passed. Because this calculation was the same up to a time of 0.1115 s, Calculation 3 was restarted at this time with the new pressure boundary and run to 0.200 s. The restarting capability saved computer and labor time. Without the dynamic pressure to pull the grid toward the axis, the jetting zone caused another time step problem. To overcome it, that zone was treated as an independent mass point (i.e., it was ignored). Grid plots at 0.129 s and 0.185 s are shown in Figures 12 and 13, respectively. From these figures it can be seen that the hole does not close. This is in contrast to Calculation 3 which does have the dynamic pressure applied (see Figs. 10 - 11).

The results of Calculations 3 and 4 confirmed the results of the Calculations 1 and 2 (the one-dimensional calculations). The hole closed with dynamic pressure and stayed open without it. One difference between calculations 3 and 1 was that the hole closed faster in Calculation 3 (2-D) than in Calculation 1 (1-D). At the two meter depth, the hole closed in 0.021 s after the passage of the

penetrator for Calculation 3. For Calculation 1, the time to closure was 0.031 s. The reasons for the shorter time are that the one-dimensional Calculation 1 had a higher shear strength because it was a simulation at the 10 m depth, and there is more shear deformation developed in the two-dimensional calculation.

Having developed the methodology for the two-dimensional calculations, six other parametric calculations that varied the penetrator velocity (and hence dynamic pressure) and sediment shear strength. The time-to-closure at the 2 m depth for the 30 and 60 m/s penetrator velocity and at the 0.5 m depth for the 15 m/s penetrator velocity are given below.

HOLE CLOSURE TIMES

Shear Strength	Penetrator Velocity 15 m/s	30 m/s Baseline	60 m/s
Baseline, Eq. 8	26 ms*	21 ms+	10 ms+
5X		22 ms+	
20X	53 ms*	31 ms+	
5 m		21 ms+	

*at 0.5 m depth

+at 2 m depth

All of the holes closed; the higher the velocity and lower the sediment shear strength the faster was the process. From the above results, it appears that hole closure is relatively assured for the assumptions made in the study. The importance of the dynamic pressure model is evident and the non-uniform pipe diameter analogy (Eqs. 5 - 7) must be implemented in the code.

The computer resources varied from run-to-run. The later two-dimensional calculations took less computer time than did Calculations 3 and 4 because the grid was dezoned earlier (at 0.08 instead of 0.09 s). This reduced the number of cycles required by approximately one thousand. The typical resources used for one two-dimensional calculation is given below:

Simulation time, s	0.190
Cycles	5000
Computer Time, s (CDC 7600)	1485
Cost, $	220

CONCLUSIONS

The hole closure behind an advancing penetrator in a deep ocean sediment was simulated in both a one- and two-dimensional version of a finite-difference wave propagation computer code. The penetrator was modeled by imposing a radial velocity history to the axis of the grid. After the passage of the penetrator, a pressure boundary was applied that was based on an analogy to flow in a pipe. Some of the techniques used in the computer simulation were automatic rezoning, row dropping, elastic-plastic material models with a depth dependent shear strength, nonreflecting boundary conditions, switching from velocity to pressure boundary conditions, geostatic stresses, and restarting capabilities.

For this study, the developed pressure boundary condition in the wake of the penetrator was simplified by assuming that the sediment flow-in was small relative to the water flow-in. This assumption is good right after the penetrator passes a point but worsens as the hole closes. The effect of this assumption on the hole closure process is unclear and must be investigated. In any event, the calculations done to date show that the hole closes behind the penetrator for penetrator velocities of 15, 30, and 60 m/s and 1X, 5X, 20X the baseline shear strength. When the 30 m/s penetrator velocity was run without the dynamic pressure term ($1/2\ \rho_w\ v_w^2$), the hole did not close. This highlights the importances of having the correct pressure boundary conditions on the side of the hole.

REFERENCES

1. Subseabed Disposal Program Plan, Volume I: Overview, SAND81-0007/I, Sandia National Laboratories, Albuquerque, NM, July 1981.

2. Karnes, C. H., Dawson, P. R., Silva, A. J. and Brown, W. T., "Sediment Mechanical Response Due to Emplacement of a Waste Canister", Proceedings of the Sixteenth Annual Conference of Marine Technology, Marine Technology Society, Washington, D.C., October 6-8, 1980.

3. Canfield, T. and Burchett, S. N., "Hole Closure Calculations Using HONDO II and MARBLE", Seabed Disposal Program Annual Report, January 1, 1981 to September 30, 1981, Volume II, Sandia National Laboratories, Albuquerque, NM.

4. Hofmann, R., STEALTH, A Lagrange Explicit Finite-Difference Code for Solids, Structural, and Thermohydraulic Analysis, EPRI NP-176-1, Revision, Electric Power Research Institute, Palo Alto, CA, April, 1978.

5. Vennard, J. K., Elementary Fluid Mechanics, 4th Edition, John Wiley and Sons, Inc., New York, 1961.

6. Karnes, C. H., Burchett, S. N. and Dzwilewski, P. T., "Optimized Design and Predicted Performance of a Deep Ocean 50 m Piston Coring System", Oceans '80 Conference, IEEE Publication Number 80CH1572-7, Seattle, WA, September 8-10, 1980.

7. Lysmer, J. and Kuhlemeyer, R. L., "Finite Dynamic Model for Infinite Media", Proc. ASCE, J. of the Eng. Mech. Div., Volume 95, EM4, August 1969.

8. Von Neumann, J. and Richtmyer, R. D., "A Method for the Numerical Calculation of Hydrodynamic Shocks", J. Appl. Physics. 21, pp. 232-237, 1950.

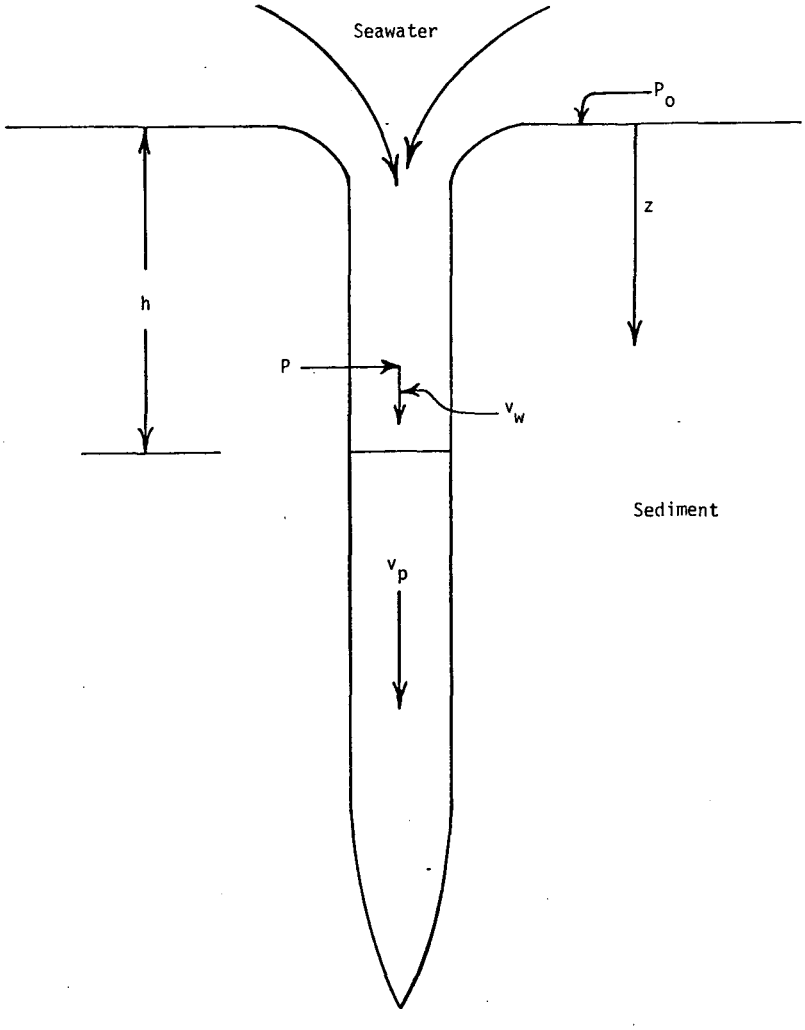


Figure 1. Schematic of Hole Closure Problem

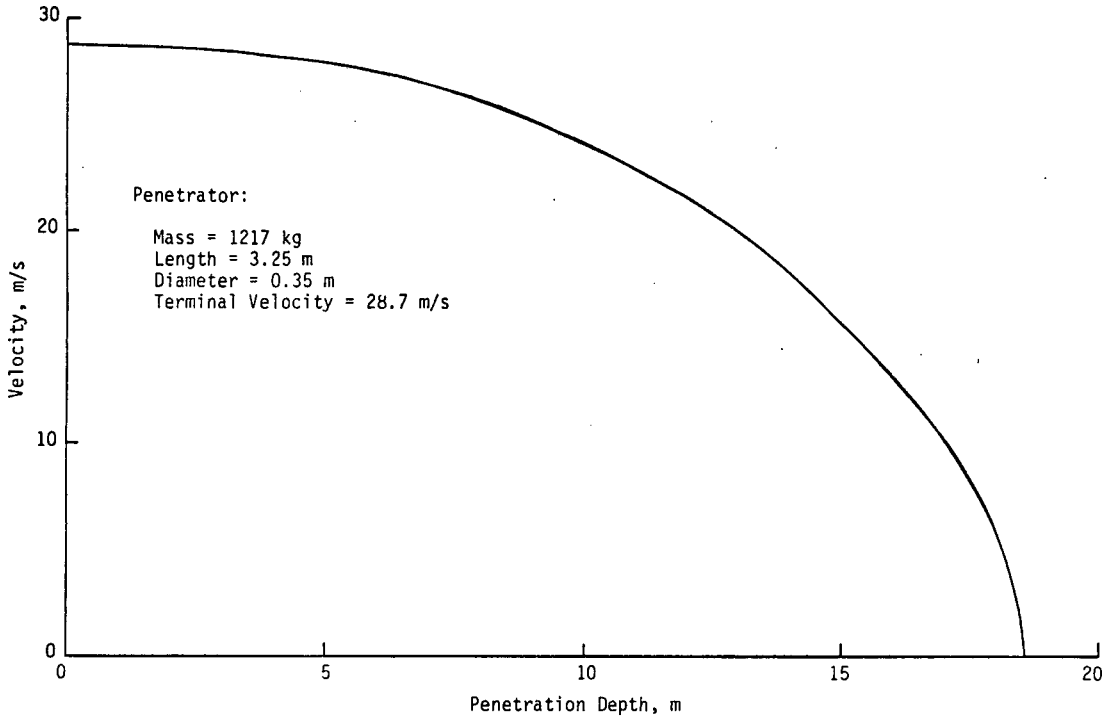


Figure 2. Velocity versus Depth for a Typical Penetrator

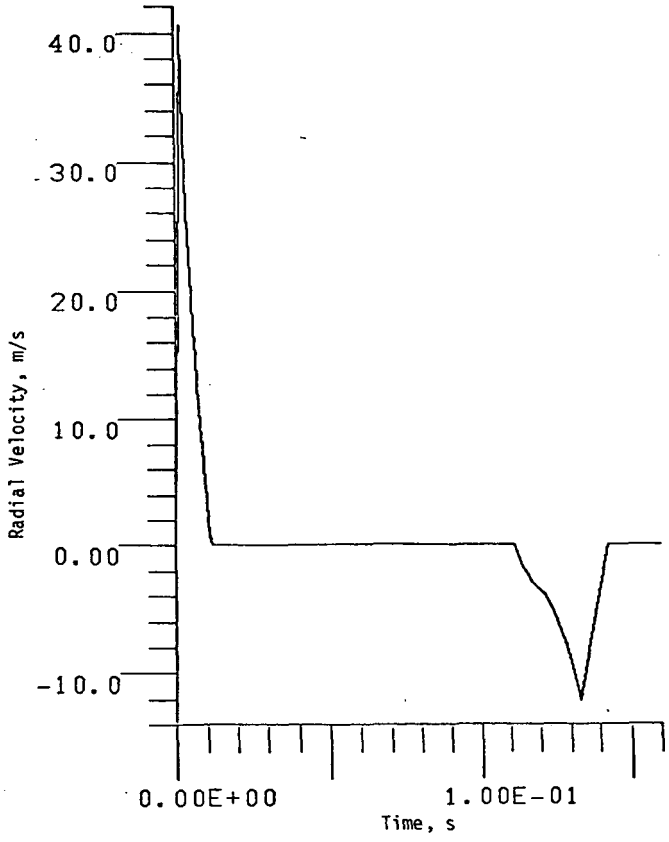


Figure 3. Radial Velocity Time History for Calculation 1 (Dynamic Pressure Included)

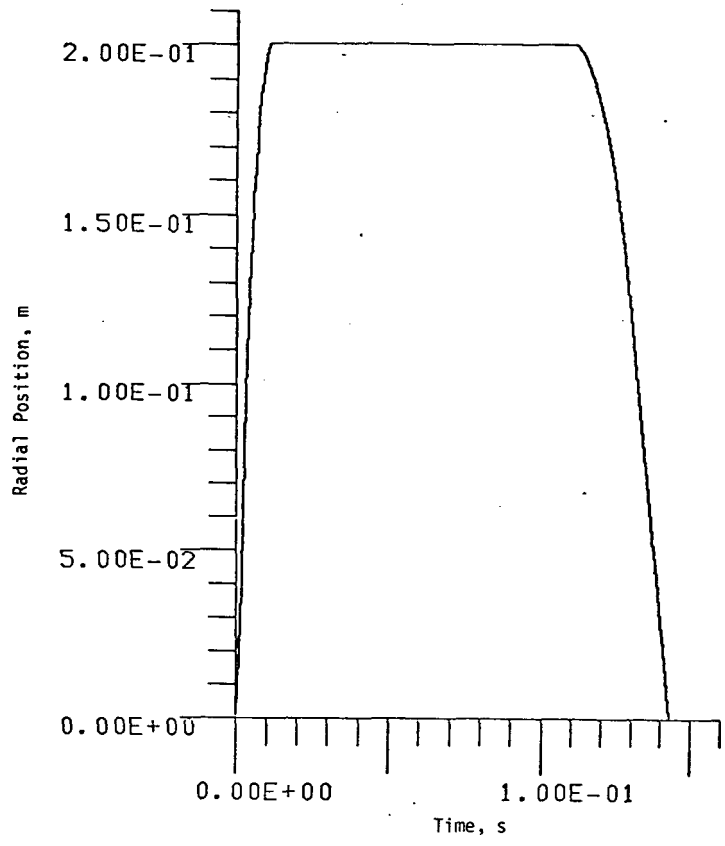


Figure 4. Radial Position Time History for Calculation 1 (Dynamic Pressure Included)

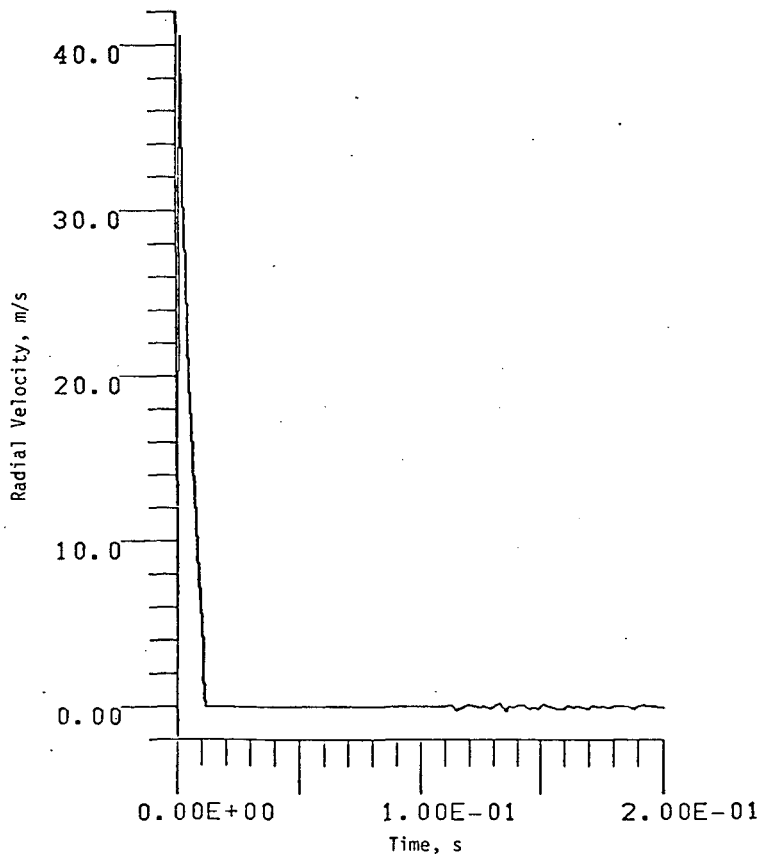


Figure 5. Radial Velocity Time History for Calculation 2 (Geostatic Stresses Only)

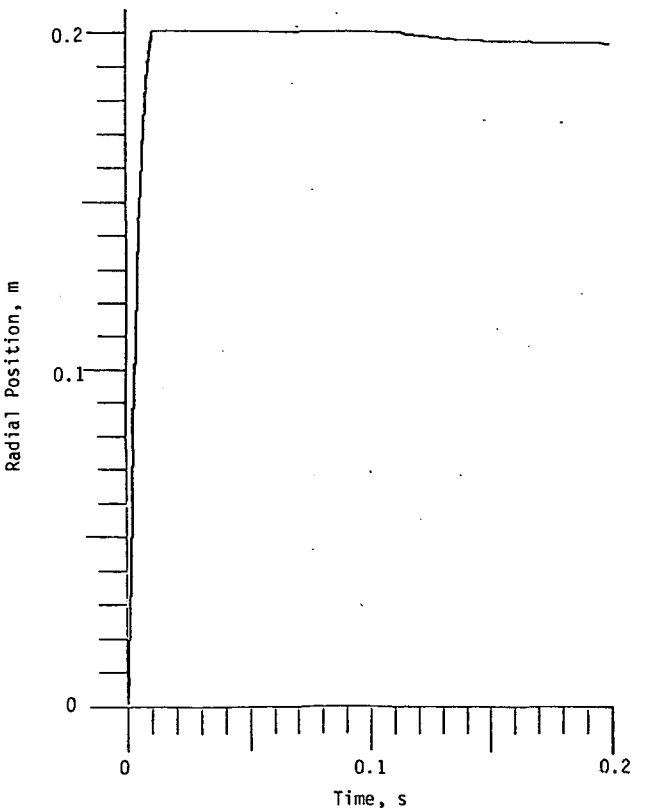


Figure 6. Radial Position Time History for Calculation 2 (Geostatic Stresses Only)

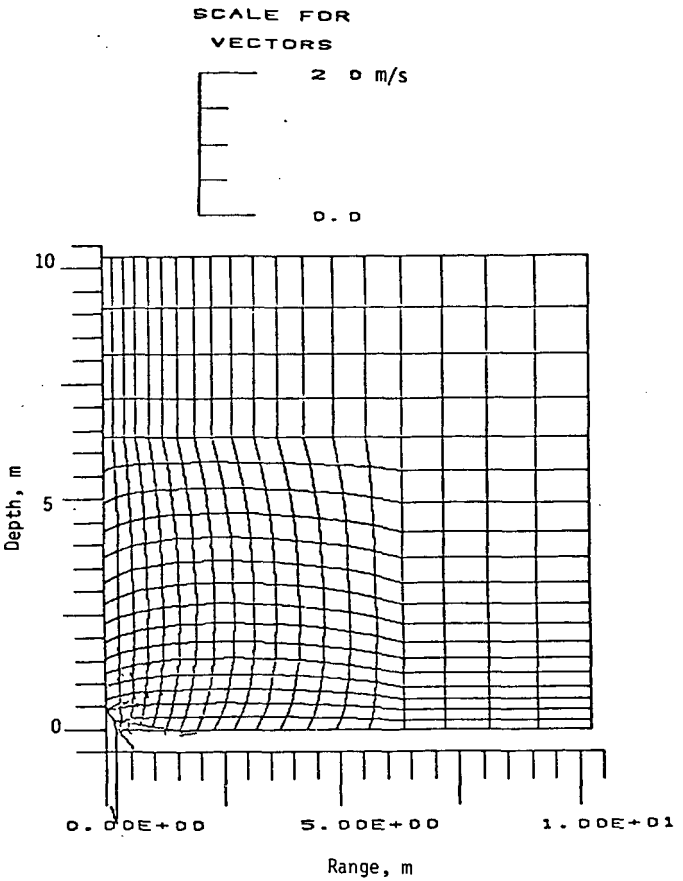


Figure 7. Grid and Velocity Vector Plot at 0.014 s for Calculation 3 (Dynamic Pressure Included)

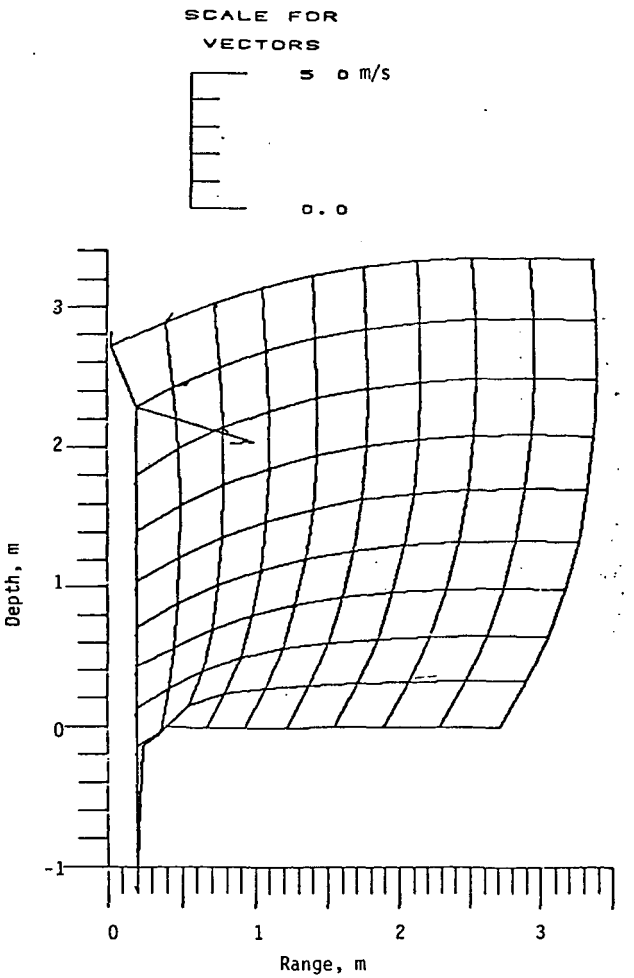


Figure 8. Grid and Velocity Vector Plot at 0.092 s for Calculation 3

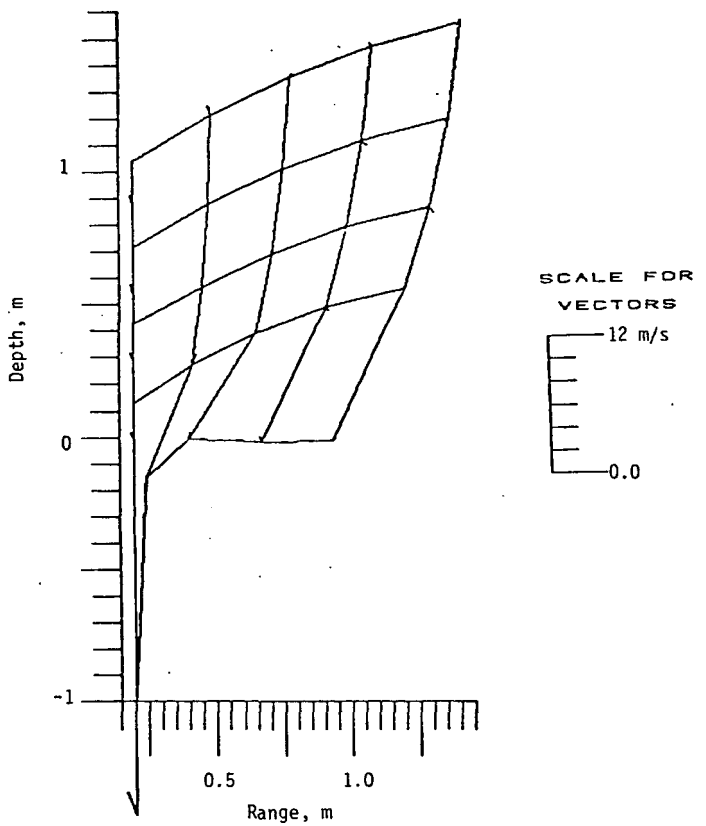


Figure 9. Expanded Grid Plot of Calculation 3 after Dezoning at 0.092 s

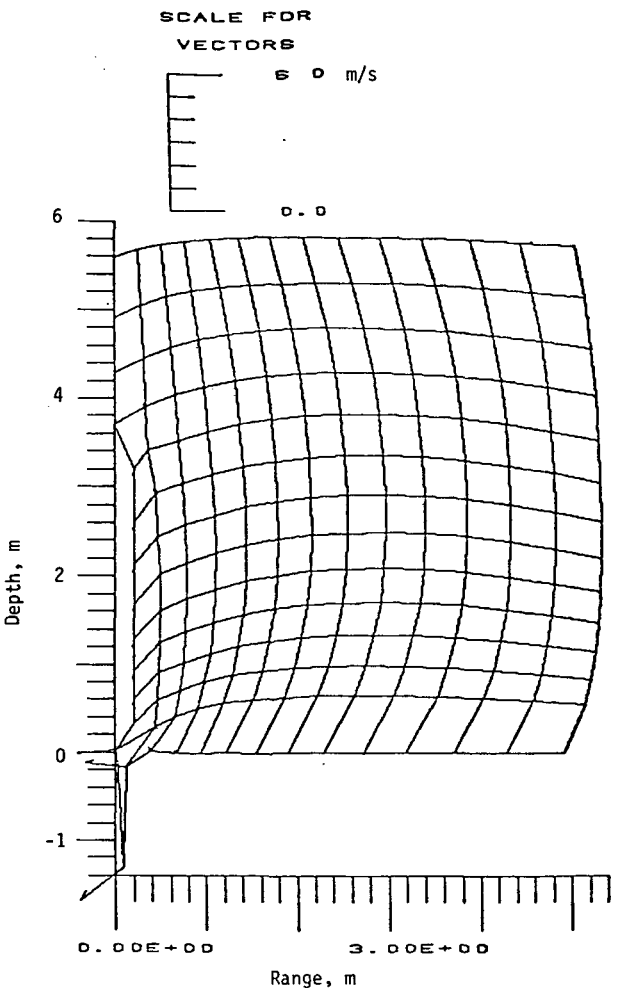


Figure 10. Grid and Velocity Vector Plot at 0.122 s for Calculation 3

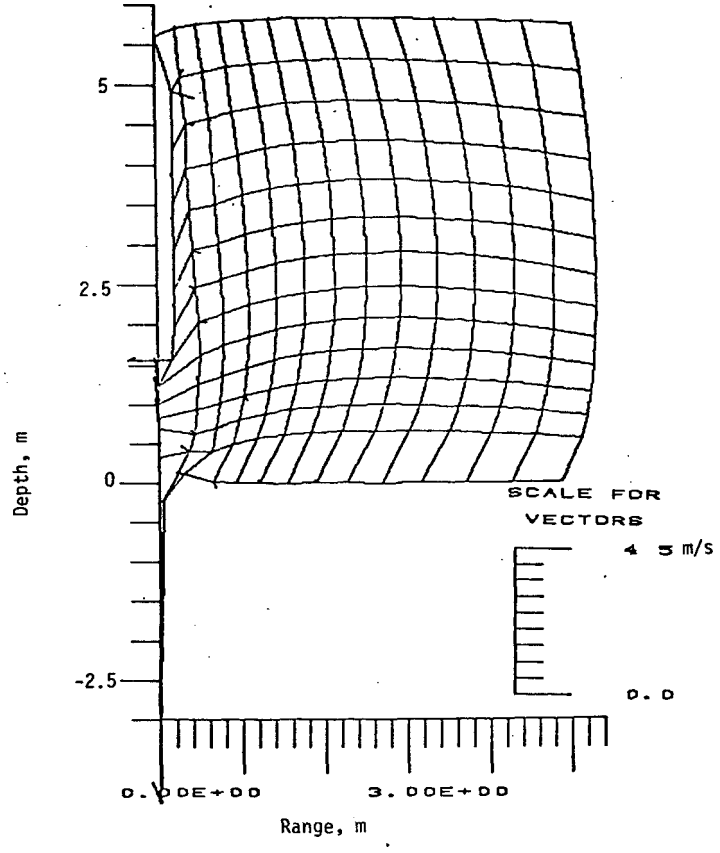


Figure 11. Grid Velocity Vector Plot at 0.173 s for Calculation 3

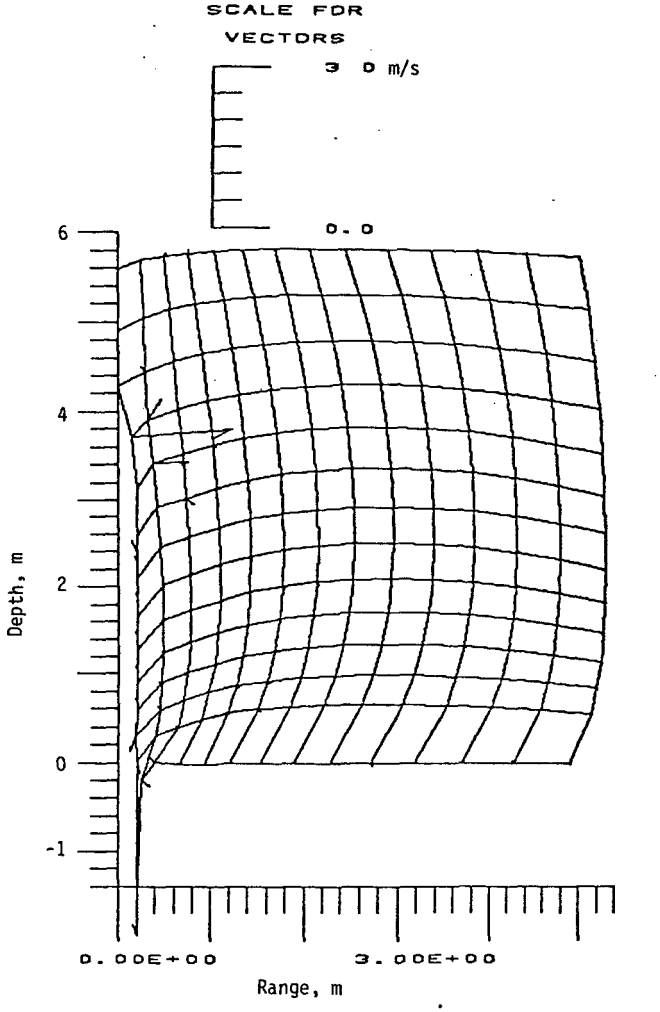


Figure 12. Grid and Velocity Vector Plot at 0.129 s for Calculation 4 (Geostatic Stress Only)

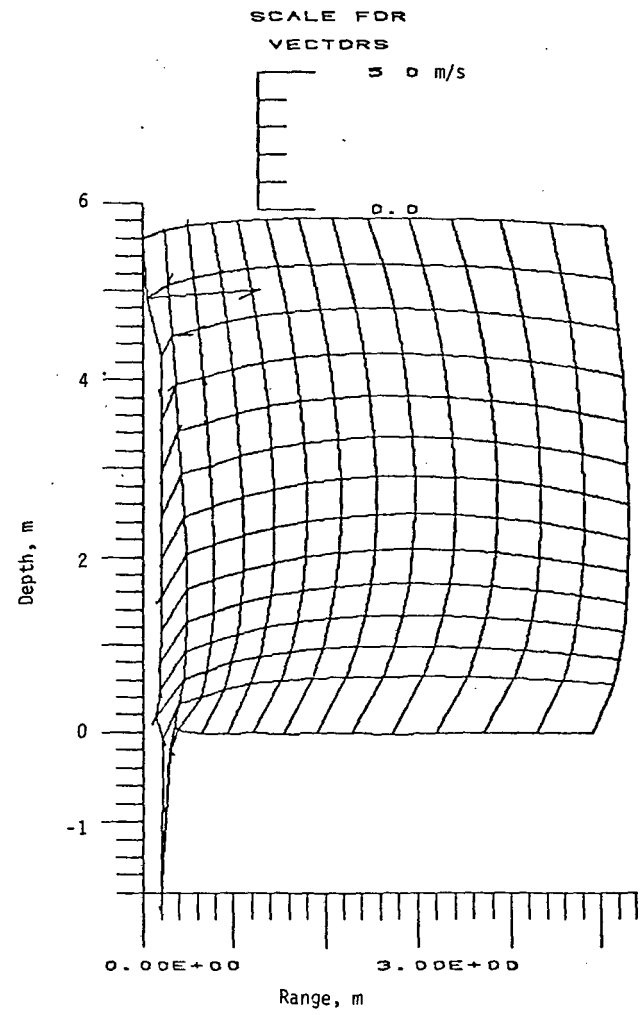


Figure 13. Grid and Velocity Vector Plot at 0.185 s for Calculation 4

APPENDIX HH

CONCEPTUAL SHIP DESCRIPTION

Marvin M. Miller and Chrys Chryssostomidis

Massachusetts Institute of Technology

(Contract #74-1104)

and

Clinton G. Shirley

Sandia National Laboratories

SUBSEABED NUCLEAR WASTE DISPOSAL: CONCEPTUAL SHIP DESCRIPTION

prepared by
Marvin M. Miller
Department of Nuclear Engineering

and
Chrys Chryssostomidis
Department of Ocean Engineering
*Massachussetts Institute of Technology (MIT)

and
Clinton G. Shirley
Transportation Technology Center (TTC)
Sandia National Laboratories

*MIT work sponsored by TTC under
Sandia Contract 74-1104

ABSTRACT

Concepts for transporting radioactive waste by ship from a specialized port facilty to an ocean site for disposal in the subseabed have been investigated to develop a reference transportation system for risk analysis purposes. The investigation included ship design requirements, radioactive material storage methods, and methods of handling this material during loading at the port and in preparation for emplacement in the subseabed. In this phase of the work, emplacement of free-fall penetrators was assumed. The design concept has been developed from a review of existing and developing technologies for handling and storage of radioactive materials and from considerations of shipboard conditions. The concept incorporates transfer casks for loading the ship with assembled penetrators, a water pool for storage aboard ship while in transit, and individual drop stations in the pool for the penetrators. The concept is described at a level of detail which elucidates the main ideas; the direction of further analyses which would be required in order to carry concept development forward is also indicated.

INTRODUCTION

The objectives of the present phase of the Subseabed Nuclear Waste Disposal Program (SDP) include the evaluation of scientific and environmental feasibility of the subseabed disposal concept. A significant effort in the evaluation of environmental feasibility involves a preliminary assessment of public and occupational risk and safety. A portion of this assessment is associated with the nuclear waste transportation segment of the disposal cycle. To perform this portion of the assessment, conceptual characterization of the transportation system, including shipping equipment, operations, and logistics, is required.

The sequence of transportation activities involved in moving nuclear waste from the generation sites to the subseabed location for disposal may be broken down into five basic steps:

1) Overland transportation of waste from generation sites to port facilities,

2) Shoreside waste storage and monitoring and disposal package preparation at port facilities,

3) Transfer of disposal packages from shoreside storage to shipboard storage,

4) In-transit shipboard storage and monitoring of disposal packages, and

5) Ship off-loading for emplacement of disposal packages in the subseabed.

To support the risk and safety assessment effort, the Transportation Technology Center (TTC) at Sandia National Laboratories is performing two tasks:

- Development of reference descriptons of the transportation equipment, operations, and logistics for a conceptual subseabed disposal transportation system; and

- Provision of technical assistance to the risk and safety analysis activities of the Subseabed Disposal Program.

The reference transportation system description will be completed in FY 1982 to support the completion of a preliminary risk and safety assessment in FY 1983, which will be included in the 1983 SDP Status Report.

In FY 1981, the Nuclear Engineering and Ocean Engineering Department of the Massachussetts Institute of Technology (MIT), under TTC sponsorship, performed an evaluation of ship design requirements and alternatives and provided recommendations for a reference ship design concept

for transporting nuclear waste at sea to subseabed disposal locations. This report describes the analyses performed and the recommendations made by the MIT investigators.

REFERENCE WASTE EMPLACEMENT CONCEPT

It is assumed that canisters of spent fuel (SF) or solidified high-level waste (HLW) from SF reprocessing have arrived at the port facility and are stored awaing transfer to ship. It is recommended that any further treatment of the waste and disposal package preparation be carried out at the shore facility instead of on board the ship. This greatly reduces the hazards and difficulties associated with waste handling on board the ship and allows centralization of disposal package preparation equipment.

Considering the free-fall penetrator method[1] to be the reference waste emplacement concept, preparation of the disposal package entails the attachment of ballast material and fins to the waste canisters. The amount of ballast material is determined by the required terminal velocity of the package as it impacts the seabed in order to achieve a desired penetration. The fins are sized in order that the package will be directionally stable and will thus fall vertically when released from the ship. The configuration for the complete disposal package (henceforth called the penetrator) used to develop the reference ship description is shown in Figure 1.

Assuming a penetrator terminal velocity of about 55 m/sec is required to achieve adequate emplacement penetration, the disposal package characteristics are estimated to have the following values:

L_p = 5.0m
l^p = 3.0m
D_p = 0.4m
d_p = 0.35m
c_p = 1.0m
h_b = 0.22m
Ballast mass = 2669.8kg.
Total mass = 3440.5kg

These parameters are defined in Figure 1. This configuration is estimated to provide a stability of $\delta = 0.0008L_p$, where δ is the position of the neutral point aft of the centre of gravity.

TRANSFER FROM SHORE STORAGE TO SHIP

The penetrator in its assembled form is assumed to be stored in the shoreside facility ready for transfer to the ship. Again, the importance of having prepared the disposal package at the shore facility is emphasized. No operations on the penetrator are considered in the reference

concept to take place on board the ship, except at the loading and disposal stages.

Two basic concepts for transfer to the ship were considered. The first involves the transfer of the penetrators through a tunnel and the second involves the use of a steel transfer cask (different from the cask used for the land transportation).

In the tunnel transfer method, the penetrator is transferred directly into the ship through the ship's side. In order to satisfy the radiation shielding requirements, the penetrators would be moved in a tunnel sufficiently filled with water or with adequate wall thicknesses. Technically, this method is feasible but a number of disadvantages exist:

1) Degradation of the structural integrity of the ship,

2) The tunnel size must accommodate and is dependent upon penetrator and transfer equipment sizes,

3) The ballasting of the ship must be very precise to assure proper alignment and may introduce an undesirable limitation on the ship size,

4) The mating requirement is difficult but not impossible.

In the transfer cask method, the penetrator is removed from the shore storage and placed in a transfer cask for transfer to the ship. The possibilities depend on whether a "hot cell" or a water pool is used to load the penetrator into the transfer cask and later to unload it aboard the ship. As described in the next section, water pool storage is the recommended shipboard waste storage method. Considering this, the most simple arrangement in terms of minimizing equipment requirements and waste handling operations would be to load and unload the transfer cask in port facility and shipboard water pools. Because the transfer cask method is is uncomplicated and is a demonstrated technology at existing nuclear facilities, it is recommended and considered as the reference method for transferring the nuclear waste from the port facility to the ship. Further details of the reference port/ship interface are being developed for risk analysis purposes and will be described in the reference transportation system description under preparation at the TTC.

SHIPBOARD WASTE STORAGE

At present, spent light-water reactor (LWR) fuel is stored under controlled conditions in water-filled pools at the reactor sites. The water serves to shield personnel from gamma radiation from the stored fuel and is also used to remove heat generated by radioactive decay. The water is continuously purified to remove both fission and corrosion products. Wet storage of LWR fuel is today a well-proven technology on an industrial scale and, therefore, the adaptation of the concept to ship conditions is

an obvious choice for temporary shipboard storage of either canistered spent fuel or high level waste prior to subseabed disposal.

Various dry storage modes are currently under development for possible application to both at-reactor (AR) and away-from-reactor (AFR) storage of canistered spent LWR fuel which has been out-of-core long enough that heat transfer from the fuel to its environment is efficient enough to ensure that fuel temperatures are well below values which would lead to significant degradation over the long-term. The basic question regarding dry storage is: what are its advantages compared to wet storage of spent LWR fuel or HLW, and are these germane in the present context?

Of the various dry storage modes now under development[2], the air-cooled vault -- wherein the canistered spent fuel is stored in closely spaced, vertical stacks in a large concrete bunker, and cooled by natural convection of air flowing directly through the structure -- seems to be the most attractive alternative to wet storage for this mission. The potential advantage of the dry storage alternative is that its packing density is comparable to that of wet storage, and there is no necessity for forced circulation of air for heat removal, thus precluding the impacts resulting from the loss of ability to circulate the coolant.

In addition, since packaging requirements for disposal in the subseabed will be quite exacting, it is unlikely that any additional packaging of the waste form will be required to facilitate heat transfer. Thus, the application of the air-cooled vault storage mode to the subseabed disposal mission merits further analysis. However, since AR pool storage is a well-proven technology for spent fuel, and its use here poses less stringent requirements than in that application, it has been chosen as the basis for the reference ship concept in this study.

GENERAL CONSIDERATIONS FOR SHIPBOARD POOL STORAGE

As previously indicated, the handling and storage of radioactive materials under water is a standard method in the nuclear industry. Spent fuel has been routinely stored in water pools for many years: the first reactor pool associated with operations of the Manhattan District, was put into service in the US in 1943, and the first commercial pools for storage of pressurized water reactor (PWR) and boiling water reactor (BWR) spent fuel were completed in 1957 and 1960, respectively. By contrast, the mission under consideration here is a new one, and at first glance, it might seem that it would pose some unique challenges. This is indeed the case, but the challenges have much more to do with the novel scheme suggested here for loading the penetrators into the ship pool and disposing of them at sea than with storage of the materials while the ship is under way. This is because, as compared with AR storage of spent fuel:

(1) The average heat load is both smaller per metric tonne of heavy metal (MTHM), and the design does not have to provide for the contingency of accepting a full core from the reactor under emergency conditions.

The heat rate of spent fuel varies with the composition of the fresh fuel, its burnup (MWD/MTHM) and specific power (MW/MTHM), and the length of time it has been out-of-core. The heat rate of typical LWR spent fuel which has been out-of-core for 10 days, 1 year, and 10 years is about 100KW/MTHM, 10KW/MTHM and 1KW/MTHM, respectively. For the purpose of this study, each penetrator was assumed to contain either one irradiated PWR assembly weighing about 0.5 MT, or the high-level waste from reprocessing three such assemblies. Since the heat from spent fuel during the first several hundred years after discharge from the reactor is primarily due the fission products contained in the high-level waste, the heat rate per penetrator would be about 0.5KW and 1.5KW for 10 year old spent fuel (SF) and for high-level waste (HLW), respectively. Thus, for a carrying capacity of 512 penetrators -- selected as a nominal capacity for the reference ship on the basis of analyses described in the remainder of this report -- the total heat rate would be about 250KW = 8.53×10^5 BTU/hr and 750KW = 2.56×10^6 BTU/hr for SF and HLW, respectively. (By contrast, the maximum design heat load at a typical LWR pool; e.g. at the 810 MWe St. Lucie 2 PWR Station in Florida, is 2.99×10^7 BTU/hr.)

(2) As in (1), the water shielding requirement is also smaller due to the smaller gamma activity of the 10-year old SF or HLW. For example, the total gamma activity per SF/HLW penetrator in curies is about $3.5 \times 10^5 / 1.1 \times 10^6$ and $4.7 \times 10^4 / 1.4 \times 10^5$ for material out-of-core for one and ten years, respectively.

(3) Credit can be taken for the fact that the waste material will have been packaged in a manner consistent with maintaining its integrity while buried in the subseabed for many years. This implies that: (i) there may be no need for a pool water purification system, especially in view of the relatively short storage period before disposal, and (ii) the probability of a criticality event for a cargo consisting of SF is low because a necessary condition would be that water penetrate the encapsulation and come into contact with the contained fuel assemblies. For HLW there is no possibilty of criticality since the fissile material has been almost entirely removed.

(4) The structural design does not have to take into account the possibility of seismic events. On the other hand, it is necessary to ensure pool integrity for the range of possible accidents at sea.

RADIATION SHIELDING

The determination of the water thickness required to reduce the dose rate at the water-air interface at the top of the pool to a specified level is a standard procedure for AR storage of SF. It is approached here in two ways: (1) an analytical approximation and (2) a computer analysis. The determination of water thickness required at the sides is not standard because land-based pools are built with thick concrete walls to maintain

structural integrity in the event of seismic disturbances, and the concrete also provides the required shielding. In the ship pool, concrete is not used, and the penetrators must be spaced far enough from the side walls to reduce the dose rate to acceptable levels. This calculation has been performed using a computer analysis only.

ANALYTIC SHIELDING APPROXIMATION

The basis for this approach is the standard buildup flux formalism[3] which is useful when a one-dimensional approximation of the source/shield geometry is a sufficiently accurate model of the physical situation; e.g., an infinite planar source emitting gamma rays isotropically from its surface, which is located at the back of an infinite slab shield of given thickness as a model for planar source and shield of finite extent in a situation where edge effects are not important. In our case, this situation applies, and the calculation for the required pool top water shielding thickness proceeds as follows:

(1) The gamma ray intensitites per energy group for a single PWR assembly of height 3.66 meter irradiated to a burnup of 33,000MWD/MTHM at a specific power of 37.3 MW/MTHM which has been out-of-core for 10 years were taken from ORIGEN code[4].

(2) The heavy metal content is assumed to be homogeneously distributed throughout each unit cell of a rectangular (16x32) penetrator storage array. Since the unit cell cross section is a 1.25 meter side square, the active source volume is $(1.25)^2 \times 3.66 \times 10^6 = 5.72 \times 10^6 cm^3$. The equivalent volume source $S_v(E)$ for each energy group (in units of $cm^{-3}sec^{-1}$) is then given by $I(E)/5.72 \times 10^6$, where I(E) is the gamma-ray intensity of the assembly at the group energy E.

(3) To convert $S_v(E)$ to an equivalent surface source, we must take into account the self-shielding of the volume source. This, in turn, is a function of the relative amounts of material within each unit cell; e.g., heavy metal and lead ballast material within the penetrator and water without. To be conservative, the attenuation was assumed to be due solely to water. The equivalent surface source density $S_A(E)$ for each energy group is then given by[5]

$$S_A(E) = \frac{S_v(E)}{\mu(E)} \left[\frac{A_1}{(1+\alpha_1)} + \frac{A_2}{(1+\alpha_2)} \right] , \qquad (1)$$

where A_1, A_2, α_1, and α_2 are tabulated functions of energy and material (water in this case) which arise in the Taylor form of the buildup factor and $\mu(E)$ is the mass attenuation coefficient for water in units of cm^{-1}.

(4) Finally, the thickness of the water shield a can be deduced from the equation for the dose rate $\dot{X}$[6].

$$\dot{X} = \sum_E \left\{ 0.0659\, E\, (\mu a/\rho)^{air} \right\} \frac{S_A(E)}{2} \left\{ A_1 E_1 [(1+\alpha_1)\mu(E)a] + A_2 [E_1(1+\alpha_2)\mu(E)a] \right\} \qquad (2)$$

where $\dot{X}$ is in units of mrem/hr., E is in Mev and $(\mu a/\rho)^{air}$ is the mass absorption coefficent for air in cm^2/g evaluated at the energy E.

Starting with a value for $\dot{X}$ as specified by the applicable radiation protection standard, the value of a can be calculated by trial and error. Two limits have been chosen here for $\dot{X}$: 0.5 mrem/hr for areas occupied continuously by occupational personnel and 5 mrem/hr for areas not occupied on a regular basis. The latter is approximately equivalent to a maximum permissable dose (MPD) of 10 rem/yr., recommended by the National Council on Radiation Protection and Measurement (NCRP) as the retrospective annual limit for whole body occupational exposure[7]. The results of the calculation are given in Table 1 below for 10-year-old SF and HLW. The values for HLW were obtained by assuming that the gamma source was three times stronger than that for SF since, by assumption, the HLW in each penetrometer arises from reprocessing three PWR assemblies.

Table 1

Water Thickness for a Given Exposure Rate

Exposure Rate	Water Thickness
Spent Fuel	
0.5 mrem/hr	2.39 m
5.0 mrem/hr	2.04 m
High Level Waste	
0.5 mrem/hr	2.56 m
5.0 mrem/hr	2.21 m

We noted that of the 12 energy groups specified in the ORIGEN code, only six contributed significantly to the exposure rate. These were centered at 0.63, 1.1, 1.55, 1.99, 2.38, and 2.75 Mev.

COMPUTER ANALYSIS OF SHIELDING

The same problem is now examined using computer analysis. The applicable codes are XSDRN[8] and NITAWL[9] which are used in sequence. NITAWL arranges the input data in a form suitable for XSDRN which carries out a one-dimensional transport calculation. A 27-18 cross section library was used. That is, the neutron/gamma spectrum was approximated by 27 and 18 groups, respectively[10]. Finally, two different configurations were used. In common with the analytic approximation, configuration 1 calculates the self-shielding in the zone containing the fuel as being due entirely to water. Configuration 2 is more realistic (for SF) in that it takes into account the presence in the fuel zone of heavy metal, the zircalloy fuel

clad, and the lead used for ballast in the penetrator, as well as water. The results are given in Table 2, where for comparison purposes the results of the analytic approximation are repeated. As before, the results for HLW were obtained by multiplying the gamma source strength by a factor of three. (Note that since the HLW waste will be solidified and incorporated into a matrix such as borosilicate glass, the inclusion of heavy metal and zircalloy cladding to calculate self-shielding is not appropriate in this case, although lead for ballast was still used).

Table 2

Water Thickness for a Given Exposure Rate

Exposure Rate	Configuration 1	Configuration 2	Analytic Appoximation
Spent Fuel			
0.5mrem/hr	2.53m	2.44m	2.39m
5.0mrem/hr	2.13m	2.08m	2.04m
High Level Waste			
0.5mrem/hr	2.69m	2.61m	2.56m
5.0mrem/hr	2.31m	2.26m	2.21m

For the pool side shielding evaluation, the pool was represented as alternating layers of volume source and water. It was found that due to self-shielding, the source is adequately represented by the contributions of two source layers. The results for an exposure rate of 0.5mrem/hr. are given in Table 3.

Table 3

Side Water Thickness for an Exposure Rate of 0.5mrem/hr

Spent Fuel	2.22m
High Level Waste	2.4m

To be conservative, it was decided to allow 3 meters of water shielding both at the top and at the sides of the pool. Because this requirement must also be met during loading of the penetrators as well as when they are in their storage position, 8 meters of water are actually required on top of the penetrator storage rack. Top and side views of the storage pool are shown in Figure 2.

RADIATION SHIELDING: TRANSFER CASK

The transfer of the penetrators from port to ship involves the use of a specially designed cask of cylindrical cross section. The thicknesses of the lead side walls required to reduce the exposure rate to 0.5 mrem/hr are found using the analytical or the computer methods described above. The results are given in Table 4.

Table 4.

Transfer Cask Wall Thickness for an Exposure Rate of 0.5mrem/hr.

Spent Fuel	16.3cm. (lead)
High Level Waste	18.5cm. (lead)

CRITICALITY ANALYSIS FOR POOL STORAGE

Nuclear Regulatory Commission regulations[11] for spent fuel pool storage require that a subcritical array with $k_{eff} \leq 0.95$ be maintained under worst-case accident scenarios with conservative assumptions regarding the spent fuel. The most conservative assumption, and the approach most commonly used today, is to assume a fuel composition that represents the most reactive fuel to be stored, at the most reactive point in the fuel assembly's life. For LWR fuels without burnable poison, this fuel composition requirement can be met by assuming the appropriate maximum initial U-235 enrichment. Sine AR storage represents a different situation, the probability of fresh fuel being placed in ship storage is zero. Nevertheless, this criterion has been used in most of the analysis because it serves to illustrate the large safety margin under actual operating conditions.

A variety of accidents were considered which could conceivably lead to a criticality condition. The conclusion is that the worst case would be an accident which resulted in all the penetrators being in contact; i.e., their center-to-center spacing would equal their diameter. In this final state, two configurations are possible: a square pitch and a more conservative (tighter packed) triangular pitch, as shown in Figure 3. As to the probability of this worst case, no attempt was made to arrive at a quantitative estimate, but note that two necessary conditions are that: (i) the structural supports which secure the penetrometers in position within the individual unit cells are inoperative, and (ii) water has penetrated the penetrator casings and come into contact with the spent fuel. Both of these events are considered to be highly unlikely, and the combination, of course, even more so. (Note that one of the major design criteria for the encapsulation is that it minimize the probability of contact between the waste form and water for many years).

The criticality analysis was done using several computer codes: NITAWL, XSDRN, BON AMI-2 and CASASIX[8,9]. Six cases were run and the

results are given in Table 5. As to the rationale for these choices, note that while a 4.0 wgt. % fresh fuel enrichment is higher than that used in current LWRs, thus both an additional measure of conservatism and allowance for possible future increases in LWR fuel enrichment in order to increase uranium utilization in the once-through cycle are provided.

Table 5

Criticality Analysis Results

Case	k_{eff}
1. 4 wgt. % enriched fresh fuel - square pitch spacing - no buckling	.9350
2. 4 wgt. % enriched fresh fuel - triangular pitch spacing - no buckling	.9722
3. 4 wgt. % enriched fresh fuel - triangular pitch spacing - 12 foot axial buckling	.9701
4. 3.5 wgt. % enriched fresh fuel - triangular pitch spacing - no buckling	.9502
5. 3.5 wgt. % enriched fresh fuel - triangular pitch spacing - 12 foot axial buckling	.9481
6. 4 wgt. % enriched fuel - 40,000 MWD/MTHM burnup - triangular pitch spacing - no buckling	.7972

The last two cases, both of which are still highly conservative, e.g. the assumption of zero neutron leakage (buckling) in case 6, illustrate that criticality should not be a problem for pool storage of spent fuel penetrators.

DECAY HEAT REMOVAL

The basic elements of the decay heat removal system are two centrifugal pumps installed in parallel, each of which is capable of circulating pool water at the design pump rate, and a tube and shell heat exchanger utilizing sea water (temperature = 70°F) as the coolant medium. Sufficient space is provided underneath and around the penetrator support structures so that natural circulation of the pool water is not restricted under normal or abnormal circumstances. In this way, there is no significant increase in the temperature of the penetrators even if the cooling system is not operating.

According to current Nuclear Regulatory Commission guidance, design temperature at AR storage pools are 120 - 125°F maximum for normal operation and 150°F for abnormal operation. (Experience to date shows pools

are operating at 100°F or less.) However, in order to provide an extra degree of conservatism for long-term AFR pool storage of spent fuel, the recently-issued ANSI/ANS standard for this type of installation[12] provides that the cooling system shall be designed to maintain an annual average normal pool water operating temperature of 90°F or less.

Since maintaining the integrity of the spent fuel cladding in the long-term is not an issue here, criteria for AR pool storage are probably more relevant. However, there would be no problem in adhering to either standard. For illustrative purposes, assume a pool outlet temperature of 100°F and an inlet temperature of 80°F. Then, the flow on the tube side of the heat exchanger for a maximum heat load of 750KW = 2.5×10^9 BTU/hr, corresponding to the storage of about 500 HLW penetrometers, would be about 300 gallons per minute (gpm).

If coolant circulation capacity were to be lost, the pool temperature would rise very slowly (about 11.7×10^{-2} °F/hr) due to the large quantity of contained pool water $\cong 10{,}000 m^3$ [13]. Assuming that the average water temperature was 90°F when coolant circulation capacity was lost, this implies that a period of approximately 40 days would elapse before boiling conditions were reached. Moreover, to maintain the pool water level under boiling conditions, makeup water would only have to be supplied at a rate of about 5 gpm.

It is concluded that the combination of low heat rate, large amount of pool water, and short storage time make the heat removal problem very tractable under both normal and accident conditions.

STORAGE AND DISPOSAL EQUIPMENT AND OPERATIONS

The penetrator storage pool will consist of a hold in the ship containing the penetrator storage rack and associated equipment, as well as the water used as a shielding and cooling medium. As stated previously, there will be a minimum of 3m above the level of the SF/HLW in the penetrator as well as a 3m border of water surrounding the penetrators storage location. For the latter condition, celluar wing tanks and tanks immediately fore and aft of the storage hold contain water for shielding and provide flood control in the event of an accident.

In the ship concept developed earlier for the TTC by Boeing[14], the canisters were stored on a rack which could operate as a conveyor belt. This would allow movement of the penetrator to a position near a drop station where the transfer to the drop station would be completed, using an overhead crane. The disadvantage of this method is the lack of positive control in securing the canisters during the sea transportation phase. Furthermore, with the increased number of penetrators considered here, it is necessary to have more conveyor racks and thus more moving parts and their attendant risks of failure.

Another similar concept would be to use a sliding/shuffling scheme where there is greater control of the penetrators. However, the possibility of jamming is very high.

An even more elaborate scheme is based on a carousel principle in which the penetrators would be placed at the circumference of a carousel. Transfer of the penetrometers to the drop station would be facilitated by rotating the carousel. The disadvantage of this concept would be the inefficient use of space, especially when a large number of penetrators are to be transported.

A simple stationary penetrator storage concept would be to employ an overhead crane for all the handling operations while at sea. Here, each penetrator station is immobile and any movement of the penetrator is accomplished by the crane. The crane required for this job must then have complete translation and rotation capabilities. Precise control is necessary. Possibly more than one crane may be required to span a large hold area.

A major shortcoming of all the above concepts is that it is necessary to use some form of transfer mechanism while at sea. This is undesirable since the risk of failure of the system is high, especially in hostile sea conditions. This was the motivation for adopting a stationary storage, individual drop station concept for the penetrators in the ship system.

An individaul drop station eliminates the use of cranes and unnecessary movement of the penetrators. Each penetrator will be secured in place using locking rings and fin guides above its own release mechanism. A suggested type of release system would involve ball or cylindrical valves. For purposes of illustration, ball valves are considered in the following discussion and the system shown in Figure 4. The ball valves are essentially solid spheres with a port whose diameter is large enough to allow the passage of the penetrator. The ball valves act as "gates", open when at the drop location to release the penetrator and closed otherwise. In principle, the 'gates' operate as ordinary ball valves found in pipes where fluid flow control and positive shut-off are required, but these are on a much larger scale. Control of these "gates" is accomplished by the use of remote controlled electric or hydraulic two-position actuator devices. Two valves are used to control any leakage, either from the storage pool or from the sea. As shown in Figure 4, the volume between the two valves is vented and a pump outlet is also included. Any leakage will therefore leak into this volume which is at atmospheric pressure and may be pumped out.

At the disposal stage, the storage hold will contain water in the load waterline of the ship. Each time a penetrator is discharged, a small volume of water is lost because of the slight change in draft but at no time does the level above the penetrometers drop below three meters. This is an essential feature of the design. Preliminary calculations show that the change in draft is small after disposal of the canisters. Alternatively, a torpedo tube concept may be employed where each penetrator may be sealed in a tube prior to disposal. After disposal, the tube is flushed and replenished as necessary. Again, the amount of replenishment fluid required is small (volume of each torpedo tube times

number of penetrators to be disposed). This latter concept has the disadvantgage of requiring a forced-circulation cooling system for the penetrators in the storage tubes.

The individual drop station system will impose design constraints on the ship. From a structural point, there may be a problem in longitudinal bending strength since there is a limited contribution from the small deck and bottom plating as a result of having large hatch and bottom openings. There may also be torsional strength problems and high stress concentrations at hatch corners, again as a result of the large openings. Clearly, the ship is an unconventional one, borrowing ideas from container ships, drill ships with a moonpool, and submarine torpedo tube openings. Extra care is necessary in ensuring sufficient stability, floodable length requirements and structural strength. In addition, the problem of corrosion must be investigated if this concept is adopted.

In spite of these ship design problems, this system is the preferred reference concept since the whole disposal operation is simple and reduces the handling of the penetrators at sea to a minimum. The remainder of this report describes ship design considerations as required to perform safety and risk assessments.

THE SHIP: DESIGN SPECIFICATIONS

Owing to the unusual mission requirements, a feasibility study of the ship was performed, recognizing the severe constraints imposed on size, strength and stability of the ship. As stated in the previous section, such a ship would borrow ideas from container ships, drilling ships, tankers, and submarines. Still, the loading conditions and mission characteristics are different and the following treatment should be regarded only as preliminary.

An attempt was made to size the ship to meet service requirements while maintaining reasonable ship proportions. For example, the length of the penetrator has a governing influence on the depth of the ship. Allowing 2.5m for the "gate" devices, 5m for the penetrator, 5m working area for the transfer and 2.5m above the tail end of the penetrator during transfer, a minimum depth (D) of 15m is required for the ship. Note that only 2.5m of overhead water is required for the transfer situation as the canister will be below the tail end of the penetrator as shown in Figure 1. The design length (L) and breadth (B) of the ship (see Figures 5 and 6) may be adjusted depending on the number of canisters to be transported per trip. Other factors influencing the main dimensions of the ship are steel weight costs, seakeeping considerations, slamming and propeller emergency characteristics, compatible dimensions for port facilities etc. Discussions on how each dimension influences these factors are found in references 15 and 16.

Assuming a nominal value of 512 penetrometers per trip, and assuming that each station occupies an area of 1.25mx1.25m, the breadth of the ship may be obtained. Breadth (B) = 16(1.25)+6(wing tanks)+4(allowance) = 30m

The allowance is for the unusable space in way of the ship centerline girder, as well as for the space taken up by adding an additional longitudinal bulkhead for collision protection.

The length (L) of the hold is (512/16)1.25 = 40m. Taking this to be 1/5 of the length of the ship, the ship length is thus 200m.

The ratios L/B=6.67; B/T=2.667; T/D=0.75; T/L=0.05 (where T is the draft taken to be 11.25m) are reasonable ship ratios with respect to the seakeeping and slamming considerations mentioned earlier.

Further, assuming a block coefficient of 0.74 for the above dimensions, a ship speed of about 16 knots is estimated and the displacement is 51200 tonnes. A deadweight of 42000 tonnes is expected with an assumed deadweight coefficient of 0.82. With rough estimates of lightship, machinery, wood, and outfit it can be shown that for a payload of 512 penetrometers (which is small compared with the total deadweight), suffificent and not excessive ballast may be added to match the displacement for the given ship dimensions.

Economic studies with alternative ships should be carried out to investigate which would be the most suitable combination of ship parameters and payload.

A plan view of the ship with the main dimensions and the position of the storage hold amidships is shown in Figure 5. A midship section is shown in Figure 6 together with approximate dimensions of wing tanks and layout of the drop stations. Other features shown include cellular type wing tanks, longitudinal collision bulkhead amidships and pontoon covers for the tanks. In Figure 7, the main structural members are shown in the midship section. These include longitudinal stiffeners for the decks, tank top, bottom shell and bulkheads; girders to support the penetrators; and a centerline keel girder. The extent of mild and high tensile steels used is also shown. The rationale behind the selection of these features is based on stability, capsizing, and collision considerations.

The stablility of a ship is measured by its ability to return to its equilibrium position after being subject to a disturbance. The displacements are known as keel and trim in the transverse and longitudinal directions, respectively. In the early design stages a useful index of transverse stability is the transverse metacentric height. In general, in the absence of other information, a positive transverse metacentric height (of the order of 4% of B) would indicate sufficient transverse stability in the intact condition. Preliminary calculations with approximate formulae show that for the characteristics of the ship selected, the metacentric height is positive, even after corrections were made to allow for the effects of fluid motion (often called free surface effects). The stability of the ship is further improved by the addition of a centerline longitudinal bulkhead and covers at the storage pool water level. These effectively minimize the motion of the pool fluid and prevent sloshing. The use of covers also allows a lower water level in the tanks to be kept

(instead of at deck level). Pontoon type covers are suggested, but other hydraulic or mechanically operated types may be used.[16] As shown in Figure 6, four pontoon type covers may be used, each 20mx10.5m and supported by the longitudinal and transverse bulkheads.

In the longitudinal direction, the longitudinal metachentric height is also a measure of a stability, being an index of the ship's resistance to change in trim. However, for a normal surface ship, the longitudinal metacenter is always far above the center of gravity and the longitudinal metacentric height is always positive.

As stated earlier, a positive metacentric height is only an initial indicator of stability. Care has to be exercised for ships with several freeboards: a capsizing may still occur even if the ship has a large metacentric height.[17] It is assumed here that there is sufficient freeboard to prevent capsizing.

For a detailed evaluation of intact transverse stability and criteria for capsizing avoidence, it is necessary to derive the "cross curves of stability".[17] This is only possible once the "linear plans" of the ship are available. The cross curves of stability will lead to the righting arm curve (curve of statical stability) for the least favorable loading condition. Together with heeling arm curves for various upsetting forces, all the data necessary for judging the adequacy of the ship's stability in the intact condition is obtained. For example, information is obtained on the effects of wave, wind, rudder and hull forces, maneuvering forces and forces during the loading and discharging of cargo. Limits may be obtained for the maximum angle of steady heel, the range of positive stability, the residual dynamic stability and the relative magnitudes of the heeling arm and maximum righting arm. The limits are set by various regulatory bodies governing safety of life at sea. Complete procedures covering the above are given in reference 18.

Another important criterion in the evaluation of stability is its function in enabling the ship to survive flooding due to damage. Such damage may occur as a result of collision or grounding. For minor damage, the side tanks, collision bulkheads, double bottom and twin valve system (see Figures 6 and 7) lessen the possibility of the extent of damage from reaching the penetrators. The design against collision or grounding may be treated in a probablistic manner.[19] More extensive work is found in the structural response aspect, energy absorption or resistance type protection schemes and other concepts developed for nuclear powered ships and ships carrying hazardous waste. Reference 20 presents a bibliography of recent work in this field. These same ideas are applicable to the proposed nuclear waste disposal ships and protection systems for the penetrators.

Should the shell of the ship be fractured as a result of the collision or grounding, the effects of flooding are change of draft, trim, heel, stability and ultimately loss of the ship through capsizing or foundering. For merchant ships, regulations are set by the regulatory

authorities for damaged stability, floodable length, and freeboard. The regulation pertaining to stability limits the changes in draft, trim, heel and stability as a result of damage to one or more specific compartments of a ship. In this way, it relates to the calculations of intact stability and buoyancy necessary to attain any particular desired equilibrium damage condition, as well as to the stability characteristics in that damaged condition.

The floodable length calculations are required to ensure that the ship can survive a prespecified damage.

The minimum permitted freeboard is allotted to ensure a sufficient reserve of buoyancy to accommodate damage. These calculations and the limits set by the US rules are found in reference 17. It is assumed that the ship is designed to comply with these rules.

A calculation was also performed to check the "damaged" stability condition, when the hold containing the penetrators was opened to the sea. In this condition, stability is reduced as a result of a "lost" water plane area. By dividing the hold into four compartments by the longitudinal and transverse midship bulkhead, this "lost" area is minimized, since at any time during the disposal, only one compartment will be "opened" to the sea. The results show that the metacentric height is still adequate in these cases. In addition, the designer can ballast the proposed ship in such a way to achieve any metacentric height deemed necessary.

In the preliminary feasibilty design, an objective was to determine the required scantlings or sizes of the structural members to withstand the expected maximum loads. Such loads may be still water bending moments and shearing forces, springing and impulsive loads, thermal loads, dynamic loads and other loads such as from launching, docking collapses etc. A combination of the most severe loads is usually selected as the normal design load for a given structure. It is assumed here that the most severe loads are caused by the still waters bending and torsional moments and the wave induced bending and torsional moment. A complete description of the underlying theories of bending moment calculations as well as the wave assumptions are found in reference 15. While a rational approach[20] is appropriate in estimating these bending loads, it is only possible here to call upon empirical formulae and accept some guidance from Classification Society Rules[21] to estimate these loads. It is recognized that under the above circumstances, the results of the calculation for the structural design have significant uncertainties, in view of the fact that the ship is an unconventional one. At best, conservative estimates and the use of high stress safety factors are maintained in the calculations.

Once a probable longitudinal bending moment acting at midships is determined, the stress distribution may be calculated for a given midship section[22] using simple beam theory. Permissable stresses are taken to be half the yield stress of the material used, that is, a safety factor of 2 is arbitrarily used. By checking that the stresses at any point in the section do not exceed the permissable stresses, the minimum scantlings

required for the section may be determined to meet bending strength requirements.

For the proposed ship, owing to its "open" deck and bottom, checks on torsional stresses are also important. This is done using a membrane analog theory[17]. At critical points such as hatch corners, interaction of torsional and bending stresses are checked using a failure criterion (such as the Von Mises criterion[20].

Figure 7 shows a feasible structural configuration obtained with the methodology described above. Features of this section include closed cellular wing tanks, longitudinal bulkheads and collision bulkheads. The closed cell construction contributes to torsional strength and stiffness, whereas the longitudinal bulkheads contribute to the bending strength. These are important as there is little structural support from the deck and bottom plating which would otherwise form a major part of the ship's strength. Scantlings were initially chosen to meet local strength requirements[20,21] but were subsequently increased to provide greater inertia of the section. To maintain scantlings within practical limits, higher tensile steel was chosen in the uppper and lower flanges of the section, and extending some distance along the side as shown in Figure 7.

Details of the reference ship concept design calculations will be included in the reference SDP transportation system description being prepared by the TTC.

CONCLUSIONS AND RECOMMENDATIONS

The ship system concept recommended by this study is offered as an improved alternative to other concepts by providing: a) a reduction in the number of penetrator handling operations, especially on ship, both in dock and at sea; and b) a simple penetrator release system; i.e. two-step valve operation.

Further development of the ship design in the engineering feasibility phase of the Subseabed Disposal Program will involve:

a) Improvements in penetrator design, including electronic monitoring devices, booster devices, and analysis of forces and damage possibility on impact with the sea bed;

b) Investigation in detail of ball valve design, including leakage rates, torque requirements, actuator devices, space requirements, manufacturing, installation, maintenance, and costs;

c) Design of cranes and control systems for the shore-ship cask transfer; and

d) Investigation of the impact of the inherent error in penetrator targeting.

Preliminary results so far suggest the feasibility of the disposal ship. However, areas of uncertainty exist, especially in the prediction of loads on the ship. It is recognized that the calculations performed need refinement in view of the unconventional nature of the ship to be designed. A further detailed static analysis (for the still water bending and torsional moment) and a probabilisitc analysis (for wave induced bending and torsional moments) should follow in the next phase of the SDP. Other important analyses to be performed include seakeeping analysis, floodable length and damaged stability, fatigue analysis, optimization studies for ship parameters, structural optimization, and an economic evaluation of the system. Seakeeping analysis perhaps is the next major study that needs to be undertaken because it will determine the operating characteristics of the proposed vessel. The level of detail of the current ship conceptual design is, however, considered to be adequate for preliminary risk and safety analyses.

GLOSSARY OF SHIP TERMS USED

ABS. American Bureau of Shipping

Block Coefficient (C_B). The ratio of the underwater volume of a ship to the volume of a rectangular block, the dimensions of which are the effective length, draft and beam. The relationship is expressed as a decimal.

Bulkhead (bhd.). A term applied to the vertical partition walls which subdivide the interior of a ship into compartments or rooms. Generally, the various types of bulkheads are distinguished by their location and use.

Center of buoyancy. This is the centroid of the underwater form of a ship and is the point through which the total force of buoyancy may be assumed to act. Its verticial height is measured from the keel and is denoted by KB.

Center of gravity. This is the point through which the total weight of the ship is assumed to act. Its vertical height is measured from the keel and is denoted by KG.

Center line girder. A vertical plate on the ship's center line extending the length of the ship.

Center line. The middle line of the ship, extending from stem to stern at any level.

Deadweight. The carrying of a ship at any draft and water density. Includes weight of cargo, fuel, lubricating oil, fresh water in tanks stores, passengers and baggage, crew and their effects.

Deck. A platform in a ship corresponding to a floor in a bulding. It is the plating, planking or covering of any tier of beams either in the hull or superstructure of a ship.

Displacement as volume (∇). The size of the hole in the water occupied by the ship measured in cubic meters.

Displacement as weight (Δ). The weight of water displaced by the ship. It is equal to the sum of lightship and deadweight. This is equal to the volume displaced multiplied by the density of sea water.

Double bottom. Compartments at the bottom of a ship between inner bottom and the shell plating, used for ballast water, fresh water, fuel oil, etc.

Draft. The depth of the ship below the waterline measured vertically to the lowest part of the hull, propellers, or other reference point.

Fore-and-aft. In line with the length of the ship; longitudinal.

Floodable length. The length of the ship which may be flooded without sinking below her safety or margin line. The floodable length of a vessel varies from point to point through her length and is usually greatest amidships and at least near the quarter length.

Freeboard. The distance from the waterline to the upper surface of the freeboard deck at side.

Freeboard deck. The uppermost continuous deck having permanent means of closing all weather openings.

Hatch. Opening in a deck through which cargo and stores are loaded and unloaded.

Heel. This is the amount of inclination of the ship in the transverse direction, and is usually measured in degrees.

Hold. Large space below deck for the storage of cargo.

Inner bottom. Plating forming the top of the double bottom; also called the tank top.

Keel. The principle fore-and-aft component of a ship's framing, located along the center line of the bottom and connected to the stem and stern frames.

Knot. A unit of speed, eualing one nautical mile per hour; the international nautical mile is 1852m.

Lightship. The weight of the ship complete, including hull, machinery, outfit, equipment and liquids in machinery.

Lines plans. The plans that show the shape or form of the ship.

Load waterline. The line on the Lines Plan of a ship, representing the intersection of the ship's form with the plane of the water surface when the ship is floating at the designed draft.

Longitudinals. Fore and aft structural shape or plate members attached to the underside of decks, flats, or to the inner bottom, or on the inboard side of the shell plating, in association with widely spaced traverses, in the longitudinal framing system.

Metacenter. The center of buoyancy of a heeled ship is not on the vertical centerline plane. A vertical line drawn through the center of buoyancy of a slightly heeled vessel intersects the centerline plane at a point called the metacenter.

Metacentric height (GM). The distance from the metacenter to the center of gravity of a ship. If the center of gravity is below the metacenter, GM is positive and is an indicator of stability.

Midships. In the vicinity of the midlength of the ship as distinguished from its ends. Technically it is exactly half way between the forward and the after perpendiculars.

Midship section. A drawing showing a typical cross section of the hull and superstructure at or near amidships, and giving the scantlings of the principle structural members.

Scantlings. The dimensions of a ship's frames, girders, plating, etc.

Shell plating. The plates forming the outer side and bottom skin of the hull.

Slamming. Heavy impact resulting from a vessel's bottom forward making sudden contact with the sea surface after having risen on a wave.

Stability. The tendency of a ship to remain upright or the ability to return to her normal upright position when heeled by the action of waves, wind, etc.

Stem. The bow frame forming the apex of the intersection of the forward sides of a ship. It is rigidly connected at its lower end to the keel and may be a flat heavy bar or of rounded plate construction.

Stern. After end of a ship.

Tank top (inner bottom). Plating forming the top of the double bottom.

Trim. This is the difference between the draft forward and draft aft.

Waterline. The line of the water's edge when the ship is afloat; technically, the intersection of any horizontal plane with the molded form.

References

1. K. R. Hinga, editor, "Subseabed Disposal Program Annual Report January to December 1980," SAND81-1095, Sandia National Laboratories.

2. For a brief description and references to the literature, see M. Miller. "Technical Considerations", in Nuclear Nonproliferation: The Spent Fuel Problem, edited by F. C. Williams and D.A. Deese, Pergamon Press, 1979, p. 127.

3. See; e.g., J. Lamarsh, Introduction to Nuclear Engineering, Addison-Wesley, 1975, Chapter 10, Part I, p. 420.

4. Supplied by S. H. Sutherland, Transportation Technology Center, Sandia National Laboratories, Albuquerque, NM, September, 1980.

5. Reference 3, p. 444, Eq. (10.52).

6. Reference 3, p. 423, Eq. (10.7) and p. 433, Eq. (10.26).

7. NCRP Report Number 39, Table 6, January 1971.

8. N. M. Greene and C. W. Craven, Jr., "XSDRN: A Discrete Ordinate Spectral Averaging Code", Oak Ridge National Laboratory Report Number ORNL-TM-2500, July 1969.

9. R. M. Westfall et. al., "SCALE: Standard Computer Analysis for Licensing Evaluation", Oak Ridge National Laboratory Report Number ORNL/NUREG/CSD-2, October 1981. Besides NITAWL, the SCALE package includes an improved version of XSDRN (XSDRN:PM) as well as the CSASIX and BON AMI-2 codes used in the criticality analysis.

10. The neutron source spectra is included to account for secondary production of gamma rays due to (n,γ) reactions with the heavy metal and water. However, due to the small size of the neutron source term -- a total spontaneous neutron fission rate of 1.308×10^{8} sec^{-1} as compared with a total gamma rate of 1.144×10^{15} sec^{-1} per 10-year-old PWR assembly -- the neutron contribution is insignificant.

11. Regulatory Standard Review Plan (SRP), Section 9.1.2.

12. American Standard Design Criteria for an Independent Spent Fuel Storage Installation (Water Pool Type), ANSI/ANS-57.7-1981, paragraph 6.3.3.2, p. 9.

13. This does not include the water in the 3 meter side border since it is separated from the penetrator array by structural walls and does not circulate.

14. J. W. Baxter, et.al., "International Nuclear Fuel Cycle Transportation System Assessment", SAND79-7115, TTC-0039, prepared for Sandia National Laboratories by Boeing Engineering and Construction, July 1980.

15. D. G. M. Watson, A. W. Gilfillan, "Some Ship Design Methods", Transactions, The Royal Society of Naval Architects, London, 1976.

16. R. Taggart (editor), Ship Design and Construction, The Society of Naval Architects and Marine Engineers, 1980.

17. I. L. Buxton et. al., Cargo Access Equipment for Merchant Ships, MacGregor publications, 1978.

18. J. P. Comstock (editor), Principles of Naval Architecture, The Society of Naval Architects and Marine Engineers, 1967.

19. M. Alexandrov, Probabilistic Approach to the Effectiveness of Life Saving Systems, Transactions, S.N.A.M.E. 1970.

20. N. Jones, A. Literature Survey On The Collision and Grounding Protection of Ships, Ship Structure Committee Report 283, 1979.

21. J. Evans (editor), Ship Structural Design Concepts, Cornell Maritime Press, 1975.

22. American Bureau of Shipping (Annual), Rules for Building and Classing Steel Vessels.

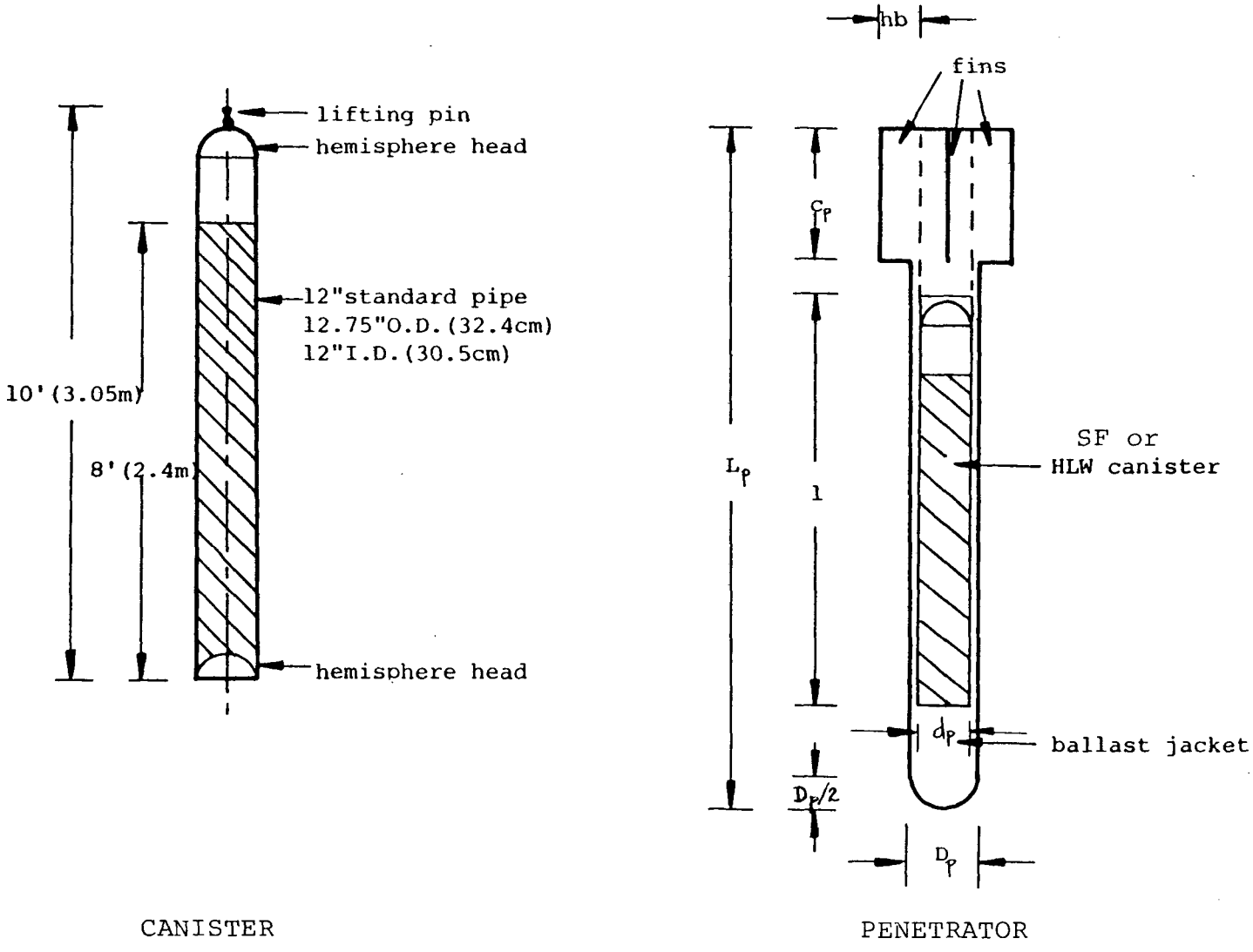


Figure 1. Reference Waste Emplacement Package

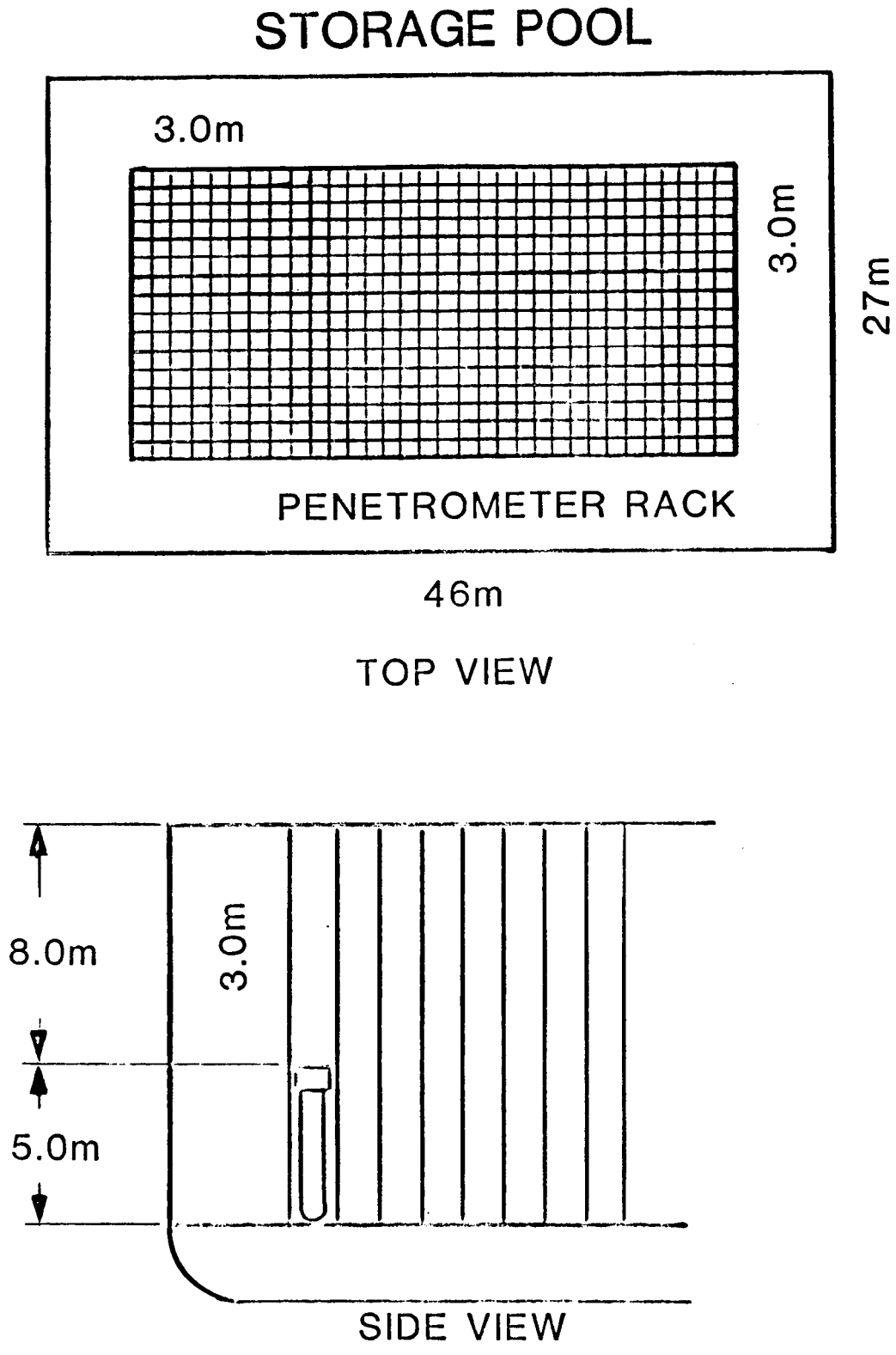


Figure 2. Shipboard Storage Pool

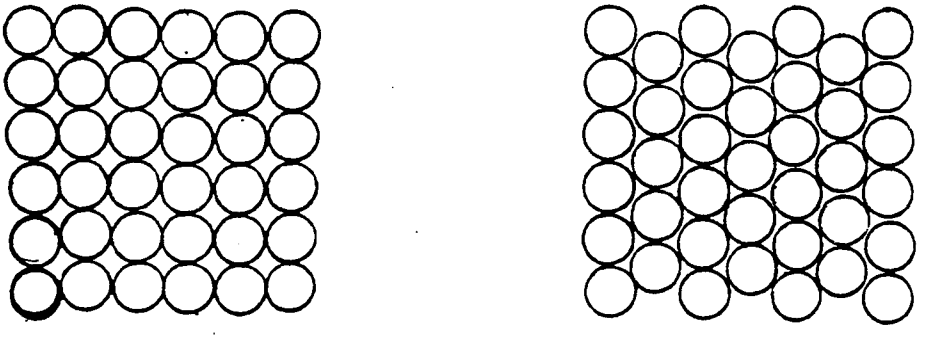


Figure 3. Worst-Case Accident Criticality Configurations

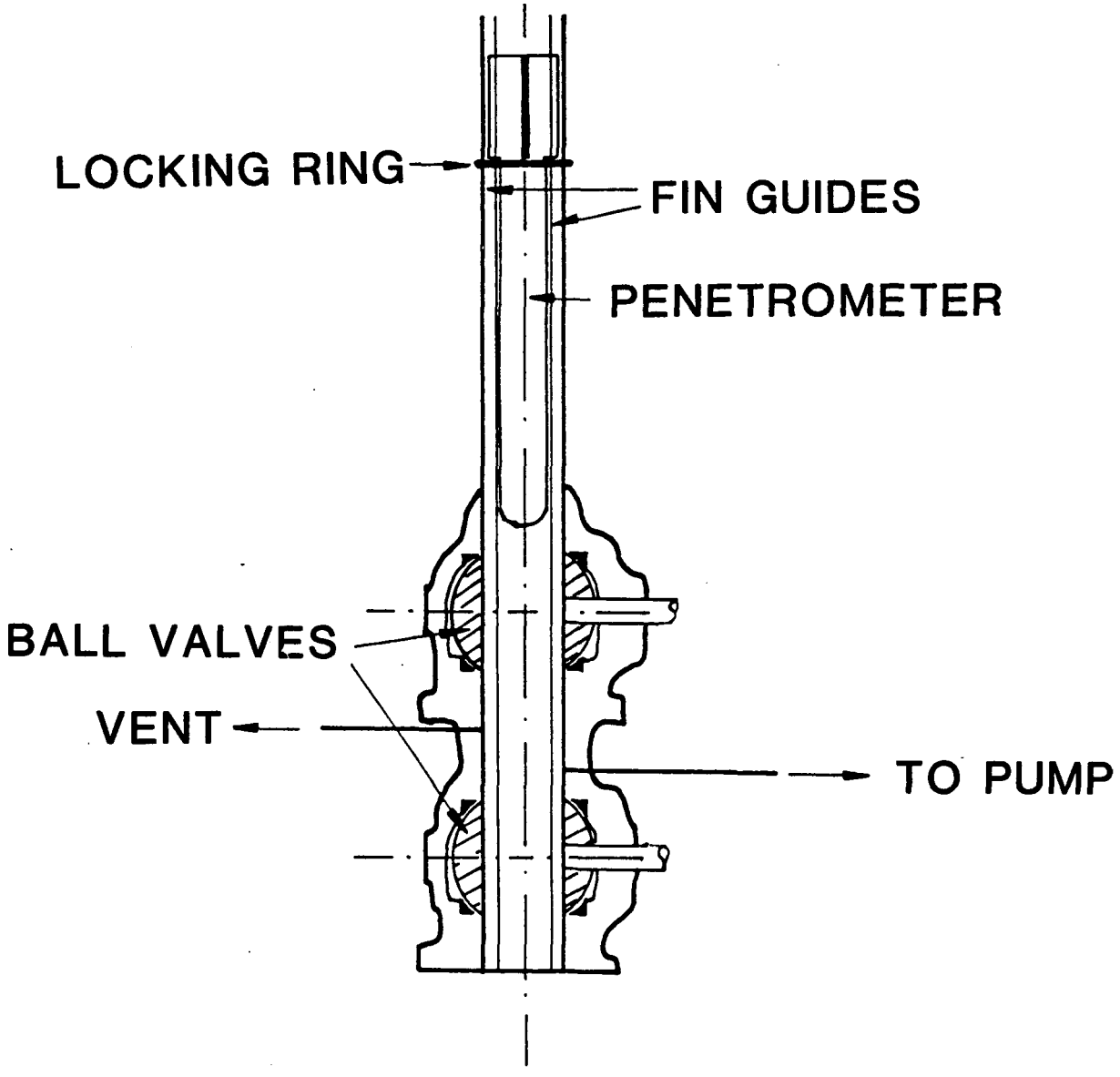


Figure 4. Penetrator Release Mechanism

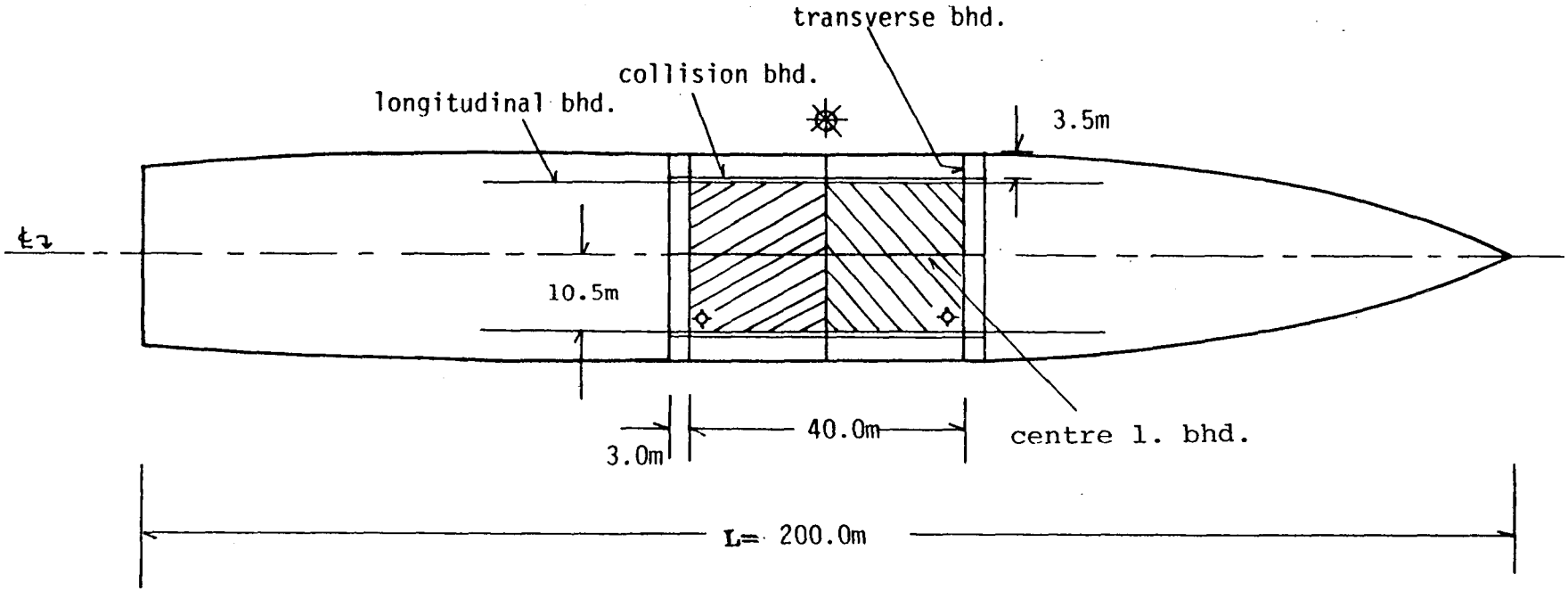


Figure 5. Plan View of Ship

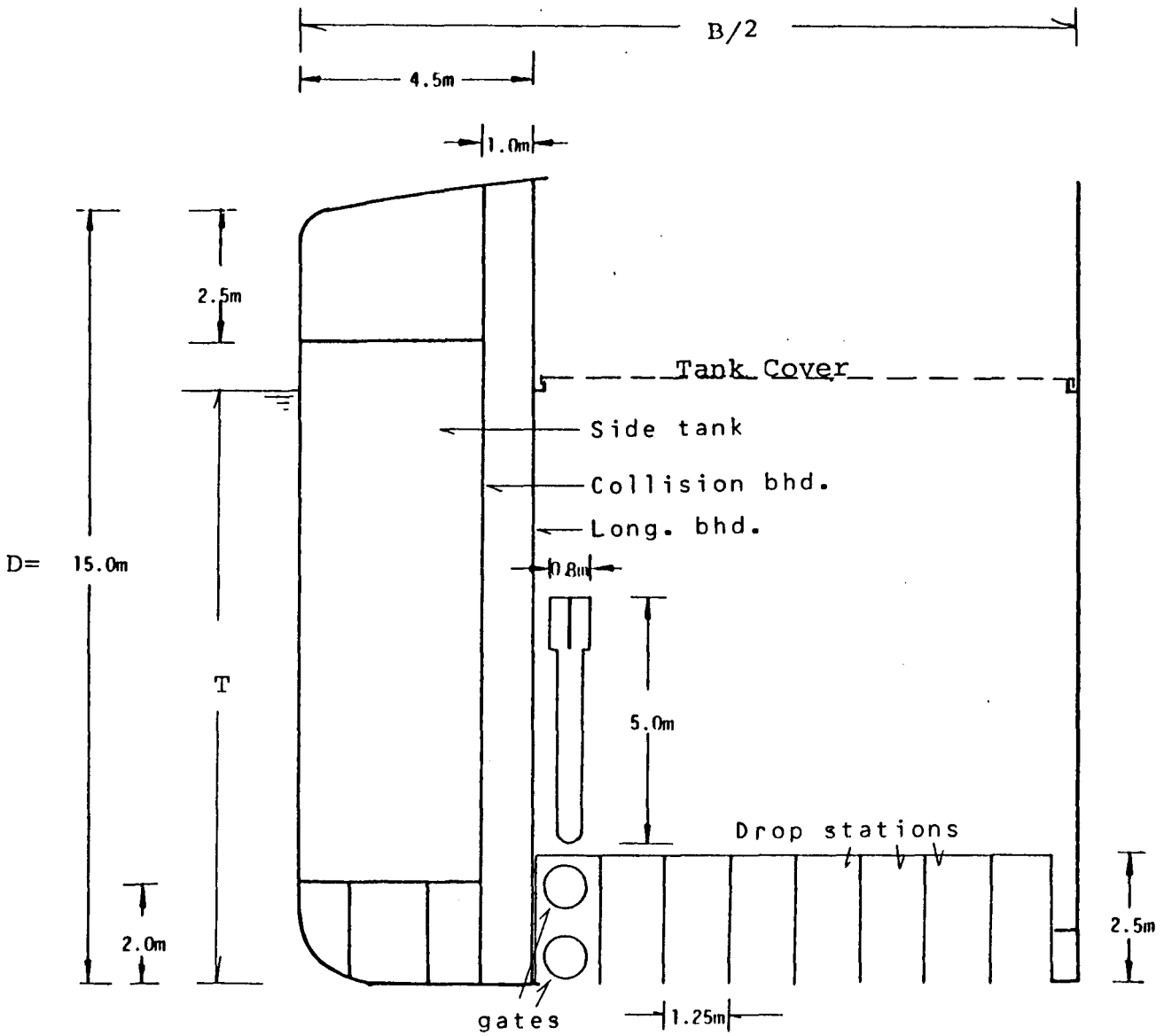


Figure 6. Midship Section of Ship

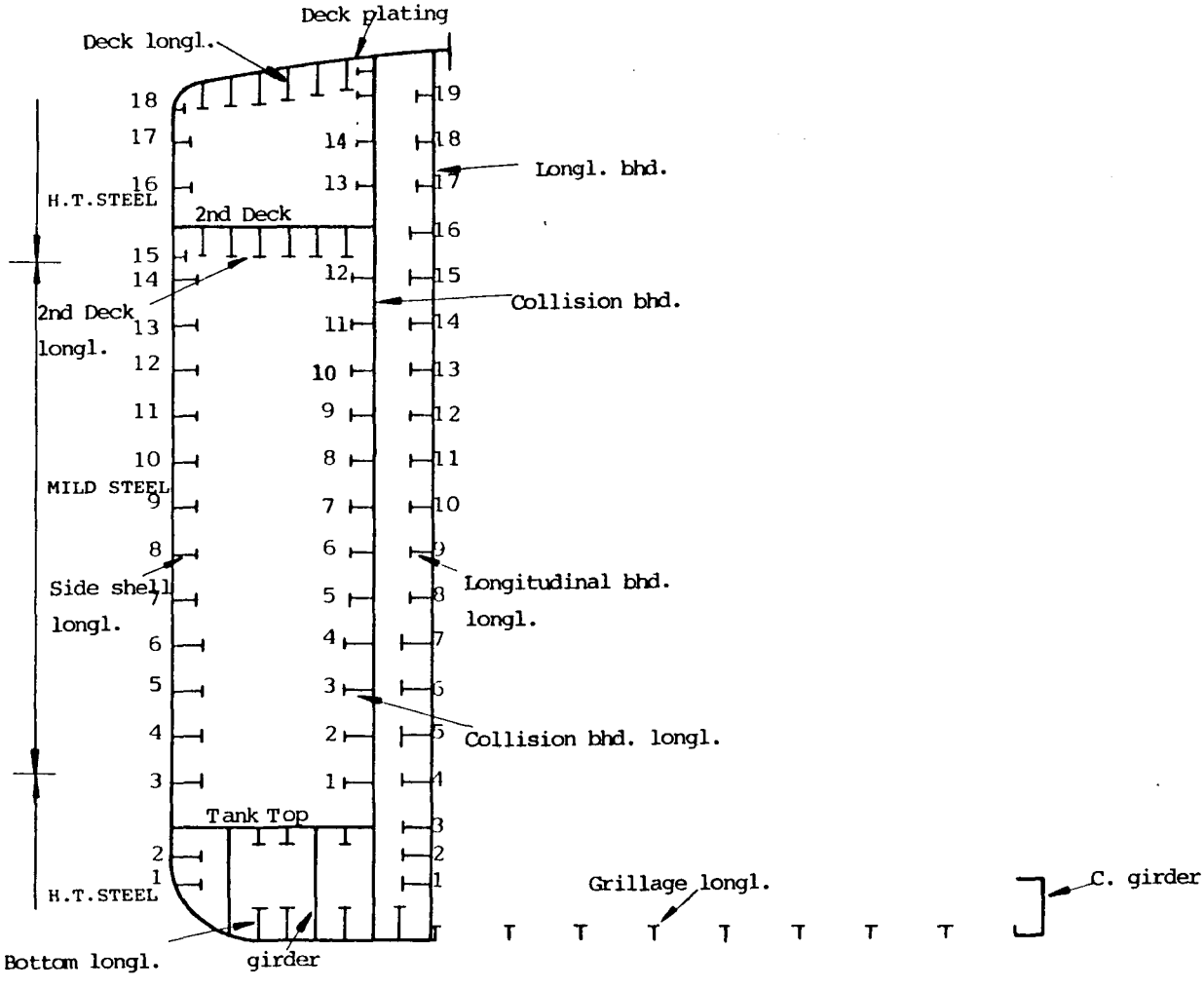


Figure 7. Structural Members at Midships

APPENDIX II

ENVIRONMENTAL MODELING

M. G. Marietta

Sandia National Laboratories

E. S. Hertel

Dikewood Corp.

(Contract #74-1013)

D. W. Jackson

Concepts Development, Inc.

(Contract #74-1162)

A. R. Robinson

Harvard University

(Contract #74-2579)

G. L. Weatherly

Florida State University

(Contract #62-8599)

Sandia National Laboratories

Albuquerque, New Mexico 87185

date: December 16, 1981

to: L. S. Gomez; S. L. Kupferman, 4516



from: M. G. Marietta, 5521

subject: SDP Environmental Modeling Progress Report

This memo represents an addenda to the n^{th} appendix of the m^{th} part of the SDP annual (minus one quarter) report for the following participants in the environmental modeling program.

Marietta, M. G., 5521

Hertel, E. S. , Dikewood Corp.
Contract #74-1013

Jackson, D. W. , Concepts Development, Inc.
Contract #74-1162

Robinson, A. R., Harvard University
Contract #74-2579

Weatherly, G. L., Florida State University
Contract #62-8599

Introduction

The environmental modeling program is concerned only with accident scenarios for the SDP since correct emplacement of the waste material within the sediments would mean that no radioactive releases would occur. However, various ongoing and future low-level waste disposal programs involve dumping on the sediment surface, and this modeling program applies directly to such dumping of low-level wastes.

The problem is to trace the radionuclide migration from a bottom source of relatively small initial dimensions through the oceanic water column, including the inorganic and living/non-living organic material within it, to wherever the waste material comes into contact with man. In order to do a complete radiological assessment for dose to man, we must know where the released radioactive material goes, how much of it gets there, and when it gets there. During the evolution of the dispersion of the release in the deep ocean, we need to know how much of the radioactive material is taken up by selected marine species in order to do a radiological assessment for dose to biota. The evolution of the released material must be studied on all space and time scales from source scales to the ultimate fate of the released radionuclides in the world ocean.

To achieve the programmatic objectives of

(i) producing a preliminary radiological assessment in FY83 for a status report,

(ii) doing a radiological assessment in FY87 that will be scientifically adequate for an EIS, and

(iii) maintaining a modeling capability that would be sufficient for post-disposal site surveillance,

a methodology combining numerical model development and other simpler but modern scientific techniques must be provided in a timely fashion for these assessments to be made whenever required. This methodology will evolve along three different approaches: (1) assembling numerical models for the various stages of the dispersion problem described above; (2) identifying and parameterizing the dominant processes for these same stages and listing scenarios of such processes that will allow estimates of the important descriptors of dispersal with

increasing space and time scales; and (3) using a descriptive oceanography approach by inferring the released material fields from known natural material fields. Simple solutions for full oceanic basin dispersion such as IAEA-211 will not be acceptable politically, socially, or institutionally for the US/SDP.

In order to make a decision on whether to move ahead with subseabed disposal of high-level waste, long-term calculations of the concentration fields for population doses plus critical pathways calculations for short-term doses are probably sufficient. In order to address the additional questions of immediate U.S. public concern plus develop a methodology that will apply to post-disposal surveillance, short-term predictive capability is required.

For the U.S. program, it is necessary to do more than just simple dose calculations in the short term. We do have a societal responsibility to respond to the reasonable public concern of what will the human and ecosystem effects be in the first few decades of a potential release from a disposal or accident site. This is essentially answering the "dose to me -- dose to my children" question. To do this, we must develop a methodology which can provide radiological assessments on time scales of tens to several hundreds of years at less than basin scales. This methodology should be state-of-the-art rather than simple calculations for this is where public concern lies.

The radionuclide transport problem is conceptualized as consisting of several modeling stages. The first stage is the release into the oceanic bottom boundary layer from either a shallowly emplaced source in the sediments or a source located on the sediment surface. This involves modeling the mixing and lateral shear within the bbl itself including important particulate, biological, and chemical processes and their interfaces with transport processes within the sediments. The second stage is the mixing and stirring of the released material that occurs in the water overlying the bbl due to the mesoscale eddy field. This stage involves tracing the plume of material as it is sheared apart into "ribbon-like" strips and advected at the mesoscale while smaller scale processes mix the material within the ribbons. There is an important interface between the first and second stages, and this is parameterizing the various exchange processes between the bbl and the water directly overlying it. Such exchange can be due to mesoscale or topographic variability and/or boundary mixing. Correct parameterization of these exchange processes involve important modeling studies that must be completed before the two stages

can be realistically interfaced. At the third stage which is the large scale dispersal problem, the released material must be traced through the full ocean basin circulation until it reaches its ultimate fate. This stage involves modeling half-oceans (N. Atlantic and N. Pacific) and the World Ocean. The interface with the smaller scale models must be carefully done since it will involve models which are computationally and physically different. Eventually, the released material finds its ultimate fate in the ocean. This may be in the Anarctic, various isolated sediment sinks, or a well-mixed ocean with a steady-state water-sediment-biology partitioning.

As the released material is traced through ever-increasing space and time scales, radiological assessments for both man and biota can be done. This involves another important interface between ocean and human dosimetry models. This will require an accumulation of fisheries and human consumption/population data plus a decision on which human dosimetry models should be used. The important criterion here is selecting models that are consistent with other waste disposal options so that differences between options in the radiological assessments can be attributed to differences in the disposal medium and transport barriers rather than differences in the human dosimetric calculations.

Thus, our programmatic modeling plan includes the development of a bottom boundary layer model, BBLM, a regional-scale open-ocean model, REM, and coarse-grid primitive-equation models, LSM, half-oceans and the world ocean. The important interfaces between these models are (1) BBL/sediment processes; (2) BBL/REM exchange processes; (3) REM/LSM embedding; (4) REM/REM embedding to build larger scale eddy-resolving general circulation models; (5) LSM/human dosimetry models, and (6) all physical models with particulate/biological/chemical processes.

This is an ambitious modeling program that must be developed under programmatic constraints on funding for manpower, computing, and field work. So, our approach has been to identify the best existing models, bring them to SNLA with the best available data, and modify them for waste disposal purposes. Whenever such models are not available, they will be developed at SNLA. There is much that is not known about the oceanic processes that bear upon this problem although the oceanographic sciences have progressed rapidly in the past few years. In such a rapidly changing field, it is important that the SDP maintain a state-of-the-art modeling capability. This will allow us to make the best radiological assessments possible when asked to do so but more importantly to record the

necessary caveats that must accompany such model output. Then, as new data and understanding becomes available, the models can be updated continuously so that a state-of-the-art capability for the SDP is maintained. Now this capability cannot immediately be covered by large numerical models since a hierarchy of such models that could represent an overall ocean model does not yet exist. So, parallel approaches must be pursued which will help us do the calculations required for radiological assessments in the short term and will also provide important input into the development of the various numerical models. These approaches are to develop a process-oriented scenario series of calculations and to use large scale tracer distributions to infer the long time scale fate of released materials. These two activities complement the modeling program and provide the conceptual framework on which we build, evaluate, and tie numerical models to real ocean data. It is in this spirit that we are developing our modeling program.

This year's activities have focused on the following efforts:

(1) finishing the Big Sky Report (SAND80-1776),

(2) supporting the Big Envelope and Jackson Hole Workshops,

(3) 1-D bbl parametric studies,

(4) barotropic (2-D) open ocean modeling studies,

(5) dispersion studies in 2-D eddy fields,

(6) analytical solutions for dispersion studies,

(7) baroclinic (3-D) open-ocean modeling studies,

(8) large-scale modeling studies,

(9) deep-ocean carbon-cycle modeling studies,

(10) using natural tracer distributions for real ocean verification of models, and

(11) supporting international activities.

Discussion

(1) The Big Sky Workshop report entitled "Proceedings of a Workshop on Physical Oceanography Related to the

Subseabed Disposal of High-Level Nuclear Waste" was issued in April, 1981. This report represents the completion of the first phase of developing a physical oceanographic program for the SDP.

(2) The Big Envelope Workshop which was a recommendation of the Big Sky Workshop was held in September, 1981. This workshop is discussed in a separate addenda. The Jackson Hole Workshop was held in January, 1981 and is also discussed in another addendum.

(3) Some parametric studies using the one-dimensional bottom boundary layer (bbl) model which was acquired from Florida State University were completed. These were used for the Big Envelope Workshop and for gaining some familiarity with modeled processes in anticipation of writing a dedicated bbl code. The one-dimensional studies included up/down slope pumping, topographic variation using a time-varying bottom boundary condition, stratification parameter studies over different oceanic regimes related to potential disposal sites.

On the basis of the understanding gained from these and previous FSU one-dimensional studies, a three-dimensional model has been outlined. An important consideration in writing this model will be the future interface between the BBLM and REM for studying exchange processes. Writing this program and beginning the bbl process studies is a task for FY82.

(4) Several studies using the Harvard Barotropic Open Ocean Model were started this year. First, a careful parameter study of the computational parameters for the non-dimensional problem was completed using MODE data. This resulted in a better understanding of the stability condition for this model. Then, a study of the physical parameter sensitivity was started. The goal of this work is to extend the model's capability from the MODE region to more energetic regions by learning how to adjust the resolution and filtering in order to successfully make long-time scale simulations. The resolution question is a further application of the computational parameter study, but the filtering question involved a significant amount of extra effort. A careful study was completed to investigate the relation between filtering, which controls the enstrophy cascade, resolution, and energy reduction in the field. We will continue with this work to improve our ability to make extension simulations. These results

will be directly useful in achieving a long-time simulation ability with the Harvard Baroclinic Open Ocean Model (#7). It will also be used to generate long-time history tapes of eddy fields (Fig. 1) in which we can do multiple realizations of material releases, as described in number five, for two-dimensional studies as a step towards doing such releases three-dimensionally.

(5) A program for solving the two-dimensional advection/diffusion equation with scavenging that is dynamically similar to the REM was written by adapting the existing structure of the Harvard Barotropic Model (REM) for solving the vorticity equation to a concentration equation. This program is intended to be used for performing multiple realizations of material releases in a single long time history eddy field generated by the REM. A parameter variation study on both the computational and physical parameters and a study of various instantaneous and continuous releases in several different shear fields was completed. Comparison of model output to a series of analytical solutions (#6) is presently underway. Further work will focus on release experiments in the various oceanic regions that will be simulated in the REM studies in 4. An additional capability to solve Lagrangian particle tracer equations (floats) will be added. A study of various diagnostics for these fields will be performed.

(6) A collection of various analytical solutions for dispersion problems which are appropriate for partial code validations has been compiled. Some of these are text book solutions while others have, to our knowledge, not been previously published. These are presently being used to carefully check the dispersion code within the assumptions that are required in order to obtain these analytical solutions.

(7) The Harvard Baroclinic Open Ocean Model was obtained, and is now being used to model a three-dimensional block of open ocean. As a result of the studies done with the Barotropic Model, the first long-time scale baroclinic simulation was performed using MODE region data with a six layer vertical resolution (Fig. 2). This was an important first step towards our goal of performing long time scale three-dimensional dispersion simulations in an eddy field. Future work will continue to be directed towards this goal.

(8) The large scale modeling activity has progressed slowly but steadily. Appropriate wind stress, temperature, salinity, and bottom topography data have been provided by GFDL to use with the previously obtained GFDL coarse grid model. These data have been interfaced with the SNLA version of this model and we now have the capability of simulating an ocean circulation at these scales (1° - 3° grids) for the N. Atlantic, N. Pacific, and World Ocean. Some problems still exist with data storage and processing and these are currently being worked out. Future work in this area will include making the program modifications provided by GFDL to improve the resolution of bottom topography and to include dispersion (and Lagrangian particle tracer) equations. Then a series of specific simulations for this scale model can be outlined.

(9) A joint project with Brookhaven National Laboratories to model the deep ocean carbon cycle began this year. This model is a combination of the SNLA marine ecosystem model and the BNL deep carbon model and their respective data sets in order to understand the carbon fluxes through the abyssopelagic ecosystem. The radionuclide transport will be partially tied to the carbon transport so if a model handles carbon in a reasonable fashion, some confidence will be gained for that model's radionuclide transport predictions in so far as the biological processes are concerned.

A model for the benthic boundary layer was constructed (Fig. 3), parameter ranges identified, and a linear, coupled set of equations for the biomass densities written. Preliminary studies to identify a steady state with realistic values for the various interactive carbon fluxes in the system were completed. Parametric and sensitivity studies will be performed; the nitrogen cycle will be considered; comparisons to known data made; and the relationship to the radionuclide transport model will be carefully defined next year.

(10) As an outgrowth of the Big Sky, Big Envelope, and various short meetings with consultants, a number of possible applications of our various models to ocean tracers, both radioactive and non-radioactive, have been identified that will serve as partial code verifications. The carbon cycle modeling exercise is one example on which work has already been done. We have also started to consider the simplest biological/particulate interactions of ^{230}Th in the water column. Others that are being

studied are Pu in the Pacific, ^{3}He from the Galapagos Heat Vents ^{210}Pb for side wall scavenging, ^{210}Po for biological processes, Mn for a large scale tracer, and Cu for bbl/sediment interaction processes. Atlantic tritium is currently being modeled at GFDL, and we maintain a close contact with this work.

(11) Various international activities have been supported as requested by SDP management. These include SWG/SATG, SWG/POTG, and IAEA/GESAMP meetings and intersessional work.

Future Work

Next year's activities will focus on tasks which are considered crucial to meeting the deadlines imposed by the FY83 status report. Due to limited funds and manpower, some previously planned activities will have to be scaled down. With present resources, our FY82 goals are to:

(1) Write the 3-D bbl model and begin process studies.

(2) Perform a careful series of release simulations using the barotropic and companion dispersion model.

(3) Write a dispersion program to be used with the baroclinic model and begin release simulations with this set of companion codes.

(4) Finish the preliminary modifications required for the large scale models of the N. Atlantic, N. Pacific, and World Ocean, and begin release simulations.

(5) Continue with the biological/chemical interfacing of these models with a goal of reproducing some natural tracer distributions.

(6) Establish reviewed biological and radioecological data bases as recommended by the Jackson Hole Workshop.

(7) Perform a "first cut" radiological assessment using the above available methodology.

The execution of this work will be strongly limited by computing contracts due to the decreased funding.

MGM:5521:njm

STREAMFUNCTION CONTOURS FROM A MODE REGION SIMULATION STARTING AT 18 PERIODS

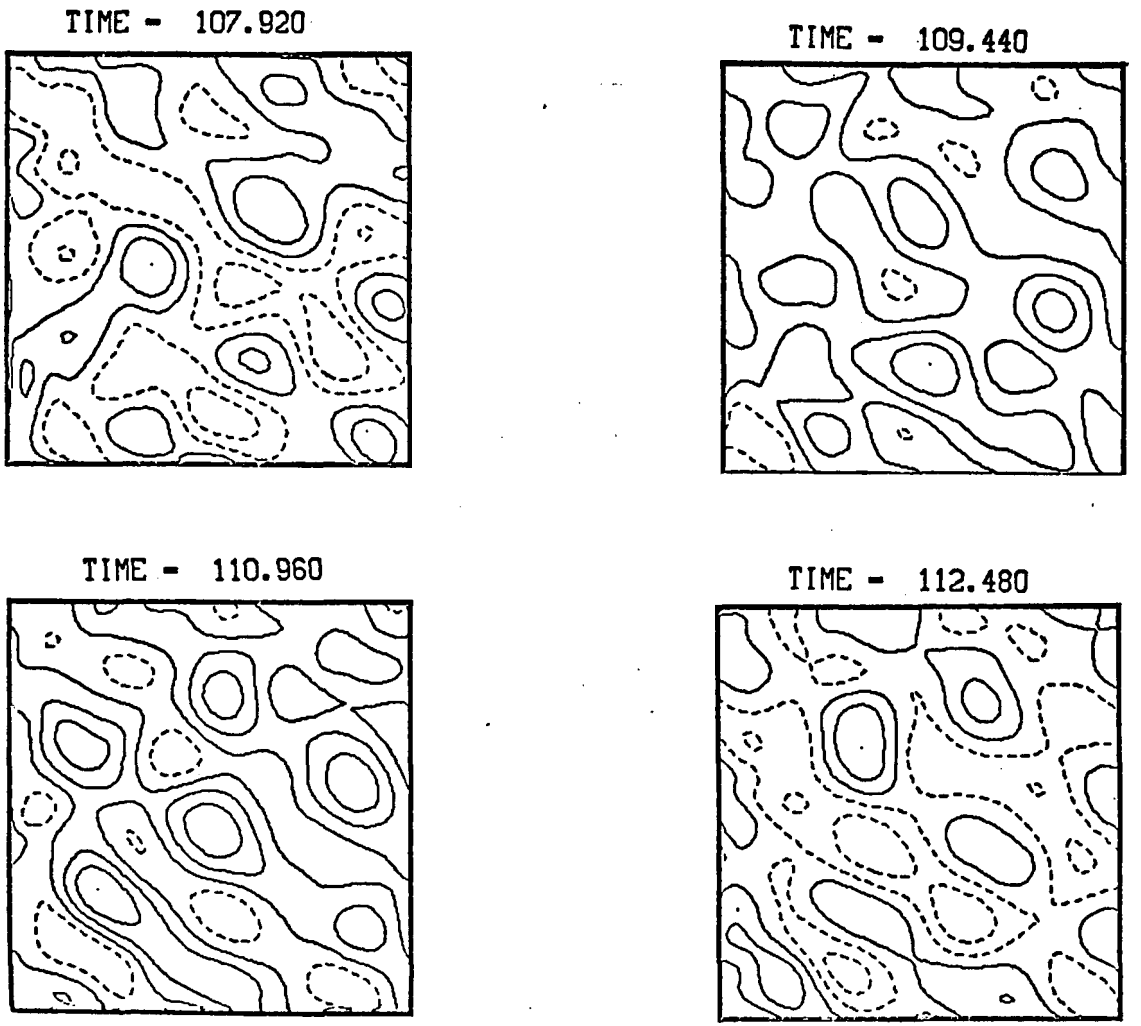


Figure 1

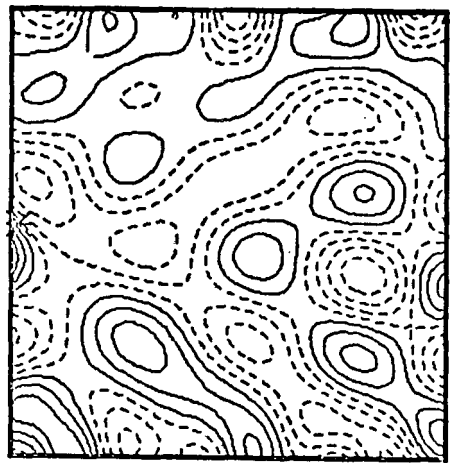
TIME- 15.17

STREAMFUNCTION CONTOURS FOR A BAROCLINIC MODE SIMULATION WITH SIX LEVELS

LEVEL- 2



LEVEL- 4



LEVEL- 6

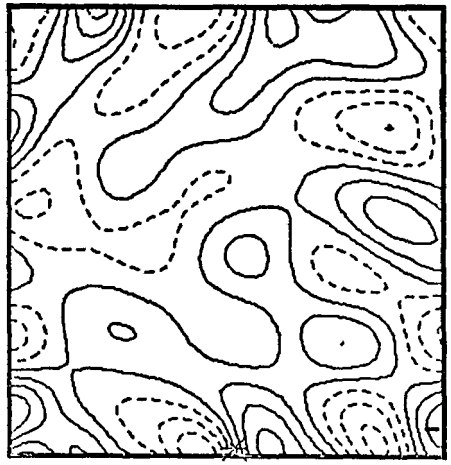


Figure 2

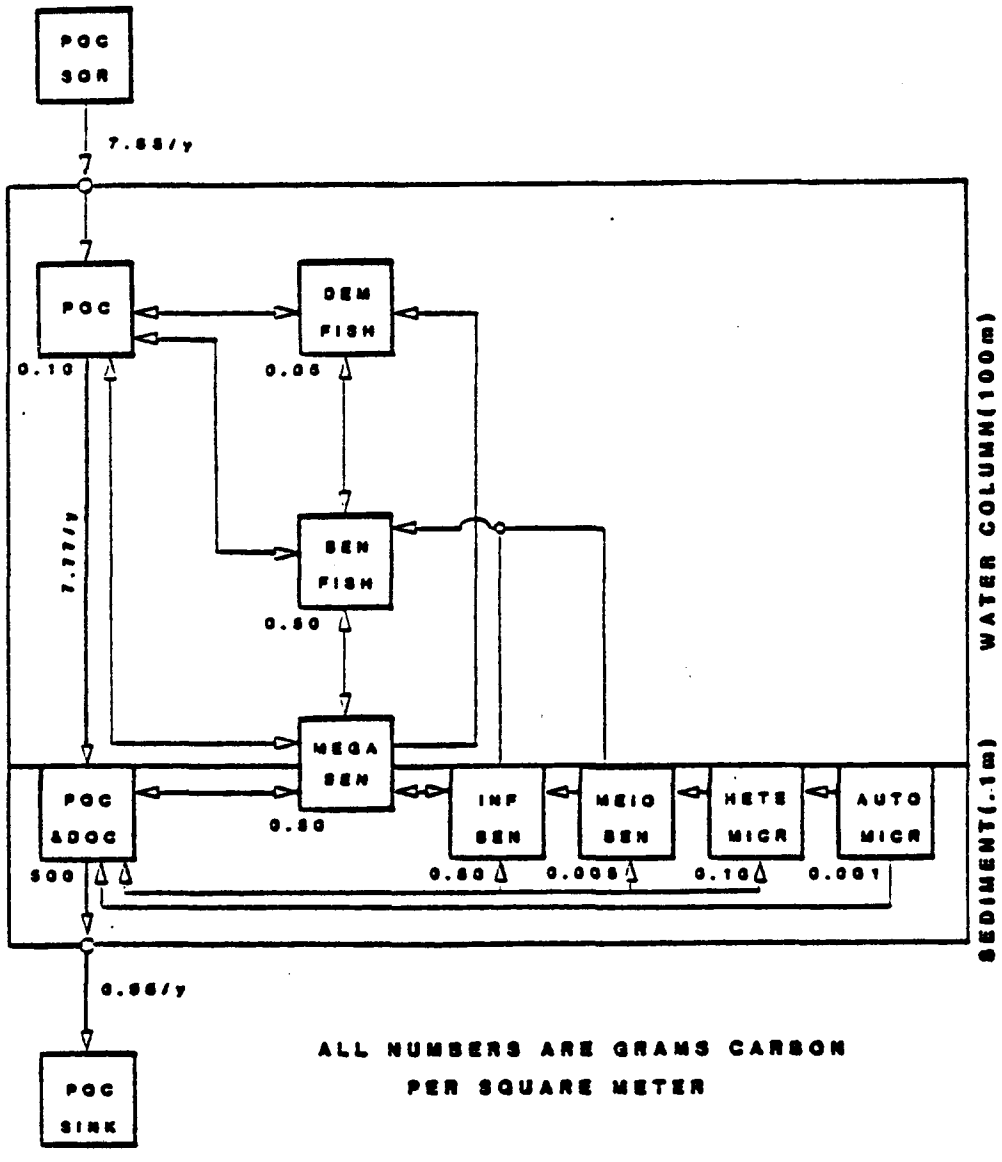

DEEP-SEA CARBON MODEL
POC SOR
7.55/y
POC
DEM FISH
0.10
0.05
SEN FISH
0.50
MEGA SEN
POC &DOC
0.50
INF SEN
MEIO SEN
HETE MICR
AUTO MICR
500
0.50
0.005
0.10
0.001
WATER COLUMN(100m)
SEDIMENT(.1m)
0.55/y
POC SINK
ALL NUMBERS ARE GRAMS CARBON
PER SQUARE METER

Figure 3

APPENDIX JJ

DEEP SEA BIOPHYSICS

A. A. Yayanos

Scripps Institution of Oceanography

(Contract #74-1165)

DEEP-SEA BIOPHYSICS

BY A. A. YAYANOS

SCRIPPS INSTITUTION OF OCEANOGRAPHY
UNIVERSITY OF CALIFORNIA, SAN DIEGO
LA JOLLA, CALIFORNIA 92093

ABSTRACT

A collection of deep-sea bacterial cultures was completed. Procedures were instituted to shelter the culture collection from accidental warming. A substantial data base on the rates of reproduction of more than 100 strains of bacteria from that collection was obtained from experiments and the analysis of that data was begun. The data on the rates of reproduction were obtained under conditions of temperature and pressure found in the deep sea. The experiments were facilitated by inexpensively fabricated pressure vessels, by the streamlining of the methods for the study of kinetics at high pressures, and by computer-assisted methods.

A polybarothermostat was used to study the growth of bacteria along temperature gradients at eight distinct pressures. This device should allow for the study of microbial processes in the temperature field simulating the environment around buried HLW. It is small enough to allow placement in a radiation field in future studies.

A flow fluorocytometer was fabricated. This device will be used to determine the DNA content per cell in bacteria grown in laboratory culture and in microorganisms in samples from the ocean. The technique will be tested for its rapidity in detemining the concentration of cells (standing stock of microorganisms) in samples from the ocean.

COMPLETION OF A COLLECTION OF CULTURES OF DEEP-SEA BACTERIA

Samples of water, sediments, animal guts and the water around decomposing animals were used as sources of deep-sea bacteria. The samples originated from depths of between 1,800 and 10,500 meters of the Pacific Ocean. Bacteria were isolated from these samples using techniques previously described (Dietz and Yayanos, 1978; Yayanos, Dietz and Van Boxtel, 1979; Yayanos, Dietz and Van Boxtel, 1981). More than 300 bacterial isolates were obtained and are maintained as a collection of deep-sea bacterial cultures.

The deep-sea bacteria from this collection reproduce under deep-sea conditions of temperature and pressure at rates rapid compared to those of organisms from other collections. Furthermore, the hallmark of these bacteria is that they all demonstrate growth that is barophilic--they reproduce most rapidly at some pressure above atmospheric.

The culture collection of several hundred bacterial isolates should suffice for the the purposes of, at least, the next 3 to 5 years.

This work was begun several years ago (about 1977). The purpose of the collection and of the studies of the bacteria in it is to address questions of the following type:

(1) To what extent can bacteria be food for other organisms?
(2) How fast can deep-sea bacteria reproduce under deep-sea temperatures and pressures?
(3) Of the bacteria in the deep sea, what fraction of them come from shallower sources? What fraction of them are active in the deep sea?
(4) What are the pathways and their capacities for the transport of bacterial biomass within and out of the deep sea? To what extent can deep-sea bacteria migrate through sediments?
(5) What is the metal and trace element composition of deep-sea bacteria?
(6) How will deep-sea bacteria respond (e.g., with a loss of viability or with an altered mutation rate) to the temperature and radiation fields around properly emplaced or improperly placed radioactive waste?
(7) How will bacteria interact with radionuclides found in the inventory of proposed HLW or SPF?

MAINTENANCE OF DEEP-SEA BACTERIA IN IN THE LABORATORY

The cultures of deep-sea bacteria are maintained in nutrient media such as type 2216 marine broth and in silica gels containing nutrients. These cultures are kept at the pressure of their depth of origin and at 2 C. The pressure vessels are kept in a walk-in cold

room connected to an emergency power source. The pressure vessels within the cold room are within additional insulated boxes that are always filled with ice. In the event of mechanical failure of the refrigeration system, the ice cooled boxes will (on the basis of tests) maintain the cultures without replenishment of the ice at less than 5 C for 3 days. These precautions along with checks of the cold room temeprature every eight hours, and an emergency notification procedure make for a reliably kept culture collection. These cultures in pressure vessels are transfered to fresh medium on a scheduled basis.

A computer program was evaluated as a means to facilitate the recording of data on the isolates that included their origin, the date of original isolation, the dates of the next four transfers to fresh medium, and the date of the last transfer to fresh medium. The data files could be sorted or searched by the computer. When fully implemented, the computerized recordkeeping of data on culture maintenance should contribute to the timely transfer of cultures to fresh medium.

Two other methods of maintaining cultures were explored--lyophilization and storage at less than -70 C. Although continually done, the evaluation of the two methods was slow due to the need to evaluate the duration of storage and to the limitations imposed by the number of available pressure vessels. That is, we usually could not afford to release pressure vessels from experiments of ecological interest in order to determine the recoverability of cells following some particular storage treatment. The high cost of pressure vessels allowed for the present only a modest study of lyophilization or of cold (<-70 C) storage of barophilic bacteria.

Studies on the lyophilization of isolate CNPT-3 found recoverable cells from lyophilization but not in a reliable manner. Controlling the temperature during the initial phases of freeze drying seemed to be critical for predictable recovery of this organism.

DESIGN OF RELATIVELY INEXPENSIVELY FABRICATED PRESSURE VESSELS

The high cost of pressure vessels has stymied the progress of deep-sea microbiology. We designed a relatively inexpensive pressure vessel with a pin-held closure having a piston seal. Such a design is shown in Figure 1, along with the fabrication steps that have resulted in a cost of less than $300 per vessel. Commercially available vessels of similar capacity (about 400 cc) cost more than $1,200 each. Hundreds of vessels are needed to properly maintain deep-sea cultures and to efficiently perform experiments.

The vessel type shown in Figure 1 also allowed for rapid and easy access to compressed samples because of the pin-held closure. The vessel was connected to the high pressure pump; the pressure in the vessel was ascertained to be the same as that at the beginning of the incubation; the vessel was decompressed; the pin was removed and the closure was removed from the vessel by lifting it off (the flexible high pressure tubing between the vessel and the pump did

not need to be disconnected); samples were taken or inserted and the vessel was repressurized. The coupling device described in a subsequent section also contributed to efficient experimentation.

KINETICS OF MICROBIAL PROCESSES AT HIGH PRESSURES--SAMPLING WITHOUT DECOMPRESSION.

A high pressure kinetics system was used to sample a culture without necessitating the decompression of the bulk of the culture and without subjecting the sample to any shear forces. The apparatus was an outgrowth of the one described previously (Yayanos, 1969).

KINETICS OF MICROBIAL PROCESSES AT HIGH PRESSURE--SAMPLING CULTURES WITH DECOMPRESSION/RECOMPRESSION CYCLES

The method decribed in the preceeding section yielded data on cultures undecompressed during the experiment. But then each experiment lasted about two to three weeks. To increase the number of experiments done, we also did experiments on cultures that were sampled with decompression-recompression cycles. The validity of this approach was tested periodically by using two pressure vessels to do experiments in parallel and identical in every way except one: the culture in one vessel was sampled without decompression; the culture in the other was sampled with brief (1 to 2 minutes) decompressions. In experiments on the effects of pressure and temperature on the reproduction of bacteria, the results from these two types of experiments were indistinguishable (in those cases where the generation times were hours long.) Therefore, in order to increase the rate at which experiments were done, the following apparatus was used.

Two platforms were constructed to each hold six pressure vessels (Figure 2). Each pressure vessel contained two syringes (appropriately modified for use at high pressures). Each syringe contained a bacterial culture and glass ball. The two racks of pressure vessels were in two different temperature-regulated water baths. The racks were attached to motors which continuously rocked the vessels causing the glass balls to mix the cultures. Each of the cultures was sampled by decompressing a pressure vessel for 1 to 2 minutes. Control experiments were done to insure that decompression is not biasing the results. The racks of pressure vessels rocking in two different temperature-regulated baths greatly enhanced the ability to study barophilic bacteria.

COUPLING DEVICE FOR QUICK HIGH PRESSURE CONNECTIONS

Laboratory work at high pressures often requires either rapid access to the contents of pressure vessels or repeated access to a large number of pressure vessels by means of a single pumping system. For example, the presssure vesels on each of the rocking platforms need to be sampled two to three times each day. Described here is a coupling device that allows a pressure vessel to be rapidly connected to and separated from a pumping system. Standard

high pressure valves can be adapted for use with the device without any modification. We have used the described coupling device to 100 MPa (1,000 bars).

The two parts of the device, a coupler and adapter, are shown in Figure 3. The coupler was secured to a high pressure pumping system with flexible tubing of type 316 stainless steel (0.76 mm i.d., 1.59 mm o.d.). The "O"-rings, made of Viton, were size 2-108 and the back-up rings, made of Buna-N rubber, were size 8-108 (Parker Hannifin Corporation, Lexington, Kentucky). The wiper rings were fabricated from Teflon and held in place with caps (Fig. 3). As many adapters, Fig. 3, as needed are made from bar stock or, as was done here, from high pressure tubing. One end of a piece of high pressure tubing was sealed with a weld, rounded and polished. The other end was coned and threaded for a standard 0.25 inch (6.35 mm) o.d. high pressure connection. A small hole was drilled through the wall of the tubing. One adapter was fastened to the valve of each pressure vessel.

A pressure vessel was joined to the pumping system by slipping the coupler over the adapter. The "O"-rings of the coupler straddled the hole in the wall of the adapter. As the pressure was increased, the "O"-rings in the coupler were pushed equally in opposite directions and the coupler remained stationary. An ethylene glycol and water mixture used as the hydraulic fluid provided sufficient lubrication for the "O"-rings in the coupler. We used the device to compress and decompress with improved efficiency as many as 40 pressure vessels each day.

We thank Eugene W. Hartlett for helpful suggestions and skillful machining.

A POLYBAROTHERMOSTAT: USE FOR DETERMINING THE DOMAIN OF GROWTH OF BACTERIA ON THE PRESSURE-TEMPERATURE (P-T) SURFACE.

Polythermostats have been used for years to determine the effects of temperature on microbial processes. The cultures are placed at specific temperatures along a single temperature gradient. The device described here was used to place cultures at 8 different pressures along a single temperature gradient. The temperature gradient was along the length of an aluminum block, 30 inches long, with 9 holes, each 30 inches long. A pressure vessel is placed in each hole except the center one. The vessels had an inner diameter of 5/16 inches. One end of the aluminum block was heated and the other end was cooled. The temperature along the length of the block was measured along the length of the center hole by using a thermistor. The inoculated culture medium was dispensed in tubes about 1.5 to 2 inches long and placed into the pressure vessels. Each pressure vessel could be independently pressurized. Thus, at eight desired pressures, the effects of a series of temperatures could be determined. The polybarothermostat is shown in Figures 4 to 7. The linearity of the temperature gradient is seen in Figure 8 and the outcome of an experiment at 580 bars with isolate CNPT-3 is shown in Figure 9. In summary, this device should allow for a rapid determination of the domain of temperature and pressure permitting

growth of isolates. It should, furthermore, allow for the study of microbially faciliated processes along temperature gradients in sediments.

DETERMINATION OF THE CONCENTRATION OF CELLS AND THEIR SIZE USING A COULTER COUNTER AND A MULRICHANNEL ANALYZER INTERFACED TO A COMPUTER

A model ZH Coulter Counter was used for both counting cells and determining their size. The model ZH had high resolution circuitry that eliminated pulses having a shape that would lead to inaccurate size estimates. Pulses having shapes unaccepatable for size information can arise when, for example, a particle flows near the wall of the orifice of an aperture tube. This circuitry was used only when size information was being collected. The size data was collected with a Nuclear Data ND66 multichannel analyzer having a particle sizing circuit board. The resulting frequency distribution of cell sizes was then transmitted to a Tektronix 4052 computer for storage on disc. The size data was processed by the Tektronix 4052.

The raw counts of a sample were logged from the model ZH Coulter Counter with the high resolution circuitry disconnected. The raw counts were entered into the Tektronix 4052 using turnkey software that allowed the following: creation of a new data file name or access to an existing one; alteration of the parameters of the data reduction algorithms (dilution series used in sampling the culture, Coulter manometer volume, diameter of aperture tube orifice); input of up to 10 raw counts per time point; correction for coincident counting of particles; input of the time of the sample; calculation of the cells/ml of culture; and, storage of the data in the appropriate disc file. The disc file allowed for sorting or accessing the experiments by geographical origin of the isolate, by isolate number, by the pressure of the experiment and by the temperature. The data in the files can be accessed by a program for plotting and for curve fitting. A back-up disc was created at the end of each week. Back-up copies of all data were stored at a location separate from this laboratory.

Note that the ND66 multichannel analyzer and 4052 computer served (simultaneously if necessary) both the Coulter Counter and the flow fluorocytometer.

FABRICATION OF A FLOW FLUOROCYTOMETER FOR THE ENUMERATION OF FLUORESCENTLY LABELLED BACTERIA

It is well known that bacteria can be labelled with various fluorescent dyes for ecological and physiolgical studies. Recently techniques have been developed that allow such enumeration at rates of several thousand cells per second. For example, Bailey, et al. (1977) used a laser flow microfluorometer to achieve such rapid data acquisition with fluorescently labelled bacteria. Also, with the use of a multichannel analyzer to acquire the intensity of fluorescent pulses, they were able to enumerate cells and simultaneously measure their relative protein content (when using FITC as the dye) or simultaneously measure their nucleic acid content (when using

acridine orange as the dye). Lindmo and Steen (1979) and Steen and Lindmo (1979) have also described a flow fluorocytometer that accomplishes similar measurements on more than 1000 cells per second. Steen (at a seminar at this institution) showed data obtained with his instrument on bacteria that appeared to be as good as that of Bailey et al. (1977). The method of Lindmo and Steen (1979) utilyzes an epifluorescence microscope which many laboratories have.

The following components have been assembled into a flow fluorocytometer similar to that of Lindmo and Steen.

SAMPLE FLOW SYSTEM (Fabricated in the SIO machine shop)
EPIFLUORESCENCE MICROSCOPE (Zeiss Universal)
PHOTOMULTIPLIER (EMI)
MULTICHANNEL ANALYZER (Nuclear Data ND66)
RS232 INTERFACE
COMPUTER (Tektronix 4052) (also, connected by modem to large Burroughs computer at UCSD)
DISC STORAGE AND HARD COPY DEVICES

Figures 10 and 11 show some of these components. The instrument will be used in 1982 to determine the standing stock of microorganisms in sea water and to determine the DNA content per cell in laboratory cultures.

COMPLETION OF EXPERIMENTS ON BACTERIAL REPRODUCTION AT DEEP-SEA TEMPERATURES AND PRESSURES IN NUTRIENT RICH MEDIA

The rate of reproduction of deep-sea bacteria from the above described culture collection, has been determined for more than 100 isolates at deep sea pressures and temperatures. The data for CY 1981 are appended to this report. The data will be analyzed and published in 1982. This data base will serve as a guide for studies on the effects of ionizing radiation on microbial processes and for determining the uptake of radionuclides by bacteria.

Among the conclusions from this data base are the following:

(1) Most of the bacteria we isolated from deep-sea samples, including a few from sediments, have shown barophilic growth in laboratory culture.

(2) The pressure at which these heterotrophic bacteria reproduce optimally is always at a pressure slightly less than that at their depth of origin.

(3) Obligately barophilic bacteria exist and appear to be confined to the hadal regions of the seas.

(4) The mean generation time of the barophilic bacteria in cultures of nutrient rich media at optimum pressures and 2 C, is within the range of 5 and 25 hours based on studies of dozens of isolates from depths of 2,000 m to over 10,500 m.

(5) The barophilic trait in itself 24es not render a bacterium inactive on decompression. That is, barophilic bacteria from abyssal depths grow at atmospheric pressure; obligately barophilic bacteria from hadal depths survive at least temporary decompressions to atmospheric pressure.

(6) The pressure at which the rate of reproduction is optimal is diagnostic for the depth of origin of the bacterium.

REFERENCES

Bailey, J.E., et al. Characterization of Bacterial Growth by Means of Flow Microfluorometry. Science 198:1175-1176 (1977).

Dietz, A.S. and Yayanos, A.A. Silica Gel Media for Isolating and Studying Bacteria under Hydrostatic Pressure. Appl. Env. Microbiol. 36:966-968 (1978).

Lindmo, T. and Steen, H.B. Characteristics of a simple high-resolution flow cytometer based on a new flow configuration. Biophys. J. 28: 33-44 (1979).

Yayanos, A. A. A technique for studying biological reactions rates at high pressure. Review of Scientific Instruments 40:961-963 (1969).

Yayanos, A. A., Dietz, A. S. and Van Boxtel, R. Obligately barophilic bacterium from the Mariana Trench. Proc. Natl. Acad. Sci., U.S.A. 78:5212-5215 (1981).

Yayanos, A. A., Dietz, A. S. and Van Boxtel, R. Isolation of a deep-sea barophilic bacterium and some of its growth characteristics. Science 205: 808-810 (1979).

FABRICATION STEPS

1. Face off bars to lengths of
   18″ (126 pcs.)
   15″ (24 pcs.)
2. Gundrill to 1.490″ (± 0.020),
   17″ deep with spherical radius at bottom
   14″ deep with spherical radius at bottom
3. 32 hone I.D. to 1.500 $\begin{cases} +0.001 \\ -0.000 \end{cases}$ to a depth of 5″
4. Ream I.D. to 1.530″ to a depth of 1 15/16″; terminate reamed portion with 30° angle with wall of cylinder.
5. Drill cross holes
6. Make cap
7. Make pins
8. 'O' ring size is 2-218

MATERIALS:

1. Body and cap: 316 steel (ASTM 479)
2. Pin: 17-4 PH stainless steel

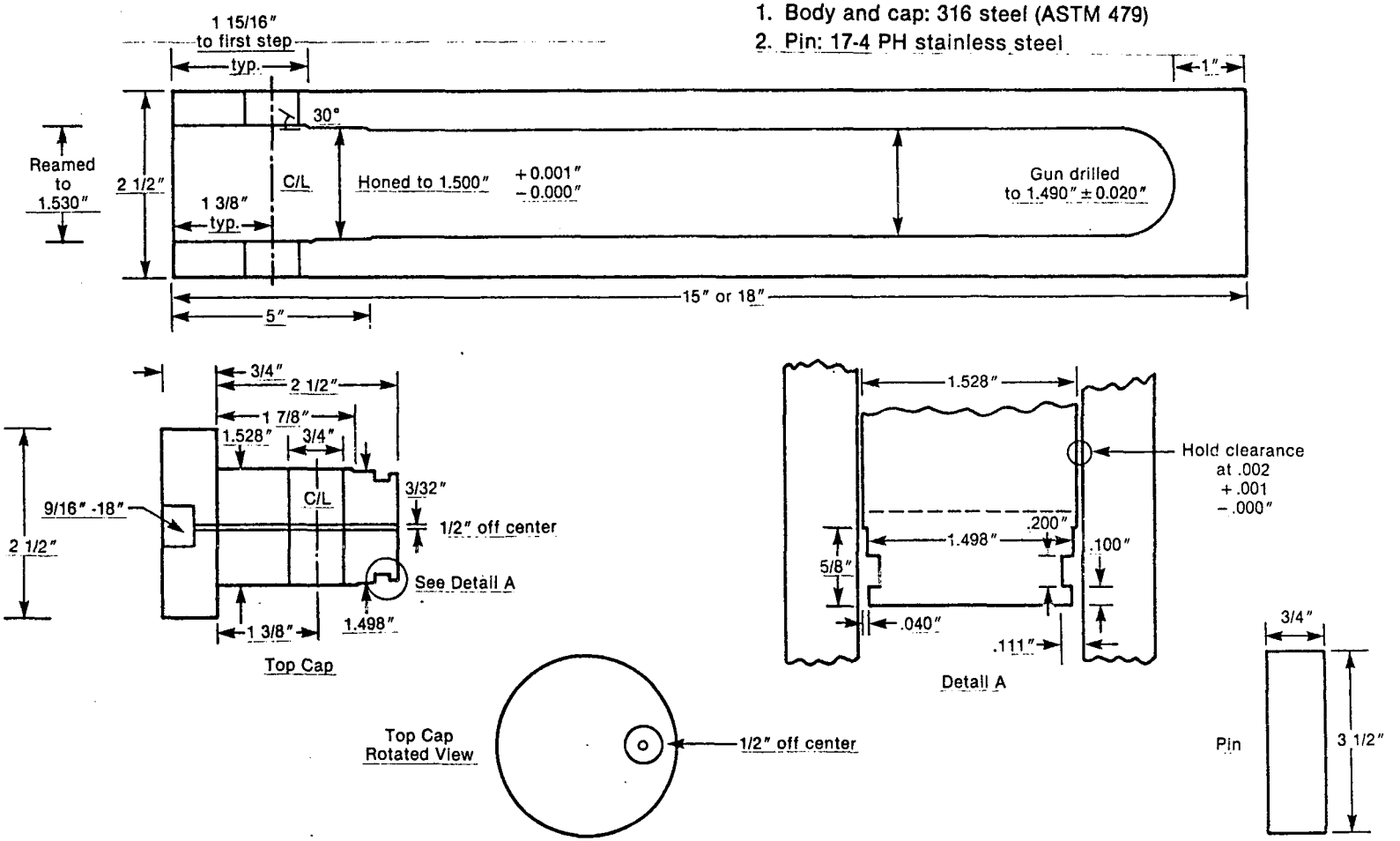


Figure 1. Details of pressure vessel fabrication.

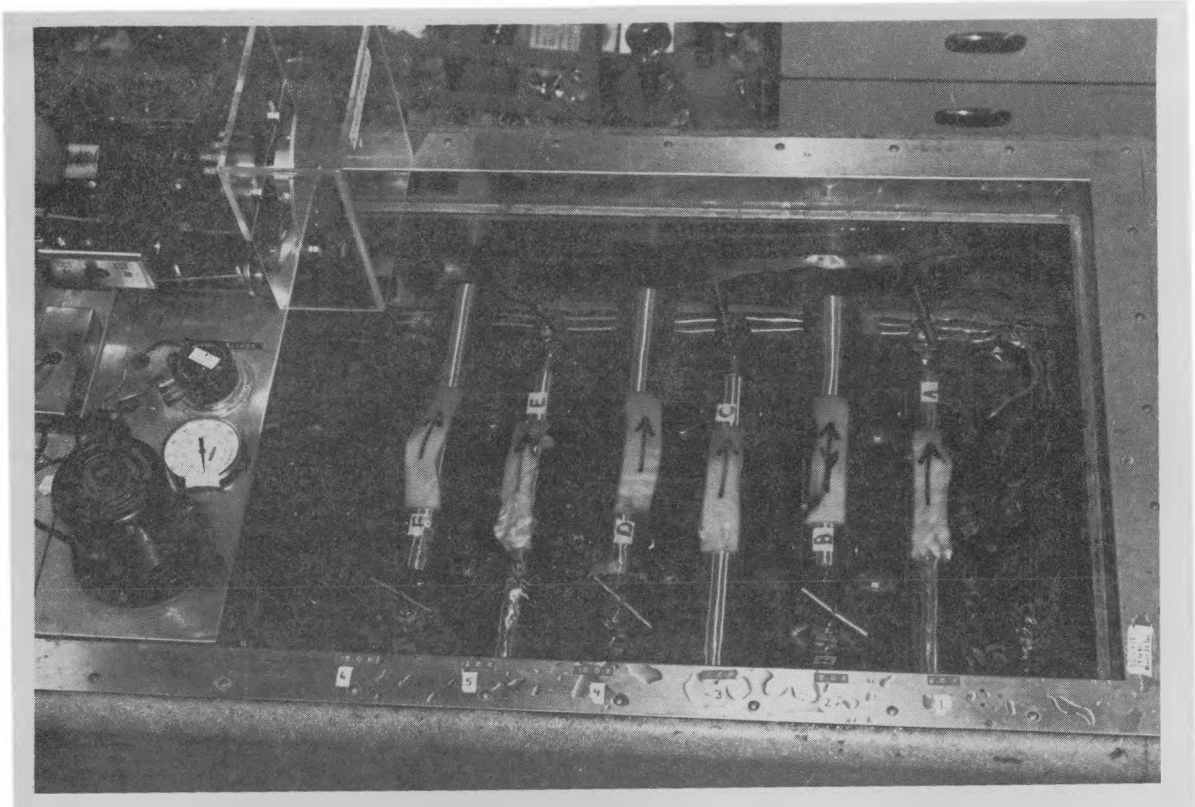


Figure 2. Six pressure vessels are shown resting on a platform in a temperature controlled water bath. The platform is rocked by a motor shown in the upper left hand corner of the picture. Each pressure vessel contains two cultures and is sampled with a decompression-compression cycle.

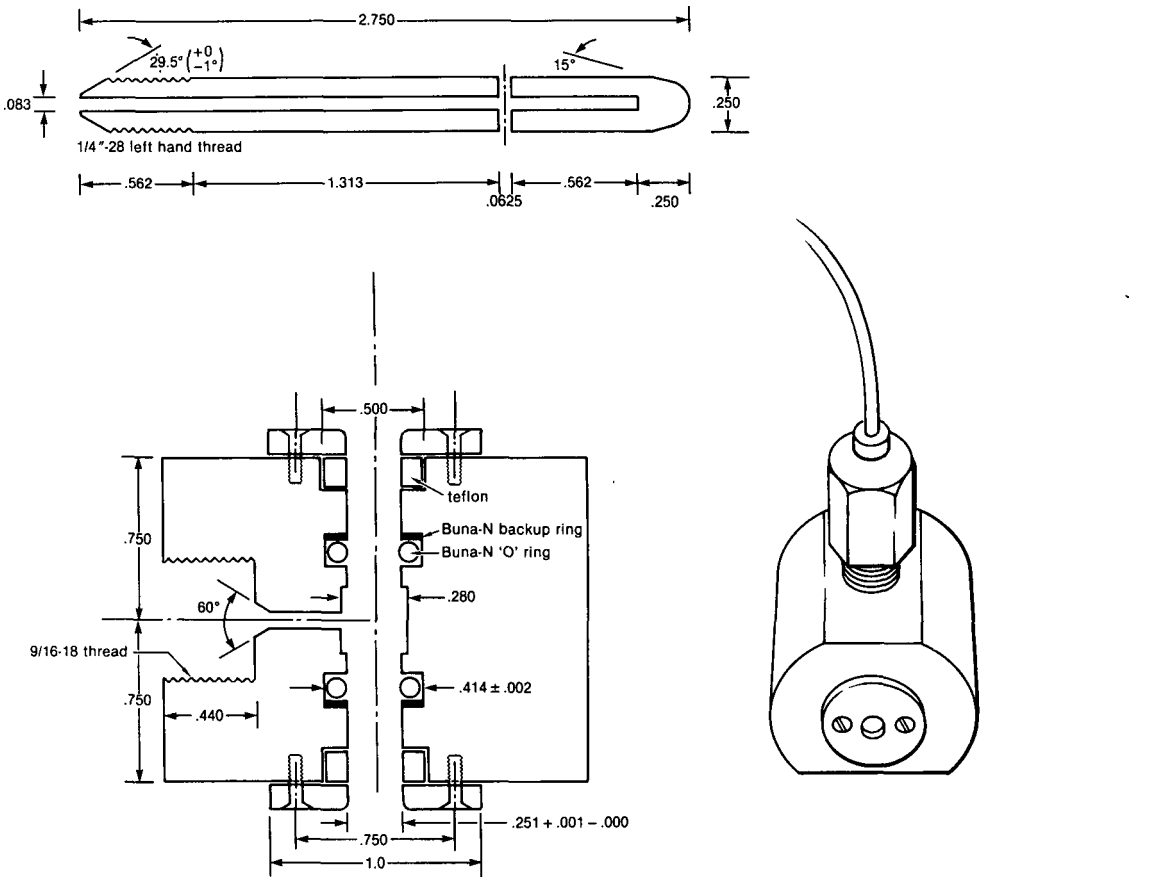


Figure 3. Shows the the parts and dimensions of the coupling device. The coupling device consisted of an adapter for pressure vessels and a coupler that was secured to a high pressure pumping system. The threaded tube with a hole in its side is the adapter that can be connected to any high pressure valve with a standard 6.35 mm high pressure connection. Either end of the coupler can be slipped over the adapter. For use to 1,000 bars (100 MPa), the coupler was secured to flexible high pressure tubing (1.59 mm o.d.) as shown in the 3-D sketch of the coupler. All dimensions are given in inches.

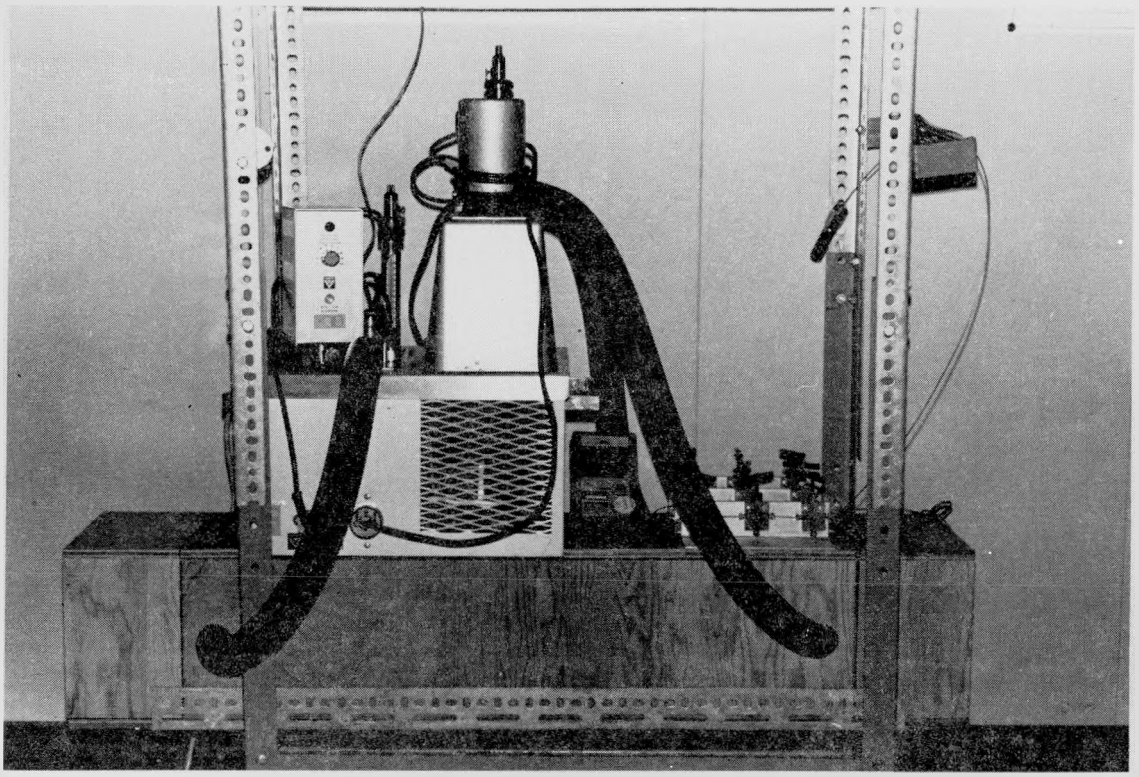


Figure 4. A polybarothermostat is shown that allows 8 pressure vessels to be placed in parallel along the same temperature gradient. The wooden box contains insulation surrounding an aluminum block in 8 holes of which are placed pressure vessels. Two temperature regulated baths are shown on top of the box and are used to cool one end of the aluminum block and to heat the other end.

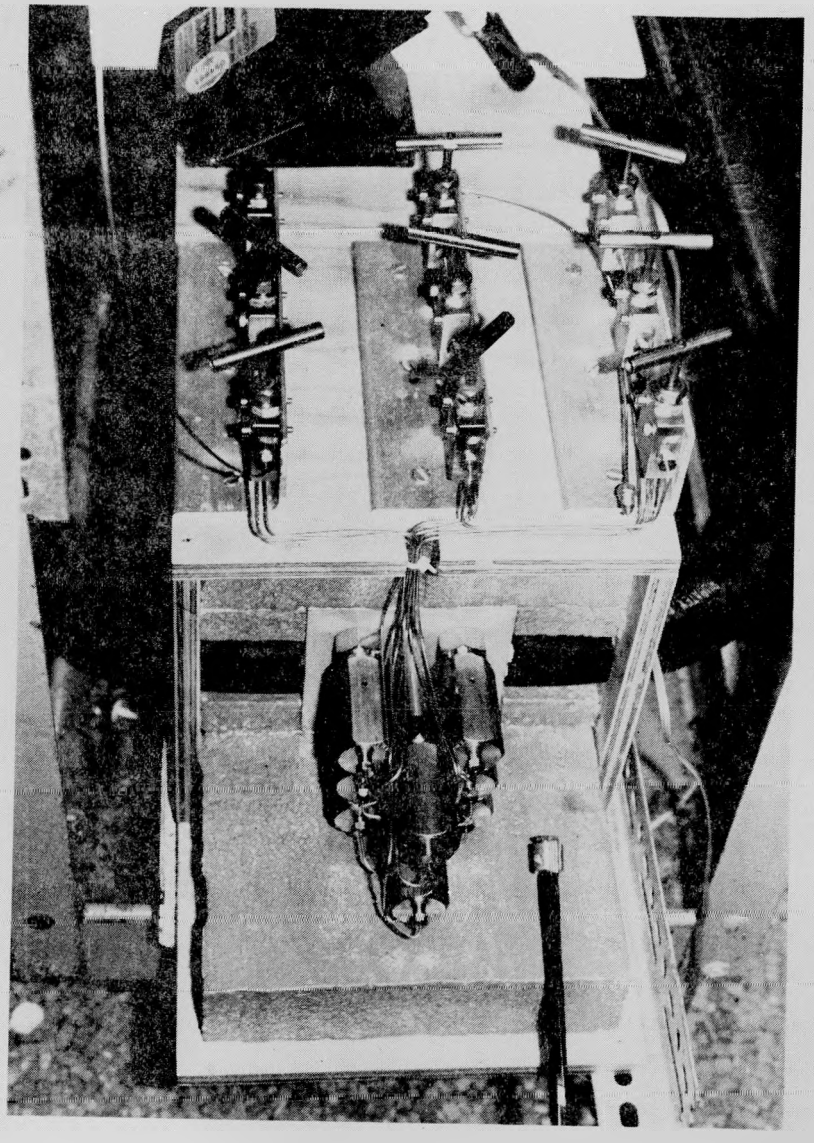


Figure 5. Shows the end of the polybarothermostat at which the pressure vessels are pressurized and the manifold of high pressure valves.

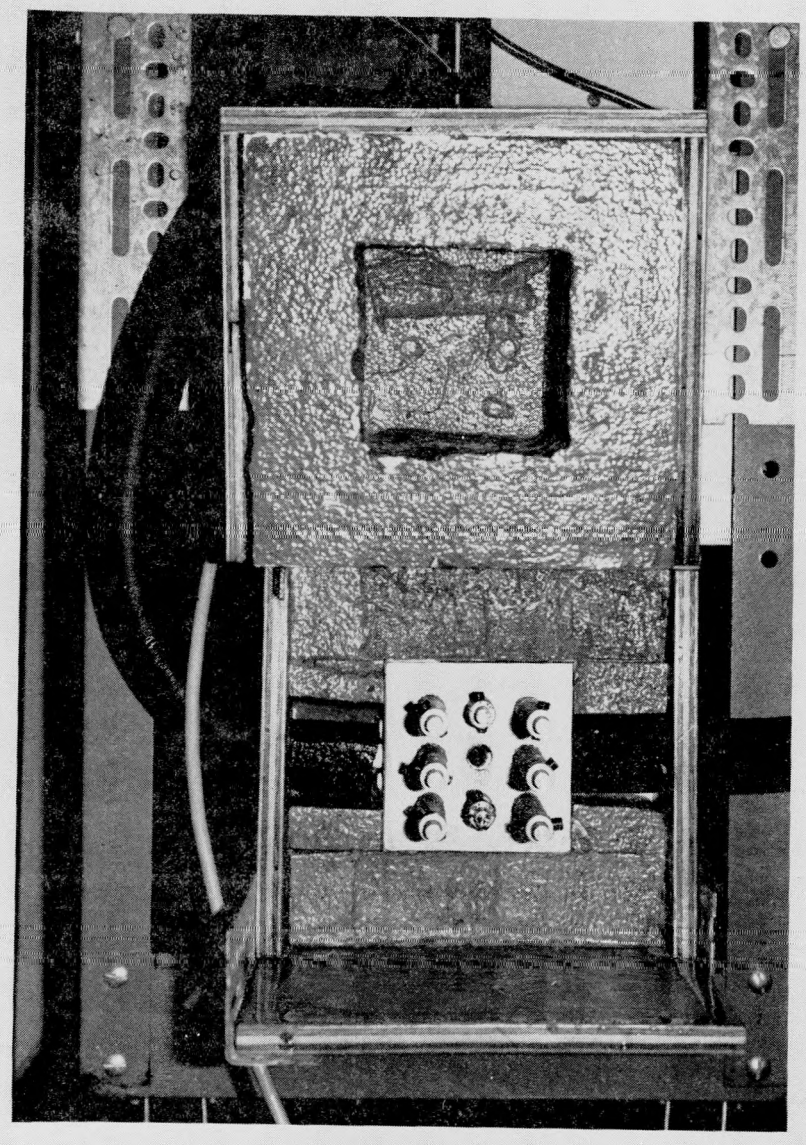


Figure 6. Shows the end of the polybarothermostat through samples are loaded into the pressure vessels. The center hole in the aluminum block is empty and is used for a thermistor to determine the temperature gradient along the length of the block.

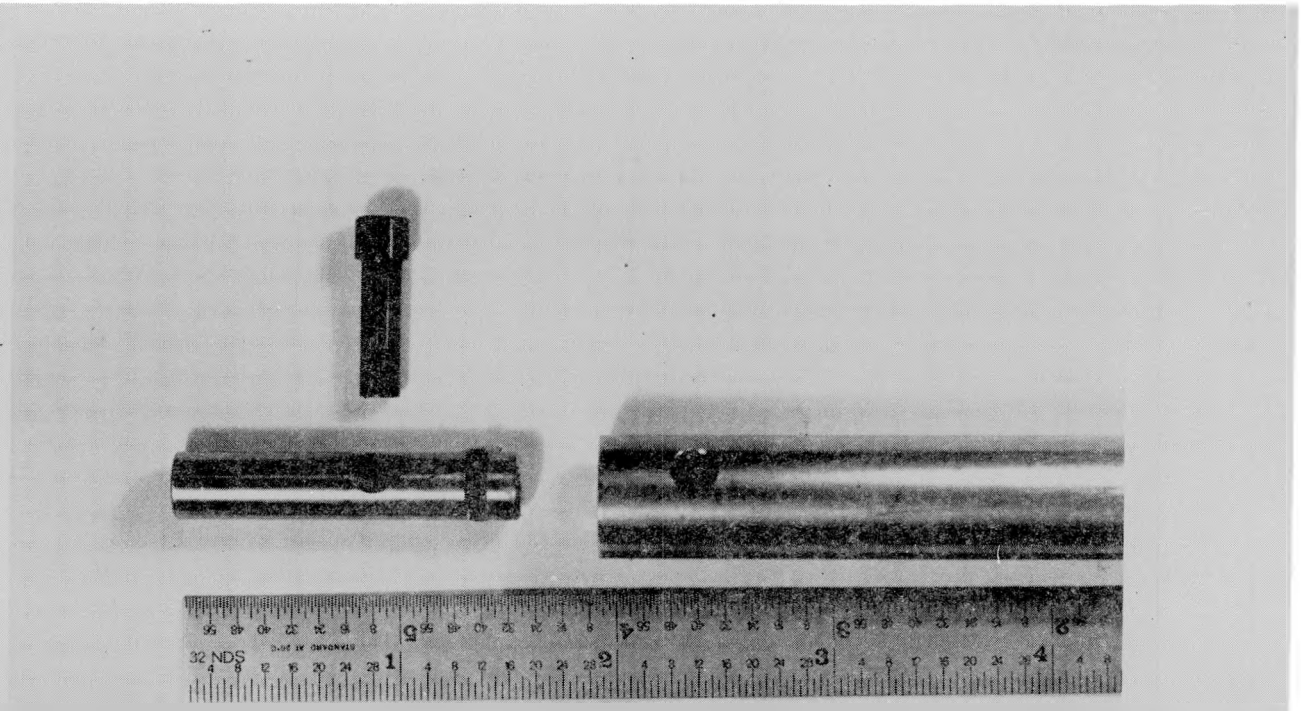


Figure 7. Shows the type of closure used on the pressure vessels of the polybarothermostat. The vessels were made of type 316 stainless steel. The pins were made type 17-4 PH stainless steel.

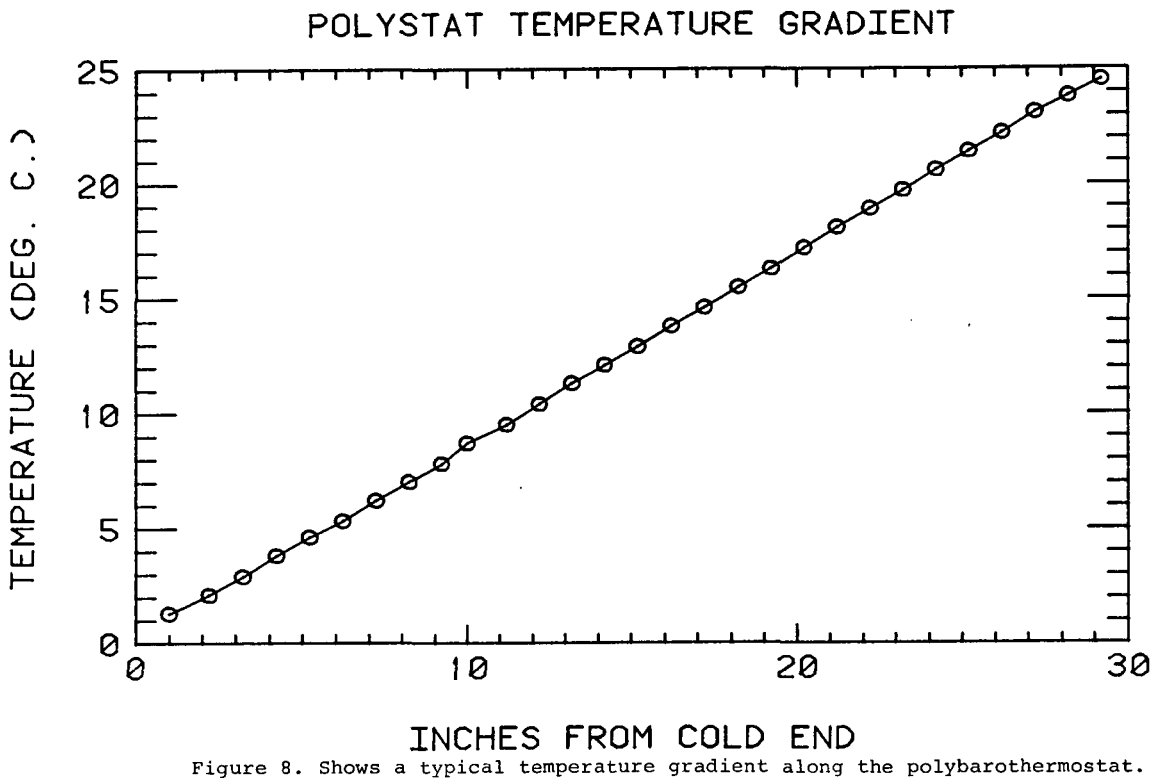


Figure 8. Shows a typical temperature gradient along the polybarothermostat.

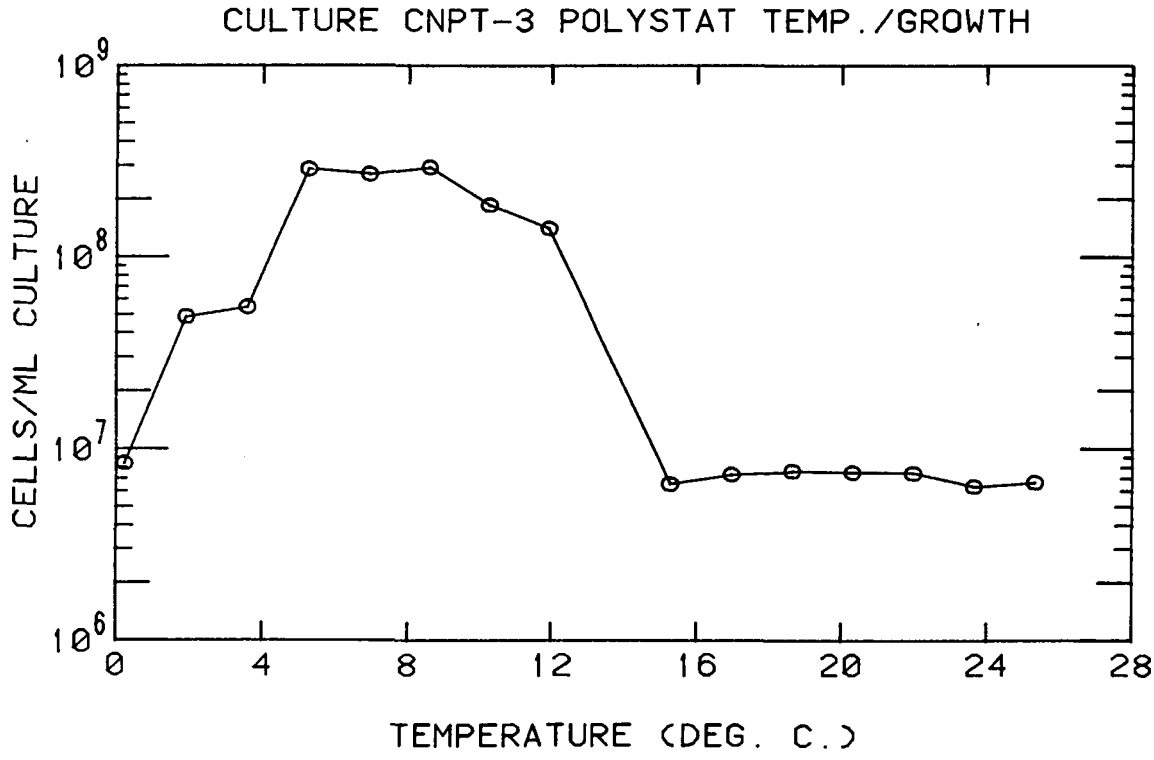


Figure 9 Shows the result of an incubation of a deep-sea bacterial culture along a temperature gradient at 580 bars.

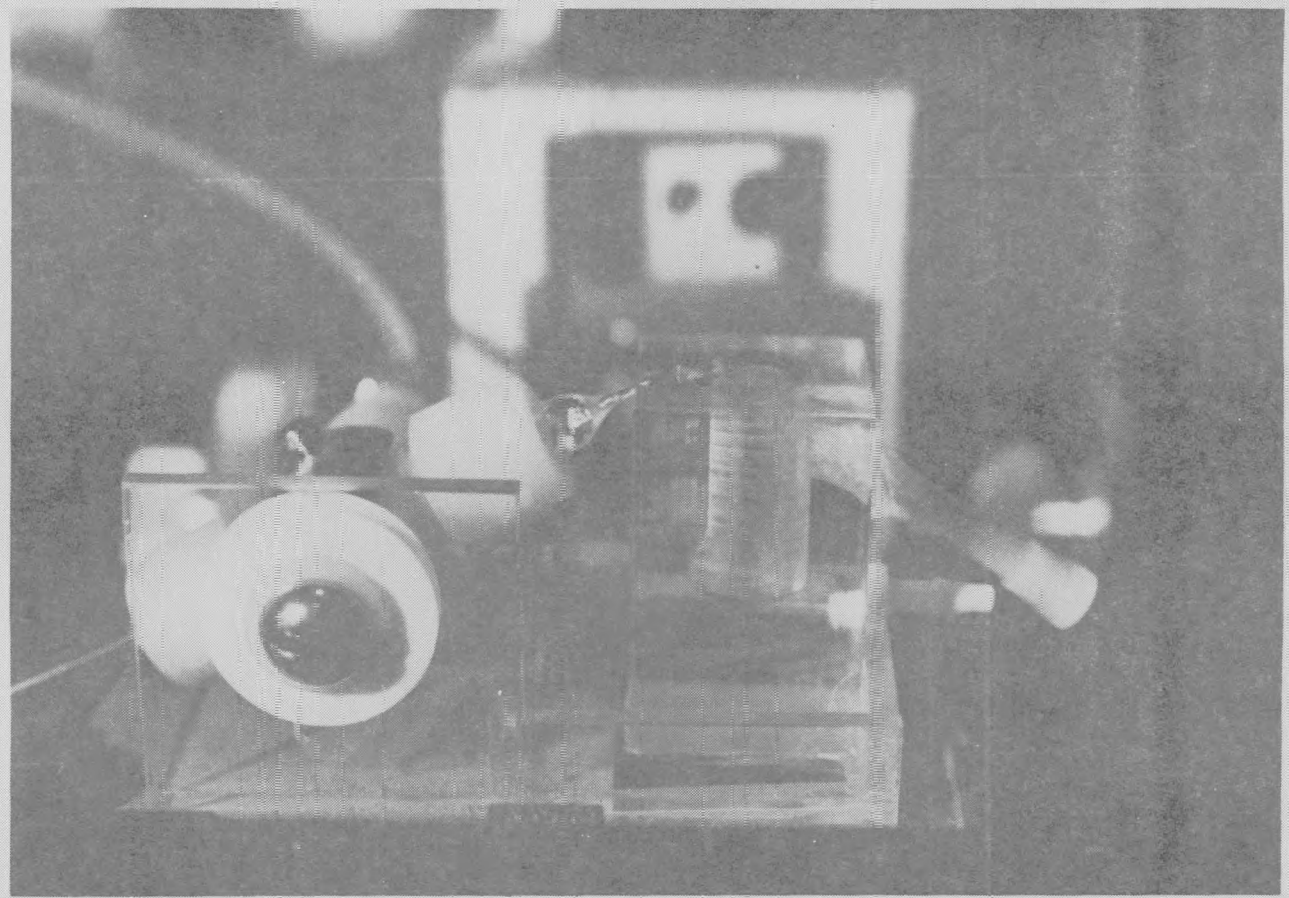


Figure 10. Shows the hydrodynamic focusing injector and aspirator used in the flow fluorocytometer similar to the one of Lindno and Steen (1979).

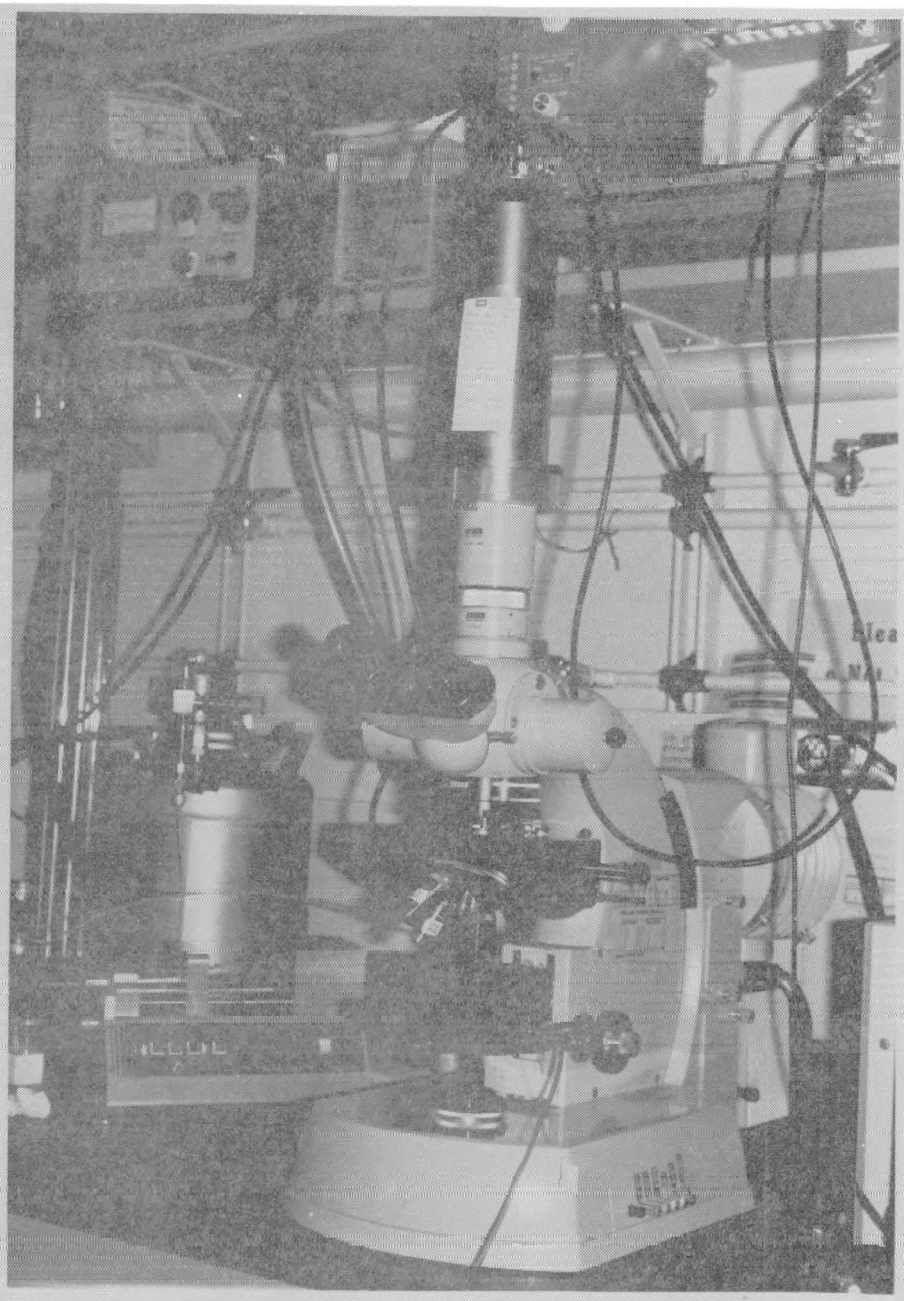


Figure 11. Shows the flow fluorocytometer components (with the exception of the multichannel analyzer). The component shown in the previous Figure is within the black box on the stage of the microscope. Pulses from the phtomultiplier on top of the microscope are sent to the multichannel analyzer. The instrument can detect over 1000 pulses per second. When the bacteria are labelled with acridine orange the pulse height is proportional to DNA content and when with fluorescene isothiocyanate the pulse height is proportional to cell size (Lindmo and Steen, 1979).

ADDENDUM TO DEEP-SEA BIOPHYSICS REPORT

BY A. A. YAYANOS

The attached addendum contains all of the data obtained in CY1981 on the reproduction of deep-sea bacteria. The file identifiers have the following meaning.

Each file identifier has 5 parts:

1 2 3 4 5
PLACE OF ORIGIN/ISOLATE NUMBER/EXPERIMENTAL TEMPERAURE/EXP. PRESSURE.DATE

PLACES OF ORIGIN ARE:

CNP	=	CENTRAL NORTH PACIFIC
HS	=	SEDIMENTS NEAR HAWAII
SC	=	SAN CLEMENTE BASIN
PE	=	PATTON ESCARPMENT AREA
AT	=	ALEUTIAN TRENCH AND VICINITY
MT	=	MARIANA TRENCH AND VICINITY
PT	=	PHILIPPINE TRENCH AND VICINITY

ISOLATE NUMBERS ARE DESIGNATED BY THE LETTER "I" FOLLOWED BY A NUMBER. THE NUMBER IS ASSIGNED TO A PARTICULAR BACTERIAL CULTURE WHEN IT IS FIRST ISOLATED FROM A DEEP-SEA SAMPLE.

THE TEMPERATURE OF AN EXPERIMENT IS INDICATED BY THE LETTER T FOLLOWED BY THE NUMBER OF DEGREES C. IF THE TEMPERATURE HAS A DECIMAL VALUE, THEN THE LETTER D IS USED TO INDICATE THE POSITION OF THE DECIMAL (E.G., 2.5 C = 2D5).

THE PRESSURE OF THE EXPERIMENT IN PSI IS INDICATED BY A NUMBER FOLLOWING THE LETTER P.

THE 4 CHARACTER CODE AT THE END OF THE FILE IDENTIFIER IS THE DATE AT WHICH THE EXPERIMENT WAS BEGUN. (J=JANUARY;F=FEBRUARY; M=MARCH; A=APRIL; Y=MAY; U=JUNE; L=JULY; G=AUGUST; S=SEPTEMBER; O-OCTOBER; N=NOVEMBER; D=DECEMBER). THE MIDDLE TWO NUMBERS OF THE LAST FOUR CHARACTERS ARE THE DAY OF THE MONTH. THE LAST NUMBER IS THE YEAR (0 BEGINS AT 1980 AND 9 ENDS AT 1989).

There are a few exceptions to this file structure that can be ignored for the purposes of this report.

Most of the data should be submitted for publication during CY1982.

AT/I4/T2/P7500.N021

Hours	Cells/ml
0.00	3.10E+006
22.47	2.64E+006
27.70	2.70E+006
43.58	2.94E+006
51.87	2.51E+006
68.42	2.64E+006
75.15	2.62E+006
91.93	2.72E+006
164.33	2.71E+006

AT/I4/T2/P9000.N021

Hours	Cells/ml
0.00	3.10E+006
22.48	3.64E+006
27.72	2.69E+006
43.60	2.69E+006
51.88	2.57E+006
68.43	2.61E+006
75.17	2.95E+006
91.95	2.67E+006
164.45	2.82E+006

AT/I4/T2/P1500.N021

Hours	Cells/ml
0.00	3.10E+006
22.08	2.67E+006
27.63	2.71E+006
43.52	3.37E+006
51.80	3.96E+006
68.33	7.28E+006
75.08	1.13E+007
91.87	3.86E+007
99.17	5.39E+007
125.68	1.10E+008
164.37	1.27E+008

AT/I4/T2/P3000.N021

Hours	Cells/ml
0.00	3.10E+006
22.10	2.76E+006
27.65	2.81E+006
43.53	3.10E+006
51.82	3.71E+006
68.35	4.72E+006
75.10	7.57E+006
91.88	2.96E+007
99.18	4.14E+007
125.68	9.67E+007
164.40	1.18E+008

AT/I4/T2/P6000.N021

Hours	Cells/ml
0.00	3.10E+006
22.45	2.58E+006
27.68	2.80E+006
43.57	2.59E+006
51.85	2.59E+006
68.40	3.14E+006
75.13	3.59E+006
91.92	5.63E+006
125.70	1.57E+007
164.42	4.36E+007

AT/I4/T2/P4500.N021

Hours	Cells/ml
0.00	3.10E+006
22.12	2.56E+006
27.67	2.61E+006
43.55	3.01E+006
51.83	3.10E+006
68.42	4.36E+006
75.12	5.42E+006
91.90	1.75E+007
99.40	2.97E+007
125.70	7.86E+007
164.42	8.94E+007

AT/I23/T2/P12000.D071

Hours	Cells/ml
0.00	1.90E+005
5.10	1.89E+005
22.15	2.63E+005
45.77	5.49E+005
70.95	2.86E+005
94.45	3.60E+005
120.23	3.80E+005
153.02	1.00E+006
166.05	3.49E+005
192.42	2.12E+005

AT/I23/T2/P6000.D071

Hours	Cells/ml
0.00	1.90E+005
4.88	1.70E+005
21.88	2.90E+005
45.72	4.42E+005
70.98	7.65E+005
94.40	3.19E+006
120.18	1.53E+007
126.53	1.43E+007
153.00	2.11E+007
166.00	1.95E+007
192.13	1.89E+007

AT/I23/T2/P2000.D071

Hours	Cells/ml
0.00	1.90E+005
4.87	2.46E+005
21.85	2.29E+005
45.68	2.41E+005
70.87	2.95E+005
94.37	3.33E+005
120.15	4.37E+005
153.00	1.02E+006
165.97	7.25E+005
192.07	1.31E+006

AT/I23/T2/P10000.D071

Hours	Cells/ml
0.00	1.90E+005
5.08	1.64E+005
22.13	3.02E+005
45.75	3.74E+005
70.95	3.06E+005
94.45	4.79E+005
120.22	8.44E+005
153.02	3.24E+006
166.03	3.36E+006
192.40	3.92E+006

AT/I23/T2/PATM.D071

Hours	Cells/ml
0.00	1.90E+005
4.72	1.55E+005
21.83	2.09E+005
45.67	2.14E+005
70.85	2.33E+005
94.35	2.37E+005
120.00	2.77E+005
152.98	1.29E+006
165.95	4.04E+005
192.05	2.89E+005

AT/I4/T2/PATM.N021

Hours	Cells/ml
0.00	3.10E+006
22.15	2.75E+006
27.62	2.61E+006
43.50	3.25E+006
51.78	4.00E+006
68.32	6.26E+006
75.07	8.91E+006
91.85	3.04E+007
99.00	4.23E+007
125.68	8.72E+007
164.37	9.28E+007

AT/I23/T2/P8000.D071

Hours	Cells/ml
0.00	1.90E+005
4.90	1.95E+005
22.10	3.16E+005
45.73	4.39E+005
70.83	4.57E+005
94.48	1.19E+006
120.20	5.27E+006
126.63	4.88E+006
153.02	1.97E+007
166.02	1.42E+007
173.07	1.51E+007
192.38	1.52E+007

AT/I23/T2/P4000.D071

Hours	Cells/ml
0.00	1.90E+005
4.87	6.79E+005
21.88	4.49E+005
45.70	4.74E+005
70.90	5.72E+005
94.38	1.21E+006
120.17	4.79E+006
126.35	6.75E+006
153.00	1.93E+007
165.98	2.01E+007
173.05	2.03E+007
192.10	1.87E+007

AT/I5/T2/P1500.N091

Hours	Cells/ml
0.00	1.14E+006
23.97	1.38E+006
41.03	4.27E+006
47.67	7.16E+006
66.52	5.11E+007
72.22	7.16E+007
89.82	9.42E+007

AT/I5/T2/P4500.N091

Hours	Cells/ml
0.00	1.14E+006
24.00	1.17E+006
41.07	2.84E+006
47.93	5.04E+006
66.53	2.10E+007
72.25	3.08E+007
89.85	5.65E+007

AT/I5/T2/P7500.N091

Hours	Cells/ml
0.00	1.14E+006
24.03	7.63E+005
41.10	7.63E+005
47.97	7.28E+005
66.57	9.45E+005
72.47	9.11E+005
89.88	8.65E+005

AT/I24/T2/P10000.D141

Hours	Cells/ml
0.00	9.10E+005
19.93	3.02E+005
44.32	6.05E+005
69.65	1.44E+006
91.72	3.04E+006
118.02	7.12E+006
150.33	6.85E+006

AT/I24/T2/P12000.D141

Hours	Cells/ml
0.00	9.10E+005
19.95	3.07E+005
44.33	2.78E+005
69.67	2.70E+005
91.73	4.35E+005
118.03	4.49E+005
150.35	1.87E+006
163.82	3.46E+005

AT/I24/T2/P6000.D141

Hours	Cells/ml
0.00	9.10E+005
19.75	5.22E+005
43.72	1.50E+006
67.72	5.77E+006
91.15	1.50E+007
117.98	1.96E+007
150.33	2.48E+007

AT/I5/T2/P3000.N091

Hours	Cells/ml
0.00	1.14E+006
24.00	1.19E+006
41.05	3.35E+006
47.68	6.43E+006
66.53	5.14E+007
72.23	6.20E+007
89.93	9.87E+007

AT/I5/T2/P6000.N091

Hours	Cells/ml
0.00	1.14E+006
24.02	1.09E+006
41.08	2.06E+006
47.95	2.91E+006
66.55	1.23E+007
72.42	1.39E+007
89.87	4.45E+007

AT/I5/T2/P9000.N091

Hours	Cells/ml
0.00	1.14E+006
24.05	9.22E+005
41.12	1.00E+006
48.00	1.02E+006
66.58	1.10E+006
72.47	9.86E+005
89.90	9.56E+005

AT/I24/T2/P4000.D141

Hours	Cells/ml
0.00	9.10E+005
19.58	4.99E+005
43.50	1.37E+006
67.70	5.37E+006
91.13	2.10E+007
117.97	2.59E+007
150.32	2.90E+007

AT/I24/T2/PATM.D141

Hours	Cells/ml
0.00	9.10E+005
19.18	2.42E+005
43.47	2.31E+005
67.65	2.63E+005
91.05	2.46E+005
117.93	3.27E+005
150.32	3.80E+005
163.77	2.89E+005

AT/I5/T2/PATM.N091

Hours	Cells/ml
0.00	1.14E+006
23.95	1.25E+006
40.90	4.45E+006
47.65	8.64E+006
66.50	5.38E+007
72.20	6.71E+007
89.80	8.23E+007

AT/I6/T2/P4500.N091

Hours	Cells/ml
0.00	1.09E+006
24.02	8.90E+005
41.07	2.45E+006
47.93	3.12E+006
66.55	1.16E+007
72.25	1.92E+007
89.87	4.99E+007

AT/I6/T2/P7500.N091

Hours	Cells/ml
0.00	1.09E+006
24.05	8.14E+005
41.12	7.56E+005
47.98	9.61E+005
66.58	8.68E+005
72.47	9.63E+005
89.90	8.18E+005

AT/I24/T2/P2000.D141

Hours	Cells/ml
0.00	9.10E+005
19.57	2.83E+005
43.48	5.24E+005
67.68	1.08E+006
91.07	2.41E+006
117.98	7.13E+006
150.32	1.78E+007
163.80	1.76E+007

AT/I6/T2/P6000.N091

Hours	Cells/ml
0.00	1.09E+006
24.03	7.14E+005
41.10	1.23E+006
47.95	1.64E+006
66.57	6.45E+006
72.45	8.29E+006
89.88	2.10E+007

AT/I6/T2/P9000.N091

Hours	Cells/ml
0.00	1.09E+006
24.07	9.00E+005
41.13	8.94E+005
48.02	1.13E+006
66.60	9.32E+005
72.48	8.28E+005
89.92	8.69E+005

AT/I24/T2/P8000.D141

Hours	Cells/ml
0.00	9.10E+005
19.77	4.71E+005
44.08	1.32E+006
69.63	5.01E+006
91.70	1.21E+007
118.03	1.95E+007
150.33	1.49E+007

AT/I25/T2/P6000.D011

Hours	Cells/ml
0.00	1.26E+006
24.53	3.93E+005
43.13	3.07E+005
73.02	4.41E+005
118.13	3.83E+006
139.00	6.81E+006
165.12	1.63E+007
189.48	1.93E+007

AT/I6/T2/P1500.N091

Hours	Cells/ml
0.00	1.09E+006
23.98	1.17E+006
41.08	3.42E+006
47.67	5.56E+006
66.52	3.84E+007
72.22	5.31E+007
89.83	8.61E+007

AT/I6/T2/PATM.N091

Hours	Cells/ml
0.00	1.09E+006
23.97	8.47E+005
40.95	3.62E+006
47.65	5.22E+006
66.50	3.43E+007
72.20	4.87E+007
89.82	7.17E+007

AT/I6/T2/P3000.N091

Hours	Cells/ml
0.00	1.09E+006
24.00	8.91E+005
41.05	2.26E+006
47.68	3.55E+006
66.53	3.66E+007
72.23	6.16E+007
89.85	8.63E+007

AT/I25/T2/P10000.D011

Hours	Cells/ml
0.00	1.26E+006
24.57	2.70E+005
43.33	2.73E+005
73.07	3.01E+005
118.12	4.48E+005
139.33	4.47E+005
165.17	5.70E+005
189.52	6.16E+005
210.85	7.91E+005
236.00	1.32E+006
308.83	1.08E+007

AT/I25/T2/P12000.D011

Hours	Cells/ml
0.00	1.26E+006
24.58	2.68E+005
43.33	2.55E+005
73.08	2.64E+005
118.13	3.77E+006
139.35	3.21E+005
165.18	3.09E+005
189.67	2.94E+005
210.85	3.45E+005
308.85	2.64E+005

AT/I26/T2/PATM.D011

Hours	Cells/ml
0.00	2.72E+005
24.47	9.30E+005
43.08	5.39E+005
72.98	5.21E+005
118.13	1.21E+006
138.97	5.13E+005
165.08	4.76E+005
189.45	5.52E+005
210.77	4.46E+005
308.67	4.57E+005

AT/I25/T2/P2000.D011

Hours	Cells/ml
0.00	1.26E+006
24.47	2.63E+005
43.08	2.11E+005
73.00	3.55E+005
118.10	4.32E+006
138.97	3.52E+005
165.08	3.26E+005
189.47	4.33E+005
210.77	4.10E+005
235.93	6.60E+005
308.68	7.28E+005

AT/I25/T2/P4000.D011

Hours	Cells/ml
0.00	1.26E+006
24.47	2.86E+005
43.12	2.61E+005
73.02	3.67E+005
118.10	2.50E+006
138.98	3.09E+006
165.10	1.12E+007
189.47	1.69E+007
210.78	1.78E+007
235.95	1.77E+007

AT/I25/T2/PATM.D011

Hours	Cells/ml
0.00	1.26E+006
24.47	2.86E+005
43.07	1.51E+005
72.98	1.74E+005
118.10	3.54E+006
138.95	5.39E+005
165.07	1.89E+005
189.45	4.94E+005
210.75	4.28E+005
308.67	2.78E+005

AT/I26/T2/P8000.D011

Hours	Cells/ml
0.00	2.72E+005
24.55	6.07E+005
43.13	5.93E+005
73.03	1.14E+006
118.15	1.22E+007
139.02	1.43E+007
165.13	1.47E+007
189.50	1.53E+007
210.82	1.57E+007

AT/I25/T2/P8000.D011

Hours	Cells/ml
0.00	1.26E+006
19.30	2.94E+005
43.30	2.81E+005
73.03	4.01E+005
118.12	5.70E+006
139.32	1.91E+006
165.15	8.10E+006
189.50	1.38E+007
210.83	1.47E+007
235.98	1.63E+007

AT/I26/T2/P8000.D011

Hours	Cells/ml
0.00	2.72E+005
24.65	5.79E+005
43.32	6.42E+005
73.05	9.21E+005
118.15	6.31E+006
139.33	9.95E+006
165.15	1.04E+007
189.52	1.09E+007
210.85	1.17E+007
235.98	1.24E+007

AT/I26/T2/P4000.D011

Hours	Cells/ml
0.00	2.72E+005
24.53	5.09E+005
43.12	5.14E+005
73.02	8.94E+005
118.15	7.06E+006
139.00	1.43E+007
165.12	1.60E+007
189.48	1.53E+007
210.80	1.52E+007
235.97	1.60E+007

AT/I1/T10/P6000.N231

Hours	Cells/ml
0.00	5.30E+006
18.78	3.88E+006
21.42	4.43E+006
26.15	5.80E+006
42.77	3.11E+007
45.87	4.53E+007
49.52	6.03E+007
169.00	1.47E+008

AT/I1/T10/P9000.N231

Hours	Cells/ml
0.00	5.30E+006
18.82	3.44E+006
21.45	3.88E+006
26.18	3.83E+006
42.80	6.23E+006
45.98	8.67E+006
49.65	1.12E+007
169.03	3.69E+007

AT/I26/T2/P10000.D011

Hours	Cells/ml
0.00	2.72E+005
24.58	5.64E+005
43.33	5.52E+005
73.07	6.17E+005
118.17	1.23E+006
139.35	1.56E+006
165.17	3.88E+006
189.53	7.85E+006
210.87	1.19E+007
236.00	1.21E+007
308.83	1.18E+007

AT/I26/T2/P12000.D011

Hours	Cells/ml
0.00	2.72E+005
24.58	5.02E+005
43.33	4.93E+005
73.08	4.33E+005
118.17	7.28E+005
139.37	3.07E+005
165.22	4.38E+005
189.67	8.87E+005
210.87	3.38E+005
308.87	5.26E+005

AT/I1/T10/P7500.N231

Hours	Cells/ml
0.00	5.30E+006
18.80	3.65E+006
21.43	4.17E+006
26.17	4.63E+006
42.78	1.97E+007
45.97	2.34E+007
49.63	2.91E+007
169.02	9.90E+007

AT/I26/T2/P2000.D011

Hours	Cells/ml
0.00	2.72E+005
24.48	8.96E+005
43.10	3.96E+005
73.00	5.40E+005
118.13	4.24E+006
138.98	9.71E+005
165.10	1.60E+006
189.47	2.41E+006
210.78	4.12E+006
235.95	8.84E+006
308.70	1.35E+007

AT/I1/T10/PATM.N231

Hours	Cells/ml
0.00	5.30E+006
18.32	3.44E+006
21.28	3.77E+006
25.95	4.42E+006
42.70	1.26E+007
45.73	1.68E+007
49.37	2.47E+007
168.93	8.04E+007

AT/I1/T10/P1500.N231

Hours	Cells/ml
0.00	5.30E+006
18.33	4.09E+006
21.18	4.41E+006
25.97	6.54E+006
42.72	2.53E+007
45.75	3.20E+007
49.38	4.39E+007
168.95	1.35E+008

AT/I1/T10/P3000.N231

Hours	Cells/ml
0.00	5.30E+006
18.48	3.31E+006
21.20	3.64E+006
25.98	3.75E+006
42.73	4.07E+006
45.77	4.97E+006
49.40	6.50E+006
168.97	2.13E+008

AT/I1/T10/P4500.N231

Hours	Cells/ml
0.00	5.30E+006
18.50	4.09E+006
21.30	5.00E+006
26.00	7.31E+006
42.75	4.08E+007
45.85	5.62E+007
49.52	7.05E+007
168.98	1.54E+008

AT/I1/T2/P4500.0191

Hours	Cells/ml
0.00	1.05E+006
4.92	9.54E+005
21.78	1.14E+006
28.93	1.84E+006
46.95	6.08E+006
53.12	1.30E+007
69.82	2.66E+007
93.98	6.47E+007
101.68	7.03E+007
166.58	8.55E+007

AT/I1/T2/P6000.0191

Hours	Cells/ml
0.00	1.05E+006
4.93	1.02E+006
21.80	1.21E+006
28.95	1.48E+006
46.95	3.68E+006
53.18	4.16E+006
69.83	1.24E+007
94.00	2.48E+007
101.70	2.92E+007
124.53	3.88E+007
147.15	4.88E+007
166.60	5.30E+007

AT/I1/T2/P7500.0191

Hours	Cells/ml
0.00	1.05E+006
4.95	9.89E+005
21.82	7.98E+005
28.97	8.45E+005
46.98	6.72E+005
53.20	6.98E+005
69.83	6.28E+005
94.02	1.04E+006
101.72	8.63E+005
166.62	1.18E+006

AT/I1/T2/P9000.0191

Hours	Cells/ml
0.00	1.05E+006
4.97	1.10E+006
21.83	1.07E+006
29.18	9.48E+005
47.00	1.02E+006
53.22	1.04E+006
69.87	9.75E+005
94.03	1.01E+006
101.73	9.60E+005
166.80	1.01E+006

AT/I27/T2/P6000.D141

Hours	Cells/ml
0.00	3.00E+005
19.77	5.02E+005
43.73	1.16E+006
67.72	3.67E+006
91.17	1.46E+007
117.98	2.07E+007
150.37	2.21E+007

AT/I1/T2/P1500.0191

Hours	Cells/ml
0.00	1.05E+006
4.90	8.66E+005
21.75	1.39E+006
28.90	2.97E+006
46.92	1.09E+007
53.10	2.21E+007
69.78	5.76E+007
93.93	9.68E+007
101.53	1.00E+008
166.55	1.39E+008

AT/I27/T2/P10000.D141

Hours	Cells/ml
0.00	3.00E+005
19.93	3.72E+005
44.32	4.27E+005
69.67	8.02E+005
91.73	1.61E+006
118.02	3.35E+006
150.38	3.77E+006

AT/I27/T2/P12000.D141

Hours	Cells/ml
0.00	3.00E+005
19.87	4.01E+005
44.33	3.48E+005
69.68	4.17E+005
91.75	4.82E+005
118.03	4.26E+005
150.38	8.57E+005
163.83	4.17E+005

AT/I1/T2/PATM.0191

Hours	Cells/ml
0.00	1.05E+006
4.88	9.27E+005
21.73	1.54E+006
28.88	3.23E+006
46.97	8.10E+006
53.08	1.61E+007
69.77	4.72E+007
93.92	8.14E+007
101.52	8.65E+007
166.53	9.95E+007

AT/I1/T2/P3000.0191

Hours	Cells/ml
0.00	1.05E+006
4.90	8.66E+005
21.77	1.29E+006
28.92	1.83E+006
46.93	1.01E+007
53.12	1.83E+007
69.80	4.79E+007
93.97	8.67E+007
101.57	9.31E+007
166.57	1.13E+008

AT/I27/T2/P4000.D141

Hours	Cells/ml
0.00	3.00E+005
19.60	4.95E+005
43.52	1.04E+006
67.70	3.52E+006
91.15	1.47E+007
117.97	2.58E+007
150.37	2.94E+007

AT/I27/T2/PATM.D141

Hours	Cells/ml
0.00	3.00E+005
19.20	3.60E+005
43.48	4.44E+005
67.67	5.04E+005
91.05	5.42E+005
117.95	5.74E+005
150.35	8.44E+005
163.78	5.89E+005

AT/I11/T2/P7500.N161

Hours	Cells/ml
0.00	3.03E+006
26.45	2.14E+006
43.05	2.18E+006
50.23	2.18E+006
67.27	2.17E+006
74.63	3.04E+006
92.45	2.62E+006
163.02	2.42E+006

AT/I27/T2/P2000.D141

Hours	Cells/ml
0.00	3.00E+005
19.58	4.40E+005
43.50	7.08E+005
67.68	1.30E+006
91.07	2.69E+006
117.95	8.03E+006
150.35	1.69E+007
163.80	1.60E+007

AT/I11/T2/P1500.N161

Hours	Cells/ml
0.00	3.03E+006
18.87	1.83E+006
26.38	2.19E+006
42.98	4.26E+006
50.02	5.59E+006
67.20	1.91E+007
74.43	4.64E+007
92.13	8.56E+007
97.67	9.38E+007
162.92	1.30E+008

AT/I11/T2/P4500.N161

Hours	Cells/ml
0.00	3.03E+006
26.42	1.91E+006
43.82	2.50E+006
50.07	2.86E+006
67.23	8.05E+006
74.48	1.47E+007
92.43	4.39E+007
97.75	4.66E+007
163.00	9.17E+007

AT/I11/T2/P9000.N161

Hours	Cells/ml
0.00	3.03E+006
18.85	2.18E+006
26.47	2.16E+006
43.07	2.16E+006
50.25	2.98E+006
67.28	1.88E+006
74.65	2.99E+006
92.47	2.21E+006
163.03	2.23E+006

AT/I27/T2/P8000.D141

Hours	Cells/ml
0.00	3.00E+005
19.78	4.31E+005
44.30	1.00E+006
67.63	2.49E+006
91.72	8.03E+006
118.13	1.61E+007
150.37	1.45E+007

AT/I11/T2/P3000.N161

Hours	Cells/ml
0.00	3.03E+006
26.40	2.11E+006
43.00	2.80E+006
50.05	4.25E+006
67.22	1.28E+007
74.43	3.35E+007
92.42	7.25E+007
97.70	8.37E+007
162.98	1.15E+008

AT/I11/T2/P6000.N161

Hours	Cells/ml
0.00	3.03E+006
26.43	2.17E+006
43.03	2.01E+006
50.22	2.19E+006
67.25	2.89E+006
74.48	3.95E+006
92.43	7.25E+006
97.77	1.69E+007
163.00	5.68E+007

AT/I2/T10/P6000.N231

Hours	Cells/ml
0.00	3.49E+006
18.80	3.62E+006
21.43	4.28E+006
26.17	5.12E+006
42.78	2.93E+007
45.88	3.86E+007
49.53	5.27E+007
169.00	1.21E+008

AT/I2/T10/P9000.N231

Hours	Cells/ml
0.00	3.49E+006
18.82	2.99E+006
21.45	3.12E+006
26.20	3.61E+006
42.80	5.56E+006
45.98	6.91E+006
49.67	1.09E+007
169.03	3.35E+007

AT/I2/T10/P7500.N231

Hours	Cells/ml
0.00	3.49E+006
18.80	3.49E+006
21.43	3.57E+006
26.18	4.44E+006
42.80	1.88E+007
45.97	2.70E+007
49.65	3.39E+007
169.02	1.01E+008

AT/I11/T2/PATM.N161

Hours	Cells/ml
0.00	3.03E+006
18.83	1.73E+006
26.37	2.00E+006
42.97	2.34E+006
50.00	3.82E+006
67.18	9.94E+006
74.42	2.52E+007
92.12	6.26E+007
97.67	7.43E+007
162.90	9.15E+007

AT/I2/T10/PATM.N231

Hours	Cells/ml
0.00	3.49E+006
18.33	3.30E+006
21.30	3.66E+006
25.97	4.15E+006
42.72	9.25E+006
45.73	1.32E+007
49.37	2.02E+007
168.95	7.46E+007

AT/I2/T10/P3000.N231

Hours	Cells/ml
0.00	3.49E+006
18.50	3.82E+006
21.22	4.38E+006
26.00	6.01E+006
42.75	2.25E+007
45.78	3.05E+007
49.38	4.44E+007
168.97	1.18E+008

AT/I2/T10/P1500.N231

Hours	Cells/ml
0.00	3.49E+006
18.35	3.66E+006
21.20	4.29E+006
25.97	5.68E+006
42.72	1.71E+007
45.77	2.44E+007
49.38	3.90E+007
168.95	1.26E+008

AT/I2/T10/P4500.N231

Hours	Cells/ml
0.00	3.49E+006
18.52	3.80E+006
21.32	4.40E+006
26.02	5.95E+006
42.75	2.79E+007
45.87	4.09E+007
49.52	5.29E+007
168.98	1.27E+008

AT/I2/T2/P4500.0191

Hours	Cells/ml
0.00	8.77E+005
4.92	7.30E+005
21.77	9.32E+005
28.95	1.48E+006
46.95	3.85E+006
53.15	7.80E+006
69.82	2.29E+007
94.00	5.24E+007
101.70	6.26E+007
166.60	8.38E+007

AT/I2/T2/P7500.0191

Hours	Cells/ml
0.00	8.77E+005
4.95	7.04E+005
21.82	6.19E+005
28.97	6.72E+005
46.98	5.04E+005
53.22	7.46E+005
69.85	4.02E+005
94.02	7.30E+005
101.72	6.05E+005
166.63	6.25E+005

AT/I21/T2/P6000.D071

Hours	Cells/ml
0.00	1.91E+005
4.85	2.49E+005
21.88	2.76E+005
45.70	4.46E+005
70.90	8.31E+005
94.40	2.24E+006
120.18	1.31E+007
126.52	1.32E+007
152.95	1.84E+007
166.00	1.72E+007
192.12	1.74E+007

AT/I2/T2/P1500.0191

Hours	Cells/ml
0.00	8.77E+005
4.88	6.60E+005
21.75	1.17E+006
28.92	2.60E+006
46.92	1.66E+007
53.10	2.37E+007
69.78	5.75E+007
93.93	1.00E+008
101.55	1.05E+008
166.55	1.26E+008

AT/I2/T2/P6000.0191

Hours	Cells/ml
0.00	8.77E+005
4.93	7.54E+005
21.80	7.90E+005
28.95	1.01E+006
46.97	1.16E+006
53.20	3.72E+006
69.83	6.91E+006
94.02	2.30E+007
101.72	2.53E+007
124.60	3.14E+007
147.15	4.25E+007
166.62	4.91E+007

AT/I2/T2/P9000.0191

Hours	Cells/ml
0.00	8.77E+005
4.97	7.84E+005
21.83	8.63E+005
29.18	8.69E+005
47.00	8.82E+005
53.23	1.02E+006
69.88	6.76E+005
94.03	7.81E+005
101.73	8.18E+005
166.65	8.51E+005

AT/I2/T2/PATM.0191

Hours	Cells/ml
0.00	8.77E+005
4.87	7.28E+005
21.73	1.28E+006
28.90	3.32E+006
46.90	1.14E+007
53.08	2.28E+007
69.77	5.53E+007
93.92	8.93E+007
101.53	9.04E+007
166.55	9.82E+007

AT/I2/T2/P3000.0191

Hours	Cells/ml
0.00	8.77E+005
4.90	7.18E+005
21.77	1.08E+006
28.93	2.02E+006
46.93	1.03E+007
53.12	2.28E+007
69.80	4.11E+007
93.97	8.81E+007
101.68	9.02E+007
166.58	1.13E+008

AT/I21/T2/P10000.D071

Hours	Cells/ml
0.00	1.91E+005
5.08	1.30E+005
22.12	5.41E+005
45.75	3.24E+005
70.93	1.56E+006
94.43	4.04E+005
120.20	5.65E+005
152.97	2.07E+006
166.03	1.41E+006
192.23	2.18E+006

AT/I21/T2/P12000.D071

Hours	Cells/ml
0.00	1.91E+005
5.10	1.48E+005
22.13	7.54E+005
45.77	2.61E+005
70.95	3.08E+005
94.45	2.04E+005
120.22	3.71E+005
152.97	8.52E+005
166.05	4.19E+005
192.42	2.08E+005

AT/I12/T2/P7500.N161

Hours	Cells/ml
0.00	3.49E+005
26.45	1.42E+006
43.05	1.45E+006
50.25	1.51E+006
67.28	1.52E+006
74.65	2.42E+006
92.47	1.59E+006
163.03	1.47E+006

AT/I21/T2/P2000.D071

Hours	Cells/ml
0.00	1.91E+005
4.72	1.45E+005
21.85	1.58E+005
45.67	2.12E+005
70.87	2.65E+005
94.37	6.58E+005
120.15	2.11E+005
152.95	8.81E+005
165.97	2.14E+005
192.07	1.99E+005

AT/I21/T2/P4000.D071

Hours	Cells/ml
0.00	1.91E+005
4.85	6.33E+005
21.87	2.22E+005
45.68	2.35E+005
70.88	5.95E+005
94.38	8.68E+005
120.17	2.84E+006
126.33	3.76E+006
152.95	1.20E+007
165.98	1.27E+007
173.03	1.36E+007
192.08	1.32E+007

AT/I21/T2/PATM.D071

Hours	Cells/ml
0.00	1.91E+005
4.70	1.90E+005
21.82	2.17E+005
45.65	2.12E+005
70.85	2.57E+005
94.35	2.07E+005
120.13	2.06E+005
152.93	2.87E+005
165.95	2.72E+005
192.05	2.60E+005

AT/I12/T2/P9000.N161

Hours	Cells/ml
0.00	3.49E+005
18.87	1.38E+006
26.47	1.45E+006
43.07	1.48E+006
50.27	1.56E+006
67.30	1.57E+006
74.70	2.53E+006
92.48	1.47E+006
163.05	1.46E+006

AT/I21/T2/P8000.D071

Hours	Cells/ml
0.00	1.91E+005
4.88	1.60E+005
22.10	3.18E+005
45.73	4.17E+005
70.92	7.51E+005
94.42	1.12E+006
120.18	5.57E+006
126.62	6.43E+006
152.97	1.43E+007
166.02	1.23E+007
173.05	1.36E+007
192.38	1.35E+007

AT/I12/T2/P1500.N161

Hours	Cells/ml
0.00	3.49E+005
18.87	1.28E+006
26.40	1.71E+006
42.98	3.04E+006
50.03	5.26E+006
67.22	1.90E+007
74.43	3.69E+007
92.40	7.87E+007
97.70	8.88E+007
162.97	1.17E+008

AT/I12/T2/P4500.N161

Hours	Cells/ml
0.00	3.49E+005
26.43	1.36E+006
43.02	1.77E+006
50.07	2.77E+006
67.25	1.11E+007
74.47	1.54E+007
92.43	4.21E+007
97.77	5.15E+007
163.00	9.04E+007

AT/I3/T2/P6000.N021

Hours	Cells/ml
0.00	2.60E+006
22.45	2.42E+006
27.67	2.44E+006
43.55	2.35E+006
51.83	2.69E+006
68.38	2.92E+006
75.12	3.45E+006
91.98	4.64E+006
99.38	5.10E+006
125.77	1.27E+007

AT/I3/T2/P9000.N021

Hours	Cells/ml
0.00	2.60E+006
22.48	2.75E+006
27.70	2.46E+006
43.60	2.56E+006
51.87	2.57E+006
68.42	2.56E+006
75.17	2.98E+006
91.83	2.60E+006
164.45	2.46E+006

AT/I12/T2/P3000.N161

Hours	Cells/ml
0.00	3.49E+005
26.42	1.63E+006
43.00	2.57E+006
50.05	4.54E+006
67.23	1.54E+007
74.45	3.48E+007
92.58	6.60E+007
97.72	8.57E+007
162.98	1.16E+008

AT/I12/T2/P6000.N161

Hours	Cells/ml
0.00	3.49E+005
26.43	1.21E+006
43.03	1.38E+006
50.23	2.02E+006
67.27	3.50E+006
74.63	6.44E+006
92.45	1.26E+007
97.78	1.84E+007
163.02	5.24E+007

AT/I3/T2/P7500.N021

Hours	Cells/ml
0.00	2.60E+006
22.47	2.53E+006
27.68	2.58E+006
43.57	2.42E+006
51.85	2.45E+006
68.40	2.48E+006
75.13	2.84E+006
91.92	2.57E+006
164.43	2.71E+006

AT/I12/T2/PATM.N161

Hours	Cells/ml
0.00	3.49E+005
18.85	1.26E+006
26.45	1.30E+006
42.97	2.66E+006
50.02	4.83E+006
67.20	1.57E+007
74.42	4.16E+007
92.12	6.79E+007
97.68	7.52E+007
162.90	9.38E+007

AT/I3/T2/PATM.N021

Hours	Cells/ml
0.00	2.60E+006
22.50	2.38E+006
27.62	2.52E+006
43.50	2.88E+006
51.77	3.94E+006
68.15	7.04E+006
75.05	1.02E+007
91.85	3.47E+007
98.98	4.99E+007
125.75	1.08E+008
164.35	1.08E+008

AT/I3/T2/P1500.N021

Hours	Cells/ml
0.00	2.60E+006
22.07	2.46E+006
27.63	2.45E+006
43.52	3.26E+006
51.78	4.17E+006
68.33	8.74E+006
75.07	1.34E+007
91.87	4.53E+007
99.17	6.52E+007
125.75	1.09E+008
164.37	1.39E+008

AT/I3/T2/P3000.N021

Hours	Cells/ml
0.00	2.60E+006
22.08	2.64E+006
27.65	2.46E+006
43.53	2.96E+006
51.80	3.57E+006
68.35	8.11E+006
75.08	1.02E+007
91.87	3.42E+007
99.18	5.36E+007
125.75	1.05E+008
164.38	1.16E+008

AT/I3/T2/P4500.N021

Hours	Cells/ml
0.00	2.60E+006
22.10	2.52E+006
27.65	2.60E+006
43.53	2.86E+006
51.82	3.29E+006
68.37	5.52E+006
75.10	7.32E+006
91.88	2.57E+007
99.38	3.38E+007
125.77	8.38E+007
164.40	9.58E+007

CNPT/I3A/T2/PATM.Y261

Hours	Cells/ml
0.00	1.72E+004
43.13	1.73E+005
65.83	4.96E+005
98.70	2.55E+006
137.88	4.42E+006

CNPT/I3A/T2/P6000.Y261

Hours	Cells/ml
0.00	1.72E+004
22.28	2.77E+004
43.18	1.47E+005
48.88	8.62E+004
65.95	9.15E+004
98.72	8.31E+004
137.97	7.68E+004
162.82	9.62E+004
312.38	9.77E+004

CNPT/I3A/T2/P8000.Y261

Hours	Cells/ml
0.00	1.72E+004
22.45	3.32E+004
43.48	8.20E+004
49.22	8.57E+004
66.17	5.30E+004
98.73	5.38E+004
138.50	5.41E+004
162.85	6.01E+004
312.40	1.04E+005

CNPT/I3A/T2/P10000.Y261

Hours	Cells/ml
0.00	1.72E+004
22.47	2.22E+004
43.42	6.82E+004
49.23	9.88E+004
66.18	7.29E+004
98.77	9.76E+004
138.53	5.85E+004
162.87	7.47E+004

CNPT/I3A/T2/P4000.Y261

Hours	Cells/ml
0.00	1.72E+004
22.27	5.41E+004
43.17	9.01E+004
48.37	2.26E+005
65.92	1.13E+005
98.72	1.46E+005
137.95	2.28E+005

CNPT/I3A/T2/P12000.Y261

Hours	Cells/ml
0.00	1.72E+004
22.48	3.27E+004
43.45	6.72E+004
49.25	7.21E+004
66.20	7.34E+004
98.78	8.10E+004

CNPT/I3A/T10/P12000.U011

Hours	Cells/ml
0.00	1.03E+005
21.28	5.38E+004
43.43	6.38E+004
68.10	7.29E+004
97.08	6.43E+004

CNPT/I3A/T10/P6000.U011

Hours	Cells/ml
0.00	1.03E+005
20.97	7.47E+004
43.38	8.00E+004
68.05	1.37E+005
97.07	1.32E+005
169.78	2.49E+005

CNPT/I3A/T10/P2000.U011

Hours	Cells/ml
0.00	1.03E+005
20.93	2.97E+005
25.62	5.73E+005
42.95	4.56E+006
49.55	5.03E+006
67.98	6.41E+006
97.05	4.80E+006

CNPT/I3A/T10/P10000.U011

Hours	Cells/ml
0.00	1.03E+005
21.27	8.83E+004
43.42	5.64E+004
68.08	5.91E+004
97.08	5.07E+004

CNPT/I3A/T10/PATM.U011

Hours	Cells/ml
0.00	1.03E+005
20.92	6.64E+005
25.60	1.57E+006
42.93	5.14E+006
49.52	5.32E+006
67.97	5.90E+006
97.03	5.61E+006
169.72	6.96E+006

CNPT/I3A/T2/P2000.Y261

Hours	Cells/ml
0.00	1.72E+004
22.25	5.07E+004
43.13	1.66E+005
48.85	1.81E+005
65.90	4.48E+005
98.70	5.16E+005
137.92	6.73E+005
162.80	8.91E+005
190.58	1.27E+006

CNPT/I3A/T10/P8000.U011

Hours	Cells/ml
0.00	1.03E+005
21.25	6.64E+004
43.40	8.41E+004
68.07	6.56E+004
97.07	5.59E+004
169.80	1.42E+005

CNPT/I3A/T10/P4000.U011

Hours	Cells/ml
0.00	1.03E+005
20.95	7.00E+004
25.63	9.04E+004
42.98	2.97E+005
49.57	2.96E+005
68.00	3.67E+005
97.05	4.61E+005
169.75	2.83E+006

CNPT/I3/T10/P8000.U011

Hours	Cells/ml
0.00	1.50E+006
21.23	1.14E+007
25.85	2.58E+007
43.38	1.50E+008
49.77	1.79E+008
68.07	1.95E+008
155.07	3.95E+008

CNPT/I3/T10/P4000.U011

Hours	Cells/ml
0.00	1.50E+006
20.93	3.91E+006
25.62	5.79E+006
42.97	1.98E+007
49.55	3.06E+007
68.00	4.14E+007
169.78	1.38E+008

CNPT/I3/T10/PATM.U011

Hours	Cells/ml
0.00	1.50E+006
20.90	1.75E+006
25.92	1.78E+006
42.92	1.94E+006
49.52	2.02E+006
67.97	2.06E+006
169.73	2.13E+006

CNPT/I3/T10/P10000.U011

Hours	Cells/ml
0.00	1.50E+006
21.25	1.08E+007
25.87	2.74E+007
43.42	2.10E+008
49.77	1.83E+008
68.08	3.73E+008

CNPT/I3/T10/P12000.U011

Hours	Cells/ml
0.00	1.50E+006
21.28	5.99E+006
25.87	1.09E+007
43.43	1.06E+008
49.78	2.04E+008
68.10	2.05E+008

CNPT/I3/T10/P6000.U011

Hours	Cells/ml
0.00	1.50E+006
20.97	8.71E+006
25.85	1.77E+007
43.37	1.11E+008
49.53	1.04E+008
68.03	1.84E+008
169.80	2.97E+008

CNPT/I3/T2/P12000.Y261

Hours	Cells/ml
0.00	1.22E+006
22.83	1.18E+006
43.43	1.24E+006
49.25	1.42E+006
66.20	1.46E+006
72.32	1.58E+006
98.78	2.57E+006

CNPT/I3/T2/P6000.Y261

Hours	Cells/ml
0.00	1.22E+006
22.28	1.46E+006
43.17	1.55E+007
48.87	2.59E+007
65.93	9.48E+007
72.28	1.39E+008
98.73	1.34E+008

CNPT/I3/T2/PATM.Y261

Hours	Cells/ml
0.00	1.22E+006
43.12	3.97E+006
65.83	1.19E+007
72.25	1.74E+007
98.68	3.30E+007
137.87	5.82E+007

CNPT/I3/T10/P2000.U011

Hours	Cells/ml
0.00	1.50E+006
20.92	2.49E+006
25.60	3.21E+006
42.95	6.01E+006
49.53	8.17E+006
67.98	1.50E+007

CNPT/I3/T2/P2000.Y261

Hours	Cells/ml
0.00	1.22E+006
22.25	1.98E+006
43.13	6.96E+006
48.83	1.03E+007
65.90	3.49E+007
72.27	4.95E+007
98.70	1.09E+008
137.90	6.99E+007
162.80	8.54E+007

CNPT/I3/T2/P10000.Y261

Hours	Cells/ml
0.00	1.22E+006
22.48	1.74E+006
43.42	4.87E+006
49.23	6.74E+006
66.18	1.59E+007
72.30	2.25E+007
98.77	4.93E+007
138.52	9.37E+007
162.87	1.16E+008

CNPT/I3/T2/P8000.Y261

Hours	Cells/ml
0.00	1.22E+006
22.47	2.54E+006
43.40	1.35E+007
49.22	2.40E+007
66.15	8.82E+007
72.28	1.24E+008
98.75	1.47E+008
138.48	2.28E+008
162.85	1.94E+008
312.42	1.54E+008

CNPT/I3/T2/P4000.Y261

Hours	Cells/ml
0.00	1.22E+006
22.27	2.68E+006
43.15	1.47E+007
48.85	2.70E+007
65.92	1.05E+008
72.28	1.65E+008
98.72	1.12E+008
137.95	1.06E+008
162.82	1.10E+008
312.43	9.34E+007

MTQNAG/I41/T2/PATM.D151

Hours	Cells/ml
0.00	5.47E+005
22.33	6.82E+005
49.42	5.81E+005
69.82	5.68E+005
127.50	6.10E+005
146.28	6.61E+005
164.28	7.74E+005
190.77	5.83E+005
482.17	6.04E+005

MTQNAG/I41/T2/P11000.D151

Hours	Cells/ml
0.00	5.47E+005
22.72	7.23E+005
49.52	1.07E+006
70.20	9.92E+005
127.62	2.20E+006
146.58	4.70E+006
164.35	7.95E+006
190.83	1.16E+007
482.23	2.02E+007

MTQNAG/I41/T2/P9000.D151

Hours	Cells/ml
0.00	5.47E+005
22.55	6.20E+005
49.48	8.15E+005
70.18	8.85E+005
146.57	2.28E+006
164.33	3.36E+006
190.82	5.68E+006
482.22	1.12E+007

MTQNAG/I41/T2/P5000.D151

Hours	Cells/ml
0.00	5.47E+005
22.35	5.81E+005
49.43	5.69E+005
69.83	5.63E+005
146.30	6.48E+005
164.30	6.20E+005
190.78	5.87E+005
482.18	6.63E+005

MTQNAG/I41/T2/P7000.D151

Hours	Cells/ml
0.00	5.47E+005
22.53	5.81E+005
49.47	6.05E+005
69.85	7.28E+005
146.32	1.02E+006
164.32	1.16E+006
190.80	1.61E+006
482.20	8.30E+006

MT/I103/T2/P7500.G171

Hours	Cells/ml
0.00	6.38E+005
26.30	2.50E+006
49.57	1.62E+007
68.50	8.16E+007
95.85	1.36E+008
168.37	1.41E+008

MT/I103/T2/P5000.G171

Hours	Cells/ml
0.00	6.38E+005
26.28	3.02E+006
49.55	2.42E+007
68.30	1.18E+008
95.72	1.72E+008
168.23	1.90E+008

MT/I103/T2/G.G171

Hours	Cells/ml
1.01	2.01E+001
173.38	8.63E+000
345.75	7.93E+000
518.12	8.40E+000
690.49	7.98E+000
862.85	1.63E+002
1035.22	9.77E+002

MT/I103/T2/P15000.G171

Hours	Cells/ml
0.00	6.38E+005
26.37	6.17E+005
49.63	6.62E+005
68.70	6.16E+005
96.08	1.49E+006
168.55	5.85E+005

MTQNAG/I41/T2/P13000.D151

Hours	Cells/ml
0.00	5.47E+005
22.73	6.65E+005
49.53	7.74E+005
70.22	5.65E+005
129.27	2.07E+006
146.60	2.77E+006
164.37	4.94E+006
190.85	8.88E+006
482.42	1.07E+007

MTQNAG/I41/T2/P15000.D151

Hours	Cells/ml
0.00	5.47E+005
22.73	7.01E+005
49.55	6.65E+005
70.23	5.68E+005
146.62	1.26E+006
164.38	1.33E+006
190.87	2.57E+006
482.43	4.93E+006

MT/I103/T2/P12500.G171

Hours	Cells/ml
0.00	6.38E+005
26.35	6.54E+005
49.62	7.97E+005
68.68	8.29E+005
96.07	1.57E+006
168.53	1.53E+006

MT/I103/T2/P10000.G171

Hours	Cells/ml
0.00	6.38E+005
26.33	1.35E+006
49.58	5.03E+006
68.52	2.60E+007
95.87	8.50E+007
168.38	1.33E+008

MT/I103/T2/P2500.G171

Hours	Cells/ml
0.00	6.38E+005
26.27	2.57E+006
49.52	1.76E+007
68.28	7.47E+007
95.70	1.70E+008
168.22	1.82E+008

MT/I103/T2/PATM.G171

Hours	Cells/ml
0.00	6.38E+005
26.25	1.23E+006
49.48	2.73E+006
68.72	4.09E+006
95.68	7.09E+006
168.20	1.35E+007

MT/I121/T2/P15000.U101

Hours	Cells/ml
0.00	2.61E+006
23.42	2.65E+006
47.32	2.56E+006
78.40	2.39E+006
114.20	2.66E+006
138.65	2.56E+006
164.47	2.56E+006
283.90	2.65E+006
313.82	2.10E+006
361.68	1.54E+006

MT/I121/T2/PATM.U101

Hours	Cells/ml
0.00	2.61E+006
22.98	2.57E+006
46.72	2.59E+006
77.80	2.31E+006
113.85	2.67E+006
138.72	2.55E+006
162.00	2.61E+006
281.87	2.78E+006
313.77	2.05E+006
337.72	2.32E+006
361.28	2.67E+006
384.28	2.86E+006
451.67	8.20E+006

MT/I41/T2/P11000.D151

Hours	Cells/ml
0.00	4.33E+005
22.70	5.56E+005
49.50	6.69E+005
70.20	7.06E+005
127.62	2.12E+006
146.57	3.38E+006
164.33	4.78E+006
190.83	9.99E+006
482.23	2.42E+007

MT/I121/T2/P10000.U101

Hours	Cells/ml
0.00	2.61E+006
23.22	2.55E+006
47.08	2.60E+006
78.37	2.23E+006
114.15	2.66E+006
138.62	2.59E+006
164.42	2.65E+006
283.95	2.81E+006
313.80	3.53E+006
337.80	2.56E+006
361.67	2.37E+006
384.33	2.81E+006
451.68	3.13E+006

MT/I121/T2/P7500.U101

Hours	Cells/ml
0.00	2.61E+006
23.20	2.55E+006
47.07	2.55E+006
78.10	2.31E+006
113.90	2.69E+006
138.40	2.73E+006
164.57	2.75E+006
283.53	3.26E+007
313.80	1.50E+008
337.78	1.43E+008
361.65	1.48E+008
384.30	1.71E+008

MT/I121/T2/P12500.U101

Hours	Cells/ml
0.00	2.61E+006
23.40	2.68E+006
47.30	2.58E+006
78.38	1.35E+006
114.17	2.70E+006
138.62	2.58E+006
164.33	2.67E+006
283.87	2.88E+006
313.82	2.31E+006
337.83	2.51E+006
361.68	2.63E+006
451.70	2.80E+006

MT/I121/T2/P5000.U101

Hours	Cells/ml
0.00	2.61E+006
23.02	2.43E+006
46.75	2.77E+006
78.08	2.40E+006
113.88	3.87E+006
138.37	2.63E+006
162.63	2.54E+006
283.52	9.67E+006
313.78	1.05E+008
337.75	1.66E+008
361.65	1.90E+008
384.30	2.04E+008

MT/I121/T2/P2500.U101

Hours	Cells/ml
0.00	2.61E+006
23.00	2.41E+006
46.73	2.65E+006
78.08	2.35E+006
113.87	2.67E+006
138.23	2.64E+006
162.62	2.55E+006
283.50	2.86E+006
313.78	2.53E+006
337.73	3.24E+006
361.63	1.44E+007
384.28	7.13E+007
451.68	1.19E+008

MT/I41/T2/P7000.D151

Hours	Cells/ml
0.00	4.33E+005
22.52	5.19E+005
49.45	5.74E+005
69.85	5.75E+005
146.30	7.53E+005
164.32	7.43E+005
190.80	8.41E+005
482.20	2.37E+006

MT/I41/T2/PATM.D151

Hours	Cells/ml
0.00	4.33E+005
22.33	6.00E+005
49.38	4.84E+005
69.82	4.37E+005
127.60	5.20E+005
146.27	5.64E+005
164.28	2.82E+005
190.75	5.23E+005

MT/I41/T2/P15000.D151

Hours	Cells/ml
0.00	4.33E+005
22.73	6.27E+005
49.53	5.73E+005
70.23	6.28E+005
146.93	1.07E+006
164.37	1.02E+006
190.87	1.69E+006
482.42	6.30E+006

MT/I41/T2/P9000.D151

Hours	Cells/ml
0.00	4.33E+005
49.47	5.40E+005
70.18	6.53E+005
146.55	2.12E+006
164.33	2.65E+006
190.73	4.05E+006
482.22	2.37E+007

MT/I122/T2/P12500.G241

Hours	Cells/ml
0.00	6.85E+005
21.83	6.58E+005
45.58	7.52E+005
70.48	8.63E+005
93.75	8.31E+005
165.55	8.23E+005

MT/I41/T2/P5000.D151

Hours	Cells/ml
0.00	4.33E+005
22.35	5.62E+005
49.43	4.84E+005
69.83	4.32E+005
146.28	5.76E+005
164.28	5.57E+005
190.78	4.86E+005
482.18	4.69E+005

MT/I122/T2/PATM.G241

Hours	Cells/ml
0.00	6.85E+005
21.75	1.10E+006
45.48	2.49E+006
70.15	3.85E+006
93.50	5.14E+006
165.27	8.45E+006

MT/I41/T2/P13000.D151

Hours	Cells/ml
0.00	4.33E+005
22.72	5.70E+005
49.52	5.97E+005
70.22	6.76E+005
129.27	3.27E+006
146.58	1.77E+006
164.35	1.96E+006
190.85	4.91E+006
482.40	7.96E+006

MT/I122/T2/P5000.G241

Hours	Cells/ml
0.00	6.85E+005
21.78	2.00E+006
45.53	1.06E+007
70.18	9.24E+007
93.53	1.62E+008
165.32	1.80E+008

MT/I122/T2/G.G241

Hours	Cells/ml
1.01	2.68E+001
173.38	1.03E+001
345.75	8.75E+000
518.12	9.03E+000
690.49	1.22E+001
862.85	1.00E+003
1035.22	1.00E+003

MT/I122/T2/P15000.G241

Hours	Cells/ml
0.00	6.85E+005
21.85	7.46E+005
45.60	7.69E+005
70.50	7.98E+005
93.67	7.88E+005
165.57	7.58E+005

MT/I104/T2/P10000.G171

Hours	Cells/ml
0.00	5.81E+005
26.33	1.54E+006
49.60	5.14E+006
68.52	2.30E+007
95.88	8.51E+007
168.40	1.21E+008

MT/I104/T2/P15000.G171

Hours	Cells/ml
0.00	5.81E+005
26.38	5.60E+005
49.65	6.43E+005
68.72	4.96E+005
96.08	1.19E+006
168.57	5.15E+005

MT/I104/T2/P7500.G171

Hours	Cells/ml
0.00	5.81E+005
26.32	2.46E+006
49.58	1.56E+007
68.50	8.78E+007
95.87	1.52E+008
168.38	1.66E+008

MT/I122/T2/P10000.G241

Hours	Cells/ml
0.00	6.85E+005
21.82	1.16E+006
45.57	3.80E+006
70.47	1.38E+007
93.73	7.36E+007
165.53	1.16E+008

MT/I122/T2/P2500.G241

Hours	Cells/ml
0.00	6.85E+005
21.75	2.00E+006
45.52	8.45E+006
70.17	5.27E+007
93.52	1.27E+008
165.28	1.41E+008

MT/I122/T2/P7500.G241

Hours	Cells/ml
0.00	6.85E+005
21.78	1.56E+006
45.38	6.65E+006
70.45	6.51E+007
93.55	1.49E+008
165.52	1.68E+008

MT/I104/T2/P2500.G171

Hours	Cells/ml
0.00	5.81E+005
26.28	2.64E+006
49.53	1.53E+007
68.30	8.75E+007
95.72	1.67E+008
168.25	1.77E+008

MT/I104/T2/PATM.G171

Hours	Cells/ml
0.00	5.81E+005
26.27	1.20E+006
49.50	2.68E+006
68.73	4.15E+006
95.68	5.95E+006
168.22	1.13E+007

MT/I104/T2/P12500.G171

Hours	Cells/ml
0.00	5.81E+005
26.35	6.72E+005
49.62	7.75E+005
68.70	8.41E+005
96.07	1.35E+006
168.55	1.16E+006

MT/I123/T2/P2500.G241

Hours	Cells/ml
0.00	1.08E+006
21.77	2.47E+006
45.52	1.26E+007
70.17	6.76E+007
93.53	1.22E+008
165.30	1.33E+008

MT/I123/T2/PATM.G241

Hours	Cells/ml
0.00	1.08E+006
21.75	1.40E+006
45.50	2.95E+006
70.17	4.86E+006
93.52	6.63E+006
165.27	9.75E+006

MT/I123/T2/P12500.G241

Hours	Cells/ml
0.00	1.08E+006
21.83	7.17E+005
45.58	9.18E+005
70.50	1.12E+006
93.75	1.00E+006
165.57	1.85E+006

MT/I123/T2/P15000.G241

Hours	Cells/ml
0.00	1.08E+006
21.87	8.35E+005
45.62	8.91E+005
70.52	8.75E+005
93.77	8.61E+005
165.58	1.04E+006

MT/I123/T2/P7500.G241

Hours	Cells/ml
0.00	1.08E+006
21.80	2.14E+006
45.55	1.01E+007
70.47	8.65E+007
93.40	1.32E+008
165.52	1.60E+008

MT/I104/T2/P5000.G171

Hours	Cells/ml
0.00	5.81E+005
26.30	2.93E+006
49.55	1.38E+007
68.32	1.20E+008
95.73	1.79E+008
168.25	1.86E+008

MT/I100/T2/P12500.L131

Hours	Cells/ml
0.00	3.36E+005
29.75	1.79E+005
52.68	2.63E+005
73.10	2.55E+005
97.08	2.47E+005
151.28	3.70E+005
196.15	2.89E+005

MT/I123/T2/P10000.G241

Hours	Cells/ml
0.00	1.08E+006
21.82	1.61E+006
45.38	4.58E+006
70.48	1.99E+007
93.73	8.92E+007
165.57	1.09E+008

MT/I123/T2/P5000.G241

Hours	Cells/ml
0.00	1.08E+006
21.78	2.46E+006
45.53	1.62E+007
70.18	1.15E+008
93.55	1.45E+008
165.32	1.60E+008

MT/I123/T2/G.G241

Hours	Cells/ml
1.01	2.70E+001
173.38	1.01E+001
345.75	8.73E+000
518.12	9.11E+000
690.49	1.13E+001
862.85	1.00E+003
1035.22	1.00E+003

MT/I100/T2/P2500.L131

Hours	Cells/ml
0.00	3.36E+005
29.65	1.57E+005
52.60	3.19E+005
72.72	3.45E+005
150.98	4.18E+005
196.08	5.56E+005
219.23	6.12E+005
266.35	6.44E+005
358.33	8.18E+005

MT/I100/T2/PATM.L131

Hours	Cells/ml
0.00	3.36E+005
29.63	2.12E+005
52.13	2.39E+005
73.07	2.40E+005
96.98	2.96E+005
150.97	2.80E+005
196.07	2.79E+005
219.22	3.52E+005
267.58	3.60E+005
358.47	4.13E+005

MT/I100/T2/P12500.L201

Hours	Cells/ml
0.00	2.78E+006
28.97	1.99E+006
52.33	2.04E+006
76.55	2.20E+006
99.10	2.54E+006
147.02	1.82E+006
170.78	3.14E+006
192.32	3.16E+006
219.92	3.97E+006
243.90	3.63E+006
264.90	3.74E+006
358.67	4.11E+006

MT/I100/T2/P10000.L131

Hours	Cells/ml
0.00	3.36E+005
29.73	1.70E+005
52.67	2.89E+005
73.08	3.37E+005
97.07	4.25E+005
151.27	4.46E+005
196.13	5.24E+005
219.28	5.96E+005

MT/I100/T2/P15000.L131

Hours	Cells/ml
0.00	3.36E+005
29.77	2.01E+005
52.70	2.62E+005
73.12	2.50E+005
97.10	5.07E+005
151.30	2.84E+005
196.25	3.09E+005
219.33	3.42E+005
268.02	3.26E+005
358.68	4.86E+005

MT/I100/T2/P7500.L131

Hours	Cells/ml
0.00	3.36E+005
29.72	2.26E+005
52.65	4.41E+005
72.75	5.22E+005
97.05	7.43E+005
151.02	4.69E+005
196.12	2.68E+006
219.27	3.77E+006
244.62	5.51E+006
267.97	1.07E+007
358.48	2.99E+007
389.02	4.58E+007
433.08	5.86E+007
504.20	6.40E+007

MT/I100/T2/P5000.L131

Hours	Cells/ml
0.00	3.36E+005
29.68	2.01E+005
52.62	4.10E+005
72.72	4.68E+005
97.02	6.69E+005
151.00	4.43E+005
196.10	2.89E+006
219.25	4.06E+006
244.60	6.03E+006
267.95	9.24E+006
358.35	4.59E+007
388.98	6.88E+007
433.07	6.57E+007

MT/I100/T2/G.L131

Hours	Cells/ml
1.01	2.44E+002
173.38	2.17E+002
345.75	4.03E+001
518.12	4.67E+001
690.49	1.75E+002
862.85	3.44E+002
1035.22	2.65E+002

MT/I108/T2/P2500.L201

Hours	Cells/ml
0.00	2.78E+006
28.88	1.91E+006
52.05	2.21E+006
76.45	2.61E+006
98.58	3.31E+006
146.75	4.13E+006
168.95	7.30E+006
191.97	9.85E+006
219.50	1.38E+007
243.58	1.86E+007
264.83	2.44E+007
358.65	7.54E+007

MT/I108/T2/PATM.L201

Hours	Cells/ml
0.00	2.78E+006
28.37	1.88E+006
51.40	1.91E+006
76.42	1.94E+006
99.22	2.02E+006
147.05	6.48E+005
168.93	1.87E+006
191.95	1.81E+006
219.48	1.96E+006
243.57	1.97E+006
264.82	1.96E+006

MT/I101/T2/P12500.G031

Hours	Cells/ml
0.00	2.64E+005
21.40	2.21E+005
47.02	2.23E+005
74.17	3.84E+005
99.13	2.33E+005
121.03	4.34E+005
170.47	2.73E+005
215.92	2.53E+005
267.10	3.11E+005
339.25	3.15E+005
388.20	4.19E+005

MT/I108/T2/P10000.L201

Hours	Cells/ml
0.00	2.78E+006
28.95	1.91E+006
52.32	2.61E+006
76.53	3.70E+006
99.07	5.36E+006
146.80	7.43E+006
169.07	1.18E+007
192.30	1.37E+007

MT/I108/T2/P15000.L201

Hours	Cells/ml
0.00	2.78E+006
28.98	1.94E+006
52.35	2.03E+006
76.57	2.06E+006
99.13	2.11E+006
147.03	1.23E+006
170.83	2.08E+006
192.33	2.01E+006
219.97	2.16E+006
243.92	2.16E+006
264.92	2.03E+006

MT/I108/T2/P7500.L201

Hours	Cells/ml
0.00	2.78E+006
28.92	1.95E+006
52.10	3.05E+006
76.48	5.01E+006
98.75	7.62E+006
146.78	1.46E+007
169.00	2.54E+007
192.05	4.13E+007
219.55	6.22E+007
243.62	6.51E+007
264.87	6.11E+007

MT/I108/T2/P5000.L201

Hours	Cells/ml
0.00	2.78E+006
28.90	1.91E+006
52.08	3.18E+006
76.47	5.26E+006
98.62	8.62E+006
146.77	3.17E+007
168.98	6.34E+007
192.00	1.17E+008
219.52	1.68E+008
243.60	1.91E+008
264.85	1.91E+008

MT/I108/T2/G.L201

Hours	Cells/ml
1.01	9.71E+002
173.38	5.64E+001
345.75	2.47E+001
518.12	3.01E+001
690.49	6.10E+001
862.85	9.71E+002
1035.22	9.71E+002

MT/I101/T2/P7500.L131

Hours	Cells/ml
0.00	2.37E+005
29.72	1.86E+005
52.65	2.86E+005
72.77	2.60E+005
97.05	3.20E+005
125.88	5.48E+005
151.02	1.32E+006
196.12	5.76E+005
219.28	7.72E+005
267.97	1.00E+006
358.50	1.49E+006

MT/I101/T2/PATM.G031

Hours	Cells/ml
0.00	2.64E+005
21.50	2.27E+005
46.65	1.80E+005
74.23	2.51E+005
99.17	2.49E+005
120.95	1.90E+005
170.35	2.23E+005
215.82	2.74E+005
266.85	2.74E+005
339.20	3.37E+005
388.15	2.84E+005

MT/I101/T2/P15000.L131

Hours	Cells/ml
0.00	2.37E+005
29.78	1.23E+005
52.72	1.38E+005
73.13	1.93E+005
151.30	1.99E+005
196.27	2.03E+005
219.35	1.86E+005
358.70	2.57E+005

MT/I101/T2/P15000.G031

Hours	Cells/ml
0.00	2.64E+005
21.42	1.94E+005
47.03	3.26E+005
74.18	4.22E+005
99.15	3.16E+005
121.05	3.09E+005
170.50	2.80E+005
215.93	2.40E+005
267.12	2.99E+005
339.28	3.60E+005
388.22	3.95E+005

MT/I101/T2/P12500.L131

Hours	Cells/ml
0.00	2.37E+005
29.75	1.09E+005
52.68	1.45E+005
73.12	1.22E+005
97.08	1.81E+005
151.28	1.71E+005
196.17	1.56E+005
219.32	1.91E+005
268.02	2.35E+005
358.68	3.26E+005

MT/I101/T2/P7500.G031

Hours	Cells/ml
0.00	2.64E+005
21.20	1.97E+005
46.98	2.15E+005
73.88	3.57E+005
98.87	2.68E+005
121.00	2.43E+005
170.43	3.77E+005
215.87	4.40E+005
267.08	7.21E+005
339.23	8.27E+005
388.17	8.90E+005

MT/I101/T2/P2500.G031

Hours	Cells/ml
0.00	2.64E+005
21.00	2.42E+005
46.67	2.15E+005
73.85	3.43E+005
98.83	2.44E+005
170.37	2.80E+005
215.83	3.07E+005
266.87	2.70E+005
339.22	3.44E+005
388.15	3.87E+005

MT/I101/T2/PATM.L131

Hours	Cells/ml
0.00	2.37E+005
29.63	1.08E+005
52.15	1.79E+005
73.07	2.11E+005
96.98	2.88E+005
150.97	2.57E+005
196.07	2.30E+005
219.23	2.35E+005
267.60	3.10E+005
358.48	3.71E+005

MT/I101/T2/P10000.L131

Hours	Cells/ml
0.00	2.37E+005
29.73	1.48E+005
52.67	1.78E+005
73.10	2.56E+005
97.07	2.47E+005
125.88	3.67E+005
151.27	2.77E+005
196.15	2.46E+005
219.30	3.36E+005
267.98	4.33E+005
358.53	4.88E+005

MT/I101/T2/P10000.G031

Hours	Cells/ml
0.00	2.64E+005
21.23	2.01E+005
47.00	2.53E+005
74.12	3.06E+005
99.12	3.15E+005
121.02	2.93E+005
170.45	4.40E+005
215.88	3.91E+005
267.10	5.02E+005
339.25	6.45E+005
388.18	6.95E+005

MT/I102/T2/PATM.G031

Hours	Cells/ml
0.00	6.20E+006
21.50	6.69E+006
46.67	6.75E+006
74.25	6.55E+006
99.17	7.02E+006
120.97	6.87E+006
170.35	8.33E+006
215.83	5.84E+006

MT/I102/T2/P12500.G031

Hours	Cells/ml
0.00	6.20E+006
21.40	8.00E+006
47.03	6.90E+006
74.18	6.92E+006
99.13	5.50E+006
121.03	9.84E+006
170.50	8.24E+006
215.93	8.69E+006

MT/I101/T2/P5000.G031

Hours	Cells/ml
0.00	2.64E+005
21.02	1.95E+005
46.70	2.86E+005
73.87	3.76E+005
98.85	4.44E+005
120.98	3.68E+005
170.42	6.79E+005
215.85	8.81E+005
266.88	1.23E+006
339.23	2.04E+006
388.17	2.39E+006
506.75	3.62E+006

MT/I101/T2/P2500.L131

Hours	Cells/ml
0.00	2.37E+005
29.68	1.17E+005
52.62	1.96E+005
72.72	2.44E+005
97.02	2.83E+005
125.97	4.63E+005
150.98	4.81E+005
196.08	2.82E+005
219.25	3.24E+005
266.37	3.14E+005
358.33	5.30E+005

MT/I102/T2/P7500.G031

Hours	Cells/ml
0.00	6.20E+006
21.22	7.47E+006
46.98	7.31E+006
73.90	7.29E+006
98.88	4.16E+007
121.00	1.19E+008
170.45	1.43E+008
215.88	1.48E+008

MT/I101/T2/P5000.L131

Hours	Cells/ml
0.00	2.37E+005
29.70	1.43E+005
52.63	3.32E+005
72.72	2.54E+005
97.03	4.20E+005
125.93	3.52E+005
151.00	1.35E+006
196.10	4.29E+005
219.27	5.81E+005
267.95	9.83E+005
358.35	1.08E+006

MT/I102/T2/P10000.G031

Hours	Cells/ml
0.00	6.20E+006
21.25	6.61E+006
47.00	7.83E+006
74.15	8.92E+006
99.12	1.83E+007
121.82	6.41E+007
170.47	9.85E+007
215.90	9.96E+007

MT/I102/T2/P2500.G031

Hours	Cells/ml
0.00	6.20E+006
21.02	7.14E+006
46.68	7.04E+006
73.85	1.34E+007
98.85	6.55E+007
120.97	1.62E+008
170.40	1.70E+008
215.85	1.69E+008

MT/I102/T2/G.G031

Hours	Cells/ml
1.01	1.08E+003
173.38	1.09E+001
345.75	1.17E+001
518.12	9.95E+000
690.49	1.21E+001
862.85	1.08E+003
1035.22	1.08E+003

MT/I102/T2/P15000.G031

Hours	Cells/ml
0.00	6.20E+006
21.42	7.69E+006
47.05	9.19E+006
74.20	6.67E+006
99.15	6.40E+006
121.07	8.16E+006
170.52	8.58E+006
215.95	6.93E+006

MT/I109/T2/PATM.L201

Hours	Cells/ml
0.00	1.74E+006
28.40	1.32E+006
51.40	1.59E+006
76.60	1.64E+006
99.23	1.63E+006
147.05	1.01E+006
168.95	1.62E+006
191.97	1.57E+006
219.50	1.57E+006
243.57	1.85E+006
264.83	1.61E+006

MT/I109/T2/P12500.L201

Hours	Cells/ml
0.00	1.74E+006
28.98	1.45E+006
52.35	1.72E+006
76.57	2.03E+006
99.10	2.39E+006
147.02	2.57E+006
170.82	4.61E+006
192.33	5.01E+006
219.93	5.84E+006

MT/I109/T2/P7500.L201

Hours	Cells/ml
0.00	1.74E+006
28.93	1.72E+006
52.32	4.66E+006
76.52	1.02E+007
98.77	2.47E+007
146.80	1.53E+008
169.07	1.83E+008
192.07	1.97E+008
219.57	2.06E+008
243.62	2.11E+008
264.88	2.01E+008

MT/I102/T2/P5000.G031

Hours	Cells/ml
0.00	6.20E+006
21.03	6.99E+006
46.70	7.13E+006
73.88	2.83E+007
98.87	1.24E+008
120.98	1.58E+008
170.42	1.70E+008
215.88	1.81E+008

MT/I109/T2/P10000.L201

Hours	Cells/ml
0.00	1.74E+006
28.95	1.51E+006
52.33	3.08E+006
76.55	6.36E+006
99.08	1.05E+007
146.82	2.29E+007
169.08	3.74E+007
192.30	5.21E+007

MT/I109/T2/P2500.L201

Hours	Cells/ml
0.00	1.74E+006
28.90	1.45E+006
52.08	2.31E+006
76.45	3.29E+006
98.60	4.87E+006
146.75	1.29E+007
168.97	1.65E+007
191.98	2.71E+007
219.52	5.25E+007
243.58	7.57E+007
264.85	9.29E+007
358.67	1.11E+008

MT/I120/T2/PATM.U101

Hours	Cells/ml
0.00	1.30E+006
22.98	1.41E+006
46.72	1.53E+006
77.80	1.67E+006
113.83	2.24E+006
138.72	2.36E+006
162.08	2.36E+006
281.87	3.54E+006

MT/I120/T2/P12500.U101

Hours	Cells/ml
23.38	1.50E+006
47.28	1.44E+006
78.38	1.39E+006
114.17	1.58E+006
120.00	1.30E+006
138.62	1.57E+006
164.43	1.62E+006
283.85	1.57E+006

MT/I109/T2/G.L201

Hours	Cells/ml
1.01	1.40E+003
173.38	3.78E+001
345.75	1.82E+001
518.12	1.86E+001
690.49	3.40E+001
862.85	9.83E+001
1035.22	1.04E+003

MT/I109/T2/P15000.L201

Hours	Cells/ml
0.00	1.74E+006
29.00	1.41E+006
52.37	1.83E+006
76.58	1.89E+006
99.13	1.98E+006
147.03	1.42E+006
170.83	1.95E+006
192.35	1.79E+006
219.97	2.10E+006
243.92	1.89E+006
264.83	1.77E+006

MT/I120/T2/P7500.U101

Hours	Cells/ml
0.00	1.30E+006
23.18	1.56E+006
47.05	2.78E+006
78.10	2.87E+007
113.90	1.26E+008
138.38	1.25E+008
164.38	1.41E+008

MT/I109/T2/P5000.L201

Hours	Cells/ml
0.00	1.74E+006
28.92	1.90E+006
52.08	4.68E+006
76.52	1.13E+007
98.62	2.72E+007
146.78	1.70E+008
168.98	1.84E+008
192.00	1.92E+008
219.53	2.03E+008
243.62	2.06E+008
264.87	1.93E+008

MT/I120/T2/P5000.U101

Hours	Cells/ml
0.00	1.30E+006
23.02	1.63E+006
46.75	3.13E+006
78.08	2.53E+007
113.88	1.57E+008
138.37	1.52E+008
162.62	1.68E+008

MT/I120/T2/P2500.U101

Hours	Cells/ml
0.00	1.30E+006
23.00	1.60E+006
46.73	2.87E+006
78.08	1.26E+007
113.85	9.35E+007
138.22	1.09E+008
162.60	1.29E+008

MT/I120/T2/P10000.U101

Hours	Cells/ml
0.00	1.30E+006
23.20	1.41E+006
47.07	1.80E+006
78.37	3.77E+006
114.13	1.53E+007
138.60	6.22E+007
164.42	1.01E+008

MT/I120/T2/P15000.U101

Hours	Cells/ml
0.00	1.30E+006
23.40	1.31E+006
47.30	1.46E+006
78.40	1.26E+006
114.20	1.33E+006
138.63	1.35E+006
164.45	1.33E+006
283.88	1.40E+006

PT/I47/T2/P15000.F021

Hours	Cells/ml
0.00	7.47E+005
19.30	4.49E+005
25.47	5.91E+005
43.08	5.73E+005
49.75	5.31E+005
67.23	5.01E+005
73.33	5.29E+005
91.87	5.25E+005
97.52	5.45E+005
162.63	5.29E+005
186.92	5.75E+005

PT/I47/T2/P7500.F021

Hours	Cells/ml
0.00	7.47E+005
19.07	9.28E+005
25.42	1.25E+006
43.42	2.72E+006
49.38	4.51E+006
67.18	1.24E+007
73.28	1.91E+007
91.73	3.37E+007
97.45	4.36E+007
163.28	1.23E+008
187.47	1.28E+008

PT/I47/T2/PATM.F021

Hours	Cells/ml
0.00	7.47E+005
19.43	1.11E+006
25.52	1.25E+006
43.75	1.61E+006
49.80	1.31E+006
67.13	1.48E+006
73.25	1.49E+006
91.77	1.74E+006
97.53	1.71E+006
163.43	3.56E+006
187.63	2.84E+006

PT/I47/T2/P12500.F021

Hours	Cells/ml
0.00	7.47E+005
19.28	5.06E+005
25.45	4.84E+005
43.20	4.31E+005
49.73	4.33E+005
67.22	4.52E+005
73.32	4.73E+005
91.85	5.62E+005
97.50	5.06E+005
162.82	4.65E+005
187.08	4.23E+005

PT/I56/T2/P12500.F231

Hours	Cells/ml
0.00	2.44E+005
19.55	3.09E+005
25.37	3.12E+005
42.87	3.85E+005
50.13	2.68E+005
68.00	3.36E+005
73.53	2.57E+005
90.87	2.95E+005
97.83	3.07E+005
120.85	4.00E+005
144.03	4.07E+005
163.05	3.36E+005

PT/I47/T2/P10000.F021

Hours	Cells/ml
0.00	7.47E+005
19.08	6.41E+005
25.43	6.58E+005
43.30	1.10E+006
49.72	1.43E+006
67.20	3.10E+006
73.30	4.41E+006
91.83	6.31E+006
97.48	1.02E+007
162.97	6.38E+007
187.22	1.11E+008

PT/I56/T2/P2500.F231

Hours	Cells/ml
0.00	2.44E+005
19.07	6.69E+005
24.97	9.40E+005
42.45	3.45E+006
49.67	5.93E+006
67.32	2.93E+007
73.87	4.70E+007
90.58	9.30E+007
97.43	9.69E+007
120.48	9.62E+007
143.65	1.05E+008

PT/I56/T2/PATM.F231

Hours	Cells/ml
0.00	2.44E+005
19.07	8.00E+005
24.93	8.88E+005
42.38	1.66E+006
49.63	1.90E+006
67.30	4.57E+006
73.07	6.45E+006

PT/I47/T2/P5000.F021

Hours	Cells/ml
0.00	7.47E+005
18.87	1.03E+006
25.40	1.40E+006
43.52	3.37E+006
49.37	5.71E+006
67.17	1.88E+007
73.27	2.22E+007
91.80	4.61E+007
97.43	6.30E+007
163.32	1.07E+008
187.50	1.10E+008

PT/I47/T2/P2500.F021

Hours	Cells/ml
0.00	7.47E+005
18.83	6.77E+005
25.25	7.58E+005
43.62	1.06E+006
49.35	1.21E+006
67.15	2.25E+006
73.25	2.99E+006
91.78	7.50E+006
97.43	1.06E+007
163.35	5.90E+007
187.52	7.26E+007

PT/I56/T2/P15000.F231

Hours	Cells/ml
0.00	2.44E+005
19.55	2.68E+005
25.50	2.57E+005
42.88	2.52E+005
50.13	2.09E+005
68.02	2.16E+005
73.53	1.67E+005
91.00	3.05E+005
97.98	3.14E+005
120.88	2.55E+005

PT/I56/T2/P7500.F231

Hours	Cells/ml
0.00	2.44E+005
19.25	6.65E+005
25.17	7.67E+005
42.65	2.39E+006
49.85	3.90E+006
67.57	1.32E+007
73.88	2.16E+007
90.75	7.51E+007
97.55	9.18E+007
120.65	1.01E+008
143.70	1.10E+008
162.75	1.09E+008

PT/I22/T2/P7500.M191

Hours	Cells/ml
0.00	4.23E+005
24.53	5.17E+005
90.98	8.24E+006
114.17	3.27E+007
120.43	3.69E+007
137.87	5.00E+007
162.22	5.63E+007
264.40	1.02E+008

PT/I56/T2/P5000.F231

Hours	Cells/ml
0.00	2.44E+005
19.08	7.79E+005
25.13	8.14E+005
42.48	8.89E+005
49.82	9.34E+005
67.53	9.64E+005

PT/I22/T2/P12500.M191

Hours	Cells/ml
0.00	4.23E+005
24.70	4.72E+005
91.13	7.32E+005
114.80	1.22E+006
120.45	1.55E+006
138.05	2.63E+006
162.42	1.03E+007
186.02	2.67E+007
264.50	3.70E+007

PT/I56/T2/P10000.F231

Hours	Cells/ml
0.00	2.44E+005
19.27	7.62E+005
25.33	5.12E+005
42.67	1.08E+006
50.12	1.33E+006
67.87	2.54E+006
73.35	3.22E+006
90.75	1.00E+007
97.72	1.21E+007
120.68	4.54E+007
144.00	5.52E+007
163.02	6.39E+007

PT/I22/T2/P10000.M191

Hours	Cells/ml
0.00	4.23E+005
24.55	4.66E+005
91.00	2.54E+006
114.20	1.84E+007
120.43	2.58E+007
137.88	4.51E+007
162.28	5.12E+007
264.35	6.48E+007

PT/I22/T2/P15000.M191

Hours	Cells/ml
0.00	4.23E+005
24.37	4.29E+005
91.15	4.18E+005
114.83	5.03E+005
120.45	5.05E+005
138.07	5.25E+005
162.45	5.09E+005
186.07	5.34E+005
264.50	5.85E+005

PT/I22/T2/P2500.M191

Hours	Cells/ml
0.00	4.23E+005
24.38	5.80E+005
90.78	1.36E+006
113.98	1.65E+006
120.42	1.81E+006
137.55	2.17E+006
161.97	2.78E+006
185.63	3.86E+006
264.18	1.00E+007

PT/I22/T2/PATM.M191

Hours	Cells/ml
0.00	4.23E+005
24.37	8.94E+005
90.77	2.15E+006
113.95	3.03E+006
120.40	3.17E+006
137.53	3.77E+006
161.95	4.27E+006
185.60	4.98E+006
264.17	5.93E+006

PT/I99/T2/PATM.S301

Hours	Cells/ml
0.00	1.95E+005
23.57	6.32E+004
50.28	7.08E+004
118.55	7.76E+004
142.67	2.38E+005
168.80	1.53E+005
190.42	2.16E+005
216.65	1.68E+005
287.15	3.57E+005
316.07	4.52E+005

PT/I99/T2/P12500.S301

Hours	Cells/ml
0.00	1.95E+005
23.65	2.69E+004
47.93	4.02E+004
118.50	1.65E+005
142.75	5.05E+005
168.90	9.59E+005
190.50	3.24E+006
216.78	9.07E+006
287.22	2.00E+007

PT/I99/T2/P5000.S301

Hours	Cells/ml
0.00	1.95E+005
23.58	2.90E+004
47.88	8.65E+004
118.60	2.07E+006
142.70	6.55E+006
168.85	2.01E+007
190.45	2.51E+007
216.73	2.61E+007
287.17	4.35E+007

PT/I99/T2/P2500.S301

Hours	Cells/ml
0.00	1.95E+005
23.58	2.53E+004
47.87	3.68E+004
118.58	8.81E+004
142.67	2.87E+005
168.82	2.86E+005
190.43	4.04E+005
216.72	3.82E+005
287.17	1.16E+006
316.08	1.49E+006
336.15	1.72E+006
359.92	2.14E+006

PT/I99/T2/P7500.S301

Hours	Cells/ml
0.00	1.95E+005
23.62	4.39E+004
47.90	8.99E+004
118.60	1.39E+006
142.72	4.92E+006
168.88	1.72E+007
190.47	3.10E+007
216.75	1.94E+007
287.18	2.80E+007

PT/I22/T2/P5000.M191

Hours	Cells/ml
0.00	4.23E+005
24.50	4.35E+005
90.80	5.19E+006
114.02	2.02E+007
120.42	2.77E+007
137.57	4.59E+007
161.98	5.75E+007
264.20	8.03E+007

PT/I99/T2/P10000.S301

Hours	Cells/ml
0.00	1.95E+005
23.63	4.29E+004
47.92	7.68E+004
118.62	2.01E+006
142.73	7.00E+006
168.88	2.38E+007
190.48	2.99E+007
216.77	3.26E+007
287.20	4.33E+007

PT/I99/T2/P15000.S301

Hours	Cells/ml
0.00	1.95E+005
23.68	1.10E+005
47.95	8.83E+004
118.67	9.80E+004
142.77	1.57E+005
190.52	1.85E+005
216.80	1.99E+005
287.23	4.34E+005
316.12	6.30E+005
336.18	3.84E+005
359.93	3.27E+005

PT/I13/T2/P10000.Y071

Hours	Cells/ml
0.00	7.22E+005
26.43	5.94E+005
93.70	7.01E+006
117.63	2.67E+007
140.87	5.96E+007
165.72	1.21E+008

PT/I13/T2/P15000.Y071

Hours	Cells/ml
0.00	7.22E+005
26.58	3.91E+005
93.88	5.29E+005
117.67	6.41E+005
141.83	5.85E+005
165.75	5.92E+005

PT/I13/T2/P7500.Y071

Hours	Cells/ml
0.00	7.22E+005
26.42	7.42E+005
93.65	2.27E+007
117.42	1.02E+008
140.85	1.55E+008
165.50	1.51E+008

PT/I4/T2/P2500.Y111

Hours	Cells/ml
0.00	2.26E+006
23.02	2.61E+006
46.80	7.55E+006
71.52	5.37E+007
93.72	9.88E+007
128.82	1.34E+008
166.42	1.51E+008

PT/I4/T2/PATM.Y111

Hours	Cells/ml
0.00	2.26E+006
21.87	2.12E+006
45.62	3.92E+006
70.27	1.33E+007
93.45	5.36E+007
127.98	8.30E+007
166.40	1.09E+008
190.55	1.27E+008

PT/I4/T2/P12500.Y111

Hours	Cells/ml
0.00	2.26E+006
23.40	2.08E+006
47.23	2.25E+006
71.78	2.11E+006
93.98	2.11E+006
128.25	2.04E+006
166.68	1.94E+006

PT/I13/T2/P2500.Y071

Hours	Cells/ml
0.00	7.22E+005
26.27	4.38E+005
93.42	4.34E+006
117.27	2.59E+007
140.63	7.34E+007
165.47	9.95E+007

PT/I13/T2/PATM.Y071

Hours	Cells/ml
0.00	7.22E+005
26.23	4.70E+005
93.12	5.24E+005
116.83	6.85E+005
140.58	8.00E+005
165.20	9.07E+005

PT/I13/T2/P12500.Y071

Hours	Cells/ml
0.00	7.22E+005
26.60	4.93E+005
93.87	6.54E+005
117.65	1.20E+006
141.02	1.38E+006
165.72	1.63E+006
189.45	1.98E+006

PT/I4/T2/P15000.Y111

Hours	Cells/ml
0.00	2.26E+006
23.42	2.31E+006
47.25	2.25E+006
71.80	2.30E+006
94.00	2.36E+006
128.27	2.23E+006
166.70	2.19E+006

PT/I4/T2/P7500.Y111

Hours	Cells/ml
0.00	2.26E+006
23.17	2.41E+006
46.97	3.85E+006
71.55	2.01E+007
93.75	6.52E+007
128.05	7.44E+007
166.45	8.98E+007
190.58	1.10E+008

PT/I13/T2/P5000.Y071

Hours	Cells/ml
0.00	7.22E+005
26.28	5.85E+005
93.43	1.96E+007
117.38	1.09E+008
140.65	1.45E+008
165.48	1.58E+008

PT/I65/T2/P7500.L061

Hours	Cells/ml
0.00	8.21E+005
27.72	8.57E+005
52.35	1.00E+006
76.27	1.37E+006
100.72	2.15E+006
149.70	3.08E+007
166.57	3.67E+007
196.18	5.20E+007
219.87	5.17E+007
341.42	5.23E+007

PT/I4/T2/P5000.Y111

Hours	Cells/ml
0.00	2.26E+006
23.03	2.65E+006
46.83	7.15E+006
71.55	5.54E+007
93.73	8.85E+007
128.03	1.13E+008
166.43	1.36E+008

PT/I65/T2/P12500.L061

Hours	Cells/ml
0.00	8.21E+005
27.75	1.06E+006
52.38	1.02E+006
76.50	1.03E+006
100.77	1.32E+006
149.72	1.75E+006
166.95	2.99E+006
196.22	1.55E+007
219.93	3.33E+007
244.55	3.07E+007

PT/I4/T2/P10000.Y111

Hours	Cells/ml
0.00	2.26E+006
23.18	2.04E+006
46.98	2.82E+006
71.75	4.51E+006
93.97	2.35E+007
128.23	3.69E+007
166.65	3.51E+007
190.60	3.95E+007

PT/I65/T2/P10000.L061

Hours	Cells/ml
0.00	8.21E+005
27.73	7.16E+005
52.37	8.35E+005
76.40	1.04E+006
100.73	1.49E+006
149.72	2.66E+007
166.93	3.82E+007
196.20	3.98E+007
219.88	4.01E+007

PT/I65/T2/P15000.L061

Hours	Cells/ml
0.00	8.21E+005
27.85	7.77E+005
52.40	9.19E+005
76.62	8.55E+005
100.78	8.95E+005
149.73	8.21E+005
167.00	9.19E+005
196.23	4.83E+005
219.95	9.05E+005
341.48	7.96E+005

PT/I65/T2/P2500.L061

Hours	Cells/ml
0.00	8.21E+005
27.42	7.64E+005
52.30	8.16E+005
76.22	8.16E+005
100.68	1.13E+006
149.68	1.17E+006
166.43	1.43E+006
196.15	1.78E+006
219.83	2.21E+006
244.50	1.59E+006
341.37	4.87E+006

PT/I65/T2/PATM.L061

Hours	Cells/ml
0.00	8.21E+005
27.40	9.22E+005
52.28	8.97E+005
76.20	9.11E+005
100.67	8.64E+005
149.67	8.88E+005
166.42	9.88E+005
196.13	9.93E+005
219.82	9.95E+005
244.50	9.69E+005
341.35	9.07E+005

PT/I23/T2/PATM.M091

Hours	Cells/ml
0.00	1.53E+006
17.05	1.65E+006
40.87	2.22E+006
65.53	2.69E+006
88.53	2.38E+006
122.42	2.28E+006
142.88	1.99E+006
165.92	3.34E+006

PT/I23/T2/P12500.M091

Hours	Cells/ml
0.00	1.53E+006
18.82	1.06E+006
42.63	1.35E+006
65.72	1.52E+006
88.95	2.13E+006
122.18	5.27E+006
142.48	1.71E+007
166.27	2.46E+007

PT/I23/T2/P5000.M091

Hours	Cells/ml
0.00	1.53E+006
18.48	1.23E+006
42.28	1.87E+006
65.23	3.97E+006
88.70	8.37E+006
121.88	2.11E+007
142.62	3.82E+007
166.00	4.70E+007

PT/I23/T2/P2500.M091

Hours	Cells/ml
0.00	1.53E+006
18.40	1.40E+006
42.27	1.69E+006
65.22	1.79E+006
88.68	1.66E+006
121.80	2.21E+006
142.63	2.71E+006
165.93	3.62E+006

PT/I23/T2/P7500.M091

Hours	Cells/ml
0.00	1.53E+006
18.63	1.42E+006
42.43	1.97E+006
65.45	4.31E+006
88.75	1.46E+007
122.00	2.75E+007
142.67	3.78E+007
166.02	4.63E+007

PT/I65/T2/P5000.L061

Hours	Cells/ml
0.00	8.21E+005
27.45	7.25E+005
52.32	8.41E+005
76.23	1.31E+006
100.70	1.30E+006
149.68	1.35E+007
166.55	2.63E+007
196.17	4.36E+007
219.85	4.72E+007

PT/I23/T2/P10000.M091

Hours	Cells/ml
0.00	1.53E+006
18.67	1.11E+006
42.45	1.54E+006
65.50	2.90E+006
88.93	1.06E+007
122.08	2.84E+007
142.70	3.75E+007
166.17	4.44E+007

PT/I23/T2/P15000.M091

Hours	Cells/ml
0.00	1.53E+006
18.83	1.35E+006
42.65	1.40E+006
65.77	1.45E+006
88.97	1.39E+006
122.32	1.46E+006
142.83	1.37E+006
166.53	1.50E+006

PT/I48/T2/P10000.G311

Hours	Cells/ml
0.00	9.25E+005
24.83	9.42E+005
48.45	1.66E+006
65.95	2.54E+006
72.47	3.70E+006
90.73	7.20E+006
190.72	6.59E+007

PT/I48/T2/P15000.G311

Hours	Cells/ml
0.00	9.25E+005
24.92	1.05E+006
48.48	1.12E+006
65.98	1.00E+006
72.50	1.08E+006
90.75	1.05E+006
190.75	9.49E+005

PT/I48/T2/P7500.G311

Hours	Cells/ml
0.00	9.25E+005
24.62	1.08E+006
48.43	3.99E+006
65.68	1.96E+007
72.23	3.97E+007
90.70	7.53E+007
190.68	1.11E+008

PT/I14/T2/P2500.Y071

Hours	Cells/ml
0.00	5.73E+005
26.27	3.49E+005
93.43	7.32E+005
117.37	1.30E+006
140.65	5.88E+006
165.47	3.05E+007
189.43	9.16E+007

PT/I14/T2/PATM.Y071

Hours	Cells/ml
0.00	5.73E+005
26.25	3.88E+005
93.12	3.77E+005
116.83	3.57E+005
140.58	4.09E+005
165.20	4.01E+005

PT/I14/T2/P12500.Y071

Hours	Cells/ml
0.00	5.73E+005
26.62	4.21E+005
93.87	1.13E+006
117.67	2.15E+006
141.02	4.16E+006
165.75	8.88E+006
189.47	1.72E+007

PT/I48/T2/P2500.G311

Hours	Cells/ml
0.00	9.25E+005
24.53	1.18E+006
48.40	6.78E+006
65.65	3.86E+007
72.20	5.79E+007
90.13	7.24E+007
190.63	9.32E+007

PT/I48/T2/PATM.G311

Hours	Cells/ml
0.00	9.25E+005
24.52	1.01E+006
48.38	2.83E+006
65.62	7.76E+006
72.18	1.12E+007
90.12	2.90E+007
190.62	7.34E+007

PT/I48/T2/P12500.G311

Hours	Cells/ml
0.00	9.25E+005
24.52	9.65E+005
48.47	1.07E+006
65.97	1.05E+006
72.48	1.07E+006
90.73	1.22E+006
190.75	1.05E+006

PT/I14/T2/P15000.Y071

Hours	Cells/ml
0.00	5.73E+005
26.58	4.17E+005
93.90	3.74E+005
117.68	4.61E+005
141.05	5.36E+005
165.77	5.41E+005

PT/I14/T2/P7500.Y071

Hours	Cells/ml
0.00	5.73E+005
26.43	4.16E+005
93.67	3.29E+006
117.43	1.54E+007
140.85	5.99E+007
165.52	1.36E+008

PT/I48/T2/P5000.G311

Hours	Cells/ml
0.00	9.25E+005
24.57	1.18E+006
48.58	6.55E+006
65.67	4.53E+007
72.22	7.09E+007
90.13	9.17E+007
190.67	1.31E+008

PT/I57/T2/P2500.U151

Hours	Cells/ml
0.00	1.64E+006
19.85	1.51E+006
42.02	5.69E+006
49.10	1.05E+007
66.50	5.47E+007
72.15	7.16E+007
89.95	9.78E+007

PT/I57/T2/P7500.U151

Hours	Cells/ml
0.00	1.66E+006
19.88	8.90E+005
42.38	1.44E+006
66.98	1.25E+007
72.35	3.05E+007
98.33	8.11E+007
162.43	1.32E+008

PT/I14/T2/P5000.Y071

Hours	Cells/ml
0.00	5.73E+005
26.28	3.76E+005
93.45	1.92E+006
117.40	1.57E+007
140.67	7.43E+007
165.50	1.32E+008

PT/XRA705/T2/P12500.A081

Hours	Cells/ml
0.00	5.43E+006
19.77	4.45E+006
47.43	4.60E+006
96.20	4.70E+006
115.77	5.66E+006
120.50	5.81E+006
138.02	7.47E+006
145.35	8.87E+006

PT/I57/T2/P1ATM.U151

Hours	Cells/ml
0.00	1.64E+006
20.17	1.81E+006
42.02	3.95E+006
49.07	6.39E+006
66.48	2.06E+007
72.13	2.89E+007
89.93	7.39E+007

PT/I57/T2/P15000.U151

Hours	Cells/ml
0.00	1.66E+006
20.08	1.78E+006
42.45	1.95E+006
67.65	2.16E+006
90.38	1.88E+006
162.50	1.93E+006

PT/I57/T2/P12500.U151

Hours	Cells/ml
0.00	1.66E+006
20.07	1.19E+006
42.43	1.36E+006
67.65	1.36E+006
90.38	1.64E+006
162.48	1.70E+006

PT/I14/T2/P10000.Y071

Hours	Cells/ml
0.00	5.73E+005
26.45	4.55E+005
93.72	2.32E+006
117.65	5.06E+006
140.88	1.12E+007
165.72	3.50E+007
189.45	7.55E+007

PT/I57/T2/P5000.U151

Hours	Cells/ml
0.00	1.64E+006
19.87	9.88E+005
42.05	3.59E+006
49.13	7.92E+006
66.83	4.97E+007
72.33	7.42E+007
89.97	1.18E+008

PT/I57/T2/P10000.U151

Hours	Cells/ml
0.00	1.64E+006
20.05	9.11E+005
42.40	1.06E+006
66.95	1.55E+006
90.35	8.35E+006
96.75	1.66E+007
162.47	5.29E+007

PT/XRA705/T2/P2500.A081

Hours	Cells/ml
0.00	5.43E+006
19.20	4.59E+006
47.13	4.90E+006
95.87	9.29E+006
115.45	1.97E+007
120.47	2.56E+007
137.72	4.00E+007
145.30	4.61E+007
167.43	8.35E+007
187.78	1.12E+008
212.37	1.41E+008
270.23	1.68E+008

PT/XRA705/T2/PATM.A081

Hours	Cells/ml
0.00	5.43E+006
19.08	5.01E+006
47.12	5.55E+006
95.85	5.59E+006
115.42	7.75E+006
120.47	7.78E+006
137.70	8.56E+006
145.30	7.83E+006
167.42	8.86E+006
187.75	9.45E+006

PT/XRA705/T2/P15000.A081

Hours	Cells/ml
0.00	5.43E+006
19.70	4.53E+006
47.45	4.67E+006
96.22	4.39E+006
115.78	5.29E+006
138.03	4.90E+006
145.37	4.96E+006
167.82	7.01E+006
187.85	5.09E+006
212.67	4.19E+006
270.58	5.26E+006

PT/XRA705/T2/P7500.A081

Hours	Cells/ml
0.00	7.02E+005
19.55	4.47E+006
47.22	5.58E+006
96.17	3.49E+007
115.60	8.96E+007
120.48	1.09E+008
137.87	2.15E+008
145.33	1.96E+008
167.47	2.17E+008

PT/I67/T2/P7500.F021

Hours	Cells/ml
0.00	5.69E+005
68.32	7.32E+005
235.22	8.30E+005
498.67	5.56E+007

PT/XRA705/T2/P5000.A081

Hours	Cells/ml
0.00	5.43E+006
19.18	4.77E+006
47.20	5.95E+006
95.88	3.44E+007
115.47	8.50E+007
120.47	9.78E+007
137.73	1.89E+008
145.32	1.84E+008
167.47	2.15E+008

PT/I67/T2/P12500.F021

Hours	Cells/ml
0.00	5.69E+005
68.35	5.97E+005
235.53	8.80E+005
500.40	7.10E+005

PT/XRA705/T2/P10000.A081

Hours	Cells/ml
0.00	5.43E+006
19.58	4.59E+006
47.42	4.78E+006
96.18	1.58E+007
115.62	4.00E+007
120.50	4.41E+007
137.88	8.14E+007
145.33	1.01E+008
167.75	1.58E+008
270.57	2.09E+008

PT/I49/T2/P12500.F021

Hours	Cells/ml
0.00	4.16E+005
19.28	5.00E+005
25.45	5.11E+005
43.20	4.91E+005
49.73	4.22E+005

PT/I67/T2/P10000.F021

Hours	Cells/ml
0.00	5.69E+005
68.33	6.28E+005
235.23	8.18E+005
500.58	3.37E+007

PT/I67/T2/P15000.F021

Hours	Cells/ml
0.00	5.69E+005
68.37	6.45E+005
235.55	9.10E+005
499.03	7.48E+005

PT/I67/T2/P5000.F021

Hours	Cells/ml
0.00	5.69E+005
68.28	7.30E+005
234.83	9.21E+005
500.45	2.51E+007

PT/I67/T2/P2500.F021

Hours	Cells/ml
0.00	5.69E+005
68.43	7.71E+005
234.80	9.80E+005
500.45	1.01E+006

PT/I67/T2/PATM.F021

Hours	Cells/ml
0.00	5.69E+005
68.25	2.06E+006
236.85	1.78E+006
500.33	3.29E+006

PT/I49/T2/P10000.F021

Hours	Cells/ml
0.00	4.16E+005
19.08	6.64E+005
25.45	8.27E+005
43.30	9.67E+005
49.72	1.36E+006
67.22	2.37E+006
73.32	3.63E+006
91.85	8.01E+006
97.48	1.05E+007
162.98	4.31E+007
187.22	4.35E+007

PT/I49/T2/PATM.F021

Hours	Cells/ml
0.00	4.16E+005
19.45	1.07E+006
25.53	1.34E+006
43.75	2.33E+006
49.82	3.17E+006
67.15	6.57E+006
73.25	8.83E+006
91.77	2.05E+007
97.55	2.74E+007
163.45	8.71E+007
187.63	9.78E+007

PT/I49/T2/P15000.F021

Hours	Cells/ml
0.00	4.16E+005
19.32	4.19E+005
25.47	4.13E+005
43.08	4.21E+005
49.75	3.42E+005
67.25	4.87E+005
73.35	3.15E+005
91.88	3.43E+005
97.53	3.03E+005
162.65	4.20E+005
186.92	4.36E+005

PT/I49/T2/P7500.F021

Hours	Cells/ml
0.00	4.16E+005
19.07	9.17E+005
25.42	9.92E+005
43.42	1.83E+006
49.38	3.25E+006
67.20	1.15E+007
73.30	1.89E+007
91.83	6.19E+007
97.47	7.00E+007
163.30	1.21E+008
187.47	1.38E+008

PT/I24/T2/PATM.M191

Hours	Cells/ml
0.00	4.89E+005
24.38	8.66E+005
113.98	2.13E+006
137.53	2.63E+006
161.95	3.09E+006
185.62	3.62E+006
264.17	4.78E+006
286.83	5.30E+006
311.57	5.82E+006
335.83	5.92E+006
354.60	6.31E+006
427.65	6.89E+006

PT/I24/T2/P12500.M191

Hours	Cells/ml
0.00	4.89E+005
24.70	6.32E+005
114.83	6.25E+005
138.07	6.70E+005
162.43	7.78E+005
186.07	7.09E+005
264.50	7.79E+005
287.08	8.74E+005
311.77	8.22E+005
336.75	9.30E+005
356.93	9.01E+005
427.70	1.03E+006

PT/I24/T2/P5000.M191

Hours	Cells/ml
0.00	4.89E+005
24.40	5.93E+005
114.03	6.77E+005
137.57	7.99E+005
162.00	8.43E+005
185.65	1.02E+006
264.20	1.16E+006
286.85	1.50E+006
311.75	2.32E+006
334.72	3.41E+006
356.90	9.20E+006
427.67	3.04E+007

PT/I24/T2/P2500.M191

Hours	Cells/ml
0.00	4.89E+005
24.40	5.25E+005
114.00	5.23E+005
137.55	5.73E+005
161.98	5.60E+005
185.63	7.03E+005
264.18	6.67E+005
286.85	7.08E+005
311.75	6.57E+005
336.47	6.83E+005
356.90	6.13E+005
427.67	7.13E+005

PT/I24/T2/P7500.M191

Hours	Cells/ml
0.00	4.89E+005
24.55	5.75E+005
114.18	7.28E+005
137.88	7.94E+005
162.23	7.87E+005
185.83	9.91E+005
264.35	3.18E+006
286.85	5.43E+006
311.75	7.84E+006
336.72	1.20E+007
356.92	2.20E+007
427.68	3.35E+007

PT/I49/T2/P5000.F021

Hours	Cells/ml
0.00	4.16E+005
18.87	1.11E+006
25.40	1.71E+006
43.52	4.31E+006
49.37	6.98E+006
67.18	3.28E+007
73.28	5.02E+007
91.80	8.69E+007
97.45	9.57E+007
163.33	1.20E+008
187.50	1.44E+008

PT/I24/T2/P10000.M191

Hours	Cells/ml
0.00	4.89E+005
24.57	5.61E+005
114.20	5.65E+005
137.90	5.76E+005
162.28	5.79E+005
185.83	5.72E+005
264.37	9.73E+005
287.07	1.52E+006
311.77	2.96E+006
336.73	6.76E+006
356.92	1.57E+007
427.68	3.02E+007

PT/I24/T2/P15000.M191

Hours	Cells/ml
0.00	4.89E+005
24.73	6.77E+005
114.85	8.47E+005
138.08	9.61E+005
162.45	1.07E+006
186.08	1.10E+006
264.52	1.31E+006
287.08	1.33E+006
311.75	1.39E+006
336.75	1.56E+006
356.93	1.35E+006
427.72	1.49E+006

PT/I15/T2/P12500.A191

Hours	Cells/ml
0.00	1.99E+005
11.90	2.86E+005
36.27	5.79E+005
58.08	1.17E+006
82.25	2.85E+006
106.18	7.61E+006
112.58	1.07E+007

PT/I15/T2/P7500.M311

Hours	Cells/ml
0.00	9.88E+005
22.63	1.09E+006
47.98	1.72E+006
66.73	4.16E+006
140.22	1.48E+008
162.42	1.44E+008

PT/I15/T2/PATM.M311

Hours	Cells/ml
0.00	9.88E+005
22.48	1.36E+006
47.75	1.62E+006
66.53	1.78E+006
139.77	2.20E+006
162.20	2.19E+006

PT/I15/T2/P12500.M311

Hours	Cells/ml
0.00	9.88E+005
22.80	1.09E+006
48.18	1.24E+006
67.03	1.38E+006
140.38	3.05E+006
162.63	4.12E+006
378.50	9.07E+007

PT/I15/T2/P7500.A291

Hours	Cells/ml
0.00	3.62E+005
23.72	4.94E+005
48.53	1.07E+006
78.60	2.81E+006
99.25	6.61E+006
117.78	2.32E+007
141.03	6.95E+007
163.55	1.43E+008
187.20	1.31E+008
285.77	1.29E+008

PT/I15/T2/PATM.A191

Hours	Cells/ml
0.00	1.99E+005
11.48	3.49E+005
36.40	5.66E+005
58.18	7.87E+005
82.35	1.12E+006
106.28	1.21E+006
178.33	1.22E+006
227.73	1.47E+006

PT/I15/T2/P12500.A291

Hours	Cells/ml
0.00	3.62E+005
24.13	4.61E+005
48.87	1.01E+006
78.63	1.43E+006
99.25	2.05E+006
118.12	2.79E+006
141.00	4.28E+006
163.73	8.21E+006
187.47	2.26E+007
285.80	3.72E+007

PT/I15/T2/P7500.A191

Hours	Cells/ml
0.00	1.99E+005
11.67	2.94E+005
36.00	6.67E+005
57.82	1.16E+006
81.97	2.92E+006
105.82	1.18E+007
112.60	1.92E+007
178.67	1.25E+008
227.80	1.32E+008

PT/I15/T2/P15000.A191

Hours	Cells/ml
0.00	1.99E+005
11.93	3.15E+005
36.28	4.18E+005
58.10	4.42E+005
82.27	4.62E+005
106.20	6.14E+005
178.90	5.05E+005

PT/I15/T2/P15000.M311

Hours	Cells/ml
0.00	9.88E+005
22.82	1.22E+006
48.20	1.18E+006
67.07	1.15E+006
140.40	1.36E+006
162.65	1.40E+006
380.17	1.20E+006

PT/I15/T2/P10000.M311

Hours	Cells/ml
0.00	9.88E+005
22.67	1.53E+006
48.02	1.76E+006
66.77	2.79E+006
140.23	6.11E+007
162.43	1.27E+008

PT/I15/T2/P15000.A291

Hours	Cells/ml
0.00	3.62E+005
24.18	4.51E+005
48.97	5.73E+005
78.65	6.10E+005
99.25	4.99E+005
118.07	5.97E+005
141.00	8.64E+005
163.75	9.65E+005
187.48	1.75E+006

PT/I15/T2/P2500.M311

Hours	Cells/ml
0.00	9.88E+005
22.48	1.24E+006
47.67	1.40E+006
66.55	1.81E+006
140.02	5.89E+007
162.22	1.24E+008

PT/I15/T2/PATM.A291

Hours	Cells/ml
0.00	3.62E+005
23.58	4.06E+005
43.00	7.41E+005
99.25	3.64E+005
115.28	4.33E+005
141.08	4.93E+005
163.10	4.53E+005
186.82	4.96E+005
283.15	4.41E+005

PT/I15/T2/P2500.A291

Hours	Cells/ml
0.00	3.62E+005
23.60	3.74E+005
48.27	4.69E+005
78.52	5.51E+005
99.25	8.39E+005
117.73	1.05E+006
141.07	1.71E+006
163.15	5.34E+006
187.00	2.22E+007
285.73	1.09E+008

PT/I15/T2/P2500.A191

Hours	Cells/ml
0.00	1.99E+005
11.47	3.21E+005
35.77	4.30E+005
57.77	5.86E+005
81.92	7.94E+005
105.77	1.14E+006
178.37	1.60E+007
227.78	7.44E+007

PT/I15/T2/P10000.A291

Hours	Cells/ml
0.00	2.15E+006
24.12	5.80E+005
48.55	1.04E+006
78.62	2.47E+006
99.25	5.52E+006
118.02	1.63E+007
141.02	3.31E+007
163.57	3.95E+007
187.22	4.48E+007
285.78	1.35E+008

PT/I15/T2/P10000.A191

Hours	Cells/ml
0.00	1.99E+005
11.68	3.42E+005
36.03	7.22E+005
58.07	1.56E+006
82.22	3.80E+006
106.17	1.49E+007
112.62	2.09E+007

PT/I15/T2/P5000.A191

Hours	Cells/ml
0.00	1.99E+005
11.48	3.44E+005
35.80	7.08E+005
57.78	1.19E+006
81.95	3.04E+006
105.80	1.55E+007
112.98	2.16E+007
178.38	1.20E+008
227.77	1.25E+008

PT/I15/T2/P5000.M311

Hours	Cells/ml
0.00	9.88E+005
22.50	1.16E+006
47.78	1.75E+006
66.57	3.43E+006
140.03	1.60E+008
162.25	1.47E+008

PT/I60/T2/PATM.U221

Hours	Cells/ml
0.00	4.94E+005
25.00	3.92E+005
49.25	6.34E+005
73.17	8.61E+005
95.73	2.37E+006
140.88	3.86E+007
163.20	9.13E+007
189.02	1.07E+008

PT/I60/T2/P12500.U221

Hours	Cells/ml
0.00	4.94E+005
25.33	4.33E+005
49.53	5.95E+005
73.25	3.61E+005
95.85	5.05E+005
141.22	5.28E+005
163.30	6.23E+005
189.05	6.93E+005
214.30	6.12E+005
241.10	6.85E+005

PT/I60/T2/P7500.U221

Hours	Cells/ml
0.00	4.94E+005
25.05	5.26E+005
49.47	5.39E+005
73.22	1.92E+006
95.78	7.70E+006
140.95	8.94E+007
163.25	8.72E+007

PT/I15/T2/P5000.A291

Hours	Cells/ml
0.00	3.62E+005
23.62	5.03E+005
48.30	8.14E+005
78.58	1.04E+006
99.25	1.89E+006
117.77	4.41E+006
141.05	1.84E+007
163.17	7.66E+007
187.03	1.73E+008
285.75	1.36E+008

PT/I60/T2/P5000.U221

Hours	Cells/ml
0.00	4.94E+005
25.03	5.82E+005
49.63	8.18E+005
73.20	3.94E+006
95.77	3.07E+007
140.93	1.08E+008
163.23	1.16E+008

PT/I60/T2/P10000.U221

Hours	Cells/ml
0.00	4.94E+005
25.32	9.98E+005
49.48	5.26E+005
73.23	5.05E+005
95.83	9.82E+005
141.22	2.36E+006
163.27	6.50E+006
189.03	3.59E+007
214.27	5.96E+007
241.07	5.74E+007

PT/I60/T2/P2500.U221

Hours	Cells/ml
0.00	4.94E+005
25.02	4.90E+005
49.27	8.11E+005
73.18	2.87E+006
95.75	1.48E+007
140.92	1.06E+008
163.22	1.34E+008

PT/I60/T2/P15000.U221

Hours	Cells/ml
0.00	4.94E+005
25.35	4.30E+005
49.55	3.12E+005
73.27	2.83E+005
95.88	5.53E+005
141.22	5.47E+005
163.32	5.64E+005
189.07	5.20E+005
214.32	5.41E+005
241.12	6.16E+005

PT/I58/T2/P15000.U151

Hours	Cells/ml
0.00	1.78E+006
20.10	1.80E+006
42.47	1.90E+006
67.65	1.94E+006
90.40	1.97E+006
162.52	2.00E+006

PT/I58/T2/PATM.U151

Hours	Cells/ml
0.00	1.78E+006
20.17	1.51E+006
42.03	3.21E+006
66.50	1.50E+007
72.15	2.06E+007
89.93	6.78E+007
161.82	1.22E+008

PT/I58/T2/P7500.U151

Hours	Cells/ml
0.00	1.78E+006
19.97	6.54E+005
42.40	1.60E+006
66.83	2.17E+007
72.37	3.69E+007
90.35	8.51E+007
162.45	1.27E+008

PT/I58/T2/P12500.U151

Hours	Cells/ml
0.00	1.78E+006
20.08	1.15E+006
42.43	1.26E+006
67.57	1.30E+006
90.38	1.41E+006
162.48	1.71E+006

PT/I25/T2/P12500.M031

Hours	Cells/ml
0.00	3.23E+005
20.97	3.29E+005
27.83	3.20E+005
45.18	3.26E+005
69.35	4.54E+005
141.05	5.44E+005
165.72	5.45E+005
189.38	5.82E+005

PT/I58/T2/P10000.U151

Hours	Cells/ml
0.00	1.78E+006
20.05	9.13E+005
42.42	8.67E+005
66.97	2.07E+006
90.37	9.92E+006
96.77	1.78E+007
162.47	5.03E+007

PT/I25/T2/P15000.M031

Hours	Cells/ml
0.00	3.23E+005
21.00	3.42E+005
45.20	3.41E+005
69.38	3.75E+005
141.07	3.94E+005
165.73	4.03E+005

PT/I25/T2/P7500.M091

Hours	Cells/ml
0.00	1.05E+006
18.65	9.44E+005
42.45	1.06E+006
65.48	1.04E+006
142.68	1.12E+006

PT/I25/T2/PATM.M031

Hours	Cells/ml
0.00	3.23E+005
20.53	7.01E+005
27.38	6.84E+005
44.72	9.61E+005
68.97	1.27E+006
140.58	2.43E+006
165.02	2.64E+006
188.78	2.91E+006

PT/I58/T2/P5000.U151

Hours	Cells/ml
0.00	1.78E+006
19.87	1.05E+006
42.07	4.76E+006
49.15	9.08E+006
66.85	4.66E+007
72.35	7.10E+007
89.97	1.15E+008
161.85	1.42E+008

PT/I58/T2/P2500.U151

Hours	Cells/ml
0.00	1.78E+006
19.85	1.45E+006
42.05	6.65E+006
49.13	1.25E+007
66.52	5.34E+007
72.17	6.73E+007
89.95	8.76E+007
161.83	1.32E+008

PT/I25/T2/PATM.M091

Hours	Cells/ml
0.00	1.05E+006
17.05	1.64E+006
40.88	2.28E+006
65.55	2.54E+006
142.88	2.48E+006

PT/I25/T2/P12500.M091

Hours	Cells/ml
0.00	1.05E+006
18.82	1.00E+006
42.63	9.25E+005
65.75	9.45E+005
142.48	9.65E+005

PT/I25/T2/P7500.M031

Hours	Cells/ml
0.00	3.23E+005
20.80	4.09E+005
27.68	3.78E+005
45.02	5.07E+005
69.20	6.28E+005
140.77	9.66E+005
165.42	1.04E+006
189.33	1.02E+006

PT/I25/T2/P10000.M031

Hours	Cells/ml
0.00	3.23E+005
20.87	7.56E+005
27.70	9.50E+005
45.05	1.40E+006
69.20	1.90E+006
148.80	3.63E+006

PT/I25/T2/P15000.M091

Hours	Cells/ml
0.00	1.05E+006
18.83	8.64E+005
42.65	1.01E+006
65.77	8.73E+005
142.83	8.83E+005

PT/I16/T2/PATM.M311

Hours	Cells/ml
0.00	1.40E+006
22.48	3.88E+006
47.77	4.82E+006
66.53	5.48E+006
139.78	6.97E+006
162.22	8.28E+006

PT/I16/T2/P12500.M311

Hours	Cells/ml
0.00	1.40E+006

PT/I25/T2/P10000.M091

Hours	Cells/ml
0.00	1.05E+006
18.68	1.08E+006
42.47	1.07E+006
65.52	1.05E+006
142.70	1.13E+006

PT/I25/T2/P2500.M091

Hours	Cells/ml
0.00	1.05E+006
18.42	8.49E+005
42.27	1.05E+006
65.23	8.91E+005
142.88	1.05E+006

PT/I25/T2/P2500.M031

Hours	Cells/ml
0.00	3.23E+005
20.63	3.39E+005
27.52	3.07E+005
44.85	3.09E+005
69.00	3.31E+005
140.52	4.43E+005
165.20	6.62E+005
189.12	4.10E+005

PT/I16/T2/P7500.M311

Hours	Cells/ml
0.00	1.40E+006
22.65	1.43E+006
48.02	1.64E+006
66.75	2.09E+006
140.05	3.94E+007
162.42	5.06E+007
380.25	6.05E+007

PT/I25/T2/P5000.M091

Hours	Cells/ml
0.00	1.05E+006
18.48	9.40E+005
42.28	1.16E+006
65.25	1.12E+006
142.67	1.19E+006

PT/I25/T2/P5000.M031

Hours	Cells/ml
0.00	3.23E+005
20.72	4.14E+005
27.53	3.89E+005
44.88	4.80E+005
69.02	5.41E+005
140.60	6.15E+005
165.22	6.18E+005
189.17	6.48E+005

PT/I16/T2/P12500.A291

Hours	Cells/ml
0.00	3.18E+005
24.15	4.00E+005
48.95	5.26E+005
78.63	6.97E+005
99.25	1.09E+006
118.05	2.07E+006
141.00	6.61E+006
163.75	1.98E+007
187.47	2.56E+007

PT/I16/T2/P7500.A191

Hours	Cells/ml
0.00	1.34E+005
11.67	1.81E+005
36.00	3.30E+005
57.82	9.21E+005
81.97	2.51E+006
105.83	1.33E+007
112.48	1.50E+007
178.67	4.51E+007
227.82	5.76E+007

PT/I16/T2/P2500.M311

Hours	Cells/ml
0.00	1.40E+006
22.48	1.44E+006
47.77	1.59E+006
66.55	1.55E+006
140.02	1.87E+006
162.23	2.08E+006
380.22	1.41E+007

PT/I16/T2/PATM.A291

Hours	Cells/ml
0.00	3.18E+005
23.60	3.34E+005
43.02	3.51E+005
99.25	3.07E+005
115.30	3.55E+005
141.08	4.89E+005
163.12	4.86E+005
186.83	3.89E+005
283.15	5.59E+005

PT/I16/T2/PATM.A191

Hours	Cells/ml
0.00	1.34E+005
11.45	2.03E+005
36.40	5.57E+005
58.18	7.83E+005
82.35	1.31E+006
106.28	1.30E+006
178.35	1.25E+006
227.75	1.78E+006

PT/I16/T2/P12500.A191

Hours	Cells/ml
0.00	1.34E+005
11.92	1.84E+005
36.27	1.62E+005
58.08	2.18E+005
82.25	3.36E+005
106.20	5.03E+005
178.88	6.15E+006
228.02	2.36E+007

PT/I16/T2/P15000.M311

Hours	Cells/ml
0.00	1.40E+006
22.83	1.39E+006
48.22	1.42E+006
67.10	1.41E+006
140.42	1.41E+006
162.67	1.61E+006
380.27	1.30E+006

PT/I16/T2/P7500.A291

Hours	Cells/ml
0.00	3.18E+005
23.72	3.47E+005
48.55	9.57E+005
78.62	3.53E+006
99.25	1.21E+007
117.80	2.48E+007
141.03	3.99E+007
163.57	5.62E+007
187.22	5.81E+007
285.78	5.49E+007

PT/I16/T2/P2500.A291

Hours	Cells/ml
0.00	3.18E+005
23.62	2.90E+005
48.28	3.82E+005
78.58	4.50E+005
99.25	5.97E+005
117.75	9.03E+005
141.07	1.09E+006
163.13	2.21E+006
187.02	3.23E+006
285.73	1.45E+007

PT/I16/T2/P2500.A191

Hours	Cells/ml
0.00	1.34E+005
11.48	1.07E+005
35.78	1.45E+005
57.77	2.41E+005
81.93	4.02E+005
105.78	5.58E+005
178.38	1.50E+006
227.77	2.85E+006

PT/I16/T2/P5000.A191

Hours	Cells/ml
0.00	1.34E+005
11.50	1.74E+005
35.82	4.12E+005
57.80	7.82E+005
81.95	1.77E+006
105.82	5.62E+006
112.65	8.03E+006
178.40	4.09E+007
227.80	4.73E+007

PT/I16/T2/P5000.M311

Hours	Cells/ml
0.00	1.40E+006
22.50	1.36E+006
47.47	1.52E+006
66.57	2.09E+006
140.05	2.70E+007
162.40	3.83E+007
380.23	5.32E+007

PT/I16/T2/P15000.A291

Hours	Cells/ml
0.00	3.18E+005
24.18	3.31E+005
48.97	3.03E+005
78.65	4.04E+005
99.25	3.84E+005
118.08	4.57E+005
141.00	4.07E+005
163.77	4.35E+005
187.50	4.51E+005

PT/I16/T2/P15000.A191

Hours	Cells/ml
0.00	1.34E+005
11.93	1.68E+005
36.30	1.99E+005
58.12	2.64E+005
82.27	2.07E+005
106.22	2.02E+005
178.40	2.80E+005
228.05	2.90E+005

PT/I16/T2/P10000.A191

Hours	Cells/ml
0.00	1.34E+005
11.70	2.07E+005
36.03	2.88E+005
58.07	5.89E+005
82.23	1.29E+006
106.18	5.37E+006
112.67	8.43E+006
178.70	5.50E+007
227.85	6.21E+007

PT/I16/T2/P10000.M311

Hours	Cells/ml
0.00	1.40E+006
22.67	1.19E+006
48.03	1.47E+006
66.78	2.66E+006
140.25	4.21E+007
162.45	5.58E+007
380.25	7.04E+007

PT/I61/T2/P7500.U291

Hours	Cells/ml
0.00	1.92E+005
23.98	9.30E+005
46.45	3.70E+006
71.50	3.95E+007
95.73	9.75E+007
161.37	1.29E+008

PT/I16/T2/P5000.A291

Hours	Cells/ml
0.00	3.18E+005
23.63	3.17E+005
48.30	6.95E+005
78.60	1.70E+006
99.25	5.27E+006
117.78	1.38E+007
141.05	2.63E+007
163.22	3.84E+007
187.03	4.73E+007
285.75	4.35E+007

PT/I61/T2/P5000.U291

Hours	Cells/ml
0.00	1.92E+005
23.95	1.37E+006
46.43	7.59E+006
71.48	8.09E+007
95.75	1.19E+008
161.35	1.44E+008

PT/I61/T2/G.U291

Hours	Cells/ml
1.01	1.19E+001
173.38	8.48E+000
345.75	8.27E+000
518.12	9.44E+000
690.49	1.62E+001
862.85	1.00E+003
1035.22	1.00E+003

PT/I61/T2/P15000.U291

Hours	Cells/ml
0.00	1.92E+005
24.23	4.30E+005
46.52	5.66E+005
71.55	5.83E+005
95.37	4.62E+005
161.80	6.33E+005

PT/I61/T2/P12500.U291

Hours	Cells/ml
0.00	1.92E+005
24.22	3.86E+005
46.48	4.40E+005
71.50	4.78E+005
95.40	4.80E+005
161.78	7.89E+005

PT/I16/T2/P10000.A291

Hours	Cells/ml
0.00	3.18E+005
24.13	2.99E+005
48.57	6.78E+005
78.63	1.73E+006
99.25	5.68E+006
118.03	2.55E+007
141.02	2.79E+007
163.58	3.68E+007
187.23	4.32E+007
285.80	4.78E+007

PT/I61/T2/P10000.U291

Hours	Cells/ml
0.00	1.92E+005
24.18	6.31E+005
46.47	1.36E+006
71.52	4.36E+006
95.72	2.35E+007
161.77	7.09E+007

PT/I61/T2/P2500.U291

Hours	Cells/ml
0.00	1.92E+005
23.93	1.49E+006
46.42	8.02E+006
71.45	6.94E+007
95.77	1.02E+008
161.33	1.30E+008

PT/I61/T2/PATM.U291

Hours	Cells/ml
0.00	1.92E+005
23.92	9.26E+005
45.78	3.20E+006
71.42	1.57E+007
95.18	4.85E+007
161.32	9.22E+007

PT/I59/T2/P15000.U221

Hours	Cells/ml
0.00	1.81E+006
25.33	1.49E+006
73.25	1.93E+006
95.87	1.72E+006
141.25	1.62E+006
163.30	1.68E+006
189.07	1.61E+006
214.30	1.67E+006
241.10	4.36E+005

PT/I59/T2/P7500.U221

Hours	Cells/ml
0.00	1.81E+006
25.03	1.61E+006
49.47	1.66E+006
73.20	1.98E+006
95.45	6.59E+006
140.97	1.04E+008
163.23	1.22E+008

PT/I59/T2/PATM.U221

Hours	Cells/ml
0.00	1.81E+006
49.23	1.62E+006
73.15	2.13E+006
95.38	3.75E+006
140.90	5.86E+007
163.18	1.02E+008
189.02	1.16E+008
214.13	1.19E+008
241.02	1.28E+008

PT/I59/T2/P12500.U221

Hours	Cells/ml
0.00	1.81E+006
25.32	1.47E+006
49.53	5.00E+005
73.23	1.51E+006
95.85	1.50E+006
141.25	1.50E+006
163.28	1.61E+006
189.05	1.54E+006
214.28	1.57E+006
241.08	4.66E+005

PT/I26/T2/P12500.M031

Hours	Cells/ml
0.00	6.85E+004
20.98	6.43E+004
27.85	5.85E+004
45.20	1.04E+005
52.13	1.34E+005
69.37	2.53E+005

PT/I59/T2/P10000.U221

Hours	Cells/ml
0.00	1.81E+006
25.20	2.09E+006
49.48	1.25E+006
73.22	1.68E+006
95.83	1.28E+006
141.25	5.96E+006
163.27	2.63E+007
189.03	4.77E+007

PT/I59/T2/P5000.U221

Hours	Cells/ml
0.00	1.81E+006
25.02	1.48E+006
95.75	7.04E+006
140.93	1.08E+008
163.22	1.30E+008

PT/I59/T2/P2500.U221

Hours	Cells/ml
0.00	1.81E+006
25.00	1.51E+006
49.27	1.86E+006
73.18	3.97E+006
95.82	3.24E+007
140.92	1.30E+008
163.20	1.46E+008

PT/I26/T2/P2500.M031

Hours	Cells/ml
0.00	6.85E+004
20.63	1.23E+005
27.52	1.13E+005
44.87	2.10E+005
51.80	2.31E+005
69.02	3.21E+005
97.95	3.56E+005
121.45	3.66E+005
140.55	7.52E+005
165.03	1.03E+006
189.15	1.29E+006

PT/I26/T2/PATM.M031

Hours	Cells/ml
0.00	6.85E+004
28.55	3.70E+005
27.38	5.16E+005
44.73	6.85E+005
51.78	7.72E+005
68.98	1.07E+006
97.93	1.08E+006
121.43	1.11E+006
140.52	1.84E+006
165.03	1.80E+006
188.80	1.95E+006

PT/I1/T2/P7500.A271

Hours	Cells/ml
0.00	2.12E+005
17.12	2.22E+005
41.15	1.60E+006
65.23	6.87E+006
89.27	6.47E+007
162.95	1.33E+008

PT/I26/T2/P5000.M031

Hours	Cells/ml
0.00	6.85E+004
20.72	1.31E+005
27.55	1.88E+005
44.88	2.73E+005
51.85	3.33E+005
69.03	4.88E+005
97.97	1.26E+006
121.48	5.05E+006
140.62	1.18E+007
165.25	1.84E+007
189.18	2.46E+007
213.98	2.84E+007

PT/I26/T2/P15000.M031

Hours	Cells/ml
0.00	6.85E+004
21.12	7.92E+004
27.87	6.04E+004
45.22	7.86E+004
52.15	6.95E+004
69.38	7.19E+004
98.32	9.56E+004
121.75	2.99E+005
141.08	1.82E+005
165.73	1.17E+005
189.68	1.29E+005

PT/I26/T2/P7500.M031

Hours	Cells/ml
0.00	6.85E+004
20.80	7.21E+004
27.70	1.07E+005
45.03	2.85E+005
51.97	4.14E+005
69.20	1.10E+006
76.42	1.94E+006
98.10	4.42E+006
121.50	1.43E+007
140.78	2.50E+007
165.43	2.83E+007
189.35	3.54E+007

PT/I1/T2/P12500.A271

Hours	Cells/ml
0.00	2.12E+005
17.30	1.23E+005
41.43	1.12E+005
65.42	2.48E+005
89.70	1.71E+005
124.83	2.80E+005
163.15	3.01E+005
186.40	2.95E+005

PT/I26/T2/P10000.M031

Hours	Cells/ml
0.00	6.85E+004
20.88	1.96E+005
27.72	3.02E+005
45.05	4.78E+005
51.98	6.76E+005
69.22	1.02E+006
76.42	1.49E+006
98.12	3.75E+006
121.72	1.79E+007
140.80	3.42E+007
165.45	4.24E+007
189.37	5.18E+007

PT/I1/T2/P10000.A271

Hours	Cells/ml
0.00	2.12E+005
17.22	1.52E+005
41.18	2.84E+005
65.25	9.84E+005
89.32	2.35E+006
144.50	3.70E+006
162.98	4.11E+006
186.42	4.11E+006

PT/I1/T2/P15000.A271

Hours	Cells/ml
0.00	2.12E+005
17.42	2.14E+005
41.45	1.74E+005
65.33	1.94E+005
89.73	1.42E+005
144.50	3.21E+005
163.17	2.84E+005
186.38	3.01E+005

PT/I1/T2/P2500.A271

Hours	Cells/ml
0.00	2.12E+005
17.08	5.21E+005
40.88	3.52E+006
64.97	3.00E+007
88.95	8.86E+007
144.50	1.33E+008
162.73	1.31E+008

PT/I1/T2/PATM.A271

Hours	Cells/ml
0.00	2.12E+005
17.58	3.53E+005
40.85	1.74E+006
64.95	1.75E+007
88.75	3.65E+007
144.50	9.17E+007
161.32	9.84E+007
186.47	1.06E+008

PT/I107/T2/PATM.0281

Hours	Cells/ml
0.00	9.28E+004
20.87	6.87E+004
44.77	1.70E+005
118.53	9.46E+004
143.70	1.31E+005
166.48	1.33E+005
189.92	1.28E+005
213.70	3.33E+005
286.88	3.22E+005

PT/I107/T2/P12500.0281

Hours	Cells/ml
0.00	9.28E+004
20.97	1.74E+005
45.10	7.32E+004
118.62	3.11E+005
145.88	4.09E+005
166.57	5.47E+005
190.02	8.77E+005
213.90	1.51E+006

PT/I107/T2/P7500.0281

Hours	Cells/ml
0.00	9.28E+004
20.92	1.48E+005
44.83	3.12E+005
118.58	1.77E+007
124.45	2.55E+007
145.85	3.17E+007
166.53	3.80E+007
189.98	4.11E+007

PT/I1/T2/P5000.A271

Hours	Cells/ml
0.00	2.12E+005
17.10	4.10E+005
40.92	3.45E+006
64.98	2.95E+007
88.98	9.72E+007
124.83	1.32E+008
162.75	1.41E+008

PT/I107/T2/P5000.0281

Hours	Cells/ml
0.00	9.28E+004
20.90	1.61E+005
44.80	2.77E+005
118.57	7.13E+006
124.42	1.05E+007
145.83	2.31E+007
166.52	3.25E+007
189.97	3.78E+007

PT/I107/T2/P2500.0281

Hours	Cells/ml
0.00	9.28E+004
20.98	1.17E+005
44.78	2.69E+005
118.55	6.76E+005
145.82	2.89E+006
166.50	1.67E+006
189.95	2.07E+006
213.88	2.26E+006
286.90	6.24E+006
335.63	8.95E+006

PT/I107/T2/P10000.0281

Hours	Cells/ml
0.00	9.28E+004
20.93	1.67E+005
45.08	2.46E+005
118.60	3.22E+006
124.45	4.44E+006
145.87	1.97E+007
166.55	3.16E+007
190.00	3.63E+007

PT/I107/T2/P15000.0281

Hours	Cells/ml
0.00	9.28E+004
20.98	9.09E+004
45.12	4.83E+004
118.63	1.55E+005
146.00	1.64E+005
166.58	2.01E+005
190.03	1.78E+005
213.92	3.20E+005
335.68	1.19E+005

PT/I100/T2/P15000.0161

Hours	Cells/ml
0.00	2.96E+005
72.70	3.25E+005
96.22	2.98E+005
123.82	3.26E+005
148.75	2.97E+005
166.90	9.63E+005
240.45	3.64E+005
264.13	5.81E+005

PT/I100/T2/P7500.0161

Hours	Cells/ml
0.00	2.96E+005
72.63	7.31E+005
96.13	3.27E+006
123.77	7.94E+006
148.72	1.96E+007
166.85	2.31E+007
240.40	3.06E+007

PT/I100/T2/PATM.0161

Hours	Cells/ml
0.00	2.96E+005
72.58	4.12E+005
96.08	6.31E+005
123.73	3.78E+005
143.82	1.93E+005
166.82	2.16E+005
240.35	3.39E+005
264.05	2.66E+005

PT/I100/T2/P12500.0161

Hours	Cells/ml
0.00	2.96E+005
72.67	3.49E+005
96.17	3.28E+005
123.80	4.81E+005
148.68	6.28E+005
166.90	1.02E+006
197.15	1.88E+006
219.57	5.26E+006
240.43	1.44E+007
264.13	1.90E+007

PT/I96/T2/P12500.S141

Hours	Cells/ml
0.00	4.32E+005
19.12	2.48E+005
42.47	2.87E+005
65.18	2.53E+005
89.08	5.84E+005
161.78	2.00E+007
185.97	4.15E+007
213.57	5.57E+007

PT/I100/T2/P10000.0161

Hours	Cells/ml
0.00	2.96E+005
72.65	3.31E+005
96.15	7.03E+005
123.78	3.97E+006
148.72	8.74E+006
166.88	2.02E+007
240.42	3.13E+007

PT/I96/T2/P2500.S141

Hours	Cells/ml
0.00	4.32E+005
18.62	1.88E+005
42.40	7.88E+005
65.22	2.08E+005
89.02	2.93E+005
161.70	4.42E+005
185.90	5.24E+005
213.55	3.28E+005
240.93	3.21E+005
258.62	3.04E+005

PT/I96/T2/PATM.S141

Hours	Cells/ml
0.00	4.32E+005
18.60	1.84E+005
42.38	2.93E+005
65.20	1.80E+005
89.00	1.96E+005
163.80	3.07E+005
185.87	3.96E+005
213.53	3.36E+005
240.92	2.52E+005

PT/I100/T2/P5000.0161

Hours	Cells/ml
0.00	2.96E+005
72.62	5.25E+005
96.12	1.42E+006
123.75	3.82E+006
148.68	1.13E+007
166.85	2.17E+007
240.38	4.40E+007

PT/I100/T2/P2500.0161

Hours	Cells/ml
0.00	2.96E+005
72.60	3.62E+005
96.10	7.12E+005
123.75	5.41E+005
148.27	4.07E+005
166.83	7.14E+005
197.12	1.09E+006
219.52	2.20E+006
240.37	3.50E+006
264.07	7.21E+006

PT/I96/T2/P15000.S141

Hours	Cells/ml
0.00	4.32E+005
19.13	2.17E+005
42.48	2.96E+005
65.28	1.63E+005
89.10	2.28E+005
161.78	4.39E+005
185.98	3.14E+005
258.65	3.15E+005
333.50	1.45E+005

PT/I96/T2/P7500.S141

Hours	Cells/ml
0.00	4.32E+005
18.08	1.83E+005
42.43	3.82E+005
65.25	1.39E+006
89.05	8.44E+006
161.73	5.29E+007
185.93	5.27E+007
258.63	5.60E+007

PT/I62/T2/P7500.U291

Hours	Cells/ml
0.00	5.04E+005
23.98	8.61E+005
46.47	3.22E+006
71.50	3.88E+007
95.73	1.06E+008
161.38	1.39E+008

PT/I96/T2/P5000.S141

Hours	Cells/ml
0.00	4.32E+005
19.07	2.49E+005
42.42	6.27E+005
65.23	8.25E+005
89.03	2.88E+006
161.72	3.51E+007
185.92	4.06E+007
213.55	4.60E+007
240.95	4.63E+007

PT/I62/T2/P12500.U291

Hours	Cells/ml
0.00	5.04E+005
24.22	3.43E+005
46.50	2.54E+005
71.55	2.80E+005
95.40	3.31E+005
161.80	4.27E+005

PT/I96/T2/P10000.S141

Hours	Cells/ml
0.00	4.58E+005
19.10	2.10E+005
42.45	3.31E+005
65.27	8.65E+005
89.07	3.44E+006
161.75	7.09E+007
185.95	7.10E+007
258.63	7.02E+007

PT/I62/T2/P5000.U291

Hours	Cells/ml
0.00	5.04E+005
23.97	1.12E+006
46.45	3.73E+006
71.48	5.88E+007
95.75	1.19E+008
161.37	1.57E+008

PT/I62/T2/G.U291

Hours	Cells/ml
1.01	1.14E+001
173.38	8.76E+000
345.75	6.29E+000
518.12	6.97E+000
690.49	9.17E+000
862.85	1.00E+003
1035.22	1.00E+003

PT/I62/T2/P15000.U291

Hours	Cells/ml
0.00	5.04E+005
24.25	2.49E+005
46.53	2.44E+005
71.57	2.40E+005
95.37	3.14E+005
161.82	4.89E+005

PT/I62/T2/P10000.U291

Hours	Cells/ml
0.00	5.04E+005
24.20	6.07E+005
46.48	1.33E+006
71.53	3.53E+006
95.72	2.19E+007
161.78	5.97E+007

PT/I62/T2/P2500.U291

Hours	Cells/ml
0.00	5.04E+005
23.93	1.44E+006
46.43	6.40E+006
71.47	6.14E+007
95.77	1.14E+008
161.33	1.51E+008

PT/I62/T2/PATM.U291

Hours	Cells/ml
0.00	5.04E+005
23.92	8.11E+005
45.85	2.95E+006
71.62	1.47E+007
95.17	4.60E+007
161.32	8.72E+007

PT/XRA710/T2/P15000.A081

Hours	Cells/ml
0.00	1.17E+005
19.78	2.15E+005
47.47	2.35E+005
96.22	1.80E+005
115.78	2.47E+005
138.05	2.62E+005
167.80	2.74E+005
187.85	2.90E+005
212.68	3.55E+005
270.60	2.92E+005

PT/XRA710/T2/P7500.A081

Hours	Cells/ml
0.00	1.17E+005
19.58	3.21E+005
47.22	2.50E+005
96.17	2.19E+005
115.60	3.98E+005
137.88	3.57E+005
167.50	4.35E+005
187.80	6.00E+005
212.38	1.56E+006
270.33	1.99E+007
289.12	2.99E+007

PT/XRA710/T2/PATM.A081

Hours	Cells/ml
0.00	1.17E+005
19.05	3.60E+005
47.12	7.60E+005
95.87	8.00E+005
115.43	1.81E+006
137.72	2.02E+006
167.43	2.24E+006
187.77	2.62E+006
212.33	2.91E+006
270.22	3.40E+006

PT/XRA710/T2/P12500.A081

Hours	Cells/ml
0.00	1.17E+005
19.77	4.54E+005
47.45	2.88E+005
96.20	2.02E+005
115.77	3.59E+005
138.03	4.91E+005
167.78	1.22E+006
187.83	3.06E+006
212.58	1.15E+007
270.60	4.16E+007
289.13	4.13E+007

PT/I54/T2/P12500.F021

Hours	Cells/ml
0.00	2.05E+005
19.75	2.15E+005
26.22	1.51E+005
44.57	8.96E+004
68.33	2.43E+005
93.70	3.45E+005
164.20	5.58E+006
188.25	1.90E+007
210.97	2.65E+007
235.62	2.79E+007
499.02	4.39E+007

PT/XRA710/T2/P10000.A081

Hours	Cells/ml
0.00	1.17E+005
19.60	2.41E+005
47.43	2.47E+005
96.18	2.73E+005
115.63	4.70E+005
137.90	6.49E+005
167.75	1.80E+006
187.82	5.84E+006
212.57	2.35E+007
270.58	5.23E+007
289.12	4.97E+007

PT/XRA710/T2/P5000.A081

Hours	Cells/ml
0.00	1.17E+005
19.18	2.65E+005
47.20	2.68E+005
95.95	2.70E+005
115.47	3.72E+005
137.75	3.58E+005
167.47	3.75E+005
187.80	3.80E+005
212.37	4.15E+005
270.25	3.71E+005

PT/XRA710/T2/P2500.A081

Hours	Cells/ml
0.00	1.17E+005
19.10	1.97E+005
47.13	2.47E+005
95.87	1.35E+005
115.45	3.91E+005
137.73	2.89E+005
167.45	3.58E+005
187.78	3.07E+005
212.33	3.72E+005
270.23	3.51E+005

PT/I54/T2/P2500.F021

Hours	Cells/ml
0.00	2.05E+005
20.08	5.03E+005
25.93	1.35E+005
43.92	1.87E+005
68.27	3.66E+005
93.63	4.82E+005
163.78	1.27E+006
187.95	1.05E+007
210.43	5.63E+007
234.78	8.69E+007
498.53	2.09E+008

PT/I54/T2/PATM.F021

Hours	Cells/ml
0.00	2.05E+005
20.38	5.17E+005
25.50	6.55E+005
43.77	1.07E+006
68.25	1.63E+006
93.60	1.99E+006
163.55	2.77E+006
187.65	2.80E+006
236.85	3.00E+006
499.83	2.11E+008

PT/I9/T2/P7500.A271

Hours	Cells/ml
0.00	3.30E+005
17.13	4.85E+005
41.17	2.40E+006
65.25	2.30E+007
89.30	6.92E+007
144.50	1.00E+008
162.97	1.09E+008

PT/I54/T2/P5000.F021

Hours	Cells/ml
0.00	2.05E+005
25.93	1.88E+005
44.08	4.14E+005
68.28	6.86E+005
93.65	1.33E+006
163.80	2.83E+007
187.97	5.40E+007
210.53	7.89E+007
234.82	9.85E+007
498.55	1.22E+008

PT/I54/T2/P15000.F021

Hours	Cells/ml
0.00	2.05E+005
19.67	1.22E+005
26.23	1.25E+005
44.60	1.74E+005
68.37	1.27E+005
93.72	2.07E+005
164.22	1.53E+005
188.37	3.32E+005
210.98	1.99E+005
235.53	2.37E+005
499.03	3.25E+005

PT/I54/T2/P7500.F021

Hours	Cells/ml
0.00	2.05E+005
19.92	2.58E+005
25.95	2.12E+005
44.12	2.22E+005
68.30	4.66E+005
93.67	1.80E+006
164.00	3.38E+007
188.05	5.11E+007
210.68	6.86E+007
235.05	1.10E+008
498.67	1.15E+008

PT/I9/T2/P12500.A271

Hours	Cells/ml
0.00	3.30E+005
17.32	3.18E+005
41.45	4.39E+005
65.43	4.47E+005
89.73	5.25E+005
124.83	5.26E+005
163.15	7.04E+005
186.40	6.12E+005

PT/I54/T2/P10000.F021

Hours	Cells/ml
0.00	2.05E+005
19.83	1.42E+005
26.20	5.17E+005
44.55	1.96E+005
68.32	2.87E+005
93.68	7.78E+005
164.02	2.79E+007
188.15	4.80E+007
210.70	4.81E+007
235.22	4.54E+007
499.02	1.04E+008

PT/I9/T2/P10000.A271

Hours	Cells/ml
0.00	3.30E+005
17.23	1.80E+005
41.20	6.00E+005
65.27	1.72E+006
89.33	7.82E+006
144.50	3.38E+007
163.00	4.03E+007
186.42	4.68E+007

PT/I9/T2/P15000.A271

Hours	Cells/ml
0.00	3.30E+005
17.42	3.60E+005
41.47	3.72E+005
65.45	4.11E+005
89.75	4.96E+005
144.50	4.44E+005
163.17	4.64E+005
186.38	5.51E+005

PT/I101/T2/PATM.0161

Hours	Cells/ml
0.00	1.53E+005
72.58	2.40E+005
96.08	2.57E+005
123.73	2.44E+005
144.85	2.24E+005
166.83	1.49E+005
240.37	2.14E+005
264.07	2.93E+005

PT/I101/T2/P12500.0161

Hours	Cells/ml
0.00	1.53E+005
72.67	2.55E+005
96.17	2.11E+005
123.82	4.09E+005
148.73	1.22E+005
166.92	3.24E+005
197.25	4.55E+005
219.58	7.05E+005

PT/I9/T2/P2500.A271

Hours	Cells/ml
0.00	3.30E+005
17.10	1.20E+006
40.87	7.70E+006
64.97	5.54E+007
88.97	1.04E+008
144.50	1.16E+008
162.73	1.22E+008

PT/I9/T2/PATM.A271

Hours	Cells/ml
0.00	3.30E+005
17.60	7.82E+005
40.87	3.52E+006
64.87	7.58E+006
88.77	3.67E+007
144.50	8.54E+007
161.32	9.79E+007
186.47	1.07E+008

PT/I101/T2/P7500.0161

Hours	Cells/ml
0.00	1.53E+005
72.63	2.43E+005
96.13	2.81E+005
123.78	7.48E+005
148.72	1.64E+006
166.88	4.67E+006
197.23	1.00E+007
219.55	1.46E+007
240.40	2.71E+007
264.10	3.59E+007

PT/I9/T2/P5000.A271

Hours	Cells/ml
0.00	3.30E+005
17.12	8.84E+005
40.92	4.83E+006
65.02	5.65E+007
88.98	1.09E+008
124.80	1.22E+008
162.77	1.35E+008

PT/I101/T2/P5000.0161

Hours	Cells/ml
0.00	1.53E+005
72.63	2.90E+005
96.12	2.99E+005
123.77	7.94E+005
148.70	1.58E+006
166.85	2.70E+006
197.22	1.05E+007
219.53	1.26E+007
240.38	3.57E+007
264.08	3.23E+007

PT/I101/T2/P2500.0161

Hours	Cells/ml
0.00	1.53E+005
72.60	2.37E+005
96.10	2.73E+005
123.75	2.49E+005
148.28	1.64E+005
166.85	1.76E+005
197.22	3.24E+005
219.52	3.80E+005
240.37	3.87E+005

PT/I101/T2/P10000.0161

Hours	Cells/ml
0.00	1.53E+005
72.48	2.77E+005
96.15	3.82E+005
123.80	1.11E+006
148.73	1.64E+006
166.90	8.61E+006
197.23	9.29E+006
219.57	1.52E+007
240.42	2.44E+007
264.12	3.31E+007

PT/I101/T2/P15000.0161

Hours	Cells/ml
0.00	1.53E+005
72.68	2.30E+005
96.23	2.99E+005
123.82	3.87E+005
148.75	1.93E+005
166.93	1.35E+005
240.47	2.74E+005
264.18	6.51E+004

PT/I97/T2/P15000.S141

Hours	Cells/ml
0.00	1.58E+006
19.15	5.14E+005
42.50	4.07E+005
65.30	4.51E+005
89.12	4.01E+005
161.80	3.73E+005
186.00	2.91E+005
258.60	2.77E+005
333.50	2.97E+005

PT/I97/T2/P7500.S141

Hours	Cells/ml
0.00	1.58E+006
19.10	4.20E+005
42.43	3.96E+005
65.25	3.88E+005
89.07	3.40E+005
161.75	5.58E+005
185.93	6.55E+005
258.58	1.64E+007
313.42	2.76E+007
333.47	3.68E+007

PT/I97/T2/PATM.S141

Hours	Cells/ml
0.00	1.58E+006
18.60	5.38E+005
42.40	4.69E+005
65.20	4.86E+005
89.03	5.97E+005
161.70	1.72E+005
185.88	5.72E+005
258.57	6.11E+005
332.03	6.43E+005

PT/I97/T2/P12500.S141

Hours	Cells/ml
0.00	1.58E+006
19.13	5.06E+005
42.48	2.71E+005
65.28	3.73E+005
89.10	3.25E+005
161.78	8.08E+005
185.98	4.02E+005
258.58	2.74E+005
313.42	3.68E+005
333.48	5.26E+005

PT/I55/T2/P12500.F231

Hours	Cells/ml
0.00	3.39E+005
19.53	4.51E+005
25.35	3.47E+005
42.85	4.85E+005
50.13	2.14E+005
68.00	4.70E+005
73.52	2.52E+005
90.83	3.41E+005
97.82	3.34E+005
120.85	4.43E+005
144.02	1.01E+006

PT/I97/T2/P10000.S141

Hours	Cells/ml
0.00	1.58E+006
19.12	5.95E+005
42.45	3.70E+005
65.27	3.43E+005
89.08	3.20E+005
161.77	3.85E+005
185.97	3.84E+005
258.58	5.70E+006
313.42	1.93E+007
333.48	3.68E+007

PT/I55/T2/P2500.F231

Hours	Cells/ml
0.00	3.39E+005
19.05	4.75E+005
24.97	4.52E+005
42.43	6.09E+005
49.65	6.84E+005
67.32	4.54E+005
73.18	6.64E+005
90.57	2.03E+006
97.43	3.10E+006
120.47	2.17E+007
143.63	7.85E+007
162.37	9.07E+007
189.58	1.09E+008

PT/I55/T2/PATM.F231

Hours	Cells/ml
0.00	3.39E+005
18.62	1.02E+006
24.95	1.12E+006
42.28	1.84E+006
49.65	7.28E+005
67.28	1.45E+006
73.07	1.62E+006
90.43	2.07E+006
97.30	2.23E+006
120.32	2.41E+006
143.62	5.27E+006
162.25	1.24E+007
189.58	5.08E+007

PT/I97/T2/P5000.S141

Hours	Cells/ml
0.00	1.58E+006
19.08	7.33E+005
42.42	4.17E+005
65.23	4.44E+005
89.05	4.11E+005
161.73	5.37E+005
185.92	5.84E+005
258.57	1.05E+006
313.42	7.09E+006
332.08	1.92E+007

PT/I97/T2/P2500.S141

Hours	Cells/ml
0.00	1.58E+006
18.62	5.16E+005
42.42	4.35E+005
65.22	4.32E+005
89.03	4.81E+005
161.72	7.42E+005
185.90	4.92E+005
258.57	4.96E+005
313.42	4.32E+005
332.13	5.14E+005

PT/I55/T2/P15000.F231

Hours	Cells/ml
0.00	3.39E+005
19.65	5.10E+005
25.50	3.90E+005
42.88	3.56E+005
50.15	3.42E+005
68.03	3.76E+005
73.53	3.89E+005
90.83	4.46E+005
97.97	4.37E+005
120.87	4.43E+005
163.07	3.35E+005
189.65	3.74E+005

PT/I55/T2/P7500.F231

Hours	Cells/ml
0.00	3.39E+005
19.23	3.86E+005
25.15	3.48E+005
42.63	5.37E+005
49.83	3.88E+005
67.53	6.71E+005
73.32	1.01E+006
90.73	2.50E+006
97.52	3.91E+006
120.63	2.49E+007
143.68	4.68E+007
162.73	5.17E+007
189.62	6.41E+007

PT/I109/T2/P7500.0281

Hours	Cells/ml
0.00	2.64E+005
20.93	4.01E+005
45.07	7.92E+005
118.58	2.42E+007
124.45	2.77E+007
145.87	2.99E+007
166.55	3.42E+007
189.98	3.73E+007

PT/I109/T2/P12500.0281

Hours	Cells/ml
0.00	2.64E+005
20.97	3.23E+005
45.12	3.42E+005
118.62	1.56E+006
145.90	2.05E+006
166.58	5.14E+006
190.03	1.48E+007
213.92	1.91E+007
286.93	2.10E+007
335.67	2.78E+007

PT/I55/T2/P5000.F231

Hours	Cells/ml
0.00	3.39E+005
19.08	3.84E+005
25.13	3.32E+005
42.47	4.45E+005
49.82	3.63E+005
67.53	8.36E+005
73.20	1.18E+006
90.57	3.34E+006
97.45	5.69E+006
120.48	3.79E+007
143.67	7.74E+007
162.38	9.84E+007
189.60	1.11E+008

PT/I55/T2/P10000.F231

Hours	Cells/ml
0.00	3.39E+005
19.27	3.86E+005
25.33	4.73E+005
42.67	4.49E+005
50.10	2.84E+005
67.98	4.25E+005
73.33	4.62E+005
90.75	1.04E+006
97.72	1.91E+006
120.67	7.24E+006
143.98	2.39E+007
163.00	3.09E+007
189.62	3.70E+007

PT/I109/T2/P10000.0281

Hours	Cells/ml
0.00	2.64E+005
20.95	4.56E+005
45.08	6.64E+005
118.60	2.21E+007
124.47	2.15E+007
145.88	2.76E+007
166.57	3.04E+007
190.02	2.72E+007

PT/I109/T2/P2500.0281

Hours	Cells/ml
0.00	2.64E+005
20.90	2.77E+005
44.80	2.50E+005
118.55	1.39E+006
145.83	1.84E+006
166.52	2.57E+006
189.95	2.52E+006
213.90	4.02E+006
286.92	3.03E+006
335.65	2.90E+006

PT/I109/T2/P15000.0281

Hours	Cells/ml
0.00	2.64E+005
20.98	2.89E+005
44.73	2.79E+005
118.63	3.73E+005
146.02	3.83E+005
166.60	2.80E+005
190.05	5.71E+005
213.93	3.91E+005
335.68	3.49E+005

PT/I109/T2/PATM.0281

Hours	Cells/ml
0.00	2.64E+005
20.88	2.62E+005
44.78	2.41E+005
118.53	2.74E+005
143.70	2.96E+005
166.50	3.46E+005
189.93	2.56E+005
213.70	5.14E+005
286.90	4.18E+005
335.62	3.13E+005

PT/I98/T2/PATM.S301

Hours	Cells/ml
0.00	1.34E+005
23.55	1.20E+005
50.28	5.23E+004
118.55	7.84E+004
142.65	1.28E+005
168.78	6.14E+004
190.40	1.37E+005
216.63	2.40E+005
287.13	1.61E+005
316.05	2.96E+005

PT/I98/T2/P12500.S301

Hours	Cells/ml
0.00	1.34E+005
23.53	9.41E+004
47.92	7.21E+004
118.63	1.25E+005
142.73	3.94E+005
168.88	7.55E+005
190.48	1.96E+006
216.78	6.13E+006
287.22	2.02E+007

PT/I98/T2/P5000.S301

Hours	Cells/ml
0.00	1.34E+005
23.58	6.40E+004
47.88	7.50E+004
118.58	1.50E+006
142.67	3.47E+006
168.82	1.51E+007
190.43	2.22E+007
216.72	3.59E+007
287.17	4.42E+007

PT/I98/T2/P2500.S301

Hours	Cells/ml
0.00	1.34E+005
23.57	6.06E+004
47.83	5.70E+004
118.57	1.20E+005
142.67	4.44E+005
168.80	2.02E+005
190.42	2.97E+005
216.65	3.52E+005
287.15	7.85E+005
316.07	6.99E+005
336.13	6.32E+005
359.90	7.92E+005

PT/I98/T2/P7500.S301

Hours	Cells/ml
0.00	1.34E+005
23.60	8.18E+004
47.90	7.32E+004
118.60	3.25E+006
142.70	1.32E+007
168.85	1.60E+007
190.45	2.64E+007
216.73	2.22E+007
287.18	3.33E+007

PT/I109/T2/P5000.0281

Hours	Cells/ml
0.00	2.64E+005
20.92	3.10E+005
44.82	5.29E+005
118.57	1.49E+007
124.43	1.84E+007
145.85	2.14E+007
166.53	2.65E+007
189.97	2.66E+007

PT/I98/T2/P10000.S301

Hours	Cells/ml
0.00	1.34E+005
23.62	2.50E+005
47.90	9.75E+004
118.62	2.69E+006
142.72	8.14E+006
168.87	2.53E+007
190.47	2.60E+007
216.75	2.66E+007
287.20	4.09E+007

PT/I98/T2/P15000.S301

Hours	Cells/ml
0.00	1.34E+005
23.65	2.17E+005
47.93	1.76E+005
118.65	7.79E+004
142.75	1.90E+005
168.90	1.42E+005
190.50	1.39E+005
216.80	1.36E+005
287.23	3.91E+005
316.10	6.47E+005
336.18	1.96E+005
359.92	1.41E+005

PT/I46/T2/P15000.G311

Hours	Cells/ml
0.00	1.09E+006
24.92	1.02E+006
48.47	1.02E+006
65.97	1.10E+006
72.50	1.07E+006
90.75	1.10E+006
190.75	1.05E+006

PT/I46/T2/P7500.G311

Hours	Cells/ml
0.00	1.09E+006
24.60	1.62E+006
48.42	5.76E+006
65.68	3.60E+007
72.22	6.05E+007
90.70	1.11E+008
190.65	1.07E+008

PT/I46/T2/PATM.G311

Hours	Cells/ml
0.00	1.09E+006
24.52	1.41E+006
48.53	5.76E+006
65.62	1.77E+007
72.18	2.47E+007
90.10	5.01E+007
190.62	7.83E+007

PT/I46/T2/P12500.G311

Hours	Cells/ml
0.00	1.09E+006
24.83	9.23E+005
48.45	9.03E+005
65.95	1.12E+006
72.48	1.11E+006
90.73	8.77E+005
190.72	1.00E+006

PT/I3/T2/PATM.Y111

Hours	Cells/ml
0.00	2.04E+006
21.87	1.86E+006
45.62	2.67E+006
70.25	6.04E+006
93.45	2.18E+007
127.98	6.77E+007
166.38	1.03E+008
190.55	1.21E+008

PT/I3/T2/P12500.Y111

Hours	Cells/ml
0.00	2.04E+006
23.40	1.91E+006
47.23	1.98E+006
71.77	1.95E+006
93.98	1.94E+006

PT/I46/T2/P10000.G311

Hours	Cells/ml
0.00	1.09E+006
24.82	9.92E+005
48.43	2.93E+006
65.93	7.86E+006
72.47	1.15E+007
90.72	2.82E+007
190.68	7.71E+007

PT/I3/T2/P7500.Y111

Hours	Cells/ml
0.00	2.04E+006
23.17	2.14E+006
46.95	3.24E+006
71.53	1.12E+007
93.73	5.81E+007
128.05	6.35E+007
166.43	8.26E+007
190.57	1.06E+008

PT/I46/T2/P5000.G311

Hours	Cells/ml
0.00	1.09E+006
24.55	1.88E+006
48.57	1.48E+007
65.67	8.34E+007

PT/I46/T2/P2500.G311

Hours	Cells/ml
0.00	1.09E+006
24.53	2.08E+006
48.38	1.58E+007
65.63	6.96E+007
72.20	7.90E+007
90.12	8.28E+007
190.63	1.08E+008

PT/I3/T2/P5000.Y111

Hours	Cells/ml
0.00	2.04E+006
23.02	2.19E+006
46.82	5.00E+006
71.52	3.13E+007
93.72	8.20E+007
128.02	1.00E+008
166.42	1.30E+008

PT/I3/T2/P2500.Y111

Hours	Cells/ml
0.00	2.04E+006
23.17	2.19E+006
46.80	4.88E+006
71.50	2.83E+007
93.80	8.36E+007
128.00	1.16E+008
166.40	1.31E+008

PT/I3/T2/P10000.Y111

Hours	Cells/ml
0.00	2.04E+006
23.18	2.02E+006
46.97	2.39E+006
71.75	3.72E+006
93.95	1.36E+007
128.23	2.44E+007
166.65	2.65E+007
190.58	3.66E+007

PT/I3/T2/P15000.Y111

Hours	Cells/ml
0.00	2.04E+006
23.42	2.00E+006
47.25	2.08E+006
71.78	2.03E+006
94.00	2.07E+006
128.27	1.86E+006
166.68	1.99E+006

PT/I64/T2/P15000.L061

Hours	Cells/ml
0.00	1.05E+006
27.83	9.33E+005
52.38	9.47E+005
76.60	9.04E+005
100.78	9.21E+005
149.73	1.26E+006
166.98	1.01E+006
196.25	1.09E+006
219.95	1.04E+006
341.47	9.25E+005

PT/I64/T2/P7500.L061

Hours	Cells/ml
0.00	1.05E+006
27.70	9.10E+005
52.33	9.85E+005
76.25	9.93E+005
100.72	1.37E+006
149.70	8.60E+006
166.55	2.24E+007
196.17	4.39E+007
219.87	4.93E+007
341.40	4.89E+007

PT/I64/T2/PATM.L061

Hours	Cells/ml
0.00	1.05E+006
27.38	9.53E+005
52.28	9.97E+005
76.20	1.00E+006
100.67	9.72E+005
149.67	9.59E+005
166.40	1.06E+006
196.12	1.10E+006
219.80	1.09E+006
244.48	1.06E+006
341.33	9.69E+005

PT/I64/T2/P12500.L061

Hours	Cells/ml
0.00	1.05E+006
27.73	9.47E+005
52.37	9.57E+005
76.50	1.03E+006
100.75	1.08E+006
149.72	1.14E+006
166.95	1.30E+006
196.20	1.62E+006
219.92	1.55E+006
244.53	1.61E+006
341.45	1.50E+006

PT/I64/T2/P5000.L061

Hours	Cells/ml
0.00	1.09E+006
27.43	9.20E+005
52.32	9.99E+005
76.23	1.06E+006
100.70	1.37E+006
149.68	2.03E+006
166.53	2.85E+006
196.15	7.39E+006
219.83	2.36E+007
244.52	3.47E+007
341.38	4.43E+007

PT/I64/T2/G.L061

Hours	Cells/ml
1.01	1.00E+003
173.38	1.00E+003
345.75	1.43E+001
518.12	1.22E+001
690.49	1.37E+001
862.85	1.00E+003
1035.22	1.00E+003

PT/I64/T2/P10000.L061

Hours	Cells/ml
0.00	1.05E+006
27.72	9.35E+005
52.35	9.24E+005
76.40	9.39E+005
100.73	1.11E+006
149.72	1.50E+006
166.92	1.90E+006
196.18	6.31E+006
219.88	2.09E+007
244.52	2.78E+007

PT/I64/T2/P2500.L061

Hours	Cells/ml
0.00	1.05E+006
27.42	9.69E+005
52.30	1.03E+006
76.22	1.00E+006
100.68	9.98E+005
149.68	1.08E+006
166.42	1.21E+006
196.13	1.50E+006
219.82	1.27E+006
265.00	4.41E+005
341.45	1.27E+006

SC/I4/T2/P4000.0121

Hours	Cells/ml
0.00	2.36E+006
24.28	3.28E+006
29.28	4.03E+006
47.18	1.06E+007
53.45	1.51E+007
71.58	4.13E+007
77.72	4.79E+007
93.85	7.26E+007
170.23	1.00E+008

SC/I4/T2/P3000.0121

Hours	Cells/ml
0.00	2.36E+006
24.28	4.17E+006
29.25	5.96E+006
47.17	2.55E+007
53.43	4.29E+007
71.33	8.48E+007
77.78	9.28E+007
93.83	1.30E+008
167.50	1.64E+008

SC/I4/T2/PATM.0121

Hours	Cells/ml
0.00	2.36E+006
24.23	9.17E+006
29.20	1.78E+007
47.12	9.51E+007
53.38	1.21E+008
71.32	2.17E+008
77.65	2.07E+008
93.78	2.08E+008

SC/I4/T2/P6000.0121

Hours	Cells/ml
0.00	2.36E+006
24.32	2.63E+006
29.35	2.27E+006
47.20	2.24E+006
53.48	2.57E+006
71.62	1.74E+006
77.75	2.41E+006
93.90	2.47E+006
167.55	2.71E+006

SC/I5/T2/P6000.0051

Hours	Cells/ml
0.00	1.57E+006
4.88	1.06E+006
20.85	1.09E+006
27.57	1.12E+006
47.15	1.01E+006
52.05	1.04E+006
68.60	1.05E+006
76.32	1.11E+006
92.82	1.02E+006

SC/I4/T2/P5000.0121

Hours	Cells/ml
0.00	2.36E+006
24.30	2.23E+006
29.33	2.36E+006
47.28	3.30E+006
53.47	3.56E+006
71.60	4.36E+006
77.73	4.74E+006
93.87	5.52E+006
167.53	7.55E+006

SC/I4/T2/P2000.0121

Hours	Cells/ml
0.00	2.36E+006
24.27	6.55E+006
29.23	8.84E+006
47.15	4.61E+007
53.42	7.95E+007
71.20	1.45E+008
77.73	1.39E+008
93.82	1.75E+008

SC/I4/T2/P1000.0121

Hours	Cells/ml
0.00	2.36E+006
24.25	7.86E+006
29.22	1.21E+007
47.13	6.64E+007
53.40	1.10E+008
71.17	1.75E+008
77.67	1.67E+008
93.82	2.12E+008

SC/I5/T2/P1000.0051

Hours	Cells/ml
0.00	1.57E+006
4.80	1.27E+006
20.75	3.07E+006
27.50	6.05E+006
47.05	4.10E+007
51.98	5.41E+007
68.52	1.20E+008
75.88	1.60E+008
92.73	1.53E+008

SC/I5/T2/PATM.0051

Hours	Cells/ml
0.00	1.57E+006
4.78	1.18E+006
20.73	3.72E+006
27.48	7.43E+006
47.02	4.54E+007
51.97	7.09E+007
68.50	1.23E+008
75.87	1.73E+008
92.22	1.64E+008

SC/I5/T2/P4000.0051

Hours	Cells/ml
0.00	1.57E+006
4.85	1.07E+006
20.80	1.57E+006
27.53	2.17E+006
47.12	6.14E+006
52.02	7.86E+006
68.55	1.75E+007
76.28	3.09E+007
92.78	3.79E+007
171.20	6.61E+007

SC/I5/T2/P3000.0051

Hours	Cells/ml
0.00	1.57E+006
4.83	1.10E+006
20.78	2.02E+006
27.52	3.17E+006
47.08	1.43E+007
52.03	1.94E+007
68.55	5.11E+007
76.27	7.74E+007
92.77	9.20E+007
171.18	1.55E+008

SC/I6/T2/P3000.0051

Hours	Cells/ml
0.00	1.77E+006
4.85	1.79E+006
20.80	3.45E+006
27.53	6.08E+006
47.10	2.51E+007
52.02	3.38E+007
68.55	7.53E+007
76.28	8.41E+007
92.77	1.05E+008
171.22	1.39E+008

SC/I5/T2/P2000.0051

Hours	Cells/ml
0.00	1.57E+006
4.82	1.88E+006
20.77	2.39E+006
27.50	4.46E+006
47.05	4.21E+007
51.98	4.03E+007
68.53	9.81E+007
76.25	1.21E+008
92.75	1.73E+008
171.18	2.20E+008

SC/I6/T2/P5000.0051

Hours	Cells/ml
0.00	1.77E+006
4.87	1.77E+006
20.83	1.97E+006
27.57	2.37E+006
47.15	3.41E+006
52.05	3.74E+006
68.58	5.15E+006
76.32	5.34E+006
92.80	6.64E+006
171.23	8.59E+006

SC/I6/T2/P4000.0051

Hours	Cells/ml
0.00	1.77E+006
4.85	1.81E+006
20.82	3.36E+006
27.55	3.96E+006
47.13	1.10E+007
52.03	1.36E+007
68.57	3.07E+007
76.30	4.01E+007
92.78	4.95E+007
171.22	7.93E+007

SC/I6/T2/P6000.0051

Hours	Cells/ml
0.00	1.77E+006
4.88	1.83E+006
20.85	1.80E+006
27.58	1.94E+006
47.17	1.93E+006
52.07	1.93E+006
68.60	1.84E+006
76.33	2.05E+006
92.82	1.93E+006

SC/I5/T2/P5000.0051

Hours	Cells/ml
0.00	1.57E+006
4.87	1.83E+006
20.82	1.13E+006
27.55	1.45E+006
47.13	1.89E+006
52.03	2.10E+006
68.58	2.87E+006
76.30	3.14E+006
92.80	3.43E+006
171.20	4.39E+006

SC/I6/T2/P1000.0051

Hours	Cells/ml
0.00	1.77E+006
4.82	1.88E+006
20.75	5.43E+006
27.50	1.11E+007
47.05	6.39E+007
51.98	9.26E+007
68.52	1.36E+008
75.90	1.91E+008
92.72	1.62E+008

SC/I6/T2/PATM.0051

Hours	Cells/ml
0.00	1.77E+006
4.88	1.86E+006
20.75	6.39E+006
27.48	1.38E+007
47.10	8.62E+007
51.97	1.12E+008
68.50	1.54E+008
75.88	2.05E+008
92.72	1.71E+008

SC/I7/T2/PATM.S141

Hours	Cells/ml
0.00	1.13E+006
22.43	2.15E+006
28.92	3.95E+006
45.35	2.12E+007
52.83	4.18E+007
70.33	1.30E+008
76.55	1.75E+008
95.12	1.88E+008
165.68	2.09E+008

SC/I7/T2/P6000.S141

Hours	Cells/ml
0.00	1.13E+006
22.20	7.19E+005
29.03	9.31E+005
45.53	7.64E+005
52.93	8.01E+005
70.63	8.35E+005
76.65	9.42E+005
95.23	1.03E+006
167.23	1.06E+006

SC/I7/T2/P3000.S141

Hours	Cells/ml
0.00	1.13E+006
22.22	9.58E+005
28.97	1.55E+006
45.40	6.61E+006
52.88	1.36E+007
70.48	4.56E+007
76.60	6.65E+007
95.18	1.13E+008
167.18	1.64E+008

SC/I6/T2/P2000.0051

Hours	Cells/ml
0.00	1.77E+006
4.83	1.84E+006
20.78	4.41E+006
27.52	8.79E+006
47.07	4.33E+007
52.00	6.05E+007
68.53	1.14E+008
76.27	1.39E+008
92.75	1.49E+008

SC/I7/T2/P2000.S141

Hours	Cells/ml
0.00	1.13E+006
22.23	1.27E+006
28.95	2.03E+006
45.38	1.17E+007
52.87	2.53E+007
70.47	9.31E+007
76.58	1.16E+008
95.15	1.46E+008
167.17	1.97E+008

SC/I7/T2/P1000.S141

Hours	Cells/ml
0.00	1.13E+006
22.23	1.64E+006
28.83	3.07E+006
45.37	1.84E+007
52.85	3.95E+007
70.40	1.29E+008
76.57	1.48E+008
95.13	1.93E+008
167.15	2.20E+008

SC/I7/T2/P5000.S141

Hours	Cells/ml
0.00	1.13E+006
22.20	7.14E+005
29.02	8.19E+005
45.45	1.13E+006
52.92	1.44E+006
70.52	2.25E+006
76.65	2.75E+006
95.22	3.53E+006
167.22	4.93E+006

SC/I7/T2/P4000.S141

Hours	Cells/ml
0.00	1.13E+006
22.22	8.08E+005
28.98	1.05E+006
45.42	3.00E+006
52.90	4.61E+006
70.50	1.44E+007
76.63	2.09E+007
95.20	5.05E+007
167.20	1.06E+008

SC/I1/T2/P4000.S211

Hours	Cells/ml
0.00	1.37E+006
22.05	1.19E+006
29.55	2.07E+006
47.25	5.83E+006
54.02	8.43E+006
72.32	3.21E+007
94.83	6.08E+007
168.57	9.20E+007

SC/I1/T2/P3000.S211

Hours	Cells/ml
0.00	1.37E+006
22.03	1.63E+006
29.45	3.13E+006
47.23	1.35E+007
54.00	2.61E+007
72.18	7.63E+007
94.83	1.17E+008
168.55	1.59E+008

SC/I1/T2/PATM.S211

Hours	Cells/ml
0.00	1.37E+006
21.97	3.67E+006
29.40	7.46E+006
47.18	4.27E+007
53.95	8.01E+007
72.10	1.65E+008
94.82	2.05E+008

SC/I1/T2/P6000.S211

Hours	Cells/ml
0.00	1.37E+006
22.08	9.30E+005
29.58	9.90E+005
47.28	9.48E+005
54.05	9.38E+005
72.35	1.08E+006
94.85	1.11E+006
168.67	1.29E+006

SC/I10/T2/P6000.S141

Hours	Cells/ml
0.00	1.08E+006
22.15	8.46E+005
29.03	9.68E+005
45.55	1.05E+006
52.93	8.44E+005
70.55	8.06E+005
76.68	9.61E+005
95.23	8.97E+005

SC/I1/T2/P5000.S211

Hours	Cells/ml
0.00	1.37E+006
22.23	1.08E+006
29.57	1.33E+006
47.27	1.94E+006
54.03	2.24E+006
72.33	3.43E+006
94.85	5.14E+006
168.58	1.29E+007

SC/I1/T2/P2000.S211

Hours	Cells/ml
0.00	1.37E+006
22.00	2.15E+006
29.43	4.49E+006
47.22	2.85E+007
53.98	4.63E+007
72.17	1.22E+008
94.83	1.59E+008

SC/I1/T2/P1000.S211

Hours	Cells/ml
0.00	1.37E+006
21.98	3.07E+006
29.42	7.05E+006
47.20	4.06E+007
53.97	7.43E+007
72.12	1.45E+008
94.82	1.85E+008

SC/I10/T2/P1000.S141

Hours	Cells/ml
0.00	1.08E+006
22.18	2.19E+006
28.95	4.02E+006
45.38	2.24E+007
52.85	4.54E+007
70.40	1.15E+008
76.57	1.32E+008
95.15	1.86E+008
167.17	2.28E+008

SC/I10/T2/PATM.S141

Hours	Cells/ml
0.00	1.08E+006
22.43	2.55E+006
28.95	4.38E+006
45.45	2.29E+007
52.83	4.21E+007
70.33	1.18E+008
76.55	1.47E+008
95.13	1.66E+008
165.70	2.32E+008

SC/I10/T2/P4000.S141

Hours	Cells/ml
0.00	1.08E+006
22.17	1.16E+006
28.98	1.49E+006
45.43	3.27E+006
52.90	4.74E+006
70.52	1.17E+007
76.65	1.65E+007
95.20	4.14E+007
167.22	7.10E+007

SC/I10/T2/P3000.S141

Hours	Cells/ml
0.00	1.08E+006
22.17	1.48E+006
28.97	2.20E+006
45.42	7.16E+006
52.88	1.27E+007
70.48	4.20E+007
76.60	5.11E+007
95.18	8.89E+007
167.20	1.59E+008

SC/I8/T2/P3000.S081

Hours	Cells/ml
0.00	3.58E+005
3.17	4.79E+005
21.42	1.30E+006
26.98	2.21E+006
44.87	9.09E+006
51.25	1.47E+007
69.77	4.98E+007
75.70	7.00E+007
145.25	1.50E+008

SC/I10/T2/P2000.S141

Hours	Cells/ml
0.00	1.08E+006
22.18	1.73E+006
28.97	3.25E+006
45.40	1.37E+007
52.87	2.61E+007
70.47	7.79E+007
76.58	1.00E+008
95.17	1.38E+008
167.18	2.15E+008

SC/I8/T2/P6000.S081

Hours	Cells/ml
0.00	3.58E+005
1.38	4.81E+005
21.65	7.16E+005
27.03	5.38E+005
44.93	5.33E+005
51.30	5.66E+005
69.65	6.67E+005
75.75	1.01E+006
145.30	5.96E+005

SC/I10/T2/P5000.S141

Hours	Cells/ml
0.00	1.08E+006
22.15	8.94E+005
29.02	1.01E+006
45.47	1.28E+006
52.92	1.22E+006
70.53	1.46E+006
76.67	1.40E+006
95.22	1.55E+006
167.23	1.71E+006

SC/I8/T2/P5000.S081

Hours	Cells/ml
0.00	3.58E+005
3.35	5.00E+005
21.63	6.47E+005
27.82	8.99E+005
44.92	1.66E+006
51.42	1.76E+006
69.63	2.19E+006
75.73	2.79E+006
145.28	2.77E+006

SC/I8/T2/P4000.S081

Hours	Cells/ml
0.00	3.58E+005
3.18	4.65E+005
21.60	1.05E+006
27.00	1.46E+006
44.90	4.13E+006
51.27	6.79E+006
69.62	2.09E+007
75.72	3.04E+007
145.27	8.84E+007

SC/I8/T2/P1000.S081

Hours	Cells/ml
0.00	3.58E+005
2.97	5.51E+005
21.38	2.42E+006
26.95	3.94E+006
44.85	2.49E+007
51.22	4.29E+007
69.58	1.22E+008
74.27	1.46E+008
145.22	2.35E+008

SC/I8/T2/PATM.S081

Hours	Cells/ml
0.00	3.58E+005
2.95	5.70E+005
21.38	2.91E+006
26.95	5.[illegible]006
44.82	3.24E+007
51.20	5.37E+007
69.57	1.53E+008
74.25	1.64E+008
145.18	2.13E+008

SC/I8/PBT/PATM.S111

Hours	Cells/ml
0.25	2.22E+008
1.85	3.10E+008
3.46	3.74E+008
5.07	4.52E+008
6.66	5.09E+008
8.27	5.04E+008
9.86	6.32E+008
11.48	6.98E+008
13.09	7.99E+008
14.68	8.93E+008
16.29	9.82E+008
17.88	1.07E+009
19.49	9.26E+008

SC/I8/PBT/P6000.S111

Hours	Cells/ml
0.25	1.20E+006
1.85	1.63E+006
3.46	1.10E+006
5.07	1.09E+006
6.66	8.49E+005
8.27	9.62E+005
9.86	1.77E+006
11.48	1.31E+007
13.09	1.36E+008
14.65	6.02E+007

SC/I8/PBT/P3000.S111

Hours	Cells/ml
0.25	2.17E+006
1.85	6.62E+006
3.46	1.10E+008
5.07	6.38E+008
6.66	1.04E+009
8.27	1.25E+009
9.86	1.23E+009
11.48	1.46E+009
13.09	1.29E+009
14.65	1.11E+009
16.29	8.95E+008
17.88	5.37E+008
19.49	5.22E+008

SC/I8/T2/P2000.S081

Hours	Cells/ml
0.00	3.58E+005
2.98	5.08E+005
21.40	1.94E+006
26.97	3.35E+006
44.87	1.74E+007
51.23	3.18E+007
69.60	9.02E+007
74.28	1.08E+008
145.23	2.20E+008

SC/I8/PBT/P5000.S111

Hours	Cells/ml
0.25	1.19E+006
1.85	9.41E+005
3.46	7.86E+005
5.07	1.60E+006
6.66	1.33E+007
8.27	2.75E+008
9.86	4.67E+008
11.48	5.04E+008
13.09	6.12E+008
14.65	4.38E+008
16.29	4.93E+008
17.88	4.00E+008
19.49	3.44E+008

SC/I8/PBT/P4000.S111

Hours	Cells/ml
0.25	1.35E+006
1.85	1.75E+006
3.46	2.51E+007
5.07	4.22E+008
6.66	5.17E+008
8.27	7.63E+008
9.86	7.61E+008
11.48	7.06E+008
13.09	5.97E+008

SC/I8/PBT/P1000.S111

Hours	Cells/ml
0.25	4.98E+006
1.85	9.62E+006
3.46	7.75E+007
5.07	3.61E+008
6.66	9.95E+008
8.27	1.14E+009
9.86	1.10E+009
11.48	1.10E+009
13.09	1.14E+009
14.68	1.01E+009
16.29	9.93E+008
17.88	8.12E+008
19.49	7.61E+008

SC/I8/PBT/P7000.S111

Hours	Cells/ml
0.25	1.02E+006
9.86	8.99E+005
11.48	1.14E+006
13.09	1.58E+006
14.65	7.66E+005
16.29	1.33E+006
17.88	1.20E+006
19.49	1.37E+006

SC/I11/T2/PATM.S281

Hours	Cells/ml
0.00	1.04E+006
21.52	4.73E+006
27.17	8.50E+006
45.25	4.83E+007
50.77	8.64E+007
67.87	1.50E+008
75.33	1.86E+008
93.12	2.07E+008
163.80	2.19E+008

SC/I11/T2/P6000.S281

Hours	Cells/ml
0.00	1.04E+006
21.75	1.20E+006
27.45	1.27E+006
45.50	1.23E+006
50.87	1.31E+006
67.97	1.21E+006
75.42	1.22E+006
93.28	1.20E+006
163.90	1.31E+006

SC/I11/T2/P3000.S281

Hours	Cells/ml
0.00	1.04E+006
21.70	1.95E+006
27.20	3.23E+006
45.30	1.37E+007
50.82	1.92E+007
67.92	6.19E+007
75.37	8.44E+007
93.23	9.14E+007
163.85	1.55E+008

SC/I8/PBT/P2000.S111

Hours	Cells/ml
0.25	4.78E+007
1.85	3.82E+008
3.46	6.36E+008
5.07	7.92E+008
6.66	9.93E+008
8.27	1.04E+009
9.86	1.09E+009
11.48	1.06E+009
13.09	9.86E+008
14.68	9.22E+008
16.29	8.83E+008
17.88	6.72E+008
19.49	5.33E+008

SC/I11/T2/P2000.S281

Hours	Cells/ml
0.00	1.04E+006
21.68	2.80E+006
27.18	4.60E+006
45.27	2.65E+007
50.80	4.22E+007
67.90	9.29E+007
75.35	1.22E+008
93.22	1.58E+008
163.83	1.87E+008

SC/I11/T2/P1000.S281

Hours	Cells/ml
0.00	1.04E+006
21.67	3.79E+006
27.18	6.49E+006
45.27	4.06E+007
50.78	5.23E+007
67.88	1.38E+008
75.35	1.49E+008
93.20	2.11E+008
163.82	1.96E+008

SC/I11/T2/P5000.S281

Hours	Cells/ml
0.00	1.04E+006
21.73	1.16E+006
27.43	1.38E+006
45.48	1.96E+006
50.85	2.40E+006
67.97	2.83E+006
75.40	3.05E+006
93.27	3.30E+006
163.88	4.17E+006

SC/I11/T2/P4000.S281

Hours	Cells/ml
0.00	1.04E+006
21.72	1.43E+006
27.42	1.99E+006
45.47	5.69E+006
50.83	8.14E+006
67.95	2.22E+007
75.38	3.69E+007
93.25	5.21E+007
163.87	7.97E+007

SC/I2/T2/P4000.S211

Hours	Cells/ml
0.00	1.83E+006
22.05	2.15E+006
29.55	3.19E+006
47.25	8.29E+006
54.02	1.22E+007
72.32	3.83E+007
94.88	6.37E+007
168.57	9.00E+007

SC/I2/T2/P3000.S211

Hours	Cells/ml
0.00	1.83E+006
22.05	2.61E+006
29.53	4.70E+006
47.23	1.93E+007
54.00	3.60E+007
72.32	8.42E+007
94.88	1.16E+008

SC/I2/T2/PATM.S211

Hours	Cells/ml
0.00	1.83E+006
21.97	5.16E+006
29.42	1.08E+007
47.18	6.95E+007
53.97	1.02E+008
72.12	1.82E+008
94.87	2.00E+008

SC/I2/T2/P6000.S211

Hours	Cells/ml
0.00	1.83E+006
22.08	1.48E+006
29.58	1.69E+006
47.28	1.74E+006
54.07	1.95E+006
72.37	1.67E+006
94.90	1.85E+006
168.68	2.04E+006

SC/I9/T2/P6000.S081

Hours	Cells/ml
0.00	3.74E+005
3.38	5.48E+005
21.67	6.49E+005
44.93	6.15E+005
44.93	6.15E+005
51.30	5.83E+005
69.67	6.51E+005
75.77	1.09E+006

SC/I2/T2/P5000.S211

Hours	Cells/ml
0.00	1.83E+006
22.07	1.46E+006
29.58	1.78E+006
47.27	2.32E+006
54.05	2.55E+006
72.35	3.57E+006
94.88	4.71E+006
168.58	6.77E+006

SC/I9/T2/P1000.S081

Hours	Cells/ml
0.00	3.74E+005
3.08	6.64E+005
21.40	2.57E+006
26.97	4.93E+006
44.85	4.84E+007
51.23	5.05E+007
69.60	1.41E+008
74.28	1.61E+008
145.22	2.41E+008

SC/I9/T2/PATM.S081

Hours	Cells/ml
0.00	3.74E+005
2.97	7.15E+005
21.38	4.96E+006
26.95	5.46E+006
44.83	3.67E+007
51.22	5.80E+007
69.58	1.51E+008
74.27	1.78E+008
145.20	4.74E+008

SC/I2/T2/P2000.S211

Hours	Cells/ml
0.00	1.83E+006
22.02	3.15E+006
29.45	6.56E+006
47.22	3.71E+007
53.98	6.39E+007
72.17	1.34E+008
94.87	1.85E+008

SC/I2/T2/P1000.S211

Hours	Cells/ml
0.00	1.83E+006
22.00	4.16E+006
29.43	9.11E+006
47.20	5.95E+007
53.98	9.88E+007
72.15	1.82E+008
94.87	2.28E+008

SC/I9/T2/P4000.S081

Hours	Cells/ml
0.00	3.74E+005
3.18	5.63E+005
21.62	1.09E+006
27.02	1.46E+006
44.90	4.48E+006
51.42	6.46E+006
69.63	1.62E+007
75.73	3.07E+007
145.28	8.47E+007

SC/I9/T2/P3000.S081

Hours	Cells/ml
0.00	3.74E+005
3.17	5.84E+005
21.43	1.44E+006
27.00	2.12E+006
44.95	8.82E+006
51.27	1.49E+007
69.78	5.36E+007
75.70	7.51E+007
145.25	1.63E+008

SC/I9/PBT/P3000.S111

Hours	Cells/ml
1.05	2.77E+006
2.66	7.46E+007
4.26	3.43E+008
5.87	8.14E+008
7.45	1.12E+009
9.07	1.12E+009
10.88	1.31E+009
12.29	1.05E+009
13.88	1.15E+009
17.08	8.63E+008
18.70	6.07E+008
20.29	4.40E+008

SC/I9/T2/P2000.S081

Hours	Cells/ml
0.00	3.74E+005
3.02	6.30E+005
21.38	2.01E+006
26.98	3.33E+006
44.87	1.80E+007
51.25	3.42E+007
69.62	9.86E+007
74.30	1.16E+008
145.25	2.49E+008

SC/I9/PBT/P1000.S111

Hours	Cells/ml
1.05	1.89E+007
2.66	9.78E+007
4.26	1.03E+008
5.87	8.67E+008
7.45	1.37E+009
9.07	1.23E+009
10.68	1.32E+009
12.27	1.20E+009
13.88	1.15E+009
15.47	1.17E+009
17.08	1.01E+009
18.70	8.13E+008
20.29	8.92E+008

SC/I9/PBT/P7000.S111

Hours	Cells/ml
1.05	1.10E+006
2.66	1.76E+006
4.26	1.33E+006
5.87	1.06E+006
7.45	1.10E+006
9.07	1.14E+006
10.68	1.60E+006
12.27	1.27E+006
13.88	1.16E+006
15.47	1.52E+006
17.08	1.67E+006
18.70	1.75E+006
20.29	2.08E+006

SC/I9/PBT/P6000.S111

Hours	Cells/ml
1.05	1.59E+006
2.66	1.75E+006
4.26	1.11E+006
5.87	1.10E+006
7.45	9.57E+005
9.07	2.38E+006
10.68	2.70E+006
12.27	4.59E+008
13.88	5.90E+008
15.47	6.25E+008
17.08	1.29E+009
18.70	5.55E+008
20.29	5.11E+008

SC/I9/T2/P5000.S081

Hours	Cells/ml
0.00	3.74E+005
3.37	5.44E+005
21.65	8.04E+005
27.03	1.02E+006
44.92	1.37E+006
51.43	1.50E+006
69.65	1.85E+006
75.75	2.20E+006
145.30	2.09E+006

SC/I9/PBT/P4000.S111

Hours	Cells/ml
1.05	1.67E+006
2.66	3.03E+006
4.26	2.24E+008
5.87	6.04E+008
7.45	5.28E+008
9.07	5.70E+008
10.68	6.94E+008
12.27	6.85E+008
13.88	5.60E+008
15.47	3.26E+008
17.08	4.70E+008
18.70	3.17E+008
20.29	4.24E+008

SC/I9/PBT/PATM.S111

Hours	Cells/ml
1.05	3.07E+008
2.66	3.09E+008
4.26	4.39E+008
5.87	5.13E+008
7.45	5.44E+008
9.07	6.02E+008
10.68	6.53E+008
12.27	6.57E+008
13.88	6.74E+008
15.47	8.67E+008
17.08	9.70E+008
18.70	9.24E+008
20.29	7.77E+008

SC/I3/T2/P3000.0121

Hours	Cells/ml
0.00	8.86E+004
24.27	4.00E+006
29.23	5.69E+006
47.15	2.17E+007
53.42	3.78E+007
71.33	7.41E+007
77.68	9.48E+007
93.83	1.21E+008
167.48	1.79E+008

SC/I9/PBT/P2000.S111

Hours	Cells/ml
1.05	4.38E+007
2.66	5.18E+008
4.26	6.05E+008
5.87	8.64E+008
7.45	9.46E+008
9.07	9.73E+008
10.68	1.03E+009
12.27	1.03E+009
13.88	8.93E+008
15.47	9.22E+008
17.08	7.60E+008
18.70	5.93E+008
20.29	4.34E+008

SC/I3/T2/P6000.0121

Hours	Cells/ml
0.00	8.86E+004
24.32	1.92E+006
29.35	2.23E+006
47.20	1.88E+006
53.47	1.94E+006
71.60	2.01E+006
77.73	2.04E+006
93.88	2.11E+006
167.53	2.48E+006

SC/I9/PBT/P5000.S111

Hours	Cells/ml
1.05	1.36E+006
2.66	1.23E+006
4.26	1.62E+006
5.87	3.43E+006
7.45	1.60E+008
9.07	2.92E+008
10.68	7.28E+008
12.27	7.54E+008
13.88	5.94E+008
15.47	4.22E+008
17.08	4.23E+008
18.70	4.19E+008
20.29	3.11E+008

SC/I3/T2/P5000.0121

Hours	Cells/ml
0.00	8.86E+004
24.30	2.09E+006
29.32	2.32E+006
47.18	3.01E+006
53.45	3.30E+006
71.58	3.73E+006
77.72	4.52E+006
93.87	5.27E+006
167.52	6.77E+006

SC/I3/T2/P4000.0121

Hours	Cells/ml
0.00	8.86E+004
24.28	2.95E+006
29.25	3.75E+006
47.17	8.98E+006
53.43	1.28E+007
71.33	3.72E+007
77.70	5.13E+007
93.85	6.92E+007
167.50	9.23E+007

SC/I3/T2/P1000.0121

Hours	Cells/ml
0.00	8.86E+004
24.23	7.17E+006
29.20	1.16E+007
47.12	5.99E+007
53.38	1.05E+008
71.17	1.63E+008
77.65	1.74E+008
93.80	2.02E+008

SC/I3/T2/PATM.0121

Hours	Cells/ml
0.00	8.86E+004
24.22	7.92E+006
29.18	1.37E+007
47.10	8.07E+007
53.37	1.18E+008
71.32	2.04E+008
77.63	1.92E+008
93.77	1.88E+008

SC/I12/T2/PATM.S281

Hours	Cells/ml
0.00	7.62E+005
21.65	3.63E+006
27.17	6.51E+006
45.25	4.03E+007
50.78	6.46E+007
67.88	1.38E+008
75.33	1.60E+008
93.12	2.16E+008
163.80	2.20E+008

SC/I12/T2/P6000.S281

Hours	Cells/ml
0.00	7.62E+005
21.77	7.03E+005
27.47	7.05E+005
45.52	6.88E+005
50.87	8.27E+005
67.98	7.26E+005
75.43	7.19E+005
93.28	7.61E+005
163.90	7.01E+005

SC/I12/T2/P2000.S281

Hours	Cells/ml
0.00	7.62E+005
21.70	2.06E+006
27.20	3.62E+006
45.28	2.10E+007
50.82	3.52E+007
67.92	8.98E+007
75.37	1.17E+008
93.22	1.62E+008
163.83	2.20E+008

SC/I12/T2/P1000.S281

Hours	Cells/ml
0.00	7.62E+005
21.82	2.84E+006
27.18	4.91E+006
45.27	3.09E+007
50.80	6.41E+007
67.90	1.18E+008
75.35	1.45E+008
93.20	2.17E+008
163.82	2.26E+008

SC/I12/T2/P3000.S281

Hours	Cells/ml
0.00	7.62E+005
21.72	1.51E+006
27.22	2.46E+006
45.30	1.01E+007
50.83	1.68E+007
67.93	5.18E+007
75.38	7.51E+007
93.23	9.90E+007
163.85	1.53E+008

SC/I3/T2/P2000.0121

Hours	Cells/ml
0.00	8.86E+004
24.25	5.58E+006
29.22	8.40E+006
47.13	4.29E+007
53.42	7.22E+007
71.18	1.40E+008
77.67	1.42E+008
93.82	1.70E+008

SC/I12/T2/P5000.S281

Hours	Cells/ml
0.00	7.62E+005
21.75	6.97E+005
27.45	9.16E+005
45.50	1.24E+006
50.85	1.45E+006
67.97	1.64E+006
75.42	1.67E+006
93.27	1.80E+006
163.88	1.72E+006

SC/I12/T2/P4000.S281

Hours	Cells/ml
0.00	7.62E+005
21.73	1.06E+006
27.42	1.63E+006
45.47	4.47E+006
50.83	6.13E+006
67.85	1.52E+007
75.48	2.49E+007
93.28	5.34E+007
163.87	7.35E+007

APPENDIX KK

BIOLOGY OF THE CENTRAL NORTH PACIFIC

Robert R. Hessler and Camilla L. Ingram

Scripps Institution of Oceanography

(Contract #74-1163)

The Biology of the Central North Pacific

Robert R. Hessler and Camilla L. Ingram

Scripps Institution of Oceanography
La Jolla, CA 92093

Sandia Contract No. 74-1163

Program Overview

Assessing the potential of the benthic biological community in the central North Pacific for incorporation of radionuclides requires the determination of the composition, abundances, and functional roles of the fauna. The organisms which compose this community fall into various size or functional groupings which facilitate their study. During the investigations of the past several years, we have concentrated our efforts on particular groups within the benthic community, because of their likely importance in biological transport of radionuclides and the availability of means to obtain and study them. Detailed results from these studies are presented as addenda. A brief summary of the status of our knowledge of the various elements of the benthic community will be given below (Table 1).

We have studied the following groups to varying extents. The nanobiota (procaryote and eucaryote organisms ≈2-50 μm) have been partially characterized for types, volume and distribution within the sediment. The meiofauna (foraminiferans and metazoans ≈50-300 μm and the macrofauna (metazoans ≈300 μm-2 cm) have been adequately characterized for taxonomic category, density, and horizontal and vertical distribution on and in the sediment. Until an actual disposal site is chosen or an in situ experiment planned, it is not necessary to do further research on these groups. Considerable data have been gathered on scavenging amphipods, one group within the highly motile megafauna. We have determined the species composition of this group and many aspects of their behavior and population dynamics. Methods for estimating scavenging amphipod density have been considered, but feasibility study of these ideas awaits future cruises. Next year's research efforts will concentrate on amphipods, because of the high potential these organisms have for transporting radionuclides.

Among the benthic organisms in the central North Pacific, little is known about those on manganese nodules, sessile or slowly motile megafauna (metazoans >2 cm), highly motile megafauna such as fish and organisms which are not scavengers, and epibenthic plankton. A combination of direct sampling and photography should be used to study these groups. A free vehicle camera system for investigating the time course activities of sessile and slowly motile megafauna has been

developed this year. A towed fish/sled stereocamera system has been partially designed, but further development has been deferred due to lack of funds.

In addition to the above work, we have been using a shallow water analog to study the energetics of the type of amphipods which would be of particular importance to radionuclide dispersal and incorporation. A full report on this research is given as an addendum. Due to lack of funds this work has been terminated.

Cruise Participation - RAMA XV

In June 1981, we participated in a cruise organized by Vaughan Bowen to the Aleutian Trench (53^{o}N 163^{o}W, 6400 m) and the Tufts Abyssal Plain (42^{o}N 136^{o}W, 4100 m). The purpose of this cruise was to investigate the origin of a layer of near-bottom water found in the North Pacific which is 2-3 times richer in plutonium than the adjacent water. The reasons for our participation was to obtain amphipod samples to be analyzed by Bowen's group for Pu and compared with previous samples from MPG-I, and to compare the composition of the scavenging amphipod communities.

These samples have been sorted to species and enumerated. The implications from comparisons to MPG-I are very tentative, because only two trap stations were obtained at each RAMA XV locality versus 31 for MPG-I.

The predominant amphipods found at both locations are the same as those found at MPG-I, Paralicella tenuipes, P. caperesca, Orchomene gerulicorbis, and Eurythenes gryllus. Other species were found, including several that were new to us, but these were uncommon.

Eurythenes gryllus, both in the Aleutian Trench and on the Tufts Abyssal Plain, may mature at a smaller size than those found at MPG-I. This is indicated by the size of the largest instars. The largest female found in the Aleutian Trench was a stage 9 female measuring 7.4 cm total body length, which is much smaller than the lower range for this instar at MPG-I (8.1 cm, $\bar{x}$ = 8.6 cm). At the Tufts Abyssal Plain mature females (stage 14) had a size range of 9.5-11.5 cm (n = 6, $\bar{x}$ = 10.4 cm). This compares with a range of 11.5-13.9 cm (n = 4, $\bar{x}$ = 12.7 cm) for MPG-I.

The abundance of E. gryllus both in the Aleutian Trench and at the Tufts Abyssal Plain may be less than at MPG-I. The density of E. gryllus changes vertically above the sediment; therefore, the numbers caught per height cannot be compared directly between areas until the abundance with height is determined for the Aleutian Trench and the

Tufts Abyssal Plain. The height range sampled at both the RAMA XV locations should include the height of peak density, because at MPG-I this height was at 20 m. As may be seen from Table 2, all of the catches from the Aleutian Trench and the Tufts Abyssal Plain are lower than those at MPG-I. Further samples are needed to determine if these populations are indeed less numerous than those at MPG-I.

Polonium 210 and Lead 210 Levels in Amphipods

During the past year we have cooperated with Robin Cherry and Mereille Heyraud at the International Laboratory of Marine Radioactivity in Monaco. They are interested in comparing the levels of ^{210}Po and ^{210}Pb in benthic and pelagic amphipods at various depths to give insights into the vertical flux of materials between the deep-sea and shallower depths.

We have sent them amphipods from MPG-I (Eurythenes gryllus, Paralicella caperesca, P. tenuipes, and Orchomene gerulicorbis, the shallow-water analog Orchomene sp., and the fish Coryphaenoides yaquinae. The analyses for ^{210}Po and ^{210}Pb have been completed on these specimens, and a report on these analyses may be obtained from Robin Cherry or Merielle Heyraud.

Table 1. The status of our knowledge of different groups of benthic organisms found at the MPG-I study area.

	ORGANISM GROUP	STATUS
1.	NANOBIOTA (2-50μm)	PARTIALLY CHARACTERIZED
2.	MEIOFAUNA (50-300μm)	ADEQUATELY CHARACTERIZED FOR NOW
3.	MACROFAUNA (300μm - 2cm)	ADEQUATELY CHARACTERIZED FOR NOW
4.	MANGANESE NODULE FAUNA	NEEDS TO BE INVESTIGATED
5.	SESSILE OR SLOWLY MOTILE FAUNA	NEEDS TO BE INVESTIGATED
6.	HIGHLY MOTILE MEGAFAUNA	AMPHIPOD PORTION PARTIALLY CHARACTERIZED
7.	EPIBENTHIC PLANKTON	NEEDS TO BE INVESTIGATED

APPENDIX LL

DEEP SEA SCAVENGING AMPHIPODS: AN IN SITU MARKING METHOD

C. R. Smith-Zaninovich and T. M. C. Present

Scripps Institution of Oceanography

(Contract #74-1163)

DEEP-SEA SCAVENGING AMPHIPODS: AN IN SITU MARKING METHOD

C. R. Smith-Zaninovich and T. M. C. Present
Marine Biology Research Division, A-002
Scripps Institution of Oceanography
La Jolla, California 92093 U.S.A.

Sandia Contract No. 74-1163

Abstract

Seven vital stains selected from the literature were tested for use in population studies of abyssal scavenging amphipods. Laboratory and field experiments with one sub-littoral and five deep-sea species of amphipods indicate that the stain Fast Green FCF, when administered through food is an appropriate marking agent in terms of (1) label visibility, (2) labeling efficiency, and (3) physiological benignity for time scales up to four weeks. Based on laboratory experiments, Nile Blue A also proves to be an acceptable feeding label for scavenging amphipods on time scales of one week. Field labeling of abyssal amphipods with Fast Green FCF-stained bait demonstrates that feeding stains may be readily used as in situ marking agents for studies of scavengers in remote environments.

Introduction

Demersal lysianassid amphipods comprise a major portion of the abyssal and hadal mobile scavenging fauna, and probably play a significant role in the dynamics of deep benthic communities (Dayton and Hessler, 1972; Paul, 1973; Hessler, 1974; Schulenberger and Hessler, 1974; Isaacs and Schwartzlose, 1975; Hessler *et al.*, 1978; Lipps *et al.*, 1979; Smith *et al.*, 1979; Thurston *et al.*, 1979). Knowledge of the population biology of these animals would increase our general understanding of deep-sea ecology as well as facilitate assessment of the consequences of deep-ocean waste disposal, for these mobile scavengers are potentially important dispersers of radioactive and toxic chemical wastes.

Lysianassid scavengers have proved difficult to study with most deep-sea data collection techniques (i.e., trawling, dredging, coring, survey photography) because of their maneuverability and/or small size (Schulenberger and Hessler, 1974). Consequently, investigations on the population biology of these amphipods are almost exclusively based on baited camera drops and trap collections. Such baited experiments have yielded some population structure and behavioral information (see above references), but as yet, little is known of deep lysianassid dispersal capabilities or population densities. The development of a labeling technique for use *in situ* in conjunction with baited trap experiments might allow analysis of the dispersal and abundance of deep-sea scavenging amphipods through mark and capture methodology.

We have focused on the development of nonradioactive labels, specifically vital stains, because of legal difficulties surrounding the use of radionuclides in international waters. We first conducted a literature survey to identify stains of potential utility (both for lysianassids and other deep-sea invertebrates) and then tested these stains on scavenging amphipods under laboratory and field conditions.

Literature Survey

Past workers have had some success using vital stains or dyes as *in vivo* marking agents (see Arnold, 1966 for a good review for aquatic organisms). As our research goals primarily concern amphipods and because of the relative selectivity of vital stains, the present survey focuses on work on invertebrates, particularly crustaceans.

Three criteria were employed in selecting stains of possible utility for *in situ* deep-sea work: (1) the method of application must be amenable to the rigorous and remote conditions of the deep-sea environment, (2) the stain must be highly visible in the target animal over an appropriate time interval (we have arbitrarily selected greater than four weeks), and (3) the stain must have no discernable effects (either deleterious or advantageous) on the physiology or ecology of the organisms.

In general, four basic techniques have been used in the application of vital stains: injection, tatooing, immersion and feeding (Arnold, 1966). As stain injection and tatooing are impractical for *in situ* deep-sea studies, only those stains administered by one or both of the latter techniques were considered in our survey.

Immersion and feeding stains offer different advantages. An immersion stain would allow the labeling of variable numbers of organisms and might be applied to both mobile epifauna attracted to traps and sessile infauna by way of reasonably unsophisticated deep-sea equipment (e.g., opening and closing traps, box corers left in the sediment for a period of time, etc.).

Stain applied in feeding would allow marking of large numbers of animals, require no special equipment, and be especially effective for organisms that are attracted to bait, such as scavenging amphipods.

Our present work primarily involves several species of scavenging lysianassid amphipods from the abyssal Central North Pacific. As these amphipods are readily collected with baited traps and feed voraciously on fish or cephalopod carcasses (Paul, 1973; Schulenberger and Hessler, 1974; Hessler *et al.*, 1978; Lipps *et al.*, 1979; Thurston, 1979), it seems most practical to mark them through stained bait. This eliminates any need for special equipment required for deep-sea application of immersion stains.

A wide variety of taxa have been successfully dyed by one or more immersion stains. Relatively little effort, however, appears to have been devoted to the isolation of effective feeding stains for invertebrates. Target species, application procedures and labeling success of past workers are summarized in Tables 1 and 2 for immersion and feeding stains used on invertebrates.

We have found no references on the use of vital stains on amphipods. A fair amount of work has been done on crustaceans, especially decapods, however, and we selected seven dyes used with some degree of success for testing on amphipods. These stains are: (1) Fast Green FCF, used as a feeding and immersion stain with marginal success on *Penaeus* spp. by Dawson (1957); (2) Nile Blue A (= Nile Blue Sulfate), an effective immersion stain for asteroids (Loosanoff, 1937; Feder, 1955), penaids (Racek, 1956; Dawson, 1957), and pelecypods (Loosanoff and Davis, 1947); (3) Methyl Violet, a dye employed as an immersion stain on *Crangon vulgaris* (Meyer-Waarden and Tiews, 1965); (4) Neutral Red, successfully administered through immersion on shrimp (Wheeler, 1963), asteroids (Vernon, 1937; Feder, 1955), pelecypods and other invertebrate taxa (Loosanoff and Davis, 1947), and through feeding on portunid crabs (Cargo, 1968); (5) Rose Bengal, a protein stain widely used for labeling protoplasm alive at the time of fixation (Mason and Yevich, 1967) (6) Sudan Black B, a lipid stain fed to carp (*Cyprinus* sp.) by Loeb, Kelly and Stafford (1961); and (7) Trypan Red, used successfully as an immersion and feeding stain on *Penaeus* sp. (Dawson, 1957).

Materials and Methods

Laboratory studies

Laboratory tests of the potential utility of the seven selected dyes as feeding stains for marking deep-sea lysianassids were carried out on a shallow-water analog, Orchomene sp. A. This apparently undescribed scavenger is readily trapped at 40-100 m depths in Scripps Canyon, La Jolla, California (32°52.5'N, 117°15.5'W). Orchomene sp. A is considered an appropriate primary test animal because it is congeneric with amphipods trapped in the central North Pacific (Schulenberger and Hessler, 1974; Schulenberger and Barnard, 1976), is comparable to abyssal species in terms of scavenging feeding strategy (as evinced by baited trap collection) and body size range (0.5-5.0 mm in length), and is easily maintained in laboratory aquaria.

Two Antarctic bathyal species of lysianassid scavengers were also used in testing Fast Green FCF because of their availability and survival capability in aquaria. These were Orchomene plebs (1.0-2.5 cm long) collected with baited traps from 600 m in McMurdo Sound (77°49.2'S, 166°12.9'W), and Orchomene sp. B (cf. rossi), an apparently new species 3.0-5.0 cm long, trapped at 600 m through the Ross Ice Shelf Project (RISP) hole (82°22.5'S, 168°37.5'W; Clough and Hansen, 1979; Lipps et al., 1979; Bruchhausen et al., 1979; Stockton, in press).

Feeding stain tests on Orchomene sp. A were conducted as follows: Ten amphipods were placed in each of 40 open-topped cylindrical, 150 nylon mesh containers (3.5 x 4.5 cm) (Toby Teaboys^{R}, available from Ocean Seismic Survey, Inc., Norwood, New Jersey) held in 5-cm deep acrylic trays. Fresh seawater (5.0°-14.0°C) was kept running across the trays at all times. Animals were allowed to acclimate to the containers for several days, then starved for a week before being exposed to experimental bait. After 24-hour exposure to experimental bait (72 hr for 8% Methyl Violet), amphipods were monitored daily with a hand-held magnifying glass (12 diopters power) and the following data recorded for each container: number live, dead and stained, location and intensity of stain, number of mature females (brooding and nonbrooding), and miscellaneous information (e.g., presence of exuviae). Dead amphipods were removed from experimental containers. Bait consisted of pieces of Pacific mackerel (Scomber japonicus) muscle cut into 125-mm^3 cubes. We prepared experimental bait by immersing mackerel cubes in 20 ml deionized water-stain solution for 15 minutes (except that in one experiment with Sudan Black B, peanut oil was used in place of deionized water as a solvent). The bait was then rinsed at least four times in deionized water and at least three times in seawater to remove excess stain, and fed to the experimental animals. The various concentrations (by weight) of the seven stains tested are presented in Table 3. The concentrations used were generally those with which previous authors had the greatest success. The Trypan Red stain used was manufactured by Gurr, High Wycomb, Bucks, England. All other stains were manufactured by Matheson, Coleman and Bell, Norwood, Ohio. After staining, all

animals except those in starvation experiments were fed weekly with an excess of unstained mackerel muscle. Animals in starvation experiments were not fed after staining, and detrital and fecal material was cleaned from their containers every two days. Control animals were treated identically to experimentals except that bait presented to them was unstained.

Experiments with the two Antarctic Orchomene species were conducted under different conditions. Animals were maintained in large aquaria at approximately -1.0°C and fed chunks of either Trematomas hansoni (for O. plebs) or smelt (for O. sp. B) stained with Fast Green FCF in a manner similar to that previously described for mackerel. The stain concentration used in these experiments was 6% by weight. Orchomene sp. B from RISP were starved for three to five days after collection and exposed to stained bait for 48 hours. Orchomene plebs were presented with stained bait the day following their capture. This labeled bait was available to them for 16 days. Again control animals received unstained bait but were otherwise treated as experimentals.

Field studies

A preliminary mark and capture experiment and two in situ stain testing experiments using Fast Green FCF dyed bait were carried out at abyssal depths in the Central North Pacific to assess the utility of this marking technique in the field. The study sites were located at approximately 31°N and 158-160°W in a water depth of 5800-5900 m.

Free-vehicle systems with flotation packages, polypropylene mooring line, timed and magnesium releases, and disposable descent weights similar to those of Smith et al. (1979) were employed in these studies. In the mark and capture experiment, four 40 cm long mackerel (S. japonicus) were sliced to the vertebral column 10-15 times per side, soaked in a 4% by weight Fast Green FCF-distilled water solution for 15 minutes, and then washed five times in distilled water and five times in seawater. Two of these stained fish were then fastened inside a bottomless half-gallon plastic jug (to prevent excessive rinsing during free vehicle descent) and attached with tarred nylon cord passed around the caudal peduncles to the free vehicle mooring line 21 m above the descent weight. The other two stained mackerel were attached in a similar fashion to the free vehicle mooring line at the level of the descent weight. Four acrylic tube traps, 152 mm diameter by 308 mm height, with screening and a funnel entrance opening of 45 mm on one end, were attached at both 20 m and 1 m above the descent weight. These trapping heights were selected to capture the small, sediment/surface associated amphipod species as well as the larger, higher ranging Eurythenes gryllus. All traps were baited with unstained chopped mackerel placed in 0.5-mm screen jars and set to open by magnesium releases 48 hr after free vehicle deployment. This free vehicle was launched August 22 and recovered August 26, 1978, 94 hr later.

The two *in situ* stain testing experiments also utilized the above mentioned acrylic tube traps. These were each baited with a small piece (3-13 cm^3) of bonito (*Sarda chiliensis*) fillets stained as above with 6% by weight Fast Green FCF and made readily available to incoming organisms (i.e., the bait was not placed in screen jars). Traps in each drop were set at 0 m and 20 m above the bottom and remained open for approximately 6 hr. The first staining-experiment free vehicle was deployed August 10 and recovered 239 hr later on August 20, 1979. The second was deployed August 20 and recovered 162 hr later on August 27, 1979.

Results

Laboratory studies

In evaluating the results of our laboratory tests, we consider four aspects of staining performance: (1) visibility of labeled body regions, (2) staining efficiency, (3) retention time, and (4) staining effects on survivorship. We define staining efficiency as the proportion of experimental animals stained after exposure to marked bait. Stain retention time is the period over which the stained state of a labeled animal is readily visible. This may be estimated directly by considering the time to fading. Most fadings, however, were not directly observed because animals remained in containers until death, rather than being removed at the time of stain fading. Thus, if one individual lost the stain while another died between monitorings, the fading could be detected only through a decrease in the proportion of amphipods stained. This appeared to occur commonly during our experiments and, consequently, it is desirable to assess stain retention time both directly and indirectly through consideration of the percentage of surviving animals stained over time. To the extent that the stain does not affect mortality (see below), one would expect the proportion of stained amphipods in a labeled sample to remain roughly constant over time until fading becomes important or the sample size becomes so small through mortality that each individual makes up a relatively large proportion of the total. With adequate sample size, enough animals should survive to allow the incidence of fading to lead to a declining proportion of labeled amphipods.

Stain visibility and mortality effects were assessed through comparison of experimental with control animals .

Fast Green FCF. Fast Green FCF labeled *Orchomene* sp. A from Scripps Canyon initially exhibited a highly visible bright to dark green coloration in the fore-, mid-, and hindgut, and the hepato-pancreatic caecae. Occasionally mouthparts were also observed to be stained. For a number of hours following staining, green feces were released. Stain concentrations of 8% yielded the darkest, most visible labeling effect, but even 1% concentrations led to an obvious green pigmentation visible to the naked eye. Over time, the body coloration diminished in

intensity, fading first in the fore- and hindguts and lastly in the midgut and hepato-pancreatic caecae.

Amphipods exposed to mackerel soaked in 8% Fast Green FCF stain solution became labeled with high efficiency (87%, see Figure 1). Experiments with lower concentrations, ranging down to 1%, yielded similar results. We detected no male-female or juvenile-adult differences in uptake efficiency.

Retention times using an 8% concentration ranged from 14 to 60 days with a median of 38 days and an average of 35 days (s.d. = 14, N = 23) to fading. Retention of 6% Fast Green FCF ranged from 22 to 96 days, with a median fading time of 46 days and a mean of 55 days (s.d. = 38, N = 3). (It should be noted that although we stained 94 amphipods with 8% and 17 amphipods with 6% solutions, most animals died before losing the stain, leading to the small sample sizes for fading.) At concentrations of Fast Green FCF of 4% to 1%, three individuals faded; these ranged from 46 to 48 days after staining. Neither leaching of stained bait for 24 hours in seawater prior to feeding nor starving of animals after staining appeared to decrease stain retention times (no fadings were recorded with individuals living up to 63 days after stain administration).

Consideration of the proportion of surviving animals stained yields results similar to those from direct fading observations. For experiments using 8% Fast Green FCF and amphipods haphazardly selected from all size classes, the percent of survivors stained began to decline at approximately the 34-day mark and reached a proportion equal to half that of those originally stained after about 54 days (Figure 2). This suggests that fading becomes important approximately 35-40 days following staining. At lower Fast Green FCF concentrations (6-1%), the proportion of survivors stained did not drop substantially until 45 days after labeling. Experiments with 8% concentrations using juveniles and adults separately indicated that juveniles lose stain more rapidly than adults, with fading becoming important 15-20 days following staining (Figure 2).

There is some indication that Orchomene sp. A from Scripps Canyon can retain the green label during at least two instars. In eight instances in which stained amphipods were observed to molt successfully, staining was retained following ecdysis with little or no reduction in labeling intensity.

Marking with Fast Green FCF did not appear to affect Orchomene sp. A mortality. Comparison of control with experimental survivorship for 8%, 6%, 4%, 2%, and 1% concentrations of Fast Green FCF yielded no significant difference at an alpha level of 0.05 (Kolmogorow-Smirnoff two sample test (two-tailed) from Tate and Clelland (1957) yielded probabilities, respectively, of $p>0.20$, $p>0.20$, $p>0.20$, $p = 0.05$, and

p>0.20 with N's of 69, 20, 20, 20 and 20). The nearly "significant" p = 0.05 for the 2% concentration is not of concern when one takes multiple testing into consideration.

There is some evidence, however, suggesting that labeling with this stain at concentrations of 4-8% may inhibit chances of survival during or immediately following ecdysis. In four out of ten instances in which stained amphipods began to molt, individuals survived less than 4 days after ecdysis. All unstained animals observed to molt survived for at least 31 days (N = 3). Both stained and unstained amphipods showed the same maximal post-molt survival periods of about 60 days, however.

A bait preference experiment suggests that mackerel stained with 8% Fast Green FCF is at most slightly less palatable than unstained mackerel to Orchomene sp. A. Seventy-five percent (N = 20) of the amphipods presented simultaneously with stained and unstained bait became labeled. This is not significantly different from the 87% efficiency obtained with stained bait alone (p = 0.109 with percentage test from Sokal and Rohlf [1969]).

Results on Fast Green FCF staining of the two Antarctic species are limited. Twenty Orchomene sp. B collected through the RISP hole were exposed to 6% Fast Green FCF stained smelt for 24 hours. All individuals became labeled (100% staining efficiency) and exhibited a dark green coloration along the entire gut. This was highly visible through the translucent exoskeleton and contrasted strongly with the normal white to orange coloration. In 12 out of 20 marked specimens, the mouthparts, the gnathopods, and the first two pairs of pereopods also stained dark green. Labeled mouthparts and forelimbs lost their coloration rapidly, fading completely in less than three days. Gut staining lasted longer; all 20 individuals retained green coloration in some area of the gut until death 3-4 days after staining. The mortality of stained animals and unstained control animals was similar; all died within four days of stained bait removal from deteriorating aquarium conditions.

Orchomene plebs from McMurdo Sound also stained with 100% efficiency. All 80 marked animals showed highly visible dark green coloration along the entire gut after 16 days with 6% Fast Green FCF labeled Trematomas hansoni. No mortality occurred in either the 10 control or 80 stained amphipods over this period.

Nile Blue A. Twenty Orchomene sp. A exposed to 4% Nile Blue A stained mackerel for 24 hours, became labeled with 100% efficiency. The label initially consisted of highly visible dark to bright green coloration along the entire gut and in the hepato-pancreatic caecae. In addition, 16 of the specimens exhibited light green pigmentation in the basal segments of the first antennae. The intensity of the label diminished over time, with dark or bright green coloration fading to greyish-green before disappearance. The stain tended to be lost first from the foregut and endured the longest in the midgut and hepato-

pancreatic caecae. Times to complete fading of the label ranged from 10 to 22 days after staining, with a median of 14 and a mean of 15 days (s.d. = 4.7, N = 6). Consideration of the proportion of survivors stained over time (Figure 3) also suggests that fading becomes important approximately 14 days after labeling. Starving of animals increased time to fading significantly ($p<0.0005$, one-tailed t-test), yielding a mean of 30 days (s.d. = 4.7, N = 6).

Mortality rates of unstained control and Nile Blue A stained amphipods were not significantly different ($p>0.20$, Kolmogorov-Smirnoff Test, Tate and Clelland, 1957).

Other Stains. The five additional stains tested as feeding labels on Orchomene sp. A exhibited low staining efficiency (Figure 1) and/or rapid fading times (Figure 3 and Table 3). There were no significant differences between survivorship of experimental and control animals, although small sample sizes (N = 20 in all cases) may have prevented detection of actual trends. Table 3 presents further data concerning the performance of these dyes.

Field studies

Upon recovery of the mark-and-capture experiment, it was observed that the stained mackerel at the 21-m level had been stripped to the bone with only the two skeletons remaining fastened to the mooring line (the stained mackerel on the descent weight were not recovered). In the traps at the 1 m level, a total of 691 lysianassid amphipods of six species were captured. Of these, 629 individuals were Orchomene gerulicorbis. Nineteen of these specimens exhibited a light to dark green coloration in the gut region, presumed to have been caused by feeding on stained bait. This coloration was highly visible against the normally whitish body color of these amphipods. Assuming that each amphipod captured in the 1-m traps had an equal chance of becoming stained, the probability that all 19 stained individuals would be O. gerulicorbis is a nonsignificant 0.163. The null hypothesis that all species can become stained with equal efficiency cannot be rejected.

Two traps at the 20 m level on the mooring line, containing an undetermined number of amphipods, were lost during free vehicle recovery. No amphipods were caught in the two remaining traps from this level.

Three species of amphipods, Eurythenes gryllus, Orchomene gerulicorbis and Paralicella caperesca were labeled during the in situ stain-testing experiments. All six intact E. gryllus and the single P. caperesca caught in the traps exhibited a highly visible bright green coloration along the length of the gut (a piece of an E. gryllus individual consisting of the head and first few pereonal segments contained no stain). The green label contrasted sharply with the

normally white to light red body coloration. Sixty-one out of 93 O. gerulicorbis captured in traps with stained bait exhibited light to bright green digestive tracts and mouthparts.

Discussion

The stain, Fast Green FCF, yielded a highly visible mark in all six species (from three genera) of scavenging amphipods stained. It also was taken up with high efficiency ($\geq$ 86%) over a 24-hr period in all species for which this could be calculated. This ability to label animals within such a short time interval makes this stain especially suitable for marking scavengers attracted to bait.

At 1-8% concentrations, Fast Green FCF labeling lasts an average of 35-55 days in our shallow-water analog species, and usually persists through ecdysis. Based on the lower metabolic rates which appear to be characteristic of deep-sea species (Smith and Hessler, 1974; Smith, 1978; Smith, in preparation), we would expect stain retention time to be at least as great in abyssal amphipods and so exceed our desired retention interval of four weeks. Hence, for both shallow and deep-sea lysianassid species, Fast Green FCF could be used to study population phenomena on time scales of days to one month.

Fast Green FCF generally meets our criterion of no discernible physiological effects, although there is a slight indication that staining inhibits molting success. While staining concentrations of 4-8% may decrease the chance of amphipod survival immediately following ecdysis, labeling does not seem to influence the overall mortality of our shallow water analog (no significant differences between survivorship of control and experimental animals). If molting animals indeed suffer differential mortality, one might expect to see discrepancies between experimental and control survivorship curves. The lack of such differences suggests either that (1) molting frequency is not high enough to allow staining to lead to significant mortality differences on the time scale of stain retention (= 96 days) with our sample sizes ($N \leq 69$), or (2) the few incidents of ecdysis for which we can consider stain-mortality effects (10 stained and 3 unstained molts) are anomalous, and labeling does not increase post-molt mortality. In either case, it seems that for labeling experiments on time-scales of up to four weeks and involving hundreds to thousands of individuals of our shallow-water Orchomene sp., the potential mortality effects of Fast Green FCF on molting animals will be small and can generally be ignored. This also is probably true for deep-sea species in which growth rates and molting frequency may be expected to be commensurate with presumptive low metabolic rates (Smith and Hessler, 1974; Smith, 1978; Smith, in press), further mitigating the impact of post-molt mortality on population levels.

We observed no other evidence of physiological or behavioral differences between Fast Green FCF stained experimental and control

animals.

It seems unlikely that staining with Fast Green FCF could affect the ecology of abyssal amphipods as, excluding bioluminescence, their environment is without light. Changes in coloration could affect shallow-water lysianassids, however, by attracting visual predators, for example. The magnitude of such ecological effects associated with staining cannot be evaluated until more is known of the natural history of these organisms.

In conclusion, Fast Green FCF, when administered through labeled food at concentrations of 1-8%, generally meets our acceptance criteria and proves to be a suitable in situ marking agent for scavenging lysianassid amphipods in general and deep-sea species in particular. Because of its high staining efficiency, visibility and palatability, Fast Green FCF has broad utility as an amphipod labeling agent. We are utilizing it not only for in situ population studies, but also in laboratory analyses of amphipod feeding physiology and behavior. It has been particularly useful as a positive indicator of feeding activity for animals at any stage of gut fullness.

Nile Blue A appears to be a suitable short-term in situ marking agent for scavenging lysianassids. Based on laboratory experiments with Orchomene sp. A from Scripps Canyon, 4% Nile Blue A meets all of our deep-sea acceptance criteria except for a minimum four-week label duration. With an average fading time of 14 days, this stain could be used for marking studies spanning days to one week, e.g., time scales relevant to the analysis of diurnal behavior patterns.

The five other feeding stains tested proved unsuitable as in situ labeling agents for lysianassids because of low staining efficiency and/or retention time.

As demonstrated by our labeling experiments in the laboratory and at 5800 m in the Central North Pacific, lysianassid amphipods may be rapidly and effectively marked in situ through use of stained bait. This technique, with the appropriate stain, would no doubt prove effective for other scavenging marine invertebrates as well, including some commercial species such as shrimp and lobsters. Labeling of scavengers with stained bait is particularly appealing for several reasons. It allows in situ marking, thus minimizing the physical and ecological disturbance effects of the marking process on target species. Scavengers in very remote environments, such as the deep-sea or beneath permanent ice shelves, may be labeled nearly as readily as those in accessible habitats. Finally, this labeling technique is very simple, demands little time, requires no special equipment, and is easily executed on shipboard. Thus, we feel that in situ marking with stained bait has broad utility for investigating the population biology of scavengers in a variety of habitats.

Acknowledgments. We thank R. R. Hessler for support and encouragement throughout this research. We are also grateful to B. R. Burnett, R. R. Hessler, C. A. Ingram, G. W. Lopez, J. P. Meador, J. F. Siebenaller and L. J. Snider for help in the field, stimulating discussion and/or critically reading the manuscript. C. D. Ross and K. M. Lingo expertly transformed our rough drafts into final copy. This research was funded under DOE Contract Nos. 05-7898, 13-2564, 13-9950 and 74-1163.

Literature Cited

Arnold, D. E.: Marking fish with dyes and other chemicals. Tech Pap. Bur. Sport Fish. & Wildl. (US) 10, 3-44 (1966)

Bruchhausen, P.M., J. A. Raymond, S. S. Jacobs, A. L. DeVries, E. M. Thorndike and H. H. DeWitt: Fish, crustaceans and the sea floor beneath the Ross Ice Shelf. Science, N.Y. 203, 449-451 (1979)

Cameron, G. R.: The staining of calcium. J. Path. Bact. 33, 929-955 (1930)

Cargo, D. H.: Crabs retain dye from stained food. Md. Tidewat. News 14, 6, 8 (1968)

Clough, J. W. and B. L. Hansen: The Ross Ice Shelf Project. Science, N.Y. 203, 433-434 (1979)

Dawson, C. E.: Studies on the marking of commercial shrimp with biological stains. U.S. Fish Wildl. Serv., Spec. Scient. Rep.-- Fish. 231, 1-24 (1957)

Dayton, P.K. and R. R. Hessler: Role of biological disturbance in mantaining diversity in the deep sea. Deep-Sea Res. 19, 199-208 (1972)

Feder, H. M.: The use of vital stains in marking Pacific coast stafish. Calif. Fish Game 41, 245-246 (1955)

Hessler, R. R.: The structure of deep benthic communities from central oceanic waters. In: The Biology of the Oceanic Pacific, pp. 79-93. Ed. by J. McGowan. Oregon State University Press (1974)

Hessler, R. R., C. L. Ingram, A. A. Yayanos and B. R. Burnett: 1978. Scavenging amphipods from the floor of the Philippine Trench. Deep-Sea Res. 25, 1029-1047 (1978)

Hidu, H. and J. E. Hanks: Vital staining of bivalve mollusc shells with alizarin sodium monosulfate. Proc. Natn. Shellfish Ass. 58, 37-41 (1968)

Isaacs, J. D. and R. A. Schwatzlose: Active animals of the deep-sea floor. Scient. Am. 233, 85-91 (1975)

Lamberts, A. E.: Alizarin deposition by corals. Ph.D. dissertation, Univ. Hawaii, 163 pp (1973)

Lamberts, A. E.: Measurement of alizarin deposition by corals. Proc. Sec. Ann. Coral Reef Symp. 2, 241-244 (1974)

Lipps, J. H., T. E. Ronan, Fr. and T. E. DeLaca: Life beneath the Ross Ice Shelf, Antarctica. Science, N.Y. 203, 447-449 (1979)

Loeb, H. H., W. H. Kelly and K. F. Stafford: Feeding dyes to carp. N.Y. Fish Game J. 8, 151-153 (1961)

Loosanoff, V. L.: Use of nile blue sulfate in marking starfish. Science, N.Y. 85, 412 (1937)

Loosanoff, V. L. and H. C. Davis.: Staining of oyster larvae as a method for studies of their movements and distribution. Science, N.Y. 106, 597-598 (1947)

Mason, W. T. and P. P. Yevich: The use of phloxine B and rose-bengal stains to facilitate benthic sorting. Trans. Amer. micro. Soc. 86, 221-223 (1967)

Meyer-Waarden, P. F. and K. Tiews: Further results of the German shrimp research. Special meeting to consider problems in the exploitation and regulations of fisheries for Crustacea, 1962. Rapp. P.v. Reun. Cons. perm. int. Explor. Mer 156, 131-138 (1965)

Paul, A. Z.: Trapping and recovery of living deep-sea amphipods from the Arctic Ocean floor. Deep-Sea Res. 20, 289-290 (1973)

Racek, A. A.: Penaid prawn fisheries of Australia with special reference to New South Wales. Proc. Indo-Pac. Fish. Counc. 6, 347-359 (1956)

Shulenberger, E. and J. L. Barnard: Amphipods from an abyssal trap set in the North Pacific Gyre. Crustaceana 31, 241-258 (1976)

Shulenberger, E. and R. R. Hessler: Scavenging abyssal benthic amphipods trapped under oligotrophic central North Pacific Gyre Waters. Mar. Biol. 28, 185-187 (1974)

Smith, G. F. D.: Factors limiting distribution and size in the starfish. J. Fish. Res. Bd Can. 5, 84-103 (1940)

Smith, K. L., Jr.: Abyssal amphipods: metabolic adaptation to an episodic food source? Nature, Lond. (in press)

Smith, K. L., Jr.: Metabolism of the abyssopelagic rattail Coryphaenoides armatus measured in situ. Nature, Lond. 274, 362-364 (1978)

Smith, K. L., Jr. and R. R. Hessler: Respiration of benthopelagic fishes: In situ measurements at 1230 m. Science, N.Y. 184, 72-73 (1974)

Smith, K. L., Jr., G. A. White, M. B. Laver, R. R. McConnaughey and J. P. Meador: Free vehicle capture of abyssopelagic animals. Deep-Sea Res. 26A, 57-64 (1979)

Stockton, W. L.: Scavenging amphipods from under the Ross Ice Shelf, at J-9, Antarctica. Deep-Sea Res. (in press)

Swan, E. F.: Some uses of colored materials in marine biological research. Turtox News 39, 290-293 (1961)

Tate, M. W. and R. C. Clelland: Nonparametric and shortcut statistics. Interstate Printers and Publishers, Inc., Danville, Illinois 171 pp. (1957)

Thurston, M. H.: Scavenging abyssal amphipods from the northeast Atlantic Ocean. Mar. Biol.51, 55-68 (1979)

Vernon, A. A.: Starfish stains. Science, N.Y. 86, 64 (1937)

Weber, D. D. and G. J. Ridgeway.: The deposition of tetracycline drugs in bones and scales of fish and its possible use for marking. Progve Fish Cult. 24, 150-155 (1962).

Wheeler, R. S.: Immersion staining of post-larval shrimp. Circ. Fish Wildl. Serv., Wash. 161, 90-91 (1963)

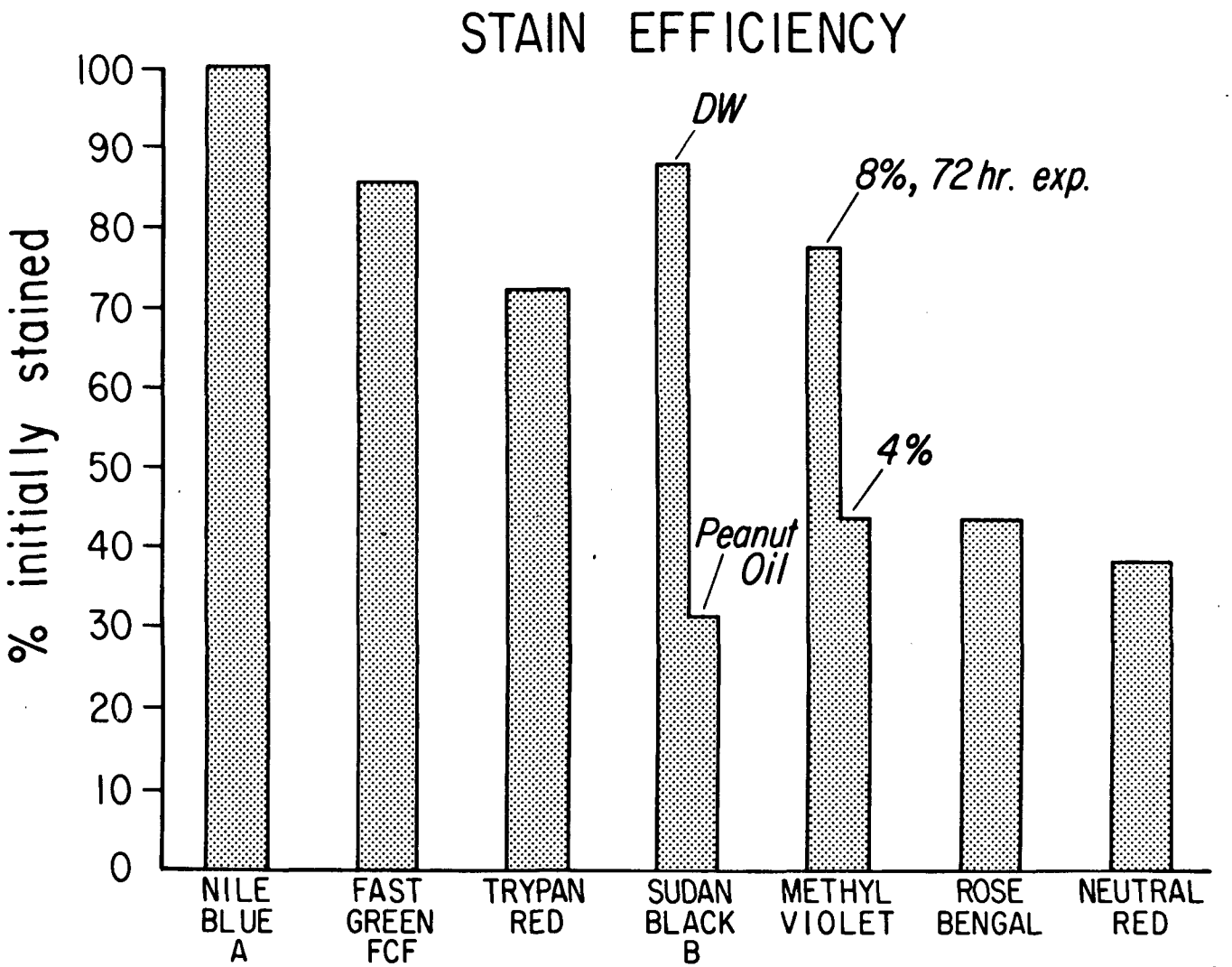

STAIN EFFICIENCY
% initially stained
100
90
80
70
60
50
40
30
20
10
0
DW
8%, 72 hr. exp.
4%
Peanut Oil
NILE BLUE A
FAST GREEN FCF
TRYPAN RED
SUDAN BLACK B
METHYL VIOLET
ROSE BENGAL
NEUTRAL RED

Fig. 1

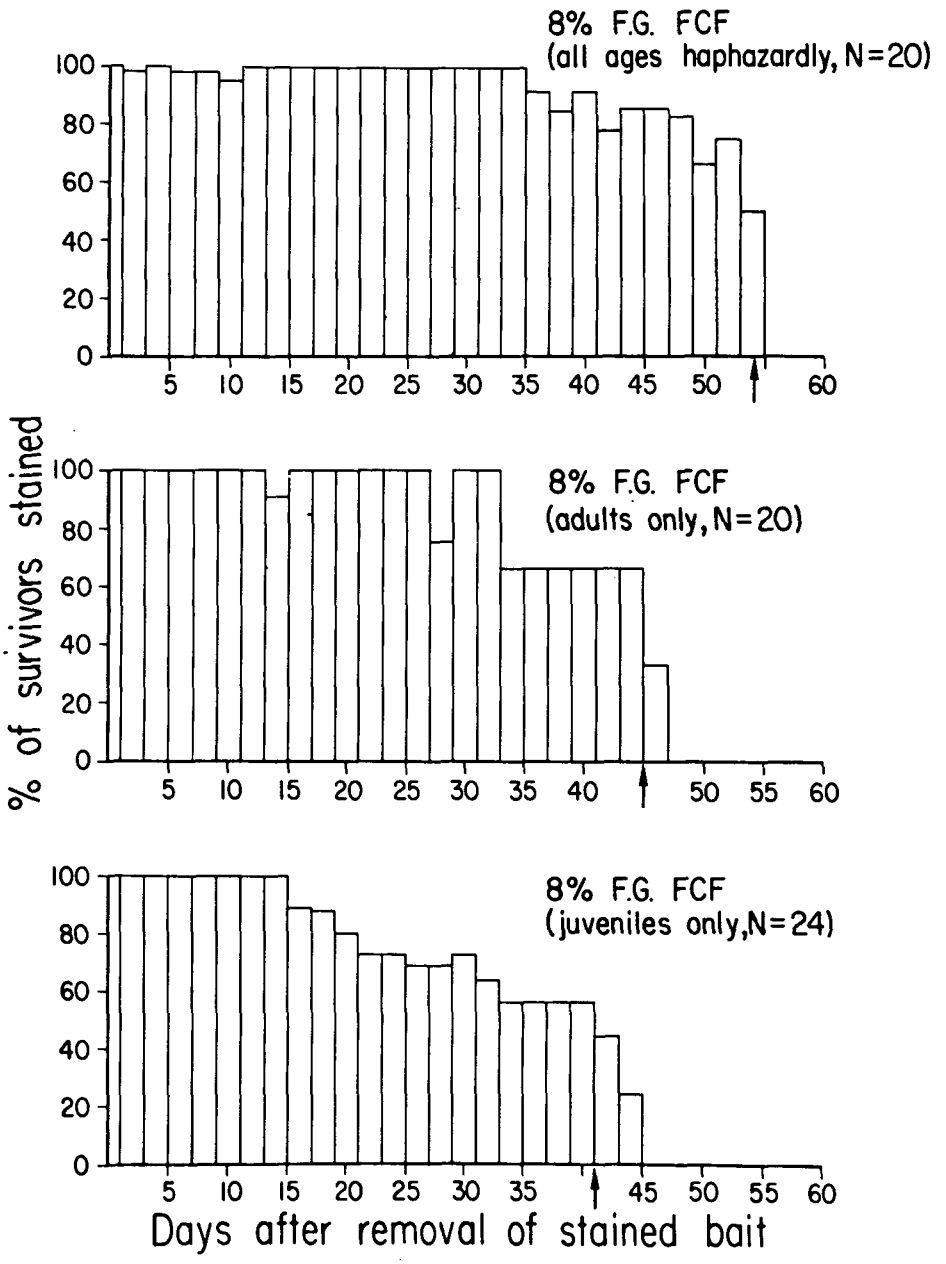

8% F.G. FCF
(all ages haphazardly, N=20)
8% F.G. FCF
(adults only, N=20)
8% F.G. FCF
(juveniles only, N=24)
% of survivors stained
Days after removal of stained bait

Fig. 2

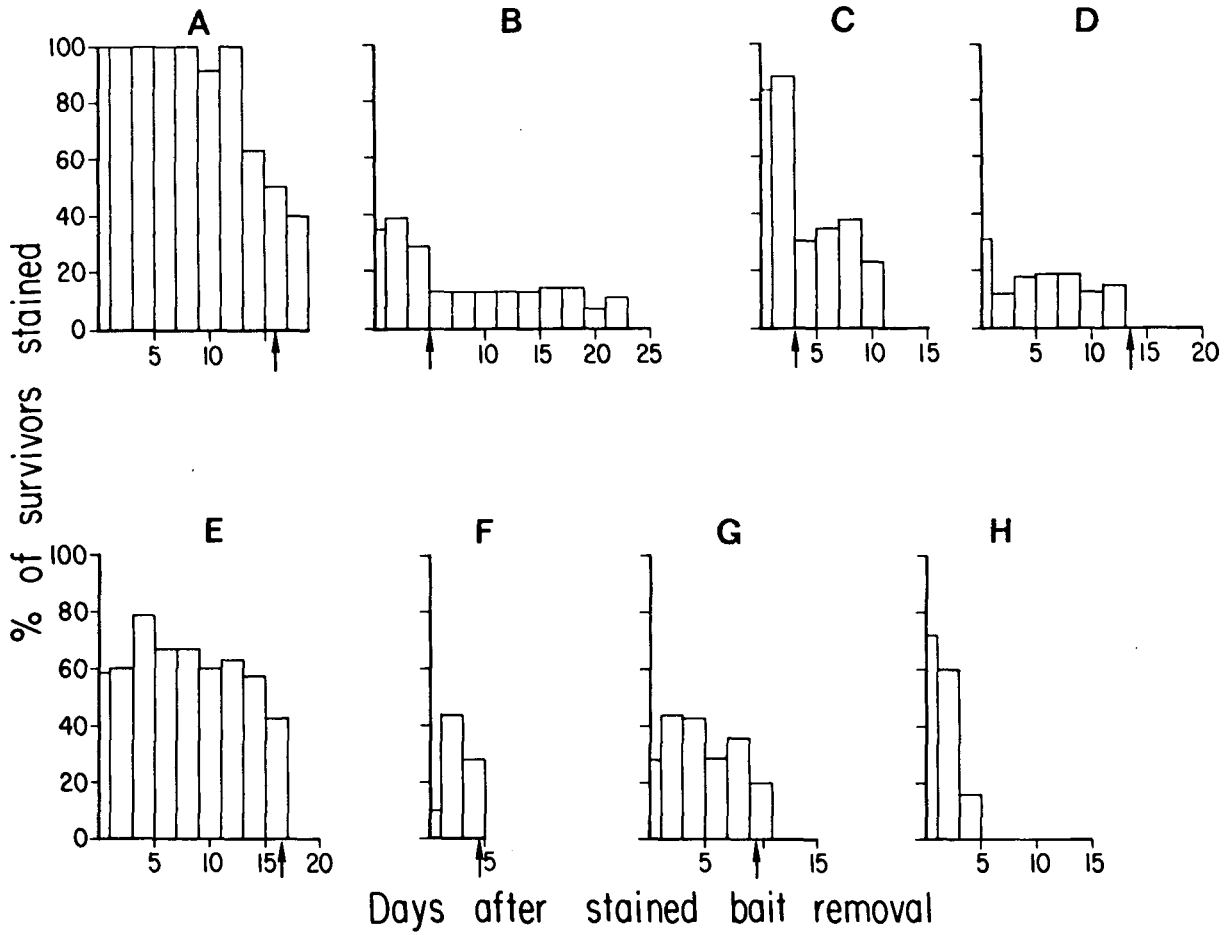

A
B
C
D
E
F
G
H
% of survivors stained
Days after stained bait removal

Fig. 3

Table 1. Alphabetical listing of vital immersion stains and the organism(s) labeled

Stain	Organism(s)	Color and location of stain	Stain retention time	Stain solution	Immersion period	Reference
Alizarin	Echinoids (*Strongylocentrotus* spp.)	Pink inner parts of teeth, ends of spines, tubercles, bases of pedicellaria, sutures	"Long-term"	Supersaturated 9° C seawater	2-4 wk	Swan, 1961
	Gastropods (*Limnaea* sp.)	Growing edge of shell	Not given	≤0.01% in tapwater	2-3 mo	Cameron, 1930
	Anthozoans (10 spp.)	Magenta coloration of coral skeleton	>5 mo	10 ppm SW	24-48 hr	Lamberts, 1973, 1974
Alizarin Red S = Alizarin sodium monosulfate	Penaids (*Penaeus* spp.)	Light pink, general	≤48 hr	0.1% (2.5%DW,SW)	10 min	Dawson, 1957
	Pelecypods (*Mercenaria* and *Mya*, adults and larvae)	Red peripheral and medial areas of shell	≥18 mo	$5\text{-}20\times10^{-4}$% SW (adults) $0.25\text{-}0.75\times10^{-4}$% SW (larvae)	1wk	Hidu and Hanks 1968
Alizarin Blue S	Echinoids (*Strongylocentrotus* spp.)	Blue parts of teeth, ends of spines, tubercles, pedicellaria bases, sutures.	"Long-term" (somewhat toxic)	≤saturation in SW	2-4 wk	Swan, 1961
Basic Brown (=an indeterminant form of Bismarck Brown)	Asteroids	Dark red (general?)	"faded slowly"	0.1% SW(?)	<5 min	Vernon, 1937
Bismarck Brown Y	Penaids (*Penaeus* spp.)	Dark brown branchiae and antennal scales	<48 hr	0.1% (2.5% DW,SW)	15 min	Dawson, 1957
	Polychaetes	Brown (location not specified).	14 days in lab, <48 hr *in situ* (intertidal)	0.1-0.05% in SW	1-2hr	Klawe, 1954
Fast Green FCF	Penaids (*Penaeus* spp.)	Light green in anterior digestive tract, branchiae and parts of exoskeleton	≤6 days	0.75% in SW	15 min	Dawson, 1957
Food Coloring	Postlarval shrimp	Red, blue and green digestive tract	≤ 7 days	100%	10 min	Wheeler, 1963
Janus Green B	Penaids (*Penaeus* spp.)	Blue-black; general, with branchial concentration	"rapid fading"	0.1% SW	10 min	Dawson, 1957
Methyl Green	Penaids (*Penaeus* spp.)	Blue-green cephalothorax, branchiae and abdomen	≤48 hr	0.75% SW	Not given	Dawson, 1957

Methyl Violet B (Gentiana Violet B)	Caridean shrimp (*Crangon vulgaris*)	Eyes as well as other parts	Several weeks (lost at molt)	0.1% FW	3-5 min	Meyer-Waarden and Tiews, 1962
Methylene Blue	Echinoids (*Strongylocentrotus* spp.)	Blue(?) tube feet	Not given (assumed long)	Saturated in SW	10 min	Swan, 1961
Neutral Red	Asteroids:					
	Asterias sp.	Red, apparently general	>4 wk	0.1% SW(?)	<5 min	Vernon, 1937
	Pisaster orchraceus	Deep red orally	≥5 mo	0.1% (dissolved in small volume of DW, then SW)	5-10 min	Feder, 1955
	Pelecypods (*Ostrea virginica* larvae) and crustaceans, ctenophores and "worm larvae" incidentally	Red generally and especially around stomach for *Ostrea* larvae	>10 days	10^{-4}% SW	20 min	Loosanoff and Davis, 1947
	Postlarval shrimp	Dark red digestive tract, light red abdominal tissue	>7 days	0.3% SW	10 min	Wheeler, 1963
Nile Blue Sulfate	Asteroids:					
	Asterias spp.	Very deep blue generally	≤10 mo	0.1% (dissolved in small volume of DW, then SW)	3-5 min	Loosanoff, 1937
	Asterias vulgaris	Not given	≥4 mo	Not given	Not given	Smith, 1940
	Pisaster ochraceus	Blue in spines and oral surface	≤7 mo	0.1% (dissolved of small volume of FW, then SW)	"a few minutes"	Feder, 1955
	Penaids:					
	"prawns"		"a long period"	0.1% (SW)	3-4 min	Racek, 1956
	Penaeus sp.	Dark blue margins of appendages and branchiae	≤4 days	0.1% (1.6% DW, SW)	20 min	Dawson, 1957
	Demosponges (*Cliona celata*)	Deep blue	"several weeks"	Not given	Not given	Loosanoff and Davis, 1947
Purpurin	Echinoids (*Strongylocentrotus* spp.)	Deep red newly deposited calcareous material (inner parts of teeth, ends of spines, surface of tubercules, pedicellariae bases, sutures).	implied as being very long-term	SW beyond saturation	2-4 wk	Swan, 1961
	Serpulid (unidentified)	Red newly deposited tube.	"	"	"	"
	Ophiuroid (*Ophiura sarsi*)	Red regenerating arms.	"	"	"	"
	Pelecypod (*Tapes japonica*)	Red newly deposited shell.	"	"	"	"
	Coralline alga (*Calliarthron regonerans*)	Red terminal portions.	"	"	"	"

Tetracyclines	Salmon (Oncorhynchus nerka)	Fluorescence of skeletal components	10 days	$5.5x10^{-5}$% FW	23-40 hr	Weber and Ridgeway, 1962
Trypan Blue	Penaids ("prawns")	Blue tint	14 days	?	2 min	Racek, 1956
Trypan Red	Penaids (Penaeus sp.)	Red in abdomen and, in one rare (unduplicated) case, in branchiae	≤17 days	1% (10% DW, 90% SW)	4 min	Dawson, 1957

Table 2. Alphabetical listing of vital feeding stains and the organism(s) labeled

Stain	Organism(s)	Color and location of stain	Stain retention time	Staining technique	Reference
Fast Green FCF	Penaids (Penaeus spp.)	Blue stomach and digestive tract	8 days	3 feedings of mullet stained in an 8% SW solution.	Dawson, 1957
Neutral Red	Portunids (Callinectes sp.)	Red ventrally behind mouth	6 wk	Pieces of fish stained dark red and fed to crabs 3 times in 1 wk	Cargo, 1968
Niagara Sky Blue	Penaids (Penaeus sp.)	Dark blue stomach and digestive tract	≤26 days	6 feedings with mullet stained in 1% soln. (10% DW, 90%SW)	Dawson, 1957
Sudan Black B	Cyprinid (Cyprinus sp.)	Dark blue, entire fish except tooth enamel	≥60 days	"Flour baits" stained in 2.7% Sudan Black B soln. fed to fish until "full."	Loeb, Kelly and Stafford, 1961
Trypan Blue	Penaids (Penaeus sp.)	Blue coloration of digestive tract	<3 days	5 feedings of mullet stained in 1% soln. (10% DW, 90% SW)	Dawson, 1957
Trypan Red	Penaids (Penaeus sp.)	Red branchiae	≥233 days	4 feedings of mullet stained in 1% soln. (10% DW, 90% SW)	Dawson, 1957

Table 3. Orchomene sp. A. Concentrations and results of stains tested in the laboratory.

Stain	Concentration by weight and solvent	Color of label and areas stained	Fading time md (days)	Fading time x̄±s.d. (days)	Fading time Range (days)	N	Comments
Methyl Violet	8% DW (72 hr exposure)	Violet in entire gut and hepato-pancreatic caecae; also often in branchiae, dorso-posterior areas of body wall, pleopods and pereopods	12	13±5	6-18	5	18% of stained amphipods showed no label until 2 days after removal of stained bait.
	4% DW	Violet along entire gut; also often in branchiae and dorso-posterior areas of of body wall	4	4±0	4-4	6	75% of stained amphipods showed no label until 2 days after removal of stained bait.
Neutral Red	4% DW	Dark red in entire gut and sometimes in hepato-pancreatic caecae.	6	10±9	4-24	4	29% of stained amphipods showed no label until 2 days after removal of stained bait.
Rose Bengal	2% DW	Red in entire gut and sometimes in hepato-pancreatic caecae.	8	9±3	6-12	4	38% of stained amphipods showed no label until 2 days after stained bait removal.
Sudan Black B	3% DW	Black along entire gut and sometimes in hepato-pancreatic caecae.	4	7±4	4-12	14	27% of stained amphipods showed no label until 2 days after stained bait removal. This stain mixed poorly with water.
	3% Peanut Oil	Black to greenish black along entire gut and sometimes hepato-pancreatic caecae.	2	6±6	2-14	6	
Trypan Red	4% DW	Red along entire gut and often also in hepato-pancreatic caecae.	4	5±2	1-10	20	
Fast Green FCF	8% DW	See text.	38	35±14	14-60	23	See text.
	6% DW	" "	46	55±38	22-96	3	" "
	4% DW	" "	47	47±1	46-48	2	" "
	2% DW	" "	-	-	-	0	" "
	1% DW	" "	46	46±0	46-46	1	" "
Nile Blue A	4% DW	See text.	14	15±5	10-24	6	See text.

APPENDIX MM

FEEDING ACTIVITY AND ENERGETICS IN ORCHOMENE N. SP.: PROJECT SUMMARY

T. M. C. Present and C. Smith-Zaninovich

Scripps Institution of Oceanography

(Contract #74-1163)

FEEDING ACTIVITY AND ENERGETICS IN ORCHOMENE N. SP.: PROJECT SUMMARY

T. M. C. Present and C. Smith-Zaninovich

INTRODUCTION

Feeding activity patterns, gut clearance times, and preliminary estimates of ingestion and egestion rates are presented for Orchomeme n. sp. maintained in experimental chambers and aquaria. (A taxonomic description is currently being prepared by J. Meador and T. Present.)

Orchomene n. sp. is a small (0.5-5.0 mm long), shallow-dwelling, scavenging lysianassid amphipod. It is readily collected throughout the year in baited traps set at 50 m to 100 m in Scripps Canyon head, located approximately 0.6 km offshore of Scripps Institution of Oceanography, La Jolla, California. Due to its convenient collection and easy laboratory maintenance, feeding observations and experiments were undertaken on Orchomene n. sp. as a representative marine scavenging amphipod species.

METHODS

Collection and Maintenance

Experimental animals were collected as needed with baited traps set 0 m to 5 m off the bottom in 50 m to 100 m depths. Traps were retrieved within 24 h of deployment except when inclement weather prevented boat launching. Trapped animals were placed in buckets of chilled and aerated seawater for transport to the lab where they were immediately placed in aquaria equipped with a flow-through seawater system.

Laboratory aquaria were maintained at 9.5°C-14.0°C. Animal survivorship decreased sharply at temperatures above 17.0°C, but feeding, growth, moulting, and reproduction were observed to continue to at least 4.5°C. Animals were briefly exposed (24 h or less) to temperatures as low as 1.5°C without observable ill effects. In situ temperature taken at time and depth of collection using a maximum-minimum thermometer was 11.75°C at 100 m on February 5, 1979, 11.30°C at 85 m on February 16, 1979, and 12.25°C at 50 m on May 4, 1979.

Animals were exposed to approximately the naturally occurring light-dark schedule. They were fed mackerel, bonita, or squid once a week unless experimental protocol dictated otherwise.

Feeding Activity Studies

Two aspects of feeding activity were studied: (1) feeding rhythmicity or the relationship between feeding activity and time of day, and (2) feeding frequency or the time between successive meals in relation to food availability.

Feeding rhythmicity study. Forty similarly sized individuals were placed separately in 150 mesh containers (Toby Teaboys®, available from Ocean Seismic Survey, Inc., Norwood, New Jersey) held in a 5-cm deep acrylic tray. Fresh seawater was kept running across the tray at all times. Animals were not fed for two weeks to standardize their level of feeding readiness. A small piece of mackerel was then added to each container. Animals were monitored every hour for 29 h from bait addition to observe if they were on the bait. Presence on the bait was taken as an indication of feeding. Pilot studies indicated that this assumption is valid. A red light was used to minimize light disturbance when monitoring the animals during the night.

Feeding frequency studies. Two experiments were conducted to characterize feeding frequency. In the initial experiment, 200 similarly sized individuals were placed separately in mesh containers as above. Forty containers were placed in each of 5 acrylic trays in running seawater (9.0°C–14.0°C). Animals were not fed for 10 days to standardize their level of feeding readiness. Mackerel was then added to the containers for 1, 3, 6, 9, or 12 days. It was replaced every 3 days to prevent spoilage and possible food avoidance. After the specified period, the food was replaced with mackerel stained with 6% Fast Green FCF. Animals were monitored daily to determine if they had ingested stained food. Time to staining of an individual represents an estimate of time until feeding following the earlier meal of unstained bait. Stained bait was changed every three days to prevent spoilage. Fast Green FCF stained food is ingested as readily as unstained food by both sexes and all ages, and has no effect on survival (Smith and Present, unpublished data).

Results of this experiment indicated a decrease in feeding frequency after a 12-day exposure to food. A second experiment was then conducted to investigate the effect of longer term exposure to food on feeding frequency. Experimental procedure was as in the initial experiment except seven groups of 35 animals each were used, and seven exposure times to unstained food were tested. Exposure times tested were 1, 3, 6, 9, 12, 15, and 18 days.

Gut Clearance Studies

Three facets of the process of food passage through the gut of Orchomene n. sp. were investigated: (1) gut clearance time, defined as the time it takes for one meal (a full gut of food) to be passed through the gut, (2) the path of food as it passes through the gut, and (3) the effect of food availability on gut clearance time and passage route of food already consumed.

The presence and location of food in the gut can be determined simply by looking through the relatively transparent exoskeleton of the animals. The accuracy of this method was verified by performing sagittal dissections through the guts of several individuals and comparing the location of the food bolus found with its location as determined in the living animal. The visibility of food in the gut can be enhanced by using naturally marked foods such as the dark muscle of mackerel or red salmon meat, or by staining food with inert substances such as carbon or carmine red.

One experiment was designed to investigate the three facets of gut clearance simultaneously. The effects of two extreme levels of food availability, no food and constant excess food, on gut clearance time and food passage path were considered. Fifty adult females were placed separately in mesh containers in a tray of running seawater (11.5°C-13.0°C), fed unstained mackerel for 3 days, and then left unfed for 1 wk to standardize their level of feeding readiness. One-half of the surviving animals were then fed canned red salmon while the remaining half were fed canned red salmon stained with carmine red. After 24 h, all individuals from both groups with full guts (12 fed unstained salmon, 10 fed stained salmon) were placed separately in acid washed experimental chambers filled with 50 ml of double GF/C filtered seawater (11.5°C-13.0°C). The chambers (Fig. 1) were designed to separate animals from any feces they might produce, and also enable an experiment to be conducted in filtered seawater. Unfiltered seawater contains variable amounts of particulate organic matter, as well as larvae, that might be used as food by Orchomene n. sp. Therefore, use of the chambers reduces the availability to the animal of two unquantifiable potential food sources. One-half of the animals in each group were given a small piece of mackerel and were continuously exposed to food for the duration of the experiment. The remaining animals were not exposed to food after being placed in the experimental chambers.

The location of food in the guts of all animals was precisely noted every 4 h for the first 24 h and daily thereafter. The seawater and food were replaced after each check to prevent oxygen depletion and contamination. Monitoring continued until all animals had cleared their initial meal (stained or unstained salmon) or had died. As animals cleared their guts or died, they were rinsed with double-filtered deionized water, dried at 60°C for 12 h, cooled, and weighed.

Gut clearance time was estimated as the time from placement in the

experimental chamber to the observation of a cleared gut. Additional estimates of gut clearance time and the effect of food availability on gut clearance time were provided by data on fecal production through time, following a known amount of ingestion, collected in the ingestion-egestion study discussed below. Gut clearance time was estimated in that study as time from ingestion to the cessation of fecal production. In animals not fed after the initial meal, cessation of fecal production corresponded with the observation of a cleared gut.

Ingestion and Egestion Studies

The small size of Orchomene n. sp., its consequent small ration size, and low level of fecal production present numerous methodological problems in attempts to quantify ingestion and egestion. Considerable time and effort were spent formulating quantitative methods for determining ration size and fecal production of an individual animal. A pilot study employing these methods was then conducted to obtain preliminary ingestion and egestion data for Orchomene n. sp.

Quantification of ration. There are two methods of directly determining ration size or the amount of food ingested by an individual. An animal can consume a known ration in its entirety or available food can be weighed before and after a feeding to determine the ration by difference. The small mouth size of Orchomene n. sp. and its tearing and shredding style of feeding preclude the first and simplest method of ration determination. The second method was employed.

Error may be introduced into estimates obtained by this method in the weighing of the food before and after feeding, and by the possibility that some weight loss or gain of the food may have occurred that is not due to ingestion. Such changes could be due to loss of food that is macerated but not ingested, leaching of food substances into the water, or infiltration of salts from seawater into the food.

Errors in weight determination can be minimized by use of a balance with an appropriate level of accuracy and by standardization of the weighing procedure. A Cahn Electrobalance 2^{R}, accurate to $\pm$0.1 µg, was used for all measurements. All items to be weighed were first dried at 60°C for 12 h and cooled in a desiccator for not more than 48 h.

Choice of a suitable food source can eliminate or reduce errors caused by weight changes in the food not due to ingestion. Squid mantle, stripped of all membranes, cut into 5 mm^2 pieces, and dried at 60°C for 12 h proved to be the best food source in the regard for ingestion studies. Squid, very likely a natural food of Orchomene n. sp., is unlikely to have considerable weight loss due to maceration because of its nonfibrous texture. The use of dried squid of known initial weight enables the calculation of a correction factor for leaching and salt infiltration in seawater through the use of blanks. To reduce variability in the correction factor, all squid was rinsed in double-filtered deionized water to eliminate excess salts before final

drying and weighing. Experimental chambers were also soaked in acid dichromate wash and filled with twice-filtered seawater that was replaced daily to inhibit bacterial growth.

Two independent experiments were conducted to investigate the feasibility of estimating correction factors for the effect of seawater exposure on the dry weight of squid. Both experiments were conducted at 20.0°C–21.0°C. As is evident in Fig. 2, the relationship between squid initial dry weight and its weight after 24-h exposure to seawater in an experimental chamber and redrying is linear and highly significant. The regressions do not differ between the two experiments and the data were combined to calculate the regression given in the figure. Clearly, correction factors can be readily calculated through the use of blanks, and used with confidence in the estimation of ingestion using dried squid as the food source.

Quantification of fecal production. Several methods of quantifying the production of particulate feces by individual animals were tested. These fall into two major categories: (1) filtration of particulate feces from experimental chambers through prepared filters and determination of dry weight or ash-free dry weight by difference from known filter weight, and (2) removal of visible feces by pipette or forceps from experimental chambers onto prepared filters or aluminum boats and determination of dry weight or ash-free dry weight by difference from known filter or boat weight.

In the filtration method, error may be introduced by (1) loss of filter weight due to the filtration process and/or (2) filtration of nonfecal organic (bacteria) and inorganic (salts) material in addition to particulate fecal matter. Efforts were made to minimize these errors by prewashing filters to reduce further filter weight loss, acid washing experimental chambers to inhibit bacterial growth, and rinsing filtered material with double-filtered deionized water to remove excess salts.

Using blanks, estimates were made of the magnitudes of the remaining error terms (filter weight loss, nonfecal organics, inorganic material) and compared to the total quantity of organics filtered from experimental chambers containing one animal producing feces for an 18-h period (Table 1).

Table 1. Comparison of quantities of material filtered from blank (no animal) and experimental (1 animal) chambers.

Quantity measured	n	$\bar{x}$ (mg)	s	$s_{\bar{x}}$	95% confidence limits (mg)
BLANK: sum dry weight effect of filter weight loss, nonfecal organics, inorganic material	14	0.2801	0.1522	0.0407	±0.0879
BLANK: ash-free dry weight of nonfecal organics	14	0.2017	0.0718	0.0192	±0.0415
EXPERIMENTAL: ash-free dry weight of fecal and nonfecal organics	7	0.2329	0.0569	0.0215	±0.0526

The large amount of nonfecal organics coupled with the inherent variability in the quantities of both fecal and nonfecal organics make the filtration method of quantifying particulate fecal production unacceptable.

The direct removal method was used for quantifying particulate fecal production. Care must be taken in using this technique. Significant and inestimable error could be introduced by not collecting all the particulate feces produced. Also, a nonfecal inorganic contribution to the apparent dry weight of the feces must be considered as salts may cling to fecal pellets collected. Methods to minimize these potential errors were developed.

Observations have established that fecal pellets of Orchomene n. sp. are discrete cylindrically shaped entities, do not break apart easily, and maintain their integrity on the scale of hours. These characteristics make them easy to identify and collect with pipette or forceps. Feeding the animals naturally marked or artificially marked food ensures that all fecal pellets present can be detected by microscope survey. Collecting with forceps reduces the nonfecal inorganic error component by reducing the volume of seawater removed with feces. This factor is further reduced by rinsing the fecal pellets with double-filtered deionized water. Feces, after collection and rinsing, were dried at 60°C for 4 h in a predried, preweighed aluminimum boat. The boat was then reweighed and the dry weight of the feces

determined by difference.

Ingestion and egestion pilot study. Thirty adult Orchomene n. sp. were placed separately in mesh containers in a tray of running seawater (14.0°C–14.5°C), fed unstained squid for 1 wk and then left unfed for 1 wk to standardize their level of feeding readiness. During the 1 wk of feeding, the food was changed every 2 days to reduce spoilage and the possibility of food avoidance. Squid mantle was prepared as described previously for use as the experimental food source and preweighed.

The 12 surviving animals were transferred to experimental chambers containing 50 ml double-filtered seawater (14.0°–14.5°C) and one piece of prepared squid. Three chambers containing only seawater and squid served as blanks. At 3, 6, 10, and 24 h into the experiment, feces in each chamber were counted, removed, rinsed, dried, and weighed as described above. After 24 h the squid was removed from all chambers including the blanks, rinsed, dried, and weighed. Initial squid dry weights were corrected for 24-h exposure to seawater using a correction factor calculated from the dry weight change of squid in the three blanks. The final dry weights were then subtracted from the corrected initial dry weights of squid in the experimental chambers to determine dry weight of squid ingested by each animal in 24 h.

In six chambers, the squid was replaced with 6% Fast Green FCF stained mackerel. The remaining six chambers were empty of food. Feces in each chamber were counted and removed daily until unstained fecal production stopped. Egestion was estimated as fecal dry weight per day and number of feces produced per day. Gut clearance time of the ingested food was estimated in animals not fed after the squid ration as the time that fecal production stopped. In animals given stained food, gut clearance time was taken as the time to appearance of stained feces. The sex and dry weight of each experimental animal was determined as soon as it had cleared it squid ration.

RESULTS

Feeding Activity

Feeding rhythmicity. The hourly feeding activities of 40 individuals over a 29-h period are depicted in Fig. 3. Although not fed for 2 wk prior to the beginning of monitoring, nearly 25% or 9 of 40 animals were not observed feeding on offered food. Four of the nonfeeding animals were adult females in reproductive condition as evidenced by the large, well-developed oocytes visible in their ovaries. It should be emphasized that the animals were held in mesh containers, not the glass experimental chambers, and so may have been feeding on organics present in the seawater. All seawater was passed through gravel and cotton to remove large particulates, but some organic matter probably remained in the seawater.

The data indicate a large amount of variability in the timing and

duration of feeding in Orchomene n. sp. Single individuals were observed feeding 0-25 times out of the total of 30 hourly observations (Fig. 4). Reproductive females showed no tendency to feed for more or less time than males or nonreproductive females ($p>0.20$, two-tailed Kolmogorov-Smirnov Two-Sample Test). The median amount of time spent feeding in the 29 h by all animals was 5 h, as estimated by the number of hourly observations of feeding.

Figure 5 summarizes the feeding activities of all individuals through the 29-h period. Considering all animals together, there appears to be a semi-diurnal rhythmicity in feeding activity with peak activity occurring near midnight and a smaller peak in the middle to late afternoon. This rhythmicity in activity is not as evident in reproductive females. Time of feeding in these individuals appears to be more random.

Feeding frequency. The great variability seen among Orchomene n. sp. in the timing and duration of feeding is also evident in meal frequency or, inversely, the time period that elapses between successive meals. Figure 6 depicts the frequencies of times to a successive meal observed after increasing periods of initial exposure to food.

In both experiments, the majority of individuals initially fed for 1, 3, 6, and 9 days resumed feeding on stained food within 24 h. Some individuals, however, did not exhibit this essentially uninterrupted feeding but waited 2-7 days to feed again. For animals initially fed for 1-9 days, time between successive meals does not appear related to the duration of the initial feeding period as the frequency distributions for the two extreme cases, 1 day and 9 days, are not significantly different ($p>0.20$ for both experiments, two-tailed Kolmogorov-Smirnov Two-Sample Test).

The frequency distributions of time between meals in 1-day and 12-day initially fed animals are very different in both experiments. Time to a successive meal is significantly longer in the 12-day groups ($p<0.005$, both experiments, one-tailed Kolmogorov-Smirnov Two-Sample Test) and is also more variable between individuals. With a further increase in initial exposure to food to 15 and 18 days, however, the majority of animals resumed feeding on stained food within 24 h, which was the same as the 1-9 day initially fed groups. The frequency distributions of time between meals are not significantly different between 15-, 18- and 1-day initially fed animals ($p>0.20$, two-tailed Kolmogorov-Smirnov Two-Sample Test).

As is evident in these data, feeding frequency is not clearly related to the length of an animal's previous exposure to food. The repeated demonstration of a significantly longer time to feeding after an initial exposure to food of 12 days suggests that there may be periodicity in feeding behavior or feeding readiness, perhaps associated with some physiological phenomenon.

Gut Clearance Studies

Gut clearance times for all experimental animals range from 6^{+}-9 h to 7^{+}-8 days, as estimated by observation of either a cleared gut or cessation of fecal production. Frequency distributions of observed gut clearance times are presented in Fig. 7. Three observations of unstained red salmon remaining in the gut for longer than 10 days are not considered real, as the red salmon lost its color and was difficult to distinguish in the gut after 7 days.

The median gut clearance time in animals continuously exposed to food appears to be less than that in animals not offered any additional food, regardless of ration. With the sample sizes used, however, there is no significant difference in gut clearance time between fed and unfed animals ($0.10<p<0.20$ for all experiments, two-tailed Mann-Whitney U Test).

Gut clearance time is not different in males and females ($p>0.20$, two-tailed Mann-Whitney U Test) for both fed and unfed animals originally given dried squid. All animals fed stained and unstained salmon were females and so sexual differences in gut clearance times could not be tested.

Figure 8 presents the observed gut clearance times in all experiments in relation to whole animal dry weight. Considering each feeding regime separately, gut clearance time is not significantly correlated to body dry weight. By combining all experiments and both sexes, however, there is a highly significant negative correlation between clearance rate and body dry weight (Spearman rank correlation coefficient, $r_s = -0.5609$, $n = 28$, $0.005>p>0.002$). Unfortunately, larger animals were more numerous in experimental groups continuously exposed to food, while smaller animals predominated in unfed groups. Therefore, it is possible that the significant correlation reflects a food availability effect rather than a body size effect, such as metabolic rate or even possibly food processing rate. Clearance rate is not significantly correlated with body dry weight in animals continuously exposed to food, all experiments considered together (Spearman rank correlation coefficient, $r_s = +0.2216$, $n = 13$, $0.50>p>0.20$) or for animals not fed further food considered together ($r_s = -0.4661$, $n = 15$, $0.10>p>0.05$). In the latter group, however, because the size range of animals is quite large, a larger sample size may have produced a significant negative correlation of clearance rate with body weight.

Monitoring of feces in the ingestion-egestion study enabled estimation of food passage time. This was measured as the time from introduction of the ration to the first appearance of feces (Fig. 9). Food passage times as defined range from 0^{+}-3 h to 10^{+}-24 h. Median passage time is 3^{+}-6 h. There is no significant difference in passage time in animals when food is present or absent ($p>0.20$, two-tailed Mann-Whitney U Test). Food passage rate is not different in males and

females ($0.20>p>0.10$, two-tailed Mann-Whitney U Test). It is also not significantly correlated with body dry weight (Spearman rank correlation coefficient, $r_s = -0.0841$, $n = 22$, $p>>0.5$).

In tracking the path of food through the gut, food was noted as being in the foregut, midgut, hindgut, and/or either hepatopancreatic ceca. Movement of food through the gut qualitatively differed between animals continuously exposed to food and those not exposed to food after their initial meal. The latter group shunt food to the digestive ceca more frequently and sooner after ingestion. In both groups there is transfer of material between the ceca and foregut in both directions. Carmine red may not be a good indicator of food movement through the gut, because food marked with this stain did not appear as frequently in the ceca as did unstained red salmon.

Ingestion-Egestion Pilot Study

Table 2 summarizes the pilot study data. Fecal pellet dry weight is not presented, because seawater was accidentally spilled into the aluminum boats containing the feces to be weighed and so invalidated any fecal weight estimates. The squid dry weight correction factor was calculated from the three blanks run with the experiment. This correction factor was used instead of that calculated previously from much larger sample sizes (Fig. 2), because it is not known what effect temperature has on the correction factor. This pilot study was conducted at $14.0^{\circ}C$–$14.5^{\circ}C$, while the initial correction factor was estimated at $20.0^{\circ}C$–$21.0^{\circ}C$.

The amount of dry squid ingested in 24 h by Orchomene n. sp. individuals ranges from 0.092 mg to 0.477 mg or from 25.63% to 91.55% of the body dry weight. The dry weight of squid ingested in positively correlated with body dry weight (Fig. 10, Spearman rank correlation coefficient, $r_s = +0.6993$, $n = 12$, $0.02>p>0.01$). Ingestion expressed as a proportion of body weight, however, is not significantly correlated with body weight ($r_s = +0.5245$, $N = 12$, $0.10>p>0.05$). Whether this body weight independence of ingestion expressed as proportion of body weight is a real phenomenon or a result of small sample size is unknown.

Fecal pellet production is quite variable between individuals and ranges from 2 to 64 pellets produced from the ingested squid. Fecal pellet production is not correlated with the quantity of squid ingested (Spearman rank correlation coefficient, $r_s = +0.3750$, $n = 11$, $0.50>p>0.20$) or with animal dry weight ($r_s = -0.0659$, $n = 11$, $p>>0.50$).

Males and females did not differ significantly in body dry weight ($p>0.20$, two-tailed Mann-Whitney U Test), in fecal pellet production ($p = 0.10$, two-tailed Mann-Whitney U Test), or in the amount of food ingested expressed as dry weight or as the proportion of body dry weight ($0.10>p>0.05$, two-tailed Mann-Whitney U Test). Females ingested $72.66 \pm 21.85\%$ ($\bar{x} \pm$ 95% C.L., $n = 4$) of their body weight in 24 h; males ingested $46.94 \pm 15.55\%$ ($n = 7$).

SUMMARY AND DISCUSSION

1) Orchomene n. sp. exhibits quite variable feeding activity between individuals. There is a suggestion of feeding rhythmicity with peak activity occurring near midnight and a smaller peak in mid to late afternoon. This rhythmicity in activity is not as evident in reproductive females as in males and nonreproductive females. Unfortunately, monitoring continued for only 29 h so it is impossible to say if the observed pattern is real and if peak activity normally corresponds to midnight or corresponds with some other factor that occurred at midnight in this case. For example, the activity peaks correspond very well with times of maximum tidal current velocities occurring in San Diego that day. If the rhythmicity is real, it is interesting that it persists in animals held in laboratory aquaria for approximately 1 mo.

2) Feeding frequency or time between feedings is also extremely variable in these animals. Time between meals is significantly longer after 12 days of food availability versus shorter term (1-9 days) or longer term (15 and 18 days) food availability. Perhaps Orchomene n. sp. has some 12-day behavioral or physiological cycle that affects feeding activity.

3) Gut clearance times range from 6^{+}-9 h to 7^{+}-8 days. Continuous exposure to food may reduce median gut clearance time but sample sizes were insufficient to demonstrate this. Clearance time may also be negatively correlated with body size. Food passage rate or the time a parcel of food takes to pass through the gut is on the scale of hours. Median passage time is 3^{+}-6 h. Passage time seems to be independent of food availability, sex or body size. Food availability did, however, affect the path of food movement through the gut, at least qualitatively. In animals not exposed to food after an initial feeding as opposed to those continuously exposed to food, ingested food is shunted to digestive ceca more rapidly and in greater amounts. Food also remains in the foregut longer in non-feeding individuals. Since both the foregut and hepatopancreatic ceca probably function in food storage in some capacity in Orchomene n. sp., these observations are not surprising.

4) Despite the small size of Orchomene n. sp., ingestion and egestion can be quantified. Dried squid is a suitable food source because it enables estimation of error factors through the use of blanks. Egestion can be estimated by counting fecal pellets produced and by collection and weighing of fecal pellets.

5) Individual Orchomene n. sp. ingest 25.63%-91.55% of their dry body weight in 24 h. There is a significant positive correlation of the dry weight of squid ingested with body dry weight. Ingestion expressed as a proportion of body weight, however, seems to remain constant with body weight. Females ingest 72.66 $\pm$ 21.85%

($x \pm$ 95% C.L.) of their body dry weight in 24 h; males ingest $46.94 \pm 15.55\%$. Egestion estimated as number of fecal pellets produced is not correlated with the quantity of food ingested and is independent of body size and sex.

Table 2. Data summary from ingestion-egestion pilot study.

Sex	Whole body dry wt (mg)	Dry wt initial squid ration (mg)	Corrected* dry wt of initial ration (mg)	Dry wt of remaining squid (mg)	Dry wt squid ingested in 24 h (mg)	% Body dry wt ingested	Food available after initial meal?	Gut passage time (h)	Gut clearance time (days)	Feces produced from ingested squid (no. pellets)
♂	0.286	8.550	6.056	5.886	0.170	59.44	Y		DIED	
♂	0.459	10.398	7.465	7.296	0.169	36.82	Y	10-24	1-2	8
♂	0.577	10.580	7.604	7.163	0.441	76.43	Y	3-6	2-3	25
♂	0.532	9.841	7.040	6.683	0.357	67.11	Y	<3	1-2	8
♂	0.469	7.407	5.185	5.043	0.142	30.28	Y	6-10	2-3	21
♂	0.425	8.517	6.031	5.850	0.181	42.59	N	3-6	1-2	2
♂	0.349	8.451	5.981	5.853	0.128	36.68	N	3-6	4-5	34
♂	0.359	7.478	5.239	5.147	0.092	25.63	N	3-6	2-3	16
♀	0.555	10.076	7.219	6.858	0.361	65.05	Y	<3	1-2	26
♀	0.521	5.895	4.493	4.016	0.477	91.55	N	3-6	2-3	41
♀	0.383	8.304	5.869	5.587	0.282	73.63	N	3-6	7-8	64
♀	0.394	7.931	5.585	5.347	0.238	60.41	N	<3	2-3	24

*Correction applied: corrected dry wt squid = -0.4605 + 0.7622 (initial dry wt squid)

$n = 3$, $r = 0.9992$, $p<0.05$

$r^2 = 0.9984$

FIGURE CAPTIONS

Figure 1. Experimental chamber used in gut clearance studies and ingestion/egestion pilot study.

Figure 2. Effect of 24-h exposure to seawater on the dry weight of squid pieces. The initial and final dry weight are highly significantly correlated ($p<<0.001; r^2 = 0.9926$); a correction factor can be applied to the final weight of squid to correct for the effect of seawater exposure.

Figure 3. Feeding activities of 39 individual Orchomene n. sp. throughout a 29-h period. Observations were made hourly. ■ indicates the individual was observed on the bait at the time of monitoring. * No feeding observed.

Figure 4. Frequency distribution of the number of times individuals were observed feeding in the 29-h period from 1100, 20 November 1978 to 1600, 21 November 1978. □ males or nonreproductive females; ■ reproductive females.

Figure 5. Frequency distribution of the number of individuals observed feeding throughout a 29-h period. Individuals were not fed for 2 wk prior to the experiment. Mackerel was offered to all animals at 1015, 20 November 1978 and remained available throughout the experiment. Water temperature was 6.0°C. □ males or nonreproductive females; ■ reproductive females.

Figure 6. Frequency distributions of time intervals between successive meals. The interval between successive meals was measured as the time to staining after being initially fed unstained food. □ males or nonreproductive females; ■ reproductive females.

Figure 7. Frequency distributions of observed gut clearance times for animals fed one of three food sources initially, followed by no further food or excess food. * indicates observations that are not considered valid estimates of gut clearance time because unstained red salmon was difficult to distinguish in the gut after 7 days.

Figure 8. Gut clearance times in Orchomene n. sp. in relation to whole body dry weights. Combining data from all experiments, there is a significant negative correlation between gut clearance time and whole body dry weight (Spearman rank correlation coefficient, $r_s = -0.5609$, $n = 28$, $0.005>p>0.002$).

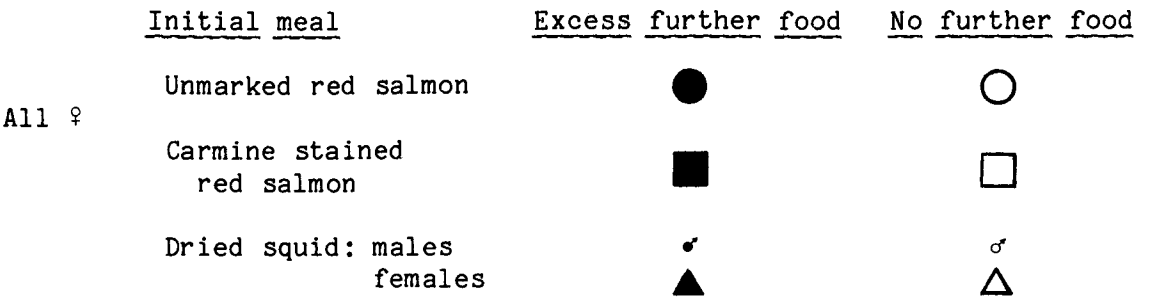


Figure 9. Frequency distribution of food passage times in Orchomene n. sp. with and without food continuously present. ☐ animals fed dried squid and then offered excess food. ▨ animals fed dried squid and then not given any more food.

Figure 10. Ration consumed by Orchomene n. sp. in 24 h compared to the animal's dry weight. A significant positive relationship between the amount of food ingested and the animal's dry weight was found (Spearman rank correlation test, $r_s = 0.6993$, $n = 12$, $0.02>p>0.01$). ○ males; ● females.

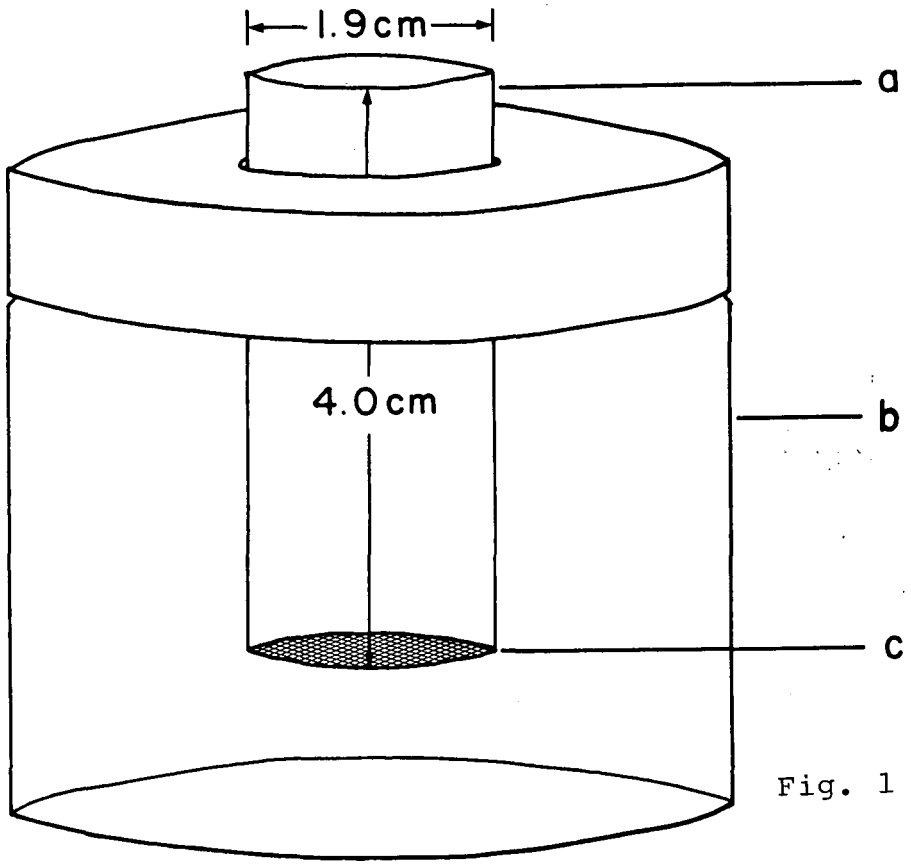

1.9cm
a
4.0cm
b
c

Fig. 1

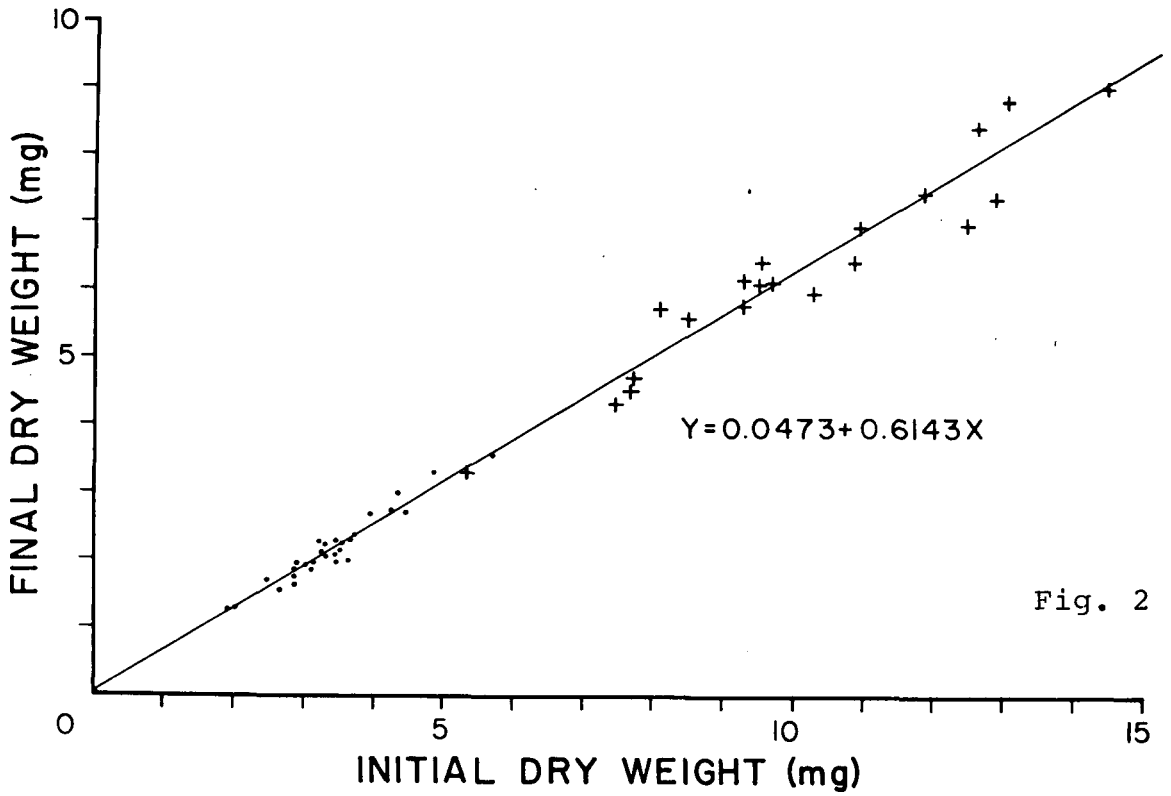

FINAL DRY WEIGHT (mg)
INITIAL DRY WEIGHT (mg)
Y=0.0473+0.6143X
0
5
10
15

Fig. 2

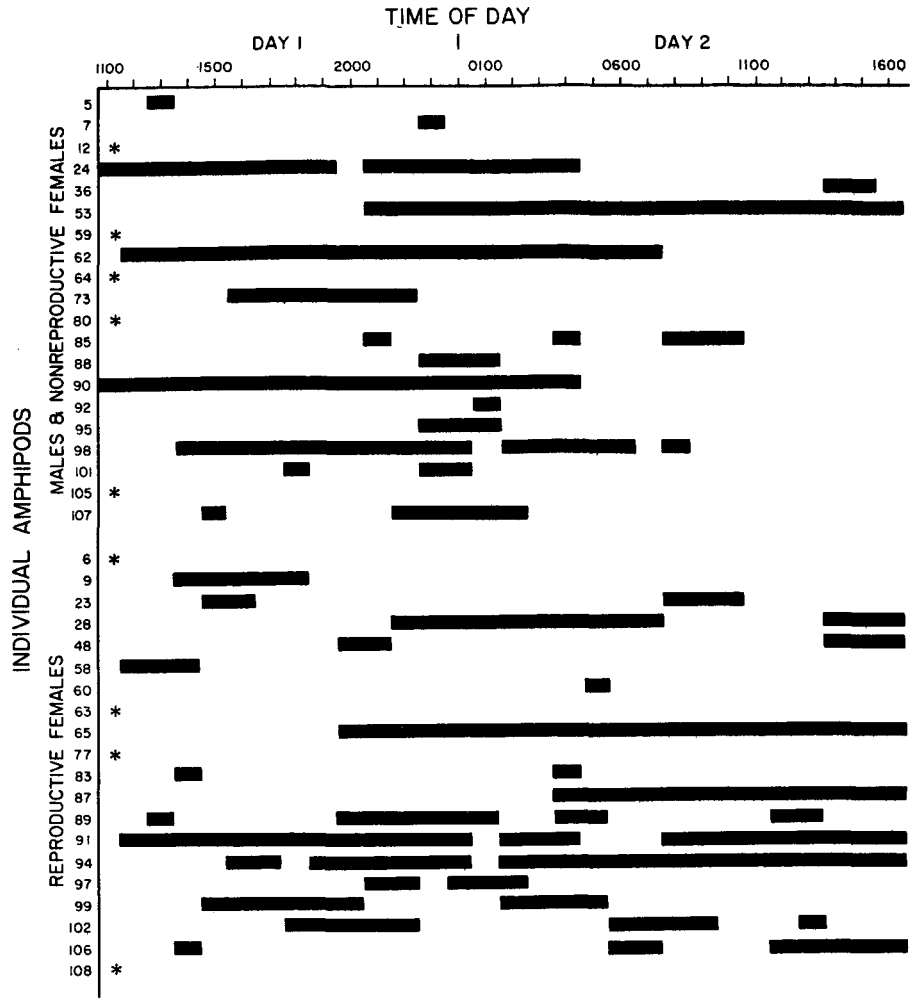

TIME OF DAY
DAY 1
DAY 2
1100
1500
2000
0100
0600
1100
1600
INDIVIDUAL AMPHIPODS
MALES & NONREPRODUCTIVE FEMALES
REPRODUCTIVE FEMALES
5
7
12
24
36
53
59
62
64
73
80
85
88
90
92
95
98
101
105
107
6
9
23
28
48
58
60
63
65
77
83
87
89
91
94
97
99
102
106
108

Fig. 3

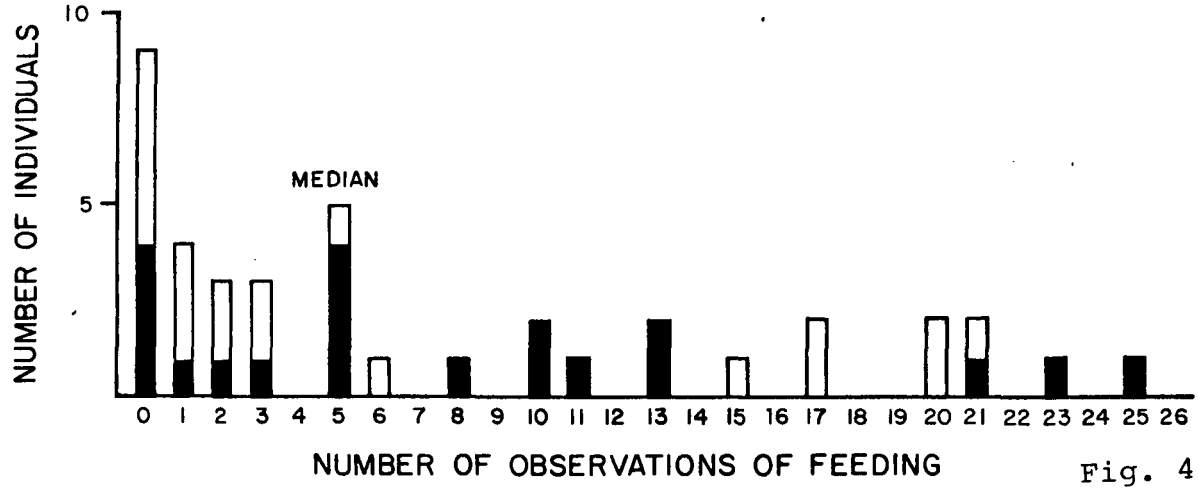

NUMBER OF INDIVIDUALS
10
5
MEDIAN
0 1 2 3 4 5 6 7 8 9 10 11 12 13 14 15 16 17 18 19 20 21 22 23 24 25 26
NUMBER OF OBSERVATIONS OF FEEDING

Fig. 4

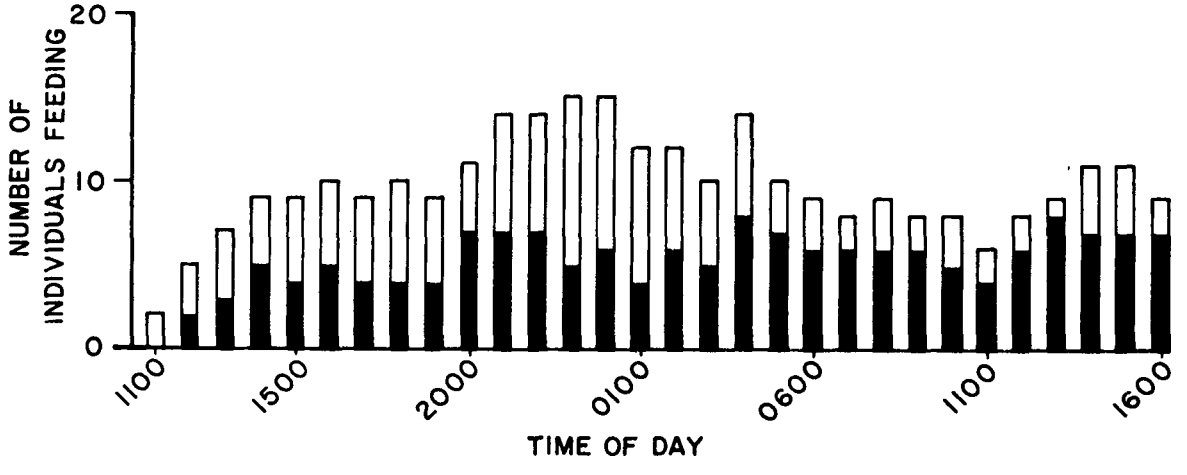

NUMBER OF INDIVIDUALS FEEDING
20
10
0
1100
1500
2000
0100
0600
1100
1600
TIME OF DAY

Fig. 5

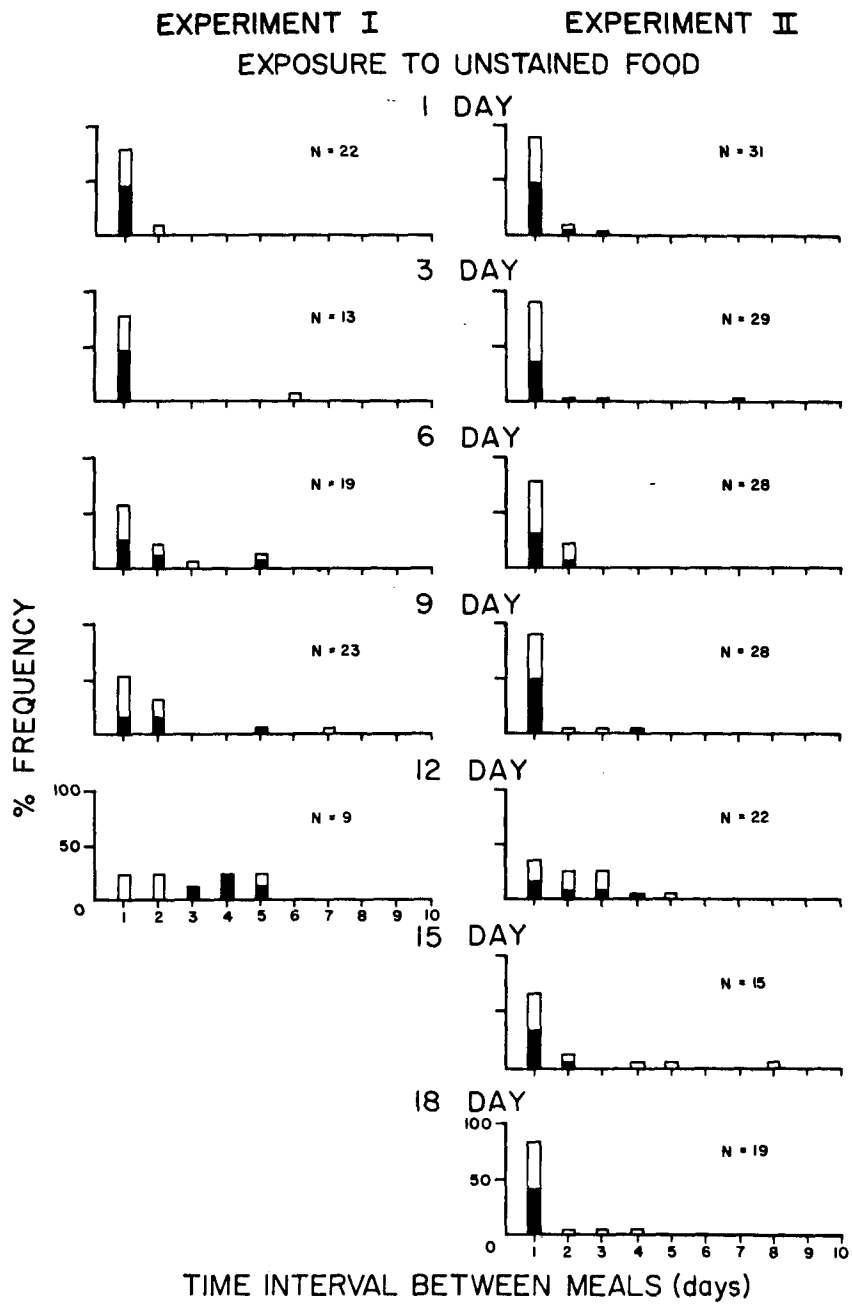

EXPERIMENT I
EXPERIMENT II
EXPOSURE TO UNSTAINED FOOD
1 DAY
N = 22
N = 31
3 DAY
N = 13
N = 29
6 DAY
N = 19
N = 28
9 DAY
N = 23
N = 28
12 DAY
N = 9
N = 22
15 DAY
N = 15
18 DAY
N = 19
% FREQUENCY
100
50
0
1 2 3 4 5 6 7 8 9 10
TIME INTERVAL BETWEEN MEALS (days)

Fig. 6

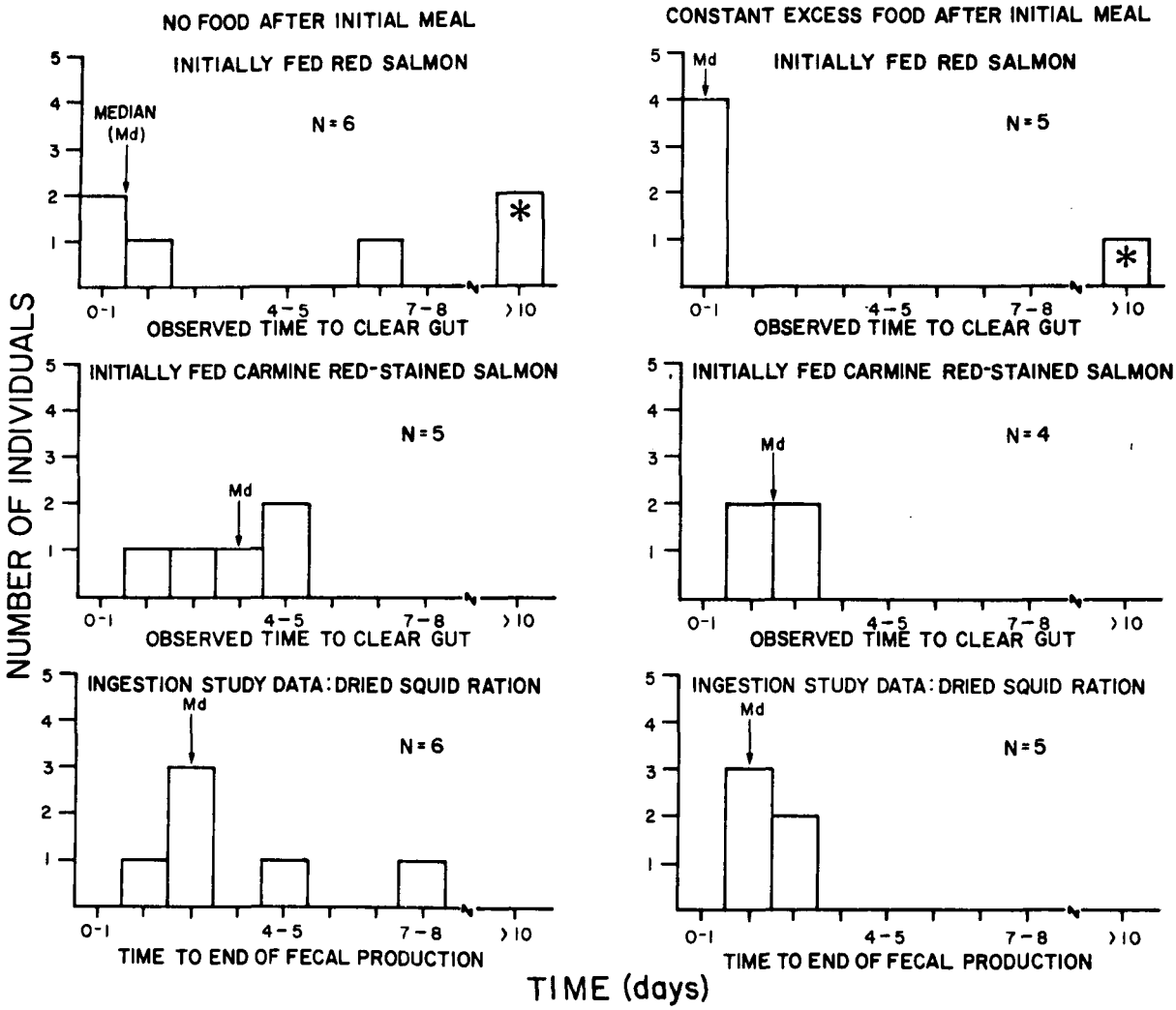

NO FOOD AFTER INITIAL MEAL
INITIALLY FED RED SALMON
MEDIAN (Md)
N=6
OBSERVED TIME TO CLEAR GUT
CONSTANT EXCESS FOOD AFTER INITIAL MEAL
INITIALLY FED RED SALMON
N=5
OBSERVED TIME TO CLEAR GUT
INITIALLY FED CARMINE RED-STAINED SALMON
N=5
OBSERVED TIME TO CLEAR GUT
INITIALLY FED CARMINE RED-STAINED SALMON
N=4
OBSERVED TIME TO CLEAR GUT
INGESTION STUDY DATA: DRIED SQUID RATION
N=6
TIME TO END OF FECAL PRODUCTION
INGESTION STUDY DATA: DRIED SQUID RATION
N=5
TIME TO END OF FECAL PRODUCTION
NUMBER OF INDIVIDUALS
TIME (days)

Fig. 7

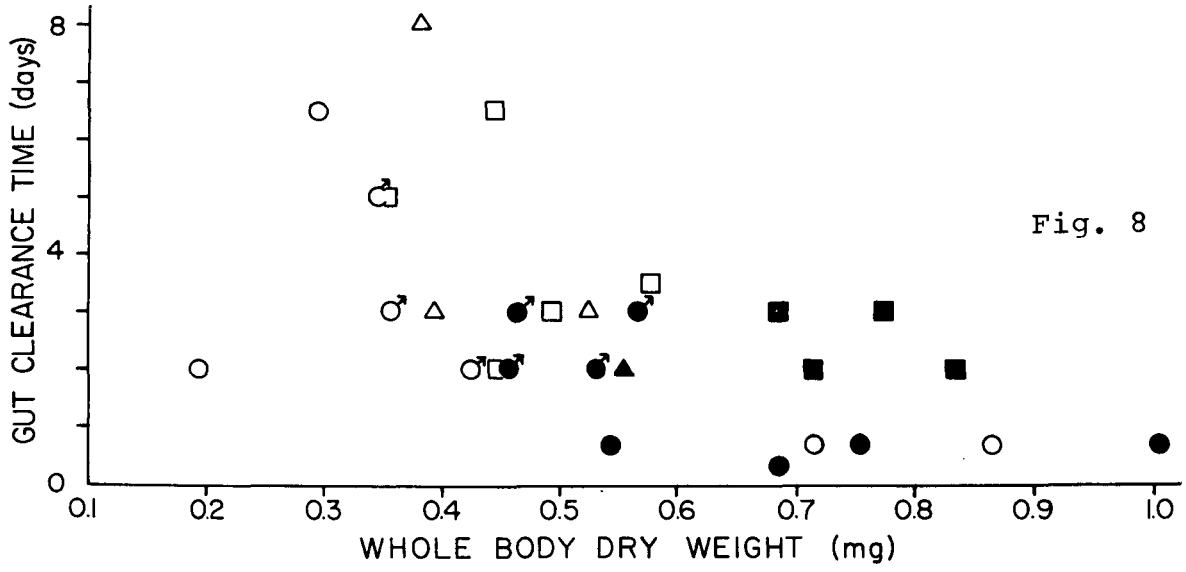

GUT CLEARANCE TIME (days)
WHOLE BODY DRY WEIGHT (mg)

Fig. 8

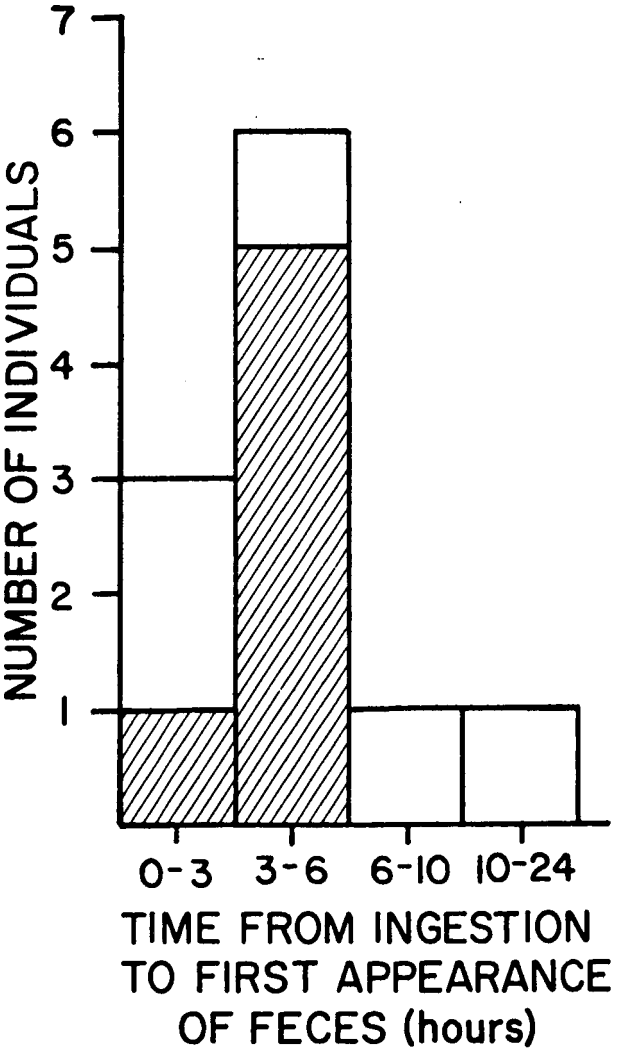

NUMBER OF INDIVIDUALS
7
6
5
4
3
2
1
0-3
3-6
6-10
10-24
TIME FROM INGESTION
TO FIRST APPEARANCE
OF FECES (hours)

Fig. 9

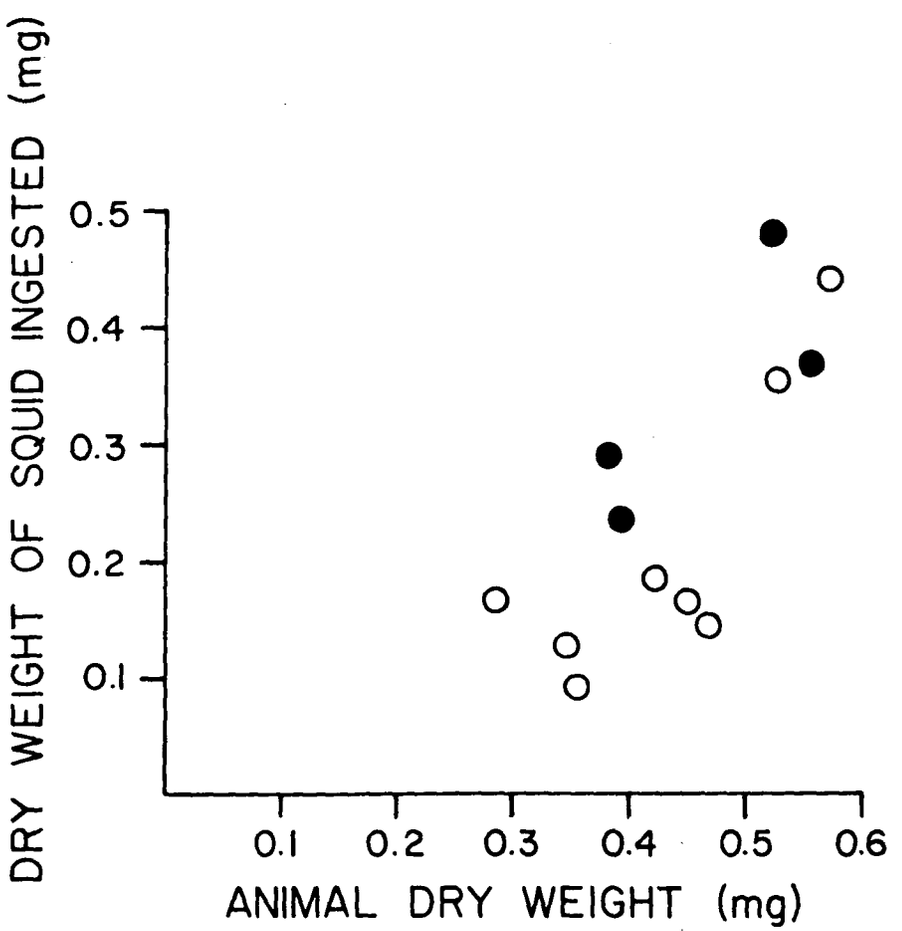

DRY WEIGHT OF SQUID INGESTED (mg)
0.5
0.4
0.3
0.2
0.1
0.1
0.2
0.3
0.4
0.5
0.6
ANIMAL DRY WEIGHT (mg)

Fig. 10

APPENDIX NN

ACTIVITY RATES OF ABYSSAL COMMUNITIES

R. J. Baldwin and K. L. Smith, Jr.

ADDENDUM 1:

Benthic Boundary Layer in the Central and Eastern North Pacific
I. A Chemical and Biological Characterization

K. L. Smith, Jr., M. L. Laver, and N. O. Brown

ADDENDUM 2:

Benthic Boundary Layer in the Central and Eastern North Pacific
II. Sediment Community Oxygen Consumption and Nutrient Exchange

K. L. Smith, Jr. and S. G. Horrigan

ADDENDUM 3:

Scavenging Deep Sea Amphipods: Effects of Food Odor on O_2 Consumption and a Proposed Metabolic Strategy

K. L. Smith, Jr. and R. J. Baldwin

ADDENDUM 4:

Energetics of the Sablefish Anoplopoma fimbria under Laboratory Conditions

K. M. Sullivan and K. L. Smith, Jr.

ADDENDUM 5:

A Comparison of Methods of Age Determination of Coryphaenoides acrolepis (Macrouridae) with a Review of Problems

R. R. Wilson, Jr.

Scripps Institution of Oceanography
(Contract #74-1164)

ACTIVITY RATES OF ABYSSAL COMMUNITIES

R. J. Baldwin and K. L. Smith, Jr.
Scripps Institution of Oceanography
La Jolla, California 92093

Contract #74-1164

ABSTRACT

Our research program is currently directed toward two major aspects of deep ocean ecology: (1) the structure and activity rates of the sediment community and (2) the estimation of abyssopelagic animal populations with determination of metabolic rates for the major animals inhabiting that zone. This research is being conducted on a transect of five stations spanning the central and eastern North Pacific, from the oligotrophic central gyre area to the eutrophic Southern California Continental Borderlands.

Sediment community biomass, abundance, oxygen consumption, organic carbon and total nitrogen increased from west to east corresponding to the increase in surface productivity. Nitrogenous nutrient profiles within and above the sediment are variable, suggesting heterogeneity of the sediments.

Abyssopelagic amphipod populations show denser aggregations on the bottom with bimodal vertical distribution at the deeper stations. Coryphaenoides yaquinae were found exclusively in the deeper western stations and at altitudes up to 1000 m. The shallower water species C. armatus were found exclusively in the bottom water (<100 m) of the easternmost stations.

Energetic and starvation studies on the sablefish Anoplopoma fimbria reveal that slow growth rates, low conversion efficiencies and low metabolic rates may be adjustments to large, infrequent meals. Preliminary studies of vertebral and scale ring count of another deep sea fish, Coryphaenoides acrolepis, imply that seasonally variable growth patterns exist even in an "aseasonal" environment.

B.2.1. Property acquisition and model development for biological uptake and movement of radionuclides in the oceans.

Our research emphasis during the past year has centered on characterizing the structure and determining the metabolic function of both the sediment community and the abyssopelagic animals of the deep-sea benthic boundary layer. The primary impetus of our ongoing study is to formulate a biological transport model based on the above components. The status of this research and its supporting equipment is outlined below.

I. Sediment community

B.2.1.5. Sediment community characterization:

Nitrogenous nutrient profiles (above and below the sediment-water interface), organic carbon, total nitrogen, and macrofaunal abundance and biomass were determined on a transect of five stations spanning the central and eastern North Pacific (Smith, Laver and Brown, Addendum 1). Water samples and undisturbed sediment were collected by the free vehicle grab respirometer, supplemented with bottom water hydrocasts and gravity cores.

Ammonium and nitrite profiles were variable within the sediments as well as in the overlying water column (up to 48 cm). Although nitrate concentrations of the overlying water were more uniform, nitrate was variable in the surface sediments (15-20 cm). Macrofaunal abundance and biomass, organic carbon and total nitrogen increased from west to east along the transect stations, corresponding to the increase in surface primary productivity.

The characterization of this transect and the model for sediment community oxygen consumption (B.2.1.6) were done in conjunction with Task #1 of our proposed research.

B.2.1.6: Sediment community oxygen consumption and nutrient exchange:

Sediment community oxygen consumption (SCOC) and nitrogenous nutrient exchange rates were determined for five transect stations across the central and eastern North Pacific using the FVGR (Smith and Horrigan, Addendum 2). Rate measurements were analyzed at three spatial levels: intergrab (on the order of centimeters), inter-substation (on the order of kilometers), and interstation (on the order of 10^2 km).

Most of the variability in SCOC at interstation and inter-substation levels can be explained by depth and macrofaunal abundance (an indicator of surface primary productivity). Analysis of these benthic boundary layer parameters allowed us to formulate a predictive equation for sediment community oxygen consumption. Nitrogenous nutrient flux rates are variable along the transect with no east to west trend. Much of the variability was due to temporal and spatial heterogeneity of the sediments.

II. Abyssopelagic fauna

B.2.1.7. Abyssopelagic animal distribution:

A variety of traps with intermittent hooks were attached to free vehicle mooring lines for sampling the large mobile scavengers attracted to bait odor (Smith and Baldwin, Addendum 3). Lines were set at altitudes up to 1800 m at 74 substations representing five

major stations along a transect of the central and eastern North Pacific.

The numerically dominant amphipod at all stations was Eurythenes gryllus. This lysianassid scavenger, caught at altitudes up to 1700 m, was trapped at higher altitudes in the western side of the transect, with dense bottom aggregations and increasing vertical bimodal distribution toward the west. Seasonal variation in amphipods caught per fishing day was more pronounced in the shallower water stations.

Similar spatial variation was noticed in the rattail species with Coryphaenoides yaquinae (central North Pacific) caught higher in the water column than the C. armatus (eastern N. Pacific). However, seasonal variability of the rattails was noted throughout the transect.

B.2.1.8. Energetics of the sablefish Anoplopoma fimbria:

To further our investigation of abyssopelagic animal metabolism (Task #3), we measured the energetics of the sablefish Anoplopoma fimbria under varying diet conditions in the laboratory (Sullivan and Smith, Addendum 4). Respiration, growth, ingestion and excretion rates were determined on laboratory specimens; water, protein and lipid content of white skeletal muscle were measured in both laboratory held and field fish.

Sablefish fed a large ration (14% of wet body weight) grew 2 to 3 times faster than those fed a reduced portion (4% of wet body weight). Although growth rates of the fish on the reduced diet was similar to growth rates reported for natural populations, the white muscle composition varied considerably.

Laboratory measurements of respiration and excretion rates indicate that sablefish have approximately 162 days of energy stored in body lipids. Energy allocation shows very slow growth rates, low conversion efficiences, and low metabolic rates as adjustments made to large, infrequent meals.

B.2.1.9. Vertebral and scale ring count as indicators of growth in Coryphaenoides acrolepis

Growth as a component of abyssopelagic animal metabolism (Task #3) is currently being investigated for the ubiquitous deep-sea rattail Coryphaenoides acrolepis (Wilson, Addendum 5). Vertebral and scale ring count are both found to be good indicators of fish length with vertebral ring count slightly more reliable in this species. Cyclic patterns of growth (on the order of one year) indicate that seasonally variable growth-influencing factors are operating in the abyssal environment.

Addendum 1

Benthic boundary layer in the central and eastern North Pacific I. A chemical and biological characterization

K. L. Smith, Jr., M. B. Laver and N. O. Brown

Submitted to Deep-Sea Research

Benthic boundary layer in the central and eastern North Pacific. I. A chemical and biological characterization

K. L. Smith, Jr., M. B. Laver and N. O. Brown

Marine Biology Research Division, A-002

Scripps Institution of Oceanography,

La Jolla, CA 92093

ABSTRACT

Nitrogenous nutrient profiles immediately above and below the sediment-water interface as well as sediment organic carbon, total nitrogen, and macrofaunal abundance and biomass were evaluated on a transect of 5 stations across the central and eastern North Pacific. This transect extended from the central gyre area north of Hawaii to the Santa Catalina Basin off the southern California coast. A free vehicle grab respirometer was used to collect nutrient water samples at close intervals from 48 cm above to 15-20 cm below the sediment-water interface. This free vehicle was also used to recover undisturbed sediment samples for macrofaunal and organic carbon and total nitrogen analyses. Bottom water hydrocasts and gravity cores supplemented the free vehicle samples. Ammonium and nitrite profiles above the sediment-water interface revealed considerable variability up to 48 cm at all stations and were distinctly different from bottom water hydrocast samples taken at 2 m altitude. Nitrate profiles were more uniform. Sediment nutrients, organic carbon and total nitrogen profiles were also erratic in these oxygenated surface sediments (15-20 cm) suggesting the heterogeneity of the sediments and of the overlapping reactions occurring in the diagenesis of organic matter. Macrofaunal abundance and biomass, and surface organic carbon and total nitrogen increased from west to east, with a trend towards larger animals at the eastern stations. These longitudinal gradients from west to east, corresponded to increasing surface primary productivity.

INTRODUCTION

Over the past several years, we have been measuring the sediment community oxygen consumption and nutrient exchange rates at abyssal and bathyal depths along a transect in the central and eastern North Pacific. The original intent of this study was to compare the observed *in situ* rate measurements with the annual primary productivity of the surface waters. Surface productivity changes considerably from the oligotrophic central gyre region to the more eutrophic areas in the eastern boundary current region off southern California.

Based on some of our initial sampling and rate measurements in these areas, we became increasingly aware of the high intra- and inter-station variability (Smith, White, Laver and Haugsness, 1978; Smith, White and Laver, 1979). We began developing new and modified instrumentation to provide more accurate and precise sampling and analyses of the sediments and the water immediately above the sediment-water interface in pursuit of information which might shed light on the causes of this variability.

Our intent, in this first of three papers on the investigation of the benthic boundary layer communities along the North Pacific transect, is to define the biological and chemical parameters which characterize the deep-sea benthic boundary layer. We present data to 1) characterize the water and sediments at each transect station, and 2) discuss and compare the methodology used in sampling this boundary layer.

METHODS

Undisturbed sediment samples and water profiles immediately above the sediment-water interface were taken with a free-vehicle grab respirometer (FVGR) (Smith and Baldwin, 1981; Smith et al., 1979). In addition, bottom-water hydrocasts were taken in the immediate vicinity of the FVGR deployments. A gravity corer was used at several of the stations to corroborate data from the FVGR sediments.

Sediment sampling and analyses

The FVGR consists of an aluminum tripod (2.4 m high, 2.7 m at the base) with a flotation package (net buoyancy 250 kg) mounted atop the frame. Four open-topped stainless-steel modified Ekman grabs (20.3 x 20.3 x 30 cm each) are mounted on a tray which is located in the center of the tripod. This tray is held above the sediment by two hydrostatic plungers. Another tray, which comprises the tops of the grab chambers, is suspended above the first by an acoustic release. After the FVGR reaches the bottom and a sufficient amount of time (about 1 hr) has elapsed to allow any disturbed sediment to dissipate, the grabs are slowly driven into the sediment to a depth of about 15 cm by the electronically actuated plungers. The separation of the top and bottom trays prevents a bow-wave effect. The top tray is then released by acoustic command, sealing to the grab chambers on silicone gaskets which border the top of each grab. Both top and bottom assemblies travel on four guide rods. After incubation of one to four days the grab closures are actuated by an electronic timer, and a second acoustic command releases the descent weights (3 x 99 kg) allowing the FVGR to return to the surface. Winnowing of the sediment as the FVGR ascends (50-55 m min^{-1}) is prevented by the chambers being completely sealed. The water overlying the sediment is usually clear

with considerable undisturbed detail observable on the sediment surface. Gravity cores (5 cm x 1.8 m length) with liner and core catcher were also taken at the FVGR deployment sites.

Immediately after the FVGR has been secured on deck, the top-water is siphoned off the sediment and two subcores taken from one of the four-grab samples. The first core is promptly frozen for onshore CHN and particle size analyses. The second is sectioned at 1-cm intervals for the top 5 cm and at 2-cm intervals for the remainder of the core. The subsections are then pressure filtered and 2-3 ml of the filtrate diluted to 40 ml with surface seawater for pore water ammonium, nitrate and nitrite content (Kalil and Goldhaber, 1973). All sectioning and squeezing is carried out at 2-4°C in a cold van, with samples kept on ice prior to analyses (3-4 h). Analysis of ammonium and nitrite follow methods of Strickland and Parsons (1972) using triplicate 5.0 ml sample volumes and scaling down reagent aliquots proportionately. Filtered surface seawater and distilled-deionized water serve as ammonium blanks. Nitrate is analyzed by the copper-coated cadmium wire method of Gardner, Wynne and Dunstan (1976). A 10.0-ml sample is reduced to four 2.0-ml replicates to which are added 0.05 ml each nitrite reagents (double strength).

The three remaining grab samples are elutriated with surface seawater which has been filtered (Teel Coldwater Filter®, exclusion approximately 10 μm) and sieved through 425 and 300 μm screens. The sieved samples are preserved in 10% buffered formalin. On shore, the samples are transferred to 95% ethanol and sorted to major taxa. Although the sieving water was filtered, we routinely found contamination by surface organisms in our samples (planktonic copepods, cyprid and decapod larvae, and chaetognaths). These animals were

eliminated from our biomass and abundance calculations (Hessler and Jumars, 1974). The Foraminifera retained in both size fractions were sorted and stained with rose bengal to distinguish the living organisms from dead tests. However, these protozoans were not included in the macrofaunal abundance and biomass estimates.

Manganese nodules when present were carefully removed from each grab sample and preserved in separate containers prior to sieving. Macrofauna associated with each nodule were removed and included in the sediment macrofauna analyses with the exception of the Foraminifera. Displacement volume measurements were performed on the combined nodules from each grab.

Sediment carbon and nitrogen concentrations were determined with a Hewlett-Packard®185B CHN analyzer. Four subsamples of the CHN core were taken at 1-cm intervals. One half of the subsamples were adjusted to pH 3.5 with 0.1 N HCl to remove carbonates. All samples were then dried under vacuum at 70°C for 16 h prior to weighing and combustion.

Water sampling and analyses

A syringe array is vertically fastened to one of the legs of the FVGR. This array consists of ten 50-ml syringes (B-D Plastipak®) which are simultaneously activated to take filtered (precombusted Whatman GF/C) water samples near the sediment-water boundary. The intake hoses to the syringes can be adjusted from 0 to 72 cm above the sediment-water interface at 2-cm intervals.

Two large-volume syringe samplers (LVS) (1.7 l each) are located on the top tray of the FVGR. These samplers are set up to take filtered water samples about 10 cm above the sediment for dissolved oxygen and nutrient

concentration analyses. The undiluted LVS and syringe array samples are analyzed for nitrate, nitrite, and ammonium as described above.

A bottom water hydrocast is taken immediately after the deployment of the free vehicle grab respirometer to determine initial oxygen, temperature, and nutrient values (Carpenter, 1965). A Nansen bottle with deep-sea reversing thermometers is attached one meter above a Benthos Model 2214 pinger. The pinger, which has a messenger-activated "double-ping" switch to determine when the bottle is tripped, is mounted directly above the hydroweight. By observing the primary signal and the bottom reflection from the pinger on a precision depth recorder, the bottle can be adjusted to within two meters of the sediment surface in calm seas.

RESULTS

Five major stations (14 substations) were occupied along a transect extending from the central North Pacific to the southern California continental borderlands (Fig. 1). Each bottom station is characterized below by describing, 1) the topographical setting, 2) the bottom water (temperature, dissolved oxygen and inorganic nitrogenous nutrient profiles), and 3) the sediments (type, organic carbon and total nitrogen content, inorganic nitrogenous nutrients of the pore waters, macrofaunal abundance and biomass and manganese nodule presence).

Station CNP:

The CNP station is located north of the Murray Fracture Zone and east of the Musicians Seamount chain. A total of seven substations were occupied at this abyssal hill site within a 48-mile radius of $30^{o}44.5'N$, $158^{o}38'W$ during

two cruises in August of 1978 and 1979. Mean water depth of these substations was 5837 m with a range of only 149 m (Fig. 2).

Water profiles

Bottom-water temperature and dissolved oxygen are predictably constant among all the substations of CNP. Temperature ranged from 1.48° to 1.61°C while the dissolved oxygen concentration of the bottom water ranged from 3.70 to 3.78 ml l^{-1}. Water column profiles of nitrogenous nutrients reflect less variability with increased altitude above the interface. Nitrate concentrations are relatively constant from the surface centimeter of the sediment up to 48 cm altitude. Nitrite decreases in concentration from the surface sediment to the overlying water column and fluctuates with increased altitude, especially at substation 189 (Fig. 3A). Ammonium decreases two orders of magnitude from the surface sediments to the concentrations in the overlying water column.

Sediment profiles

Sediments in this area are characterized as quartz-illite rich clays of continental origin. Organic carbon content in the upper centimeter of the sediment column varies from 2.5 to 8.9 mg C gm^{-1} of sediment with comparable variability exhibited in total nitrogen, ranging from undetectible to 0.8 mg N gm^{-1} sediment (Fig. 2). Vertical profiles of organic carbon and total nitrogen at substations 173 and 189 reveal some digression from the expected decrease with increased depth of sediment. Organic carbon at substation 189 decreased with increased sediment depth to 9 cm contrasting the uniform distribution of total nitrogen with depth (Fig. 3A). The ratio of carbon to nitrogen decreased from a high of 5 at the surface to values between 4 and 4.4

at depths of 2 to 9 cm. The vertical profile at substation 173 deviated significantly from the first substation (Fig. 3B). Organic carbon increased with sediment depth reaching peaks at intermediate depths (2-4 and 5-7 cm), twice that found at comparable depths at substation 189. In contrast, total nitrogen decreased with increased depth of sediment. Carbon to nitrogen ratios were considerably higher than those measured at substation 189 and generally increased with sediment depth, indicative of the increased refractive carbon.

Inorganic nitrogenous nutrients in the pore water at substations 173 and 189 agreed more closely than the organic carbon and nitrogen profiles. Nitrate increased in concentration from the sediment-water interface to a sediment depth of 4 to 6 cm (Fig. 3A). The concentration of nitrite was more variable, spanning two orders of magnitude. Initially, nitrite decreased from the surface (0-1 cm) to a low at 2 cm and then significantly increased to 10 cm depth. Nitrite for substation 189 was an order of magnitude higher in the top centimeter than at substation 173, and then decreased to undetectable limits below that depth. Ammonium pore water concentrations were similar at both substations, exhibiting an initial decrease in the upper 3 to 4 cm followed by an abrupt increase to 6 cm and then slight oscillation to 10 cm (Figs. 3A,B). The decreasing ammonium and increasing nitrate concentrations in the surface layers are indicative of nitrification. Ammonium buildup in the subsurface layers suggests nitrate reduction on denitrification. The high degree of variability in nitrite may be a reflection of its intermediate status in the nitrogen cycle.

Macrofaunal abundance was highly variable among 6 substations in the CNP, ranging from 84 to 531 individuals m^{-2} at substations 246 and 204 respectively

(Fig. 2). Abundance was generally higher in the western group of substations, which were not significantly different from one another. However, statistically there was only a significant difference ($P < 0.05$) between western substations 139 and 204 and eastern substations 189 and 246 (Fig. 2).

The four dominant taxa of macrofauna were polychaetes, nematodes, copepods, and tanaids, comprising from 70 to 94% of the total macrofaunal abundance (Fig. 4A). The relative composition of these four taxa was similar in the small (300 µm screen) and large fractions (> 425 µm screen) (Fig. 4C). Even the nematodes which dominated in overall abundance in the western substations, were similarly distributed in the two size fractions.

Intergrab variation was higher in the eastern than the western substations. This variation in abundance ranged by a factor of 2 to 10 between individual grabs at the same substation. Variation in abundance between individual grabs in the western area is no greater than a factor of two.

Biomass of the macrofauna varies from a low of 1.7 mg m^{-2} at substation 204 to 58.0 mg m^{-2} at substation 189. However, the intrastation variability is great enough to eliminate any significant differences between any of the six substations (Fig. 2). There is a general tendency for higher abundance to biomass ratios at the western than eastern substations. This suggests a greater number of smaller animals at the western substations.

At substations 204, 189, 246 and 281, the polychaetes, nematodes, copepods, and tanaids dominated the biomass (Fig. 4B). In the other two substations (173, 139), other groups such as the bivalves, amphipods and incertae sedis, were expressed significantly relative to the four normally

dominant taxa (Fig. 4B).

The number of foraminiferan tests at the six CNP stations reveal a general pattern of decreasing numbers toward the east ranging from 18,988 tests m^{-2} at CNP-139 to 6452 tests m^{-2} at CNP-281. The number of living Foraminifera ranged from 8982 individuals m^{-2} at substation 139 to 394 individuals m^{-2} at substation 173, accounting for 47% to 3% of the total Foraminifera tests, respectively. The agglutinated Foraminifera were more abundant than the calcareous forms or Komokiacea.

Surface manganese nodules were present in all grabs from each CNP substation and revealed no longitudinal trend in numerical or volumetric distribution. Number of nodules per grab ranged from 9 $\pm$ 2 at substation 173 to 25 $\pm$ 3 at substation 189. Total displacement volume of the collected nodules ranged from 65 $\pm$ 10 ml at substation 204 to 245 $\pm$ 25 ml per grab at substation 189. The few macrofauna associated with these nodules included Komokiacea (substation 139) and a single hydroid (substation 281).

Station G:

Station G is located east of the Murray Fracture Zone in the northwest portion of the Baja California seamount province. This station is comprised of two substations, 109 and 132, each occupied during September 1980, and occurs at a depth approximately 1000 m shallower than the CNP station (Fig. 2).

Water profiles

The overlying water column immediately above the sediment has a temperature of 1.60°C and a dissolved oxygen content of 3.50 ml l^{-1}. The

oxygen content is lower than that of the CNP, and exemplifies the generally eastward flow of the North Pacific deep water (Reid, Roden and Wyllie, 1958). Nitrogenous nutrient profiles in the overlying water at substation 132 exhibit some variability up to an altitude of 20 cm above the interface (Fig. 3C). Nitrate at 0-2 cm altitude is significantly lower than pore water concentrations. However, with the above and two exceptions at 6 and 24 cm, nitrate maintains the same relative concentrations as in the sediments to 48 cm altitude. Nitrite is an order of magnitude lower in concentration in the overlying water compared to pore water values (Fig. 3C). The profiles of nitrite exhibit a general decline in concentration with increased altitude to 2 m. Concentrations of ammonium are also an order of magnitude lower in the overlying water than in the sediment pore waters, being detectable only to an altitude of 16 cm above the sediment-water interface (Fig. 3C).

Sediment profiles

The clay sediments of this area have a surface organic carbon and total nitrogen content similar to that measured at the CNP station. In vertical profile, organic carbon increased with depth in the upper 3 cm and then decreased to a value slightly below that of the surface at 8 cm depth (Fig. 3C). Total nitrogen was significantly more variable than carbon, showing peaks at 3 and 6 cm, both an order of magnitude higher than surface and deeper sediment values. Ratios of organic carbon to total nitrogen are highest at the surface (10.8) and lowest at intermediate depths where nitrogen is highest (1.1 to 1.3).

Nitrogenous nutrient profiles from the pore waters at substation 132 are similar to those measured in the CNP stations (Fig. 3A,B). Nitrate remains relatively constant with depth to 8 cm. Nitrite is variable,

increasing and then decreasing with depth into the sediment. A more irregular pattern is exhibited by ammonium which reaches a significant peak between 2-3 cm corresponding to similar peaks in organic carbon and total nitrogen.

Macrofaunal abundance at station G, substations 109 and 132, were comparable to the lowest values measured at the three east substations in the CNP (Fig. 2). However the dominant taxa changed from the western CNP to station G, exhibiting a transition from nematodes (> 45% total abundance) at the western CNP substations to polychaetes (70% total abundance) at station G (Fig. 4A). The eastern CNP substations show no clear dominance of either taxa.

In the 425 μm fraction of the macrofauna, polychaetes dominated the other taxa in abundance, as well as biomass (Fig. 4C, 4D). The nematodes dominated in the 300 μm fraction at substation 109 (Fig. 4C, 4D). The copepods were found exclusively in the 300 μm fraction and the tanaids in the 425 μm.

There is an order of magnitude difference in biomass of the macrofauna between substations 109 and 132 (Fig. 2). However, the large variation between grabs at each substation precludes the determination of a significant inter-substation difference.

Very few foraminiferan tests were found at station G. The total number of tests ranged from 640 to 1415 m^{-2}. All of the Foraminifera with stained protoplasm were agglutinated, and they constituted only 7% to 9% of the total.

The number and size of manganese nodules significantly decreased at station G when compared to station CNP. Only substation 132 had nodules present, 2 ± 1 per grab with a total displacement volume of 7.5 ± 1.5 ml per grab.

Station F:

The third station on the transect is also located in the Baja California Seamount Province on a flat plain area at a depth of 4392 m (Fig. 2).

Water profiles

Water overlying the sediment at station F has a temperature of 1.64°C and a dissolved oxygen concentration (3.55 ml l^{-1}), within 0.05 ml l^{-1} of the measured value at station G (Fig. 2). Nitrate concentrations are relatively constant across the sediment-water interface and reveal a gradual decrease with increased altitude up to 32 cm. At 2 m altitude an increase is indicated. Nitrite is present only at 24 and 32 cm altitudes, and not detectable immediately above the sediment-water interface. Ammonium concentrations are much lower in the overlying water than in the sediment and become undetectable at 2 m altitude (Fig. 3D).

Sediment profiles

The predominately clay sediment of this area has a surface organic carbon content similar to those stations to the west but the total nitrogen is considerably higher. In profile, the organic carbon fluctuates considerably between 3 and 10 cm depth but generally remains constant to a depth of 14 cm (Fig. 3D). Total nitrogen, although variable, decreases an order of magnitude to 14 cm. Ratios of organic carbon to nitrogen increase with increased depth from 5.3 at the surface to 33.5 at 14 cm, suggesting a direct relationship between the refractory quality of the organic matter and depth in the sediment.

Pore water nutrients at this station exhibit greater variability, especially nitrite and ammonium, when compared to stations to the west (Fig. 3D). Nitrate shows a gradual increase in concentration from the surface sediment to a depth of 4 cm then a gradual decrease back to surface concentrations at a depth of 8 cm. This increase corresponds with a more erratic increase in ammonium, spanning an order of magnitude, and two orders of magnitude decrease in nitrite at mid depth. These mid depth fluctuations overlap with decreases in total nitrogen at similar levels (Fig. 3D).

Abundance of macrofauna increases significantly over that found in the stations to the west (Fig. 2). Polychaetes and nematodes account for over 75% of the total number of macrofauna with nematodes being the dominant of the two (42% vs 35%) (Fig. 4A). Biomass is not significantly different from substation 132. Hence, the abundance to biomass ratio indicates a reduction in animal size between station G and F. Polychaetes are the dominant taxa contributing 86% of the total biomass. Amphipods, the only other significant contributor, account for 8% of the total biomass (Fig. 4B).

The polychaetes dominated by weight and abundance in the 425 μm screen. In the 300 μm fraction, the nematodes dominated the relative abundance while the amphipods dominated the biomass (Fig. 4C, 4D).

The agglutinated Foraminifera continued to dominate the total number of tests, 588 m^{-2}. The number of Foraminifera with stained protoplasm were 10% of the total number of tests.

Manganese nodules were present in each grab at station F representing a slight increase in number and size from station G to the west but significantly reduced compared to station CNP. Total number of nodules per

grab ranged from 3 to 6 while the displacement volume ranged from 8 to 130 ml.

Station C:

Station C is located immediately west of the southern California Continental Borderlands at the base of the Patton Escarpment (Fig. 2). The depth of the station is 3815 m.

Water profiles

Water temperature immediately above the sediment-water interface is 1.55°C with a dissolved oxygen concentration of 3.10 ml l^{-1}, somewhat reduced from the western stations. Nutrient profiles in the overlying water are similar to those observed at the other stations (Fig. 3E). Nitrate is lower than the concentration in the surface sediments, and remains fairly constant in the water column up to 2 m altitude. Nitrite and ammonium concentrations are significantly reduced in the bottom water when compared to concentrations in the sediment and are undetectable at 2 m altitude (Fig. 3E).

Sediment profiles

The silty clay sediment at station C had a surface organic carbon content significantly higher than that measured to the west (Fig. 2). However, the total nitrogen was comparable to that measured at station F resulting in a high carbon to nitrogen ratio of 9.8. These carbon and nitrogen ratios are similar to those measured at the same stations in November 1977 (Smith et al., 1979). Organic carbon and total nitrogen profiles exhibit similar patterns, the most notable being a significant decrease between 2 and 5 cm depth (Fig. 3E). The C:N ratio increases with depth from the surface (9.8) to 12 cm (20.4). Nitrate decreases an order of magnitude from the surface to 12 cm

depth in contrast to the relatively constant profile seen in all the stations to the west (Fig. 3). Nitrite concentration shows an initial increase to 3 cm depth but then follows a similar decrease to that exhibited by nitrate. Ammonium, on the other hand, decreases initially in the upper 4 cm, corresponding to depletions in nitrogen and carbon, but then gradually increases. This pattern in nitrogenous nutrients suggests nitrification in the surface sediments and nitrate reduction or denitrification in the subsurface sediments.

There is a precipitous increase in both abundance and biomass of the macrofauna at station C compared to all the previous stations (Fig. 2). The mean abundance is 8 times higher and the biomass 6 times higher than that measured at station F. These abundance values compare reasonably well with those obtained at the same station in November 1977 (Smith et al., 1979). However, the biomass values are considerably lower, which may be a result of spatial or temporal variation.

The numerically dominant taxa were the polychaetes and nematodes with polychaetes remaining the dominant group in biomass (Fig. 4A, 4B). The amphipods replaced the nematodes as the second most dominant group in biomass. The nematodes continued to dominate the 300 m fraction in abundance (Fig. 4C). The 425 μm fraction had a similar number of polychaetes and nematodes (Fig. 4C).

There was an order of magnitude increase in the total number of foraminiferan tests over the previous station to the west with the calcareous forms becoming the clearly dominant group. The total number of foraminiferan tests was 132,257 m^{-2} which was the highest mean quantity we found at any station. Of this total, only 1% were deemed living at the time of collection.

Station SCB:

The Santa Catalina Basin station is located in the southern California Continental Borderlands due west of the island of Catalina at a depth of 1300 m (Figs. 1 and 2).

Water profiles

The most variation in physical characteristics of the overlying water column occurs at this station. Bottom water temperature ranged from 1.9 to 3.5°C, with the cause and periodicity at this time unknown. A similar variability is exhibited in the dissolved oxygen concentration which ranges from 0.31 to 1.5 ml l^{-1} over a single tidal cycle. At the time our measurements were initiated, the dissolved oxygen concentration was 0.41 ml l^{-1}.

Nitrate showed little variation in the overlying water column, and was significantly higher than in sediment pore waters (Fig. 3F). Nitrite and ammonium were detectable at varying intervals above the sediment-water interface and always at lower concentrations than found in the sediment pore water (Fig. 3F). Ammonium was not detectable 2 m above the interface.

Sediment profiles

The sediments of this basin are a silty clay similar to that found at the base of the Patton Escarpment (station C). However, they have significantly higher amounts of organic carbon and total nitrogen (Fig. 2). Neither carbon nor total nitrogen vary substantially in concentration with depth when compared to the previous stations examined (Fig. 3). However, the C:N ratio increases with sediment depth from 13.9 at the surface to 21.4 at 16 cm. Pore

water nutrient profiles do not exhibit easily discernable patterns with depth to 16 cm (Fig. 3F). Nitrate varies considerably with depth decreasing to a low at 12 cm and then increasing. Nitrite concentrations are less variable than the other stations, but are of comparable magnitude. Ammonium concentrations are consistantly higher and show less variability than previously observed in other station profiles (Fig. 3F).

There was a tenfold increase in macrofaunal biomass at substation 110 with overall abundance remaining fairly consistent with station C (Fig. 2). The polychaetes dominated in number (89%), and in biomass (53%). An exception was the presence of one large ophiuroid which was responsible for 70% of the biomass in one grab. The nematodes were more abundant than the polychaetes in the 300 m fraction although, the polychaetes had a higher biomass in the 425 μm and 300 μm fractions (Fig. 4C, 4D).

The benthic foraminiferan tests were very abundant, 117,562 m^{-2}, and dominated by the calcareous forms as at station C. Only 1% of these tests stained positive with rose bengal indicating living protoplasm. No Komokiacea were identified in the 3 grab samples.

Summary of Results

Water profiles

Bottom water taken by hydrocast showed little variation in the physical properties we examined at each station with the exception of the anomalous temperature and dissolved oxygen data from SCB. Water temperature at the six western substations (Fig. 2) ranged from 1.48°C to 1.64°C and dissolved oxygen from 3.78 ml l^{-1} to 3.10 ml l^{-1}, with a generally eastward trend toward higher bottom temperatures and lower O_2 content. Nitrate in bottom samples was

predictably high at all stations, with nitrite and ammonium low or absent (Fig. 3). The transect showed no longitudinal trends in nutrient profiles of the water overlying the sediment and no gross anomalies were present as nutrient concentrations tended to remain between that of the hydrocast bottom water and that of the sediment surface pore water.

Sediment Profiles

Sediments at all stations were clay or silty-clay. Surface carbon and nitrogen show a general west to east increase corresponding to increases in biomass (see below) (Fig. 3). Sediment nutrient profiles, as well as those in the water overlying the sediment, show no clear easterly trends, and variability within the individual profiles is high.

Going west to east along the transect, there are apparent trends seen in the macrofaunal composition. A transition from the dominance of nematodes to polychaetes begins at station G and continues in the subsequent eastern stations. There is an overall increase in the abundance and biomass of macrofauna from the central North Pacific to the Santa Catalina Basin. The increase in macrofauna abundance is 20 times greater and the biomass increases by three orders of magnitude.

Total numbers of Foraminifera (living + dead) spanned three orders of magnitude along our transect ranging from a low of 640 individuals m^{-2} at station G-109 to 132,257 individuals m^{-2} at station C-125. A significant increasing trend in total numbers is evident at the easternmost stations at the base of the Patton Escarpment and the Catalina Basin. The predominate Foraminifera change from the agglutinating form in the central North Pacific to the calcareous in the eastern stations with a general increase in the total

number of tests (living and dead) at the eastern stations. Percent of living Foraminifera decreased in an eastward direction from a high of 47% at CNP-139 to a low of 1% at SCB-110 and C-125.

Manganese nodules were present in the surface sediments at only 3 western stations and exhibited a general trend of decreasing numbers and size to the east. There were only a few macrofauna associated with these nodules at two substations in CNP.

DISCUSSION

Water profiles

Our 2000-mile transect runs from the highly oligotrophic surface waters of the central North Pacific to the eutrophic Catalina Basin, representing relative extremes in surface productivity (Fig. 2). However, the bulk water (> 2 m altitude), or what is generally characterized as deep-sea bottom water, shows remarkable uniformity in the molecular species we analyzed. In all cases, nitrate was high (> 30 μM) and other nitrogenous species, nitrite and ammonium, absent or in the case of SCB and station G, nitrite, very low (Fig. 3). These features are characteristic of total nitrification in oxygenated water. Yet in true bottom water, that is, the water immediately overlying the sediment, the above pattern breaks down. Nitrite and ammonium are present above the sediment-water interface at all stations (Fig. 3). Although nitrate concentrations remain close to that of the bulk overlying water, it is apparent that calculations of diffusive fluxes of nitrogenous compounds across the sediment must take into account the nature of nutrient concentrations in the water immediately overlying the sediment. Wilson (1978) has estimated oxygen and nitrogen fluxes from pore water profiles relative to concentrations in standard hydrocast bottom water. Wada, Koike and Hattori (1975) have used water taken 5 m above the bottom as a control for measurements of nitrate metabolism at 50 cm above the sediment-water interface. The physical limitations of deep-sea hydrocast sampling (e.g., sea surface state, wire angle, PDR resolution, and location of the bottle on the wire) prevent sediment-free water samples from being taken closer than 2 m above the bottom, even under ideal conditions. Alternative methods of sampling bottom water have included devices which trip on contact with the sediment surface (Wada *et*

al., 1975; Rittenberg, Emery and Orr, 1955), submarine controlled devices (Kajihara, Matsunaga and Maita, 1974; Smith and Laver, 1981; Smith, in press), and instruments which take bottom water, pore water and/or sediment cores simultaneously (Sayles, Wilson, Hume and Mangelsdorf, 1973; Wilson, 1978; Smith et al., 1979). Morse (1974) and Wimbush (1970) have proposed a stagnant benthic boundary layer about 1 cm thick through which molecular species transport is purely diffusive. Our results indicate a layer with distinct stratification of nitrogenous species occurs up to 0.5 m above the sediment-water interface.

Many boundary-layer interval water sampling methods have been described (Blaker, 1979; Kajihara et al., 1974; Sholkovitz, 1970; Clasby, Reeburgh and Alexander, 1972; Broenkow, 1969 and others). To our knowledge, only that of Sholkovitz (1970) may be used at abyssal depths to sample immediately above the sediment. Even so, the samples taken are unfiltered and the intervals large (20 cm), and as he has pointed out, the altitude at which water is taken cannot be determined with precision. Blaker (1979) has noted that in the close-interval samplers, the actual tripping mechanism may cause enough disturbance in the water column to disrupt small gradients. Our syringe array may suffer from this design flaw, although the release mechanism is 50 cm from the intakes of the syringes. A more pertinent problem might be the disruption of the gradient by the "landing" of the FVGR and the expression of surface pore water nutrients by compression and disruption of the surface sediments. Also, the presence of a large sampler on the sea floor may create eddys in the bottom current which would tend to mix the boundary layer. We feel a long enough time interval is allowed (at least 48 h) prior to tripping the syringe array for re-stratification to occur. The efficacy of our method, as with the methods of others, is still open to question.

We can find no account of closely spaced profiling of nutrients above the sediment-water interface, with the exception of Kajihara et al. (1974), who sampled in relatively shallow water (20-70 m). They found similar patterns in nutrient profiles to those we find in the deep sea. They propose a model in which large particles of organic matter settle to the bottom and are broken up and resuspended by shear forces of bottom currents. These shear forces are presumed to release the nutrients generated by organic diagenesis within the particles to the surrounding water, resulting in localized peaks of nutrient enrichment above the sediment where the particles are broken up. Although similar patterns are seen in our profiles (Fig. 3) resuspension of particles would probably be low at the deep stations (> 3500 m) due to low current velocities (0.6-3 cm s^{-1}) (Ramp, 1976; Ingram and Hessler, in prep.). However, such resuspension could be a reasonable mechanism at the Catalina Basin station, where tidal current velocities may be high (22 cm s^{-1}) (Smith and Laver, 1981; Shepard, Marshall, McLoughlin and Sullivan, 1979) and we have observed obvious lenses of suspended material from the submersible Alvin. Because we did not measure distributions of suspended matter, we cannot evaluate the correlation between particulate dissolution and nutrient enrichment.

Another possible explanation for the distribution of nitrogen cycle intermediates in the overlying water is the differential location of microbially mediated processes of nitrification, nitrate reduction and denitrification in stratified layers overlying the sediment-water interface. Although denitrification is generally thought not to occur in oxygenated environments, localized anoxic microhabitats may be generated close to the sediment-water interface such as interstices of decomposing marine "snow." Measurements of oxygen, nitrous oxide, hydrogen sulfide, and dissolved organic

nitrogen (Seitzinger, Nixon, Pilson and Burke, 1980; Barnes, 1979) combined with nephelometer recordings would clarify the processes involved. We must also consider the source of the chemical species involved. In denitrification processes, the nitrate would primarily come from the overlying bulk water, and to a lesser extent from diffusion out of the sediment. If nitrification processes are involved, the main source of nitrite and ammonium would be the sediment. At all stations the nitrite and ammonium concentrations are lower in the water 0.5 cm above the interface than in the top layer of sediment, suggesting a diffusive chemical gradient out of the sediment. This gradient could be enhanced by bioturbation (McCaffrey, Meyers, Davey, Morrison, Bender, Luedtke, Cullen, Froelich and Klinkhammer, 1980), and by bottom currents. Nitrate concentrations in the water column are generally similar to those in the surface sediment with an evident diffusion gradient into the sediment only in the Santa Catalina Basin.

Sediment profiles

Many methods of obtaining sediment cores for pore water analyses have been developed, ranging from the massive Deep Sea Drilling Project (DSDP) cores to our FVGR samples. Gravity corers with and without core catchers and liners have been used, as well as box corers and Reineck corers (Emerson, Jahnke, Bender, Froelich, Klinkhammer, Bowser and Setlock, 1980; Suess, Müller, Powell and Reimers, 1980; Rowe, Clifford and Smith, 1977). Where pore water only was required, in situ filtration devices have been used (Sayles et al., 1973; Wilson, 1978). A full discussion of coring methods is not relevant here, yet an examination of certain limitations of the methods is in order. In studies such as ours where micro-stratification of pore-water chemicals is being examined, retaining the integrity of the surface layers is imperative.

To this end, we feel that subcoring of large corers, such as the Ekman or Reineck devices, with thin-walled liners provides the least disturbance of the sediment (Rowe et al., 1977). Gravity corers, even without liners and core catchers, tend to disrupt the surface sediment by the force of impact and angle of penetration. Gravity cores taken at station G show pore water nitrogenous nutrient profiles which are similar in magnitude and direction to those taken concurrently with the FVGR, but the gravity core gradients are much smoother. This difference may be the result of a variety of factors. 1) Compression of the sediments in the gravity core and a subsequent mixing of the pore water down the core could occur. In contrast, the FVGR grabs are slowly pushed into the sediment (1-5 cm min^{-1}) compared to a normal gravity core impact velocity of 60 to 120 m min^{-1}. 2) Enclosure and incubation of grab samples on the bottom for periods of 1 to 4 days in the FVGR may cause alterations in pore water nutrient profiles when compared to non-incubated gravity core profiles. 3) Spatial heterogeneity of the sediments between sampling sites cannot be discounted. 4) Decompression and temperature increase during core retrieval have been shown to alter the relative concentrations of pore water compounds (Sayles et al., 1973; Bischoff, Greer and Luistro, 1970) and is a common problem with currently used deep-sea coring methods including the FVGR. We are currently planning to evaluate the importance of the first 3 factors by concurrently sampling a small area with the FVGR and submersible manipulated cores and grabs.

The remineralization of nitrogenous organic matter in oxygenated sediments begins with the formation of ammonium by the process of ammonification. Ammonium is then oxidized to nitrite and finally to nitrate by the process of nitrification. Suess et al. (1980) have proposed that in oxygenated sediments there should be two layers, an upper layer characterized

by ammonium and nitrite formation and a lower layer characterized by nitrate formation. Our nutrient profiles reveal that ammonium, nitrite and nitrate are generally present at all levels examined (Fig. 3). The depletion of ammonium and nitrite with a corresponding increase in nitrate is only evident in one deep gravity core taken to a depth of 30 cm at station G. Our FVGR cores are perhaps too shallow to indicate any large scale processes which might be occurring in deep-sea sediment. However, in the surface sediments, the pore water profiles we obtained are irregular (Fig. 3) and the distribution cannot be explained totally by ammonification and nitrification processes. The subsurface depletion of nitrate with concurrent increases in nitrite and ammonium in the eastern stations suggest that dissimilatory nitrate reduction and denitrification are proceeding in low oxygen and anaerobic microcosms (Wilson, 1978; Barnes, 1979), and that assimilatory nitrate reduction is possibly occurring in contiguous oxygenated areas.

Our results do not suggest any significant longitudinal gradients in pore water nitrogenous nutrients. Rowe and Staresinic (1979) have noted a general increase in nitrate and decrease in ammonium with distance from shore in the western North Atlantic. Our data indicate this same trend for surface pore water ammonium from station SCB to station G, but nitrate surface concentrations seem to vary independently, correlating to the concentrations immediately above the sediment-water interface (Fig. 3). Also, nitrate values of 200-300 μM in abyssal plain surface sediment found by Rowe and Staresinic (1979) are an order of magnitude higher than ours in a comparable study area. In a southern California Basin study, Rittenberg et al. (1955) found nitrate values of 240 μM in the surface sediments of Catalina Basin, more than 10 times our reported concentration, and ammonium values 30 times higher than ours at the same station. However, bottom water nitrate concentrations were

in close agreement with our data. We do not know if these discrepancies represent sampling errors, variation in analytical procedure, or true variability as a result of temporal or spatial changes.

Profiles of sediment organic carbon and total nitrogen reveal few clear correlations to the nutrient data. In our analyses, we have not differentiated between the organic and inorganic nitrogen (ammonium) bound to the clays either in an exchangeable or fixed state. In Pacific clay sediments, Arrhenius (1952) and Müller (1975; 1977) have found decreasing organic carbon to total nitrogen ratios with depth into the sediment. At CNP-189 and station G we found similar decreases in the upper 10 cm which may be attributable either to bound inorganic or organic nitrogenous compounds with their sorption serving as protection from microbial remineralization (Müller, 1977). Both ammonium and organic nitrogen bind to the highly charged lattice structure of alumina silicates such as illite (Stevenson and Tilo, 1969; Müller, 1977), which dominates the CNP station sediments. In contrast, the other CNP substations and Stations F, C, and SCB exhibit a general increase in organic carbon to total nitrogen ratio with depth indicative of the preferential utilization of nitrogenous compounds (Emery and Rittenberg, 1952) and the resulting increase in the refractive nature of the organic matter with time.

A clear pattern does develop in surface organic carbon and total nitrogen concentrations when compared to biomass and abundance of macrofauna. An easterly trend of increasing surface sediment organic carbon and total nitrogen corresponds to increases in macrofaunal biomass and abundance (Fig. 2). There is also a general eastward increase in the ratio of organic carbon to total nitrogen which could be attributable to two factors, 1) increasing contribution of terrestrial and shallow water organic matter, and 2) increased

biogenic activity. Marine macrophytes and terrestrial plants have high carbon to nitrogen ratios (> 10) and become increasingly important as a source of organic matter to sediments with decreasing distance from land (Bordowskiy, 1965; Müller, 1977). Rates of sediment community oxygen consumption and nitrogenous nutrient exchange increased along the same transect toward the east (Smith and Horrigan, in prep.). This increased biogenic activity coupled with preferential decomposition of nitrogenous compounds may be of sufficient magnitude to allow accumulation of refractory organic matter.

The range of total macrofaunal abundance (84-531 individuals m^{-2}) from substations in the CNP station are comparable to samples taken from the central North Pacific with a 0.25 m^2 box core (84-160 individuals m^{-2}) (Hessler and Jumars, 1974). The abundance of macrofauna per unit area at station G compares reasonably well with the eastern CNP substations and falls within the range found by Sanders, Hessler, and Hampson (1965) the lower Bermuda slope. Station F with 1098 individuals m^{-2} compares with abundance measurements from the abyssal rise on the Gay Head-Bermuda transect (Sanders et al., 1965). Macrofaunal abundance at station F is five times greater than station G, although the biomass values are very similar. Total biomass data from stations F and G were lower than reported values (> 420 μm) in the abyssal northwestern Atlantic but higher than those found in the northern Gulf of Mexico at abyssal depths (Rowe, Polloni and Horner, 1974).

The macrofaunal abundance at station C is comparable to a 1977 study in the same area using the same methodology (Smith et al., 1979). The difference between biomass values was approximately an order of magnitude and may be a result of temporal (seasonal) changes.

Total biomass from station SCB (7.3 g m^{-2}) compared well with results

collected in the summer and fall in the Catalina Basin (8.7 g m^{-2}) (Hartman and Barnard, 1958; 1960). However, our abundance values were 2 orders of magnitude greater. This may be explained by a variety of factors including 1) differences in sampling techniques, and 2) spatial and temporal variability. Hartman and Barnard (1958; 1960) employed coarser screens to sort the macrofauna (1000 μm) than we employed (300 μm) therefore losing the smaller fraction which are numerically important. They also used orange peel and Campbell grabs for sample collection which create shock waves on impact with the sediment that are capable of sweeping away surface organisms (Smith and Howard, 1972). In addition, spatial and temporal variability cannot be discounted in explaining the differences between the two studies in light of the previous discussion concerning intragrab variability and possible seasonal changes at station C.

Corresponding to the observed increase in macrofaunal abundance and biomass toward the east (Fig. 2) there is a transition in dominant taxa from the nematodes in the western CNP to polychaetes in SCB (Fig. 4A). In the eastern CNP substations, there is no apparent dominance of either taxa. The dominance of nematodes in the central North Pacific has been recorded before (Hessler and Jumars, 1974), while the dominance of polychaetes has been noted to decrease with distance from the continent (Sanders et al., 1965). The number of different taxonomic groups excluding the polychaetes, nematodes, copepods and tanaids, also increases in the eastern substations. With the increase of these other taxa, the copepods and tanaids become relatively less prominent (Fig. 4A).

Individual macrofauna are generally larger as well as more abundant in the eastern substations. A reduction in the average size of individual

organisms with increasing depth has been recorded previously in many benthic environments (Rowe and Menzel, 1971; Gage, 1978; Thiel, 1975, Smith, 1978). Smith et al. (1978) noted a decrease in wet weight biomass of macrofauna from shallow stations (17 m) to deep stations (2750 m). While most of the biomass was found in the larger fraction, (425 µm), up to 76% of the animals occur in the smaller fraction (Smith et al., 1978). Thiel (1979) and Gage (1978) have suggested factors, such as food supply, in the benthic deep-sea environment which may account for the small size of the deep-sea benthos.

In our estimates of macrofaunal abundance and biomass, the contribution of the Foraminifera have been excluded because of the difficulty in identifying living from dead forms. Our values of total numbers of Foraminifera for the CNP station agree closely with those obtained by Bernstein, Hessler, Smith and Jumars (1978) in the same area. The reliability of the rose bengal method we used to determine living from dead Foraminifera is questionable. Smith and associates (1978) attempted sorting the living Foraminifera by crushing each test and then estimating the biomass of the enclosed protoplasm. They found that Foraminifera were a very significant component of the deep sea benthic community at a 2200 m station in the western North Atlantic. In the 420 µm fraction alone, a total of 17,766 Foraminifera m^{-2} were recorded with a wet weight biomass of 861.5 mg m^{-2}. These abundance and biomass values were greater than all the other macrofaunal taxa combined (420 and 297 µm). Our highest estimate of living Foraminifera abundance (CNP-139, 8982 individuals m^{-2}) is half that reported for the deep slope station in the western North Atlantic.

A west-to-east gradient is evident in the total number of benthic Foraminifera. The agglutinating forms are dominant in the western substations

and the calcareous forms are most prevalent in the eastern substations. The dominance of agglutinating Foraminifera in the CNP has been observed in previous studies (Hessler and Jumars, 1974; Bernstein et al., 1978). The precipitous change to a dominance of calcareous foraminiferan test was first observed at station C. The apparent lack of calcareous foraminiferan tests in the western stations can be attributed to the undersaturation of deep water with respect to calcite and rapid dissolution rates (Honjo, 1977; Takahashi and Broecker, 1977).

Manganese nodules decreased numerically and volumetrically from west to east being absent beyond station F. This distributional pattern supports the premise that manganese nodules are most abundant in pelagic sediment regions characterized by low sedimentation rates (Crerar and Barnes, 1974).

We found few macrofauna associated with the manganese nodules and then only with those at the CNP station. However, Burnett and Nealson (1981) report a variety of microorganisms associated with manganese nodules from a similar area in the central North Pacific. These microorganisms may be important in the overall metabolic processes which influence the chemical profiles we observed. There are no obvious correlations between the number or size of manganese nodules and the other parameters we have measured.

SUMMARY

It is apparent from our deep-sea bottom water profiles at all stations that a layer exists above the sediment-water interface, perhaps as large as 50 cm, which is enriched in nitrogenous nutrients (Fig. 3); nutrient concentrations in the bulk overlying water are not equivalent to this narrow zone above the sediment. These nutrients occur in highest concentrations near

the sediment-water interface, the bottom 10 cm of our profiles, with the exception of nitrate which remains relatively constant with altitude. These increased concentrations of nutrients can be a result of diffusion from the sediments and/or direct microbial activity in the bottom water. Profiles of dissolved oxygen, nitrogen, particulate and dissolved organic nitrogen and carbon would help clarify our results.

The most pronounced longitudinal trend in our sediment data is the increase in surface organic carbon and total nitrogen corresponding to an increase in infaunal abundance and biomass from west to east. Increases in surface C:N ratios, carbon and nitrogen, abundance, biomass, and surface productivity, indicate preferential decomposition of nitrogenous organic matter in the richer environments (Fig. 2).

Pore water profiles of nitrate, nitrite, ammonium, organic carbon and total nitrogen exhibited no obvious patterns in these oxygenated sediments. Ammonification and nitrification processes are occurring in the surface sediments but our results are insufficient to explain the observed profiles. We propose that these surface sediments are not homogeneous. Distinct gradients of nitrogenous nutrients should not be evident considering the qualitatively and quantitatively heterogeneous supply of organic matter to the sediment, bioturbation, bottom currents and, diffusion across the sediment-water interface. Other concurrent microbial processes such as assimilatory and dissimilatory nitrate reduction, and denitrification are proceeding in the top 10-20 cm of the sediment column either in aerobic or anaerobic microcosms. We feel that these processes must be examined in greater detail in the surface sediments through additional analyses of dissolved oxygen, nitrogen, nitrous oxide, and dissolved organic nitrogen and carbon to understand the

stoichiometry and exchange rates across the sediment-water interface. Deep subsurface sediment profiles of these species, as those in the overlying bulk water, do not provide the necessary information to decipher such boundary layer reactions.

Acknowledgements

This research was supported by two grants from the National Science Foundation (OCE-78-08640 and OCE-76-10728) and by a contract from the Sandia Laboratories, Subseabed disposal program. We thank R. Baldwin, S. Hamilton, P. Klement, P. Rishel, M. Unwin, and A. White for technical assistance during various stages of this research. The full cooperation of the crews of the research vessels Thomas Washington and New Horizon and in particular, Captain Arsenault, L. Smith and J. Stankaitus are gratefully acknowledged. Invaluable comments on the manuscript were provided by R. Baldwin, A. Carlucci, and S. Horrigan.

REFERENCES

Arrhenius G. (1952) Sediment cores from the East Pacific. Reports of the Swedish Deep-Sea Expdition 1947-1948, 5, 1-227.

Barnes R. O. (1979) Nitrogen diagenesis in marine sediments: Evidence for suboxic and anoxic conversion of organic N to N_2 gas. Fourth International Symposium on Environmental Biogeochemistry, Canberra, Australia, 26-31 August 1979.

Bernstein B. B., R. R. Hessler, R. Smith and P. A. Jumars (1978) Spatial dispersion of benthic Foraminifera in the abyssal central North Pacific. Limnology and Oceanography, 23, 401-416.

Bischoff J. L., R. E. Greer and A. O. Luistro (1970) Composition of interstitial waters of marine sediments: Temperature of squeezing effect. Science, 167, 1245-1246.

Blakar I. A. (1979) A close-interval water sampler with minimal disturbance properties. Limnology and Oceanography, 24, 983-987.

Bordowskiy O. K. (1965) Accumulation of organic matter in bottom sediments. Marine Geology, 3, 33-82.

Broenkow W. W. (1969) An interface sampler using spring-activated syringes. Limnology and Oceanography, 14, 288-290.

Burnett B. R. and K. H. Nealson (1981) Organic films and microorganisms associated with manganese nodules. Deep-Sea Research, 28A, 637-645.

Carpenter J. H. (1965) The Chesapeake Bay Institute technique for the Winkler dissolved oxygen method. Limnology and Oceanography, 10, 141-143.

Clasby R. C., W. S. Reeburgh and V. Alexander (1972) A close-interval syringe sampler. Limnology and Oceanography, 17, 632.

Crerar D. A. and H. L. Barnes (1974) Deposition of deep-sea manganese nodules. Geochimica et Cosmochimica Acta, 38, 279-300.

Emerson S., R. Jahnke, M. Bender, P. Froelich, G. Klinkhammer, C. Bowser and G. Setlock (1980) Early diagenesis in sediments from the eastern equatorial Pacific. I. Pore water nutrient and carbonate results. Earth and Planetary Science Letters, 49, 57-80.

Emory K. O. and S. C. Rittenberg (1952) Early diagenesis of California basin sediments in relation to origin of oil. American Association of Petroleum Geologists Bulletin, 36, 735-806.

Gage J. D. (1978) Animals in deep sea sediments. Proceedings of the Royal Society of Edinburgh, 76B, 77-93.

Gardner W. S., D. S. Wynne and W. M. Dunstan (1976) Simplified procedure for the manual analysis of nitrate in seawater. Marine Chemistry, 4, 393-396.

Hartman O. and J. L. Barnard (1958) The benthic fauna of the deep basins off southern California, Part I. Allan Hancock Foundation Pacific Expeditions, 22, 1-67.

Hartman O. and J. L. Barnard (1960) The benthic fauna of the deep basins off southern California, Part II. Allan Hancock Foundation Pacific Expeditions, 22, 69-297.

Hessler R. R. and P. A. Jumars (1974) Abyssal community analysis from replicate box cores in the central North Pacific. Deep-Sea Research, 21, 185-209.

Honjo S. (1977) Biogenic carbonate particles in the ocean; do they dissolve in the water column? In: The Fate of Fossil Fuel CO_2, N. Andersen and A. Malahoff, editors, Plenum Press, pp. 269-294.

Kajihara M., K. Matsunaga and Y. Maita (1974) Anomalous distribution of suspended matter and some chemical compositions in seawater near the seabed: transport processes. Journal of Oceanographical Society of

Japan, 30, 232-240.

Kalil E. and M. G. Goldhaber (1973) A sediment squeezer for removal of pore waters without air contact. Journal of Sedimentary Petrology, 43, 553-558.

McCaffrey R. J., A. C. Meyers, E. Davey, G. Morrison, M. Bender, N. Luedtke, D. Cullen, P. Froelich and G. Klinkhammer (1980) The relationship between pore water chemistry and benthic fluxes of nutrients and manganese in Narragansett Bay. Limnology and Oceanography, 25, 31-44.

Morse J. W. (1974) Calculation of diffusive fluxes across the sediment-water interface. Journal of Geophysical Research, 79, 5045-5048.

Müller P. J. (1975) Diagenese stickstofataltiger organischer substanzen inoxischen und anöxischen marinen sedimenten. Meteor Forsch Evgebnisse, 22, 1-60.

Müller P. J. (1977) C/N ratios in Pacific deep-sea sediments: Effect of inorganic ammonium and organic nitrogen compounds sorbed by clays. Geochimica et Cosmochimica Acta, 41, 765-776.

Ramp S. R. (1976) The measurement and analysis of low frequency currents in the deep central N. Pacific Ocean. Master's Thesis, University of Washington, 76 pp.

Reid J. L., G. I. Roden and J. G. Wyllie (1958) Studies of the California current system. Progress Report California Cooperative Oceanographic and Fisheries Investigations, 6, 28-57.

Rittenberg S. C., K. O. Emery and W. L. Orr (1955) Regeneration of nutrients in sediments of marine basins. Deep-Sea Research, 3, 23-45.

Rowe G. T. and N. Staresinic (1979) Sources of organic matter to the deep-sea benthos. Ambio Special Report No. 6, 19-23.

Rowe G. T., C. H. Clifford and K. L. Smith, Jr. (1977) Nutrient regeneration

in sediments off Cap Blanc, Spanish Sahara. Deep-Sea Research, 24, 57-63.

Rowe G. T., P. T. Polloni and S. G. Horner (1974) Benthic biomass estimates from the northwestern Atlantic Ocean and the northern Gulf of Mexico. Deep-Sea Research, 21, 641-650.

Rowe G. T. and D. W. Menzel (1971) Quantitative benthic samples from the deep Gulf of Mexico with some comments on the measurement of deep-sea biomass. Bulletin of Marine Science, 21, 555-566.

Sanders H. L., R. R. Hessler and G. R. Hampson (1965) An introduction to the study of deep-sea benthic faunal assemblages along the Gay Head-Bermuda transect. Deep-Sea Research, 12, 845-867.

Sayles F. L., T. R. S. Wilson, D. N. Hume and P. C. Mangelsdorf, Jr. (1973) In situ sampler for marine sedimentary pore waters: evidence for potassium depletion and calcium enrichment. Science, 181, 154-156.

Seitzinger S., S. Nixon, M. E. Q. Pilson and S. Burke (1980) Denitrification and N_2O production in near-shore marine sediments. Geochimica et Cosmochimica Acta, 44, 1853-1860.

Shepard F. P., N. F. Marshall, P. A. McLoughlin and G. G. Sullivan (1979) Currents in submarine canyons and other seavalleys. American Association of Petroleum Geologists, 173 pp.

Sholkovitz E. R. (1970) A free-vehicle bottom-water sampler. Limnology and Oceanography, 15, 641-643.

Smith K. L., Jr. (1978) Benthic community respiration in the N.W. Atlantic Ocean: in situ measurements from 40 to 5200 m. Marine Biology, 47, 337-347.

Smith K. L., Jr. Zooplankton of a bathyal benthic boundary layer: in situ rates of oxygen consumption and ammonium excretion. Limnology and

Oceanography, (in press).

Smith K. L., Jr. and R. J. Baldwin (1981) Deep Sea Respirometry: In situ techniques. In: Handbook on poloragraphic oxygen sensors: aquatic and physiological applications, H. Forstner and E. Gnaiger, editors, Springer-Verlag, (in press).

Smith K. L., Jr. and J. D. Howard (1972) Comparison of a grab sampler and large volume corer. Limnology and Oceanography, 17, 142-145.

Smith K. L., Jr. and M. B. Laver (1981) Respiration of the bathypelagic fish Cyclothone acclinidens. Marine Biology, 61, 261-266.

Smith K. L., Jr., G. A. White and M. B. Laver (1979) Oxygen uptake and nutrient exchange of sediments measured in situ using a free vehicle grab respirometer. Deep-Sea Research, 26, 337-346.

Smith K. L., Jr., G. A. White, M. B. Laver and J. A. Haugsness (1978) Nutrient exchange and oxygen consumption by deep-sea benthic communities: preliminary in situ measurements. Limnology and Oceanography, 23, 997-1005.

Stevenson F. J. and S. N. Tilo (1969) Nitrogenous constituents in deep-sea sediments. In: Advances in Organic Geochemistry, 1966, G. D. Hobson and G. C. Speers, editors, Pergamon Press, pp. 237-263.

Strickland J. D. H. and T. R. Parsons (1972) A practical handbook of seawater analysis. Fisheries Research Board of Canada Bulletin, 167, 1-310.

Suess E., P. J. Muller, H. S. Powell and C. E. Reimers (1980) A closer look at nitrification in pelagic sediments. Geochemical Journal, 14, 129-137.

Takahashi T. and W. S. Broecker (1977) Mechanisms of calcite dissolution on the sea floor. In Fate of Fossil Fuel CO_2, N. Andersen and A. Malahoff, editors, Plenum Press, pp. 455-477.

Thiel H. (1975) The size structure of the deep-sea benthos. International

Revue ges. Hydrobiologia, 60, 575-606.

Thiel H. (1979) Structural aspects of the deep-sea benthos. Ambio Special Report No. 6, 25-31.

Wada E., I. Koike and A. Hattori (1975) Nitrate metabolism in abyssal waters. Marine Biology, 29, 119-124.

Wilson T. R. S. (1978) Evidence for denitrification in aerobic pelagic sediments. Nature, 274, 354-356.

Wimbush M. (1970) Temperature gradient above the deep sea floor. Nature, 227, 1041-1043.

Figure Legends

Figure 1. A transect of 5 stations across the central and eastern North Pacific.

Figure 2. Characterization of 5 stations (14 substations) along a transect from 160°W to 118°W longitude between 30° and 34°N latitude. Parameters measured include depth, sediment organic carbon and total nitrogen, macrofaunal abundance and biomass, bottom water temperature, and dissolved oxygen.

Figure 3. Vertical profiles of nitrogenous nutrients (nitrate, nitrite, and ammonium) in the sediment and overlying water column, and sediment organic carbon (open circle, solid line) and sediment organic nitrogen (open circle, dashed line) at selected substations within the major stations (CNP, G, F, C, and SCB). (Note log scale for nutrient concentrations.)

Figure 4. Relative composition of dominant taxa of macrofauna at 11 substations along the transect. Total abundance (A), abundance by size fraction (C), total biomass (B), and biomass by size fraction (D). The component abundance (individuals m^{-2}) and biomass (mg wet wt. m^{-2}) of each faunal group is given within the bars and the substation totals presented above each bar. Number of grab samples per substation is given in parentheses. The size fractions are ASTM #40 = 425 µm and ASTM #50 = 300 µm.

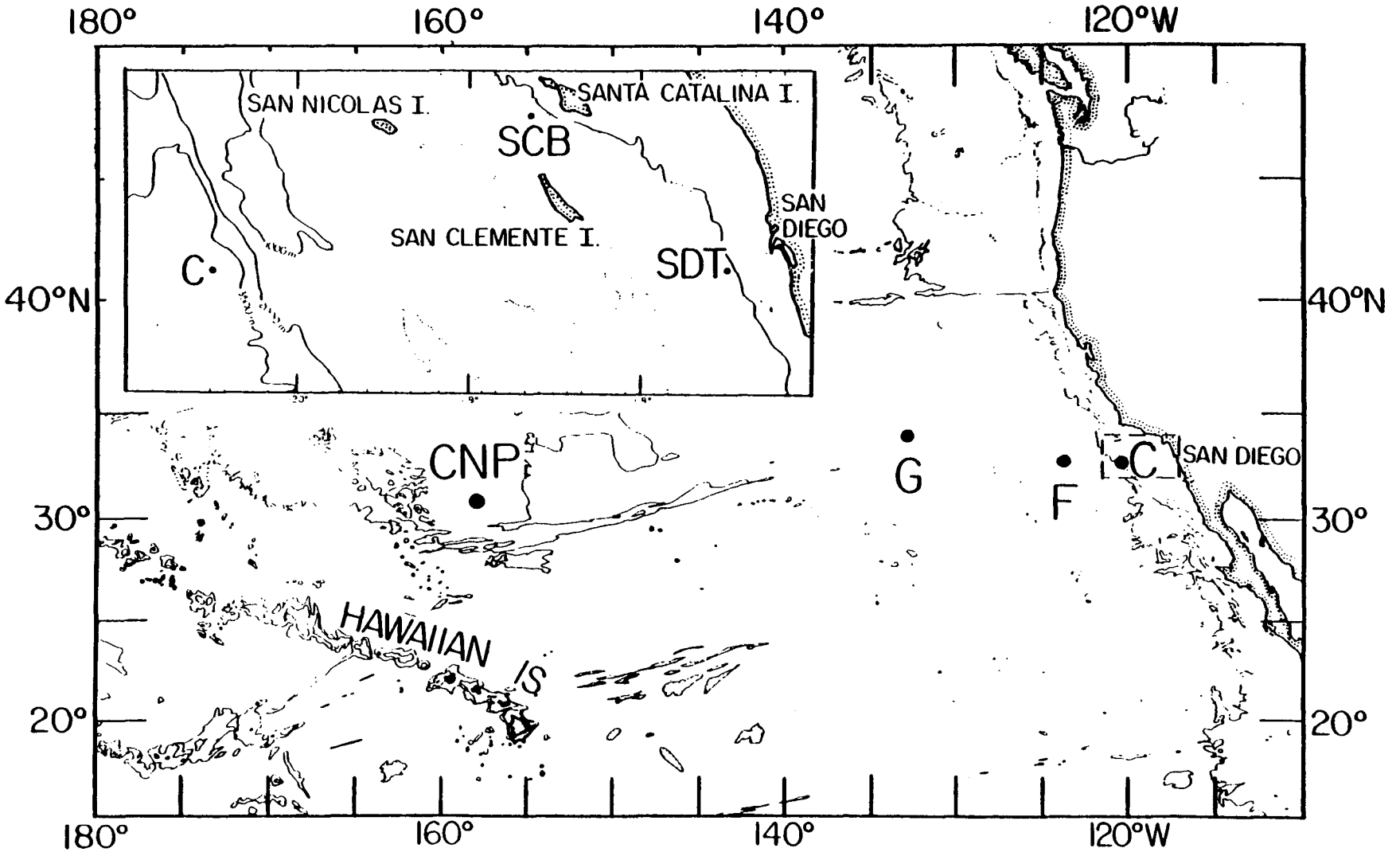

180°
160°
140°
120°W
40°N
30°
20°
SAN NICOLAS I.
SANTA CATALINA I.
SCB
SAN CLEMENTE I.
SAN DIEGO
C
SDT
CNP
G
F
C
SAN DIEGO
HAWAIIAN IS

Fig. 1

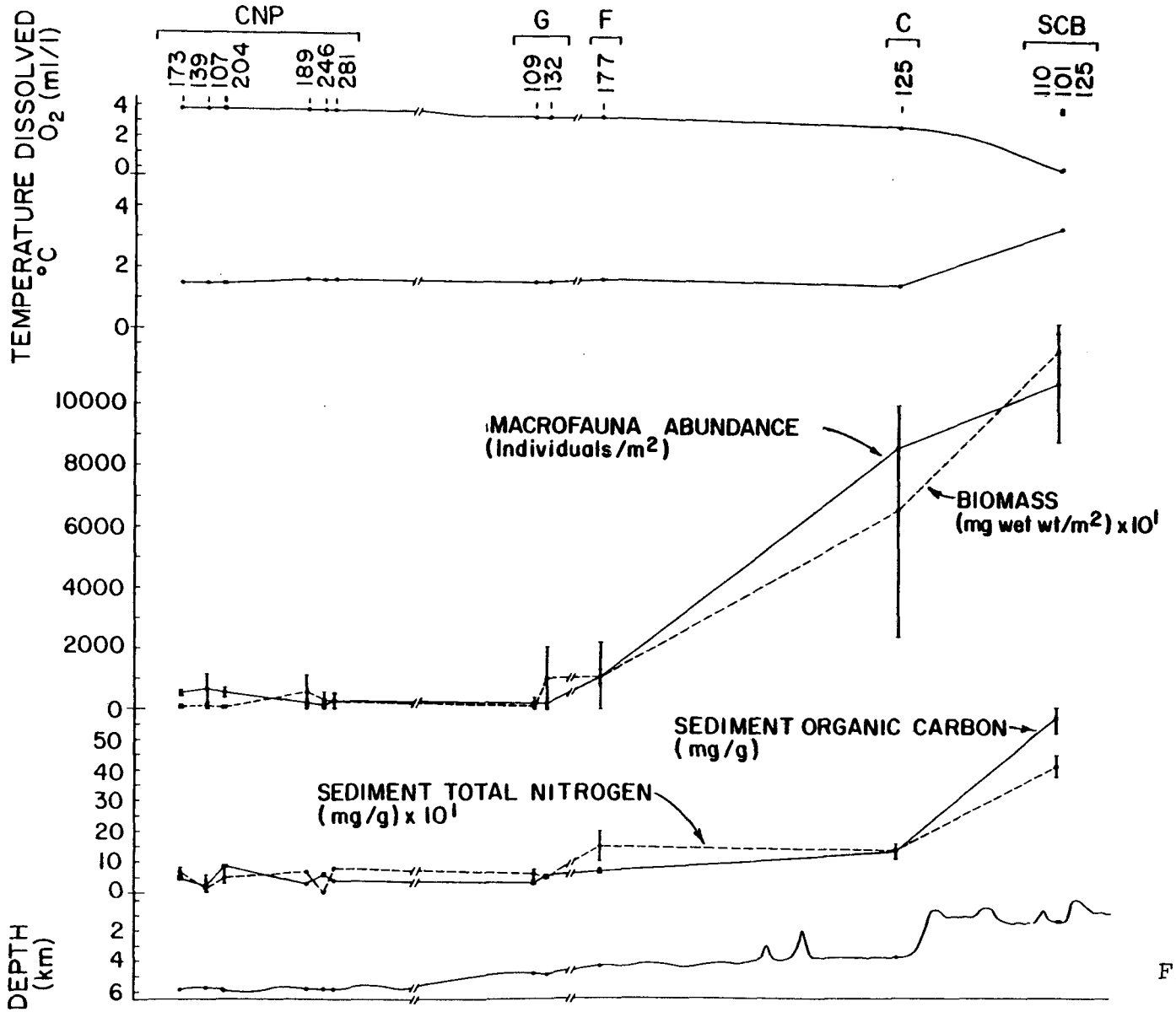

CNP
G
F
C
SCB
173
139
107
204
189
246
281
109
132
177
125
110
101
125
TEMPERATURE DISSOLVED O2 (ml/l)
°C
4
2
0
4
2
0
10000
8000
6000
4000
2000
0
MACROFAUNA ABUNDANCE
(Individuals/m2)
BIOMASS
(mg wet wt/m2) x 10'
SEDIMENT ORGANIC CARBON
(mg/g)
50
40
30
20
10
0
SEDIMENT TOTAL NITROGEN
(mg/g) x 10'
DEPTH
(km)
2
4
6

Fig. 2

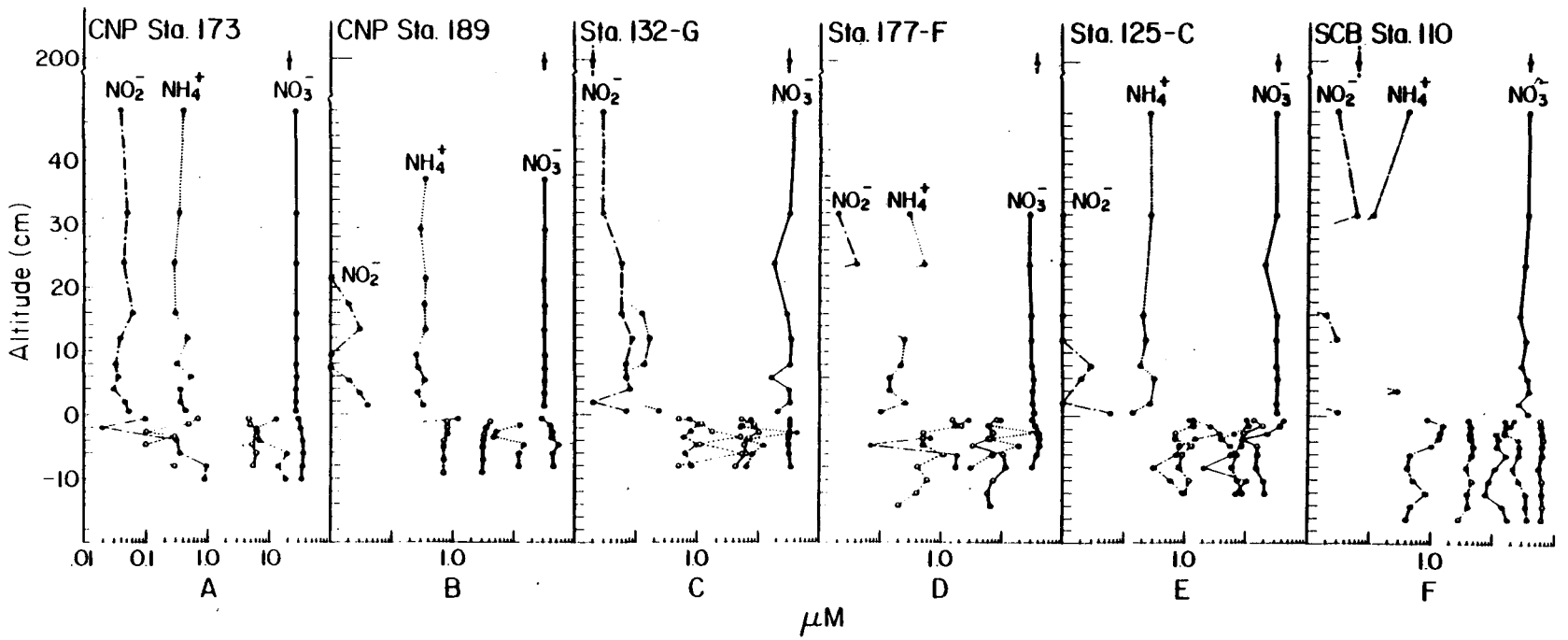

CNP Sta. 173
CNP Sta. 189
Sta. 132-G
Sta. 177-F
Sta. 125-C
SCB Sta. 110
Altitude (cm)
200
40
30
20
10
0
-10
NO_2^-
NH_4^+
NO_3^-
.01
0.1
1.0
10
A
B
C
D
E
F
μM

Fig. 3

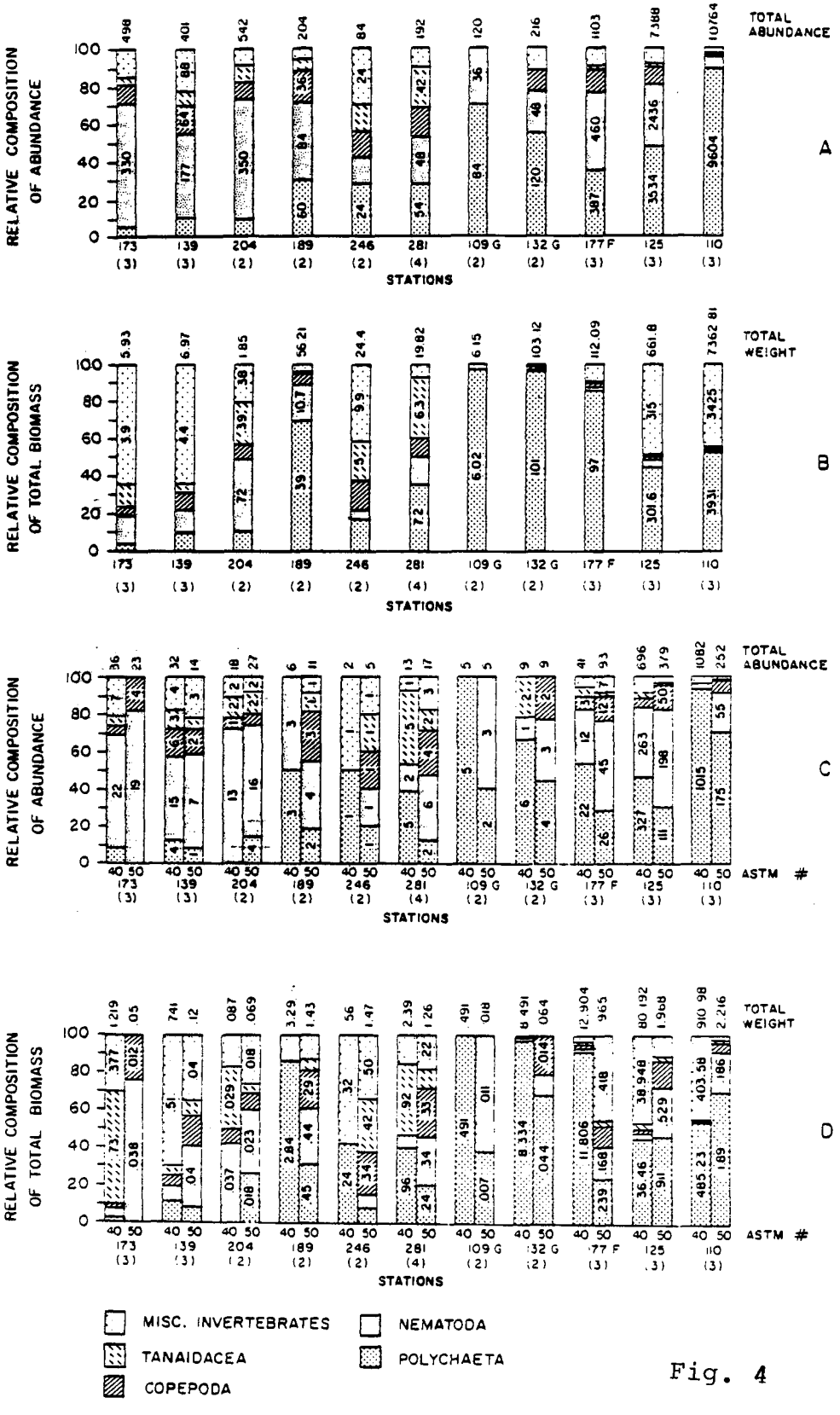

RELATIVE COMPOSITION OF ABUNDANCE
TOTAL ABUNDANCE
A
RELATIVE COMPOSITION OF TOTAL BIOMASS
TOTAL WEIGHT
B
RELATIVE COMPOSITION OF ABUNDANCE
TOTAL ABUNDANCE
C
ASTM #
RELATIVE COMPOSITION OF TOTAL BIOMASS
TOTAL WEIGHT
D
ASTM #
173 (3)
139 (3)
204 (2)
189 (2)
246 (2)
281 (4)
109 G (2)
132 G (2)
177 F (3)
125 (3)
110 (3)
STATIONS
MISC. INVERTEBRATES
NEMATODA
TANAIDACEA
POLYCHAETA
COPEPODA

Fig. 4

Addendum 2

Benthic boundary layer in the central and eastern North Pacific. II. Sediment community oxygen consumption and nutrient exchange

K. L. Smith, Jr. and S. G. Horrigan

Submitted to Deep-Sea Research

Addendum 2:

Benthic boundary layer in the central and eastern North Pacific. II. Sediment community oxygen consumption and nutrient exchange

K. L. Smith, Jr. and S. G. Horrigan

Scripps Institution of Oceanography, A-002

La Jolla, California 92093 USA

Abstract--Sediment community oxygen consumption (SCOC) and nutrient exchange rates (NH_4^+, NO_3^-, NO_2^-) were measured along a transect of five stations from the oligotrophic central North Pacific to the eutrophic upwelling off the coast of southern California. These rates were measured using a free vehicle grab respirometer at three spatial scales, intergrab (cm), intersubstation (km), and interstation (10^2 km). Sediment community oxygen consumption increased along a gradient of increasing surface primary productivity from west to east. Most of the variability in SCOC at both the interstation and substation level are correlated to depth and macrofaunal abundance. Predictive equations for SCOC were generated using these parameters. Nitrogenous nutrient exchange rates were highly variable and showed no east-west trends. Much of the small scale variability in nitrogenous nutrient exchange rates is attributable to temporal and spatial heterogeneity in the sediments. Measured nutrient exchange rates did not agree with predicted fluxes estimated from pore water profiles which is attributed to differences in temporal scaling. Predicted fluxes represent overall processes which occur on long time scales. Measured fluxes represent a composite of short- and long-term processes monitored across the sediment-water interface. Concurrent estimates of organic matter supply to and demand of the sediment community at the easternmost station on the transect revealed insufficient supply of carbon and nitrogen.

Measurements of oxygen consumption and nutrient exchange rates of deep-sea sediments in aerobic environments provide some indication of the rate at which organic matter that reaches the bottom is remineralized. Organic matter in most regions of the ocean is produced in the overlying surface water and is transported to the sea floor at various rates depending on its form and the transformations undergone through the water column. The amount of organic matter which reaches the benthic boundary layer, as measured by sedimentation traps, is directly proportional to the primary productivity of the overlying surface water. If sediment community oxygen consumption (SCOC) and nutrient exchange rates are related to the amount of organic matter which reaches the benthic boundary layer, a similar direct proportionality should exist between surface primary productivity and SCOC and nutrient exchange rates. Such a relationship has been proposed (Smith, 1974; Smith, White and Laver, 1979; Smith and Hinga, in press).

To test this hypothesis, we established a transect of stations along a gradient of surface productivity, consisting of a series of five stations from the oligotrophic central North Pacific to the eutrophic upwelling off the coast of southern California. Each station has been characterized with respect to biological and chemical parameters in the sediments and the overlying water column (Smith, Laver and Brown, submitted). Four of the measured parameters (macrofaunal abundance, macrofaunal biomass, sediment organic carbon, sediment total nitrogen) varied directly with surface primary productivity, increasing from west to east.

Here we present data on the sediment community oxygen consumption and nitrogenous nutrient exchange rates obtained at each station along the transect. Rate measurements were analyzed at three spatial levels: inter-

grab (on the order of centimeters), inter-substation (on the order of kilometers), and inter-station (on the order of 10^2 km). Analysis of a variety of benthic boundary layer parameters allowed us to identify relationships among the parameters and to formulate a predictive equation for sediment community oxygen consumption.

MATERIALS AND METHODS

Sediment community oxygen consumption and nitrogenous nutrient exchange rates were measured in situ using a free vehicle grab respirometer (FVGR) (Smith, White and Laver, 1979; Smith and Baldwin, in press). This device consists of an aluminium tripod supporting a central instrumentation package and a flotation array. The central instrumentation package consists of two trays, a lower one with four stainless steel grabs (20.3 cm x 20.3 cm x 30 cm) and an upper one consisting of the grab tops. Inserted into each top are a polarographic oxygen sensor, a solid state stirring motor, and two syringe systems. The polarographic oxygen sensors (Kanwisher, 1959), when coupled to an autoscaling amplifier and recorder housed in an electronics cylinder atop the tray, provide a continuous record of dissolved oxygen tension within the overlying water enclosed in each grab. The solid state stirring motor slowly circulates the water within each grab, preventing stratification and maintaining a constant flow over the oxygen sensor. Two syringe samplers attached to each grab withdraw 50 ml water samples, one at the beginning and one at the end of an incubation, from the overlying water for nutrient analyses aboard ship.

On deployment, the FVGR with flotation, instrumentation tripod and ballast, is 95 kg negative and descends to the bottom at a rate of 50-60m min^{-1} (Smith and Baldwin, in press). A period of 1 h is allowed once the FVGR

reaches the bottom before the bottom grab tray is slowly guided into the sediment on four vertical rods by two hydrostatic pistons activated by an electronic timer. The four grabs on this tray enter the sediment to a depth of approximate 15±2 cm at a speed of 1-4 cm min^{-1}. No bow wave is created by these grabs because they enter the sediment at slow speed and are open at the top. Once the grab tray is positioned in the sediment, the top instrumentation tray is released acoustically and falls on the guide rods to the lower tray, sealing each grab. Two types of initial water samples are taken after the two trays are sealed, one from each grab, using a withdrawal syringe, and a control bottom water sampler using a large-volume water sampler mounted on the instrumentation tray. Both samplers are activated simultaneously with a preset electronic timer.

The sediment and overlying water in each grab is incubated for a sufficient period of time to obtain a measureable change (≤25%) in dissolved oxygen tension and nutrient concentration. At Stas CNP and G, incubations lasted for a period of 3-4 days, while at Stas F, C, and SCB, incubations lasted for a period of 1-3 days. At the end of the incubation, the final grab syringe and external control water samples are taken and the spring-loaded grab jaws closed, sealing the sediment and water in each grab. The FVGR is then recalled to the surface by acoustic command and the ballast weights were dropped.

On deck the initial, final, and control water samplers are immediately removed and the samples analyzed for nitrogenous nutrients and dissolved oxygen. Ammonium, nitrate and nitrite were analyzed using the methodology outlined by Strickland and Parsons (1972) and nitrate determined by the copper-coated cadmium wire method (Gardner, Wynne and Dunstan, 1976).

Dissolved oxygen was determined using the modified Winkler method (Carpenter, 1965).

Sediments were removed from all but one grab and sieved through a 297-μm sieve for macrofaunal abundance and wet weight biomass analysis in the laboratory. Manganese nodules, when present, were counted and their displacement volumes were determined. One grab of the four was subcored for sediment organic carbon, sediment total nitrogen, and pore water nutrient analysis. The methodology used in these sediment analyses is fully described in Smith, Laver and Brown (submitted).

Oxygen consumption rates were determined from continuous recordings of dissolved oxygen tensions. Each sensor was calibrated using chilled, nitrogen-purged and oxygen-saturated seawater as limits. The effects of pressure were corrected for each individual sensor using laboratory-generated output/pressure curves.

RESULTS

Sediment community oxygen consumption (SCOC) and nitrogenous nutrient exchange rates were measured at five stations (13 substations, or deployments of the FVGR) along a transect from the central to the eastern North Pacific (Fig. 1). Chemical and biological descriptions of each of these stations are given in Smith, Laver and Brown (submitted). Oxygen consumption of the sediment community along this transect increased from west to east (Fig. 2), ranging over two orders of magnitude from a low of 3.6 μmoles O_2 m^{-2} h^{-1} at substation 189 (CNP) to 118 μmoles O_2 m^{-2} h^{-1} at substation 125 (C). Nutrient flux rates across the sediment-water interface were highly variable at the five transect stations (Fig. 3), showing no marked trend from west to east and

great variability among grabs from a single deployment. Nitrate and ammonium were the most significant contributors to the nitrogen flux; the intermediate compound, nitrite, showed smaller fluxes.

Station CNP

This station, occupied in August of 1978 and 1979, consisted of seven independent substations within an 89-km radius in an abyssal hill region (water depth = 5755-5904 m) north of Hawaii (Fig. 1; Smith et al., submitted). Bottom water temperature was 1.5°C; bottom dissolved oxygen concentration was 3.74 ml O_2 l^{-1}. Sediment organic carbon ranged from 2.5 to 8.9 mg C g^{-1}. Macrofaunal abundance was generally higher in the western substations, but biomass exhibited no obvious trends. Manganese nodules were present at each substation.

Sediment community oxygen consumption at station CNP averaged 5.8±1.9 μmoles O_2 m^{-2} h^{-1}. Intrastation variability exhibited no discernable longitudinal trends (Fig. 2), and ranged from an average of 3.46 μmoles O_2 m^{-2} h^{-1} (station 189) to 7.32 μmoles O_2 m^{-2} h^{-1} (station 139). Substation 189, in addition to showing the lowest average SCOC, had the highest number of manganese nodules (Smith et al., submitted).

Variability at the grab level, ≈0.1 m^2, can be seen in comparing the SCOC measured by each grab at a single deployment. The greatest variability was seen at substations 173 and 107 (range = 4.5 μmoles O_2 m^{-2} h^{-1}). The least variability was seen at substation 189 (range = 2.2 μmoles O_2 m^{-2} h^{-1}).

Generally at the substations of the CNP station, nitrogenous nutrient fluxes across the sediment-water interface showed a net flux out of the sediments. The sole exception was substation 189, where the net flux of

nitrate and ammonium was into the sediments. The combined flux of nitrate, nitrite and ammonium ranged from 0.65 μmoles N m^{-2} h^{-1} at substation 173 to 10.1 μmoles N m^{-1} h^{-1} at substation 107.

Considerable variability at the grab level exists in nutrient exchange rates. Adjacent grabs on the same deployment of the FVGR can exhibit opposite fluxes of the same species. Specific examples are nitrate at substations 173 and 139, and ammonium at substation 107 (see range bars, Fig. 3).

Both the sediment community oxygen consumption and nitrogenous nutrient exchange rates represent a summation of a variety of processes, both aerobic and anaerobic, occurring simultaneously in the sediment. To evaluate the overall exchange of dissolved oxygen and nitrogenous nutrients and provide a relative index for comparison at various spatial levels, we calculated the ratio of oxygen consumption to total nitrogen flux. The two western substations 173 and 139 exhibited the highest O:N values on a grab level, 1.47 to 3.83, while those ratios for substations 107 and 189 were an order of magnitude lower, 0.17 to 0.37. These ratios reflect the increased nitrogenous flux of the species we measured at the eastern substations.

Station G

Station G is located 2670 km to the east of station CNP in the Baja California seamount province (Fig. 1). The two substations comprising this station, 109 and 132, were occupied in September 1980. The bottom water of this station has a similar temperature and dissolved oxygen content to that of station CNP, despite its 1000-m shallower depth (Smith et al., submitted). Sediment organic carbon and total nitrogen and macrofaunal abundance were similar to that measured at the western CNP station, although the macrofaunal

biomass at one substation, 132, was an order of magnitude greater. The number of manganese nodules was lower at station G than at CNP, and were in fact present only at substation 132.

Sediment community oxygen consumption rates were distinctly higher at station G than at Sta CNP to the west (Fig. 2). The two substations comprising this station did not exhibit sediment community oxygen consumption rates significantly different from one another ($P>0.05$), with an overall mean value of 13 ± 3.1 μmoles O_2 m^{-2} h^{-1}. Both substations revealed considerable intergrab variation in SCOC rates with ranges as great as 7.1 μmoles O_2 m^{-2} h^{-1} at substation 132.

Nutrient exchange rates were measured at only one of the substations (132) at Sta G. The net flux of all three species of nitrogenous nutrients combined, 4.0 μmoles N m^{-2} h^{-1}, was into the sediments, estimated from a mean of the four grab measurements made on a single FVGR deployment. However, there was considerable intergrab variability in the nitrate and nitrite fluxes, exhibiting the full gamut from evolution to uptake by the sediments (Fig. 3). Two grabs displayed an uptake of both nitrate and nitrite while the other two showed evolution of both species. Ammonium was evolved in all four grabs and displayed little variability. The mean exchange rate of ammonium for all four determinations was higher than that measured at any other station (Fig. 3). Uptake of nitrate and nitrite suggests a preponderance of either nitrate reduction or denitrification processes while the release of these same species along with ammonium indicates ammonification and nitrification coupled with denitrification and nitrate reduction processes.

Oxygen consumption to nitrogenous nutrient flux ratios for substation G-132 are of the same order of magnitude as the eastern substations of Sta CNP.

exception of one grab and ranged from 0.11 to 0.47. The similarity in values between the CNP and G stations reflect a consistency in the relationship between oxygen consumption and nitrogenous flux, with both increasng proportionately.

Station F

To the east of Sta G and still in the Baja California seamount province is the third station on the transect, F (Fig. 1), at a water depth of 4392 m. Bottom water temperature and dissolved oxygen concentration were similar to the stations to the west. The surface sediments, however, showed increased total nitrogen and macrofaunal abundance when compared to the previous stations. Manganese nodules were present in each grab taken on the single FVGR deployment (Smith et al., submitted).

Oxygen consumption rates of sediments increase significantly over the western stations in approaching the North American continent. At Sta F, which consisted of one substation (177), the rates of SCOC in September were more than double those at Sta G. The intergrab variation at this station was greater than that measured at previous stations, ranging from 27.2 to 37.5 μmoles O_2 m^{-2} h^{-1}.

Net evolution of nitrogenous nutrients from the sediments at Sta F was 7.2 μmoles N m^{-2} h^{-1}. All three species of nitrogen were evolved, on the average, with nitrate being the dominant species (Fig. 3). In one grab, ammonium and nitrite fluxes were undetectable, but all other measurements showed evolution of all three species from the sediments. The grab in which nitrate only was evolved strongly suggests nitrification processes.

The O:N ratio for SCOC and nutrient exchange at this station increases an

order of magnitude in value over the previous station and is comparable to those values obtained for the westernmost substations of the CNP station, 173 and 39. Individual grab O:N ratios ranged from 1.58 to 3.87. The increased values over the previous station primarily reflects the increase in SCOC.

Station C

Station C, at the base of the Patton Escarpment, exhibits sediment community oxygen consumption rates an order of magnitude greater than Sta F. Macrofaunal abundance and biomass at this station is also markedly higher than any of the stations to the west. The mean abundance and biomass is 8 and 6 times higher, respectively, over those measured at Sta F (Smith et al., submitted). Only two measurements of SCOC were made at this station, 62.5 and 78.6 μmoles O_2 m^{-2} h^{-1}.

The net flux of the combined nitrogenous nutrients is out of the sediments at substation 125, 7.0 μmoles N m^{-2} h^{-1}, and is similar in magnitude to that measured at Sta G. However, there is a distinct difference between Stas C and F in the direction but not the magnitude of the nitrite flux. At station C nitrite is taken up by the sediments. There is little variability in the flux of each nutrient between grabs; all are in the same direction and of the same order of magnitude.

An examination of the O:N ratios for station C reveal an increase of up to one order of magnitude over station F. Intergrab variability in the O:N ratio is greater than at any of the previous stations, with values of 5.32 and 10.21 for the two grabs from which oxygen consumption and nutrient exchange data exist. The increase in the O:N ratio at this station again reflects increasing SCOC which is not matched by the nitrogenous nutrient fluxes.

Station SCB

The highest rates of SCOC we measured along the transect were at Sta SCB in the Santa Catalina basin during January and February. This basin is located at a depth of 1300 m due west of Santa Catalina Island in the Southern California Continental Borderlands. Sediment community oxygen consumption measurements at two substations, 110 and 125, were not significantly different ($P>0.05$) from one another and revealed less intergrab variability than recorded at Sta C. Station SCB differs from other stations in having increased temperature, sediment organic carbon and total nitrogen, and macrofaunal abundance and biomass, and decreased bottom water oxygen concentration, lower than the other stations by an order of magnitude.

The three substations which consititute Sta SCB show considerable variability in the direction and magnitude of flux of all three nutrients, especially nitrate (Fig. 3). Nitrate is consumed by the sediments at two substations, 101 and 125, but is evolved at the third, 110. Substations 110 and 101 were occupied within a temporal range of 2 days and a spatial range of 0.7 km. Nitrite fluxes also exhibited considerable variability. Ammonium is evolved at all three substations and fluxes show considerable variability in magnitude, although they are within the range measured at the other substations along the transect. The net flux of nitrogenous nutrients is into the sediments at substations 101 and 125, 16.1 and 9.0 μmoles N m^{-2} h^{-1}, and out of the sediments at substation 110, 1.91 μmoles N m^{-2} h^{-1}.

On a smaller scale, the measurements made from each grab at all three substations exhibit a large variability in magnitude and direction (Fig. 3). Nitrate was the most variable, being evolved and consumed at similar magnitudes in adjacent grabs. Ammonium was evolved in all grabs with one

exception at substation 125.

The O:N ratios calculated for the two substations, 110 and 125, exhibited considerable variability but are within the same order of magnitude ranges as values from Sta C. At the substation level, the greatest variability is between the two grabs of substation 125 which have O:N values of 2.34 and 68.97. Much of this variability is attributable to the erratic nitrogenous nutrient fluxes in each grab.

Transect Analysis

Both SCOC and nitrogenous nutrient exchange rates should provide an indication of the rate at which organic matter is remineralized in deep-sea aerobic sediments. A plot of SCOC vs total nitrogen flux for all substations shows a general trend of increasing O:N ratio toward the east (Fig. 4). Total nitrogen flux does not, however, increase at the same rate as SCOC. Anomalous individual measurements are present from Stas G and SCB. All O:N ratios with one exception fall below the predicted value for the decomposition of organic matter in seawater of 17.25:1 (Redfield, Ketchum and Richards, 1963).

The major components of the total nitrogen flux we measured are fluxes of ammonium and nitrate, representing the processes of ammonification and nitrification. Dividing the total nitrogen flux into these two components and comparing the components with SCOC showed no obvious trends not expressed in the total nitrogen flux. The lack of a clear relationship between SCOC and nitrogenous nutrient flux may be due to several factors: 1) Our "total nitrogen flux" is comprised of the fluxes of nitrate, nitrite, and ammonium. Other nitrogen species, such as N_2 gas, nitrous oxide, and dissolved organic nitrogen, were not measured, and may in fact contribute to the total nitrogen

flux. 2) Our analyses on various spatial scales show a great deal of heterogeneity in the sediments on all scales. 3) Processes which occur in these alleged "aerobic sediments" are complex, and may include processes usually considered to be anaerobic, such as denitrification (Smith et al., submitted).

The dependence of SCOC and nitrogenous nutrient exchange on other measured parameters was examined using a multiple regression analysis (Ryan, Joiner and Ryan, 1976). From this analysis, we can generate a simple predictive equation for the flux rates of O_2 and nitrogen species. The analysis was performed on three levels, grab, substation and station, to examine possible associations on fine to coarse spatial scales.

Inter-grab level.--A single deployment of the FVGR (one substation) is composed of four grabs. The parameters measured in each grab were oxygen consumption, nitrogenous nutrient flux (nitrate, nitrite, ammonium), macrofaunal abundance, macrofaunal biomass, manganese nodule number, and manganese nodule displacement volume. Manganese nodules were present only at the three westernmost stations, and were included in the intergrab analysis only at the CNP station.

Among the grabs which comprise the CNP station (seven deployments), SCOC was positively correlated with macrofaunal abundance ($r = 0.86$) and negatively correlated with manganese nodule number ($r = -0.93$). Attempts to generate a predictive equation of SCOC based on macrofaunal abundance and manganese nodule number from all the grab measurements failed to provide a regression line with a slope significantly different from zero. This was primarily a result of two extreme macrofaunal abundance values, separated by two orders of magnitude: 24 individuals m^{-2} (246c) and 1210 individuals m^{-2} (139c). The

inclusion of additional independent variables or various transformations did not improve the fit.

Inter-substation level.--Each substation is a single deployment of the FVGR. The number of substations per station ranges from 7 (CNP) to 1 (F and C). Parameters measured on the substation level but not on the grab level include: depth, bottom water measurements of dissolved O_2 (ml l^{-1}), ammonium (μM), nitrite (μM), nitrate (μM), surface sediment measurements of organic carbon (mg g^{-1}) and total nitrogen (mg g^{-1}) and pore water measurements of ammonium, nitrite and nitrate. A single grab was selected randomly from each substation to provide values for the parameters measured on the grab level (see above), and a correlation matrix of all these parameters was generated.

Four parameters were highly associated with SCOC: depth ($r = -0.988$), macrofaunal abundance ($r = 0.949$), bottom water dissolved oxygen ($r = -0.928$), and sediment total nitrogen ($r = 0.947$). There were no obvious relationships between the fluxes of nitrogenous nutrients and any of the other variables. A randomly selected grab was chosen from each substation for SCOC and macrofaunal number and combined with substation data for dissolved oxygen, depth, and sediment total nitrogen in a stepwise regression analysis. An attempt was made to select an equation which accounted for the highest variability in SCOC while maintaining a minimum number of independent variables because of the very limited degrees of freedom. The resulting equation was:

$$Y = 75.6 - 0.012\ Z + 0.005\ MA \qquad (1)$$

where Y is sediment community oxygen consumption (μmoles O_2 m^{-2} h^{-1}), Z is water depth (m) and MA is macrofaunal abundance (individuals m^{-2}). This equation accounts for 99.7% of the variability in SCOC with a standard

deviation of 2.34 about the regression line and 9 degrees of freedom. Depth alone accounted for 87.6% of the variation in SCOC. The inclusion of additional independent variables or various transformations did not improve the fit. This equation, generated from 12 individual measurements of SCOC from each of 12 substations, is a reasonable predictor for the other measured values of SCOC (Fig. 5a).

Inter-station level.--Each of the five stations which constitute the CNP-ENP transect is composed of 1-7 substations. One substation was selected randomly from each station and one grab was selected randomly from within that substation to represent the parameters measured on the grab level for that station. SCOC was highly correlated with depth ($r = -0.93$) and macrofaunal abundance ($r = 0.95$). A predictive equation for SCOC was generated from a stepwise regression analysis with depth (Z) and macrofaunal abundance (MA) as independent variables:

$$Y = 115.0 - 0.020\ Z + 0.004\ MA \qquad (2)$$

This equation accounts for 99.1% of the variability in SCOC with a standard deviation of 4.71 around the regression line and 2 degrees of freedom.

There is a marked similarity between the station and substation predictive equations. In the station analysis, we eliminated the bias of unequal numbers of substations while sacrificing degrees of freedom. The predictive quality of the station equation is less than that of the substation equation (Fig. 5b). Predictive values for SCOC in the CNP station are underestimates and are frequently below zero, while those for Stas G, C, and SCB are overestimates. The reduction in the number of measurements used to generate the station equation and the resulting reduction in the number of degrees of freedom influence the quality of the regression equation.

Sediment community oxygen consumption is highly correlated positively with macrofaunal abundance and negatively with water depth at each of the three spatial levels we have examined. In addition, manganese nodule number was negatively correlated with SCOC at the grab level. The flux of nitrogenous nutrients was not obviously correlated with any of the variables we measured.

Expectedly, the predictive equations of SCOC mirrored the correlation matrix analyses in that depth and macrofaunal number were the best predictive variables. The exception was at the grab level, where the spatial variability in macrofaunal number was sufficient to prevent the generation of a statistically acceptable predictive equation for SCOC. On the substation and station levels, depth is the most important variable in predicting SCOC.

DISCUSSION

Three methods have been used to measure sediment community oxygen consumption (SCOC) in the deep sea: the electron transport system method (ETS) (Christensen and Packard, 1977), the laboratory core method (Pamatmat, 1973) and the *in situ* method (Smith and Teal, 1973; Smith *et al.*, 1979; Hinga, Sieburth and Heath, 1979). Both the ETS and laboratory core methods involve the use of decompressed sediment samples for biochemical analyses and direct oxygen consumption measurements in the laboratory. SCOC measurements made with all three methods exhibit a decrease in magnitude with increasing water depth over a range from 250 m in the eastern North Pacific off the Columbia River to 7000 m in the Aleutian Trench (Fig. 5). The least depth dependence is exhibited by the laboratory core incubation measurements, which vary from 50 to 214 μmoles O_2 m^{-2} h^{-1} over the depth range from 150 to 700 m (Pamatmat, 1973); depth accounts for only 4% of the variability in laboratory-measured

SCOC. In contrast, the in situ measurements in the Atlantic and Pacific span three orders of magnitude although they are measured over a smaller depth range. The best fit of these in situ SCOC measurements with depth was to a logarithmic function with a regression coefficient of 0.72. The in situ SCOC measurements fall between the higher SCOC measured with the laboratory core method and the lower estimates obtained with the ETS method. In a comparison of the laboratory core method and in situ method at a 3000-m station in the western North Atlantic, order of magnitude higher values of SCOC were obtained with the laboratory method (Smith, 1978).

The comparisons above indicate that the various methods used to measure SCOC contribute to the wide range of reported values. Our results reported here along the CNP-ENP transect indicate that variation can occur in measurements obtained by a single method. We attribute the observed variability within the in situ measurements in spatial and temporal variation. All of the measurements of SCOC in Fig. 6 represent mean values for stations or substations which are generally separated by distances greater than 100 km. SCOC measured at the same station at the same time of year in the central North Pacific exhibits considerable variation within a radius of 89 km (Sta CNP, Fig. 2). On a smaller scale, we have observed variation in SCOC even between grabs on the same FVGR deployment, a distance of less than 1 m. Greater small-scale variability in SCOC has been reported by Hinga and associates (1979) in the North Atlantic and Gulf of Mexico. On single deployments of an in situ respirometer, they recorded order of magnitude differences in SCOC in the Gulf of Guinea at 4000 m and in the western North Atlantic at 1345 m.

Temporal variation in SCOC in the deep sea is also important to consider.

Measurements of SCOC at Sta C at two different seasons in our study and that of Smith et al. (1979) exhibit an order of magnitude change at a depth of 3815 m (Fig. 6). However, rates of sediment community oxygen consumption at the oligotrophic stations in the western North Atlantic at slope and rise depths off New England reveal no significant difference ($P>0.05$) between seasons (Smith, 1978).

Depth of the water column overlying the sediment community has been shown to be an important variable for predicting SCOC in the deep ocean. Smith (1978) developed a predictive equation for SCOC along a transect of stations in the western North Atlantic Ocean:

$$\ln Y = 2.93 - 0.001\ (D) + 0.15\ (C{:}N) + 0.11\ (1/N) - 0.65\ (T) + 142.7\ (1/B)$$

where D is depth (m), C:N is organic carbon to nitrogen ratio in surface sediment, N is total nitrogen, T is bottom water temperature, and B is macrofaunal biomass. The depth parameter accounted for 83.1% of the variation in SCOC. We applied this equation to our measurements of SCOC from the CNP-ENP transect and to other in situ measurements from the literature where values for the independent variables were available. The western North Atlantic equation generally over-predicts SCOC by one to 20 orders of magnitude in the central North Pacific stations where there is very low macrofaunal biomass (Fig. 7a). At those CNP substations with higher biomass and great depth, there was closer agreement between observed and predicted SCOC (substations 173, 189 and 281) (Smith et al., submitted). At stations of intermediate depth along the CNP-ENP transect, the underestimate of SCOC increased with increasing macrofaunal biomass and surface productivity, and decreasing depth. At the other extreme of the transect, where stations exhibited high macrofaunal biomass and shallow depth, the western North

Atlantic equation again overestimated SCOC by a factor of 2 to 20.

For comparative purposes, we can ask how well our predictive equation for the CNP-ENP transect predicts SCOC measurements made in other areas of the World Ocean. We have taken measurements of SCOC reported in the literature which were made using comparable *in situ* methods and where macrofaunal abundance estimates were available. Our substation equation (1) generally overestimates SCOC measurements from the western North Atlantic stations and deviates notably from those stations on the continental margin off New England (Fig. 7b). Observed values of SCOC measured at two stations, one on the continental slope off Cape Hatteras and one on the abyssal plain in the Gulf of Mexico (Hinga *et al.*, 1979) are predicted well by our equation. Measurements of SCOC made in the San Diego Trough (Smith, 1974), which is adjacent to the Santa Catalina Basin on the Southern California Continental Borderlands, also shows close agreements with predicted rates (Fig. 7b).

There are two measurements of SCOC which are conspicuously underestimated by the CNP-ENP transect predictive equation (1), one in the Tongue of the Ocean, and one in the eastern North Pacific at the base of the Patton Escarpment. The Tongue of the Ocean station is located at a depth of 2000 m in close proximity to land and has a high SCOC (Smith in Wiebe, Boyd and Winget, 1976) with a low abundance of macrofauna. The macrofaunal abundance at this station is an order of magnitude lower than that estimated for stations at comparable depths in the western North Atlantic and North Pacific. The second measurements of SCOC which are strongly underestimated by the CNP-ENP transect equation were made at station C on the same transect but at a different time of the year (Smith *et al.*, 1979). This seemingly anomalous measurement was made in November while those measurements presented in our

study were made in February. This temporal variation may be a reflection of the seasonal supply of organic matter from the continent and the overlying water column. The higher rates of SCOC in November correspond to increased rates of ammonium evolution from the sediments. A seasonal variation in sedimenting particulate organic matter has been measured in the western North Atlantic at abyssal depths which correlates directly with primary productivity in the surface waters (Deuser and Ross, 1980). There is no reason not to expect the same seasonal variation in SCOC, especially in a highly productive region influenced by seasonal upwelling as off southern California. However, Smith (1978) did not find seasonal differences in SCOC between 300 and 3650 m in the western North Atlantic. We are currently examining the seasonal variation in SCOC and sedimentation rates along the entire CNP-ENP transect.

There are few measurements of nitrogenous nutrient flux across the sediment-water interface in the deep sea to compare with our measurements. Smith and associates (1979) measured ammonium, nitrate, and nitrite flux at two stations in the eastern North Pacific, one on the CNP-ENP transect (Sta C) in the eastern North Pacific and one in the Southern California Continental Borderlands in the San Diego Trough, immediately adjacent to Sta SCB. Ammonium was evolved at both of these stations and in significantly higher amounts than in our measurements at Stations C and SCB (Fig. 8). However, these fluxes were an order of magnitude lower than the *in situ* flux rates of ammonium measured at shallow slope depths (278 m) in the Gulf of Guinea (Hinga *et al.*, 1979). At deep slope depths (2200-2750 m) in the western North Atlantic, ammonium evolution from the sediemnts (Smith *et al.*, 1978) was comparable to that measured at most of our CNP-ENP stations (Fig. 8).

Nitrate flux measurements both in our study and those of others are

highly variable in magnitude and direction. In the San Diego Trough (A-26), nitrate was consumed by the sediments at a rate within the wide range we measured at Sta SCB (Smith et al., 1979) (Fig. 8 and Fig. 3). However, at Sta C-66 nitrate was evolved at an order of magnitude higher rate during November (Smith et al., 1979) than during our study (C-125) in February. Flux rates of nitrate measured at both stations in the western North Atlantic are negative and fall within the range of values measured along the CNP-ENP transect (Fig. 8 and Fig. 3).

Nitrite fluxes are of low and comparable magnitude in the western North Atlantic, eastern North Pacific and along our CNP-ENP transect (Fig. 8 and Fig. 3). One exception is the high nitrite evolution measurements made in the San Diego Trough (station A-26) (Smith et al., 1979).

The comparison of nitrogenous nutrient flux rates across the sediment-water interface measured in a variety of environments reveal considerable variability in magnitude and direction. It is not unreasonable to expect such variability, which can be a result of both spatial and temporal differences as exhibited in SCOC. The wide range of nutrient flux rates between grabs of a single FVGR deployment demonstrates the small scale spatial variation (Fig. 3). Seasonal differences are also apparent when comparing measurements made at Sta C in November (Smith et al., 1979) and in February (this study) (Fig. 8).

A net production or consumption of a given nutrient will result in a measured flux of that nutrient on the short (1-4 days) time scales of incubation. Alternatively, fluxes of nutrients from the sediments can be inferred from pore water nutrient profiles (see, for example, Sayles, 1979, 1981) on the much longer time scales of sediment accumulation.

Fluxes across the sediment-water interface are controlled by processes occurring at the interface or within the sediment column. Many of these processes, resulting in changes in the oxidation state of nitrogen, are biologically mediated by bacteria. Ammonium is produced in the heterotrophic breakdown of organic matter that reaches the sediment. Two processes may contribute: microbial ammonification and animal excretion. Apparent "consumption" of ammonium may occur by adsorption of the cation to sediment particles (Rosenfeld, 1979). Microbially, ammonium can be consumed in the process of nitrification, in which it is transformed in two stages to nitrite and then nitrate. Nitrite, considered to be an intermediate in bacterial nitrification, is also produced in the process of denitrification, generally thought to be an anaerobic bacterial process. Nitrite produced by denitrification may be further reduced to nitrogen, N_2. N_2 was not measured in this study, but has been shown to be an important component of the nitrogen cycle in shallow water (Seitzinger, Nixon, Pilson and Burke, 1980) and deep-sea sediments (Barnes, Bertine and Goldberg, 1975). Nitrate is consumed in the process of denitrification and is produced in the process of nitrification.

We can compare the measured fluxes made on short time scales with predicted fluxes estimated on longer time scales from pore water profiles. A similar exercise was done by Klump and Martens (1981) in a high organic coastal marine basin. They point out that observed and predicted fluxes should agree only if net interface processes are unimportant. In our study, fluxes of nitrogenous nutrients across the sediment-water interface were measured directly during the short-term incubation of the FVGR by taking the difference in initial and final nutrient concentrations. The flux thus measured is the sum of various processes which produce or consume the measured

nitrogenous nutrients during the course of an incubation in the sediment enclosed by a single grab. These measurements made in a closed system are subject to errors resulting from the lack of natural current flow and ion concentration gradients which are of unknown importance.

Spatial heterogeneity of the processes which produce and consume nitrogenous nutrients exists on a centimeter-to-meter scale (see Fig. 3, measurements and range bars). The flux of a given nutrient may differ not only by orders of magnitude, but may also differ in direction (into or out of the sediments) between grabs in a single deployment. Due to this spatial heterogeneity, we chose to compare the predicted diffusive flux with the measured flux from the single grab in the deployment from which pore water measurements were made. If the pore water nutrient profile represents the long-term sum of processes which produce or consume nitrogenous nutrients, and if our measured fluxes represent only those processes which occur during the 1- to 4-day incubation, comparison of the observed and calculated fluxes should give an indication of the temporal heterogeneity of the processes. For the purposes of comparison, the mean flux of nitrogenous nutrients from a given substation (deployment) are also presented in Table 1.

The predicted flux of nitrogenous nutrients across the sediment-water interface can be calculated from the gradient of the nutrient, using the nutrient concentrations measured in pore water and in the overlying water, assuming a diffusive flux across the sediment-water interface. For comparison with direct flux measurements, we have made these calculations for ammonium, nitrite, and nitrate. We used two measured nutrient concentration points, one immediately above (0-1 cm) and one immediately below (0-1 cm) the sediment-water interface (Smith *et al.*, submitted). Admittedly, this forces us to

place a great deal of emphasis on only two measured points. However, we felt there was little theoretical basis to fit a curve to the highly irregular pore water nutrient profiles (Fig. 9). For ammonium only, we also calculated the expected flux by disregarding the irregularities in the profiles and drawing a curve by eye through the measured points (solid continuous line in Fig. 9). The resulting ammonium concentration at 5 cm depth was then used in the diffusive equation assuming a linear flux across the upper 5 cm of the sediment column. This is similar to the method used by Sayles (1981) which he claims gives an approximation by underestimates the flux of his model by up to 50%.

The simple diffusive equation:

$$J = \phi D_b \frac{\Delta c}{\Delta d}$$

where J = flux in moles m^{-2} h^{-1};

ϕ = porosity (taken as 0.75 cm_p^3 cm_b^{-1} [McDuff and Gieskes, 1976]);

D_b = diffusion coefficient (taken as 10^{-6} cm_b^2 sec^{-1} [McDuff and Gieskes, 1976]);

$\frac{\Delta c}{\Delta z}$ = concentration gradient of the ion in question

is used in our calculations, where z is 0.5 or 5 cm. This equation ignores the process of bioturbation which has been shown to be an important mechanism in the transport of ions across the sediment-water interface in shallow water (Aller, 1980; McCaffrey, Myers, Davey, Morrison, Bender, Luedtke, Cullen, Froelich and Klinkhammer, 1980). The magnitude and resulting effect of bioturbation in deep-sea sediments cannot be assessed. Macrofaunal bioturbation has little effect on nitrogenous nutrient fluxes even in shallow water, however (Aller, 1980).

The comparison of the measured fluxes with the predicted fluxes using the

two methods of estimating the concentration gradient are summarized in Table 1. All predicted values for ammonium flux are small and positive with the exception of Sta CNP-189, which may be anomalous due to large numbers of manganese nodules or to bioturbation because the macrofaunal biomass is unusually high at this substation (Smith et al., submitted). Predicted fluxes of ammonium calculated from two points over the 0.5 cm depth interval agree more closely with the measured fluxes than do those estimated from the 5 cm depth interval. The positive flux indicates net production of ammonium in the sediments, most likely from the breakdown of organic matter. The small values indicate either a small supply of organic matter to the sediments or coupled consumption of ammonium by the process of nitrification. Measured fluxes are sometimes much larger than predicted values (132-G, 177-F). This could indicate increased heterotrophic breakdown due to a large input of organic matter. Differences in observed and predicted fluxes were seen by Klump and Martens (1981) in shallow water. The environment they studied is not analogous to the deep sea; nevertheless, their conclusion that processes occurring at the sediment-water interface may override diffusive fluxes calculated from pore water nutrient profiles is pertinent to our work.

All predicted values of nitrite flux are small and positive, indicating net production of nitrite in the sediment, due most likely to the process of bacterial nitrification. Measured fluxes of nitrite are also low, but indicate that nitrite can be either produced or consumed. Two explanations exist: 1) on the short time scale, the two stages of nitrification may not be closely coupled, or 2) denitrification may occur at certain places (e.g., 132-G and 125-C). Denitrification, thought to be an anerobic process, may occur locally in otherwise aerobic sediments (Wilson, 1978). The enzyme system involved in denitrification and nitrate reduction can be produced in

bacteria under oxygenated conditions (Sugahara, Sugiyama and Kawai, 1974).

Predicted values of nitrate flux are small compared to measured fluxes and both predicted and measured fluxes vary in direction, indicating that either production or consumption of nitrate may occur. We assume this represents the fluctuating importance of the processes of nitrification (production of nitrate) and denitrification (consumption of nitrate). The low predicted fluxes indicate that these processes are of equivalent importance, or else occur very slowly, in the sediment. On a short time scale, however, at the interface, one process may be much more important than the other, as indicated by large positive and negative values in the measured fluxes. Predicted fluxes represent the overall processes which occur on long time scales in the sediment. They do not, however, represent the short-term processes which occur at the sediment-water interface, such as the remineralization of non-refractory organic matter, which is not recorded in the "historic" pore water profiles. The measured fluxes are a composite of short-term processes and the long-term processes, while the pore water profile calculations are an underestimate of the total metabolic activity. The comparison of the quality and quantity of the organic material entering the benthic boundary layer and that in the surface sediments certainly illustrates this discrepancy (Rowe and Gardner, 1979; Honjo, 1980).

Dissolved oxygen profiles for pore waters in the central equatorial Pacific (Murray and Grundmanis, 1980) should be evaluated in light of these same temporal and spatial scales when compared to measured sediment-water interface fluxes of oxygen. Our reported measurements of SCOC have been made on a short time scale and probably do not equal oxygen consumption rates estimated from pore water profiles of dissolved oxygen, which reflect long

time scales, in excess of our 1- to 4-day incubation periods.

The question arises as to what does influence sediment community metabolism (oxygen consumption and nitrogenous nutrient exchange). Are there important controlling parameters we have ignored in the above analysis, such as surface water primary productivity, or sedimentation rate? We have reported increases in rates of SCOC and nitrogenous nutrient exchange rates from the central toward the eastern Pacific. Although depth accounts for the major part of the variability at least in the SCOC values, this does not imply that depth per se (i.e., hydrostatic pressure) is a controlling factor of these rates. The primary productivity of the overlying surface water along the transect increases toward the east. Primary productivity estimates, based on ^{14}C-HCO_3^- incubations range from 60 g C m^{-2} yr^{-1} in the central gyre area (Sta CNP) to 300 g C m^{-2} yr^{-1} in the midcurrent area of the California upwelling system off southern California (Sta C). These estimates of annual productivity are difficult to compare specifically with our sediment community metabolism measurements because 1) our measurements have been made at only one point in time and 2) the annual productivity estimates are themselves based on a limited number of 1-day measurements made at different times throughout the year.

Seasonal differences may have a significant impact when comparing sediment activity and surface water productivity measurements. Deuser and Ross (1980) reported that the rate of sedimenting particulate organic matter in the Sargasso Sea is seasonal and reflects, even at abyssal depths, the seasonality of primary productivity in the overlying water. There is no observed phase shift between the periodicities in these two fluxes, suggesting a bulk settling rate of particulate organic matter of less than 60 days at

3200 m depth (Deuser, Ross and Anderson, 1981). Sediment community oxygen consumption and nitrogenous nutrient exchange rates we measured at Sta C in February were significantly lower than similar measurements made at the same station in November (Smith et al., 1979). There is seasonality in primary productivity along the CNP-ENP transect. Seasonal peaks in productivity occur in late winter/early spring for the central North Pacific (McGowan, 1974) and in the spring for the eastern North Pacific (Eppley, Reid and Strickland, 1970). These observations, coupled with the fact that organic matter produced in the surface water is transported rapidly to the bottom in the form of fecal pellets (Wiebe, Boyd and Winget, 1976; Turner, 1977; Honjo and Roman, 1978) have prompted us to compare sediment metabolism rates with daily productivity rates measured during the same season and, when available, the same month.

Sediment community oxygen consumption and nitrogenous nutrient exchange rates measured in this study are not obviously related to surface water primary productivity using either seasonal or annual estimates. Regression analysis revealed that only a small percentage of the variation in SCOC and nutrient flux is attributable to daily rates of primary productivity available in the literature. Adding other SCOC and nutrient exchange rate measurements for two stations in the eastern North Pacific (Smith et al., 1979) and two stations in the western North Atlantic (Smith, White, Laver and Haugsness, 1978) to the regression analysis did not improve the relationship with surface primary productivity.

Two factors which complicate the comparison of sediment community metabolism with surface primary productivity are remineralization of organic matter in the water column and midwater repackaging and advective processes. A large percentage of the organic matter produced in the euphotic zone is

remineralized there (Eppley and Peterson, 1979). The amount of this organic matter present in the aphotic water column which escapes decreases with depth (Honjo, 1980). However, Knauer and Martin (1981) have found a general decrease in organic matter with depth to 1500 m where they report a significant increase. This increase corresponds to an increase in the number of fecal pellets which are quantitatively different from those trapped at shallower depths, which implies repackaging and horizontal advection from other areas (Knauer and Martin, 1981; Urrere and Knauer, 1981).

A more vaid comparison would be between sediment community metabolism (oxygen consumption and nutrient exchange) and the rate at which sedimenting particulate organic matter enters the benthic boundary layer. Synoptic measurements of these rates in the deep sea have been made at only one of our stations (SCB) and at two stations in the western North Atlantic (DWD and ADS) (Smith et al., 1978; Rowe and Gardner, 1979).

We have calculated the carbon and nitrogen demand in the Santa Catalina basin stations and compared it to the carbon and nitrogen supply measured at the same station and time (Table 2). Sediment community oxygen consumption was converted to organic carbon, assuming a respiratory quotient of 0.85. Total nitrogenous nutrient exchange was a summation of ammonium, nitrate and nitrite rates of flux, regardless of the direction of the flux.

The carbon supply as determined from particle interceptor traps (Soutar, Singleton, Butler and Baxter, 1978) was insufficient to meet the carbon demands estimated from sediment community oxygen consumption, providing only 37-40% (Table 2). A comparison of the supply and demand of nitrogen produced erratic results due to the high variability in nitrogenous nutrient exchange rates between grabs in a single substation. In two grabs, one from each

substation, the supply of nitrogen was more than sufficient to meet the estimated demands of the sediment community (Table 2). However, the input of particulate nitrogen was less than sufficient to meet the estimated demands in the other two grabs.

These estimates of supply and demand for the Santa Catalina Basin contrast those calculated for two deep slope stations in the western North Atlantic (Smith et al., 1978; Rowe and Gardner, 1979). The supply of organic carbon to these stations is in excess of the estimated demand at both stations (Table 2). However, the supply of particulate nitrogen is sufficient to meet the estimated sediment community demand only at station DWD and is insufficient at station ADS.

Other sources of organic matter to the sediment community not measured with the particle interceptor traps include large organic falls (e.g., fish, kelp) and migration of prey species. The discrepancy between the supply and demand of organic carbon in the Santa Catalina Basin can most probably be explained by these unmeasured sources, especially the kelp Macrocystis which is often observed on the bottom in this nearshore environment (K. Smith, pers. obs.). In the more oligotrophic stations further from shore on the slope in the western North Atlantic, the sedimenting small particulate matter is probably the predominant supply of organic matter.

In these comparisons, we have ignored other consumer components of the benthic boundary layer, such as the plankton, benthopelagic animals, and epibenthic megafauna. These consumer groups have generally been discounted in past considerations of carbon flow as being insignificant. Smith (in press) has recently shown that one group, the plankton, consisting of microorganisms and zooplankton, constitutes a very significant consumer of food energy in the

benthic boundary layer community of the Santa Catalina Basin (1300 m). The plankton in the 50-m water column above the bottom has an estimated carbon demand of 30.8 mg C m^{-2} day^{-1}, of which 98% is attributed to bacterioplankton. This demand of the plankton is equal to that of the sediment community at the same station (Table 2). It must be kept in mind, however, that the SCOC and plankton metabolism measurements were not made synoptically, the plankton measurements being made in June and the SCOC in January/February. Regardless, these results stress the possible importance of other benthic boundary layer consumer components in the utilization of organic matter entering the system. We are currently investigating the importance of other BBL consumer components.

Furthermore, we can compare our measured nutrient fluxes with those which would be expected from model estimates. Craig (1969) and Munk (1966) produced early two-dimensional models which predict oxygen utilization in the water column. More recently, Fiadeiro (1975) has presented a three-dimensional model for the distribution of tracers such as NO_3^- or O_2. Fiadeiro found the best fit for observed NO_3^- distributions to have a production consumption term J such that

$$J = J_1 \exp(-\beta(z-1))$$

where $J_1 = 45 \times 10^{-3}$ µmoles kg^{-1} yr^{-1};

$\beta = 1.2$ km^{-1};

z = depth in kilometers.

By integrating this equation over the distance from 1 to 4 km (limits imposed by Fiadeiro's model), we find the production of NO_3^- in the water column over this distance to be 36 µmoles m^{-2} yr^{-1}.

A reasonable value for primary production in the central North Pacific is

5 moles C m^{-2} yr^{-1} (T. Hayward, pers. comm.). Using the Redfield ratio for C:N, we expect 0.7 moles N m^{-2} yr^{-1} to be produced in the euphotic zone. About 5%, 36 μmoles m^{-2} yr^{-1}, of this organic N is remineralized in the water column from 1 to 4 km, according to the model.

If 90% of organic N is recycled in the euphotic zone (Eppley, Sharp, Renger, Perry and Harrison, 1977), then half the remineralization of N which occurs should happen in the water column between 1 and 4 km. According to our calculated values of NO_3^- flux, 1.2 μmoles N m^{-2} yr^{-1} are produced in the sediments at Sta CNP-173. This is <0.2% of the organic N produced in the euphotic zone, and is consistent with much of the remineralization of N occurring in the water column.

We have found an increase in SCOC along a transect of stations along a gradient of increasing surface primary productivity in the North Pacific Ocean. Most of the variability in SCOC at both the inter-station and inter-substation level can be explained by the parameters of depth and macrofaunal abundance. Predictive equations for SCOC based on these parameters were generated. Nitrogenous nutrient flux measurements along the same transect were highly variable and showed no east-west trend. We propose that much of the small-scale variability in nitrogenous nutrient flux is due to temporal and spatial heterogeneity in the sediments.

Acknowedgements:

This research was supported by NSF grants OCE-76-10728, OCE-78-08640 and OCE-81-17661 and a contract from Sandia Laboratories to KLS. We thank M. Laver, R. Baldwin, N. Brown, P. Klement, S. Hamilton and A. White for expert technical assistance and T. Dingler for help with the statistical analyses.

REFERENCES

ALLER, R. C. (1980) Relationships of tube-dwelling benthos with sediment and overlying water chemistry. In: Marine Benthic Dynamics, K. R. TENORE and B. C. COULL, editors, University of South Carolina Press, pp. 285-308.

BARNES, R. O., K. K. BERTINE and E. D. GOLDBERG (1975) N_2:Ar nitrification and dentrification in southern California borderland basin sediments. Limnology and Oceanography, 20, 962-970.

CARPENTER, J. H. (1965) The Chesapeake Bay Institute technique for the Winkler dissolved oxygen method. Limnology and Oceanography, 10, 141-143.

CHRISTENSEN, J. P. and T. T. PACKARD (1977) Sediment metabolism from the northwest African upwelling system. Deep-Sea Research, 24, 331-343.

CRAIG, H. (1969) Abyssal carbon and radiocarbon in the Pacific. Journal of Geophysical Research, 74, 5491-5506.

DEUSER, W. G. and E. H. ROSS (1980) Seasonal change in the flux of organic carbon to the deep Sargasso Sea. Nature, 283, 364-365.

DEUSER, W. G., E. H. ROSS and R. F. ANDERSON (1981) Seasonality in the supply of sediment to the deep Sargasso Sea and implications for the rapid transfer of matter to the deep ocean. Deep-Sea Research, 28A, 495-505.

EPPLEY, R. W. and B. J. PETERSEN (1979) Particulate organic matter flux and plankton new production in the deep ocean. Nature, 282, 677-680.

EPPLEY, R. W., F. M. H. REID and J. D. H. STRICKLAND (1970) Estimates of phytoplankton crop size, growth rate, and primary productions. In: The Ecology of the Plankton off La Jolla, California, in the Period April through September, 1967, Bulletin Scripps Institution of Oceanography 17, pp. 33-42.

EPPLEY, R. W., J. H. SHARP, E. H. RENGER, M. J. PERRY and W. G. HARRISON (1977) Nitrogen assimilation by phytoplankton and other microorganisms in

the surface waters of the central North Pacific Ocean. Marine Biology, 39, 111-120.

FIADEIRO, M. E. (1975) Numerical modeling of tracer distributions in the deep Pacific Ocean. Ph.D. thesis, University of California, San Diego, 226 pp.

GARDNER, W. S., D. S. WYNNE and W. M. DUNSTAN (1976) Simplified procedure for the manual analysis of nitrate in seawater. Marine Chemistry, 4, 393-396.

HINGA, K. R., J. McN. SIEBURTH and G. R. HEATH (1979) The supply and use of organic material at the deep-sea floor. Journal of Marine Research, 37, 557-579.

HONJO, S. (1980) Material fluxes and modes of sedimentation in the mesopelagic and bathypelagic zones. Journal of Marine Research, 38, 53-97.

HONJO, S. and M. R. ROMAN (1978) Marine copepod fecal pellets: production, preservation and sedimentation. Journal of Marine Research, 36, 45-57.

KANWISHER, J. (1959) Polarographic oxygen electrode. Limnology and Oceanography, 4, 210-217.

KLUMP, J. V. and C. S. MARTENS (1981) Biogeochemical cycling in an organic rich coastal marine basin - II. Nutrient sediment - water exchange processes, Geochimica et Cosmochimica Acta, 45, 101-121.

KNAUER, G. A. and J. H. MARTIN (1981) Primary production and carbon-nitrogen fluxes in the upper 1500 m of the northeast Pacific. Limnology and Oceanography, 26, 181-186.

McCAFFREY, R. J., A. C. MYERS, E. DAVEY, G. MORRISON, M. BENDER, N. LUEDTKE, D. CULLEN, P. FROELICH and G. KLINKHAMMER (1980) The relation between pore water chemistry and benthic fluxes of nutrients and manganese in Narragansett Bay, Rhode Island. Limnology and Oceanography, 25, 31-44.

McDUFF, R. E. and J. M. GIESKES (1976) Calcium and magnesium profiles in DSDP waters: diffusion or reaction? Earth and Planetary Science Letters, 33, 1-10.

McGOWAN, J. A. (1974) The nature of oceanic ecosystems. In: The Biology of the Oceanic Pacific, C. B. MILLER, editor, Oregon State University Press, pp. 9-28.

MENZIES, R. J. and G. T. ROWE (1968) The LUBS, a large undisturbed bottom sampler. Limnology and Oceanography, 13, 708-714.

MUNK, W. (1966) Abyssal recipes. Deep-Sea Research, 13, 707-730.

MURRAY, J. W. and V. GRUNDMANIS (1980) Oxygen consumption in pelagic marine sediments. Science, 209, 1527-1530.

PAMATMAT, M. M. (1973) Benthic community metabolism on the continental terrace and in the deep sea in the North Pacific. International Revue ges Hydrobiologia, 58, 345-368.

REDFIELD, A. C., B. H. KETCHUM and F. A. RICHARDS (1963) The influence of organisms on the composition of sea water. In: The Sea, Vol. 2, M. N. HILL, editor, Wiley-Interscience, pp. 26-77.

ROSENFELD, J. K. (1979) Ammonium adsorption in nearshore anoxic sediments. Limnology and Oceanography, 24, 356-364.

ROWE, G. T. and W. D. GARDNER (1979) Sedimentation rates in the slope water of the northwest Atlantic Ocean measured directly with sediment traps. Journal of Marine Research, 37, 581-600.

ROWE, G. T., P. T. POLLONI and S. G. HORNER (1974) Benthic biomass estimates from the northwestern Atlantic Ocean and the northern Gulf of Mexico. Deep-Sea Research, 21, 641-650.

RYAN, T. A., B. L. JOINER and B. F. RYAN (1976) MINITAB Student Handbook, Duxbury Press, 341 pp.

SAYLES, F. L. (1981) The composition and diagenesis of interstitial solutions - II. Fluxes and diagenesis at the water-sediment interface in the high latitude North and South Atlantic. Geochimica et Cosmochimica Acta, 45, 1061-1086.

SAYLES, F. L. (1979) The composition and diagenesis of interstitial solutions - I. Fluxes across the seawater-sediment interface in the Atlantic Ocean. Geochimica et Cosmochimica Acta, 43, 527-545.

SEITZINGER, S., S. NIXON, M. E. Q. PILSON and S. BURKE (1980) Denitrification and N_2O production in near-shore marine sediments. Geochimica et Cosmochimica Acta, 44, 1853-1860.

SMITH, K. L., Jr. (in press) Zooplankton of a bathyal benthic boundary layer: in situ rates of oxygen consumption and ammonium excretion. Limnology and Oceanography.

SMITH, K. L., Jr. (1978) Benthic community respiration in the N.W. Atlantic Ocean: in situ measurements from 40 to 5200 m. Marine Biology, 47, 337-347.

SMITH, K. L., Jr. (1974) Oxygen demands of San Diego Trough sediments: an in situ study. Limnology and Oceanography, 19, 939-944.

SMITH, K. L., Jr. and R. J. BALDWIN (1981) Deep Sea Respirometry: In situ techniques. In: Handbook on polarographic oxygen sensors:aquatic and physiological applications, H. FORSTNER and E. GNAIGER, editors, Springer-Verlag, (in press).

SMITH, K. L., Jr. and K. R. HINGA. Sediment community respiration in the deep sea. In: The Sea, Vol. 8, Deep-Sea Biology, G. T. ROWE, editor, Wiley-Interscience (in press).

SMITH, K. L., Jr., M. B. LAVER and N. O. BROWN Benthic boundary layer in the central and eastern North Pacific. I. A chemical and biological

characterization. Deep-Sea Research, (submitted).

SMITH, K. L., Jr. and J. M. TEAL (1973) Deep-sea benthic community respiration: an in situ study at 1850 meters. Science, 179, 282-283.

SMITH, K. L., Jr., G. A. WHITE and M. B. LAVER (1979) Oxygen uptake and nutrient exchange of sediments measured in situ using a free vehicle grab respirometer. Deep-Sea Research, 26A, 337-346.

SMITH, K. L., Jr., G. A. WHITE, M. B. LAVER, and J. A. HAUGSNESS (1978) Nutrient exchange and oxygen consumption by deep-sea benthic communities: preliminary in situ measurements. Limnology and Oceanography 23, 997-1005.

SOUTAR, A., J. SINGLETON, M. BUTLER and D. BAXTER (1978) Collection of pelagic sediment samples for geochemical analysis (PIT deployment). Science Applications Report 2(13), 15 pp.

STRICKLAND, J. D. H. and T. R. PARSONS (1972) A practical handbook of sea-water analysis. Bulletin of the Fisheries Research Board of Canada, 167, 310 pp.

SUGAHARA, I., M. SUGIYAMA and A. KAWAI (1974) Distribution and activity of nitrogen-cycle bacteria in water-sediment systems with different concentrations of oxygen. In: Effect of the Ocean Environment on Microbial Activities, R. R. COLWELL and R. Y. MORITA, editors, University Park Press, pp. 327-340.

TURNER, J. T. (1977) Sinking rates of fecal pellets from the marine copepod Pontella meadii. Marine Biology, 40, 249-259.

URRERE, M. A. and G. A. KNAUER (1981) Zooplankton fecal pellet fluxes and vertical transport of particulate organic material in the pelagic environment. Journal of Plankton Research, 3, 369-387.

WIEBE, P. H., S. H. BOYD and C. WINGET (1976) Particulate matter sinking to

the deep-sea floor at 2000 m in the Tongue of the Ocean, Bahamas, with a description of a new sedimentation trap. Journal of Marine Research, 34, 341-354.

WILSON, T. R. S. (1978) Evidence for denitrification in aerobic pelagic sediments. Nature, 274, 354-356.

Table 1. Calculated and measured fluxes of nitrogenous nutrients at six substations on the CNP-ENP transect. a = exchange rates from single grab of the deployment (substation); b = mean exchange rate for all grabs of the deployment (substation).

	NH_4^+ flux (μmoles m^{-2} h^{-1}				NO_2^- flux (μmoles m^{-2} h^{-1}			NO_3^- flux (μmoles m^{-2} h^{-1})		
Station	Measured[a]	Measured[b]	Calculated 0.5 cm	Calculated 5.0 cm	Measured[a]	Measured[b]	Calculated 0.5cm	Measured[a]	Measured[b]	Calculated 0.5 cm
CNP 173	+0.16	+0.55	+0.69	+.081	+0.07	+0.08	+0.002	-1.14	+0.02	+0.14
CNP 189	-2.87	-2.92	+6.69	+.076	+0.15	+0.15	+0.06	-3.51	-4.86	-0.17
132 G	+3.87	+3.39	+0.41	+.059	-0.24	-0.05	+0.04	-38.7	-7.32	+0.67
177 F	+2.90	+1.29	+0.51	+.081	+0.07	+0.10	+0.15	+3.14	+5.80	-0.14
125 C	+0.74	+0.45	+0.56	+.54	-0.06	-0.08	+0.06	+10.2	+6.59	+0.49
SCB 110	+0.72	+0.36	+0.86	+.124	+0.14	-0.06	+0.04	+9.11	+1.61	-0.81

Table 2. Comparison of the organic carbon and nitrogen demand (sediment community oxygen consumption and nitrogenous nutrient flux) of and organic carbon and nitrogen supply (particulate organic matter flux) to the deep-sea sediment community at three stations. The demand estimates for the Santa Catalina Basin (SCB-110 and 125) are from this study, while those for the western North Atlantic stations (DWD and ADS) are from Smith et al. (1978). The supply estimates for the Santa Catalina Basin station were measured with particle interceptor traps designed by Soutar et al. (1978) synoptically with the demand measurements. Particulate organic matter flux for stations DWD and ADS were taken from Rowe and Gardner (1979) for sedimentation traps moored at 36 m (DWD) and 500 m (ADS) above the bottom.

			Demand							Supply particulate organic matter mg m^{-2} d^{-1}		Supply: Demand	
			Sediment community oxygen consumption		Nitrogenous nutrient flux								
Station	Grab	Depth (m)	µmoles O_2 m^{-2} h^{-1}	mg C m^{-2} d^{-1}	µmoles N m^{-2} h^{-1}				mg N m^{-2} d^{-1}				
					NH_4^+	NO_3^-	NO_2^-	Total	Total	C	N	C	N
SCB-110	C	1300	111.50	27.60	0.18	11.89	0.09	12.16	4.09	11.13	3.12	0.40	0.76
	D		104.81	25.94	0.44	2.53	0.13	3.10	1.04	11.13	3.12	0.43	3.00
SCB-125	A	1300	113.28	28.04	2.73	21.49	0.06	24.28	8.16	11.13	3.12	0.40	0.38
	B		122.65	30.36	0.71	0.18	<0.01	0.89	0.30	11.13	3.12	0.37	10.40
DWD		2200	20.52	5.08	0.95	0.95	0.06	1.96	0.66	18.30	2.40	3.60	3.64
ADS		2750	17.39	4.32	0.61	0.80	0.01	1.42	0.48	7.00	0.40	1.62	0.83

FIGURE LEGENDS

FIGURE 1. A transect of five stations across the central and eastern North Pacific.

FIGURE 2. Sediment community oxygen consumption at five stations (13 substations) along the transect from 160°W to 110°W longitude and between 30°N and 34°N latitude. Rates are given as means with standard error bars and the number of replicates. Note log scale.

FIGURE 3. Nitrogenous nutrient exchange rates of ammonium, nitrite and nitrate at five stations (10 substations) along a transect from 160°W to 118°W longitude between 30°N and 34°N latitude. Rates are given as means with range values. Number of replicates are given in parentheses. Note log scale.

FIGURE 4. A plot of sediment community oxygen consumption and total nitrogenous nutrient flux for all substations on the CNP-ENP transect.

FIGURE 5. Measured and predicted sediment community oxygen consumption for all substations. A) Predicted values were calculated using substation equation (1). B) Predicted values were calculated using the station equation (2). Circled values were used to generate the predictive equation.

FIGURE 6. Sediment community oxygen consumption measured by three methods: in situ (IS), laboratory core (LC) and electron transport system (ETS) presented as a function of depth.

FIGURE 7. Measured and predicted sediment community oxygen consumption for available *in situ* stations. A) Predicted values were derived using equation for western North Atlantic stations: $\ln Y = 2.93 - 0.001(D) + 0.15\ (C:N) + 0.11\ (1/N) - 0.65\ (T) + 142.7\ (1/B)$ (Smith, 1978). B) Predicted values were calculated using the CNP-ENP transect substation equation (1): $Y = 75.6 - 0.012\ Z + 0.0005\ MA$. Macrofaunal abundance values for the stations of Hinga *et al.*, and Smith in Wiebe *et al.* (1976) were estimated from measurements made in close proximity (Menzies and Rowe, 1968; Rowe, Polloni and Horner, 1974; F. Grassle, pers. comm.).

FIGURE 8. Comparison of nitrogenous nutrient exchange rates across the sediment-water interface at six deep-sea stations. Two stations are located in the eastern North Pacific, one in the San Diego Trough (A-26), and one at the base of the Patton Escarpment common with Sta C of this study (C-66) (Smith *et al.*, 1979). Exchange rates in the western North Atlantic were measured at slope stations DWD and AWS (Smith *et al.*, 1978). Substations C-125 and SCB-101 are from this study. Range bars are given and the number of measurements are presented in parentheses.

FIGURE 9. Pore water nutrient profiles and overlying nutrient water concentrations from all substations. Solid continuous line in ammonium pore water profiles were used for nutrient flux estimates from 5 cm (see text).

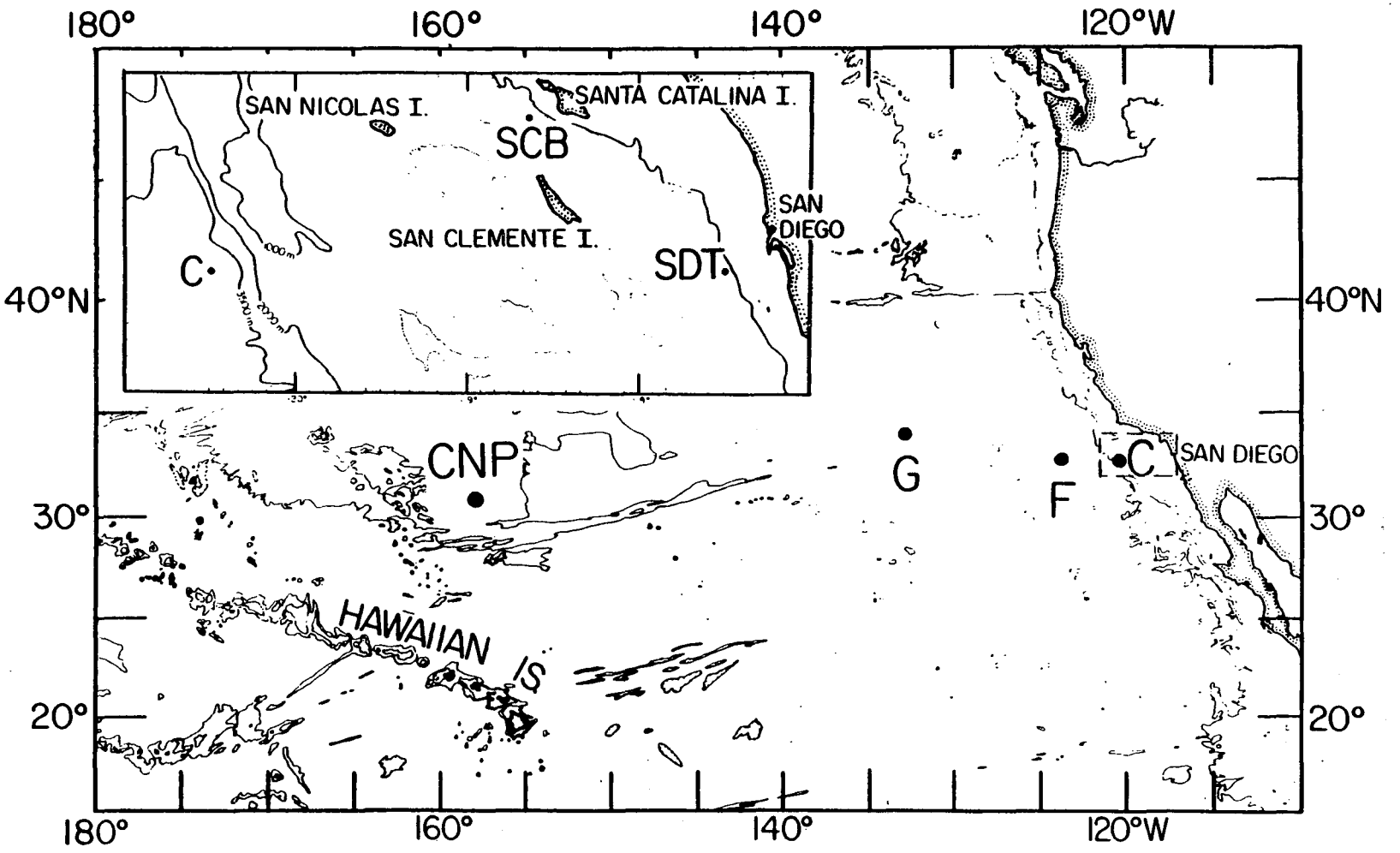

180°
160°
140°
120°W
40°N
30°
20°
SAN NICOLAS I.
SANTA CATALINA I.
SCB
SAN CLEMENTE I.
SAN DIEGO
SDT
C
CNP
G
F
C
SAN DIEGO
HAWAIIAN IS

Fig. 1

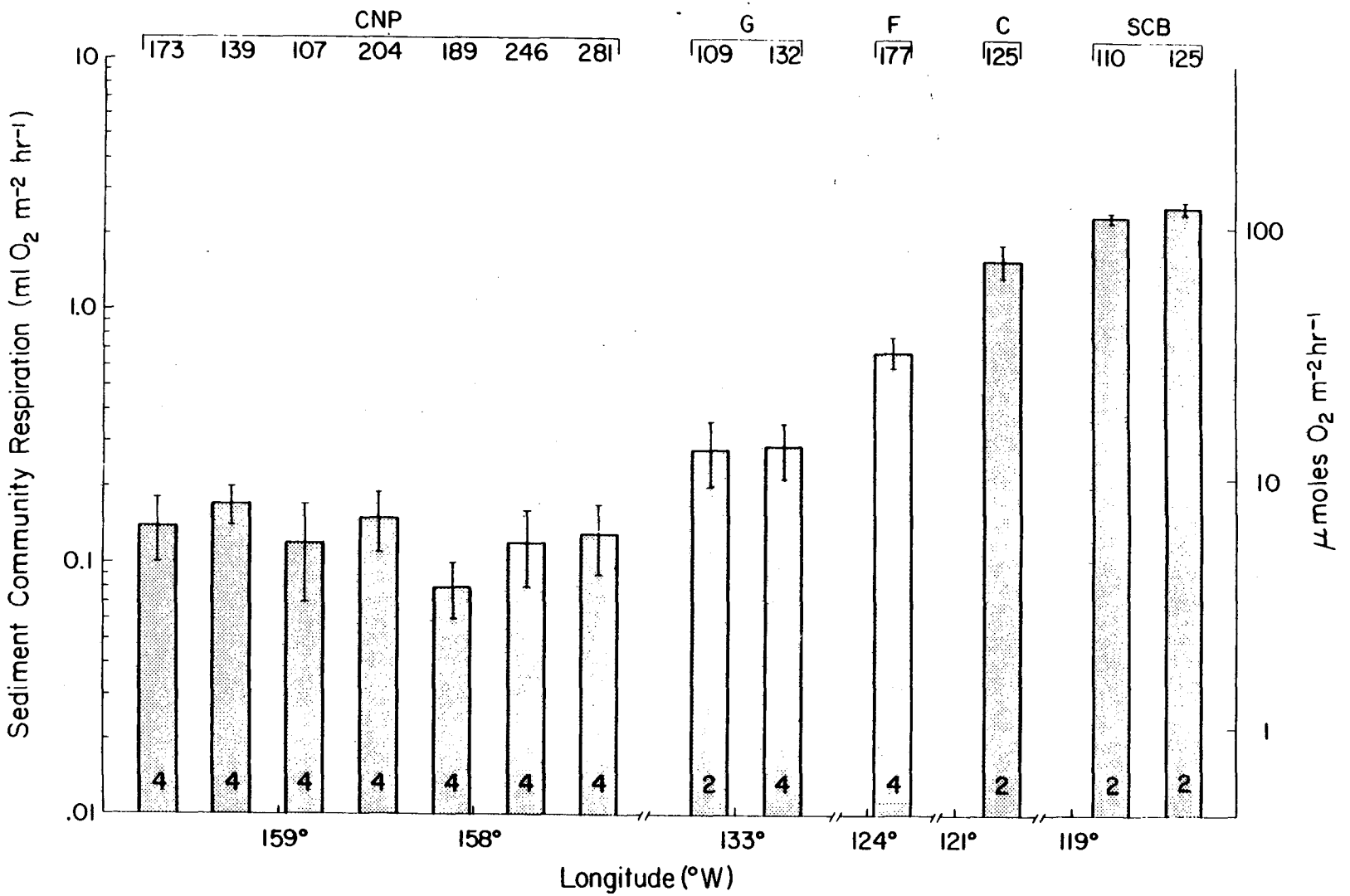

CNP
G
F
C
SCB
173
139
107
204
189
246
281
109
132
177
125
110
125
10
1.0
0.1
.01
100
10
1
Sediment Community Respiration (ml O_2 m^{-2} hr^{-1})
μmoles O_2 $m^{-2}hr^{-1}$
4
4
4
4
4
4
4
2
4
4
2
2
2
159°
158°
133°
124°
121°
119°
Longitude (°W)

Fig. 2

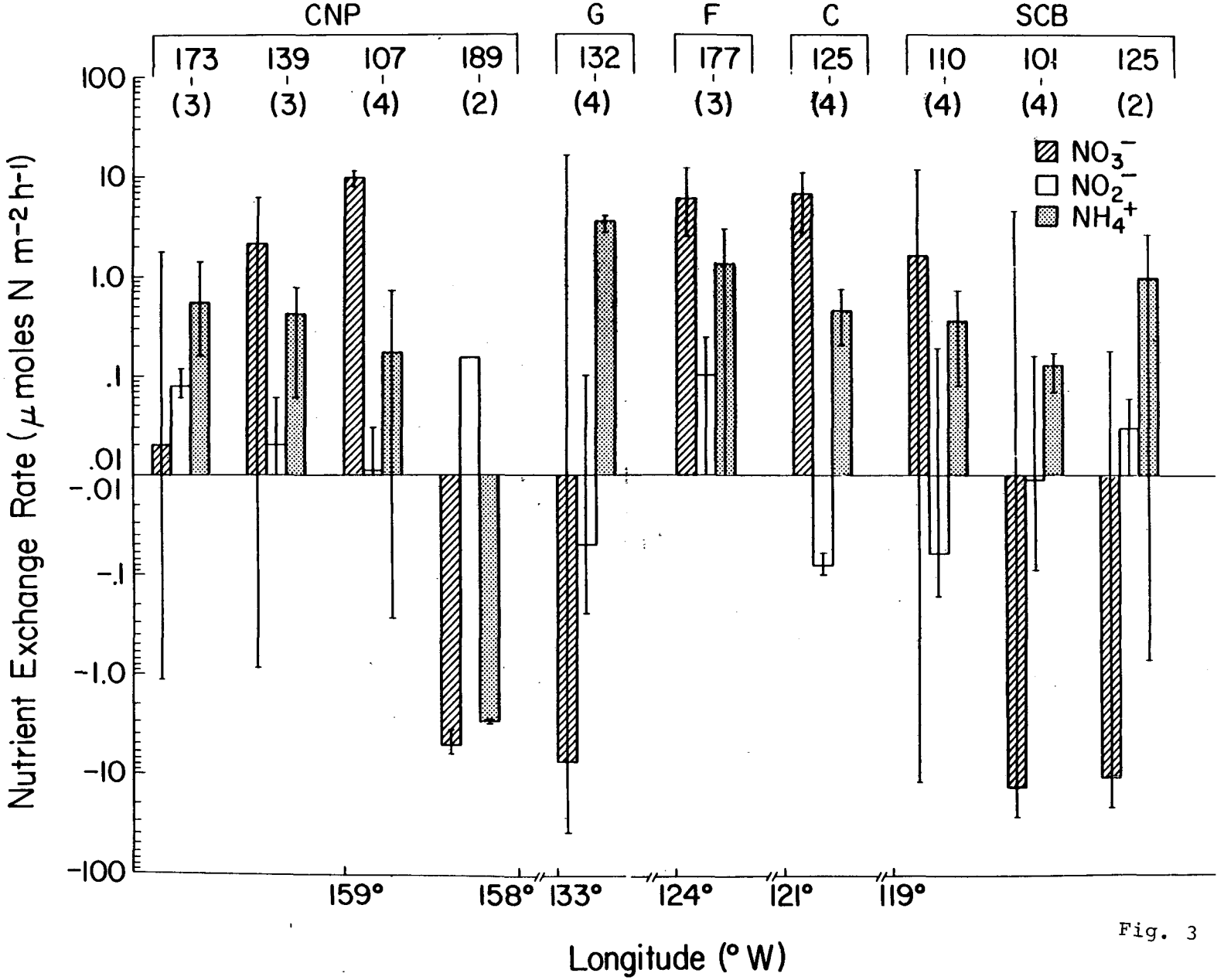

CNP
G
F
C
SCB
173
139
107
189
132
177
125
110
101
125
(3)
(3)
(4)
(2)
(4)
(3)
(4)
(4)
(4)
(2)
NO_3^-
NO_2^-
NH_4^+
100
10
1.0
.1
.01
-.01
-.1
-1.0
-10
-100
Nutrient Exchange Rate (μ moles N m^{-2} h^{-1})
159°
158°
133°
124°
121°
119°
Longitude (° W)

Fig. 3

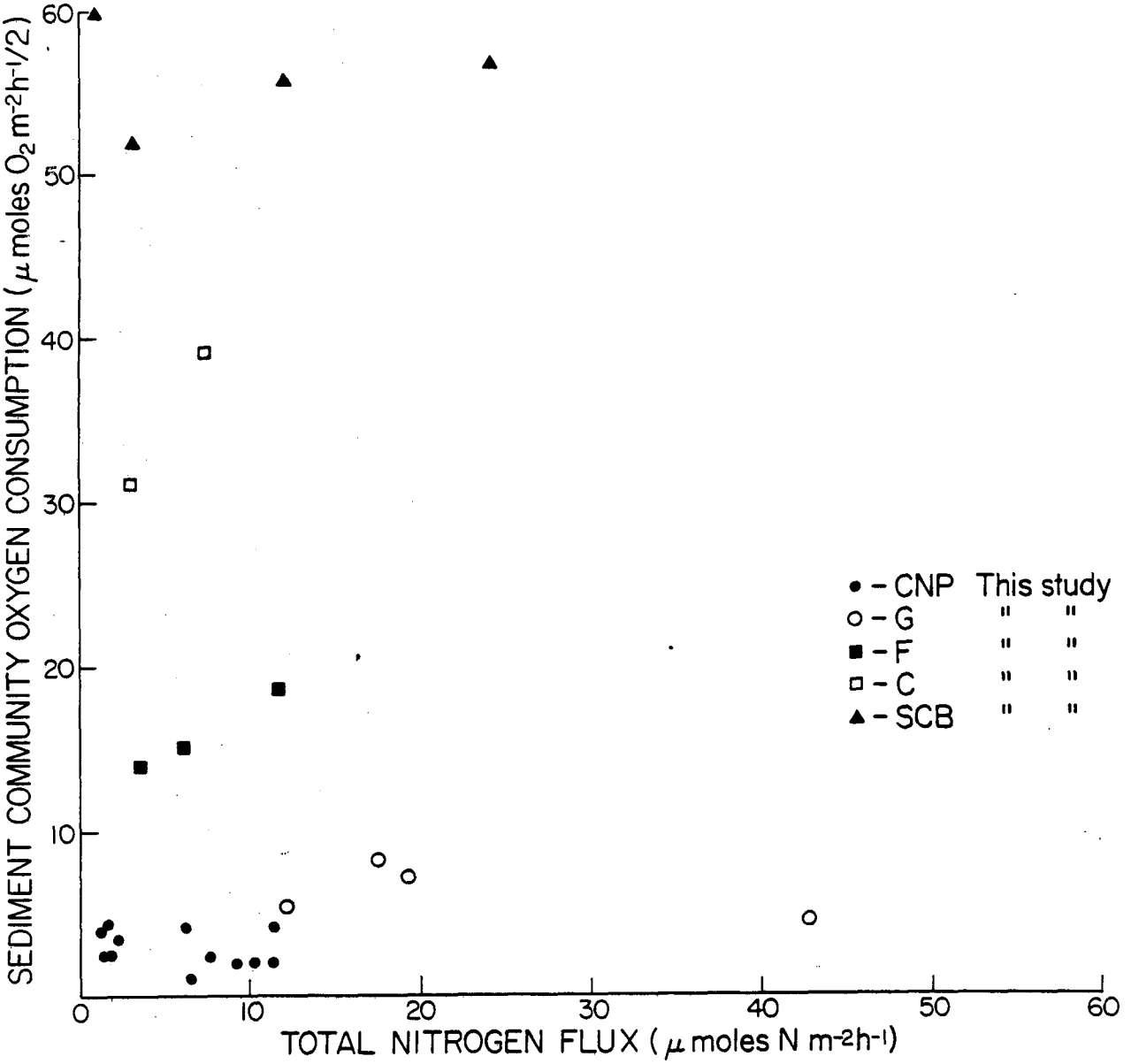

SEDIMENT COMMUNITY OXYGEN CONSUMPTION (μ moles O_2 $m^{-2}h^{-1}/2$)
TOTAL NITROGEN FLUX (μ moles N $m^{-2}h^{-1}$)
0
10
20
30
40
50
60
● – CNP This study
○ – G " "
■ – F " "
□ – C " "
▲ – SCB " "

Fig. 4

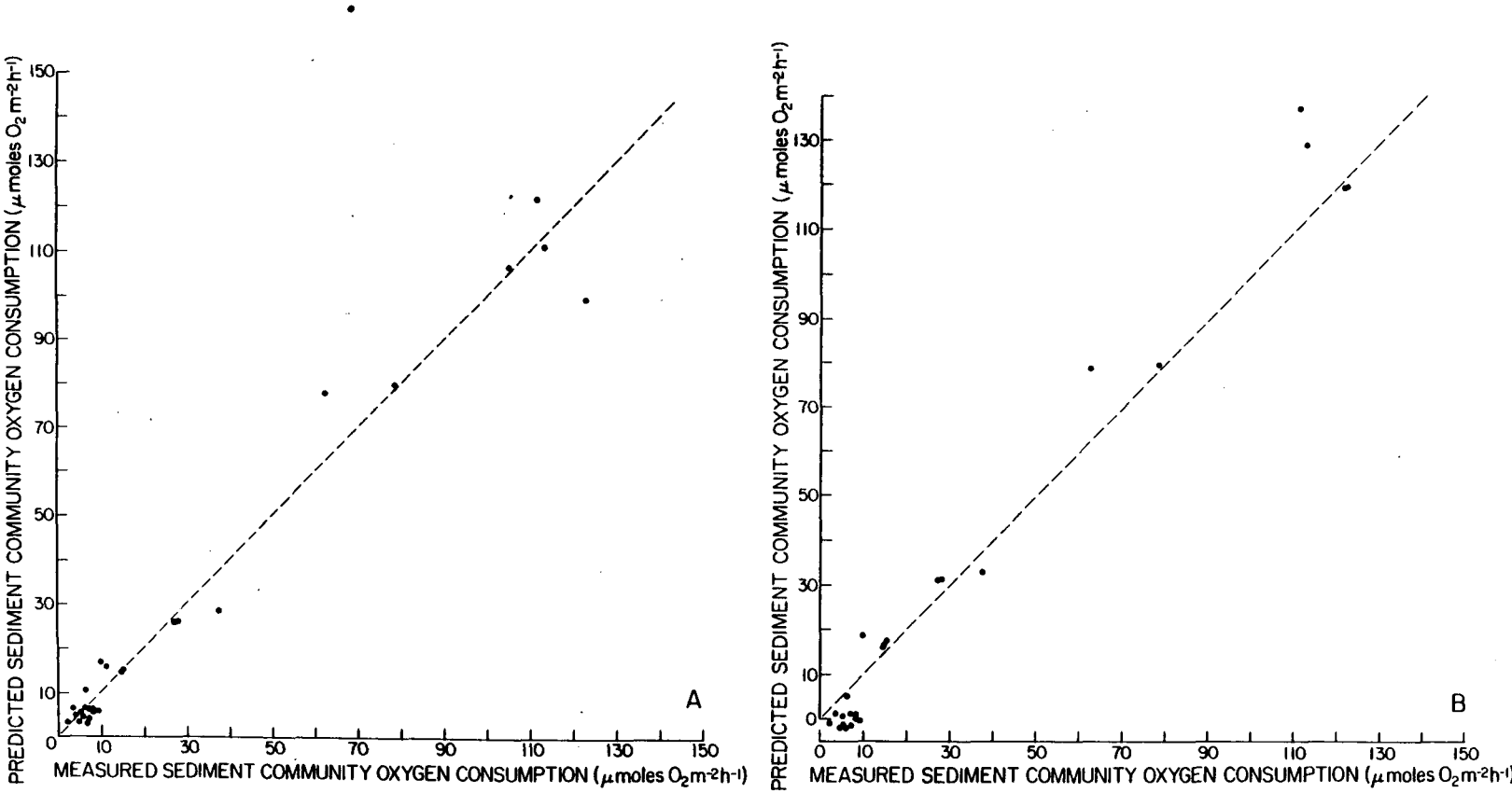

PREDICTED SEDIMENT COMMUNITY OXYGEN CONSUMPTION (μmoles O2 m-2h-1)
MEASURED SEDIMENT COMMUNITY OXYGEN CONSUMPTION (μmoles O2m-2h-1)
0
10
30
50
70
90
110
130
150
A
B

Fig. 5

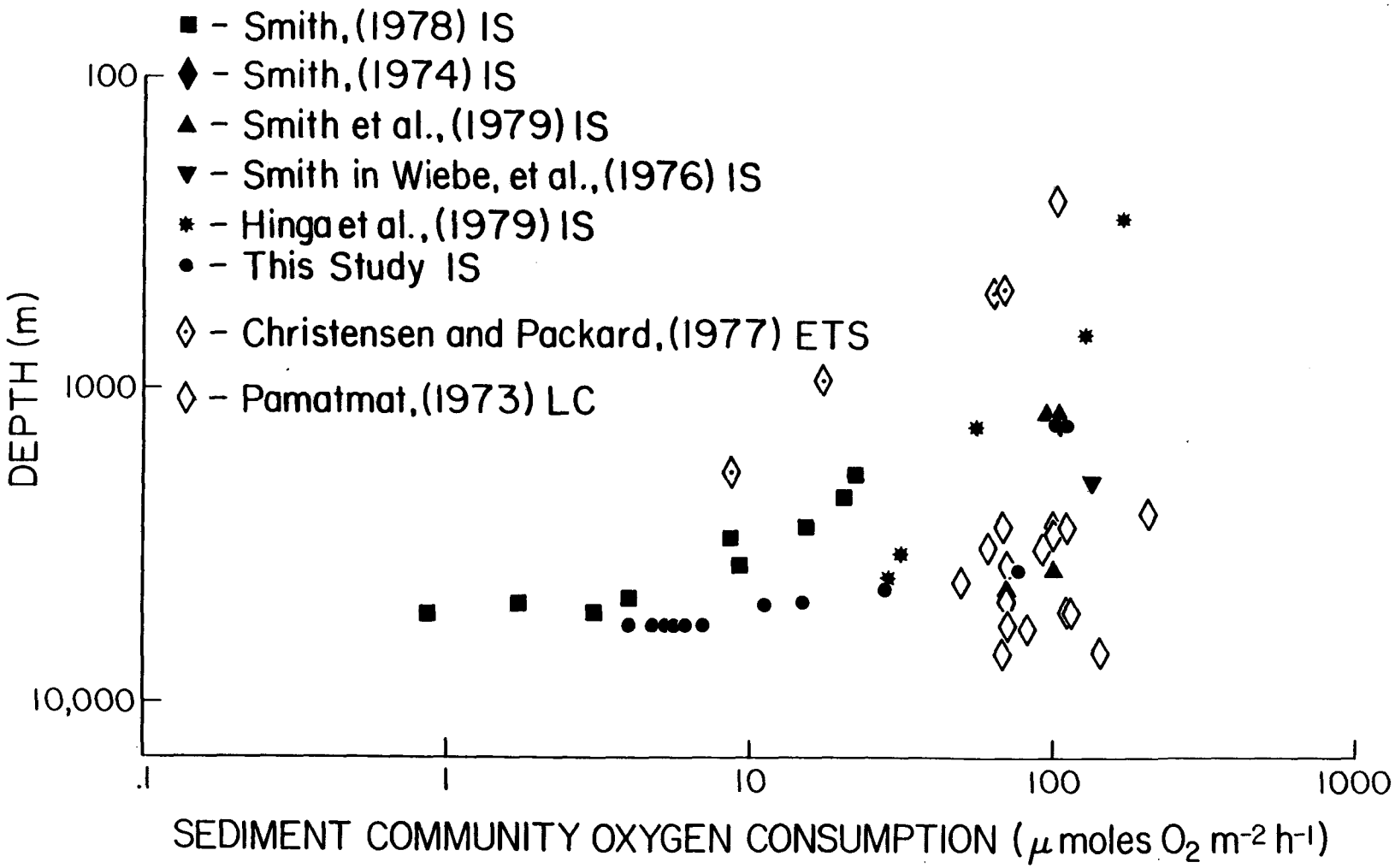

■ - Smith, (1978) IS
♦ - Smith, (1974) IS
▲ - Smith et al., (1979) IS
▼ - Smith in Wiebe, et al., (1976) IS
* - Hinga et al., (1979) IS
● - This Study IS
◊ - Christensen and Packard, (1977) ETS
◊ - Pamatmat, (1973) LC
DEPTH (m)
100
1000
10,000
.1
1
10
100
1000
SEDIMENT COMMUNITY OXYGEN CONSUMPTION (μ moles O_2 m^{-2} h^{-1})

Fig. 6

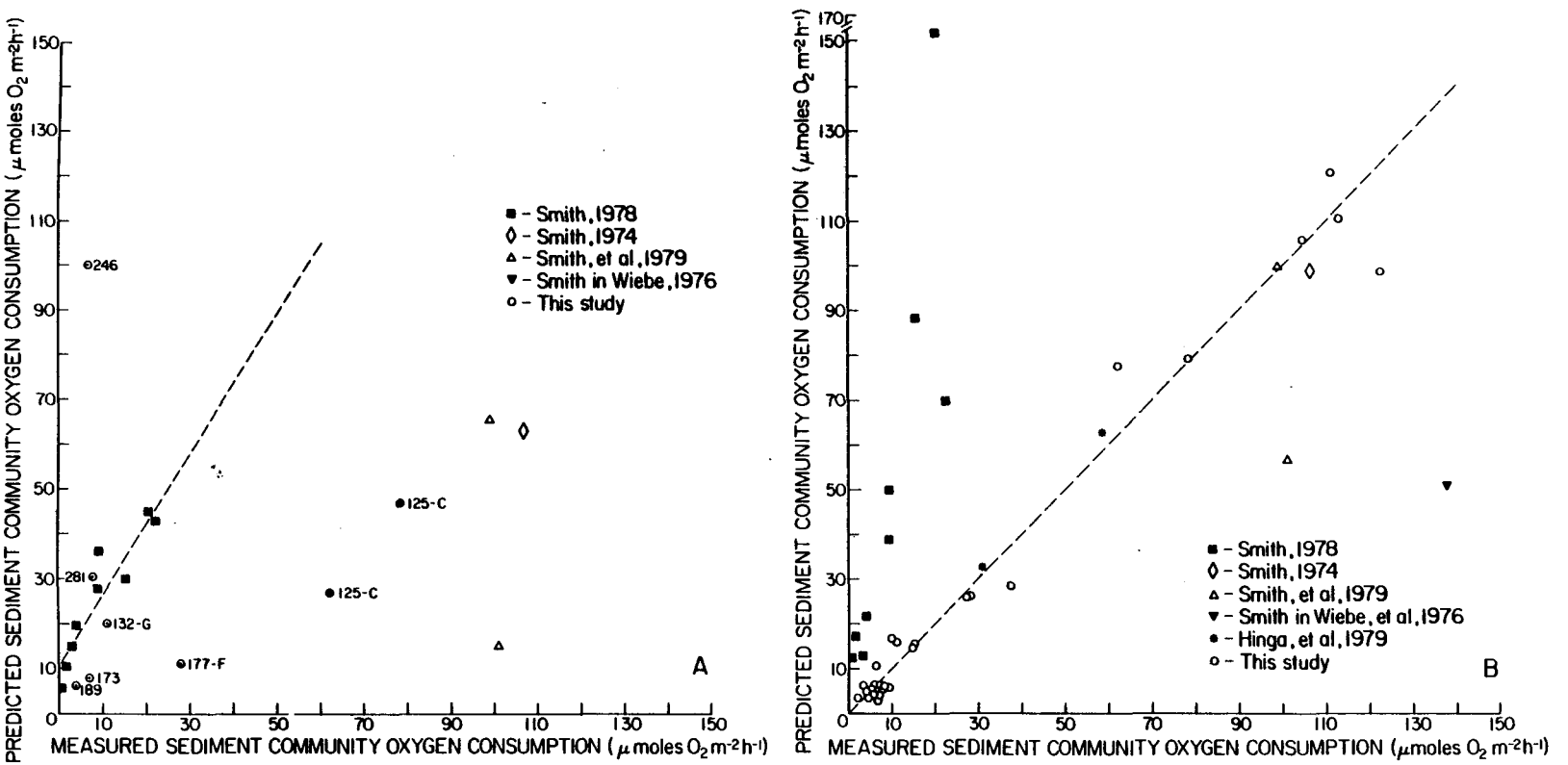

PREDICTED SEDIMENT COMMUNITY OXYGEN CONSUMPTION (μmoles O2 m-2h-1)
MEASURED SEDIMENT COMMUNITY OXYGEN CONSUMPTION (μmoles O2 m-2h-1)
■ - Smith, 1978
◊ - Smith, 1974
△ - Smith, et al, 1979
▼ - Smith in Wiebe, 1976
○ - This study
246
281
132-G
173
189
177-F
125-C
125-C
A
■ - Smith, 1978
◊ - Smith, 1974
△ - Smith, et al, 1979
▼ - Smith in Wiebe, et al, 1976
• - Hinga, et al, 1979
○ - This study
B

Fig. 7

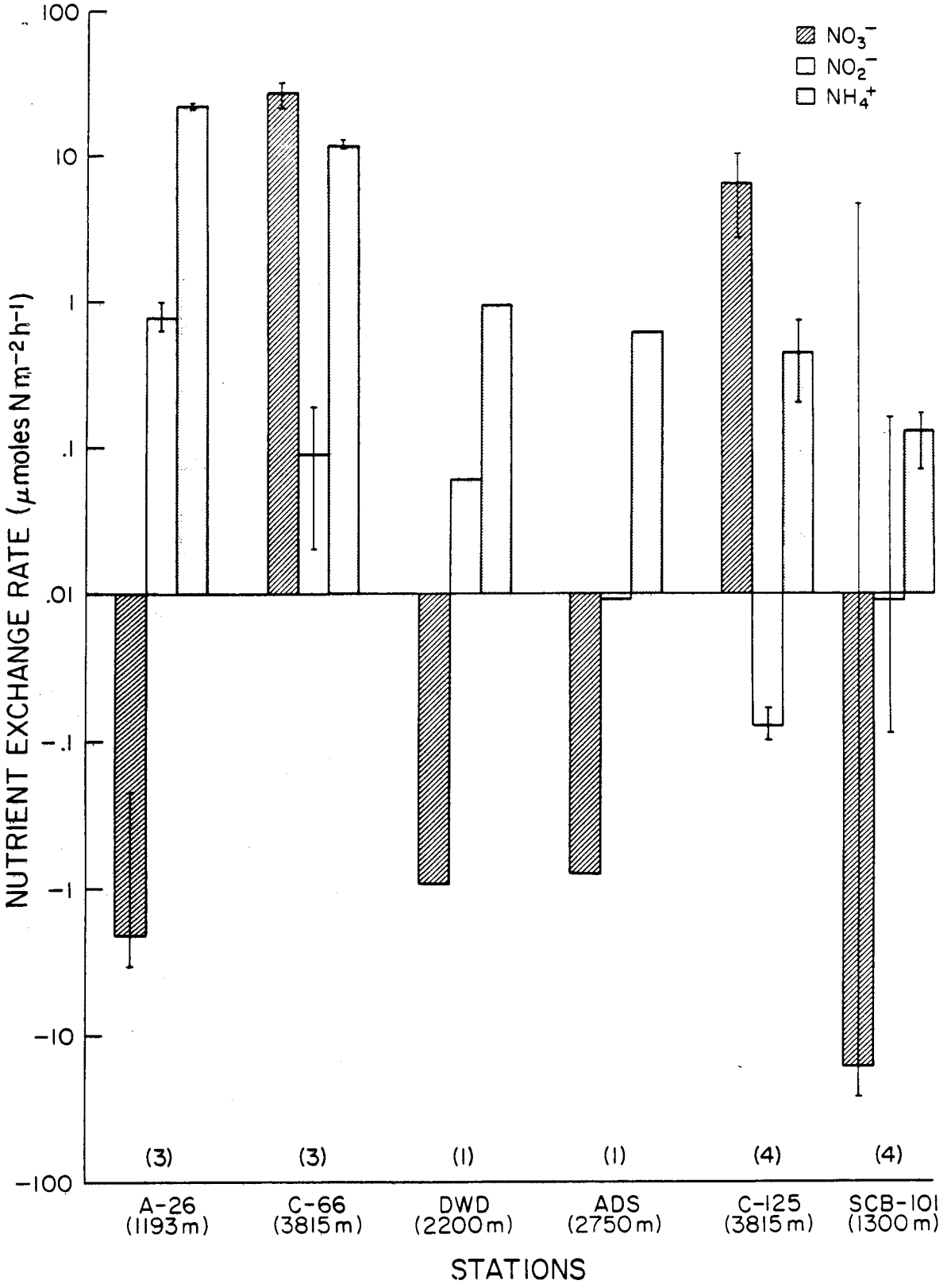

100
10
1
.1
.01
-.1
-1
-10
-100
NUTRIENT EXCHANGE RATE (μmoles N m⁻² h⁻¹)
NO3⁻
NO2⁻
NH4⁺
(3)
(3)
(1)
(1)
(4)
(4)
A-26 (1193m)
C-66 (3815m)
DWD (2200m)
ADS (2750m)
C-125 (3815m)
SCB-101 (1300m)
STATIONS

Fig. 8

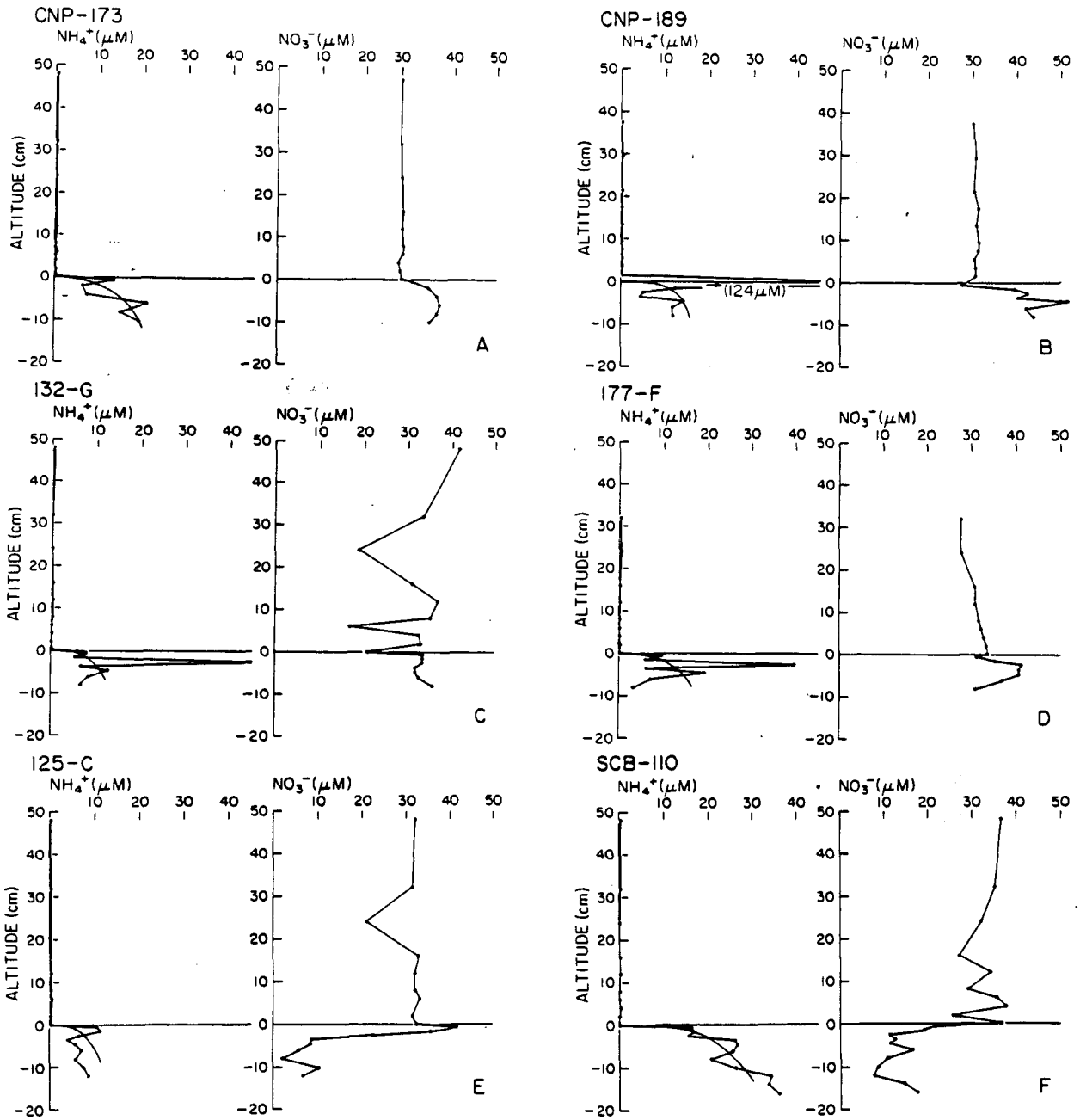

CNP-173
CNP-189
132-G
177-F
125-C
SCB-110
NH4+(μM)
NO3−(μM)
ALTITUDE (cm)
(124μM)
A
B
C
D
E
F

Fig. 9

Addendum 3

Scavenging deep-sea amphipods: Effects of food odor on O_2 consumption and a proposed metabolic strategy.

K. L. Smith, Jr. and R. J. Baldwin

In press: Marine Biology

Addendum 3:

Scavenging deep-sea amphipods: effects of food odor on O_2 consumption and a proposed metabolic strategy

K. L. Smith, Jr. and R. J. Baldwin

Marine Biology Research Division, A-002, Scripps Institution of Oceanography, La Jolla, CA 92093, USA

Running Title: Effects of Food Odor on Amphipod Respiration

Abstract

In situ respiration rates as a response to the odor of food, were measured for two species of scavenging amphipods, *Paralicella caperesca* from 3650 m in the western N. Atlantic and *Orchomene* sp. B from 1300 m in the Santa Catalina Basin off southern California. In addition, complementary laboratory starvation/respiration rates for a shallow-water species, *Orchomene* sp. A, were determined. Initial elevated O_2 consumption rates were found for up to 8 h in all deep-sea amphipods exposed to bait odor, followed by a period of lowered respiration equivalent to rates observed in animals not exposed to bait. *Orchomene* sp. A revealed a response similar to that observed in the deep-sea species. A metabolic strategy is proposed whereby scavenging amphipods efficiently utilize large episodic organic falls in the food-limited environment of the deep sea. This strategy involves (1) the ability to withstand long periods of starvation, (2) rapid response to an organic fall, (3) rapid location of the organic fall, (4) maximal rate of food consumption with maximal quantity ingested, and (5) efficient utilization of the consumed food. Each of these attributes are explored with the expected and observed mechanisms employed to achieve them.

Introduction

Lysianassid amphipods represent a significant component of the fauna inhabiting the benthic boundary layer at bathyl to hadal depths. Although rarely captured by trawl, dredge, grab or corer, these scavenging amphipods are attracted rapidly to baited cameras and traps in large numbers (Bowman and Manning, 1972; Dayton and Hessler, 1972; Paul, 1973; Shulenberger and Hessler, 1974; Hessler et al., 1978; Thurston, 1979). In comparison to lysianassids, other scavengers such as fishes, decapods, octopods, ophiuroids, holothurians, and polychaetes are usually less abundant at bait sites (Isaacs, 1969; Dayton and Hessler, 1972).

Our interest in the food energy utilization in the deep sea and the abundance of these amphipods prompted us to first address the question of establishing the metabolic requirements of these scavengers. Preliminary in situ measurements of O_2 consumption on one species of amphipod, Paralicella caperesca at abyssal depths suggested the following hypothesis: scavenging deep-sea amphipods are energetically adapted to a sporadic food source in a food-limited environment by having (1) two states of metabolism, a resting rate much like a state of torpor or dormancy and an active rate for optimal utilization of a bait fall when available, and (2) energy storage capabilities for long-term sustenance. In our quest to verify this hypothesis, we have examined two other species of scavenging amphipods from bathyal and shallow-water environments, Orchomene sp. A and sp. B (Table 1).

Materials and Methods

Field Studies

The slurp gun respirometer, designed to be operated visually from the submersible Alvin, gently captures pelagic animals that may not be attracted to bait (Smith and Baldwin, in press; Smith and Laver, 1981). The modular unit of the slurp gun respirometer is a horizontally mounted acrylic cylinder (38 cm x 9 cm ID) connected on either end to two right-angle plunger valves. The volume of the chamber can be adjusted to meet the behavioral requirements of the captured animal by a piston. Three or four of these modules constitute a slurp gun respirometer, permitting measurements of up to three individual animals plus a control per submersible dive. Polarographic O_2 sensors continuously monitor the O_2 tension in each chamber and are calibrated by a modified Winkler procedure (Strickland and Parsons, 1972); limits are established with O_2-free seawater (nitrogen purged). Oxygen consumption rates are calculated over intervals of time which are sufficient to record a significant difference, generally on the order of 2-3 h. The resulting values are presented per hour but plotted at the median of the time interval. Hence, exact time periods for the various phases of the O_2 consumption curves are not available.

During capture operations in the western North Atlantic at a depth of 3650 m, the submersible sat on the bottom while the mechanical arm positioned the intake funnel near a swimming Paralicella caperesca which had been attracted by the sliced mackerel bait during an in situ measurement of rattail fish respiration. With all valves of the slurp gun respirometer open, the pump was turned on and the amphipod (P. caperesca #1) gently "slurped" into the animal chamber. After the first capture, the intake and outlet

manifold engaged the second module and the same procedure followed in capturing P. caperesca #2. Chamber volumes were then adjusted to 0.25 l (P. caperesca #1) and 1.50 l (P. caperesca #2). A control fish trap set at the same station within 1 h of initiating the amphipod experiment showed no measureable O_2 consumption by the bottom water for incubations of up to 22 h.

During capture operations of Orchomene sp. B in the Santa Catalina Basin at 1300 m, nitex mesh (200 μm) enclosed mackerel bait was used to lure the amphipods from the surrounding sediment. An attempt was made to capture one large isolated amphipod with the slurp gun respirometer. However, with limited visibility and many small swarming animals, two smaller Orchomene sp. B were slurped up with the larger specimen. The chamber volume was then constricted to 0.85 l.

In both in situ experiments, the animals were observed for 2 h and then the entire slurp gun respirometer was detached from the submersible and tethered to a previously deployed free vehicle bottom mooring line (Smith et al., 1979). The purpose of mooring the respirometer was to allow in situ incubation of the amphipods in excess of the normal dive time of the Alvin (8–10 h).

As with the slurp gun respirometer, the megafauna respirometer is also manipulated visually from Alvin to select and sample animals occupying the sediment surface. Dual respirometer chambers (29 cm diam x 9.5 cm high) with a single hinged top plate are mounted on a rectangular acrylic base (35 cm x 72 cm) (Smith and Baldwin, in press). When the top pivots to a closed position, the chambers seal and lock to the base. The megafauna respirometer is designed for animals that are scooped from the sediment with a mesh basket and deposited (sediment free) on the respirometer base. However, in a

fortuitous event, 4 specimens of Orchomene sp. B amphipods entered one otherwise empty chamber before it was closed, thereby providing respiration rates for animals not exposed to the scent of bait. Following capture operations, the megafauna respirometer was attached to a free vehicle mooring line and allowed to incubate in situ for 25.2 h prior to acoustic recall.

On recovery the amphipods were removed from the animal chambers of both respirometers and quickly frozen for laboratory analyses of water content, lipid, and glycogen. The volume of each chamber was determined and corrected for the displacement volume of the amphipod. Bottom water samples taken at the time of each amphipod capture by Alvin-operated Niskin bottles were analyzed for initial dissolved O_2 concentration.

Laboratory Studies

The rationale for conducting the shallow-water studies was (1) to compare the O_2 consumption response to the odor of bait for the deep-sea scavengers to that of a shallow-water species, and (2) to examine the effects of starvation periods on that response. We chose to study a shallow-water amphipod, Orchomene sp. A, which was easily trapped and could be maintained in the laboratory for extended periods of time. This amphipod was of comparable size (0.31-0.86 mg dry weight) to Orchomene sp. B but considerably smaller than Paralicella caperesca.

The traps were simple 1.9 l nalgene jars with a 4 mm mesh plastic screen holding the entrance funnel in position. Bait (cat food or mackerel) was placed in two 160 µm nitex mesh cups so that animals were unable to feed prior to recovery. Traps were tethered to a 24 h set line and on recovery, were transported to the lab in a chilled water bath to maintain sea water at

approximately 10°C. Amphipods to be used for biochemical analyses were immediately frozen at -70°C, the remainder were isolated in 160-µm mesh cups (for starvation purposes) and maintained on an acrylic tray with fresh chilled sea water (10-13°C) introduced into a over-flow system. These nitex mesh cups allow microplankton, nanoplankton and bacteria to enter the "starvation" chamber and undoubtedly to grow in the cup itself, probably constituting a limited food source for the amphipods.

Laboratory respirometry was conducted with a carousel respirometer system and six 29-ml respirometers. Each respirometer consists of an acrylic cylinder (3.1 cm diam., 4.6 cm height) closed at the base, with an inserted acrylic support for the O_2 sensor (calibrated as above) and magnetic stir bar; a screw-on top holds the sensor firmly against the support. The carousel is a modified turbine-action stirrer with water driven magnetic blades which provide continual stir bar rotation for the externally mounted chambers. The entire carousel system is maintained in a refrigerated aquarium at in situ temperatures with O_2 tension continuously monitored.

Exposure to bait scent was conducted with one cm^3 of mackerel tissue enclosed in 250 µm nitex screening. Bait was placed with the amphipods for 5 min and removed prior to initiation of respiration measurements.

The possible bias of respiration rates due to either low O_2 concentration within the chambers or diurnal foraging behavior was examined. Since O_2 consumption rates of Orchomene sp. A did not conform to O_2 concentrations above 3.0 ml l^{-1} (bottom water = 2.71 ml l^{-1}), our analyses of respiration rates were terminated at chamber concentrations of 3 ml l^{-1}. Variations in respiration rates due to possible diurnal foraging behavior were reduced by starting all experiments at approximately the same time of day.

Biochemical Analyses

Nineteen amphipods representing the three species were identified, measured and weighed prior to lyophilization and then reweighed to determine water content. Each animal was homogenized in 10-100 v/w distilled water at 2°C with a Tekmar Tissumizer for 2 min and replicate subsamples of the homogenate were taken for total lipid (Bligh and Dyer, 1959; Marsh and Weinstein, 1966) and glycogen determination (Holland and Gabbott, 1971; Nahorski and Rogers, 1972).

Results

Respiration

Paralicella caperesca

Two specimens of the scavenging amphipod, Paralicella caperesca, were captured after being exposed briefly to the odor of bait at a depth of 3650 m in the western North Atlantic. At the time of the initial exposure to the bait odor, P. caperesca came from the surrounding sediments and swam toward the food source located approximately 1 m above the sediment surface. The area influenced by the bait scent could not be adequately determined because of the visual constraints of the submersible viewing ports and lights.

The two captured amphipods exhibited a rapid swimming behavior similar to that of the surrounding population of amphipods which had been attracted by bait in a nearby fish respiration chamber. This behavior continued throughout our 2-h period of observation and paralleled the activity of the surrounding amphipod populations. The fortuitous presence of bait had two benefits: (1) the amphipods migrated out of the sediment in search of the bait, facilitating

their capture by the slurp gun respirometer, and (2) amphipod respiration could be measured while the animals were in a seemingly natural excited state.

Oxygen consumption rates of these two specimens of Paralicella caperesca (6.69 and 13.00 mg dry weight, respectively) were measured continuously for a period of 21 h. The weight specific O_2 consumption rates of both specimens (Fig. 1a) were high for the first 6-8 h of incubation in the slurp gun respirometer and then dropped precipitously by an order of magnitude to a "resting" rate for the duration of the measurements. It is not possible in P. caperesca to distinguish increased rates due to excitement versus those due to capture since there was no control; however, considering the results from Orchomene sp. B, we interpret this response as being attributable to the presence of bait. Total O_2 consumption by P. caperesca in both SGR chambers depleted the O_2 concentration by 5.5% and 1.2% with final values of 6.17 ml O_2 l^{-1} for specimen #2 and 6.45 ml O_2 l^{-1} for specimen #1 at the end of the incubation period.

Weight specific O_2 consumption rates were higher in the larger animal (Paralicella caperesca #2, Fig. 1a). This is contrary to the expected inverse relationship and may be a result of sex, instar stage, physiological condition, etc. A small amount of fecal material observed with the smaller specimen also could have biased the respiration values.

Orchomene sp. B

The abundant scavenging amphipod of the Santa Catalina Basin is Orchomene sp. B. These animals are considerably smaller (0.11-1.28 mg dry wt) than the specimens of Paralicella caperesca and include two males and one female attracted to bait scent in the slurp gun respirometer, and three females and

one male not lured by bait in the megafauna respirometer. The behavior of only the largest specimens could be observed in each chamber, since the other specimens were too small to be visible from the submersible viewport. The large amphipods behavior was similar to that of unrestrained specimens swarming in the bottom water in the immediate vicinity of the bait.

Oxygen consumption rates of the three combined Orchomene sp. B exposed to the odor of bait (Fig. 1b) fluctuated similarly to the rates described above for Paralicella caperesca. There was an initial active or excitatory rate of O_2 consumption for a period of approximately 6-7 h, followed by a rapid decline to a resting rate for the duration of the incubation, more than 4.5 times lower than the active rates.

The four animals in the megafauna respirometer were captured without any exposure to bait odor. These animals were about the same size (0.11-1.28 mg dry wt) as those exposed to bait (0.88-1.23 mg dry wt). Unlike the exposed Orchomene sp. B, there was no obvious change in the respiration rate (Fig. 1b). Concentration of dissolved O_2 in the experimental and control chambers were depleted by 32.3% and 2.8% leaving final concentrations of 0.77 and 1.03 ml O_2 l^{-1}, respectively.

Weight specific O_2 consumption rates of the Orchomene sp. B are significantly higher in the control than in the exposed group when the resting rates are compared (Fig. 1b). This may be a result of the larger percentage of smaller individuals in the control and therefore a higher weight specific O_2 consumption.

Orchomene sp. A

We first examined the response of Orchomene sp. A to bait odor as a function of length of starvation. Oxygen consumption rates were determined for animals exposed and unexposed to the scent of bait after various periods of starvation (Fig. 2.). Prior to starvation, there was no increase in O_2 consumption immediately following exposure to bait odor (Fig. 2a). After 2 days of starvation following capture, the amphipods exposed to the odor of bait showed a slight initial increase in weight specific O_2 consumption over the unexposed animals and then steadily increased to peaks at between 8 and 11 h of incubation (Fig. 2b). In both of these cases, initial response to the scent appears negligible, but the O_2 consumption rates during evening and early morning hours (1830-0200 h) were considerably heightened in animals exposed to the scent as compared to those unexposed. A period of 4 days' starvation prior to exposure to bait did not alter the trend observed after starvation for 2 days (Fig. 2c). However, after 5 days of starvation, exposure to the odor of bait caused a significant increase in weight specific O_2 consumption when compared to unexposed specimens of comparable size (Fig. 2d). The period of active O_2 consumption declined precipitously within the first 4 h following exposure, showing no increase in consumption rates during the evening hours. This same pattern persists after 7 days of starvation (Fig. 2e). After 9 days of starvation, exposure to bait odor elicited a slower response, peaking after 3 h incubation and then gradually declining through evening hours. The increase in weight specific O_2 consumption for the exposed animals of the 9 day test may reflect their smaller size.

One series of experiments was run on Orchomene sp. A following 13 days' starvation. The few animals that survived this length of deprivation (5%)

exhibited a very limited or lethargic response to handling and the O_2 consumption rates for the duration of the incubation (19 h) of both the exposed and unexposed animals were not detectable above the control with no amphipods. Orchomene sp. A, exposed to bait odor, were initially more active at night (starvation periods of up to 4 days) with the concomitant increase in O_2 consumption rates especially during the evening and early morning hours. Animals starved for longer periods of time (5-9 days) show less elevated O_2 consumption in evening hours but their active rates initiated by exposure to bait odor are slightly higher (15.5 $\pm$ 2.2 µl O_2 mg dry wt^{-1} h^{-1}) than the evening rates of the animals starved for 2-4 days (11.7 $\pm$ 1.3 µl O_2 mg dry wt^{-1} h^{-1}).

Chemical Composition

We measured water, total lipid and glycogen content of the three species of scavenging amphipods to identify possible similarities in animals occupying a similar niche. The animals used in these analyses are either the same or belong to a similar size class as those in the respiration studies.

The wet weight of the four species of scavenging amphipods on the bottom increases with increasing depth from 1.29 mg for Orchomene sp. A at 56 m to 59.09 mg for Paralicella caperesca at 3650 m (Table 2). Water content ranged from a low of 59% in Orchomene sp. A (Scripps Canyon) to a high of 78% in Orchomene sp. B (Santa Catalina Basin) and P. caperesca (western North Atlantic) (Table 2).

Total lipid content of the four species of amphipods was variable ranging from a low of 1.9% in Paralicella caperesca to a high of 4.7% in Orchomene sp. A. The glycogen levels were also variable and exhibit no obvious trends with

highest concentrations found in P. caperesca (1%) and lowest concentrations in Orchomene sp. B (0.11%) (Table 2).

Discussion

Respiration

In comparing the rates of O_2 consumption in situ for two species of amphipods (Paralicella caperesca, 3650 m and Orchomene sp. B, 1300 m), it is not surprising to find that both active and resting rates are lower in the deeper living P. caperesca (Table 3). Similar trends of decreasing metabolism with increased depth have been noted for the bathyal decapod Parapagurus pilosimanus from 1000 m depth (9-24 µl O_2 g^{-1} h^{-1}) (George, 1979a) as compared to the red crab from 850 m Geryon quinquidens (17-35 µl O_2 g^{-1} h^{-1} and the shallow-water intertidal crab Callinectes sapidus (30-150 µl O_2 g^{-1} h^{-1}) (George, 1979b). Childress (1977) reports that Gaussia princeps, a diurnal vertical migrating copepod (200-400 m), has considerably lower respiration rates than the shallower living copepods, and a study of 28 species of midwater crustaceans substantiates the general trend of decreasing O_2 consumption with increasing depth (Childress, 1975). Comparisons of O_2 consumption rates for deep and shallow-living amphipods sometimes conform to this pattern but sometimes do not. In a comparison of the shallow-living Hyperia galba (25-650 m) with the deep-living Paracallisoma coecus (500-1100 m), respiration rates ranged from 0.08-0.14 µl O_2 mg wet wt^{-1} h^{-1} for the shallow amphipod to 0.04-0.05 µl O_2 mg wet wt^{-1} h^{-1} for the deeper living species (Childress, 1975). George (1979a), however, reported no significant difference in the respiration rates for two cold-adapted species of amphipods from two depths: Eurythenes gryllus from a depth of 1850 m (60-64 µl O_2 g^{-1} h^{-1} over a hydrostatic pressure range of 1-325 atm) and Anonyn nugax, a

shallow-water species from the Arctic shelf (30-115 µl O_2 g^{-1} h^{-1}). George hypothesized that active scavengers such as E. gryllus may have higher growth and metabolic rates than either deep-living species that are lethargic or species occupying the O_2 minimum zone at abyssal depths.

Oxygen consumption rates for the Paralicella caperesca and Orchomene sp. B exposed to bait are higher than most published rates for cold-adapted amphipods tested in the laboratory (Table 3). This may be a response to the presence of bait and/or a manifestation of environmental changes inherent in laboratory analysis of animals (Smith and Baldwin, in press). Since respiration rates of the Orchomene sp. B not exposed to bait were within the ranges reported for other cold adapted species, we assume the bait attraction was a major factor in influencing O_2 consumption. A heightened metabolic state on exposure to bait has been noted in plaice (Edwards et al., 1969) with subsequent adjustment to a lower metabolism such that their growth would be restricted during low food periods while conversion efficiency remained stable. The energetic advantages of such a system are obvious in the deep sea and will be explored further in this paper.

Elevated respiration rates with exposure to food odor have also been noted for the gastropod Nassarius reticulatus (Crisp et al., 1978). After 2 weeks' starvation, the introduction of full strength crab extract more than doubled the respiration rate of the gastropod, a response similar to Orchomene sp. A after 4 days' starvation. However, whereas increased respiration rates persisted only 20-25 min for N. reticulatus, Orchomene sp. A exposed to bait continued to respire at a high rate throughout the 8- to 13-h test period.

For starvation periods up to 4 days, Orchomene sp. A exposed to bait odor exhibit a strong diurnal respiration pattern with high evening rates; all

remnants of the pattern are lost by the fifth day (Fig. 2). A similar loss of diurnal rhythm was noted for an intertidal amphipod, Marinogammarus marinus L., after 4 days in the laboratory (Fincham, 1972), and cyclic respiration in a crab, Cancer pagurus, decreased during starvation but returned upon resumed feeding (Ansel, 1973).

It must be noted that specimens of Orchomene sp. A not exposed to bait odor respired at consistently low rates throughout the test periods. It is possible that these animals may maintain a low metabolic state until food is available, at which time foraging behavior is initiated and O_2 uptake increases. Decreased activity with starvation has been reported for the shallow-water amphipod, Marinogammarus obtusatus (Mackintosh, 1973), and in the crab Cancer pagurus (Ansel, 1973), which resumed its normal activity and O_2 consumption rates when fed. It is possible that exposure to bait odor elicits the same response as the feeding of the animal, i.e., to resume a cylic respiration pattern for starvation periods less than 5 days.

Chemical Composition and Depth

Our measurements of lipid as percent wet weight (1.9-4.7%) (Table 2) are within those reported for most amphipods (0.25-7.0% wet wt) (Childress, 1974; Yayanos and Nevenzel, 1978; Percy, 1979) but considerably lower than the Antarctic amphipods Cheirimedon forigneri and Orchomenella plebs (9.1-13.8%) (Pearse and Giese, 1965). Lipid composition remains relatively unchanged with depth for Orchomene sp. A and sp. B. This is consistent with results of Childress and Nygaard (1974) who found insignificant lipid variation in 21 species of midwater crustaceans for depths of 0-150 m versus 900-1200 m (deepest sampled depth). Although Paralicella caperesca is significantly lower in lipids than the shallow-water Orchomene sp. A, the apparent trend of

lower lipid concentration with increased depth breaks down when a wider range of depths is examined. Five species of Eurythenes gryllus from the central N. Pacific (5900 m) showed a lipid concentration of 4.83 ± 2.67% wet weight (Smith, unpub. data), a concentration equal to that in the shallow-water Orchomene sp. A.

Water contents for Orchomene sp. B and Paralicella caperesca (Table 2) are similar to the 74% value reported by Cummins and Weycheck (1971) for two species of gammarid amphipods. The percentages in shallow-water Orchomene sp. A were slightly lower (65.57 ± 5.58). Similar studies on a variety of crustaceans have revealed little difference in water content between shallow-living (0-150 m) and deeper-living (900-1200 m) animals (Childress and Nygaard, 1974).

Interspecific comparisons of chemical composition must be made with care due to variations in physiological states such as sex, growth, reproduction, and storage and utilization of reserves (Ansel, 1972; Morris, 1973) as well as season and depth of capture (Lee, 1974). Even so, in the sections that follow, we present some tentative ideas on the probable energy reserves available to the individual animals.

Metabolic Strategy for Deep-sea Scavengers

In dicussing metabolic strategy for deep-sea scavengers, we will assume (1) the deep-sea environment is food energy limited, (2) there is a selective advantage for an animal in such an environment to optimally utilize the available food energy, and (3) large organic falls represent the prime source of food of scavengers. Allowing these three basic assumptions, we can identify five attributes which would constitute an energy strategy for a

deep-sea scavenger (1) to withstand long periods of starvation, (2) to respond rapidly to an organic fall, (3) to locate rapidly an organic fall, (4) to maximize the rate of consumption and quantity ingested of the organic fall and, (5) to utilize the consumed food efficiently. Each of these attributes can be further refined by defining specific expected mechanisms to achieve them.

Starvation

Resistance to starvation would possibly involve a state of temporary "torpor": the respiration rate would be lowered while the animal subsisted on a high energy reserve such as lipid. During this inactive state, the amphipods would maintain an acute sensitivity to the presence of potential food falls while retaining some degree of protection from predation (e.g., by hiding in the sediment). We interpret our resting O_2 consumption rates when amphipods are not exposed to the scent of bait as being such a state of torpor.

Torpor is used by a variety of animals when food supply is low. The metabolic rate of bumblebees is 3 orders of magnitude lower during torpor than during active foraging (Heinrich, 1975). Hummingbirds also expend significantly less energy in a torpid state (Pearson, 1950). The total lipid in the four species of scavenging amphipods we examined (Table 2), and the lipids found in Hirondellea gigas being predominantly triglyceride (Yayanos and Nevenzel, 1978) suggests a high energy fuel reserve. The total lipid content of the two Paralicella caperesca used in our O_2 consumption measurements is sufficient to maintain these animals at the resting rate of respiration for between 40 and 96 days (Table 4). If we assume conservatively that only 50% of this lipid is an energy reserve such as neutral lipid then it still will be able to sustain these animals in a resting period for 20-48

days. If one takes glycogen reserves into account, P. caparesca could be sustained at a resting level for up to 126 days based on total lipid, or 78 days based on 50% of the lipid.

Sustenance times are much shorter in the shallower living Orchomene sp. A and sp. B (Table 4). Orchomene sp. B from 1300 m can subsist on the total lipid at a resting rate of metabolism for up to 9 days or almost 9.5 days on combined glycogen and lipid. Whereas, the shallowest species Orchomene sp. A can live at the resting rate for only 1.1 days on the total lipid energy resource. Since concentrations of glycogen are relatively low, they do not appreciably extend this period. Hence, it would appear that the shallower living species must forage for food more often than the deeper living species, Paralicella caperesca.

While in a state of torpor, animals would have to maintain an acute sensitivity to the presence of organic falls within a certain surrounding radius. Dahl (1979) has reported that lysianassid amphipods, including Eurythenes gryllus, have dense accumulations of chemosensory setae for reception of odors carried by water currents. This does not preclude the possible use of mechanosensory mechanisms to detect the presence of food such as pressure waves generated either by the impact of a bait fall on the bottom or by the increased swimming activity of scavengers directed to or at such a fall (Horridge, 1966).

During torpor, as with terrestrial animals which hibernate or undergo torpor, there is a period of increased vulnerability to predation and hence some protection would be required such as hiding in the sediments or being of sufficient size to escape predation. In support of this hypothesis, examination of 311 Paralicella caperesca showed that only individuals <7 mm

had sediment in their guts (286 specimens <7 mm, 26% with sediment, total size range 3-16 mm) (R. R. Hessler and C. L. Ingram, unpublished data). A higher incidence of gut sediment was also found in smaller individuals of Hirondellea gigas from the Philippine Trench (Hessler et al., 1978). Direct observations from the submersible Alvin substantiate this behavior since P. caperesca and Orchomene sp. B were seen to emerge from the sediments when disturbed or in the presence of bait odor (K. Smith, pers. observation).

Response to a Food Fall

When a large organic fall is available, a scavenger must be able to sense its presence almost immediately, while still in a state of torpor because of the intense intra- and interspecific competition. Once the food is sensed, the animal must switch immediately into an active metabolic mode with an immediate fuel source, such as glycogen, to migrate rapidly to the meal. We interpret the rapid increase in respiration rate of Paralicella caperesca and Orchomene sp. B when exposed to bait as a response to the presence of food. The shallow-water scavenger Orchomene sp. A exhibits a similar response after a starvation period of 5 days (Fig. 2). Such increased activity resulting from a stimulus such as food odor has been routinely reported in a wide variety of marine animals both behaviorally and electrophysiologically (Laverack, 1963; Kleerekoper, 1967; Hindley, 1975; Fuzessary and Childress, 1975; Crisp et al., 1978).

Glycogen reserves are present as a ready energy reserve in all four species of scavenging amphipods we examined, being highest in Paralicella caperesca (Table 2). Glycogen reserves in P. caperesca, Orchomene sp. B and Orchomene sp. A were compared to the active metabolic rates of these animals (Table 4). Given a mean "active" rate of energy consumption, the deeper

living P. caperesca could be sustained for a period of 0.34-1.42 days or 8-34 h. The active or excitatory phase in P. caperesca lasted from 6 to 8 h (Fig. 1a). Hence, this glycogen reserve without additional lipid or protein reserve and ingestion of new food, could sustain four unsuccessful sorties in P. caperesca #1 and only one in P. caperesca sorties in P. caperesca #1 and only one in P. caperesca #2. However, the physiological state of the animal, previous history of starvation, and the small sample size must be considered in critically evaluating these estimates. This sustenance time on glycogen reserves alone, based on active rates of O_2 consumption, ranges from 0.10 days (2.4 h) in Orchomene sp. B to 0.01 days (14.4 min) in Orchomene sp. A for animals starved 5 days (Table 4). Obviously, these glycogen reserves alone would be insufficient to maintain the period of active metabolic rate suggested in Fig. 1b and 2d. However, the combined energy reserve, of glycogen and lipid would be enough to maintain both Orchomene sp. B and Orchomene sp. A for many unsuccessful sorties (Table 4).

There is a discrepancy of many days between the length of starvation period we imposed on Orchomene sp. A and the estimated sustenance time on the glycogen and lipid reserves for freshly caught specimens. Assuming that the freshly caught amphipods were not starved and total lipid represented an energy reserve, one can calculate that they could be sustained at a resting rate of O_2 consumption for up to 1.1 days and not 12 days as indicated by our starvation experiments. Additional energy sources are obviously required, perhaps through breakdown of some structural proteins and carbohydrates or by uptake in the form of dissolved organic matter or small particulate organic material which passed through the 160-μ mesh of the holding chambers.

In comparing the three species of scavenging amphipods, estimated

sustenance time tends to increase with increasing depth and could be related to food supply, being more plentiful in the shallower waters off southern California than in the more oligotrophic western North Atlantic on the continental rise.

Location of Food Source

Once activated, scavengers must be able to locate the food fall directionally and efficiently orient to it. Detection limits may be sufficiently rigid to sensitize the animal only when it is so close that there will be a net energy gain for the entire sortie. the probability of success. During this location and homing period, the locomotion of the scavenger should be rapid and efficient using both hydrodynamic lift and buoyancy mechanisms in an effort to conserve fuel.

There is extensive literature available on optimal foraging strategies of animals (Schoener, 1971; Pyke et al., 1977). In a food-limited environment, scavenging amphipods would be predicted to optimize the resource yield while limiting the risk of predation (Covich, 1976). A spiral foraging pattern would be the most energy efficient per unit area covered with the lowest risk of predation strategy when compared to meandering and linear foraging patterns (Kitchell, 1979). Smaller amphipods would restrict such a foraging pattern closer to the refuge of the sediment while larger individuals could forage with less risk from predation further above the sediment surface and take advantage of possible vertical diffusion of chemical cues from a organic fall site (Jumars and Gallagher, in press).

The chemosensory setae associated with the antennules on lysianassid amphipods have a terminal sensory pore and numerous cilia, which probably

serve not only in sensing the presence of food but in active location while swimming (Dahl, 1979). These chemosensory mechanisms would be most effective in rheotaxis so that the amphipod could locate bait by following an odor against a flowing current; such mechanisms have been found in other crustaceans and fishes (Hindley, 1975; Kleerekoper, 1967). Chemotactic responses are questionable in such an environment where turbulent mixing in the benthic boundary layer would eliminate the odor gradient any distance from the source. However, recent laboratory studies with Orchomene sp. A from Scripps Canyon indicate that the response to bait odor is orthokinetic (increased swimming activity with increasing chemical concentration) and not a directional response to the odor bearing current (Meador, 1981). Deeper living species of scavenging amphipods may very well exhibit a more efficient rheotactic response, since food resources are more limited. Deeper living species of crustaceans, such as the bathypelagic mysid Gnathophausia ingens, exhibit a highly developed chemoreceptive ability and can detect amino acid concentrations as low as 10^{-10} to 10^{-12} M (Fuzessery and Childress, 1975).

It is difficult to evaluate the locomotory aspect of our hypothesis. There is substantial evidence that deep-sea scavenging amphipods appear within 30 to 40 min after bait has reached the bottom (Hessler et al., 1978; Thurston, 1979). Thurston (1979) noted that these amphipods appeared from down current for the first 13 h of exposure. The distance from which these animals orient to the bait and the energetic efficiency with which they make such migrations is not known. Lysianassids have well developed natatory pleopods and are generally considered strong swimmers (Hessler et al., 1972; Bowman and Manning, 1972). In addition, the preponderance of low density neutral lipids in the deep-sea lysianassids, such as Hirondellea gigas (Yayanos and Nevenzel, 1978), would provide substantial buoyancy to these

animals reducing the amount of energy to be expended in hydrodynamic lift.

From in situ observations of swimming speeds, one can estimate the potential distance traveled during the active phase in O_2 consumption. Paralicella caperesca excited by the presence of bait were observed from the submersible, and their swimming speeds were timed with reference to a structural component of known length on the respirometer. A mean swimming speed of 2.46 ± 0.45 cm sec^{-1} was determined from measurements made on 12 different P. caperesca within the size range of those used in the O_2 consumption measurements. Given a speed of 2.46 cm sec^{-1} and a 7-h activity period (Fig. 1a), P. caperesca could follow a foraging pattern for 620 m (ignoring the time necessary to mobilize the animal once stimulated by the presence of food). Such a forage by the two P. caperesca used in our respiration studies would involve an energy expenditure of from 0.35 cal (P. caperesca #1) to 1.32 cal (P. caperesca #2) thus requiring 5% and 11%, respectively, of the total energy reserves of each animal (Table 4). Based on only 50% of the lipid being available as an energy store, 7.5-20% of the energy reserve would be required for such a sortie. A similar calculation was made for Orchomene sp. B based on observations of swimming speeds from Alvin for excited animals. A mean swimming speed of 3.06 ± 0.33 cm sec^{-1} (mean ±1 SD) was calculated from 16 independent speed measurements of Orchomene sp. B. Given this swimming speed and an active rate of respiration for 7 h (see Fig. 1b), we calculated that the animal could swim a distance of 771 m, an effort that would require an energy expenditure of 0.14 cal and consume 13% of the total energy reserve or 25% of the energy reserve if only 50% of the lipid is available as energy. The shallow-water species, Orchomene (sp. A), swam faster when disturbed (5.66 ± 1.90 cm sec^{-1} (Meador, 1981) than the deeper species, and could cover a distance of 204 m in 1 h, the period of active

metabolism in animals starved 5 days (Fig. 2d). Such activity would cost Orchomene sp. A 8% of its total energy reserve for each 1-h foray (Table 4).

Consumption of Meal

On arrival at the organic fall the scavenger must cope with intense inter- and intraspecific competition for food while trying to maximize the net energy gain from the forage. The scavenger must eat as much as possible in as short a time as possible. In addition, the animal must have a large food storage capacity.

Most lysianassid scavengers from the deep sea, especially Paralicella spp. and Eurythenes spp., are well adapted for efficiently consuming large quantities of bait. The mandibles are nontriturative and adapted for cutting or slicing large chunks of flesh (Dahl, 1979). With the mandibles in a closed position, these large food particles are funneled into the foregut. In contrast, Orchomene spp. have a triturating mandible which is adapted to pulverizing small chunks of food. Thurston (1979) found that the Orchomene spp. from baited traps had smaller fragments of bait which had been chewed in their guts as compared to Paralicella spp. which tended to ingest muscle and fatty tissue from carrion leaving the more refractory structural tissue on the carcass (Shulenberger and Hessler, 1974).

Deep-sea lysianassid amphipods are capable of storing large quantities of food in their guts. Paralicella spp., with a soft extendible body wall, are capable of expanding its volume 3-5 times with food (Shulenberger and Hessler, 1974) which is stored in the midgut and can expand to fill the entire body cavity (Dahl, 1979). Such a capacity to fill the entire body cavity is also observed in Eurythenes spp. and Hirondellea spp. In Orchomene spp., the

distensible food storage portion of the alimentary tract is the relatively smaller foregut which is restricted by a thicker and more rigid exoskeleton (Thurston, 1979).

Assimilation

After scavengers have eaten to satiation, they should disperse a short distance from the fall site to avoid possible predation or cannibalism and then efficiently digest the food with the aid of gut symbiotic microflora. Digestion rate would probably be slow to maximize assimilation of available nutriment.

Predation and/or cannibalism routinely occur in scavenging amphipods collected in baited traps (Hessler et al., 1978; Thurston, 1979). After feeding to satiation, amphipods such as Paralicella spp. are so engorged with food their appendages are held in abnormal positions preventing normal ambulation (Shulenberger and Hessler, 1974). To reduce the risk of predation while either on the bait or swimming away, and to minimize excessive energy expenditures during the period of extreme distension, we would predict these amphipods would disperse only a short distance from the bait source to seek refuge. Because of this strategy one would predict that amphipods aggregate or clump in distribution. There is evidence of such clumping. Wolff (1971) observed large aggregations of swimming amphipods and isopods just above the bottom from a submersible at 4160 m. Moreover, trapped amphipods <2 cm in length exhibit extreme patchiness at depths of 5800 m (C. Ingram and R. Hessler, in prep.).

In a preliminary study of assimilation of ^{14}C-labeled fish tissue by unidentified deep-sea scavenging amphipods, Jannasch et al. (1980) found that

amphipods incorporated a relatively large fraction of the ^{14}C label into lipid over a 5-day *in situ* incubation.

Microflora have been identified and isolated from the gut contents of scavenging deep-sea amphipods (Hessler *et al.*, 1978; Schwarz *et al.*, 1976; Jannasch *et al.*, 1980). Isolates of the gut microflora incorporate significant quantities of ^{14}C label from the fish tissue into a nucleic acid-polysaccharide fraction indicating nucleic acid synthesis and growth (Jannasch *et al.*, 1980). Gut microflora taken from the guts of *Hirondellea* sp. collected in the Aleutian Trench revealed accelerated growth and substrate conversion rates on artificial media such as starch, urea and glucosamine as compared to activity rates of microorganisms in the sediment and overlying water from the same environment (Schwarz *et al.*, 1976). Such efficient conversion of sporadic bait falls by intestinal microflora might further enable the scavenging amphipod to utilize its limited food source maximally.

Acknowledgements. This research was supported by the National Science Foundation grants OCE-76-10728 and OCE-78-08640. We thank M. Laver, M. Unwin and G. A. White for technical assistance through various stages of this research and C. Ingram for amphipod identifications. The Alvin group provided their usual high quality support. Our manuscript benefited greatly from the comments by R. Hessler, C. Ingram, N. Holland, J. Meador and W. Stockton.

Literature Cited

Ansell, A. D.: Distribution, growth and seasonal changes in biochemical composition for the bivalve Donax vittatus (da Costa) from Kames Bay, Millport. J. exp. mar. Biol. Ecol. 10, 137-150 (1972)

Ansell, A. D.: Changes in O_2 consumption, heart rate and ventilation accompanying starvation in the decapod crustacean Cancer pagurus. Neth. J. Sea Res. 7, 455-475 (1973)

Armitage, K. B.: Temperature and O_2 consumption of Orchomonella chilensis (Heller) (Amphipoda:Gammaroidea). Biol. Bull. mar. biol. Lab., Woods Hole 123, 225-232 (1962)

Bligh, E. G. and W. J. Dyer: A rapid method of total lipid extraction and purification. Can. J. Biochem. and Physiol. 37-8, 911-917 (1959)

Bowman, T. E. and R. B. Manning: Two arctic bathyal crustaceans: the shrimp Bythocaris cryonesus new species, and the amphipod Eurythenes gryllus, with in situ photographs from Ice Island T-3. Crustaceana 23, 187-201 (1972)

Busdosh, M. and R. M. Atlas: Response of two Arctic amphipods, Gammarus zaddachi and Boeckosimus (Onisimus) affinis, to variations in temperature and salinity. J. Fish. Res. Bd. Can. 32, 2564-2568 (1975)

Childress, J. J.: The respiratory rates of midwater crustaceans as a function of depth of occurrence and relation to the O_2 minimum layer off southern California. Comp. Biochem. Physiol. 50A, 787-799 (1975)

Childress, J. J.: Effects of pressure, temperature and O_2 on the O_2 consumption rate of the midwater copepod Gaussia princeps. Mar. Biol. 39, 19-24 (1977)

Childress, J. J. and M. H. Nygaard: The chemical composition of midwater fishes as a function of depth of occurrence off southern California.

Deep-Sea Res. 20, 1093-1109 (1973)

Childress, J. J. and M. H. Nygaard: Chemical composition and buoyancy of midwater crustaceans as function of depth of occurrence off southern California. Mar. Biol. 27, 225-238 (1974)

Covich, A.: Analyzing shapes of foraging areas: some ecological and economic theories. Ann. Rev. Ecol. Systemat. 7, 235-258 (1976)

Crisp, M., J. Davenport and S. E. Shumway: Effects of feeding and of chemical stimulation on the O_2 uptake of Nassarius reticulatus (Gastropoda: Prosobranchia). J. mar. biol. Ass. U.K. 58, 387-399 (1978)

Cummins, K. W. and J. C. Weycheck: Caloric equivalents for investigations in ecological energetics. Mitt. Internat. Verein. Limnol. 18, 1-158 (1971)

Dahl, E.: Deep-sea carrion feeding amphipods: evolutionary patterns in niche adaptation. Oikos 33, 167-175 (1979)

Dayton, P. K. and R. R. Hessler: Role of biological disturbance in maintaining diversity in the deep sea. Deep-Sea Res. 19, 199-208 (1972)

Edwards, R. R. C., D. M. Finlayson and J. H. Steele: The ecology of 0-group plaice and common dabs in Lock Ewe. II. Experimental studies in metabolism. J. exp. mar. Biol. Ecol. 3, 1-17 (1969)

Emery, K. O. and J. Hulsemann: Submarine canyons of southern California. Part I. Topography, water and sediments. Allan Hancock Pacific Expeditions, 27(1), 1-80 (1963)

Fincham, A. A.: Rhythmic swimming and rheotropism in the amphipod Marinogammarus marinus (Leach). J. exp. mar. Biol. Ecol. 8, 19-26 (1972)

Fish, J. D. and G. S. Preece: The ecophysiological complex of Bathyporeia pilosa and B. pelagica (Crustacea:Amphipoda) I. Respiration rates. Mar. Biol. 5, 22-28 (1970)

Fuzessery, Z. M. and J. J. Childress: Comparative chemosensitivity to amino acids and their role in the feeding activity of bathypelagic and littoral crustaceans. Biol. Bull. mar biol. Woods Hole 149, 522-538 (1975)

George, R. Y.: What adaptive strategies promote immigration and speciation in deep-sea environment. Sarsia 64, 61-65 (1979a)

George, R. Y.: Behavioral and metabolic adaptations of polar and deep-sea crustaceans: a hypothesis concerning physiological basis for evolution of cold adapted crustaceans. Bull. Biol. Soc. Wash. No. 3, 283-296 (1979b)

Haedrich, R. L. and G. T. Rowe: Megafaunal biomass in the deep sea. Nature, Lond. 269, 141-142 (1977)

Halcrow, K. and C. M. Boyd: The O_2 consumption and swimming activity of the amphipod Gammarus oceanicus at different temperatures. Comp. Biochem. Physiol. 23, 233-242 (1967)

Heinrich, B.: Energetics of pollination. Ann. Rev. Ecol. Systemat. 6, 139-170 (1975)

Hessler, R. R., C. L. Ingram, A. A. Yayanos and B. R. Burnett: Scavenging amphipods from the floor of the Philippine Trench. Deep-Sea Res. 25, 1029-1047 (1978)

Hessler, R. R., J. D. Isaacs and E. L. Mills: Giant amphipod from the abyssal Pacific Ocean. Science, N.Y. 175, 636-637 (1972)

Hindley, J. P. R.: The detection, location and recognition of food by juvenile banan prawns, Penaeus merguiensis (de Man). Mar. Behav. Physiol. 3, 193-210 (1975)

Holland, D. L. and P. A. Gabbott: A micro-analytical scheme for the determination of protein, carbohydrate, lipid and RNA levels in marine invertebrate larvae. J. mar. Biol. Ass. U.K. 51, 659-668 (1971)

Horridge, G. A.: Some recently discovered underwater vibration receptors in invertebrates. In: Some contemporary studies in marine science, pp 395-405. Ed. by H. Barnes. London:George Allen and Unwin Ltd. 1966

Ikeda, T.: Nutritional ecology of marine zooplankton. Mem. Fac. Fish. Hokkaido Univ. 22, 1-97 (1974)

Isaacs, J. D.: The nature of oceanic life. Sci. Amer. 221, 146-162 (1969)

Jannasch, H. W., R. L. Cuhel, C. O. Wirsen and C. D. Taylor: An approach for in situ studies of deep-sea amphipods and their microbial gut flora. Deep-Sea Res. 27A, 867-872 (1980)

Jumars, P. A. and E. D. Gallagher: Deep-sea community structure: three plays on the benthic proscenium. In: The environment of the deep sea. Ed. by W. G. Ernst and J. Morin. Englewood Cliffs, New Jersey:Prentice-Hall (in press)

Kitchell, J. A.: Deep-sea foraging pathways: an analysis of randomness and resource exploitation. Paleobiology 5, 107-125 (1979)

Kleerekoper, H.: Some aspects of olfaction in fishes with special reference to orientation. Amer. Zool. 7, 385-395 (1967)

Klekowski, R. Z., K. W. Opalinski and S. Rakusa-Suszcewski: Respiration of antarctic Amphipoda Paramoera walkeri Stebbing during the winter season. Pol. Arch. Hydrobiol. 20, 301-308 (1973)

Krog, J.: The influence of seasonal environment changes upon the metabolism, lethal temperature and rate of heart beat of Gammarus limnaeus (Smith) taken from an Alaskan lake. Biol. Bull. mar. biol. Woods Hole 107, 397-410 (1954)

Laverack, M. S.: Aspects of chemoreception in Crustacea. Comp. Biochem. Physiol. 8, 141-151 (1963)

Lee, R. F.: Lipid composition of the copepod Calanus hyperboreus from the Arctic Ocean. Changes with depth and season. Mar. Biol. 26, 313-318 (1974)

MacDonald, A. G. and J. M. Teal: Tolerance of oceanic and shallow-water Crustacea to high hydrostatic pressure. Deep-Sea Res. 22, 131-144 (1975)

Mackintosh, J.: The effect of hunger and satiety on swimming activity in the amphipod, Marinogammarus obtusatus Dahl. Comp. Biochem. Physiol. 45A, 483-487 (1973)

Marsh, J. B. and D. B. Weinstein: Simple charring method for determination of lipids. J. Lipid Res. 7, 574-576 (1966)

Meador, J. P.: Chemoreception and food finding abilities of a lysianassid amphipod. 108 pp. MS Thesis, San Diego State University, San Diego, CA 1981

Morris, R. J.: Changes in the lipid composition of Acanthephyra purpurea Milne Edwards (Crustacea:Decapoda) during its diurnal migration: a preliminary investigation. J. exp. mar. Biol. Ecol. 13, 55-61 (1973)

Nahorski, S. R. and K. J. Rogers: An enzymic fluorometric micro method for determination of glycogen. Anal. Biochem. 49, 492-497 (1972)

Opalinski, K. W.: Standard, routine and active metabolism of the Antarctic amphipod Paramoera walkeri Stebbing. Pol. Arch. Hydrobiol. 21, 423-429 (1974)

Paul, A. Z.: Trapping and recovery of living deep-sea amphipods from the Arctic Ocean floor. Deep-Sea Res. 20, 289-290 (1973)

Pearse, J. S. and A. C. Giese: The organic constitution of several benthonic invertebrates. Comp. Biochem. Physiol. 18, 47-57 (1965)

Pearson, O. P.: The metabolism of hummingbirds. Condor 52, 145-152 (1950)

Percy, J. A.: Seasonal changes in organic composition and caloric content of an Arctic marine amphipod Onisimus (=Boeckosimus) affinis H. J. Hansen. J. exp. mar. Biol. Ecol. 40, 183-192 (1979)

Pyke, G. H., H. R. Pulliam and E. L. Charnov: Optimal foraging: a selective review of theory and tests. Quart. Rev. Biol. 52, 137-154 (1977)

Schoener, T. W.: Theory of feeding strategies. Ann. Rev. Ecol. Systemat. 2, 369-404 (1971)

Schwarz, J. R., A. A. Yayanos and R. R. Colwell: Metabolic activities of the intestinal microflora of a deep-sea invertebrate. Appl. Environ. Mirobiol. 31, 46-48 (1976)

Shulenberger, E. and R. R. Hessler: Scavenging abyssal benthic amphipods trapped under oligotrophic central North Pacific Gyre waters. Mar. Biol. 28, 185-187 (1974)

Smith, K. L., Jr.: Benthic community respiration in the N.W. Atlantic Ocean: in situ measurements from 40-5200 m. Mar. Biol. 47, 337-347 (1978a)

Smith, K. L., Jr. and R. J. Baldwin: Deep-Sea respirometry: in situ techniques. In: Handbook on polarographic O_2 sensors: aquatic and physiological applications. Ed. by H. Forstner and E. Gnaiger. Berlin: Springer-Verlag (in press)

Smith, K. L., Jr. and M. B. Laver: Respiration of the bathypelagic fish Cyclothone acclinidens. Mar. Biol. 61, 261-266 (1981)

Smith, K. L., Jr., G. A. White, M. B. Laver, R. R. McConnaughey and J. P. Meador: Free vehicle capture of abyssoppelagic animals. Deep-Sea Res. 26A, 57-64 (1979)

Smith, P. E. and R. W. Eppley: Primary production and the anchovy population in the southern California Bight: comparison of time series. Limnol. Oceanogr. (in press)

Strickland, J. D. H. and T. R. Parsons: A practical handbook of seawater analysis, 2nd ed. Bull Fish. Res. Bd. Can. 167, 1-310 (1972)

Thurston, M. H.: Scavenging abyssal amphipods from the North-East Atlantic Ocean. Mar. Biol. 51, 55-68 (1979)

Wolff, T.: Archimede Dive 7 to 4160 metres at Madeira: observations and collecting results. Vidensk. Meddr. dansk naturh. Foren. 134, 127-147 (1971)

Yayanos, A. A. and J. C. Nevenzel: Rising-particle hypothesis: rapid ascent of matter from the deep ocean. Naturwiss. 65, 255-256 (1978)

Table 1. *Paralicella caperesca*, *Orchomene* sp. B and *Orchomene* sp. A. Summary of capture site data and *in situ* observations.

	P. caperesca	*Orchomene* sp. B	*Orchomene* sp. A
Geographic location	Western North Atlantic	Santa Catalina Basin	Scripps Canyon
Latitude and longitude	38°18.4'N; 69°35.6'W	33°18.6'N; 118°36.2'W	32°52.7'N; 117°15.3'W
Description	Continental Rise	Depression in Calif. continental borderlands	Near-shore canyon
Surface primary productivity g C m^{-2} yr^{-1}	100	143	143
Sediment	Clayey silt	Silty clay	Silty sand[c]
% Organic carbon	1.3	5.8	0.51[c]
% Organic nitrogen	0.09	0.4	0.06[c]
Depth	3650 m	1300 m	56 m
Station designation	DOS-2 (Smith, 1978)	SCB (Smith et al., in prep.)	SC
Temperature at capture depth	3°C	3°C	10-13°C
Oxygen conc. at capture depth	6.54 ml l^{-1}	1.06 ml l^{-1}	2.71 ml l^{-1}
Number of individuals exposed to bait smell before respirometry	2[a]	3[b]	18[a]
Number of individuals not exposed to bait smell before respirometry	0	4[b]	18[a]
Date of capture		June 1979	Dec. 1980-Jan. 1981
Hours of direct observation	2	2	NA
Hours of respirometry	22	21-25.2	8-13

[a]Each animal respired individually in its own respirometry chamber. [b]All animals respired as a group in a single respirometry chamber. [c]Emery and Hulseman, 1963.

Table 2. Glycogen, lipid and water as % total wet weight for three species of scavenging amphipods. Values for P. caperesca were determined on the same animals used in the respiration experiment whereas the other values were derived from animals trapped specifically for proximate analyses.

Species	Location	Depth (m)	Weight (mg)	n	% Water	% Lipid	% Glycogen
Orchomene sp. A	Scripps Canyon	55	1.29 ± 0.76	4	59.1 ± 10.1	4.7 ± 2.0	0.13 ± 0.09
Orchomene sp. B	Santa Catalina Basin	1300	7.37 ± 1.33	8	77.9 ± 3.1	2.5 ± 1.3	0.11 ± 0.09
Paralicella caperesca	Western N. Atlantic	3650	30.40, 59.09	2	78.0 ± 6.0	1.9 ± 0.1	1.02 ± 0.55

Table 3. Comparison of previously published respiration rates of intertidal and midwater amphipods with the in situ respiration of Paralicella caperesca and Orchomene sp. B

Species	Respiration (lO_2 mg wet wt^{-1} h^{-1})	Temperature (°C)	Depth of capture (m)	Reference
Orchomene sp. B	0.21–0.98	3.0	1,300	Present paper
Paralicella caperesca	0.02–0.66	3.0	3,650	Present paper
Paracallisoma coecus	0.04–0.05	5.5	500+	Childress, 1975
Bathyporeia pelagica	0.10–0.52	5.0	0	Fish and Preece, 1970
Gammarus oceanicus	0.04–0.12	5.0	0	Halcrow and Boyd, 1967
Parathemisto japonica	0.33–0.45	6.5–7.0	10	Ikeda, 1974
Boeckosimus affinis	0.58	0	6	Busdosh and Atlas, 1975
Paramoera walkeri	0.06–0.14	2.0	50	Klekowski, 1973
Paramoera walkeri	0.03–0.06	1.9	5	Opalinski, 1974

Table 4. Glycogen and lipid energy reserves potentially available to three species of scavenging amphipods with the estimated sustenance time for each, assuming a mean oxygen consumption expenditure for both resting and active periods. Energy reserves and oxygen consumption of Paralicella caperesca were determined on the same animals whereas those determinations for the other species represent mean values derived from a composite group not necessarily used in both the oxygen consumption and chemical composition analysis. Oxygen consumption values for Orchomene sp. A were derived for animals starved 5 days (Fig. 2d). An oxycalorific equivalent of 4.86 cal ml^{-1} O_2 was used to convert oxygen consumption values into calories. Lipid and glycogen values were converted to caloric equivalents using 9.30 cal mg^{-1} and 4.19 cal mg^{-1}, respectively. A: active; R: resting

Species	Wet wt	Energy reserve (cal)		Oxygen consumption		Estimated sustenance time (days)		
	(mg)	Glycogen	Lipid	Rate	Cal/day	Glycogen	Lipid	Combined
Paralicella				A	1.26	1.42	4.54	5.96
caperesca #1	30.40	1.80	5.77	R	0.06	30.00	96.17	126.17
Paralicella				A	4.52	0.34	2.22	2.56
caperesca #2	59.10	1.55	10.04	R	0.25	6.20	40.16	46.36
Orchomene				A	0.49	0.04	2.08	2.12
sp. B	4.31	0.02	1.02	R	0.11	0.18	9.27	9.45
Orchomene				A	1.55	0.01	0.49	0.50
sp. A	1.76	0.01	0.76	R	0.70	0.01	1.09	1.10

Figure Legends

Fig. 1. Weight specific O_2 consumption as a function of incubation time for 2 groups of scavenging deep-sea amphipods. a. Rates of two individual Paralicella caperesca initially exposed to the odor of bait, measured in situ in western North Atlantic. b. Rates of two groups of Orchomene sp. B, one exposed to the odor of bait (solid line) and one unexposed (broken line) measured in situ in Catalina Basin. * midnight.

Fig. 2. Orchomene sp. A: Weight specific O_2 consumption as a function of incubation time for 6 periods of starvation (0 days-9 days). Solid lines indicate animals exposed to bait scent; dashed lines indicate animals not exposed to bait scent. Dry weights (mg) and sample number (in parenthesis) are noted for each set. *midnight

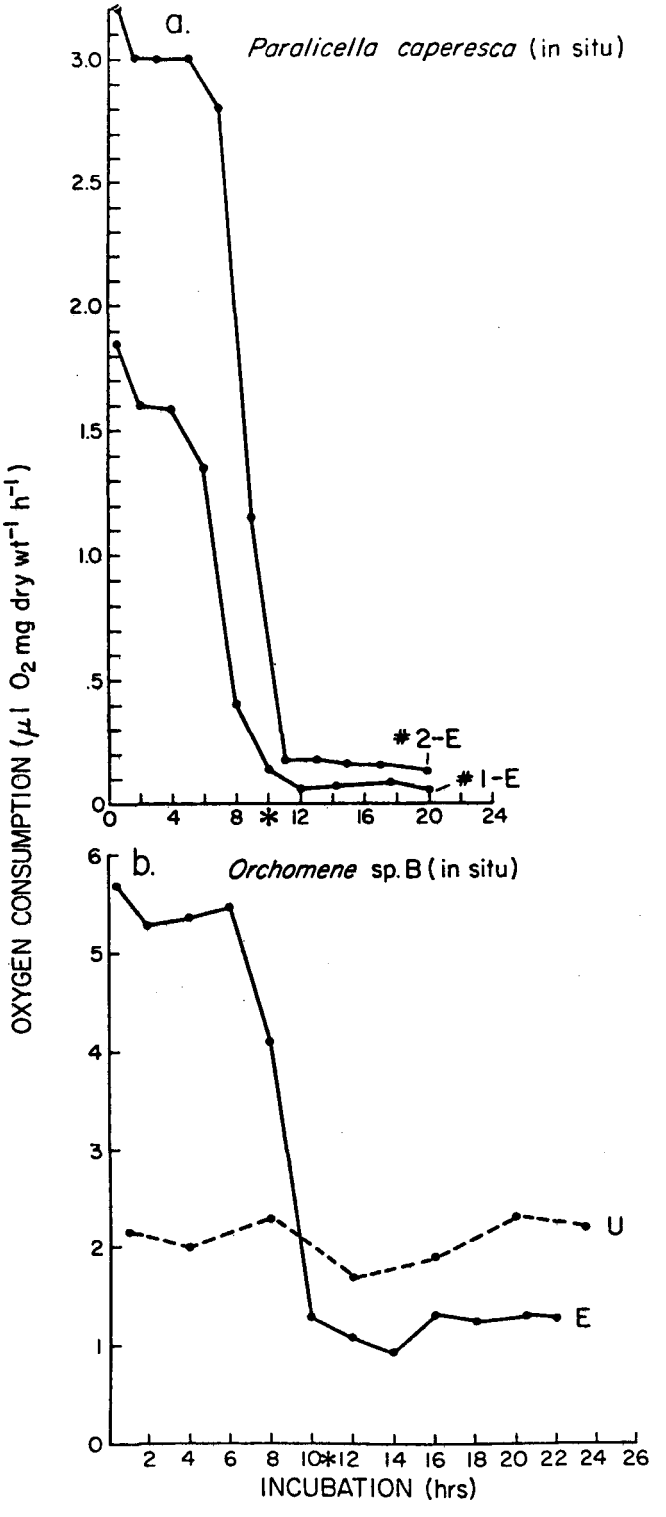

a.
Paralicella caperesca (in situ)
3.0
2.5
2.0
1.5
1.0
.5
0
#2-E
#1-E
0 4 8 * 12 16 20 24
b.
Orchomene sp. B (in situ)
6
5
4
3
2
1
0
U
E
2 4 6 8 10*12 14 16 18 20 22 24 26
INCUBATION (hrs)
OXYGEN CONSUMPTION (µl O2 mg dry wt-1 h-1)

Fig. 1

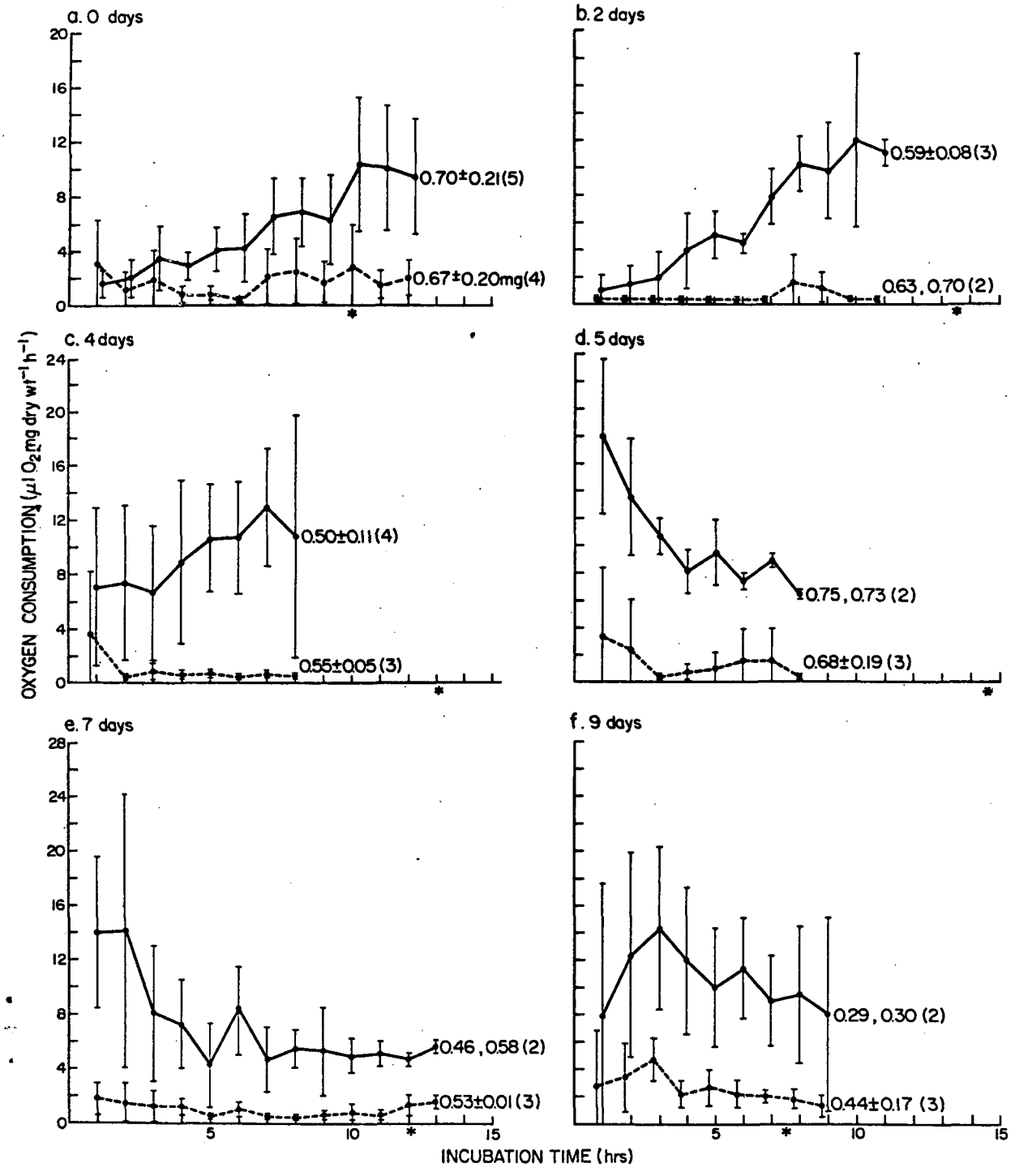

a. 0 days
0.70±0.21(5)
0.67±0.20mg(4)
b. 2 days
0.59±0.08(3)
0.63, 0.70 (2)
c. 4 days
0.50±0.11(4)
0.55±0.05 (3)
d. 5 days
0.75, 0.73 (2)
0.68±0.19 (3)
e. 7 days
0.46, 0.58 (2)
0.53±0.01 (3)
f. 9 days
0.29, 0.30 (2)
0.44±0.17 (3)
OXYGEN CONSUMPTION (µl O2 mg dry wt-1 h-1)
INCUBATION TIME (hrs)

Fig. 2

Addendum 4

Energetics of the sablefish *Anoplopoma fimbria* under laboratory conditions

K. M. Sullivan and K. L. Smith, Jr.

In press: Fisheries Reseach Board of Canada Journal

Energetics of the Sablefish, Anoplopoma fimbria, under Laboratory Conditions

Kathleen M. Sullivan and Kenneth L. Smith, Jr.

Scripps Institution of Oceanography A-002, University of California, San Diego, La Jolla, California 92093

RUNNING HEAD: SULLIVAN AND SMITH: SABLEFISH ENERGETICS

SULLIVAN, K. M. AND K. L. SMITH, JR. Energetics of the Sablefish, Anoplopoma fimbria, under Laboratory Conditions.

We measured respiration, growth, ingestion and excretion rates for sablefish, Anoplopoma fimbria collected off southern California at a depth of 500 m and maintained in the laboratory. We also measured the water, protein and lipid content of white skeletal muscle in both laboratory-held and field fish. Sablefish fed a large ration (14% of wet body weight) every 7 - 10 d showed growth rates two to three times higher than known growth rates for field fish. On a reduced ration (4% of wet body weight) A. fimbria grew at rates similar to field fish, but white muscle composition varied significantly from field fish. Oxygen consumption rates under constant temperature conditions showed a decrease in the weight specific oxygen consumption rates with increase in body weight, ranging from routine metabolic rates of 195.8 mg $O_2 \cdot kg^{-1} \cdot h^{-1}$ for a 0.25 kg fish to 60.8 mg $O_2 \cdot kg^{-1} \cdot h^{-1}$ for a 2.78 kg fish. Based on measurements of respiration and excretion, sablefish were estimated to have 162 days of energy stored in the body lipids, and did not show signs of starvation stress with food deprivation up to 6 months in the laboratory. Energy allocation show very slow growth rates, low conversion efficiencies, and low metabolic rates as adjustments made to large, infrequent meals.

Introduction

Laboratory studies can provide important types of information on fish energetics not generally obtainable from field studies. The range of growth, metabolic and excretion rates measured under controlled laboratory conditions offer insights into the physiological scope of a marine fish which may have some predictive value as to the ecology of the fish in its own environment. Subsequently, energetics studies often serve to illustrate the biological adaptations utilized by a species to cope with one particular biotic or abiotic factor in the environment. Therefore, one way of understanding the physiological consequences of a limited food supply or large infrequent rations, for example, would be to investigate the energetics of a species under such conditions in the laboratory.

Energetics studies of Anoplopoma fimbria were initiated to learn more about the energy allocation of a relatively deep living benthopelagic fish. Large deep-living benthopelagic fishes such as macrourids are known to feed on large episodic carcass falls, and have extremely low metabolic rates 2 orders of magnitude lower than comparable sized shallow-living fish when attracted to baited in situ respirometry chambers (Smith 1978). Anoplopoma fimbria has an extremely broad geographic range along the continental slope from Mexico to the Bering Sea and westward to Japan. Its bathymetric distribution is equally broad, extending from the surface water in the northermost areas of its range to over 1550 meters off southern California (Hart 1973, Phleger et al. 1970). Sablefish belong to the family Anoplomatidae (Order Scopaeniformes) which has two monotypic genera. The skilfish (Erilepis zonifer), the other family member is also a deep-living fish but does not occur south of Monterey Bay, California; both species show greatest abundance off Alaska. Because it has

no swimbladder, A. fimbria can be brought to the surface in good physiological condition unlike the majority of deep-living fishes.

Field data have been collected on the food relationships and general population ecology of A. fimbria off southern California (Conway 1967) and off Oregon and Washington (Holmberg and Jones 1954, Pruter 1954). An attempt to hold A. fimbria in large floating pens off British Columbia succeeded in maintaining a large number of fish over a period of several years on a diet of herring (Clupea harengus pallasi) and chopped dogfish (Squalas acanthias) (summarized by Kennedy, 1974). However, A. fimbria has not been studied under laboratory conditions, especially with respect to its ability to thrive on large (15% of wet weight), infrequent meals. Measurements of growth, metabolic or excretion rates have not been made on individual fish.

The purpose of this study was to examine the physiological responses of A. fimbria collected off southern California, and maintained in the laboratory on varying ration levels fed at 7 to 10 day intervals. Along with the aquarium studies, we made corresponding biochemical analyses of muscle tissue composition. This study offers insights into the changes both physiological and biochemical, that occur as a fish inhabits greater depths, experiences potentially lower rations, and longer intervals between meals.

Materials and Methods

All A. fimbria used in the aquarium experiments were collected from Scripps Canyon off San Diego, California at a depth of 468 meters with the exception of one 0.25 kg fish caught in Monterey Bay, California. All fish were collected on either electric fishing reels or longlines, and transported back to the laboratory in chilled water. In the laboratory, fish were held in 2100-l chilled running seawater tanks which had seasonal temperature fluctuations ranging from 6.0 to 10.0°C. These tanks were located in a darkened enclosure and were covered to minimize disturbances. All fish, both experimental fish and field fish sacrificed for biochemical assays were collected in June or November.

Within the tanks, A. fimbria were confined individually by nylon mesh barriers in order to minimize activity and to identify individuals. Typically fish occupied a space 1.0 x 0.5 x 0.8 m. Tanks were cleaned once a week, however, there was very little fouling over the 4- to 6-month experiments because of the darkness and the chilled water. Fish were fed every 7 to 10 days; three separate experiments were conducted, each with 4 to 8 fish.

Experiment I ran from November 1978 to June 1979 with 4 fish fed a ration of chopped mackerel and squid. Two fish were sacrificed after 100 days, and the remaining 2 fish were sacrificed after 209 days. The purpose of this experiment was to evaluate laboratory survival and maximum growth rates on weekly feedings.

Experiment II ran from June 1979 until December 1979 with 6 fish fed chopped mackerel every 8 to 10 days and 2 fish starved that entire period of time. The purpose of this experiment was to evaluate growth on varying ration

size, and time course of starvation.

Experiment III ran from November 1979 to April 1980 with 7 fish fed synthetic diets (mackerel puree, corn oil and agar, and a filler food with just agar). The purpose of this experiment was to look at varying composition of ration and starvation; fish were fed every 8 to 10 days.

The composition of the various foods was assayed and this information along with energy content of food in joules is given in Table 1. After 24 h, any uneaten food was removed from the tanks, dried and weighed. Controls were run with all food items where the loss of weight with soaking times of 6, 12 and 24 hours was measured; there was no significant loss of weight in any of the food (Student's t-test $p = 0.05$). Mackerel used were eviscerated, and sliced into 3 cm slices. Ingestion rates were determined by subtracting the uneaten food from total ration given to the fish.

Growth of Anoplopoma fimbria

Growth of A. fimbria was monitored by weighing fish every 2 to 3 wk, and by measuring changes in chemical composition of the white skeletal muscle. Fish were weighed in a handling net tared on a 9-kg capacity scale calibrated in 10-g increments. The fish were not anesthetized prior to weighing, but were removed quickly with a wet handling net, weighed and returned to the water in less than 4 min. The fish occasionally regurgitated food or refused to eat for periods up to 2 wk after this handling, but controls run on fish not weighed for 6 months compared to fish weighed biweekly showed no significant differences in growth rates ($n = 3$, Student's t-test, $p = 0.05$) over a 6-month period.

A second qualitative estimate of growth involved measuring changes in the gross chemical composition of white muscle after a fish had been on a specific dietary regime for the experimental period. When fish were collected from the field for a given experiment, 5 individuals were sacrificed immediately, and muscle tissue assayed as wild fish for comparison to experimental fish held in the laboratory.

Water contents were determined from two 1-g muscle samples taken from frozen tissue according to the procedure outlined in Sullivan and Somero (1980). Protein concentration of white muscle was determined using a modified micro-biuret method (Itzhati and Gill 1964) also described in Sullivan and Somero (1980). Lipid contents of white muscle was determined by a chloroform/methanol extraction and a simple charring method (Marsh and Weinstein 1966). Tripalmitin was used as a standard.

Respiration and Excretion

Oxygen consumption rates were determined by placing individual fish in a respiration chamber equipped with a circulating pump, and with an oxygen sensor. Fish were starved for 1 wk prior to any respiration experiments (except when noted) and allowed to acclimate in the chamber 24-36 h. The respiration chambers were usually placed in the same tank as the fish, and fish readily swam into the chambers with little coaxing. The chambers were 89.9 and 68.6 l plexiglass rectangular boxes. A Kanwisher-type polarographic electrode, amplifier and recorder system monitored the depletion of oxygen (Kanwisher 1959). These electrodes were calibrated with Winkler titrations, and with air-saturated and nitrogen-purged seawater as limits.

The chambers were set up as either flow-through, or closed systems. Closed systems were used to monitor respiration rates down to very low oxygen tensions, experiments were run with and without chemical filters that removed ammonia and urea. Open system respirometry was used to examine respiration rates over 48 hour periods at relatively constant, high oxygen tensions (85-90% saturated). Both open and closed respiration measurements are interpreted as routine metabolic rates. Routine metabolic rate is defined as the rate of oxygen consumption during normal spontaneous activity for organisms in a postabsorbtive state, and thermally acclimated (Brett and Groves 1978). This describes the condition of sablefish starved for one week, and unrestrained within the chambers.

Several control experiments were run to determine bacterial metabolism and bacterial scavenging of ammonia produced. There was no change in oxygen tension in a closed chamber over a 48 hour period and a chamber pulsed with ammonia equal to the maximum values seen in excretion experiments (84 mg/l) showed no change in the ammonia levels over 48 hours. Therefore, we found no microbial interference either in the consumption of oxygen or in the scavenging of ammonia.

Excretion was evaluated by the production of ammonia in the respiration chambers. 18 urea determinations made on 6 fish showed urea to be less than 1% of the ammonia concentration with no detectable variation over time. Thus, monitoring of urea was discontinued. Both urea and ammonia were determined by methods outlined in Strickland and Parsons (1972). Excretion rates determined from ammonia assays are expressed as mg nitrogen excreted $\cdot$ $kg^{-1} \cdot h$.

In experiments where both oxygen consumption and nitrogen excretion were measured, oxygen to nitrogen ratios were calculated.

Results

Growth

Growth, ingestion rates and conversion efficiencies of all experiments are presented in Table 2. In the first experiment growth rates ranged from 0.066 to 0.085 kg gained per month. Conversion efficiencies were between 15 and 20% for fish on a mixed diet of mackerel and squid. The average ingested food per week was very similar between fish, with very high standard deviations, indicating large variations in ingestion rates from week to week. The smallest fish initially (1.38 kg) showed the largest conversion efficiency and greatest growth rate. There was a general decrease in growth rate and conversion efficiency with increased size.

In experiment II, fish on varying ration levels again showed large fluctuations in weekly ingestion rates, as indicated by the large standard deviations. Figure 1 illustrates the weekly ingested ration over the course of the experiment. All fish responded very similarly, and all fish varied their ingestion levels, even fish on limited rations. Conversion efficiencies were less for fish on mackerel diet alone ranging from 8 to 17%. Fish on restricted rations had roughly one third the growth rate, and one third the conversion efficiency of fish on large rations.

In experiment III, fish ate a larger proportion of the ration presented, but had low growth rates, and low conversion efficiencies on the synthetic high lipid diet. Fish on the filler diet also ate a large percentage of the ration presented. Fish on the filler diet lost weight more quickly than fish deprived of any food, starved fish in experiment II were quiescent a majority of the time compared to fish fed filler food which tended to have more short

bursts of activity. Percent water, protein and lipid of white muscle for laboratory and field sablefish is given in Table 3. In experiment I, two fish were sacrificed after 100 days, and two fish were sacrificed after 209 days. There was no significant difference between those four fish, indicating that changes from field-type muscle composition to laboratory type composition occurs within the first 100 days of feeding in the laboratory. Laboratory fish, both fed and starved, had lower water content and higher protein and lipid contents than field fish.

A plot of growth vs. ration level for 17 laboratory A. fimbria (Fig. 2) in all 3 experiments exhibits a linear relationship between ration size and growth. Both ration and growth are expressed as percent wet weight of the fish. The maintenance ration, a theoretical ingestion level at which a fish neither gains nor loses weight, is about 2% of the wet body weight per week. Maximum ingestion levels for fish fed at 7 to 10 day intervals averaged over the 5- to 7-month experiments is 10% of the wet body weight per week. The mixed diet of squid and mackerel yielded slightly higher growth rates per ration level than a diet of chopped mackerel alone.

Respiration

Oxygen consumption vs. body weight for A. fimbria measured in an open respirometry system at 8.0°C (Fig. 3) showed a decrease in the weight specific respiration rate with increase in size. Measurements represent an average oxygen consumption rate over 3 to 12 hour experiments for fish in a post-absorptive state (one week after eating) and acclimated to the chamber for 24 hours. The b exponent for the allometric equation $E_m = a\ M^b$ is 0.72 where E_m is oxygen consumption per hour. In Fig. 3, weight specific respiration rate plotted against weight yields a slope of -0.28. The b-value from the

allometric equation is very similar to the theoretical value of 0.75 found for reptiles, mammals, and fresh water fish mass-related changes in metabolic rate. The size range includes both mature and immature fish. This scaling relationship suggests that there are no ontogenetic changes in the metabolic rate during growth over the size range examined in the laboratory.

Oxygen consumption vs. external oxygen tension in closed respiration chambers at 10.0°C for starved and fed fish (Experiment II) showed a decrease in the weight specific respiration rate with a lowering of oxygen tension (Fig. 4). Starved fish, with already depressed respiration rates showed little change in oxygen consumption rates over a wide range of oxygen tensions. Fed fish showed a sharp decrease in respiration rates with a lowering in oxygen tension to rates comparable to the starved fish. In these closed chamber experiments, ammonia was chemically scrubbed from the circulating water, thus the build up of toxic waste products did not compound the effects seen in the closed system. Fish did not appear stressed at the conclusion of the closed experiments, but were quiescent.

Excretion

Ammonia excretion rates are plotted against day of the week for starved and fed A. fimbria (Experiment II) in Fig. 5. Fed fish were fed the morning of Day 1 and water samples collected at 4 to 10 h intervals throughout the week in an open chamber. Starved fish showed a low nitrogen excretion rate that did not vary over the course of the week. Fed fish showed a peak in ammonia excretion 12 to 24 h after feeding. Nitrogen excretion rates remained elevated up to 4 d after feeding, however, by the end of the week excretion rates of fed fish were similar to those of starved fish. Patterns of nitrogen excretion suggest that a fish is not in a post-absorptive state for up to 5 d

after feeding, thus allowing a week after feeding for all respiration experiments would remove food processing costs from oxygen consumption measurements.

Muscle Composition

A. fimbria maintained on a limited ration or starved in the laboratory have a higher muscle protein and lipid content that wild fish caught off southern California (Table 3). The variation between fish is much lower than for fish caught in the field as indicated by the lower coefficients of variation for the muscle composition parameters. Field fish from Scripps Canyon, San Diego Trough and San Clemente Canyon all had very similar white muscle compositions. Scripps Canyon fish were used for comparisons to laboratory fish; 5 fish were sacrificed and analyzed at the beginning of each of the 3 experiments. Fish from experiments I and II are represented in the laboratory fish. There was no significant difference between lab fish (Student's t-test, $p = 0.05$) on either full or partial/starved rations. Fish collected in Santa Catalina Basin showed the highest muscle water content, and the lowest protein and lipid contents; the muscle characteristics of these fish varied significantly from other fish collected (Student's t-test, $p = 0.10$).

The muscle composition of wild vs. laboratory fish, the variation in ingestion rates (Fig. 1) and the extended period of elevated nitrogen excretion rates (Fig. 5) suggest that A. fimbria occurring off southern California are capable of surviving well on large, very infrequent meals. The laboratory evidence suggests the fish is physiologically capable of eating very infrequently, and in fact laboratory fish were not starved in the sense of catabolizing muscle protein by food deprivation of 4 to 5 months.

Discussion

Food deprivation for a number of months does not result in starvation for A. fimbria maintained in the laboratory. A. fimbria appear to be capable of a wide range of respiration, ingestion and growth rates, and seem to thrive well on large, infrequent meals. Starvation in shallow living fish such as plaice (Pleuronectes platessa L.) has been shown to result in a significant change in white muscle composition, with an increase in water content and a drop in protein and lipid content after 35 d without food (Jobling 1980). Sablefish held in the laboratory for 5 months without food did not differ significantly in muscle composition from those fed weekly. The energy allocation of a fish ingesting large, infrequent meals has not been investigated previously, and may hold valuable insights to feeding and energetics of very deep-living marine fishes.

Growth and Ingestion

Growth of laboratory A. fimbria varies with both size and composition of ration, and growth rates measured in the lab ranged from growth rates calculated from penned-reared and wild sablefish (Table 4) to four times that of known growth rates. Initial lengths of the fish suggest that the A. fimbria used in the experiments were 3- to 4-year old fish, and probably sexually immature (Conway 1967). Generally, conversion efficiencies are higher for smaller fish on high ration levels, and not necessarily associated with the highest growth rates (Huisman 1976). Smaller A. fimbria tend to show the highest conversion efficiencies, but not always the highest growth rates. Smaller fish typically devote a large percentage of energy to growth (Brett 1976), and this is seen in the energy budget of three A. fimbria ranging from 0.25 to 2.7 kg (Table 5). The wide range of growth rates seen in the

laboratory helps explain the extremely wide variability in lengths for a given age class of A. fimbria in the field. Pruter (1954) found that the forklength of a 2-year old fish caught off Oregon and aged by otoliths can range from 350 to 590 mm in forklength, the range for 3 year old fish is from 390 to 670 mm and the range for 4 year old fish 440 to 720 mm. This range of sizes for a given age class has also been encountered by Conway (1967) for A. fimbria collected off southern California. In the northern end of their range, A. fimbria spawns from December to April, with the peak months being January and February (Phillips 1969). The difficulty in aging field fish is complicated not only by the long spawning season, but also by the range of potential growth rates for this species. Changes in food availability both with season and with depth could result in variable growth rates for cohorts.

Ingestion rates of A. fimbria were extremely variable, even after the fish had been in the laboratory for several months. This variability in ingestion rates has two posible explanations. First, large marine fish, A. fimbria may not be well suited for laboratory study. This seems unlikely because of the very high growth rates seen in the laboratory. However, fish in chemical contact with one another have very similar ingestion patterns (Fig. 1) suggesting a social aspect to their feeding behavior may be disrupted in the laboratory. Secondly, ingestion rates may be very variable because the periodicity of feeding in the field is even greater than one week. Field fish may be feeding at irregular, infrequent intervals.

If indeed, sablefish feed very infrequently in the field, this would explain the lack of starvation stress after several months of food deprivation, as reflected in the similar muscle compositions of fed and starved fish. Smith (1978) measured very low in situ respiration rates for

the abyssopelagic rattail Coryphaenoides armatus, and estimated from neutral lipid stores that the animal had 189 days of energy stored in lipid reserves. Sablefish have an order of magnitude higher lipid content than the rattail, and estimating that 70% of the lipid is neutral (or triglycerides) based on several fractionations, field fish from Scripps Canyon had 163 days of energy stored in lipid reserves. This calculation was based on respiration rates measured on laboratory fish of the same size. Exercise and burst swimming activity are energetic costs not accounted for in the laboratory. Burst swimming can elevate metabolic rates two orders of magnitude (Webb 1975); while fish in the laboratory did show bursts of activity, they were confined to spaces so small that they could not accelerate to any speed. Until levels of activity of swimming ability can be estimated for field fish, it is impossible to estimate the added expense of exercise on the daily energy requirements and growth of the fish.

Respiration and Excretion

Oxygen consumption rates were determined under constant temperature conditions, there appeared to be two important factors influencing oxygen consumption in A. fimbria: body weight and external oxygen tension. There is an order of magnitude difference in the respiration rates of the smallest (0.25 kg) and largest (2.78 kg) fish (Fig. 3). Individual fish of varying sizes are able to survive under a wide range of external oxygen tensions. Starved fish have a very constant, low rate of oxygen consumption (40 - 80 mg $O_2 \cdot kg^{-1} \cdot h$) over a wide range of oxygen tensions. Fed fish decreased their rate of oxygen consumption with a decrease in oxygen tension from 235 to 62 mg $O_2 \cdot kg^{-1} \cdot h$. Environmental oxygen tensions encountered by A. fimbria off southern California range from 0.34 to 0.80 mg O_2/l at depths greater than

450 m in the various basins (Emory 1960). Oxygen tensions have been found as high as 2.0 mg O_2/l at a depth of 1300 m on a seasonal basis in Santa Catalina Basin (Smith and Laver 1981). A. fimbria collected off southern California spend at least part of their time in colder and less oxygenated water than provided by our study. Temperatures in the depth range where the laboratory fish were collected range from 3.5 to 5°C. Measurements made under lower oxygen tensions, and information on the change in respiration rates with lowering of temperature in fish (Brett and Glass 1973) suggests that in situ respiration rates would be much lower than those measured in the laboratory. Lowering the oxygen tension and respiration rates of the fish would lengthen the amount of time a fish could survive without feeding. Known in situ respiration rates for large (0.5 to 1.2 kg) macrourids at depths of 2750 to 3650 m at 3.5°C range from 3.9 to 5.3 mg $O_2 \cdot kg^{-1} \cdot h^{-1}$ (Smith and Hessler 1974, Smith 1978). The larger sablefish may respire at comparable rates at this low temperature, the lowest weight specific respiration rate for a 2.78 kg fish at 8.0°C was 18.6 mg $O_2 \cdot kg^{-1} \cdot h^{-1}$.

Carnivorous fish normally use protein as an energy source unless starved (Brett and Groves, 1979), thus each mg of nitrogen produced in the form of ammonia represents 6.25 mg of protein metabolized, based on an average nitrogen content of proteins of 16% (Houk and Ue 1974). Proteins metabolized by fish yield 20.1 x 10^3 Joules/g (Brett 1979). Energetic costs of growth (Table 5) are based on a final composition of A. fimbria muscle of 14.5% protein and 10% lipid. The calculated cost to add 1 g of muscle is 4.31 x 10^3 Joules. The 0.25, 0.88 and 2.78 kg fish gained 35, 28 and 22 g on 15%, 7% and 6% rations respectively.

A smaller proportion of the ingested energy can be accounted for in the largest fish, perhaps due to the development of energy-dense gonadal tissue or mucus production. In contrast, the smaller fish have 86% and 99% of the ingested energy accounted for in growth, metabolism and nitrogen excretion. Feces from the sablefish were often a fine, flocculant material that was very difficult to collect quantitatively, and there seemed to be very little produced in small fish except for the expulsion of bones. In addition, the cost of food processing, the post-prandial oxygen consumption (= specific dynamic action, Beamish 1974) was not accounted for in the energy budgets. From the patterns of nitrogen excretion, A. fimbria would most likely have small, long-term cost of food processing resulting in a slightly elevated oxygen consumption rate stretching over the period of several days.

In comparison to other fish energetics studies, the sablefish grow very slowly and have very low food to flesh conversion efficiencies. Carp and trout can convert over 50% of the ration wet weight into flesh under laboratory conditions (Huisman 1976) while the sablefish in the laboratory at best can convert 10-15% of ration wet weight to body weight (Table 6). The frequency and size of the meal plays an important role in conversion efficiencies and growth rates. By ingesting large, infrequent meals A. fimbria may grow very slowly, but is also able to survive well on a variable food supply. Energetics of sablefish collected off southern California may give some insight as to how very deep-living fish allocate energy when feeding on random, episodic bait falls.

Acknowledgments

This research was supported by Sandia contract No. 74-1164 and NSF grant OCE78-08640 to K. L. Smith, Jr. We thank R. R. McConnaughey, and R. R. Wilson for help in collecting fish, and G. N. Somero, G. W. Boehlert and R. H. Rosenblatt for critical evaluation of the manuscript.

References

Beamish, F. W. H. 1974. Apparent specific dynamic action of largemouth bass Micropterus salmoides. J. Fish. Res. Board Can. 31: 1763-1769.

Brett, J. R. 1976. Feeding metabolic rates of young sockeye salmon Onchorhynchus nerka in relation to ration level and temperature. Fisheries and Marine Science Technical Report # 675, Canada 43 p.

Brett, J. R. 1979. Environmental factors and growth. In W. S. Hoar, D. J. Randall and J. R. Brett [ed.] Fish physiology Vol. VIII. Academic Press, New York and London.

Brett, J. R., and N. R. Glass. 1973. Metabolic rates and critical swimming speeds of sockeye salmon (Oncorhynchus nerka) in relation to size and temperature. J. Fish. Res. Board Can. 30: 379-387.

Brett, J. R., and T. D. D. Groves. 1979. Physiological energetics. In W. S. Hoar, D. J. Randall and J. R. Brett [ed.] Fish physiology Vol. VIII. Academic Press, New York and London.

Brett, J. R., and C. A. Zala. 1975. Daily patterns in nitrogen excretion and oxygen consumption of sockeye salmon (Oncorhynchus nerka) under controlled conditions. J. Fish. Res. Board Can. 32: 2479-2486.

Conway, J. B. 1967. Food relationships and general population ecology of the sablefish, Anoplopoma fimbria and the Pacific hake Merluccius productus. Masters Thesis, San Diego State University. 109 p.

Emory, K. O. 1960. The sea off southern California: A modern habitat of petroleum. John Wiley and Sons Ltd., New York. 366 p.

Hart, J. L. 1973. Pacific fishes of Canada. Fish. Res. Bd. of Canada, Bulletin 180. 732 p.

Holmberg, E. K., and W. G. Jones. 1954. Results of sablefish tagging experiments in Washington, Oregon and California. Pac. Marine Fish.

Comm. Bull. 3: 105-112.

Houk, T. W., and K. Ue. 1974. The measurement of actin concentration in solution: A comparison of methods. Anal. Biochem. 62: 66-74.

Huisman, E. A. 1976. Food conversion efficiencies at maintenance and production levels for carp (Cyprinus carpio L.) and rainbow trout (Salmo gairdneri Richardson). Aquaculture 9: 259-273.

Itzhati, R. F., and D. M. Gill. 1964. A micro-biuret method for estimating proteins. Anal. Biochem. 9: 401-410.

Jobling, M. 1980. Effects of starvation on proximate chemical composition and energy utilization of plaice, Pleuronectes platessa L. J. Fish. Biol. 17: 325-334.

Kanwisher, J. 1959. Polarographic oxygen electrode. Limnol. and Oceanogr. 4: 210-217.

Kennedy, W. A. 1974. Final Report on British Columbia sablefish culture experiments. Fish. Res. Bd. of Can. 103 p. Technical Report #452.

Marsh, J. B., and D. B. Weinstein. 1966. Simple charring method for determination of lipids. J. Lipid Res. 7: 574-576.

Phillips, J. B. 1969. A review of sablefish trapping experiments in California. Pac. Marine Fish Comm. Bull. 7: 81-88.

Phleger, C. F., N. Schultz, A. Soutar, and E. Duffrin. 1970. Experimental sablefish fishing off San Diego, California. Commercial Fish. Review June: 31-39.

Pruter, A. T. 1954. Age and growth of Oregon sablefish, Anoplopoma fimbria. Pac. Marine Fish. Comm. Bull. 3: 122-128.

Smith, K. L., Jr. 1978. Metabolism of the abyssopelagic rattail Corphaenoides armatus measured in situ. Nature 272: 362-364.

Smith, K. L., Jr., and R. R. Hessler. 1974. Respiration of benthopelagic

fishes: *in situ* measurements at 1230 meters. Science 184: 72-73.

Smith, K. L., Jr., and M. B. Laver. 1981. Respiration of the bathypelagic fish *Cyclothone acclinidens*. Mar. Biol. 61: 261-266.

Strickland, J. D., and T. R. Parsons. 1972. A practical handbook of seawater analysis. Bull. Fish. Res. Board Can. 167: 310 p.

Sullivan, K. M., and G. N. Somero. 1980. Enzyme activities of fish skeletal muscle and bran as influenced by depth of occurrence and habits of feeding and locomotion. Mar. Biol. 60: 91-99.

Webb, P. W. 1975. Hydrodynamics and energetics of fish propulsion. Bull. Fish. Res. Board Can. 190: 158 p.

Table 1. Proximate chemical composition of squid, Pacific mackerel and synthetic foods used in *Anoplopoma fimbria* growth experiments. All values are expressed as percent wet weight with standard deviation and sample size. Joules per gram of food are calculated from average composition and conversion of 18.8×10^3 Joules $\cdot g^{-1}$ protein and 33.5 J $\times 10^3 \cdot g^{-1}$ lipid (Brett and Groves 1979).

Food	Percent water	Percent protein	Percent lipid	Joules per gram
Squid	82.0 ± 3.3	11.4 ± 2.7	2.3 ± 1.6	2.92×10^3
(*Loligo operensus*)	n = 12	n = 12	n = 12	
Pacific mackerel	72.5 ± 4.2	18.6 ± 3.7	3.0 ± 2.4	4.51×10^3
(*Scomber japonicus*)	n = 16	n = 16	n = 16	
High lipid	76.0 ± 2.1	4.8 ± 2.2	16.0 ± 1.9	6.26×10^3
synthetic diet	n = 23	n = 23	n = 23	
No-calorie	96.0 ± 1.4	1.2 ± 0.7	0.0 ± 0	0.23×10^3
synthetic diet	n = 17	n = 17	n = 17	

Table 2. Growth, ingestion, and conversion efficiencies of laboratory Anoplopoma fimbria from three growth experiments. The diet in experiment I was chopped mackerel and squid, the diet in experiment II was chopped mackerel, and the diet in experiment III was synthetic high lipid food and synthetic filler-food. See text for explanation. Conversion efficiency is defined as kg wet body weight gained per kg food.

Initial weight kg	Final weight kg	Ration (g/wk)	Ingestion (average g/wk eaten) $\bar{x} \pm$ S.D.	Months observed	Kg gained per month	Conversion efficiency
			Experiment I			
1.88	2.32	200	118.3 ± 54	3.3	0.070	0.15
1.80	2.24	200	118.2 ± 41	6.9	0.066	0.17
1.69	2.17	200	116.6 ± 58	3.3	0.075	0.17
1.38	1.83	200	101.0 ± 38	6.9	0.085	0.20
			Experiment II			
2.140	2.80	350	179.2 ± 63	7.2	0.091	0.12
1.96	2.70	350	173.6 ± 67	5.8	0.128	0.17
1.35	1.57	200	123.2 ± 45	5.8	0.041	0.08
1.44	1.57	90	66.5 ± 39	5.8	0.022	0.08
1.35	1.24	90	58.1 ± 23	5.8	-0.019	---
1.57	1.45	0	0	5.8	-0.020	---
0.81	0.69	0	0	5.8	-0.021	---
			Experiment III - high lipid			
2.25	2.37	250	241.0 ± 46	4.0	0.029	0.03
1.09	1.17	200	166.5 ± 37	4.0	0.020	0.03
0.990	1.10	200	175.0 ± 42	4.0	0.028	0.04
			Experiment III - filler food			
1.91	1.79	200	178.4 ± 44	4.0	-0.029	---
1.90	1.74	200	175.7 ± 33	4.0	-0.040	---
1.80	1.68	200	184.3 ± 37	4.0	-0.030	---

Table 3. Percent water, protein and lipid of white muscle of Anoplopoma fimbria kept in the laboratory for 3 months *Experiments I and II), or collected from three sites in the Southern California Bight. Means are given with standard deviation (S.D.), coefficient of variation (C.V.) and sample size (n).

Site	Average weight (kg)	Average length (mm)		Percent water	Percent protein	Percent lipid
Laboratory Fish - high rations	1.827	577	x	71.6	13.9	10.1
			S.D.	± 1.8	± 2.8	± 2.6
			C.V.	3.0%	20.1%	26.0%
			n	7	7	7
Laboratory Fish - starved or low ration	1.850	570	x	70.3	16.0	9.5
			S.D.	± 1.2	± 3.0	± 1.7
			C.V.	1.7%	18.8%	17.9%
			n	4	4	4
Scripps Canyon - San Diego Trough	2.170	588	x	7.63	12.8	8.4
			S.D.	± 5.7	± 3.2	± 3.0
			C.V.	7.5%	25.0%	37.5%
			n	15	15	13
San Clemente Canyon Fish	1.480	527	x	76.9	11.5	5.6
			S.D.	± 6.6	± 3.2	± 2.8
			C.V.	8.6%	27.8%	50.0%
			n	7	7	5
Santa Catalina Basin Fish	1.284	514	x	84.2	9.8	5.2
			S.D.	± 6.8	± 3.4	± 2.0
			C.V.	8.1%	34.7%	38.5%
			n	6	6	4

Table 4. Available growth rates and conversion efficiencies for pen-reared (Kennedy 1970) and wild tagged (Pruter 1954) Anoplopoma fimbria.

Study	Initial weight (kg)	Months observed	Gain per month (kg)	Conversion efficiency (kg flesh/kg food)
Penned-reared sablefish held off Naniamo, Canada (Kennedy 1970)	0.35 - 1.90	18	0.11 - 0.15	0.11
Wild tagged sablefish caught off Oregon (Pruter 1954)				
2 year old fish	0.69	12	0.033	--
3 year old fish	1.14	12	0.038	--
4 year old fish	1.69	12	0.042	--

Table 5. Energy budget for laboratory-reared Anoplopoma fimbria based on measurements of growth, respiration and nitrogenous excretion. Values are expressed in Joules per week, with percent of ingested calories in parentheses. All fish were held in the lab for four months on a high-lipid synthetic diet containing 6.26×10^3 per gram of food. Based on the composition of white muscle when the fish were sacrificed at the end of four months, 4.31×10^3 Joules are needed to add one gram of muscle tissue to fish.

Fish Weight (kg)	Average Ingestion (Joules/wk) $\times 10^3$	joules/kg $\times 10^3$	Metabolism (Joules/wk) $\times 10^3$	Growth (Joules/wk) $\times 10^3$	Excretion (Joules/wk) $\times 10^3$
0.250	247.9 (100%)	991.6	54.8 (22%)	151.1 (60%)	11.7 (4.7%)
0.880	371.8 (100%)	422.5	223.1 (60%)	119.7 (32%)	28.5 (8.0%)
2.780	929.5 (100%)	334.3	197.2 (21%)	95.0 (10%)	85.8 (9.2%)

Table 6. Growth expressed as percent wet weight on a given ration level for carp, brown trout and A. fimbria of comparable size. All fish reared between 8° and 10°C with the exception of A. fimbria reared in surface-floating pens experiencing summer high temperatures of 18°C (Kennedy 1969).

Fish Species	Growth (% wet weight · d^{-1})	Ration (% wet weight · d^{-1})	Reference
Carp (Cyprinus carpio)	1.3	2	Huisman (1976)
Carp (Cyprinus carpio)	2.2	4	Huisman (1976)
Brown trout (Salmo gairdneri)	1.1	2	Huisman (1976)
Sablefish (Anoplopoma fimbria)	0.3	2	this study (Experiment I)
Sablefish	0.2	2	this study (Experiment II)
Sablefish	0.2	2	Kennedy (1969)

Figure Legends

Fig. 1. Ingestion reates of IAnoplopoma fimbria in Experiment II. Dashed lines represent restricted ration levels; Fish E received 80 grams of chopped mackerel per week, Fish D received 90 g/w, Fish C received 200 g/w. Fish A and B were essentially on unlimited rations. Maximum ingestion rate for any one week period was 330 g mackerel. Ration limitations were imposed after Day 50 for Fish C, D and E.

Fig. 2. Growth wate, expressed as % wet weight increase per week, is plotted against Ration, expressed as of fish wet weight eaten per week for A. fimbria in experiments I, II and III. Growth rates were evaluated after a minimum of 100 days on a specific diet. Ration level represents an average ingestion rate over the entire experimental period. A linear regression run on all values yield an r-value of 0.91.

Fig. 3. Log-Log plot of weight specific oxygen consumption vs. wet body weight for A. fimbria at 8.0°C for fish starved for one week prior to the experiment. Respiration measurements were made in an open respirometry system over 3 to 36 hours with 5 to 22 measurements made on individual fish. Line represents linear regression curve fit to the equation $y = 0.28x + 315$.

Fig. 4. Weight specific oxygen consumption of A. fimbria vs. external oxygen tension for fish starved and fed in a closed respirometry chamber. All measurements were made at 8.0°C. High ration represents fish ingesting greater than 150 g food per week, low ration represents fish ingesting less than 150 g food per week.

Fig. 5. Ammonia excretion in mg nitrogen /kg wet weight/h over the course of a week for starved and fed A. fimbria. All measurements were made at 8.0°C, high ration represents fish ingesting over 150 g food/wk, and low ration represents fish ingesting less than 150 g food/wk. Fish were fed on the morning of day 1. Fish weights ranged from 1.0 to 1.9 kg.

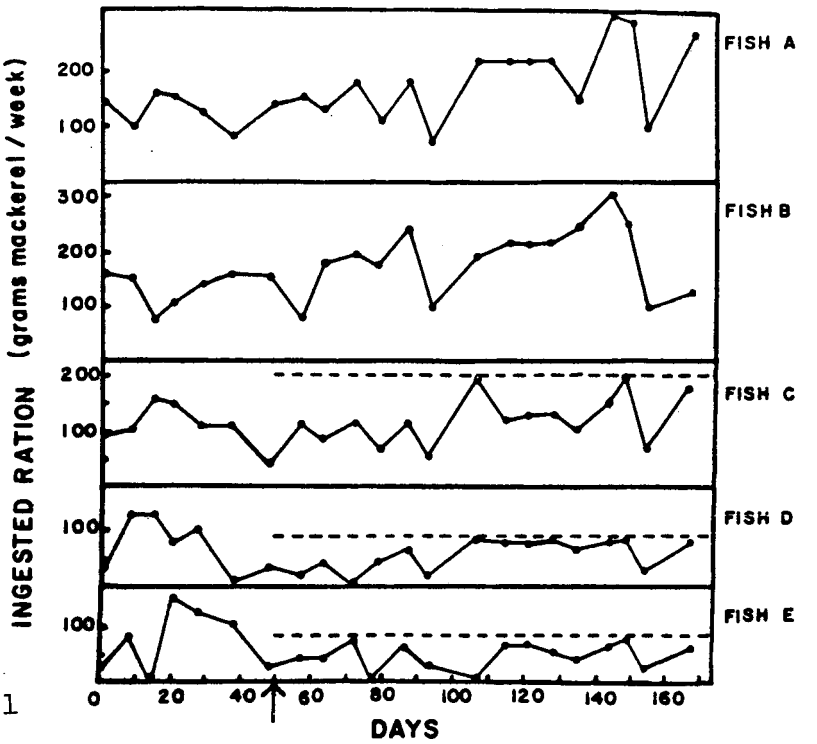

INGESTED RATION (grams mackerel / week)
FISH A
FISH B
FISH C
FISH D
FISH E
200
100
300
200
100
200
100
100
100
0
20
40
60
80
100
120
140
160
DAYS

Fig. 1

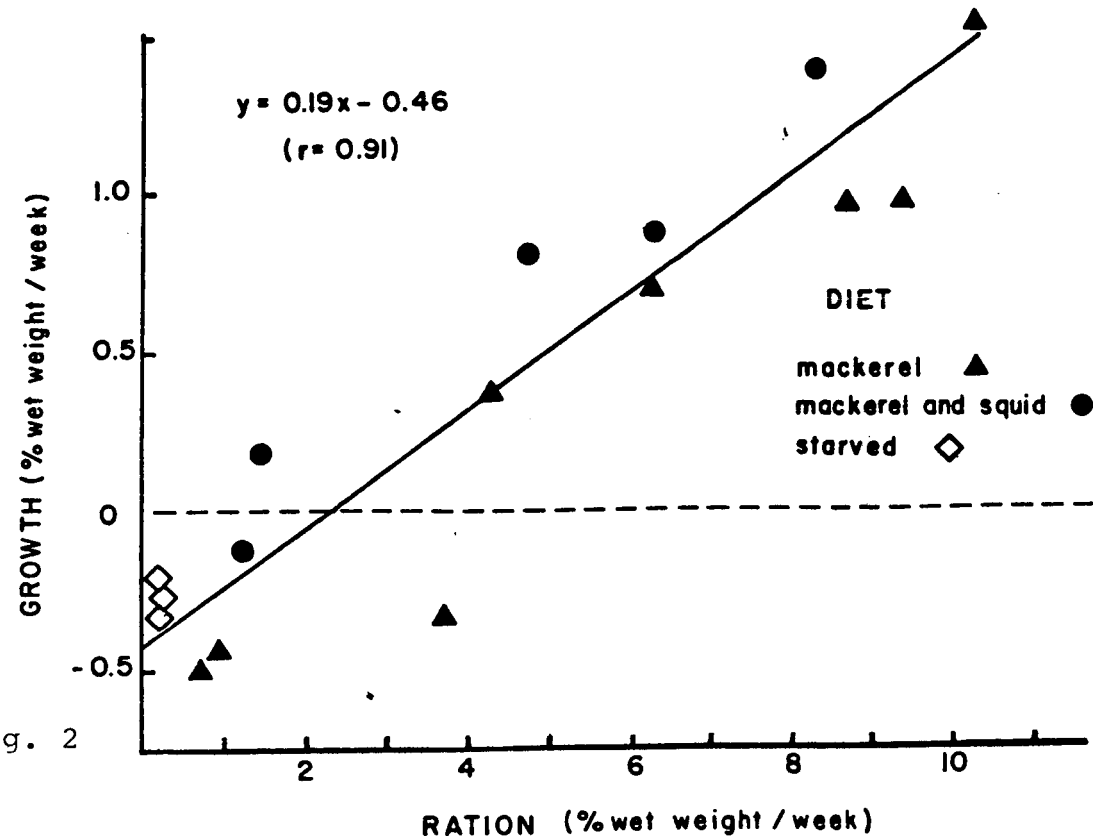

y = 0.19x - 0.46
(r = 0.91)
GROWTH (% wet weight / week)
1.0
0.5
0
-0.5
DIET
mackerel
mackerel and squid
starved
2
4
6
8
10
RATION (% wet weight / week)

Fig. 2

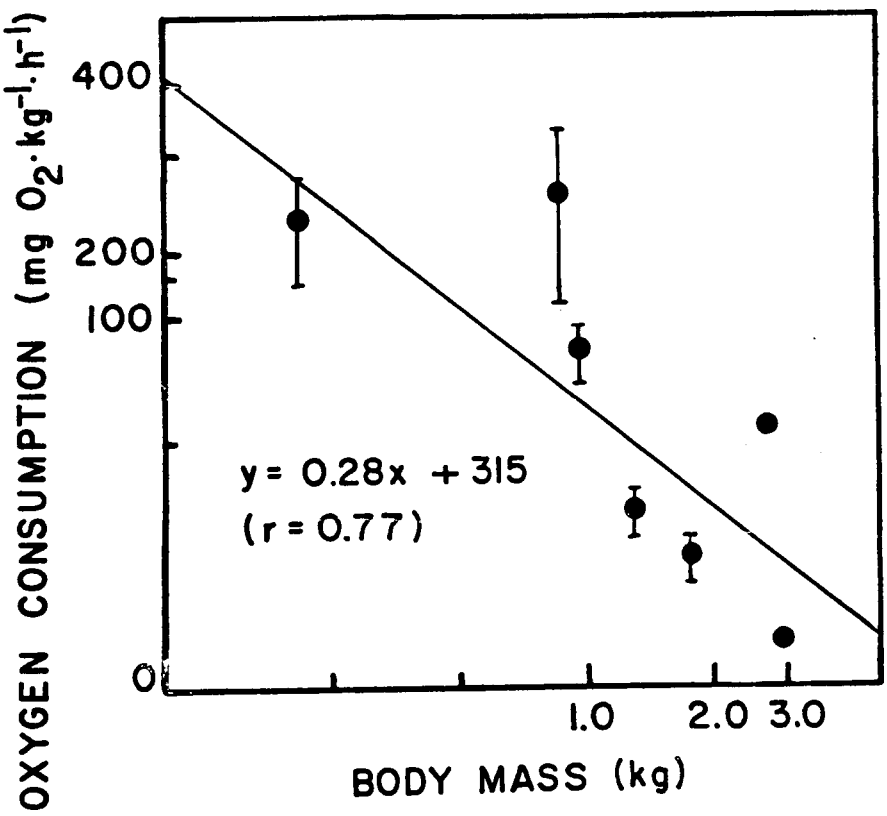

OXYGEN CONSUMPTION (mg $O_2 \cdot kg^{-1} \cdot h^{-1}$)
400
200
100
0
y = 0.28x + 315
(r = 0.77)
1.0
2.0
3.0
BODY MASS (kg)

Fig. 3

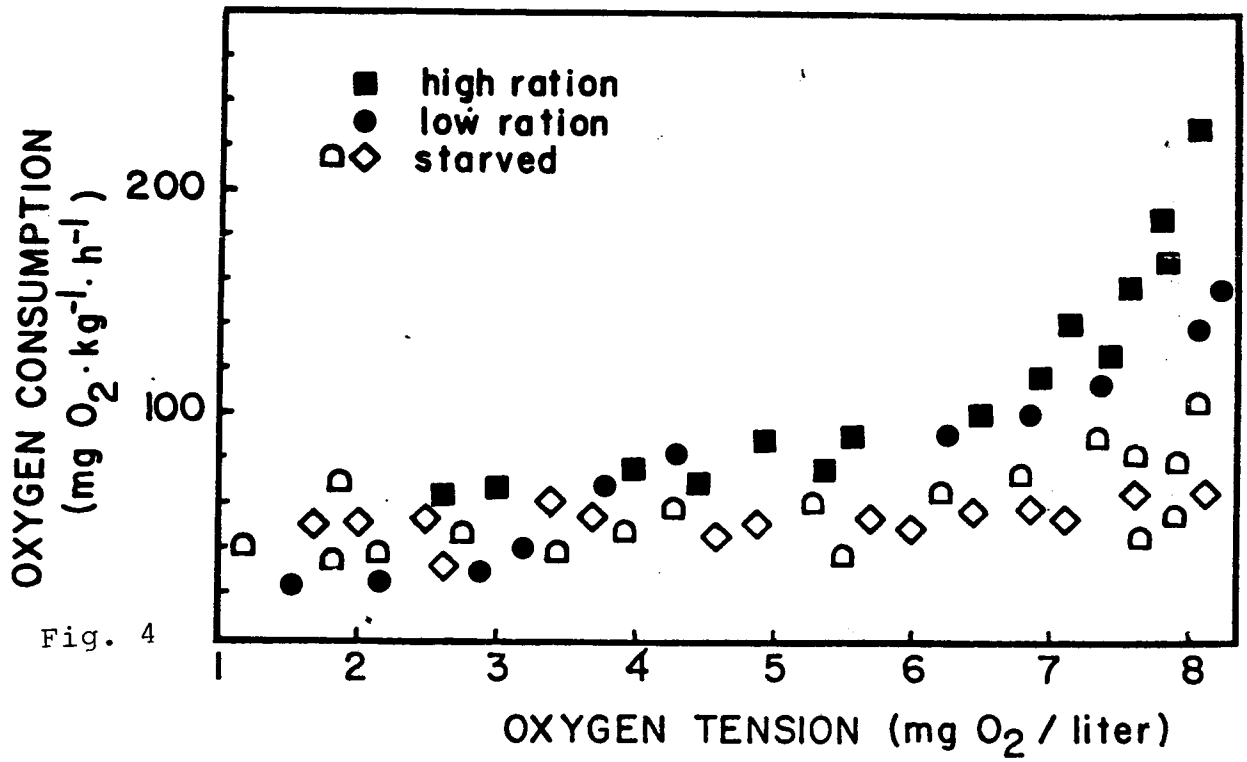
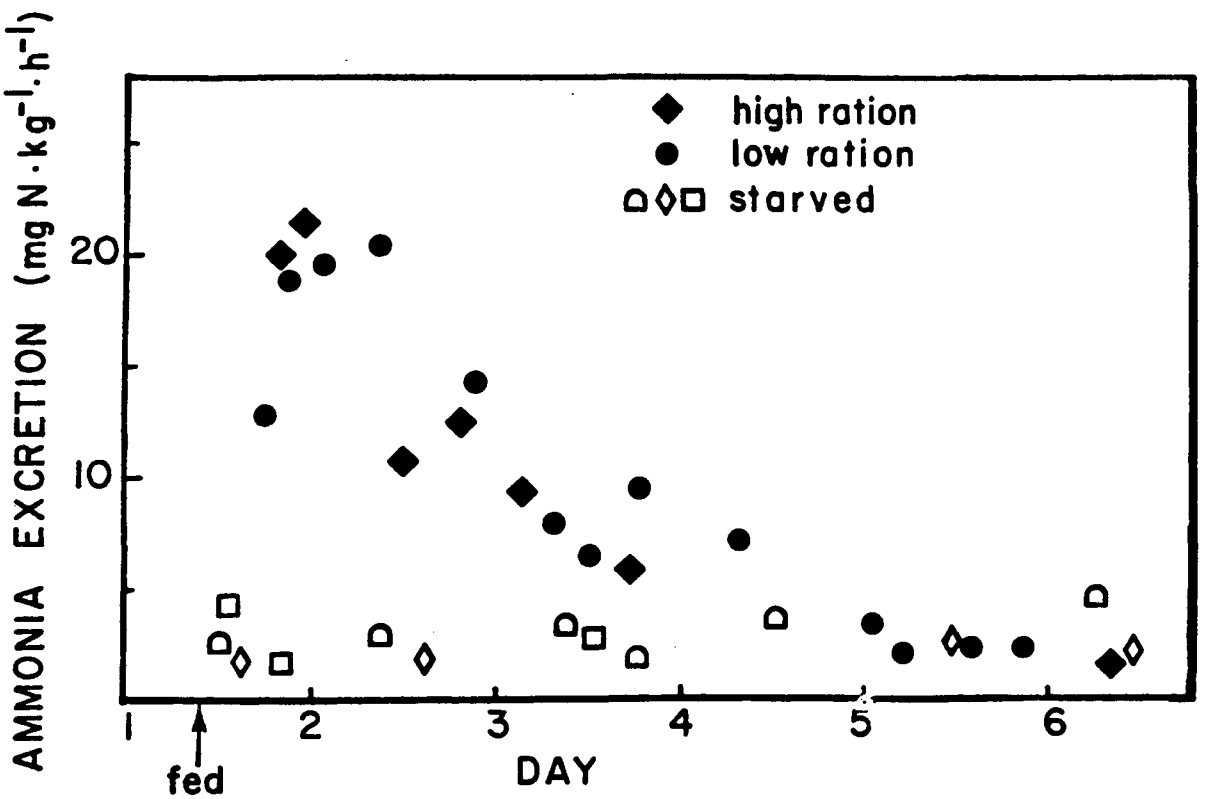

high ration
low ration
starved
OXYGEN CONSUMPTION (mg $O_2 \cdot kg^{-1} \cdot h^{-1}$)
200
100
1
2
3
4
5
6
7
8
OXYGEN TENSION (mg O_2 / liter)

Fig. 4

Fig. 5


high ration
low ration
starved
AMMONIA EXCRETION (mg N·kg⁻¹·h⁻¹)
20
10
1
2
3
4
5
6
fed
DAY

Addendum 5

A comparison of methods of age determination of *Coryphaenoides acrolepis* (Macrouridae) with a review of problems

R. R. Wilson, Jr.

Submitted to *Deep-Sea Research*

ABSTRACT:

Growth marks of scales seen by the use of polarized light are compared to those of vertebral centra in age and growth determinations of Coryphaenoides acrolepis. The two techniques are found to be comparable although the vertebrae are more reliable predictors of fish length. Logistic growth curves for the females are presented based on two different length measurements. General problems of age determinations in grenadiers are discussed.

INTRODUCTION

The age of shallow marine and fresh water fishes is often determined by counting the yearly or daily growth marks deposited on their hard structures (Bagenal 1974, Pannella 1974, Weatherley 1972, Pannella 1971, and Graham 1928). The most commonly used structures are the scales and the saccular otoliths, both of which have been employed in attempts to age populations of deep-sea grenadiers (Gordon 1979, review). However, there are difficulties in utilizing both of these structures.

Grenadier otoliths are thick, opaque, and, especially in older individuals, difficult to read by any of the reported methods (Mulcahy, Killingley, Phleger, and Berger 1979, Koch 1976, and Savvatimskii 1971). Grenadier scales do not show the typical periodic compression of the striae normally signifying annual growth marks which has led to the application of transmitted plane polarized light as described by Savage (1919) and Farran (1924) to identify what are presumed to be annual growth marks. Age and growth relationships of grenadiers derived by using polarized light (Kosswig 1974, Rannou 1973, Savvatimskii 1972 and 1971) are credible and consistent, but it is unclear that these polarized light rings do, or should, bear any relationship to growth marks of the scales, otoliths, and vertebrae which, in the same structures of shallow marine and fresh water fishes, have been shown repeatedly to be of a yearly nature (Graham 1928, review).

Savvatimskii, Kokh, and Yernst (1977) compared the ring patterns of Coryphaenoides rupestris Gunnerus from the North Atlantic seen with polarized light reading of the scales to those seen in the otoliths with normal lighting. They concluded that age determination by the two methods should be comparable, but did not make any age-length or growth rate comparisons. Such

a comparison is needed to validate the use of polarized light in the ageing of grenadiers. It is the purpose of this paper to determine whether the polarized light method does yield the same results when compared with another age indicator in the Pacific Grenadier Coryphaenoides acrolepis (Bean) and to review the underlying assumption that growth marks observed on the various hard parts of grenadiers are indicative of age, in years, of the fish.

TERMS AND DEFINITIONS

A list of terms and their definitions is given below.

Growth Mark: A general term referring collectively to any mark seen on any hard structure of the fish using any technique. The term "growth" mark implies that the marks are deposited as a result of periodic variations in the growth rate of the fish.

Annulus (pl. annuli): The growth mark seen on fish scales with ordinary light. This mark is identified by a compression, or sudden bending of the scale striae.

Striae (sing. stria): The regular, usually concentric, superficial ridges seen on all fish scales with reflected or transmitted ordinary light (see Wallin 1957).

Bands: The alternating dark and light areas of grenadier scales seen with transmitted plane polarized light and the alternating dark and light areas seen in sectioned otoliths with transmitted ordinary light (Blacker 1974 and Farran 1924, discussions).

Rings: One pair of scale or otolith bands, i.e., one dark and one light seen as indicated above. Also, the narrow concentric ridges seen in the vertebral centra of C. acrolepis with reflected ordinary light.

MATERIALS AND METHODS

Specimens were obtained from the basins of the Southern California Continental Borderland, viz., the San Diego Trough (32°41.7'N, 117°41.7'W, 1200 m), Santa Catalina Basin (33°35.8'N, 118°37.3'W, 1300 m), and San Clemente Basin (32°35.8'N, 118°6.2'W, 2100 m) between October 1979 and August 1980. They were captured using a combination of free-vehicle setlines (Phleger and Soutar 1971) and 7.6 m otter trawls. The former method is highly selective for the larger individuals, and the latter collects mainly smaller ones. The proportion of free-vehicle fishing time was much greater than that of the trawls, i.e., 42 deployments totalling 320 hours of bottom time versus 7 trawls totalling 5.5 hours of bottom time. Consequently smaller individuals were rare in the population sample, thus requiring that preserved specimens collected previously from the same basins and housed in the Scripps Institution fish collection be included as part of the total population sample. All of the free-vehicle drops and trawls were conducted on the flat part of the basins, a logistical requirement for the trawls. Evidence from previous studies on these fish suggests that the males are more numerous on the basin slopes, regardless of whether the slope lies in the upper or lower depth range of the species (R. H. Rosenblatt and T. Matsui, personal communication, Scripps Institution of Oceanography). Because this study could be performed with one sex, I concentrated on collecting the apparently more numerous and more easily obtained females. Consequently, the males were underrepresented in the collections in both numbers and size range, and no

data analysis was performed on their ring counts.

After capture, the weight, snout-vent length (SVL), total length (TL), and sex were determined for each fish. Fish with regenerated tails were included in the total length measurements. Scales were taken from the area between the base of the first dorsal fin and the lateral line. Vertebrae were taken from below the first dorsal fin (usually four to six) and both saccular otoliths were collected.

The vertebrae were cleaned by cooking in boiling water for 10-20 minutes and then picking away the tissue. They were then soaked several minutes in detergent, rinsed in tap water, and dried at 35°C. Next they were stained with alizarin (modified from Galtsoff 1952), rinsed, and air dried. The rings of the centra were counted using reflected light under a low power binocular microscope by taking two vertebrae for each fish, counting the anterior and posterior face of the centrum of each vertebrae, and then averaging the four counts, rounding off to the nearest whole integer. On some of the smaller preserved specimens only two or three of the centra faces could be counted for any two vertebrae. Therefore, averages were taken on the obtainable counts viz., two of my averages were based on two counts and three were based on three counts. The choice of using two vertebrae to obtain the counts rather than three or four was an arbitrary one. However, the standard deviations of the mean counts indicate that in most cases four counts are adequate.

The scales were treated by washing with tap water and air drying. They were prepared for counting by placing them on a glass slide, applying a drop of water, and pressing with another slide to flatten. The preparation was viewed using transmitted plane polarized light as described by Savage (1919) and Savvatimskii (1971). The concentric dark and light bands seen with this

treatment were counted on four scales from each fish. Often several scales had to be examined due to the occurrence of regenerated scales in the samples. The four counts were averaged, as with the vertebrae, to give the final estimate of the ring count. On two of the preserved specimens only two scales could be found; therefore, averages were taken based on these.

The otoliths were cleaned with tap water and air dried. Some of these were combined with previously collected C. acrolepis otoliths from specimens of the San Diego Trough and on hand in the Scripps Institution fish collection. This combination generated a sample of about 130 saccular otoliths which were embedded in casting resin and sectioned through the medial plane with a diamond blade on a low-speed circular saw. The sections, usually less then 1 mm thick, were then immersed in either water or glycerol and viewed with transmitted ordinary light through a low-power binocular microscope. The rings of all the sectioned otoliths were counted in this fashion, but the agreement between successive counts was poor, and it was decided that the otoliths were too ambiguous for further use in this study.

After generating the two data sets from the scale and vertebral ring counts, log-transformed regressions were calculated relating the total length (TL) of the female and immature fish to their mean scale ring count ($\overline{SRC}$) and mean vertebral ring count ($\overline{VRC}$). These were then plotted against the length data. Log-transformed regressions were used to achieve linearity and thereby facilitate comparisons of the two methods. Total length was used in spite of the variability introduced by regenerated tails in order to allow comparison of my results with Savvatimskii (1971, 1972) and Novikov (1970), who apparently did not exclude those measurements.

The Spearman rank correlation was determined for the two data sets to

ascertain whether any correlation exists between the $\overline{SRC}$ and $\overline{VRC}$ from the same individuals. Next, for the females and immatures, the mean snout-vent length ($\overline{SVL}$) and mean total ($\overline{TL}$) at each $\overline{SRC}$ and $\overline{VRC}$ were calculated. Using the $\overline{SVL}$ and $\overline{VRC}$ data sets, I attempted to fit three different sigmoidal curves by the method of Ricker (1979). These were the Gompertz, Putter No. 2, and logistic. The one giving the best fit to those data was then fitted to the $\overline{SVL}$ versus $\overline{SRC}$, $\overline{TL}$ versus $\overline{SRC}$, and $\overline{TL}$ versus $\overline{VRC}$ data sets. My criteria for deciding which of the three curves provided the best fit to the data included a consideration of the R^2 values associated with each and known aspects of the developmental history of C. acrolepis (Stein 1980). The fitted curves of the four data sets were then plotted.

RESULTS

Specimens ranged in size from 18 cm to 82 cm total length with 79% of those with intact tails larger than 60 cm. Those with regenerated tails constituted 8% of the sample. The wet weights ranged from 15 g to 2600 g. Ripe females were taken throughout the sampling period and females dominated our collections by a 3:1 ratio over the males. This ratio, however, may reflect my bias toward collecting the females.

The mean vertebral ring count ($\overline{VRC}$) and mean scale ring count ($\overline{SRC}$) values for the females and immatures ranged from 3 to 18 and from 3 to 20, respectively. The Spearman rank correlation relating these two data sets is significant ($p<0.01$, $N = 100$). Ring counts on the otoliths ranged from 8 to 35. The vertebrae were consistently more difficult to read than the scales. Growth marks are usually discernable near the foci of the centra but become closely spaced and less obvious towards the margins. A comparison of stained

versus unstained vertebrae indicated no significant enhancement of the growth marks by staining. An analysis of the standard deviations of the vertebral averages based on four counts where the paired scale averages were also based on four counts (N = 94 pairs of counts) showed that 83% of the deviations were less than or equal to 1.3 and 95% less than or equal to 2.1. The associated scale data is 73% less than or equal to 1.3 and 92.5% less than or equal to 2.1.

The scale rings made visible by the polarized light varied in readability. Some scales displayed the rings nicely showing a clear concentric pattern of alternating dark and light bands from the center to the margin of the scale. In others the pattern was more ambiguous, especially near the centers of the scales. Usually scales from the same fish were of comparable readability with those from younger fish being the most difficult to read.

In site of these difficulties, $\overline{VRC}$ and $\overline{SRC}$ were found to be good predictors of fish length. The results of the log-transfomed regressions relating total length to $\overline{VRC}$ and $\overline{SRC}$ are given in Figure 1. Even though a somewhat higher correlation is seen between TL and $\overline{VRC}$ than TL and $\overline{SRC}$ ($r = 0.94$ versus 0.91,respectively), both generate essentially identical regression curves in that neither the slopes or the y-intercepts are significantly different ($p>0.05$). However, it is apparent from the correlation coefficients and the analysis of the standard deviations that $\overline{VRC}$ is a more reliable predictor of length.

The comparability of these two predictors is again seen when mean total length ($\overline{TL}$) and mean snout-vent length ($\overline{SVL}$) are plotted against $\overline{VRC}$ and $\overline{SRC}$ (Figure 2). The logistic, of those curves tested, was found to give the best

fit to the data. The Gompertz curve calculated on the basis of $\overline{SVL}$ versus $\overline{VRC}$ actually yielded a slightly higher R^2 value than the logistic. However, the equation for this curve predicts a 1-year-old fish to be only 2.2 mm SVL. Stein (1980) reported mature oocytes of C. acrolepis to be a least 2 mm in diameter. Therefore, the Gompertz was discarded in favor of the logistic which predicts a 1-year-old fish of 31 mm SVL. This is more reasonable since Stein (1980) reports that scale and rostral-scute formation begins in juveniles of 16.5 mm head length (ca. 24 mm SVL).

The form of the logistic curve fitted to these data is:

$$L_t = \frac{L_{max}}{1 + Ce^{-gt}}$$

where L_{max} is the theoretical maximum length attained by members of the population, C and g are derived constants, and t is the age or mean ring count. L_t is the calculated mean length at age.

DISCUSSION

The earliest reported attempt to age grenadiers by their scales was that of Gilbert and Hubbs (1920). Using ordinary light they observed scale marks in Gadomus denticulatus Gilbert and Hubbs that appeared similar in form to the annuli of scales seen in shallow marine fishes. These marks were recognized by a slight compression of the striae near the focus of the scale and by irregular zig-zag patterns of striae perpendicular to the basal margin of the scales. Species of Gadomus from deeper than 600 m lacked any semblance of these marks, which Gilbert and Hubbs regarded as evidence for the lack of seasonality at these depths. Okamura (1970) noted in his comparison of scales from temperate and tropical grenadiers that annuli were lacking in the

tropical forms.

Farran (1924) using ordinary and polarized light, investigated scales from several grenadier species (Table 1) of the temperate northeast Atlantic. In none of his specimens, while using ordinary light, did he see a compression of the striae but noted the presence of annuli by a "sudden bending of the striae along a line perpendicular to the margin of the scale." Viewing the scales under polarized light, he attempted to define the relationship between the concentric alternating dark and light bands thus seen and the annuli as determined by the striae. He found that occasionally the total number of band pairs, i.e., rings, agreed with the number of annuli. However, he noted that the number of bands per interval distance between the annuli is not constant, but becomes progressively fewer toward the margin of the scale. This is the same condition reported by Savage (1919) for herring scales, except that the band-pairs were always more numerous than the annuli. Farran's final conclusion was that it is not possible to assign a definite age to grenadiers based on annuli determined by the striae. This rested on the observation that different scales from the same fish showed a different number of annuli and that in but few scales were the annuli clearly marked all around. Apparently, it was not his intent that polarized light rings themselves be regarded as yearly growth marks.

Kulikova (1957) and Novikov (1970) conducted age and growth determinations on four North Pacific grenadier species (Table 1) presumably using the bending of the striae to identify the annuli, which they regarded as annual. In C. acrolepis and C. pectoralis (Gilbert), two of the four species examined by Kulikova, maximum "ages" of 6 and 8 years, respectively, were assigned to individuals of about 80 cm total length. Novikov, also working

with C. pectoralis, concluded that 11 years was nearer the age of an 80 cm fish and that 15 years corresponded to a 100 cm one. Neither Kulikova nor Novikov attempted to verify the periodicity of the annuli.

Savvatimskii (1972 and 1971) working with C. rupestris and Macrurus berglax (Lacèpéde) collected from the northern Newfoundland Banks concluded that the traditional scale and otolith techniques were too ambiguous for use in the age determination of these species. Using transmitted plane polarized light to view the scale rings, an age-length relationship for C. rupestris was calculated on the assumption that each pair of dark and light bands seen represented one year's growth. The assumption was justified by the statement that polarized light rings seen in the scales of haddock and redfish are coincident with the scale annuli, which are presumably of a yearly periodicity. Savvatimskii reported an apparent difference in growth rate between the males and females of C. rupestris but no statistical analysis of the data was presented.

Rannou (1973), again using polarized light, calculated age-length regression equations for three geographically separated populations of Coelorhynchus coelorhynchus Risso. The areas collected were the Azores seamount region, the western Mediterranean, and the southern Celtic shelf ($47^{o}56.3'N$, $7^{o}32.8'W$). Comparison of these regressions showed no difference in the slopes, indicating essentially no difference in growth rates of the individuals from these different regions. Population subsamples from within these regions, however, showed slight growth rate differences. His age estimates based on the scales ranged from 1 to 6 years. The justification for assuming annularity of the ring structures was a citation (Savvatimskii 1971) to the effect that a one-to-one relationship exists between scale rings and

scale annuli in the haddock and redfish.

Confirming that the growth marks seen in the hard parts of grenadiers represent age in years is difficult. The five classical methods of confirmation given by Graham (1928) are as follows:

1) Agreement with Petersen's method.

2) The seasonal record.

3) The observation of a stock over a period of years; and marked scales.

4) Marking experiments.

5) Tank or pond experiments with fish of known age.

Method number 5 is, of course, impossible. Number 4 might be done if large numbers of grenadiers could be marked in situ and then sampled repeatedly. Number 3 requires the examination of the hard parts of a dominant year class in successive years. Fishery-quantities of specimens would have to be collected and the method requires that the stock under investigation spawns at discrete times of the year, a life history trait that has been established in only a few grenadier species (see Gordon 1979 for review of spawning periodicities). Method number 2, the seasonal record, requires an examination of the margins of the hard structures of relatively few specimens over the course of one or two years. If the growth marks are annual, then one should see an alternation from one marginal structure to the other over the course of one year. With otoliths, for example, one should see the formation of a dark band at the margin during one part of the year followed by the formation of a light band. Motais (1960) found seasonal alternations of dark and light bands at the margins of unsectioned otoliths of Trachyrhynchus trachyrhynchus Risso collected from the northwestern Mediterranean. This allowed him to determine the ages of his specimens which ranged from 3 to 7 years old with the mean total length of a 6-year-old fish being 41.6 cm. Savvatimskii, et al. (1977)

and Koch (1976) have reported that the margins of C. rupestris otoliths are ambiguous, precluding verification by the seasonal method. This same ambiguity exists at the margins of C. acrolepis otoliths and scales, especially in the older individuals.

Agreement with the Petersen method requires, for best results, an unbiased population sample large enough to reveal through size-frequency analysis the size structure of the population. Graphically, for species with discrete yearly spawning periods, the size-frequency classes appear as a series of humps, usually diminishing in height in the direction of the larger size-classes. If the hard structures of specimens taken from the size-frequency classes contain growth marks which, when counted, fall numerically in the same sequential order as the classes which they represent, then agreement with Petersen's method is established and the growth marks may be regarded as yearly. For the technique to be very effective, however, smaller size classes should be well represented. Since the young of grenadiers are notoriously difficult to collect in substantial quantities (Gunther 1887, Merret 1978, and Stein 1980), they are unlikely candidates for this method of conformation. Furthermore, the technique breaks down completely with species that recruit young throughout the year (Weatherley 1972), which is apparently the case with C. acrolepis. Nevertheless, Rannou (1976) showed that the successive addition of rings in the otoliths of Nezumia sclerorhynchus (Valenciennes) from the eastern Mediterranean coincided with the progression of the size-frequency classes as determined by head-length measurements. The relationship was most evident in the smaller size classes as would be expected by the Petersen method. Without makihg the assumption that the rings represented age in years, Rannou calculated a von Bertalanffy growth curve for the males and females combined, but noted that, at any given ring count, the

females were larger. The smallest specimens available to him were 15 mm HL and possessed 6 rings, the largest were 43-44 mm HL possessing 14-23 rings.

Table 1 summarizes the reported occurrences of growth marks in grenadier species and shows that the various types are well known in temperate species inhabiting depths from 200-5800 m. Furthermore, it is apparent that these growth marks are similar in form to those of shallow marine fishes. For example, Rannou and Thiriot Quevreaux (1975) have shown by electron microscopy that the ring structures in the otoliths of Coryphaenoides guetheri (Vaillant) collected from about 1900 m are the same as those found in the hake of the photic zone. By comparing the work of Farran (1924) and Savage (1919), it is apparent that the polarized light rings in grenadier scales are essentially the same as in shallow living fishes (i.e., herring) but it is still unclear what the relationship is between the scale annuli and the scale rings. It appears, however, in view of the comments of Gilbert and Hubbs (1920) and Okamura (1970) concerning the disappearance of scale annuli in specimens inhabiting ostensibly aseasonal environments, that scale annuli of grenadiers are labile features which tend to become ambiguous or absent with decreasing latitudes or increasing depth. The use of annuli in ageing populations of grenadiers should probably be avoided since it is certain that an underestimate of age will be obtained.

My results indicate agreement between two different ~~age~~ length predictors in C. acrolepis although the causal relationship between them is not understood. This in itself does not confirm the annual nature of the growth marks (Graham 1928), but it does indicate that there is nothing particularly unique or unexpected in the manner of growth of grenadiers. That my results do not agree with those of Kulikova (1957) for C. acrolepis is attributable to the

difference in age estimates obtained from reading the annuli directly versus reading the polarized light rings. Although a yearly periodicity of growth marks in grenadiers has been clearly confirmed only in the otoliths of *T. trachyrhynchus* by Motais (1960), the widespread occurrence and similarity of these ring structures suggest that in both shallow and deep-living grenadiers cyclical patterns of growth on the order of one year are present. The indication that these patterns persist in the abyssal grenadiers *C. armatus* (Hector) and *C. yaquinae* Iwamoto and Stein (Table 1) implies that seasonally variable growth-influencing factors are operating in the abyssal environment.

ACKNOWLEDGEMENTS

I would like to thank all of those who participated in the SABRAT cruise series I-IV for help in collecting the specimens. Particular thanks goes to K. M. Sullivan, S. C. Cary, M. Olsson, R. Chastain, and C. Stack who assisted with the specimen preparations. I would like to thank M. J. Allen, T. M. Present and A. P. Klimley for helpful discussions on this problem and T. M. Present for assisting with the French translations. Thanks also goes to K. L. Smith for reading and commenting on earlier drafts of this paper and providing shiptime for collecting. Special thanks goes to R. H. Rosenblatt for providing previously collected material, for reading and commenting on earlier drafts of this paper, and for many helpful discussions and advice. This work was supported by Sandia grant #74-1164 and NSF grant OCE78-08640 to K. L. Smith.

REFERENCES

Bagenal T.B., editor (1974) The Ageing of Fish. Unwin Brothers Limited, 234 pp.

Farran G.P. (1924) Seventh report of the fishes of the Irish Atlantic slope, the macrurid fishes (Coryphaenoididae). Proceedings of the Royal Irish Academy Dublin, 36, 91-143.

Galtsoff P.S. (1952) Staining of growth rings in the vertebrae of tuna (Thunnus thynnus). Copeia 1952, No. 2, 103-105.

Gilbert C.H. and C.L. Hubbs (1920) The macrouroid fishes of the Phillipine Islands and the East Indies. United States National Museum Bulletin No. 100, Vol. 1, part 7, 395-396.

Gordon J.D.M. (1979) Lifestyle and phenology in deep-sea anacanthine teleosts. In: Fish phenology: anabolic adaptiveness in teleosts, P.J. Miller, editor. Symposia of the Zoological Society of London No. 44, 327-355.

Graham M. (1928) Studies of age-determination in fish, part 2, a survey of the literature. Great Britain. Ministry of Agriculture, Fisheries, and Food, Fishery Investigations, series 2, Vol. 11, No. 3, 50 pp.

Gunther A.C. (1887) Report on the deep-sea fishes collected by H.M.S. Challenger during the years 1873-1876. Report on the Scientific Results of the Voyage of H.M.S. Challenger during the years 1873-1876, Zoology, Vol. 22, p. 123.

Iwamoto T. and D.L. Stein (1974) A systematic review of the rattail fishes (Macrouridae:Gadiformes) from Oregon and adjacent waters. Occasional Papers of the California Academy of Sciences, 111, 1-79.

Koch H. (1976) A contribution on the methods of age determination in roundnose grenadier (Coryphaenoides rupestris Gunn.). International Commission for the Northwest Atlantic Fisheries Research Document, Vol. 6, No. 28

(revised), 3 pp.

Kosswig K. (1974) Alter und wachstum des grenadierfisches in Nordatlantic. Informationen fur die Fischwirtschaft des Auslandes, 21, 6-7.

Kulikova E.B. (1957) [Growth and age of deep-water fishes.] Trudy Akademiia Nauk SSSR Institut Okeanologii, 20, 347-355. [In Russian] Translation In: Marine Biology, B.N. Nikitin, editor (1959), American Institute of Biological Sciences, pp. 284-290.

Marshall N.B., and T. Iwamoto (1973) Family Macrouridae. In: Fishes of the Western North Atlantic, D.M. Cohen, editor-in-chief. Memoir Sears Foundation for Marine Research, 1, part 6, pp. 496-537.

Merret N.R. (1978) On the identity and pelagic occurrence of larval and juvenile stages of rattail fishes (family Macrouridae) from 60°N, 20°W and 53°N, 20°W. Deep-Sea Research, 25, 147-160.

Motais R. (1960) Quelques observations sur la biologie d'un poisson abyssal Trachyrinchus trachyrinchus Risso et sur les conditions de vie en mer profond. Bulletin de l'Institute Océanographique, Monaco, No. 1165, 79 pp.

Mulcahy S.A., J.S. Killingley, C.F. Phleger, and W.H. Berger (1979) Isotopic composition of otoliths from a benthopelagic fish Coryphaenoides acrolepis, Macrouridae:Gadiformes. Oceanologica Acta, 2, 423-427.

Novikov N.P. (1970) Biology of Chalinura pectoralis in the North Pacific. In: Soviet fisheries investigations in the northwestern Pacific, P.A. Moiseev, editor. Proceedings of the All-Union Scientific Research Institute of Marine Fisheries and Oceanography (VNIRO), 70. Jerusalem: Israel Program for Scientific Translations 1972, pp. 304-331.

Okamura O. (1970) Studies on the macrouroid fishes of Japan--morphology, ecology and phylogeny. Reports of the Usa Marine Biological Station Vol.

17, Nos. 1-2, p. 19.

Pannella G. (1971) Fish otoliths: daily growth layers and periodical patterns. Science, 173, 1124-1127.

Pannella G. (1974) Otoliths growth patterns: an aid in age determination in temperate and tropical fishes. *In:* The Ageing of Fish, T.B. Bagenal, editor, Unwin Brothers Limited, pp. 28-39.

Phleger C.F. and A. Soutar (1971) Free vehicles and deep-sea biology. American Zoologist, 11, 409-418.

Rannou M. (1973) Étude de la croissance de Coelorhynchus coelorhynchus (Téléostéens, Gadiformes). Bulletin du Muséum National d'Historie Naturelle, series 3, No. 160, Écologie Général, 16, 273-281.

Rannou M. (1975) Données nouvelles l'activité reproductrice cyclique des poissons benthiques bathyaux et abyssaux. Académie des Sciences, Paris, Comptes Rendus Hebdomadires des Séances, serie D: Sciences Naturelles, 281, 1023-1025.

Rannou M. (1976) Age et croissance d'un poisson bathyal: Nezumia sclerorhynchus (Macrouridae:Gadiformes) de la mer d'Alboran. Cahiers de Biologie Marine, 17, 413-421.

Rannou M. and C. Thiriot-Quievereux (1975) Structure des otolith d'un Macrouridae (Poisson:Gadiforme) bathyal. Étude au microscope électronique a balayage. Annales Institut Océanographique, Paris, 51, 195-201.

Ricker W.E. (1979) Growth rates and models. *In:* Bioenergetics and Growth, Fish Physiology Vol. 8, W.S. Hoar, D.L. Randal, and J.R. Brett, editors, Academic Press, pp. 667-741.

Savage R.E. (1919) Report on age determination of scales of young herrings, with special reference to the use of polarized light. Great Britain.

Ministry of Agriculture, Fisheries and Food. Fisheries Investigation, series 2, Vol. 4, No. 1, 31 pp.

Savvatimskii P.I. (1971) Determination of the age of grenadiers (Order Macruriformes). Journal of Ichthyology, 11, 397-403.

Savvatimskii P.I. (1972) [The age of the rock grenadier in the north west Atlantic and a possible influence on its population numbers.] Trudy Polyarnyi Nauchno Issledovatel'skii i Proektnii Institut Morskogo Rybnogo Khozyaistva Okeanografii, 28, 116-127. [In Russian]. Fisheries Research Board of Canada Translation series No. 2491 (1973), 26 pp.

Stein D.L. (1980) Description and occurrence of macrourid larvae and juveniles in the northeast Pacific Ocean off Oregon, U.S.A. Deep-Sea Research, 27, 839-900.

van Oosten J. (1923) A study of the scales of whitefish of known ages. Zoologica, 2, 381-412.

Wallin O. (1957) On the growth and developmental physiology of the scale of fishes. Drottningholm, Sweden. Statens Undersoeknings Och Foersoeksanstalt foer Soetvattensfisket, Report, 38, 385-447.

Weatherley A. H. (1972) Growth and Ecology of Fish Populations. Academic Press, 273 pp.

TABLE 1

Grenadier species whose hard structures are reported to contain growth marks

Species	Region collected	Depth (m)	Type	Reference
Chalinura leptolepis	Temperate NE Atlantic	4256	Otolith rings	Rannou (1975)
Chalinura murrayi[1]	Temperate NE Atlantic	770-795	Scale annuli and rings	Farran (1924)
Coelorhynchus coelorhynchus	Temperate NE Atlantic and western Mediterranean	180-810	Scale annuli and rings	Farran (1924), Rannou (1973)
Coelorhynchus occa[2]	Temperate NE Atlantic	864-1350	Scale annuli and rings	Farran (1924)
Coryphaenoides acrolepis	Temperate NW Pacific	> 1430	Scale annuli	Kulikova (1957)
Coryphaenoides acrolepis	Temperate NE Pacific	1200-2000	Scale, otolith, and vertebral rings	Wilson (this paper)
Coryphaenoides angustifrons	Temperate NW Pacific	1030-1430	Scale annuli	Kulikova (1957)
Coryphaenoides armatus	Temperate NE Atlantic	2750-4256	Otolith rings	Rannou (1975)
Coryphaenoides armatus	Temperate NE Pacific	3790	Scale, otolith, and vertebral rings	Wilson (unpublished data)
Coryphaenoides cinereus	Temperate NW Pacific	1030-1430	Scale annuli	Kulikova (1957)
Coryphaenoides guentheri	Temperate NE Atlantic	1900	Otolith rings	Rannou and Thiriot Quievreux (1975)
Coryphaenoides pectoralis[3]	Temperate NW Pacific	260-2170	Scale annuli	Novikov (1970)
Coryphaenoides rupestris	Temperate NW Atlantic	600-200	Scale annuli, scale and otolith rings	Farran (1924), Koch (1976)
Coryphaenoides yaquinae	Temperate North Central Pacific	5800	Scale, otolith, and vertebral rings	Wilson (unpublished data)
Gadomus denticulatus	Tropical NW Pacific	518	Scale annuli	Gilbert and Hubbs (1920)
Macrurus berglax	Temperate NW Atlantic	200-600	Scale rings	Savvatimskii (1971)
Nezumia aequalis[4]	Temperate NE Atlantic	450-1350	Scale annuli and rings	Farran (1924)
Nezumia liolepis	Temperate NE Pacific	1000-1300	Otolith rings	Wilson (unpublished data)
Nezumia sclerorhynchus	Eastern Mediterannean	500-800	Otolith rings	Rannou (1976)
Trachyrhynchus trachyrhynchus	Western Mediterranean	700-1100	Otolith rings	Motais (1960)
Trachyrhynchus trachyrhynchus	Temperate NE Atlantic	607-1440	Scale annuli and rings	Farran (1924)

FOOTNOTES TO TABLE 1

1 Reported as Coryphaenoides murrayi, current nomenclature that of Marshall and Iwamoto (1973).

2 Reported as Coelorhynchus labiatus, current nomenclature that of Marshall and Iwamoto (1973).

3 Reported as Chalinura pectoralis, current nomenclature that of Iwamoto and Stein (1974).

4 Reported as Lionurus aequalis, current nomenclature that of Marshall and Iwamoto (1973).

Figure 1: Total length versus Mean Ring Count from the scales and vertebrae of C. acrolepis females. Scale Ring Counts ($\overline{SRC}$) are reresented by the solid circles and broken line. Vertebral Ring Counts ($\overline{VRC}$) are reresented by the open squares and the solid line. The regression equations are (1) $Log_{10}TL=0.85(\pm0.04)\log_{10}\overline{SRC} + 1.90(\pm0.04)$ and (2) $Log_{10}TL=0.91(\pm0.03)\log_{10}\overline{VRC} + 1.83(\pm0.03)$ where for (1) $R^2=0.85$, N=89 and for (2) $R^2=0.89$, N=94. Not all points are plotted due to coincidence.

Figure 2a: Mean Total Length at a given Mean Ring Count versus Mean Ring Count fitted to a logistic growth curve. Vertical bars are the 95% confidence interval estimates of the mean length. Scale counts are represented by the solid circles and broken lines, vertebral counts by the open squares and solid lines. The equations of the curves are (1) $\overline{TL}_t = (800\ mm) \times [1 + 8.31e^{-0.32(\overline{SRC})}]^{-1}$ and (2) $\overline{TL}_t = (800\ mm) \times [1 + 8.80e^{-0.32(\overline{VRC})}]^{-1}$.

Figure 2b: Mean Snout-Vent Length at a given Mean Ring Count versus Mean Ring Count fitted to a logistic curve. Symbols are as in Figure 2a. The equations of the curves are: (1) $\overline{SVL}_t = (270\ mm) \times [1 + 9.25e^{-0.33(\overline{SRC})}]^{-1}$ and (2) $\overline{SVL}_t = (270\ mm) \times [1 + 11.0e^{-0.35(\overline{VRC})}]^{-1}$.

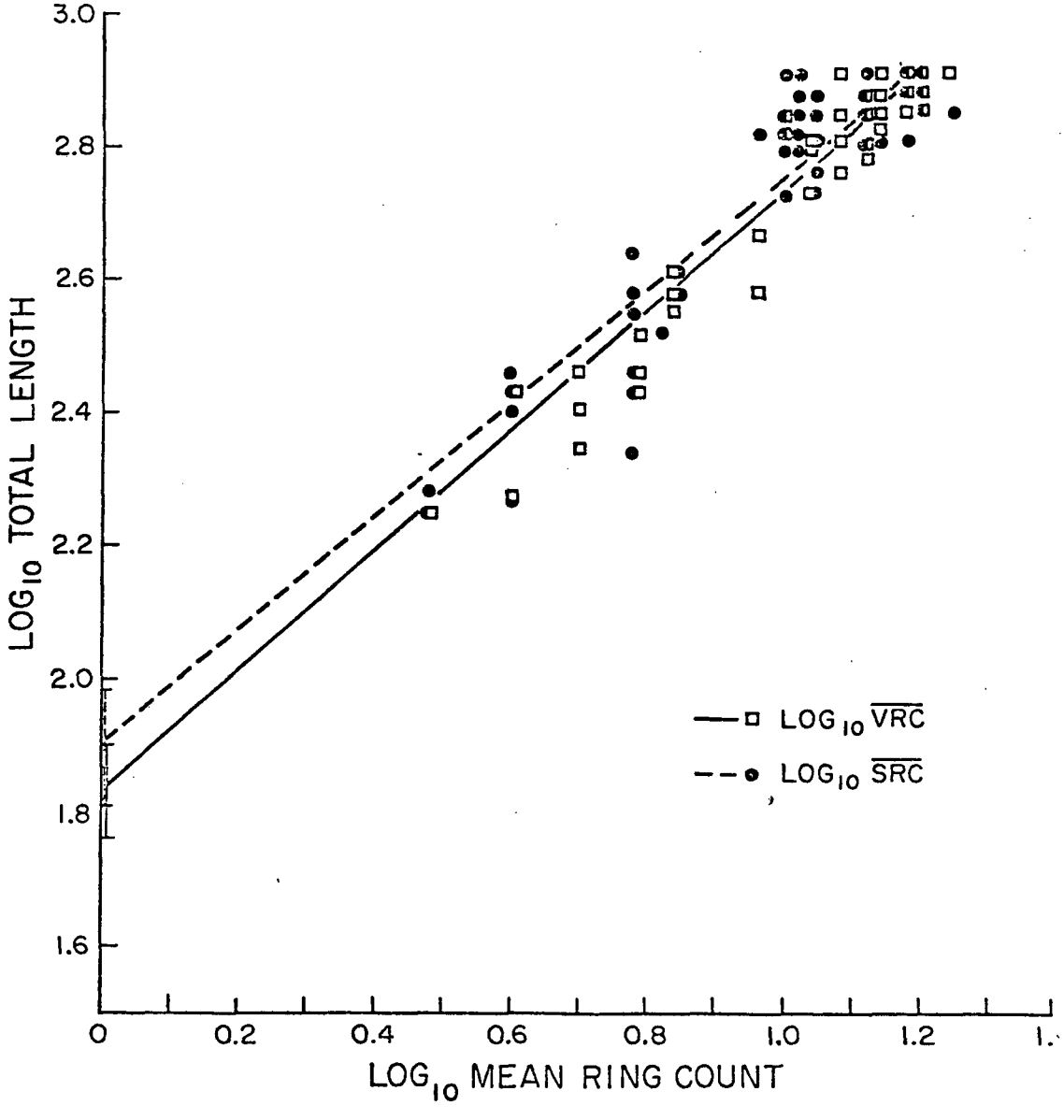

3.0
2.8
2.6
2.4
2.2
2.0
1.8
1.6
LOG10 TOTAL LENGTH
0
0.2
0.4
0.6
0.8
1.0
1.2
LOG10 MEAN RING COUNT
LOG10 VRC
LOG10 SRC

Fig. 1

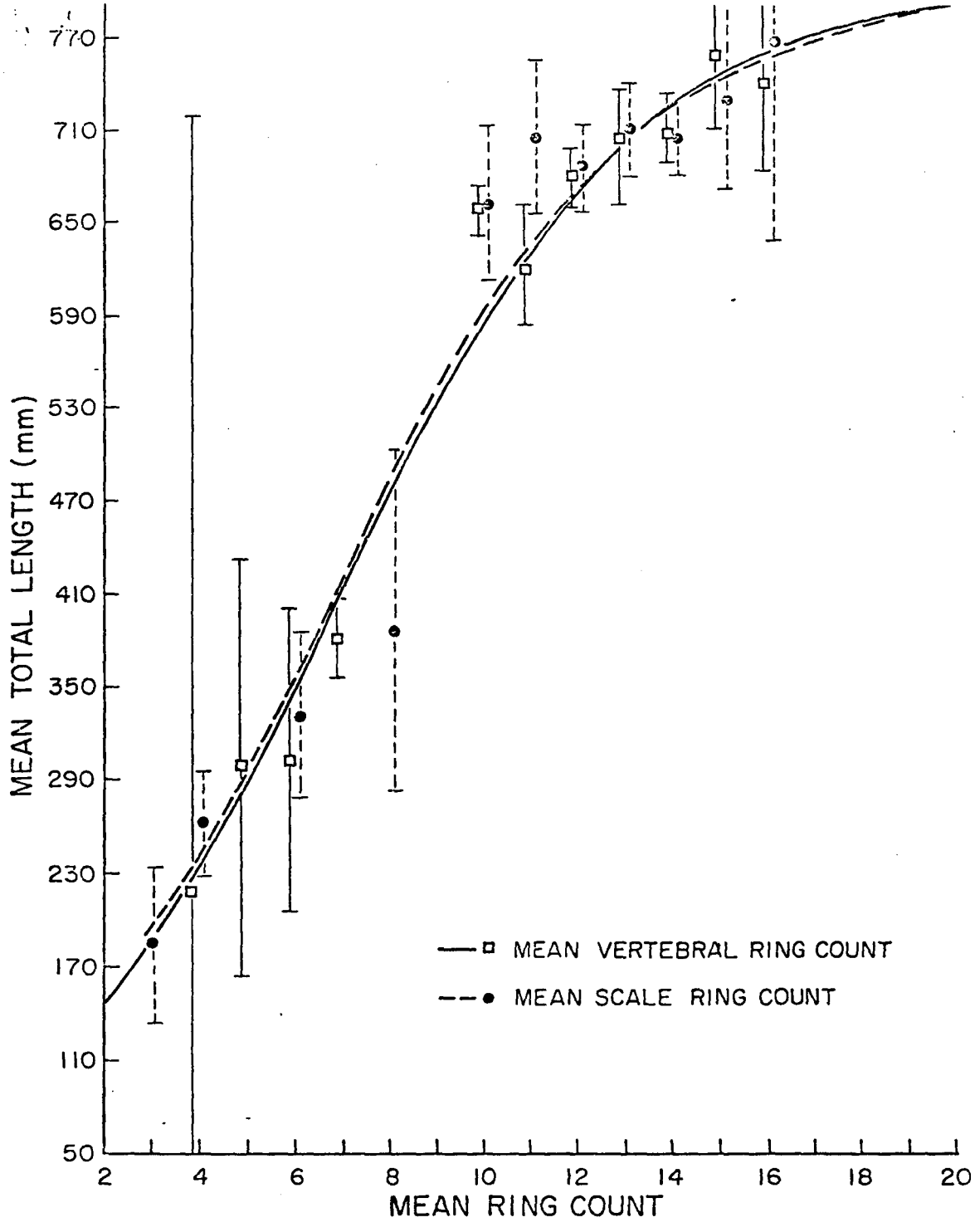

MEAN TOTAL LENGTH (mm)
770
710
650
590
530
470
410
350
290
230
170
110
50
2
4
6
8
10
12
14
16
18
20
MEAN RING COUNT
MEAN VERTEBRAL RING COUNT
MEAN SCALE RING COUNT

Fig. 2a

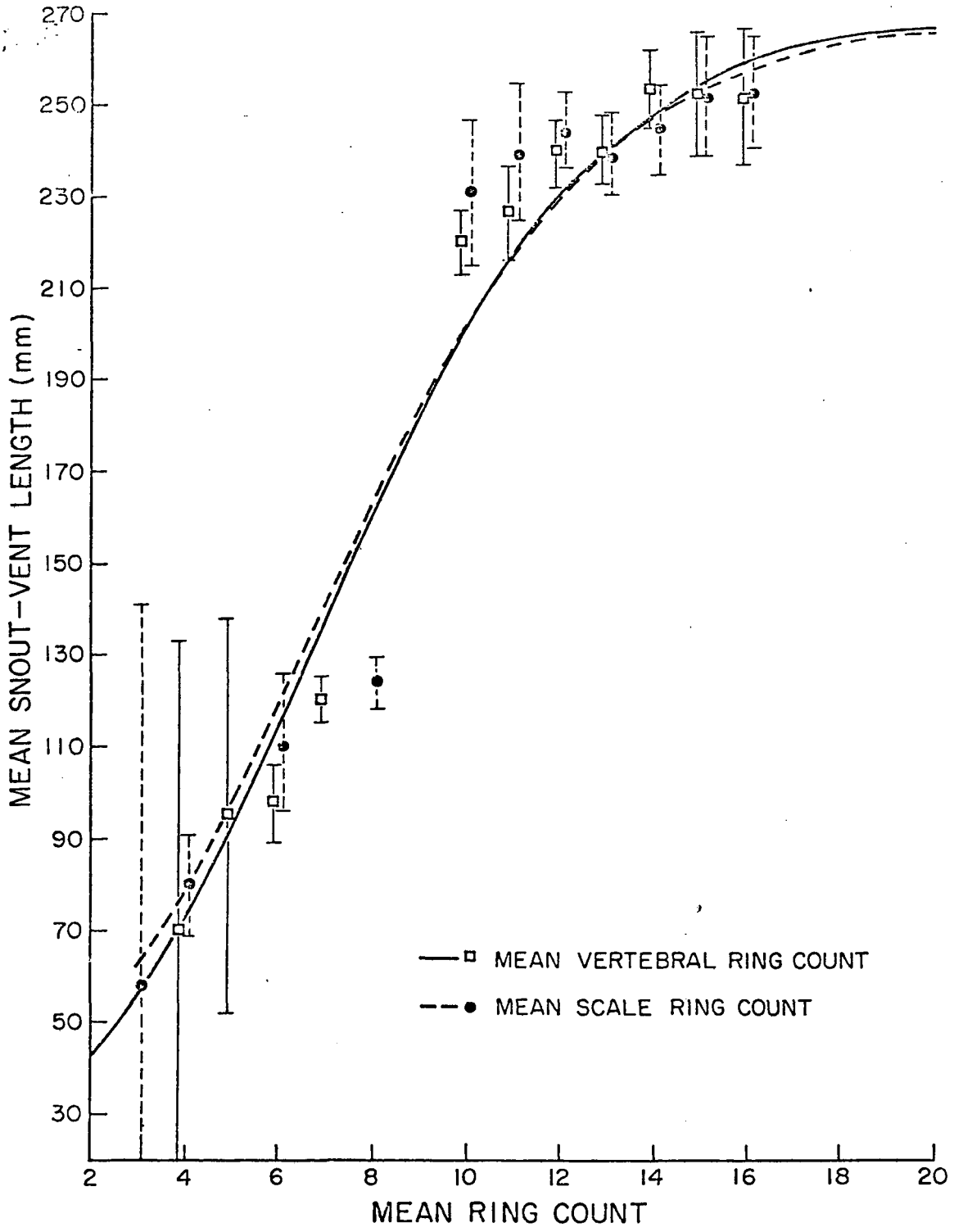

MEAN SNOUT-VENT LENGTH (mm)
270
250
230
210
190
170
150
130
110
90
70
50
30
2
4
6
8
10
12
14
16
18
20
MEAN RING COUNT
MEAN VERTEBRAL RING COUNT
MEAN SCALE RING COUNT

Fig. 2b

APPENDIX OO

LONG CORE FACILITY

Alan H. Driscoll

University of Rhode Island

(Contract #46-7036)

SUBSEABED DISPOSAL PROGRAM

The Long Core Facility, 1981

Sandia National Laboratories Contract 46-7036
Progress Report for Period 1 January, 81 to 31 December, 81

Alan H. Driscoll
Graduate School of Oceanography
University of Rhode Island
Narragansett, Rhode Island 02882-1197

Abstract

During the 1981 performance period the bulk of the work carried out as part of the Engineering Design of the Long Core Facility has centered around the refinement and design of the core head instrumentation systems. The end result has been the identification of a specific instrument configuration which will be produced during calender 1982, and which will yield data necessary to the confirmation of the computer models developed early in this program. The computer modeling work associated with this program has been brought to a point where actual field data from conventional coring systems will be required in order to finalize the models.

The scope of the work carried out during 1981 has been in keeping with the goals of the Subseabed Disposal Program and the project is considered to be on schedule relative to the program at this time.

Introduction

As in previous years, support for the Long Core Facility, (LCF) is a duality shared by the Department of Energy, Sandia National Laboratory, (DOE/SNL) and the National Science Foundation, (NSF). Under this funding scheme the development of the predictive corer models and the design of the core head instrument system are supported by DOE/SNL and the mechanical design of the complete corer/ship system by NSF. During the 1981 performance period work on the LCF has progressed at a level consistent with available funding.

The stated objective of the Long Core Facility, (LCF), Figure 1 remains that of the design, development, and production of a highly reliable deep sea coring system capable of recovering 50 meter long cores of 11 cm diameter from oceanic depths while utilizing a select number of support vessels. Previous modeling work performed by Sandia has confirmed the feasibility of this technique and the current work is concerned with the engineering design of the various subsystems which compose the LCF. To date, the URI Design Group and LCF Working Group have determined that the 50 meter coring system can be produced utilizing exisiting technology.

The DOE/SNL work supported during the 1981 performance period has con-

centrated on the refinement and preliminary design of an active piston control system and the selection of a suitable core barrel coupling design. These two tasks represent an interface between the Sandia modeling effort and the mechanical design aspects of the program as supported by NSF. In addition, the design of the core head instrumentation system was carried out with the assistance of the DOE/SNL supported consultant at URI. During this period active input was received from the Sandia Modeling Group under the direction of Charles Karnes and through scueduled meeting between the URI Design Group and the LCF Working Group.

Work Performed During 1981

The following describes the specific task performed during 1981 as part of the engineering design of the LCF and covers their development and the results achieved as of December 31, 1981.

1. Active Piston Control

At present two approaches to this problem are being actively pursued by the design group at URI. The first, and primary system is the Hydrostatic Accumulator Piston (HAP) which was selected for development based on its ability to recover a usable sample even in the event of a piston control system failure. In this unlikely event a core would be obtained of no less a quality than that obtainable with conventional coring devices.

The HAP system (Figures 2 & 3) is based on the use of a parachute to provide a restraining force on the piston during coring. The motion of the piston would be controlled by a valve between the evacuated upper section of the HAP and the oil filled lower section. The HAP will be capable of reducing its length during coring thereby maintaining a consistent piston position during the sequence. This ability will compensate for increases in internal wall friction which result in corer plugging and sample disturbance in conventional devices. (Addenda 1)

Development of this design is at a point where a reduced length model of the valving and body will be tested during 1982 along with its associated control electronics.

The second alternative the Free Activating Piston, (FAP) (Figures 4 & 5) is under study. Conceptually this system would utilize an independent piston within the barrel string, but unlike the HAP there would be no connection to the deployment cable. Movement of the piston would be controlled by a two stage valve located between the piston and an evacuated chamber in the core head.

By controlling this valve the movement of the piston can be controlled during coring and would be capable of responding to the forces generated by sample drag in the core barrel.

As a means of marking milestone within the project a system of Information Notes was initiated during 1981. These notes are representative of the thinking of the Working Group at a specific point in the project and are not a refined technical document. The Information Note, No.1 found

in Addenda 1 is presented as a means of understanding the philosophy of active piston control with a parachute controlled LCF.

2. Barrel Coupling Design

During FY 80 two barrel coupling types were identified for further study (Figure 6). These include a slipover design which has been used successfully in previous coring systems and a Sandia proposed wedge type coupling of three parts designed to produce high barrel string rigidity. Both of these coupling designs have been subjected to preliminary analytical modeling by Sandia in an attempt to identify the most suitable joint or coupling design but the data resulting from these analysis have been inconclusive. The wedge type will probably produce a more rigid joint but it is much more complex in that each joint is made up of three sections.

A finite element model is being used by Sandia to analyse the coupling designs. However, the model is limited and only partial success has been realized in determining failure potential and stress concentrations of the couplings. The use of three dimensional modeling was considered but it has been decided that full scale tests would be more appropriate to determine the suitability of the coupling configurations. These tests will supplement Sandia's modeling effort and provide experimental data to assess the various coupling designs. Details of this program are presented in Appendix 5.

The testing program will involve the construction of full scale prototype couplings fabricated from mild steel. The physical models will be tested in the URI Civil Engineering Laboratory Facilities using a Tinius Olsen machine with a 300,000 lb. capacity.

The first series of tests will involve models with 1" wall thicknesses as well as reduction couplings of 1" to .5" wall thickness. These thicknesses are considered realistic for a first test based on the size and load capacity of the machine selected. Based on results of these tests a second series may be performed in FY 81 using thicker walled models to duplicate the upper core barrel sections. Some combination of tension, compression, and bending loading situations are planned for this test series. Also, pressure tests will be conducted to assess the effectiveness of the seals.

Since the coupling design will influence barrel buckling during penetration the testing program will be designed to determine the stiffness of each coupling design. The axial and bending stresses, as well as data relative to the alignment and sealing capacity of each design. In addition, the results will be used to evaluate the Sandia modeling results so that other possible coupling concepts can be studied and a final design selected.

3. Core Head Instrumentation

During 1981 a suite of core head electronic systems was designed which would monitor both the mechanical performance of the corer and provide a sample quality monitoring function. The suite of instruments being developed include 1) Acoustic Release/Altimeter, 2) Rotation and Tilt Recorder, 3) Power and Control Unit 4) Piston Motion Sensor, 5) Cable Angle

Sensor, 6) Telemetry Package, and 7) Deck Unit (Figure 7).

Each individual instrument had been designed to include three distinct subassemblies per unit. Under this design scenario the power supply and digital subassemblies are common to all instruments and the remaining sensor interface is the only unique subassembly. This approach was taken to reduce design time and to provide as high a level of commonality between instruments as is possible.

During this performance period a decision was made to approach the development of the required core head instrumentation in selected phases. Under this scenario instruments crucial to the confirmation of the Sandia predictive models would be produced during Phase 1, the development and testing of the core head telemetry system and cable angle sensor in phase 2, and finally in phase 3 a field test of the fully integrated instrumentation system. The vehicle that was selected for the purposes of this test was the standard piston core as designed by A.H. Driscoll. This device has currently wide usage and had been a source of field data from which the Sandia models were initially developed.

In September 1981 a working group meeting was held at URI to discuss the specific requirements of the core head instrumentation and to define the actual system configuration for the phase 1 work scheduled for 1982. During this meeting the concept of individual instruments assigned specific function was eliminated as to costly and a concept of a central digital package fed by various sensors was adopted (Figure 8). This decision, based on the economics of the program, has resulted in the necessity to modify the instrument designs developed earlier in the year.

The re-design of the system has resulted in approximately 2 lost man months to the project. However, with adequate funding in 1982, this loss can be negated through a consolidation of instrument design and a testable system fielded in late 1982. The construction and fielding of the phase 1 suite of instruments is necessary to obtain accurate base line coring data for use in the confirmation of the Sandia predictive models prior to any final mechanical systems design.

Discussion

The development of the LCF is currently at a point where the basic components of the system are known and where the commencement of final design phase can begin. During 1981 the LCF system was presented at the Oceans 81 conference in Boston (Addenda 2) in order to further acquaint the community with the progress of the systems development. The maintaining of a progressive development of the LCF will be dependent upon adequate funding being provided for that purpose from the agencies involved.

The project is presently suffering from delay in receiving funding support due to the existing economic conditions. Initial support for the scheduled DOE/SNL work scheduled for October 81 was not received until December 81 and at that point only one instrument was funded. The remainder of the instrument support is scheduled for early 1982 and its

receipt will dictate the schedule of development relative to the project.

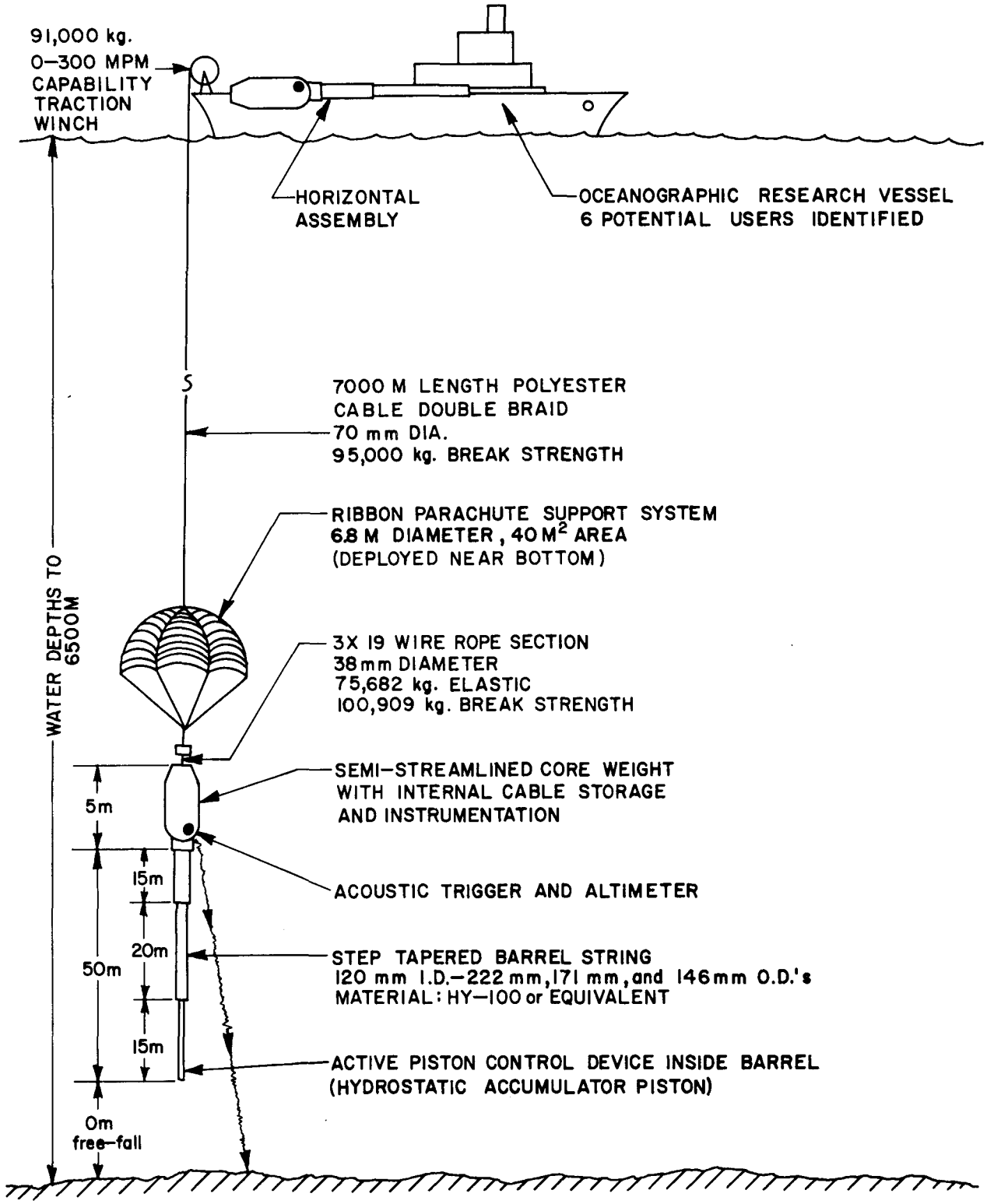
References

1. Driscoll, A.H., Devine, M.C., and Webman, K.W. "Operational Philosophy of Piston Control as Implemented with the Hydrostatic Accumulator Piston, (HAP) and a Ribbon Parachute." March 1981, LCF Information Note No.1, Unpublished manuscript.

2. Driscoll, A.H., The Long Core Facility,"New Techniques in Deep Ocean Coring" September 1981 Oceans 81, Boston.

Fig. 1

LONG CORING FACILITY
GENERAL CONFIGURATION OF SYSTEM

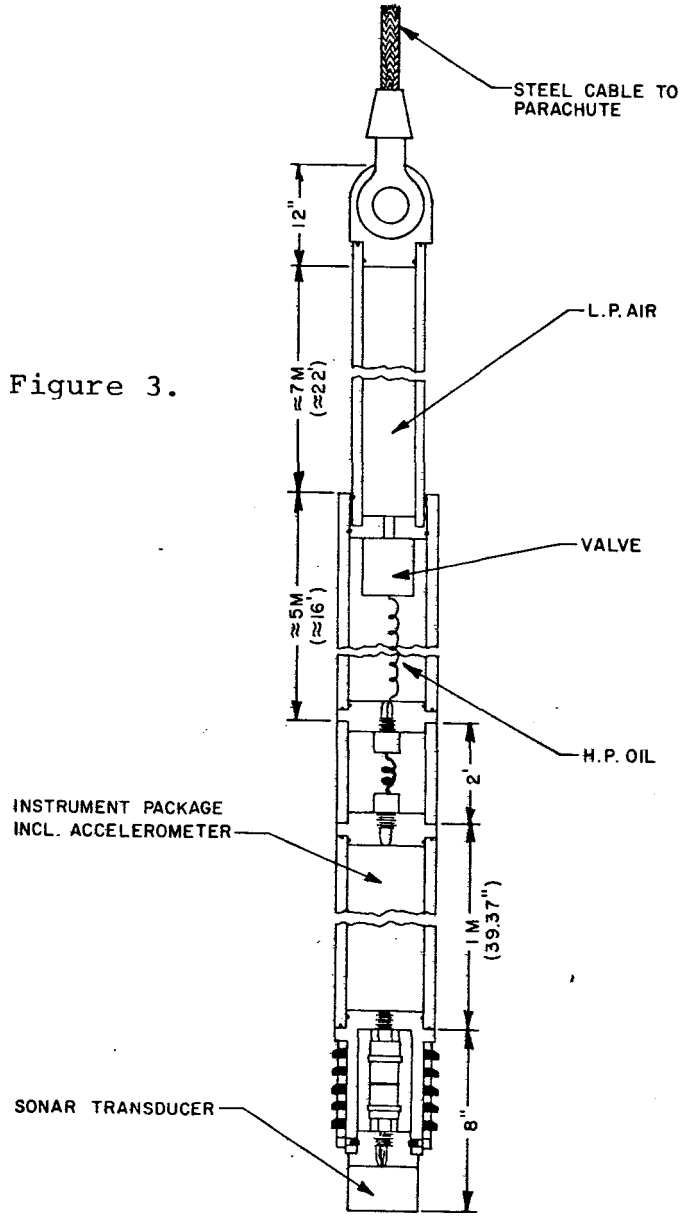


HYDROSTATIC ACCUMULATOR PISTON (HAP)

ALWAYS GET CORE - EVEN IF IT DOESN'T WORK
MINIMAL MAINTENANCE - REPLACE ENTIRE H.A.P. AT SEA
REQUIRES VALVE OPERATION AT 10,000 PSI
VALVE OPERATES IN A CLEAN ENVIRONMENT
HIGH RELIABILITY
REQUIRES MINIMAL R & D - OTHER THAN VALVE
REQUIRES PARACHUTE & SEPARATE CABLE
PHYSICAL SIZE REQUIRES H.A.P. TO EXTEND INTO CORE
WEIGHT AFTER PENETRATION
EASY ADAPTABILITY TO OTHER PISTON CORERS

Figure 2.

Figure 3.



FREE PISTON

IF IT DOESN'T WORK - NOR CORE
NO PARACHUTE OR CABLE TO PISTON REQUIRED
TWO STAGE SERVOVALVE USED
VALVE OPERATION AT 10,000 PSI REQUIRED
VALVE MAY REQUIRE SOME DEVELOPMENT
REQUIRES CHAMBER (S) TO STORE BARREL WATER
ALSO NEEDS CHAMBERS FOR HYDRAULIC OIL & NITROGEN
REDUCES CORE WEIGHT AVAILABLE VOLUME
CONCEPT REQUIRES PIPING OR HOSES, FITTINGS, ETC.
POSSIBLE FOULING OF VALVE SECOND STAGE WITH DEBRIS COULD BE A PROBLEM
MAINTENANCE REQUIRED - MORE THAN H.A.P.
REQUIRES MORE DEVELOPMENT THAN H.A.P.

Figure 4.

PISTON CONTROL
FREE PISTON

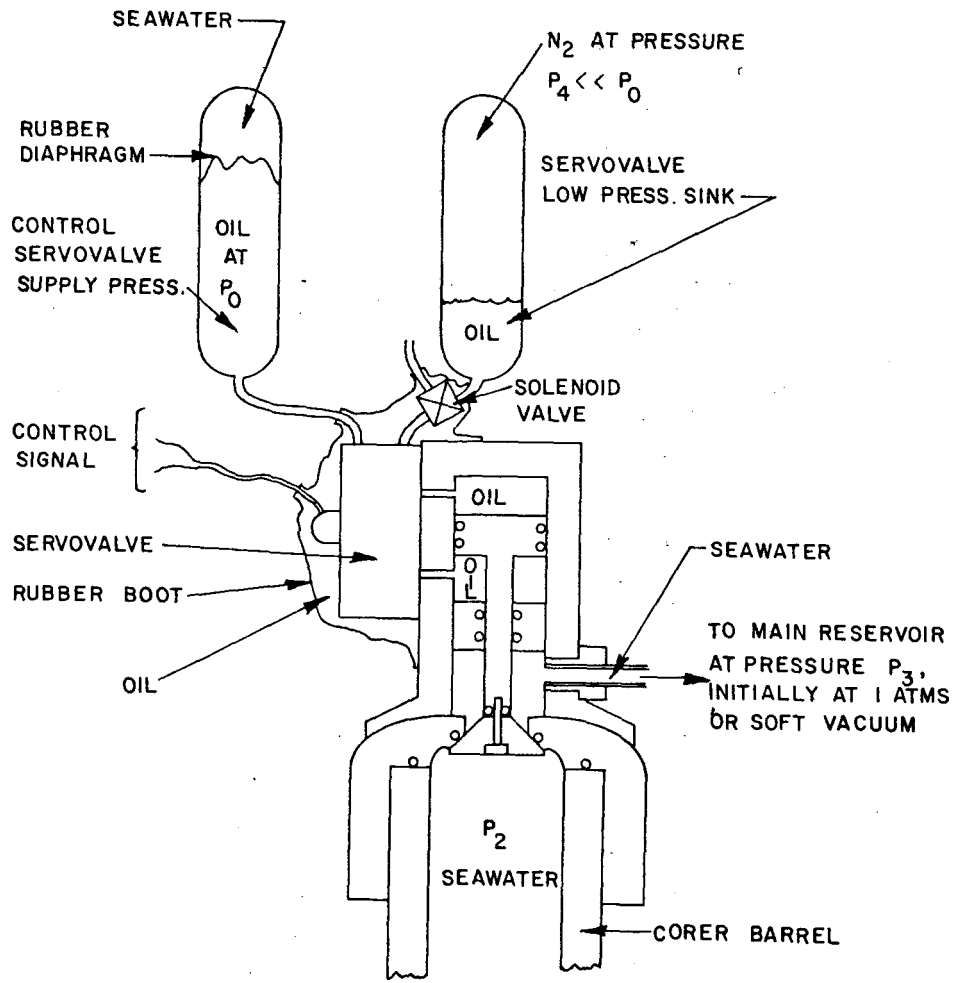


Figure 5.

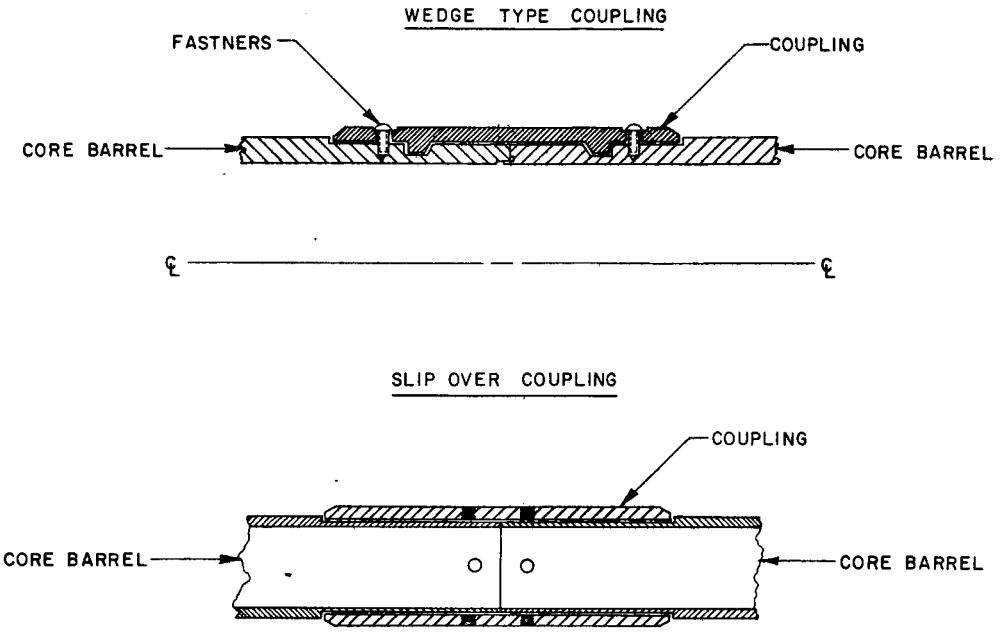


Figure 6.

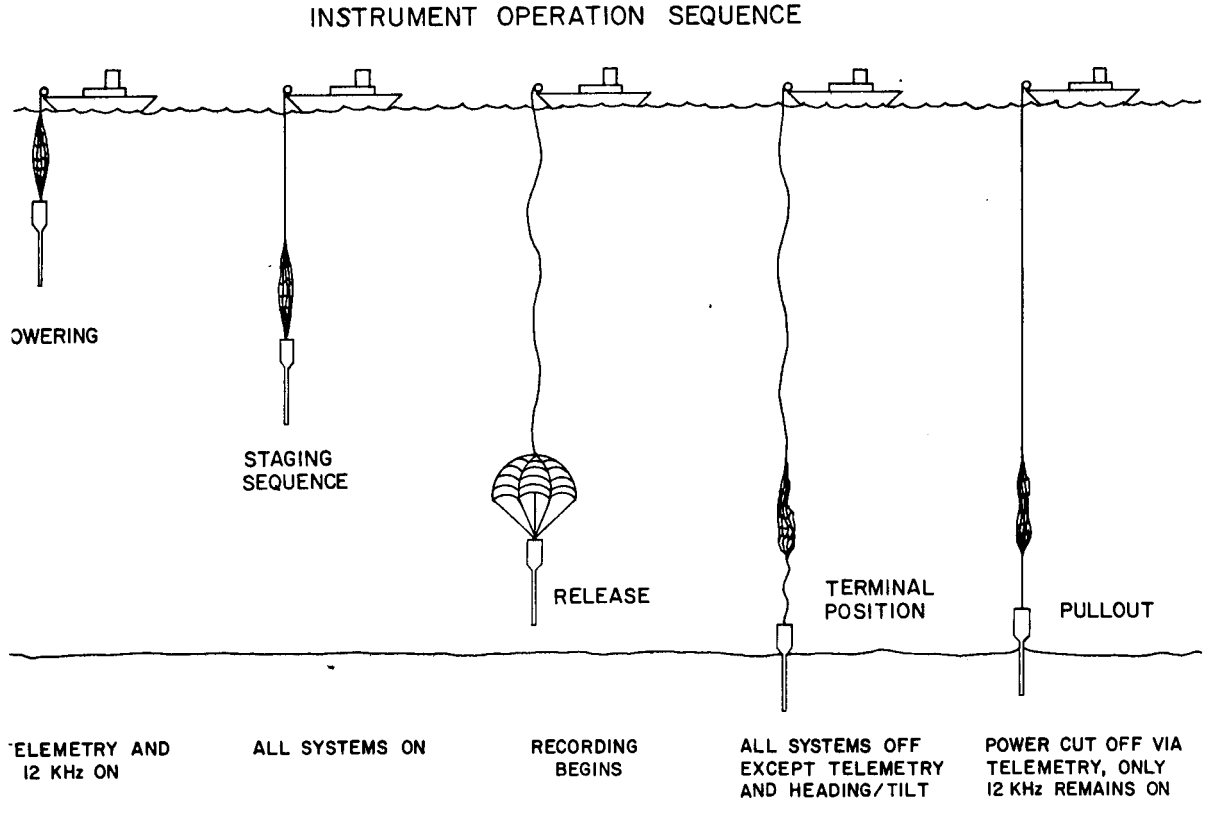
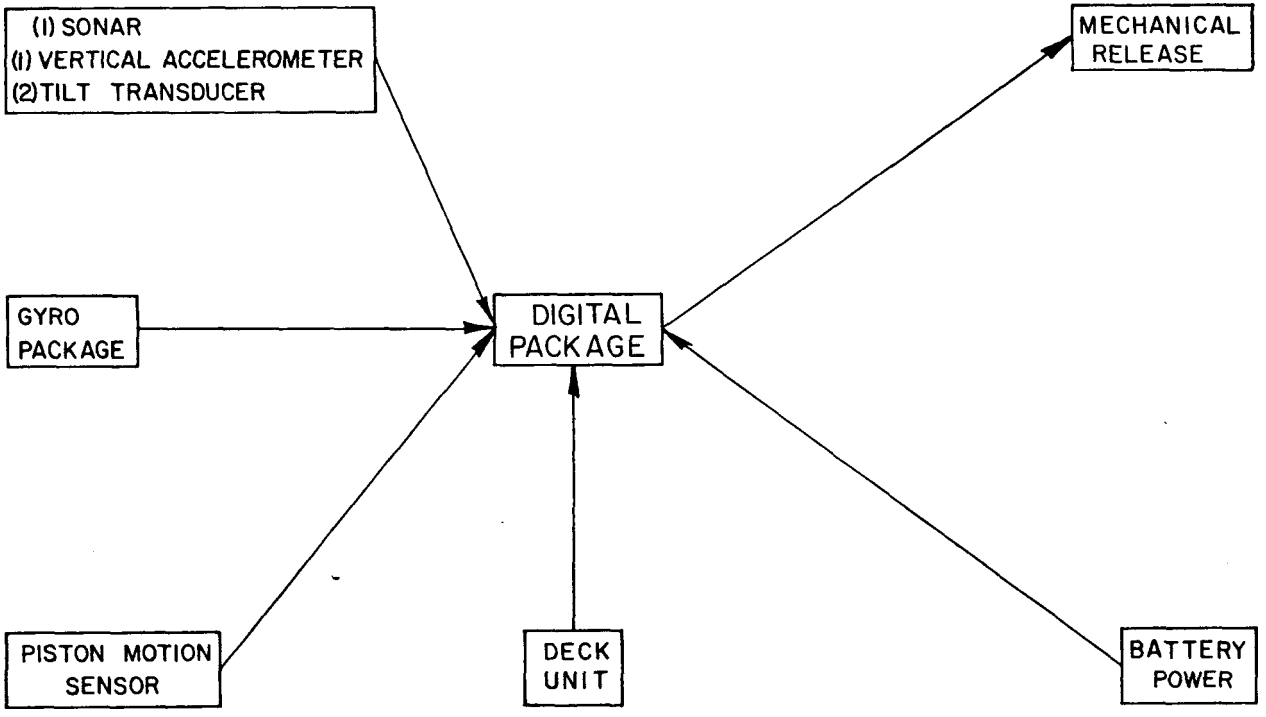


Figure 7.

FIGURE 8

LCF CORE HEAD INSTRUMENTATION
PHASE I CONFIGURATION



Addendum 1

LONG CORING FACILITY PROGRAM

INFORMATION NOTE NO. 1

OPERATIONAL PHILOSOPHY OF PISTON CONTROL AS IMPLEMENTED WITH THE HYDROSTATIC ACCUMULATOR PISTON (HAP), AND A RIBBON PARACHUTE

MARCH 1981

BY

ALAN H. DRISCOLL
DIRECTOR OF CORING FACILITIES GSO/URI

MAURICE C. DEVINE
WATCH-HILL SYSTEMS COMPANY, INC.

KENNETH M. WEBMAN
ANALYSIS & TECHNOLOGY, INC.

INTRODUCTION

The following technical note describes the use of a 40 m^2 ribbon parachute in combination with an active piston control system, the Hydrostatic Accumulator Piston (HAP) as found in the 50 meter Long Coring Facility, (LCF) system. The HAP is a telescoping device consisting of two concentric cylindrical chambers. The lower chamber contains oil which is pressurized by the ambient sea pressure tending to force the chambers together. The upper chamber is at atmospheric pressure. A valve between the two chambers is actuated by a self-contained system which allows the assembly to contract at a controlled rate. The primary purpose of the ribbon chute is two fold in this application. First the parachute is utilized to support the entire weight of the coring system during its near bottom approach while at the same time allowing the polyester rope used to deploy and recover the coring system to reach a state of equilibrium in the water column. Secondly, the parachute acts as a predictable piston control system retardent during the three to five seconds required to complete the coring sequence.

The following text describes the coring sequence and the operation of the ribbon parachute and HAP at its present state of development.

DISCUSSION

1. After deployment from the support vessel the entire coring system is lowered towards the bottom using the polyester rope and traction winch system developed for this purpose. At a predetermined distance above the bottom the winch speed is increased in order to allow the parachute to take the full weight of the suspended coring system. This is chosen to be greater than the parachute sink rate.

2. The winch continues to pay out rope at this higher rate of speed as the corer, suspended by the parachute, continues to sink toward the bottom. This high rate of speed is necessary in order to guarantee that the rope is completely slack at the time of corer trip, as any residual strain in the rope will cause an immediate rebounding of the rope at the moment of release, collapsing the parachute, and nullifying the operation of the piston control device. The corer sink rate will be determined by the operational parameters of the specific parachute used; at present two options are available, either a $20m^2$ chute or a larger $40m^2$ chute. At this point a decision has not been reached as to the most desireable option for this application.

3. As the parachute suspended coring system descends its closure with the sea floor in monitored by two devices, the first a 12 KH_z long range deep sea pinger mounted in the core head, and secondly a high frequency 200 KH_z short range sonar altimeter also mounted in the core head, (Figure 1). This short range sonar is intergrated into the suite of core head instrumentation which is activated shortly before actual bottom closure. Internal monitoring of closure will begin as soon as the sonar altimeter senses a return signal from the bottom.

4. Once the sea floor has been sensed and verified by the sonar altimeter initation of the corer triggering sequence lies with this device. At a predetermined altitude above the sea floor the sonar altimeter activates a mechanical release system in the core head. Upon command from the altimeter the release activates. The core head and barrel are then allowed to fall and penetrate the sediment under their own weight. The time required to achieve full penetration in sediments of 380 gr/cm^2 shear strength is approximately 3 to 5 seconds.

5. During the descent and parachute retarded descent period the Hydrostatic Accumulator Piston is located in the lower end of the barrel string and is held in position by a series of mechanical stops located immediately above the core cutter. The electronics within the piston are maintained in a "powered down" condition during this time period. The HAP is connected to the parachute by a single length of 38 mm steel cable which is in an unloaded condition prior to actual triggering of the coring device. A connective device coupling the polyester rope to the steel cable occurs

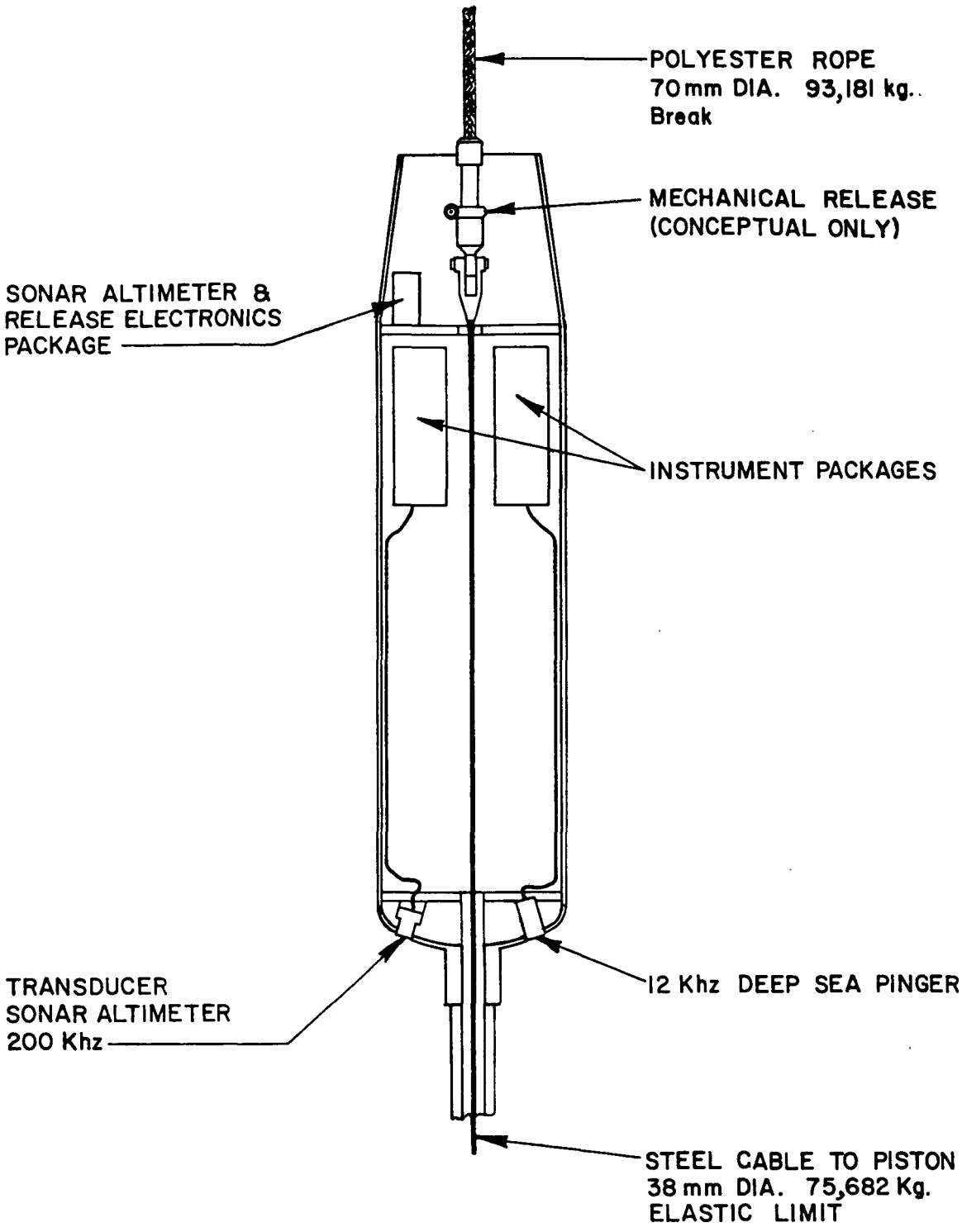

POLYESTER ROPE
70mm DIA. 93,181 kg.
Break
MECHANICAL RELEASE
(CONCEPTUAL ONLY)
SONAR ALTIMETER &
RELEASE ELECTRONICS
PACKAGE
INSTRUMENT PACKAGES
TRANSDUCER
SONAR ALTIMETER
200 Khz
12 Khz DEEP SEA PINGER
STEEL CABLE TO PISTON
38 mm DIA. 75,682 Kg.
ELASTIC LIMIT

FIGURE 1

at the point where the mechanical release mechanism contacts the cable and where the parachute is attached. Up until the point of release the steel cable attached to the piston is in an unloaded condition; at release the cable immediately feels the drag produced by the inflated parachute and begins to act upon the HAP.

6. At the moment of release, when the barrel string and core weight begin to fall, (See #4), strain is placed upon the steel cable connected to the HAP causing the piston control device to be lifted off the mechanical stops at the lower end of the barrel by the drag of the attached parachute. At this point, sensors in the piston detect departure from the rest position on the mechanical stops and immediately activate the piston electronics.

7. This scenario assumes that there is no free fall of the coring system prior to activation of the piston control device. Present thinking is that the incorporation of a free fall potential would result in a partial collapse of the parachute before the free fall period had ended and tension was placed on the cable attached to the HAP. Triggering of the corer will occur when the core cutter is at a altitude of 1 to 1.5 meters above the sediment. At this altitude the face of the piston within the core barrel is approximately 2 meters above the sediment. This dictates that a 2 meter column of water will be present above the cored sample in the worst case which will translate to approximately 48.0 meters of sediment recovery. This spacing between the piston face and the sediment surface will be held constant during the full coring sequence.

8. During the coring sequence the parachute experiences a predictable downward drag due to the force placed on it by the piston and tractive forces involved in the coring process, (Figure 2). The contraction rate of the HAP will be equal to the sink rate of the parachute resulting in the maintenance of the desired positon of the piston relative to the surface of the cored sediment.

9. Contraction of the two sections of the HAP is controlled by the operation of a valve between the two piston chambers, (Figures 3 & 4). The activation rate and duty cycle of this valve are determined by the control system within the piston itself, (Figure 5). One approach to controlling the contraction of the HAP would be to have the piston control system measure the sink rate of the parachute which can be accomplished by any one of the following methods which are being considered.

    a) If the sink rate vs force characteristics of the parachute can be defined accurately and are representative of all parachutes of this specific manufacture then a certain repeatability can be assumed. With this assumption, a force measurement using strain gages or a load cell can be performed at the top section of the piston control device which experiences the same loading as the steel cable attached to the parachute. This load measurement can be related to the parachute sink rate and can be used to compensate for that sink rate in the piston by contracting the sections accordingly.

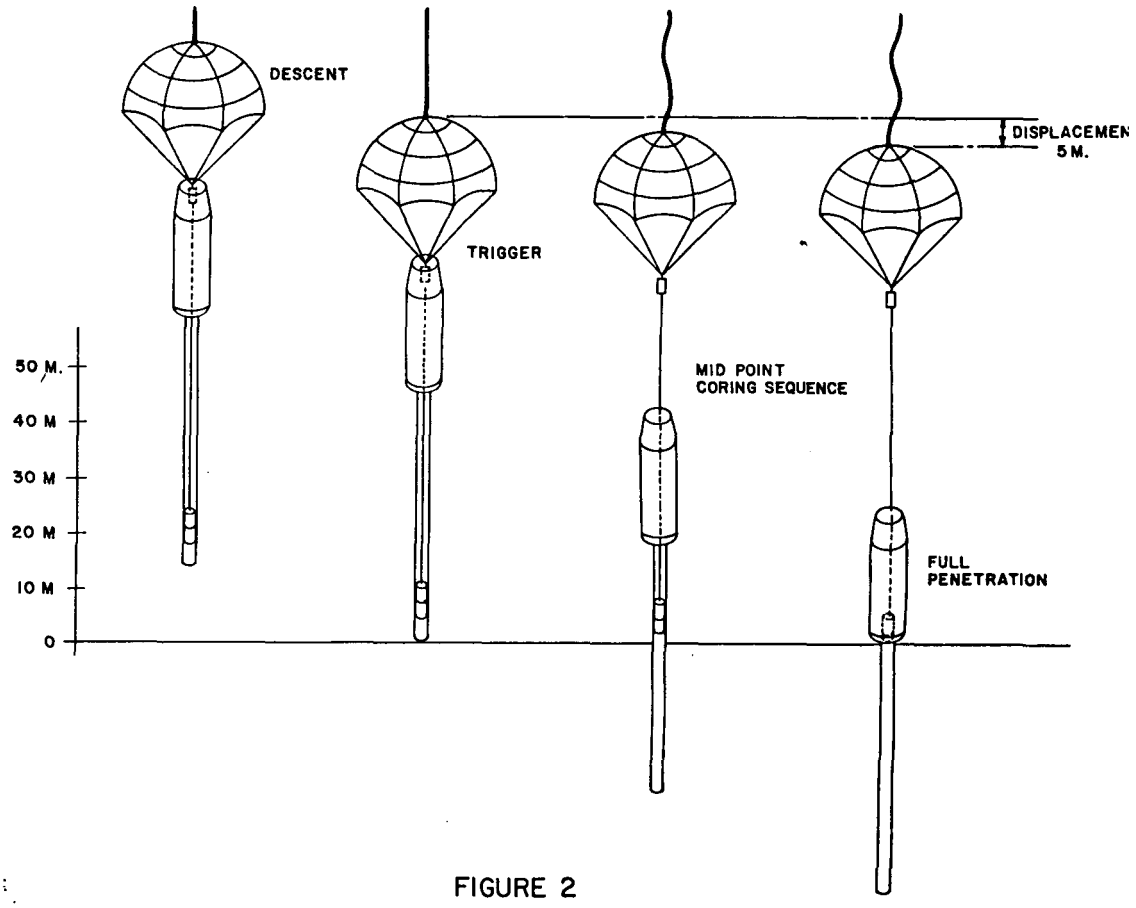


FIGURE 2

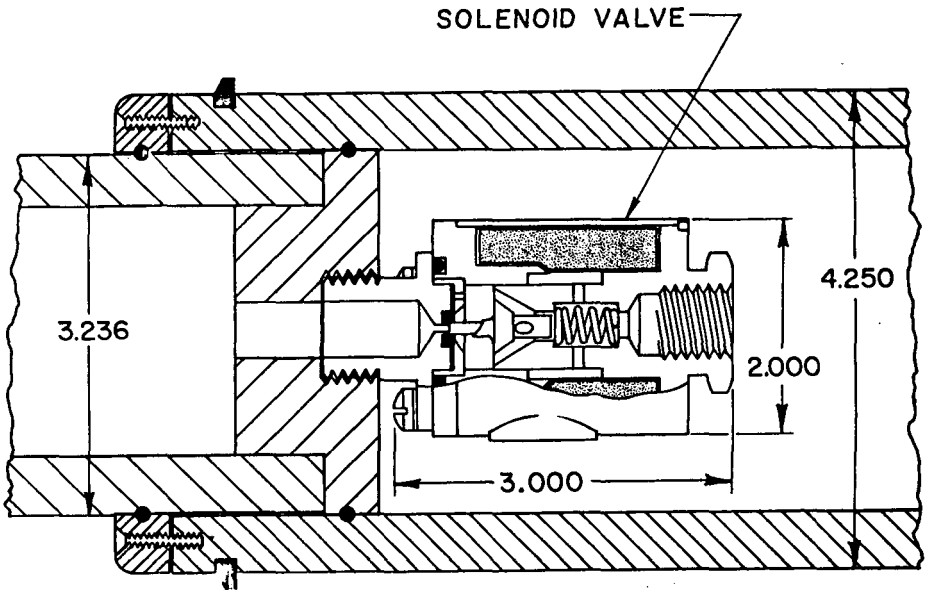


FIGURE 3

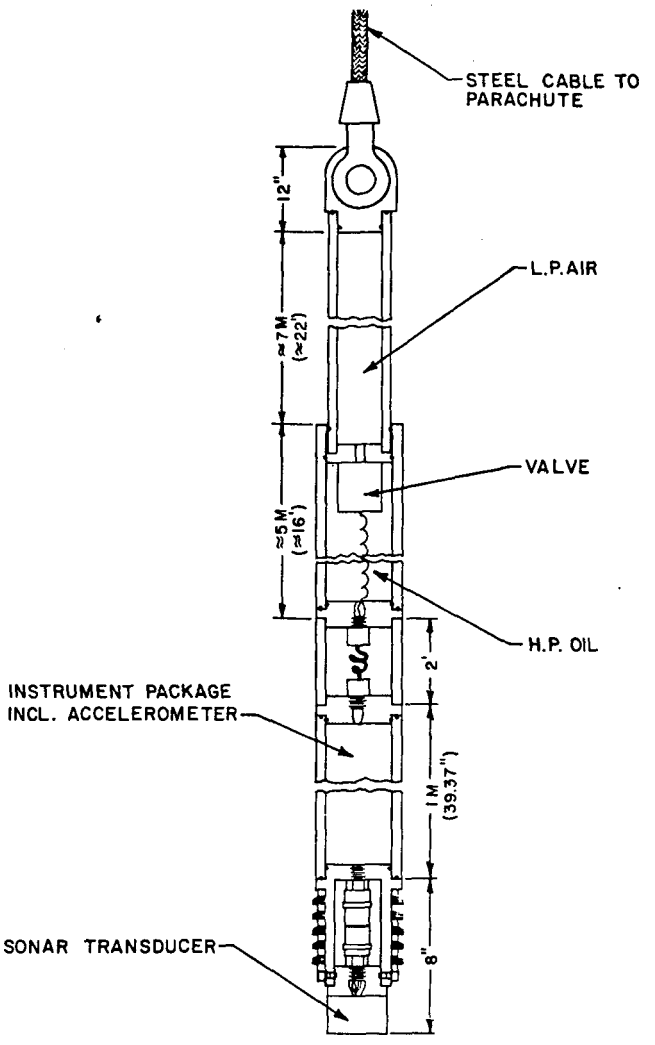


FIGURE 4

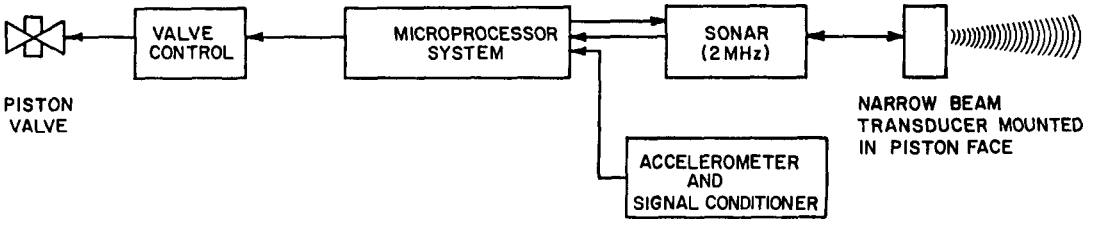


FIGURE 5

b) Under this option, a direct measurement of the sink rate of the top of the piston may be made. This rate should be equal to the sink rate of the parachute, and can be accomplished by integrating the output of an accelerometer located in the piston top section. This is combined with the initial downward velocity of the system (i.e. the sink rate of the parachute at the time of release), to yield positional change data for the top half of the piston. Note, the top half of the piston always sinks at the same rate as the parachute does .

The initial velocity of the piston relative to the bottom at the time immediately following release but before bottom contact is made by the core cutter, is obtained by the piston sonar. When the piston is activated, and before bottom contact occurs, the sonar in the piston will repeatedly echo range off the bottom. The range rate observed in this interval will be equal to the sink rate of the parachute, since the piston length is unchanging during this time.

Note, that the sonar measurements of velocity are used only to provide the initial reference for the integrations performed by the system during penetration of the corer. Of course, once the core cutter has contacted the sediment, sonar measurements of piston altitude can no longer be interpreted as being due to the parachute sink rate, and cannot be used for control.

Using the initial velocity thus obtained, and the accelerations measured, an accurate determination of the sink rate of the parachute can be continuously made. The contraction rate of the piston can be controlled so as to match this sink rate, and piston lower face position will remain constant.

c) An alternative approach to controlling the piston during coring, is to measure and double integrate piston lower section accelerations during penetrations. Again, the initial velocity of the system will be determined by the piston sonar as described above. The contraction rate of the piston will be controlled to drive the net positional error to zero, thereby maintaining a constant piston altitude above the sediment, (approximately 2 meters).

10. In the approaches to piston control mentioned above the best available data on parachute sink rate characteristics may be incorporated into the algorithm as limits for the operation of the device.

It should be noted that the narrow beam sonar system in the piston face is not only required as a part of active piston control, but is also included as a data recording device which is important to later penetration vs sample recovery ratio data.

The sonar system in the core weight, in addition to performing the actual release of the corer, will also record altitude data during penetration. This will provide additional data on the recovered sample.

TECHNICAL NOTE NO. 1

DRAWING REFERENCE SHEET

The drawings listed on this sheet relate to components either in a conceptual state or in final form at the time of the writing of this technical note. Changes in both the concepts and the details of the drawings may occur during further development.

DRAWING NUMBER	TITLE	DATE
001-0105-0010	LCF CONCEPTUAL DWG	8-8-80
001-0101-0047	HAP CONCEPTUAL DWG	2-13-81
001-0101-0060	HAP CONCEPTUAL DWG	*

* Drawing Currently in Progress

Addendum 2

THE LONG CORING FACILITY, NEW TECHNIQUES IN DEEP OCEAN CORING

Alan H. Driscoll

Graduate School of Oceanography
University of Rhode Island
Narragansett, R.I. 02882

ABSTRACT

A new technique, the Long Coring Facility (LCF), is currently being developed which will enable the recovery of 50 meter piston corer from oceanic depths of up to 6500 meters. The LCF will be completely portable and is designed for use aboard a selected number of research vessels.The need for a device of this nature has arisen from requirements identified by both the scientific and engineering community for the acquisition of long, high quality cores for use in interdisciplinary studies.

The development of the LCF has relied on previous coring experience and the creation of a series of computer models designed to predict the performance of the developing system. Based on the results of these analysis it is apparent that a reliable, and efficient coring system can be produced utilizing existing technology.

1. INTRODUCTION

The overall objective of the Long Coring Facility (LCF) is to develop, design and produce a highly reliable deep sea coring system capable of routinely recovering 50 meter long cores of 11 cm diameter from oceanic depths while utilizing a select number of support vessels from the Oceanographic Research Fleet. Previous work has proven the feasibility of this approach and currently on going research is concerned with the engineering design of the various sub-systems involved in the LCF. To date, it has been determined, by the design team at URI that the LCF and its associated sub-systems can be produced utilizing existing technology.

Justification for the development of the LCF has been derived from the solicitation of an interest survey within the scientific community in 1977 and from a series of meetings and workshops carried out during 1977. The first, an Engineering Workshop, (Driscoll-Silva June 1978)[1] was convened in order to review all available technology capable of recovering very high quality, 50 m long large diameter cores from oceanic depths. Within the framework of this workshop all available and developing technologies relevant to the problem were assessed including both the Giant Piston Core and the Hydraulic Piston Core. The Engineering Workshop concluded with the recommendation that current state of the art Giant Piston Core technology be expanded and a major redesign program be carried out to upgrade this technology to a point where 50 meter sample recovery could be obtained and a reliable, rapidly recycleable system designed.

Following the Engineering Workshop a broad spectrum Scientific Workshop was held at the University of Rhode Island in March of 1978. (Heath, Silva, and Driscoll, 1978).[2] The purpose of this workshop was to bring together a majority of the potential scientific user community in order to establish the need for a facility of this type and to identify specific problem areas which could be investigated with an LCF device. At the conclusion of this workshop the 40 participants representing 15 various institutions and organizations concluded that a long coring capability was a definite national requirement and that the establishment of such a facility should proceed along well planned lines.

The scientific needs for the development of an LCF lie in its application to a wide variety of scientific and engineering problems. These areas include Paleoceanography, Paleoclinatology, Paleomagnetism, Geochemistry, Stratigraphy, Bacteriology, and Geotechnical Engineering. The large (11 cm) diameter of the sample allows for multidisciplinary work to be carried out on the same core while still providing adequate material to be archived for future work on the same core.

2. BACKGROUND

With the determination that a 50 meter LCF device would be an asset to the scientific community an engineering feasibility study was begun in 1979. This study relied heavily on previous experience with the Grant Piston Core, (Hollister et all,1973[3] and Driscoll and Hollister, 1974[4]) as well as data obtained from conventional piston coring experience. Where possible cores that had been instrumented relative to deceleration profiles and rotation were selected for inclusion in a data base that would be intergrated with the computer models being developed at Sandia National Laboratories.

The model studies initiated by Sandia National Laboratories were concerned with the analysis of a conceptual 50 meter long coring system. These analysis concentrated on the hydrodynamic stability, penetration mechanics, corer pullout, and corer buckling

potential of the conceptual system. The results of these analysis indicated that within the limits of the model studies, a 50 meter system was feasible and could be developed utilizing existing technology. (Karne et all)[5]

In addition to the analytical work performed during 1979, a survey of the presently existing oceanographic fleet was made in order to determine specific vessels which would be useable as support platforms for the LCF. The intent was to identify a suite of vessels capable of supporting LCF operations and to maintain the concept of total LCF system portability. The analysis of the ship data was accomplished by Gibbs and Cox Naval Architects of New York and utilized the conceptual system data generated by the Sandia group.

Other tasks that were begun during this period included the determination of core head instrumentation parameters and the definition of each instruments resolution capabilities. Preliminary work was begun on the cable system that would ultimately be used with the LCF and a variety of rope and cable types were identified for further study.

The work carried out during 1980 concentrated on the refinement and finalization of the computer models developed earlier. These models were then used by the URI Design Group as a means of evaluating the coring system during the development of the preliminary designs. In addition, modeling of the synthetic rope selected for use with the LCF was accomplished by Civil Systems Inc. as consultants to the Sandia Modeling Group.

The mechanical design of the coring system, as carried out by the URI design group, concentrated on several critical tasks during this period. The main task addressed was the preliminary analysis of three piston control concepts which had been previously identified by the LCF Working Group: a water turbine system, a Hydrostatic Accumulator Piston (HAP) and a Free Active Piston (FAP). The results of the preliminary analysis carried out by Analysis and Technology Inc. ranked the three piston control options as to their feasibility of development and produced a recommendation that the HAP system be developed as a first order system while the FAP was to be developed as a second order system. The water turbine concept was eliminated from consideration due to the time and development costs that would be involved.

The other activity carried out during this period was the identification and selection of a suitable barrel and coupling system. Two couplings, a joint types, were evaluated by the Sandia Modeling Group utilizing a finite element approach (Figure 1). The results of this limited modeling effort indicated that physical model tests should be conducted to verify or refine the models, compare the behavior of the different types and provide a sound basis for the final selection of the coupling design. The design of the testing program then became the responsibility of the URI Design Group and will be completed in 1980.

The ship survey and analysis that was begun in 1979 was completed during the 1980 period. The analysis performed by Gibbs and Cox resulted in the identification of six vessels suitable for the deployment and recovery of the 50 meter LCF. The vessels identified were the R.V. ATLANTIS II, USNS HAYES, C.S. HUDSON, R.V.KNORR, R.V. MELVILLE and R.V. MOANA WAVE which would accept a somewhat shorter coring system. Analysis of vessels capable of handling an LCF system shorter than the projected 50 meter design length has been limited to the R.V. MOANA WAVE at this time.

With the analysis of the available oceanographic research vessels and the coring parameters developed by the Sandia Modeling Group now available it was recognized that a specialized winch system would be required to handle the LCF at sea. Specifications for a double drum traction winch system were developed and a suitable winch manufacturer was identified. The criteria used in the selection of both a winch type and specific manufacturer were as follows: a) the winch system was to be capable of producing a sustained line pull of 200,000 lbs. at speeds of up to 25 mpm during pullout and recovery and b) speeds of up to 300 mpm during final deployment. This high line speed would be necessary for the parachute deployment with synthetic line.

One primary concern in the selection of a manufacturer was that they possess a demonstrable ability to produce a stock winch system that was not a first generation prototype. Ultimately, this criterion was met by the Smatco Winch Co. and the Model 20 winch system. With the exception of a limited amount of engineering designed to meet the power and portability requirements of the LCF the winch design is essentially complete.

Various types of cable capable of handling the load requirements of the LCF were investigated during FY 80. Initially three types were investigated; Steel Cable, Kevlar Rope, and Polyester Braid. Each rope type was assessed primarily on its weight in water, elongation at LCF operation loads, cyclic life, ability to be produced in a single 7,000 m length, and acquisition cost. Based on these criteria a decision was made early in FY 80 to concentrate on a Samson Polyester Stable Braided Rope. Subsequent analysis of specific cable, (Dzwilewski and Driscoll, 1980)[6], has shown that it is suitable for all aspects of LCF operations and is compatible with the selected winch option.

The core head instrumentation task of the LCF project has been funded by the Subseabed Disposal Program (SDP) through a contract from Sandia National Laboratory to the University of Rhode Island. As part of this task an electrical engineering consultant was hired in early 1980 and active development of the core head instrumentation was accelerated. During FY 80 the decision was made that the mission requirements of the LCF were best met through a system of distributed instrumentation packages having a common and redundant power source. The objective was to develop a series of instruments which possess a high commonality of components in order to simplify the training of personnel and to reduce the amount of spare parts required. In addition, it was decided to design all LCF instrument-

ation for continuous operations without the need to open the pressure housings except for repair.

3. STATUS OF THE LCF

With the completion of the initial feasibility study and preliminary design work it was possible to fix a majority of the subsystems that make up the LCF. At this point the design effort was broken down into six major sub-tasks as follows: Core Weight Design, Barrel String, Corer Handling System, Winch and Cable System, Piston Control, and the Core Head Instrumentation. Each of these groups will be discussed in the following text.

Core Weight Design

Based on the hydrodynamic analysis performed by the Sandia Modeling Group early in the project, an optimized weight shape capable of meeting the requirements of the project was developed, (Barnett, 1980[7]). Since it had been determined that the coring system would not be required to achieve terminal velocities prior to entering the sediment, the final shape design was orientated around the system requirements. Even though the shape selected is unstable it is felt that the inertia of the 12,900 to 15,400 kg coring system is of sufficient magnitude, given an operating time of 5 seconds, that the inherent instabilities of the system will not present a problem.

The core weight, Figure 2, has been designed to accommodate not only the various instruments crucial to the monitoring of the corers mechanical performance and quality of cored material, but also to accept additional instrumentation which may be carried as add on experiments in the future, i.e. cameras, heat flow recorders, etc. A variable weight option has also been designed into the core head in order to be able to tailor the total mass of the system relative to the free fall selected for the corer.

TABLE 1

CORER MASS AND PULLOUT FORCES[5]

Free Fall Distance m	Entry Velocity m/s	Required Mass kg	Net Pullout Force kg
0	0	15,400	33,720
25	18	12,900	31,676

In addition, the core weight will allow for the use of two different piston control devices currently under development at URI. Both the Hydrostatic Accumulator Piston and the Free Activating Piston can be housed within the core head without prejudicing the options mentioned previously or to the exclusion of a free fall loop should it be required.

Barrel String

Due to the axial stresses that would be encountered during either a nonvertical entry or pullout of the corer from the sediment it has been necessary to design a step tapered barrel string utilizing either an NY80 or NY100 grade steel. A 120 mm core barrel I.D. has been selected as the most efficient size for the operational system when combined with the varying barrel wall thickness dictated by the step tapers. Based on the material that has been identified the upper 15 m of the string will consist of a 51 mm thick wall section, the middle barrel sections will be composed of 25 mm thick wall section and the 15 m lower section will utilize a thin 13 mm thick wall section. An additional advantage to the step tapered string is a reduction in the frictional forces involved in corer pullout.

For ease of handling aboard ship and during the corer assembly process each barrel section has been limited to 3.048 m. The 120 mm I.D. also allows for the use of a thin walled polycarbonate liner to be inserted in each section. This will eliminate the need to extrude the cored sample which ultimately induce a degree of sample disburbance.

With the determination of a suitable core barrel configuration the problem of coupling these individual sections together into a rigid unit was approached. A variety of coupling designs were discussed and ultimately two were selected for analysis by the Sandia Mideling Group (Figure 1). The result of these analyses were inconclusive and a decision was made to initiate a physical model testing program in order to verify the model and identify a suitable coupling design.

The two designs being evaluated are a traditional slip over type coupling and a somewhat more complex three piece wedge type coupling. Both coupling designs are configured to create a sealed system against the intrusion of water from outside the barrel during coring. The two couplings differ in the manner in which this is achieved, but the maintenance of a sealed system relys on the coupling method.

Corer Handling System

In order to assemble and disassemble the corer at sea with any factor of safety a specialized handling system will be required. Because of the variety of vessels capable of supporting the LCF, it will be necessary to design the handling system with a high commonality of components and to restrict the specialized sub assemblies to a system of sockets and base plates unique to each vessel. Once effected , the system can be moved from vessel to vessel with a minimum of effort involved in its assembly.

The basic handling system will be composed of a rotating core platform designed to control the cores during launch and recovery as well as providing a work platform for maintenance of the core weight at sea. Assembly and disassembly of the barrel string will be aided by a monorail system supported by davits, erected along the side of the support vessel. A series of powered falls will assist in the removal of individual barrel sections and their transport to storage racks on the deck. During assembly of the system the process will be reversed.

Within the suite of equipment being designed for the corer handling system the largest single item will be an A-frame unique to the LCF. The function of this frame will be to assist in the initial placement of the core weight in the outboard cradle and to support the launch and recovery of the corer. The frame is designed against the 95.000 kg breaking strength of the polyester rope that will be used to deploy the corer and will incorporate an adequate safety factor.

Power for the A-frame will be derived from the diesel-hydraulic power unit associated with the winch system. Adequate space has been provided for the large sheaves required by the rope system and intermediate recovery winch used in returning the core to its cradle. During the design of the equipment the concept of total system portability has been preserved.

WINCH AND CABLE SYSTEM

As was mentioned earlier, a suitable winch system has been identified which meets the requirements of continuous line pull, portability, and performance in the field. The Smatco Model 20 is a double drum traction winch designed to handle synthetic rope at relatively high loads and speeds. The winch is powered by a remote diesel hydraulic power unit which possesses adequate reserve power to accommodate A-frame, deck hydraulic requirements and a future wire rope storage reel.

The winch system will be capable of delivering a 95.000 kg line pull at speeds up to 25 mpm and speeds of up to 300 mpm with system loads of 15.000 kg. Incidental to the original design of the winch is its unique ability to be modified to handle both wire rope and electro-mechanical cables with a minimum of modification to the traction unit. This feature makes the LCF winch system highly versatile when not involved in coring operations.

The decision to acquire a specialized winch system for the LCF resulted from an assessment of the available fleet capabilities within both the University National Oceanographic Laboratory System (UNOLS) and other vessels surveyed. Without exception the deep sea winch capabilities aboard these vessels were inadequate compared to the anticipated coring loads. (Table 1)

Initially the search for a rope or cable which could be used to support the demands of the coring system was confined to three major types: Steel Rope, Kevlar, and a Polyester Cable. A series of criterion were developed for a preliminary evaluation of each cable type relative to the requirements of the system.

The selection criteria were mainly based on the anticipated loads that the cable and winch would be subjected to during the deployment of the coring system, and on portability. The loads were obtained from a study which optimized the design of the 50 m piston coring system with respect to penetration, structural stability, pullout, and core quality. Other criteria were based on operating conditions, splices and terminations, manufactured lengths, and cost.

The braided polyester cables met all the criteria for the main operating cable for the LCF and the 70 mm diameter one was chosen. It can be manufactured in a single 7000 m length which eliminates splicing problems, it has the smallest bending radius of the three types of cables considered here, the fatique life is several thousand cycles when working to 50 percent of the rated strength, the termination problems have been solved by the manufacturer, and it is the least expensive.

One unique feature of polyester cable is that the stressed cable cannot be stored on a reel because it requires thirty minutes to recover 75 percent of the residual strain upon unloading and maybe more than 24 hours to recover the remaining amount (McKenna and Wong 1979[8]). If this type of cable is stored on a reel, the strain recovery would exert tremendous forces on the reel and damage it. The solution is to store the cable loose in a container on the deck of the ship. Previous at sea experience with this concept aboard the USNS Attacapa (Samson Ocean Systems[9]) has shown that the technique is both feasible and satisfactory in dealing with the recovered cable.

Analysis of the Polyester cable (Dzwilewski and Driscoll, 1980[6]) have indicated that the transient cable motion occurring at the time of corer trip would have a decidedly adverse effect upon both the operation of the corer and the quality of the sample recovered. This problem will be reduced through the use of a parachute deployment scheme (Figure 2), and through the incorporation of an active piston control device. In addition, the stretch of the cable induced by the pullout loading will be substantial; approximately 66 m. Although the stretch of the cable is of a greater length than the corer the analysis of the cable indicates that the cable drag will be sufficient to damp out any large vibrations which could result in corer repenetration and possible structural damage.

PISTON CONTROL

The development of an active piston control device is presently confined to two options; the Hydrostatic Accumulator Piston (HAP) Figure 3 and a Free Activating Piston (FAP) Figure 4. At present, the mechanical design is concentrating upon the HAP system as the primary device. The FAP is still in a conceptual phase although volving systems have been identified which are applicable to both devices. The HAP system is based upon the use of a parachute deployment concept. Under this concept the HAP would react to the downward drag of the parachute by collapsing back upon itself at a rate equal to the downward movement of the parachute. The effect would be to stabilize the face of the piston relative to the cored sediment. In this way the cored sediment column would be stabilized and coring effects such as plugging etc. would be sensed and compensated for (Driscoll, Devine, Webman, 1981[10]).

Conceptually the FAP would utilize an independent piston within the barrel string, but unlike the HAP there would be not connection to the 70 mm deploy-

ment cable. Movement of the piston would be controlled by a series of valves located between the piston and an evacuated chamber in the core head. By contolling the valve system water trapped in the barrel above the piston would be transferred to the chamber and result in an upward movement of the piston during coring.

This system would rely heavily upon the core head instrumentation system for data relative to corer position relative to the sediment, velocity, and piston position. By utilizing the instrumentation it will be possible to accurately control the movement of the piston and to insure the quality of the recovered sample. As with the HAP, the FAP will be housed inside the already designed core weight.

CORE HEAD INSTRUMENTATION

With the definition of the LCF mission requirements it has been possible to identify a suite or core head instrumentation which will be used to monitor the corers mechanical performance, control various on bottom experiments, and act as a quality control device for the cored sample. At present, a majority of the instruments have been produced and preliminary testing completed. Individual instruments have been sized for use with standard piston cores in order to obtain initial field data prior to use with the LCF.

The instrumentation that was designed for use with the LCF by the Watch Hill Systems Co. as consultants to the URI Design Group included the following:

a. Recording Altimeter/Acoustic Release
This unit echo ranges to find a preset release point and activates the release mechanism allowing the corer to penetrate. All altitude data from the point of release for a period of 10 seconds is stored internally for later integration with other sensor input.

b. Tilt Alarm Instrument
Compares tilt sensor reading with preset limits, and sends alarm status signal to telemetry package. At pullout, accepts signals from cable angle and heading transducers, rotation sensor final heading, and its own tilt transducers, formats these and performs slow serial transmission to the telemetry package.

c. Rotation Recorder Using Compass and Rotation Sensor
Records one ganetic compass reading at release time combines this with integrated rotation rate, records time history of rotational position for 10 sec. Waits for signal from tilt alarm package and supplies final heading data to it.

d. 3-Axis Acceleration Recorder
Records from 3 self contained acceleromenters for a period of 10 sec. activated at release.

e. Cable Angle and Heading Transducers
Mechanical arrangement to permit the generation of electrical signals cooresponding to the measured variables. Provides inputs to the tilt alarm package, which also functions as a processor for these signals.

f. Piston Pisition
Intelligent H.A.P. Electronic System makes acoustic measurements off the bottom, operates to maintain a constant height (1.om or initial value) over the bottom, sends control signals to valve in the H.A.P. controlling the contraction of the cylinders. If transducer for the sonar is buried in mud or fails to provide a good signal the intelligent H.A.P. will follow a predetermined profile for controlled contraction of the cylinders. The 200khz sonar will be either purchased as a subassembly from others, or developed in cooperation with others already having the components.

Piston Position Measuring System F.A.P.
In the case of a non-intelligent piston (having no measurement and contrl system of its own), the problem of determining the position of the piston relative to the corer exists. This position is to be compared to the corer altitude to permit computation of the control signal to be sent to the piston positioning mechanism. Various alternatives have been looked at to perform this function, ranging from the use of sonar signals within the core barrel to the use of a simple pinch-roller mechanism driven by the piston cable passing through it.

This portion of the design cannot be persued until the piston control method (free piston, HAP, etc.) is determined. In the case of the intelligent HAP (with its own control system), the requirement for an individual piston position measurement is eliminated.

g. Acoustic Telemetry Package
The function of this package is to provide a status and data link with the surface vessel, as well as to permit the reception at the corer of two or three commands from the surface. Prior to release of the core, the telemetry package will accept and telemeter the alarm/no alarm status from the tilt alarm sensor.

Following penetration of the bottom sediment by the corer, the telemetry package will accept corer heading and tilt information from the rotation and tilt alarm devices and also cable angle and relative heading information from the associated transducers and instruments. This information will be slowly telemetered to the surface vessel at a rate of 1/3 to 1 bit/sec.

Commands received from the surface vessel will be used to activate selected functions on the corer prior to release. It is expected that the telemetry package will be purchased from others either as major subassemblies or as a completed device.

h. Power and Control Package
Centralized power storage and distribution are incorporated as part of the instrumentation design. The power source has been selected as ni-cad batteries. Exact sizing of the battery pack will be done when the instrument package power requirements have been defined further.

4 SUMMARY

Within the realm of geological sampling tools the LCF, when operational, introduces a new dimension into the practice of obtaining continuous long cores from the deep ocean as a routine operation. The portability of the complete system will allow its use aboard a wide variety of research vessels and will subsequently reduce the time required for the investigator to access the system. In addition, the variety of vessels permits usage of the system over a wide theater of operations on relatively short notice. This condition would not exist were the LCF restricted to a single support vessel with a fixed mission profile.

The following table reflects the versatility of the LCF and summarixes the capabilities of the system.

TABLE 2

System Cost Per Day at Sea	$10,000
Cost per 50m Core in 5000m Water	2,000
Available Support Vessels	6
System Access Time	1 year or less
Flexibility of Support Vessel to Perform Other Science.	No restrictions
Cores that can be obtained per 24 hour day	2 to 3
System Cost on Shore	7-$800 per day
Ability to Use Modified System on Other Vessels	Most of UNOLS Fleet
Water Depth Limitations	Unlimited
Weather Limitations	Sea State 5 or 6
Maximum Sediment Shear Strength Penetrateable	Design 380 gm cm^2 Max. 600 gm cm^2
Sample Diameter	11.4 cm
Sample Area	45 cm^2
50m Sample Volume	6.13 m^3
System Components Available for other Applications	Winch System, Barrel Sections, Core Head Inst.
Core Head Instrumentation	Altitude, Trigger, Rotation, Inclination 3 Axis Piston Position, Telemetry

ACKNOWLEDGEMENTS

The author wishes to acknowledge support for the project from the National Science Foundation under Grant Number OCE 78-24975 and from the Department of Energy through Sandia National Laboratory under Contract 46-7036. Also thanks are extended to C.D. Hollister, C. Karnes, and A.J. Silva for their help and support on the project.

REFERENCES

1. Driscoll, A.H. and A.J. Silva, Ed., "Report of the Engineering Workshop on Deep Sea Coring", Vols. 1 and 2, Woods Hole Oceanographic Inst., November, 1977.

2. Heath, R.S., A.H. Silva and A.H. Driscoll, "Report of Scientific Workshop on Deep Sea Coring", Univ. of Rhode Island, March, 1978.

3. Hollister C.D., A.J. Silva, and A.H. Driscoll, "A Giant Piston Core", Ocean Eng., Vol 2, pp 159 - 168, 1973.

4. Driscoll, A.H. and C.D. Hollister, "The W.H.O.I. Giant Piston Core; State of the Art", Marine Technology Society, 10th Annual Conference, 1974.

5. Karnes, C.H., S.N. Burchett, and P.T. Dzwilewski, "optimized Design and Predicted Performance of a Deep Ocean 50 m Piston Coring System", Proceedings of Oceans 80, Seattle, 1980.

6. Dzwilweski, P.T. and A.H. Driscoll, "Long Core Facility Winch and Cable System", American Society of Mechanical Engineers, Winter Annual Meeting, Chicago, 1980.

7. Barnett, D.W., "Dynamic Elastic Analysis of a Slender Body with Application to a Seabed Corer" Sandia National Laboratory, SAND 80-0908, October, 1980.

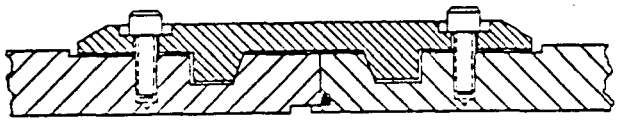
8. McKenna, H.A., and Wong, R.K., "Synthetic Fiber Rope, Properties and Calculations Relating to Mooring Systems," Proceedings of the Winter Annual Meeting of the American Society of Mechanical Engineers, New York, New York, December 2-7, 1979

9. Samson Ocean Systems, Inc., Traction Winch Systems, TW2-48, Boston, 8 pp.

10. Driscoll, A.H., M.C. Device, and K.M. Webman, "Operational Philosophy of Piston Control as Implemented with the Hydrostatic Accumulator Piston (HAP), and a Ribbon Parachute", Long Core Facility Information Note No. 1, March, 1981.



SLIP-OVER TYPE COUPLING



WEDGE TYPE COUPLING

FIGURE 1 COUPLING DESIGNS

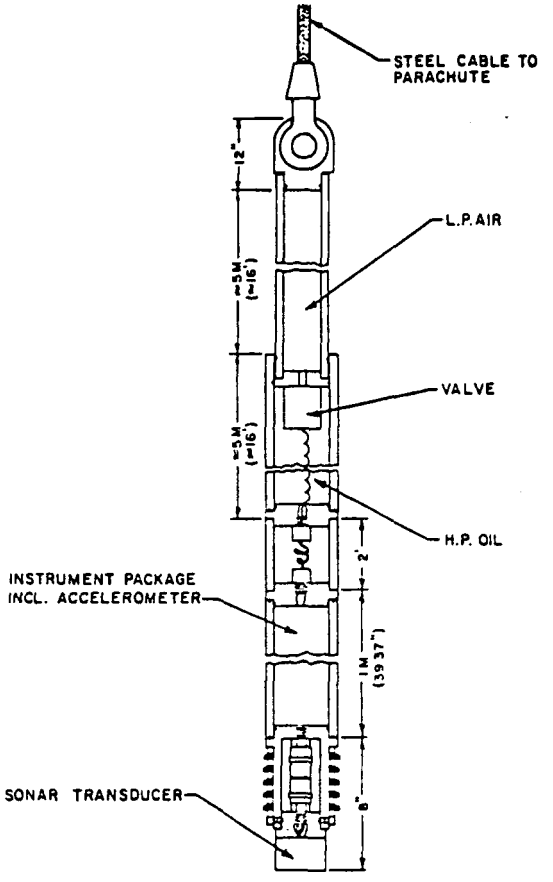


FIGURE 3 HYDROSTATIC ACCUMULATOR PISTON (HAP)

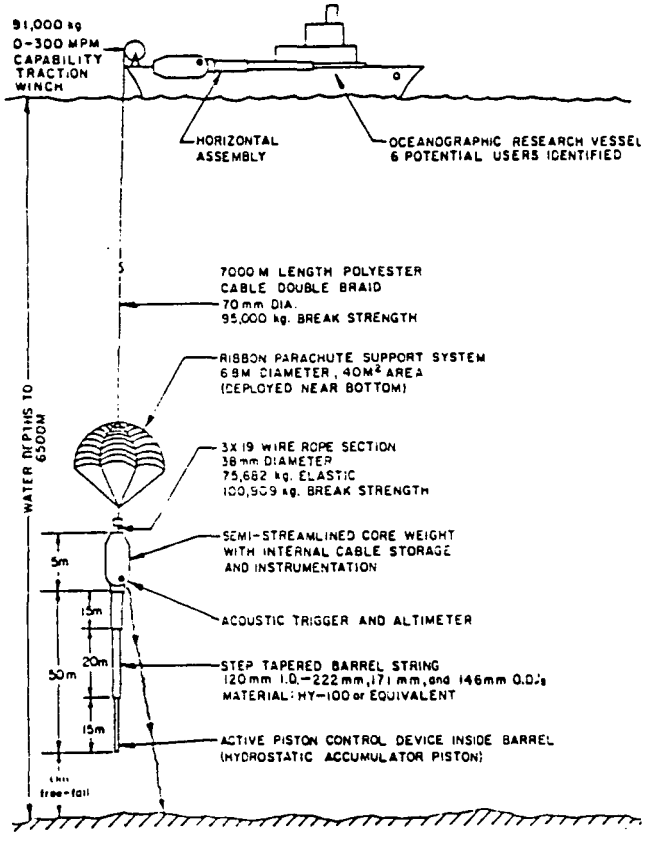


FIGURE 2 LCF SYSTEM CONFIGURATION

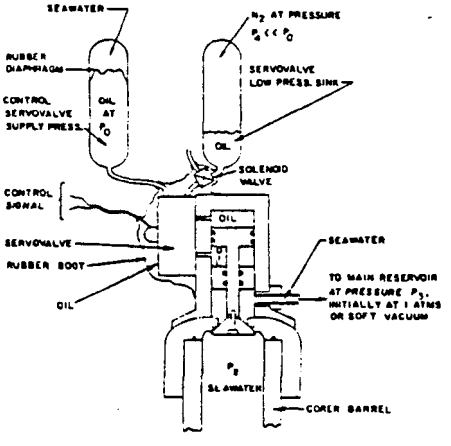


FIGURE 4 FREE ACTIVATING PISTON (FAP)

APPENDIX PP

MODELING STUDIES FOR LONG CORING FACILITY

C. H. Karnes, S. N. Burchett, and E. A. Aronson

Sandia National Laboratories

Modeling Studies For Long Coring Facility

C. H. Karnes, S. N. Burchett, E. A. Aronson
Sandia National Labs

The computer modeling studies for the Long Coring Facility has been in two areas during FY'81. The first is a refinement of the structural response affecting buckling and bending due to non-normal entry into standard and 50 percent stiffer sediments, and the second is the development of a model for the transient response of the hydraulic actuator piston control system.

The bending response is presented for the geometry presented in Fig. 1 identified as Corer F1 having a 13 mm wall thickness in the lower section, 25 mm in the center and 63.5 mm in the upper section. Since the 50 m long corer is very long and slender and may not be released in exactly a vertical orientation, the calculations have been performed for orientations deviating from vertical by up to three degrees. Figs. 2 and 3 show the lateral deflection and bending stresses for the core barrel as a function of entry angle measured from vertical. It shows that the addition of a drag term due to the lateral motion of the weight stand has a negligible effect on the peak bending deflection.

The results represented by the circles and squares are for penetration into the sediment considered standard for the LCF design, that from LL44-GPC3 having a logarithmic function of sediment depth. A set of calculations was also done for a sediment which was 50 percent stiffer than the standard sediment to determine its response to a surprisingly stiff sediment. Fig. 3 shows that even a 1.5 degree entry angle into the standard sediment will cause a stress of 200 MPa which is the yield stress for mild steel. These calculations predict uniform bending stress neglecting the effects of stress concentrations in joints and couplings. It is concluded that entry angles must be controlled very carefully and even with a barrel wall thickness of 63.5 mm in the upper 15 m section, a medium-to-high strength steel must be used with careful attention paid to coupling stress concentrations.

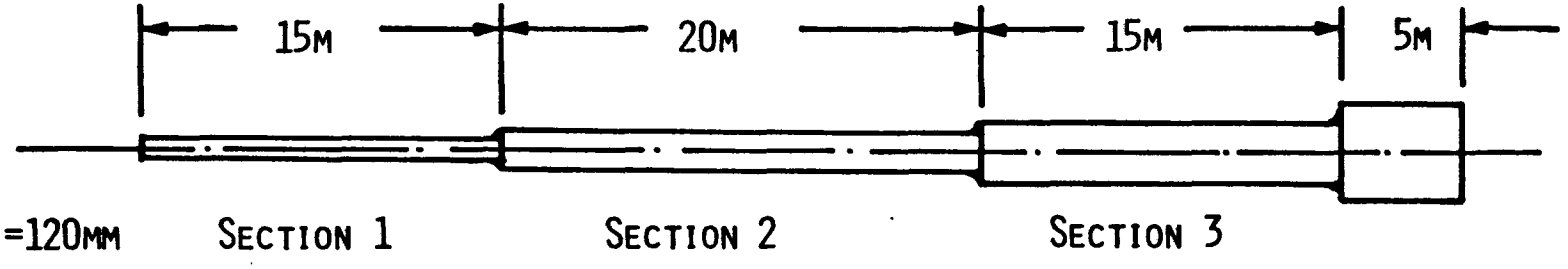
For the analysis of the piston control system, it is important to recall that the piston must be held stationary once the corer enters the sediment in order to prevent mechanical distortion of core sample. One of two proposed piston control systems is the hydraulic actuator piston which is attached to a parachute similar to that used on

The parachute used alone as a passive piston restraint would be pulled down several meters by the force required to hold the piston stationary. The hydraulic actuator shown schematically in Fig. 4 contains the piston (lower part of Unit 2) and a low pressure cavity (Unit 1). The ambient pressure, Pw, pressurizes the oil reservoir in Unit 2 and supplies the energy to contract the actuator as the control valve discharges the oil into the low pressure cavity. The control valve receives its signal from an accelerometer, integrator and microprocessor built into Unit 2. This feedback control loop opens and closes the control valve in such a way to keep Unit 2, the coring piston, at zero velocity. A short-range acoustic device built into Unit 2 determines the velocity of Unit 2 as it approaches the sediment after corer trip and after the parachute lifts the hydraulic actuator piston off its electronic start switch. This supplies the electronic integrating circuit with an initial velocity so that the piston can be controlled to zero velocity.

A preliminary, transient analysis of the control system has been accomplished by obtaining a numerical solution to the set of coupled differential equations which describe the motion of Units 1 and 2. The motion of Unit 3, the core barrel is prescribed as a result of a previous solution with the piston being held fixed. The following effects are considered: parachute drag, buoyancy, mass changes of Units 1 and 2, pressure differences, friction between components and between the core sample and core barrel, the sediment shear strength versus depth, and the sediment bearing capacity.

Fig. 5 shows the results of the first series of calculations for the piston position versus time after the control system is turned on. The gain shown as a parameter is the factor relating the piston velocity (to be controlled to zero) to the signal which drives the control valve open. These results show that a gain of 100 is required to keep the piston stationary within the 10 cm goal.

Future work on the mechanical response of the coring system will be to confirm the validity of the final mechanical design. Additional analyses of the hydraulic actuator piston control system will be performed to determine the sensitivity to other control parameters such as control valve response characteristics. An effort will also be initiated to analyze the response of the free piston control concept which also uses the ambient pressure as a power source.



	WALL THICKNESS (MM)				
CORER	SECTION 1	SECTION 2	SECTION 3	M_B(KG)	MWS(KG)
F1	13	25	63.5	6770	7379
F2	13	38.5	63.5	7922	6653

FIG. 1 Stepped Tapered Barrel Geometry

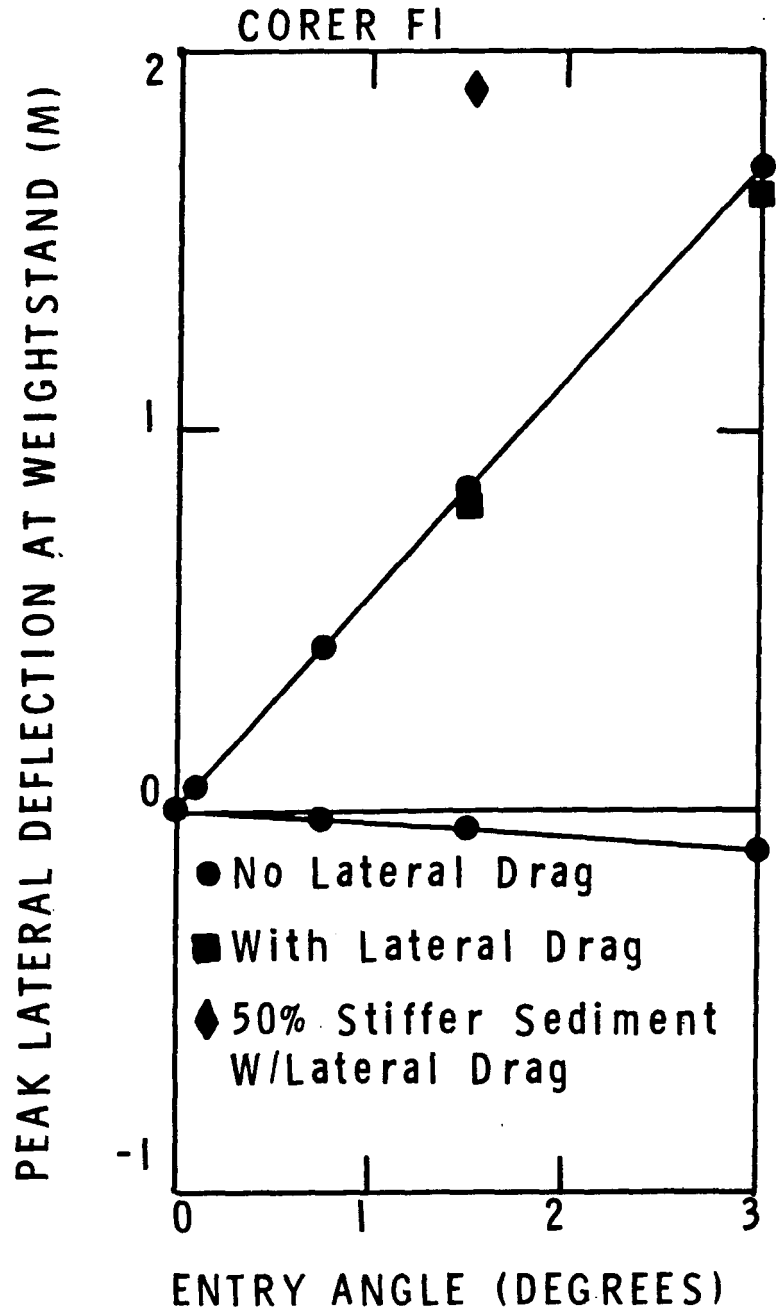


FIG. 2 Peak Deflection Due To Non-Normal Entry

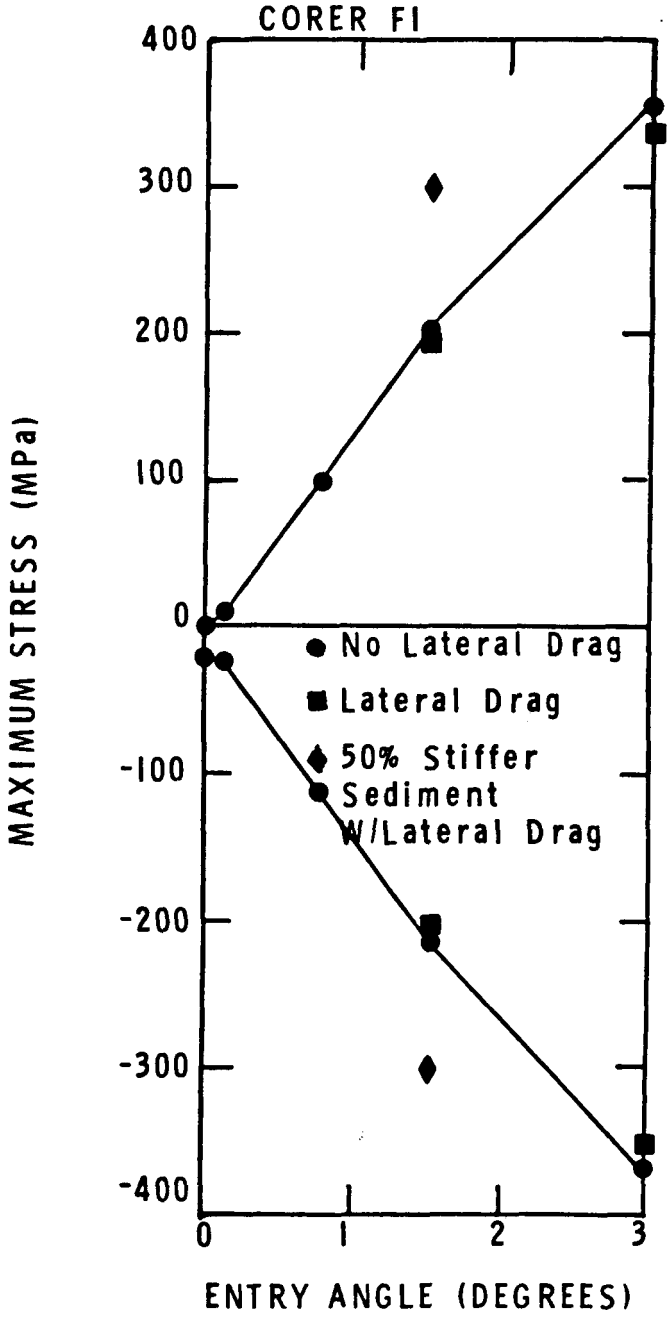


FIG. 3 Bending Stress Due To Non-Normal Entry

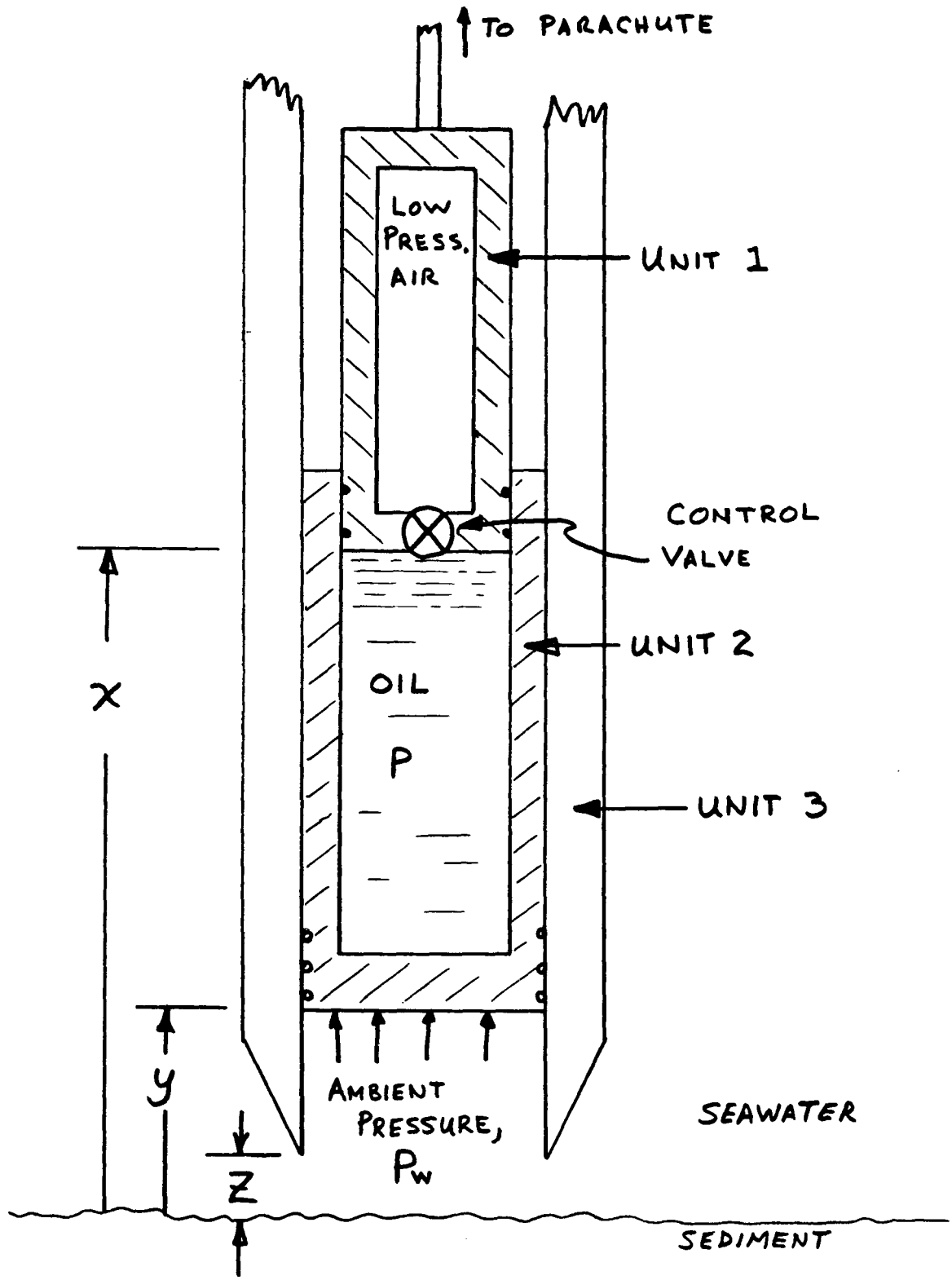


FIG. 4 Schematic Of Hydraulic Actuator Piston Control System

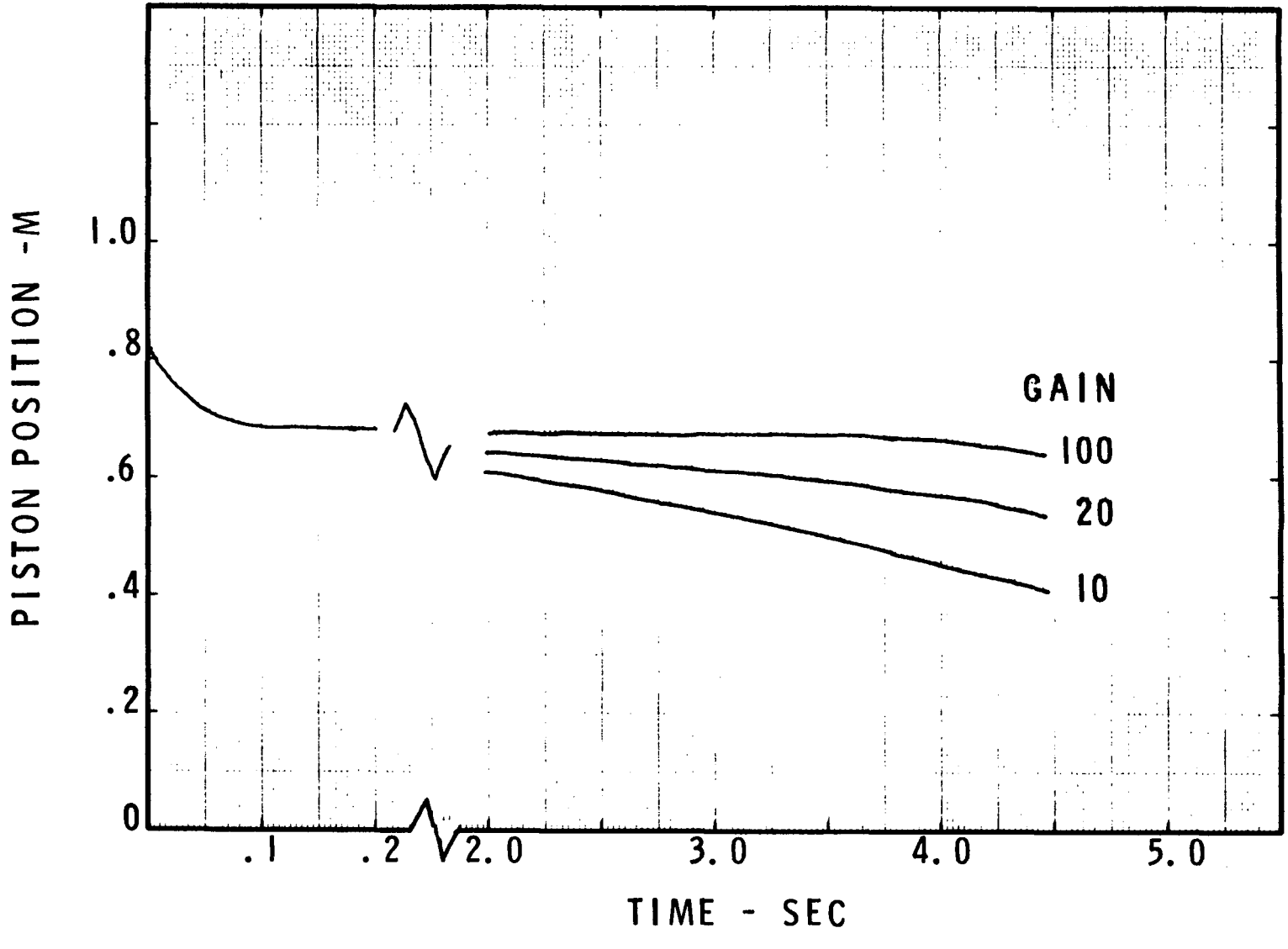


FIG. 5 Effects Of Gain On Piston Control Response

APPENDIX QQ

INSTRUMENTED SEABED PENETRATOR PROJECT

L. T. James

Sandia National Laboratories

Sandia Laboratories

Albuquerque, New Mexico
Livermore, California

date: January 7, 1982

[redacted] D. M. Talbert, 4516

S. T. James

from: L. T. James, 5627

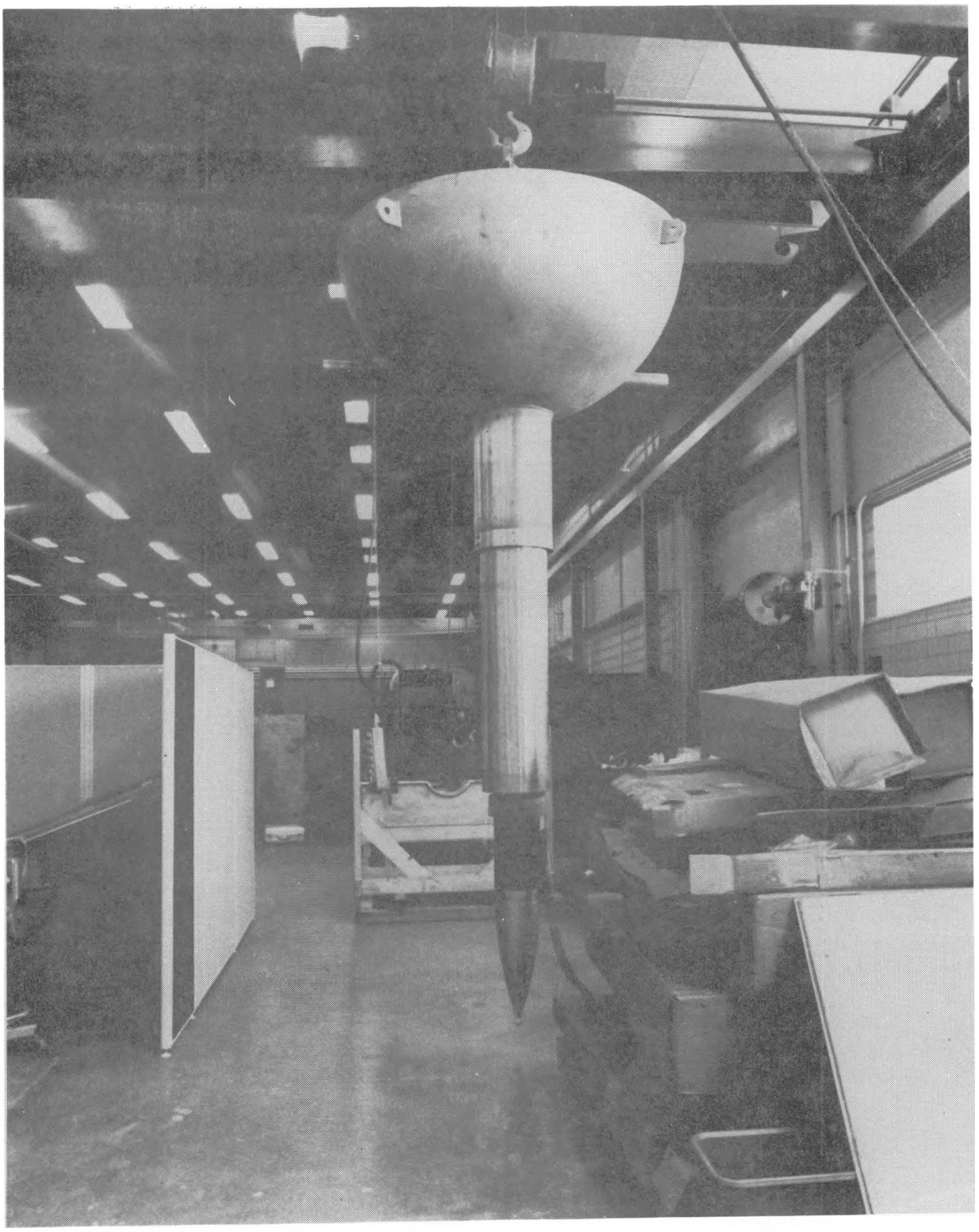
subject: Instrumented Seabed Penetrator (ISP) Project; Summary of Progress During CY 1981

Fabrication of the first-generation gun-launched instrumented seabed penetrator system (ISP-1) was completed during 1981. Pictures of the gun and penetrator assembly are attached.

Shallow-water tests of the ISP-1 were scheduled for late September, but these tests were canceled in late August when it was learned that the telemetry electronics failed to operate after shock-table tests. The telemetry subsystem is now being redesigned to eliminate those components which are most likely to fail when subjected to large shocks.

LTJ:5627:ecg

Copy to:
5620 M. M. Newsom
5627 T. S. Edrington
5627 L. T. James



801-802

APPENDIX RR

SOCIOPOLITICAL ASPECTS OF A SUBSEABED DISPOSAL PROGRAM FOR HIGH LEVEL NUCLEAR WASTE

Judith L. Kildow

Massachusetts Institute of Technology

(Contract #74-2545)

SOCIO-POLITICAL ASPECTS OF A SUBSEABED DISPOSAL PROGRAM FOR HIGH LEVEL NUCLEAR WASTE

FINAL REPORT

FEBRUARY 1982

For: Sandia Laboratories
Albuquerque, N.M.

Contract No. 74-2545

ABSTRACT: The research included in this report provides data describing and assessing the basic national and international socio-political and legal factors which could influence the formation and implementation of a Subseabed Disposal Program for High Level Radioactive Waste and Spent Fuel. Using the particulars identified in this research effort, the report summarizes the basic socio-political constraints and aids which currently exist or might come about which would influence a Subseabed Disposal Program.

Submitted by: Dr. Judith T. Kildow, Principal Investigator

Massachusetts Institute of Technology
Department of Ocean Engineering
Cambridge, Massachusetts 02139

TABLE OF CONTENTS

INTRODUCTION . . . . . .

TASK I: MODEL THE LINKAGES AMONG THE SCIENTIFIC AND TECHNICAL ASPECTS OF THE SUBSEABED EMPLACEMENT OPTION FOR HIGH LEVEL WASTE OR SPENT FUEL AND THE PUBLIC POLICY CONCERNS.

TASK II: IDENTIFY DOMESTIC LAWS, POLICIES AND PRACTICES RELEVANT TO THE SUBSEABED DISPOSAL ASSESSMENT PROGRAM WHICH MIGHT AFFECT THE CONTINUANCE OF THE RESEARCH PROGRAM OR THE DEPLOYMENT OF THE SUBSEABED DISPOSAL SYSTEM IF IT BECOMES TECHNICALLY FEASIBLE.

TASK III: ASSESS MAJOR US FOREIGN POLICIES AND ACCOMPANYING ON-GOING ACTIVITIES AS THEY MAY RELATE TO THE CONTINUANCE OF THE SUBSEABED DISPOSAL RESEARCH PROGRAM AND AS THEY MIGHT RELATE TO THE FEASIBILITY OF DEPLOYING A SUBSEABED DISPOSAL SYSTEM.

TASK IV: ESTABLISH WHICH US FOREIGN POLICIES MIGHT CONFLICT WITH DOMESTIC POLICIES RELEVANT TO THE SUBSEABED DISPOSAL ASSESSMENT PROGRAM.

TASK V: IDENTIFY INTERNATIONAL CONDITIONS WHICH MIGHT AFFECT THE ESTABLISHMENT OF A MANAGEMENT SYSTEM FOR IMPLEMENTING SUBSEABED DISPOSAL OF HIGH LEVEL NUCLEAR WASTE.

TASK VI: IDENTIFY EXISTING INTERNATIONAL ORGANIZATIONS, GROUPS, TREATIES, REGULATIONS, ETC., WHICH COULD HAVE SOME INFLUENCE OVER OR BE INFLUENCED BY THE DEPLOYMENT OF A SUBSEABED DISPOSAL PROGRAM.

ADDENDA I: . . . . . .

ADDENDA II: . . . . . .

TASK VII: DESCRIBE AND ASSESS THE RELEVANCE FOR THE SUBSEABED DISPOSAL ASSESSMENT PROGRAM OF THE POLICIES AND PERCEPTIONS OF THOSE ISLAND NATIONS IN GEOGRAPHIC PROXIMITY TO SITES BEING ASSESSED.

ADDENDA I: . . . . . .

ADDENDA II: . . . . . .

TASK VIII: DESCRIBE AND ASSESS THE TRENDS IN POLICIES AND . . . PERCEPTIONS OF GOVERNMENTS OF OTHER NATIONS WHICH HAVE THE NEED TO DISPOSE OF THEIR HIGH LEVEL NUCLEAR WASTE.

ADDENDA I: . . . . . .

ADDENDA II: . . . . . .

ADDENDA III: . . . . . .

TASK IX: DESCRIBE AND ASSESS THE ROLE OF NATIONS NOT YET . . . . FACED WITH NEED FOR A DISPOSAL METHOD AS WELL AS THEIR PARTICIPATION IN A COOPERATIVE PROGRAM ASSESSED IN TERMS OF CONSTRAINTS AND OPPORTUNITIES FOR MULTI-NATION SUBSEABED COOPERATION.

TASK X: DESCRIBE AND ASSESS THE ROLE OF NATIONS THAT . . . . . MIGHT NEVER HAVE THE NEED FOR HIGH LEVEL WASTE DISPOSAL AND THEIR POTENTIAL INFLUENCE ON COOPERATIVE PROGRAMS.

TASK XI: INTERPRET AND ANALYZE THE INFORMATION TO GIVE . . . . INITIAL INDICATORS OF THE AREAS OF GREATEST CONCERN AND THE MORE POSITIVE AREAS OF SUPPORT.

TASK XII: PRODUCE THE FOLLOWING WORKING PAPERS: 1) A . . REVIEW, INTERPRETATION, ASSESSMENT AND IDENTIFICATION OF THE CONSTRAINING AND SUPPORTING FACTORS TOWARD ESTABLISHMENT OF A SUBSEABED PROGRAM; 2) A GENERAL DESCRIPTION AND ANALYSIS OF TRADE-OFFS AND NEGOTIATING STRATEGIES.

ADDENDA I: SUBSEABED CONFERENCE PARTICIPANTS, 6-7 JULY 1981 . . .

ADDENDA II: MEMORANDUM 6-7 JULY 1981. . . .

ADDENDA III: CONFERENCE HANDOUTS. . . . . .

BIBLIOGRAPHY . . . . . .

INTRODUCTION

The radioactive waste disposal programs of most countries, including the United States, are focused on investigations of geologic formations on land as possible containment media for nuclear wastes. However, in recent years several countries in addition to the United States have initiated programs to investigate the potential of geologic formations in the subsea floor for such use.[1] The U.S. program was conceived in 1973 as part of the Federal Waste Management Program. It is currently one of four project elements of the U.S. Deparment of Energy's National Waste Terminal Storage (NWTS) program, managed and operated by the Sandia National Laboratories in Albuquerque, New Mexico, the sponsor of this report. The Subseabed Disposal Program (SDP) is being considered as a supplement to the other three land-based options, and as an option for longer-term disposal than the others.[2]

Although the SDP is not a top priority option for the U.S., since land-disposal options seem more probable and imminent, the U.S. SDP research program to date has spent more money than all other nations' expenditures in this regard taken together, and therefore is considered to be farther along. However, a group of nations that does not include the U.S. may not be able to avail themselves of land-based options due to political and/or physical limitations, and therefore perceive the SDP as their principal option.

The U.S. currently meets together with some of these other nations within the international Nuclear Energy Agency (NEA) seabed working group of the Organization of Economic Cooperation and Development (OECD) to maintain a cooperative program to exchange information and coordinate research.

The international nature of the SDP and the unevenness of other options available to nations that have or want nuclear power and who have a current or potential need to dispose of nuclear wastes compels the U.S. and those other nations with current needs to consider seriously how to manage development of a SDP option that could someday prove viable. The problem is magnified by the trends toward commitments to nuclear power throughout the international system of nation-states. Wastes must be disposed of which not only result from domestic operations, but from international contracts and arrangements designed to meet non-proliferation standards. The increase in the numbers of nuclear fuel export licenses and the unpredictability of reprocessing policies makes uncertain the ultimate path to be chosen for the disposal of spent fuel.[3]

As the SDP has matured, it has become apparent to the U.S. managers of this program that resolution of the scientific, environmental and technical aspects of seabed disposal, while difficult enough to establish, was only part of the problem; implementation and management of the actual program might prove to be just as difficult, or even more so. Hence, the Sandia Laboratories sponsored a project in 1980-81 to set out a social science research program for the SDP.[4] The major management problems that were identified included: broad public concern over use of the oceans for disposal; diversity of interests and objectives of nations; the international scope of the problem, and the high probability that disposal sites would, for scientific and environmental reasons, be optimal in international waters, an area to be managed for the "heritage of mankind."

This report focuses on one set of recommendations from the Social Science Research Program, issued Summer 1981: the parameters of social scientific factors that could influence the SDP favorably and unfavorably.

The following tasks build upon work initiated by Urban Systems Research and Engineering, Inc.[5] However, it branches into some new areas, gives alternative assessments, and updates information within a rapidly-changing political and economic climate. The work included in this report attempts to establish the foundations for a data base necessary to build a viable and effective program management system.

The report, organized according to the Task Order of the current contract, answers the requirements to:

1. Model the linkages among the scientific and technological aspects of the subseabed emplacement option for high level waste or spent fuel and the public policy concerns.

2. Identify domestic laws, policies and practices relevant to the Subseabed Disposal Assessment Program which might affect the continuance of the research program or the deployment of the subseabed disposal system if it becomes technically feasible.

3. Assess major U.S. foreign policies and accompanying on-going activities as they may relate to the continuance of the Subseabed Disposal Research Program and as they might relate to the feasibility of deploying a subseabed disposal system.

4. Establish which U.S. foreign policies might conflict with domestic policies relevant to the Subseabed Disposal Assessment Program.

5. Identify international conditions which might affect the establishment of a management system for implementing subseabed disposal of high level nuclear waste.

6. Identify existing international organizations, groups, treaties, regulations, etc. which could have some influence over or be influenced by the deployment of a subseabed disposal program.

7. Describe and assess the relevance for the Subseabed Disposal Assessment Program of the policies and perceptions of those island nations in geographic proximity to sites being assessed.

8. Describe and assess the trends in policies and perceptions of governments of other nations which have the need to dispose of their high level nuclear waste.

9. Describe and assess the role of nations not yet faced with need for a disposal method as well as their participation in a cooperative program assessed in terms of constraints and opportunities for multination subseabed cooperation.

10. Describe and assess the role of nations that might never have the need for high level waste disposal and their potential influence on cooperative programs.

11. Interpret and analyze the information to give initial indicators of the areas of greatest concern and the more positive areas of support.

12. Produce the following working papers: 1) A review, interpretation, assessment and identification of the constraining and supporting factors toward establishment of a subseabed program; 2) A general description and analysis of trade-offs and negotiating strategies.

FOOTNOTES: INTRODUCTION

1. Sandia Laboratories, Subseabed Disposal Program Plan, vol. I, July 1981, p. 28.

2. Ibid., p. 7.

3. Nuclear Fuel, 11 May 1981, pp. 6-8.

4. Judith T. Kildow, Principal Investigator, Social Science Research Agenda for Subseabed Disposal of High Level Nuclear Waste and Spent Fuel Program, Final Report, Sandia Laboratories, 1981.

5. Urban Systems Research and Engineering, Inc.(Deese, Innes, et al), Political and Institutional Implications of the Seabed Assessment Program for Radioactive Waste Disposal, Final Report, 24 February 1981.

TASK I:

Model the Linkages Among the Scientific and Technological Aspects of the Subseabed Emplacement Option for High Level Waste or Spent Fuel and the Public Policy Concerns.

A discussion of the feasibility of subseabed disposal of high level wastes and/or spent fuel must address the interrelationships between technical system design and the impacting political environment. Some assumptions are necessarily made at the earliest stages of the investigation. We have assumed:

1) That subseabed emplacement of high level nuclear waste will be available as an alternative disposal option by the year 2000;

2) That no civilian reprocessing facilities will be operating in the United States by that time. The policies of the current administration seem favorable to the reprocessing option, but the existing plant at Barnwell, South Carolina is technically out of date, and the capital investment necessary for its replacement is prohibitive to the private sector;[1]

3) That fifty years of domestic nuclear generated power production will have produced fifty years' worth of spent fuel in storage at reactor sites around the United States, with larger amounts east of the Mississippi than in the West;[2]

4) That spent fuel being considered for disposal in the subseabed will have been in storage for 15 years after irradiation and before preparation for emplacement;

5) That high level wastes generated by military research and development and by weapons production will remain stored at Hanford, Washington, Idaho Falls, Idaho, and Barnewll, South Carolina;

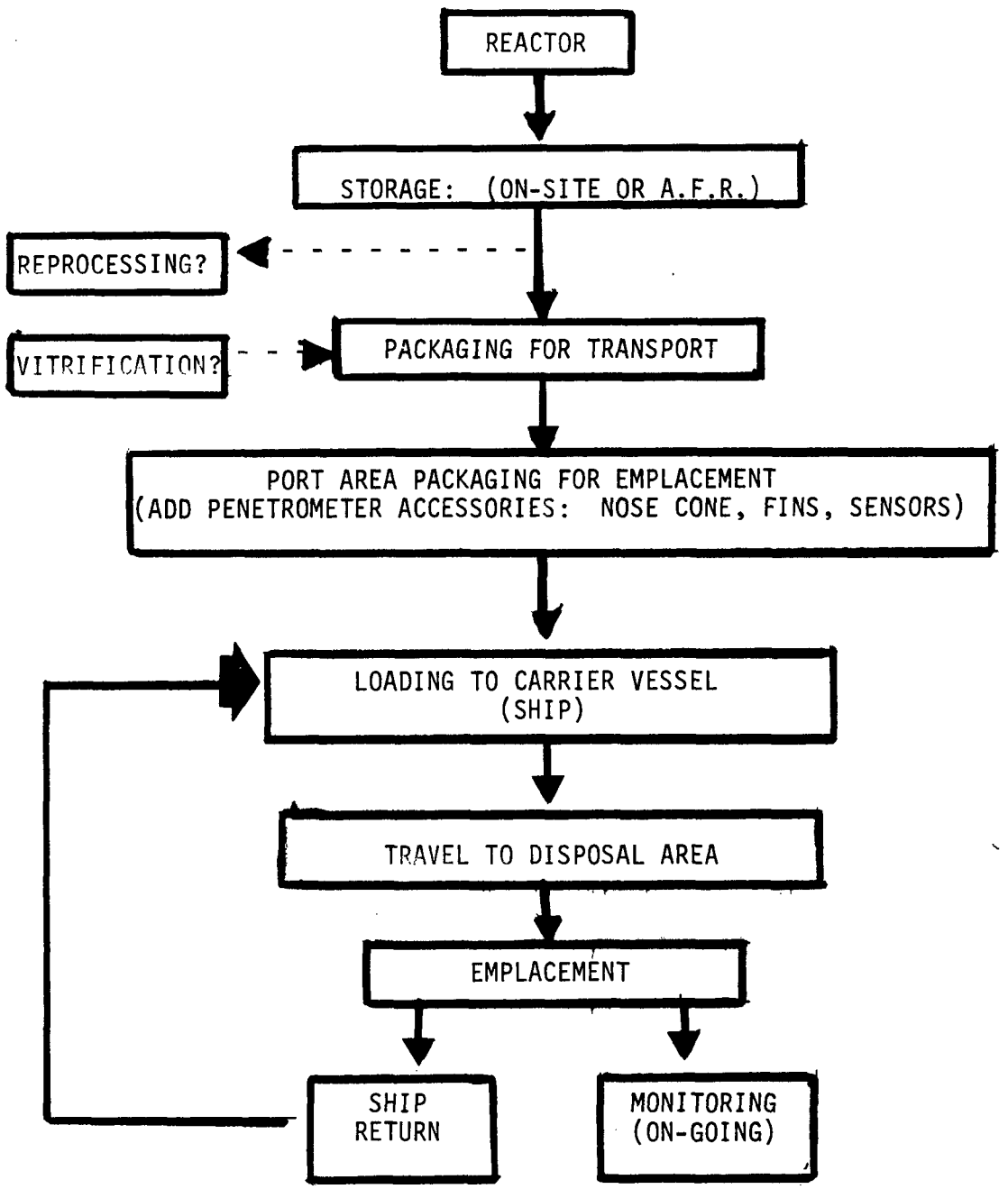
6) That emplacement of military waste in the International Commons area of the subseabed will add political obstacles to an already politically complicated program development procedure, and therefore should not be considered. The philosophy underlying the development of an international locale for military waste disposal may run counter to the pacifist discouragement of weapons production. Such an enterprise may also raise questions at the national level concerning the release of classified information about amounts and types of waste in existence;

7) That at least two regionally located disposal sites will be necessary within the United States to minimize land transportation distances between storage and disposal areas. Land based western sites located in Nevada and New Mexico are under consideration and probably will be available by the year 2000;

8) The subseabed option could be utilized to dispose of spent fuel which has accumulated at U.S. East Coast reactors, if reprocessing is available;

9) An Atlantic dumpsite is chosen as well as an East Coast port facility;

10) The path from reactor to emplacement area will be similar to that schematically represented below:



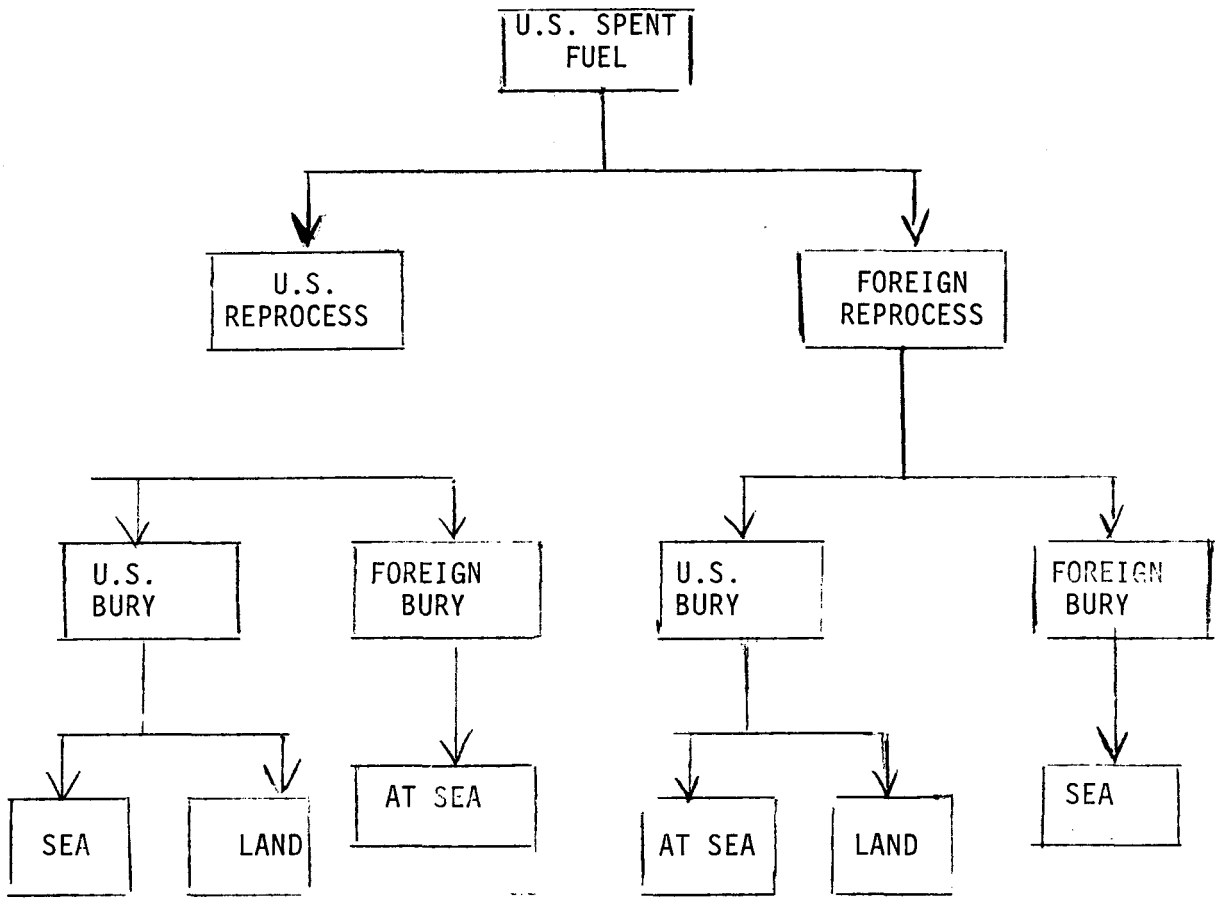
Observations:

1) The assumption that spent fuel will be the material disposed of, implies different system design parameters from the assumption that high level waste from reprocessing is the candidate. Packaged spent fuel rods contain fewer fission fragments than the same volume of high level waste, making the early containment problem easier from a technical perspective when spent fuel is the waste form under consideration. It is, however, current Department of Energy (DOE) policy that nothing of value should be emplaced in the deep-sea sediments,[3] suggesting that only high level waste is suitable. While retrieval of the waste canisters may not pose a technical difficulty, it may be safest from environmental and safeguards standpoints to leave them in the seabed after emplacement, and require retrieval for monitoring purposes only.

A difficulty is inherent in the fact that current and predictable future high level reprocessed wastes in the United States are of military origin and therefore are unsuitable under our assumption six. The Department of Energy does have responsibility to plan for the disposal of defense generated wastes. However, current policy considerations appear to favor transferring that responsibility to the Department of Defense.

Spent fuel contains an industrially valuable resource only if reprocessing is developed and breeder technology or plutonium recycling become acceptable alternatives to present fuel cycle practices. There is no commercial market for plutonium otherwise.[4] While plutonium obtained from spent fuel is less than ideal for weapons production due to the presence of substantial quantities of non-thermally fissionable isotopes, it is not difficult to envision cases in which a less optimal bomb would be preferable to none.[5]

Whether or not the United States chooses to reprocess by the time subseabed disposal is available is only half the issue. Other nations currently participating in OECD/NEA studies of subseabed disposal, notably France and Great Britain, have been reprocessing spent fuel for several years. It has been suggested that these countries may proceed with a subseabed program on their own prior to U.S. involvement.[6] It would be most prudent of the United States to design the technical system with high level waste as the disposal candidate to retain consistency with European research and development. Although this might at first seem contrary to current U.S. policy on reprocessing,[7] the U.S. could become the customer for the French and/or British reprocessing programs if return of the plutonium were guaranteed. See below for the range of possible U.S. options. It can also be argued, however, that the large amounts of spent fuel currently in storage and expected to accumulate by the year 2000, could not all be reprocessed even if the technology were available within the next ten years. Therefore, it is necessary to plan as well for spent fuel disposal.



2) Transportation of spent fuel and/or high level waste packages is the most troublesome link in any disposal system. It is most susceptible to the threat of theft, to the interference of distressed publics, and to the restrictions imposed by state and local legislations. Any mechanism which reduces the time spent transporting wastes between reactor storage and disposal areas is beneficial to the smooth operation of the program. Two of the assumptions we have listed are explainable by this concept:

1. The necessity for several regional (U.S.) disposal sites.

2. The choice of an Atlantic port site, if seabed disposal is used in the United States.

Given the location of high level waste and spent fuel storage sites throughout the U.S. (See Figure 1), the concept of two or three regional disposal sites is attractive for minimizing and spreading transportation risks. Western land based disposal sites are being researched in Nevada and New Mexico, Gulf Coast salt domes, if publicly acceptable, might service the central United States, and subseabed disposal can answer some of the disposal problems of the East Coast.

An Atlantic port facility is chosen for several reasons, it most importantly follows logically from the selection of an Atlantic disposal site. The concentration of spent fuel storage facilities/reactors in the eastern United States is also a factor.

A series of tradeoffs are implied between technical quality and policy decisions concerning Atlantic dumpsite selection. Informally, general agreement has been established between the nations of the OECD/NEA Seabed Working Group to consider an Atlantic site with top priority. All of the nations which are most interested in the program have Atlantic coastlines,[8] and the shortest time spent at sea implies the lowest probability of accident.

From the oceanographer's point of view, the North Atlantic is not optimal for site selection. Tectonically, it is a much less stable ocean and therefore has much smaller site-suitable seabed area than does the Pacific. (See Figure 2.) The Atlantic in general is far more heavily trafficked, adding to the hazard of collision at sea and the necessity of avoidance of regularly used shipping lanes.

Choice of a Pacific site, however technically appealing, would be less efficient politically, and more dangerous due to the greater transportation distances required either on land or at sea. Recent protests over the siting of low level waste disposal facilities on Pacific islands has illustrated the strength of potential opposition within the island communities of the Pacific,[9] and suggests that attempts to locate high level disposal sites in the region might meet similar response. Transporting wastes by sea to Pacific sites implies travel off the coastlines of many nations not involved with the seabed disposal program, nor likely to have need for the option. Political opposition can be expected. These technical/political tradeoffs will undoubtedly impact final site selection.

3) Within the technical system of port and ship facilities are many interrelationships which need to be defined and resolved before designs can be finalized. Each parameter implies different policy decisions, impacts of which must also be considered. The establishment of the inter-linkages and precise design of the system around them is crucial to the success of the project.

For example, the establishment of a set of shipment logistics is of critical importance. Permissible loading capacities for each type of waste, shipment frequencies and fleet size must be determined. Underlying these decisions is the concept of the definition of an accident (vs. "disaster") scenario.

In order to proceed with technical design tasks it is necessary to decide whether a possible event has the characteristics of an accident or a disaster. Presumably, an accident can be defined as an occurrence which is reasonably acceptable, and a disaster is that which will irreparably damage the technical integrity or public credibility of the system. Total loss of ship and payload is the worst case scenario facing subseabed disposal. The question of whether the worst case would carry disaster

status depends on the volume and type of waste carried on the definitions of wastes acceptable for dumping at sea and on recommended release rates established by the IAEA.

The London Dumping Convention Revised IAEA Definition and Recommendations of 1974 establish waste categories unsuitable for dumping and acceptable upper-limit release rates for ocean dumped materials at a single site and for a finite ocean basin. (See Figures IIIa, and IIIb.)

These release rate limits are translatable to concentrations at a single site and assumed upper limits on mass dumping rates as follows:

100,000 tonnes*/year = mass dumping rate limit concentration limits:

a) 10 Curies/tonne/year for α-emitters; limited to 10^{-1} Curies/tonne for ^{226}Ra and supported ^{210}Po;

b) 10^{2} Curies/tonne for β/γ-emitters with $t_{\frac{1}{2}} > 0.5$ years excluding tritium and β/γ-emmitters of unknown half lives.

c) 10^{6} Curies/tonne for tritium and β/γ-emitters of $t_{\frac{1}{2}} < 0.5$ years.[10]

The assumed assimilative capacity of the ocean basin and the ICRP dose limits for public exposure are the bases of development for these recommendations.

Ship design proceeds around a pre-specified payload capacity expressed as weight in tonnes. Payload capacity for subseabed disposal implies the definition of an accident scenario. The worst case accident; loss of payload and containment in shallow coastal waters must be considered within the framework of the acceptable release rates established by the IAEA. Canister weight and content are prerequisite pieces of information. Ocean basin dumping activities from all sources must be taken into account. Clear presentation to technical system designers of these decisions is imperative to ensure maximum safety and efficiency.

An accident management scheme should also be closely coordinated with technical system design. Any perceivable gap between the two may result in public acceptance difficulties and therefore may retard the forward development of the program. Gaps between accident management plans and technical designs also raise the probability of the occurrence of the disaster scenario, which should be avoided at all cost.

---

*1 metric ton = tonne = 1.1 U.S. tons.

Conclusions:

By extrapolation from observed technical-public policy interrelationships it can be noted that two or perhaps three basic decisions are necessary:

1. Decision to accept the seabed for disposal by the U.S. and others (crucial to system development!);

2. Selection of the "Ocean of Choice" for a disposal site (Atlantic vs Pacific);

3. Definition of accident/disaster scenarios in terms of percent of mass dumping and release rate limits.

Technical designs can proceed most efficiently only after these choices have been made. The type of waste to be emplaced is also an important consideration, but is secondary to the first three considerations.

The most crucial is obviously the choice of the seabed as a disposal medium. East Coast waste/spent fuel stores require a regional disposal site, and the eastern United States poses problems for siting land based repositories due to the large population concentrations in the region, and the lack of easily accessible suitable geologic formations. Precluding economic consideration, seabed disposal of eastern wastes may be the best alternative to cross country transport for burial in western repositories. Domestically, this seems the most favorable argument for subseabed emplacement.

Two other factors should force U.S. considerations of subseabed disposal of high level waste, (1) the selected land-based sites may not be capable of processing and isolating the large amounts of wastes requiring disposal and a supplementary system may become necessary, (2) the land disposal sites might prove to be hazardous ultimately, and their use discontinued, in which case subseabed could become the option. In either case, an Atlantic site would not be essential, but rather a viable supplement.

There is an additional consideration which skews the technical/policy work which should be noted here. As stated in preceding paragraphs, the Subseabed Program scientists claim the Pacific geology and clays are much more suitable than Atlantic.[11] The political scientists claim the Atlantic is too busy and risky. The technical designers for the program are proceeding with the assumption that a penetrometer will be the burial vehicle. The Pacific clays are soft enough for the penetrometer, while the Atlantic muds would require a drill hole. Thus, all indicators would seem to favor the Pacific site. Yet, current NEA research programs are focusing on the Atlantic sites with the Europeans eyeing their proximity; this report indicates there could be direct U.S. interest in an Atlantic site; and

the Pacific island states are adamant about protecting the Pacific Ocean from any more radioactive contamination. This final point illuminates a problem area affecting the current program. Some inconsistencies may need to be resolved among technical design and site operations as well as site selection.

Internationally, the United States must concern itself with the probability that other interested nations may opt for subseabed disposal due to the absence of land-based sites as options within their borders. Whether directly or indirectly interested, it is to the advantage of the U.S. to retain adequate political and technical control during the process of the program's development.

Figure I A

Table 2–4. High Level Waste and Spent Fuel Storage in the United States.

Existing high level reprocessing waste (as of 10/1/77):

Site		*Volume (thousands of cu. ft.[a])*	
DOE-operated			
Savannah River, South Carolina		2900	
Idaho Falls, Idaho (Idaho National Engineering Laboratory)		404	
Hanford, Washington		6102.5	
	Subtotal	9406.5	
West Valley, New York (Nuclear Fuel Services)			
Neutralized (Purex waste)		80.2	(600,000 gallons)
Acidic (Thorex waste)		1.6	(12,000 gallons)
	Subtotal	81.8	
	Total	9488.3	

Spent fuel storage (as of 12/31/78):

1. At the end of 1978, there were approximately 4,400 metric tons of commercial spent reactor fuel in storage at reactor sites and the three nonfunctioning reprocessing plants (GE–Morris; West Valley, New York; AGNS–Barnwell).[b]
2. The Tennessee Valley Authority has announced tentative plans to construct a large away from reactor spent fuel storage facility by 1984. The facility may be located at Oak Ridge, Tennessee.
3. The federal government intends to construct an away from reactor spent fuel storage facility by 1984–1985. Interim storage of spent fuel may take place at the three nonfunctioning reprocessing plants.
4. Spent fuel storage experiments are planned for Hanford, Washington, and the Nevada Test Site for 1979–1980. The Waste Isolation Pilot Plant may include "demonstration" storage of up to 1,000 spent fuel assemblies in a retrievable mode, but the project will not commence before 1985.
5. Spent reactor fuel is presently accumulating at the rate of about 1,300 metric tons per year.

[a] 1 cubic foot = approximately 7.5 gallons of liquid; much of the defense waste is solidified.

[b] 1 metric ton = 2,200 pounds. Volume is about 13.1 cubic feet per metric ton of spent fuel.

Source: IRG (1978).

stored at the government reservations at Hanford, Idaho Falls, and Savannah River. At the end of 1978, about 4,400 metric tons of spent reactor fuel were in storage at reactor sites (Figure 2–9), and the Department of Energy has estimated that, on the basis of a minimum of 148 GWe of nuclear electrical generating capacity at century's end—about three times current nuclear capacity—the cumulative spent fuel discharge by domestic light water reactors will total

SOURCE: Radioactive Waste: Politics, Technology, and Risk
R. Lipschutz Ballinger Publishing Co. page 48

Figure I B

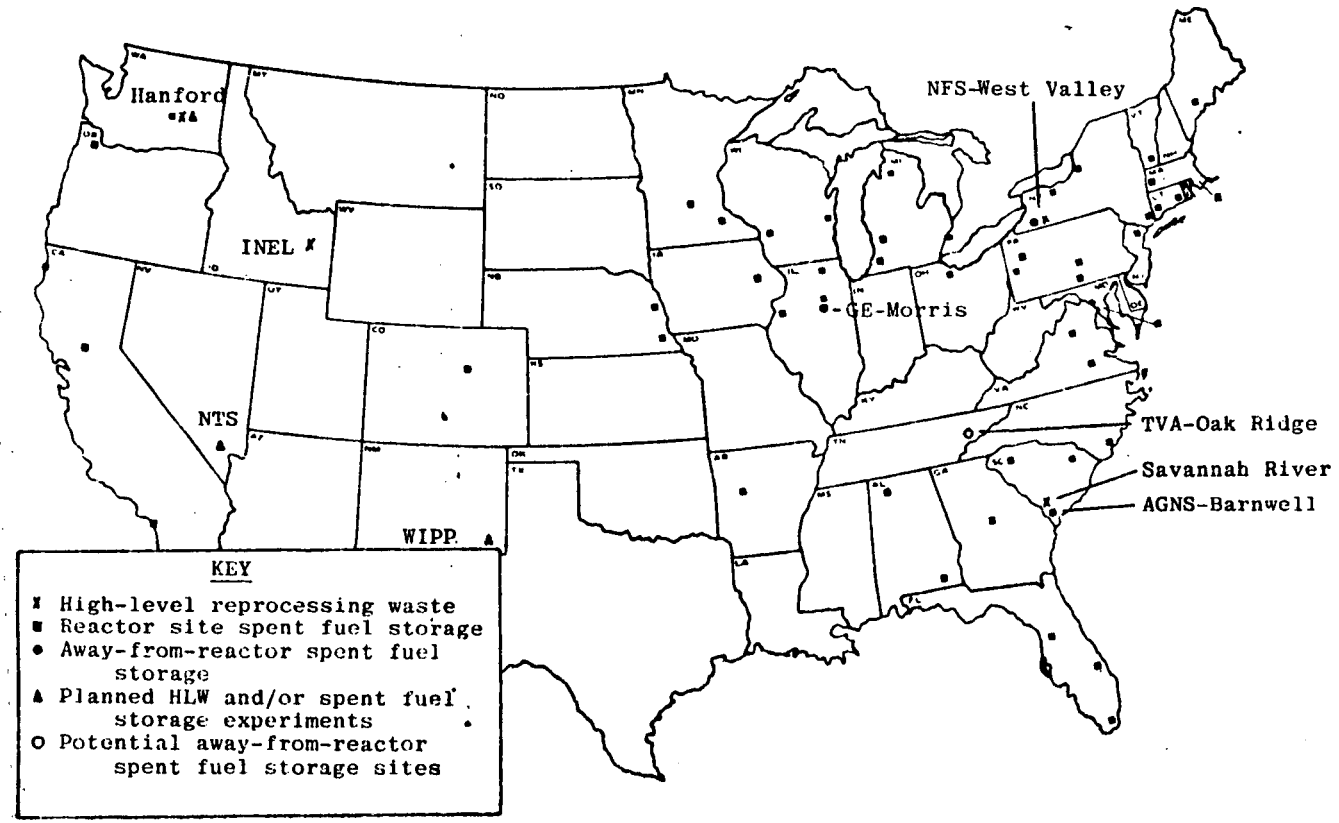
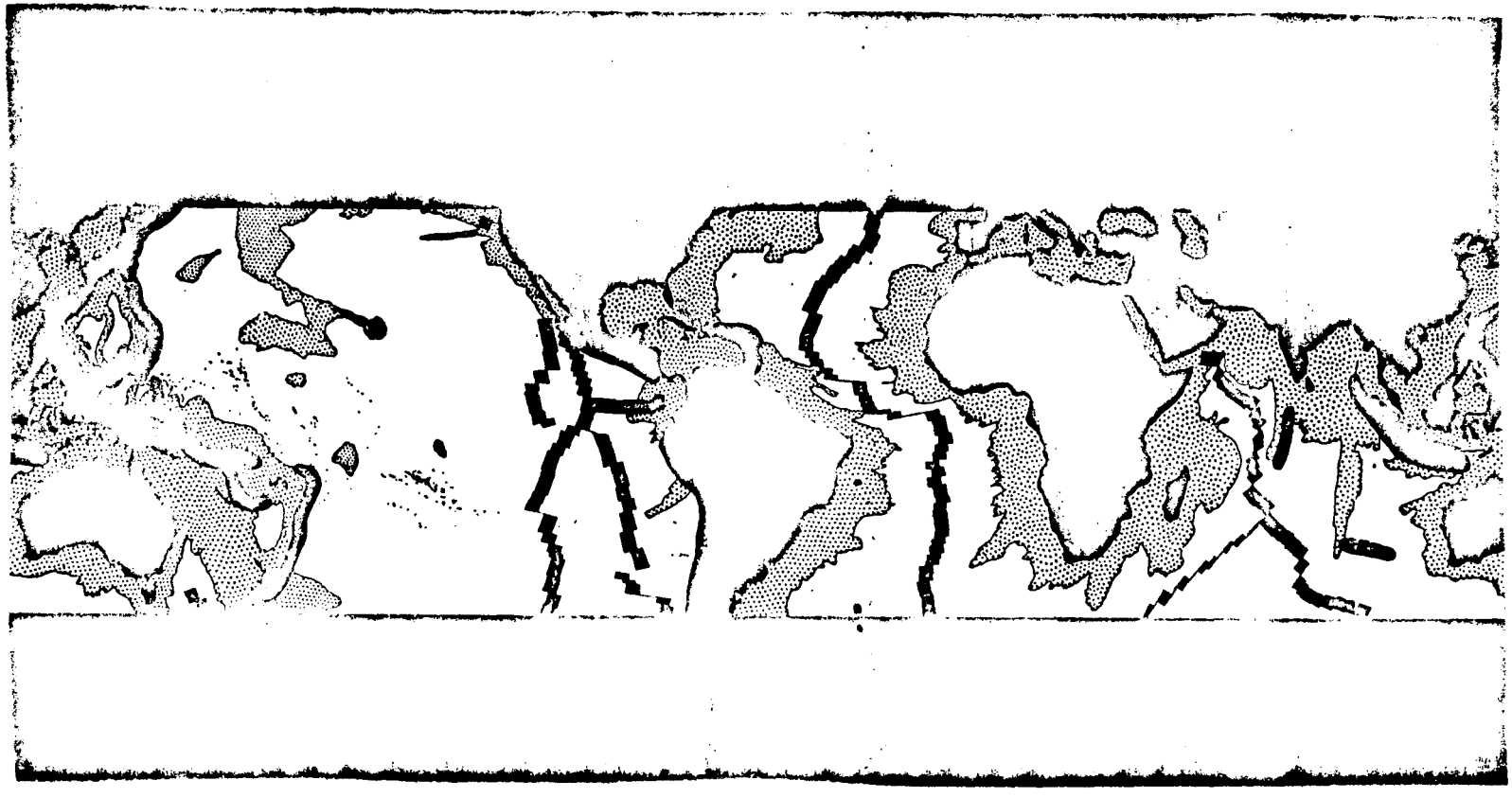


Figure 2–9. High Level Waste and Spent Fuel Storage Sites in the United States.

Source: Prepared by author from DOE (1979c:4) and IRG (1978).

Figure II a



White areas hold some potential for the disposal of high level wastes within the subseabed sediments.

Source: "Nuclear Waste Into Deep Sea Sediments", Hollister and Anderson, 1979

Figure IIb

FIGURE 2

Site Suitability Criteria Applied to the World Map

Areas blackened out are: a) at latitudes higher than 40° north, b) within a hundred miles of a spreading center, c) within 100 miles of active volcanoes, d) within 100 miles of the floor of a deep sea trench/island arc system, and e) on dry land. Continental margins, inland seas, aseismic ridges and abyssal plains are stippled. All of these areas are, at present, not thought to be potential repositories for reasons discussed in the text. Areas that appear to hold some potential for the disposal of high level waste (if it is inserted into the seabed sediment) are white. The next critical need for total assessment of white areas is an accurate determination of thickness and uniformity of the formation. Areas blanketed by less than 50 meters of sediment will generally extend at least another 200 miles from the black regions (denoting the crest and upper flanks of the mid-oceanic ridges and their transform faults); these areas are probably not suitable for this disposal concept.

SOURCE: Nuclear Waste Into Deep Sea Sediments, Hollister and Anderson, 1979.

Figure 3a

London Dumping Convention of 1972:

Provisional Definition (IAEA) of 1974:

High-level waste unsuitable for dumping = material with concentration (Curies/tonne) exceeding:

(a) 10 Ci/tonne: α-active waste with $t_{\frac{1}{2}} > 50$ years.
< 100 Ci/year of ^{226}Ra at any given site.

(b) 10^3 Ci/tonne β/γ-active waste excluding tritium (H_3)
10^2 Ci/tonne limit for ^{90}Sr and ^{137}Cs.

(c) 10^6 Ci/tonne for tritium.

Assumed volume of ocean basin = $10^{17} m^3$

Assumed upper limit on dumping rate = 100,000 tonnes/year at any given site.
(averaged over gross mass not to exceed 100 tonnes)

SOURCE: Marine Radioecology: Proceedings of the Third N.E.A. Seminar "Radiological Aspects of Seabed Dumping in the Deep Oceans," W.L. Templeton, page 24 NEA/OECD 1980.

Figure 3b

1974 IAEA Recommendations:

Estimated Annual Release Rate Limits:

	Release Rate Limits (Ci/year)	
	Single Site	Finite Ocean Volume $10^{17} m^3$ *
α-emitters (limited to 10^4 Ci/yr for ^{226}Ra and supported ^{210}Po)	10^5	10^5
β/γ-emitters ($t_{1/2}$ > 0.5 yr. excluding tritium) and β/γ-emitters of $t_{1/2}$ unknown	10^7	10^8
Tritium and β/γ-emitters with $t_{1/2}$ < 0.5 year	10^{11}	10^{12}

*$10^{17} m^3$ is an ocean basin volume slightly smaller than the North Atlantic.

SOURCE: Marine Radioecology: Proceedings of the Third N.E.A. Seminar W.L. Templeton, page 28 NEA/OECD 1980.

FOOTNOTES: TASK I

1. According to industry executives present at a meeting with DOE secretary, James Edwards, on 23 April 1981, to discuss the possibility of an industry take-over of the Barnwell station as suggested by President Reagan on 20 March. Nuclear News, June 1981.

2. See Figure I. Wastes may also be stored at away-from-reactor facilities located regionally.

3. Dr. D.R. Anderson, Interview, 7 July 1981 meeting.

4. Op. Cit., meeting of industry executives, 23 April 1981.

5. Wohlstetter, Albert, Swords From Plowshares, pp. 40-42.

6. Dr. C. Hollister, Interview, 7 July 1981 meeting.

7. The Nuclear Non Proliferation Act of 1978 discourages foreign nations from reprocessing spent fuels of U.S. origin. Current U.S. policy also prohibits domestic reprocessing, DOE Statement of Position in the Matter of Proposed Rolemaking on the Storage and Disposal of Nuclear Waste, 15 April 1980.

8. Great Britain, France, United States, The Netherlands.

9. New York Times, 18 March 1981.

10. W.L. Templeton, "Radiological Aspects of Subseabed Dumping in the Deep Oceans." Marine Radioecology, Proceedings of the Third NEA Seminar NEA/OECD, 1980, p. 31.

11. Charles D. Hollister, D. Richard Anderson, G. Ross Heath, "Subseabed Disposal of Nuclear Wastes," Science, vol. 213, 18 September 1981, pp. 1321-1326.

TASK II:

Identify Domestic Laws, Policies and Practices Relevant to the Subseabed Disposal Assessment Program Which Might Affect the Continuance of the Research Program or the Deployment of the Subseabed Disposal System if it Becomes Technically Feasible.

Federal legal parameters which may affect a subseabed disposal option generally fall into two categories: (1) 'Energy-Related' legislation (nuclear energy-related legislation in particular) and (2) 'Environmental/Marine' legislation.

Nuclear Energy-Related Legislation

The Atomic Energy Act of 1954 defined the role of the Atomic Energy Commission as the lead agency for review and licensing of commercial nuclear power generating facilities.[1] Later, the Energy Reorganization Act of 1974 transferred that role to the Nuclear Regulatory Commission (NRC). These laws do not directly impact on subseabed disposal or its legality, however, but merely provide some guidelines for possible federal management and regulatory schemes. Subseabed disposal was not considered during the passage of either law. In fact, nuclear waste disposal seems in general to have been neglected as an issue until recently.[2]

The purpose of the Atomic Energy Act of 1954 was to establish the Federal government as regulator and licensor of the emerging nuclear power industry. Of primary concern was the separation of defense and commercial reactor regulation with little or no specifics as to waste disposal technique. Since the subseabed program only began in 1973, there is no mention of subseabed emplacement of high-level wastes or spent fuel.

This legislation was supplemented and, in effect, superceded in 1974 by the Energy Reorganization Act. The Atomic Energy Commission (AEC) established under the 1954 Act was replaced by the Nuclear Regulatory Commission as lead regulatory agency and the Energy Research and Development Agency (ERDA) as research and development supervisory agency. The Nuclear Regulatory Commission is defined specifically in this Act as responsible for "licensing and relating regulatory functions of the Atomic Energy Commission...(and specifically)...facilities used primarily for the receipt and storage of high-level radioactive wastes..."[3] This is as close as the legislation comes to defining NRC's role for subseabed disposal. Although waste disposal is mentioned, the emphasis in 1974 was government reorganization of an outdated management system for nuclear power in the wake of the oil crisis of the early 1970s, and a forecasted growth in demand for the alternative energy source provided by the nuclear industry.

Although the subseabed option would seem to be free of much of the confusion surrounding Federal vs. State authority over land-based disposal site selections, it is not without State-Federal jurisdictional obstacles. It will be necessary, for example, to transport wastes from the sites of production either to packaging stations and then to the port, or directly to port-area packaging facilities. States through which the wastes will travel may object. The Price-Anderson Act of 1957 serves to establish

insurance against transportation accidents involving nuclear materials. It has been seen that this provides small reassurance to city and state officials.[4]

Radioactive waste management was not addressed as a legislative issue in and of itself until the recent (December 1980) passage of the Low-Level Radioactive Waste Policy Act (P.L. 96-573). This statute began as S.2189, the Nuclear Waste Policy Act, which focused primarily on spent fuel and high-level waste management.[5] The necessity of developing away-from-reactor storage was the issue that led to the Senate acceptance of S.2189 over another bill, S.2890, introduced at the same time, which called for permanent disposal.[6] In the final session of Congress, after having passed the House, the Nuclear Waste Policy Act lost its high-level waste provisions in a battle over defense waste regulations. Several members of the Armed Services Committee (Senate) objected to a clause which would have required the preparation of an Environmental Impact Statement (EIS) for defense waste management.[7] In the hurry and determination to pass some kind of nuclear waste management law, the lame-duck Congress scratched the offending high-level waste sections and passed the revised S.2189 as the Low-Level Waste Policy Act of 1980.

Several characteristics of the legislative history of P.L. 96-573 are worthy of note here. The first is that some attempt was made to legislate high-level radioactive waste policy. The second noticeable trend is the emphasis which was placed on the debate between away-from-reactor storage and permanent disposal as concepts for radioactive waste management schemes. The third factor of note is the concern over the legislation of defense waste management in conjunction with commercially generated waste management.

Each of these issues may affect the development of legislation directly related to subseabed disposal should such legislation be deemed necessary. National policies which underlie them have shifted with changes in the Administration and the Congress. Emphasis placed on the storage and disposal of commercially generated spent fuel by the Carter Administration may give way to consideration of disposal of high-level reprocessed wastes as a result of the Reagan Administration's support for reprocessing and the breeder.[8] Should defense wastes come under consideration for subseabed emplacement, it is possible that controversy might ensue in developing legislation to cover the subseabed program. The subseabed program could benefit from military support, however, if the military wanted and needed the program.

The Carter Administration, in the Nuclear Non-Proliferation Act (NNPA) of 1978 set out its policies on the diversion of nuclear materials for military purposes.[9] While NNPA is directly concerned with strengthening safeguards attached to nuclear fuel and technology exports, it may relate to any other U.S. bilateral agreement or multilateral arrangement having to do with the nuclear fuel cycle.[10]

The Act emphasized the "...imperative need to increase the effectiveness of international safeguards and controls on peaceful nuclear activities,.,"[11] and restricts U.S. cooperation in peaceful nuclear energy pursuits to those nations which have ratified the NPT of 1970.[12]

Recently released safety standards proposed by the Nuclear Regulatory Commission will directly impact program design and implementation if not amended. The current draft rules require packaging to prevent leakage for 1000 years, retrieval for the first 50 years, and involve the multi-barrier concept in repository design to prevent nuclide escape.[13]

An amendment to the Omnibus Territories authorization bill was offered by Senator Matsunaga (Democrat, Hawaii) and enacted by the Congress in 1979. The amendment, Section 605 of P.L. 96-205, requires that Congress be kept fully informed of any actions by the Federal government involving nuclear waste storage in the U.S. territories. It also requires an Act of Congress before the Federal government would be authorized to begin implementing any plan for storage or transportation of nuclear wastes within the jurisdictional boundaries of any U.S. territory or possession anywhere in the world.[14]

While it is unlikely that burial of the wastes would take place within territorial limits of 3 miles (or 12 miles in the event of enactment of a new Sea Treaty), transportation of the waste might take place within these regions and therefore be subject to this law.

Environmental/Marine-Related Legislation

The legal feasibility of subseabed disposal under Federal statutes requires an overview of existing environmental legislation. However, consideration must also be given to the possible differences between national policies and their reflected attitudes, popular at the time of enactment, and those currently prevalent, which could alter the course of future decisions.

The National Environmental Policy Act of 1969 (NEPA) is considered the bulwark of modern environmental legislation. It established the Environmental Protection Agency (EPA), the Environmental Impact Statement (EIS) process, and set forth the notion of measureable environmental quality standards. Prevailing attitudes of concern for the environment prompted its passage. NEPA is not an anti-dumping law. It is a pro-regulation law, and it gives the EPA jurisdiction over review of a Subseabed Disposal Program.

NEPA requires detailed assessments of environmental impacts inherent in any federal action significantly affecting the quality of the human environment.[15] Environmental Impact Statements are required on Federal actions in areas outside the jurisdiction of the United States as well.[16]

A prevalent social attitude in the early 1970s was concern for the environment and the preservation of its integrity and the sanctity of the oceans space. Prevention of oil spills was a goal as well, following the Torrey Canyon Disaster, and later, the Argo Merchant Spill.

Concurrent to the international consideration of the London Dumping Convention (1972) and the International Convention for Prevention of Pollution from Ships (1973), much environmental (marine-oriented) legislation was passed in the United States.

Marine Protection Research and Sanctuaries Act

Perhaps the most relevant legislation put into force was the Marine Protection Research and Sanctuaries Act of 1972 (MPRSA).

The MPRSA has been interpreted by some as an obstacle to subseabed disposal, [17] both in the banning of the transport to sea of high-level waste for the purpose of 'dumping', [18] and by the definition of 'dumping' as presented in the Act. Under MPRSA, 'dumping' is:

"... the addition of any material or combination of materials to that part of the oceans, coastal or other waters beyond the territorial jurisdiction of the United States...(but)...does not include...intentional placement of a device either in the water...or on or in the submerged lands beneath such water, if the placement of the device is for a purpose other than disposal, and if the placement of the device is otherwise regulated...as part of an authorized Federal or State program."[19]

It seems that the interpretation of subseabed emplacement of nuclear wastes as 'dumping' is valid only if the emplacement is considered permanent. Given a method for waste retrieval, perhaps subseabed nuclear waste emplacement might not be considered 'dumping' under MPRSA. The transportation clause might, however, still be sufficient to hinder program implementation. Amendments to the Act seem necessary before the subseabed program would be considered legal under its provision.

Amendments to Marine Protection Research and Sanctuaries Act (MPRSA)

A recently passed piece of legislation may serve as a precedent for continued amendment to the MPRSA to accommodate the subseabed disposal concept. The 1980 Amendment to the Marine Protection Research and Sanctuaries Act and authorizations (P.L. 96-572) has as its main focus the discontinuation of dumping of hazardous wastes under interim permits outstanding by December 31, 1981. A clause has been designed for the current purposes of the Subseabed Disposal Program. It reads, "(limited permits for dumping of industrial waste will be made available to)... conduct research on new technology or to determine whether or not the ocean dumping of a new or relatively little understood substance will in fact be harmful..."[20] These permits would be available after the

December 1981 deadline. The legislation was developed and considered concurrently with the Low-Level Waste Policy Act. Subseabed disposal, while not the issue of primary importance in the drafting and consideration of either piece of legislation, was nevertheless a consideration. MPRSA amendment is feasible and ongoing.

The Federal Water Pollution Act

The Federal Water Pollution Control Act (1948) and its various amendments explicitly forbid any discharge of high-level radioactive wastes into the oceans.[21] It would seem that the concept of emplacement of packaged wastes in the deep sea floor might not be covered by a general prohibition on discharge.

The Coastal Zone Management Act

State control over protection of the coastal area provided under the Coastal Zone Management Act of 1972 (P.L. 92-583) might encourage states to take steps to ensure that nuclear waste transports into and out of port towns are highly regulated, if not prohibited.[22] This would exacerbate Federal-State conflicts over nuclear waste shipments. The Federal consistency and national interest provisions of this Act could be useful in facilitating the necessary arrangements if the appropriate Federal agencies argued to its importance, and if the respective states didn't effectively counter such moves.

Environment/Marine Transport

Safe transportation of nuclear materials is the responsibility of the Department of Transportation (DOT) and the Nuclear Regulatory Commission (NRC).[23] Under the Hazardous Materials Transportation Act of 1974 (P.L. 93-633) DOT is authorized to protect "the nation adequately against the risks to life and property...inherent in the transportation of hazardous materials in commerce."[24] Although NRC's authority under the Atomic Energy Act of 1954 and the Energy Reorganization Act of 1974 (P.L. 93-438) extends over all persons possessing using or transporting nuclear material, common and contract carriers have been exempted due to regulatory authority exercised by DOT. However, the NRC would have licensing responsibilities if it was decided that the port facility would serve as away-from-reactor (AFR) storage. The NRC derives this responsibility from the Atomic Energy Act of 1954 and the Energy Reorganization Act of 1974.

Ports and Waterways Safety Act

The Ports and Waterways Safety Act of 1972 (P.L. 92-340) subjects vessels carrying hazardous materials (as defined by the Water Pollution Control Act and Amendments: to controls established by the Coast Guard

within U.S. ports. Handling and loading of hazardous materials are also discussed in the Act.[25] These parameters will affect the establishment of procedures for the transfer of packaged nuclear waste from land to sea transportation systems in port areas.

The Deepwater Port Act

The Deepwater Port Act of 1974 (P.L. 93-627) provides for regulation of the construction and operation of such facilities off the coasts of the U.S. Primarily considered as oil tanker way stations, they may feasibly play a role in nuclear waste transportation system. Section 18 of the Act sets a precedent for assessing charges against private entities with respect to government accident response activities. A Deepwater Port Liability Fund is set up to compensate shoreline property owners in case of accidents at deepwater port facilities. The Fund, patterned after the Alaskan Pipeline Liabilities Fund, may serve as a precedent for establishment of such a fund related to activities involved in the subseabed project.

Port and Tanker Safety Act of 1978 and Act to Prevent Pollution from Ships of 1980

The Port and Tanker Safety Act of 1978 (P.L. 95-474) and the Act to Prevent Pollution from Ships of 1980 (P.L. 96-478) are this country's implementation of the 1978 Marpol Protocol, developed from the unratified International Convention for the Prevention of Pollution from Ships (1973).[26] The 1980 Act implements Annexes I and II of the convention, which deal with the prevention of pollution by oil and noxious liquid substances. The three optional Annexes, dealing with pollution from packaged substances, are not implemented.[27] These would most likely need to be implemented under amendment to the legislation, or in new legislation. Since radioactive materials are regulated as packaged forms,[28] they would be covered by Annex III to the Convention, and therefore are not discussed in the 1980 Act.

Intervention on the High Seas Act and Amendments

A final piece of environmental legislation which may impact a Subseabed Disposal Program is the 1978 Amendment to the Intervention on the High Seas Act (P.L. 95-302) which extends 'intervention' to substances other than oil.[29] The original 1974 Act (P.L. 93-248) implemented the International Convention Relating to Intervention on the High Seas (1969: Brussels).[30] It delegates responsibility to the U.S. Coast Guard to intervene in case of accidents involving oil or other hazardous substances on the high seas.

Other U.S. Regulations for Transport

All packages of high-level waste (HLW) passing through a U.S. port must be in compliance with the applicable regulations of the U.S. Coast Guard (46 CFR 146), the Department of Transportation (49 CFR 173 & 176), and the Nuclear Regulatory Commission (10 CFR 71).

The U.S. Coast Guard regulations (46 CFR 146) specify marking and labeling reguirements, handling and stowage procedures, personnel identification, and segregation of irradiated wastes. The purpose of these regulations is to make more effective the provisions of the 1960 International Convention for the safety of Life at Sea.

The Department of Transportation's regulation 49 CFR 173 is concerned with the packaging and preparation for transport requirements. In addition, 49 CFR 176 is concerned with regulations for carriage by vessel. These regulations specify operating requirements, general handling and stowage procedures, segration requirements, and procedures for contamination control.

The Nuclear Regulatory Commission's regulations 10 CFR 71 is concerned with the packaging of radioactive material for transport and the transportation of radioactive material. These regulations specify the necessary licenses, package standards, and operating procedures for the transport of radioactive materials.

In addition to compliance with all Federal regulations, the shipper or carrier will need to comply with local and "state agencies, EPA offices, Port Authorities and Corps of Engineers additional requirements, and obtain any related licenses, permits, or approvals required for the planned operations." [31]

Analogous Situations

LNG Facility Siting

Liquified natural gas (LNG) is natural gas cooled to -259^{o} Fahrenheit. The liquid takes up 1/600th the volume of the gas facilitating storage and shipment. However, this reduction in volume also increases its explosive properties. The average LNG tanker has the explosive potential of 50 times that of the atomic bomb dropped on Hiroshima. Both LNG tankers and LNG terminal sites pose catastrophic possibilities if an explosion was to occur near a populated area. The need to strictly regulate the handling, storage, and transport of LNG is obvious.[32]

The problems encountered in trying to site an LNG facility can be enormous. For nearly ten years, utility companies in California have been trying to site an LNG terminal along the California coast. An accumulation of well-intentioned regulations designed to protect public health and safety, as well as the environment make it difficult to site the LNG facility. The state of California even attempted to circumvent its own

facility siting, coastal protection, and environmental impact assessment laws and to preempt local regulatory authority and still failed to site a facility despite predictions of commercial and industrial dislocations causing dramatic increases in unemployment. This attempt to preempt normal procedures only tended to stimulate suspicion, ill will, and law suits against the siting of the facility.

Similarly, port siting of a nuclear waste transport facility may prove to be one of the more difficult issues to resolve in a subseabed program. In part, the difficulties may hinge on three factors:

(1) Will it be a military or public site?

(2) Will it be one of several ports, or a single port which processes all the wastes?

(3) Will the ports serve as away-from-reactor storage sites as well as transfer points for disposal operations?

To a large extent, these issues will have to be settled by the public via lengthy environmental reviews. Not only scientists and engineers, but also an active public needs to calculate the dangers inherent in a nuclear waste transport facility, especially the risks of an accident. Port siting of a transport facility will inevitably be difficult. But if anything is to be learned from the LNG facility siting experience, attempts to preempt normal siting procedures will inevitably exacerbate the inherent problems.

Thought might be given to the choice of a military port rather than a public port. Military ports are often more remote from adjacent population centers and have security systems in place which might be sufficient for subseabed needs. Public acceptance might be more readily obtainable if the port were sited where it would interfere least with their daily lives.

The number of ports to be developed will depend somewhat on the level of participation in a subseabed program. For example, if several European countries decide to participate, installation of one "central" port facility might suffice, although inducing one country to accept the wastes of the others may not be easy. The French may be more willing than others to set up such a port. The French nuclear program seems to have a strong government backing and sizeable public support, factors which have been sufficient to propel their program beyond that of other countries.

The potential interest of a single country (such as an LDC) to provide a port facility on a fee for service basis for economic benefit is also possible. This may be practical if the country is located near the emplacement site. The port would serve as the collection point where wastes would be prepared for emplacement. It would be augmented by a series of intermediate storage ports distributed among the participating countries which would serve as "temporary" collection sites for wastes

prior to shipment to the central facility. Financially, these intermediate ports could serve to ease high shipping costs by reducing port stops. The advantage to this system might be that the "temporary" nature assigned to the other ports would ease public disapproval of their operation, eliminating one of the barriers to subseabed implementation.

The third point of controversy may arise from an intent to use a port for an AFR facility, as well as for a transfer point for wastes. This would increase the inventories of wastes present at the port site, which may result in intensified public resistance to its presence. Also, if increased land area is necessary to accommodate the greater volumes of waste, the number of potential adequately-sized port sites may diminish.

The Deep Seabed Hard Minerals Resources Act

The controversial Deep Seabed Hard Mineral Resources Act of 1980 (P.L. 96-283) is the only piece of U.S. legislation directing the use of the seabed. It provides a regulatory framework for allocation of access to the minerals of the deep seabed and provides environmental protection provisions. The Act establishes the United States policy that seabed mining is a freedom of the high seas.

This unilateral action on the part of the United States was not well received by other nations participating in the Law of the Sea negotiations. The only other nations which have legislation currently in force regarding the right to seabed resources are West Germany and Japan. However, France also has national legislation pending.

Unilateral actions such as those reflected in the Deep Seabed Minerals Act and in the recent U.S. slow down of negotiations at the U.N. Conference, may impede progress towards an international agreement which may be necessary to implement subseabed disposal.

Yet, the implementation of this domestic legislation sets a framework for many aspects of a Subseabed Program and may eliminate many of the obstacles.

Policies and Trends

Some further observations of policies and trends worth noting which could affect the Subseabed Program: EPA/NOAA monitoring program of low-level waste. The Office of Radiation Programs of the EPA recently released information concerning the NOAA/EPA program monitoring the impact of dumping LLW in the marine environment off U.S. waters from 1946 to 1970. It may have a disquieting effect due to some of the alarming results, and may hinder any attempts to isolate high or low level radioactive wastes in the marine environment.

On the other hand, the collection of this data further aids in scientific and environmental understanding of the use of waters for disposal of radioactive waste.

Trends Away From Focus on Environmental Protection

The emphasis on deregulation in the current Reagan Administration brings to the surface several factors which could ultimately affect the Subseabed Program.

--With deregulation goes the power and priority of many energy and environmental programs and their supervisory agencies/departments.

For example, the organization plan of the Administration for the Executive Branch includes abolishing the Department of Energy under which the Subseabed Program and, more generally, waste disposal programs currently lie. If that occurs, what happens to these programs? At worst, they wither away; at best, they go to other departments. In the first case, although amendments to legislation have been proposed to sustain the Subseabed Program as a viable option, there are not financial guarantees for the program as waste disposal becomes a low priority item. In the other case, if the department responsible for waste disposal programs changes, the bureaucratic and committee oversight of Congress change for it and the political leverage achieved over time is likely to become undermined. In competition with other programs in the same situation, i.e., land disposal, a strong competitor, could push the Subseabed Program to such low priority that it can't survive.

The EPA, the other agency responsible for administering the MPRSA and the regulator of NEPA, which would require an EIS is changing so rapidly, it is difficult to assess its impact on attempts to proceed with a Subseabed Program, if the Subseabed Program were to rely on the MPRSA or NEPA for its strength. It might be much easier under the potential relaxation of the laws for pollution (although NRC could be a balancer) but on the other hand, might be difficult to get EPA attention and assistance, if this is not a priority item.

Recent Administration statements in Congressional testimony have indicated clear signals favoring an emphasis on nuclear energy. This could indicate emphasis on all waste disposal programs. However, the deemphasis on environmental consideration in general could, on balance, be detrimental to any rapid progress in a Subseabed Program. And, in November 1981 official Administration policy was to emphasize land disposal options at the expense of all others.

The rapid proliferation of Marine environmental legislation during the 70s and the recent reflections on their necessity and possible endurance make the conclusions of a study by the Department of Commerce, released in 1978, quite relevant. The following issues remain outstanding and there is need for their resolution.

(1) The nature of long-term Federal policy toward the disposal of chemical, municipal, nuclear, and other potentially hazardous wastes in ocean waters.

(2) "Need for a comprehensive Federal policy, and the appropriate Federal role, in dealing with hazardous materials...in the marine environment."

(3) "Need for a Federal policy on comprehenisve liability and compensation for damage from spills of hazardous materials.[35]

Without resolution of these issues, the status of the Subseabed Program from year to year will remain uncertain and possibly the U.S. ability to retain control over the international aspects will decline.

One might draw some analogies to seabed mining here. For, in the 1960s and early 1970s the U.S. was the undisputed technological leader for this industry. The lack of U.S. government initiative or even consistent policy toward the deepsea mining program inhibited U.S. industrial progress in all but one corporation which was able to proceed for other reasons. However, French German and Japanese industries, subsidized and encouraged by their governments, proceeded unhindered and in some instances have surpassed U.S. know how in this area once dominated by U.S. expertise. The lack of consistent U.S. policies on this program had very damaging effects on the U.S. participation in this program. Such wavering at a critical time for a Subseabed Program could have the same results.*

*See Addenda III, at end of Task XII, titled Conference Handouts for a comprehensive and further elaboration of the relevant Federal Executive agencies and Legislative committees which have an interest in nuclear waste disposal.

FOOTNOTES: TASK II

1. Atomic Energy Act of 1954.

2. The United States has been accused of "benign neglect" in the management of both low- and high-level radioactive wastes. A Nuclear Waste Primer, League of Women Voters, 1980, p. 26.

3. Energy Reorganization Act of 1974, P.L.93-438, section 202, (3) and (4).

4. Roger Kasperson, The Dark Side of the Radioactive Waste Problem, p. 15.

5. S.2189, The Nuclear Waste Policy Act (Senate Energy and Natural Resources Committee).

6. Legislative History of P.L.96-573 as reported in the U.S. Congressional and Administrative News, 1970-present.

7. Ibid.

8. Nucleonics Week, 8 January, 19 January, 22 January 1981.

9. Nuclear Non-Proliferation Act of 1978, P.L.95-242.

10. Ibid., section 104 (a).

11. Ibid., section 2.

12. Ibid., section 104 (d).

13. New York Times, 17 June 1981.

14. Congressional Record (Senate), 30 July 1980.

15. National Environmental Policy Act of 1969, P.L.91-190.

16. Memorandum to Heads of Agencies on Applying the E.I.S. Requirement to Environmental Impacts Abroad, Council on Environmental Quality, 24 September 1976.

17. Hearings on Nuclear Waste Disposal Before the Subcommittee on Oceanography of the House Committee on Merchant Marine and Fisheries, 95th Congress, Second Session, p. 248-249.

18. Marine Protection Research and Sanctuaries Act, P.L.92-532, Title I, section 101 (a).

19. Ibid., Title I: Definitions.

20. Amendment to MPRSA, 1980, P.L. 96-572, section 2 (b):1.

21. Federal Water Pollution Control Act Amendments of 1942, P.L.92-500, section 301.

22. Coastal Zone Management Act, P.L.92-583.

23. Federal Environmental Law. Dolgin & Gilbert, eds. (St. Paul: West Publishing Co., 1974), p. 1051.

24. Transportation Safety Act of 1974, P.L.93-633, Title I (Also called "The Hazardous Materials Transportation Act").

25. Ports and Waterways Safety Act of 1972, P.L.92-340.

26. House Report No. 96-1224, Merchant Marine and Fisheries Committee, 18 August 1980, p. 2.

27. Ibid., p. 8.

28. Federal Environmental Law, Dolgin & Guilbert, p. 1051, and IMCO Regulations on Maritime and Transport of Nuclear Materials.

29. House Report No. 96-1224, Merchant Marine and Fisheries Committee, 18 August 1980, p. 8.

30. Intervention on the High Seas Act, P.L.93-248.

31. From an Allied General Nuclear Services memo dated 31 July 1980, on the American National Standard Proposed Guide for Water Transportation of Irradiated Nuclear Fuel, Obtober 1976.

32. Lawrence E. Susskind and Stephen R. Cassella, The Dangers of Preempted Legislation: The Case of LNG Facility Siting in California (1980).

33. "House Report No. 96-41, Part II,"August 1980, p. 43, as reprinted in U.S. Code and Administrative News, 96th Congress, p. 3077.

34. Lee, Kimball, "Implications of the Arrangements Made for Deepsea Mining for Other Joint Exploitations," The Columbia Journal of World Business, Winter 1980, p. 58.

35. U.S. Ocean Policy in the 1970's: Status and Issues (Policy Overview), U.S. Department of Commerce, October 1978, p. 34.

TASK III: Assess Major U.S. Foreign Policies and Accompanying On-going Activities as They May Relate to the Continuance of the Subseabed Disposal Research Program and As They Might Relate to the Feasibility of Deploying a Subseabed Disposal System.

TASK IV: Establish Which U.S. Foreign Policies Might Conflict With Domestic Policies Relevant to the Subseabed Disposal Assessment Program

TASK V: Identify International Conditions Which Might Affect the Establishment of a Management System for Implementing Subseabed Disposal of High Level Nuclear Waste

TASKS III, IV, V.

Foreign Policy Considerations

During the past decade, the U.S. position in the changing world political and economic order has undergone dramatic transition. Its hegemonous political, economic, and technological leadership of the 1950s has evolved into one of cooperative leadership in international affairs with a strong commitment to international law and international cooperation. In the past five years of the UN Conference on the Law of the Sea, there has been further diminishment of U.S. initiatives and more responsiveness to the demands of other nations, particularly disadvantaged or Third World nations. These foreign policy trends reflect how U.S. leaders perceived the changing international environment and sought to integrate new nations into an effective international order, not only on U.S. terms but on the terms of those nations which believed that the current system was inequitable. In this process, "equity" became a major demand within international affairs: an attempt to rectify the inequities of the past.

A reasonable guess for the future course of the SDP, based upon foreign policies of the last decade, would take it further along this global route, an extension of the sort of negotiating position developed in the establishment of the Seabed Regime within the UN. This would be the logical next step in solidifying management of the international waters proclaimed to be part of the Heritage of Mankind.

The UNCLOS negotiations for the Seabed Regime can be viewed from another perspective as well. The negotiations could have been limited to those nations affected directly by the mining of the seabed: the net consumers, those advanced industrial nations with a need for access to the supplies; and the net suppliers, those nations which were the principal suppliers of the materials to be mined from the seafloor--these latter because their markets might be interrupted and their economies might experience dislocations. But many of the supplier nations were also disadvantaged nations without much political or economic leverage against the major industrialized nations. The negotiations would have been tilted against them. These weaker supplier nations insisted on bringing in their disadvantaged nation-partners--adding to their strength in a series of negotiating sessions that came to consider many other matters important to the industrialized world, and giving the less advantaged nations, supplier and non-supplier, far more negotiating strength than ever before. Thus, the results of the Seabed Mining Regime negotiations were far more favorable for the lesser developed nations than they might have been in a context limited to consumers and suppliers.

Why would the United States and other industrialized nations agree to rules and procedures that would seem so clearly to work to their disadvantage?

There were two underlying reasons for this. One concerns the gradual growth of technological capability in other nations; the other, awareness of a growing interdependence among all nations.

Technology Dispersion

U.S. leadership in technology, which had been the bulwark of much of its power for several decades, was being shared. When there was only one place to go for technology, the U.S. bargaining position in international relations was very strong. But when the West Germans, the Japanese, the French and others began to challenge the unilateral strength of the U.S. leadership in technology, nations who wanted to obtain technology had a marketplace to go to and several vendors from which to choose. This change had major implications for the latitude of U.S. force and initiative, compelling the U.S. to negotiate in many forums in a cooperative way.

In seabed mining, for example, the U.S. lead in underwater technology held only for a short time before the West Germans, French and Japanese provided a viable challenge. The U.S. had no choice but to act in cooperation with those nations and their diverse interests, a contrast to U.S. behavior during INTELSAT negotiations, when it alone held the technology. In the case of subseabed disposal of high-level nuclear wastes, those nations with capabilities in underwater technology--from military and deepsea mining experience--also force the U.S. to cooperate. The U.S. cannot proceed unilaterally with the assurance of the past that it alone could do so, but must consider either reciprocal arrangements or an international framework which meets the demands of other nations that hold the technology.

Interdependence

Another factor which emerged in the past decade with great constraining force upon the United States is the interdependence among nations. Not only is the U.S. dependent upon its traditional allies for supplies and support, but it receives much of its strategic raw materials from Third World nations. The OPEC embargo of 1974 was a highly visible part of a growing realization that the U.S. could not ignore or alienate such nations as Zaire and Gabon that supply almost solely several of the strategic materials most necessary to keep our economy and military establishment going. To decide to carry out multilateral negotiations for a subseabed disposal system limited to users would cause some of the nations upon whom the U.S. relies for certain strategic materials to protest their right to participate in the process and help dictate the result. Agreement upon the IMCO/IAEA framework for disposal of low-level wastes might not now be possible to achieve without consideration of second or third order effects from nations who were not parties to those negotiations. but who might demand a voice today. The complete nuclear fuel cycle is one of the most intricate examples of interdependence that exists. The "back end" of that cycle--disposal--may prove difficult to negotiate if balance in interdependencies

can't be achieved.

The Example of INTELSAT

During the decade of the sixties, when the United States sought to exploit the use of another technological achievement, communications satellites, the INTELSAT negotiations reflected a far different perception of the U.S. role in international affairs and far greater initiative from the U.S. In that case, the U.S. entered negotiations under a set of circumstances similar in some respects to the case of subseabed disposal: a lead in the technology, the desire to use the technology and the desire to share some of the benefits with the rest of the world--and with the U.S., having made the R&D investment, getting its fair share. In the case of INTELSAT, the U.S. ran into far more problems with their sought-after European partners than anticipated. The Europeans insisted that the U.S. allow them more of a share of the benefits from the technology than merely using the communications services for a fee. They wanted to gain the know-how. They wanted to participate in the production of the system as a means to modernize their industries. And they wanted to have more to say about the operations than the U.S. was originally willing to allow. The developing nations were on the periphery of these negotiations in the beginning because the technology did not interest them at the time, and since there were far fewer developing nations able to exert their political influence. The result of the INTELSAT negotiations was a viable international organization in which power was phased from other nations. In 1964, the agreement permitted the U.S. essentially to guide the operations, allowing the technology to develop efficently to culmination without political interference. However, the Europeans got a specified percentage of the R&D contracts and a promise to renegotiate in five years, at which time more of an international partnership was to be established for the operations of the organization. The concessions reflected a decisive and cooperative spirit of initiative on the part of the U.S., which wanted to assure that its costly R&D efforts came to fruition.

The U.S. came to the negotiations with proven technologies, and with a negotiating team based on an experimental public/private corporation composed primarily of the communications industry and the U.S. government --Comsat. While this partnership was far from perfect--the industry dominated the negotiations due to the need to understand the technology and the State Department lacked technical competence--Comsat brought a very strong and unified voice to the negotiations. Comsat's objective was clear: to launch a communications satellite which would become a key part of global network of communications and support it by means of user fees. The allocation of the radio frequency spectrum for INTELSAT demonstrates the sharing of an international resource, an example that can be compared with use of the seabed for mining and the subseabed for disposal. Certainly, much can be learned from assessing both the process and the substance of the INTELSAT negotiations, as well as the international climate in which they took place.

Policy by Default

With these two examples of international organizational structures for handling major technological programs--INTELSAT and the International Seabed Regime--it must be asked why two such different structures resulted to utilize common property resources. Was it differences in technology and what the technology required? Was it a difference in international conditions? Would it have been possible to construct an INTELSAT-like organization to mine the seabed? And is it still possible to use that same model for the SDP?

As a possible precursor to a SDP, the NEA Working Group might be viewed as a core for international negotiations aimed at forming a management structure; that is, the group of nations that want and need a disposal system for high level waste (HLW). If the INTELSAT model is relevant--a limited multilateral organization of those with vested interests in the outcome, instead of a Seabed Regime of global scope including those without direct interest in the outcome--then it is necessary to examine what is missing and what might be consistent with current foreign policies of the United States. It is also necessary to consider if such an approach would be in line with current international conditions, which, under the new "Heritage of Mankind" concept, may already have bypassed that possibility and precluded any restrictive attempts to use international waters.

From the U.S. perspective, what is apparently missing is any organized body--public or private--to devise a workable waste disposal program and then to negotiate its implementation on an international scale. Because of the internal fragmentation of radioactive waste disposal responsibilities among agencies,[1] it is difficult to discern any program or governmental group with uniform objectives that can implement a program, nationally or internationally. Currently, diverse groups of scientists, policy makers and others work informally at an international level without formal direction and without uniform objectives. It appears that U.S. governmental policies regarding waste disposal, non-proliferation and international trade in nuclear power facilities are without coordination. The NRC, which has cognizance over final licensing, has evidenced much confusion over dealing with at least three completely separated sets of policies.

A business partnership among the utilities industry, the producers of the equipment, the Federal government and a segment of the public, formed under Congressional mandate as was done in the case of Comsat, might begin to establish a consistent set of policies to meet the multiple needs of the United States. Then, with a strong, integrated body of those most heavily involved in this process, the United States would have a forceful negotiating arm with a clear idea of how to proceed, which could then assert some leadership in the international arena regarding either

the internationalization of the fuel cycle, or, at the least, a cooperative program of waste disposal to meet standards for non-proliferation. Current policy is evolving from a number of separate ad hoc actions by unofficial groups, with industry proceeding in its own direction until obstructed; with scientists and technicians participating in international discussions without responsibility or accountability to the policy/decision makers who answer to the President and the Congress; with only sketchy media reports to formulate public and official perceptions. As an interim measure, this format may be necessary during the period in which an organized effort gets underway, but certainly such a method cannot be expected to substitute for a strongly organized, federally endorsed partnership of visible, accountable persons authorized by law to negotiate for the United States, particularly in such serious matters as radioactive waste disposal and non-proliferation policies. But there seems to be no apparent organized effort underway to move away from this unaccountable course of disconnected activities that threaten to establish global policies through default.

Policies of the '80s

The policies of the '60s that created INTELSAT were replaced with the foreign policies of the '70s, which are creating the Seabed Regime. The question is: What are the policies of the current Administration? Are they a return to the '60s, creating a national framework for attempting a major public/private partnership? Are they similar to the '70s, under which global negotiations will be inevitable? Or are they different from both, dictating that industry take responsibility itself, removing the government from the scene? It appears unlikely that the various interested publics in the United States and abroad would stand by and allow the private sector to dictate policies regulating something as dangerous as radioactive wastes.

The NEA process, then, appears to be a viable first step--although without an official negotiating arm to carry out a consistent set of policies toward a set of objectives, the U.S. effort will remain weak. The U.S. position regarding the SDP should be part of an array of U.S. policies regarding the entire nuclear fuel cycle--nuclear power, non-proliferation and waste disposal. Even if the U.S. chooses to use only its own land-based sites for HLW disposal, the international aspects of the remainder of the problem cannot be ignored and must be part of any waste disposal decisions. At this time, it is not apparent that they are.

Whether the U.S. decides to act unilaterally, multilaterally or globally in the case of a Subseabed Disposal Program, if it chooses to participate at all, will depend upon the degree of control and leadership it perceives for itself in the nuclear arena. Isolationist policies might dictate a unilateral mode. Attempts to strengthen the position of the industrialized group of nations might dictate a limited multilateral user approach open to others. Or, attempts to strengthen international efforts and international law, as opposed to coalition building, as well

as an overriding fear of reprisals from outside nations, might dictate a global effort.

Foreign Policies Toward the Pacific

If Pacific Ocean sites turn out to be the best for disposal, accommodation between those who want to use them and those who live in the Pacific region will have to be reached. Currently, many of the Pacific islands have attained independence and are strongly asserting sovereignty, especially in relationships with their former colonial sponsors. The Japanese have actively sought strong economic ties with many of these island nations and have established firm economic footholds in the Pacific region. The United States, on the other hand, has spent the past two decades focusing on the Far East, Middle East and the European nations. With the emergence of independence, military bases, among other things which have been taken for granted for so long, are at risk, and must be renegotiated under far different circumstances than they were originally. The price for renewal of the bases appears higher than the U.S. has thus far offered to pay, in foreign assistance and through other means. Since the islands are of strategic importance, the U.S. is not in a position to make strong demands for things other than the bases from the Pacific islanders. Unless subseabed disposal is assigned top priority in U.S. foreign and domestic policies, it seems doubtful the U.S. will do much to endanger its already fragile relationships within this area. The Japanese have similar difficulties with these islands, as evidenced by their backing off in the face of the outcry from the peoples of these islands from a plan to dispose of low-level wastes in the Pacific under international standards agreed to under the IMCO treaty. If the Japanese and neighboring Taiwan and Korea can arrange to transfer their wastes to their European suppliers for disposal, they might be willing to pay an extra high price for that service as a trade-off for better relationships in the Pacific.

Foreign Policy Toward Business

U.S. foreign policies toward industry appear to be somewhat in conflict with U.S. domestic policies regarding nuclear power and nuclear waste. While U.S. industry contracts with other nations and promises to take back their wastes, and U.S. utilities lope along waiting for licensing decisions from the NRC, domestic policy makers struggle to accommodate public concerns about what to do with overflowing interim waste storage areas.

Domestic outcries to stop emplacement of radioactive waste on land near, or downstream from, population centers, fall in large contrast to industry attempts to promise their customers that the U.S. government will acquire major additions for already bulging storage areas, and that the wastes will ultimately be placed in repositories that the public is currently opposing. How can the U.S. government allow waste generated by others to be stored on U.S. territory, threatening the health and safety of U.S. citizens, when domestically there is major opposition to isolating wastes

generated within the U.S. in that way? Perhaps the SDP provides an avenue for resolution of this inconsistency between domestic and international conditions and policies.

U.S. Foreign Policies Toward Non-Proliferation

Policies of non-proliferation have varied with Administrations over the past decade. While it is not yet clear what the policies of the current Administration will be, there appears to be a definite shift toward handling each case on an individual basis and weighing its merits, as opposed to a blanket policy for all nations.[2] Certain key areas of this policy directly affect the subseabed program. If recent statements of the Secretary of Energy, James Edwards, are correct, almost any nation can use spent fuel rods for warheads on missiles, provided they have missile technologies. If this is the case, a decision to sell nuclear power plants abroad is a decision to allow proliferation of nuclear weapons, unless under very strict controls.

Another problem involves the degree to which the U.S. will adhere to current international agreements regarding non-proliferation, specifically whether the U.S. will sell fuel to nations that do not abide by IAEA guides and requirements. All of this bears upon whether the U.S. and other industrial nations will unendingly supply nuclear power to nations that seek to build economies based on nuclear energy. Ultimately, it bears upon how much radioactive waste will need to be disposed of.

U.S. Policies and Middle East Energy Supplies

The Middle East situation will also dictate energy uses throughout the world for as long as it remains unstable. Those nations unable to withstand unreliability of access to Middle East sources of energy are forced to seek alternatives, and nuclear is the only one with assured results at this time. Therefore, the industrial growth of many new nations, their need for additional energy sources and their inability to afford the unabated rise in petroleum prices will increase pressures on more new nations to turn to, or increase their capacity for, nuclear power. This trend is exacerbated by the use of petroleum as a foreign policy weapon. Taken along with similar circumstances in industrialized nations, this could increase not only the total amounts of nuclear wastes to be isolated, but also increase the amounts generated in areas without any land disposal options and without the capital necessary to launch a disposal program. This has the potential for creating a situation in which the industrialized nations will have to agree to dispose of the wastes in order to sell power plants. The lack of a disposal option will either limit the sales of nuclear power plants or will force the international community to come up with a viable international disposal option. A SDP would be a likely candidate, if scientific evidence is promising.

Those nations unable to build another power plant until a disposal option is found may be blazing a path for others, whether by helping to stifle nuclear power development or compelling a waste disposal solution.

Clearly, this one option could lead to subseabed disposal; the stifling of nuclear power development would make subseabed disposal less urgent and less desirable to a range of nations that might have needed a disposal site were there nuclear expansion.

International Environmental Considerations and Policies

U.S. policies for protecting the international ocean environment have been stronger than most other nations until recently. The U.S. stopped dumping low-level wastes in 1970 and has closely monitored where others have dumped ever since, although other nations dump according to IMCO regulations.

The U.S. passed one of the strictest coastal environmental acts of all nations when it passed the Tanker Safety Act in 1978.

The United States, after IMCO established regulations for incineration at sea, endorsed incineration at sea, and is moving to build its own incinerator vessel. Regulations in the U.S. Executive Branch are under review to enable a smooth implementation of this program through the Maritime Administration.

U.S. special legislation for seabed minerals development includes sections for environmental protection, and the Environmental Protection Agency recently added international EIS requirements to make sure that the U.S. environmental regulations were carried out beyond U.S. jurisdiction.

All of these factors indicate that if the U.S. participates in a SDP, the conditions would be based on conservative estimates of environmental needs.

The only possible change--which could turn out to be a major one--is if the short-term trends of the current U.S. Administration were to establish long-term consequences for policy. Then, in the event the Subseabed Disposal Program becomes essential for the nuclear industry to continue, under Administration policy that favors such an option, SDP environmental concerns might be subordinated for expediency.

FOOTNOTES: TASKS III, IV, V

1. Jackie L. Burns, "Institutional Issues in the Planning and Implementation of a Program to Dispose of High-Level Radioactive Wastes," Rand Corporation. Note: Prepared for the U.S. Department of Energy (N-1650-DOE), February 1981; and Dorothy S. Zinberg and David Deese, "Radioactive Waste Management: A Comparative Study of National Decision-Making Processes," Harvard University, Cambridge, Mass. Prepared for the U.S. Energy Research and Development Administration, Final Report, January 25, 1979.

2. Stephanie Cork, Nuclear Fuel, May 1981, p. 8.

TASK VI:

Identify Existing International Organizations, Groups, Treaties, Regulations, etc., Which Could Have Some Influence Over or Be Influenced by the Deployment of a Subseabed Disposal Program.

PART I: INTERNATIONAL TREATIES AND REGULATIONS

Stockholm Convention:

The Declaration on the Human Environment which resulted from a United Nations Conference on the Human Environment at Stockholm in June 1972 is a documentation of the principles underlying the environmental movement of the late 1960s and early 1970s. It has been called "...a landmark effort to achieve world-wide consensus on how to deal with...preserving the earth's environment."[1] It was the precursor and inspiration for the flood of marine and other pollution legislation following 1972, and as such is worth considering here. Most notable is the call for international cooperation for the betterment of the human environment.[2] The marine pollution recommendations call for nations to implement conventions on marine pollution to ensure the control of ocean dumping.

Principle number 1 states that man has the responsibility to "protect and improve the environment for present and future generations." This concept of man's responsibility for future generations should influence any disposal concept for long-lived radioactive wastes.

The legal framework in which subseabed disposal must work, and the decisions of nations considering it are influenced by the concepts contained in the Stockholm Declaration. Deese, et al have stated that the international climate surrounding environmental practices has changed since the early 1970s and therefore that pollution is not seen as a primary consideration in state decisions.[3] Another point of view is, however, that protection of the marine environment retains its stronghold as an influence in national decision-making processes, having been institutionalized over the past decade through the national and international conventions which follow, as well as through legislation at national levels. It is beyond the scope and expertise of the authors of this paper to offer a legal opinion. We can but document the legal parameters.

The London Dumping Convention:

The London Dumping Convention of December 29, 1972 raises two issues which need to be addressed regarding subseabed emplacement of nuclear wastes. As discussed by Deese,[4] at issue are the interpretation of "dumping" and the nature of the waste to be emplaced as defined in the Convention.

The Dumping Issue

Article III: Section (1)

a) '"Dumping" means:

(i) any deliberate disposal at sea of wastes or other matter from vessels, aircraft, platforms or other man-made structures at sea;

(ii) any deliberate disposal at sea of vessels, aircraft, platform or other man-made structures at sea;

b) "Dumping" does not include:

(i) the disposal at sea of wastes or other matter incidental to, or derived from the normal operations of ships...

(ii) placement of matter for a purpose other than the mere disposal thereof, provided that such emplacement is not contrary to the aims of this convention.'

Annexes to the Convention list substances under consideration: High-level radioactive wastes are listed in Annex I: prohibited substances.[5]

The Nature of the Waste:

"Annex I: (6) High-level radioactive wastes or other high-level radioactive matter, defined on public health, biological or other grounds by the competent international body in this field, at present the International Atomic Energy Agency, as unsuitable for dumping at sea."[6]

This may or may not leave room for IAEA interpretation of 'suitability' for 'dumping' on a case-by-case basis.

Annex II lists those substances which require special controls and permits before 'dumping' is permissible.[7]

"Annex II: (d) Radioactive wastes or other radioactive matter not included in Annex I."[8] Again, in combination with Annex I, Section 6, there may be room for IAEA interpretation.

Should subseabed emplacement of radioactive substances as proposed by the subseabed program be considered 'dumping' as defined in Article III, Section (1) a), or should the concept be viewed in the light of Article III, Section (1) b) as "placement for a purpose other than the mere disposal thereof..."? Therein lies the conflict.

Legal opinions vary. The IAEA has indicated that the Convention does not prohibit seabed disposal, and this is the prevailing international attitude. The U.S. State Department holds the opinion that subseabed waste emplacement is dumping as defined under the convention.[9]

The Marpol Convention and Protocol

Another treaty related in concept to the London Convention is the International Convention for the Prevention of Pollution from Ships (1973.)[10]

Its purpose was:

"...to achieve the complete elimination of intentional pollution of the marine environment by oil and other harmful substances..."[11]

"...in order to prevent...pollution...by the discharge of harmful substances or effluents..."[12] The argument here is that the subseabed waste emplacement is not intentional marine pollution, and that efforts to insure nuclide containment indicate the desire to avoid such pollution by the activity in question.

"Discharge" is defined as:

"a) ...any release howsoever caused from a ship and includes any escape, disposal, spilling, leaking, dumping, emitting or emptying.

b) Discharge does not include:

(i) dumping within the meaning of the Convention on the Prevention of Marine Pollution by Dumping of Wastes and other matter..." (London Dumping Convention).[13]

This reference back to the London Convention yields the controversies discussed earlier related to the interpretation of "dumping" and waste form suitability.

Five Annexes follow the Convention, each consisting of regulations on some aspect of maritime carriage of toxic substances. Optional Annex III, "Regulations for the Protection of Pollution by Harmful Substances Carried by Sea in Packaged Forms or in Freight Containers, Portable Tanks or Road and Rail Tank Wagons" seems the most applicable to our consideration. (See Addenda I in this section)

The Oslo Convention

The Convention for the Prevention of Marine Pollution by Dumping from Ships and Aircraft done at Oslo, Norway on February 15, 1972 may also need to be considered in planning a management scheme for subseabed waste emplacement. It represents the first multilateral agreement in the field of prevention of marine pollution by dumping and served as a model for the development of the London Convention.[14]

Radioactive materials are not expressly prohibited under Annex I. They may possibly be included in "...other persistent synthetic materials which may float or remain in suspension in the sea..." 15

Article 19 defines "dumping":

"...any deliberate disposal of substances and material by or from ships or aircraft other than:

a) any discharge incidental to...normal operation...

b) the placing of substances and materials for a purpose other than the mere disposal thereof, if not contrary to the aims of this Convention."[16]

The London Dumping Convention Article III, Section (i): b) directly paraphrases this and implies the same set of uncertainties.

A Commission is established of representatives of each of the contracting parties to be consulted by a contracting party having decided that an Annex I substance "cannot be disposed of on land without unacceptable danger or damage..."[17]

Unilateral action by states party to the Oslo Convention relating to subseabed waste emplacement may come under the consideration of this Commission.

The SOLAS Convention

Although the International Convention on the Safety of Life at Sea (SOLAS) 6/17/60) does not directly refer to protection of the marine environment, it should be mentioned here. Some subsequent conventions on marine pollution have been based on its provisions on the carriage of dangerous goods. SOLAS also contains special provisions on the safety of nuclear ships.[18]

Chapter VII of SOLAS contains regulations on carriage of dangerous goods divided into classes. Radioactive materials are listed under Class 7. The regulations relate to packing, labelling and stowage of dangerous goods. The Convention also empowers the Inter-Governmental Maritime Consultive Organization (IMCO) to establish shipping routes for the purpose of separation of traffic. Presumably, if a subseabed nuclear waste disposal were implemented, IMCO would establish routing for vessels transporting nuclear waste to the disposal sites.

Marpol Protocol

The IMCO Safety Committee has prepared our international maritime dangerous goods code which contains detailed provisions on Class 7 materials carriage. The code is based on the safety standards from the IAEA transport regulations. [19]

The Tanker Safety and Pollution Prevention Conference, held in London in February 1978 produced two treaties, one of which was the previously mentioned 1978 Marpol Protocol, and also a Protocol of 1978 Relating to the International Convention for the Safety of Life at Sea (SOLAS Protocol). Stricter requirements on the safety of vessels were established within the treaty.[20]

International treaties relating to nuclear power, nuclear weapons, nuclear ships and maritime carriage of nuclear materials may affect the perceptions of governments toward a subseabed disposal option for radioactive waste isolation.

Nuclear energy and nuclear weaponry have been associated in the public's minds since the earliest days of power generation from fissile materials.[21] Within the context of the types of waste to be emplaced, questions concerning non-proliferation may arise not only in the public sector but at the international legal level. As suggested by Lester and Willrich:

"...other governments may specially object to any disposal by the United States of radioactive waste of military origin in an area beyond its national jurisdiction. The motive for such an objection may be general concern with the impact on the environment, or it may be political concern with the military origin of the waste involved."[22] Spent fuel may be considered to contain materials suitable for nuclear weapons production. High-level radioactive wastes produced from weapons manufacture may be unacceptable to national governments for disposing in the subseabed, or they may not. Such questions need close examination and negotiation by international lawyers. Perhaps resolution will come from amendments to existing treaties or the establishment of new international arrangements.

Non-Proliferation Treaty

The significance of the Non-Proliferation Treaty to a Subseabed Disposal Program lies primarily in the question of application of safeguards to port and transportation facilities and the disposal area.

Under the Treaty, non-nuclear weapons states party must accept International Atomic Energy Agency safeguards to ensure that nuclear energy has not been diverted from peaceful purposes to nuclear weapons. The safeguards apply to all peaceful nuclear materials and activities in national territory and elsewhere.[23]

The nuclear weapons states are not required to submit to these safeguards, however, but merely pledge to find means to end the arms race.[24]

Should an agreement on subseabed disposal be reached between states which are weapons states and those which are not, or those which are signatories and those which are not, there may be a question about the applicability of the safeguards to the several facilities involved.

The question of the type of waste emplaced is a strong influence as well. Spent fuel requires stronger safeguards to prevent plutonium diversion than does high-level reprocessing waste. Weapons waste may be by virtue of its origin prohibited from a Subseabed Disposal Program, as its acceptance may be interpreted as an approval of weapons production.

However, according to Dr. B. Goldschmidt (the Chairman of the Board of Governors of the IAEA) the Treaty's implications for activities of its signers can be summed up in one phrase:

"...a nuclear explosion is prohibited, but everything not prohibited is allowed, including all stages of the fuel cycle, even if they make it possible to produce nuclear explosives."[25]

So the real significance is the applicability of IAEA standards to a multinationally controlled nuclear waste repository located in an international area. These safeguards are continuously evolving, and have reached different stages of development for different types of facilities, simply because the Agency's experience is limited in safeguarding some types of facilities.

IAEA safeguards systems appear in two documents published by the Agency: INFCIRC/66/Rev. 2 and INFCIRC/153. The former forms the basis for project agreements, transfer agreements and unilateral submission agreements under which equipment, facilities and other materials are subject to safeguards. The second document is the basis for all agreements with non-nuclear weapons states party to the NPT under which all nuclear material in all peaceful nuclear activities is subject to safeguards.

While there are no existing safeguards procedures for a disposal facility situated in international territory, they do exist for some of the parts of the process.

In the event that spent fuel is disposed of, continuous inspection is necessary when the fuel is transferred out of the storage pool and placed in canisters. Frequent spent fuel shipments require at least a fixed interval surveillance camera set to photograph each cask leaving the building, and primary verification on receipt of the cask at the receiving facility at the disposal site, which could be considered a material balance area.[26]

These are, of course, only hypotheses, since the specifics regarding types of waste are still uncertain. The Agency, in carrying out its responsibilities "to establish and administer safeguards...to ensure that special fissionable and other materials, services equipment, facilities and information...are not used in such a way as to further any military purpose..."[27] may need to consider the development of special safeguards procedures for the subseabed disposal concept.

The Treaty Banning Nuclear Weapons Tests in the Atmosphere, Outer Space, and Under Water

The Treaty Banning Nuclear Weapons Tests in the Atmosphere, Outer Space, and Under Water (1963), Nuclear Test Ban Treaty, has as its goal a general disarmament policy. Thus, subseabed disposal of radioactive wastes generated from weapons production may cause controversy. Although it is not clear that weapons waste will ever be included for this mode of disposal, a catalogue of possibly influential treaties must include those which apply in any forseeable situation. While the Test Ban Treaty itself is not likely to obstruct a Subseabed Disposal Program, it may influence aspects of the management framework.

Seabed Weapons Treaty

Although the Treaty on the Prohibition of the Emplacement of Nuclear Weapons and Other Weapons of Mass Destruction on the Seabed and Ocean Floor and in the Subsoil Thereof (hereafter referrred to as the Seabed Weapons Treaty) contains no specific provisions on radioactive marine pollution, it may impact on a Subseabed Disposal Program in so far as the emplacement of military wastes are concerned. The Preamble to the Treaty states that it "constitutes a step towards the exclusion of the seabed, the ocean floor, and the subsoil thereof from the arms race."[28] and it would seem that facilitating weapons waste disposal might be taken as an action contrary to that goal.

Article I of the Seabed Weapons Treaty goes on to state:

"(1) The States party to this Treaty undertake not to emplant or emplace on the seabed and the ocean floor and in the subsoil thereof beyond the outer limit of a seabed zone, as defined in Article 2, any nuclear weapons or...any other facilities specifically designed for storing, testing or using such weapons.

(2) The undertakings of paragraph 1 of this Article shall also apply to the seabed zone referred to in the same paragraph, except that within such a seabed zone, they shall not apply either to the coastal state or to the seabed beneath its territorial waters.

(3) The States party to this Treaty undertake not to assist, encourage, or induce any state to carry out activities referred to in paragraph 1 of this Article and not to participate in any other way in such actions."[29]

Article I, Section 2 may infer that weapons waste emplacement at sites within a nation's territorial limits could not be prohibited under the Treaty.

Article III gives each State party to the Seabed Weapons Treaty verification rights on other States party.

Member States of the Euratom Treaty must communicate to each other through a commission any measures they intend to take for the disposal of radioactive wastes.[30]

A Convention on the Physical Protection of Nuclear Material was opened for signature on March 3, 1980 in Vienna and New York. It applies directly to the establishment of guidelines for safeguarding fissionable materials in international transport and domestic use and storage. Materials are categorized in Article I, Section (a) and (b) and international transport is defined in Section (c). Such transport is defined by "facilities" in national countries at both ends of the shipment, and seems not to be applicable to the procedure in question. A copy of the Convention is addended to this section.

Should damage to the ocean environment occur from burial of radioactive waste materials, it may become apparent long after the date of the emplacement. This complicates the question of liability within the frame of management schemes of finite lifetimes. Who will bear responsibility for the possibility of environmental damage by a Subseabed Program?

Existing Conventions on liability applicable to all nuclear activities reflect the principle of liability for the hazard created (absolute liability) rather than liability for fault.[31]

The Conventions that apply in the case of radioactive pollution that are caused by substances carried on a ship are (1) the Paris and Vienna Conventions,[32] which provide that:

"...in the case of damage caused by a nuclear incident occuring in the course of maritime carriage of nuclear material covered by such Conventions, the operator of a nuclear installation is the person liable for such damage," [33] and (2) the subsequently developed Convention Relating to Civil Liability in the Field of Maritime Carriage of Nuclear Material (12/71).

General liability in "The Field of Nuclear Energy" is covered under the Paris and Vienna Conventions.

The success of these different Conventions will be based mainly on the goodwill of countries wishing to observe and enforce the obligations implied. International bodies responsible for their application are not generally vested with powers directly binding on the contracting parties.[34]

Subseabed emplacement of radioactive wastes may necessitate new multilateral agreements on liability for damages, if the program is attempted by a few nations in mutual cooperation. The difficulty in the development of such instruments binding liability to hazards to the global commons are not to be overlooked as a possible impediment to the implementation of the Subseabed Disposal Program.

The establishment of an international regime for the transport of nuclear wastes over international waters for disposal in the subseabed would nearly assure compliance with international standards and regulations and would "fix firmly the allocation for responsibility for vessel design, maintenance, and performance as well as ensuring high operational

performance of crew." [35]

Although no precedent exists for the creation of such a regime at least one private company operates that incinerates hazardous waste at sea. The M/T Vulcanus, a hazardous waste incinerator ship, was originally a cargo ship but in 1972 was converted to a chemical tanker with two large incinerators. The ship complies with all IMCO regulations concerning transport of dangerous cargo. Although it was owned by a Dutch company for a number of years, it is presently owned by an American company, although it flies a foreign flag. The Vulcanus, has been hired by several countries throughout the world for incineration of hazardous chemicals. Recently it was hired by the U.S. Department of Defense for incineration of Agent Orange, a chemical used during the Vietnam War. The IMCO promptly amended the appropriate conventions to regulate this activity when it was ready for operation.

An international regime could serve a managerial function, supervising and licensing existing national or private companies. "If the organization were associated with the U.N. it might also consider leasing vessels directly and operating them under the U.N. flag." [36] However, such functions operating under U.N. auspices must be carefully considered so that assurances against unjustified political interference could be precluded. Otherwise other multilateral forums must be considered preferable.

PART II: INTERNATIONAL ORGANIZATIONS AND STRUCTURES*

Council for Mutual Economic Assistance

Purpose: Contribute through the union and coordination of the forces of member countries to the planned development of the national economy and an acceleration of economic and technical progress of these countries; raising the level of industrialization of the underdeveloped countries; an uninterrupted growth in labor productivity; and a steady rise in the well being of the peoples of the member countries.

Structure: Council, principal political organ, has authority to discuss all matters within the domain of the organization and to make appropriate recommendations and decisions. Standing Commissions provide main focus of intergovernmental work, each composed of experts from all member states.

Relation to Subseabed Disposal Program (SDP): Standing Commission on peaceful uses of atomic energy; established a waste management coordinating council (1971) possible regional organization role.

---

*See chart at end of chapter for organization memberships, Figure I

European Economic Community

Purpose: Establish Common Market, promote "harmonious" development of economic activities, a continued and balanced expansion, increased stability and closer relations between its members.

Relation to SDP: Much interest in promoting regional energy policy-pushing expansion of member nuclear programs as answer to energy problems, regional support agency.

Euratom

Purpose: Develop research, disseminate information, enforce uniforn safety standards, facilitate investment, ensure regular and equitable distribution of supplies of nuclear material, guarantee nuclear materials are not diverted from their designated uses, exercise certain property rights in regard to such materials, create common market for free movement of capital for investment and personnel for nuclear industries and to promote peaceful uses of atomic energy.

Relation to SDP: Coordinates (currently) national nuclear research programs, operates supply agency for fissionable material and conducts inspections of nuclear installations using such supplies to ensure material is not diverted from peaceful use, mandate to examine any radioactive waste disposal plan to determine its potential for contamination of water, soil or airspace of another member, establish basic standards including maximum public and occupational doses and enforces their implementation.

Food and Agriculture Organization (UN specialized Agency)

Purpose: Promote common welfare by furthering separate and collective action for raising levels of nutrition and standards of living of the peoples under their jurisdiction.

Relation to SDP: Interest in any activity with potential to influence supply of world's food requirements; may perceive SDP to endanger food source of oceans therefore would monitor Subseabed Disposal program carefully; assists IAEA in studying radioactive waste disposal in marine areas; may assist in establishing recommended standards and procedures and to comment on state practices relating to SDP.

Joint Group of Experts on the Scientific Aspects of Marine Pollution (GESAMP)

Purpose: Studies technical problems related to pollution; composed of IMCO, FAO, UNESCO, WMO, WHO, IAEA.

Relation to SDP: Information exchange - has studied environmental effects of seabed exploration and exploitation; done some work on waste disposal in sea, particularly site selection, although avoided specific mention of radioactivity.

International Atomic Energy Agency (IAEA)

Purpose: Assist in nuclear R & D and its application; establish health and safety standards and conventions on civil liability for damage; administer safeguards programs to ensure peaceful atomic energy activities not diverted to military uses; provide technical assistance.

Relation to SDP: As presented by Deese:[37]

1. Establish safety standards and publication of recommendations on radiological protection and waste management; were supposed to have drawn up specific set of standards for waste disposal at sea by 1978.

   a) legal/administrative measures for control of radioactive waste disposal into seas and oceans;

   b) studies of the effects of radioactivity on aquatic organisms and ecosystems, as well as the interaction of rad contaminants with constituents of the marine environment;

   c) development of guidelines for geologic disposal of high level and alpha-bearing wastes;

2. Recommendations on safe transport of radioactive materials--widely accepted regulations already established by them.

3. Regional training and technical assistance.

   a) research contracts and agreements on marine science and pollution;

   b) special missions on siting of nuclear facilities on seacoasts and offshore.

Other points to be considered: May develop international guidelines on spent fuel storage and high level waste solidification; however, agency seems to want to avoid "political" problems which are inherent in such guideline specification. Tension observed at IAEA because it serves two regimes: the safeguards regime and a second older regime for promotion of nuclear technology. "The Agency cannot easily judge any technology to be inherently unsafe, guardable--and therefore not a candidate for wide-spread international diffusion and dissemination--without risking a disruptive internal fight."[38]

International Council of Scientific Unions (ICSU)

Purpose: Coordinate and facilitate activities of international scientific unions in the field of exact and natural sciences; act as coordinating center for national adhering organization; promote scientific research within countries through national organizations or their government; consultative status with UNESCO, FAO, IAEA, and others.

Relation to SDP: Information exchange and monitoring of program; seem to be concerned with world environmental problems; was instrumental in setting up World Weather Watch & Earthwatch, facilitating the research which made setting up their monitoring efforts feasible; the special monitoring commissions of the Scientific Committee on Problems of the Environment (SCOPE) may monitor SDP development and operation.

International Commission on Radiological Protection (ICRP)

Purpose: Establish international standards on radiological protection, particularly occupational exposure; investigate exposure from the release of rad materials into the environment, including disposal of solid wastes. Specific regulatory and dose assessment procedures also cover direct external exposure from industrial sources and the monitoring of exposure after planned and accidental releases of radioactivity into the environment.

Relation to SDP: Occupational and public exposure standards as set up by ICRP will need to be followed within program.

International Energy Agency (IEA)

Purpose: Coordinate responses of participating states to world energy crisis, and to develop oil-sharing mechanism for use in times of supply difficulties; currently evaluating potential danger of plutonium as a nuclear fuel.

Relation to SDP: Because its "sister"agency NEA is not a policy-oriented agency, political acceptance or rejection of SDP by the industrial nations will probably have to come from the IEA. In turn, IEA'S reaction will undoubtedly depend upon success or failure of the joint R & D program which IEA and NEA have on SDP members are concerned with solving the nuclear waste disposal problem which they regard as a major obstacle to the development of national energy resources. Some general problems with IEA program on long term cooperation in energy.

Intergovernmental Oceanographic Commission (IOC)

Purpose: Promote scientific investigation of oceans to learn more about their nature and resources; under auspices of UNESCO investigates the routes, fares and effects of pollutants in the marine environment.

Relation to SDP: Possible monitoring/research role in program.

Intergovernmental Marine Consultative Organization (IMCO)

Purpose: Formal secretariat for London Dumping Convention; facilitates cooperation among governments in the field of government regulations and practices relating to technical matters of all kinds of affective shipping engaged in international trade; encourage adoption of standards of maritime safety, efficiency of navigation, and prevention and control of marine pollution from ships; and to deal with legal matters related to these purposes.

Relation to SDP: Shipping regulation, ship safety, routing schemes; IMCO's secretariat; main association-considerable technical expertise which is widely recognized; IMCO largely tech-oriented, not very politically oriented; so far, most of its enforcement done by national agencies, IMCO may do eventually.

If the SDP regulated under London Convention, IMCO would be influential in program because it is secretariat, but other than that, its "political influence" is open to question; International Convention relating to Civil Liability in the Field of Maritime Carriage of Nuclear Material (Brussels Convention) ensures that nuclear installation operator is liable under the Paris or Vienna Conventions on Civil Liability or under national law. Shipowners are also free from liability for damage to vessels or nuclear installations.

Nuclear Energy Agency (NEA)

Purpose: A future role contributing toward economic progress and encouraging cooperation between governments for optimum development of nuclear energy; encourage harmonization of the government's regulatory policies and practices in nuclear field of particular reference to health and safety; radioactive waste management and nuclear third party liability and insurance; forecasts of uranium resources, production and demand; operation of common services and encouragement of cooperation in field of nuclear energy information; sponsorship of R & D undertakings jointly operated by OECD countries.

Structure: Steering Committee composed of all member governments' representatives and representatives from European communities; IAEA observer; committees and study groups; Committee on Radiation Protection and Public Health; Radioactive Waste Management Committee; Committee on the Safety of Nuclear Installations; Study Group on Long-term Role of Nuclear Energy; Group of Governmental Experts on Third Party Liability in the Field of Nuclear Energy, and a few others.

IGO Relations With IAEA, IMCO, European Communities

Relation to SDP: Established in 1977, a multilateral consultation and surveillance mechanism for sea dumping of rad waste; legal and administrative measures include OECD Convention on Third Party Liability in Field of Nuclear Energy; some powers to regulate and to more limited extent, enforce rad waste guidelines in member states; its formal regulatory role limited to innocuous areas of rad protection; traditionally it has been devoted to

promotion of technical developments in nuclear energy with little capability or willingness to become involved in the politically controversial task of regulation. As NEA's role contracted from its establishment its role in organizational hierarchy became more firmly established-primary responsibility for rad protection and health and safety standards among its member states.

Agency for the Prohibition of Nuclear Weapons in Latin America (OPANAL)

Purpose: Established in 1969 to administer treaty for the prohibition of nuclear weapons in Latin America without prejudice to peaceful uses of atomic energy. Treaty (of Tlateloco) was designed to make Latin America a nuclear free zone; thus it prohibits all testing, manufacture, acquisition, installation, and development of nuclear weapons.

Members: Bahamas, Barbados, Bolivia, Brazil, Chile, Colombia, Costa Rica, Dominican Republic, Ecuador, El Salvador, Granada, Guatemala, Haiti, Honduras, Jamaica, Mexico, Nicaragua, Panama, Paraguay, Peru, Suriname, Trinidad and Tobago, Uraguay, Venezuela.

Relation to SDP: Activities of organization include encouraging peaceful uses of atomic energy; if at some point Latin American country enters into Subseabed Disposal Program might be under the auspices of OPANAL.

UN Conference on Trade and Development (UNCTAD)

Purpose: Promote international trade with a view to accelerating the economic growth of less-developed countries; to formulate and implement policies related to trade and development to review and facilitate the coordination of various institutions within the United Nations system in regard to international trade and development; to initiate action for the negotiation and adoption of multilateral legal instruments in the field of trade, to harmonize trade and related development policies of governments and regional economic groups.

Relation to SDP: Shipping Commission may have interest in shipping if a lesser-developed country was to decide to take over shipping in SDP; or may be a means to stop SDP if lesser-developed countries decide the program would be against their better interests.

UN Development Programme (UNDP)

Purpose: Coordinate and administer technical assistance provided through the UN system, in order to assist less-developed countries in their efforts to accelerate social and economic development.

Relation to SDP: One of the major activities-transfer of appropriate technologies and stimulating growth of local technological capabilities.

UN Environmental Programme (UNEP)

Purpose: To facilitate international cooperation in all matters affecting the human environment; to ensure that environmental problems of wide international significance receive appropriate governmental consideration; and to provide the acquisition, assessment, and exchange of environmental knowledge; set up by Stockholm Conference in 1972; financed by voluntary contributions, but assured base level of funding; set up Global Environmental Monitoring System which records information obtained on world environment from national and regional bodies and from other specialized agencies; an international repository for potential toxic chemicals--both these part of "Earthwatch" whose aim is to examine the level and effect of pollution in different environments and to recommend the international measures needed.

Relation to SDP: Earthwatch special interest in problems of preserving the marine environment.

UN Educational, Scientific and Cultural Organization (UNESCO)

Purpose: (Natural Sciences Division) increase and diffuse knowledge; develop international scientific cooperation by organizing meetings among scientists, assisting activities of international scientific organizations and by promoting exchange of scientific information; cooperative with ICSU to set up World Scientific and Technical Information System. Endeavors to apply scientific knowledge to relations between peoples on the national as well as the international level.

Relation to SDP: Scientific information exchange, will probably "Monitor"any SDP effort.

Western European Union (WEU)

Purpose: Collective self defense and political collaboration in support of European unity.

Relation to SDP: Focus of activity in recent years (one of the foci) state of European nuclear energy programs probably through the Committee on Scientific, Technological, and Aerospace Questions.

World Health Organization (WHO)

Purpose: Attain highest possible level of health for all peoples; conducts studies, subsidizes research and furnishes technical assistance to this end (largest budget of UN special agency).

Relation to SDP: Interest in environmental problems and its participation in GESAMP may induce its involvement in program of SDP.

World Meteoroligical Organization (WMO)

Purpose: Facilitate worldwide cooperation in establishment of meteorological observation stations; promote establishment and maintenance of systems for rapid exchange of weather information; promote standardization of meteorological observations and ensure uniform publication of observations and statistics.

Relation to SDP: World Weather Watch system coordinated with Global Atmospheric Research Program (ICSU); complementary effort with this system global measurement of atmospheric pollutants, interest in environmental issues and participation in GESAMP may also tie it into a Subseabed Disposal Program-probably "monitor" its progress.

INTERNATIONAL ORGANIZATIONS AND COUNTRY MEMBERSHIP

ORGANIZATION / COUNTRY	CMEA	EEC	-EURATOM	IATTC	ICCAT	ICES	ICRP	ICSU	-SCOR	IWC	NATO	OECD	-IEA	-NEA	UN	-FAO	-GESAMP	-IAEA	-ILO	-IMCO	-UNCTAD	-UNDP	-UNEP	-UNESCO	--IOC	--EONR	-WHO	WEU	WTO
Argentina								X	X	X					X	X		X	X	X	X	X	X	X			X		
Australia								X	X	X		X			X	X		X	X	X	X	X		X			X		
Belgium		X	X			X		X	X		X	X	X	X	X	X		X	X	X	X	X	X	X		X	X	X	
Bulgaria	X							X							X	X		X	X	X	X	X	X	X			X		X
Canada				X	X	X		X	X	X	X	X		X	X	X		X	X	X	X	X	X	X			X		
Czechoslovakia	X							X							X	X		X	X	X	X	X		X			X		
Finland						X		X	X			X			X	X		X	X	X	X	X		X			X		
France		X	X	X	X	X		X	X	X	X	X			X	X		X	X	X	X	X	X	X		X	X	X	
GDR	X					X		X	X						X			X	X	X	X			X			X		X
GFR		X	X			X		X	X		X	X		X	X	X		X	X	X	X	X	X	X		X	X	X	
India								X	X						X			X	X	X	X			X			X		
Italy		X	X					X	X		X	X		X	X	X		X	X	X	X	X		X		X	X	X	
Japan				X	X			X	X	X		X		X	X	X		X	X	X	X	X	X	X			X		
Netherlands		X	X			X		X	X	X	X	X		X	X	X		X	X	X	X	X	X	X		X	X	X	
Pakistan								X							X	X		X	X	X	X	X	X	X			X		
Spain					X	X		X	X			X		X	X	X		X	X	X	X	X	X	X			X		
South Korea								X							X	X		X		X	X			X			X		
Sweden						X		X	X			X		X	X	X		X	X	X	X		X	X		X	X		
Switzerland								X	X			X		X		X		X	X	X	X		X	X		X	X		
Taiwan																													
UK		X	X			X		X	X	X	X	X		X	X	X		X	X	X	X		X	X		X	X	X	
US				X	X	X		X	X	X	X	X		X	X	X		X	X	X	X		X	X			X		
USSR	X				X	X		X	X	X					X			X	X	X	X		X	X			X		X

FIGURE I

ANNEX III

REGULATIONS FOR THE PREVENTION OF POLLUTION BY HARMFUL SUBSTANCES CARRIED BY SEA IN PACKAGED FORMS, OR IN FREIGHT CONTAINERS, PORTABLE TANKS OR ROAD AND RAIL TANK WAGONS

Regulation 1

Application

(1) Unless expressly provided otherwise, the Regulations of this Annex apply to all ships carrying harmful substances in packaged forms, or in freight containers, portable tanks or road and rail tank wagons.

(2) Such carriage of harmful substances is prohibited except in accordance with the provisions of this Annex.

(3) To supplement the provisions of this Annex the Government of each Party to the Convention shall issue, or cause to be issued, detailed requirements on packaging, marking and labelling, documentation, stowage, quantity limitations, exceptions and notification, for preventing or minimizing pollution of the marine environment by harmful substances.

(4) For the purpose of this Annex, empty receptacles, freight containers, portable tanks and road and rail tank wagons which have been used previously for the carriage of harmful substances shall themselves be treated as harmful substances unless adequate precautions have been taken to ensure that they contain no residue that is hazardous to the marine environment.

Regulation 2

Packaging

Packagings, freight containers, portable tanks and road and rail tank wagons shall be adequate to minimize the hazard to the marine environment having regard to their specific contents.

Regulation 3

Marking and Labelling

Packages, whether shipped individually or in units or in freight containers, freight containers, portable tanks or road and rail tank wagons containing a harmful substance, shall be durably marked with the correct technical name (trade names shall not be used as the correct technical name), and further marked with a distinctive label or stencil or label, indicating that the contents are harmful. Such identification shall be supplemented where possible by any other means, for example by the use of the United Nations number.

SOURCE: New Directions in the Law of the Sea, Volume IV.

Regulation 4

Documentation

(1) In all documents relating to the carriage of harmful substances by sea where such substances are named, the correct technical name of the substances shall be used (trade names shall not be used).

(2) The shipping documents supplied by the shipper shall include a certificate or declaration that the shipment offered for carriage is properly packed, marked and labelled and in proper condition for carriage to minimize the hazard to the marine environment.

(3) Each ship carrying harmful substances shall have a special list or manifest setting forth the harmful substances on board and the location thereof. A detailed stowage plan which sets out the location of all harmful substances on board may be used in place of such special list or manifest. Copies of such documents shall also be retained on shore by the owner of the ship or his representative until the harmful substances are unloaded.

(4) In a case where the ship carries a special list or manifest or a detailed stowage plan, required for the carriage of dangerous goods by the International Convention for the Safety of Life at Sea in force, the documents required for the purpose of this Annex may be combined with those for dangerous goods. Where documents are combined, a clear distinction shall be made between dangerous goods and other harmful substances.

Regulation 5

Stowage

Harmful substances shall be both properly stowed and secured so as to minimize the hazards to the marine environment without impairing the safety of ship and persons on board.

Regulation 6

Quantity Limitations

Certain harmful substances which are very hazardous to the marine environment may, for sound scientific and technical reasons, need to be prohibited for carriage or be limited as to the quantity which may be carried aboard any one ship. In limiting the quantity due consideration shall be given to size, construction and equipment of the ship as well as the packaging and the inherent nature of the substance.

Regulation 7

Exceptions

(1) Discharge by jettisoning of harmful substances carried in packaged forms, freight containers, portable tanks or road and rail tank wagons shall be prohibited except where necessary for the purpose of securing the safety of the ship or saving life at sea.

(2) Subject to the provisions of the present Convention, appropriate measures based on the physical, chemical and biological properties of harmful substances shall be taken to regulate the washing of leakages overboard provided that compliance with such measures would not impair the safety of the ship and persons on board.

Regulation 8

Notification

With respect to certain harmful substances, as may be designated by the Government of a Party to the Convention, the master or owner of the ship or his representative shall notify the appropriate port authority of the intent to load or unload such substances at least 24 hours prior to such action.

ADDENDA II

TEXT OF CONVENTION ON THE PHYSICAL PROTECTION OF NUCLEAR MATERIAL

TEXTS

• *International Atomic Energy Agency*

PHYSICAL PROTECTION OF NUCLEAR MATERIAL

The Meeting of Governmental Representatives to Consider the Drafting of a Convention on the Physical Protection of Nuclear Material was held in Vienna at the Headquarters of the International Atomic Energy Agency from 31st October to 10th November 1977, from 10th to 20th April 1978, from 5th to 16th February and from 15th to 26th October 1979. Informal consultations between Governmental Representatives took place from 4th to 7th September 1978 and from 24th to 25th September 1979.

Representatives of fifty-eight States and one Organisation participated, namely, representatives of:

Algeria
Argentina
Australia
Austria
Belgium
Brazil
Bulgaria
Canada
Chile
Colombia
Costa Rica
Cuba
Czechoslovakia
Denmark
Ecuador
Egypt
Finland
France
German Democratic Republic
Germany, Federal Republic of
Greece
Guatemala
Holy See
Hungary
India
Indonesia
Ireland
Israel
Italy
Japan
Korea, Republic of
Libyan Arab Jamahiriya
Luxembourg
Mexico
Netherlands
Niger
Norway
Pakistan
Panama
Paraguay
Peru
Philippines
Poland
Qatar
Romania
South Africa
Spain
Sweden
Switzerland
Tunisia
Turkey
Union of Soviet Socialist Republics
United Arab Emirates
United Kingdom of Great Britain and Northern Ireland
United States of America
Venezuela
Yugoslavia
Zaire
European Atomic Energy Community

The following States and international organisations participated as observers:

Iran
Lebanon
Malaysia
Thailand
OECD Nuclear Energy Agency

Secretariat services were provided by the International Atomic Energy Agency.

The Meeting had before it the following documents:

(a) Draft Convention on the Physical Protection of Nuclear Materials, Facilities and Transports, as contained in document CPNM/1;

(b) IAEA Document INFCIRC/225/Rev.1: The Physical Protection of Nuclear Material;

(c) IAEA Document INFCIRC/254; Communications Received from Certain Member States regarding Guidelines for the Export of Nuclear Material, Equipment or Technology.

The Meeting completed consideration of a Convention, the text of which follows. Certain delegations expressed reservations with regard to particular provisions in the text. These are recorded in the documents and in the Daily Reports of the Meeting. It was agreed that the text will be referred by delegations to their authorities for consideration.

The Meeting recommended that the text of the Convention be transmitted for information to the Twenty-third General Conference of the International Atomic Energy Agency.

The Convention will, in accordance with its terms, be opened for signature from 3rd March, 1980, at the Headquarters of the International Atomic Energy Agency in Vienna and at the Headquarters of the United Nations in New York.*

* This Note is an extract from the Final Act of the Meeting.

CONVENTION ON THE PHYSICAL PROTECTION OF NUCLEAR MATERIAL

THE STATES PARTIES TO THIS CONVENTION,

RECOGNIZING the right of all States to develop and apply nuclear energy for peaceful purposes and their legitimate interests in the potential benefits to be derived from the peaceful application of nuclear energy,

CONVINCED of the need for facilitating international co-operation in the peaceful application of nuclear energy,

DESIRING to avert the potential dangers posed by the unlawful taking and use of nuclear material,

CONVINCED that offences relating to nuclear material are a matter of grave concern and that there is an urgent need to adopt appropriate and effective measures to ensure the prevention, detection and punishment of such offences,

AWARE OF THE NEED FOR international co-operation to establish, in conformity with the national law of each State Party and with this Convention, effective measures for the physical protection of nuclear material,

CONVINCED that this Convention should facilitate the safe transfer of nuclear material,

STRESSING also the importance of the physical protection of nuclear material in domestic use, storage and transport,

RECOGNIZING the importance of effective physical protection of nuclear material used for military purposes, and understanding that such material is and will continue to be accorded stringent physical protection,

HAVE AGREED as follows:

Article 1

For the purposes of this Convention:

(a) "nuclear material" means plutonium except that with isotopic concentration exceeding 80% in plutonium-238; uranium-233; uranium enriched in the isotopes 235 or 233; uranium containing the mixture of isotopes as occurring in nature other than in the form of ore or ore-residue; any material containing one or more of the foregoing;

(b) "uranium enriched in the isotope 235 or 233" means uranium containing the isotopes 235 or 233 or both in an amount such that the abundance ratio of the sum of these isotopes to the isotope 238 is greater than the ratio of the isotope 235 to the isotope 238 occurring in nature;

(c) "international nuclear transport" means the carriage of a consignment of nuclear material by any means of transportation intended to go beyond the territory of the State where the shipment originates beginning with the departure from a facility of the shipper in that State and ending with the arrival at a facility of the receiver within the State of ultimate destination.

Article 2

1. This Convention shall apply to nuclear material used for peaceful purposes while in international nuclear transport.

2. With the exception of Articles 3 and 4 and paragraph 3 of Article 5, this Convention shall also apply to nuclear material used for peaceful purposes while in domestic use, storage and transport.

3. Apart from the commitments expressly undertaken by States Parties in the Articles covered by paragraph 2 with respect to nuclear material used for peaceful purposes while in domestic use, storage and transport, nothing in this Convention shall be interpreted as affecting the sovereign rights of a State regarding the domestic use, storage and transport of such nuclear material.

Article 3

Each State Party shall take appropriate steps within the framework of its national law and consistent with international law to ensure as far as practicable that, during international nuclear transport, nuclear material within its territory, or on board a ship or aircraft under its jurisdiction insofar as such ship or aircraft is engaged in the transport to or from that State, is protected at the levels described in Annex I.

Article 4

1. Each State Party shall not export or authorize the export of nuclear material unless the State Party has received assurances that such material will be protected during the international nuclear transport at the levels described in Annex I.

2. Each State Party shall not import or authorize the import of nuclear material from a State not party to this Convention unless the State Party has received assurances that such material will during the international nuclear transport be protected at the levels described in Annex I.

3. A State Party shall not allow the transit of its territory by land or internal waterways or through its airports or seaports of nuclear material between States that are not parties to this Convention unless the State Party has received assurances as far as practicable that this nuclear material will be protected during international nuclear transport at the levels described in Annex I.

4. Each State Party shall apply within the framework of its national law the levels of physical protection described in Annex I to nuclear material being transported from a part of that State to another part of the same State through international waters or airspace.

5. The State Party responsible for receiving assurances that the nuclear material will be protected at the levels described in Annex I according to paragraphs 1 to 3 shall identify and inform in advance States which the nuclear material is expected to transit by land or internal waterways, or whose airports or seaports it is expected to enter.

6. The responsibility for obtaining assurances referred to in paragraph 1 may be transferred, by mutual agreement, to the State Party involved in the transport as the importing State.

7. Nothing in this Article shall be interpreted as in any way affecting the territorial sovereignty and jurisdiction of a State, including that over its airspace and territorial sea.

Article 5

1. States Parties shall identify and make known to each other directly or through the International Atomic Energy Agency their central authority and point of contact having responsibility for physical protection of nuclear material and for co-ordinating recovery and response operations in the event of any unauthorized removal, use or alteration of nuclear material or in the event of credible threat thereof.

2. In the case of theft, robbery or any other unlawful taking of nuclear material or of credible threat thereof, States Parties shall, in accordance with their national law, provide co-operation and assistance to the maximum feasible extent in the recovery and protection of such material to any State that so requests. In particular:

(a) a State Party shall take appropriate steps to inform as soon as possible other States, which appear to it to be concerned, of any theft, robbery or other unlawful taking of nuclear material or credible threat thereof and to inform, where appropriate, international organisations;

(b) as appropriate, the States Parties concerned shall exchange information with each other or international organisations with a view to protecting threatened nuclear material, verifying the integrity of the shipping container, or recovering unlawfully taken nuclear material and shall:

(i) co-ordinate their efforts through diplomatic and other agreed channels;

(ii) render assistance, if requested;

(iii) ensure the return of nuclear material stolen or missing as a consequence of the above-mentioned events.

The means of implementation of this co-operation shall be determined by the States Parties concerned.

3. States Parties shall co-operate and consult as appropriate, with each other directly or through international organisations, with a view to obtaining guidance on the design, maintenance and improvement of systems of physical protection of nuclear material in international transport.

Article 6

1. States Parties shall take appropriate measures consistent with their national law to protect the confidentiality of any information which they receive in confidence by virtue of the provisions of this Convention from another State Party or through participation in an activity carried out for the implementation of this Convention. If States Parties provide information to international organisations in confidence, steps shall be taken to ensure that the confidentiality of such information is protected.

2. States Parties shall not be required by this Convention to provide any information which they are not permitted to communicate pursuant to national law or which would jeopardize the security of the State concerned or the physical protection of nuclear material.

Article 7

1. The intentional commission of:

(a) an act without lawful authority which constitutes the receipt, possession, use, transfer, alteration, disposal or dispersal of nuclear material and which causes or is likely to cause death or serious injury to any person or substantial damage to property;

(b) a theft or robbery of nuclear material;

(c) an embezzlement or fraudulent obtaining of nuclear material;

(d) an act constituting a demand for nuclear material by threat or use of force or by any other form of intimidation;

(e) a threat:

(i) to use nuclear material to cause death or serious injury to any person or substantial property damage, or

(ii) to commit an offence described in sub-paragraph (b) in order to compel a natural or legal person, international organisation or State to do or to refrain from doing any act;

(f) an attempt to commit any offence described in paragraphs (a), (b) or (c); and

(g) an act which constitutes participation in any offence described in paragraphs (a) to (f)

shall be made a punishable offence by each State Party under its national law.

2. Each State Party shall make the offences described in this Article punishable by appropriate penalties which take into account their grave nature.

Article 8

1. Each State Party shall take such measures as may be necessary to establish its jurisdiction over the offences set forth in Article 7 in the following cases:

(a) when the offence is committed in the territory of that State or on board a ship or aircraft registered in that State;

(b) when the alleged offender is a national of that State.

2. Each State Party shall likewise take such measures as may be necessary to establish its jurisdiction over these offences in cases where the alleged offender is present in its territory and it does not extradite him pursuant to Article 11 to any of the States mentioned in paragraph 1.

3. This Convention does not exclude any criminal jurisdiction exercised in accordance with national law.

4. In addition to the States Parties mentioned in paragraphs 1 and 2, each State Party may, consistent with international law, establish its jurisdiction over the offences set forth in Article 7 when it is involved in international nuclear transport as the exporting or importing State.

Article 9

Upon being satisfied that the circumstances so warrant, the State Party in whose territory the alleged offender is present shall take appropriate measures, including detention, under its national law to ensure his presence for the purpose of prosecution or extradition. Measures taken according to this Article shall be notified without delay to the States required to establish jurisdiction pursuant to Article 8 and, where appropriate, all other States concerned.

Article 10

The State Party in whose territory the alleged offender is present shall, if it does not extradite him, submit, without exception whatsoever and without undue delay, the case to its competent authorities for the purpose of prosecution, through proceedings in accordance with the laws of that State.

Article 11

1. The offences in Article 7 shall be deemed to be included as extraditable offences in any extradition treaty existing between States Parties. States Parties undertake to include those offences as extraditable offences in every future extradition treaty to be concluded between them.

2. If a State Party which makes extradition conditional on the existence of a treaty receives a request for extradition from another State Party with which it has no extradition treaty, it may at its option consider this Convention as the legal basis for extradition in respect of those offences. Extradition shall be subject to the other conditions provided by the law of the requested State.

3. States Parties which do not make extradition conditional on the existence of a treaty shall recognize those offences as extraditable offences between themselves subject to the conditions provided by the law of the requested State.

4. Each of the offences shall be treated, for the purpose of extradition between States Parties, as if it had been committed not only in the place in which it occurred but also in the territories of the States Parties required to establish their jurisdiction in accordance with paragraph 1 of Article 8.

Article 12

Any person regarding whom proceedings are being carried out in connection with any of the offences set forth in Article 7 shall be guaranteed fair treatment at all stages of the proceedings.

Article 13

1. States Parties shall afford one another the greatest measure of assistance in connection with criminal proceedings brought in respect of the offences set forth in Article 7, including the supply of evidence at their disposal necessary for the proceedings. The law of the State requested shall apply in all cases.

2. The provisions of paragraph 1 shall not affect obligations under any other treaty, bilateral or multilateral, which governs or will govern, in whole or in part, mutual assistance in criminal matters.

Article 14

1. Each State Party shall inform the depositary of its laws and regulations which give effect to this Convention. The depositary shall communicate such information periodically to all States Parties.

2. The State Party where an alleged offender is prosecuted shall, wherever practicable, first communicate the final outcome of the proceedings to the States directly concerned. The State Party shall also communicate the final outcome of the depositary who shall inform all States.

3. Where an offence involves nuclear material used for peaceful purposes in domestic use, storage or transport, and both the alleged offender and the nuclear material remain in the territory of the State Party in which the offence was committed, nothing in this Convention shall be interpreted as requiring that State Party to provide information concerning criminal proceedings arising out of such an offence.

Article 15

The Annexes constitute an integral part of this Convention.

Article 16

1. A conference of States Parties shall be convened by the depositary five years after the entry into force of this Convention to review the implementation of the Convention and its adequacy as concerns the preamble, the whole of the operative part and the annexes in the light of the then prevailing situation.

2. At intervals of not less than five years thereafter, the majority of States Parties may obtain, by submitting a proposal to this effect to the depositary, the convening of further conferences with the same objective.

Article 17

1. In the event of a dispute between two or more States Parties concerning the interpretation or application of this Convention, such States Parties shall consult with a view to the settlement of the dispute by negotiation, or by any other peaceful means of settling disputes acceptable to all parties to the dispute.

2. Any dispute of this character which cannot be settled in the manner prescribed in paragraph 1 shall, at the request of any part to such dispute, be submitted to arbitration or referred to the International Court of Justice for decision. Where a dispute is submitted to arbitration, if, within six months from the date of the request, the parties to the dispute are unable to agree on the organisation of the arbitration, a party may request the President of the International Court of Justice or the Secretary-General of the United Nations to appoint one or more arbitrators. In case of conflicting requests by the parties to the dispute, the request to the Secretary-General of the United Nations shall have priority.

3. Each State Party may at the time of signature, ratification, acceptance or approval of this Convention or accession thereto declare that it does not consider itself bound by either or both of the dispute settlement procedures provided for in paragraph 2. The other States Parties shall not be bound by a dispute settlement procedure provided for in paragraph 2, with respect to a State Party which has made a reservation to that procedure.

4. Any State Party which has made a reservation in accordance with paragraph 3 may at any time withdraw that reservation by notification to the depositary.

Article 18

1. This Convention shall be open for signature by all States at the Headquarters of the International Atomic Energy Agency in Vienna and at the Headquarters of the United Nations in New York from 3rd March 1980 until its entry into force.

2. This Convention is subject to ratification, acceptance or approval by the Signatory States.

3. After its entry into force, this Convention will be open for accession by all States.

4. (a) This Convention shall be open for signature or accession by international organisations and regional organisations of an integration or other nature, provided that any such organisation is constituted by sovereign States and has competence in respect of the negotiation, conclusion and application of international agreements in matters covered by this Convention.

(b) In matters within their competence, such organisations shall, on their own behalf, exercise the rights and fulfil the responsibilities which this Convention attributes to States Parties.

(c) When becoming party to this Convention such an organisation shall communicate to the depositary a declaration indicating which States are members thereof and which Articles of this Convention do not apply to it.

(d) Such an organisation shall not hold any vote additional to those of its Member States.

5. Instruments of ratification, acceptance, approval or accession shall be deposited with the depositary.

Article 19

1. This Convention shall enter into force on the thirtieth day following the date of deposit of the twenty first instrument of ratification, acceptance or approval with the depositary.

2. For each State ratifying, accepting, approving or acceding to the Convention after the date of deposit of the twenty-first instrument of ratification, acceptance or approval, the Convention shall enter into force on the thirtieth day after the deposit by such State of its instrument of ratification, acceptance, approval or accession.

Article 20

1. Without prejudice to Article 16 a State Party may propose amendments to this Convention. The proposed amendment shall be submitted to the depositary who shall circulate it immediately to all States Parties. If a majority of States Parties request the depositary to convene a conference to consider the proposed amendments, the depositary shall invite all States Parties to attend such a conference to begin not sooner than thirty days after the invitations are issued. Any amendment adopted at the conference by a two-thirds majority of all States Parties shall be promptly circulated by the depositary to all States Parties.

2. The amendment shall enter into force for each State Party that deposits its instrument of ratification, acceptance or approval of the amendment on the thirtieth day after the date on which two-thirds of the States Parties have deposited their instruments of ratification, acceptance or approval with the depositary. Thereafter, the amendment shall enter into force for any other State Party on the day on which that State Party deposits its instrument of ratification, acceptance or approval of the amendment.

Article 21

1. Any State Party may denounce this Convention by written notification to the depositary.

2. Denunciation shall take effect one hundred and eighty days following the date on which notification is received by the depositary.

Article 22

The depositary shall promptly notify all States of:

(a) each signature of this Convention;

(b) each deposit of an instrument of ratification, acceptance, approval or accession;

(c) any reservation or withdrawal in accordance with Article 17;

(d) any communication made by an organisation in accordance with paragraph 4(c) of Article 18;

(e) the entry into force of this Convention;

(f) the entry into force of any amendment to this Convention; and

(g) any denunciation made under Article 21.

Article 23

The original of this Convention, of which the Arabic, Chinese, English, French, Russian and Spanish texts are equally authentic, shall be deposited with the Director-General of the International Atomic Energy Agency who shall send certified copies thereof to all States.

IN WITNESS WHEREOF, the undersigned, being duly authorized, have signed this Convention, opened for signature at Vienna and at New York on 3rd March, 1980.

ANNEX I

LEVELS OF PHYSICAL PROTECTION TO BE APPLIED IN INTERNATIONAL TRANSPORT OF NUCLEAR MATERIAL AS CATEGORIZED IN ANNEX II

1. Levels of physical protection for nuclear material during storage incidental to international nuclear transport include:

(a) For Category III materials, storage within an area to which access is controlled;

(b) For Category II materials, storage within an area under constant surveillance by guards or electronic devices, surrounded by a physical barrier with a limited number of points of entry under appropriate control or any area with an equivalent level of physical protection;

(c) For Category I material, storage within a protected area as defined for Category II above, to which, in addition, access is restricted to persons whose trustworthiness has been determined, and which is under surveillance by guards who are in close communication with appropriate response forces. Specific measures taken in this context should have as their object the detection and prevention of any assault, unauthorized access or unauthorized removal of material.

2. Levels of physical protection for nuclear material during international transport include:

(a) For Category II and III materials, transportation shall take place under special precautions including prior arrangements among sender, receiver, and carrier, and prior agreement between natural or legal persons subject to the jurisdiction and regulation of exporting and importing States, specifying time, place and procedures for transferring transport responsibility;

(b) For Category I materials, transportation shall take place under special precautions identified above for transportation of Category II and III materials, and in addition, under constant surveillance by escorts and under conditions which assure close communication with appropriate response forces;

(c) For natural uranium other than in the form of ore or ore-residue, transportation protection for quantities exceeding 500 kilograms U shall include advance notification of shipment specifying mode of transport, expected time of arrival and confirmation of receipt of shipment.

ANNEX II

TABLE: CATEGORIZATION OF NUCLEAR MATERIAL

Material	Form	Category		
		I	II	III[c]
1. Plutonium[a]	Unirradiated[b]	2 kg or more	Less than 2 kg but more than 500 g	500 g or less but more than 15 g
2. Uranium-235	Unirradiated[b]			
	- uranium enriched to 20% ^{235}U or more	5 kg or more	Less than 5 kg but more than 1 kg	1 kg or less but more than 15 g
	- uranium enriched to 10% ^{235}U but less than 20%		10 kg or more	Less than 10 kg but more than 1 kg
	- uranium enriched above natural, but less than 10% ^{235}U			10 kg or more
3. Uranium-233	Unirradiated[b]	2 kg or more	Less than 2 kg but more than 500 g	500 g or less but more than 15 g
4. Irradiated fuel			Depleted or natural uranium, thorium or low-enriched fuel (less than 10% fissile content)(d)(e)	

(a) All plutonium except that with isotopic concentration exceeding 80% in plutonium-238.

(b) Material not irradiated in a reactor or material irradiated in a reactor but with a radiation level equal to or less than 100 rads/hour at one metre unshielded.

(c) Quantities not falling in Category III and natural uranium should be protected in accordance with prudent management practice.

(d) Although this level of protection is recommended, it would be open to States, upon evaluation of the specific circumstances, to assign a different category of physical protection.

(e) Other fuel which by virtue of its original fissile material content is classified as Category I and II before irradiation may be reduced one category level while the radiation level from the fuel exceeds 100 rads/hour at one metre unshielded.

FOOTNOTES: TASK VI

1. Lay, Churchill, Nordquist, New Directions in the Law of the Sea, Introduction, volume I, p.xx.

2. Stockholm Declaration on the Human Environment, Preamble and Principle 24.

3. "Political and Institutional Implications of the Seabed Assessment Program for Radioactive Waste Disposal," Urban Systems Research and Engineering, Inc., p. 1.

4. D. Deese, Nuclear Power and Radioactive Wastes, pp. 83-85.

5. Convention on the Prevention of Marine Pollution by Dumping of Wastes and Other Matter, London, 29 December 1972, article IV, section (1) part (a).

6. Ibid., annex I (6).

7. Ibid., article IV, section I (b).

8. Ibid., annex II (d).

9. John Norton Moore, Esq., Interview, 12 June 1981 (As of this date, there was no one at the State Department available for comment).

10. As the 1973 Convention was not accepted by a sufficient number of nations to permit it to enter into force, it was superceded by the Protocol of 1978 Relating to the International Convention for the Prevention of Pollution from Ships, 1973. (The Marpol Protocol)
    The 1978 Marpol Protocol includes most of the requirements of Marpol 1973 Annexes I and II remain obligatory, and Annexes III, IV and V remain optional.
    From House Report No. 96-1224, Merchant Marine and Fisheries Committee, 18 August 1980, p. 4.

11. International Convention for the Prevention of Pollution From Ships 1973, Preamble.

12. Ibid., article I, section (1).

13. Ibid., article II, section (3).

14. Lay, Churchill, Nordquist, New Directions in the Law of the Sea, volume I, Introduction, p. xx.

15. Convention for the Prevention of Marine Pollution by Dumping From Ships and Aircraft (Oslo), annex I, section (6).

16. Ibid., article 19, section (1).

17. Ibid., article 16.

18. Ibid., article 9.

19. Nuclear Law Bulletin No. 13 (OECD/NEA),April 1974, p. 43-44.

20. House Report No. 96-1224, Merchant Marine and Fisheries Committee, 18 August 1980.

21. Dorothy Zinberg, "The Public and Nuclear Waste Management," The Bulletin of the Atomic Scientists, January 1979, p. 34.

22. Mason Willrich and Richard Lester, Radioactive Waste: Management and Regulation, 1977, p. 77.

23. Dr. B. Goldschmidt, "The Negotiation of the Non Proliferation Treaty (NPT)," IAEA Bulletin, volume 22, nos. 3-4, August 1980, p. 77.

24. Ibid.

25. Ibid., p. 78.

26. "The Present Status of the IAEA Safeguards on Nuclear Fuel Cycle Facilities," IAEA Bulletin, volume 22, nos. 3-4, August 1980, p. 17.

27. IAEA Statute, article III.5.

28. Treaty on the Prohibition of the Emplacement of Nuclear Weapons and Other Weapons of Mass Destruction on the Seabed and Ocean Floor and in the Subsoil Thereof, Preamble, 11 February 1971.

29. Ibid., article I, sections I, II, III.

30. Treaty Establishing the European Atomic Energy Community, chapter III, article 37.

31. Nuclear Law Bulletin, No. 13 (OECD/NEA), April 1974, p. 53.

32. Convention on Third Party Liability in the Field of Nuclear Energy April 1960, Paris.

33. Convention Relating to Civil Liability in the Field of Maritime Carriage of Nuclear Material, Preamble, December 1971.

34. John Norton Moore, Esq., Interview 12 June 1981.

35. G.I. Rochlin, Plutonium, Power, and Politics, University of California Press, 1979, p. 253.

36. Ibid, p. 252.

37. David Deese, Nuclear Power and Radioactive Waste, p. 98.

38. Rochlin, Plutonium, Power, and Politics, University of California Press, p. 197.

TASK VII:

Describe and Assess the Relevance for the Subseabed Disposal Assessment Program of the Policies and Perceptions of Those Island Nations in Geographic Proximity to Sites Being Assessed.

During the Senate hearings on S.2189, the bill which in abridged form became the Low-Level Waste Policy Act of 1980, Senator Spark Matsunaga of Hawaii left little doubt that the Pacific island nations and U.S. trust territories are concerned about the possibility of the implementation of subseabed disposal option in that area.[1]

In his statement, Senator Matsunaga pointed out several issues relating to the response of Pacific nations to a possible subseabed nuclear waste disposal option.

His first observation was that the Department of Energy (DOE) consideration of ocean bed storage of nuclear waste materials outside of U.S. territorial jurisdictions is "most disconcerting" to the people of Hawaii and the Pacific trust territories. Consideration of internationally located sites is "almost as alarming to the people of the Pacific as would be nuclear waste storage withing the territorial boundaries of the American Pacific."[2]

Senator Matsunaga's second point concerned the fact that his Amendment (Sec. 605 of P.L. 96-205) to the Omnibus Territories authorization bill requires "an Act of Congress before the Federal government would be authorized to begin the implementation of any plan to store nuclear wastes within the jurisdictional boundaries of any U.S. territory or possession anywhere in the world."[3] The international nature of sites under consideration by DOE for subseabed disposal mean, he stated, that the protections provided here to the people of the territories may not be effective.

His third point discusses the possibility that significant risks to the health and safety of the peoples of the Pacific are inherent in subseabed nuclear waste emplacement.

Extensive hearings by the Energy and Natural Resources Committee are called for, he states, before a decision is made by the Federal government to begin implementing plans to store nuclear wastes on the ocean floor. Senator Matsunaga received assurance from Senator Johnston, the floor manager of the Waste Policy Bill (S.2189) that such hearings would occur.

Expressions of concern over possible nuclear waste management schemes in the Pacific region have been numerous within the past year. Australia's government expressed concern in May 1980 about a U.S. proposal to store nuclear wastes on Midway, Wake or Palmyra Islands.[4] The United States had hoped to locate an Away-From-Reactor storage site (AFR) in the Pacific region, in cooperation with the Japanese. United States interest in studying a Pacific site was reportedly based on non-proliferation concerns. Our knowledge of the Japanese, South Korean and Taiwanese nuclear power programs and the fact that Japan will not be reprocessing all its spent fuel inspired the study.[5]

Nuclear power opponents from sixteen nations met to oppose the joint Japanese-U.S. plan pledging resistance to use of any Pacific Ocean locale for spent fuel storage. The so-called "Nuclear Free Pacific Conference" consisted of members of a range of environmental groups from Australia, Canada, Japan, the Phillipines, New Zealand, the U.S. and Pacific nations and territories.[6]

Final agreement on a study of the feasibility of Pacific island nuclear waste storage was not reached between the U.S. and Japan until November 1980.[7] Protests continued, however. Antonia Boya Won Pat, U.S. representative from Guam indicated her displeasure in a letter to Secretary of State Muskie in August.[8] A governors' meeting in Honolulu on October 2-3 produced a statement of opposition drafted by the governors of Hawaii, Guam, American Samoa, and the northern Mariana Islands.[9]

It is clear, therefore, that any discussion of the subseabed disposal option could arouse severe political opposition in the Pacific. Antagonism stems in part from anti-colonial sentiments and part from mistrust inspired by the history of nuclear weapons tests in the region.[10] Plans are underway presently by the displaced people of Bikini Atoll to file a 450 Million dollar suit against the United States for injuries, damages to the islands and the failure of the American government to live up to its obligations.[11]

Japan's plans to dump small quantities of low-level wastes 1,000 miles north of Guam were rescheduled following protests by Pacific island governments, anti-nuclear, and fishermen's groups.[12] Low-level waste disposal projects also generated the islanders' opposition, which could prove a severe roadblock to any Subseabed Program implementation.

FOOTNOTES: TASK VII

1. Congressional Record (Senate), 30 July 1980,S.10264-65.
2. Ibid., S.10265.
3. Ibid.
4. New York Times, 12 May 1980, p. 21.
5. Nucleonics Week, 12 June 1980.
6. Ibid.
7. Nucleonics Week, 24 November 1980
8. New York Times, 17 August 1980, p. 13.
9. New York Times, 5 October 1980, p. 13.
10. Nucleonics Week, 12 June 1981, p. 15.
11. New York Times, 15 March 1981, p. 15.
12. New York Times, 18 March 1981, p. 7.

TASK VIII

Description and Analyses of Policies of Governments Having the Need for High-Level Nuclear Waste/Spent Fuel Disposal*

"Energy itself has become an inescapably international issue. The policies of individual states, even if intended to affect only the management of energy within their own borders, have an international impact.[1] Nuclear waste disposal programs, as components of energy policies, contribute to the international energy scenario. Consideration of the issues impacting a subseabed nuclear waste disposal program which may be managed at the multilateral or international level must include assessments, periodically updated, of waste disposal needs and programs and a general survey of political atmosphere in possible participant states.

Here, most emphasis was placed on nations of the "western industrialized" sector. While it may be useful, given the possible international nature of the Subseabed Disposal Program to determine eastern European bloc nations' positions, those nations have not been as open with information regarding their needs as have their western neighbors. Although some speculation has been made about several eastern European countries' waste disposal needs,[2] consideration was focused on those governments likely to be receptive politically and economically to a multilateral or international enterprise undertaken jointly with the United States or with each other.

What follows is a summary of these nations' current policies regarding nuclear energy, nuclear waste disposal research and development programs, and the political environment currently affecting them. Assessment of each nation's possible acceptance, participation, or tolerance of a Subseabed Disposal Program is also included. Less developed countries of Latin America and the Pacific will be discussed under a separate heading.

Eighteen nations currently produce electricity from uranium fuels.[3] Others must demonstrate the capability to dispose of nuclear wastes before atomic power generation can commence.

Australia

Australia currently owns and operates no nuclear power generating facilities. Mining and milling wastes are produced from uranium mining activities. Australia is the principal source of uncertainty about the world's uranium resources, having many known ore deposits and a minerals policy characterized by a wariness of foreigners.[4] For this reason, Australia is an influential actor with respect to the other nations' waste disposal practices. Assurances of uranium supply may affect a nation's decision regarding reprocessing facilities; and therefore generation of high-level wastes for disposal. Australia's reputation adds to the uncertainty surrounding uranium resource availability for

*See chart at end of Task VIII.

nuclear nations. She permits exports under strict controls and in small quantities as assurance against proliferation.[5]

The Australian government decided in December 1980 to permit countries buying Australian uranium to reprocess spent fuel with the condition that they follow strict safeguard provisions. Canada and the U.S. and the other major world exporters of uranium for nuclear fuel currently do not permit reprocessing.[6]

Australia is a party to the NPT and currently has IAEA/NPT safeguards in force.[7] Deese has indicated that Australia might be more receptive to the Subseabed Disposal Program if it were part of a broader non-proliferation arrangement.[8] A large, stable land area makes Australia one of the three countries considered geologically most promising for land-based disposal facilities. It is questionable whether Australia would be considered as a host state given a possible international land-based disposal site as conceived by the International Nuclear Fuel Cycle Evaluation Working Group 7.[9] The possibility cannot have escaped the Australian government. However, for that reason, the substitution of an internationally located site (such as the subseabed) for an international waste disposal facility may be more attractive to the Australians.

Austria

All nuclear energy related activities were suspended following a referendum of November 1978. Prior to the vote, Austria was actively pursuing investigations of hard rock as a disposal medium.[10] Austria is not currently researching radioactive waste disposal alternatives and is not a member of the Seabed Working Group of the OECD/NEA.[11]

Her status as the "mother country" of the IAEA (Vienna is the organization's base) might make her receptive to a Subseabed Disposal Program if it were part of a broader non-proliferation arrangement.

Austria is a non-weapons state, and a signatory of the Non-Proliferation Treaty. Austria is a party to the London Dumping Convention, although her lack of a coastline reduces her oceans policy to a question of principle.

Belgium

Belgium's current power generating capacity is 1,744 megawatts (Mw) at three stations.[12] She contracts with France through the Cogema Agreements for reprocessing the spent fuel from her reactor programs.[13] Belgian research and development work is carried out with the participation of the Commission of the European Communities.[14] Belgium has taken advantage of the ocean as a disposal site for low and intermediate level wastes through the disposal practices of the NEA community.[15] Belgium is also investigating nuclear waste disposal in clay formations underlying the reactor at Mol.[16] The economies of scale implied by multilateral disposal facilities and Belgium's observed willingness to centralize the

waste from her reactors through the Cogema process imply that she may become interested in the subseabed disposal option once one is established. Belgium is not currently participating in the activities of the Seabed Working Group, however.

Britain

With current nuclear power generating capacity of 9,013 megawatts, the United Kingdom is highly dependent on her nuclear generated power supplies.[17] The third member of the United Reprocessors Gmbh, with France and West Germany, she is economically committed to reprocessing.[18] However, the reportedly high levels of radioactive waste pollution eminating from the Windscale plant may not be allowed to continue indefinitely.

Britain is tightly constrained in her search for a land-based disposal option by the availability of sites within her borders and political opposition to development of the possibly useful sites which have been located in the granite of southwestern Scotland.[19]

Subseabed waste disposal appears particularly attractive to the United Kingdom in light of the fact that ocean dumping of low-level waste is an established practice.[20] An ocean disposal program for high-level wastes might therefore meet with less public opposition in Britain than elsewhere. Given the impact on the world environmental movement of the Torrey Canyon incident off her coasts, Britain's participation in the London Dumping Convention and her continued interest in subseabed disposal make her an interesting case for other European nations who might consider participation in a Subseabed Disposal Program.

Canada

Canada's nuclear generating capacity stands presently at 5,588 Mw.[21] She mirrors U.S. policies, and stores her spent fuel at reactor sites without reprocessing.[22]

Canada is a supplier of CANDU reactor technology and uranium for nuclear fuel. Currently, the Canadian nuclear industry is percieved as struggling, and many jobs may be lost unless export contracts go through with Rumania, Mexico, and South Korea. In 1977, following the United States' example, Canada sought renegotiation of uranium supply agreements to include stronger safeguards, notably the prohibition of reprocessing of nuclear fuel of Canadian origin. The strict standards have lessened the attractiveness of Canadian export services, but the government has voted not to moderate them.[23]

Canadian waste management has been heavily focused on disposal in hard rock formations.[24] Canada's abundant stable land area makes her appear to the geologist to be one of the three non-communist nations possessing adequate land-based disposal sites.[25] She is, however, an

active member of the Seabed Working Group of the OECD/NEA.

Canada has a reputation as an international leader in marine protection. For Example, the Canadian Arctic Water Pollution Prevention Act (1970) imposes strict controls over vessels within the Canadian economic zone; a philosophy not jointly shared with other nations.[26]

Canada's reputation for strict environmental and safeguard controls indicate that she would look most favorably on a Subseabed Disposal Program that would be operated within a larger framework encompassing non-proliferation as well as waste disposal goals. In international seabed mining negotiations, Canada, with its own mineral interests, has often sided with the Third World "Group of 77" positions on seabed minerals issues.

Denmark

Nuclear fission may not be considered for power generating purposes here until geologic disposal facilities have been demonstrated within national boundaries.[27] While the Danish government might be receptive to some international agreement for high-level waste disposal in territory other than Danish soil, strict assurances of availability would be necessary. Such institutional assurances are difficult to insure over the length of time required for nuclear waste disposal.

Salt is being considered as a disposal medium with the assistance of the Commission of the European Communities.[28]

Finland

Finland has a current nuclear generating capacity of 2,296 Mw.[29] She does not contract with Cogema for reprocessing services.

International cooperation in waste disposal programs is important to Finland, as her land-based options are limited. Currently, plans call for shipment of spent fuel abroad to Sweden which shares the problem of disposal site scarcity, but has developed a temporary repository for spent fuel storage. A high-level waste repository is also being investigated by the industry and government.[30] Finland is not actively participating in the Seabed Working Group.

France

Nuclear generating capability of 18,300 Mw from 25 plants is currently available.[31] Strong emphasis has been placed on breeder development and reprocessing. Facilities at Cap de La Hague are capable of reprocessing lightwater reactor (LWR) fuel, low enriched uranium and breeder reactor fuels. The facility services French

reactors, with extra capacity contracted out through Cogema, a subsidiary of The Commissariat al'Energie Atomique, to Japan, Sweden, the Federal Republic of Germany, The Netherlands, Belgium and Switzerland. The acceptance of their fuel for reprocessing serves to centralize the European waste disposal problem somewhat. Cogema is free to retain plutonium extracted from foreign spent fuel for its own use, placing it under international controls. Contract provisions are secret, however. The facilities at La Hague are experiencing difficulties with waste build up. There is one ton of radioactive sludge from degraded gas graphite fuel which has been left in storage tanks too long. Cogema has no idea what to do with it according to dissatisfied workers at the La Hague plant.[32]

French policy under Giscard d'Estaing did support the development of European fuel cycle independence based on interdependence through bilateral and multilateral agreements such as the Cogema arrangements and United Reprocessors Gimbh. In particular, he supported France's ambition to be in a unique position to offer technological knowledge in all stages of the fuel cycle, idea being that no matter what the energy situation presently in other nations, they would eventually step up their own nuclear programs, and turn to France for assistance.[33]

D. Deese, citing Barbreau (1977),[34] has suggested that France may have come closest of all nations to a national policy incorporating subseabed disposal of transuranic wastes. Although France has not carried out ocean dumping operations since 1971, at one time she did dispose of radioactive wastes within the framework of the NEA/London Dumping Convention agreements. France is a member of the Seabed Working Group. Research and development of final disposal facilities in granite are also underway.

The current political situation in France may have implications for the direction of her nuclear industry over the next decade. Francois Mitterand, the socialist leader, has replaced M. Giscard d'Estaing as French president and he has the support of the nation behind his socialist policies as reflected in the parliamentary elections of June 14 and 21 of this year.[35] During his campaign, Mitterand promised decreased emphasis on nuclear power production and a slow down of reprocessing at Cap de La Hague.* French ecologists are urging that he live up to his promises. Should he implement these policies, France would have to pursue new paths for resolving its nuclear waste problem, and the other nations which depend on the La Hague facility to alleviate some of their nuclear waste problems would also have to consider other alternatives. Subseabed disposal might then come under closer scrutiny by France and her Cogema contractors, notably Japan.[36]

France's status as a non-NPT weapons state could prove an obstacle to her participation in any program involving disposal of wastes in the international commons of the subseabed although the U.S. has supported French nuclear activities despite this. The near absence of IAEA overview of waste and spent fuel stores in France and the concurrent possibility that France might attempt to dispose of defense wastes through the seabed program facilities raises questions about her current political

---

*Science magazine, 27 November 1981, p. 1006, reports Mitterand appears to be continuing the reprocessing policies of his predecessor despite campaign promises.

status regarding implementation of the Subseabed Disposal Program. She is, however, a participant in the Seabed Working Group of the OECD/NEA.

Federal Republic of Germany

German nuclear generating capacity is 8,996 Mw.[37] Spent fuel is not considered a waste and reprocessing is established in Germany, the third partner in the United Reprocessors Gmbh and a Cogema contractor. One hundred percent of German uranium is imported.[38]

German progress on waste disposal research and development at the Asse salt mine and at Gorleben has been held up by local politics. Asse is not to be reopened for use by the industry, but will be used only for government managed experimental work.[39] Difficulties at Asse and Gorleben have led to a general agreement that the outlook for nuclear programs in Germany hinges totally on political decisions.[40] German law requires that no additional plant licenses will be considered until a fuel management procedure has been decided upon.[41]

Recent statements by German political leaders indicate that nuclear power will continue to be emphasized, to reduce German dependence on imported oil which is seen as a major contribution to German economic difficulty.[42]

Continued German political controversy over the back end of the nuclear fuel cycle and legal constraints for reactor licensing imply growing pressure for solutions to her waste disposal problems. In 1980, Germany indicated an interest in the Seabed Working Group studies,[43] and as early as 1978 it was suggested that any solution situated outside German national boundaries would be welcomed.[44] Such a solution would certainly alleviate conflicts between the Federal government and the states which have final say over disposal sites within their boundaries.

Germany has not carried out ocean dumping of low-level radioactive wastes since 1971, although earlier she had participated in the NEA/London Dumping Convention disposal in the North Atlantic.

Italy

Italian research and development programs are assessing disposal feasibility in argillaceous (clay) formations. Acceptance of clay as a feasible geologic disposal medium may make nuclear waste disposal in subsea clays an attractive option technically to the Italians.

Japan

Japan is dependent on 23 nuclear stations with 15,676 Mw total capacity for the generation of nuclear energy. No licenses for additional nuclear plants are permitted without explicit arrangements for handling the spent fuel produced.[46] Waste disposal is therefore a primary concern of the Japanese power industry and the Japanese government. Japan contracts out through the Cogema arrangements for spent fuel reprocessing as part of the solution to her waste management problems. Japan requires U.S. approval for spent fuel transfers to Britain and France for reprocessing.[47]

Although an extremely limited land area constrains Japan's development of disposal sites within her national boundaries, site surveying and some studies of hydrogeological conditions at existing deep mines have been conducted. Japanese focus, however, has long been concentrated on the possibility of the subseabed disposal of high-level waste. Plans to dispose of low-level waste in the seas have been considered seriously, and have aroused the indignation of Japan's island neighbors.[48] Japan has ratified the London Dumping Convention. Although concerned about possible Soviet opposition to waste disposal at sea, the policy seems to be to forge ahead and see what results.

Waste disposal considerations are driven often by proliferation policies. Local opposition was especially strong in Japan and Europe for the shipment of spent fuel from Japan to European reprocessors.[49]

Netherlands

A very limited nuclear power generating capability (530 Mw) and the consideration of salt domes as repository sites provide the framework for nuclear waste disposal considerations in the Netherlands. The Dutch hold Cogema contracts and are considering high-level wastes for disposal. Several of the sites considered are located in salt formations under the sea off the Dutch coastline.[50] The Netherlands is a member of the Seabed Working Group of OECD/NEA. She has been a party of ocean dumping practices organized by the NEA through the mechanism of the London Dumping Convention.[51]

Norway

No nuclear power reactors presently exist in the country, although two research reactors have been producing low and intermediate level waste since 1951. No disposal studies are currently occurring in Norway, although participation in joint Scandinavian research is ongoing.[52]

Spain

Spanish nuclear generating capacity stands at 1,117 Mw.[53] The nuclear program has been characterized by a series of terrorist incidents perpetrated by Basque rebels.

Broad theoretical evaluations of geologic formations located within Spanish jurisdiction have been undertaken to determine their acceptability as high-level waste disposal sites. Currently, low-level wastes are disposed of in an abandoned uranium mine.[54]

Sweden

Current Swedish nuclear generating capacity is 6,710 MW.[55] Sweden accepts spent fuel from Finland, and holds contracts for reprocessing with Cogema.[56]

To comply with Sweden's Nuclear Stipulation Law which requires demonstration of waste disposal technology before new licenses can be approved, the Swedish power industry set up the Nuclear Fuel Safety Project. Swedish policy has focused on the spent fuel storage and disposal illustrated by the development of a spent fuel/reprocessed waste carrier ship may be interesting to the Subseabed Program, although the ship is designed for carriage over coastal waters.[57]

An Abandoned Iron Ore Mine Near Stripa: Sweden is the site of a recently organized international research project investigating granite as a host rock. The project, under the auspices of the OECD/NEA includes members from Finland, Japan, Sweden, Switzerland and the United States. France and Canada are expected to participate as associate members.[58]

Although the Stripa mine is not to be used as a final disposal site, since the value of the iron ore deposits in the area has been recognized, the project provides the most recent example of international cooperation in radioactive waste management.

Sweden has participated in the ocean disposal of low and intermediate level wastes under the auspices of the NEA/London Dumping Convention in the North Atlantic, although not since 1971.[59]

Sweden's decision to store spent fuel rather than reprocess may affect her policy towards a subseabed disposal project should one become available. The question is whether or not spent fuel would be (1) acceptable for disposal in such a facility, (2) a resource that the Swedes would look favorably on relinquishing.

Switzerland

Swiss nuclear generating capacity presently is 2,034 Mw,[60] and she holds Cogema contracts for reprocessing of spent fuel. Safe disposal of all kinds of nuclear waste must be demonstrated by 1984 under the recently enacted Atomic Law. Geological host sites are under investigation within Swiss borders, and Switzerland will be a participant in the OECD/NEA research in granite as a host medium at Sweden's Stripa mine.[61] The Swiss also participate in the Seabed Working Group.

As previously mentioned, the Swiss are currently attempting to negotiate a bilateral agreement with Australia concerning uranium fuel supply. The Canadians, who had been suppliers until 1977 imposed an embargo on Swiss shipments in that year.[62]

Switzerland was one of the INFCE participants strongly in favor of allowing countries the right to decide whether reprocessing was in their best interest.[63]

The Swiss have utilized the NEA ocean dumping site in the North Atlantic for disposal of low-level radioactive wastes.[64]

ADDENDA I

NATIONS WITH POTENTIAL NEED FOR HLW/SPENT FUEL REPOSITORY

CURRENT NEED

Significant and Large Existing Stock HLW	Significant and Small Existing Stock HLW
* Canada	Argentina
* France	● * Belgium
● * Germany, Fed. Rep.	Bulgaria
● * Japan	Czechoslovakia
* United Kingdom	Finland
● * United States	Germany, Dem. Rep.
USSR	India
	Italy
	Korea
	* Netherlands
	Pakistan
	Spain
	● * Sweden
	● * Switzerland
	Taiwan

* express interest in Subseabed Disposal Program.

● self-imposed deadline for HLW repository prior to year 2000.

NATION	CURRENT NUCLEAR POWER GENERATING CAPACITY ① (MW gross)	REPROCESSING? ②	GOVERNMENT GENERALLY FAVORABLE TO NUCLEAR PROGRAMS?	RESPONSIBILITY FOR FUEL CYCLE BACK-END/ DISPOSAL IMPLEMENTATION	STIPULATION LAW? Ⓐ ②	OCEAN DUMPING OF LLW? ③ (NEA OR OTHER)	SWS MEMBER?
BELGIUM	1744	yes — own plants and COGEMA	yes		NO	YES (NEA)	NO
CANADA	5588	NO — indefinitely deferred	yes	STATE: SPENT FUEL STORAGE / STATE	NO	NO	YES
FRANCE	18,283	yes — contracted out only	yes, BUT... Ⓑ	STATE / STATE	NO	YES (NEA) not since 1971	YES
FEDERAL REPUBLIC OF GERMANY	8996	yes — own plants and COGEMA contracts	yes, BUT... Ⓒ	MIXED (STATE AND PRIVATE) AND CONTRACTED / MIXED	YES	YES (NEA) not since 1981	NO
JAPAN	15,676	yes — own plant and COGEMA contracts	yes	PRIVATE AND CONTRACTED / MIXED	YES	YES (OTHER) (unilateral action)	YES
SWEDEN	6710	yes — only contracted. recent emphasis on SPENT FUEL AFR STORAGE	divided	MIXED: SPENT FUEL STORAGE AND CONTRACTED REPR. / MIXED	YES	YES (NEA) not since 1971	NO
SWITZERLAND	2034	yes — only contracted	divided		YES	YES (NEA)	NO: OBSERVER
UNITED KINGDOM	9012	yes — own plants	yes	STATE / STATE	NO	YES (NEA) also unilateral: ex: windscale discharges	YES
UNITED STATES	56,604	NO — indefinitely deferred	divided, but shifting: favor Ⓓ	PRIVATE SECTOR / MIXED MOSTLY STATE	NO: national; yes: states (1 state)	YES (OTHER) unilateral action in US coastal waters not since 1970	YES

① APRIL 1981: NUCLEONICS WEEK

② Report by International Energy Associates Ltd for U.S. DOE. Fall 1980

③ Vanlis and Forster "Disposal of Radionuclides in the Sea" IAEA BULLETIN VOL 21 #4 AUGUST 1979

Ⓐ NEW REACTOR LICENSING DEPENDENT ON WASTE MANAGEMENT DEMONSTRATION.

Ⓑ MITTERAND'S SOCIALISTS MAY LESSEN NATIONAL EMPHASIS ON NUCLEAR POWER: FREEZE NEW PROJECTS. (SCIENCE JUNE 1981.)

Ⓒ FUEL CYCLE 'BACK END' POLITICS HAVE HAD NEGATIVE IMPACT ON NUCLEAR POWER POLICIES AND PUBLIC PERCEPTIONS

Ⓓ US POLICY UNDER REAGAN WILL BE SUPPORTIVE OF NUCLEAR INDUSTRY

ADDENDA III

Special Report

Fuel Reprocessing & Storage

Jimmy Carter's attempt to kill off reprocessing around the world seems to have failed, for the news stories in this Nucleonics Week/NuclearFuel Special Report portray a matter-of-fact advance toward it in country after country – other than the U.S. Look at just a handful of the stories:

> *French deny they're reconsidering selling reprocessing plant to Pakistan. . . . West Germany starts licensing proceedings for a reprocessing plant, a prerequisite for power plant operating licenses. . . . Critics present litany of complaints about La Hague plant, and mishaps occur there, but Cogema defends its profitable operations. . . . Sweden pressing for generic U.S. approval of reprocessing. . . . India plans more at-reactor small reprocessing units.*

And the idea of reprocessing refuses to die even in the U.S., what with a Texas advisory group calling for its approval, a committee of scientists urging Carter to reconsider his stand, DOE pondering use of AGNS' Barnwell plant for plutonium production, the ghost of Gesmo hovering over Congress and NRC – and then the election of Reagan suggesting a reversal of U.S. policy.

But, one way or the other, nations must provide spent fuel storage, and the raging pro and con, the estimates and re-estimates of when the crunch will come, the moves toward establishment of away-from-reactor storage facilities, the different options for these, the more-immediate job of getting reactor storage pools reracked – and getting them approved for use – make for a fascinating and exciting story of what 1980 held in this nuclear power arena.

It's all here in FUEL REPROCESSING & STORAGE, a compilation of everything of importance and interest on those topics that was carried last year in Nucleonics Week and NuclearFuel. This 47-page Special Report's repackaging of the material gives you a review of the events and a perspective that help you make business sense out of the chaotic conditions of the market.

Order FUEL REPROCESSING & STORAGE today; price $85, but *please specify Series 7* so as to distinguish from the Special Reports of previous years. Telephone toll-free 800-223-6180 (if within New York State call collect 212-997-6410), or write Nucleonics Week/NuclearFuel, 1221 Avenue of the Americas, New York, N.Y. 10020.

A PENNSYLVANIA ANTINUCLEAR GROUP SAYS THAT PHILADELPHIA ELECTRIC SPIES on its demonstrations and has been taking photographs of demonstrators "in order to distort the image of the opposition" to Philadelphia Electric participation in nuclear power plant operation and construction, according to a source at the Keystone Alliance. The group has brought an action before the Pennsylvania Public Utility Commission to block the use of ratepayer funds for the alleged surveillance. The utility's public relations department, which according to the alliance has been handling the utility's alleged surveillance activities, has denied the group's charges, calling them "an excuse to get their foot in the door so that, through interrogatories, they can get every piece of paper we've printed in the past four years. They're trying to grab media attention with these outrageous charges."

The case before the PUC, which also involves the alliance's objections to the use of rate revenues for what a source in the antinuclear group called "the promotion of nuclear power through advertising and contributions to the Edison Electric Institute and the Atomic Industrial Forum," is being heard by an administrative law judge who will probably not render an opinion until the end of the year, according to sources on both sides of the matter. The commission is then free to accept, amend or reject the judge's opinion.

While the Keystone Alliance has accused Philadelphia Electric of conducting "ongoing" surveillance of antinuclear demonstrations, including "taking a lot of pictures and [automobile] license numbers," a utility

REPRINTED BY PERMISSION

source denied the charges. He said that on one occasion photographs had been taken of a demonstration in order to "notify the local [television] stations that they were coming out to cover programs listing different [antinuclear] organizations, when they were really all the same."

The beginning of the PUC case last month was preceded by the release of a report written by the Center for National Security Studies, a project of the American Civil Liberties Union, charging that there has been "a significant amount of spying on and disruption of the antinuclear movement" in the U.S., according to an ACLU source. He added, "Most of the spying is legal, even though it violates an intuitive sense of privacy rights." According to the report, open antinuclear meetings are monitored, demonstrations are photographed by local police, and antinuclear groups are infiltrated, all by state and local police, the federal government, utility operatives and, to a "surprisingly large extent," privately owned intelligence services. The source, who said that he and his group had not taken a position on nuclear power, said, "The situation fits the subject of spying on groups not because of their illegal acts but because they are politically unpopular or irritating." Yet, the source added, "The nuclear industry does have some national security significance, and the rationale is to protect it against hostile acts."

SUPER-SARA HAS BEEN ALLOCATED ABOUT $46-MILLION BY THE EEC Council of Ministers. The project at the EEC Joint Research Center in Ispra, Italy, is designed to simulate various kinds of loss-of-coolant accidents in PWRs and BWRs. Following Three Mile Island, the program was revamped to include work on small and medium loss-of-coolant breaks as well as large ones. The funds voted by the council assure the project's continuation through 1983.

REACTOR NOTES PERTAINING TO NUCLEAR ELECTRICITY GENERATING TABLE which starts on the next page: Enel's Latina unit, off line since last September for maintenance, returned to service April 14. . . . Also in Italy, Caorso was shut down May 2 for six days when a damaged valve in the auxiliary circuit of the primary containment vessel caused some water loss and increased radioactivity. Repair of the valve was immediate but the unit remained down for inspection of the suspensions on fastenings for recycle water pipes. . . . According to Kyushu Electric Power, Genkai-1 has set a record for continuous operation of a Japanese nuclear plant. The unit had run for 322 consecutive days as of May 7, and is expected to remain in operation through May 30, completing a 345-day run before being brought down for refueling and maintenance. . . . Sacramento Municipal Utility District shut down Ranch Seco May 17 when a small leak in one or more of the steam generator tubes set off a radiation alarm. Babcock & Wilcox, manufacturer of the reactor and generators, and Smud officials are inspecting for further leaks. . . . Baltimore Gas & Electric's Calvert Cliffs-1 was out of service April 3-9 for periodic inspection of reactor snubbers. Thirty snubbers required reinforcement to insure adequate seal life. . . . The Power Authority of the State of New York's Indian Point-3 returned to operation April 2 after repairs of the turbine. The unit operated at partial power throughout the month, however, while voltage conversion equipment in the switchyard was under repair.

Explanation of symbols used in generating table on following pages

[a]amended total corrects previous error [b]awaiting licensing action as result of TMI accident [c]down for modification [f]down for refueling [k]permanently shut down; figures, representing final power generation in March, remain as they were at end of that month and are retained to provide proper U.K. total generation in 1981 [m]down for maintenance and inspection [p]in power testing stage [r]down for repair [s]includes 1,342 Mwh equivalent in steam production [w]coastdown toward refueling [z]licensed for partial power

Nucleonics Week is published every Thursday by McGraw-Hill, Inc., 1221 Avenue of the Americas, New York, N.Y. 10020. Corporate officers: Harold W. McGraw, Jr., president, chief executive officer and chairman of the board; Robert N. Landes, senior vice president and secretary; Ralph J. Webb, treasurer.

TELEPHONES

Subscription information:
Call (212) 997-3916 or
TOLL-FREE 800-223-6180
News offices:
Brussels (32-2) 513-4516, -7
New York (212) 997-3194
Washington (202) 624-7590

Nuclear Publications' staff and primary responsibilities:

Roger Newburger, manager
Mickey (Madeline) Epstein, editorial assistant
Rob Laufer, chief editor (Nucleonics Week)
Don Martin, chief editor (NuclearFuel and Inside N.R.C.)
Sandy Cannon, Washington editor (Nucleonics Week)
Stephanie Cooke, assistant editor (NuclearFuel)
Joanne Dann, Washington editor (Inside N.R.C.)
Brad Ferguson, assistant editor (Nucleonics Week)
Douglas Glucroft, European editor
Patricia Hinsberg, Washington editor (Inside N.R.C.)
Michael Knapik, Washington editor (NuclearFuel)

Nucleonics Week subscription rates: $670 per year in U.S. and Canada, $810 elsewhere (air mail delivered). Additional subscriptions after the first, to same address, in same envelope: $580 per year in U.S. and Canada, $670 each elsewhere.

© Copyright 1981 by McGraw-Hill, Inc. All rights reserved. Reproduction in any form whatsoever forbidden without express permission of the copyright owner. NUCLEONICS WEEK is Reg. U.S. Pat. Off.
ISSN 0048-105X

NUCLEAR GENERATING TABLE FOR APRIL 1981

	Capacity (Mw gross)	Mwh gross in April	Plant factor April	Total Mwh gross in 1981	Plant factor 1981	Lifetime total Mwh gross
ARGENTINA:						
Atucha	357	232,178	90.3%	931,853	90.6%	16,621,392
BELGIUM:						
Doel-1	412	0[f]	0	835,800	70.4	18,482,420
Doel-2	412	273,900	92.3	1,104,500	93.1	15,743,460
Tihange-1	920	411,000	62.0	1,476,000	55.7	34,291,000
Total, Belgium		*684,900*		*3,416,300*		
BRITAIN (*figures are for 4-week period)						
Berkeley (2 units)	334.4	0*[mr]	0	239,000	25.0	40,045,000
Bradwell (2 units)	374.1	0*[mr]	0	0	0	37,012,000
Dungeness A (2 units)	576.6	0*[mr]	0	0	0	45,371,000
Hinkley Point A (2 units)	663.9	302,000*	67.7	1,422,000	75.0	54,128,000
Hinkley Point B (2 units)	1,320	271,000*[mr]	30.6	2,021,000	53.6	20,693,000
Oldbury (2 units)	633.5	276,000*	64.8	1,276,000	70.5	39,342,000
Sizewell (2 units)	652.5	275,000*[mr]	62.7	1,263,000	67.8	54,129,000
Trawsfynydd (2 units)	584.8	268,000*	68.2	939,000	56.2	48,923,000
Wylfa (2 units)	1,352	486,000*[mr]	53.5	2,673,000	69.2	46,571,000
Calder Hall (4 units)	240	156,918	90.8	530,302	76.7	36,591,983
Chapelcross (4 units)	240	141,906	82.1	607,874	87.9	37,034,220
Hunterston A-1	169	94,282*	83.0	427,610	88.6	20,720,025
Hunterston A-2	169	85,072*	74.9	413,875	85.7	21,372,994
Hunterston B-1	660	62,040*[r]	14.0	1,029,550	54.6	11,116,170
Hunterston B-2	660	242,160*[fr]	54.6	928,650	49.3	4,997,200
Dounreay PFR	250	30,370[r]	16.9	112,430	15.6	1,008,820
Windscale AGR	32			57,998[k]	83.9	3,707,444
Winfrith SGHWR	100	70,781	98.3	286,205	99.4	6,515,156
Total, Britain		*2,761,529*		*14,227,494*		
CANADA:						
Douglas Point	220	102,130	64.5	408,920	64.5	12,269,607
Pickering-1	542	387,900	99.4	1,522,640	97.5	38,279,240
Pickering-2	542	390,060	100.0	1,532,250	98.2	37,270,060
Pickering-3	542	319,510	81.9	1,203,190	77.1	32,489,130
Pickering-4	542	392,500	100.6	1,555,910	99.7	29,829,340
Bruce-1	800	526,100	91.3	2,229,900	96.8	22,610,670
Bruce-2	800	569,100	98.8	2,042,200	88.6	22,605,840
Bruce-3	800	46,000[m]	8.0	1,744,000	75.7	19,232,320
Bruce-4	800	569,800	98.9	1,726,600	74.9	12,647,200
Total, Canada		*3,303,700*		*13,966,210*		
FINLAND:						
Loviisa-1	465	315,269	94.2	1,313,280	98.1	11,753,543
Loviisa-2	465	314,937[p]	94.1	1,122,933	83.9	1,477,577
Olkiluoto-1	683	466,648	94.9	1,755,450	89.2	9,880,797
Olkiluoto-2	683	445,890[p]	90.7	916,592	46.6	1,611,075
Total, Finland		*1,542,744*		*5,108,255*		
FRANCE:						
Bugey-1	560	372,830	92.5	1,460,050	90.5	28,136,390
Bugey-2	957	636,340	92.4	2,522,130	91.5	12,584,180
Bugey-3	957	0[m]	0	1,630,210	59.1	11,973,710
Bugey-4	957	604,910	87.8	2,606,700	94.6	11,781,660
Bugey-5	957	0[m]	0	674,010	24.5	9,031,980
Chinon-2	242	151,369	86.9	592,072	85.0	20,647,930
Chinon-3	500	201,602[m]	56.0	988,483	68.6	23,585,996
Chooz (Sena)	325	231,000	98.7	917,000	98.0	22,582,691
Dampierre-1	957	648,840	94.2	2,552,720	92.6	5,550,450
Dampierre-2	957	647,320	93.9	2,275,560	82.6	2,344,830
Dampierre-3	957	432,990[p]	62.8	1,164,720	42.3	1,164,720
Fessenheim-1	930	660,600	98.7	2,000,910	74.7	19,687,561
Fessenheim-2	930	641,540	95.8	2,551,900	95.3	19,289,201
Gravelines-B1	957	683,260	99.2	2,511,380	91.1	4,668,540
Gravelines-B2	957	524,570	76.1	2,399,570	87.1	3,786,799
Gravelines-B3	957	166,480[p]	24.2	1,303,830	47.3	1,417,030
Marcoule	43	27,119	87.6%	105,733	85.4%	10,969,479
Monts d'Arree	75	40,461	74.9	198,192	91.8	5,313,359
Phenix	250	30,020	16.7	459,760	63.9	8,870,740
St. Laurent-des-Eaux-A1	500	136,901[r]	38.0	695,746	48.3	28,977,155
St. Laurent-des-Eaux-A2	530	0[r]	0	0	0	28,457,034
St. Laurent-des-Eaux-B1	957	0[p]	0	160,650	5.8	160,650
Tricastin-1	957	235,180[r]	34.1	1,841,530	66.8	4,673,168
Tricastin-2	957	649,980	94.3	2,365,512	85.8	4,093,647
Tricastin-3	957	540,650	78.5	981,570	35.6	981,570
Total, France		*8,263,962*		*34,959,938*		
INDIA:						
Rapp-1	220	111,268	70.2	286,473	45.2	5,828,962
Rapp-2	220	58,551[p]	37.0	216,560	34.2	252,412
Tarapur-1	210	62,376	41.3	308,900	51.1	10,740,849
Tarapur-2	210	82,171	54.3	115,857	19.2	10,980,123[a]
Total, India		*314,366*		*927,790*		
ITALY:						
Caorso	860	523,699[p]	84.6	1,056,421	42.7	3,894,667
Garigliano	160	0[c]	0	0	0	12,476,362
Latina	200	58,315[m]	40.5	58,315	10.1	19,542,860
Trino	270	0[c]	0	0	0	19,682,019
Total, Italy		*582,014*		*1,114,736*		
JAPAN:						
Fukushima-1	460	95,274[fm]	28.8	991,503	74.8	16,578,128
Fukushima-2	784	533,084	94.4	2,058,134	91.2	21,077,888
Fukushima-3	784	0[m]	0	276,874	12.3	23,312,586
Fukushima-4	784	553,173	98.0	2,182,833	96.7	14,021,243
Fukushima-5	784	529,165	93.7	2,119,123	93.9	16,526,225
Fukushima-6	1,100	792,000	100.0	2,639,840[a]	83.3	12,695,290[a]
Genkai-1	559	401,816	99.8	1,606,703	99.8	21,219,341
Genkai-2	559	402,355	100.0	1,074,949	66.8	2,807,570
Hamaoka-1	540	0[fm]	0	194,728	12.5	13,862,690
Hamaoka-2	840	563,110	90.1	2,313,008	95.6	14,526,245
Ikata	566	407,492	100.0	1,333,179	81.8	13,164,241
Mihama-1	340	240,436	98.2	952,926	97.3	7,582,836
Mihama-2	500	17,879[fm]	5.0	17,879	1.2	19,539,467
Mihama-3	826	592,800	99.7	1,321,168	55.5	19,788,749
Ohi-1	1,175	0[fm]	0	1,109,750	32.8	11,493,822
Ohi-2	1,175	845,250	99.9	3,259,180	96.3	13,426,525
Takahama-1	826	444,014	74.7	2,159,319	90.8	21,548,025
Takahama-2	826	592,802	99.7	1,035,156	43.5	25,179,692
Shimane	460	0[fm]	0	476,233	35.9	20,039,441
Tokai-1	166	85,963	71.9	236,770	49.5	13,921,630
Tokai-2	1,100	792,000	100.0	3,032,350	95.7	19,160,900
Tsuruga	357	6,822[fm]	2.7	700,084	68.1	21,774,503
Fugen	165	0[r]	0	0	0	1,988,046
Total, Japan		*7,895,435*		*31,091,689*		
NETHERLANDS:						
Borssele-1	475.5	337,020	98.4	609,020	44.5	25,224,700
Dodewaard	54	25,230	64.9	122,980	79.1	4,686,325
Total, Netherlands		*362,250*		*732,000*		
PAKISTAN:						
Kanupp	137	0[m]	0	30,830	7.8	3,031,140
SOUTH KOREA:						
Kori-1	587	0[fm]	0	282,695	16.7	9,307,595
SPAIN:						
Garona	460	329,000	99.3	1,189,980	89.8	24,563,490
Vandellos	497.4	156,639[fm]	43.7	1,021,066	71.3	29,365,322
Zorita	160	106,900	92.8	435,800	94.6	12,592,800
Total, Spain		*592,539*		*2,646,846*		

	Capacity (Mw gross)	Mwh gross in April	Plant factor April	Total Mwh gross in 1981	Plant factor 1981	Lifetime total Mwh gross
SWEDEN:						
Barsebaeck-1	590	409,053	96.3%	1,615,177	95.1%	19,534,393
Barsebaeck-2	590	408,197	96.1	1,601,559	94.3	16,215,746
Forsmark-1	940	614,091	90.7	2,443,683	90.3	4,702,942
Forsmark-2	940	225,425[p]	33.3	692,214	25.6	692,214
Oskarshamn-1	460	157,331[fm]	47.5	1,024,172	77.3	23,299,640
Oskarshamn-2	590	409,058	96.3	1,652,340	97.2	23,902,920
Ringhals-1	780	547,363	97.5	2,188,029	97.4	22,169,914
Ringhals-2	840	49,586[m]	8.2	1,660,876	68.7	26,721,825
Ringhals-3	980	468,687[p]	66.4	1,207,562	42.8	1,589,085
Total, Sweden		*3,288,791*		*14,085,612*		
SWITZERLAND:						
Beznau-1	364	261,220	99.7	1,049,770	100.1	27,305,820
Beznau-2	364	267,800	102.2	1,071,730	102.2	25,457,650
Goesgen	970	673,500	96.4	2,719,900	97.4	12,676,600
Muehleberg	336	242,520	100.2	973,260	100.6	21,209,810
Total, Switzerland		*1,445,040*		*5,814,660*		
TAIWAN:						
Chinshan-1	636	403,668	88.2	1,614,948	88.2	11,514,902
Chinshan-2	636	356,421	77.8	1,554,125	84.8	8,950,718
Total, Taiwan		*760,089*		*3,169,073*		
WEST GERMANY:						
Biblis A	1,200	740,910	85.6	3,012,970	87.2	42,978,050
Biblis B	1,300	890,720	95.2	3,583,950	95.7	31,566,153
Brunsbuettel	806	334,321[m]	57.6	1,673,048	72.1	9,413,258
Isar (Ohu)	900	524,919	81.0	2,166,798	83.6	14,544,099
MZFR	57	31,513[s]	76.8	152,395	92.8	4,671,193
Neckar	856	599,260	97.2	2,406,461	97.6	24,713,176
Obrigheim	345	213,860	86.1	950,850	95.7	29,792,590
Philippsburg-1	900.3	0[c]	0	0	0	3,674,950
Stade-1	662	463,912	97.3	1,891,448	99.2	44,600,700
Unterweser	1,300	240,414[fm]	25.7	2,156,727	57.6	21,422,081
Wuergassen	670	382,797	79.4	972,938	50.4	21,993,605
Total, West Germany		*4,422,626*		*18,967,585*		
U.S.:						
New England:						
Connecticut Yankee	616	429,058	96.7	1,694,437	95.5	54,797,635
Millstone-1	690	4,500[fr]	0.9	4,500	0.2	38,800,396
Millstone-2	881	635,610	100.2	2,138,060	84.3	25,978,495
Pilgrim	685	453,930	92.0	1,551,960	78.7	29,457,273
Yankee, Rowe	185	82,641[w]	62.0	394,391	74.0	22,779,533
Vermont Yankee	540	388,974	100.0	1,462,687	94.1	27,575,534
Maine Yankee	864	606,350	97.5	2,437,150	97.9	41,639,310
Total, New England		*2,601,063*		*9,683,185*		
Middle Atlantic:						
Indian Point-2	1,022	0[cfm]	0	0	0	31,148,356
Indian Point-3	1,022	286,980[r]	39.0	890,990	30.3	23,765,780
Ginna	496	197,381[f]	55.3	1,240,349	86.8	33,180,448
FitzPatrick	850	432,480[mr]	70.7	2,023,310	82.7	24,952,156
Nine Mile Point-1	640	0[fm]	0	813,568	44.1	39,146,289
Oyster Creek	650	184,440[c]	39.4	1,324,150	70.7	42,482,740[a]
Salem-1	1,136	29,000[r]	3.5	1,902,450	58.1	18,823,960
Peach Bottom-2	1,098	576,770[r]	73.0	2,745,600	86.8	43,833,470
Peach Bottom-3	1,098	0[f]	0	1,643,900	52.0	40,670,960
Three Mile Island-1	871	0[b]	0	0	0	26,029,947
Three Mile Island-2	961	0[r]	0	0	0	2,125,528
Beaver Valley	923	297,100[r]	59.8	936,900	35.2	9,571,300
Shippingport	72	33,417[m]	64.5	153,419	74.0	6,842,336
Total, Middle Atlantic		*2,037,568*		*13,674,636*		
South Atlantic:						
Calvert Cliffs-1	890	509,307[mr]	79.5	2,121,044	82.7	32,585,748
Calvert Cliffs-2	880	473,443[4]	74.7	978,829	38.6	25,391,885
Surry-1	824	0[r]	0	0	0	31,545,342
Surry-2	824	370,225	62.4	2,070,685	87.3	30,654,782
North Anna-1	947	362,965[cfm]	53.2%	362,965	13.3%	14,699,877
North Anna-2	947	606,095	88.9	2,407,996	88.3	3,597,675
Brunswick-2	849	181,833[mr]	29.7	852,657	34.9	18,229,893
Brunswick-1	849	104,910[mr]	17.2	1,256,185	51.4	16,589,799
Robinson-2	739	495,211	93.1	1,916,693	90.1	44,269,275
Oconee-1	911	650,040	99.1	1,960,670	74.7	38,529,560
Oconee-2	911	631,290	96.2	1,994,740	76.0	33,429,740
Oconee-3	911	605,170	92.3	923,250	35.2	32,746,304
Hatch-1	813	0[f]	0	709,680	30.3	25,304,151
Hatch-2	820	507,300[r]	85.9	888,210	37.6	9,488,750
Farley-1	861	360,936[mr]	58.2	360,936	14.6	14,147,552
Turkey Point-3	728	0[fm]	0	980,415	46.8	34,719,687
Turkey Point-4	728	492,180	93.9	1,661,670	79.3	31,909,978
St. Lucie-1	853	496,710	80.9	2,303,440	93.8	24,606,550
Crystal River-3	868	195,932[r]	31.4	1,459,615	58.4	16,919,056
Total, South Atlantic		*7,043,547*		*25,209,680*		
East North Central:						
Big Rock Point	75	45,691	84.6	127,755	59.1	6,292,844
Palisades	810	550,890	94.5	2,212,520	94.8	26,776,930
Cook-1	1,089	781,190	99.6	2,946,920	94.0	38,802,580
Cook-2	1,133	0[f]	0	1,897,710	58.2	18,989,540
Davis-Besse	934	170,048[r]	25.3	1,250,814	46.5	10,226,137
Dresden-1	215	0[m]	0	0	0	16,799,254
Dresden-2	834	4[fm]	0	22,055	0.9	43,894,926
Dresden-3	832	476,981[r]	79.6	2,103,141	87.8	40,103,715
Quad Cities-1	833	579,972	96.7	2,024,114	84.4	39,403,021
Quad Cities-2	833	499,989[r]	83.4	2,047,887	85.4	38,769,438
Zion-1	1,085	129,130[fr]	16.5	424,070	13.6	40,686,035
Zion-2	1,085	656,775	84.1	2,609,380	83.5	38,063,786
Kewaunee	563	254,900	62.9	1,384,400	85.4	25,753,171
LaCrosse	55	30,325	76.6	80,394	50.8	2,511,033
Point Beach-1	524	282,160	74.8	1,120,400	74.2	34,580,120
Point Beach-2	524	190,320[fm]	50.4	1,284,440	85.1	31,408,290
Total, East North Central		*4,648,375*		*21,536,000*		
East South Central:						
Browns Ferry-1	1,098	247,330[f]	31.3	2,474,200	78.2	36,056,660
Browns Ferry-2	1,098	766,430	96.9	2,851,140	90.2	32,652,078
Browns Ferry-3	1,098	716,280[m]	90.6	2,228,230	70.5	29,665,880
Sequoyah-1	1,183	633,923[p]	74.4	1,507,723	44.3	2,064,814
Total, East South Central		*2,363,963*		*9,061,293*		
West North Central:						
Monticello	580	196,523[f]	47.1	1,263,860	75.7	36,063,955
Prairie Island-1	560	383,020	95.0	1,559,480	96.7	25,060,450
Prairie Island-2	560	241,590[f]	59.9	903,900	56.0	23,662,840
Arnold	566	0[fm]	0	931,165	57.1	18,051,217
Fort Calhoun	481	152,236[mr]	44.0	936,054	67.6	20,724,326
Cooper	801	278,852[f]	48.4	1,636,217	70.9	30,265,051
Fort St. Vrain	342	69,848[z]	28.4	335,739	34.1	2,265,655
Total, West North Central		*1,322,069*		*7,566,415*		
West South Central:						
Arkansas Nuclear I-1	910	596,882	91.1	827,242	31.6	29,002,002
Arkansas Nuclear I-2	943	0[f]	0	1,673,589	61.6	6,978,920
Total, West South Central		*596,882*		*2,500,831*		
Pacific:						
Hanford-1 (N reactor)	862	337,109[r]	54.3	443,920	17.9	48,842,707
Rancho Seco	967	0[f]	0	670,368	24.1	28,167,449
San Onofre-1	456	0[r]	0	0	0	35,526,434
EBR-2	6.0	0[r]	0	14,789	61.4	1,252,918
Trojan	1,216	760,670	86.9	2,745,495	78.4	25,726,855
Total, Pacific		*1,097,779*		*3,874,572*		
TOTAL, U.S.		21,711,246		93,106,612		

TASK VIII: FOOTNOTES

1. IAEA Bulletin, vol. 22, no. 1, February 1980, p. 1.

2. V.A. Morozov, "Waste Management Practices in Selected European Countries," IAEA Bulletin, vol. 21, no. 4, August 1979.

3. "Nuclear Generating Table for April 1981," Nucleonics Week, 28 May 1981 (Addenda to this task).

4. National Academy of Sciences, Energy in Transition 1985-2010, p. 319.

5. IAEA Bulletin, vol. 22, nos. 3-4, August 1980.

6. Nucleonics Week, 4 December 1980.

7. Treaties in Force, 1 January 1981, U.S. Department of State, p. 321.

8. David A. Deese, Nuclear Power and Radioactive Waste, p. 137.

9. International Nuclear Fuel Cycle Evaluation (INFCE), Report of Working Group 7: Waste Management and Disposal, 1980, p. 12.

10. F. Gera and J.P. Olivier, "OECD Countries Pursue Geological Disposal," Nuclear Engineering International, January 1978, p. 35.

11. IAEA Bulletin, vol. 22, nos. 3-4, August 1980.

12. "Nuclear Generating Table for April 1981," Nucleonics Week, 28 May 1981 (Addenda to this task)

13. Nucleonics Week, 20 March 1980.

14. F. Gera and H.Y. Tammemagi, "Disposal of Nuclear Wastes: A National and International Perspective," Radioactive Waste Management, vol. 1, January 1981, p. 215.

15. D. Van As and W.O. Forster, "Disposal of Radionuclides in the Sea," IAEA Bulletin, volume 21, no. 4, August 1979, p. 24.

16. Op. Cit., Gera and Tammemagi.

17. Nucleonics Week, 28 May 1981 (Addenda to this task).

18. David Deese, "A Cross National Perspective on the Politics of Nuclear Waste," The Politics of Nuclear Waste, E. William Colgrazier, ed., chapter 2.

19. Ibid.

20. "Why Not Bury the Nuclear Waste Issue in Davy Jones's Locker?" The Economist, 15 September 1979, p. 113.

21. Nucleonics Week, 28 May 1981 (Addenda to this task).

22. Nuclear News, volume 24, no. 8.

23. Nucleonics Week, 11 June 1981.

24. Op. Cit., Gera and Olivier (Footnote no. 10).

25. With the U.S. and Australia.

26. Dr. John Norton Moore, Interview, June 1981.

27. Op. Cit., Gera and Tammemagi (Footnote no. 14), p. 218.

28. Ibid.

29. Nucleonics Week,28 May 1981 (Addenda to this task).

30. Op. Cit., Gera and Tammemagi.

31. Nucleonics Week, 28 May 1981 (Addenda to this task).

32. Nucleonics Week, 20 March 1980.

33. Ibid.

34. Op. Cit., D. Deese, Nuclear Power and Radioactive Waste, p. 134.

35. New York Times, 22 June 1981.

36. Dr. Hiroaki Wakabayashi, "Strategic Viewpoint of a National Plan of High Level Waste Management," Nuclear Engineering Research Laboratory (NERL), University of Tokyo, Japan.

37. See Addenda to this section.

38. "The Federal Republic of Germany has a commitment from Cogema to reprocess all uncommitted German fuel discharged through 1985." Nuclear Engineering International, April 1980.

39. Nuclear Engineering International, March 1980.

40. Nucleonics Week, 2 April 1981.

41. Op. Cit., D. Deese, The Politics of Nuclear Waste, E. William Colgrazier, ed.

42. Helmut Schmidt in Nuclear Engineering International, January 1981. and Research Minister Andreas Von Bulow in Nuclear News, May 1981.

43. Proceedings of the Fifth Annual NEA-Seabed Working Group Meeting, Bristol, England, 3-5 March 1980.

44. Op. Cit., David Deese, Nuclear Power and Radioactive Waste.

45. Op. Cit., Van As and Forster.

46. Op. Cit., David Deese, The Politics of Nuclear Waste.

47. Ibid.

48. New York Times, 10 March, 1981, p. A7.

49. Op. Cit., David Deese, The Politics of Nuclear Waste.

50. Op. Cit., Gera and Tammemagi, p. 221.

51. Op. Cit., Van As and Forster.

52. Op. Cit., Gera and Tammemagi, p. 221.

53. See Addenda this section.

54. Op. Cit., Gera and Tammemagi, p. 223.

55. See Addenda this section.

56. Nucleonics Week, 20 March 1980.

57. Nuclear News, November 1980.

58. Nuclear News, June 1981, p. 126.

59. Op. Cit., Van As and Forster.

60. See Addenda this section.

61. Nuclear News, June 1981, p. 126.

62. Ibid.

63. Op. Cit., INFCE: Report of Working Group 7.

64. Op. Cit., Van As and Forster.

TASK IX: Describe and Assess the Role of Nations* Not Yet Faced with Need for a Disposal Method as Well as Their Participation in a Cooperative Program Assessed in Terms of Constraints and Opportunities for Multi-nation Subseabed Cooperation.

Nations not faced with disposal needs for spent fuel but which will probably have the need in twenty years (see chart at end of this section), will at least be carefully watching events unfold toward the formation of a regulatory mechanism for subseabed disposal. At the most, they will want to participate in the evolutionary activities to assure their future interests are considered.

This group of nations represents a varied set of political and economic interests, mostly Eastern bloc and Third World plus Australia. Several of these nations may have land disposal options if they choose that course (Brazil, Australia, Mexico) with vast currently uninhabited territories as potential sites. Others will either have to rely on other nations for land disposal. For example, the Eastern Bloc nations could turn to the Soviet Union, or they could perceive the subseabed option as preferable. Several of these nations (Brazil, Mexico, Iran and Iraq), while at varying stages of promoting nuclear power, also have major domestic sources of natural gas and petroleum to strengthen their bargaining powers as well as giving them a choice of energy options. While these nations are not the ones which are visibly interested in a SDP at this time, several factors could dictate their firm participation in the formation of a SDP.

Since almost half of these nations are Eastern bloc nations, they may choose to rely on the Soviet Union's land options. On the other hand, the Soviet Union, as a major maritime power, will surely assert some leverage on the formation of any system which utilizes international territory, and depending on the relationships among these Eastern European nations and the Soviet Union, could choose to do so through any one or several of them.

One might look to the position the Soviets achieved for representation of Eastern bloc nations on the chief decision-making body, the Council of the proposed Seabed Regime, to see an example of its policies in this regard. While none of these nations has a direct vested interest at this time in mining the seabed, they have negotiated guaranteed seats on the Council of the seabed authority for their current political and future economic interests. If this pattern is in any way replicated for subseabed disposal, this group of nations will impose their interests as well on the formation of the SDP, further diluting the set of objectives the arrangements for a SDP would have to consider and meet.

Australia has a unique position, already discussed in another section. It has strict controls over uranium production, use, and sales; it has very conservative policies regarding nuclear power and nuclear wastes; it is one of the three optimal stable geologic land areas cited for high level waste disposal, and it is located geographically in the Pacific, in close enough proximity to proposed burial sites to be concerned. Depending upon other

---

*See chart at end of Task IX, Addenda I

foreign policy considerations which will evolve over the next decade and the stability of its current domestic nuclear policies, Australia could oppose a SDP at the worst, and remain neutral at best, demanding a major voice in the regulation and enforcement mechanisms.

Brazil and Mexico, even if they have other energy and/or disposal options, may seek a major voice in the formation of any SDP because they both seek leadership positions in the Third World nation bloc, if an homogeneity is to be found among those nations. Citing their major roles in the UNCLOS III negotiations, acting on behalf of the "disadvantaged" states, they may, as the more developed of these nations, act on their behalf to protect the interests of Third World nations. If this becomes the case, the formation of a SDP could evolve into a global system much like the proposed Seabed Authority, in which case there will be protracted negotiations over many matters only peripheral to the disposal program. Projecting into the future for the duration of time necessary for the subseabed disposal technology to be refined and useful, the evolution of the power configurations of the international system will surely reflect a much strengthened role for these two nations. It would seem short-sighted to neglect their probable and potential roles.

ADDENDA I

NATIONS WITH POTENTIAL NEED FOR HLW/SPENT FUEL REPOSITORY

NEED IN 20 YEARS:

Australia

* Brazil

* Hungary

Iran

* Mexico

* Phillipines

* Poland

* Romania

* Yugoslavia

* Need based on currently accelerating national nuclear power program.

TASK X:

Describe and Assess the Role of Nations That Never Have the Need for High Level Waste Disposal and Their Potential Influence on Cooperative Programs.

There will most likely be a small group of nations who by choice will not use nuclear technologies and therefore will not have the problem of disposal. There will also be nations whose economies and demands will not necessitate nuclear activities and who, therefore, won't have this problem either. There will also be nations which have a land disposal option. It is difficult to tell which nations these may be in twenty years at this point in time, but it is probably safe to assume they will represent a mixture of developed and not very developed nations. Whether or not they will have a role in determining the outcome of a subseabed program will depend heavily on whether those nations wishing to implement a Subseabed Disposal Program (SDP) are able to negotiate a limited multilateral arrangement among users, or whether under similar circumstances to the UNCLOS Seabed Regime, they are forced into a mode of global negotiation. If the latter case is the reality, this last group of nations without a need for disposal could play a role by extracting something from the negotiations before agreement. This assumes that this group of nations were able to wield power as the Group of 77 have been able to do in the UNCLOS negotiations. Not knowing who or how many nations this group may represent, it is presumptuous to predict. In the worst case, they could try to bar a Subseabed Disposal Program unless financial payment for use of "Heritage of Mankind" territory were made in compensation for the use of the international seabed as a storage area for other nations' wastes. They might try to force a payment schedule through the UN or some alternative organization by which they received sizeable sums. In this case, the situation should be calculated as a possible cost in deriving the price of a SDP and ultimately in the cost of nuclear energy. On the other hand, these nations might not be able to do anything at all, if the force of necessity is strong enough and many powerful and diverse nations provide a unified front to achieve a Subseabed Program. The "non-need" nations could also play a role of dividing those nations attempting to form a SDP. They might try to use whatever powers they have to bargain and deal, fragmenting attempts at unity among those attempting to negotiate a very difficult program.

These nations will be important to watch in the next five to ten years, for if they grow in number, they represent a veritable threat to a Subseabed Disposal Program in international waters. However, if nations find suitable disposal areas within their jurisdictional boundaries offshore, these nations could be irrelevant.

TASK XI: Interpret and Analyze the Information to Give Initial Indicators of the Areas of Greatest Concern and the More Positive Areas of Support

CATEGORIES	CONSTRAINTS	AIDS
TECHNICAL VS. PUBLIC POLICY ISSUES	(1) Lack of consensus (U.S.) about type of waste to be emplaced--and need to coordinate the part of program development with European nations considering Subseabed Disposal Program. (2) Pacific site better tectonically; Atlantic site better politically. (3) "Other National" port development: Must all ports be developed to same standards? If so, who sets standards. (4) In fact, should whole system be based on uniform set of standards? Is it reasonable to assume that if Britain and France go ahead with SDP that they will follow U.S. "suggestions" about ship design, etc.?	(1) Should design system to be equal to the task of disposing "worst case" candidate and adjust later should it be shown that it's reasonable to do so. (2) Possible need for U.S. East Coast disposal site. (3) If it is shown that uniformity/ consensus are necessary between U.S. and European nations considering SDP U.S. dollars have been spent which means other nations don't need to spend as much money. They will perhaps want to accept U.S. design standards in order to save time and financial obligation.

CATEGORIES	CONSTRAINTS	AIDS
INTERNATIONAL TREATIES	(1) London Dumping Convention a necessity to develop "accident scenario" within the framework established by 1974 Recommendations and Definition: requires international (all signatories) consensus; adds difficulties in that many signatories will not feel the need for program development in even the distant future, but many wish to constrain SDP in order to use it as a lever in other areas of considera-ation.	(1) On the positive side, at least some framework is intact! (Revise Definition and Recommendations).
	(2) Spent fuel disposal implies stronger safe-guards than HLW disposal in so far as transport emplacement and monitoring are concerned. Goal of signatory nations is to strengthen the creditability of NPT safeguards; Would "allowing" France to participate in a multilateral management system mean that she would need to sign the NPT? Or, if she goes ahead with the Subseabed Disposal Program, can U.S. become involved?	(2) Existence of IAEA and IMCO regulations, no necessity to specifically redevelop these--only amend.
	(3) No international agreement is pending. Even if one were set up expressly for SDP program: nations are not "legally" bound to it. There are no "dire consequences" inherent in overstepping treaties other than international "disapproval" (see Israel-Iraq situation).	

CATEGORIES	CONSTRAINTS	AIDS
OTHER NATIONS	(1) Strong anti-seabed feelings in Pacific; solution in part is an Atlantic site.	(1) Lack of geologic disposal facilities or sites on land in other nations makes SDP concept attractive.
	(2) Stipulation laws 'presence' may inspire nations to "quick fix" solutions, which SDP is not. (Length of time before implementation/demonstration makes SDP unattractive.) Law requiring demonstration of needed waste disposal and final isolation before continuation or having any nuclear energy plants.	(2) U.S. R & D expenditure make SDP more economically appealing than otherwise to Europeans.
	(3) Necessity to resolve U.S. policy/ European policy re: reprocessing. European states which are net importers of uranium, etc., do not want to dispose of spent fuel. U.S. policy is confused on the issue.	(3) "Stipulation Laws" inspires other nations with need to seek a solution as soon as possible; seabed R & D established and attractive to nations with no land based formations or which have experienced difficulty in the area of public response to siting studies (United Kingdom, Germany, etc.).

CATEGORIES	CONSTRAINTS	AIDS
U.S. DOMESTIC	(1) Necessity to resolve confusion (which does exist) over spent fuel vs HLW to be emplaced. U.S. neeeds to make policy decisions not only about what we will emplace, but must state opinion about what other nations can emplace under a U.S. backed program. And U.S. money and R & D are involved no matter what, so a policy statement is necessary for clarity before final development.	(1) Amendment process to MPRSA is in place; framework within which the limits on the program can be established.
	(2) Establishment of lines of responsibility in U.S. for the various phases of the program. For instance, if port is to be an AFR, who has jurisdiction? NRC over licensing? DOE over R & D? State over development of waterfront areas--adjacent, local, etc.? Necessity for "Federal Preemption?"	(2) Necessity to dispose of East Coast stored wastes: Atlantic dumpsite. SDP removes some of the problems associated with travel to west which would otherwise be required.
	(3) Necessity of long, complex EIS process for each stage of program development cannot but slow progress. Also necessity for NRC specialized regulations will slow progress.	
	(4) Expenditures are unknown.	
	(5) Recent U.S. attempts to link supply and back-end activities (reprocessing) have resulted in lowered respect for U.S. as a supplier country may have a negative impact on other nations' acceptance of SDP program, if they feel that strings are attached.	

TASK XII:

Produce the Following Working Papers: 1) A Review, Interpretation, Assessment and Identification of the Constraining and Supporting Factors Toward Establishment of a Subseabed Program; 2) A General Description and Analysis of Trade-offs and Negotiating Strategies.

PART I:

REVIEW, INTERPRETATION, ASSESSMENT AND IDENTIFICATION OF THE CONSTRAINING AND SUPPORTING FACTORS TOWARD ESTABLISHEMENT OF A SUBSEABED PROGRAM FOR DISPOSAL OF HIGH LEVEL NUCLEAR WASTES

Constraints

The major constraints to implementing a Subseabed Disposal system for high level radioactive wastes are summarized below.

1. The absence of a convincing argument for the subseabed option as a necessary or technically viable option.

2. The uncertainty of the location of potential sites for disposal; whether they are to be in international waters or whether they might be in 200 mile exclusive economic zones under national jurisdictions; whether the best sites would be in the Atlantic or in the Pacific, based on uncertain scientific/environmental information as well as socio-political and economic considerations.

3. The absence of a technical reference system precludes a thorough eveluation, political or economic, of the merits of this option.

4. The absence of a clear definition and evaluation of the potential risks from the operation of a Subseabed Disposal system a) on its own merits, and b) compared to land-based systems due to the absence of a clear reference from which to derive an evaluation.

5. The absence of national legislation to define the scope and nature of the regulatory framework for high level waste, which must underlie and prelude the implementation of a Subseabed Program.

6. The uncertainties of interpretation in prevailing U.S. legislation which indirectly and directly relates to a Subseabed Disposal option, and the necessity, at the least, for amendment to cover this option.

7. The absence of international controls and standards to address high level wastes, apart from prohibitions.

8. The misunderstandings in definition, particularly between "dumping and emplacement" emanating from the London Dumping Convention, leading many to believe the option has already been outlawed, and thereby creating unnecessary opposition.

9. The political uncertainties in the positions of key national governments regarding nuclear policies and waste policies. Depending on the long-term decisions of the U.S., France, West Germany, Japan, Taiwan, Korea, Canada, and Australia, for example, subseabed options could be either unnecessary or very necessary.

10. The uncertain status of the UNCLOS treaty and the uncertain and nonuniform perceptions of the ultimate relevance of certain articles of the treaty.

11. The yearly uncertainties related to funding the program in the U.S. (which influences other nations) and uncertainties as to its survival places the credibility of this option in question as well as possibly compromising the quality of the program by forcing "short cuts" for lack of funds.

12. Unresolved problems related to liability by identifying the potential entities which should be held responsible for specific operations of the system, including allocation of responsibility for every part of the system. The Price Anderson legislation would be relevant here.

13. No viable ownership/management configurations for a program to assist solving the liability and responsibility of issues of number 12. Determine where and whether there would be private sector incentives for investments, or whether public ownership and management is essential or some combination thereof.

14. The unclear policy positions regarding the role, if any, the U.S. wants to play in any subseabed activities for the disposal of high level nuclear wastes. That is, does the U.S. want to have the scientific and technical as well as political and legal lead, or is it willing to permit other nations such as France and Great Britain to take the lead? Is SDP really going to be necessary?

15. The unclear U.S. policies, if the U.S. prefers some control over the events leading to a Subseabed Disposal system, regarding what should be done about changing certain international and national regulations to bring them into some consistency with the necessary requirements for a subseabed system of disposal. For example, the U.S. should prepare a list of items which should be included in an amendment to the London Dumping Convention; it should take a position on the relevance or irrelevance of the proposed Law of the Sea Treaty regarding the permissibility of such a program, etc.

In essence, the United States cannot much longer keep the Subseabed Program at such a low profile and low concern level, if it

has any intention of directing or influencing the outcomes of a subseabed system, either carried out unilaterally or multilaterally. The uncertainties which are illuminated in the 15 items of constraints listed above which characterize U.S. policies regarding this mode of disposal have a twofold result. On the one hand, the low profile keeps much of the controversy about a program from surfacing in the public eye and therefore keeps public objections at bay. However, at the same time, other nations continue to carry out their own policy objectives, some of which relate to pushing ahead with steps toward the use of the subseabed for disposal of their high level wastes. This ambivalence will ultimately function as a decisive measure to abort leadership in this program for the United States, leaving it to West European nations to push ahead. While this may be the right move for the United States, it would better serve this nation if the policy were the result of thoughtful decision rather than default, such as was discussed earlier regarding deepsea mining.

Aids To a Subseabed Disposal Program (SDP)

There are several positive areas that would assist the process in moving toward a Subseabed Disposal Program (SDP).

In the technical/political area the following have or would have a positive effect:

1. Design a system equal to the task of disposing "worst case" candidates and adjust the design as improved information indicates that it is reasonable and acceptable.

2. There is a possible need for a U.S. East Coast disposal site, and if the Atlantic proves feasible, that might be a solution.

3. If it is shown that uniformity and consensus are necessary for U.S. and European nations considering a SDP regarding the system's parameters, the U.S. by proceeding with its R & D program including past expenditures would have provided a major portion of the expenses toward a design which might make it unnecessary for other nations to do the same, and such savings in time and money might make other nations more likely to accept a U.S. design and standards, thus giving the U.S. control over the system's reliability and configuration to a larger extent than if the Europeans are permitted to take over by a U.S. default.

From the perspective of the U.S. domestic scene, there are several positive features:

4. The amendment process to the MPRSA is in place. This could be a framework through which the limits on the program can be established.

5. The recent recommendations of a National Academy of Sciences (NAS) panel on nuclear waste recommending several disposal sites distributed geographically around the United States, might make an offshore East Coast site tempting.

On the international side, there are also some positive aspects:

6. The London Dumping Convention provides a framework as well to work from to negotiate high level waste disposal.

7. The existence of the IAEA and its precedence setting nature for regulations regarding nuclear activities.

8. The formation of the NEA Subseabed Working Group and the gradually increasing interest on the part of more nations provides an excellent information exchange and forum.

9. The rapid amending to the IMCO regulations to accommodate incinerator ships for chemicals provides a welcome environment.

PART II:

A GENERAL DESCRIPTION AND ANALYSIS OF TRADE-OFFS AND NEGOTIATING STRATEGIES

There are several categories of constraints and aids which must be considered in the assessment of a seabed disposal option. The first set of them relate directly to the physical configuration of the technical delivery system and the points at which societal concerns are apparent. The other set of important factors to consider is the existing political/legal environment of institutions laws and policies which must provide suitable building blocks for a management system; second, be able to establish a suitable structure for management; and third, assure appropriate implementation and operation of a safe and reliable system of disposal as accepted by those groups influential in the political system.

In the first category (see Task I), the largest constraint is the absence of a reference system that is known to be technically feasible. Based on the assumptions found in Task I of this report, it appears that the subseabed program would be well advised to proceed with a design equal to the task of disposing "worst case" candidates and then adjust should it be shown that is is reasonable to do so. Proceeding with such a design might then alleviate several of the constraints which currently prevail in the vacuum without one, such as the lack of consensus in the U.S. about the type of waste to be emplaced--military and civilian, reprocessed or spent fuel rods, etc. This part might have to be coordinated with European and other nations interested in the program and therefore

should be carefully considered. Military waste disposal adds difficulty from a political point of view, although being reprocessed makes them technically and socially more desirable.

Another constraint appears to be the current inconsistencies regarding Atlantic and Pacific sites for disposal. On the one hand, there may be a need for an Atlantic site for the United States and that could drive the program domestically, and act as an aid. Europeans, in addition, see the Atlantic favorably due to its proximity and the short transport costs and risks. On the other hand, scientists indicate that the Pacific sites are probably much more suitable for disposal, being in a much more stable area, geologically, and in a much less crowded area functionally. However, the use of Pacific sites does not solve any U.S. problems and appears to serve Japanese, Korean, and Taiwanese principally, also arousing the ire of the Pacific Island nations who have suffered the results of nuclear activities in the past. Problem areas which will act as constraints because of societal concerns will occur over the transport routes on land for the wastes on the way to port facilities, the points of departure for the wastes if they in fact become AFR's and are not contained on large segments of military bases, but rather in public port areas, the work rules and possible labor concerns in the transport and burial process, and the reliability and safety of the burial of the wastes and the monitoring systems for determining and eliminating hazards afterwards. Public information and the political process will largely determine the resolution of the sensitive points and it is not the purpose of this paper to handle public reaction; rather, the domestic and international vehicles that are part of the orchestration of the political process are a subject covered here. Where are the weaknesses and where are the strengths of the current system to deal with these concerns?

Another fundamental constraint is the absence of a clear policy on the part of the United States regarding the role it wishes to take in launching a Subseabed Disposal system. While activities continue politically, fiscally, and technically and environmentally, there appears to be an absence of any clear direction or objective on the part of the United States. Domestically, it would seem that the Subseabed Disposal Program is insignificant and exists only at the urging of those involved in the program and due to the past President's policies of leaving several options open to abide the EPA regulations. Internationally, the United States funding of the program relative to the several other member nations of the NEA was equal to the total amount allocated by all the others, in which case it would seem that the U.S. had a leading interest. There is evidence to be an option either geographically or politically. These nations are demonstrating increases of interest and are stressing greater participation as well as greater political initiative. Some American scientists currently involved in the international cooperative efforts claim the U.S. has already given up its lead deferring to the French and British in this case. If it is demonstrated that some uniformity and concensus are necessary between the U.S. and European nations considering a SDP, the lack of U.S. political leadership would appear to be an impediment, unless the U.S. merely wants to foot the bills and follow in the lead of the other member participating nations.

Another stumbling block, which could be resolved with appropriate public information strategies is the misperception of this program. It is either confused with ocean dumping, likened to the option of shooting the wastes into space and therefore not a credible option, or seen as a threat to land based disposal which has the support of most of the "nuclear community." These and other misconceptions about the program need to be cleared away before rational political processes can move ahead toward a credible management system.

Finally, constraints in the system can also be seen as the absence of the information and understanding of particularly important sensitive aspects to a management system which must be researched for realistic and effective work to begin toward building a system of ocean disposal--e.g., liability assignment for the various portions of the system, changes in the laws which pose constraints, and structural changes for ownership options/management options.

Of all the aids to a Subseabed Disposal Program, the most reasonable and obvious one is the probability that land disposal options will not be suitable for a significant portion of nations needing disposal. Therefore, if the scientific and technical feasibility of a SDP appear commensurate with the assurances of land disposal options, or possibly better, it would seem almost inevitable that some form of SDP will emerge. With this assumption in mind, it does not seem too early to begin planning for the guidelines and scope of such a system, anticipating the problems and benefits accruing from its evolution and formations.

ADDENDA I

SUBSEABED CONFERENCE PARTICIPANTS - 6-7 JULY 1981

Dr. D.R. Anderson
Sandia Laboratories
Albuquerque, N.M. 87185

Professor Irwin ("Chip") Bupp
Harvard Business School
Harvard University
Allston, MA 02163

Luther Carter
Journalist
4522 Lowell Street
Westshire Heights
Washington, D.C. 20016

Stephen Cassella
Research Supervisor
Department of Ocean Engineering
Massachusetts Institute of Technology
Cambridge, MA 02139

Chris Chryssostomidis
Associate Professor
Department of Ocean Engineering
Massachusetts Institute of Technology
Cambridge, MA 02139

Dr. David A. Deese
John F. Kennedy School of Government
Center for Science and International Affairs
Harvard University
79 Boylston Street
Cambridge, MA 02138

Carol Eberhard
Research Assistant (MIT)
(Nuclear Regulator Commission Intern)
Washington, D.C.

Joseph Ferriera
Associate Professor
Department of Urban Studies and Planning
Massachusetts Institute of Technology
Cambridge, MA 02139

Ken Hinga
Sandia Laboratories
Albuquerque, N.M. 87185

Charles D. Hollister, Dean
Woods Hole Oceanographic Institution
Woods Hole, MA 02543

Judith T. Kildow
Associate Professor
Department of Ocean Engineering
Massachusetts Institute of Technology
Cambridge, MA 02139

Alfred Kildow
Rapporteur
50 Stoneleigh Circle
Watertown, MA 02172

John Knauss, Dean
Graduate School of Oceanography
University of Rhode Island
Kingston, R.I. 02881

Martin Krieger
Visiting Assistant Professor
Department of Urban Studies and Planning
Massachusetts Institute of Technology
Cambridge, MA 02139

Henry "Hank" Marcus
Associate Professor
Department of Ocean Engineering
Massachusetts Institute of Technology
Cambridge, MA 02139

Robert MacDougall
Nuclear Regulatory Commission
905 SS USNRC
Washington, D.C. 20555

Marvin Miller
Department of Nuclear Energy/Energy Lab
Massachusetts Institute of Technology
Cambridge, MA 02139

John Norton Moore, Director
Center for Oceans Law and Policy
University of Virginia
Charlottesville, VA 22901

Jerry Murphy
Energy Research Group
400-1 Totten Pond Road
Waltham, MA 02154

Larry Susskind, Head
Department of Urban Studies and Planning
Massachusetts Institute of Technology
Cambridge, MA 02139

Howell Thomas
Senior Associate
Center for Energy Policy
1000 Statler Office Building
Boston, MA 02116

Ann Weeks
Research Assistant
Department of Ocean Engineering
Massachusetts Institute of Technology
Cambridge, MA 02139

Michael Wheeler
Visiting Professor
Department of Urban Studies and Planning
Massachusetts Institute of Technology
Cambridge, MA 02139

Susan Wiltshire
77 Fox Run Road
South Hamilton, MA 01982

INTERNAL USE ONLY ADDENDA II

MEMORANDUM July 10, 1981

To: File

From: J.T. Kildow

Subject: Report of July 7, 1981, meeting to review applied social science work for subseabed program, Kildow and Susskind contracts.

The meeting took place in Cambridge, Mass., and was attended by persons representing scientific and engineering professions as well as a range of social scientific and legal areas of interest. See attachment

The meeting opened with brief comments by Dr. D.R. Anderson, who gave a brief update on the status of the Subseabed Disposal Program. Dr. Irwin C. Bupp of the Harvard Business School followed with a report of the efforts of the National Academy of Sciences Panel on Nuclear Waste to assess what a fully operating industrial system for handling spent fuel/HLW would look like.

From these two reports, two clear reference points emerged:

1. Dr. Anderson said that the NEA/OECD group of nations had decided to focus money and efforts for the forseeable future on Atlantic Ocean sites as opposed to the previous focus on the more geologically stable Pacific sites, reflecting the advantage of proximity of the sites for easier transport.

2. Dr. Bupp said the National Academy study had thus far concluded that the U.S. could not settle for a single repository for its nuclear wastes, but would probably need three sites, regionalizing the transport of waste fuels to avoid overloading logistical systems and to lower risks inherent in transporting wastes over long distances. Implicit in this conclusion was the question of equitably distributing the risks throughout the country rather than among just a few states. As extrapolated, Anderson said this means that if there were to be a subseabed program for disposal of nuclear wastes, then the probability is that the wastes that would be emplaced would be those from the East Coast. Land repositories in the West, if they prove to be technically feasible and safe, would serve the needs of the West and Midwest.

Professors Kildow and Susskind led morning discussions that focused on the two memoranda included in the handout packet (see attached) and an afternoon session that addressed the research tasks for the follow-on to the current work. The morning session derived a simple technical and managerial reference system for a first round of analysis. If problems arise using that system, then alternatives would be substituted to test the feasibility. Reports were made of the status of technical design of the ship, of the retrieval possibilities, and of the portside requirements. These were coupled in the discussion that followed with the social/political and managerial issues, resulting in realistic perspectives leading toward evolution of an actual system. While still reflecting some unanswered questions of key significance, the reference system emerged as follows:

--The technical system would rely on an East Coast port, perhaps at a military installation in the Southeast, e.g., South Carolina;

--This would probably be the reception point for East Coast civilian commercial wastes, most probably spent fuel wastes;

--The system would consist of five steps:

1. Transport of spent fuel from reactor storage area to a packaging facility;

2. Transport from the packaging facility to the port storage facility;

3. Preparation for ship transport by the addition of special packaging and placed by completely remotely-controlled devices upon the ship. The ship would be able to transport 144 to 500 casks, would be as large as affordable for purposes of stability in bad weather, and would include a water-cooled storage (dry storage might also be possible). The ship could be designed either with or without retrieval capability, depending upon the specifications for design, or another ship could supplement the transport ship with capability for retrieval, monitoring and research.

4. The transport ship would carry the waste to the designated sites in the Atlantic for disposal via penetrometer to 50 meters depth in the sediments, dropping the casks at a specified rate.

5. The ship would return to port to prepare for the next load. Here the technical reference system specifications are limited by the scope and substance of political agreements as well as by ownership and operating arrangements that are to be worked out. For example, depending on the size and number of ships used for transport at sea, the ship could be cycled to another port in another nation, either through joint ownership or user fees, however, the need to share the costs of the ship were not felt to be imperative. In fact, the concensus, based on very gross estimates for the various components of the system, was that the driving force as far as costs are concerned is the cost of storage casks, about $1 million each, with other costs relatively minor.

On the political/social side of the equation emerged the following reference system, which would permit the operation enumerated above: The United States would steer a negotiating course leading toward a policy decision determining the degree of control the U.S. requires over the disposal system. The U.S. should seek a balance between unilateral and broad multilateral control, allowing unilateral moves, but broadening the base of participation multilaterally to avoid neglecting those other nations that will be using the subseabed for disposal of high level wastes and spent fuel. The U.S. should keep open the possibility of international cooperation in each phase or component of the system's operation in accordance with managerial requirements laid down as complementary U.S. laws evolve.

The afternoon session included detailed discussions of controversies which need addressing and of the principal information gaps. The result was a research agenda divided into:

1. Legal steps that need to be researched.

2. Risk perception research.

3. Political strategies to consider.

The research items agreed upon included the following recommendations:

1. Perceived risk: While work proceeds about the probability of actual risks that will be confronted in the technical system, there should be

simultaneous work to assess how various publics perceive the risks. Questions of how to identify, assess and understand the ramifications of perceived risks need to be tackled. Perceived risks include those associated with affected communities as well as risks to economic participants. Risk assessments should include considerations of liability and accident management and responsibility.

2. Design a management system based on a simple reference system with the following specifications:

   a. Least possible risk.

   b. Alternative entities responsible for specific points of the system.

   c. Systematic analysis of what elements of the technical system would be best served by public, private, foreign and domestic management and ownership.

3. Perform a legal exercise for building a management system with the following considerations:

   a. Assume a scenario in which a new chapter must be written for the London Dumping Convention. In doing a sensitivity analysis allowing for some variation, define what that chapter should include as to scope, military waste, shipping rules, site selection guides, media for negotiation, cost sharing, and regulations for encapsulation, monitoring and emplacement, and who the participants would be. All of this would be done while considering technical system constraints and the need for latitude in the technical system, so as not to compromise it.

   b. Model Federal law according to the following considerations:

      --Whether to change the anti-dumping law or create new legislation to supercede it;

      --How to implement potential international regulations from a Federal perspective;

      --Where to reserve Federal preemption;

      --Where to permit state and local participation, keeping in mind current state and local laws and regulations already in place.

      --Whether this relates to EPA/NEPA regulations, or something different, requiring its own area of law.

      --How to handle liability, i.e., through insurance or upper limits.

   c. Suggestions for what the U.S. legal position should be regarding the London Dumping Convention. For example, using care not to preclude establishment of a subseabed disposal regime, but preventing that action until negotiations have been concluded, would be one possible position. What should the U.S. position be regarding the UNCLOS negotiations? Remove the ambiguity regarding its relevance, and avoid the complications of global negotiations.

4. Perform a political sensitivity analysis regarding the chief foreign policy issues, enumerating the consequences of various alternatives.

5. Make persuasive cases for key decisions along the way, such as why use Atlantic instead of Pacific sites? Why dispose of wastes in the seafloor instead of on land? Etc.

(Foreign and domestic work should be carried out simultaneously, because they will complement each other.)

6. Create a strategic planning chart, indicating at what point significant changes will occur in an evolutionary process. The principal reason for doing this work is to prioritize the research to cover urgent areas first.

Enclosures

CC: Glen Boyer
Rip Anderson
Ken Hinga
Charles Hollister
Larry Susskind

ISSUES \ DEPARTMENTS →	DEPARTMENT OF COMMERCE	DEPARTMENT OF DEFENSE.	DEPARTMENT OF THE NAVY.	DEPARTMENT OF ENERGY	DEPARTMENT OF THE INTERIOR
NUCLEAR WASTE		DEFENSE NUCLEAR AGENCY (defense wastes only)		OFFICE OF NUCLEAR WASTE ISOLATION	LANDBASED DISPOSAL OPTIONS / SITING (BUREAU OF LAND MANGMNT)
OCEAN ENVIRONMENT	-NOAA -MARAD (RESEARCH ON MARINE POLLUTION) ↓ FROM COMMERCIAL SHIPS	JOINT CHIEFS OF STAFF REPRESENTATIVE ON THE LAW OF THE SEA.	OCEANOGRAPHER OF THE NAVY (SUPPORT TO ALL NATIONAL OBJECTIVES)	ASSISTANT SECRETARY FOR THE ENVIRONMENT ··· ALL DOE ACTIVITIES ARE CONSISTANT W/ ENVIR. LAWS, POLICIES + REGULATIONS	-ASST SECRETARY: FISH AND WILDLIFE AND PARKS (marine environmental quality) - OCEAN MINING ADMINISTRATION
OCEAN TRANSPORTATION	- MARAD (Maritime Administration) (- development of smpst port facilities)				
NATIONAL SECURITY ISSUES		WHOLE DEPARTMENT: - ARMS CONTROL - NON PROLIF. - AGREEMENTS / FOREIGN COUNTRIES - INTELLIGENCE ANALYSIS (MONITORING S.S.D) -DEFENSE INTELLIGENCE AGENCY →	-NAVAL MATERIAL COMMAND (S.S.D. AS RELATES TO SUBMARINE DECOMMISSIONING) - NAVAL INTELLIGENCE (SSD - MONITORING) ↙		
INTERNATIONAL RELATIONS / S.S.D.	-INDUSTRY + TRADE ADMINISTR. (BUREAU OF TRADE REGULATN)	- ASST SECRETARY OF DEFENSE (INTERNATIONAL RELATIONS) - DEFENSE SECURITY ASSISTANCE AGENCY (TECHNOLOGY SALES, SSD)		ASST SEC'Y FOR INTERNATIONAL AFFAIRS (International aspects of overall energy policy) - (NON PROLIFERATION) - INTERNATIONAL FUEL CYCLE	- OCEAN MINING ADMINISTRATION (LOS, OCEAN MINERAL RESOURCES)
ENERGY POLICY (S.S.D.)		- ASSISTANT TO THE SECRETARY OF DEFENSE FOR LEGISLATIVE AFFAIRS	NAVAL NUCLEAR PROPULSION PROGRAM - JOINT WITH DOE (4 DECOMMISSIONINGS)	- ASST SEC'Y FOR POLICY AND EVALUATION. OFFICE OF - PROCUREMENT AND CONTRACTS MANAGEMENT	ASST SECRETARY: ENERGY AND MINERALS - OCEAN MINING ADMINISTRATION - S.S.D POLICY ANALYSIS
REGULATION (NUCLEAR (SSD)				FEDERAL ENERGY REGULATORY COMMISSION	
FUNDING		ASST TO THE SECRETARY OF DEFENSE FOR LEGISLATIVE AFFAIRS	- CHIEF OF INFORMATION		
PUBLIC INFORMATION	NATIONAL TECHNICAL INFORMATN SERVICE	ASSISTANT SEC'Y OF DEFENSE (PUBLIC AFFAIRS): military waste disposal options		- ASST SECRETARY FOR INTER-GOVERNMENTAL AND INSTITUTIONAL RELATIONS: DOE relations with: - congress - Media - regional / local agencies - consumer interests / private gas	
RESEARCH AND DEVELOPMENT	- MARAD (PORT + SHIP DEVELOPMENT) - NOAA (OCEAN ENVIRONMENT) (SEA GRANT)		OFFICE OF NAVAL RESEARCH NAVAL MATERIAL COMMAND	-OFFICE OF ENERGY RESEARCH ASST SEC'Y FOR ENERGY TECHNOLOGY	

DEPARTMENTS / INDEPENDENT AGENCIES — ISSUES / S.S.D.	DEPARTMENT OF STATE	DEPARTMENT OF TRANSPORTATION	ENVIRONMENTAL PROTECTION AGENCY	FEDERAL MARITIME COMMISSION	NUCLEAR REGULATORY COMMISSION
NUCLEAR WASTE			-national strategy - toxic substance management standards. E.I.S. review		-OFFICE OF NUCLEAR MATERIAL SAFETY + SAFEGUARDS -LICENSING OF NUCLEAR WASTE DISPOSAL FACILITIES
OCEAN ENVIRONMENT	-BUREAU OF OCEANS AND INTERNATIONAL ENVIRONMENTAL & SCIENTIFIC AFFAIRS	-COASTGUARD - ACCIDENT PLANS - MARINE POLLUTION -MARINE SAFETY COUNCIL (CG)	-E.I.S. OCEAN DUMPING INTERIM PERMITS.	ADMINISTERS FUNCTIONS/ DISCHARGES REGULATIONS: FED'L WATER POLLUTION CONTROL ACT. / CLEAN WATER ACT	
OCEAN TRANSPORTATION		-COASTGUARD - COMMERCIAL VESSEL SAFETY		APPROVAL: COMMON CARRIERS' AGREEMENTS REGULATION: COMM. CARRIERS BY WATER VESSEL CERTIFICATION	- LICENSING - N WASTE DISPOSAL FACILITIES, INCLUDING SHIPS.
NATIONAL SECURITY ISSUES	BUREAU OF POLITICO-MILITARY AFFAIRS (NUCLEAR POLICY, NONPROLIFERATION) -MONITORING EMPLACED WASTES				INTEREST IN MONITORING EMPLACED WASTES: REGULATIONS FOR SUCH ACTIVITY
INTERNATIONAL RELATIONS (S.S.D.)	-BUREAU OF OCEANS & INTERNATIONAL ENVIRONMENTAL & SCIENTIFIC AFFAIRS -BUREAU OF INTERNATIONAL ORGANIZATION AFFAIRS (Coordination of U.S. - IAEA relations, etc)	ASST SECRETARY FOR POLICY + INTERNATIONAL AFFAIRS			
ENERGY POLICY	-BUREAU OF POLITICO-MILITARY AFFAIRS (NUCLEAR POLICY -BUR. OF INTERNAT'L ORGANIZ. AFFAIRS (Coordination U.S. - IAEA relationship)				
REGULATION (NUCLEAR + S.S.D.)		-COASTGUARD - COMMERCIAL VESSEL SAFETY	E.I.S. REVIEW	OF COMMON CARRIERS BY WATER - FOREIGN + DOMESTIC OFFSHORE COMMERCE.	-LICENSING OF ALL NUCLEAR WASTE FACILITIES, CARRIERS, ETC. -REGULATION OF S.S.D. ACTIVITIES
FUNDING					
PUBLIC INFORMATION	BUREAU OF PUBLIC AFFAIRS (INTERNATIONAL PUBLIC INFO...)				
RESEARCH AND DEVELOPMENT			OFFICE OF THE ASST ADMINISTRATOR FOR RESEARCH + DEV. - TECH. CONTROLS - ALL FORMS OF POLLUTION		

	APPROPRIATIONS	ARMED SERVICES	ENERGY AND COMMERCE **✱**
NUCLEAR WASTE	- subcommittee on energy and water development	✱ WHOLE COMMITTEE / RE DEFENSE WASTES SUBCOMMITTEE: SEAPOWER AND STRATEGIC / CRITICAL MATERIALS	- subcomm on energy and power ✱ WHOLE COMMITTEE: NUCLEAR REGULATION
OCEAN ENVIRONMENT ("dumping")	- SUBCOMMITTEE ON ENERGY / WATER DEVELOPMENT		- subcommittee on health and environment
OCEAN TRANSPORTATION			- subcommittee on energy and commerce (foreign commerce)
NATIONAL SECURITY ISSUES	- ~~DOE/DEFENSE~~ Subcommittee on Defense	✱ WHOLE COMMITTEE (IN THEORY) SUBCOMM. ON SEA POWER AND STRATEGIC / CRITICAL MATERIALS	
INTERNATIONAL RELATIONS / S.S.D.	- SUBCOMMITTEE ON FOREIGN OPERATIONS - SUBCOMMITTEE ON DEFENSE	~~✱ WHOLE~~ SUBCOMM. ON SEA POWER AND STRATEGIC / CRITICAL MATERIALS	- subcommittee on energy / commerce (foreign commerce) ✱ Whole committee: foreign commerce generally
ENERGY POLICY (natl policy re. subseabed)	- SUBCOMM. ON INDEPENDENT AGENCIES	SUB COMM. ON SEAPOWER AND STRATEGIC / CRITICAL MATERIALS ✱ WHOLE COMMITTEE: RE DEFENSE MATERIALS / WASTE	- subcommittee on energy and power ✱ National Energy - DOE-OVERSIGHT Federal Energy Regulatory Commission
REGULATION (S.S.D.)	- SUBCOMMITTEE ON INDEPENDENT AGENCIES		- subcommittee on energy and power - subcommittee on health and environment. (DOE) - oversight ✱ WHOLE COMMITTEE - NUCLEAR REGULATION
FUNDING (S.S.D.)	- subcommittee on defense - subcommittee on energy / water development - subcommittee on foreign operations - subcommittee on independent agencies ✱ INTAERY: WHOLE COMMITTEE		- subcommittee on energy and power
PUBLIC INFORMATION	- SUBCOMMITTEE ON FOREIGN OPERATIONS		
RESEARCH & DEVELOPMENT	- SUBCOMMITTEE ON INDEPENDENT AGENCIES		subcommittee on energy and power

✱✱ ANEW COMMITTEE; BORN OF THE OLD INTERSTATE + FOREIGN COMMERCE COMMITTEE

ISSUES	FOREIGN AFFAIRS	GOVERNMENT OPERATIONS	INTERIOR & INSULAR AFFAIRS
NUCLEAR WASTE	INTERNATIONAL SECURITY / SCIENTIFIC AFFAIRS	ENVIRONMENT, ENERGY, AND NATURAL RESOURCES	-ENERGY AND THE ENVIRONMENT -PUBLIC LANDS ↓ (NUCLEAR REG. GENERALLY) *WHOLE COMMITTEE: OVERSIGHT OF ALL NUCLEAR WASTE DISPOSAL PROGRAMS.
OCEAN ENVIRONMENT ("dumping")	ASIAN AND PACIFIC AFFAIRS COMMITTEE HAS OVERSIGHT FUNCTIONS RELATING TO INTERNATIONAL FISHING AGREEMENTS	ENVIRONMENT, ENERGY, NATURAL RESOURCES	-ENERGY AND THE ENVIRONMENT -PACIFIC AFFAIRS -WATER AND POWER RESOURCES
OCEAN TRANSPORTATION		GOVERNMENT ACTIVITIES AND TRANSPORTATION	
NATIONAL SECURITY ISSUES	INTERNATIONAL SECURITY / SCIENTIFIC AFFAIRS (NON-PROLIFERATION)	INTERGOVERNMENTAL ~~ORGANIZATIONS~~ RELATIONS / HUMAN RESOURCES	-PACIFIC AFFAIRS
INTERNATIONAL RELATIONS / S.S.D.	ASIAN AND PACIFIC AFFAIRS INTERNATIONAL SECURITY / SCIENTIFIC AFFAIRS INTERNATIONAL ORGANIZATIONS INTERNATIONAL ECONOMIC POLICY & TRADE * WHOLE COMMITTEE	INTERGOVERNMENTAL ~~ORGANIZATIONS~~ RELATIONS / HUMAN RESOURCES	-PACIFIC AFFAIRS
ENERGY POLICY (POLICY RE SSD especially)	INTERNATIONAL ECONOMIC POLICY & TRADE	ENVIRONMENT, ENERGY, NATURAL RESOURCES INTERGOVERNMENTAL ~~ORGANIZATIONS~~ RELATIONS	-ENERGY AND THE ENVIRONMENT -PACIFIC AFFAIRS -WATER AND POWER RESOURCES
REGULATION (S.S.D and NUCLEAR)	INTERNATIONAL ORGANIZATIONS		-ENERGY AND THE ENVIRONMENT (NUCLEAR REGULATION GENERALLY) *WHOLE COMMITTEE: REGULATION OF THE NUCLEAR ENERGY INDUSTRY
FUNDING	INTERNATIONAL ECONOMIC POLICY AND TRADE *	* BUDGET AND ACCOUNTING, OTHER THAN APPROPRIATIONS - WHOLE COMMITTEE	
PUBLIC INFORMATION	-INTERNATIONAL OPERATIONS	INTERGOVERNMENTAL RELATIONS + HUMAN RESOURCES	-ENERGY AND THE ENVIRONMENT -PACIFIC AFFAIRS -PUBLIC LANDS
RESEARCH and DEVELOPMENT	INTERNATIONAL ECONOMIC POLICY AND TRADE (TECHNOLOGY TRANSFER)		ENERGY AND THE ENVIRONMENT ↑ (NUCLEAR ENERGY R+D) NUCLEAR WASTE DISPOSAL R+D OVERSIGHT IS A SPECIFIC DUTY OF THE WHOLE COMMITTEE

ISSUES	MERCHANT MARINE AND FISHERIES	PUBLIC WORKS AND TRANSPORTATION	SCIENCE AND TECHNOLOGY
NUCLEAR WASTE		* WHOLE COMMITTEE ··· LAND BASED ESPECIALLY DISPOSAL →	-ENERGY DEVELOPMENT AND APPLICATIONS -ENERGY RESEARCH AND PRODUCTION -NATURAL RESOURCES AND ENVIRONMENT -AGRICULTURE, NATURAL RESOURCES, RESEARCH AND ENVIRONMENT
OCEAN ENVIRONMENT ("dumping")	-FISHERIES, WILDLIFE, CONSERVATION, AND ENVIRONMENT -OCEANOGRAPHY	-WATER RESOURCES * WHOLE COMMITTEE : OIL AND OTHER POLLUTION OF NAVIGABLE WATERS	-NATURAL RESOURCES AND ENVIRONMENT -AGRICULTURE, NATURAL RESOURCES, RESEARCH & ENVIRONMENT
OCEAN TRANSPORTATION	-COAST GUARD AND NAVIGATION -MERCHANT MARINE -OCEANOGRAPHY * WHOLE COMMITTEE: REGISTERING AND LICENSING VESSELS	-SURFACE TRANSPORTATION: WATER TRANSPORTATION SUBJECT TO I.C.C. RULES. *WHOLE COMMITTEE: TRANSPORT. REGULATORY AGENCIES EXCEPT: I.C.C./RAILROADS, FED'L R ADMIN., AMTRAK	
NATIONAL SECURITY ISSUES			
INTERNATIONAL RELATIONS (S.S.D.)			
ENERGY POLICY (S.S.D. especially)	-COAST GUARD AND NAVIGATION -FISHERIES, WILDLIFE, CONSERVATION AND ENVIRONMENT.		-ENERGY DEVELOPMENT/APPLICATIONS -ENERGY RESEARCH AND PRODUCTION -NATURAL RESOURCES AND ENVIRONMENT -AGRICULTURE, NATURAL RESOURCES RESEARCH AND ENVIRONMENT
REGULATION (S.S.D AND NUCLEAR)	-COAST GUARD AND NAVIGATION -FISHERIES, WILDLIFE, CONSERVATION AND ENVIRONMENT -OCEANOGRAPHY	-SURFACE TRANSPORTATION -WATER RESOURCES	-NATURAL RESOURCES AND ENVIRONMENT -ENERGY RESEARCH AND PRODUCTION -AGRICULTURE, NATURAL RESOURCES, RESEARCH AND ENVIRONMENT
FUNDING	* WHOLE COMMITTEE		
PUBLIC INFORMATION	-FISHERIES, WILDLIFE, CONSERVATION AND ENVIRONMENT -MERCHANT MARINE -OCEANOGRAPHY		-ENERGY DEVELOPMENT AND APPLICATIONS -ENERGY RESEARCH AND PRODUCTION -NATURAL RESOURCES AND ENVIRONMENT
RESEARCH AND DEVELOPMENT	-FISHERIES, WILDLIFE, CONSERVATION AND ENVIRONMENT -OCEANOGRAPHY	-SURFACE TRANSPORTATION	-ENERGY DEVELOPMENT AND APPLICATIONS -ENERGY RESEARCH AND PRODUCTION -NATURAL RESOURCES AND ENVIRONMENT -SCIENCE RESEARCH AND TECHNOLOGY -AGRICULTURE, NATURAL RESOURCES, RESEARCH

INTERVIEWS

Anderson, Dr. D. Richard of Sandia Laboratories. 7 July 1981 meeting.

Hollister, Dr. Charles D., Dean, Woods Hole Oceanographic Institution. 7 July 1981 meeting.

Moore, Dr. John Norton, Director, Center for Oceans Law and Policy. 12 June 1981.

BIBLIOGRAPHY

Allday, C. "International Cooperation in the Supply of Nuclear Fuel Cycle Services." International Conference on Nuclear Power and its Fuel Cycles. Salzburg, Austria, 2-13 May 1977.

"Alternative Waste Disposal Concepts and Interim Technical Assessment." (ONWI) Bechtel, Inc. San Francisco, California, November 1979.

Anderson, Dr. D. Richard. "Nuclear Waste Disposal in Subseabed Geologic Formations: The Seabed Disposal Program." Sandia Laboratories, SAND 78-2211, May 1979.

Baxter, Kildow and Nyhart. Ocean Resources Management: Legal and Policy Aspects, Materials, and Cases. Massachusetts Institute of Technology, July 1974.

Bibbington, W. "The Reprocessing of Nuclear Fuels." Scientific American. December 1976, pp. 30-41.

Bohme, E. and Kehden, M.I. From the Law of the Sea to an Ocean Space Regime: Practical and Legal Implications of the Marine Revolution. Hamburg, Germany, 1972.

Bulletin of the Atomic Scientists. Article on the Convention on the Physical Protection of Nuclear Material. May 1980, p. 34.

Burns, J.L. Institutional Issues in the Planning and Implementation of a Program to Dispose of High Level Radioactive Wastes. Rand Corporation (N-1650 DOE), February 1981.

Center for Oceans Law and Policy, University of Virginia. The Oceans and U.S. Foreign Policy. April 1978.

Chayes, A. and Lewis, W. Bennett. International Arrangements for Nuclear Fuel Reprocessing. Cambridge: Ballinger Publishing Co., 1977.

Cloett, C.; Greene, M.; Morris, F.; Rankin, W.; and Weiss, C. Identification and Assessment of the Social Impacts of Transportation of Radioactive Materials in Urban Environments. Seattle: Battelle Human Affairs Research Centers, NUREG/CR-0744, SAND 79-7032.

The Columbia Journal of World Business. Focus: Law of the Sea. Volume XV no. 4, Winter 1980.

Congressional Quarterly-Weekly Report. January 1980 to present.

Consultation and Concurrence Workshop Proceedings. Orcas Meeting, Eastsound, Washington (ONWI/DOE), September 1979.

Curlin, J.W. "Status of Ocean Policy: A Report to the President." Oceans, 11:57-60, November 1978.

deCarmoy, G. Energy for Europe: Economic and Political Implications Washington, D.C.: American Enterprise Institute for Public Policy Research, 1977.

Deese, David A. "A Cross-National Perspective on the Politics of Nuclear Waste." Forthcoming as chapter 2 in The Politics of Nuclear Waste, ed. E. William Colglazier. New York: Pergamon Press, Fall 1980.

-------. Nuclear Power and Radioactive Waste. Mass: Lexington Books, 1978.

Deese, D.A. and Williams, F. "Nuclear Non Proliferation and the International Management of Spent Reactor Fuel." Harvard University, May 1978.

Deese, David A. "Seabed Emplacement and Political Reality." Oceanus, vol. 20, no. 1 (Winter 1977), pp. 47-63.

Dolgin, Erica and Guilbert, Thomas, eds. Environmental Law Institute. Federal Environmental Law. St. Paul, Minnesota: West Publishing Co., 1974.

Draft Convention on Environmental Cooperation Among Nations. World Peace Through Law Center. Geneva, Switzerland, 1972.

Faltermeyer, Edmond. "Burying Nuclear Trash Where it Will Stay Put." Fortune, 26 March 1979, pp. 98-105.

Farley, P.J. "Institutional and International Aspects of Spent Fuel Management." Institutional Support Group, International Energy Associates, Ltd., July 1978.

Fischer, A. "What are we going to do about Nuclear Waste?" Popular Science, December 1978.

Flemming, N.C. The Undersea. New York: MacMillan & Co., 1977.

Gera, F. and Olivier, Jean-Pierre. "OECD Countries Pursue Geological Disposal." Nuclear Engineering International, January 1978, p. 35.

Gera, F. and H.Y. Tammemagi. "Disposal of Nuclear Wastes: A National and International Perspective." Radioactive Waste Management. Harwood Academic Publishers, January 1981.

Goldschmidt, D. B. "The Negotiation of the Non-Proliferation Treaty (NPT)." IAEA Bulletin, vol. 22, nos. 3-4. August 1980, p. 77.

Gorizontov, B. "The World Ocean-Economics, Ecology, and Cooperation." International Affairs, December 1978, pp. 48-57.

Greenwood, Ted. "Radioactive Waste Management in the United States." Aspen Institute Conference on Resolving the Social, Political, and Institutional Conflicts over Permanent Siting of Radioactive Wastes. Cambridge, Massachusetts, November 1979.

Grimwood, P. and Webb, G. "Can Nuclear Wastes be Buried at Sea?" New Scientist, 24 March 1977.

Hammond, R.P. "Nuclear Wastes and Public Acceptance." American Scientist, vol. 67, pp. 146-150.

Harris, W.R. and Solomon, K.A. "Institutional Alternatives for International Nuclear Service Centers (INSC's)." Rand Corporation, November 1977.

Harrison, J.M. Preliminary Report on the Review of Research and Development on the Disposal of High Level Nuclear Wastes (ICSU), August 1980.

Harry, J.R. Deep Seabed Mining in the Law of the Sea Negotiations. Center for Oceans Law and Policy. University of Virginia, February 1978.

Hollister, Charles D.; Anderson, Richard D.; and Heath, G. Ross. "Subseabed Disposal of Nuclear Wastes." Science, vol. 213, 18 September 1981, pp. 1321-1326.

Hull, E.W. Seabrook and Koers, Alber. Introduction to a Convention on the International Environment Protection Agency. Law of the Sea Institute, University of Rhode Isand, September 1971.

IAEA. Agency's Program for 1979-1984. Vienna, Austria, 1979.

-------. "Background Information Papers Related to the IAEA's Responsibility Under the London Convention of 1972 on the Prevention of Marine Pollution by Dumping of Wastes and Other Matter." Vienna, Austria, 1974.

-------. "Convention on the Prevention of Marine Pollution by Dumping of Waste and Other Matter." Information Circular (INFCIRC/205/Add.1/ REV.1:, August 1978.

-------. IMCO: Making the Seas Safer and Cleaner." IAEA Bulletin, vol. 21, no. 4.

IAEA. International Atomic Energy Agency Bulletin. Several issues: vol. 19, no. 5, 1977; vol. 22, no. 1, February 1980; vol 22, nos. 3-4 August 1980; vol. 21, no. 4 August 1979.

-------. International Conference on Nuclear Power and its Fuel Cycle. IAEA-CN-36/81. Salzburg, Austria, 2-13 May 1977.

-------. International Legal Conference on Maritime Carriage of Nuclear Substances, Brussels, 1971. Vienna, Austria, 1972.

-------. "International Nuclear Fuel Cycle Evaluation Report of Working Group of 7: Waste Management and Disposal." Vienna, 1980.

-------. "Legal Implications of the Disposal of Radioactive Waste Into the Sea." Rousseau Panel, 1963.

-------. Maritime Carriage of Nuclear Materials: Proceedings of a Symposium, June 1972. Vienna, Austria, 1973.

-------. "Oceanographic Basis of the IAEA Revised Provisional Definition and Recommendations Concerning High Level Radioactive Waste Unsuitable for Dumping at Sea." Vienna, Austria, 1978.

-------. "The Present Status of IAEA Safeguards on Nuclear Fuel Cycle Facilities." IAEA Bulletin, vol. 22, nos. 3-4, August 1980, p. 17.

-------. "Radiological Basis of the IAEA Revised Provisional Definition..." Vienna, Austria, 1978.

-------. "Radioactive Waste Disposal Into the Sea." Safety Series, no. 5, Vienna, Austria, 1961.

-------. Regional Nuclear Fuel Cycle Centre Study: Institutional and Legal Framework Aspects. July 1976.

IMCO. "Activities of the IMCO in Relation to Marine Pollution." IMCO Secretariat, London, July 1970.

-------. "IMCO and its Activities: Information Summary." London, England, 1971.

Innes, R. "Legal and Regulatory Constraints on Subseabed Disposal of Radioactive Waste." Cambridge: Urban Systems Research and Engineering, August 1980.

International Council of Scientific Unions (ICSU) Yearbook: 1979.

International Energy Associates, Ltd. Report for Department of Energy on Comparative National Positions on Nuclear Energy. Fall 1980.

"Islanders Fight Japan's Plan to Dump Atom Waste." New York Times, 18 March 1981, p. 97.

Kasperson, Roger. The Dark Side of the Radioactive Waste Problem. Clark University Center for Technology, Environment, and Development, 1980.

Kildow, Judith T. Social Science Research Agenda for Subseabed Disposal of High Level Nuclear Waste and Spent Fuel Program. Sandia Laboratories, Final Report, 1981.

Knight, G. The Law of the Sea: Cases, Documents, and Readings.(vol. I and vol. II), Baton Rouge, Louisiana.

Kovler, P. "Who Owns the Bottom of the Sea?" Politics Today, 5:54-6, November 1978.

Krommiller, T. The Lawfulness of Deep Seabed Mining, Vols.I and II. Oceana Publications, 1980.

Krugmann, Hartmut of Princeton University. "West German's Efforts to Close the Nuclear Fuel Cycle: Strategies for Radioactive Waste Management." Energy Research, vol. 2, 1978, pp. 107-121.

LaPorte, T. "Nuclear Waste: Increasing Scale and Sociopolitical Impacts." Science, vol. 201, July 1978.

Lay, S. Houston; Churchill, Robin; and Nordquist, Myron. New Directions in the Law of the Sea, Volumes I, II, III, IV, New York: Oceana Publications, Inc./British Institute of International and Comparative Law, 1973-1975.

League of Women Voters. A Nuclear Waste Primer. L.O.W.V. Education Fund, 1980.

Lee, Kimball. "A Federalist Strategy for Nuclear Waste Management." Science, vol. 208, 16 May 1980.

-------. "Implications of the Arrangements Made for Deepsea Mining for other Joint Exploitations." The Columbia Journal of World Business, Winter 1980, p. 58.

Lippek, Henry and Schulter, C. Richard. "Legal, Institutional and Political Issues in Transportation of Nuclear Materials at the Back End of the LWR Nuclear Fuel Cycle." Seattle: Battelle Human Affairs Research Center, September 1977.

Lipshutz, R. Radioactive Waste: Politics, Technology and Risk: Report of the Union of Concerned Scientists. Cambridge: Ballinger Publishing Company, 1980.

Lonnroth, Mans. The Politics of the Back End of the Nuclear Fuel Cycle in Sweden. September 1979.

Mangone, G.J. Marine Policy for America: The United States at Sea. Mass: Lexington Books, 1977.

"Marine Radioecology: Proceedings of the Third NEA Seminar, Tokyo, Japan, 1-5 October 1979." NEA/OECD, 1980.

Maynard, Nealey, et al. "Public Values Associated with Nuclear Waste Disposal." Battelle Memorial Institute, Human Affairs Research Center, April 1978.

Mensat, T.A. "The IMCO Experience." Law Institutions and the Global Environment. Ocean Publications, 1972.

Morozov, V.A. "Waste Management Practices in Selected European Countries." IAEA Bulletin, vol. 21, no. 4, August 1979.

National Academy of Sciences. "Disposal in the Marine Environment: An Oceanographic Assessment." Washington, D.C., 1976.

National Academy of Sciences (Washington, D.C. 1979). Energy in Transition 1985-2010. San Francisco: W.H. Freeman & Company, 1980.

Nealey and Rankin. "Attitudes of the Public about Nuclear Wastes." Nuclear News, June 1978, pp. 117-122.

Nealey and Schilling. "Public Participation in Nuclear Waste Management." Battelle Memorial Institute, Human Affairs Research Center, April 1979.

New York Times articles: 22 May, 17 August, 5 October, 1980; 8 March, 10 March, 15 March, 18 March, 17 June, 22 June 1981.

Nuclear Engineering International. Volume 25, nos. 296, 298, 300, 301, 302, 305. March, April, June, July, August, October 1980; January, June 1981.

Nuclear Fuel. 11 May 1981, pp. 6-8.

Nuclear Law Bulletin. No. 13. OECD/NEA April 1974; no. 19, NEA/OECD May 1977; and no. 24.

Nuclear News. January 1980 to present.

Nucleonics Week. McGraw-Hill Publishers. Volumes 21, and 22, January 1980 to present.

O'Brien, J. "Regulating Nuclear Security." The Bulletin of the Atomic Scientists, November 1979.

Oceans. Vol. 14, no. 3, May, June 1981.

Oceanus. Vol. 24, no. 1, Spring 1981.

Pattermann, Dr. C. "International Implications of Radioactive Waste Management." Keystone Workshop on International Implications of Radioactive Waste Management, Keystone, Colorado, 15-17 September 1979.

Plane, J.C. International Approaches to the Problems of Marine Pollution. Institute for the Study of International Organization Univervity of Sussex, England, 1972.

Roberts, L. The U.K. Position on Radioactive Waste Management. Paper for the Keystone Workshop on International Implications of Radioactive Waste Management, September 1979.

Rochlin, G.I. "Nuclear Fuel Cycle Internationalization: The Uncertain Political Context." Institute of Governmental Studies, University of California at Berkeley, September 1979.

-------. "Nuclear Waste Disposal: Two Social Criteria." Science, 17 January 1977.

-------. Plutonium, Power, and Politics. University of California Press, 1979.

Sandia Laboratories. Subseabed Disposal Program Plan (vol. I). July 1981.

"Salty Solution to a Hot Nuclear Problem." New Scientist, 30 October, 1980, p. 296.

Schmidt, Helmut in Nuclear Engineering International, January 1981.

Springer, A. "Toward a Meaningful Concept of Pollution in International Law." 19 February 1975.

Stockholm International Peace Research Institute. Internationalization to Prevent the Spread of Nuclear Weapons. New York: Crane, Russak & Co., 1980.

Urban Systems Research and Engineering, Inc. Political and Institutional Implications of the Seabed Assessment Program for Radioactive Waste Disposal. Cambridge, Mass. Final Report, February 1981.

U.S. Code: Congressional and Administrative News. U.S. Statutes and Legislative Histories, 1970-present.

U.S. Congress. Congressional Research Service, Library of Congress. Nuclear Proliferation Factbook. December 1980.

U.S. Congress, House. "New Directions for Nuclear R & D, POST-INFCE." Hearings Before the Subcommittee on Energy Research and Production Committee on Science and Technology, 4-5 June 1980.

U.S. Congress, House. "Nuclear Waste Disposal." Hearings Before Subcommittee on Oceanography, Committee on Merchant Marine and Fisheries, 95th Congress, 2d session.

U.S. Congress, House. Report No. 96-1224. Merchant Marine and Fisheries Committee, 18 August 1980.

U.S. Congress, Office of Technology Assessment. Nuclear Proliferation Safeguards, 1977.

U.S. Council on Environmental Quality. Memorandum to the Heads of Agencies on Applying the Environmental Impact Statement Requirement to Environmental Impacts Abroad, 24 September 1976.

U.S. Congress, Senate. Committee on Governmental Affairs. Reader on Nuclear Proliferation, December 1980.

U.S. Congress, Senate. Congressional Record. Consideration of S.2189, Nuclear Waste Policy Bill, 30 July 1980.

U.S. Delegation Report: Tenth Session of the Third United Nations Conference on the Law of the Sea, New York, 9 March-24 April 1981.

U.S. Department of Commerce. Report to the President by the Interagency Review Group of Nuclear Waste Management. National Technical Information Service (TID29442), March 1979.

U.S. Department of Commerce. U.S. Ocean Policy in the 1970's: Status and Issues, October 1978.

U.S. Department of Energy. Cross-Statement on Proposed Rulemaking: Storage and Disposal of Radioactive Waste, September 1980.

U.S. Department of Energy. Nuclear Proliferation and Civilian Nuclear Power. Report of the Nonproliferation Alternative Systems Assessment Program, December 1979.

U.S. Department of Energy. "President's Policy Statement on Comprehensive Radioactive Waste Management Program: Fact Sheet on Radioactive Waste Management," 12 February 1980.

U.S. Department of State. "Ocean Development in the 1980's." Address by Thomas Pickering, assistant secretary for Oceans International Environmental and Scientific Affairs, Washington, D.C., March 1980.

U.S. Department of State. Treaties in Force. 1 January 1981.

Utton, A.E. and Henning, Daniel. Environmental Policy: Concepts and International Implications. New York: Praeger Publishers.

Van As and Forster. "Disposal of Radionuclides in the Sea." IAEA Bulletin, vol. 21, no. 4, August 1979.

Wakabashi, Dr. Hiroaki. "Strategic Viewpoint of a National Plan of High Level Waste Management." Nuclear Engineering Research Laboratory (NERL), University of Tokyo, Japan.

"Why Not Bury the Nuclear Waste Disposal Issue in Davy Jones's Locker?" The Economist, September 1979.

Willrich, Mason and Lester, Richard K. Radioactive Waste: Management and Regulation. New York: MacMillan & Company, 1977.

Willrich, Mason and Taylor, Theodore. Nuclear Theft: Risks and Safeguards. Cambridge: Ballinger Publishing Co., 1974.

Wohlstetter, Albert, et al. Swords From Plowshares: The Military Potential of Civilian Nuclear Energy. Chicago: University of Chicago Press, 1977.

Young, E. "Law of the Sea: An Arms Control Issue." Bulletin of the Atomic Scientists, 34:53-6, November 1978.

Zinberg, Dorothy S. and Deese, David. Radioactive Waste Management: A Comparative Study of National Decision-Making Processes. Harvard University, Cambridge, Mass. Prepared for the U.S. Energy Research and Development Administration. Final Report, 25 January 1979.

Zinberg, Dorothy. "The Public and Nuclear Waste Management." The Bulletin of the Atomic Scientists, January 1979, p. 34-39.

APPENDIX SS

PUBLIC EDUCATION AND PARTICIPATION

John E. Kelly

University of New Hampshire

(Contract #74-2546)

Abstract

Annual Report, FY 81

Public Education and Participation

As prescribed in Step 1 of the Public Education and Participation Process (attachment 1), industry, public interest groups, and decision-makers were briefed about the Subseabed Disposal Program. In regard to public interest groups, Drs. Hollister and Kelly were invited to present the technical and policy aspects of the Subseabed Program at a public forum in Hawaii sponsored by the Hawaii League of Women Voters, the Health Physics Society, and the East-West Center. The sponsors videotaped the forum for a film, entitled "Slowly Dying Embers: Radioactive Waste and the Pacific," which will be shown on television in Hawaii. In response to requests for information about the Subseabed Program, Congressional Staff, Representatives, and Senators (attachment 2) were briefed about the Subseabed Program as legislation related to the Program moved through Congress (attachment 3). Science oriented publications also were contacted about the Program (attachment 4).

Submitted by
Prof. John E. Kelly
Complex Systems Research Center
O'Kane House
Univ. of New Hampshire
Durham, NH 03824

Attachment 1

Public Education and Participation Process

STEP 1	BRIEFINGS WITH INDUSTRY, PUBLIC INTEREST GROUPS, AND DECISION-MAKERS (1981---)
STEP 2	WORKSHOPS WITH SUBGROUPS FROM STEP 1 (1982-84)
STEP 3	SCOPING SESSION WITH STEP 2 PARTICIPANTS AND OTHER INTERESTED PARTIES (1985-86)
STEP 4	PUBLIC PARTICIPATION UNDER THE NATIONAL ENVIRONMENTAL POLICY ACT (NEPA) (1986-88)

Attachment 2

Public Participation in the Subseabed Program FY 81

Participants:

Industry

Electric Power Research Institute (EPRI)
Gulf States Utilities
Potomac Electric Power Company (PEPCO)

Public Interest

Hawaii Health Physics Society
League of Women Voters:
League of Women Voters - Hawaii

Decision-Makers

Senate:

Asseltine, Jim
Staff-Environment and Public Works' Nuclear Regulation Subcommittee

Burgess, Barbara
Legislative Assistant (L.A.) to Sen. Laxalt (R-NV)
(Appropriations Committee)

Chakoff, Elliot
Staff-Energy Committee
(Sen. McClure R-ID)

Cooper, Ben
Staff-Energy Committee
(Sen. Johnston D-LA)

Crow, Steve
Staff-Appropriations' Energy and Water Subcommittee
(Sen. Hatfield R-OR)

Freihoffer, Dan
L.A. to Sen. Humphrey (R-NH)
(Energy Committee)

Participants

Gilman, Paul
Staff-Energy Committee
(Sen. Domenici R-NM)

Gleason, Jack
L.A. to Sen. Weicker (R-CT)
(Appropriations, Energy Committees)

Granger, Dick
L.A. to Sen. Hatfield (R-OR)
(Appropriations, Energy)

Gwaltney, David
Staff-Appropriations' Energy and
Water Subcommittee

Jordan, Jim
L.A. to Sen. Stennis (D-MS)
(Appropriations)

Lane, Carol
Staff-Sen. Schmitt (R-NM)
(Appropriations, Commerce)

Maginnis, Tom
L.A. to Sen. Hatfield
(Appropriations, Energy)

McCluskey, Bill
Staff-Commerce's Ocean Policy Study
(Sen. Packwood R-OR)

Moore, Curtis
Staff-Environment and Public Works'
Toxic Substances Subcommittee

Peterson, Andy
L.A. to Sen. Rudman (R-NH)
(Appropriations)

Tsongas, Sen. Paul (D-MA)
Energy Committee
Foreign Relations Committee

Tyson, Mitch
L.A. to Sen. Tsongas (D-MA)
(Energy, Foreign Relations)

Vance, Ann
L.A. to Sen. Wallop (R-WY)
(Energy)

Participants

Walsh, Tom
L.A. to Sen. Bumpers (D-AR)
(Energy, Appropriations)

Wicklund, Bob
L.A. to Sen. Weicker (R-CT)
(Energy, Appropriations)

House:

Dravo, Andrea
Staff-Interior Committee
(Rep. Udall D-AZ)

Dugan, Jack
Subcommittee Staff Director
Science and Technology's Energy Research and
Production Subcommittee
(Rep. Bouquard D-TN)

Durkin, Patrick
L.A. to Rep. Gregg (R-NH)
(Science and Technology)

Eustaquio, George
Administrative Assistant (A.A.) to Rep. Won Pat (D-Guam)
(Interior)

Freiwale, Joyce
Staff-Science & Technology's Energy Research Subcommittee
(Rep. Lujan R-NM)

Godown, Lee
L.A. to Rep. Ottinger (D-NY)
(Science and Technology)

Greer, Mel
Staff-Appropriations

Gregg, Rep. Judd (R-NH)
Science and Technology Committee

Hobson, Priscilla
L.A. to Rep. Lowery (R-CA)
(Science and Technology)

Ketcham, Rob
Special Energy Assistant
Science and Technology Committee
(Rep. Fuqua D-Fla.)

Participants

Krebs, Martha
Subcommittee Staff Director
Science and Technology's Energy Dev. and Applications

Lundine, Rep. Stanley (D-NY)
Science and Technology Committee

Malow, Dick
Staff-Appropriations' HUD-Independent Agencies
Subcommittee

Markey, Rep. Edward (D-MA)
Energy Committee
Interior Committee

Moss, Tom
Science and Technology's Science Subcommittee

Potter, Frank
Staff Director
Energy and Commerce Committee

Richardson, Mary Ann
L.A. to Rep. Lundine (D-NY)
(Science and Technology)

Schaeffer, Eric
L.A. to Rep. Schneider (R-RI)
(Science and Technology)

Schneider, Rep. Claudine (R-RI)

Star, Roger
L.A. to Rep. Gore (D-TN)
(Science and Technology, Energy and Commerce)

Stein, Ralph
DOE Fellow
Science and Technology's Energy Research Subcommittee

Wallace, Lee
Minority Staff Director
Energy Research Subcommittee

Ward, Mike
Counsel
Energy and Commerce's Energy Conservation Subcommittee

Won Pat, Rep. Antonio (D-Guam)
Interior Committee

Office of Technology Assessment

Barnard, Bill

Attachment 3

DEPARTMENT OF ENERGY AUTHORIZATION

HOUSE ACTION

SUBCOMMITTEE ON ENERGY RESEARCH AND PRODUCTION

In March the Subcommittee asked DoE to reduce its Civilian Waste Management budget of $206.241 million by $15 million (7%). DoE responded by reducing Subseabed by $3 million, from $6.5 million (Reagan Request) to $3.5 million (46%).

COMMITTEE ON SCIENCE AND TECHNOLOGY

Congressman Judd Gregg attached Report Language to the full Committee bill in May: "Radioactive waste management is a long-term scientific and institutional problem... an international as well as national problem... The Subseabed Disposal Program is an efficient, well-managed international research and development project... (and) should be continued as an international option as well as a national alternative...It should be funded at sufficient levels to determine whether subseabed disposal is scientifically and technically feasible."

But the $3.5 million funding level for Subseabed was maintained by the full Committee.

RECONCILIATION CONFERENCE

The Reconciliation Conference is a new step in the authorization process in which all authorization bills are considered as one rather than as separate bills.

The Reconciliation Conference eliminated detailed budget items, such as Subseabed $3.5 million item, in July. DoE was authorized to spend $194.124 for Civilian Waste Management on programs of its choice. However, nuclear waste legislation now moving through Congress will determine which programs DoE will support.

SENATE ACTION

COMMITTEE ON ENERGY AND NATURAL RESOURCES

The Committee authorized DoE to spend a bulk sum on all research activities.

97TH CONGRESS
1ST SESSION

S. 1662

To establish a limited program for Federal storage of spent fuel from civilian nuclear powerplants, to set forth a Federal policy, initiate a program, and establish a national schedule for the disposal of nuclear waste from civilian activities, and for other purposes.

IN THE SENATE OF THE UNITED STATES

SEPTEMBER 24 (legislative day, SEPTEMBER 9), 1981

Mr. MCCLURE (for himself, Mr. STAFFORD, Mr. DOMENICI, Mr. SIMPSON, and Mr. SYMMS) introduced the following bill; which was read twice and referred jointly to the Committee on Energy and Natural Resources and the Committee on Environment and Public Works, with the proviso that if either committee reports the bill, the other committee shall be obligated to report the bill in thirty calendar days (not including days on which the Senate is in recess for more than three days) or be discharged from further consideration thereof

---

A BILL

To establish a limited program for Federal storage of spent fuel from civilian nuclear powerplants, to set forth a Federal policy, initiate a program, and establish a national schedule for the disposal of nuclear waste from civilian activities, and for other purposes.

Be it enacted by the Senate and House of Representatives of the United States of America in Congress assembled,

NUCLEAR WASTE LEGISLATION

SENATE ACTION

THE PROPOSED NUCLEAR WASTE POLICY ACT OF 1981 (SENATE BILL #1662) CONTAINED NO PROVISION FOR CONTINUING RESEARCH AND DEVELOPMENT OF ALTERNATIVE WASTE DISPOSAL TECHNOLOGIES, SUCH AS SUBSEABED DISPOSAL.

SENATOR WALLOP (R-WYOMING) PROPOSED, AND SENATOR TSONGAS (D-MA) SECONDED, THE FOLLOWING AMENDMENT WHICH THE ENERGY COMMITTEE ACCEPTED BY UNANIMOUS CONSENT ON 21 OCTOBER 1981. THE COMMITTEE THEN PASSED S-1662 AND SENT IT TO THE FULL SENATE WHERE IT IS EXPECTED TO PASS.

> The Secretary shall continue and accelerate a program of research, development, and investigation of alternative means and technologies for the permanent disposal of high-level radioactive wastes from civilian activities, atomic energy defense activities of the Secretary and Federal research and development activities. Such program shall include examination of various waste disposal options.

HOUSE ACTION

THERE ARE SIX NUCLEAR WASTE BILLS IN VARIOUS STAGES OF DEVELOPMENT IN THE HOUSE. SOME OF THESE PROVIDE FOR CONTINUATION OF ALTERNATIVE TECHNOLOGIES. IT IS UNCERTAIN WHICH, IF ANY, OF THESE BILLS WILL SUCCEED IN THE HOUSE AND THEN GO TO THE HOUSE/SENATE CONFERENCE.

Attachment 4

SCIENCE ORIENTED PUBLICATIONS CONTACTED

AAPG EXPLORER

BIOSCIENCE *

DISCOVER

EOS *

GEOTIMES

NATURAL HISTORY +

NUCLEAR NEWS

OCEAN SCIENCE NEWS

OCEANS *

OMNI

SCIENCE DIGEST

SCIENCE NEWS

SCIENCE 81

SCIENTIFIC AMERICAN

SCIQUEST

SEA FRONTIERS +

SMITHSONIAN +

OVERVIEW ARTICLES

SCIENCE
ENVIRONMENTAL SCIENCE AND TECHNOLOGY

* article

+ Contact by Nancy Penrose

APPENDIX TT

MANAGEMENT SYSTEM DESIGN GROUP

Lawrence Susskind

Massachusetts Institute of Technology

(Contract #74-5192)

ANNUAL REPORT OF THE MANAGEMENT SYSTEM

DESIGN GROUP - SUBSEABED DISPOSAL PROGRAM

1980-1981

Prepared by Professor Lawrence Susskind
Massachusetts Institute of Technology

Annual Report of the Management System Design Group at the Massachusetts Institute of Technology

Our task is to design a management system capable of delivering high level waste (HLW) to carefully selected and monitored subseabed sites at the lowest feasible cost, in a fashion that respects all appropriate national and international regulations and protects the environment. The design of the management system must not only fit the complex regulatory framework of the United States, but also minimize political conflict as well.

To do this, we have specified a "most likely case" that presumes reprocessing, presumes retrievability, presumes (at least at the outset) one East Coast port, and presume a U.S. - initiated effort.

We have analysed (in a prelminary way) the likely sources of institutional and interest group opposition to subseabed disposal of HLW given our initial design assumptions.

We are now beginning the task of specifying the ways in which changes in the "most likely case" could respond to (and minimize) opposition to subseabed disposal. We are also identifying the basic management science and social science research needed to build a minimally acceptable understanding of the conflicts likely to arise. We are especially interested in analyzing the ways in which perceptions of risk develop.

A management system for subseabed disposal of HLW must, as best as we can determine, have at least nine components: (1) a land transportation component, (2) a storage and reprocessing component, (2) a port transfer component, (4) a sea transport, emplacement, and retrieval component, (5) a monitoring component, (6) a security component, (7) a safety and accident prevention

component, (8) an emergency response component, and (9) a development and administration component. We have attempted to outline the key questions that must still be answered before the design of an effective management system can proceed.

1. LAND TRANSPORTATION COMPONENT

The land transportation component of the subseabed management system must be designed to move HLW from reactor sites to interim storage sites and to port facilities that will prepare the waste for ocean transport to designated emplacement sites for subseabed disposal. We assume that the transportation engineering feasibility is not in question. In selecting specific transportation routes and specifying the mode(s) of transportation to be used, the following questions, however, need to be addressed:

1.1. What are the specific geographic locations of the routes and what will the timing and frequency of the shipments be? How should these decisions determine or affect the mode of transportation selected?

1.2. What criteria will be used in determining route selection (e.g. population concentrations, environmental sensitivities, proximity to port, etc.)?

1.3. What kind of regional (geographic) "equity" should there be in the actual distribution of routes (i.e., should the "risk" associated with transporting HLW through states and local jurisdicitions be evenly distributed throughout the country)?

1.4. Which political jurisdiction(s) should have responsiblity for the HLW during transportation?

1.5. What efforts should be made to address public perception and concerns about the trans-shipment of HLW?

1.6. Which jurisdiction(s) should have responsibility for HLW loading and off-loading and how should this responsibility link to the assignment of responsibility in case of accidents or other emergencies?

Many of these and related questions are being addressed by Sandia staff and consultants (other than ourselves). Our task is to synthesize the results already completed and to fill in where key management system design issues have not yet been addressed.

2. STORAGE AND REPROCESSING COMPONENT

When HLW is not being transported from one location to another, storage becomes a key management issue. While the feasibility of designing storage facilities that can meet all the applicable codes is not in question, various political decisions will have to be made. In addition, the question of "reprocessing" raises an array of sensitive political and economic questions.

2.1. How will storage and reprocessing sites be selected? What criteria will be used in evaluating various locations?

2.2. What will be the geographic distribution of such sites (nationally and regionally)?

2.3. Will states that have few or no reactor sites within their borders be considered as sites for storage?

2.4. Which political jurisdiction(s) will have responsibility for HLW while it is being stored? Who will have responsibility in a state of emergency while HLW is being stored? Who will control "access" to these facilities?

2.5. What safety and security measures will be employed in the design of storage facilities (above and beyond minimal technical design requirements)?

2.6. Will private contractors or a federal agency have primary responsiblity for reprocessing? If such activities are contracted-out to the private sector, will NRC licensing requirements still have to be met?

2.7. What kind of jurisdictional status will reprocessing sites have? Will such sites (whether commercial or government-owned and operated) be allowed to reprocess materials supplied by foreign governments (to increase the cost/effectiveness of such operations)?

2.8. What should the relationship be between reprocessing facilities and packaging, loading, and storage sites? Will all these activities be controlled by the same entity?

Many of these and related questions have been addressed by researchers working on a range of high level waste disposal options. Our task whenever possible into synthesize existing studies and results already in hand.

3. PORT TRANSFER COMPONENT

Ports located along the coastlines of the United States vary dramatically in both the size and type of activities they support. These variations, in addition to geographic relationship to subseabed disposal sites, will become factors in the selection of ports for the handling and transfer of HLW. Several management questions relate to port selection. Additional questions relate to the actual activities at ports that are selected.

3.1. How many port sites are needed to handle HLW for eventual subseabed emplacement?

3.2. What volume of HLW storage and transfer is necessary/acceptable at each port site?

3.2. What political and environmental criteria will be used to determin whether port locations are acceptable as HLW transfer points.

3.4. How should the history of conditions in existing ports be taken into account in evaluating potential port transfer sites?

3.5. Would the selection of numerous port transfer sites reduce the perception and distribution of risk for any one port?

4. SEA TRANSPORT, EMPLACEMENT, AND RETRIEVAL COMPONENT

HLW must be transported from designated port facilities to actual emplacement sites. We assume that the necessary sea transport, emplacement and retrieval equipment can be designed to code. The subseabed management system must, once again, respond to a variety of non-engineering issues.

4.1. How will ocean routes actually be selected? What environmental criteria and political concerns must be addressed in this selection process?

4.2. How will national and international responsibilities be divided for both the specification of ocean routes and the selection of emplacement sites?

4.3. What criteria (above and beyond engineering considerations) should be taken into account in designing the carrier and emplacement units?

4.4. What criteria should shape the design of a retrieval system (assuming HLW may need to be retrieved at some future time)?

4.5. Should retrieval become necessary, where and how will retrieval material be stored and under what conditions?

4.6. How should various kinds of risks be accounted for in the design of the sea transport, emplacement, and retrieval component of the management system?

4.7. What criteria should be used in the selection of emplacement sites?

We are concerned about three types of retrieval. If are dropped accidentally, what retrieval technology and strategy would be appropriate? If repositories fail, what retrieval capacity will be essential to forestall environmental damage and danger to human health? If the United States wants to retrieve waste materials to reuse them as a resource, what technological capacity will be needed?

6. THE MONITORING COMPONENT

A monitoring and evaluation component must be an integral part of the overall subseabed management system. Such a monitoring component should be operational from the initial point of transport of the HLW from reactor sites, to the storage facilities, through the port handling phase, and well past the point at which the HLW is emplaced in the designated subseabed geologic

formation. In addition to generating routine surveillance data on the condition of HLW, a monitoring system must warn against outside intrusion, (human or otherwise) and alert those responsible as to the particular nature of any emergencies that arise. Thus, our definition of monitoring encompasses awareness of the movements of emplaced waste, instances of security breaches baseline environmental monitoring (both thermal and chemical), and overall surveillance of the efficiency of the entire management system and its operation.

In addition, the type of data generated by the monitoring component must be sufficient to convince various publics that surveillance is adequate. A variety of questions will arise regarding the appropriate source of standards and regulations for monitoring and enforcement. American system must be compatible with international conventions and protocols. Questions surrounding the design of the monitoring component of the management system include:

6.1. What should the scope of the monitoring effort be?

6.2. How will the design of the monitoring system address current environmental standards, worker safety standards, and general human health standards in the immediate geographic area (and region), especially in the event of an accident or emergency?

6.3. Which jurisdiction(s) will have primary responsibility for monitoring and data analysis and interpretation? How will monitoring data be stored and retrieved?

6.4. How will conficts among national and international standards for monitoring be resolved?

6.5. How will various public be involved in the design of the monitoring component in order to ensure that perceptions of risk are addressed?

6.6. What provisions should be made for back-up in the event of a failure of the primary monitoring component?

6.7. What kinds of security and relatedly "access" will be attached to the information generated by the monitoring component? What kinds of information will be provided to the general public on a routine basis?

5. SECURITY COMPONENT

The security component of the management system will be perceived by many to be the most crucial component of the entire system. As with the monitoring component, the security component must be designed to ensure the protection of HLW from the reactor site, during emplacement and retrieval, and throughout the duration of its emplacement in the subseabed. The design of the security component must take account of a range of considerations.

5.1. What is the scope of security that must be provided? How extensive or exhaustive must security be for HLW - thoroughout the various stages of its radioactive life - and at what point would the cost of security make the entire subseabed option economically or politically impossible? Must daily (and costly) monitoring of HLW continue for 100 years, 500 years? Will the enitre security system be run at a "maintenance" level or at a more agressive "defensive" level?

5.2. Which jurisdiction(s) will have primary responsibility for security? How will conflicts regarding the assignment of national and international responsibility be resolved?

5.3. What will constitute a security violation and how will this definition relate to standards for response in emergency situations? Will such standards address the question of potential "sabotage"?

5.4. How will public perceptions of risk and security be addressed in designing the security component?

5.5. Will provision(s) for new or expanded protection be designed into the original security system in the event that the original system is compromised in some fashion?

5.6. How will decisions be made (and by whom) with respect to informing the public about security problems when and if they arise? What rights to information will the general public and the press have during an emergency situation?

7. EMERGENCY RESPONSE COMPONENT

There must be an emergency response component to the management system that can assure a timely and efficient response to a range of problem situations including spills or accidental ocean drops, lack of availability of cannisters and packaging materials, lack of availability of transport vehicles or unexpected barriers to transport, sabotage, personnel shortages, etc.

7.1. What will trigger an emergency response (i.e., under what circumstances will an emergency response be deemed necessary and prudents)?

7.2. What jurisdiction(s) will have responsibility for determining that such a response is necessary? Which jurisdiction(s) should have responsibility for implementing emergency response plans?

7.3. How will any conflicts between responsible jurisdictions be resolved?

7.4. What "checks and balances" should be built into an emergency response situation?

7.5. What specific plans and procedures will be utilized in an emergency response situation and where will legal liability reside? When emergencies occur in international waters, what different procedures or plans should be put into effect?

8. SAFETY AND QUALITY ASSURANCE* COMPONENT

Public perceptions of acceptable risk may vary dramatically from the results of formal risk assessment. The design of a safety and quality assurance component of the management system must respond to public perceptions of risk and not just to formal risk analyses.

8.1. How should responsibility for safety and quality assurance be assigned? What national and international conflicts might this raise? How should jurisdictional conflicts be resolved? How will the answer to this question be incorporated into the American legal and regulatory framework?

8.2. How will standards be set for worker safety and the protection of the general public in areas through which HLW is transported or in areas where HLW is stored? What standards for environmental protection should be employed?

8.3. What quality performance standards should constrain the engineering design of the components of the subseabed system? Which jurisdiction(s) should set these standards? How will various agency concerns be addressed (i.e. what kinds of interagency and intergovernmental arrangement must be developed)?

* When we speak of quality assurance we are concerned about such things as the weight of newly produced and filled cannisters, the construction of the ship and other modes of transport, the thermal output of cannisters, the depth at which cannisters are placed, etc.

8.4. What type of public education efforts will be undertaken to advise and up-date the general public on on-going safety precautions and emergency procedures?

8.5. How will public perception(s) of risk be determined and subsequently incorporated into the design of a safety and accident prevention component?

9. DEVELOPMENT AND ADMINISTRATION COMPONENT

The overall administration of a subseabed disposal system fit into national and international governmental structures. The design of an administrative component must involve key groups. All relevant regulatory guidelines must be observed.

The development and administration component of the management system must indicate how financing, engineering and construction of the system will be handled. The administrative componenet must also encompass personnel selection and supervision for all aspects of system design and operation. The administrative component must be designed in a manner that will ensure the cost-effectiveness of the system as a whole.

Specific issues surrounding the design of the development and administration component include:

9.1. What kind of "ownership" and financing mechanisms should be created for subseabed disposal? Or, for each phase of the system? Is public ownership or private ownership to be preferred. Is some combination of the two possible? Under what circumstances?

9.2. Should ownership options relate to the system as a whole or should different ownership options be considered for each component?

9.3. What kind of "checks and balances" should be built into the operation of the administrative component of the system?

9.4. For which jurisdiction(s) should system employees and contractors work? What if any, special selection criterial should be used in choosing contractors or personnel?

9.5. What kind of regulatory review and compliance mechanisms can enure that the system meets all relevant national and international guidelines at all times?

9.6. Which jurisdiction(s) will assume responsibility for non-compliance with established guidelines?

9.7. How will responsibility for preparing new legislation or regulatory guidelines be assigned if such are needed to permit implementation of a subseabed system?

9.8 How should affected local, state, and federal agencies be involved in the design and subsequent administration of a subseabed system?

9.9. What measures of acceptable cost should be imposed on each component of the subseabed system?

During the coming year, the MIT Management Systems Design Group will attempt to answer (or, at least, work with others to answer) the questions listed above.

Do Not Microfilm

DISTRIBUTION:

Lamont-Doherty Geological Observatory
Palisades, NY 10964
Attn: D. Hayes

Argonne National Laboratory
Chemistry Division
9700 South Cass Avenue
Argonne, IL 60439
Attn: S. Fried

University of Rhode Island (4)
Graduate School of Oceanography
South Ferry Road
Narragansett, RI 02882
Attn: A. H. Driscoll
E. Laine
A. J. Silva
M. Leinen

University of Washington
Applied Physics Laboratory
1013 Northeast 40th Street
Seattle, WA 98198
Attn: L. Olson

Oregon State University
Corvallis, OR 97331
Attn: G. R. Heath

Waterways Experiment Station
Structures Laboratory
PO Box 631
Vicksburg, MS 39120
Attn: B. Rohani

Massachusetts Institute of Technology
77 Massachusetts Avenue
Cambridge, MA 02139
Attn: L. Susskind

AOML/NOAA
15 Rickenbacker Causeway
Miami, FL 33149
Attn: R. Bennett

University of New Hampshire
O'Kane House
Durham, NH 03824
Attn: J. Kelly

The Analytic Sciences Corp.
6 Jacob Way
Reading, MA 01867
Attn: C. Koplik

Scripps Institution of Oceanography (3)
La Jolla, CA 92037
Attn: A. A. Yayanos
R. R. Hessler
K. Smith

Woods Hole Oceanographic Institution (4)
Woods Hole, MA 02543
Attn: V. T. Bowen
C. D. Hollister
B. Tucholke
F. Sayles

University of Minnesota
Department of Geology and Geophysics
Minneapolis, MN 55455
Attn: W. E. Seyfried

University of California
Civil Engineering Dept.
Berkeley, CA 94720
Attn: W. Houston

Cornell University
254 Upson Hall
Ithaca, NY 14853
Attn: P. R. Dawson

Scripps Institution of Oceanography
La Jolla, CA 92037
Attn: P. Doyle

University of Washington
Institute for Marine Studies
Seattle, WA 98195
Attn: E. Miles

5511 C. E. Hickox
5521 S. N. Burchett
5521 M. G. Marietta
5531 T. R. Canfield
5541 J. L. Krumhansl

Distribution, cont'd.

5627 L. T. James
5812 K. L. Erickson
5835 C. H. Karnes
5840 N. J. Magnani
9734 D. R. Anderson
9734 L. H. Brush
9734 L. S. Gomez
9734 R. D. Klett
9734 S. L. Kupferman
9734 J. Lipkin
9734 C. M. Percival
9734 L. E. Shephard
9734 D. M. Talbert
9734 K. R. Hinga (2)
9783 G. C. Allen, Jr.
8214 M. A. Pound
3141 L. J. Erickson
3151 W. L. Garner
For DOE/TIC (Unlimited Release)
3154-3 C. Dalin
(For DOE/TIC)